CRETACEOUS SEDIMENTOLOGY OF THE BARMER BASIN, RAJASTHAN, INDIA

HAZEL BEAUMONT

Ph.D.

JUNE, 2017

KEELE UNIVERSITY

Abstract

The Barmer Basin, western India, is a well-known and prospected petroleum system. However, the Lower Cretaceous Ghaggar-Hakra Formation has not been recognised as basin fill and not documented prior to this study. The formation outcrops in rotational fault blocks at the Sarnoo Hills and surrounding areas, on the eastern Barmer Basin margin. The thesis here describes and analyses the nature and evolution of the formation at both outcrop and within the subsurface, producing facies and depositional models.

At outcrop, the deposits of the Ghaggar-Hakra Formation contain three dominant fluvial sandstone successions, known as the Darjaniyon-ki Dhani, Sarnoo and Nosar sandstones. The Darjaniyon-ki Dhani Sandstone is a gravel bedload dominated, low sinuosity fluvial system, the Sarnoo Sandstone represents a mixed-load, high sinuosity fluvial system and the Nosar Sandstone is highly erosive well-developed, bedload dominated, low sinuosity fluvial system. The intervening mudrocks represent floodplain deposits.

The growth and development of the fluvial system between the Darjaniyon-ki Dhani and Sarnoo sandstones indicates that the climate and tectonics were stable at the time of deposition. However, the Nosar Sandstone represents rejuvenation of the fluvial system as it is suggested that this change in deposition style is due to the activation of the fault network forming the Barmer Basin and West Indian Rift System.

The facies models derived from this work are applied to the subsurface to provide interpretations of the Cretaceous succession. This provides significant insights into the sedimentology, geometries of the sediment packages with the net to gross and the petrography, all indicating the reservoir quality of the Ghaggar-Hakra subsurface material.

Acknowledgements

The completion of this thesis is due to the guidance and support of my many supervisors Dr Stu Clarke, Dr Andrew Taylor, Thomas Gould and Prof. Stuart Burley – I am truly indebted to you. I thank Cairn India and Keele University for providing all financial and logistical support. I am so very thankful for this amazing chance I have been given and all the opportunities it will lead onto.

I would not have completed this research without Andrew Bladon and his many personalities while in India. Andy, I love you and without you, my life would be lacking. Without the kind assistance of Bhanwar Lal and James Solan my second and fourth fieldwork seasons would not have occurred. While in India Dr Nicholas Whiteley, Pinakadhar Mohapatra, Dr Stephen Goodlad and Pranjal Sharma your kindness and support was unwavering. In-house, the technician staff Rich Burgess, Ian Wilshaw, Pete Greatbatch and Dave Wilde – honestly without you, life would be horrific.

I am truly grateful to those who have provided their time and effort in every way from just being there, to (occasionally) helpful discussions from the BDRG clan (Amy, Molly, Rachel, Tom and Tom), other postgraduate students at Keele and my home-grown friends in the shape of Chloe, Kirstin, Lucy and Lucy. To my climbing guys (mainly Paddy) who allow me to rant on and be 'geeky' about rocks I owe you many bottles of wine and beer and to my proof readers, you guys are amazing!

Pippa, without you the last few years would have been unimaginable. You have been my rock; I truly do need you as you are silly, brilliant, beautiful, sometimes-crazy, always-amazeballs and will be one of my partners-for-life.

Finally, this research, my Masters, my degree, the person who I am today would not have been achievable without my incredible mother and admirable stepfather, who is more like a dad to me than he will ever know. To my wonderful but pain-in-the-arse brothers, Nicholas and William, I do love you both (surprisingly). Lastly, dad, I know you have wanted me to get a 'proper job' for years now – maybe it will be possible? Genuinely, mum, Tony, dad, Nicholas, William and (of course) the dogs (Tess and Horace), I do love you and I thank you for all the support (both loving and in monetary form) over the last 26 years – you literally have no idea how much it means to me.

Contents

List of figures

Chapter 9

List of tables

1 Chapter One: Introduction

The Barmer Basin is situated within the West Indian Rift System of Rajasthan, northwest India (Figure 1.1). It is an extensional intracratonic basin, 190 km long, 45 km wide and 6 km deep (Compton, 2009) and orientated in a north northeast – south southwest direction. The basin formed predominantly within the Palaeogene Period (Biswas, 1982, Bladon *et al.,* 2015a), but early, controlling lineaments formed within the Triassic Period.

The plate tectonic setting of Rajasthan is complex. The current configuration of the Barmer Basin, and the Indian plate in which it resides, has resulted from the fragmentation of Gondwana (Reeves, 2014). Two main rifting events contributed towards the formation of the Barmer Basin: the separation of India from Madagascar (Upper Cretaceous Epoch) and the rifting of the Seychelles microcontinent (latest Cretaceous – earliest Paleogene periods; Bladon *et al.,* 2015b). The current setting of the Barmer Basin and the Indian plate is approximately 25° north of the equator and within the Tropic of Cancer. The plate is still slowly moving northwards into the Eurasian Plate creating uplift to the north of the basin forming a southeast tilt.

The sedimentary fill of the basin is recognised to be of primarily Paleogene age (Compton 2009; Dolson *et al.,* 2015). However, there is evidence of Mesozoic to Quaternary sediments (Figure 1.2). The basement of the basin is composed of the Malani Igneous Suite and is Precambrian in age (Sisodia and Singh, 2000). The Jurassic to early Cretaceous pre-rift sediments of the Barmer Basin are primarily fluvial in origin (Bladon *et al.,* 2015a, b; Dolson *et al.,* 2015). The main syn-rift phase spanned the Late Cretaceous to Eocene periods during which sediments from fluvial, alluvial, lacustrine and coastal environments were deposited, culminating in coastal, delta and shallow marine environments by the Eocene Period. The post-rift sediments are Neogene and Quaternary in age and dominantly fluvially-derived.

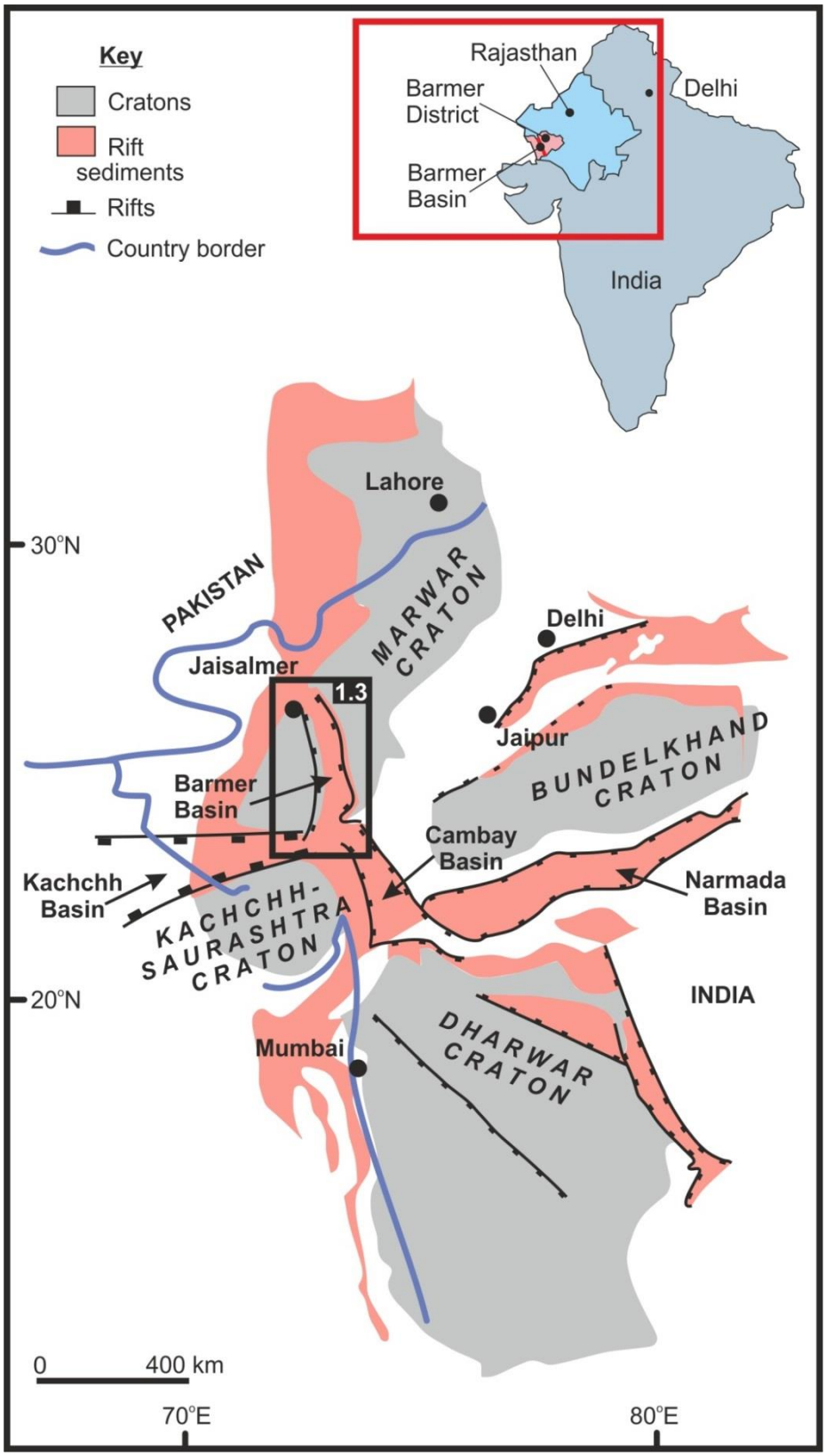

Figure 1.1: The current geography and location of the Barmer Basin and the West Indian Rift System, Rajasthan. The basins of the West Indian Rift System are Cambay, Barmer, Kachchh and Narmada basins, displayed in pink is the rift sedimentation within the basins. The blue line is the country border between India and Pakistan. Inset: map of India displaying where Rajasthan is and the location of the Barmer Basin (Balakrishnan *et al.*, 2009).

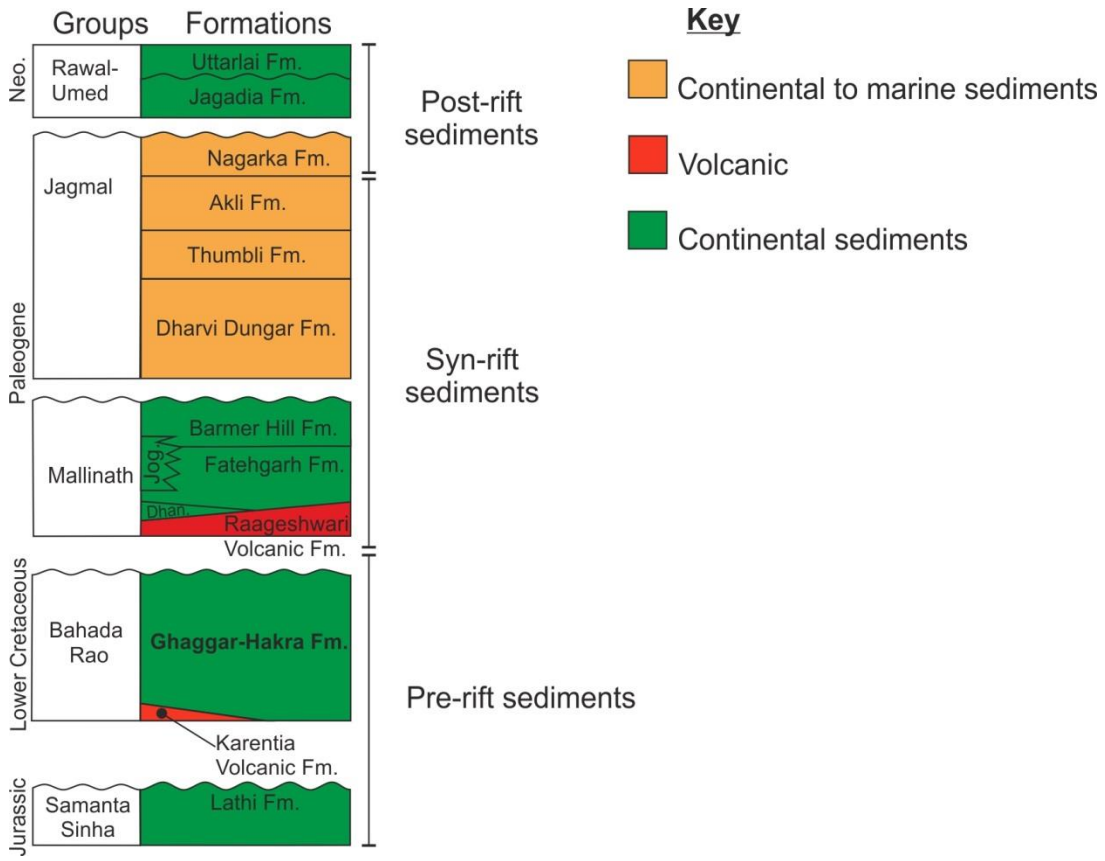

Figure 1.2: Generalised vertical succession of the Barmer Basin displaying the pre-rift, syn-rift and post-rift sedimentology, as assumed prior to this study (Dolson et al., 2015).

This research concentrates on the newly-defined Lower Cretaceous, the Ghaggar-Hakra Formation of the Barmer Basin, assumed to be pre-rift sedimentation. The Ghaggar-Hakra Formation has received comparatively little past attention (Sisodia and Singh, 2000; Bower, 2004a, b; Clarke, 2011; Bladon *et al.,* 2015a, b) when compared to the remainder of the stratigraphy of the basin. This is because it has not been recognised to date as forming part of the subsurface basin succession, despite being exposed in rotated faulted blocks on the basin's eastern margin. At outcrop, the succession constitutes three fluvial sandstone packages, dominantly composed of quartzarenites with sedimentary structures that indicate a south-westerly palaeocurrent (Sisodia and Singh, 2000). The sandstone packages are separated by mudstones and siltstones attributed either to lake-bed sedimentation (Bower, 2004a; Clarke, 2011), or to deposition upon an immature floodplain (Bladon *et al.,* 2015b).

However, previous studies of the Ghaggar-Hakra Formation at outcrop fail to describe and document the facies and architectural elements to determine the exact nature of the fluvial system along with the controls upon it. The previous studies do not provide a detailed analysis of palaeoflow for all the sandstone packages, nor do they describe and interpret the petrography of the succession. Consequently, the provenance of the fluvial system has not been established. The lack of any systematic study of the Ghaggar-Hakra Formation means that its relationships to the subsurface sedimentary fill of the Barmer Basin are yet to be established. Consequently, the possible contribution of the Ghaggar-Hakra Formation to the petroleum system of the Barmer Basin is not yet understood.

Fluvially-dominated systems are amongst the most prevalent of continental environments both present day and within the rock record. They form from the proximal edge of a basin and drain into basin centre and they interact with contemporaneous depositional systems such as alluvial fans, lacustrine systems and the shallow marine environment. The nature of fluvial system is strongly dependent upon the localised structure, subsidence rates, climate, sediment accumulation and base level (Arguden and Rodolfo, 1986; Leeder *et al.,* 1998; Gupta *et al.,* 1999; Gawthorpe and Leeder, 2000). Early research into fluvial systems has established facies and architectural element schemes (Allen, 1965; Miall, 1988; Schumm, 1972) which build together to form three-dimensional facies models to determine the type of fluvial system that is noted within the rock record (Miall, 1985, 1988). The architectural elements within fluvial systems can produce areas of high quality hydrocarbon reservoirs and consequently fluvial environments have received much study and are reasonably well understood (Allen, 1965; Schumm, 1972; Miall, 1985, 1988; Cain and Mountney, 2009).

This research provides the first comprehensive and detailed study into the Cretaceous aged Ghaggar-Hakra Formation within the Barmer Basin, India (Figure 1.1). Outcrop studies concentrate upon three, relatively small, hills on the eastern margin of the basin

where the Ghaggar-Hakra Formation is exposed in extensive quarries (Figure 1.3). Within these areas, sediments are exposed within a series of rotated fault blocks that throw down towards the basin centre and tilt the sediments towards the basin margin. The thee field areas are named (from south to north): Sarnoo, Karentia and Nosar (Figure 1.3).

Facies and architectural element analysis has been completed on these sediments to determine the nature and type of fluvial system for this part of the stratigraphy. Petrographical analysis has concluded that the formation is composed of quartzarenites but with differing amount of detrital quartz and lithic fragment grains likely related to the fluvial regime. Statistical analysis of palaeocurrent data has revealed that each of the sandstone packages flows in different directions related in part to the nature and style of fluvial regime, but also a result of strong extrinsic influences of tectonics, climate, sediment supply and base level.

The outcrop data from the proximal setting of the Ghaggar-Hakra Formation are then related to the distal basin deposits through examination and analysis of core data. The core data are described in terms of facies, facies associations and petrography, but they are interpreted with reference to the outcrop. This approach enables a basin wide analysis and synthesis of the Ghaggar-Hakra Formation to determine the contribution of tectonics and climate to the evolution of the system and sedimentology.

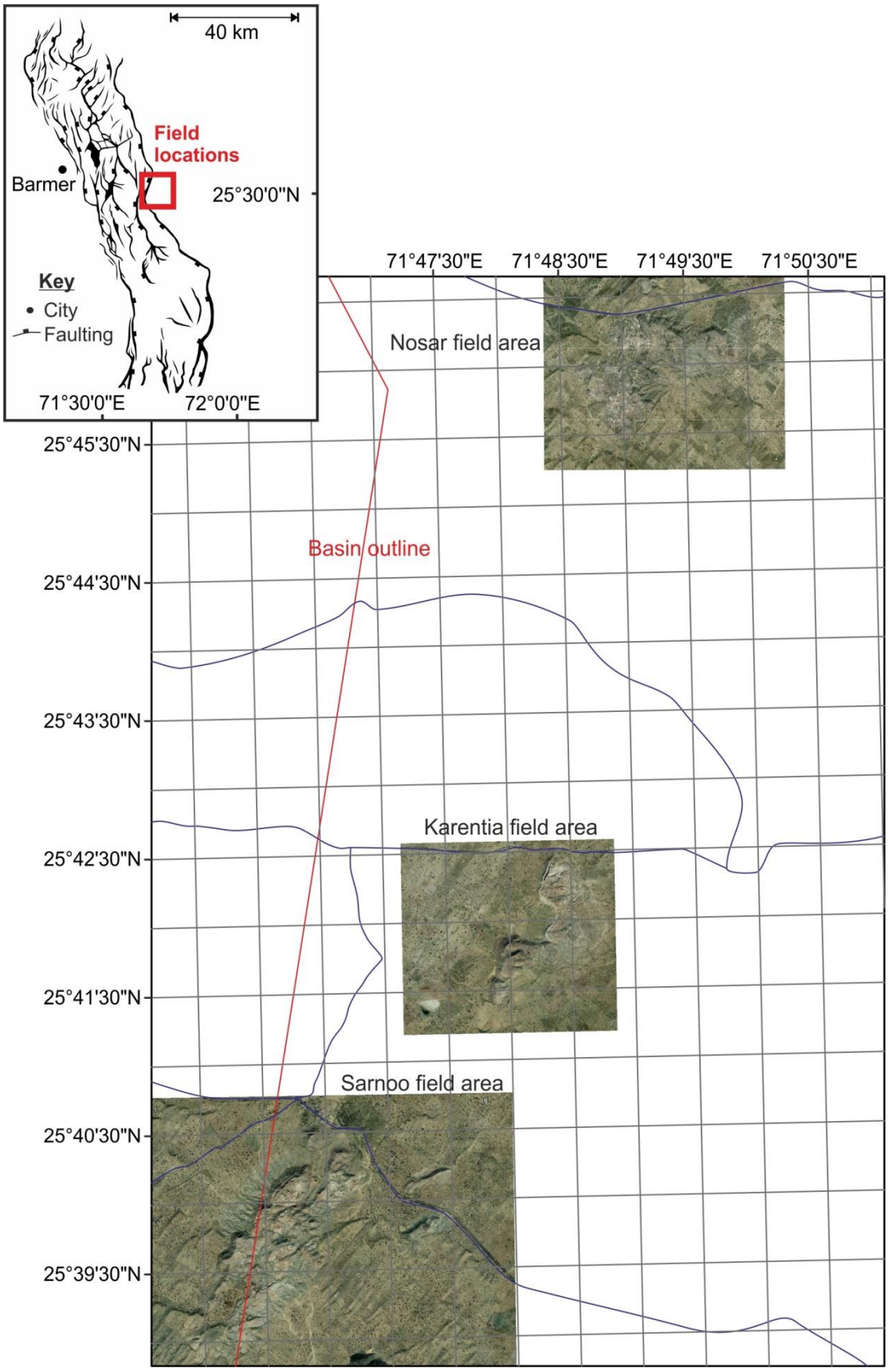

Figure 1.3: Aerial photographs of the field areas which are in the central eastern margin of the basin; with Sarnoo in the south which is approximately 2 km north to south, Karentia slightly northeast by 1 km and Nosar in the north. Inset: Structural geometry map of the Barmer Basin displaying where the field areas are.

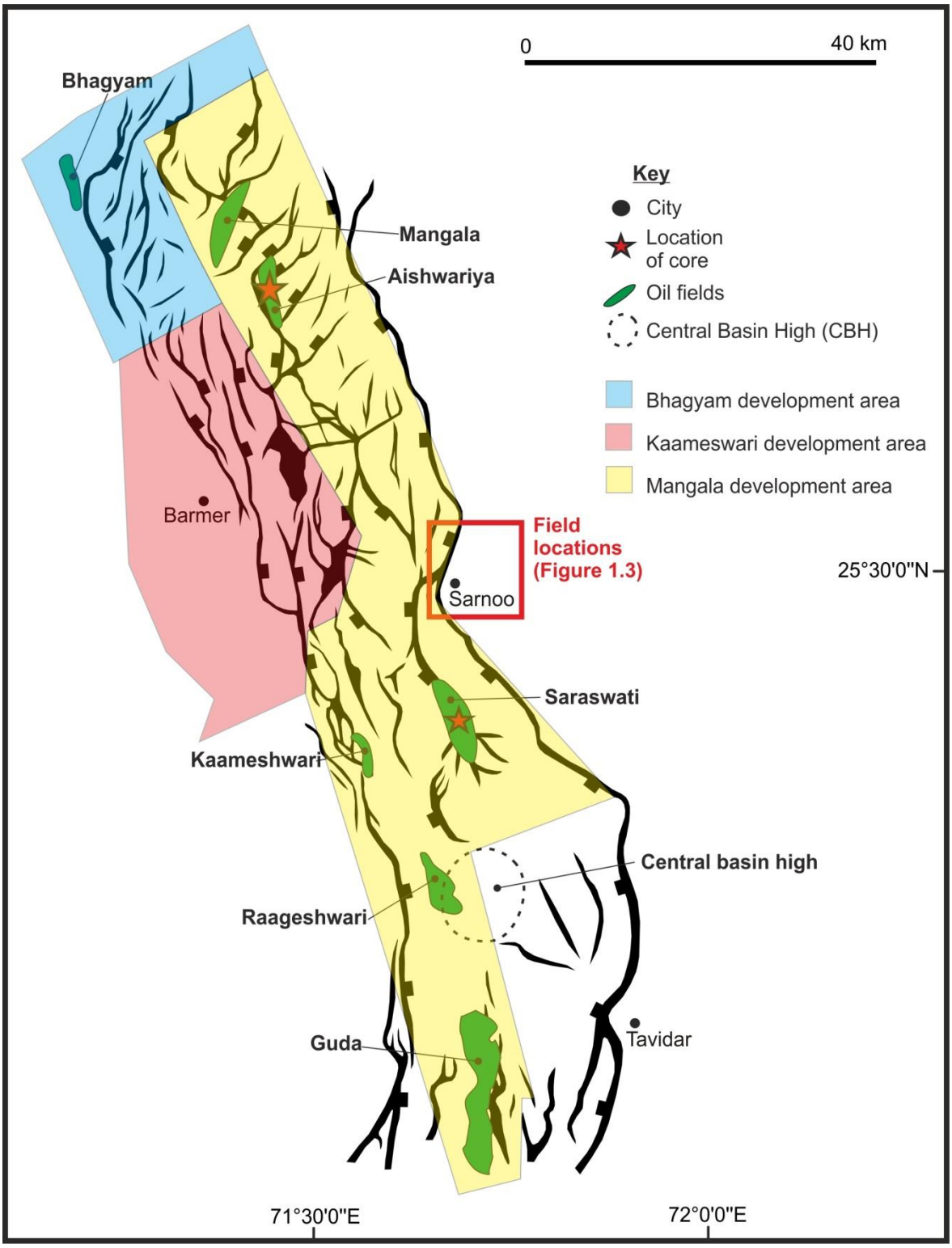

Figure 1.4: The base Paleogene structural geometry of the Barmer Basin displaying the location of the field areas, core log locations, and key oil fields. The development areas are also highlighted. See Figure 1.1 for the location of this figure within the West Indian Rift System (Dolson *et al.,* 2015).

1.1 Summary of the hydrocarbon history of the Barmer Basin

During the 1970's, the acquisition of the first two-dimensional dataset over the Barmer Basin and in 1989 this dataset was augmented with relatively poor-quality gravity data (Dolson *et al.,* 2015), which displayed some potential hydrocarbon reserves. These datasets led to an exploration partnership forming between Shell India Petroleum Development (SIPD), Natural Gas Commission of India (ONGC) and the Government of India (GoI). Using the datasets above the partnership obtained further 150 km two-dimensional dataset in the south of the basin. In 1995, the partnership established an exploration licence over the basin known as Block RJ-ON-90/1 and acquired a further 1613 km of two-dimensional seismic data and three-dimensional survey over a structural high in the south-central basin called the Central Basin High (Figure 1.4). In 1997, Cairn Energy India Ltd. (CEIL) joined the partnership with 27.5% equity (Dolson *et al.,* 2015) in the block. CEIL acquired a further 1267 km of high-density, two-dimensional seismic data and a 650 km^2 three-dimensional dataset over the Central Basin High (Figure 1.4) and subsequently discovered the Saraswati and Raageshwari oil fields (Dolson *et al.,* 2015). These prospects contain 500BOE commutatively (Cairn, 2016) and were deemed small so the SIPD and ONGC withdrew from the Barmer Basin leaving CEIL as the sole operator. Here, the reservoir is the Fatehgarh Formation of Paleogene age. CEIL then made additional discoveries in 2003 in the Kaameshwari Field on the western margin of the basin, and the Guda Field in the very south of the basin (Figure 1.4, Dolson *et al.,* 2015), again the reservoir is the Fatehgarh Formation of Paleogene age.

Up to 2003, all of the discoveries in the Barmer Basin were in poor-quality reservoirs of fluvial sandstones. In late 2004, CEIL almost withdrew from the basin but tested a large, shallow, fault block in the north of the basin, which had previously been considered a high-risk prospect. Exploration wells were successful and the discovery was named the Mangala Field. This field contained 1.3 billion barrels STOIP (Zalawadia and Powde, 2013) within a high-quality reservoir (Compton, 2009; Dolson *et al.,* 2015), in dominantly

fluvial strata of the Fatehgarh Formation deposited in the Upper Cretaceous to Paleocene intervals (Compton, 2009; Dolson *et al.,* 2015).

In 2005, ONGC joined CEIL with 30:70 equity. The joint venture converted the exploration licence over RJ-ON-90/ block into three development licences named: The Mangala development area (awarded 2004), Bhagyam development area (175,000BOE) is within the north of the basin and was awarded in 2005. Oil production here started in 2012. The Kaameswari development area was awarded in 2008 and is within the north eastern part of the basin (Figure 1.4). The main reservoir here is the Fatehgarh Formation of Paleogene age. Within the Mangala, Aishwariya and Bhagyam fields there is up to $3.6x10^9$ BOE (Compton, 2009). In 2013, exploration activities resumed within the basin. At the time of writing (Spring, 2016) there are five active fields which are: Mangala, Bhagyam, Aishwariya, Saraswati and Raageshwari (Dolson *et al.,* 2015; Carin, 2016). The basin is currently producing 6 BNBOE where the main reservoir is the medium- to coarse-grained, cross-bedded Fatehgarh Formation. Currently, there are no exploration targets for the Cretaceous-aged Ghaggar-Hakra Formation (Cairn, 2016).

1.2 Research rationale, aims and objectivities

This work will provide a fully integrated and quantitative set of three-dimensional depositional facies models for the Ghaggar-Hakra Formation of the Barmer Basin. These models, augmented with geometrical statistics for architectural elements, petrographical details, and relationships to syn- and post-depositional structure, provide the basis for interpretation of this part of the Barmer Basin stratigraphy. The models will be set in context to look at basin evolution and the provenance of the fluvial system in order to help characterise the formation at outcrop and within the subsurface.

This project will characterise the Ghaggar-Hakra Formation in its entirety by completing the following objectives:

Undertaking detailed facies analysis of all Ghaggar-Hakra sediments to understand the stratigraphy and nature of the succession.

- Gathering data on the geometric parameters of the architectural elements to add to facies data in order to distinguish the depositional environment and its evolution through time.

- Undertaking detailed petrographical analysis to examine the provenance for the fluvial system.

- Analysing palaeocurrent data to determine the palaeoflow of the sediments and the sediment routing; this will also help with the provenance of the fluvial system.

- Producing three-dimensional facies models from all strands of the research to determine the depositional environments of the formation and integrating these models into the post-depositional history.

- Describing and interpreting core data to analyse the subsurface and determine potential links to the outcrop data.

- Interpreting field data at the large scale, providing stratigraphical detail for the Ghaggar-Hakra Formation to correlate with the core data.

1.3 Thesis overview

This thesis aims to present the geological evolution of the Ghaggar-Hakra Formation of the Barmer Basin through facies, architectural element, petrographical and palaeocurrent analysis (Chapter 1). In order to complete the objectives listed in Section 1.2 a detailed literature review of fluvial systems has been undertaken (Chapter 2), allowing for the interpretation of the logged sediments in term of facies and architectural elements (Chapter 4 and 5). This interpretation has facilitated development of three-dimensional facies models (depositional elements) for each sandstone package and the mudstone successions.

The thesis then moves onto the petrographical data which are used to determine the diagenetic history and the provenance of the fluvial system (Chapter 6). The next dataset is the palaeocurrent data, analysed by using moving average techniques to determine of the flow directions and sediment pathways of the outcrop material. In-conjunction with the petrographical data, palaeocurrent analysis can be used to determine in-part, the provenance and flow directions to the centre of the basin (Chapter 7). These three datasets are brought together to give a large-scale interpretation of the formation considered in the context of the evolving eastern margin of the Barmer Basin (Chapter 8). The final dataset is the core data analysed through facies and facies associations and then related to the outcrop data. This determines the nature of the depositional environment of the subsurface Ghaggar-Hakra using the outcrop analogue (Chapter 9). Finally, this thesis draws to a close by summarising each dataset and discussing the potential future research of the Ghaggar-Hakra Formation.

A summary of the content of each thesis chapter are presented below:

- **Chapter 2** presents a literature review of the relevant topics relating to this research including: 1) dynamics of flow, transport mechanisms and bedform morphology; 2) facies and architectural elements of fluvial systems, including floodplains, and; 3) the influence of tectonics, climate, base level, sediment supply and avulsion.

- **Chapter 3** outlines the geological setting and stratigraphical context of the Barmer Basin. It considers the current literature that relates to the depositional setting of the Ghaggar-Hakra Formation in great detail.

- **Chapter 4** develops in detail the sub-facies, facies and facies associations of the Ghaggar-Hakra Formation.

- **Chapter 5** builds upon the facies and facies associations outlined in chapter four to develop architectural elements representing the dominant fluvial depositional styles. Spatial occurrences of these elements are combined to represent different fluvial facies models.

- **Chapter 6** examines the petrography of the Ghaggar-Hakra Formation. It discusses the literature pertaining to the detrital and authigenic mineralogy of fluvial systems. It then analyses the literature to examine the mineral relationships and previous interpretations of the Ghaggar-Hakra Formation to date. The data collected measures grainsize, detrital and authigenic mineralogy and porosity of the samples. This data is then used to delineate the provenance and diagenetic history of the Ghaggar-Hakra Formation.

- **Chapter 7** explores the palaeocurrent evidence of the formation. Presented first is the literature examining the analysis of palaeocurrents and how palaeocurrent data can help to determine the type of fluvial system within a basin. The limited data on the palaeocurrents of the formation are then examined. The palaeocurrent data of the formation provides palaeoflow directions, these directions are then interpolated in-conjunction with the published literature on the Lower Cretaceous fluvial systems of the West Indian Rift System to give a regional palaeoflow interpretation (Sisodia and Singh 2000, Racey *et al.,* In Review).

- **Chapter 8** discusses the results of chapters four through to seven and brings them together to provide an integrated depositional model for the formation. This is used to further the understanding of the Cretaceous succession. Also discussed are the tectonic, climatic, avulsion and base level influences upon the fluvial environment within the Barmer Basin and the West Indian Rift System. The chapter concludes with

a discussion of the limitations of the datasets and an exploration of the implications this research has for hydrocarbon exploration within the Barmer Basin.

- **Chapter 9** investigates the subsurface core data for the Ghaggar-Hakra Formation. This chapter outlines the facies interpreted from the core data which are combined to form facies associations. Next analysed are the detrital and authigenic minerals for comparison to the outcrop. Based on the facies and petrographical datasets depositional environments are suggested. The chapter then discusses how the distal environments relate to the proximal environments and places the Cretaceous stratigraphy within the context of the evolving Barmer Basin.

- **Chapter 10** concludes the research by summarising the results and suggesting future directions for research into the Ghaggar-Hakra Formation.

2 Chapter Two: Fluvial Literature Review

Fluvially-dominated depositional systems are among the most prolific of continental environments at the present day and within the rock record. The arrangements of the facies and architectural elements within fluvial systems have the potential to form good hydrocarbon reservoirs and stratigraphical traps. Consequently, mature fluvial environments have received much study and are reasonably well understood. Their nature has been analysed by multiple authors (Jackson, 1976; Allen, 1965; Miall, 1985; Gulliford *et al.,* 2014) who have developed many schemes for analysing fluvial systems - including facies, bounding surface analysis and architectural element analysis - that are widely accepted and applied frequently to the analysis of outcrop.

This chapter reviews the literature in relation to fluid flow in unconfined and confined settings within fluvial systems, starting with Newtonian concepts. Also reviewed are the intrinsic properties that are derived from these ideas - the Reynolds Number, Shields Criterion and the Froude Number - providing the basis for sediment transportation and bedform formation.

Bedforms are deposited through different processes of sediment transport and therefore relate to the preserved facies in different ways. The arrangement of facies can form different architectural elements which in turn form different types of fluvial systems. The types of fluvial systems discussed within this chapter are bedload-dominant, low-sinuosity, fluvial systems, mixed-load, high-sinuosity fluvial systems and suspended-load fluvial systems, along with their associated floodplain deposits. The fluvial systems themselves are influenced by extrinsic processes including tectonics, climate, base level, sediment supply and intrinsic processes such as avulsion (Leeder *et al.,* 1998; Gawthorpe and Leeder, 2000). These influences are discussed in detail.

2.1 Fluvial systems

Fluvial systems are characterised by their sediment load, sinuosity, bank stability, channel geometry, sediment transport and discharge, and these factors result in recognisable styles of fluvial deposition. Well-recognised types of fluvial system are bedload-dominant, low-sinuosity systems, mixed-load high-sinuosity systems and suspended-load systems (Miall, 1988; Bridge, 1993). However, in all fluvial systems, the transport and deposition of sediment are governed by the physical properties of both the fluid (water) and the solid (sediment), and controlled ultimately by processes related to Newtonian fluid flow.

Water is composed of two hydrogen gas molecules and one oxygen molecule which combine together to form one water molecule. The two hydrogen molecules possess positive charges and the oxygen molecule has a negative charge. Consequently, the positively charged hydrogen molecules of the water molecule are attracted to the negatively charged oxygen one to form a hydrogen bond (Chaplin, 2015). Water is made up from thousands of water molecules joined together through hydrogen bonding. Consider a model of a fluid being formed of individual ‘layers’ that all interact with one another as the water molecules are constantly bonding and releasing away from one-another (Chaplin, 2015).

Water, like any Newtonian fluid, yields immediately to shear or tangential stress and will deform when acted upon by an external force. The resistance of any fluid to deformation under an applied external force is governed by the fluid’s viscosity which, in water, is controlled by the internal friction of the individual ‘layers’ and the water’s hydrogen bonding (Leeder, 2011). Viscosity can be described in two ways: molecule and kinematic. Molecule viscosity is the measure of the shear stress between the individual ‘layers’ of the fluid flow. Low viscosity fluids flow easily whereas high viscosity fluids flow with difficulty because of the strength of the hydrogen bounding (Elert, 2015). Kinematic viscosity is the

ratio of the molecule viscosity to the density of the fluid (Elert, 2015). It defines a fluid's ability to resist deformation under acceleration (Leeder, 2011).

Fluids have the ability to carry solid material such as sedimentary grains. This material is known as the ‘granular solid’ and is defined mathematically as ‘a large conglomeration of discrete macroscopic particles’ (Wassgren, 2015). The particles of a granular solid are non-cohesive and held together by gravity acting upon their mass and by containment of any external boundaries (Jaeger *et al.,* 1996). Granular solids possess two properties when in motion that are derived from Newton’s Laws: momentum and inertia. Momentum is defined as a ‘mass in motion’ (Chapman, 1995), indicating that the granular solid is in constant motion. Inertia works against momentum and is the reaction of the granular solid to an applied force (Chapman, 1995). The shape and size of the granular solid not only has a mass but a weight and a density as well, which all affect how difficult it can be for the water molecules to move the granular solid. The mass and weight of the granular solid can change as the granular solid loses and gains macroscopic particles affecting the fluid’s ability to move the granular solid as a whole (Baiamonte and Ferro, 1997, Figure 2.1).

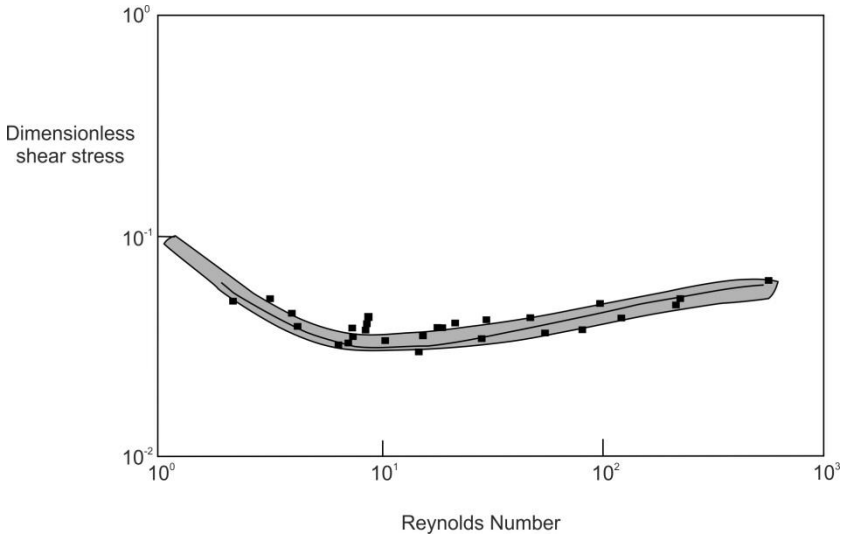

Figure 2.1: Shield’s Criterion diagram displaying the ratio between Reynolds number and dimensional shear stress; the velocity at which fluid picks up sediment vs the grainsize of the sediments. The data on the graph are not within one line but scattered within a narrow band (Miller *et al.,* 1977) due to the differences in grain size. The Shield’s Criterion is used to demonstrate the initial motion of sediment.

2.2 Derived properties

Newtonian fluids can flow in one of two states; laminar or turbulent. Laminar flow is defined as 'individual 'layers' of flowing water moving smoothly over one another with little or no diffusion' (Figure 2.2, Leeder, 2011). It occurs in fluids with high viscosities or in fluids that are moving with low velocities (Tucker, 2001). Turbulent flow is defined as 'the random motion of eddies causing diffusion of the individual 'layers' (Tucker, 2001). The eddy's move locally in random directions, but taken together they represent a fluid that as a whole moves in a definable direction. Turbulent flow occurs at high velocities and in fluids with low viscosity (Tucker, 2001; Haff, 2007).

The transition from laminar flow to turbulent flow with increasing fluid velocity or decreasing viscosity is given by the Reynolds Number (Re) (Equation 2.1; from Burr *et al.* 2006):

$$Re = \frac{\rho d u}{\mu} \qquad [2.1]$$

Where:
ρ = density of the fluid
d = depth
u = molecular viscosity
μ = kinematic viscosity

The state of the flow (laminar or turbulent) strongly affects the flow's ability to pick up and transport any granular solid, and therefore it strongly affects the ability of water to transport sediment. Between the flow of the water and the layer of sediment along the bottom of a channel there is a transfer zone known as the viscous layer (Miller *et al.,* 1977, Figure 2.2). As laminar flow involves 'layers' of water flowing over one another it does not break through the viscous layer and does not entrain sediment into the flow. Conversely, turbulent flow contains eddies which push through the viscous layer to pick up and entrain sediment (Figure 2.2).

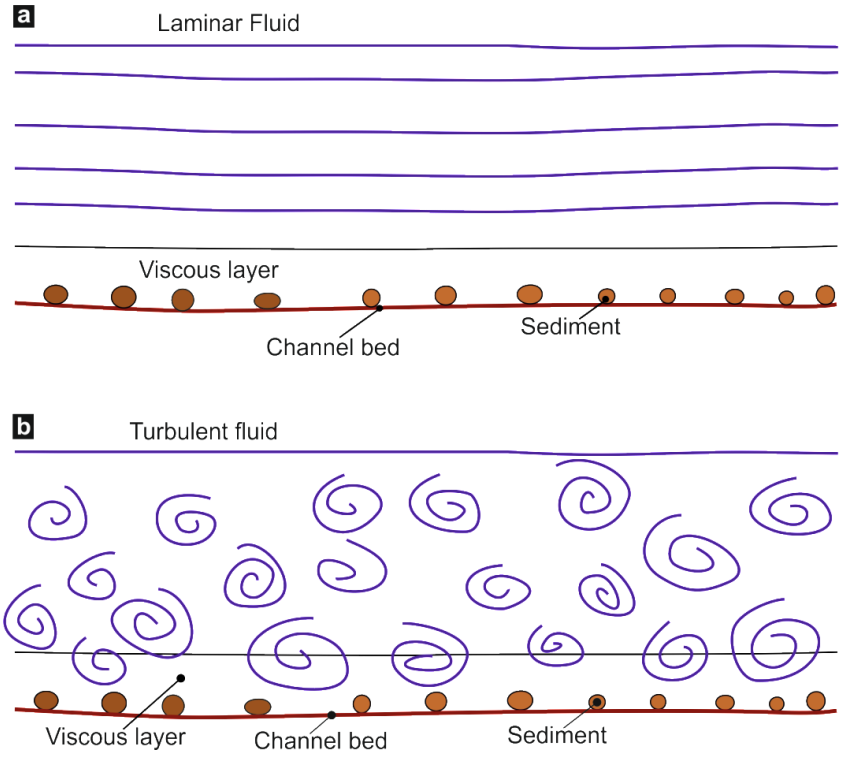

Figure 2.2: The two different types of flow from (a) laminar and (b) turbulent. (b) Turbulent flow breaks through the viscous layer to pick up the sediment whereas the laminar flow does not.

The velocity of flow required to entrain sediment of a given mas is given by the Shield's Criterion (Equation 2.2; Hsu, 2004):

$$r = 0.06\sqrt{(\rho_s - \rho_f)gD} \quad [2.2]$$

Where:
r = is the shear velocity
ρ_s = density of the sediment
ρ_f = density of the fluid
g = gravity
D = particle diameter

Shields Criterion is the ratio between the non-dimensional bed shear stress and the Reynolds Number (Miller *et al.,* 1977). The bed shear stress displays that the conditions for sediment motion are dependent on the gravity acting on the sediment, grain diameter and fluid viscosity (Leeder, 2011). This ratio determines the shear velocity which maybe faster than the velocity that is needed to pick up the particles (D, Figure 2.1, Hsu, 2004). In general, turbulent flow is the interaction of two variables, the initial movement of bed

material and local instantaneous bed shear stress caused by depositional events (Leeder, 2011). The sediment within depositional events can form bedforms, the type of bedform produced is determined by the Froude Number.

The Froude Number (Fr) describes the ratio of velocity and depth for a body of moving water, via the equation: (Equation 2.3 from Rahn, 1966):

$$Fr = \frac{v}{\sqrt{gd}}$$

[2.3]

Where:

v = stream velocity
g = gravity
d = depth of the flow

Froude numbers less than 1 define ‘subcritical’ or ‘lower flow regime’ conditions where turbulent water is flowing relatively slowly and waves propagate downstream. Froude numbers greater than 1 define ‘supercritical’ or ‘upper flow regime’ conditions with high depths standing waves form and break upstream as well as downstream. Upper flow regime conditions with shallow depths produce bedforms with long wavelengths and small amplitudes.

Sediments within fluid flows form as bedforms under conditions of turbulent water in either lower flow regime or upper flow regime conditions. The Froude Number determines the general style of bedform such that, for a given grainsize, increases in flow velocity (or decrease in flow depth) produce a predictable progression of bedforms from lower flow regime plane beds, ripples to dune-forms. The upper flow regime conditions produce upper stage plane beds and antidunes (Figure 2.3).

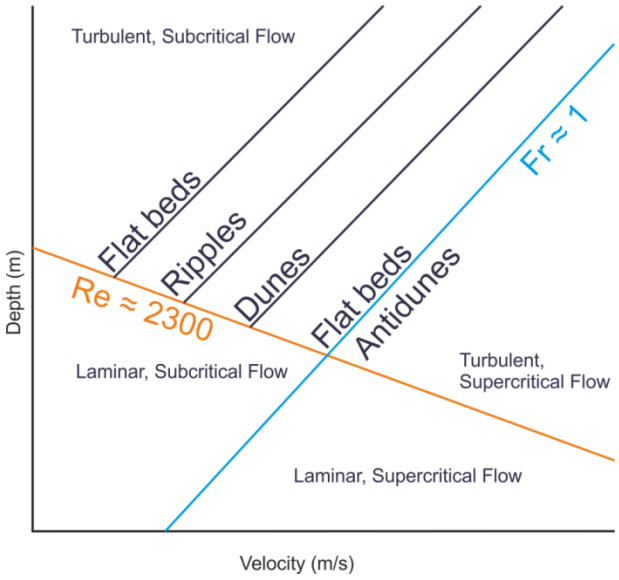

Figure 2.3: Distinctions between laminar, turbulent, subcritcal and supercritical flows, the Froude Number (Fr) of 1 displays the relationship between the lower and upper flow regimes, within turbulent flow, where bedforms are deposited. Distinct bedforms are deposited within fields defined by the Froude Number (Rahn, 1966; Tucker, 2001).

2.3 Transport processes

Sediments within fluvial systems are transported either by bedload or by suspended load, with some interaction between the two (Mather *et al.,* 2008). Bedload generally comprises coarse sand grains and gravel-grade material transported in the flow largely in contact with the bed and via the processes of rolling, saltation and reptation. The sediments are deposited on a mid-channel bars, gravel bars, or braided bars. Suspended load sediments are the finer sands and silts carried in suspension by turbulent eddies or carried as washload. They are generally deposited in low energy environments (Burr *et al.,* 2006). Clay and silt plugs are common in fluvial systems and are formed when channels are abandoned and the silt and clay can settle in stationary water following flooding events (Donselaar and Overeem, 2008).

However, clay grains have short-range atomic attractions causing clays grains to come-together (Leeder, 2011) and behave as non-granular solids (Section 2.1). Consequently, highly turbulent flow may be necessary in order to erode clay, dependent upon the clay type, fluid chemistry and organic concentration. Short-range atomic attractions between clay grains transported in the flow may cause them to clump and act as granular solids

equivalent to much coarser grains. Examples include the collection of clays grains around a central point or object in the flow to form ‘mudballs’ which essentially forms a clast requiring a higher Froude Number for transportation (Mather *et al.,* 2008). Mudballs are generally transported through rolling as bedload.

2.4 Formation of ripples, dunes, plane beds and antidunes

Confined flow with a Froude number of ≤0.84, forms lower flow regime conditions in which plane beds, ripples and dunes commonly form. Plane beds within the lower flow regime form only within coarse-grained sediments (≥0.6 mm) where the flow velocity is above that required for erosion (Leeder, 2011), but below the dune-forming velocity. Siliciclastic sediments within the lower flow regime plane beds are generally well sorted (Leeder, 2011).

Ripples and dunes form freely due to turbulence within the flow (Tucker, 2001) promoted by irregularities in the bed and resulting in both localised entrainment of sediment and localised deposition. Sediment migrates downstream as the flow transports sediment up the stoss slope (generally through saltation) and deposits on the lee slope as the sediment goes over the peak of the ripple or dune-form and falls down the slip surfaces. The migration velocity of the bedforms is determined by the amount of sediment within the system (Tjerry and Fredsøe, 2005).

Ripple-scale bedforms form when eddie currents close to the bed are sufficient to entrain sediment into the flow but insufficient enough to disturb the shallower water or to break through to the surface (Figure 2.4a). As a general rule, ripples have a maximum height of 4 mm and a maximum wavelength of 50 cm with an ripple indices of 10 – 40 (Leeder, 2011), although each individual ripple will be a different height and have a different wavelength, so the ripples within a train will vary. There is no clear relationship between flow depth, flow strength and the wavelength / height of a ripple. The spacing of ripples

becomes irregular as they migrate downstream (Simons *et al.,* 1960) as the ripples cannibalise each other (Wong *et al.,* 2003).

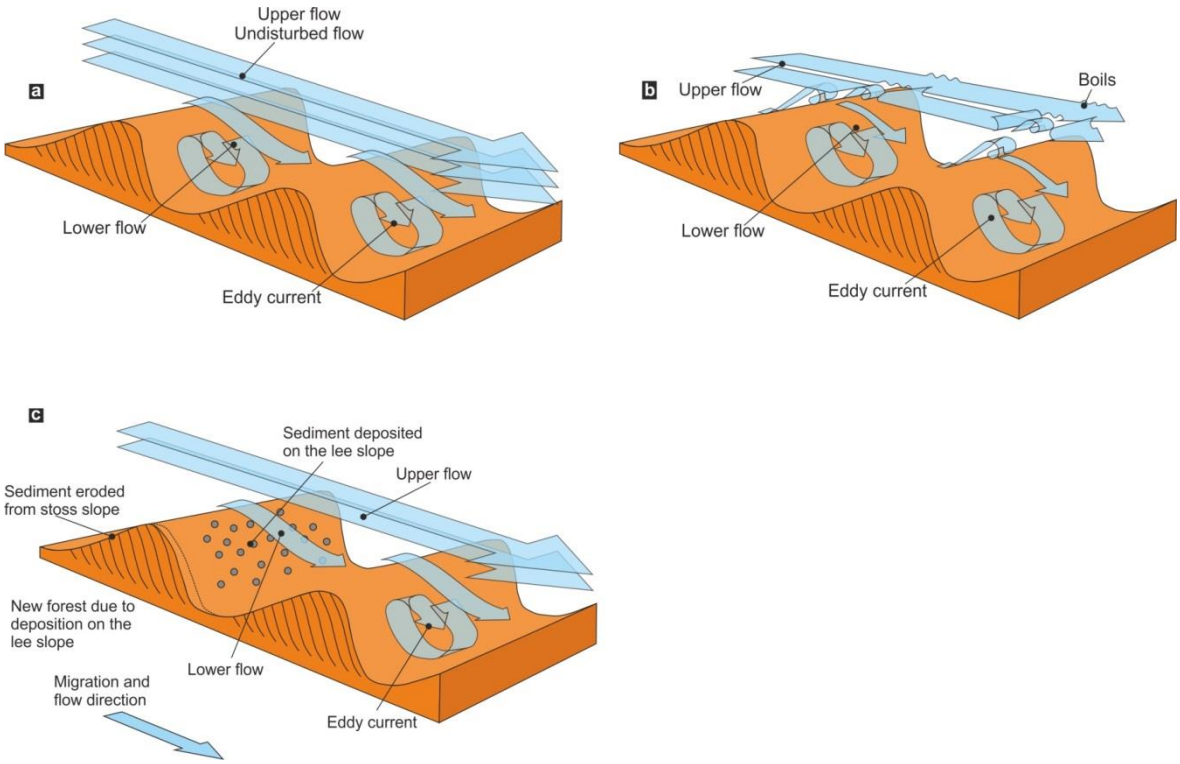

Figure 2.4: Differences in the formation of ripple- to dune-scale bedforms. (a) Ripple formation only disrupts the lower part of the flow, (b) dune formation disrupts the upper and lower flow as the eddy currents are given off the crest as 'boils', and (c) the migration of bedforms, where new sediment is added to the lee slope and eroded from the stoss slope (Simons *et al.,* 1960; Leeder, 2011).

Dune-scale bedforms are generated when the eddy currents close to the bed are sufficiently turbulent to effect the shallower water and cause turbulent 'boils' on the surface (Figure 2.4b, Simons *et al.,* 1960; Leeder, 2011). Consequently, dune-forms generally require higher energy flows than ripples do. Dunes form in bedload sediment only and their shape is governed by the bed shear stress acting upon the sediment movement (Tjerry and Fredsøe, 2005, Section 2.1). Dune-form geometry is influenced by the dune crestline, where the crestline of a dune-form is straight the resultant deposits are planar cross-bedding and sinuous-crested dune-forms produce trough cross-bedded deposits. The height of the dune and the wavelength of the dune are essentially governed by the Shield's Criterion and the amount of sediment within the system (Tjerry and

Fredsøe, 2005). The transition from ripple-scale to dune-scale bedforms is marked by: (1) wavelength and height of the bedform relative to flow depth; (2) grainsize increase, and; (3) increase in bedform migration and sediment transport rate (Simons *et al.* 1960; Mazumder, 2003; Lin and Venditti, 2013).

Upper-stage plane beds generally form the upper flow regime with high flow velocities and shallow water depths creating low-amplitude bedforms (0.75 mm – 11 mm; Leeder, 2011) with long wavelengths (0.7 m to 1 m). As the flow goes over the crests of the bedforms the speed of the flow increases and as the flow enters the troughs of the bedforms the flow velocity decelerates (Leeder, 2011). Primary current lineation forms flow-parallel ridges which occur primarily within the transition zone and are superimposed upon the plane beds.

Confined flow, with a Froude number greater than 1, forms the upper flow regime antidunes. Antidunes form as standing waves and break in the upstream direction depositing sediment on the stoss side of a developed dune-form to create bedforms that migrate upstream. The sediment deposited when a standing wave breaks is generally picked-up again within the turbulent flow (Kennedy, 1969). As antidunes move downstream their pattern does not become irregular like ripples or dunes, but if the flow increases in speed then antidunes increase in amplitude (Kennedy, 1969).

2.4.1 Bedform preservation

The potential for bedforms to be preserved as sediments in the rock record is zero unless each bedform in the train climbs upwards slightly as it migrates downstream over the bedform in front, burying and preserving at least part of that bedform. The relationship between the angle of climb of the bedforms from the horizontal and the angle of the stoss slopes of the bedforms defines three separate ‘states’ of climb. Subcritical climbing occurs when the angle of climb is less than that of the bedform stoss slope (Hunter, 1977a).

Subcritical climb preserves only the toesets of the migrating dune-forms. Set-bounding surfaces are also preserved and represent the climb of one bedform over another. Critical climbing occurs when the angle of climb is equal to that of the stoss slope (Hunter, 1977a). Critical climbing preserves the full foreset of the bedform, as a cross-bedded set, as the bedform migrates (Hunter, 1977b). Supercritical climb describes an angle of climb that is greater than that of the stoss slope where sediment is deposited on the stoss slope as well as the lee slope. Supercritical climb preserves both the stoss and lee slopes of the migrating dune-forms (Hunter, 1977a). In terms of the dynamics of the fluvial system, the angle of bedform climb is governed by the ratio of the rate of down-stream bedform migration and the rate of aggradation of the bed of the flow, preserving both ripples and dunes. Consequently, bedforms climb at increasing angles with increasing sediment load, and the angle of climb can be used to estimate sediment accumulation rates.

Antidunes are preserved in slightly different way, as the antidunes move upstream as the surface waves break (Section 2.4). As these waves break there is a short-lived movement of the water in the upstream direction allowing for sediment to fall out of suspension onto the river bed, this action allows for the antidunes to be preserved (Kenndy, 1961; Allen, 1966).

2.5 Non-Newtonian flows

Non-Newtonian fluids are not governed by the Newtonian Laws. These fluids can be known as plastic materials defined as: a material with a yield strength above which the deformation to the fluid is permanent (Postma, 1986). Plastic materials flow as plastic fluids which are defined as: the flow of material will not move below a certain yield stress (Postma, 1986). Yield stress with regards to non-Newtonian fluids, is defined as an initial resistance to shear stress (Figure 2.5). Plastic behaviour can be induced from a Newtonian fluid as sediment is added to the fluid and the change in fluid behaviour changes at 30% sediment 70% fluid (Leeder, 2011), influencing the fluid consistency.

Plastic fluids have a variable viscosity (Section 2.1) and shear rates in such flows can make grain settling impossible.

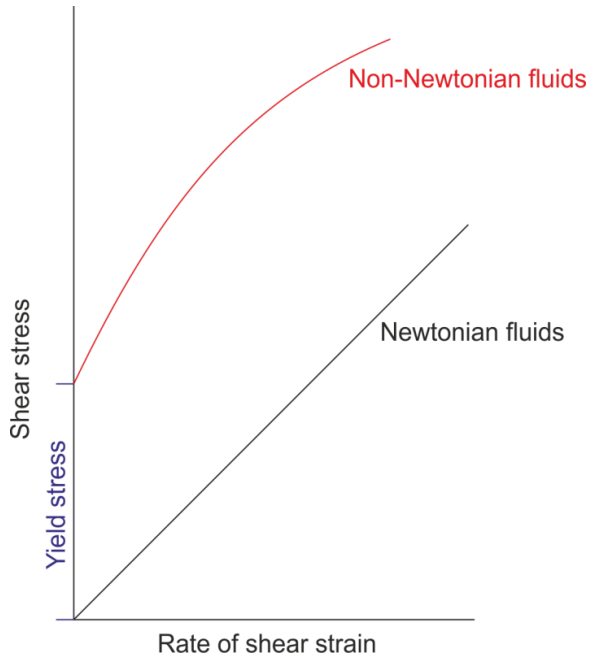

Figure 2.5: Behaviour of both Newtonian and non-Newtonian flows. Newtonian flows move instantaneously. However, non-Newtonian flows have to exceed the yield stress before they move (Leeder, 2011).

2.5.1 Transport processes

Processes in which non-Newtonian flows transport sediments are on a spectrum of plasticity and mass coherency. The transport mechanisms include cohesive flows, grainflows and debris flows. The mechanism with the highest plasticity and mass coherency is the cohesive flow. The grainfall transport mechanism incorporates rock falls and avalanches where the flow incorporates water therefore reducing the mass coherency of the flow. Rock falls are caused by gravity-driven failures of boulder- to cobble-grade fragments (Blair and McPherson, 1994). Avalanches are granular failures of large-scale brecciated bedrock.

Fluvial systems can involve all of the above transport mechanisms; however, the most common type of non-Newtonian flow within fluvial systems are debris flows (Blair and McPherson, 1994). Debris flows formed through plastic non-Newtonian laminar flows characterised by an increasing amount of fluid when compared to the processes above.

The mass coherency of debris flows is also lower than the processes mentioned above. Debris flows form when unconsolidated material moves downslope due to gravity where the main mechanism is when fast-flowing waters intersect the basin drainage slope which has abundant sediment (Blair and McPherson, 1994).

2.5.2 Sediment deposition

Each transport process has its own type of sediment deposition. Cohesive flows pick up, transport and deposit sediment that in no way changes as it moves from its starting point to its end point. Rock falls deposit angular, moderately spherical boulder- to cobble-grade sediments, commonly with clay-grained sediments which are poorly sorted. Avalanches are comprised of poorly-sorted, angular boulders which are matrix-supported (Blair and McPherson, 1994).

Debris flows deposit sediment that can be both matrix-supported and clast-supported facies. Both facies contain poorly sorted sediments with a structureless nature. The deposits are generally coarse-grained with discontinuous beds deposited within one flow event. The deposits can be either clast rich or clast poor; it depends on the sediment available when the debris flow starts to move (Blair and McPherson, 1994). Sometimes the deposits are lacking in clays and the sediments have indistinct cross-beds or indistinct laminations. This is because debris flows can evolve into high sediment load Newtonian flows as they deposit material. These indistinct laminations form from a high-concentration of sediment suspended within water where multiple beds may form from one single event (Blair and McPherson, 1994).

2.6 Geomorphological elements of fluvial systems

The formation of bedforms build together to form geomorphological elements such as channels, meander bends, mid-channel bars and the floodplain. The geomorphological elements are affected by the discharge of the fluvial system and the localised climate and tectonics (Section 2.8).

2.6.1 Channel styles

Channel styles are described by different characteristics within fluvial systems such as bedload, sediment sorting, discharge and basin drainage. There are three common types of fluvial system where the characteristics described above are different depending on the successions: bedload, low sinuosity fluvial systems; mixed load, high sinuosity fluvial system, and; suspended load, highly sinuous systems.

Bedload, low sinuosity fluvial systems are either characterised by gravel-grade bedload and sand-grade bedload systems. Gravel bedload rivers have a gravel high bedload with a low sediment sorting (Schumm and Khan, 1972). Bedload fluvial systems are associated with a low discharge volume (Parker, 1976) which can change seasonally due to flash floods and monsoon periods. Gravel bedload river have small drainage areas. The width / depth ratio is greater than 12.2 m^3 with wide shallow channels (Schumm, 1972). The bank stability is low as the system is lacking in vegetation. The mid-channel bars and floodplain locations change frequently due to the high avulsion rates.

Sandy bedload fluvial systems are dominated by medium- to coarse-grained sands with a moderate sorting (Schumm and Khan, 1972). The discharge within the system is generally fairly constant with a moderate drainage area. This type of channel style has a high width / depth ratio. The channels have low bank stability with high avulsion rate.

Mixed-load, moderately sinuous rivers carry little bedload with a high proportion of well-sorted, fine-grained sand (Schumm and Khan, 1972). The fluvial system has a moderate discharge volume with a moderately-sized drainage area. Mixed-load channels have a high width / depth ratio between 3.5 m^3 to 12.2 m^3 with a channel sinuosity between 1.3 and 2 (Schumm, 1972). The channels have a low stability and therefore the channels are constantly migrating.

Suspended-load, high sinuosity systems carry no bedload sediment, small amount of sands and are dominated by high amounts of well sorted clays and silts (Schumm and Khan, 1972). This type of fluvial system has a high discharge volume and drainage area. This type of channel style has a low width / depth ratio, where the depth is high but the channel width is narrow, typically less than 3.5 m (Schumm, 1972). The channel bank stability is high due to the amount of the vegetation. The sinuosity of these channels is greater than 2.

2.6.2 Meander bends

When meander bends are preserved they are known as point bars. Meander bends are formed due to the water flow changing directions within the channel and this causes a changing velocity within the water flow of the channel. This implies that the velocity changes from where the water flow enters the meander bend when compared to the velocity of the water when it leaves the meander bend (Figure 2.6a). This change is known as radial acceleration and occurs in a broad range of sedimentary environments (Kneller, 2003; Leeder, 2011; Ielpi and Ghinazzi, 2014). It is the reaction from the change in direction which forms the hydrostatic head (Figure 2.6). The hydrostatic head itself is maintained by helical flow (Leeder, 2011; Ielpi and Ghinassi, 2014). Helical flow is a cork-screw like flow where the circulation of the flow is in a perpendicular direction to the dominant flow current. As the flow is circular, rises and falls, where the flow rises there is sediment deposition and channel migration; this occurs on the outside of the channel bend (Krigstrom, 1962). Where the flow falls there is sediment erosion and migration on the outside of the channel (Krigstrom, 1962). This indicates channel migration laterally (Donselaar and Overeem, 2008).

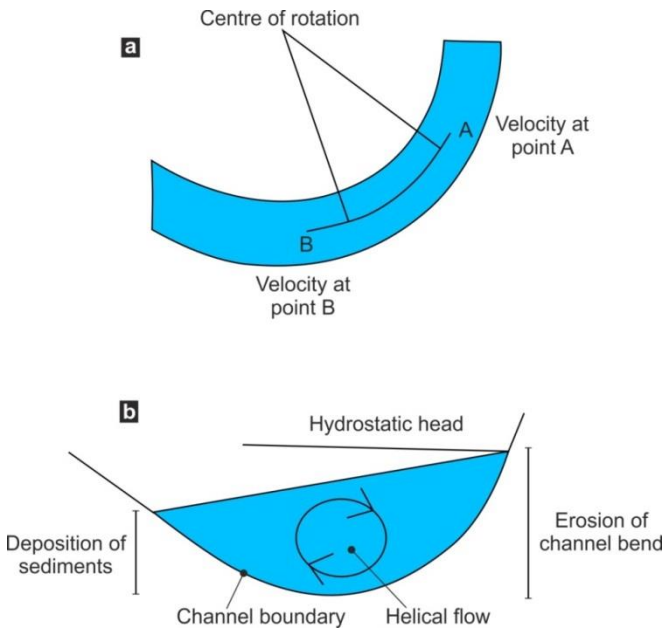

Figure 2.6: Formation of a meander bend, (a) as the fluid flow enters a curve in a confined environment the velocity changes from point A to point B, due to the curved nature of the channel forcing the flow to change direction. The reaction of this forms a hydrostatic head (b), which is maintained by a helical flow (Leeder, 2011, Ielpi and Ghinassi, 2014).

2.6.3 Mid-channel bars / transverse bars

Mid-channel bars form as small- medium- and large-scale barforms, from heights from ≤1 m, ≤4 m and ≤8 m, respectively (Best *et al.,* 2003). The bar is situated within the middle of the channel and the flanks may undergo erosion, while bar deposition is lateral and vertical (Krigstrom, 1962; Best *et al.,* 2003). The geometry of the bar grows with an asymmetrical shape. A transverse bar is the dominant type of a mid-channel bar which has a tabular geometry with a flat top. The bars can appear solitary or with multiple other bodies. Upon the transverse bars are small ripple-scale bedforms which transport the sediments to the edges of the transverse bars (Smith, 1971) indicating flow over the top of the bar. The surface areas of the bars vary between 1 to 2 square metres with a length over 200 m and a height somewhere between a few centimetres to over a metre (Smith, 1971).

2.6.4 Floodplain

The floodplain is prone to flooding from the channels and is an area of flat land adjacent to the channel system with deposits of alluvium. Material is generally deposited upon the floodplain during a flood event with coarser material closer to the channel banks as it is generally heavier therefore deposited first. Further away from the channel the finer material is deposited as this material is generally lighter or carried in suspension. The associated sub-environments are crevasse splays, chute channels and rill channels and they act as depositional centres when the fluvial system floods (Figures 2.7 to 2.9).

Crevasse splays occur within all fluvial systems but commonly in high sinuous systems. Their occurrence is primarily downstream (within the lower courses of the fluvial system; Donselaar *et al.,* 2013). The succession deposited by a crevasse splay generally consists of amalgamated silt and fine sand sheets that contain organic debris. The top of the succession can be covered rapidly by vegetation (Bristow *et al.,* 1999). Crevasse splays flow away from the channel. Their geometry can vary. For example the crevasse splays of the Niobrara River can form lobes and can also be elongated (Bristow *et al.,* 1999).

Chute channels commonly occur within high sinuosity systems where they form meander cut-off. Meander cut-off is where a new channel forms and becomes the main channel through repeated flooding (Johnson and Paynter, 1967; Ghinassi, 2010). This occurs in four stages: (1) initial erosion into the floodplain on the upstream side of a meander bend; (2) erosion and development of a chute delta; (3) flooding which allows for continued erosion of the chute channel to reach to the other end of the point bar, so the flow enters the main channel again, and; (4) lastly the channel deepens and widens (Ghinassi, 2010). The chute channel succession varies between each channel but there typical succession starts with pebble-grade clasts fining from coarse- to fine-grained sandstones that are cross-bedded. These sandstones are overlain by pedogenic clays (Ghinassi, 2010, Banham and Mountney, 2013).

Rill channels generally occur close to the main channel (Donselaar *et al.,* 2013) and vary in width, thickness, sinuosity, sedimentary textures and sedimentary structures (Torri and Poesen, 1988). Rill channels can account for up to 75% of the soil loss upon a floodplain. There are up to four stages of rill development starting with: unconfined sheet-like flows, then the flows become confined with an increase in turbulence potential to supercritical flow. The flow of the water begins to slow and is within defined channels allowing for turbulence to become pronounced and the development of ripple-scale bedforms. Finally, the flow tapers and becomes steady as the channels widen and deepen (Merritt, 1984).

2.7 Facies, associations and models

Allen (1965), Jackson (1976) and Miall (1985) have built upon each other's work and have formed a fluvial facies scheme which predicts the process of deposition of sediments (Table 2.1). Facies schemes are developed from the logging of sedimentary sections (Miall, 1985).

Facies are built into facies associations by linking together facies that have similar depositional processes, such as the linking together of the St and Sp facies (Table 2.1). Both these facies contain medium- to very coarse-grained sands with either planar or trough cross-beds interpreted as lower flow regime dune-scale bedforms. Each type of fluvial system mentioned (Section 2.6.1) deposits a combination of different facies, as seen in Table 2.1 and it's the arrangement of the different facies which leads to different interpretations. We build up from facies analysis through facies associations into bounding surface analysis and architectural element analysis.

Facies code	Lithofacies	Sedimentary structures	Interpretation	Fluvial system
Gmm	Matrix supported gravel	Grading	Debris flow deposits	Bedload, low sinuosity fluvial system
Gm	Gravel	Massive	Debris flows	Sandy bedload, low sinuosity, fluvial system
Gt	Gravel, stratified	Trough cross-beds	Minor channel fill	
Gp	Gravel, stratified	Planar cross-beds	Linguoid bars or deltaic growths from older bar remnants	
Gh	Clast supported, indistinct bedded gravel;	Horizontal bedding, imbrication	Longitudinal bedfroms, lag forms, deltaic growths, sieve deposits	
St	Sands, medium to very coarse may be pebbly	Solitary or grouped trough cross-beds	Dune-scale bedforms – lower flow regime	
Sp	Sands, medium to very coarse may be pebbly	Solitary or grouped planar cross-beds	Dune-scale bedforms, transverse bars – lower flow regime	
Sm	Sands, medium to very coarse may be pebbly	Structureless	Rapid sediment deposition	
Sr	Sand, very fine to coarse	Various ripple types	Ripple-scale bedforms – lower flow regime	Mixed-load, high sinuosity fluvial system
Sh	Sand, very fine to coarse, may be pebbly	Horizontal lamination, streaming lineation or parting	Planar beds – lower and upper flow regimes	Suspended-load, high sinuosity fluvial system
Sl	Sand, fine	Low angle cross-beds	Scours fills, crevasse splays, antidunes	
Se	Erosional scours with intraclasts	Crude cross-bedding	Scour fills	
Ss	Sand, very fine to coarse, may be pebbly	Broad, shallow scours, cross stratification	Scour fills	
Fl	Sand, silt, mud	Fine laminations, very small ripples	Overbank or waning flood deposits	
Fsc	Silt, mud	Laminated to massive	Backswamp deposits	
Fcl	Mud	Massive, with freshwater molluscs	Backswamp pond deposits	
Fm	Mud, silt	Massive, desiccation cracks	Overbank or drape deposits	
Fr	Silt, mud	Rootlets	Seatearth	
C	Coal, carbonaceous mud	Plants, mud films	Swamp deposits	
P	Carbonate	Pedogenic features	Soil	

Table 2.1: 'Standard' fluvial channel facies scheme (adapted from Miall, 1977).

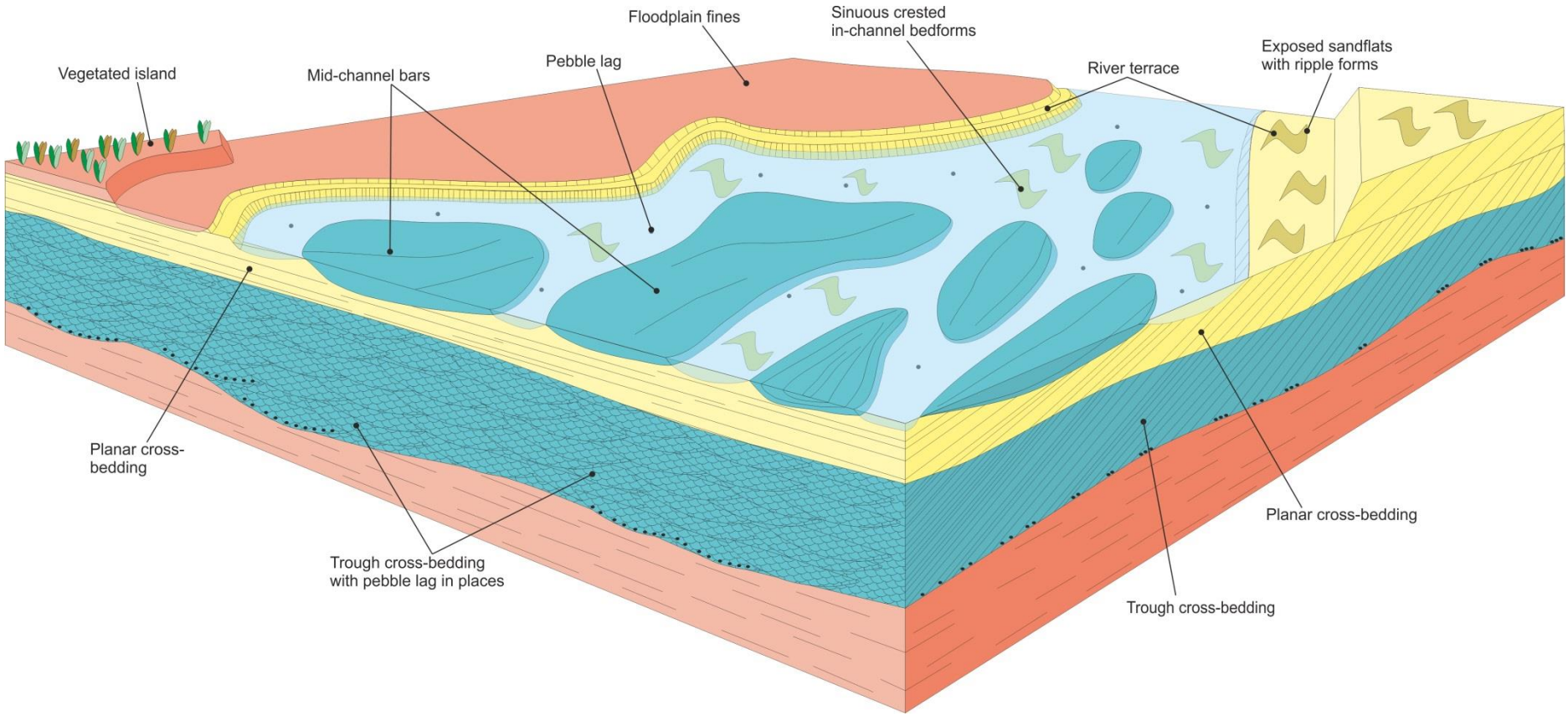

Figure 2.7: The three-dimensional facies model of a low-sinuous fluvial system displays mid-channel bars where sediment is deposited and eroded, depending on the flow. The subsurface exhibits high energy sediment deposition; diagrams adapted from Allen (1965), Walker and James (1992) and Nichols (2009), key for three-dimensional facies model in Appendix 1.

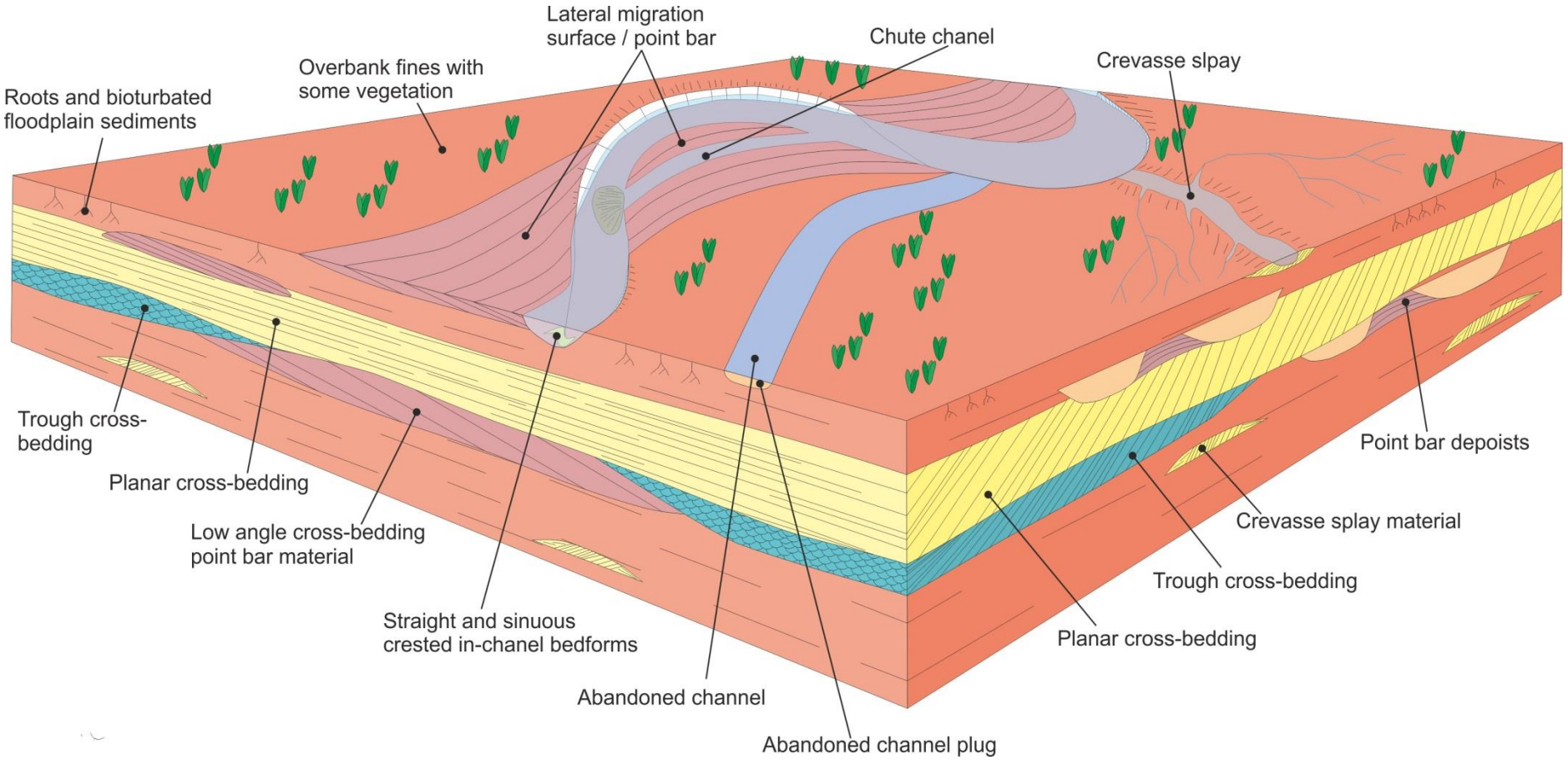

Figure 2.8: The three-dimensional facies model displays a highly sinuous fluvial system where sediment is deposited and eroded on point bars. Crevasse splays are also characteristic of high sinuosity fluvial system. The subsurface displays multiple abandoned channels and abandoned chute channels from natural channel avulsion and the deposition of sediments; diagrams adapted from Allen (1965), Walker and James (1992), Nichols (2009), and Ghazi and Mountney (2009), key for three-dimensional facies model is in Appendix 1.

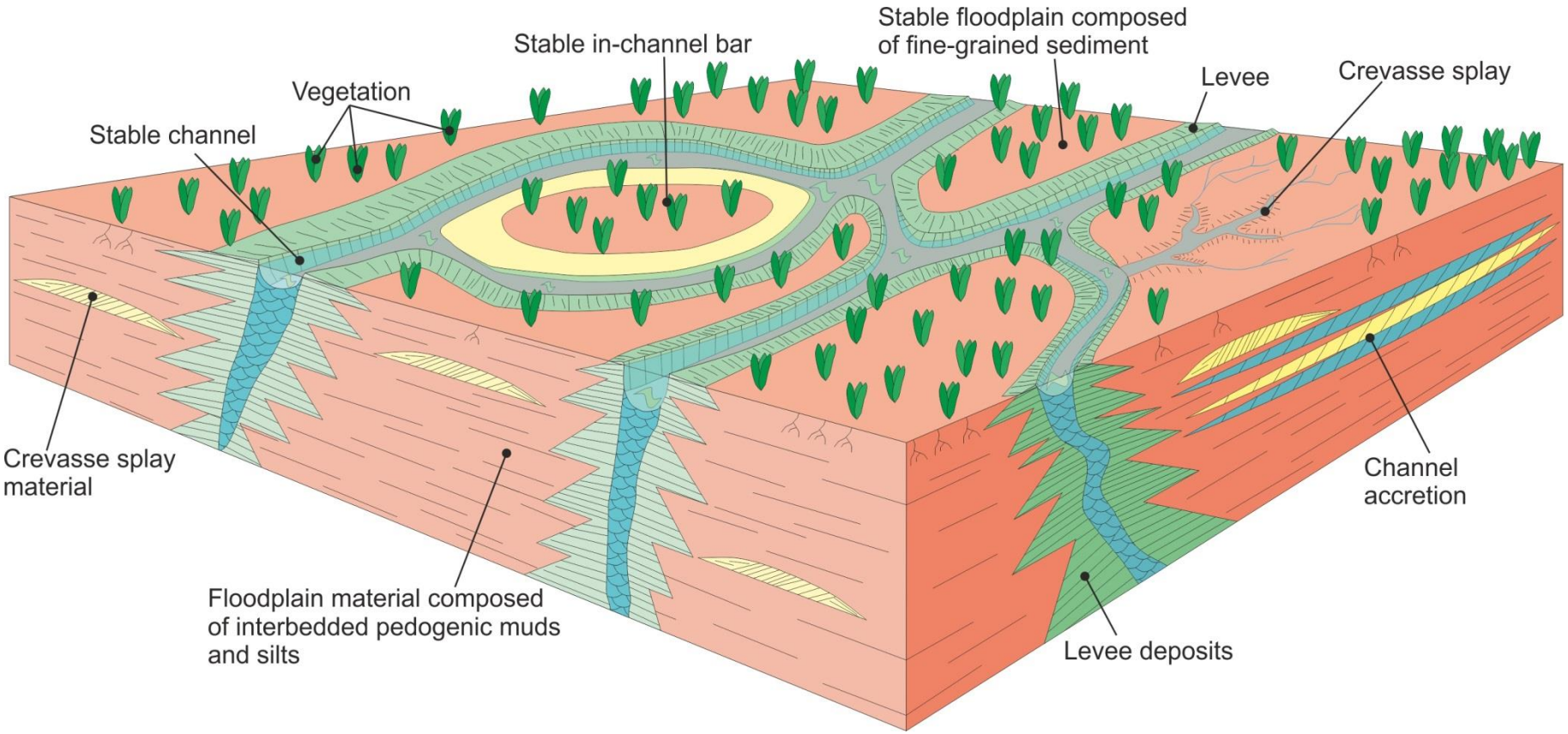

Figure 2.9: The three-dimensional facies model of a suspended load fluvial system that displays mid-channel bars which are highly stable with vegetation. The subsurface displays few abandoned channels from natural channel avulsion with predicted channel fill; diagrams adapted from Emery and Myers (1996), key for three-dimensional facies model in Appendix 1.

Bounding surfaces are used to determine the relationship between each of the facies and the individual bedforms within that facies. Bedforms within fluvial systems can form on one of three scales: (1) microforms; (2) mesoforms, and; (3) macroforms (Jackson, 1976). These scales describe the different size of bedforms related to the bounding surfaces as dictated by the bounding surface hierarchy (Table 2.2, Figure 2.10). Various authors (Brookfield, 1977; Allen, 1983; Miall, 1988) have developed bounding surface schemes, this scheme help the interpretations of sedimentary systems from the small-scale features such as individual dunes to the large-scale features such as fluvial belts.

Bounding surface hierarchy	Definition
1st order	Cross-bed set: Little or no internal erosion represented within a cross-bed set (microform), represents a continuous sediment supply.
2nd order	Coset bounding surface: where there are changes in lithofacies or flow conditions (mesoforms).
3rd order	Cross-cutting erosion surfaces: generally dip at a low angle and extend form the top to the bottom of the macroform.
4th order	Bounding surfaces: they generally form the upper bounding surface for marcoforms and represent a major change in facies distribution; where the 1st to 3rd order surfaces truncate against them.
5th order	Bounding major sand sheets: these surfaces are laterally extensive over an area (10's of m).
6th order	Mappable stratigraphic subdivisions: the distinction between member and units within the fluvial domain.

Table 2.2: Hierarchy of bounding surface within sedimentary systems; adapted from Brookfield (1977), Allen (1983) and Miall (1988)

First order bounding surfaces have little or no internal erosion on the lower boundary of the set. These surfaces represent ripple-scale or cross-bedded sets (microform) where there is a continuous sediment supply (Table 2.2, Figure 2.10; Miall, 1988).

Second order bounding surfaces are recognised where there is a change in the lithofacies or flow conditions, in either direction or magnitude. The bedforms deposited are mesoforms in scale and are representative of cosets within the sediments. There can be significant grainsize changes through the cosets where the coarser material will line the bottom boundary of the coset. Finally, first order surfaces will truncate against them and they can truncate against themselves (Table 2.2, Figure 2.10; McKee and Weir; 1953, Miall, 1988).

Third order bounding surfaces are low angle surfaces that cross-cut the marcoforms. These surfaces extend from the top to the bottom of the macroform and form reactivation surfaces (Brookfield, 1997). A reactivation surface is a discontinuity foreset where the flow strength has changed and caused erosion or a change in direction of the flow where after the flow reverts back and forward migration of bedforms will begin to occur again (Figure 2.4c). The first and second order surface will truncate against them (Table 2.2, Figure 2.10).

Fourth order bounding surfaces form the upper bounding surface of a macroform and represent a major change in facies distribution, which is not erosive (Miall, 1988). The first to third order surfaces will truncate against them.

Fifth order bounding surfaces represent a major change in the mappable units over 10's of metres therefore' they are laterally extensive over a substantial area. They mark a significant change in the facies distribution are erosive and can be the bottom of architectural elements (Table 2.2, Figure 2.10; Miall, 1988). While all the previous surfaces (first to fourth order) can truncate against the fifth order surface it is likely that the third and fourth order surfaces truncate against the fifth order surface most frequently.

Sixth order bounding surfaces are the distinctive elements separating up members and units from the surrounding material. These surfaces are highly erosive and are frequently draped by layers of pebbles. All the other bounding surfaces terminate against them; however most notably the fourth and fifth order surfaces (Table 2.2, Figure 2.10; Brookfield, 1997).

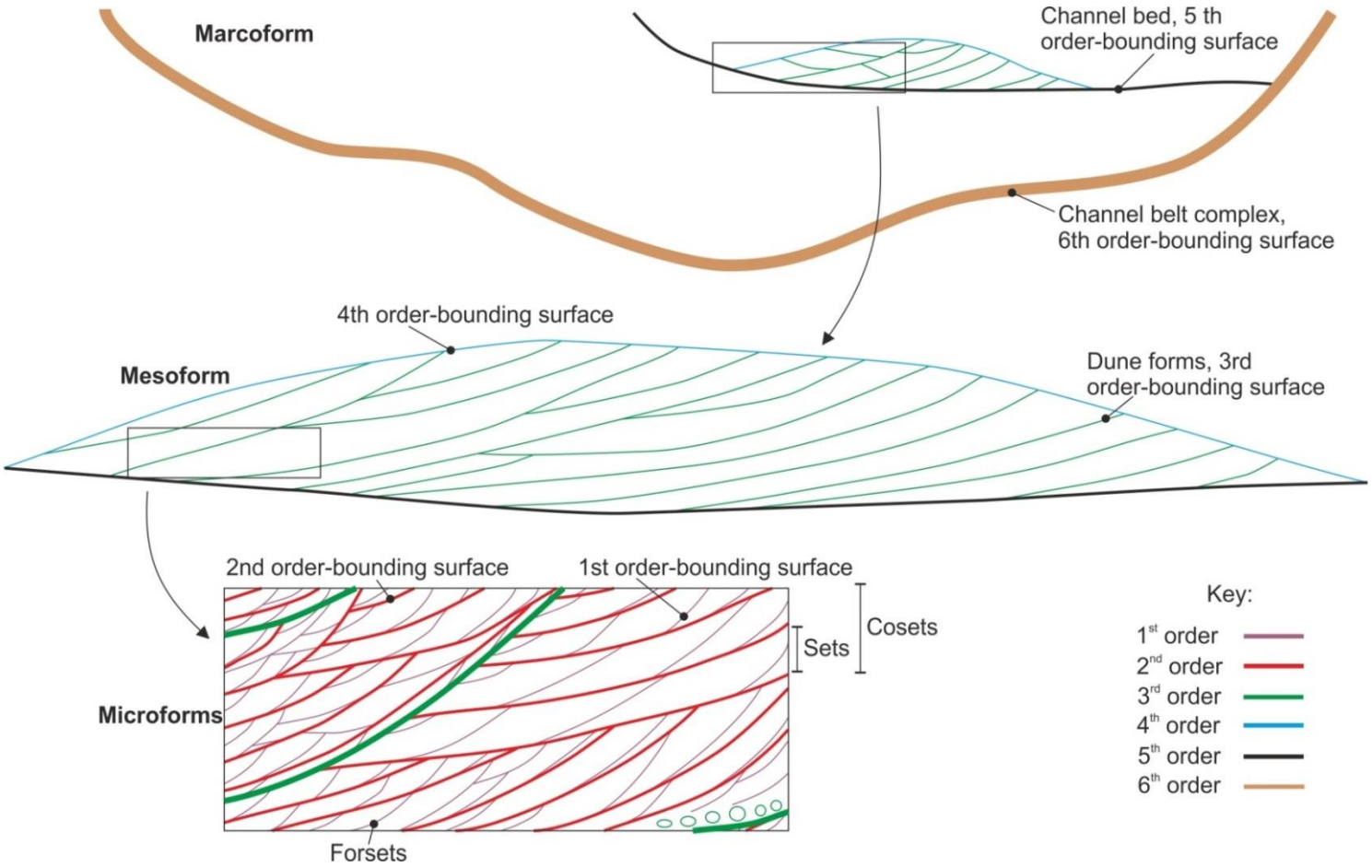

Figure 2.10: Bounding surfaces are displayed and are indicative of the bounding surfaces within fluvial systems. Bounding surfaces have a hierarchy from one to six. The first order surfaces represent foresets, where there is little or no erosion. The second order surfaces depict change in lithofacies which can be related to sets and cosets. The third order surfaces are low-angle surfaces that extend from the top to the bottom of the macroform. The fourth order bounding surface represents the lower boundary to architectural elements. The fifth order bounding surfaces delineate major bounding sheets and the sixth order bounding surface represents mappable stratigraphic units (Brookfield, 1977; Miall, 1988).

The arrangement of facies and bounding surfaces form architectural elements that are defined by: (1) the nature of the upper and lower boundaries; (2) the internal and external geometries, and; (3) scale (Miall, 1985). The benefits of modelling on an element scale are the attention to geometry of the facies and bounding surfaces (Tables 2.1, 2.2; Miall 1985, 1988).

Researchers use architectural elements to understand the three-dimensional nature of a sedimentary succession and these elements can then be combined to identify various sedimentary environments For example fluvial systems are composed of the same facies forming multiple architectural elements and it is the particular pattern of these elements that determines the type of fluvial system that is preserved. Therefore are the four types of fluvial systems as determined by Schumm (1972) are discussed below. These are: (a) bedload dominant, low sinuosity fluvial systems, (b) mixed-load, high sinuosity fluvial systems, (c) suspended load and (d) their associated floodplain deposits.

2.7.1 Bedload-dominant, low-sinuosity fluvial system

A bedload dominant, low sinuosity fluvial system can be seen in Figure 2.7 and the likely facies seen within the system are noted in Table 2.1. The three-dimensional model (Figure 2.7) exhibits multiple abandoned channels in the subsurface and little vegetation. There are two main mechanisms that are key to understanding the formation of a low sinuosity system they are the development of gravel bars and the formation of channels (Bridge, 1993). The channels within these types of systems are generally stacked and amalgamated. Channel avulsion is common within these systems due to the lack of plant life (Cant, 1977). Bedload-dominant, low-sinuosity fluvial systems are generally found in the proximal areas of the land surface, in the upper parts of the river profile.

Bedload-dominant, low-sinuosity fluvial systems can form in arid environments where the climate has limited rainfalls and the most common sediment-transport medium may be

viscous, likely non-Newtonian depositing debris flows. Debris flows are matrix-supported and therefore the clasts will not be aligned with the direction of the flow, nor do they show rounding and any sedimentary structures that are formed are indistinct when preserved.

2.7.2 Mixed-load, high-sinuosity fluvial system

The three-dimensional model of a mixed-load, high-sinuosity fluvial system can be seen in Figure 2.8 and the dominant facies are within Table 2.1. Generally mixed-load, high sinuosity fluvial systems are found in the low lying, medial-distal areas of the land surface, along the river profile. Point bar deposits can be distinctive of mixed load fluvial systems and are due to channel accretion through the development of meander bends (Section 2.4). These bar forms migrate laterally and downstream the difference is determined by the dip direction of the point bar strata (Ielpi and Ghinassi, 2014). The lateral migration can be measured by their sweep and swing. These systems have a high lateral migration and low avulsion rate due to vegetation producing stable banks.

2.7.3 Suspended-load fluvial system

Suspended-load fluvial systems display an interconnected network of deep channels (Figure 2.9) and the dominant facies are within Table 2.1. These types of fluvial systems are characterised by deep and narrow channels and mid-channel bars which are highly stable. Thick floodplains are composed of fine sands, silts and clays and are heavily vegetated with little channel avulsion. The sinuosity in these systems is variable (Emery and Myers, 1996). These systems can be 100’s of metres or kilometres long and experience low-energy conditions (Makaske, 2001).

2.7.4 Floodplain

The dominant floodplain facies are noted in Table 2.3. Facies build up into architectural elements (Section 2.7). Here these elements are the sub-environments of the floodplain setting; such as chute channels, rill channels and crevasse splays (Section 2.6.4). The

thickness of each flood event varies; this can be seen in the rock record from less than 50 mm (Lunt *et al.,* 2004) of material in one event to a thickness of 1500 mm in a different event which is noted within the floodplain conglomerates of the Old Red Sandstone, northern Scotland (Clarke and Parnell, 1999). The difference in the flooding events is due to the discharge speed, volume and the amount of sediments within the system and therefore relates to the climatic regime (Section 2.8.2) and sediment supply (Section 2.8.4).

Facies code	Lithofacies	Sedimentary structures	Interpretation
Fl	Sand, silt, mud	Fine laminations, very small ripples	Overbank or waning flood deposits
Fsc	Silt, mud	Laminated to massive	Backswamp deposits
Fcl	Mud	Massive, with freshwater molluscs	Backswamp pond deposits
Fm	Mud, silt	Massive, desiccation cracks	Overbank or drape deposits
Fr	Silt, mud	Rootlets	Seatearth
C	Coal, carbonaceous mud	Plants, mud films	Swamp deposits
P	Carbonate	Pedogenic features	Soil

Table 2.3: Typical facies associated with a flood plain environment (Miall, 1977, 1985).

The floodplain environment is dominated by soils which develop when there is land surface stability (Kraus, 1999). This environment can be exposed to bioturbation, from plants and organisms and the development of peds, soil slickenlines and fractures (Kraus and Hasiotis, 2006). Over time soils become palaeosols through pedogenesis. There are three dominant types of palaeosols that can develop known as (1) cumulative; (2) composite, and; (3) compound; these are the result of varying sediment supply (Kraus, 1999). Cumulative soils are formed from a continuous and a steady supply of sediment, where there is little or no erosion. Composite and compound sediments are formed from rapid and an unsteady amount of sediment deposition to the floodplain, where there is erosion (Kraus, 1999). This can create soils that are younger but much more developed (Wright and Marriott, 1996). Palaeosols give indications into the water table and how effectively they drained themselves, where they fall into one of three categories (Table 2.4, Simonson and Boersma, 1972; Kraus and Hasiotis, 2006): moderately to well

drained, imperfectly to poorly drained and very poorly drained. Based on this information the type of palaeosols and the conditions on its deposition can be determined and can allude to the climatic regime.

Type of soil	Characteristics	Climate
Moderately to well drained	**Red muds and silts with weak pedogenes is with carbonate nodules and slickenlines; haematite rich**	**Season wetting and drying within the tropics and subtropics**
Imperfectly to poorly drained	**Purple to greys mudstones with yellow reduction spots and large slickenlines**	**Season rainfalls within the subtropics**
Very poorly drained	**Grey clays and silts with relict bedding, jarosite nodules and gypsum crystals, with slickenlines**	**Swamps, with seasonal standing water – humid environment (tropical)**

Table 2.4: Information on the characteristics of soil drainage (adapted from Kraus and Hasiotis, 2006).

2.8 Influences upon a river

Fluvial systems are influenced by intrinsic and extrinsic time-variant processes. Extrinsic processes are external to the fluvial system and include tectonics, climate and base level (Leeder, 1978; Gupta *et al.,* 1999; Gawthrope and Leeder, 2000; Fossen, 2010). The intrinsic influences are processes which are within the fluvial system and include avulsion (Leeder, 1978; Gawthrope and Leeder, 2000; Fossen, 2010). The sediment supply within fluvial systems can be both extrinsic and intrinsic (Schumm, 1981; Fraser and DeCelles, 1992; Vazquez-Urbez and Osacar, 2013).

2.8.1 Tectonic influences

All tectonic regimes influence fluvial systems. However here, only extensional tectonics are discussed as the Barmer Basin is part of an extensional rift system.

As extension occurs, accommodation space is created for fluvial systems to aggrade in (Fossen, 2010; Gawthorpe and Leeder, 2000). Subsidence can be too slow and steady to influence a fluvial system and therefore growth of the extensional regime and the fluvial system has reached equilibrium (Leeder, 1993). The relationship between the subsidence rate and avulsion rate determines the connectedness of the channels (Figure 2.11), there can be a low subsidence rate and a low avulsion rate producing well connected channels.

There can also be high subsidence rates and high avulsion rates producing well connected channels (Figure 2.11). Contrary to this, a high subsidence rate with low avulsion rate will create poor channel connections. Low subsidence will form well-developed but isolated floodplains whereas high subsidence will form thick but under-developed floodplains. The floodplains here aggrade quickly with poorly-developed soils (Ouchi, 1985; Wright and Marriott, 1993).

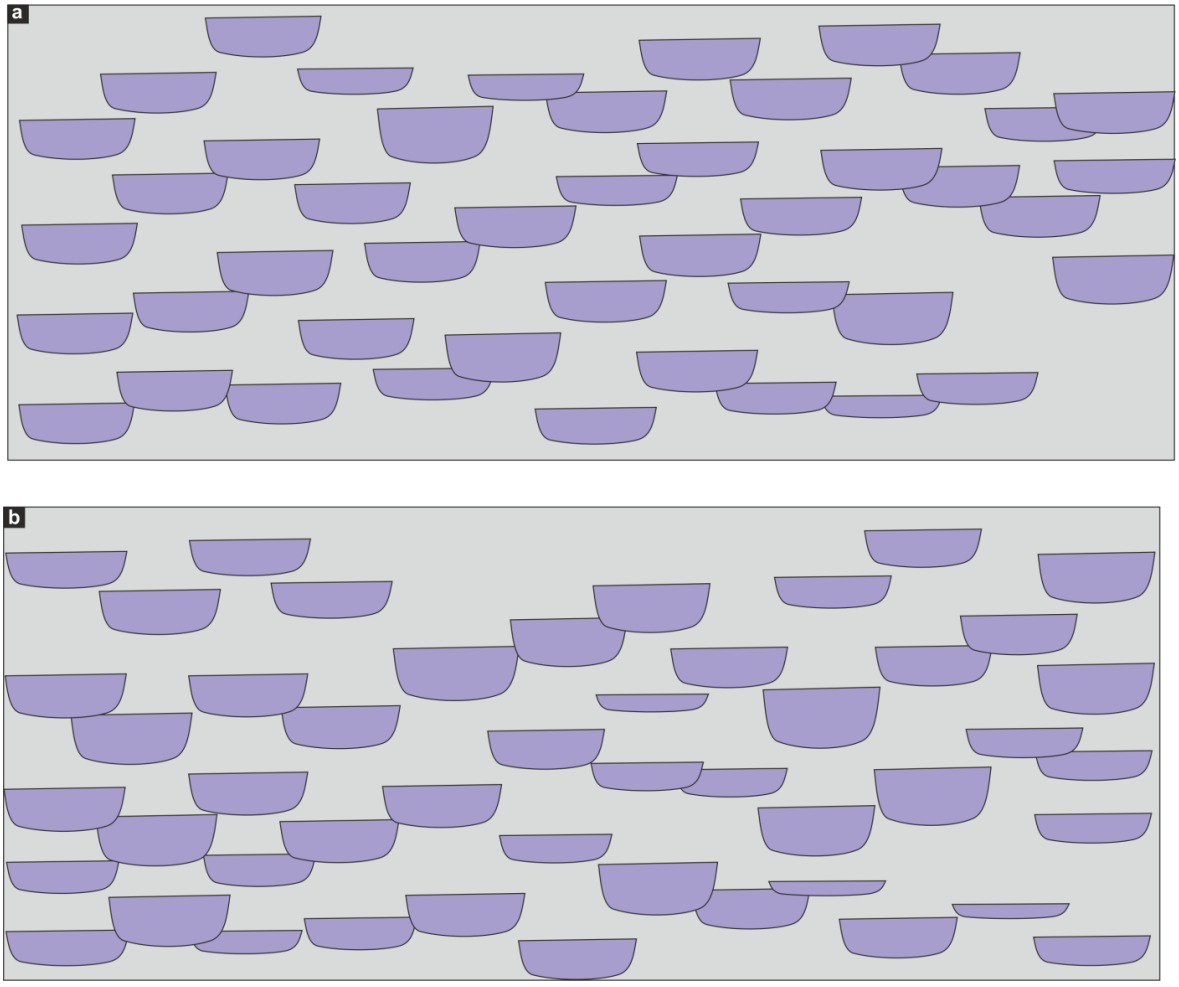

Figure 2.11: Simulated cross-section of channel avulsion and graben subsidence where the interconnectedness of the channels is slightly decreased by fault movements compared to when there is no fault movement at all (a) 890 years ago (no fault movement) and (b) 89 years ago (fault movement; adapted from Bridge and Leeder, 1979).

The development of fault networks can be complex and sediment deposited within syn-rift systems are linked to the structural geometry evolving at the basin margin (Leeder, 1993) and influences the channel growth and stacking patterns. Relay ramps are an excellent example of this evolving geometry and form in four stages (Figure 2.12):

Stage 1: In the first stage of relay ramp growth the normal faults are isolated and do not interact with one another (Figure 2.12, Peacock and Sanderson, 1994), therefore not influencing the channel patterns.

Stage 2: During the second stage of relay ramp growth the isolated faults begin to propagate towards one another but they do not join (Figure 2.12). As the fault propagates a ramp begins to develop connecting the hanging wall and footwall together with little displacement along the ramp (Peacock and Sanderson, 1994), this slowly starts to influence the drainage patterns of the fluvial systems and therefore the channel stacking patterns. The beds within the relay ramp can be rotated towards the hanging wall where folding will form (Peacock and Sanderson, 1994).

Stage 3: Across the top of the ramp there are fractures and faults with some slip to take away some of the stress applied to the system, these faults allow for the interaction of the main relay ramp forming faults (Peacock and Sanderson, 1994). This now fully influences the drainage of the fluvial systems and therefore the channel stacking patterns (Leeder, 1993). These faults / fractures are termed oblique or transfer faults (Figure 2.12, Larsen, 1988).

Stage 4: The system is now a single composite fault, as the separate segments have fully overstepped and now interact (Figure 2.12). If displacement along the fault continues at rates of 10 mm/yr (Ouchi, 1985) then deformation within the hanging wall will continue (Peacock and Sanderson, 1994). Now, the drainage patterns of sedimentary systems have fully changed due to the relay ramp evolution.

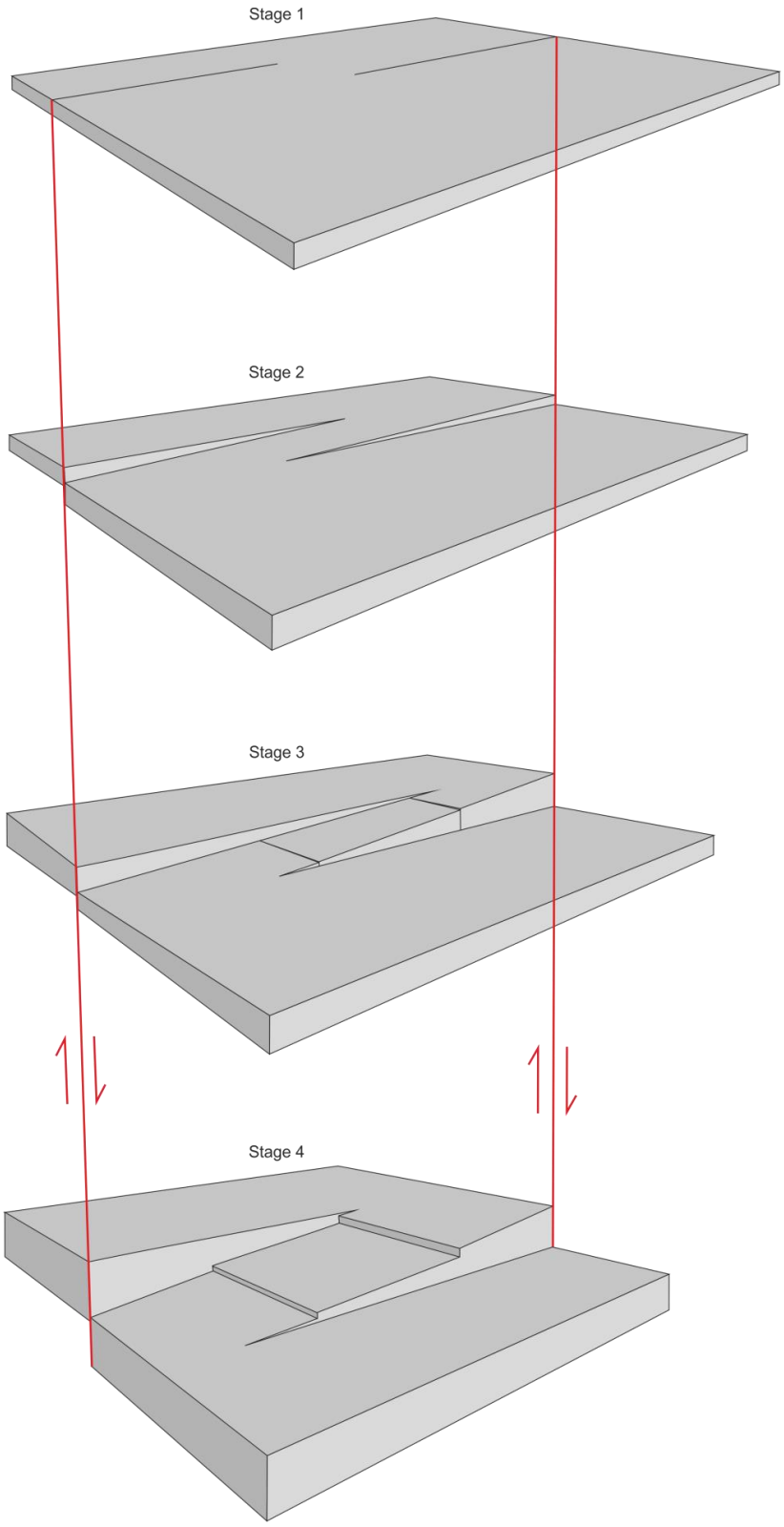

Figure 2.12: The formation of relay ramps occurs in four stages. Stage 1 isolated faults develop; Stage 2 sees propagation of the faults towards one another where the hanging wall and footwall of the relay ramp begins to form; Stage 3 is where the relay ramp start to become breached, and; Stage 4 is where the system is acting as a single composite fault network (Peacock and Sanderson, 1994).

2.8.2 Climate

The climate controls weathering rates, erosion rates, vegetation and water balance (Gawthorpe and Leeder, 2000) within fluvial systems and useful information about these processes can be gained from the floodplain environment. The discharge of the river is dependent on the annual rainfall. Discharge generally has a constant speed (Shaw *et al.,* 2011) and will influence sediment transportation. The amount of grains moved within the flow is governed by flow capacity influenced by discharge. Flow competence influences the sediment directly as it is the flow's ability to move sediment of different grainsizes which is directly dependent upon the Shields Criterion (Section 2.2, Figure 2.1). Discharge is increased due to high precipitation and more sediment is transported downstream. As this happens there is an increased risk of flooding and incision (Haff, 2007; Donselaar *et al.,* 2013). If discharge is decreased, incision will not occur and sediment will not be transported downstream. As the climate controls the amount of rainfall and discharge therefore the facies, architectural elements and the type of fluvial system can be predicted (Table 2.5, Miall, 1996).

Low sinuosity fluvial systems	
Climate type	**Lithofacies and characteristics of fluvial systems**
1. Hot-arid systems	Typical lithofacies are: Gmm, Gci and Gm The typical architectures are: sheets, lenses and lobes The major bounding surfaces are: fifth and sixth order Autogenic cyclicity: debris flow events Petrography: chemically unstable lithologies such as carbonate and feldspar Other structures: silcrete, calcrete, dreikanters, aeolian lenses and evaporitric cements
2. Hot-humid systems	Typical lithofacies are: Gh, Gt and Gp The typical architectures are: channel-forms, sheets and lenses The major bounding surfaces are: fourth, fifth and sixth order Autogenic cyclicity: channel-fill cycles Petrography: chemically unstable lithologies such as carbonate and feldspar with a diagenetic clay matrix Other structures: bauxite, laterite and coal
3. Temperate-humid systems	Typical lithofacies are: Gh, Gt and Gp The typical architectures are: channel-forms, sheets and lenses The major bounding surfaces are: fourth, fifth and sixth order Autogenic cyclicity: channel-fill cycles Petrography: N/A Other structures: Coal
High-sinuosity fluvial systems	
4. Hot-arid systems	Braid plains with playas, terminal fans, flash floods Typical lithofacies are: St, Sh, Sl, Sr, Sp, Fl and Fm

	The typical architectures are: Proximal: step-sided wadis, Medial: broad channels with marcoforms, Distal: unchannelised sheet bodies The major bounding surfaces are: fifth order surfaces with macroforms with second and third order surfaces Autogenic cyclicity: flood cycles Petrography: detrital quartz and carbonates are common Other structures: intraclast siltstones, desiccation cracks, silcrete, calcrete, evaporate lenses, nodules, dreikanters and eolain lenses
5. Hot-humid systems	<u>High sinuosity, anastomosing styles with floodplains and peat bogs</u> Typical lithofacies are: St, Sp, Sm, Sr, Sr, Sh, Sl, Se, Ss, Fl, Fsc, Fcl and Fm The typical architectures are: meanders and channels The major bounding surfaces are: channels with fifth order surfaces with fourth order marcoforms Autogenic cyclicity: macroforms and channel fills Petrography: chemically unstable lithologies such as carbonate and feldspar with a diagenetic clay matrix Other structures: peat swamps, bauxites and laterites
6. Tropical to semitropical systems	<u>Most fluvial styles with perennial but with seasonally dry floodplains</u> Typical lithofacies are: St, Sp, Sm, Sr, Sr, Sh, Sl, Se, Ss, Fl, Fsc, Fcl and Fm The typical architectures are: varying channel characteristics with meander bends The major bounding surfaces are: channels form fifth order surfaces, with fourth-order marcoforms that have second and third order surfaces within Autogenic cyclicity: macroforms and channel fills Petrography: N/A Other structures: peat swamps, drab soils, calcretes and desiccation in the upstream areas
7. Temperate systems	<u>Most fluvial styles, seasonal discharge variations</u> Typical lithofacies are: St, Sp, Sm, Sr, Sr, Sh, Sl, Se, Ss, Fl, Fsc, Fcl and Fm The typical architectures are: varying channel characteristics with meander bends The major bounding surfaces are: channels form fifth order surfaces, with fourth-order marcoforms that have second and third order surfaces within Autogenic cyclicity: macroforms and channel fills Petrography: N/A Other structures: peat swamps and drab soils

Table 2.5: The climatic influence on the fluvial systems, displaying the facies and architectural elements that are produced depending on the climatic regime, the facies codes can be seen in Tables 2.1 and 2.3 (Miall, 1996).

Both low and high sinuosity fluvial systems occur in all types of climates (Table 2.5). Low sinuosity systems can occur in environments that are hot and arid, hot and humid and temperate and humid whereas high sinuosity systems occur in hot and arid, hot and humid, tropical – semitropical and temperate systems (Table 2.5). Each of these different climatic regimes produces different fluvial systems and therefore gives different facies and different architectural elements (Miall, 1996). Being that the focus of this study is on the Barmer Basin the climatic review above ignores glacial environments.

Hot and arid systems produce debris flow and sediment gravity flows (Section 2.5) with deposits that are non-Newtonian. These systems also produce Newtonian flow deposits forming through rolling, saltation and reptation. The facies contain gravels and coarse-grained sandstones (Table 2.5). The architectural elements that form are sandsheets and lenses (Table 2.5; Miall, 1996).

Hot, humid and temperate climatic regimes produce fluvial systems of varying thickness as the deposits are from intense rainfalls which produce highly erosional surfaces. In normal weather conditions the deposits are formed through both non-Newtonian and Newtonian processes where the system has a steady discharge (Jones, 1977). The facies are formed from sands, silts and clays with channels (Table 2.5).

Tropical environments have both monsoonal areas where the flow is continuous due to the high rainfall amounts forming an irregular discharge due to the varying discharge (Jones, 1977). The deposits of the flow can vary from gravel-grade to silt-grained sediments depending on the amount of discharge to the fluvial system and the length of the flooding period (Table 2.5, Jones, 1977).

Climate is a larger-scale factor and can override the effects of local variations in tectonics (Ouchi, 1985). For examples at high relief the climate during the Triassic Period was cool as the temperature did not exceed 25°C and low relief zones such as the tropical zones are warmer (Péron *et al.,* 2005). The rainfall patterns for the globe are dependent on location as the seasons of winter and spring over the equator and subtropics (low relief) are generally wetter than the summer and autumn (Péron *et al.,* 2005). At high relief the precipitation is highest during the spring. Rainfall and temperature can be measured from present day soils; therefore, key to understanding palaeoclimate and its controls upon the palaeo-precipitation and palaeo-temperatures of fluvial systems is the palaeogeoraphy and the palaeosols of floodplain deposits. This is because the pedogeneic features are

directly related to the climate (Kraus, 1999). Examples of the differences within the palaeo-precipitation and palaeo-temperatures can be modelled, for example low relief climate can be dominated by warm and dry climate where during the Triassic Period the global temperature of 17.3°C and a global precipitation rate of 3.2 mm/day (Péron *et al.,* 2005).

2.8.3 Base level

Base level is another control on fluvial systems and defined as 'an imaginary level surface, and to define it simply as the level base with respect to which normal sub-aerial erosion' (Schumm, 1993). The base level is the height of the eustatic or relative sea level, lake level or groundwater level and controlled by the tectonic subsidence or uplift. Also, depending on whether the system is either endoreic or exoreic, base level can be controlled by regional climate as well as tectonic processes (Péron *et al.,* 2005). Base level controls accommodation space and incision on fluvial systems. Therefore, base level controls the graded profile of a fluvial system. If the base level is lowered then a fluvial system will incise (Figure 2.13) and migrate distally, whereas with an increase base level the fluvial system will migrate proximally (Figure 2.14).

A decrease in base level produces a steeper graded profile, creating an increase in stream power, erosion and therefore sediment supply. The decrease in base level can be due to increased tectonic uplift or / and a cooler global climate. The fluvial system becomes straighter in its character and incises down (Figure 2.13, c.f. Allen, 1964) as the fluvial style changes. Base level drop also indicates new drainage areas for a river; this can lower the gradient (Miall, 1996) and see the lateral migration of the rivers nickpoint. Overall there is a decrease in the accommodation space.

Base level increases then fluvial systems will migrate proximally. An increase in base level produces a shallow graded profile and the fluvial system becomes meandering to accommodate the reduction in stream power and transportation of sediment (Allen and

Allen, 2005). The increase in base level can be due to tectonic subsidence or / and a globally warmer climate. Laterally migrating high sinuosity systems create well-connected channel sandstones with little but very well-developed floodplains (Figure 2.14; Wright and Marriott, 1993; Allen, 1964). There can be an increase in avulsion (Allen, 1964). Changing the base level forces the fluvial system to respond, but this has a major lag time. Overall there is an increase in the accommodation space.

2.8.4 Sediment supply

Sediment supply can vary throughout the year due to higher discharge and subsidence and therefore a change in climate or tectonics will have a direct effect on the sediment supply. The sediment supply itself is controlled by the tectonic influences and the climate (Péron *et al.,* 2005). It is also complex and variable within continental settings due to the proximity to the source. Sediment supply rates are very difficult to quantify and depend on: bedrock denudation, surface stabilisation, type of lithology, climate and tectonics (Leeder *et al.,* 1998).

Sediment supply changes in space (nonuniformity) and time (unsteadiness). Nonuniformity occurs within given climatic regimes due to changes in the land surface from tectonic evolution or bedrock denudation. Unsteadiness results from unroofing of sediments (Coloumbo, 1994) but mostly a change in the climate regime (Leeder *et al.,* 1998). The supply rate is partially controlled by what sediments are available vs the discharge rate and the amount of precipitation (Péron *et al.,* 2005). A particularly arid environment with little vegetation will have high sediment yields when compared to heavily vegetated areas such as the tropics (Leeder *et al.,* 1998).

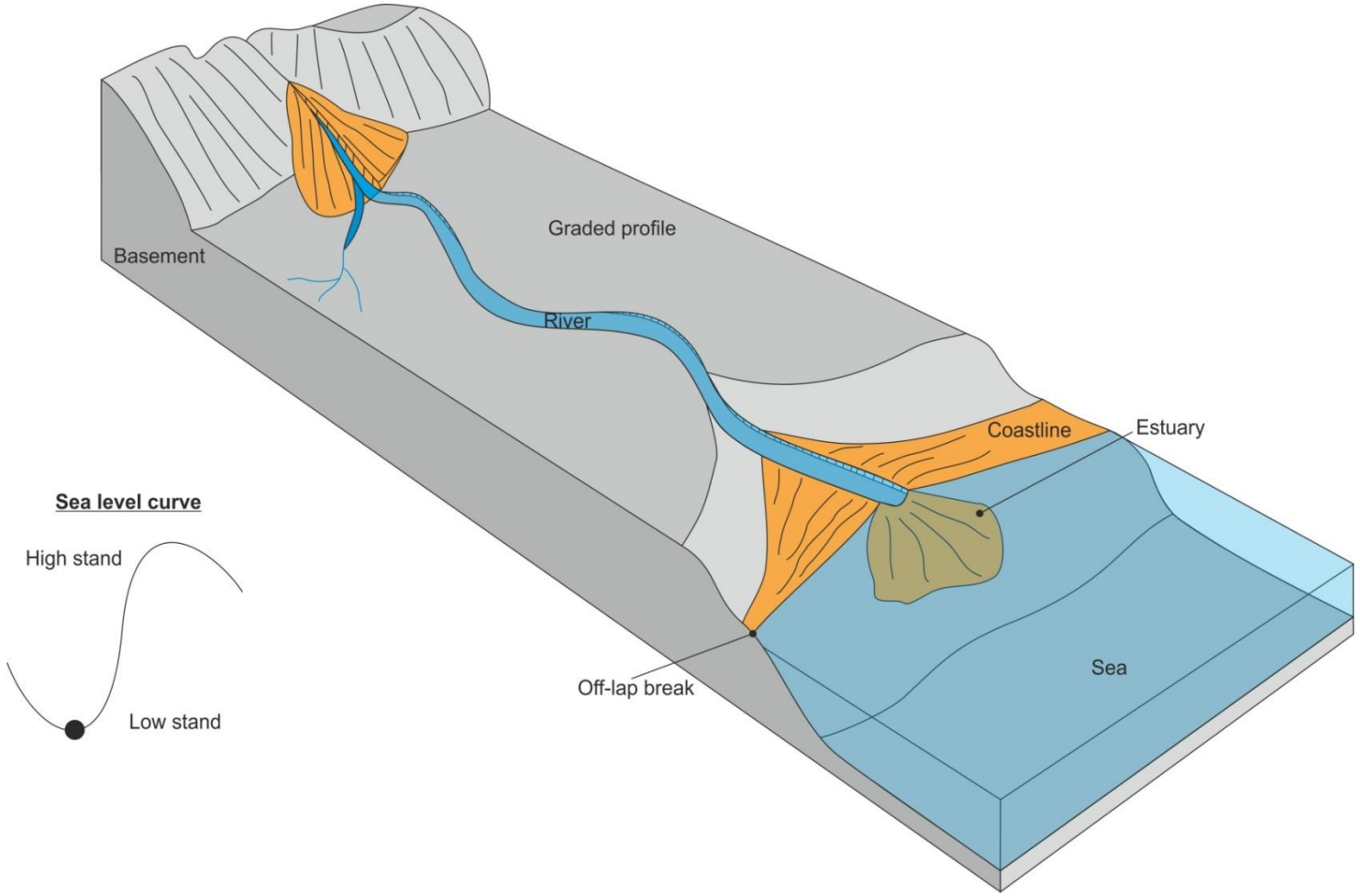

Figure 2.13: Base level decreases here and therefore the river incises and becomes straighter in order to reach the base level (Emery and Meyers, 1996; Allen and Allen, 2005).

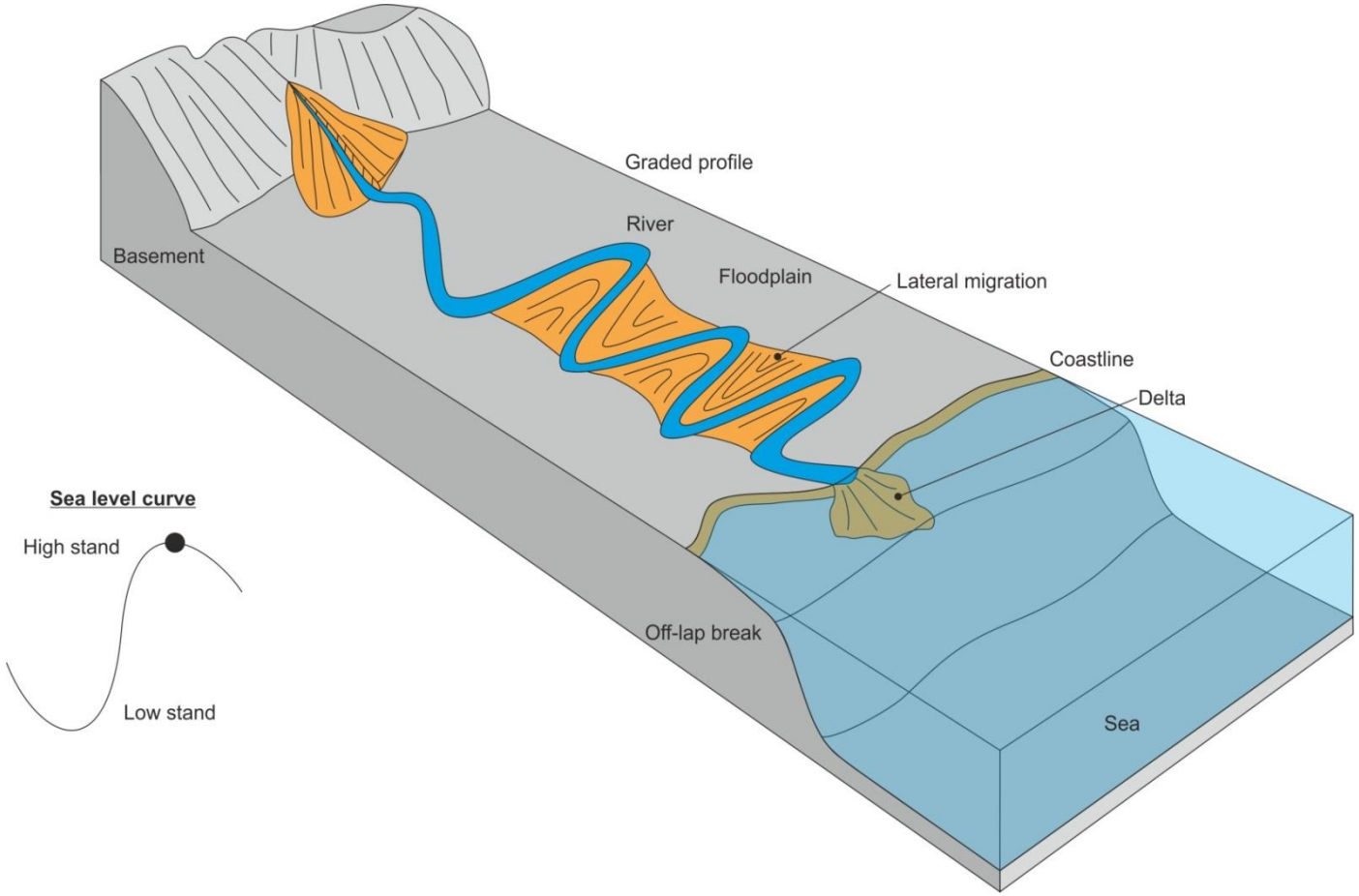

Figure 2.14: Base level increases here and therefore the river retreats proximally and becomes higher in its sinuosity in order to retreat from the increasing base level (Emery and Meyers, 1996; Allen and Allen, 2005).

Accommodation space also affects the sediment supply of a fluvial system. If the fluvial system carries enough sediment to fill the basin then preservation is high, if the sediment supply overtakes the accommodation space then the sediments can be subject to erosion and likely preserving the coastal and shoreface environments over a fluvial one (Péron *et al.,* 2005). It is suggested that climate has a higher influence on sediment supply than tectonic systems do. Currently, there is a lack of accurate dating methods available for terrestrial systems; therefore it is difficult to determine denudation rates and sediment supply.

2.8.5 Avulsion

Avulsion is defined as 'a river flow diversion from an established channel and relocated to a new position on the floodplain' (Mohrig *et al.,* 2000; Slingerland and Smith, 2004; Jones and Hajek, 2007) and occurs on time-scales of roughly 10^5 to 10^7 years (Leeder, 1993; Flood and Hampson, 2014). Avulsion happens for two reasons either; 1) channel annexation and channel incision by the flooding of the fluvial system with a general lack of floodplain deposits (Mohrig *et al.,* 2000; Donselaar *et al.,* 2013; Flood and Hampson, 2014), and / or; 2) progradation of the channel where the initial diversion away from the parent channel into the new channel is via crevasse splays (Flood and Hampson, 2014).

The deposits of channel annexation and channel incision are generally confined to the channels with limited floodplain aggradation (Slingerland and Smith, 2004) for example the Guadalope-Matarranya system, Spain (Mohrig *et al.,* 2000). The deposits of the progradational avulsion are recognized by five different depositional processes: 1) bounding strata; 2) mudstones; 3) sheet sandstone bodies; 4) ribbon sandstone bodies and; 5) large channel sandstone bodies (Slingerland and Smith, 2004). Jones and Hajek (2007) have determined a separate scheme to that defined by Slingerland and Smith (2004) looking at avulsion processes in terms of stratigraphy. There are two types of

avulsion here known as stratigraphically transitional avulsion and stratigraphically abrupt avulsion. Stratigraphically transitional avulsion produces deposits similar to avulsion by progradation (Jones and Hajek, 2007) and stratigraphically abrupt avulsion produces deposits similar to channel annexation and incision. The key differences between the two are related to crevasse splays which are more likely to be preserved within stratigraphically transitional avulsion (Jones and Hajek, 2007).

Avulsion can also be linked to the sediment supply to an area. If the sediment accumulation rate and the avulsion rate are equal then the channels are generally isolated (Figure 2.15). If the sediment accumulation rate is higher or lower than the avulsion rate then the channels can overlap or become isolated. It is noted that when the sediment accumulation rate is higher than the avulsion rate then the channel become isolated higher up the sediment package (Figure 2.15b). If the sediment accumulation rate is lower than the avulsion rate then the channels will become connected higher up the sediment package (Figure 2.15c).

Overall fluvial systems are controlled by large spatial and temporal variations (Donselaar *et al.,* 2013), the combinations of the above processes display that fluvial systems are very complex and need careful attention when analysed.

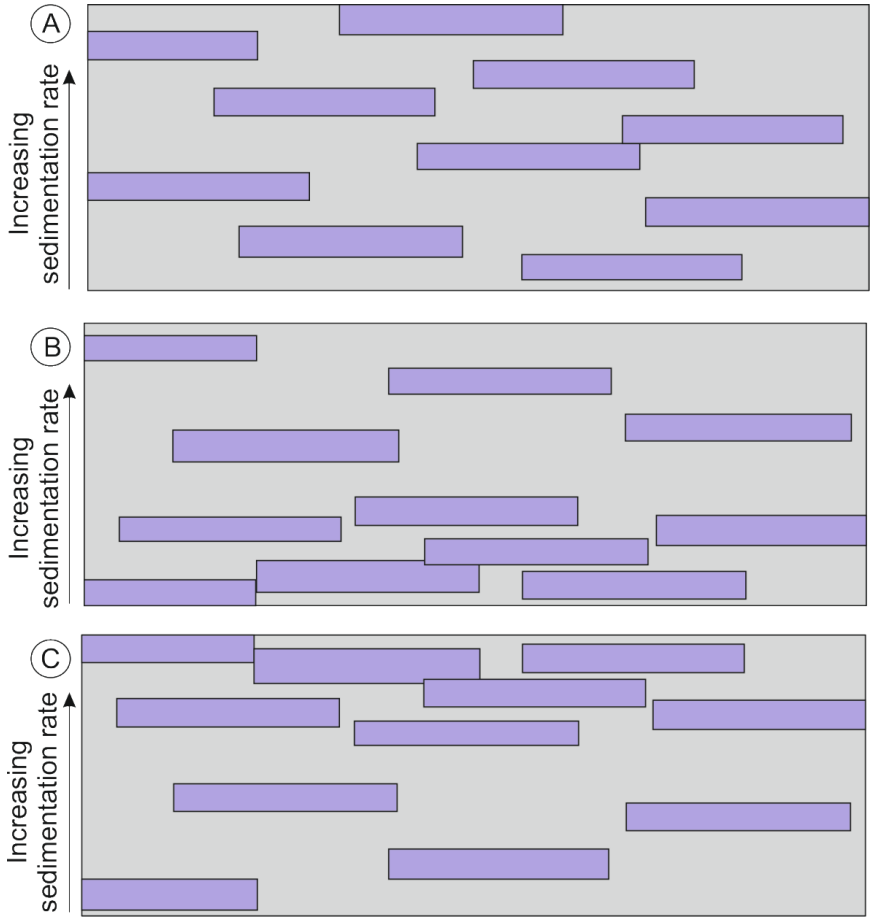

Figure 2.15: Subsidence rate within a basin versus fluvial incision with an increasing sedimentation rate where (a) is where the sedimentation rate is equal to that of the avulsion rate; (b) is where the sediment accumulation rate is above the avulsion rate, and; (c) is where the avulsion rate is higher than the sediment accumulation rates (Heller and Paola, 1996).

2.9 Summary

As discussed, fluvial systems flow as Newtonian or non-Newtonian fluids. All Newtonian fluids such as water, flow in two states (laminar or turbulent); as determined by the Reynolds Number. Sediment is picked up, transported and deposited only in turbulent flow as depicted by the Shields Criterion.

Sediment forms geomorphic bodies that may be analysed through identification of facies, bounding surfaces and architectural elements. These analyses allow for the interpretation of ancient sedimentary systems and three-dimensional models to be built. There are four depositional systems that are discussed here. They are: the bedload dominant, low sinuosity fluvial systems which are characterised by stacked and amalgamated channels.

The mixed load, high sinuosity fluvial systems characterised by point bars; suspended load fluvial system which are composed of dominantly fine-grained material; the floodplain environment which is identified by fine-grain sands, silts, clays and palaeosols.

These systems are influenced by tectonics, climate, base level, sediment supply and avulsion. Extensional tectonic regimes can influence the drainage of sedimentary systems, including fluvial environments due to the formation of relay ramps. Extensional tectonics can also influence channel avulsion and therefore the connectedness of the preserved channel deposits. Climate influences weathering rates, erosion rates, vegetation and the water balance therefore the influences of the climate combined with the localised tectonic regime implies that these large-scale influences on sedimentary systems will control the sediment supply and accumulation.

Base level will control the gradient of the fluvial system and therefore the interconnectedness of the channels. The base level can be controlled by the tectonic regime as uplift will increase the base level and tectonic subsidence will cause a sea level decrease. Sediment supply and avulsion can also influence the fluvial system; however, both of these processes are directly influenced by either climate or tectonics. These two processes are also directly related to one another as sediment rate increases the avulsion rate will decrease.

This chapter covers the literature pertaining to the fluvial system of the Ghaggar-Hakra Formation. The next chapter (3) documents the literature of the evolution of India, particularly the West India Rift System.

3 Chapter Three: The Geological Evolution of India and the Stratigraphy of the Barmer Basin.

The geological evolution of north-western India is complex and varied. The surface and subsurface strata preserve evidence of several plate reorganisations (Reeves, 2014), four separate orogenies (Gombos *et al.,* 1995), multiple extensional events with sedimentary basin formation (Reeves, 2014), and the Himalayan collision (Biswas, 1987). This complex evolution may be summarised by three key periods of geological history that have affected north-western India significantly: 1) late Triassic break-up of Pangaea; 2) late Cretaceous separation of Madagascar from India in a northeast-southwest orientation, and; 3) the Indian-Asian collision during the Paleogene Period; forming the Himalayas. The break-up of Pangaea and the separation of Madagascar and India resulted in the formation of the West Indian Rift System, comprising four basins: the Kachchh (Kutch), Barmer, Cambay, and Narmada basins.

The focus of this work is the sedimentology and stratigraphy of the Cretaceous section of the Barmer Basin. Consequently, this chapter will discuss the geological evolution of the Barmer Basin in detail but within the context of the evolution of north–western India. The lithostratigraphical subdivision of the sedimentary fill of the Barmer Basin is discussed in depth, with emphasis placed on the current and most widely accepted framework for the Lower Cretaceous succession, in order to provide context for this research (Chapters 4 – 8).

3.1 The Geological Evolution of India

The Indian Shield can be subdivided into four cratons known as the Marwar, Bundelkhand, Kachchh - Saurashtra and Dharwar cratons (Figure 3.1). Today, the preserved basement remnants of these mountain ranges manifest themselves as four basement lineament trends: the Dharwar Trend, the Aravalli-Delhi Trend, the Satpura Trend, and the Eastern Ghats Trend (Figure 3.1). Each of these trends represents

separate orogenies (Biswas, 1987) that have affected the structural evolution of India (particularly the West Indian Rift System). The Precambrian (Neoarchean, 2600-2500 Ma, Goodwin, 1991) Dharwar Trend traverses 2000 km of south-western India in an approximately north-northeastern orientation, from the present day locations of Bombay to Palghat.

The Aravalli-Delhi Trend is in a northwest-southeast orientation, in the north northwest of India stretching from Delhi to Jodphur (Figure 3.1) and is 800 km long. The Aravalli-Delhi Trend splits in the north into two separate trends known as the Aravalli and Delhi trends. The trend was formed in the Precambrian (Orosirian – Stenian periods, 2000-1100 Ma, Goodwin, 1991).

Satpura Trend is in an east-west orientation, within central India (Figure 3.1), from the east to west coastlines. This trend formed at 1600 Ma during the Precambrian (Statherian – Calymmian boundary, Collier *et al.,* 2008). This trend divides the Indian plate into north and south; in the north there are the older Precambrian-Cambrian marine deposits and in the south there are the Permian Period paralic deposits (Biswas, 1987).

Eastern Ghats Trend in a northeast-southwest direction, within eastern India (Figure 3.1) stretches from the present day locations of Kurool to Simlipad. The trend formed in the Precambrian Period (between the Mesoarchean – Stenian periods, 3000-1000 Ma; Goodwin, 1991). The Eastern Ghats Trend is approximately 600 km long.

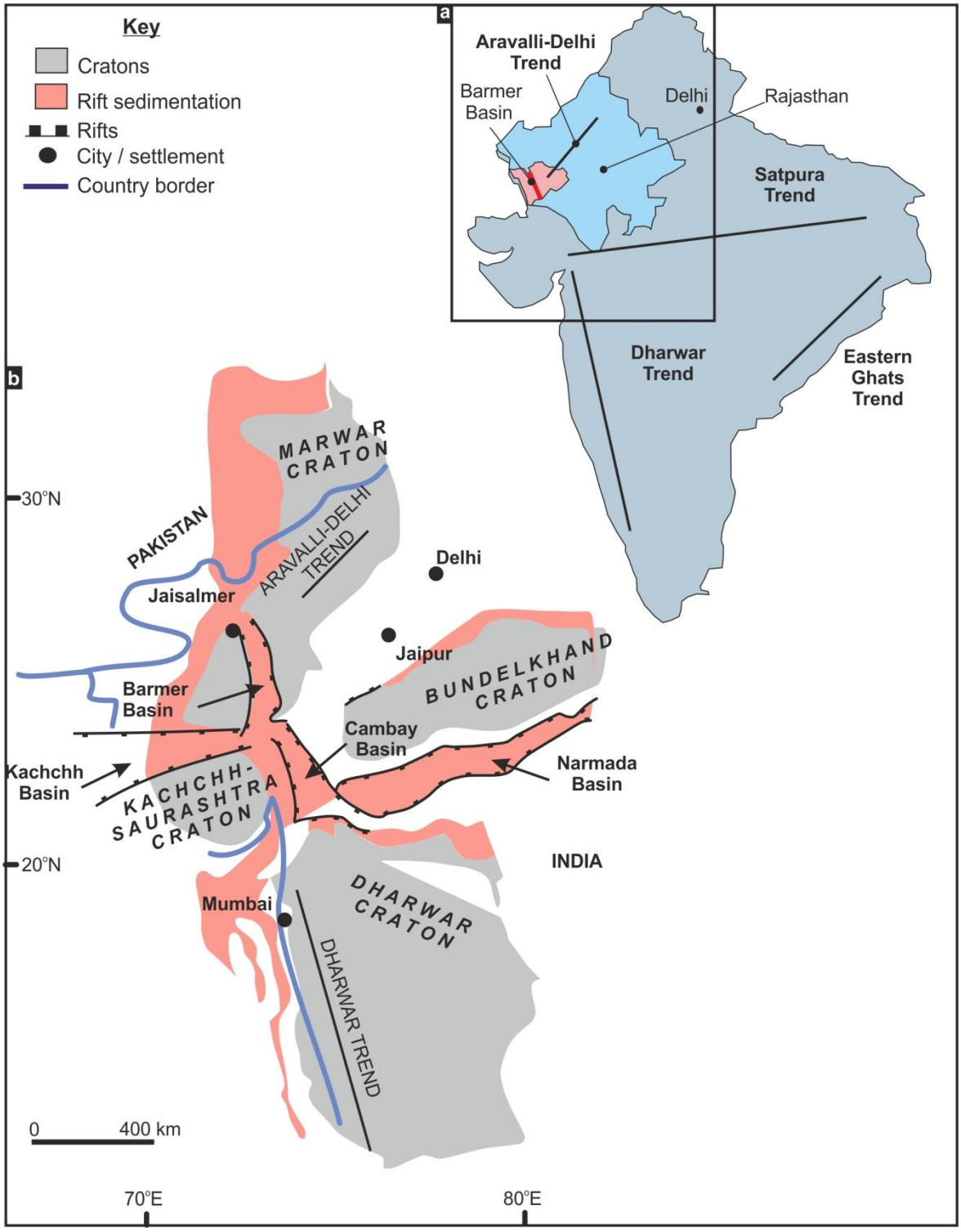

Figure 3.1: Maps of India and the West Indian Rift System; (a) Index Map of India and the locations of the Precambrian structural trends and; (b) the West Indian Rift System displaying the Kachchh, Barmer, Cambay and Narmada Basins, and the associated cratons, adapted from Balakrishnan *et al.*, (2009)

From the Cambrian Period to the Permian Period the greater Indian Plate was part of Gondawanaland which experienced collisions with Laurasia forming Pangaea. Pangaea began to slowly break-up during the Permian Period reactivating the intra-plate sutures (Biswas, 1999) of the Indian plate causing sag basins during the late Permian Period. The rifting occurring as a result of the defragmentation of Pangaea that formed the West Indian Rift System most likely initiated within the Permian Period and was long-lived through to the Paleogene Period.

Break-up of Pangaea continued into the early Triassic Period when there was regional uplift within the north Indian plate causing rifting of the Lhasa block from the north of Gondwana (Figure 3.2a, Biswas, 1999; Biswas, 2005). The east coast of India started to evolve as rifting between India and Antarctica developed during the late Triassic (Figure 3.2b, Gaina *et al.,* 2007).

During the late Jurassic to early Cretaceous periods, first phase of rifting between Madagascar and India occurred (120 Ma, Figure 3.2c, Compton, 2009) due to sea floor spreading between Australia and Antarctica as the Tethys Ocean closed (Hus and Cathro, 2010). This phase of rifting caused the reactivation of the Aravalli-Delhi Trend influencing the incipient faults of the West Indian Rift System. The second phase of Indian-Madagascar rifting occurred between 88 – 84 Ma (Figure 3.2e, Upper Cretaceous; Collier *et al.,* 2008), due to India drifting northwards; this movement is inherently preserved offshore.

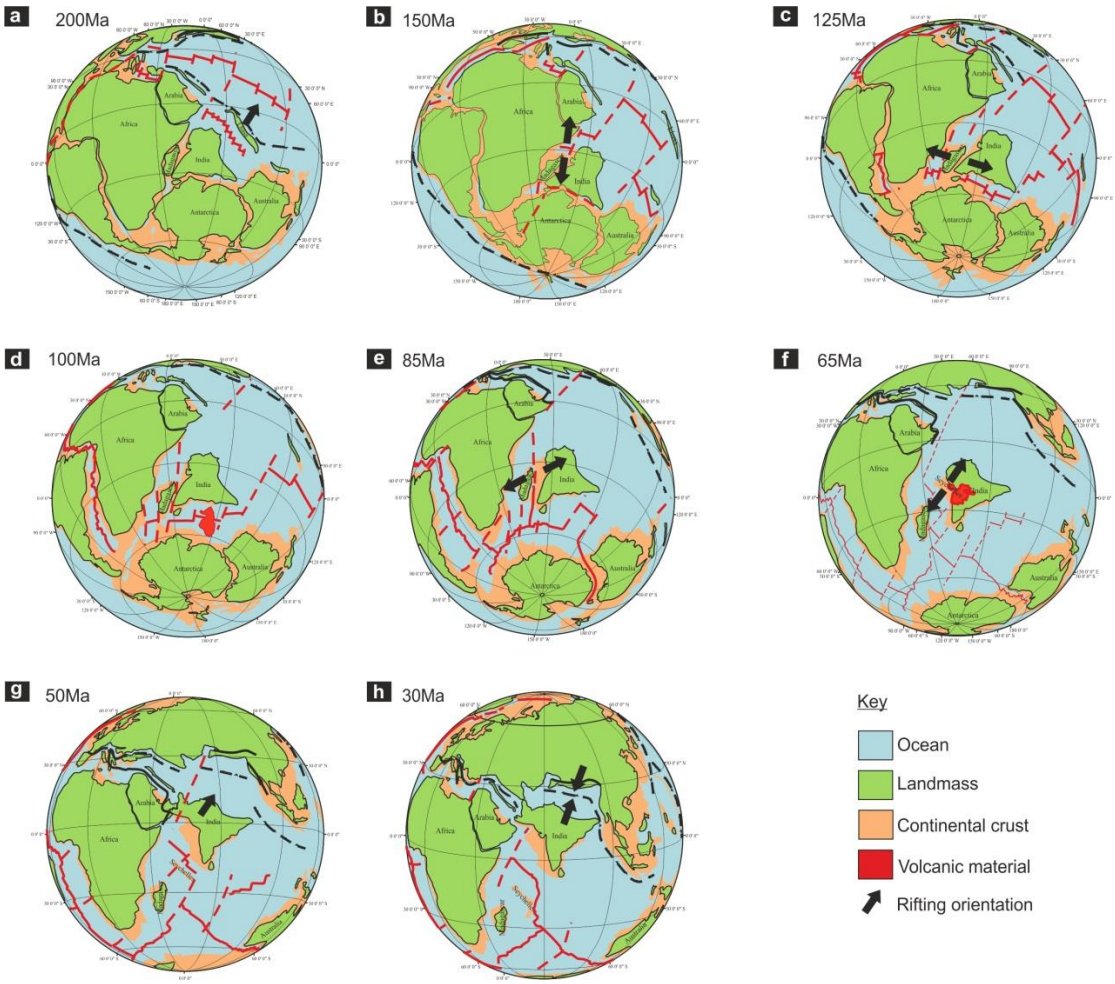

Figure 3.2: Palaeogeographical reconstructions of India. From the Jurassic Period forward it is suggested that the effects of rifting may have affected the Barmer Basin; (a, b, c) from 200 Ma – 125 Ma the break-up of Gondwana; (c, d, e) from 120 Ma – 65 Ma the rifting of India and Madagascar and the passing of the Reunion Hotspot (f, g, h) 65 Ma to present India moved northwards and collided with Asia forming the Himalayan Mountains; adapted after Hus and Cathro (2010).

Late Cretaceous rifting of the Indian plate from the African plate and opening of the Indian Ocean promotes further subsidence within the West Indian Rift System, promoting deposition of the late Cretaceous sediments. On the boundary of the Cretaceous and Paleogene periods (63.4 Ma) the Seychelles micro-continent began to separate from central west margin of India with a northwest – southeast strike (Gaina *et al.,* 2007; Collier *et al.,* 2008, Figure 3.2f, g, h), also promoting subsidence of the West Indian Rift System. This rifting of the Indian plate from the African plate and the Seychelles micro-continent coincides with the Deccan Traps eruption (Figure 3.2f, 67 – 63 Ma, Upper Cretaceous – Paleocene; Collier *et al.,* 2008) potentially originating from the same plume as the

Reunion Hotspot (Sheth, 2005). The uplift associated with this is plate-wide, forcing changes in drainage patterns of fluvial systems as before the uplift fluvial systems flowed westwards into the Arabian Sea and after the uplift fluvial systems flowed to the east, into the Bay of Bengal (Cox, 1989; Gombos *et al.,* 1995; Sheth, 2007). The uplift associated with the Reunion Hotspot also created regional planation surfaces (Figure 3.3, Sheth, 2007).

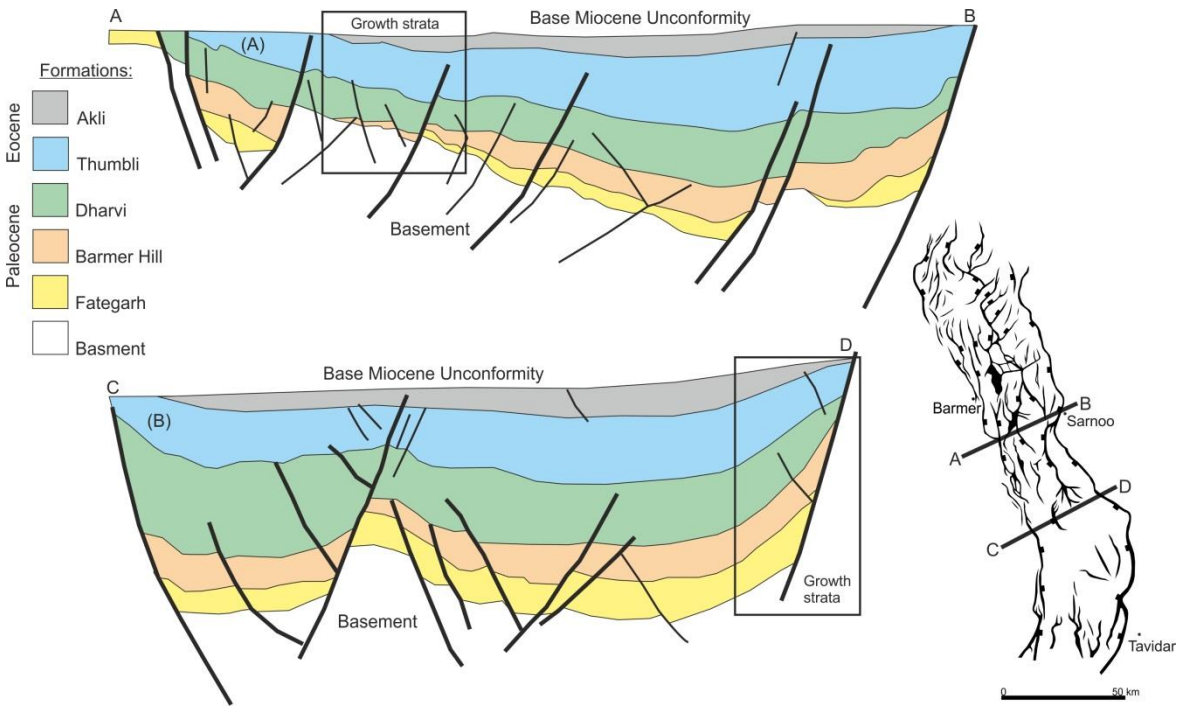

Figure 3.3: Regional cross sections of the Barmer Basin displaying the graben and growth strata of the Barmer Hill and Dharvi-Dungar formations; (a) the northern section and (b) the southern section; from Compton (2009), for basin location see Figure 3.1.

The early Eocene Epoch saw the collision of India with Asia with ~1000 m of uplift and erosion in north–western India. A widespread unconformity (Base Miocene Unconformity – BMU, Compton, 2009; Figure 3.3) developed throughout the West Indian Rift System. From the mid-Miocene (Serravallian Age) onwards there has been deposition of the continental to marine sediments within the West India Rift System.

3.2 Evolution of the Northwest India

Evolution of north-western India is depicted by numerous pericratonic basins within the West India Rift System (Biswas, 1982, 1987, 1999; Sisodia and Singh, 2000) that formed from the late Triassic to the early Paleogene periods (Figure 3.1, Biswas, 2005). The West Indian Rift System contains four interconnected rifts which are the Kachchh, Cambay, Narmada and Barmer basins. The formation of these basins within the West Indian Rift System occurred in six stages (Biswas, 1982, 1987; Bladon *et al.,* 2015b):

3.2.1 Stage one – late Triassic Period

Continental break-up of Pangaea started with the southwards rifting of Gondwana. Lhasa a continent previously situated in the north of Gondwana also started to move northwards (Section 3.1, Figure 3.2a; Biswas, 1982; Bladon *et al.,* 2015b). The regional palaeostresses associated with these rifting events caused activation along the Aravalli-Delhi Trend. This activation formed incipient faults within the location of the present day Kachchh Basin.

3.2.2 Stage two – late Jurassic Period

In the late Jurassic Period, India began to move northwards and the stress regime created by this motion resulted in the separation of Africa from East Gondwana and the reactivation of the Aravalli-Delhi Trend (Section 3.1, Figure 3.1). This plate movement allowed for a series of strike-slip faults to form the Kachchh Basin and commenced the formation of incipient faults that eventually become the Barmer Basin margin (Biswas, 1987; Bladon *et al.,* 2015a). These incipient faults provided enough accommodation space for the fluvial Lathi Formation to be deposited (Figure 3.4, Bladon *et al.,* 2015b). The Lathi Formation is the lateral equivalent to the fluvial Nirona Formation in the Kachchh Basin (Sunder *et al.,* 2013).

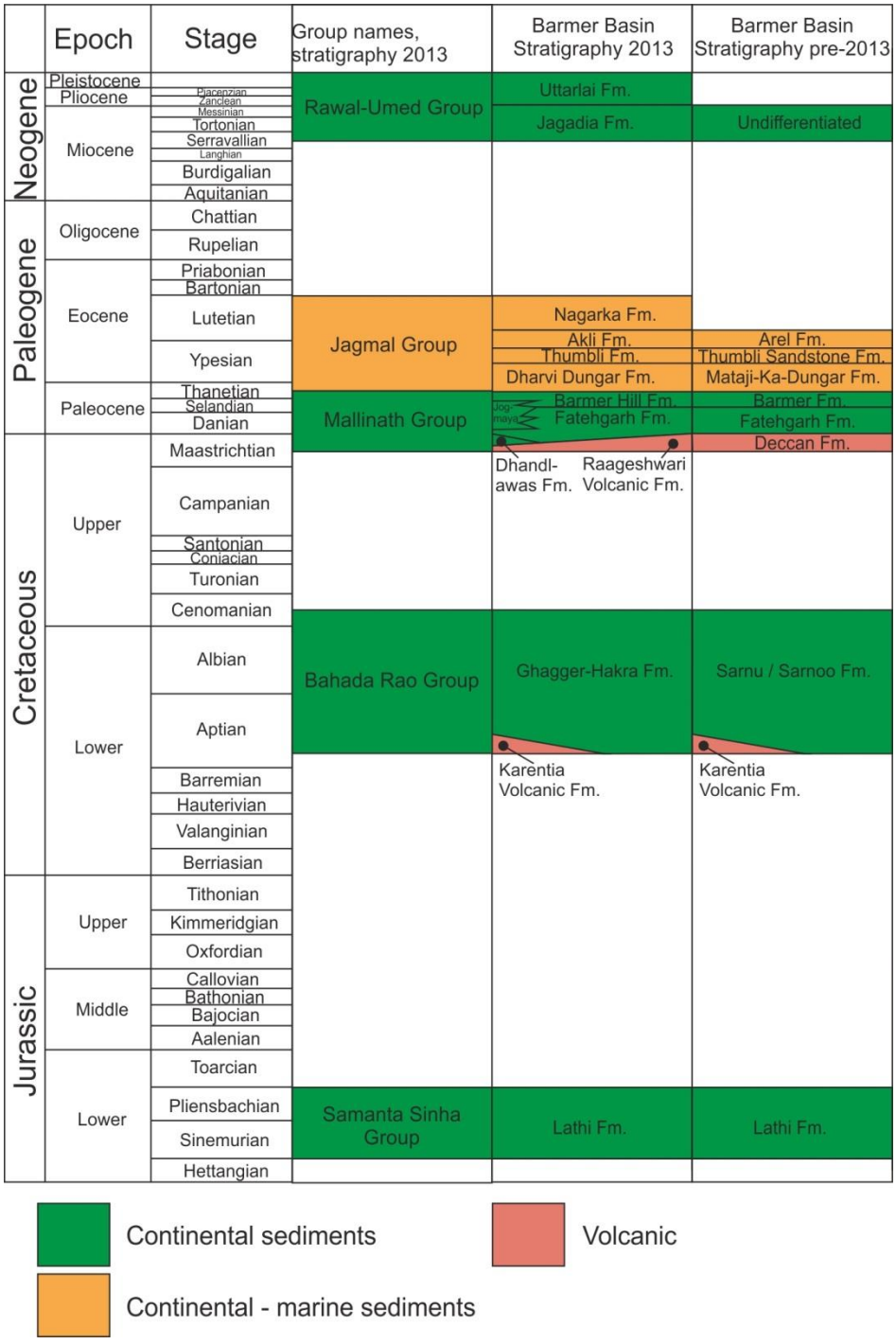

Figure 3.4: The new formation names compared to the old formation names in the Barmer Basin as described by Sisodia and Singh, 2000; Bower, 2004a; Sunder *et al.,* 2013.

3.2.3 Stage three – early Cretaceous Period

In early Cretaceous times, northeast–southwest stresses resulting from Indian Plate rotations and the first phase of rifting between India and Madagascar (Figure 3.2c) caused reactivation of the thrust faulting in the Aravalli-Delhi Trend. This reactivation formed the East Cambay Basinal Fault and deepened incipient faults where the eastern margin of the

Barmer Basin is today (Bladon *et al.,* 2015b). The reactivation also initiated the formation of the northern side of the Narmada Basin (Figure 3.1; Biswas, 1987). Sedimentation continued in the Kachchh Basin with the shallow marine sediments of the Bhuj Formation (Figures 3.2c, d, 3.4; Biswas, 1987; Singh, 2006) and in the Barmer Basin with the fluvial Ghaggar-Hakra Formation.

3.2.4 Stage four – late Cretaceous Period

In late Cretaceous times, a second phase of rifting between India and Madagascar occurred in a northeast–southwest orientation (Section 3.1). This, coupled with the Indian Plate passing over the Reunion Hotspot created tension favourable for the formation of the West Cambay Basinal Fault and the formation of the western margin of the Barmer Basin, where continental deposition occurred with the Viramgam Formation in the Cambay Basin and the Fatehgarh Formation in the Barmer Basin (Figures 3.4, 3.5; Biswas, 1982, 1987). The Narmada Basin continued to deepen and widen towards the west as seen by sediment thickness (Biswas, 1987) in the upper Nimars Sandstone succession deposited within a fluvial to shallow marine setting (Figure 3.5, Racey *et al.,* In review).

3.2.5 Stage five – early Paleogene Period

As the Indian plate moved northwards regional tension was created as the plate passed over the Reunion Hotspot and as the Seychelles micro-continent rifted away (in a north-northwest–south-southeast orientation). These two events caused extensive subsidence of the Cambay and Barmer basins (Bladon *et al.,* 2015b). The Deccan Traps erupted into the Cambay, Kachchh and Narmada basins and are laterally equivalent to the Raageshwari Volcanic Formation in the Barmer basin (Section 3.3.1.2; Figure 3.5, Biswas, 1987; Rohrman, 2007; Hus and Cathro, 2010). The Deccan Traps within the Cambay Basin produced thermal subsidence, this plus extensional subsidence in the Cambay and Barmer basin allowed for deposition of continental to marine-influenced

sediments (Figure 3.4). The deposition within the Kachchh and Narmada basins slowed (Biswas, 1987).

3.2.6 Stage six – late Paleogene Period (Oligocene Epoch)

The Indian plate continued to move northwards and collided with the Eurasian plate to form the Himalayas (Biswas, 1987). This created tensional stresses resulting in the reactivation of multiple normal faults within the West Indian Rift System. This event has also created approximately 1000 m of uplift and erosion of the basins in the West Indian Rift System (Bladon *et al.,* 2015b), thus forming the Base Miocene Unconformity (Compton, 2009). This event has caused tilting of the basins at approximately 15° in a southeast direction (Bladon *et al.,* 2015a).

3.3 Barmer Basin

The Barmer Basin is situated in the middle of the West Indian Rift System and surrounded by the Kachchh, Cambay, Narmada and Jaisalmer basins. The surface topography is a peneplained stoney desert with ephemeral rivers and sand dunes (Dolson *et al.,* 2015). The evolution of the Barmer Basin is complex and outlined above (Section 3.1.2) and brief overviews of the present day fault networks are given here. The stratigraphy of the basin has been through many revisions and the aim here is to clarify these revisions to make a coherent useful stratigraphy to be used within this research and throughout the future literature (Figure 3.4).

3.3.1 Structure

The Barmer Basin has two dominant fault networks: pre-existing west-striking, north dipping faults and the younger southwest-striking, northwest dipping fault network. The central eastern margin of the Barmer Basin has evolved to form an atypical relay ramp due to the growth of these fault networks interacting as a result of external plate boundary forces during the first phase of Indian-Madagascan rifting during the mid-Cretaceous

Period (Bladon *et al.,* 2015b, Figure 3.2). This Cretaceous rifting event occurred before the main Barmer Basin rifting event in the Paleocene Epoch and likely happened during the Aptian to Albian ages (Bladon *et al.,* 2015a, Figure 3.2).

The central western margin of the basin formed during the main Barmer Basin rifting event within the Paleogene Period (Figure 3.2; Bladon *et al.,* 2015b; Dolson *et al.,* 2015) and the centre of this margin is characterised by a breached relay ramp. This breached relay ramp has resulted from palaeostresses from the second phase of rifting between India and Madagascar, the separation of the Seychelles microcontinent and the passing over the Reunion Plume (Bladon *et al.,* 2015b). During the formation of the eastern margin the western margin was characterised by incipient faults. The sediments deposited during this time within the subsurface display growth strata (Figure 3.3).

3.3.2 Stratigraphy

The stratigraphy of the Barmer Basin has been through many revisions and here the aim is to clarify these revisions (Figure 3.4). The lithostratigraphical breakdown is within five groups: Samanta Sinha, Bahada Rao, Mallinath, Jagmal, and Rawal-Umed groups (Figures 3.4, 3.6). The sediments are of primarily Paleogene age (Dolson *et al.,* 2015, Figure 3.6). The first two groups, the Samanta Sinha and the Bahada Rao groups, represent deposition in fluvial environments. While the Samanta Sinha Group presents pre-rift stratigraphy, it is only implied to that the Bahada Rao Group does (Compton, 2009). The Mallinath Group represents fluvial to lacustrine deposition and the Jagmal Group delineates lacustrine to shallow marine deposition. Together these two groups represent the syn-rift phase of basin evolution. The Rawal-Umed Group composes fluvial to upper shoreface deposits and represents post-rift sedimentation in the basin.

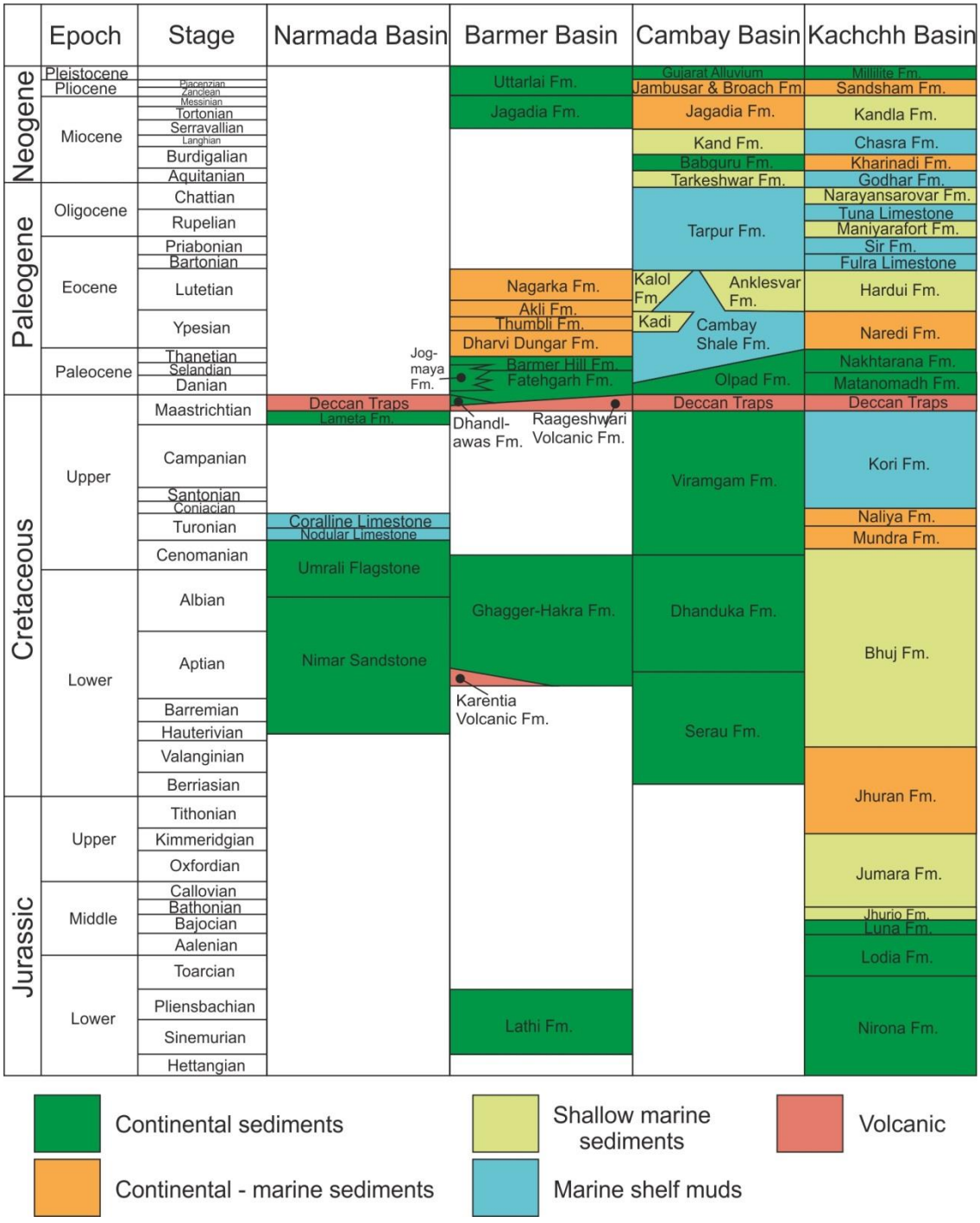

Figure 3.5: The Stratigraphy of the Narmada, Barmer, Cambay and Kachchh basins; the Ghaggar-Hakra Formation is the focus of this study, of Lower Cretaceous age and contemporaneous with the continental sediments of the Dhanduka and Serau formations of the Cambay Basin, the Umrali and Nimar formations of the Narmada Basin and the shallow marine sediments of the Bhuj Formation of the Kachchh Basin (Akhtar and Ahmad, 1991; Gould and Jones, 2012; Jones, 2013; Sunder *et al.,* 2013; Dolson *et al.,* 2015; Racey *et al.,* In review). These sediments of Lower Cretaceous age are draining towards the southwest (Srivastava *et al.,* 1980; Mukherjee, 1983; Biswas, 1987; Desai and Desai, 1989; Racey *et al.,* In review) indicating that the continental sediments are draining into the shallow marine sediments.

The oldest stratigraphy is the Malani Igneous Suite, which is the basement of the basin and therefore not included within the sedimentary groups. The Malani Igneous Suite is composed of rhyolite and trachytic flows (Sisodia and Singh, 2000), dated to the Neo-proterozoic Era at 745 ± 10 Ma (Crawford and Compton, 1969).

3.3.2.1 Pre-rift stratigraphy

The pre-rift succession of the Barmer Basin is formed of the Birmania and Randha formations and the Samanta Sinha and the Bahada Rao groups (Figures 3.4, 3.6).

Above the Malani Igneous Suite there are two Cambrian formations; the Birmania and Randha formations, which are part of the pre-rift sedimentation but are not included within the five lithostratigraphical groups that comprise the majority of the basin fill. The Birmania Formation contains three distinct marine facies assemblages (Mahashwari *et al.,* 2007). The oldest assemblage comprises microsparitic dolostone which grades into quartz-arenite with wavy to lenticular bedding and small-scale cross-bedding; these sediments are overlain by an assemblage of stromatolitic horizons and laminated to bedded phosphorites. The youngest assemblage contains thickly bedded microsparitic dolostones and massive micritic dolostones (Mahashwari *et al.,* 2000). The Birmania Formation was likely deposited within a shallow marine environment (Mahashwari *et al.,* 2007). The Randha Formation comprises mudstone interbedded with thick cross-bedded sandstone successions (Sisodia and Singh, 2000) which were likely deposited within a littoral setting (Mahashwari *et al.,* 2000).

Samanta Sinha Group

The Samanta Sinha Group unconformably overlies the Randha Formation and is subdivided into the Lathi Formation only (Figures 3.4, 3.5).

Lathi Formation

The Lathi Formation comprises medium-grained sandstones, with heavily trough cross-bedded sandstone containing fossilised wood deposited within a braided fluvial system. Data from the trough cross-beds indicate palaeoflow towards the southeast (Taylor *et al.,* 2010).

Bahada Rao Group

The Bahada Rao Group overlies the Samanta Group and is subdivided into the Karentia Volcanic Formation and the Ghaggar-Hakra Formation (Figures 3.4, 3.6).

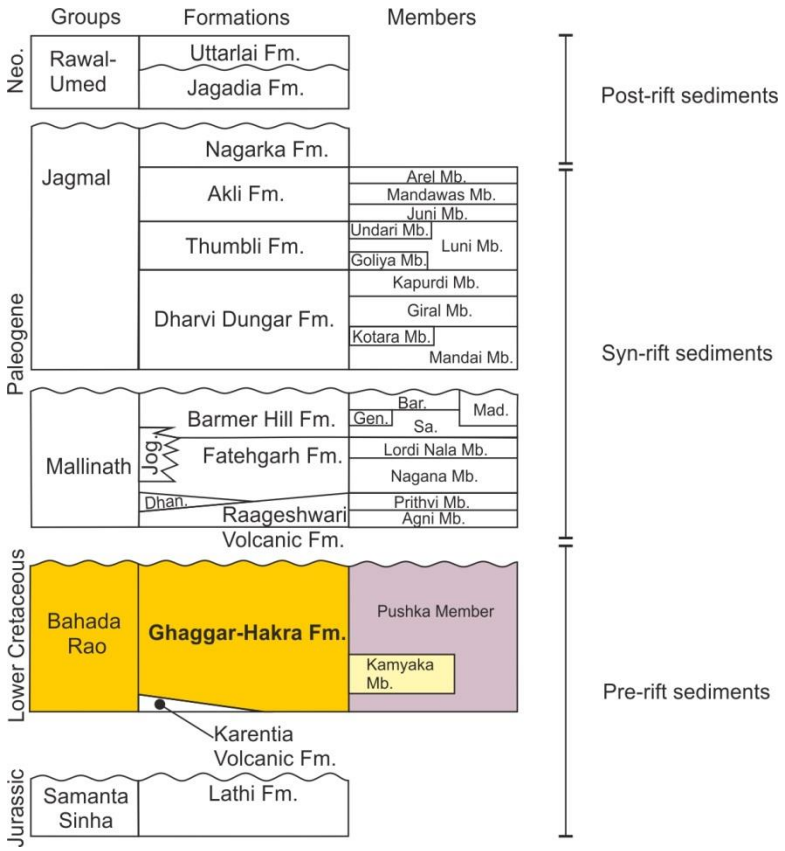

Figure 3.6: The lithostratigraphical breakdown of the Barmer Basin including the groups, formations and members, where Sa. is Sarovar Member, Gen. is Genhu Hill Member, Mad. is Madpura Member and Bar. is Bariyada Member. Highlighted to the right of the diagram are the stages of rifting and which formations were affected and when; the pre-rift sedimentation contains the Samanta Sinha Group and the assumed Bahada Rao Group, the syn-rift sedimentation contains the Mallinath and Jagmal groups and the post-rift sedimentation contains the Nagarka Formation and the Rawal-Umed Group (Bladon *et al.,* 2015a, Dolson *et al.,* 2015).

Karentia Volcanic Formation

The Karentia Volcanic Formation predominantly consists of microcrystalline and plagioclase-phyric basalts that are heavily weathered and fractured (Roy and Jokhar, 2002; Bladon *et al.,* 2015a). Other characteristics include irregular chlorite filled amygdales indicative of shallow emplacement (Bladon, 2014) into the surrounding country rocks which are the Ghaggar-Hakra sediments.

Ghaggar-Hakra Formation

The Ghaggar-Hakra Formation crops out throughout the Sarnoo and adjacent hills on the central eastern Barmer Basin margin (Figures 1.3) within rotated fault blocks (Bladon *et al.,* 2015a). The formation (formerly named the Sarnu / Sarnoo Formation, Figure 3.4; Baksi and Naskar, 1981) at outcrop comprises siltstones (undivided) interbedded with three distinct sandstone-dominated successions (Figure 3.7) that comprise informal units known as the Darjaniyon-ki Dhani Sandstone, the Sarnoo Sandstone and the Nosar Sandstone (Bladon *et al.,* 2015a). The overall thickness of the formation varies between 30 m (Baksi and Naskar, 1981) and 83 m thick (Mishra *et al.,* 1993). Palaeocurrent data is to the southwest (Sisodia and Singh, 2000) suggesting that the fluvial system will drain into the Arabian Sea, however other authors suggest that the fluvial system drains into the Goru and Pariwar marine shelfal sands (Compton, 2009) which is to the northwest of the Sarnoo area.

The base of the Darjaniyon-ki Dhani Sandstone (Figure 3.7) is marked by an erosional unconformity on the underlying siltstones and the unit comprises pebble-grade poorly sorted quartz and lithic clasts (20 – 50 mm, Sisodia and Singh, 2000) to medium-grained structureless sandstones (Bladon *et al.,* 2015a). There are trough and planar cross-beds sets and cosets which can be indistinct; the majority of the sandstone is structureless. The top of the unit grades into fine sands and red siltstones (Sisodia and Singh, 2000). From

the medium- to pebble-grained sandstones few sedimentary structures suggesting deposition within a low sinuosity system (Bladon *et al.,* 2015a).

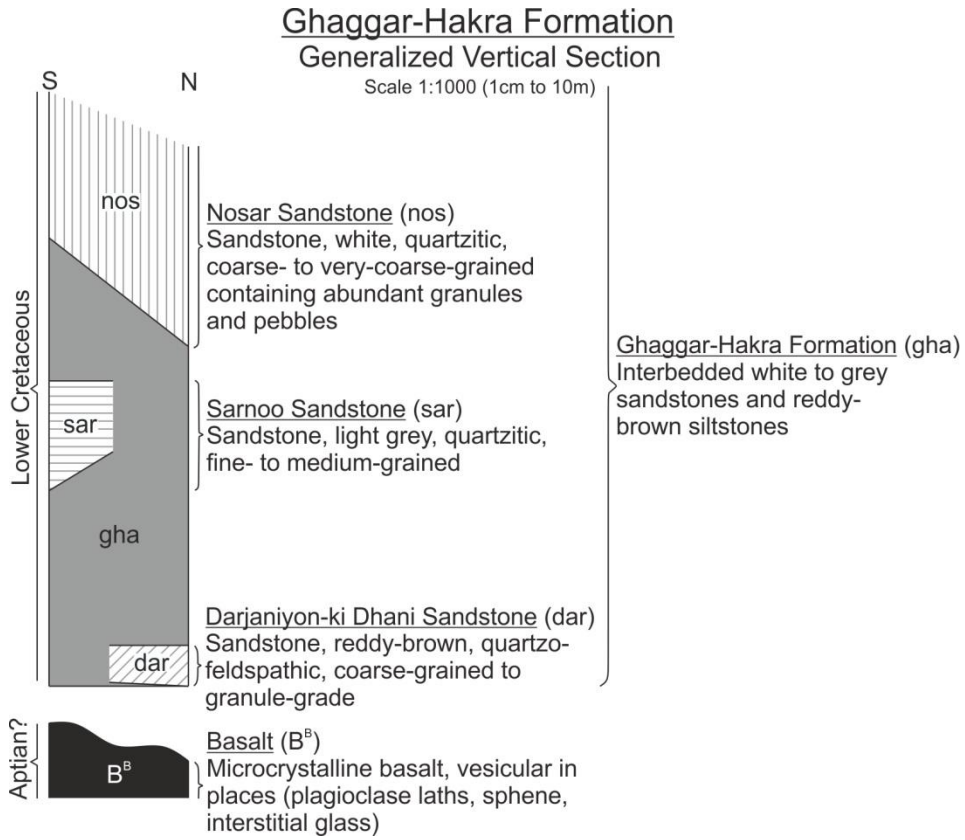

Figure 3.7: General Vertical Section of the Ghaggar-Hakra Formtiaon at outcrop displaying the breakdown of the formation into the Darjaniyon-ki Dhani, Sarnoo and Nosar Sandstones.

The Sarnoo Sandstone (Figure 3.7) displays cyclic successions, from coarse- to fine-grained sandstone with cross-bedding (Sisodia and Singh, 2000; Bladon *et al.,* 2015a). The Sarnoo Sandstone succession was deposited within a meandering fluvial environment (Bladon *et al.,* 2015a). Plant leaves (*Phlebopteris athgarhensis Jain, Ptilophyllum acutifolium Morris* and *? Sphenopteris sp.*) have been found within this sandstone which have dated the formation to the Upper Jurassic – Lower Cretaceous epochs (Baksi and Naskar, 1981; Compton, 2009). Pollen has also been analysed dating the sandstones to the Jurassic – Cretaceous periods (Papanikolaou 2016 pers. comms.).

The Nosar Sandstone (Figure 3.7) is medium- to coarse- grained sandstones with heavily cross-bedded sets and channel geometries with highly erosive bases and siltstone rip-up clasts (Bladon *et al.,* 2015a), suggesting rapidly migrating barforms where the depositional environment was a well-developed low sinuosity fluvial system (Clarke, 2011; Bladon *et al.,* 2015a). Pollen has been found within this sandstone succession dating it to the Jurassic – Cretaceous periods (Papanikolaou 2016 pers. comms.).

The intervening siltstone successions of the formation comprise red siltstones and micaceous sandstones. There are also rooted horizons and a pedogenic nature attributed to subaerial exposure, suggesting genesis on accompanying floodplain for the fluvial system (Bladon e*t al.,* 2015a). However, the siltstone packages have not been extensively studied. It has also been suggested that this succession may have formed within a lacustrine system, due to the fining- and coarsening-upwards successions within these packages (Clarke, 2011).

Within the subsurface of the Barmer Basin the Ghaggar-Hakra Formation is subdivided into two members (Figure 3.6). The older Pushka Member comprises fine- to coarse-grained, planar cross-bedded fluvial deposits (Gould and Jones, 2012; Jones, 2013). Fine-grained sands with wave and current ripples and soft-sediment deformation from load and flame structures and organisms form the Kamyaka Member and represent deposition within a lacustrine setting (Gould and Jones, 2012; Jones, 2013).

3.3.2.2 Syn-rift stratigraphy

The Mallinath and Jagmal groups form the syn-rift strata of the Barmer Basin (Figures 3.4, 3.6). The Mallinath Group represents fluvial to lacustrine deposition, with the Jagmal Group delineating lacustrine to shallow marine deposition. A significant marine transgression marks the transition from the Mallinath to the Jagmal groups.

Mallinath Group

The Maillinath Group comprises five formations: the Raageshwari Volcanic Formation, along with the Dhandlawas, Fatehgarh, Jogmaya Mandir and Barmer Hill formations. With the exception of the Raageshwari Volcanic Formation, the remaining formations of the group are dominantly terrestrial and fluvially-dominated, with alluvial fan and lacustrine interactions (Figures 3.5 and 3.6).

Raageshwari Volcanic Formation

Raageshwari Volcanic Formation has two members known as the Agni and Prithvi and dominantly composed of acidic pyroclastics and basalt lavas up to 1140 m thick (Compton, 2009). The Agni Member is composed of coarse- to fine-grained lapili acidic tuffs including lithic, crystal and vitric tuffs. Also cored are felsic lavas with large elongate feldspar crystals (Sunder *et al.,* 2013). The Prithvi Member is composed of basaltic porphyritic and amygdaloidal lava flows exhibiting phenocrysts of plagioclase feldspar, olivine and augite, with a chlorite groundmass. This member is distinctive as there are amygdales of zeolite, chlorite, calcite and hydrothermal mineralisation has occurred (Sunder *et al.,* 2013). The acidic nature of the pyroclastics and tuffs (Sunder *et al.,* 2013), suggests an explosive volcanic environment and the formation is believed to be the lateral equivalent to the Deccan Traps in central India (Compton, 2009) and the similar deposits within the Kachchh, Cambay and Narmada basins.

Dhandlawas Formation

The Dhandlawas Formation in the Barmer Basin is the lateral equivalent of the Olpad Formation in the Cambay Basin (Figure 3.5). The formation consists of muddy conglomerates and pebbly claystones (Sunder *et al.,* 2013) which are structureless and were probably deposited in a high energy alluvial fan environment (Sunder *et al.,* 2013).

Fatehgarh Formation

The Fatehgarh Formation (Figure 3.6) is fine- to coarse-grained quartz arenites with trough cross-bedding and erosive bases. It is divided into two members on the basis of sedimentary textures and structures and these are known as the Nagana and Lordi Narla members. The Nagana Member consists of coarsening upwards trough cross-bedded quartzite successions (Clarke, 2011). Above this is an erosive conglomeratic layer fining from pebble-grade conglomerates into fine-grained sandstones (Sisodia and Singh, 2000). The upper stage of the member is cyclic and constitutes fine-grained sands with cross-bedding, with a variety of ripples and well-developed palaeosols (Clarke, 2011). The Lordi Narla Member overlies the Nagana Member and consists of current and wave rippled quartzose sandstones and siltstones. There are subaqueous fauna of fish bones. At the top of the formation there is a fossiliferous layer, containing gastropods – *Campylostylus* – dating the formation to the end Cretaceous – early Paleocene periods (Compton, 2009). The origin of this formation is in dispute between several authors as it is speculated that the formation is primarily fluvial in origin due to erosive bases and trough cross-bedding, indicating high energy processes. This, combined with the palaeosols and fine-grained deposition of overbank and shallow lakes, suggests a stable (Compton, 2009), possibly meandering fluvial system. However, the gastropods and fine-grained sediments suggest a tidal flat setting (Sisodia and Singh, 2000).

Barmer Hill Formation

The Barmer Hill Formation (renamed from the Barmer Formation, Bower, 2004a; Figure 3.4) consists of fine sands with rootlets interbedded with clays and calcareous sediment and a porcellanite texture. The formation is subdivided into four members which are: Sarovar, Genhu Hill, Bariyada and Madpura members (Dolson *et al.,* 2015). The Sarovar Member is composed of fine-grained ripple laminated sandstone, interlayered with silts and muds. Above this, the Genhu Hill Member is composed of cyclic successions which are marked by erosive bases with pebble lags fining up into bioturbated siltstones (Clarke,

2011). The Bariyada Member typically exposes porcellanite texture with claystones interbedded. The uppermost Madpura Member constitutes siltstones interbedded with fine-grained ripple laminated sandstones. The Sarovar, Bariyada and Madpura members were deposited within lacustrine environment (Sunder *et al.,* 2013). The deposition of the Genhu Hill Member is high energy and suggests a lake delta environment (Taylor *et al.,* 2010) or an alluvial fan setting (Tabaei and Singh, 2002).

Jogmaya Mandir Formation

The Jogmaya Mandir Formation (Figure 3.5) is the lateral equivalent to the Fatehgarh and Barmer Hill formations. The formation is composed of boulder- to pebble- grade conglomerates containing clasts of the Malani Igneous Suite (Taylor *et al.,* 2010). *Skolithos* and *Taenidium* burrows are observed in fine-grained sands on top of the conglomerates (Sunder *et al.,* 2013). The sediments are deposited dominantly through mass and debris flows suggesting a distal alluvial fan setting. The fine-grained sediments at the top of the formation suggest a fluid flow influence possibly that of a fluvial system (Sunder *et al.,* 2013).

Jagmal Group

The deposition of the Jagmal Group is shallow marine (Sunder *et al.,* 2013) suggesting a transgression to accommodate this new depositional environment in the Barmer Basin (Figures 3.4, 3.6). The formation is subdivided into four formations, Dharvi Dungar, Thumbli, Akli and Nagarka formations; however the Nagarka Formation is regarded as part of the post-rift succession.

Dharvi Dungar Formation

The background sedimentation to the Dharvi Dungar Formation (Figures 3.4, 3.5, 3.6) is claystones, with lignites and few sandstone packages. This formation has four members known as the Mandia, Kotara, Giral and Kapurdi. The Mandia Member is composed of

predominantly massive claystones (Sunder *et al.,* 2013). The Kotara Member is formed from sand-rich beds, but this member has not been widely accepted and therefore there are no descriptions within the literature (Sunder *et al.,* 2013). Giral Member constitutes massive carbonate claystones with thinly interbedded silts and lignites (Sisodia and Singh, 2000). There are some diatoms present. The youngest member, the Kapurdi Member consists of coarse- to fine-grained sandstones, with quartz pebbles up to 5 cm in diameter (Sisodia and Singh, 2000). There are limestones and carbonate clays which are likely to contain fish fossils and echinoderms (Sunder *et al.,* 2013). The palaeoenvironment for the formation represents a marine transgression from lacustrine deposition in the Mandia Member to a shallow marine environment in the Kapurdi Member (Sunder *et al.,* 2013).

Thumbli Formation

Goliya, Luni and Undari members comprise the Thumbli Formation, assessed completely from subsurface material and composed of claystones, siltstones with minor fine-grained sandstones (Sunder *et al.,* 2013). The Goliya Member comprises a mudstone succession. The Luni Member constitutes laminated claystones with negligible siltstone intervals. Undari Member constitutes a fining upwards succession from coarse- to medium-grained cross-bedded sandstone to fine- to very fine-grained ripple-laminated sandstones and laminated claystones (Sunder *et al.,* 2013). There may be possible limestones (Bower, 2004a). The suggested depositional environment is a coastal plain with fresh water influences (Bower, 2004a), or a lacustrine setting (Sunder *et al.,* 2013).

Akli Formation

The Akli Formation is 32 m thick (Figures 3.4, 3.5, 3.6; Tripath *et al.,* 2009) and comprises shelly limestone, calcareous claystones and minor sandstone packages. The formation comprises three members: Juni Bali, Mandawas and Arel. The Juni Member is composed of massive claystones, thin sandstone and subtle lignites (Sunder *et al.,* 2013). Within this member there are trace fossils such as burrows and microfossils of leafs and wood. The

Mandawas Member is composed of lignites and claystones (Bower, 2004a). The Arel Member starts with mudstone interbedded with rare limestones, above this are claystones with shelly fragments and the top of the member is formed by a shelly limestone interbedded with rare sandstone packages (Bower, 2004a). Within all the claystones in the formation there are microforaminiferal linings which are from benthic assemblages, pollen, and algal cysts (Tripath *et al.* 2009, Figure 4) have been used for dating. The sedimentary textures and structures suggest a low salinity, shallow marine environment (Tabaei and Singh 2002, Tripath *et al.* 2009).

3.3.2.3 Post-rift stratigraphy

The Nagarka Formation and the Rawal Umed Group form the post-rift stratigraphy of the Barmer Basin (Figures 3.5; 3.6). The Nagarka Formation represents littoral to shallow marine sedimentation. From end deposition of the Nagarka Formation to the deposition of the terrestrial Rawal Umed Group there is an unconformity of 24 Ma allowing for a base level decrease.

Nagarka Formation

The Nagarka Formation is the first formation of the post-rift sedimentation (Figure 3.6, Dolson *et al.,* 2015) and is composed of dominantly massive claystones with thin lignites, limestones. Sandstone packages are noted in the south of the basin. The formation contains three distinct successions with the first succession varying laterally in thickness and between granule-grade cross-bedded to fine-grains rippled sandstones, with claystone stringers (Bower, 2004a). The second succession has coarse-grained cross-bedded sandstones and claystones which contain algal crysts of *Spiniferites ramosus Group, Adnatosphaeridium vittatum* and *Homotryblium* (Bower, 2004a). Third succession contains claystone interbedded with very coarse-grained, cross-bedded sandstones and has traces of coal, and fresh water algae – *Botryococcus spp.* (Bower, 2004a). Palaeoenvironmental interpretations place the first and third successions within a

lacustrine environment on a coastal plain, due to the freshwater algae (Bower, 2004a). The sedimentary textures, structures and fossils in the second succession probably represent a transition from a swamp to a shoreface environment (Bower, 2004a; Sunder *et al.,* 2013).

Rawal Umed Group

The Rawal Umed Group contains two formations, the Jagadia and Uttarlai formations that are terrestrial in origin.

Jagadia Formation

The literature of the Jagadia Formation is sparse. The claystones and lignites of the Jagadia Formation are terrestrial in origin due to their palynomorphs (Sunder *et al.,* 2013). The palynomorphs of ferns are exclusively found in freshwater presenting possibly fluvial or lacustrine shoreface environments.

Uttarlai Formation

The literature of the Uttarlai Formation is scarce. Uttarlai Formation displays unconsolidated massive sandstones, limestones and claystones, deposited within an alluvial to fluvial plain, with intermittent aeolian dunes (Bower, 2004a; Sunder *et al.,* 2013).

3.4 Summary

There have been several plate reorganisations within the Indian Plate that have led to a complex geological evolution for the West Indian Rift System. The geological evolution has been subdivided into six key stages by Bladon *et al.,* (2015b). The first stage, during the Triassic Period, experienced regional palaeostresses across the Indian plate giving way to the incipient faults in the area of the now Kachchh Basin. During the second stage India moved northwards as a result of the rifting of Africa and East Gondwana and incipient faults developed in the area of the Cambay Basin, this occurred in the Jurassic

Period. The Lower Cretaceous Epoch saw the third stage where the first phase of separation between India and Madagascar occurred. This reactivated the Aravalli-Delhi Trend and formed the eastern margin of the Cambay Basin and incipient faults formed in the location of the Barmer Basin. The second phase of rifting between India and Madagascar occurred within the fourth stage in the latest Cretaceous Period. This rifting plus the passage of the Indian Plate across the Reunion Hotspot caused the west margins of the Cambay and Barmer basins to form as the eastern margins of both basins continued to develop. The fifth stage is within the early Paleogene Period; the rifting of the Seychelles microcontinent occurred, creating regional tension across the Indian plate. During this time the Deccan Traps also erupted causing further subsidence of the Cambay and Barmer Basins. The final stage during the late Paleogene Period (Oligocene Epoch) saw the collision of the Indian plate with the Eurasian plate.

Clarification of the stratigraphy of the Barmer Basin has been achieved here by the means of a detailed literature review, using the most updated formation names. The groups and formations deposited within the Barmer Basin are the product of a series of epeirogenic and orogenic movements and climatic changes recognised within the West Indian Rift System. The pre-rift sedimentation was predominantly within fluvial environments, the syn-rift sediments were deposited within continental to marine settings and the post-rift sedimentation was deposited within a terrestrial setting.

This research focuses on the sediments within the Bahada Rao Group, which have been allocated to formations based on lithological changes. The detailed literature review provided here concludes that the Ghaggar-Hakra Formation is dominantly fluvial in origin and a lithostratigraphical analysis of the formation has identified three distinctive sandstone successions at outcrop which are the Darjaniyon-ki Dhani, Sarnoo and Nosar sandstones. The following chapters (4 – 8) will look at these sediments in greater detail to

determine the exact nature of the sedimentary environments that prevailed in this region during the Lower Cretaceous Epoch and the controls upon that environment.

4 Chapter Four: Facies and Depositional Environments of the Ghaggar-Hakra Formation

Facies analysis is a well-established tool for the interpretation of preserved sedimentary deposits (Cant, 1977; Miall, 1985). Facies and architectural element schemes within a broad range of fluvial systems have been developed by Cant (1977), Allen (1983) and Miall (1977, 1985). The dominant facies observed within fluvial successions can be attributed to the flow of water within confined channels, and to deposition of sediment on the floodplain between channels by gravitational settling and regular flooding (Miall, 1977; Bordy *et al.,* 2004). However, systems with high sediment load and / or significantly variable discharge commonly can also display additional facies broadly attributable to debris-driven (rather than fluid-driven) processes (Bordy *et al.,* 2004; Gomez *et al.,* 2009) and to the suppression of bedform development by a high suspended sediment load (Lowe, 1988; Leeder, 2011).

This chapter describes and discusses the fluvial facies of the Ghaggar-Hakra Formation. The work has identified fourteen facies that can be attributed to deposition by fluid driven, debris driven or subaerial processes. Many of these facies can be subdivided into a series of subfacies on the basis of Jackson (1976), Anderton (1985) and Dawson and Smith (2000) often reflecting different energy levels of essentially the same process. The facies and subfacies are described below and then grouped by the dominant transport process and then grouped into ten facies associations (Section 4.4).

4.1 Fluid flow facies

Within the Ghaggar-Hakra Formation, ten facies have been identified that are the product of sediment transport and deposition by Newtonian flows (Table 4.1).

Facies code	Facies	Subfacies code	Description	Interpretation	Figure number
G	Grain-supported conglomerates	Gg Gc	Pebble grade (52 mm), poorly sorted sediment. Pebbles – rounded. Structures – erosional surfaces, grading and crude foresets Grading of pebbles and occasional rip-up clasts Indistinct foresets with graded clasts and reactivation surfaces	Unconfined flow regime, migration of dune-scale bedforms	4.1
Stx	Trough cross-bedded sandstone	Stxc Stxm Stxf	Fine- to coarse-grained, well to moderately sorted, rounded to sub-angular sediment, clasts (22 mm), trough cross-bedding and erosional surfaces Coarse-grained quartz-arenites Medium-grained quartz-arenites Fine-grained quartz-arenites	Migration of sinuous crested dune-scale bedforms in the lower-flow regime	4.2
Sx	Cross-bedded sandstone	Sxc Sxm Sxf	Fine- to coarse-grained, well sorted, sub-rounded grains, clasts (50 mm), cross-bedding, channel structures, reactivation and erosional surfaces Coarse-grained quartz-arenites Medium-grained quartz-arenites Fine-grained quartz-arenites	Migration of straight crested dune-scale bedforms in the lower-flow regime	4.3
Sb	Parallel-bedded sandstone	Sbc Sbmf Sbvf	Very-fine- to coarse-grained, well to moderately sorted, sub-rounded to angular sediment, clasts (22 mm). There are parallel beds, indistinct ripples and trace fossils Coarse-grained quartz-arenites Fine- to medium-grained quartz-arenites Very fine-grained quartz-arenites	Non- or partially-confined flow events within the upper-flow regime	4.4
Sm	Massive sandstone	Smc Smm Smf	Fine- to coarse-grained, moderately sorted, sub-rounded, massive sands Coarse-grained quartz-arenites Medium-grained quartz-arenites Fine-grained quartz-arenites	Rapid deposition from suspension	4.5
Im	Massive siltstone		Massive siltstone	Rapid deposition from suspension	4.6
Sla	Low angle cross-bedded sandstone	Slac Slam Slaf	Fine- to coarse-grained sands, moderately sorted, sub-rounded to sub-angular grains, low-angle cross-bedding Coarse-grained quartz-arenites Medium-grained quartz-arenites Fine-grained quartz-arenites	Dune-scale bedforms in the lower-flow regime, perpendicular to flow	4.7

Sr	Rippled sandstone		Very fine- to fine-grained, well sorted, sub-rounded grains, rippled	Ripple-scale bedforms in the lower-flow regime	4.8
Scl	Cross-laminated sandstone	Sclf Sclvf	Fine-grained sands, well sorted, sub-angular sediment with cross-lamination Fine-grained quartz-arenites Very fine-grained quartz-arenites	Ripple-scale bedforms in the lower-flow regime	4.9
Sh	Horizontally-laminated sandstone	Shm Shf	Very fine- to medium-grained sands, moderately sorted, sub-angular to angular grains. Main structures are: horizontal laminations Medium-grained sublithic-arenites Fine-grained sublithic-arenites	Low amplitude, long wavelength bedforms in the upper flow regime	4.10
M	Matrix-supported Conglomerates	Mg Mc	<27 cm boulders, matrix-supported Graded Indistinct cross-beds	Gravity driven debris flows within a partially / non-confined environment	4.11
Sp	Pedogenic Sandstone		Mottled red and white, has a pedogenic nature and rhizoliths	Soil formation and associated bioturbation	4.12
Ip	Pedogenic		Mottled red and white, pedogenic nature, soil slickenlines, fractures root traces and rhizoliths.	Soil formation and associated bioturbation	4.13
Ihe	Haematitic siltstones		Mottled red and white, has a pedogenic nature, haematitic	Soil formation and associated bioturbation	4.14

Table 4.1: Fluid, debris flow and subaerial facies and subfacies of the Ghaggar-Hakra Formation

*4.1.1 Grain-Supported Conglomerate; **G***

Description: The G facies deposits (Figure 4.1, Table 4.1) are white to grey and brown, with granule- to upper pebble-grade (≤52 mm) clasts. The clasts are moderately to poorly sorted, sub-rounded with a moderate sphericity and composed of quartz and occasionally basaltic fragments. The facies is clast-supported with a subordinate matrix that, where present, is very fine-grained, sub-rounded and composed of quartz grains. The facies is generally massive; however there are erosional surfaces and indistinct foresets (≤30 cm high). This facies is present within all the sandstone successions of the Ghaggar-Hakra Formation (Figure 3.7) and accounts for 35% of the Darjaniyon-ki Dhani Sandstone, 5% of the Sarnoo Sandstone and 17% of the Nosar Sandstone, respectively.

Two subfacies can be observed:

- *Grain-Supported Conglomerates, Graded; **Gg**:* The clasts within this subfacies are normally graded. There are intermittent rip-up clasts, up to 1 m in height and width and are composed of silt- to very fine-grained sandstone and display remnant sedimentary structures such as parallel laminations.
- *Grain-Supported Conglomerates, Indistinct Cross-bedded; **Gc**:* Gc subfacies contains indistinct foresets up to 5 cm thick with clasts that line the foresets. There are no consistent sets or cosets within.

Interpretation: The grain-supported conglomerate facies are likely to represent deposition within confined / unconfined fluid flow, via rapid deposition as evidenced by the indistinct foresets (Svendsen *et al.,* 2003). The pebble-grade clasts, rip-up clasts and erosional surfaces represent high-energy deposits and reworking of local sediment (Bordy *et al.,* 2004) most likely to be the M facies (Section 4.2.1). The normally graded clasts upon the foresets of the Gc subfacies are deposited through grainflow (Hillier, 2002) and this, along with the indistinct foresets, indicates some migration of dune-scale bedforms.

Grain-Supported Conglomerates; G

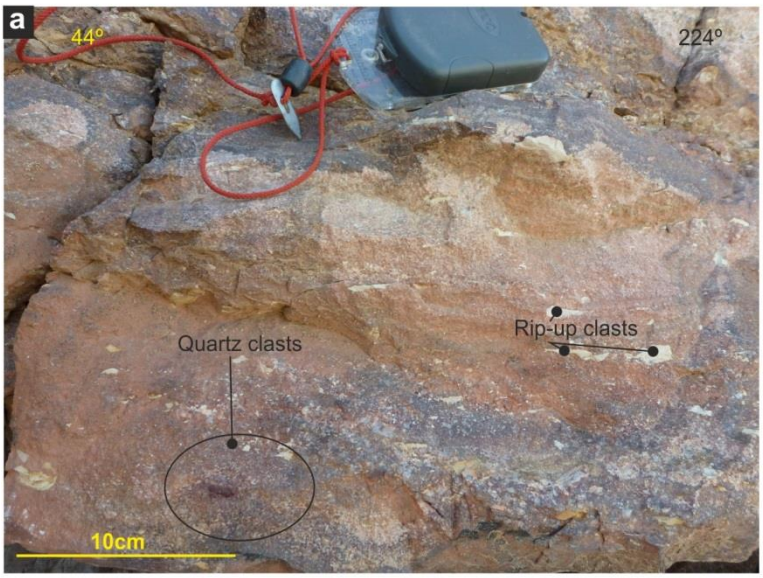

Description

Colour - white to brown

Grainsize - pebble-grade

Texture - moderately to poorly sorted, subrounded

Structures - erosional surfaces, normal grading and crude foresets

Subfacies

Subfacies - Gg

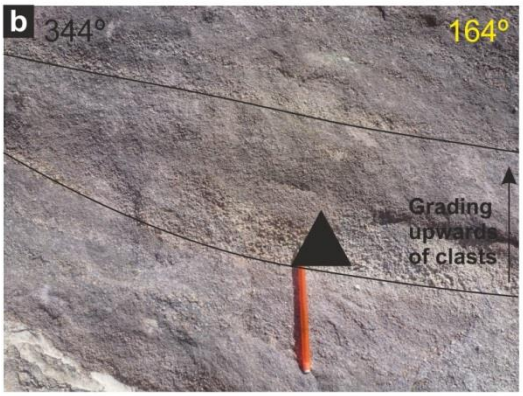

Key features - Graded clasts, rip-up clasts

Subfacies - Gc

Key features - Crude foresets

Interpretation - Reworked local sediment within a high energy, confined fluid flow.

Location - All

Succession - All minus the Siltstone successions

Figure 4.1: Summary of representative texture and structure for the grain-supported conglomerate facies; G, (a) evidence of quartz clasts and rip up clasts within the G facies (UTM 0777247, 2841083) (b) displaying confirmation of graded clasts (UTM 0777865, 2841891) and (c) evidence of indistinct cross-bedding (UTM 0777865, 2841891).

4.1.2 Trough Cross-Bedded Sandstone; ***Stx***

Description: Stx facies (Figure 4.2, Table 4.1) is composed of white to grey and pale red, coarse- to fine-grained quartz grains, which are well to moderately sorted, rounded to sub-angular and have a low to high sphericity. There are very occasional quartz clasts up to 22 mm and are rounded to sub-rounded with a high sphericity. Trough cross-beds have a foreset thickness of approximately 5 cm, which can contain quartz pebbles lining the bottom of the foreset. The foresets are arranged into sets (25 cm thick) exhibiting subcritical climb. These sets form cosets (1 m) that are regular and consistent and there is incision into the underlying units along the bottom boundary of the cosets. This facies is dominant within the Nosar Sandstone at 15% and limited within the Sarnoo Sandstone (5%).

Three subfacies are recognised by dominant sand grainsize:

- *Trough Cross-Bedded Coarse-Grained Sandstone*; **Stxc**
- *Trough Cross-Bedded Medium-Grained Sandstone*; **Stxm**
- *Trough Cross-Bedded Fine-Grained Sandstone*; **Stxf**

Interpretation: The Stx facies represents migration of sinuous-crested dune-scale bedforms (Haszeldine, 1983; Bordy *et al.,* 2004) within a confined subaqueous fluid-flow. The Stxf subfacies displays a lack of incision along the lower boundary of the cosets, suggesting less turbulent water and therefore less energy than the deposits of Stxc and Stxm subfacies. This is suggestive of variable turbulence within the lower-flow regime (Miall, 1977; North and Taylor, 1996). Subcritical climbing of the sets suggests there is a low sediment yield. The quartz clasts within the facies suggest local reworking of facies G or M (Sections 4.1.1, 4.2.1).

Trough Cross-bedded Sandstone Facies - Stx

Description

Colour - Grey to pale red

Texture - Well to moderately sorted, rounded to subangular

Structures - Trough cross -bedding and erosional surfacues

Subfacies

Subfacies - Stxc

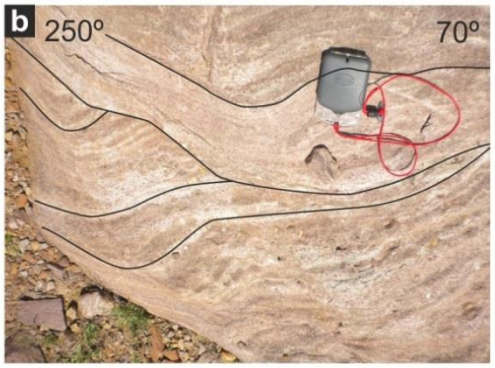

Grainsize - Coarse-grained quartz-arenites

Subfacies - Stxm

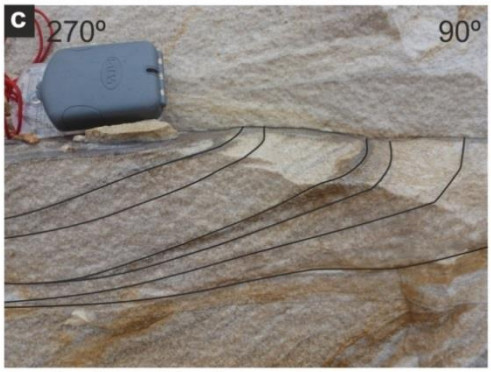

Grainsize - Medium-grained quartz-arenites

Subfacies - Stxf

Grainsize - Fine-grained quartz-arenites

Interpretation - Migration of sinuous crested bedforms within a confined fluid flow

Location - Nosar Hills

Succession - Nosar Member

Figure 4.2: Summary of representative texture and structure for the trough cross-bedded sandstone facies; Stx, (a - d) display evidence of trough-cross bedded sandstone (a) UTM 0778735, 2842021; (b) UTM 0778591, 2842109; (c) UTM 0777666, 2841371; and (d) UTM 0777181, 2841039.

*4.1.3 Planar Cross-Bedded Sandstone; **Sx***

Description: The sandstones of the Sx facies (Figure 4.3, Table 4.1) are white to grey, coarse- to fine-grained quartz-arenites. The facies is well to moderately sorted, rounded to sub-angular, with a moderate sphericity. There are quartz clasts ≤50 mm which are rounded with a high to low sphericity. The deposits are heavily cemented with calcite. The dominant sedimentary structures are planar cross-bedding with foresets with a thickness of approximately 5 cm. Set packages are on the order of 30 cm and illustrate subcritical climb. The cosets are up to 95 cm in height, have erosive bases and are generally consistent. The clasts are dominantly on the foresets that are along the lower boundary of the cosets, and can be normally graded in places. There are symmetrical, asymmetrical ripples towards the upper boundaries of the cosets. Other sedimentary structures include small channel-shaped structures up to 9 cm in width and 5 cm high. Less frequent sedimentary structures include reactivation surfaces, muddy rip-up clasts (up to 11.7 cm by 7.2 cm), soft-sediment deformation (slumps or / and load and flame structures) and tree fragments. There can be a purple discolouration. This facies is within all the sandstone successions, constituting 10% of the Darjaniyon-ki Sandstone, 15% of the Sarnoo Sandstone and up to 30% of the Nosar Sandstone.

The Sx facies consists of three subfacies recognised by different grainsizes:

- *Cross-Bedded Coarse-Grained Sandstone; **Sxc**:* The deposits are poorly sorted. This subfacies contains distinct packages of quartz clasts, which are up to 11 cm thick, along set bounding surfaces.
- *Cross-Bedded Medium-Grained Sandstone; **Sxm***
- *Cross-Bedded Fine-Grained Sandstone; **Sxf***

Cross-bedded Sandstone Facies - Sx

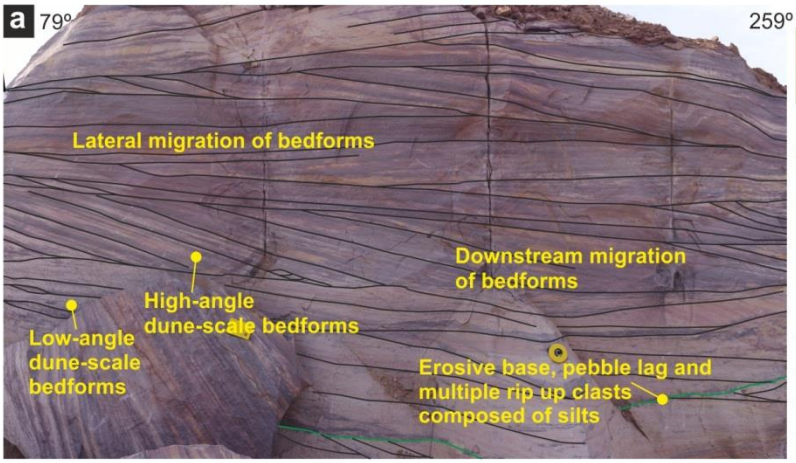

Description

Colour - Grey to grey

Texture - Well to moderately sorted, rounded to subangular

Structures - Cross -bedding reactivation and erosional surfaces and channel structures

Subfacies

Subfacies - Stxc

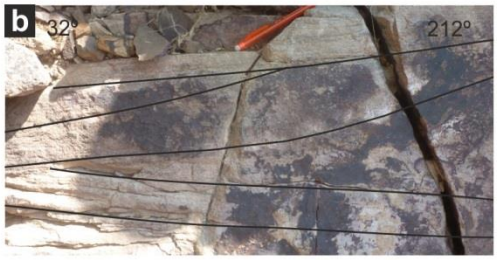

Grainsize - Coarse-grained quartz-arenites

Key features - Clast layers up to 11 cm

Subfacies - Stxm

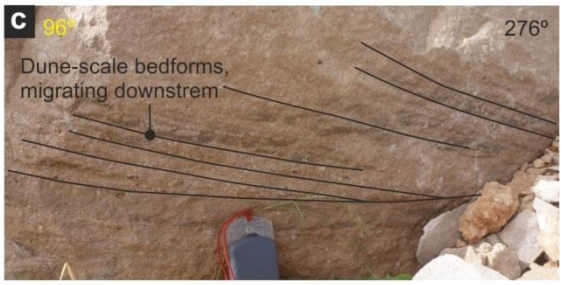

Grainsize - Medium-grained quartz-arenites

Subfacies - Stxf

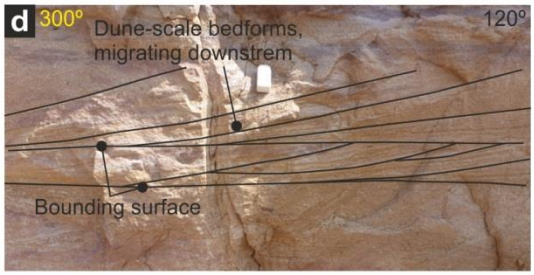

Grainsize - Very fine- to fine-grained sandstone

Interpretation - Migration of straight crested bedforms within a confined fluid flow

Location - All

Succession - Whole succession

Figure 4.3 Summary of representative texture and structure for the planar cross-bedded sandstone facies; Sx, (a - d) display evidence of planar cross-bedded sandstone (a) UTM 0782621, 2853326; (b) UTM; (c) UTM; and (d) UTM.

Interpretation: The Sx facies represents the migration of straight-crested duneforms (Miall, 1977, 1985) within a confined fluid flow, under lower flow regime conditions (Miall, 1977, 1985; Ghazi and Mountney, 2009). The cosets, with large clasts along erosional lower boundaries suggest incision and high energy. The rippled upper boundary of the cosets suggests a waning flow throughout the coset deposition. Subcritical climbing of the sets suggests there is a low sediment yield. The soft-sediment deformation is due to low shear strength within water-logged sediments causing slumping and from rapid deposition causing load casts and flame structures (Collinson *et al.,* 2006). The quartz clasts are from the reworking of facies G and M (Sections 4.1.1, 4.2.1), where normal grading occurs the deposition occurred through grainflow (Hillier, 2002). The purple discolouration is from post depositional water percolation.

4.1.4 Parallel-Bedded Sandstone: ***Sb***

Description: The deposits of the Sb facies (Figure 4.4, Table 4.1) have a white to pale brown and are coarse- to fine-grained quartz-arenites. The facies can both coarsen and fine upwards over multiple beds. The facies is moderately to well sorted, sub-rounded to angular and has a moderate sphericity. The quartz clasts vary in size from 5 mm to 22 mm they are rounded to sub-angular and have a high to low sphericity. The main sedimentary structure is parallel bedding, in beds that range in thickness from 3 – 70 cm. The facies can contain indistinct and partially restricted foresets and erosional surfaces. There are indistinct ripples (2 mm high and 60 mm wavelength) structures near the top of the facies within the Sarnoo Sandstone. This facies is mainly noted within the Sarnoo Sandstone (18%) where meniscate backfill trace fossils are prominent at the top of the facies and occasionally towards the top of the Nosar Sandstone (5%).

Parallel-bedded Sandstone Facies - Sb

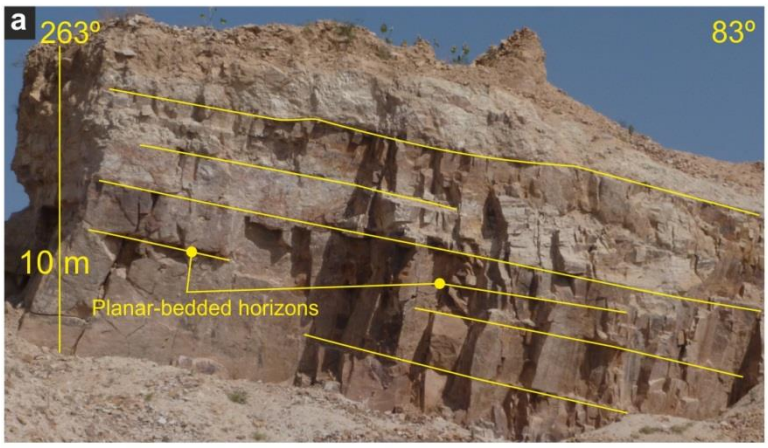

Description

Colour - White to pale brown

Texture - Well to moderately sorted, subrounded to angular

Structures - Parallel -bedding

Subfacies

Subfacies - Sbc

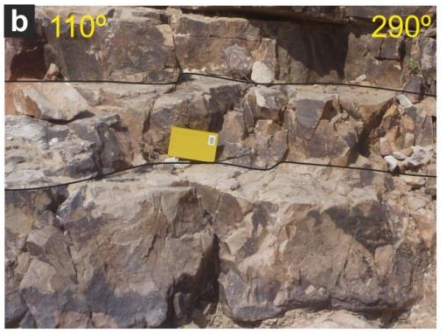

Grainsize - Coarse-grained quartz-arenites

Subfacies - Sbmf

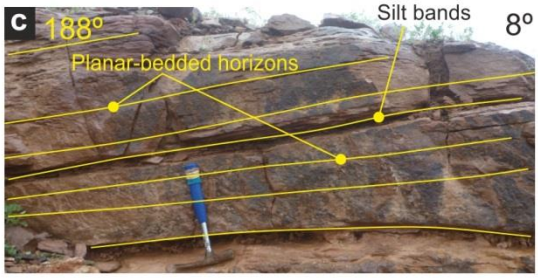

Grainsize - Medium- to fine-grained quartz -arenites

Subfacies - Sbvf

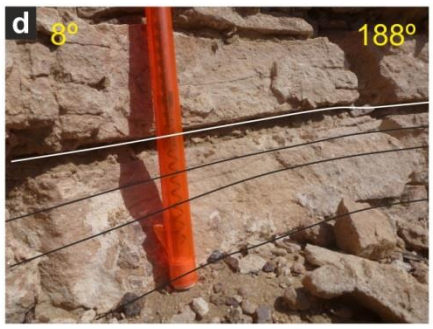

Grainsize - Very fine-grained quartz-arenites

Interpretation - Partially / non-confined fluid flow events, within the upper flow regime

Location - All **Succession** - Top of the Sarnoo and Nosar Sandstone

Figure 4.4: Summary of representative texture and structure for the parallel bedded sandstone facies; Sb, (a - d) displaying evidence of parallel bedding (a) UTM 0782621, 2853326; (b) UTM 0777598, 2840794; (c) there can be silt horizons interbedded with the sandstone beds, UTM 0782659, 2852890; and (d) UTM 0777786, 2840926.

Three subfacies are recognised:

- *Parallel-Bedded Coarse-Grained Sandstone*; **Sbc**
- *Parallel-Bedded Medium- to Fine-Grained Sandstone*; **Sbmf**
- *Parallel-Bedded Very Fine-Grained Sandstone*; **Sbvf**

Interpretation: The deposits of the parallel bedded facies are likely to represent non- or partially-confined flow events (Tunbridge, 1981) within the upper flow regime. The grainsize distribution throughout the facies indicates turbulence within the fluid flow. Clasts are reworked from the G or M facies (Sections 4.1.1, 4.2.1). The indistinct ripple-scale bedforms indicate a waning flow from the upper-flow regime into the lower-flow regime. Trace fossils colonisations suggest quiescence periods within deposition.

*4.1.5 Massive Sandstone; **Sm***

Description: The deposits of the Sm facies (Figure 4.5, Table 4.1) are red and grey to brown sublithic-arenites. The grainsize varies from coarse- to fine-grained sands which are moderately sorted, sub-rounded and moderately spherical. Clasts are up to 19 mm in diameter which are rounded and have a low sphericity. The sediments can be normally and reverse graded. This facies constitutes 10% of the Darjaniyon-ki Dhani Sandstone, 2% of the Sarnoo sandstone and 4% of the Nosar Sandstone.

The Sm facies varies in sand grainsize:

- *Massive Coarse-Grained Sandstone*; **Smc**
- *Massive Medium-Grained Sandstone*; **Smm**
- *Massive Fine-Grained Sandstone*; **Smfs**

Interpretation: It is likely that the Sm facies was deposited rapidly from suspension within stationary waters, producing a structure-less sandstone (Jones and Rust, 1982, Banham and Mountney, 2013). This process occurs as there is a high concentration of water and sediment mix (Martin and Turner, 1998) and can lead to reverse grading.

Massive Sandstone Facies - Sm

Description

Colour - Brown

Texture - Moderately sorted, sub-rounded

Structures - Massive, normal grading and clasts

Subfacies

Subfacies - Smc

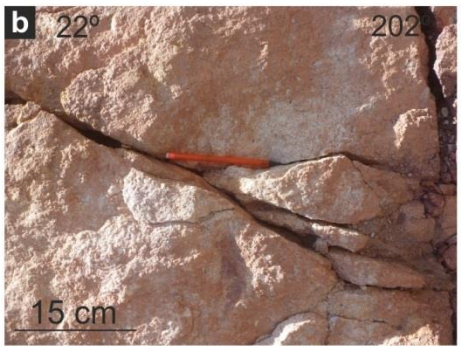

Grainsize - Coarse-grained sublithic-arenites

Subfacies - Smm

Grainsize - Medium-grained sublithic-arenites

Subfacies - Smfs

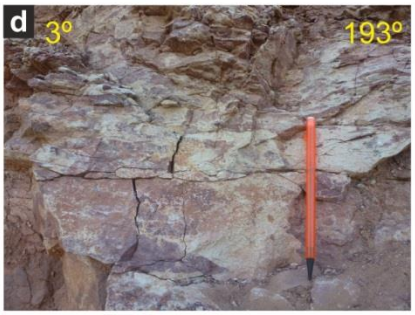

Grainsize - Very fine- to fine-grained sublithic-arenites which is mottled and is pedogeneic

Interpretation - High concentration of water / sediment mix, creating a suppressed turbulence

Location - All

Succession - All

Figure 4.5: Summary of representative texture and structure for the massive sandstone facies; Sm; (a) evidence of mottling within the Sm facies, UTM 0777543, 2840807; (b) UTM 0778635, 2842386; (c) displaying quartz pebbles (yellow circle) as part of the nature of the massive sandstone facies, UTM 0777107, 2840577; and (d) UTM 0778621, 2842360.

4.1.6 Massive Siltstone; ***Im***

Description: The Im facies (Figure 4.6, Table 4.1) is dominantly red with white mottling and composed of silt. The facies is intensely bioturbated by pedogenic processes rendering the siltstones largely structure-less. The facies is dominant within the Ghaggar-Hakra Undivided.

Interpretation: The siltstones of the Im facies were deposited through gravitational settling of the sediment within stationary waters. All primary bedding structures have been destroyed due to pedoturbation.

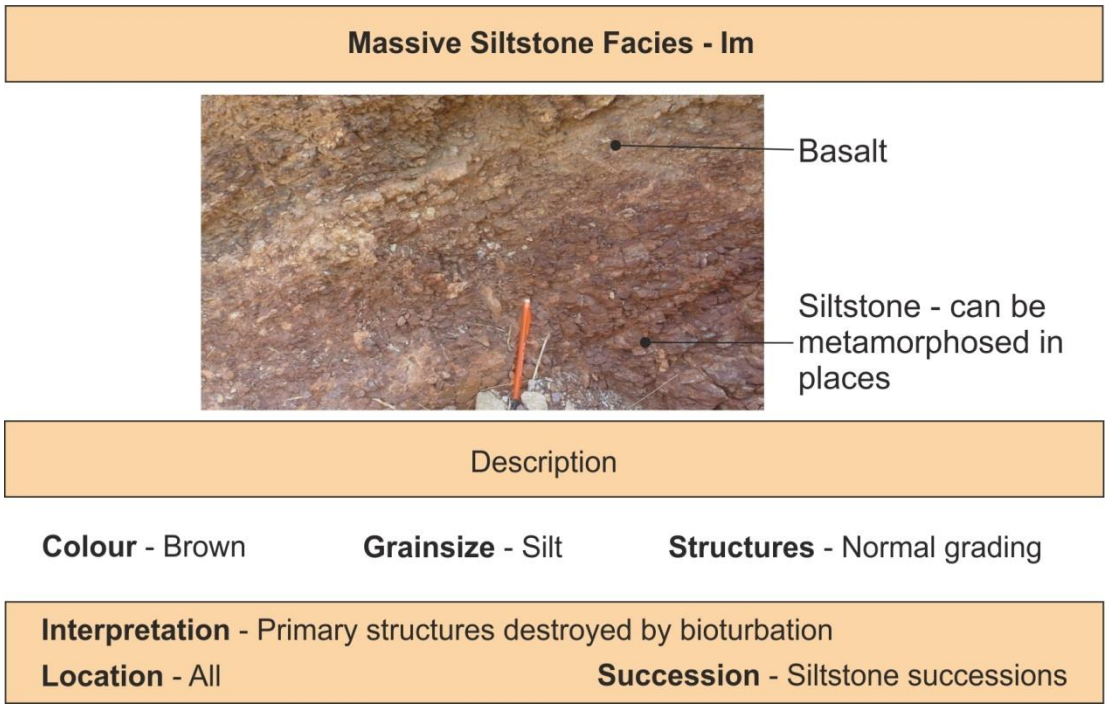

Figure 4.6: Summary of representative texture and structure for the massive siltstone facies; Im; UTM 0777181, 2841039

4.1.7 Low-Angle Cross-Bedded Sandstone; ***Sla***

Description: Sla facies (Figure 4.7, Table 4.1) is white to grey quartz-arenites. The quartz grains are coarse- to fine-grained, moderately sorted, sub-rounded with a high to moderate sphericity. The dominant sedimentary structures are low-angle cross-beds with foresets approximately 10 cm thick, arranged into sets 75 cm high and coset packages up to 2 m in thickness. The lower boundaries of the cosets are commonly erosive. Their

upper boundaries of the cosets can be eroded into by the Stx or Sx facies, making them incomplete. On the upper boundaries of the cosets the grainsize can become very fine-grained and there are meniscate trace fossils within the facies. This facies is dominant within the Sarnoo Sandstone (22%) and rarely within the Nosar Sandstone (5%).

There are three variations on sand grainsize:

- *Low-Angle Cross-Bedded Coarse-Grained Sandstone*; **Slac**
- *Low-Angle Cross-Bedded Medium-Grained Sandstone*; **Slam**
- *Low-Angle Cross-Bedded Fine-Grained Sandstone*; **Slaf**

Interpretation: The Sla facies represents cross-flow migration of sandy dune-scale bedforms (Jackson, 1976) that are laterally accreting (Ielpi and Ghinassi, 2014). The trace fossil colonisations suggest frequent pauses in sedimentation rate.

4.1.8 Rippled Sandstone; ***Sr***

Description: Sr facies (Figure 4.8, Table 4.1) is white to red; the quartz-arenites are fine- to very fine-grained, well sorted, rounded to sub-angular with a moderate sphericity and are variably micaceus. There are two types of ripples noted here, wave ripples and current ripples. Commonly noted are sinuous-crested wave ripples which are up to 5 mm high with a wavelength up to 55 mm, a set height of 10 cm and a maximum Ripple Index (RI) of 11. Current ripples are up to 10 mm in height with a wavelength up to 60 mm, set height of 5 cm and a RI of 6. There is ripple cross-lamination where the sets subcritically climb at 5° however, in the Sarnoo Sandstone, supercritcal climbing averages at 15° but the highest angle is at 29°. The sets of ripples are separated by mud drapes. Occasionally the facies is intensely weathered. Interference ripples are rarely preserved. This facies is in the Sarnoo (15%) and Nosar (7%) sandstones and within the siltstone successions (5%).

Low-Angle Cross-Bedded Sandstone Facies - Sla

Description

Colour - White to grey

Texture - Moderately sorted, subrounded

Structures - Low-angle cross-beds

Subfacies

Subfacies - Slac

Grainsize - Coarse-grained quartz-arenites

Subfacies - Slam

Grainsize - Medium-grained quartz-arenites

Subfacies - Slaf

Grainsize - Fine-grained quartz-arenites

Interpretation - Dune-scale bedforms laterally migrating, perpendicular to flow

Location - All locations

Succession - Entire succession

Figure 4.7: Summary of representative texture and structure for the low-angle cross-bedded facies, Sla; (a – d) display evidence of low-angle cross-beds; (a) UTM 0778271, 2842071; (b) UTM 0783234, 2853298; (c) UTM 0777865, 2841981; and (d) UTM 0777898, 2840794.

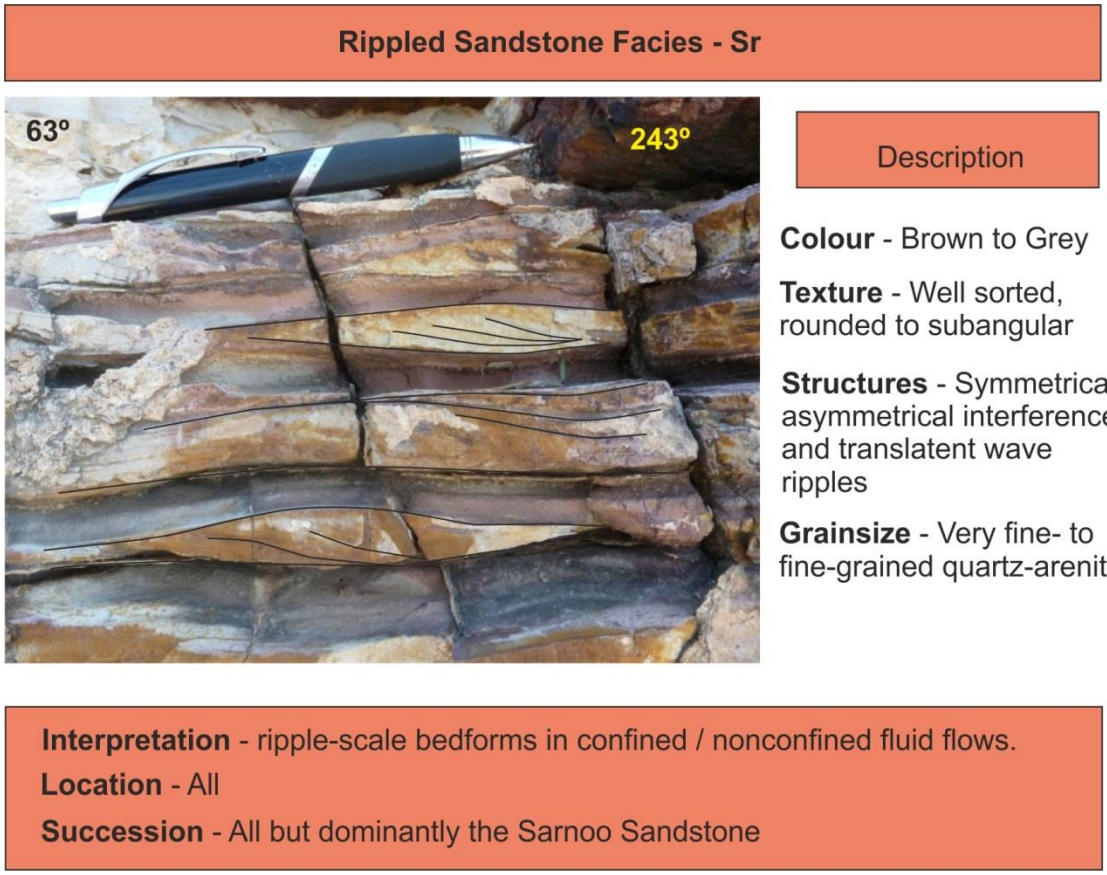

Figure 4.8: Summary of representative texture and structure for the rippled sandstone facies, Sr; UTM 0778635, 2842386

Interpretation: The Sr facies represents the migration of ripple-scale bedforms within the lower flow regime (Miall, 1977; North and Taylor, 1996). The sinuous wave ripples are formed due to wind-driven oscillations within a shallow water body, creating a migration of sinuous-crested ripple-scale bedforms. Current ripples are formed within shallow waters with a unidirectional flow. All types of ripples require lower flow regime conditions. Subcritical climbing of the sets suggests there is a low sediment yield, whereas superclimbing of sediment is suggestive of a high sediment yield (Hunter, 1977a, b). The mud drapes in-between the rippled sets are indicative of deposition of suspended load in shallow waters. Interference ripples suggest a wind influence is modifying ripple formation in very shallow water.

4.1.9 Cross-Laminated Sandstone; ***Scl***

Description: The Scl facies (Figure 4.9, Table 4.1) is red and grey which are fine- to very fine-grained quartz-arenites. The quartz grains are well sorted, sub-angular and have a high to moderate sphericity. The dominant sedimentary structure is planar cross-lamination. The laminations have a thickness of 0.7 cm. The sets have a subcritical climb at approximately 10°. This facies accounts for 10% of the siltstone successions.

There are two subfacies separated by sands grainsize:

- *Cross-Laminated Fine-Grained Sandstone*; **Sclf**
- *Cross-Laminated Very Fine-Grained Sandstone*; **Sclvf**

Interpretation: The deposits of the cross-laminated facies were deposited within both confined and unconfined fluid flows, under lower-flow regime conditions. These ripple-scale bedforms are migrating. Subcritical climb states there is a low sediment yield.

4.1.10 Horizontally-Laminated Sandstone; ***Sh***

Description: Sh facies is white to grey and red and a sublithic-arenite (Figure 4.10, Table 4.1). The grains are medium- to fine-grained, moderately sorted, sub-rounded to angular, with a varying sphericity. The main structures are horizontal laminations up to 9 mm in thickness. There is minor slumping noted. This facies accounts for 10% of the Darjaniyon-ki Dhani Sandstone, 4% of the Sarnoo Sandstone, 7% of the Nosar Sandstone and 5% of the siltstone successions.

Subfacies of various sand grainsize:

- *Horizontally-Laminated Medium-Grained Sandstone*; **Shm**
- *Horizontally-Laminated Fine-Grained Sandstone*; **Shf:** There are quartz clasts which are 1 - 2 mm, rounded and highly spherical.

Cross-Laminated Sandstone Facies - Scl

Description

Colour - Red to grey

Texture - Well sorted, subangular

Structures - Cross-lamination, symmetrical ripples

Subfacies

Subfacies - Sclf

Grainsize - Fine-grained quartz-arenites

Subfacies - Sclvf

Grainsize - Very fine-grained quartz-arenites

Interpretation - Ripple-scale bedforms migrating downstream within a confined fluid flow

Location - Sarnoo and Karentia hills **Succession** - Siltstone successions

Figure 4.9: Summary of representative texture and structure for the cross-laminated sandstone facies, Scl; (a – c) display evidence of cross-laminations; (a) UTM 0783859, 2853121; (b) UTM 0777110, 2840592; (c) UTM 0777181, 2841039.

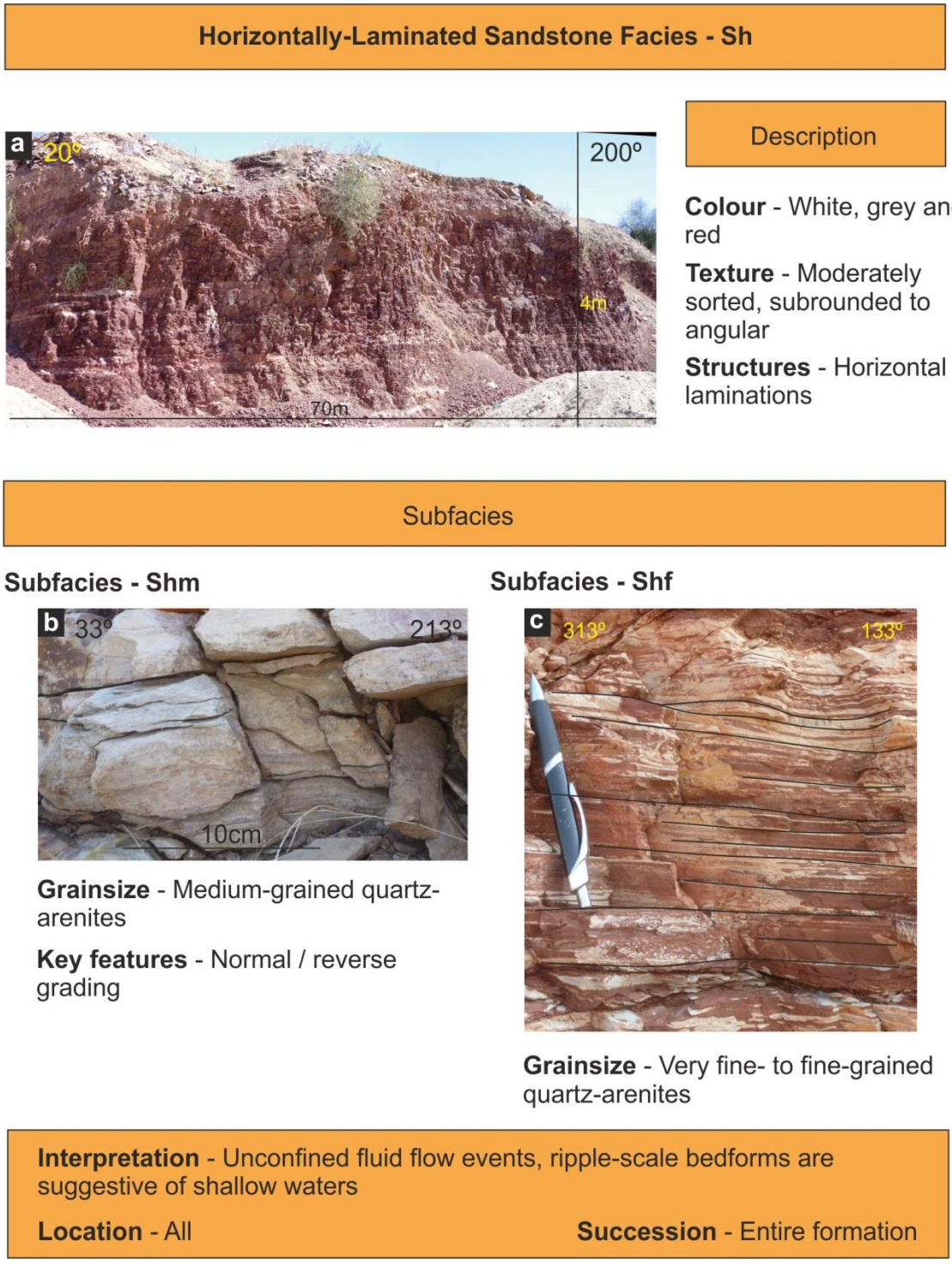

Figure 4.10: Summary of representative texture and structure for the horizontally-laminated sandstone facies, Sh; (a) evidence of mottling within the Sh facies UTM 0781500, 2846100; (b) UTM UTM 0777110, 2840592, and; (c) UTM 0783727, 2853017.

Interpretation: The horizontally-laminated facies was deposited within the upper flow regime conditions (Ghazi and Mountney, 2009) where a high flow velocity and shallow waters are needed. The sedimentary structures are formed through flooding events. This flooding is cyclic and unconfined. Slumping within the facies is caused by low shear

strength within water-logged sediments. The quartz clasts are reworked from the local area, most likely the Stx or Sx facies (Sections 4.1.2, 4.1.3).

4.2 Debris Flow Facies

The Ghaggar-Hakra Formation displays one facies that is the product of transportation and deposition by non-Newtonian flows (Table 4.1).

*4.2.1 Matrix-Supported Conglomerates; **M***

Description: The M facies comprises white to brown and red, granule- to boulder-grade (≤27 cm) conglomerates which are poorly sorted, sub-rounded to sub-angular and have a high to moderate sphericity (Figure 4.11, Table 4.1). The conglomeratic grains are composed of quartz and lithic fragments of rhyolite or basalt. The facies is matrix-supported by very fine-grained sand and is dominantly massive, but there can be occasional indistinct cross-beds. It forms 20% of the Darjaniyon-ki Dhani Sandstone and 3% of the Nosar Sandstone.

Two subfacies, based on crude sedimentary structures:

- *Matrix-Supported Conglomerates, Graded; **Mg**:* The Mg subfacies is generally reversely graded. Very occasionally the subfacies normally graded.
- *Matrix-Supported Conglomerates Indistinct Cross-Bedding; **Mc**:* The Mc subfacies has indistinct foresets in it, which are up 1 m in height with a foreset thickness of 25 cm. There are no sets or cosets.

Figure 4.11: Summary of representative texture and structure for the matrix-supported conglomerates, M; (a) evidence of matrix supported sediment, UTM 0777865, 2841891 (b) evidence of reverse grading, UTM 0777865, 2841891 and (c) evidence of indistinct cross-bedding, UTM 0778635, 2842386.

Interpretation: The deposits of the matrix-supported conglomerate facies are formed through gravity driven debris flows (Miall, 1977; Blair and McPherson, 1994). The rhyolitic and basaltic conglomeratic grains are extraformational and from the Malani Igneous Suite or / and the Karentia Volcanic Formation. The quartz grains are reworked from local material. When the Mg subfacies is normally graded, the debris flow occurred

subaqueously. The indistinct foresets are indicative of the migration of sediment. Normal grading and indistinct cross-bedding are indicative of Newtonian fluid flow, however the matrix-supported nature of the sediment suggests non-Newtonian fluid flow, suggesting there is a high fluid content within the debris flow system accounting for the mixture of fluid and debris flow properties (Blair and McPherson, 1994; Leeder, 2011).

4.3 Subaerial Facies

The Ghaggar-Hakra Formation displays three subaerial facies which have been identified here based on their grainsize and mineralogical content (Table 4.1).

*4.3.1 Pedogenic Sandstone; **Sp** and pedogenic siltstone; **Ip***

Description: The Sp facies is mottled red and white (Figure 4.12, Table 4.1). The facies varies from fine- to very fine-grained well sorted, rounded, highly spherical quartz grains. The **Ip** facies is composed of clay- to silt-grains (Figure 4.13, Table 4.1). Both facies have a pedogenic texture with soil slickenlines and calcite filled fractures.

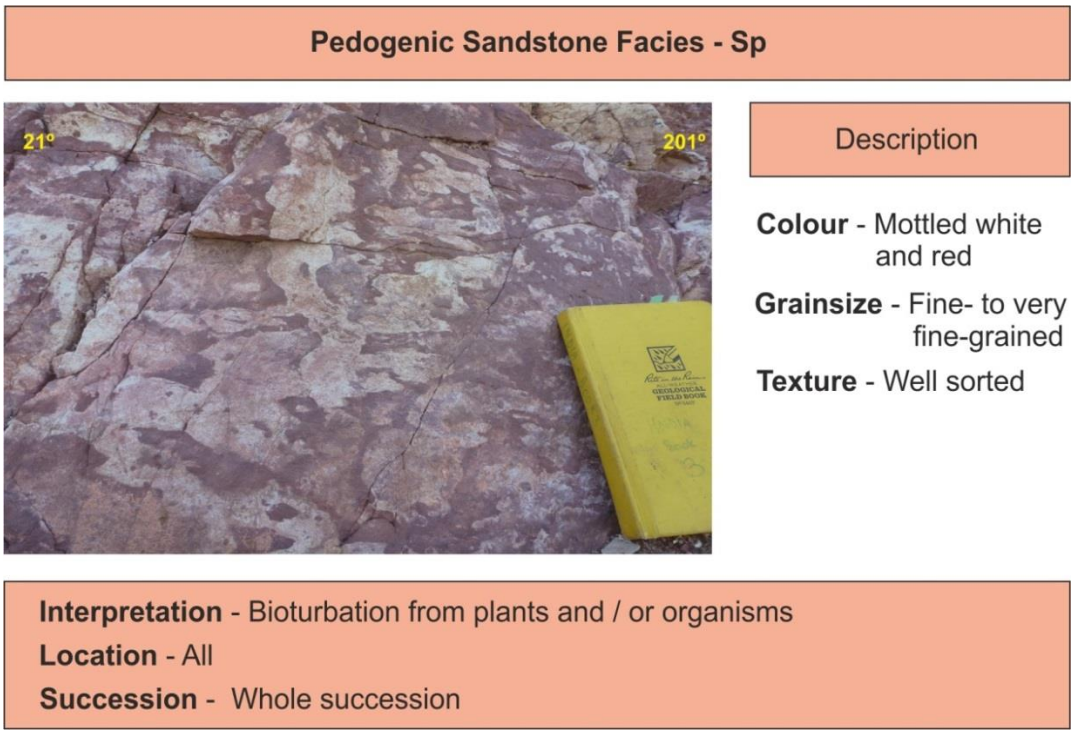

Figure 4.12: Summary of representative texture and structure for the pedogenic sandstone facies, Sp; UTM 0778635, 2842386.

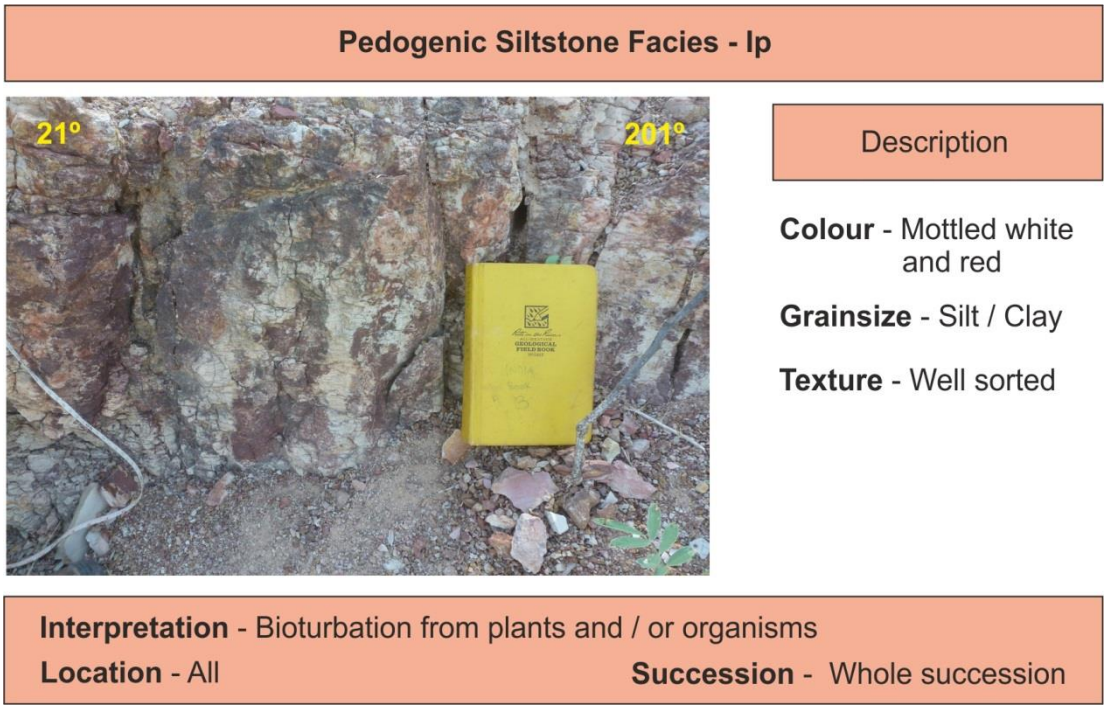

Figure 4.13: Summary of representative texture and structure for the pedogenic siltstone facies, lp; UTM 0778640, 2842381.

Interpretation: The mottled texture, fractures and roots traces are all due to the soil forming processes (Plint, 1983). Mottled colouring is from reduction and related to the draining of the soils (Simonson and Boersma, 1972).

4.3.2 Haematitic pedogenic siltstone; ***lhe***

Description: lhe facies is composed of mottled red and white sediments (Figure 4.14, Table 4.1). The facies has clay- to silt-grade sediment and there are occasional horizontal laminations. The facies has a pedogenic nature and is rich in haematite.

Interpretation: The mottled nature, fractures and roots traces are due to the soil forming processes (Plint, 1983). The haematitic nature is due to diagenesis and secondary waters, the haematite is not due to primary deposition.

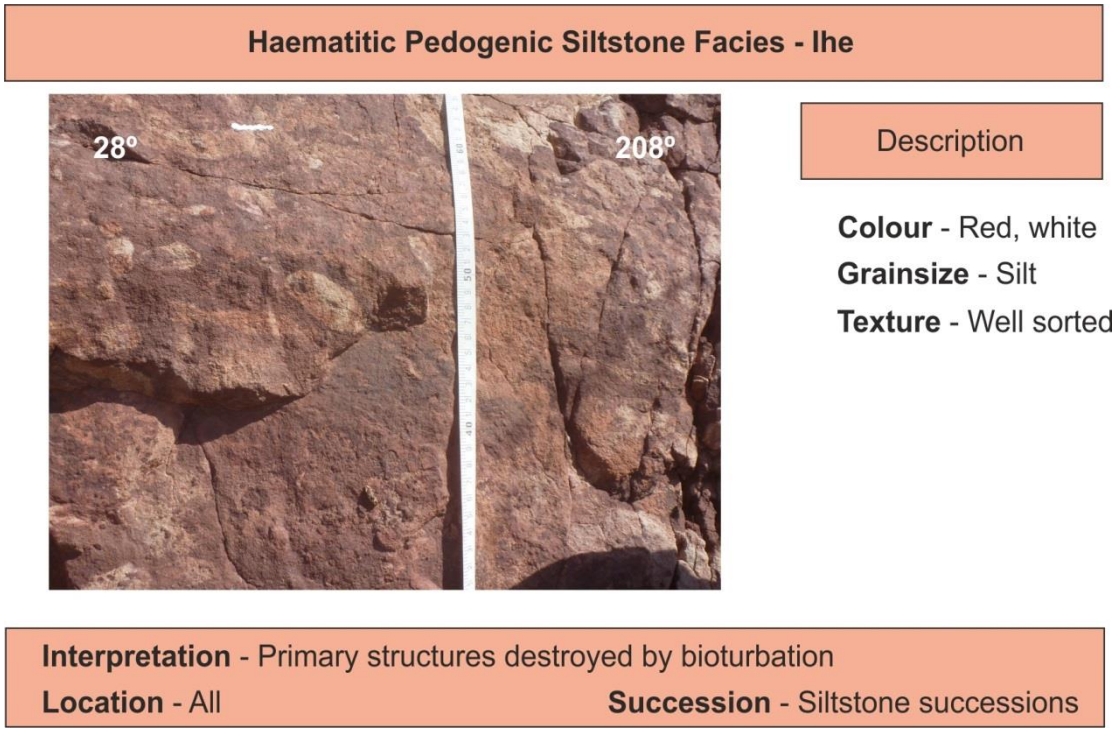

Figure 4.14: Summary of representative texture and structure for the haematitic pedogenic siltstone, lhe; UTM 0778635, 2842386.

4.4 Facies Associations

Ten facies associations have been identified that are the product of similar transport and depositional regimes, and occur together within the logged sections (Table 4.2, Figure 4.15, Appendix 1, Miall 1977; Cant 1977). There are confined environments such as channels (Cdd, Lcf, Lrf, Lfb, Lfa, Ler) and unconfined environments such as floodplain settings (Uuf, Luf, Fa, Pa).

4.4.1 Confined debris driven flow association; ***Cdd***

Description: The Cdd association relates G, M, Smc, Smf, Sh and Sr facies together (Figure 4.15). The base of the association is characterised by either the G or M facies, with Sm, Sh or Sr above. Average percentages of facies within the association are: G (or M) 50 - 90%, Sm at 20% and either Sh or Sr which varies between 30 - 10%. This association is best developed within Darjaniyon-ki Dhani Sandstone.

Association code	Association	Facies codes	Description	Interpretation	Architectural element	Figure number
Cdd	Confined debris driven flow association	G, M, Smc, Smf, Sh, Sr	G or M then Sm or Sh	Confined setting, lower flow regime	F1, F3	4.15
Uuf	Unconstricted Upper Flow Regime Association	Sbmf, G, M, Sbvf	G or M then Sb	Upper flow regime bedforms in an unrestricted setting.	F2, F3, F4	4.16
Luf	Unconfined Lower Flow Regime Association	Smm, Shf, Sr, Im, Sclf, Sclvf	Any order	Lower flow regime in an unconfined setting	F7, F8	4.17
Lcf	Confined Lower Flow Regime Association	M, Gg, Sx	M or Gc, Sx	Upper flow regime and wanes into the lower flow regime, confined flow	F2, F3	4.18
Lrf	Constricted Lower Flow Regime Association	Sx, Shm, Smm, Shf, Sr,	Sx at the bottom then any order	Lower flow regime, confined flow	F1, F2, F4, F5, F6	4.19
Lfb	In-Flow Barforms Association	Stxc, Stxm, Sxc, Sxm	Any order	Confined settings, dune-scale migrating bedforms	F1	4.20
Lfa	Laterally Accreting Barform Association	Slam, Sr, Slaf, Sxm	Any order: Sx, Sla, Sr always on top	Migration of lateral and down-stream dune-scale bedforms	F2, F5	4.21
Cuf	Confined to Unconfined Upper Flow Regime Association	Sb, Sx	At Sarnoo, Sx then Sb At Karentia / Nosar Sb then Sx	Upper flow regime and wanes into the lower flow regime, confined and unconfined settings	F7, F8	4.22
Fa	Flooding Association	Sb, Shf, Ip, Smf, Smm	Any order	Gravitional settling in stationary waters within an unconfined setting	F4, F6, F7, F8	4.23
Pa	Palaeosol Association	Ip, Sp, Ihe, Sm, Im	Any order	Primary sedimentary structures are destroyed due to bioturbation	F1, F2, F7, F8	4.24

Table 4.2: Describing the facies associations and relating them to the architectural elements seen within the Ghaggar-Hakra Formation, Architectural element key: F1 – Channel element, F2 – Channel margin element, F3 – Gravel bar element, F4 – Chute channel element, F5 – Point bar element, F6 – Sheetflood element, F7 – Floodplain element and F8 – Pond element.

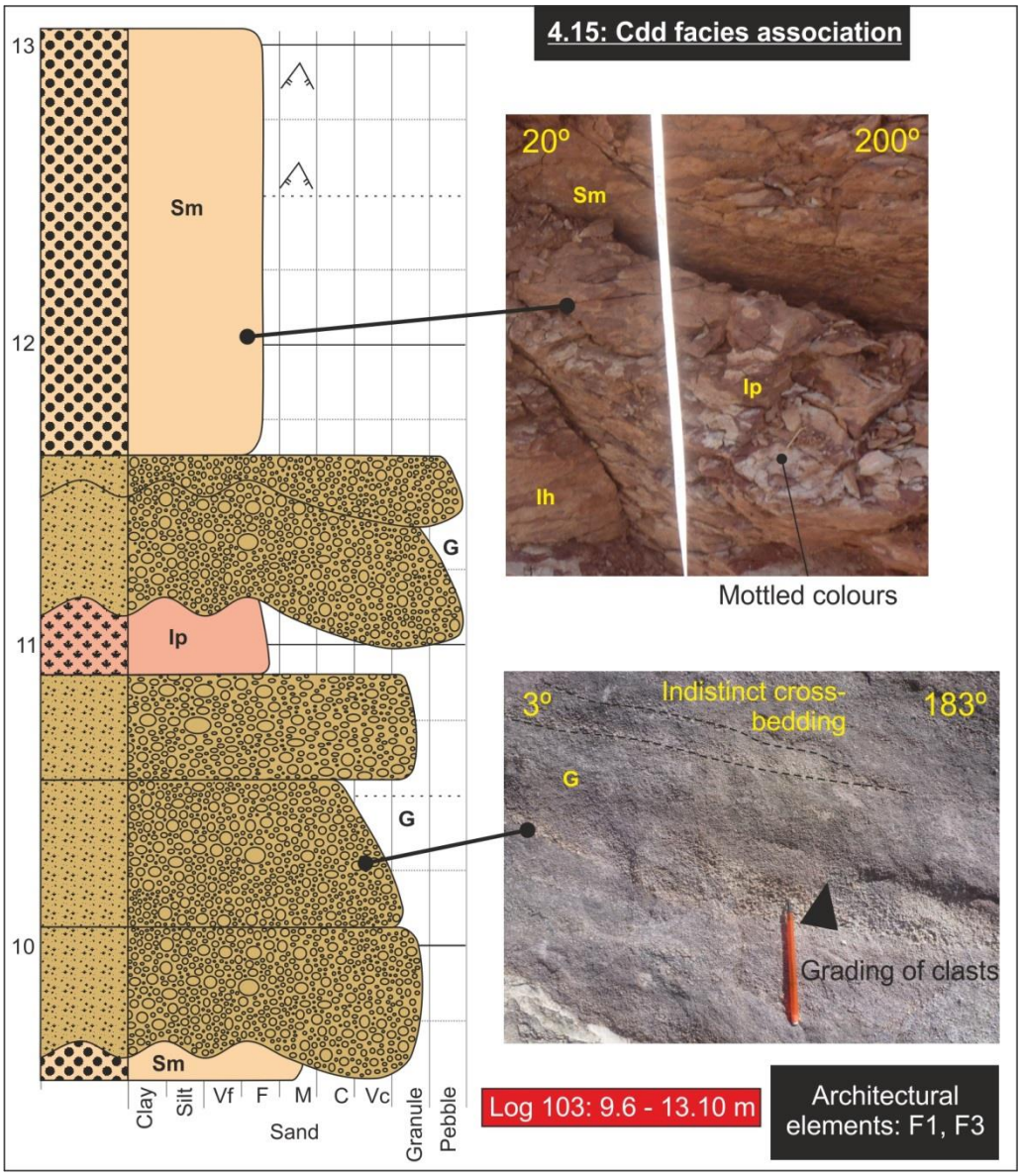

Figure 4.15: Summary of representative facies associations displaying logged data and photographs of the Cdd facies association.

Interpretation: The association was deposited within confined to partially confined, debris driven flow events. The conglomerates were deposited rapidly and likely had a waning flow towards the end of deposition. The Sm, Sh and Sr facies are within a confined flow within the lower flow regime. The deposits would have had high concentrations of water / sediment mixtures. Overall there is a waning flow.

4.4.2 Unconstricted Upper Flow Regime Association; ***Uuf***

Description: Within the Uuf association there are the M, G facies and Sbmf and Sbvf, (Figure 4.16, Table 4.2) subfacies, where M or G is overlain by the Sb facies. The G or M

facies constitutes 50%, the G facies is more common. The Sb facies forms the other 50%. The Uuf association is confined to the Sarnoo Sandstone.

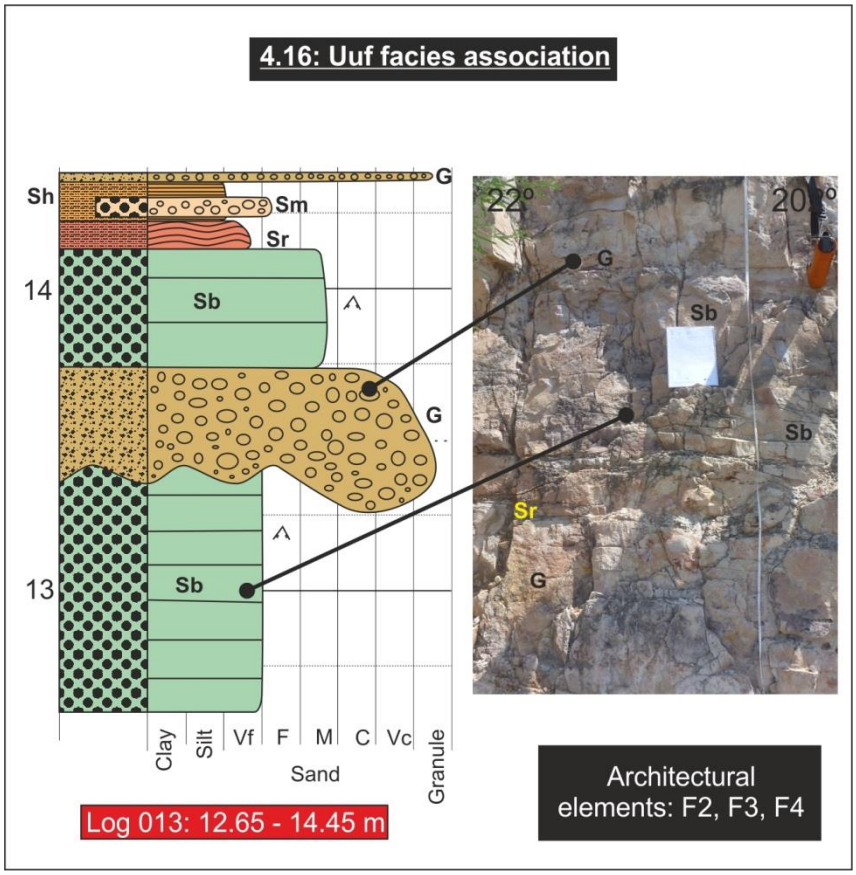

Figure 4.16: Summary of representative facies associations displaying logged data and photographs of the Uuf facies association.

Interpretation: The conglomerates and planar bedforms were deposited within cyclic unrestricted flooding events. The G or M facies here deposited is dependent upon the sediment – water mix, as the M facies represents flows with higher sediment concentrations than the G facies. The Sb facies lack of sedimentary structures indicates suppression of bedforms due to higher flow velocity's in shallower waters; indicating an unconfined area of deposition.

4.4.3 Unconfined Lower Flow Regime Association; ***Luf***

Description: The Luf association relates Smm, Im, Sclf, Sclvf, Sr, Shf, Sp and Ip facies together (Figure 4.17, Table 4.2). The Sr and Sh facies are at the base of the association,

overlain by the Sm or Im facies. Above this is the Slc facies and the association is capped by the Sp or Ip facies. The Sr and Sh constitute 40% each, the Sm / Im facies equates to 10%. The Scl facies accounts for 5% but becomes more significant in the southwest of the field areas accounting for 15% there. At the top the Sp / Ip facies forms 5% of the association. The association fines upwards. This association occurs within the siltstone successions.

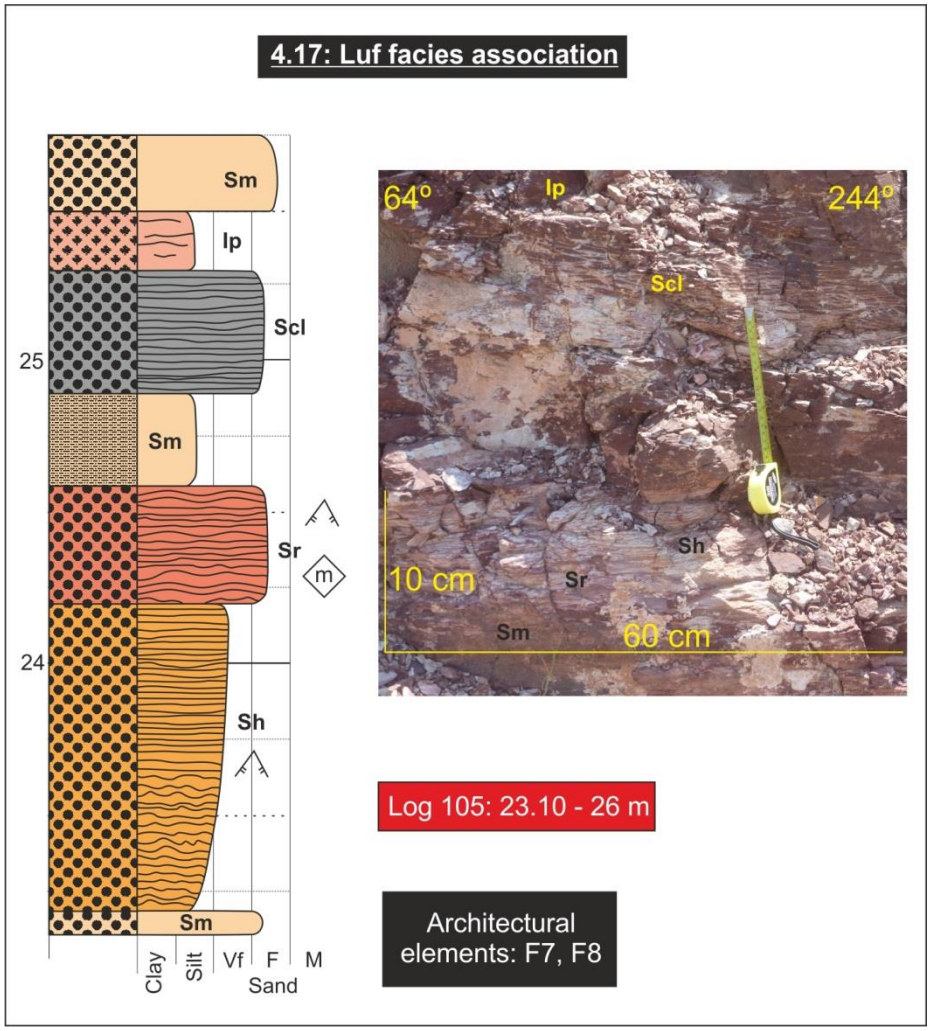

Figure 4.17: Summary of representative facies associations displaying logged data and photographs of the Luf facies association.

Interpretation: The association was deposited within unconfined shallow waters within the lower flow regime (Miall, 1977; Ghazi and Mountney, 2009) with a waning flow marked by a decrease in grainsize. There is limited bioturbation at the top of the association (Sp / Ip facies).

4.4.4 Confined Lower Flow Regime Association; ***Lcf***

Description: Lcf association relates Gc, M, and Sx facies together (Figure 4.18, Table 4.2). The facies association is split approximately 50:50 between the G or M facies and the Sx facies. Where M facies is noted it replaces the Gc subfacies. The Sx facies becomes more abundant towards the north of the field area with increased continuity within the sets and cosets. This is most common within the Nosar Sandstone.

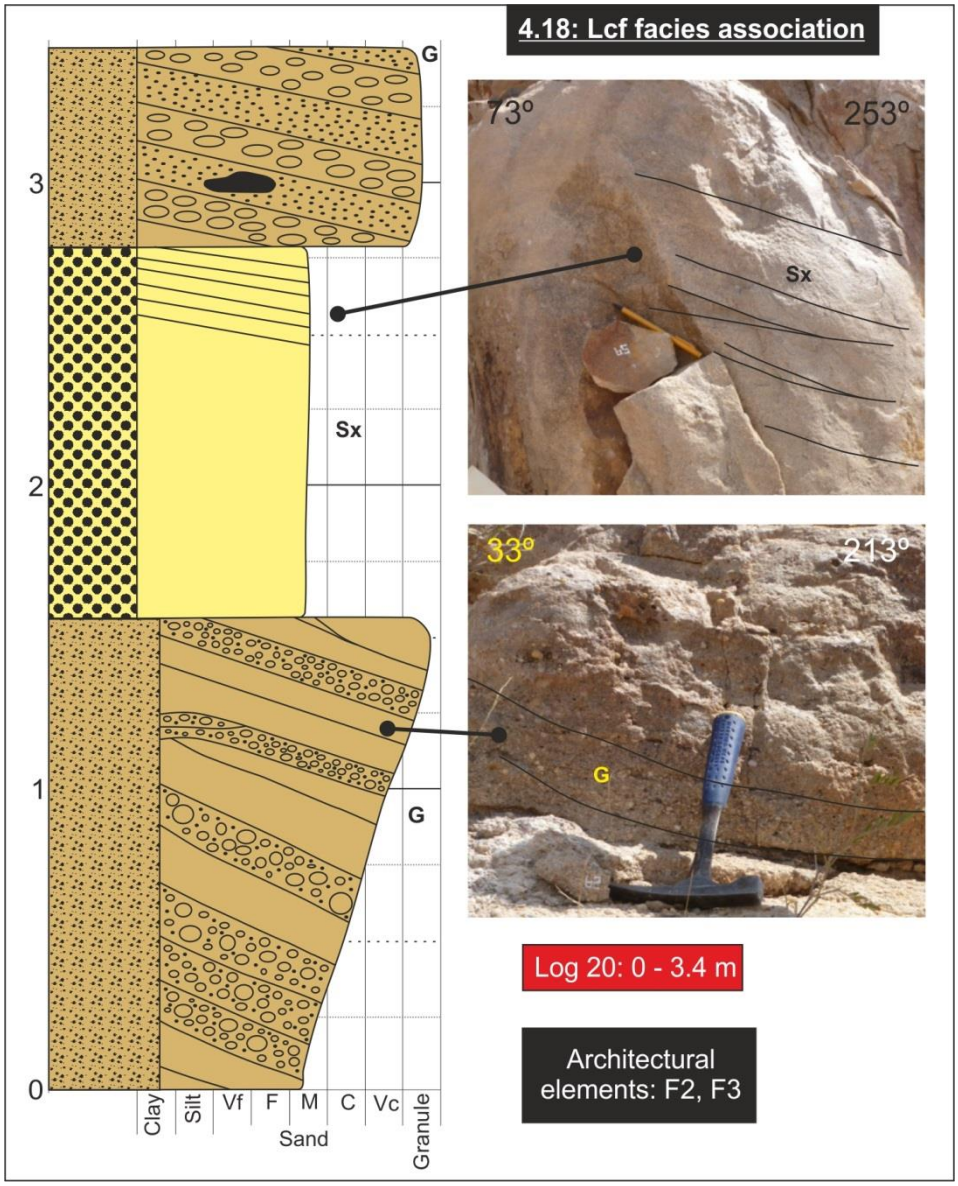

Figure 4.18: Summary of representative facies associations displaying logged data and photographs of the Lcf facies association.

Interpretation: The sediments within the Lcf association were deposited within a confined fluid flow environment, exhibiting a waning flow. Cross-bedding within indicates migration of the dune-scale bedforms.

4.4.5 Constricted Lower Flow Regime Association; ***Lrf***

Description: Lrf facies association relates Sxm, Shm, Smm, Sr and Shf subfacies together (Figure 4.19, Table 4.2). Lrf association starts with Sxm subfacies (55%) which is overlain by Smm or Sr or Shf (45%). Occasionally Smm, Shf and Sr are missing leaving only Sxm and Sh forming 90% and 10%, respectively. This association occurs mostly within the Nosar Sandstone (Nosar Hills, Figure 1.3) and the lower part of the Sarnoo Sandstone.

Interpretation: The vertical change in grainsize and dune- to ripple-scale barforms are highly suggestive of a waning flow. These structures are indicative of the lower flow regime (Miall, 1977; North and Taylor, 1996) and were deposited within a restricted setting. The barforms contain consistent sets but erratic cosets suggesting a variable fluid flow.

4.4.6 In-Flow Barforms Association; ***Lfb***

Description: The Lfb facies association is composed of Stxc, Stxm, Sxc and Sxm subfacies (Figure 4.20, Table 4.2). The Sx facies can comprise 100% of the Lfb sequence but when the Stx is observed the Sx facies constitutes 70% and the Stx facies accounts for 30%. This association is present in all the sandstone successions. The sets and cosets within the Sarnoo Sandstone are regular; whereas within the Darjaniyon-ki Dhani and Nosar sandstones the sets and cosets are irregular.

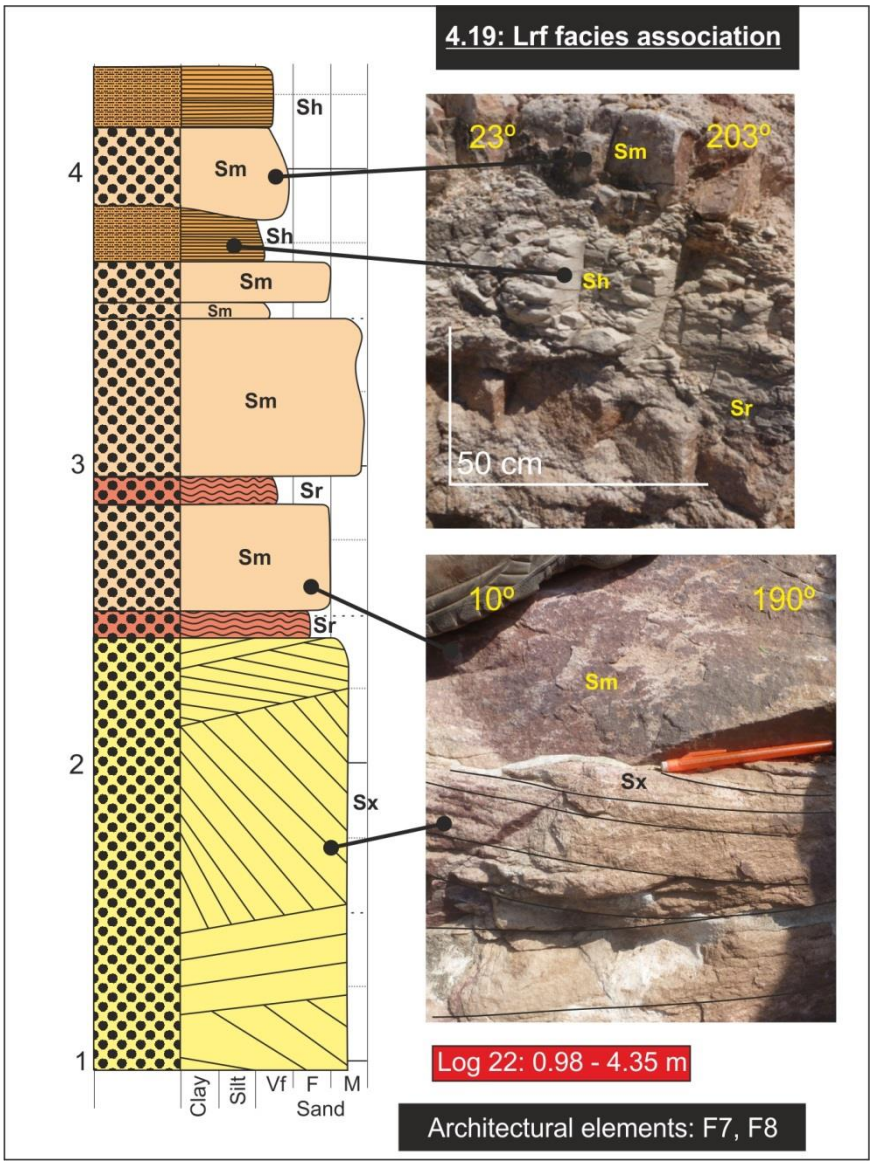

Figure 4.19: Summary of representative facies associations displaying logged data and photographs of the Lrf facies association.

Interpretation: The various types of cross-bedding within the Stx and Sx facies represent the migration of subaqueous sinuous and planar dune-scale bedforms and barforms deposited within the lower flow regime. The Lfb association was deposited within a confined flow. The consistency of the sets and cosets is dependent on the regularity of the fluid flow.

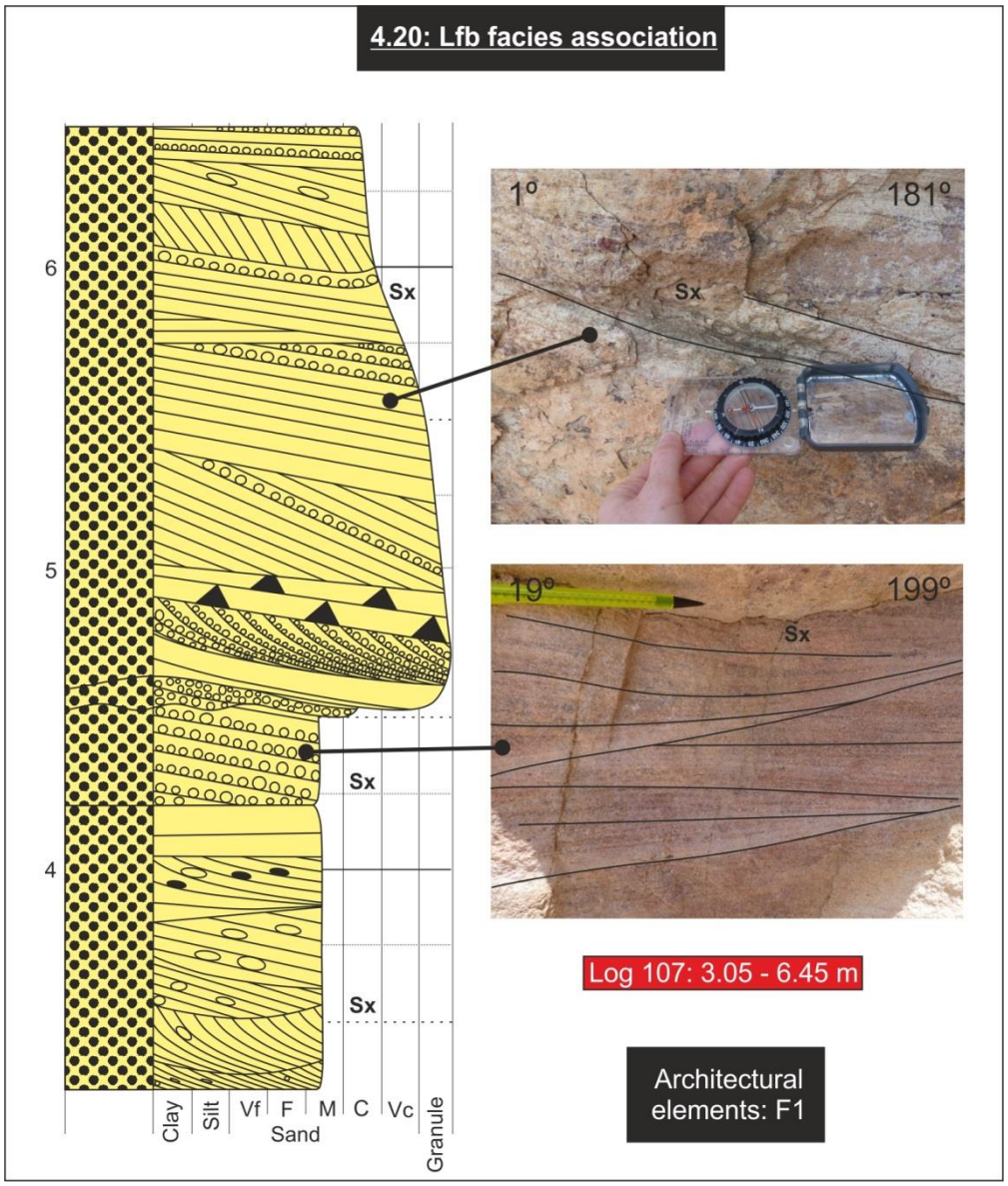

Figure 4.20: Summary of representative facies associations displaying logged data and photographs of the Lfb facies association.

*4.4.7 Laterally Accreting Barform Association; **Lfa***

Description: The relationships between Sxm, Slam, Slaf and Sr subfacies (Figure 4.21, Table 4.2) form the Lfa facies association. The order of the Lfa association varies as the Sx facies can underlie the Sla and vice-versa. The Sr subfacies packages are always on top and form less than 5% of the bedforms. The percentage of each facies is variable and the association changes laterally. The association is mainly in the Sarnoo Sandstone and rarely in the Nosar Sandstone.

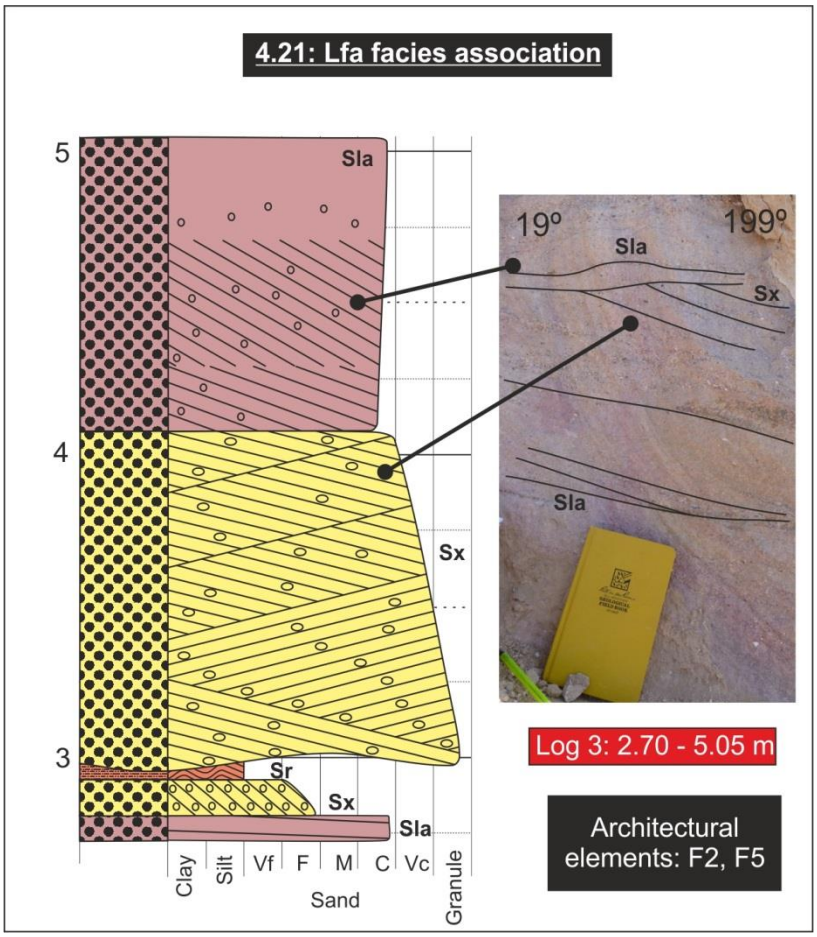

Figure 4.21: Summary of representative facies associations displaying logged data and photographs of the Lfa facies association.

Interpretation: Both the Sx and Sla facies represent straight crested duneforms, whereas the Sr facies represents ripple-scale bedforms. The barform migration within the Sx and Sla facies occur perpendicular to each other which is suggestive of lateral and down-flow movement of barforms. The ripple-scale bedforms at the top of the association indicate waning flow conditions.

4.4.8 Confined to Unconfined Upper Flow Regime Association; ***Urf***

Description: The deposits of the Sx and Sb facies form the Urf association (Figure 4.22). the division is 60% of the Sx facies and 40% of the Sb facies. This association occurs within the Sarnoo and Nosar sandstones.

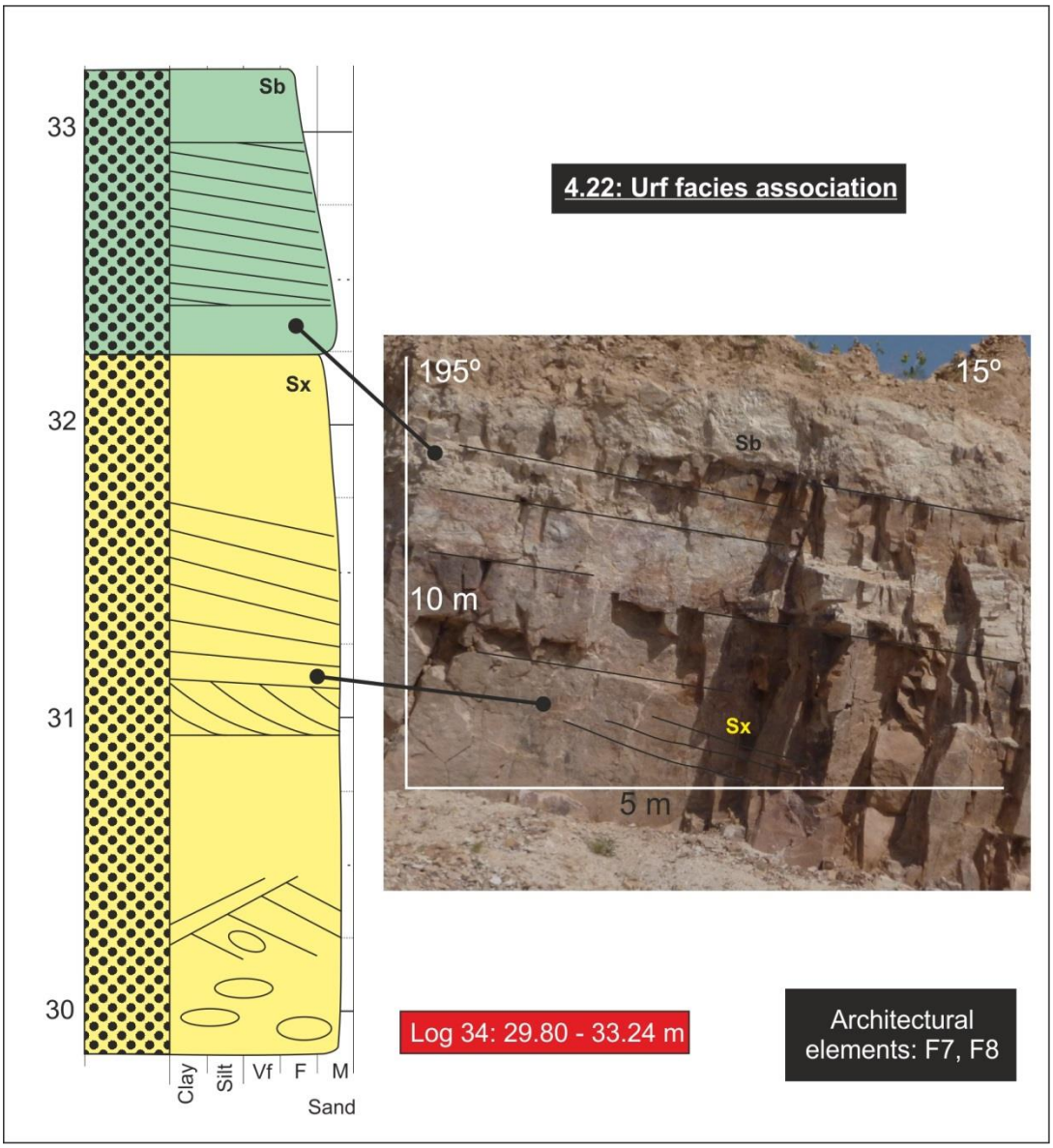

Figure 4.22: Summary of representative facies associations displaying logged data and photographs of the Urf facies association.

Interpretation: The Urf association was deposited at the transition from upper to lower flow regime within both confined and unconfined flow conditions.

4.4.9 Flooding Association; ***Fa***

Description: The deposits of the Fa association contain Sb, Smm, Smf, Sr, Shf, and Ip facies (Figure 4.23, Table 4.2) and are all deposited within unconfined fluid flows. The facies can occur in any order within the association. The percentage of the Sb facies increases south-westerly across the Sarnoo field area from 20% to 60%. The Sm and Sr facies account for 10% each. The Ip facies caps the association and accounts for 20%.

This association is within the upper successions of the Sarnoo Sandstone and the siltstone successions.

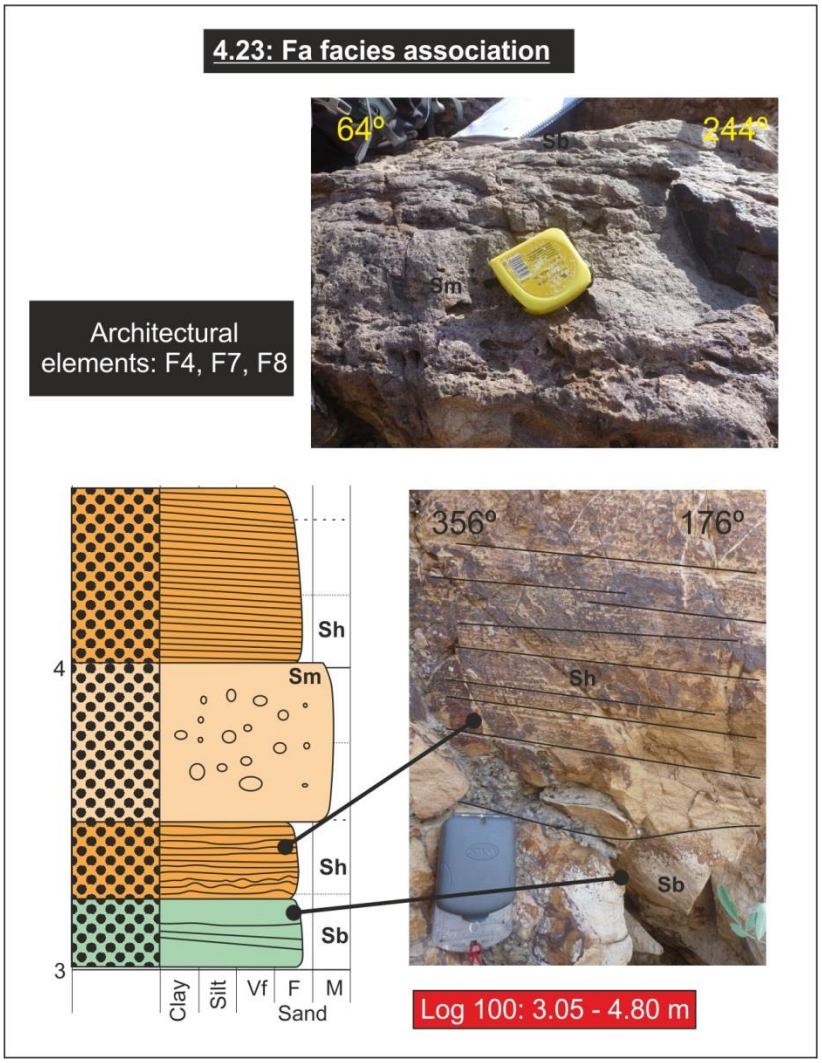

Figure 4.23: Summary of representative facies associations displaying logged data and photographs of the Fa facies association.

Interpretation: The planar bedding / horizontal laminations of the association represent cyclic deposits from unconfined flow events. The association has no particular order, indicating fluctuating energies within cyclic unconfined flow events to deposit the sediment. The ripple structures (Sr facies) were formed as the currents moved across an unconfined area due to the turbulence within the water. Bioturbation has obliterated some of the primary bedding structures (Ip facies).

4.4.10 Palaeosol Association; ***Pa***

Description: The Pa association contains Sp, Ip, Ihe, Sm and Im facies (Figure 4.24, Table 4.2) that occur in no particular order. The Ihe facies is dominant here (75%), Ip and Sp account for 15% and the Sm / Im facies take the remainder 10%. This association is laterally extensive throughout the field area. Within the sandstone successions the association has at most a 2 m lateral extent, preserved at outcrop. The association is seen throughout the entire succession.

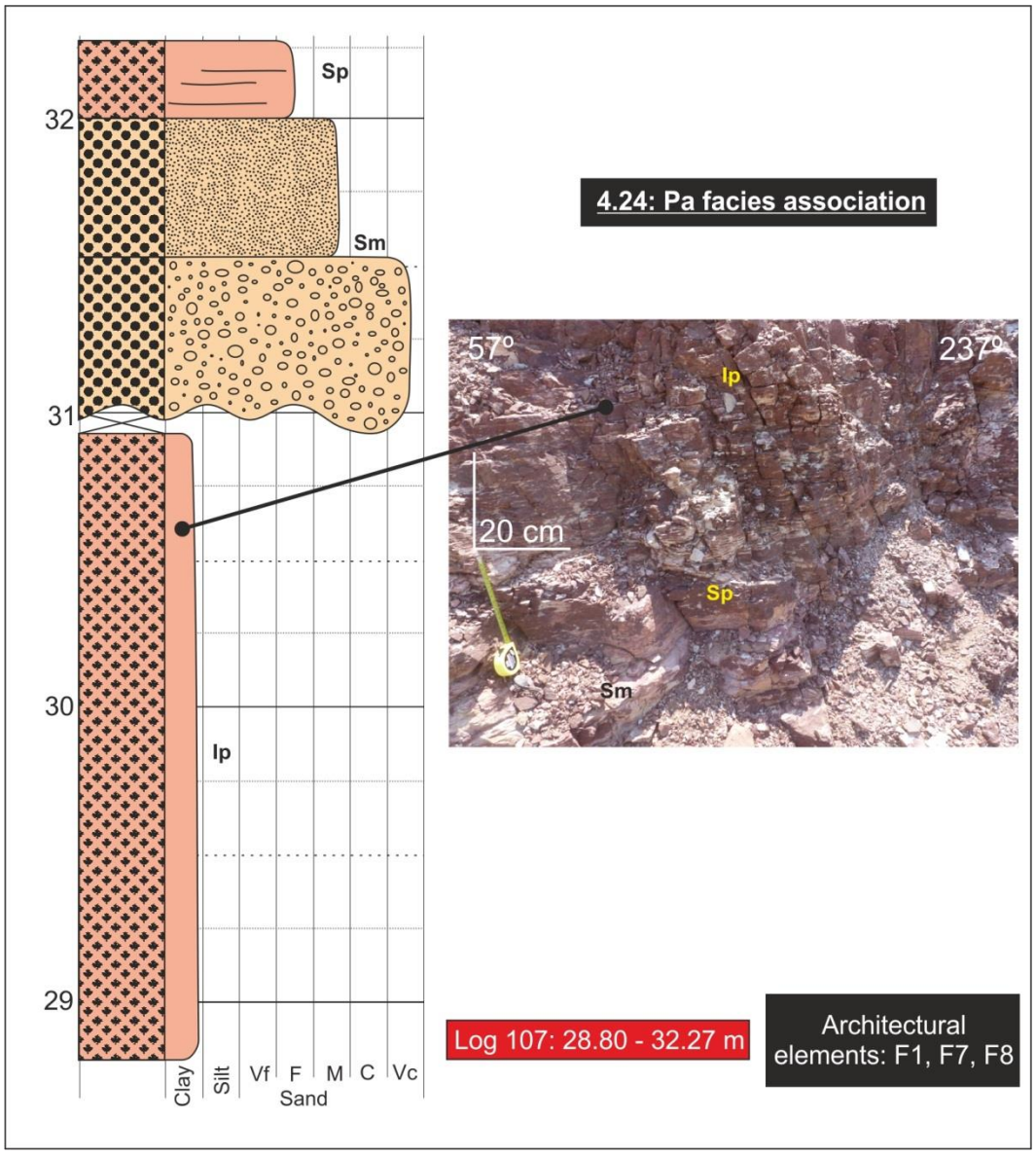

Figure 4.24: Summary of representative facies associations displaying logged data and photographs of the Pa facies association.

Interpretation: The primary structures of the Pa deposits have been destroyed by pedogenic processes. The lack of erosion within this facies association is suggestive of a cumulative soil.

4.5 Summary

Fourteen different facies have been identified based on sedimentary textures and structures. These fourteen facies have been deposited through variations in fluid flow, debris flow and subaerial exposure. Subfacies are determined by the grainsize variation that highlights the different energy levels of the same process of deposition. The fluid flow facies consist of both confined (Stx, Sx, Sla, Sr, Sla facies) and unconfined flows (G, Sb, Sm, Im and Sh facies). The debris flows are unconfined (M facies). Subaerial facies record periods of depositional quiescence allowing for colonisation leading to bioturbation of the substrate (Sp, Ip and Ihe facies). These facies were linked together based on similar depositional and transport processes forming facies associations. Two subsections are recognised and based on confined (Cdd, Hec, Lec, Lfb, Lfa, Ler) and unconfined (Heu, Luf, Fa, Pa) sediment deposition.

The next chapter (5) will bring these facies associations together to interpret the sediments of the Ghaggar-Hakra Formation, in terms of architectural elements, three-dimensional facies models and a final depositional model.

5 Chapter Five: Bounding Surfaces, Architectural Elements and Facies Models of the Ghaggar-Hakra Formation

Bounding surface analysis is widely used for characterising aeolian environments (McKee and Weir, 1953; Brookfield, 1977; Kocurek, 1981). Various authors (e.g. Miall, 1988; Doyle and Sweet, 1995; Colombera *et al.,* 2012; Gulliford *et al.,* 2014) have applied similar schemes to fluvial environments where hierarchical schemes can be applied to similar surfaces (Section 2.7). For example six orders of bounding surfaces can be recognised by their cross-cutting relationships and sedimentological features; first order surfaces are recognised by the truncation of foresets while sixth order surfaces reflect regionally significant events.

The classification of architectural elements can be applied to multiple facies associations and bounding surfaces alike (Miall, 1988). These relationships give the architectural elements geometry in three-dimensions. Although many authors have documented different architectural elements for fluvial strata, to date there is no accepted model for all fluvial systems (Miall, 1988; Ghazi and Mountney, 2009). This is because fluvial systems are inherently varied. For example, fluvial systems within arid environments are generally ephemeral and contain non- and poorly-channelised sheets of sand (e.g. Glen Canyon Group, North and Taylor, 1996; Staircase Falls, Yosemite National Park; Table 2.5). In humid environments fluvial systems can be sinuous, giving rise to architectural elements such as sandy bedforms, channels, downstream and lateral accretion (Ghazi and Mountney, 2009; e.g. Amazon River, Brazil; Table 2.5).

This chapter describes and interprets the hierarchy of bounding surfaces within the Ghaggar-Hakra Formation. The orders and relationships between bounding surfaces, when combined with the associated facies associations (Section 4.4), define eight architectural elements, where the locations from outcrop are displayed in Figure 5.1. The architectural elements are combined together in different proportions to form four separate

facies models for the formation. The chapter ends with the discussion of the evolution of the depositional environment for the Ghaggar-Hakra Formation.

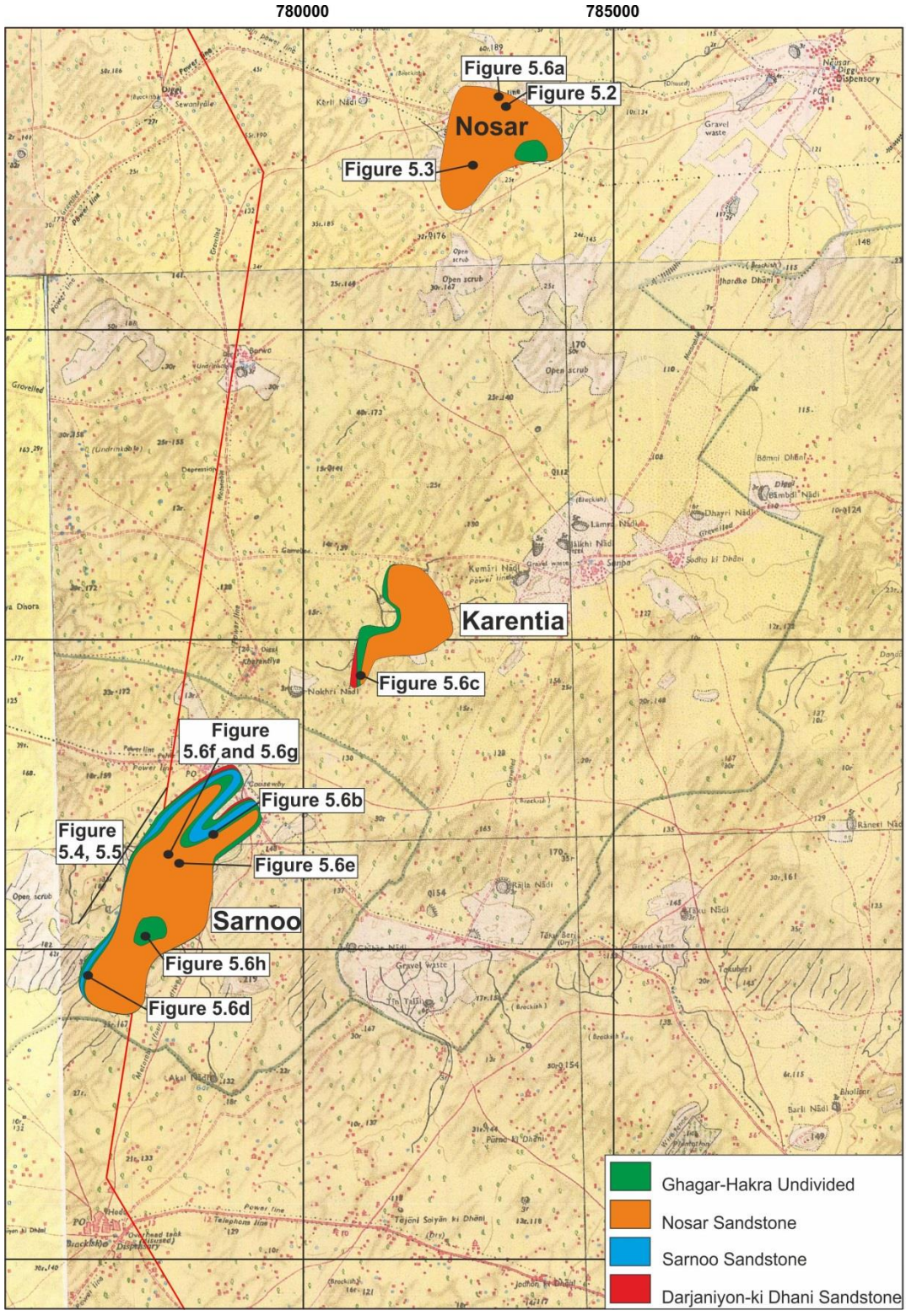

Figure 5.1: (a) Index map displaying the locations of the photographs from Figures 5.2 – 5.6 and the extent of the separate sandstone successions and the Ghaggar-Hakra Undivided. For location of field areas see Figure 1.3.

5.1 Bounding Surfaces

The scheme of Miall (1988) is adapted to fit the Ghaggar-Hakra Formation and is described below.

First order bounding surfaces are the lower boundaries of cross-bedded and ripple-laminated sets with average height of 25 cm (Figure 5.2). The surface has an angle of approximately 8°. This surface is undulose over its spatial extent but does not erode into the underlying sediment. Coarse-grained sediment lines the upper side of the surface. The cross-bedded or rippled foresets have asymptotic bases. These surfaces are akin to the first order surfaces of Miall (1988).

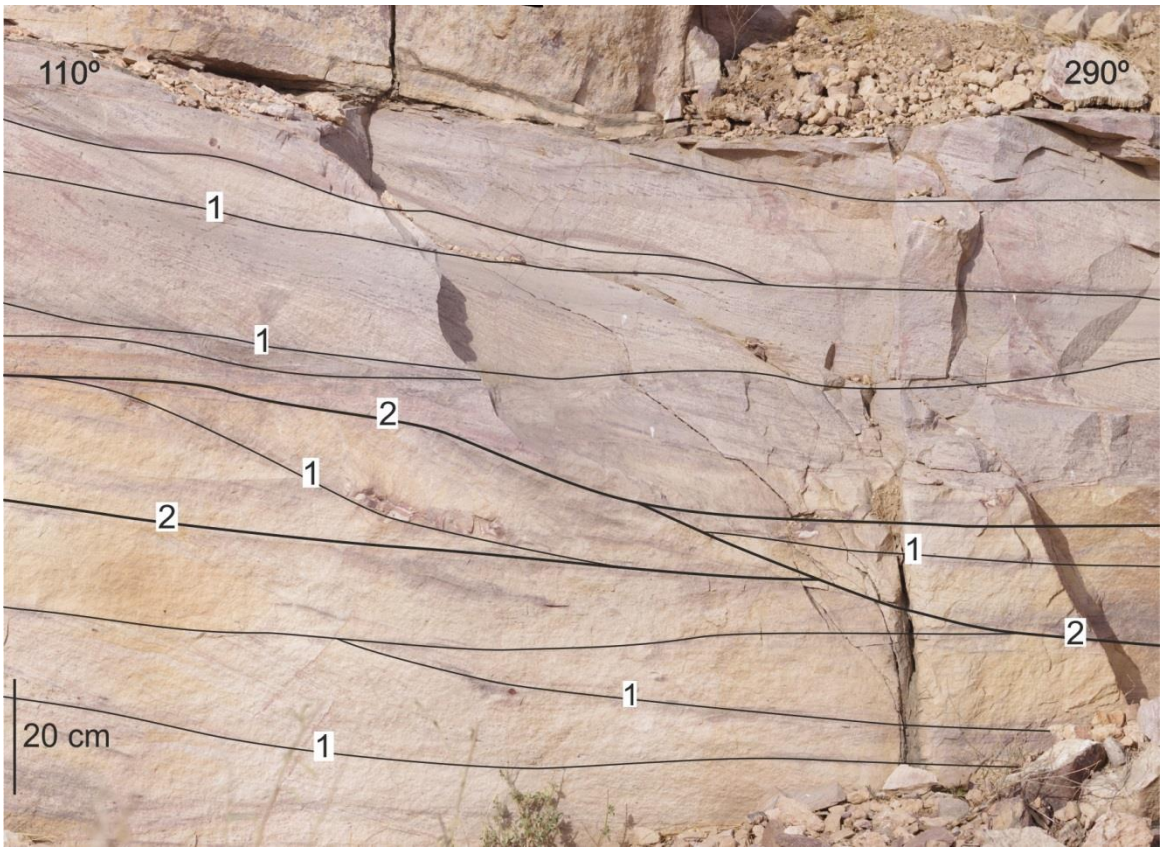

Figure 5.2: Examples of bounding surfaces orders 1 and 2 as seen dominantly within the channel elements of the Nosar Sandstone (GR: UTM 0782800, 2853527). First order surfaces are recognised by the truncation of the foresets against them, second order surfaces are recognised by the truncation of the first order surfaces against them and the surfaces have a shallow climb to them.

Second order bounding surfaces are the bottom boundary of the cosets which are up to 95 cm in height. The boundary has an angle of 5°. Granule-grade quartzite pebbles can

line the upper-side of this erosional boundary. The first order surfaces can both truncate against and be asymptotic against the second order surfaces. Where the second order surfaces truncate against each other this can represents a change in the facies or facies association (Figures 2.10, 5.2, 5.3). This definition is similar to the surfaces seen by McKee and Weir (1953).

Third order bounding surfaces laterally accrete throughout bedforms (Section 2.7). The surfaces are approximately 3.5 m long. The surfaces dip at approximately 14°. Although the surfaces are not down-cutting they do cross-cut the marcoforms. The first and second order surfaces truncate against these third order surfaces (Figure 5.3). These surfaces represent reactivation surfaces (where the flow has reversed or increased erosion has occurred; Section 2.7) and are similar to the third order surfaces of Brookfield (1977) and McKee and Weir (1953).

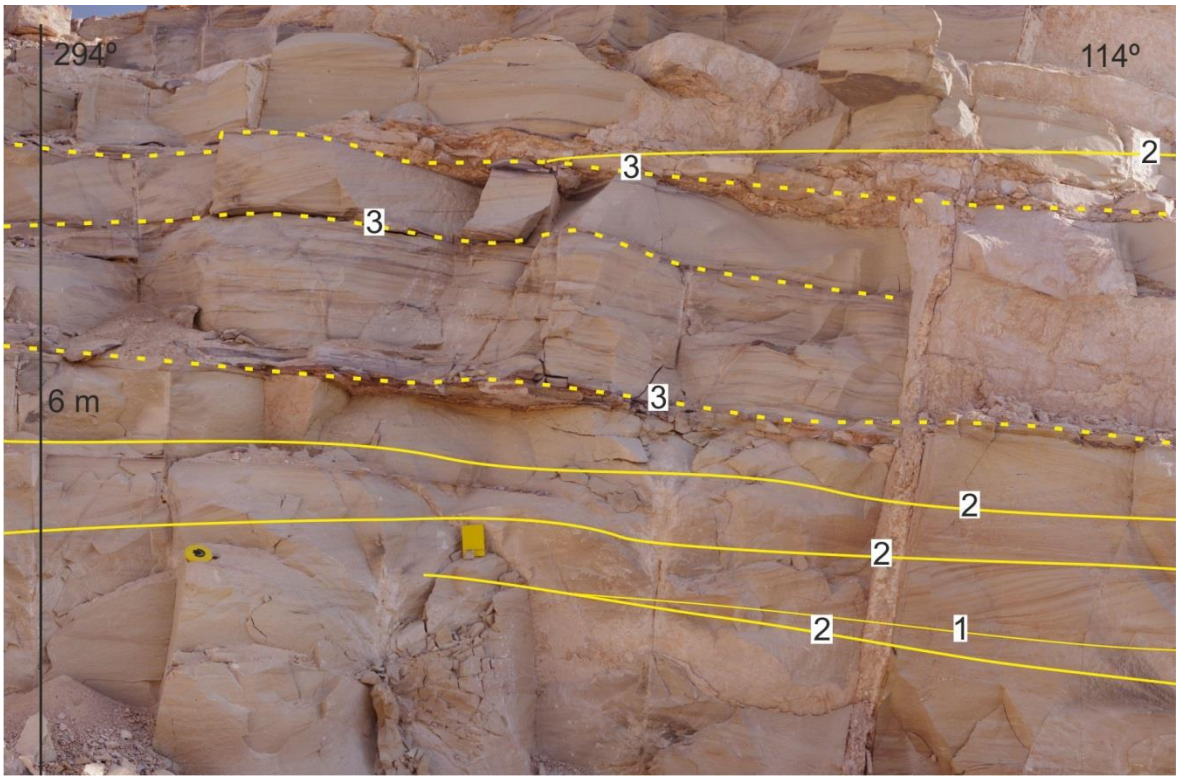

Figure 5.3: An example of the third order bounding surfaces which are identified using the angle of climb and the truncation of first and second order surfaces against it, (GR: UTM 0782563, 2852257).

Fourth order bounding surfaces are flat or convex-upward and vary in length from 1 m to 30 m. The boundary climbs at shallow angles (5° - 8°). The surface is not erosive. The first to third order surfaces truncate against this boundary at shallow angles (Figures 5.2, 5.3, 5.4). This surface is similar to the fourth order bounding surface of Miall (1988) and forms the top of sediment packages.

Fifth order bounding surfaces represent major sand sheets and are laterally mappable over 10's of metres. The boundary has no climb. This surface can be erosive and / or sharp and is lined with granule- to pebble-grade quartzite (rarely basaltic) clasts and / or mud- to very fine-grained sands forming rip-up clasts. Truncated against this surface are dominantly third and fourth order surfaces. However, occasionally the fifth order surface truncates first and second order surfaces directly (Figures 5.4, 5.5, 5.6). This surface forms the bottom of larger sedimentary packages and is similar to the fifth order bounding surface of Miall (1988).

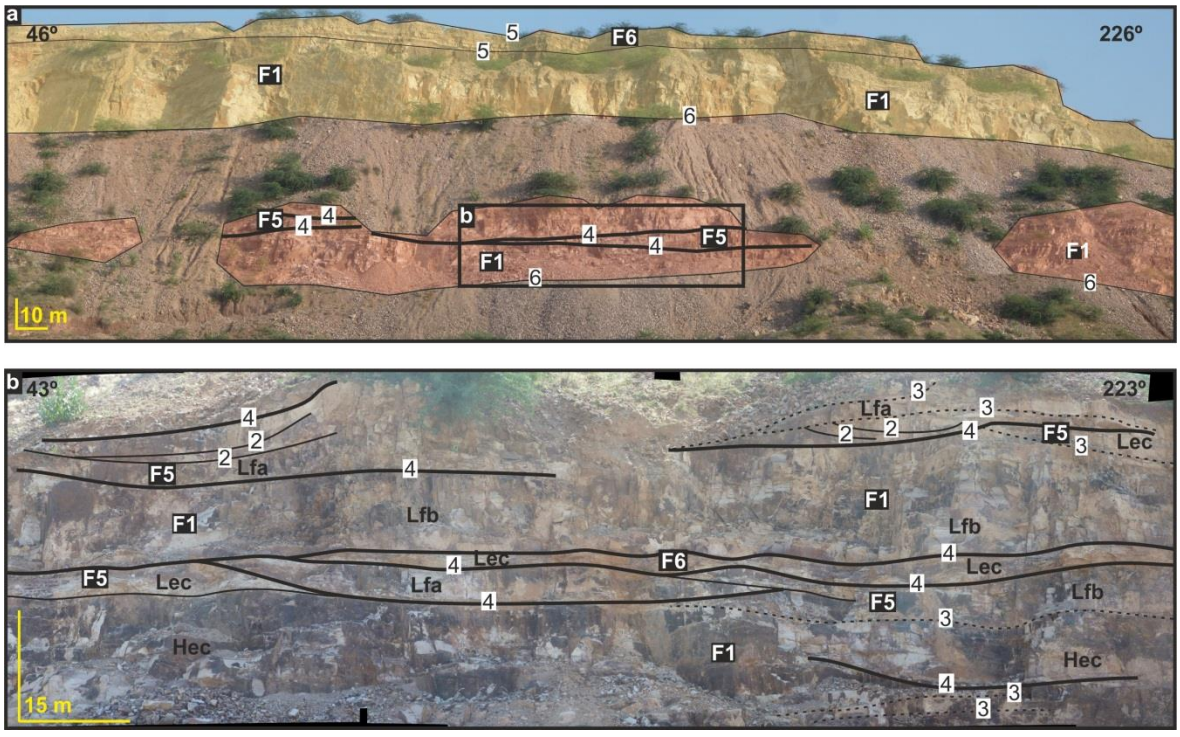

Figure 5.4: (a) Sarnoo panel displaying the larger-scale interactions of the channel (F1), point bar (F5) and sheetflood (F6) elements, with the relevant bounding surfaces (4 – 6) labelled. The fourth order surfaces are determined by their convex-upward and concordant nature, the fifth order surface are recognised by their erosive nature and lined with quartz and basaltic clasts. The sixth order surfaces

are recognised by the distinct erosive nature, change in lithology across the surface and their extensive nature; (b) Zoomed in section within the Sarnoo Sandstone, displaying bounding surfaces 2 – 4. Second order bounding surfaces are recognised by the shallow angles of climb, whereas the third order bounding surfaces have a steeper climb and the second and first order surface truncate against them. Fourth order surfaces are determined by their convex-upward nature (GR: UTM: 0777865, 2841891). Facies associations and architectural elements labelled.

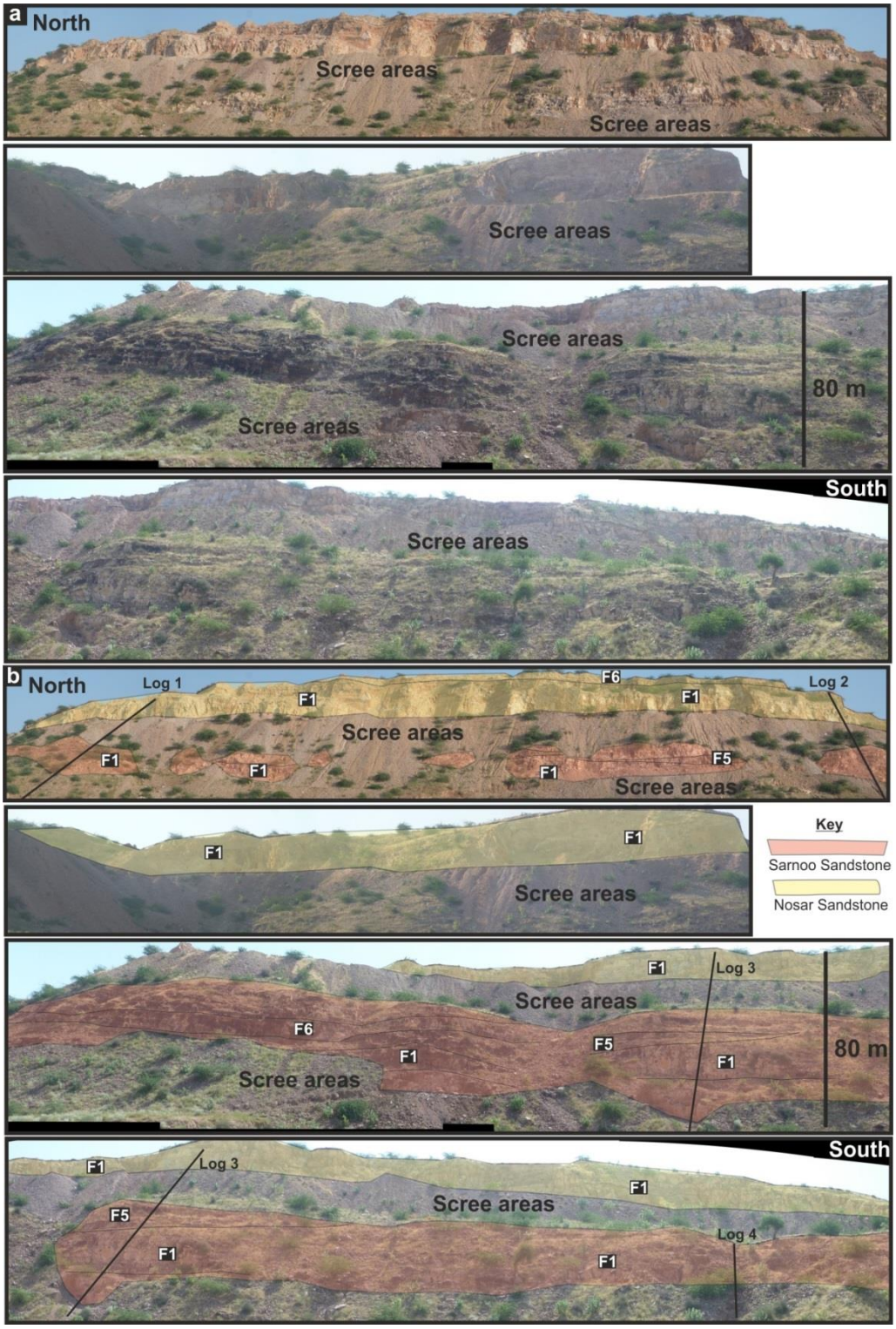

Figure 5.5: Panel correlation along the western edge of the Sarnoo Hills, displaying various bounding surfaces and architectural elements (a) uninterpreted photo montage (b) interpreted photo montage displaying the Sarnoo and Nosar Sandstones. For location see Figure 5.1 and log interpretation see Figure 5.6. The architectural elements labelled.

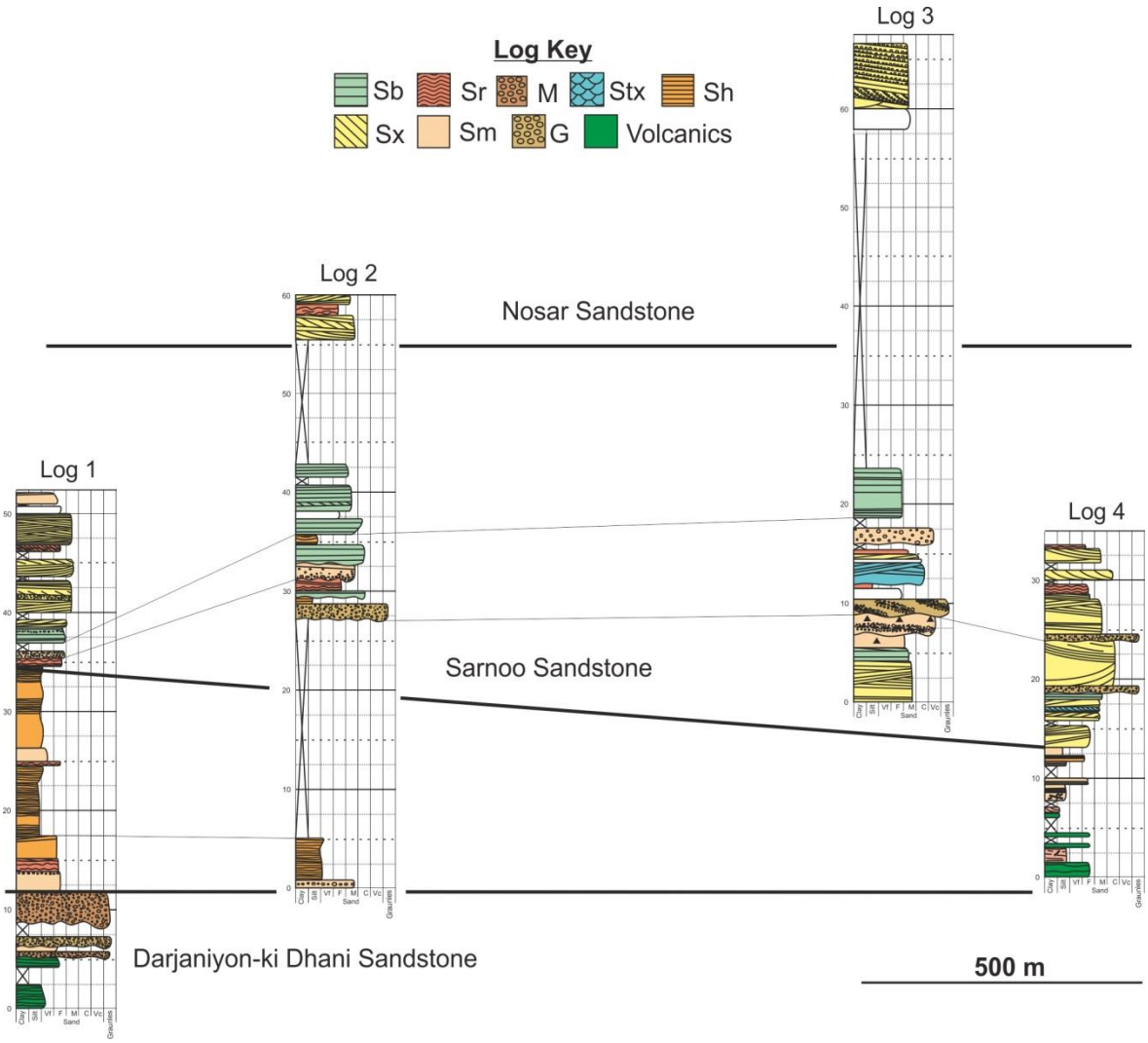

Figure 5.6: Log correlation along the western edge of the Sarnoo Hills and based on facies associations and sandstone bases. The thick black lines are tie lines linking the bases of the separate sandstone successions and therefore the sixth order bounding surface. The thin black lines link together the various facies associations and therefore represent the fourth order bounding surfaces. For locations of the logs see Figure 5.5.

Sixth order bounding surfaces represent the start of a member or unit and are mappable over large areas. These surfaces are noted throughout the extent of the field area (up to 10 km, Figure 1.3) and they have a shallow dip (approximately 5° to the south). Lining the erosional surface there are generally granule- to large pebble-grade clasts composed of quartz and / or basalt. There can also be rip-up clasts (from 1 mm by 1 mm to 130 mm by 180 mm). Fourth and fifth order surfaces truncate against this surface (Figures 5.4, 5.5, 5.6). This surface forms the base to new sandstone successions within the field areas and the surfaces are similar to those of Miall (1988) and Brookfield (1977).

5.2 Architectural Elements

Architectural elements are well-established within fluvial regimes; they bring together separate facies associations which extend laterally and vertically as sedimentary packages (Figures 5.5, 5.6). These packages have a three-dimensional geometry with defined upper and lower boundaries. They are described below:

5.2.1 Sandy bar element – F1

The deposits of sandy bar element contain the Cdd, Lcf, Lrf, Lfb, Urf and Fa facies associations (Figure 5.7a, 5.8a). The geometry of the element is channel-shaped. The lower boundary is a fifth order bounding surface and can be erosional, sharp and concave down (cut) into the floodplain (F7) element, into other sandy bars (F1) or into the channel margin element (F2). Where seen, the upper boundary is a fourth order surface and is gradational into the floodplain element (F7). The channel widths and depths vary in size from 1 m to 23 m and 50 cm to 3 m, respectively.

Within larger bars (widths above 5 m and depths below 1.25 m) the internal sedimentary structures are planar and trough cross-bedded sets and cosets (first and second order bounding surfaces) which can be stacked and amalgamated (Figure 5.9). Within the smaller bars the sedimentary structures are planar cross-bedding and ripple-laminated, or occasionally, the bars are structureless.

The sets and cosets are arranged vertically within the element to produce a well-recognised succession. The succession starts with a fifth order surface and the grain-supported conglomerates (G facies). Then there is cross-bedding (Stx / Sx facies) containing bounding surfaces order one, two and three. The succession ends with ripple-laminated horizons, plane beds and bioturbation (Sr / Sh / Sp / Ip facies). The full depositional succession is observed rarely as it is truncated frequently by the start of new cycles. Commonly, only the G, Stx and Sx facies are preserved within the succession.

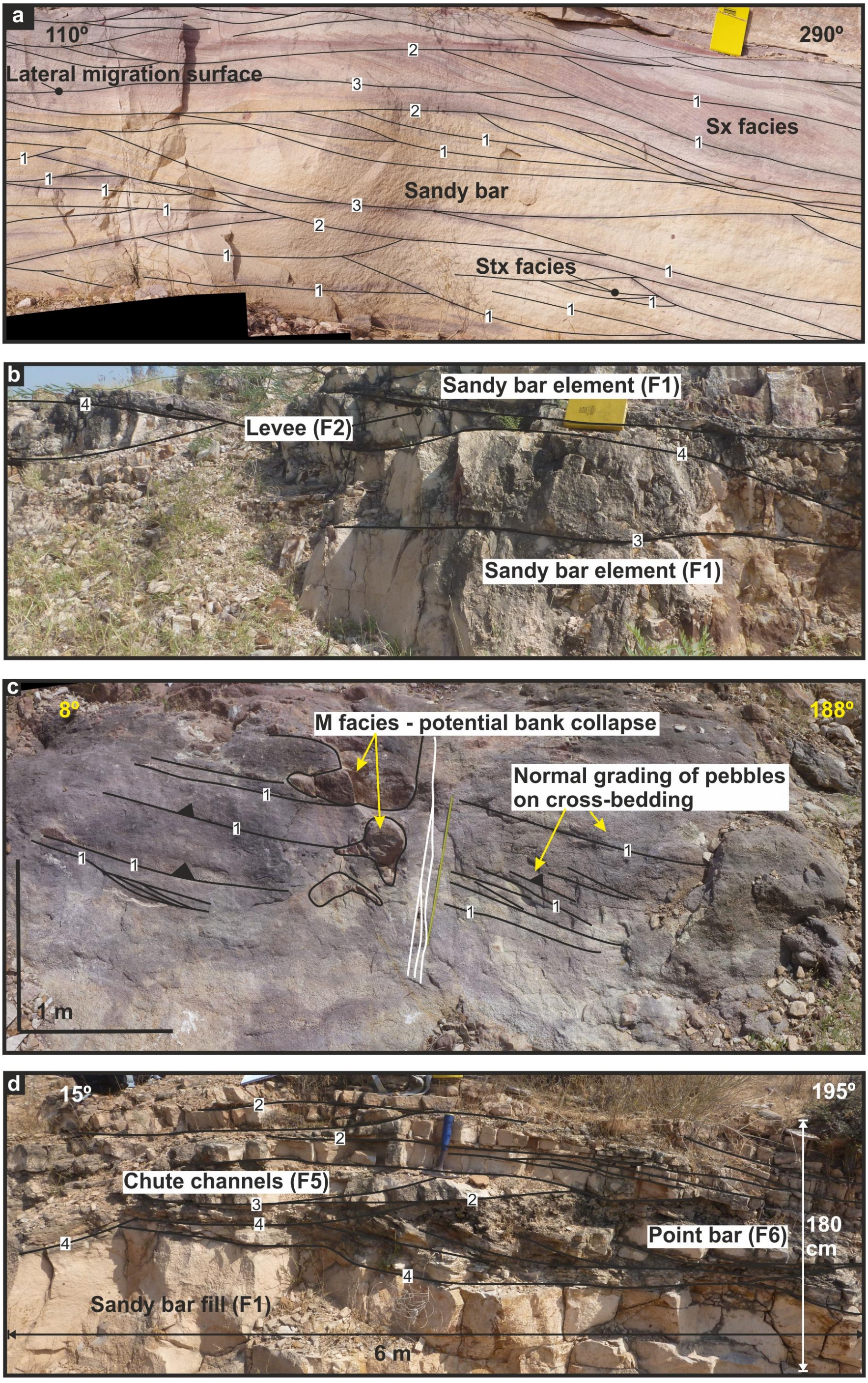
a
110º
290º
Lateral migration surface
Sx facies
Sandy bar
Stx facies
b
Sandy bar element (F1)
Levee (F2)
Sandy bar element (F1)
c
8º
188º
M facies - potential bank collapse
Normal grading of pebbles on cross-bedding
1 m
d
15º
195º
Chute channels (F5)
Point bar (F6)
180 cm
Sandy bar fill (F1)
6 m

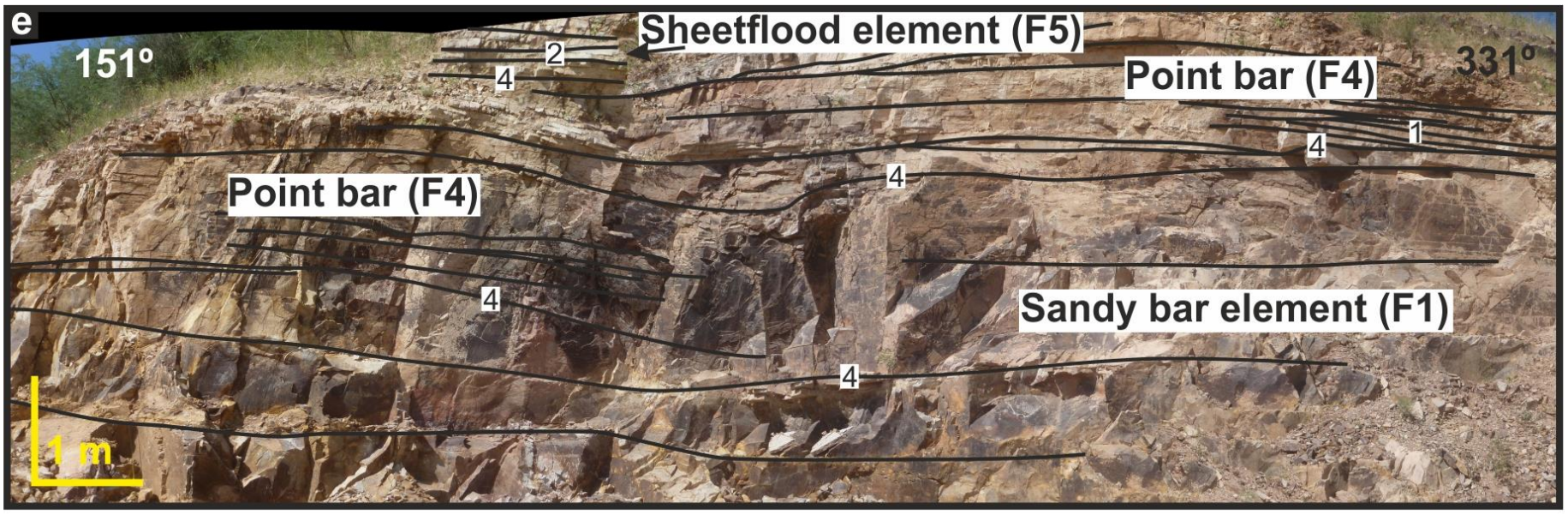

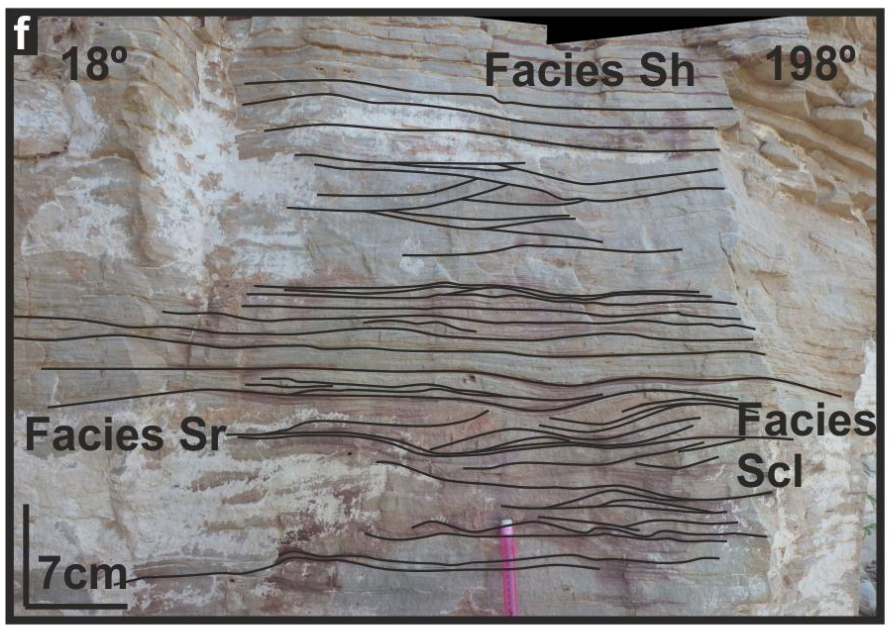

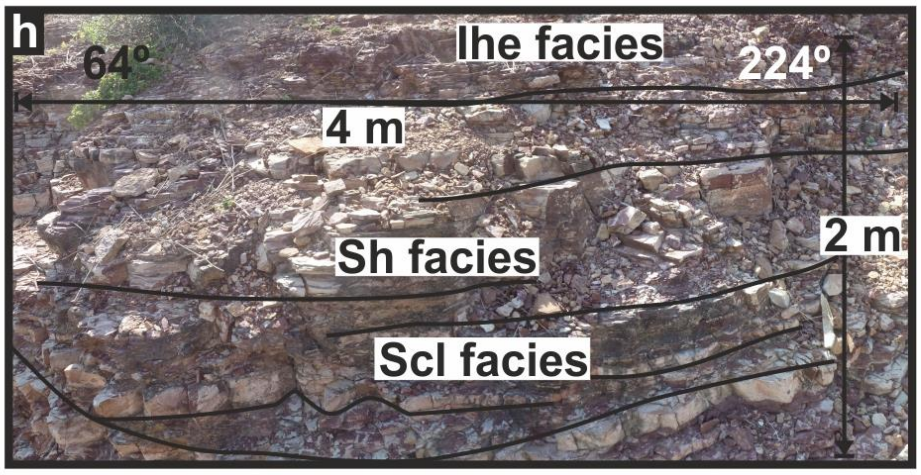

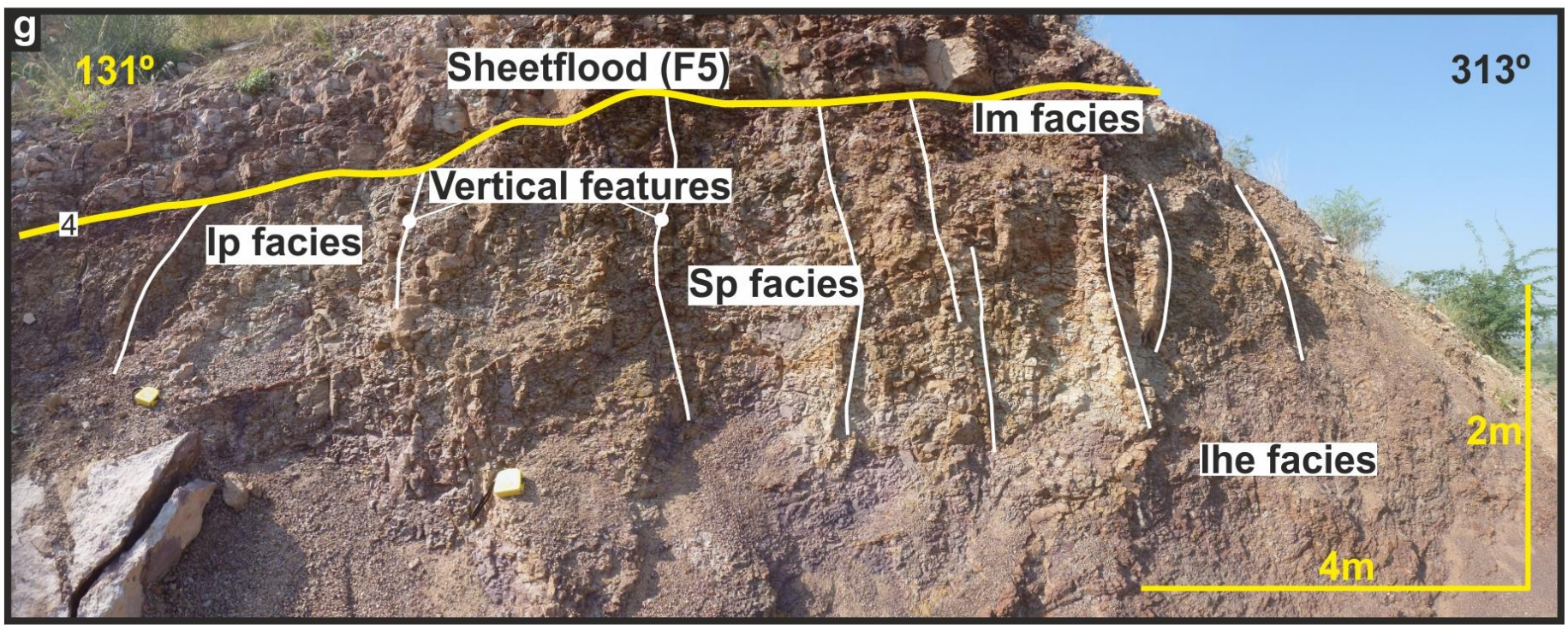

Figure 5.7: Photograph representative architectural elements: (a) sandy bar (F1); GR UTM 0782835, 28535389, Nosar Hills, Locality 117; (b) channel margin (F2); GR UTM 0778635, 2842386, Sarnoo Hills, Locality 001; (c) gravel bar (F3), GR UTM 0780744, 2844534, Karentia Hills, Locality 011; (d) chute channel (F4), GR UTM 0776966, 2840369, Sarnoo Hills, Locality 16; (e) point bar (F5), GR UTM 0778271, 2842071, Sarnoo Hills, Locality 374; (f) sheetflood (F6), GR UTM 0777801, 2841812, Sarnoo Hills, Locality 135; (g) floodplain (F7), GR UTM 0778133, 2842095, Sarnoo Hills, Locality 366; and (h) pond (F8), GR UTM 0777544, 2840797, Sarnoo Hills, Locality 300. For all locations see Figure 5.1.

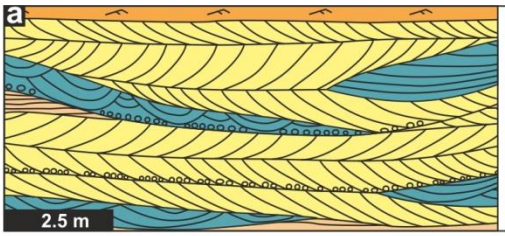

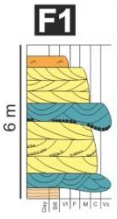

Sandy bar element

Channel complexes, with fourth order bounding surfaces, most common within the Nosar Sandstone. Grainsize decreases vertically; planar cross-bedding most prominent.

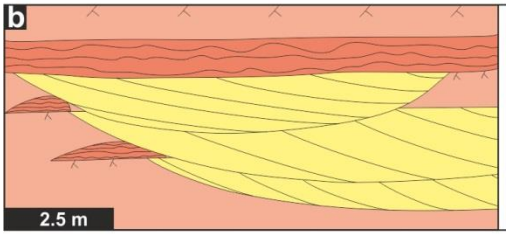

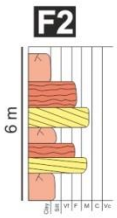

Channel margin element

Units of rippled sediment which can be bioturbated, bounded by fourth order bounding surfaces. Grainsizes decrease vertically. Eroded into by channels; Sarnoo Sandstone only.

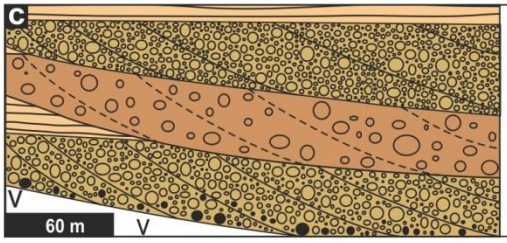

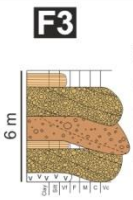

Gravel bar element

≤6 m thick, convex downwards, composed of pebble-grade conglomerates, with fourth order bounding surfaces. Within the Darjaniyon-ki Dhani and the Nosar Sandstones.

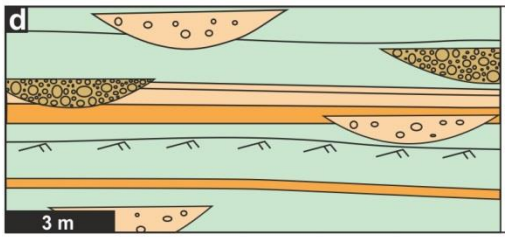

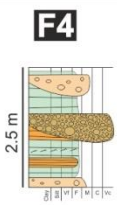

Chute channel element

Chute channels are ≤2 m in width ≤ 70 cm in height and surrounded by fourth order surfaces. Observed within the Sarnoo Sandstone only.

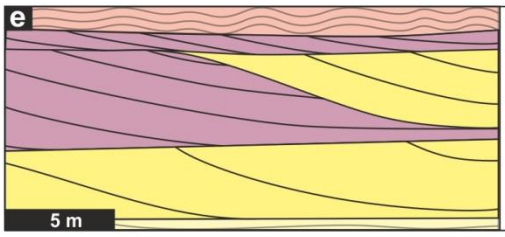

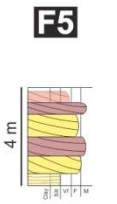

Point bar element

Point bar element is composed of fine- to medium-grained sands. Lateral thickness is ~20 m, with fourth order surfaces. Observed in the Sarnoo Sandstone.

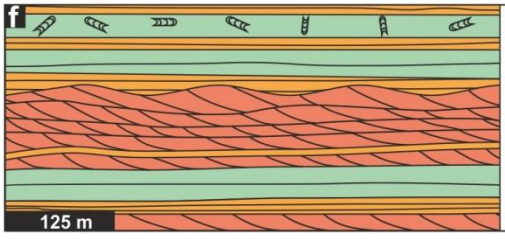

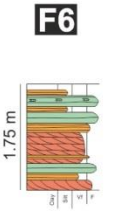

Sheetflood element

Laterally extensive sheet-like bodies, noted by a fifth order surface and composed of silt to fine-grained sands. Within the Sarnoo Sandstone and Nosar Sandstone.

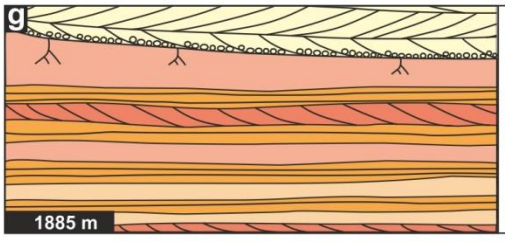

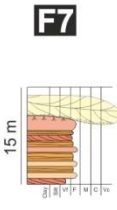

Floodplain element

≤30 m thick, laterally extensive, mud to very fine-grained sands, forming a sixth order surface. Horizontally- and ripple-laminated horizons and palaeosols evident. Extensively seen throughout the field area.

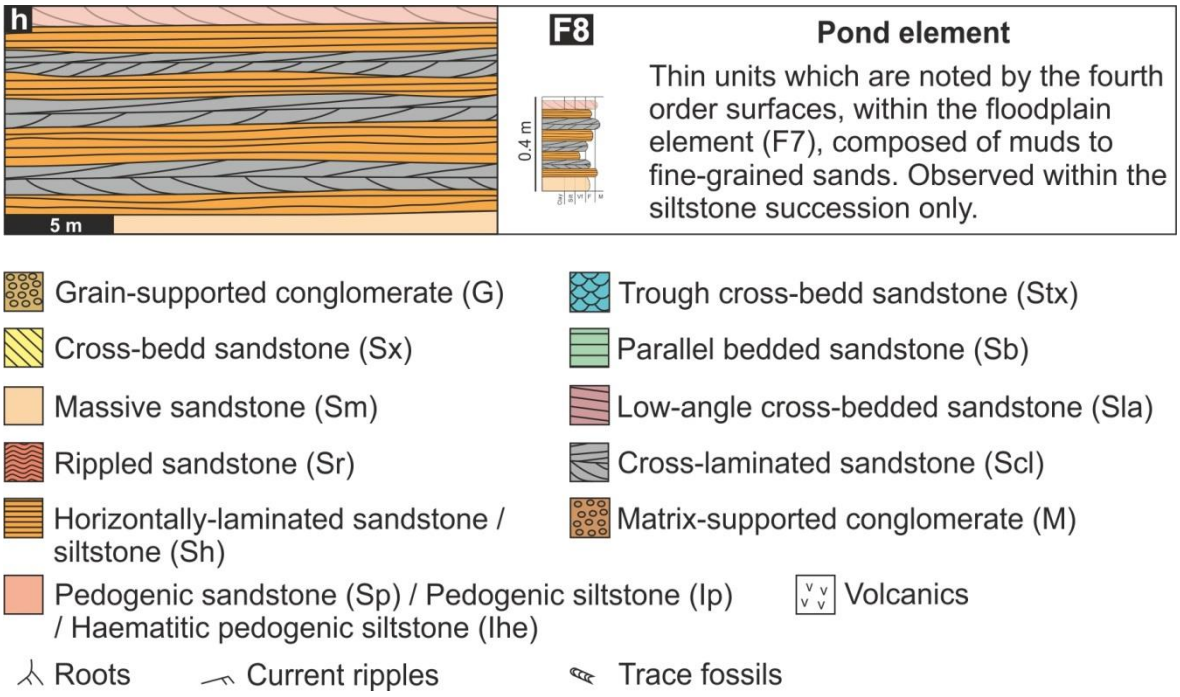

Figure 5.8: Two-dimensional representations of architectural elements drawn schematically. The sketches display the external and internal geometries, facies and facies associations observed at outcrop; the logs are representative of the facies associations noted within the architectural elements; (a) sandy bar, (b) channel margin (c) gravel bar, (d) chute channel, (e) point bar, (f) sheetflood, (g) floodplain and (h) pond. Note, that the scales alongside each sketch element are different.

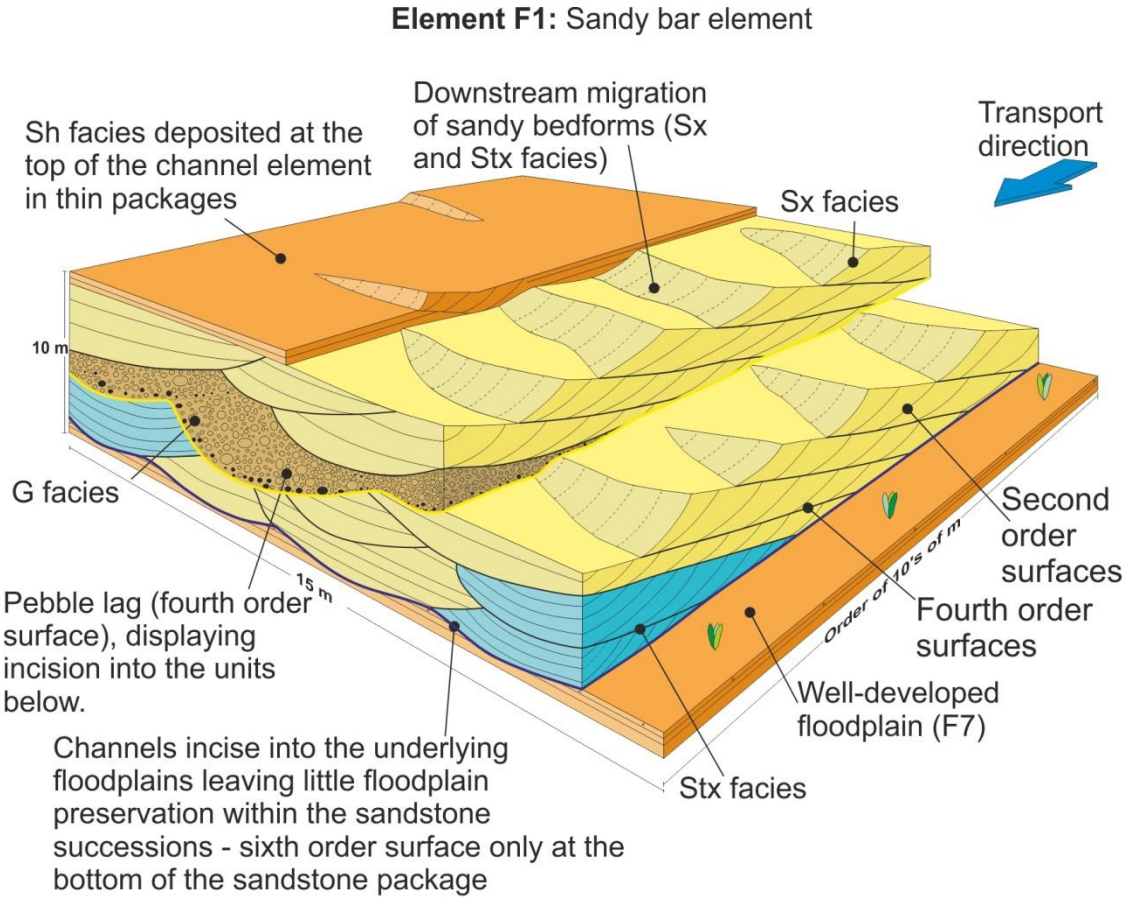

Figure 5.9: The three-dimensional schematic model of the sandy bar element displays sixth order bounding surface demonstrating the start of the new fluvial regime (Miall, 1988). The model demonstrates that the pebble lag (Cdd facies association) creates a fifth order surface as the pebble lag can be traced out within the field area. The model also exhibits a waning flow from the pebble-lag through to poorly developed floodplain deposits (F7).

5.2.2 Channel margin element – F2

The facies associations at the channel margin are Uuf, Lrf, Lfa, Fa and Pa (Figure 5.7b, 5.87b). The geometry is wedged and tabular. The lower boundary is a fifth order bounding surface which is concordant or rarely gradational to the underlying sandy bar elements (F1). Upper boundary is a fourth order surface and is gradational into the gravel bar (F3) and floodplain (F7) elements. The height is up to 5 m and the width is up to 10 m.

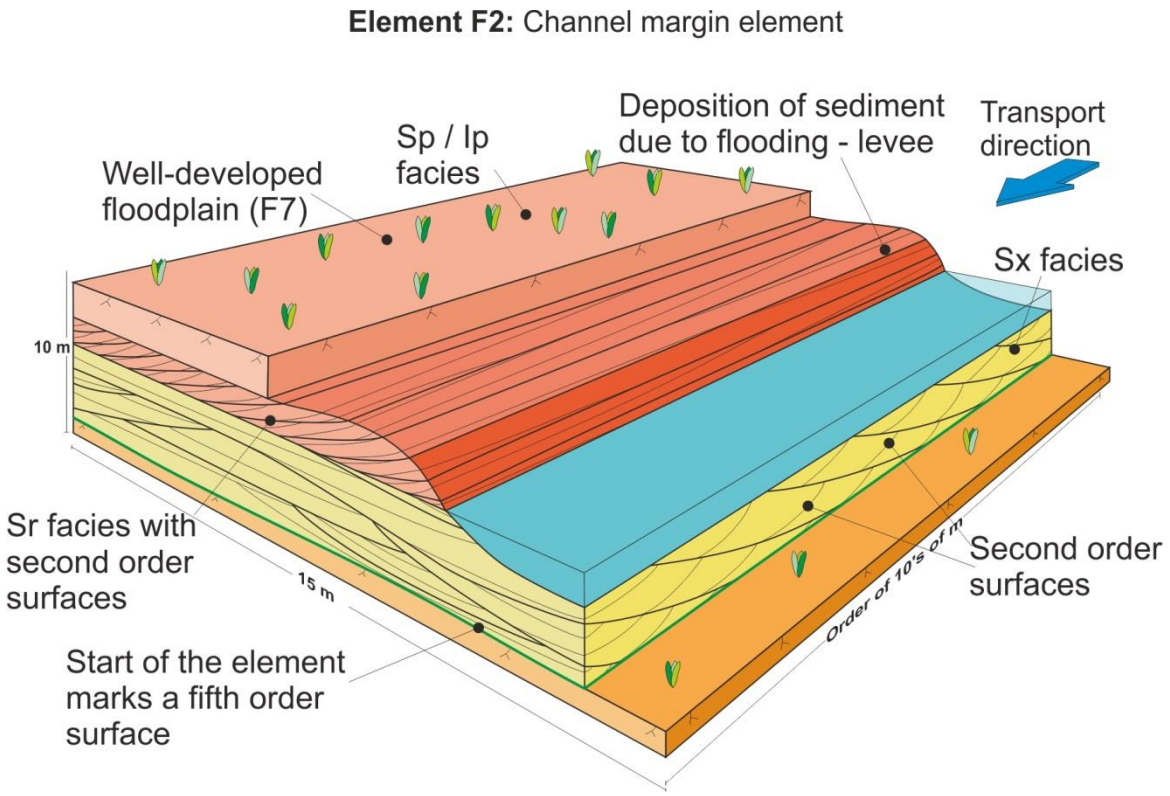

Figure 5.10: The three-dimensional architectural element model of the channel margin element. The lower boundary marks a fifth order surface from the sandy bar element (F1), the upper boundary is gradational into the floodplain element (F7). Internally the structures are from the Sr facies, into the Sp / lp facies, waning flow evident.

Internally the structures consist of stacked and amalgamated trough and planar cross-bedded sets and cosets (containing first, second and third order surfaces) of the Lrf and Lfa facies associations. Above this are the restricted flow deposits of the Uuf and Fa facies associations, which contain indistinct trough and planar cross-bedded sets (Figure

5.10). This indicates the movement of water from the sandy bar (F1) element onto the floodplain element (F7), therefore the sediment and the fluid flow moves from confined to unconfined flow.

5.2.3 Gravel bar element – F3

The associations within the gravel bar element are Cdd, Uuf and Lcf (Figure 5.7c, 5.8c). The geometry is lenticular. The lower boundary of the element is sharp and erosional into the sandy bar element (F1) and forms a fifth order surface. The upper boundary represents a fourth order bounding surface and can either be sharp or gradational into the sandy bar (F1), channel margin (F2) or floodplain (F7) elements. The width is up to 75 m and the height is up to 4 m.

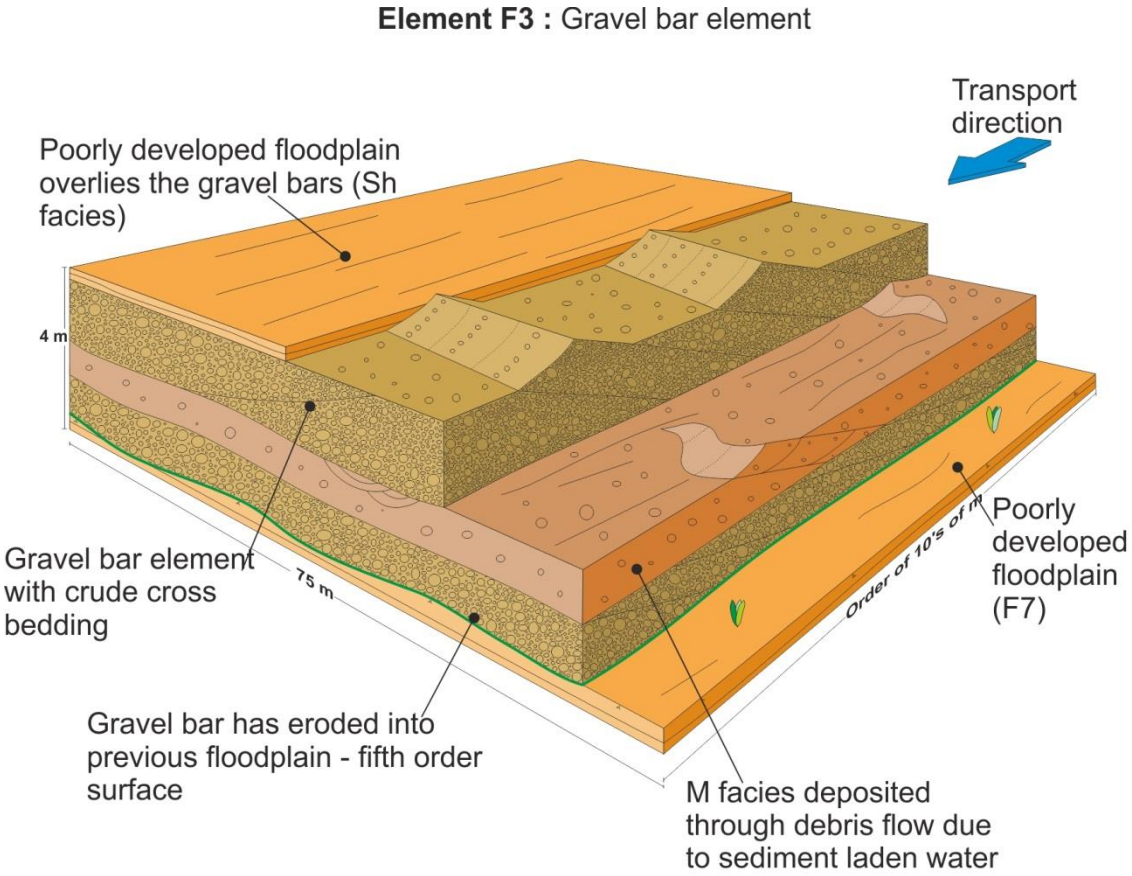

Figure 5.11: The three-dimensional schematic model displays the gravel bar facies associations, where it is observed that the sediments grade from the bar deposits to the floodplain element (F7), displaying an overall waning flow. The gravel bars throughout the succession form fifth order surfaces.

The internal geometries consist of the indistinct planar cross-bedded sets. There is also a significant amount of termination of first to third order bounding surfaces, within these deposits. This indicates the migration of barforms implying that the gravel bars are transient (c.f. Bridge 1993, Figure 5.11).

The facies associations are commonly arranged within the element into recognisable succession starting with a fifth order surface and the Cdd or Lcf facies association which contain first to third order surfaces. The succession ends with the Uuf association.

5.2.4 Chute channel element – F4

The chute channel element contains Uuf, Lrf and Fa facies associations (Figure 5.7d, 5.8d). The geometry is channel-shaped. The lower boundary is a fifth order bounding surface and is an erosional contact more commonly into the point bar element (F5) or occasionally into the floodplain element (F7). The upper boundary of the element grades into the floodplain element (F7) and forms a fourth order surface. The chute channels are up to 70 cm in height and 2 m in width. This element only occurs within the Sarnoo Sandstone only.

The chute channels are generally structureless but can display graded bedding (Figure 5.12).

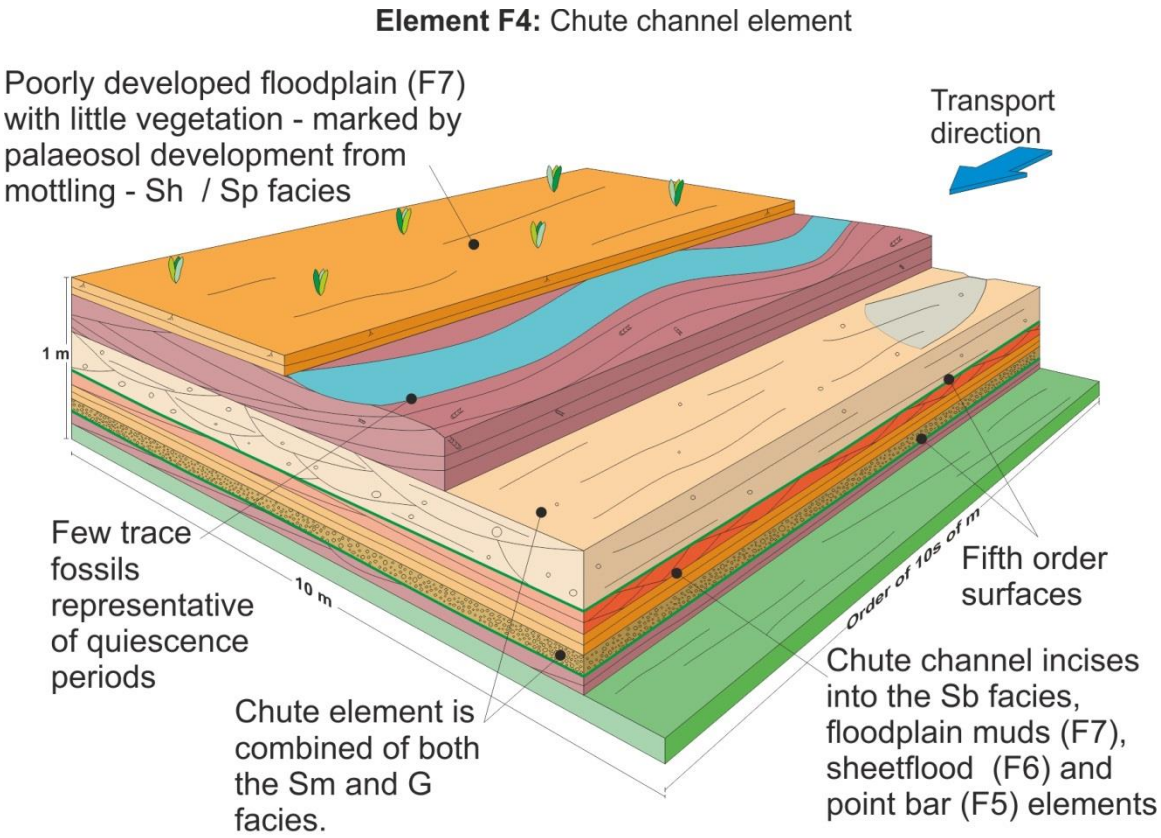

Figure 5.12: The three-dimensional architectural element model displays the chute channel eroding into the point bar (F5), sheetflood (F6), floodplain (F7) elements, forming fifth order bounding surfaces. The channels are generally formed of Sm facies as they were deposited with a highly concentrated sediment–water mix, which would have formed during flooding events from the fluvial channel.

5.2.5 Point bar element – F5

The point bar contains the Lrf and Lfa facies associations (Figure 5.7e, 5.8e). The geometry is wedge-shaped. Lower boundary is a fifth order surface and is either concordant or gradational to the sandy bar element (F1). The upper boundary is gradational into the floodplain (F7) and channel margin (F2) elements and represents a fourth order surface. The height of the element is up to 4 m and the width at most 15 m.

Internally, the geometries and boundaries are sets and cosets of low-angle cross-beds truncating against third and fourth order bounding surfaces (Figure 5.13). The sets and cosets of the element are consistent. These sets and are commonly arranged starting with the Lfa and the Lrf is generally above dominated by the Sla facies, thus forming laterally migrating barforms.

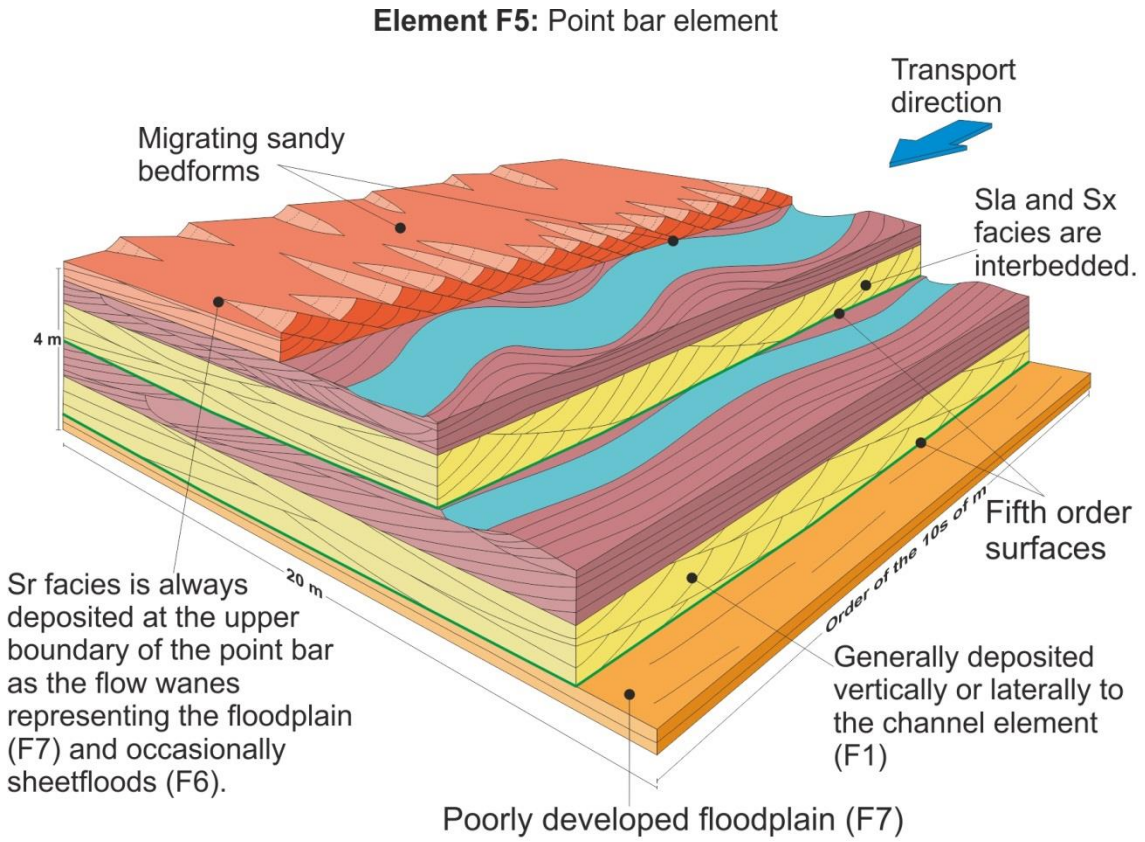

Figure 5.13: The three-dimensional representative model of the point bar model displays the fifth order lower boundary from the sandy bar element (F1) and the fourth order upper boundary is either the floodplain element (F7) or the sheeflood element (F6). The internal boundaries generally form low-angle cross-bedding. The point bar element passes laterally into the channel element (F1). The model displays the migration of sandy bedforms in the flow direction.

5.2.6 Sheetflood element – F6

The facies associations within the sheetflood element are Lrf and Fa (Figure 5.7f, 5.8f). The geometry is sheet-like, tabular and laterally extensive throughout the Sarnoo Sandstone and tabular within the Nosar Sandstone. The lower boundary forms a fifth order bounding surface and is concordant from underlying sandy bar (F1) or gravel bar (F3) elements. The upper boundary is a fourth order surface and is gradational, or has been eroded into by the sandy bar (F1), chute channel (F4), point bar (F5) or floodplain (F7) elements. The sheetflood has a vertical thickness between 0.5 – 2 m.

The internal structures consist of sets of ripple lamina (Sr facies) and plane beds (Sb facies; Figure 5.14). There can be supercritical climbing indicating a high sediment yield.

These sediments can be bioturbated after deposition. Plant leafs have been found in the sheetfloods of the Sarnoo Sandstone.

They are typically organised with a fifth order bounding surface and ripple lamina (Sr, Scl, first and second order surfaces), structureless beds horizontal laminations (Sh facies), and finally overlain by plane beds (Sb facies).

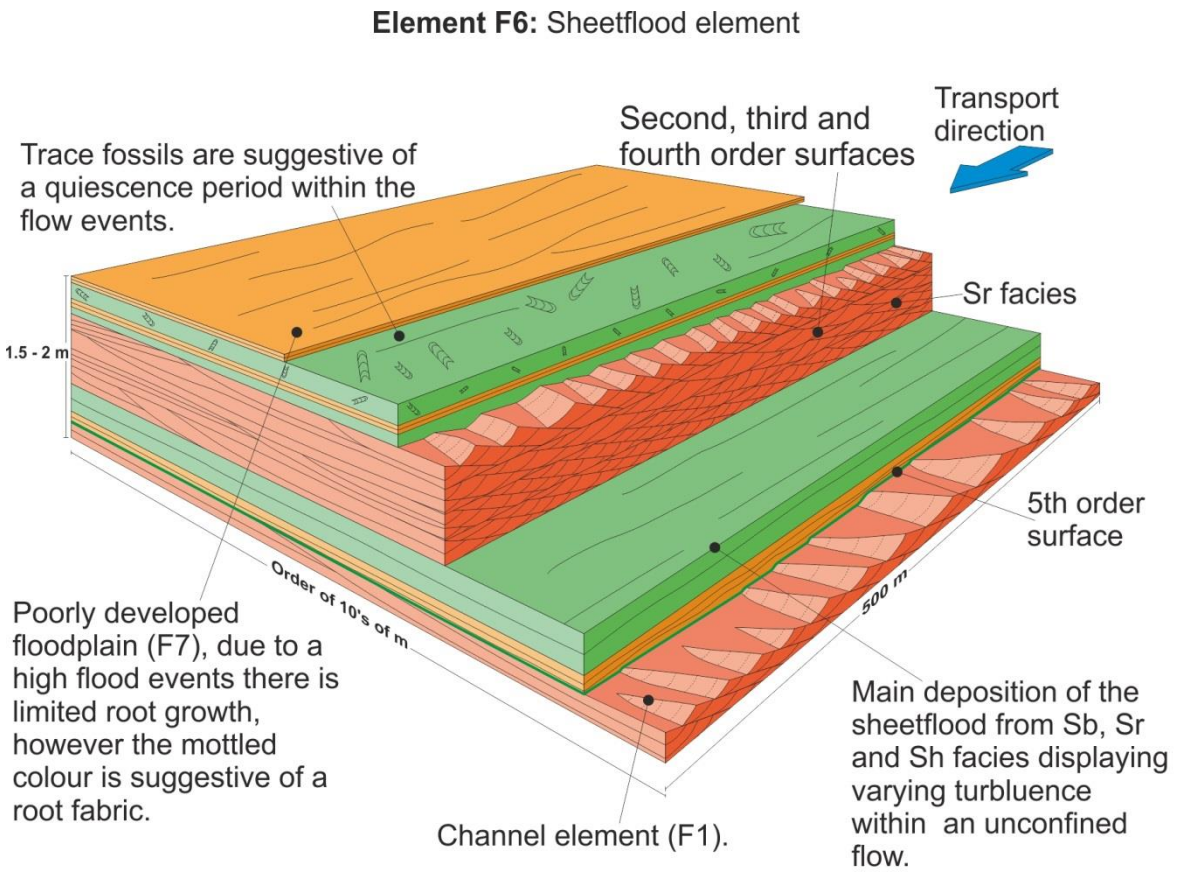

Figure 5.14: The summary model displays the sheetflood element encompassed within the sandy bar element (F1) and the floodplain element (F7). The start of the sedimentary package indicates a fifth order surface. The model exhibits a waning flow from Sb to Sr and waxing flows from Sr to Sb as the velocity of the flow is unsteady. The model demonstrates the migration of sandy bedforms in the downstream direction. Lastly the model demonstrates trace fossils within the sedimentary environment which occur during quiescence periods.

5.2.7 Floodplain element – F7

Luf, Fa and Pa facies associations form the floodplain element (Figure 5.7g, 5.8g). The geometry is tabular and laterally extensive. The lower boundary forms a sixth order surface for the siltstone successions and a fourth order surface when noted within the sandstone successions. The boundary is gradational from the sandy bar (F1), gravel bar

(F3) and point bar (F5) elements. The upper boundary marks a fourth order surface, is sharp and eroded into by the sandy bar element (F1). The lateral extension of the floodplain extends across all the field areas up to 10 km and ≤30 m in thickness. The remnants of floodplain deposition within the sandstone successions are small (≤2 m in width and ≤1 m in thickness) and lenticular.

The internal boundaries are limited and occasionally preserve first and second order surfaces (Figure 5.15). However, the internal surfaces are obscured by bioturbation. There are fourth order surfaces where the pond element (F8) is noted. There are subaerially exposed surfaces preserved (Figure 5.7g). Areas within the floodplain element are heavily mottled and have pedogenic textures. There is no distinct idealised facies succession, but the succession forms from cumulative soils and occasionally vertisols.

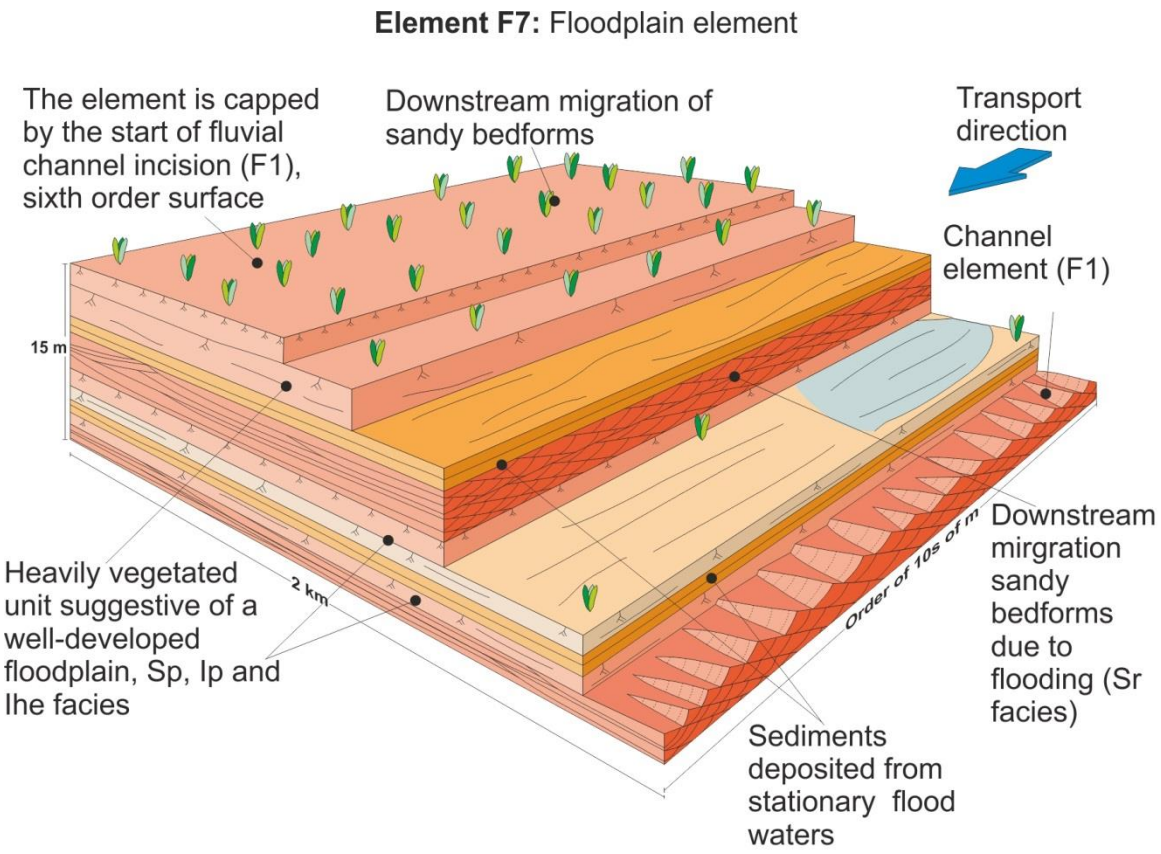

Figure 5.15: The floodplain element three-dimensional architectural element model displays Lrf and Cdd facies associations. The model demonstrates relationships to the channel element (F1), as the lower boundary grade from the channel into the floodplain; whereas the upper boundary is sharp due

to the erosion from the channels (F1). There are roots, soil structures and rhizoliths noted, forming a palaeosols and vertisols in places.

5.2.8 Pond element – F8

The Luf and Fa facies association are within the pond element (Figure 5.7h, 5.8h). The lower and upper boundaries form fourth order surfaces and grade into the floodplain (F7) element. The vertical height is 2 m and the lateral extent is at most 50 m. The geometry is lenticular.

The internal geometries consist of ripple-scale bedforms (first and second order surfaces) and horizontal laminations (Sh facies, Figure 5.16).

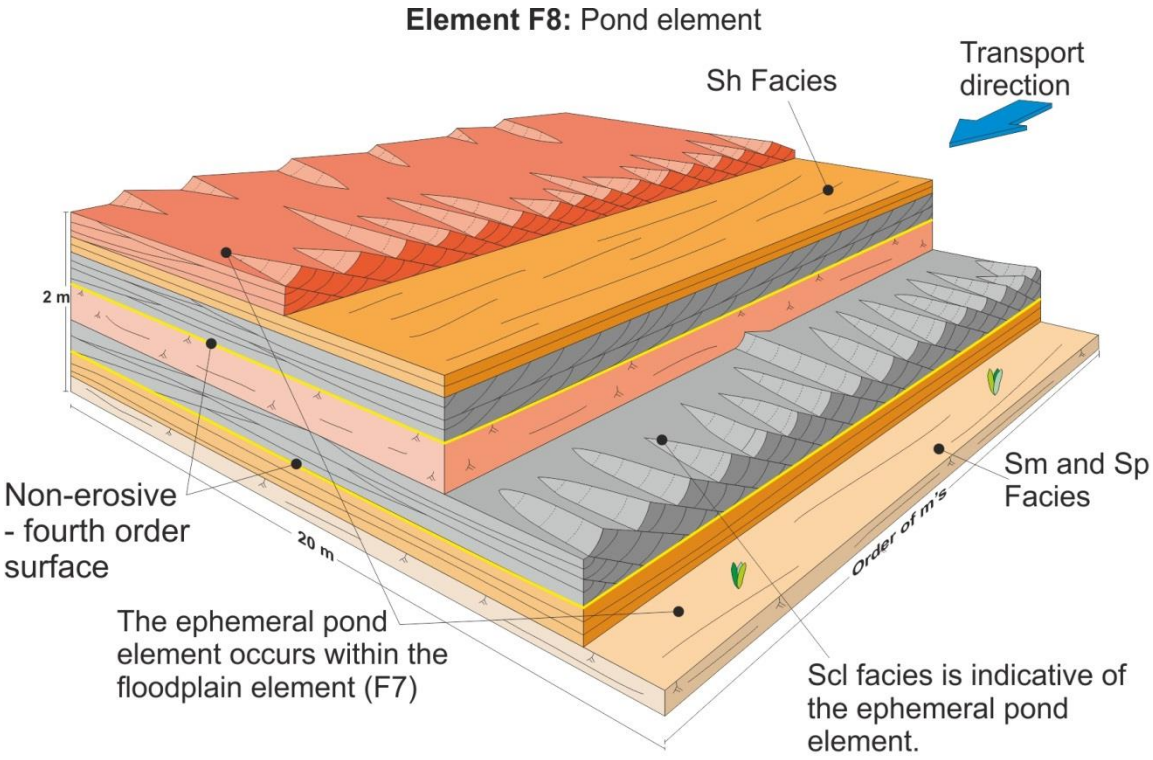

Figure 5.16: The three-dimensional architectural element pond model delineates the interbedded nature of the Sh / Scl facies. The Scl facies is indicative of the ephemeral ponds. The ephemeral pond element is surrounded by the floodplain element (F7). The model displays the migration of the sandy bedforms in the modern environment.

5.3 Facies models

The facies models are built directly from the field area which benefits from numerous small quarries that provide three-dimensional exposures. The channelised sandstones form the dominant fluvial regime, with the background claystone and siltstones forming the

associated floodplain environment. Four styles of fluvial deposition were modelled: (1) a gravel-bedload dominated, low sinuosity fluvial system, (2) a mixed bedload, high sinuosity fluvial system, (3) a sandy-bedload dominant, well-developed, low sinuosity fluvial system, and (4) the floodplain environment.

5.3.1 Gravel bedload-dominated low sinuosity fluvial system

The base of the bedload-dominated low sinuous fluvial facies model (Figure 5.17) is highly erosive and composed the gravel bar element of both matrix- and clasts-supported conglomerates (F3). Other architectural elements are sandy bars (F1) and the floodplain (F7). The gravel bar elements within this facies model are fairly tabular and they eroded into one-another, forming fourth, fifth and sixth order bounding surfaces. The channel elements here are isolated. The bedform and barform migration of the gravel bars were not long lived and easily eroded. This system has no consistent cosets, suggesting a high avulsion rate, multiple fluvial channels and transient bars (Bridge, 1993). The high avulsion rate plus multiple gravel bars observed at outcrop is suggestive of fluvial immaturity, as the sediment input is seasonally high regardless of the water level as there are both debris and fluid flow deposits, as seen in the modern environments on the facies model (Figure 5.17). There are areas within the succession that hold boulder size clasts of sediment that are from fluvial bank collapse (Figure 4.11a). The proportion of channels and gravel bars to floodplain is approximately 90:10. The floodplain is very limited which is likely to be because of the high avulsion rate and transient bars. Although it cannot be ruled out that the sparse exposure of the outcrop could be the reason for the limited amount of floodplain.

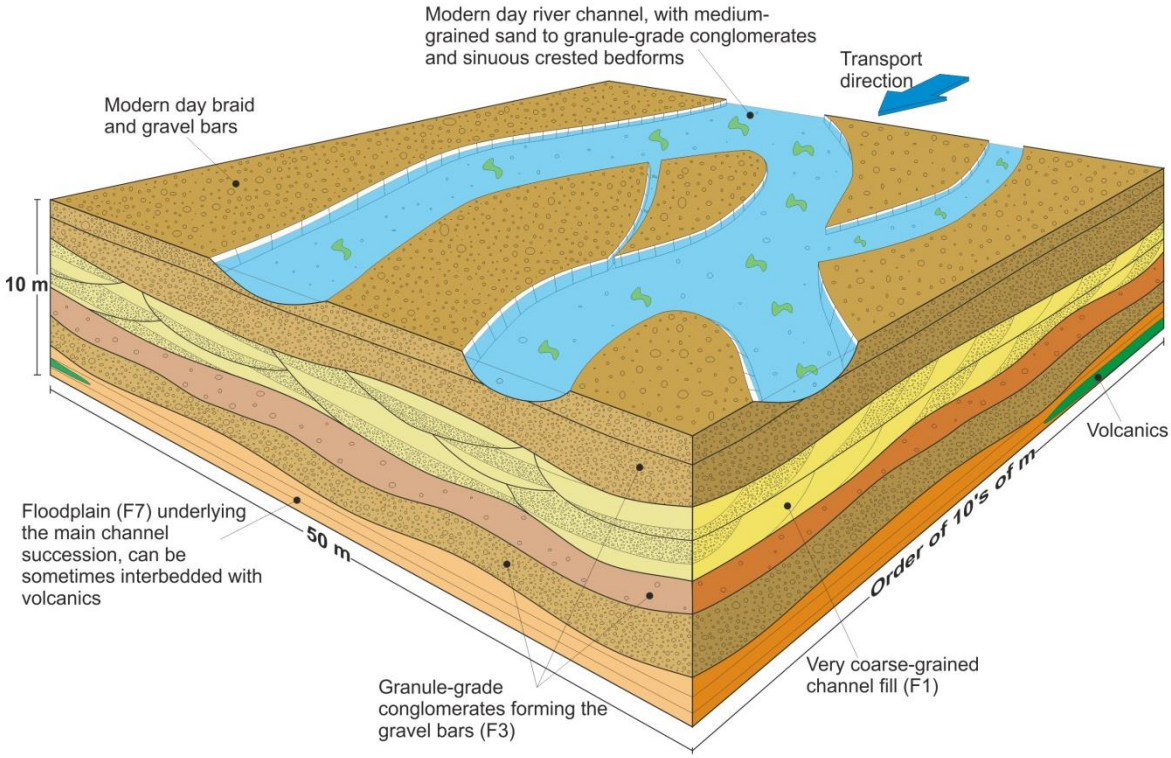

Figure 5.17: Facies model of the bedload dominant low sinuosity fluvial system, which contains the sandy bar (F1), gravel bar (F3) and the floodplain (F7) architectural elements. There are fourth to sixth order bounding surfaces within. The sets and cosets within are inconsistent suggesting the gravel bars are transient, suggesting fluvial immaturity. The proportion of channels to floodplain is 90% to 10%, respectively.

5.3.2 Mixed-bedload high sinuosity fluvial system

Observed extensively at outcrop are low-angle cross-beds representing point bar deposits (F5) there are also sandy bars (F1), channel margin (F2), gravel bars (F3), chute channels (F4) sheetfloods (F6) and floodplain (F7) architectural elements. The gravel bars, sheetflood and floodplain elements are generally tabular and there are concordant contacts between these and the other elements. The channel and point bar elements are erosive and form in-channel and wedged-shaped geometries, respectively. The sets and cosets (containing first and second order surfaces) within this sandstone are regular and consistent. Third to fifth order surfaces are frequent and attest to the variability within the bedform and barform migration within or adjacent to a fluvial channel system (Figure 5.18). In the lower part of the facies model there are coarse-grained sandstones and granule-grained conglomerates, with trough and planar cross-bedding. Whereas the upper part of the facies model contains fine-grained sandstones with ripple-scale bedforms; this suggests declining flow velocities. The amount of sediment within the system becomes

less through time as noted by the decrease in climbing angle and the increased consistency of the cosets. The fluvial channels start to amalgamate and laterally accrete producing point bars (Figures 5.3, 5.4, 5.18). The top of the succession is dominated by the floodplain element with associated vegetation, bioturbation and meniscate backfill trace fossils, as denoted within the modern environment. The proportion of sand to mud increases up through the facies model from 80% sand and 20% mud to 60% sand and 40% mud towards the top.

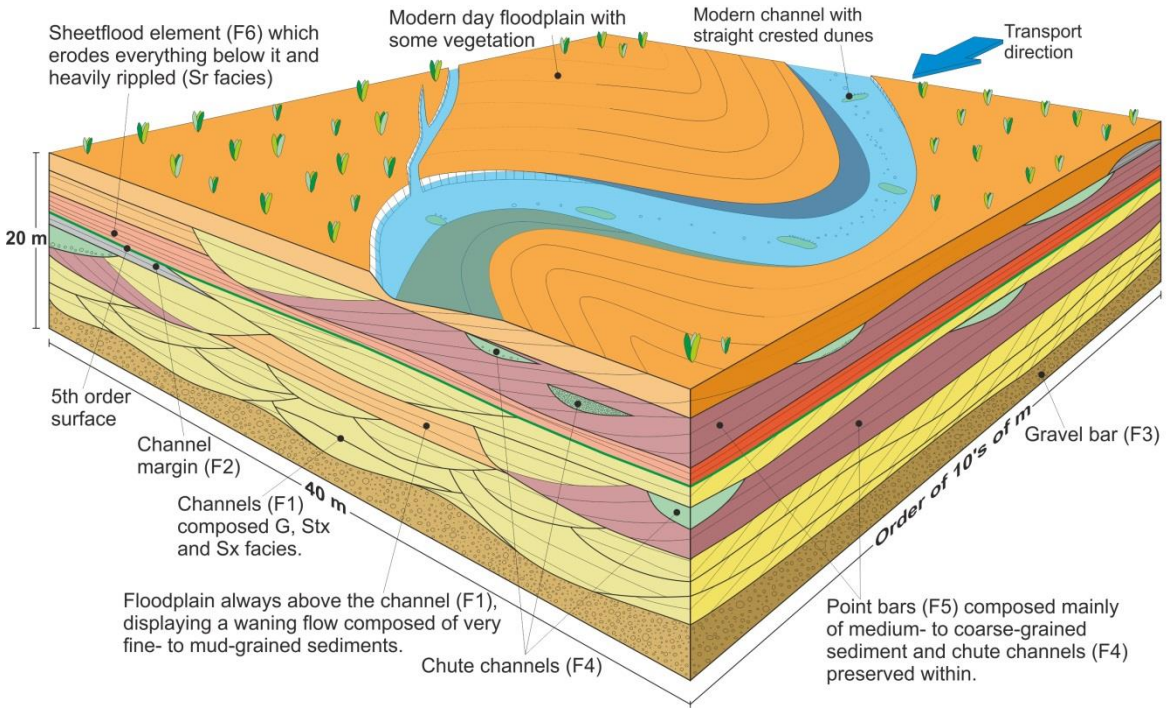

Figure 5.18: Facies model of the mixed load high sinuosity fluvial system, as evidenced by the sandy bars (F1), channel margin (F2), gravel bars (F3), chute channels (F4) sheetfloods (F6) and floodplain (F7) architectural elements. The consistency of sets and cosets representing the migration of in-channel bedforms suggests discharge stability. The proportion of sand to mud increases from 80% sand and 20% mud to 60% sand and 40% mud throughout the facies model.

5.3.3 Sandy bedload-dominant well-developed low sinuosity fluvial system

The well-developed low sinuosity fluvial system (Figure 5.19) contains four architectural elements which are stacked and amalgamated sandy bars (F1) with little floodplain material (F7), gravel bars (F3) and sheetfloods (F6). The amalgamated channels together have a tabular geometry, as do the gravel bars and sheetfloods, and they are both bounded by a fifth order bounding surfaces, which are erosive. The sets and cosets within

the channels and barforms are erratic (Figure 5.2) indicating migration of bedforms and barforms. This indicates a varying sediment supply and discharge throughout deposition. In places the facies is structureless potentially from rapid deposition due to hyperconcentrated sediment-laden floods (Bordy *et al.,* 2004), as displayed in the modern environment. The floodplain geometry here is lenticular and the preservation is scarce. The proportion of channels to floodplain is approximately 90:10 indicating a high net to gross.

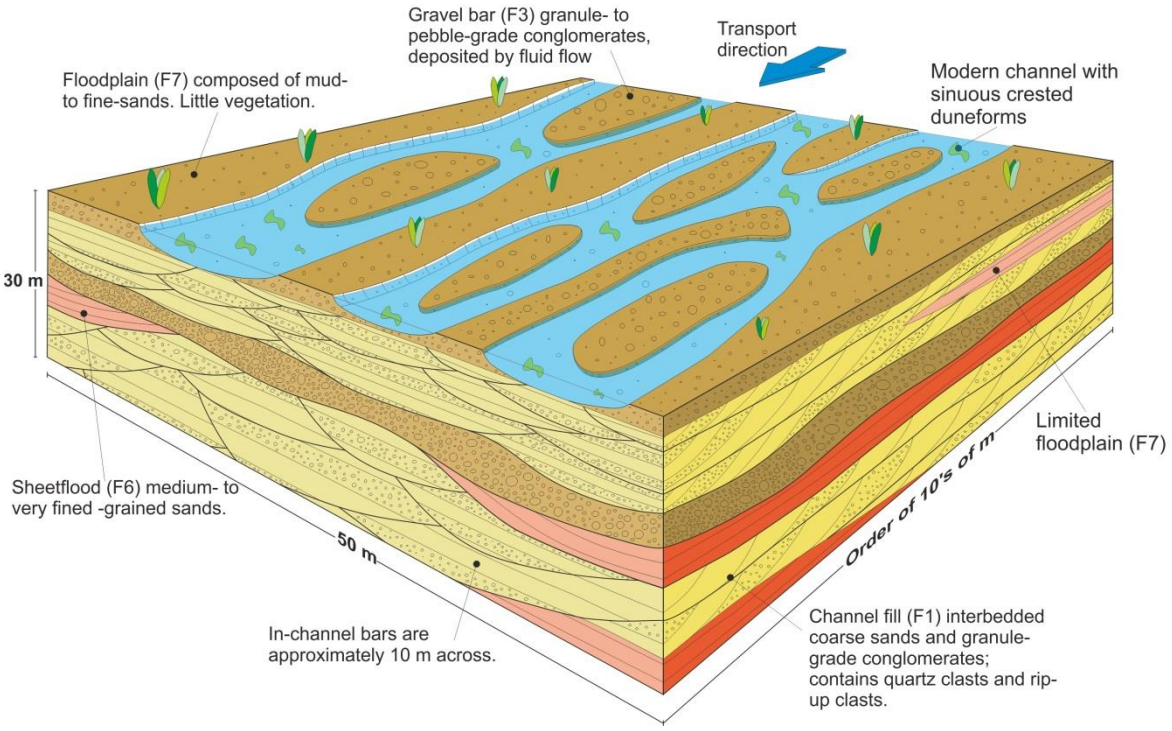

Figure 5.19: Facies model of a well-developed, bedload dominant, low sinuosity fluvial system displaying sandy bars (F1), floodplain (F7), gravel bars (F3) and sheetflood (F6) elements. There are all six types of bounding surfaces within indicating erratic surfaces and multiple truncations. This suggests discharge irregularity and a high level of channel migration. The proportion of sand to mud is at 90:10.

5.3.4 Floodplain

The siltstones are red and with white patches and formed of two architectural elements; the floodplain (F7) and pond (F8) environments (Figure 5.20). They both interbed and boundaries are concordant fourth order surfaces. These siltstones are pedogenically altered indicating soil development. As the soils form from a continuous sediment supply with little to no erosion indicating cumulative soil growth. Within the soil packages there

are roots, rhizoliths, haematite filled fractures and haematite filled nodules. The rhizoliths here are white, grey and orange in colour, where the grey and white represents the depletion zone from the organic material which can be up to 30 cm in length and the orange is from the goethite impregnation (Figure 5.21), indicating vertisols, similar rhizoliths are also seen by Kraus and Hasiotis (2006, Figure 5.21d). The proportion of floodplain sands to floodplains muds is 40% to 60% respectively.

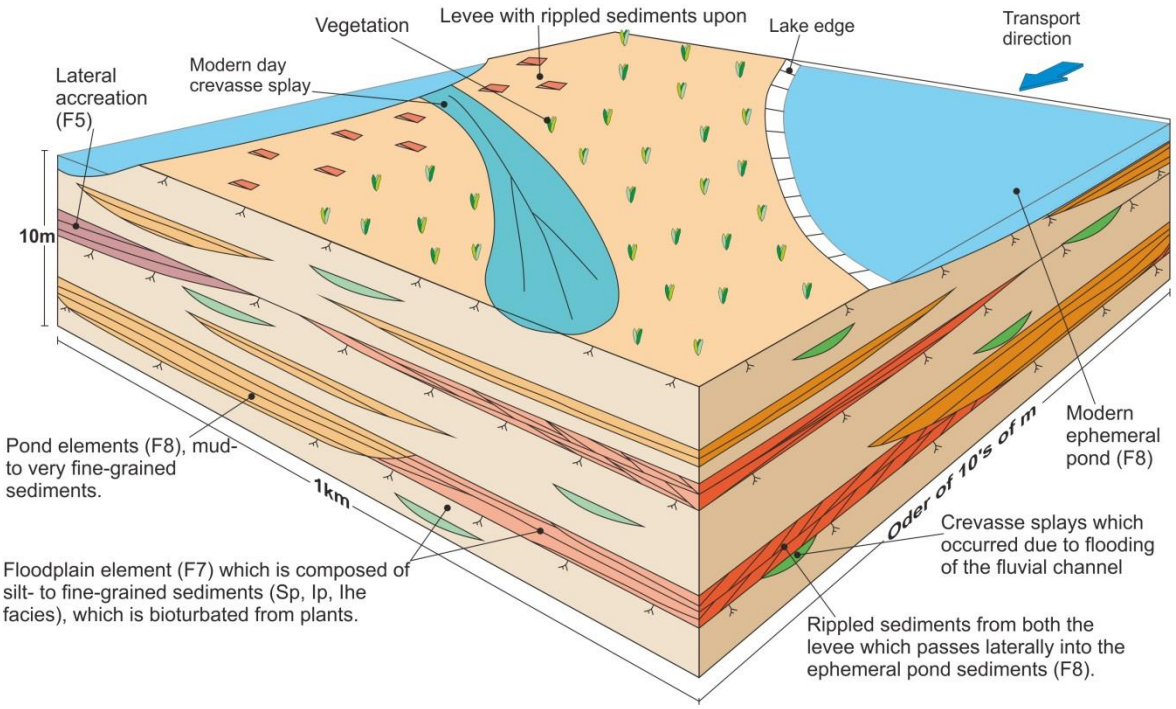

Figure 5.20: Facies model of the floodplain environment, displaying thick and well vegetated floodplains (F7) and pond (F8) elements.

5.4 Depositional elements

The Ghaggar-Hakra Formation can be characterised by these four facies models (Figure 5.22). The Ghaggar-Hakra Formation at outcrop is approximately 100 m thick and can be divided into six separate depositional elements (DE).

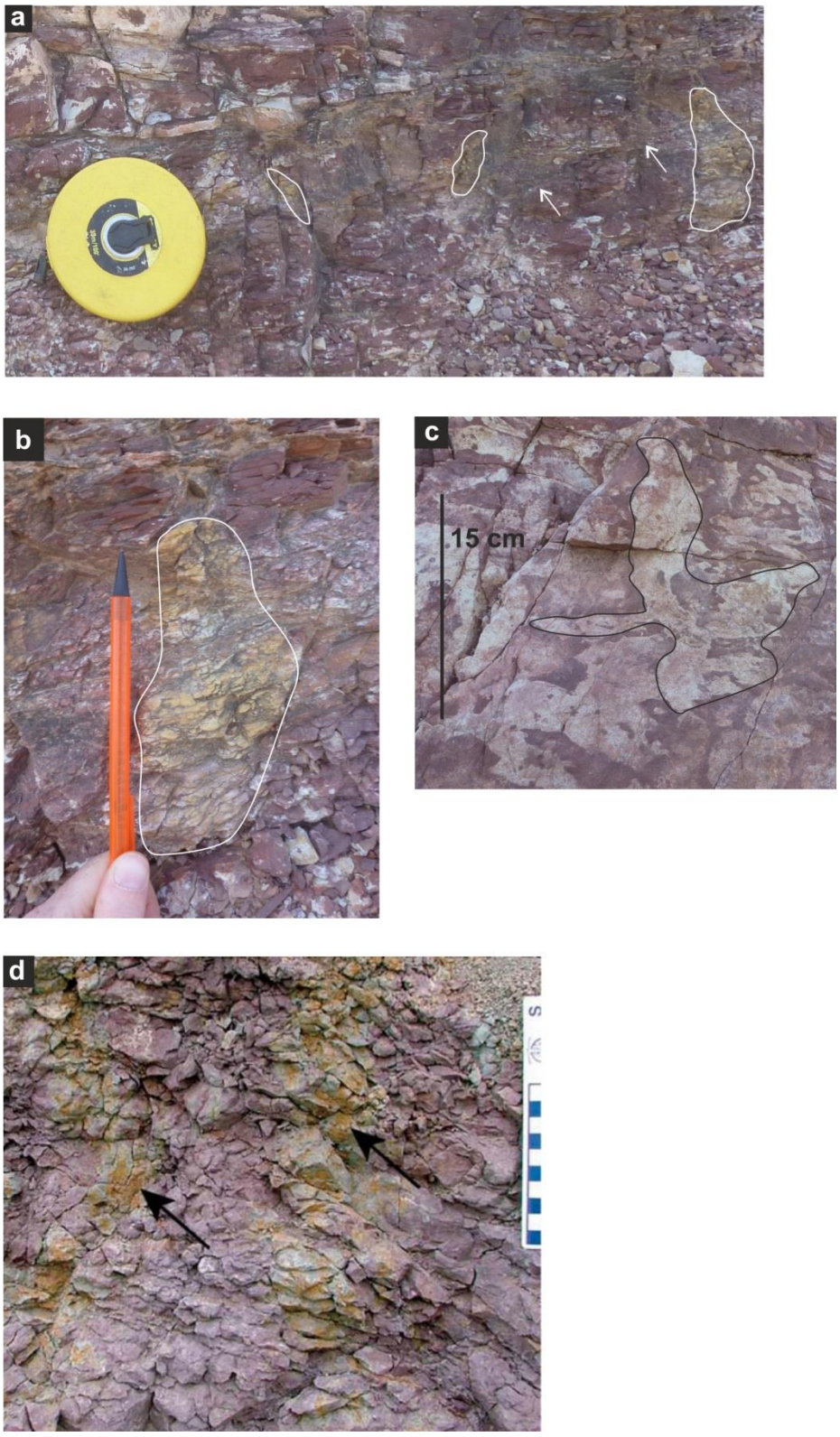

Figure 5.21: Rhizoliths within the floodplain sediments of the formation (a) and (b) orange rhizoliths within the formation; (c) white reduction zones due to the organic material within the roots and rhizoliths, and; (d) the orange rhizoliths from Kraus and Hasiotis (2006), to allow for an easy comparison.

DE1

The base of the formation and the first depositional element is marked by a sixth order surface. The thickness of this sedimentary package is at most 6 m. This sedimentary package is comprised of isolated sandy bars (F1) which have third to fifth order surfaces within them and gravel bars (F3) with either fourth or fifth order surfaces, third order surfaces internally and they are amalgamated representing a bedload dominated, low sinuosity fluvial system. This sandstone succession is equivalent to the lithostratigraphical package of the Darjaniyon-ki Dhani Sandstone and is representative of an immature fluvial system.

DE2

Above DE1 there is a sharp contact marking the start of the siltstone succession (Figure 5.22) where the sedimentary package is up to 25 m thick. Within the sedimentary package there are fining and coarsening upwards successions representing the floodplain (F7) and pond (F8) elements, respectively. The floodplain element contains well-developed ferricate palaeosols, with soil slickenlines and a haematitic nature. The isolated pond elements are up to 2 m deep and at most 50 m wide and are noted by the first and second order bounding surfaces within the ripple-scale strata. There is a regional vegetated surface (fifth order surface) approximately three-quarters of the way up the sedimentary package with calcite-filled fractures which terminate against the regional surface (Figure 5.7g). This surface marks the top of a well-developed vertisol.

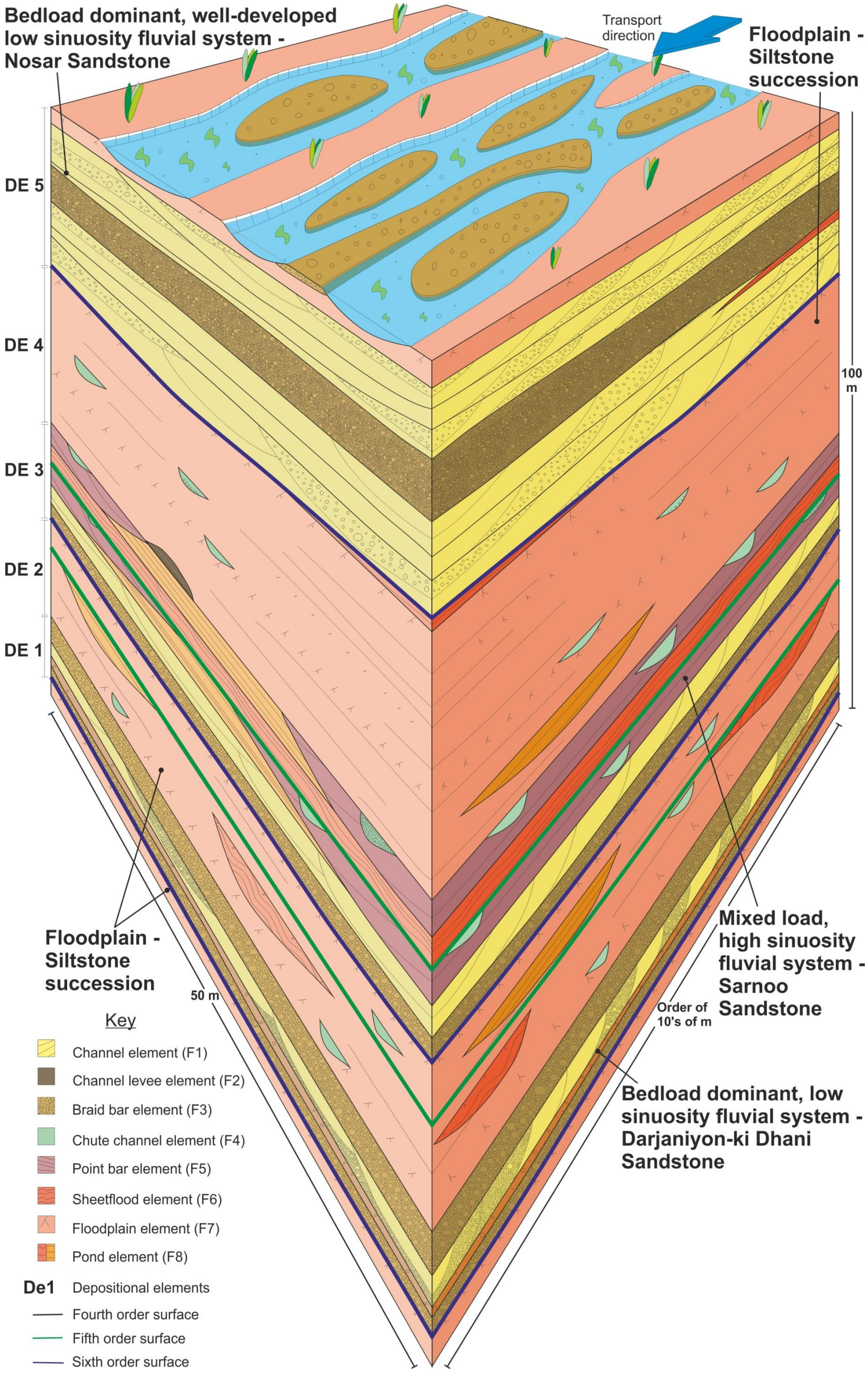

Figure 5.22: Depositional model of the Ghaggar-Hakra Formation displaying six depositional elements (DE). Depositional elements 2 and 4 are formed from the floodplain facies model and form a concordant lower boundary to the underlying sedimentary packages. The first depositional element (DE1) is the bedload dominant, low sinuosity fluvial system facies model which relates to the Darjaniyon-ki Dhani Sandstone. The third depositional element (DE3) is the mixed load, high sinuosity fluvial system facies model which directly relates to the Sarnoo Sandstone. The fifth depositional element (DE5) is formed from the bedload dominant, well-developed, low sinuosity fluvial system relating to the Nosar Sandstone. Depositional elements one through four represent a maturation of the fluvial system from low to high sinuosity. The fifth depositional element represents rejuvenation of the fluvial system.

This well-established floodplain incorporates palaeosols and fourth order surfaces relating to ephemeral ponding from the flooding of the fluvial system. The fifth order surface within this package represents a regional drying out of the floodplain environment and a depositional quiescence period. This floodplain environment is well-developed and argues for a long-lived floodplain.

DE3

The third depositional element (Figure 5.22) is up to 20 m thick and composed of a fining upwards succession. There are consistent sets and cosets containing first to third order surfaces. There are fourth and fifth order surfaces marking the bases of the channels, gravel bars and point bar elements. Around 2/3 of the way up the succession there is a distinct 2 m thick sheetflood package with ripple strata (Sr, Scl facies) with both subcritical and supercritical climbing. The package also contains chute channels cross-cutting the point bar and floodplain deposits.

The consistent sets and cosets within the channel and point bar elements represent the mixed bedload, high sinuosity facies model which is equivalent to the Sarnoo Sandstone. This fluvial system is mature. The increased consistency of the sets and cosets and the decrease in fifth order bounding surfaces suggests stabilisation of the fluvial system from the Darjaniyon-ki Dhani to Sarnoo sandstones.

DE4

The fourth depositional element is the upper siltstone package (Figure 5.22) which has a sharp contact with the underlying sandstone succession. The siltstone succession is up to 20 m thick. This package of sediment displays upwards fining relating to the waning flows from the channel leading to deposition on the floodplain element (F7). The floodplain

contains abundant well-developed palaeosols throughout. This sedimentary package contains fewer ponds then the siltstones below, again suggesting a stable fluvial system.

The floodplain is well-developed as noted through the development of the palaeosols. There are first and second order sets representing the flooding of the fluvial system. There is a distinct lack of ponding within this floodplain when compared to the lower floodplain environment.

DE5

The final depositional element (Figure 5.22) is at least 25 m thick. The base of the element is a highly erosive sixth order surface. The succession is composed of the fining upwards sandstone successions representing amalgamated and stacked sandy bars (F1) with gravel bars (F3) marked by a fifth order surfaces. The sedimentary fill from first to fourth order surfaces. There are small (up 1 m thick and 2 m wide), lenticular packages of floodplain (F7) material preserved above the channel element.

The final depositional element is a bedload dominant, well-developed, low sinuosity fluvial system which relates to the Nosar Sandstone. The highly erosive nature, multiple rip-up clasts, and sporadic sets and cosets provide evidence of varying sediment supply and discharge. The Nosar Sandstone displays rejuvenation of the fluvial system from high to low sinuosity.

5.5 Summary

The bounding surface analysis here is based on Miall's (1988) interpretation of first to sixth order bounding surfaces. These surfaces indicate different relationships between each of the facies, facies associations, bedforms and barforms. The bounding surface analysis and the facies association have been combined to form eight architectural

elements that are attributed to confined (F1, F2, F3, F4, F5) and unconfined elements (F6, F7, F8).

The architectural elements within the formation combine to form four separate facies models which determine the relative proportions and interactions of the architectural elements and the bounding surfaces separating them. The *bedload-dominant, low sinuosity fluvial system* is dominantly composed of the gravel bar elements and amalgamated channels with a highly variable discharge and is laterally equivalent to the Darjaniyon-ki Dhani Sandstone, DE1.

The *mixed-load, high sinuosity fluvial system* is dominantly identified with channels, point bars and gravel bar elements and there is an increased consistency of sets and cosets representing the migration of in-channel bedforms and barforms. This succession is laterally equivalent to the Sarnoo Sandstone (DE3). This suggests increased discharge stability, when compared to the other sandstone successions.

The third facies model is a *sandy bedload-dominant, well-developed, low sinuosity fluvial system*, where there was a high level of channel migration (channel and gravel bar elements) indicating irregularity in discharge evidenced by the first and second order surfaces. The lower surface of this model is highly erosive. This model is best represented by the Nosar Sandstone, DE5.

The final facies model is composed of the floodplain and pond architectural elements and was deposited within a floodplain environment heavily influenced by bioturbation. This model is represented by the floodplain deposits, DE2 and DE4.

In summary, the Ghaggar-Hakra Formation is interpreted here as a fluvial system that evolves through time and is affected by extrinsic processes. These processes are

discussed in Chapters 7 and 8. The next chapter (6) supplements the field evidence with petrographical evidence which allows for extrinsic processes and provenance to be assessed.

6 Chapter Six: Petrography and SEM analysis of the Ghaggar-Hakra Formation

Petrography and SEM analysis of sedimentary and igneous rocks is a well-established investigatory process (Dickinson *et al.,* 1983; Dickinson, 1985; Poppe *et al.,* 1989; Besra *et al.,* 2000; Tucker, 2001; Garzanti *et al.,* 2003; Garzanti *et al.,* 2008; Garzanti *et al.,* 2013a, b) that is often used to reconstruct provenance, erosional history, transport history and diagenetic evolution (Burley *et al.,* 1985; Weltje and Eynatten, 2004). Furthermore, combined petrography, heavy-mineral and SEM analyses can determine the type of plate-tectonic setting of sediment provenance (Dickinson and Suczek, 1979; Garzanti *et al.,* 2003; Garzanti *et al.,* 2008; Garzanti *et al.,* 2013a, b). Analysis of both the detrital grains and authigenic cements can determine the compositional maturity and pore-space availability.

The petrographical and SEM analyse presented here, not only determines the provenance of the Ghaggar-Hakra Formation, but also justifies the sediment transport systems, and provide insights into diagenetic evolution and reservoir quality controls. They also quantify the fieldwork observations.

This chapter introduces and discusses the minerals that are typically present within sandstone successions and how they relate to their provenance and their indication of the type of sedimentary system they were deposited in. The chapter also discusses past petrographical work on the Ghaggar-Hakra Formation and then goes on to discuss the implications with measured porosity from thin section analysis. The chapter concludes by discussing the results from the petrographical analysis of the fifty samples.

6.1 Literature synthesis

Detailed here is the applicability of detrital siliciclastic minerals for provenance analysis. Additional consideration is given to how provenance, textural and compositional maturity

affects the hydrocarbon prospectivity. The previous work carried out on the Ghaggar-Hakra Formation is also discussed (Sisodia and Singh, 2000; Bower, 2004a; Gould and Jones, 2012; Jones, 2013).

6.1.1 Classification of siliciclastic sediments

Using the detrital minerals within siliciclastic sediment it is possible to classify the sediment objectively and fully, and to determine the provenance (Dickinson *et al.,* 1983; Garzanti *et al.,* 2007). Several objective classification schemes for siliciclastic rocks exist, but the QFL (Quartz, Feldspar, Lithics) scheme (Pettijohn 1955) is used most commonly. It derives a descriptive name for sediments based on the relative proportions of quartz, feldspar and lithic detrital minerals within a sample. These observations can then be related to provenance models of Dickinson (1985) and Garzanti *et al.,* (2013a) to determine the geological terrane or the plate tectonic setting.

Quartz is the most common, geologically stable, detrital mineral within sandstones. Average sandstone compositions comprise about 65% detrital quartz grains (Pettijohn 1955; Tucker 2001). Two separate types of detrital quartz grains can be recognised; monocrystalline quartz (Qm) and polycrystalline quartz (Qp) grains. Monocrystalline quartz can be characterised as strained or unstrained and is characteristically derived from a metamorphic origin. Polycrystalline quartz grains are commonly derived from metamorphic and plutonic igneous rocks (Blatt and Christie, 1963). Quartz can be derived from continental blocks, magmatic arcs, and from recycled orogens, and the plate type can be determined from the relative proportions of the detrital quartz grains (Dickinson and Suczek, 1979; Dickinson *et al.,* 1983).

Feldspar types include potassium (alkali) and plagioclase (calcic) feldspar. Alkali (K) feldspar is generally more common as a detrital grain in sedimentary rocks and indicates an igneous provenance (Adams *et al.,* 1984). Both types of feldspar are highly unstable

and breakdown into, or are replaced by, micas and clays, mainly as a result of mesogenesis but can also occur as a result of chemical weathering. When feldspar breaks down during mesogenesis it forms illite, filling the intergranular areas and coating detrital grains when chemical weathering breaks down plagioclase albite will form. Although alkali feldspar is more resilient then plagioclase it commonly breaks down to anatase (Adams *et al.,* 1984) during diagenesis.

Lithics within this research are termed rigid rock fragments, are generally coarse-grained and formed from sedimentary, metamorphic and / or igneous fragments. These fragments can be related to a plate-tectonic setting, as igneous fragments are derived from an igneous setting and metamorphic fragments are from metamorphic settings.

Sedimentary rock fragments within sandstone successions are mainly chert or sandstone fragments. Chert fragments are stable and resistant to weathering. Large sandstone fragments are common (Adams *et al.,* 1984) and predominantly consist of composite detrital quartz grains. Fracturing of large fragments can reduce the porosity of siliciclastic sediment (Chuhan *et al.,* 2002). Calcite, dolomite and limestone grains can also be common within sandstone packages, and again indicate the provenance of the sedimentary system. Other grains include fossils, which can be useful for palynological age and environmental constraints.

Igneous rock fragments are generally composed of plagioclase lath sets within an altered groundmass comprising plagioclase, hornblende, pyroxene or olivine (Adams *et al.,* 1984; Tucker, 2001). The igneous rock fragments can be unstable when they are dominantly composed of feldspar, as feldspar easily breaks down due to diagenesis or chemical weathering (Dickinson, 1985).

Metamorphic rock fragments are commonly defined by one of two textures, slatey or schistose, each resulting from differing amounts of temperature and pressure to which the parent rock has been exposed, and the development of metamorphic minerals. A five-stage scheme to the 'rank' metamorphism of rock fragments contained within sedimentary rocks is commonly employed based upon texture and metamorphic minerals (Table 6.1). Increasing rank represents a general increase in metamorphic pressure and temperature.

Rank	Description
1	Weak development of slaty cleavage
2	Display strong fabric realignment
3	Development of schistosity
4	Well-developed muscovite or amphiboles
5	Coarse polyhedral crystals of biotite or hornblende

Table 6.1: Rank of metamorphism (Garazanti and Vezzoli 2003; Garazanti *et al.,* 2007).

Lithic fragments can indicate if the source of the sedimentary succession was sedimentary, igneous or metamorphic in origin, leading to the geological terrane or the plate tectonic setting (Figure 6.1). Generally, the plate tectonic settings for sedimentary fragments are stable cratons or through recycled orogeny (Figure 6.1). Igneous fragments are predominantly derived from magmatic arcs, whereas metamorphic fragments are from areas of basement uplift (Figure 6.1, Dickinson, 1985).

Micas can be divided into muscovite and biotite and commonly form only a minor percentage of the bulk composition of sedimentary rocks. Both minerals occur as detrital flakes concentrated along bedding planes and fractures. Muscovite is more chemically stable then biotite (Tucker, 2001). Detrital micas originate from igneous rocks and accumulate in fine sands and silts (Tucker, 2001).

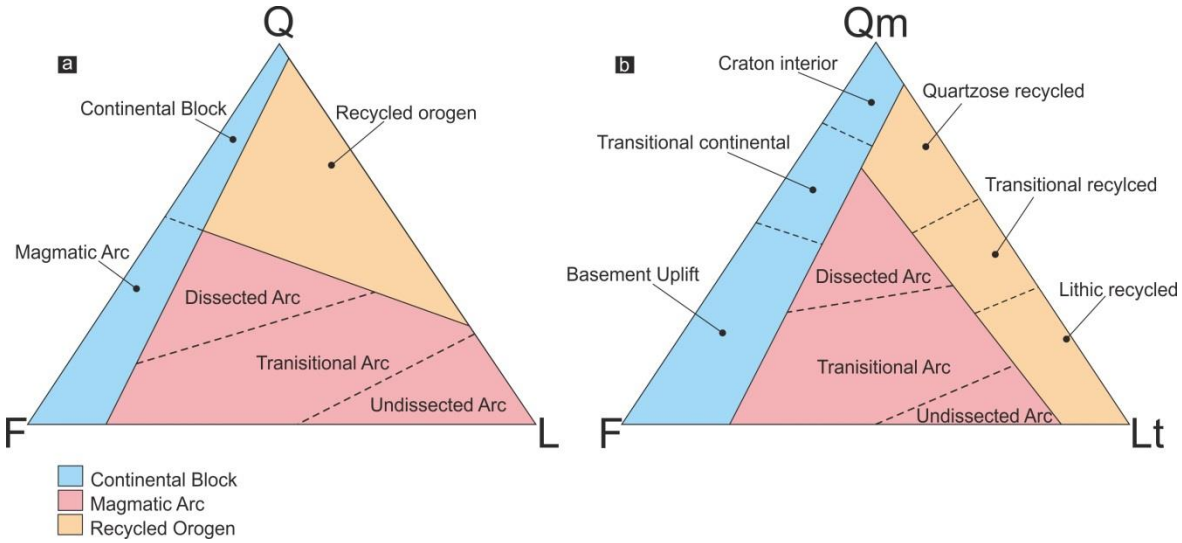

Figure 6.1: QFL plot of the framework models for sandstone suites and their likely plate tectonic provenance, a) Q – quartz grains, F – feldspar grains and L – unstable lithic fragments and; b) Qm – monocrystalline quartz grains, F – feldspar grains and Lt – total polycrystalline lithic fragments including stable polycrystalline quartz and unstable lithic fragments (Dickinson *et al.,* 1983).

Heavy minerals are very minor within the detrital content of siliciclastic rocks (>1% of the bulk composition), and commonly include grains of the non-optically opaque minerals apatite, epidote, garnet, rutile, staurolite, tourmaline, zircons, and the optically-opaque minerals illmenite and magnetite. In general, heavy minerals are ultra-stable, and are therefore resistant to chemical and mechanical weathering and may indicate a variety of parent rocks. Common sources of heavy minerals (Table 6.2) can lead to confusion over their provenance and heavy minerals alone should not be used to determine the source of the sediment (Tucker, 2001). Due to differences in chemical stability, heavy minerals can determine how local the sedimentary source is.

Source Rock	Heavy minerals
Basic Igneous	Augite, ilmenite, rutile
Felsic Igneous	Apatite, hornblende, biotite, zircon, magnetite
Low grade metamorphic	Biotite, tourmaline
High grade metamorphic	Epidote, garnet, kyanite, sillimanite
Pegmatite	Flurite, garnet, tourmaline
Sedimentary	Rounded tourmaline and zircon (reworked)

Table 6.2: Sources of heavy minerals adapted from Tucker (2001)

Detrital and authigenic clays can only be noted when under SEM. In general, clays infill intergranular areas and coat the detrital grains, this can alter the texture and compositional maturity of a rock (Blatt, 1982; Tucker, 2001). Detrital clays reflect the

source-area geology, climate and weathering processes whereas the authigenic clays are generated in situ.

There are many types of clay common in sedimentary rocks such as: kaolinite, illite, chlorite, gibbsite and smectite. These clay types form under a wide variety of temperatures and pressure conditions, implying that the type of clay is influenced by the diagenetic processes, stratigraphical succession and depositional environment (Carrigy and Mellon, 1964). If diagenesis occurs clays can form a pseudomatrix.

Kaolinite booklets can have cementing phases and dominantly result from authigenic processes. They typically infill pore space, and can form around the edges of the detrital grains. Kaolinite forms between depths of 600 m to 2000 m (Nyman *et al.,* 2014). At depths of 2500 m and below kaolinite will start to morph into dickite (at 3000 m) and the dickite will be disorganised. At 4500 m the dickite is highly organised (Beaufort *et al.,* 1998). At depths between 600 m and 3000 m feldspar dissolution can influence the pore waters and therefore can increase the influence of the kaolinite to dickite transformation (Lanson *et al.,* 2002). Below 3000 m burial depths feldspar is mostly dissolved and is unlikely to influence the transition between kaolinite and dickite, it is suggested by some authors that for dickite to form feldspar dissolution has to take place (McAulay *et al.,* 1993). The transition is kinetically controlled (Beaufort *et al.,* 1998; Lanson *et al.,* 2002) and below 4500 m kaolinite is absent, however it is reported that in the Hutton Field, North Sea, kaolinite is absent below 3300 m (McAulay *et al.,* 1993).

Illite is a micaceous mineral formed from silica within alkaline pore waters along with magnesium and iron. Illite will not form below temperatures of 100°C (Eberl and Hower, 1976; Wilkinson and Haszeldine, 2002) suggesting it is likely to form during diagenesis. Illite forms at depths between 3000 m to 5000 m (Bjorkum and Gjelsvik, 1998; Bove *et al.,* 2002). Illite will not form in reservoirs unless there is a change in the geological conditions

such as: oil charging, an influx in highly acidic pore fluids or an increase in pore pressure rates (Wilkinson and Haszeldine, 2002). The change in the geological conditions needs to be enough to overcome the kinetic barrier to allow illite growth. The illite acts as both pore coating and pore filling.

Authigenic cements include microcrystalline quartz, quartz overgrowths, anatase, calcite and dolomite. These cements are used to gain an understanding of the diagenetic history of the formation. With regards to hydrocarbons and reservoir forming sandstones the authigenic cements can occlude the pore space, therefore reducing the reservoir quality of any given sandstone succession. If there is the formation of authigenic cements then hydrocarbons were not present at the time. The following minerals are formed through diagenesis.

Microcrystalline quartz forms through pressure dissolution of in-situ volcanic rock fragments or by the passage of groundwater causing silica enrichment (French and Worden, 2013). Microcrystalline quartz forms at temperatures of approximately 100°C - 125°C, with depths of 2000 – 3000 m and the crystals generally grow up to 5 µm in length (Worden and Morad, 2000; Worden *et al.,* 2012; Fischer *et al.,* 2013). Microcrystalline quartz does not grow at the same rate as the host grains (Vagle *et al.,* 1994) and is generally responsible for approximately 40% of the porosity occlusion (Worden and Morad, 2000). The amount of quartz cementation is controlled by the source of the dissolved silica, the transport of the silica, and the reprecipitation as quartz cement (Worden and Morad, 2000). The quartz cementation can control the amount of hydrocarbons within a reservoir, for example samples from the Brent Field, North Sea display a clear relationship between high reservoir quality and the optimal amount of microquartz (Aase *et al.,* 1996).

Microcrystalline quartz generally grows on its a-axis but occasionally it does grow on its c-axis, this growth is controlled by the orientation of the detrital grains (French and Worden, 2013) and the amount of pore space. Examples of c-axis growth can be seen within the Fontainebleau Formation in central France and the Heidelberg Sandstone, Subhercynian Cretaceous Basin, Germany (French and Worden, 2013). This growth produces high porosity high microcrystalline quartz.

Quartz overgrowths grow around the detrital grains due to silica precipitation. Pressure dissolution of minerals such as feldspar creates silica enrichment and when silica becomes supersaturated overgrowths occur, these overgrowths occur around 80°C (Wilkinson and Haszeldine, 2002). Cryptocrystalline quartz overgrowths are more likely to form on euhedral monocrystalline quartz grains than polycrystalline quartz grains (Lander *et al.,* 2008), due to the differences in crystal shape.

Haematite cement occurs as rims around the detrital grains, as a result of post depositional processes such as suspension or precipitation from the iron-rich groundwaters within continental environments (Burley *et al.,* 1985). Iron cements generally develop above the water table; however, occasionally they can develop under the water table providing that the ground waters are both alkaline and oxidising (Tucker, 2001). Haematite cement can be spatially distributed in relation to lithology, depositional structures (facies, architectural elements), faults and fractures, and permeability (Chan *et al.,* 2000).

Anatase cement forms at temperatures of 300°C and forms through alkaline cements (Batzill *et al.,* 2006).

Calcite cement morphologies are poikilotopic and drusy calcite spar. Calcite cements form at temperatures between 10°C to 90°C (Heydari and Moore, 1989). The cements can be

precipitated due to the introduction of alkaline pore waters into cracks within the detrital grains or through the infilling of interstitial porosity (Nyman *et al.,* 2014). Calcite cements can replace the detrital grains. The alkaline pore waters associated with calcite can etch and corrode the detrital grains and hinder overgrowths (such as quartz and feldspar; Tucker, 2001). Whether the overgrowths are etched indicates whether the calcite formed after or before the overgrowths. However, calcite can be precipitated after overgrowths due to increasing pH and / or temperature within the rock mass (Tucker, 2001; Nyman *et al.,* 2014).

Dolomite cements vary from poikilotopic to microcrystalline pore-filling cements. They are more commonly iron-rich suggesting conditions are being reduced. Dolomite forms at temperatures between 50°C and 100°C (Heydari and Moore, 1989). Magnesium and alkaline pore waters are needed before dolomite cement can be produced from clays or silicates (Tucker, 2001). The cements form within pore spaces and can etch, corrode and replace grains.

6.1.2 Textural and compositional maturity

Sediments that are poorly sorted, with idiomorphic grains and have a high amount of matrix are classed as texturally immature sediments, whereas moderately sorted, sub-rounded and low-matrix sediments are classed as texturally mature sediments. Finally, well sorted, sediments, with no matrix are considered supermature sediments (Figure 6.2). Transportation processes can affect the textural maturity of a sedimentary rock, as the more texturally mature the sediments are in theory the further they have travelled. Therefore immature sediments are generally closer to their source area, having not travelled far, suggesting they have experienced little reworking (Tucker, 2001). Mature sediments experience the opposite. These simple concepts are not applicable when the source area is compositionally mature for example, a polycyclic littoral setting (Tucker, 2001).

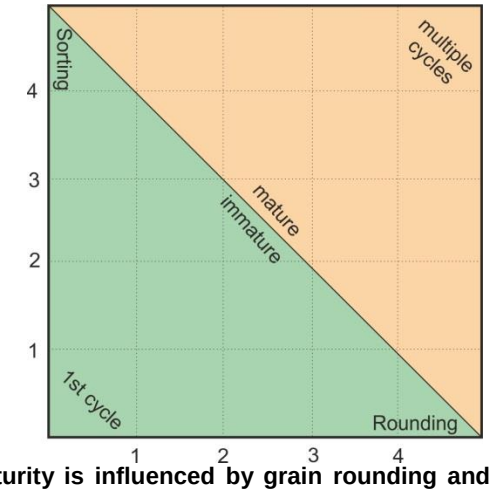

Figure 6.2: Sedimentary maturity is influenced by grain rounding and sorting, a higher sorting and rounding displays a high maturity and a lower sorting and rounding displays a lower maturity. If there are multiple cycles of sediment reworking then it is likely that these sediments have a higher maturity (Amy Gough, 2016; pers comms).

Compositional maturity is defined as the degree of weathering that the source area underwent, affecting the detrital grains and the degree of reworking of the grains during transportation (Tucker, 2001). Both processes can influence the composition and textural maturity of the sediment. If an arenite contains unstable grains, such as rock fragments and feldspars, then it is classed as immature. If an arenite is composed of dominantly quartz and some feldspars then it is compositionally mature. Supermature arenites are formed of dominantly quartz grains with little to no matrix. Compositional maturity reflects chemical weathering processes in the source and depositional areas (Tucker, 2001).

6.1.3 Mineral relationship to provenance

Detrital grains form the framework of most sandstones, conglomerates and breccias. Between these detrital grains there is a matrix composed of authigenic minerals which bind the detrital grains together (Tucker, 2001). Any naturally occurring minerals can occur within clastic sediments, but the relative abundance of a particular mineral is dependent on its abundance within the source area and the amount of weathering (mechanical and chemical) it undergoes along the transport pathway (Tucker, 2001; Limonta, 2012). Climate influences the weathering of minerals as mineral dissolution within quartz-rich sediments occurs more prominently within hot humid, semi-arid and polar regions (Burley *et al.,* 1985; Potter, 1997; Nesbitt *et al.,* 2013).

6.1.3.1 Other controls

Other controls on the mineralogical content are tectonics (primary control), transport mechanisms, the depositional environment, and diagenetic alteration (Dickinson *et al.,* 1983). Plate tectonic settings affect all the mineral composition within the deposits. Rigid rock fragments and detrital quartz grains are affected by temperature and pressure changes within the plate (Dickinson and Suczek, 1979; Dickinson, 1985; Garazanti and Vezzoli, 2003; Tucker, 2001).

Geological terranes

There are four major geological terranes or plate settings in which sandstones are derived; these are recycled orogens, magnatic arcs, continental blocks and basement uplifts (Figure 6.1, Dickinson *et al.,* 1983; Dickinson, 1985; Garzanti *et al.,* 2014).

Recycled orogens occur within subduction complexes and within fold and thrust belts where the crust is uplifted. The lithologies tend to be quartz-rich and volcanic (Dickinson, 1985), such as the Betic Cordillera, Almeria. Sediments at outcrop contain well-sorted, rounded detrital quartz grains, and heavy minerals such as hornblende, biotite, zircon, magnetite, ilmenite and rutile.

Magmatic arcs display positive relief and are mainly composed of volcanic and plutonic rocks that are produced by continuing subduction along arc-trench systems (Dickinson, 1985) e.g. island and continental arcs (Garzanti *et al.,* 2014), such as the Mariana Islands. Noted within the sediments that are derived from these areas are igneous heavy minerals (Table 6.2) and durable igneous rock fragments.

Continental blocks are consolidated regions of amalgamated ancient orogenic belts (Dickinson, 1985). Continental blocks form within the continental interior or on passive platforms and within the rock record, they are dominantly composed from poorly sorted,

quartz-arenites but can contain feldspars and lithic fragments (Garzanti *et al.,* 2014). Basement uplifts, such as the Colorado Plateau, occur along the rift shoulder, and produce sandstones composed of quartz, feldspar and a limited amount of lithic fragments (Dickinson, 1985).

Diagenesis

There are three types of diagenesis: 1) eogenesis (early, shallow burial); 2) mesogenesis (later, deep burial); and 3) telogenesis (tectonic burial and uplift; Burley *et al.,* 1985; Tucker, 2001). Diagenesis is controlled by depth of burial, compaction of sediments and pressure dissolution. 'Early' (eogenesis) events take place due to precipitation from depositional pore waters and their evolving derivatives at relatively shallow depths, whereas 'later' (mesogenesis) events largely involve fluids isolated from surface recharge that are subject to increasing temperatures and pressures as burial proceeds.

Eogenesis is noted from four main processes: compaction, grain dissolution, grain replacement, and precipitation of authigenic minerals. The compaction of the sediment is mechanical and can be up to 50% of the intergranular area; in general 25% of the bulk sandstone will be lost (McAulay *et al.,* 1993). Grain dissolution includes the leaching of detrital grains and the breakdown of detrital grains such as igneous fragments and feldspar (Burley, 1984). Both of these mechanisms allow for the development of secondary pore spaces. Grain replacement is where the authigenic minerals partially, or completely, replace the detrital grains such as, clays, haematite, and carbonate. This replacement is especially noted through the gradual change of detrital muscovite mica into authigenic kaolinite, and of authigenic illite into smectite (Burley, 1984). Authigenic minerals precipitate during this time and their appearance can indicate the depth and temperature of the sedimentary package. Quartz and feldspar overgrowths will form during this time, authigenic clays will coat detrital grains and infill the intergranular areas.

The mesogenesis stage of diagenesis is noted by a massive increase in the secondary porosity and the precipitation of the authigenic minerals (Burley, 1984). Secondary porosity is generated by widespread removal of pore-filling cements. Pore space is also formed by the etching of detrital quartz grains and quartz overgrowth's. The precipitation of authigenic cements is likely to come from the transformation of kaolinite to dickite (Beaufort *et al.,* 1998; Lanson *et al.,* 2002) and illite with low magnesium and iron contents (Burley, 1984) and minor amounts of chlorite and kandite. Precipitation of these cements infill the intergranular areas. Pore-filling and grain coating pyrite will also form, but in the latest of the mesogenesis stages (Burley, 1984). Beyond 10,000 m at around 200°C the processes become akin to burial metamorphism.

Telogenetic processes relate to the fault-generated uplift influenced the meteoric waters (McAulay *et al.,* 1993); where the dip of the rocks can influence the types of groundwaters (Burley, 1984), there are three major changes: (1) unconfined aquifer with oxidizing groundwaters capable of dissolving carbonate; (2) shallow, confined aquifer with reducing groundwaters capable of dissolving carbonate, and; (3) deeper, confined aquifer with reducing groundwaters but are capable of dissolving gypsum (Burley, 1984) and not carbonate.

Arid and humid continental sediments experience similar diagenetic regimes of eogenesis, mesogenesis and telogenesis, however, the dominant difference between the two is the amount of iron which is mobile. Within warm, wet conditions (tropical areas) the pore water is dominantly meteoric and can be either anoxic or oxygenated. During burial the clay minerals become unstable and dissolve, reprecipitating as authigenic cements and clays (Tucker, 2001). If the pore waters are oxygenated, then diagenesis forms kaolinite clays, quartz overgrowths and then calcite cements, (Burley *et al.,* 1985) as feldspar and volcanic rigid rock fragments are dissolved. These cements make reservoir character hard

to predict (Burley *et al.,* 1985). If telogenesis occurs, the sediments can be heavily modified by haematitic cements, providing the pore waters are alkaline in nature.

6.1.4 Previous petrographical interpretations of the Ghaggar-Hakra Formation

The detrital and authigenic mineralogy of the Ghaggar-Hakra Formation has been studied by previous authors (Sisodia and Singh, 2000; Bower, 2004b; Gould and Jones, 2013). This work suggests that the sandstone successions of the Ghaggar-Hakra Formation is composed of fine- to coarse-grained, well sorted quartzarenites with iron oxide, micas, heavy minerals (tourmaline and zircon) and very few feldspar components (Gould and Jones, 2013).

Limited outcrop studies of the Ghaggar-Hakra Formation undertaken in the vicinity of Sarnoo field area recognised three separate sandstone successions (Section 3.3.1.1, Figures 3.5, 3.7; Clarke, 2011; Bladon *et al.,* 2015a, b), that display distinctive petrography (Bower, 2004b). Darjaniyon-ki Dhani Sandstone comprises fine- to coarse-grained sandstone composed of strained monocrystalline and polycrystalline quartz detrital grains often with quartz overgrowths. No feldspar grains were recorded and the cement is comprised of kaolinite and haematite (Sisodia and Singh, 2000; Bower, 2004b). Zircon and tourmaline make up the heavy minerals. The porosity is poorly connected with both primary and secondary pores present (Bower, 2004b).

The Sarnoo Sandstone contains fine- to coarse-grained strained detrital quartz grains. The mineralogy is similar to the Darjaniyon-ki Dhani Sandstone; however, here there are minor components of lithic fragments and heavy minerals (Bower, 2004b). Feldspars are absent. There are primary and secondary pores are poorly connected.

The Nosar Sandstone ranges from fine- to coarse-grained with poor- to well-sorted detrital monocrystalline quartz grains (Bower, 2004b). There are traces of haematite, calcite and

kaolinite cements. The pore spaces are primary and secondary with a poor connectivity (Bower, 2004b).

The petrography reveals a dominantly quartz-arenite succession where the depositional environment was fluvial (Chapter 5; Sisodia and Singh, 2000). The source rock for the sediments of the fluvial system is likely to be metamorphic (Bower, 2004b) due to the strained monocrystalline and polycrystalline grains. Quartz overgrowths and grain replacement suggests little diagenesis has occurred within the outcrop sediments (Bower, 2004b; Gould, 2012; Gould and Jones, 2013). It is likely that the secondary pore spaces are from the dissolution of feldspar.

6.1.5 Porosity

Sedimentary textures, sediment composition, porosity, and permeability all have implications for hydrocarbons. The roundness and sorting of the grains will affect the packing of the grains therefore affecting the porosity of the sandstones; whereas the grainsize of the sandstone does not affect the porosity. There are multiple types of porosity influencing the reservoir quality (Figure 6.3), which are:

- *Primary:* porosity spaces are within the intergranular / intercrystalline areas and are the primary distribution of pores (McAulay *et al.,* 1993).
- *Secondary:* porosity is caused by dissolution of grains such as feldspar or dissolutions of rigid rock fragments. The porosity is noted as secondary intragranular (partial dissolution) and secondary oversized (complete dissolution) porosity (McAulay *et al.,* 1993), caused by pressure due to increasing compaction.
- *Interconnected:* porosity is the volume of connected space allowing for fluid or electrical current to flow between the pores.

- *Effective:* porosity is the pore volume that holds the potential to store hydrocarbons. This excludes non-connected, dead-end pore space and the volume of water bound on clays.

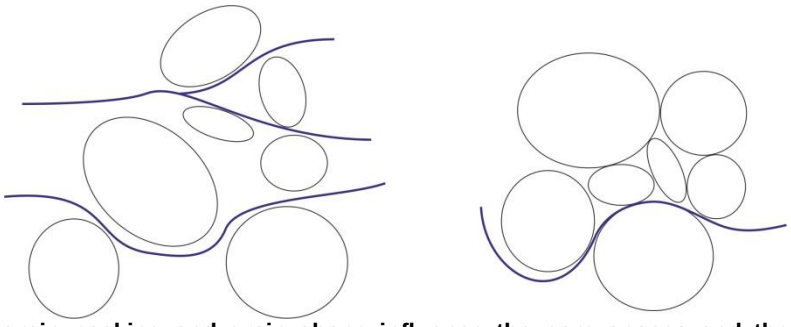

Figure 6.3: The grain packing and grain shape influence the pore spaces and the permeability, a) lightly packed grains, and; b) densely packed grains.

Measured porosity from petrographical analysis in this study is directly measured from polished thin-sections in two-dimensions and therefore, is estimated and not the exact measurement of the porosity in three-dimensions. However, the two-dimensional porosity measures the microstructural information such as the nature of the pore connectivity and any secondary obstruction to the pore space (i.e. through cements). This information cannot be gained from three-dimensional porosity measurements (Meillie and Garboczi, 2001) made through core plugs. The main problem that needs to be overcome in relation to two-dimensional porosity is the connectedness of the porosity, which is often underestimated (Meillie and Garboczi, 2001). Three-dimensional modelling of porosity and cementation can be completed through both well-log and outcrop scale GPR (ground penetrating radar) imaging (Nyman *et al.,* 2014). This has led to more realistic interpretations and proves that two-dimensional analysis can overestimate porosity (Nyman *et al.,* 2014). However, three-dimensional porosity can incorporate statistical fluctuations and resolution errors when computed through GPR. Materials with a lower porosity can be more accurately modelled in both two- and three-dimensions (Meillie and Garboczi, 2001) when compared to materials with a higher porosity.

6.2 Petrographical and SEM analysis of the Ghaggar-Hakra Formation

The petrographic samples were collected from each of the three sandstone successions, from the type localities (Figure 6.4, Appendix 4) at logs 1, 13, 23, 34, and 55. A sample was collected every time the grainsize changed going up the log within the sandstone packages. From the samples collected, careful hammering and sand paper were used to remove all foreign material and create fresh surfaces (Vine and Tourtelot, 1970). Here, 108 samples (100 sandstones and 8 volcanic samples) were impregnated with blue-stained epoxy resin for porosity identification. However, only 50 of the samples were analysed under a transmitted light standard petrographic microscope using the MicroStepper with PETROG^{TM} software. Only 54 samples were analysed due to time constraints on this research, 50 sandstone samples and 4 volcanic samples (Appendix 4). Grainsize and sorting were measured by analysing 100 grains within each sample. Modal composition of each sample was determined by point counting (200 points were counted per sample). Point counting subdivides minerals on their species which forms the modal constituents of the samples and allows for the assessment of the internal textures and fabrics of the samples.

SEM analysis was completed on 9 sandstone samples. Analysis composed of photographs and Bruker EDX analytical system, which enables area analysis, spot analysis, line profiles and image-mapping of the separate elements.

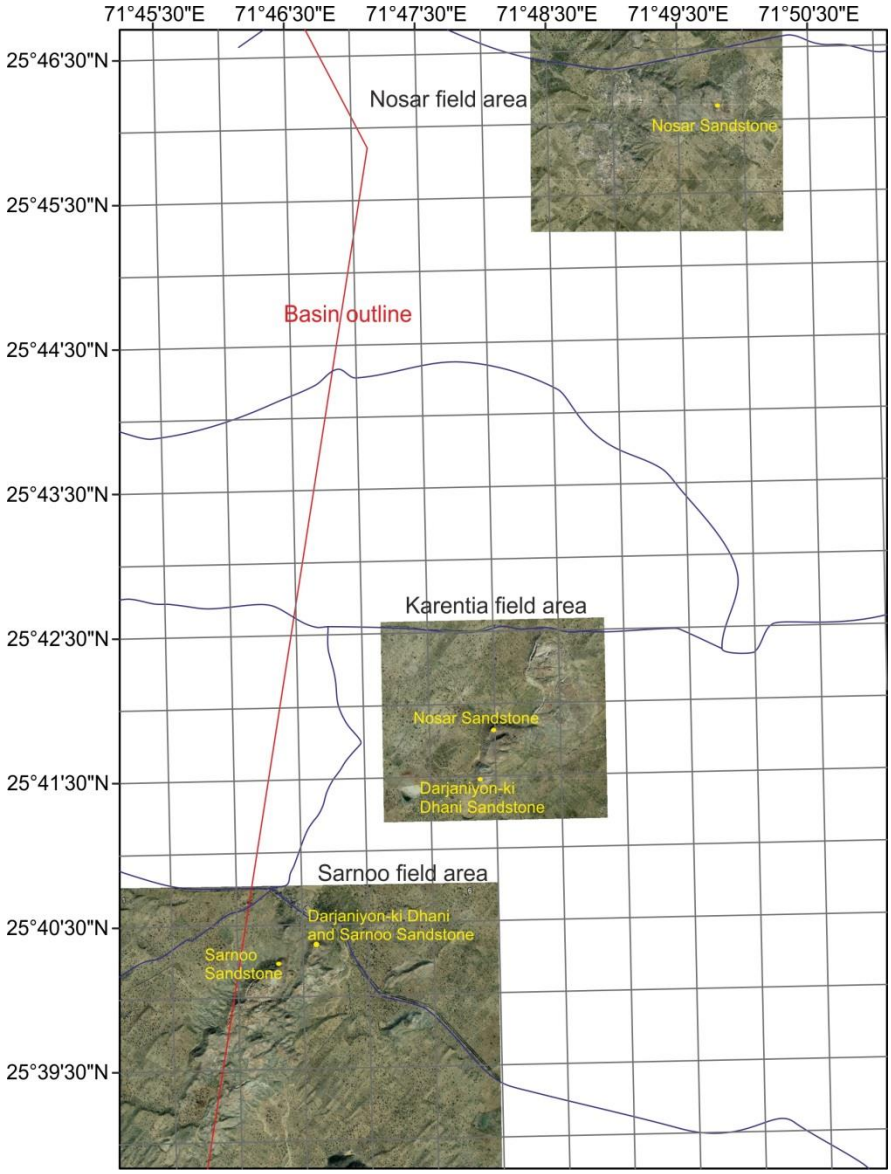

Figure 6.4: Locations of the logs used for sample collection.

6.2.1 Grainsize and sorting

Grainsize is measured using the Udden-Wentworth grainsize classification and varies from lower very fine- to upper very coarse-grained within the measured samples (Figures 6.5; Appendix 3). On samples 6 (within the Darjaniyon-ki Dhani Sandstone) and 104 (within the Nosar Sandstone, Figure 6.6) the grainsize analysis was quality controlled by Stacie Jones (from Ichron, part of the RPS Group), to determine if the grainsize analysis was accurate. These two graphs display the grainsize sampling by both the author and by Jones and suggest that this analysis is subject to anthropogenic interpretation, as both graphs vary, although the grainsize is relatively stable as the trends are similar. The

Darjaniyon-ki Dhani Sandstone varies from fine-grained to pebble-grade sediment, where its mode is upper coarse sand. This sandstone is poorly to moderately sorted. The Sarnoo Sandstone varies in grainsize from silt- to upper coarse-sand, with its mode being lower fine sand. The Sarnoo Sandstone has the most mature sorting (Figure 6.7) varying from moderate to well sorted. The Nosar Sandstone varies from fine-grained to pebble-grade sediment, where the mode is at upper medium sand. The sandstone is poor to well sorted.

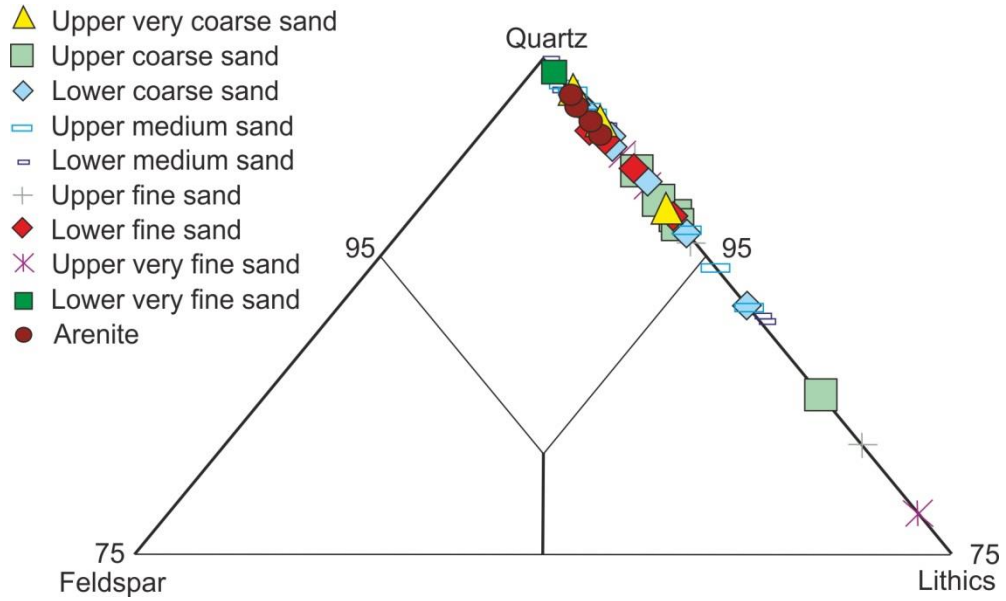

Figure 6.5: QFL diagram displaying the variations of grainsize within the sandstone successions, this relates to the compositional maturity; all data points are within the sublithic-quartzarenite to quartz-arenite range.

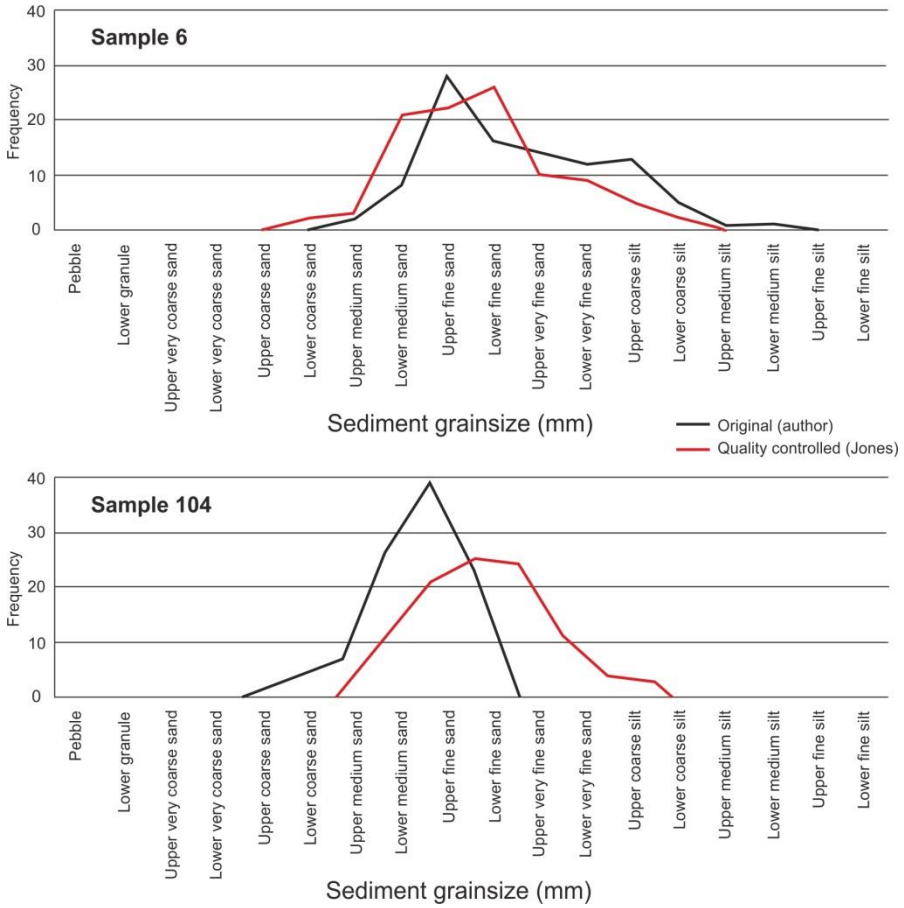

Figure 6.6: Grainsize analysis of samples 6 (Darjaniyon-ki Dhani Sandstone) and 104 (Nosar Sandstone) with the original data (black line) and the quality controlled data (by Jones, Ichron, red line); displaying how subjective PETROG can be, between different interpreters.

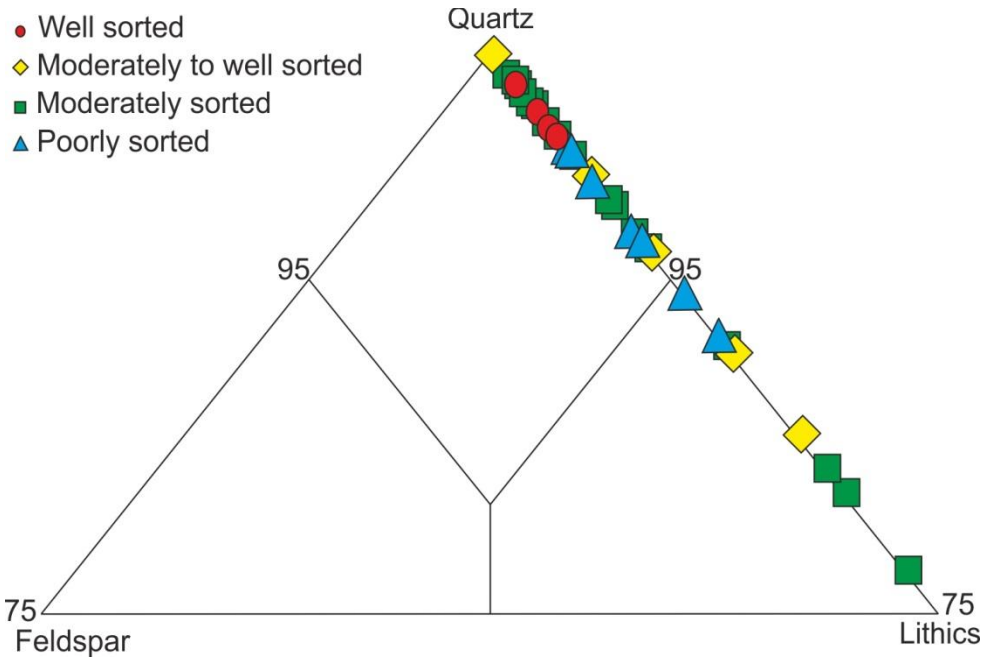

Figure 6.7: QFL diagram of the sorting of the assessed samples, suggesting that the textural and compositional maturities are related and the samples are all within the sublithic-quartzarenite to quartz-arenite range.

6.2.2 Detrital mineralogy and textures

The detrital mineralogy within the three sandstone successions consists of monocrystalline quartz, polycrystalline quartz, sedimentary, metamorphic and igneous rock fragments, undifferentiated grains, heavy minerals (tourmaline, zircon and rutile), muscovite mica, non-resolvable detrital pore-filling clays, non-resolvable pseudomatrix clays and non-resolvable undifferentiated clays.

Monocrystalline Quartz is the most common detrital mineral (Figures 6.8, 6.9, 6.10). The monocrystalline quartz is unstrained to slightly-strained as observed by the undulose extinction. The quartz grains vary from very fine-grained to pebble-grade; the grains are generally well sorted, sub-rounded to rounded with a moderate sphericity. The majority of the grains have concave-convex contacts. A few of the grains are corroded and etched due to chemical weathering. Individual grains have internal porosity and are occasionally in-filled with heavy minerals or haematite. The **Polycrystalline Quartz** grains are coarse, sub-rounded, moderately spherical, and can be slightly elongated. The grain contacts are generally sutured.

Rock fragments are sedimentary, igneous and metamorphic in origin.

Sedimentary fragments are composed of chert (Figure 6.9) which is more common in the Darjaniyon-ki Dhani Sandstone. The chert clasts are medium- to very coarse-grained, sub-rounded and moderately spherical.

Igneous fragments are coarse-grained, sub-rounded and spherical. They are composed of quartz (generally monocrystalline) with inclusions of muscovite grains and are most common in the Nosar Sandstone. These were identified due to their porphyritic nature.

Metamorphic fragments are composed of sutured polycrystalline quartz, which are elongated and most common within the Darjaniyon-ki Dhani Sandstone. These grains are up to pebble-sized, sub-rounded with a moderate sphericity. The metamorphic ranks of rock fragments are based on the Garzanti and Vezzoli (2003) models. This work exhibits ranks of metamorphism between one and two, where there are rough cleavages and elongated grains, indicating a psammite / felsite source.

The identified **heavy minerals** are tourmaline, zircon and rutile. The tourmaline and zircon minerals occur throughout the succession with no particular order to them. Tourmaline grains are subhedral, blocky in appearance, up to medium-grained, sub-angular to sub-rounded with a high sphericity. The birefringence is second-order. The zircons are medium-grained, rounded with a high sphericity and have third-order birefringence colours. The rutile minerals are rounded, with a low sphericity, thin and elongated within the detrital monocrystalline quartz grains. The birefringence is third-order.

The **muscovite mica** expands into the intergranular areas and grows from the rigid detrital minerals (Figure 6.6). The muscovite is very fine- to medium-grained, rounded with a low sphericity. The grains are elongated with third order birefringence colours. Locally the muscovite is being replaced by kaolinite at its terminations.

Non-resolvable clays are composed of detrital pore-filling clays which coat the detrital grains and infill a limited amount of the pore space. The pseudomatrix is a light brown and both fill the pores and coat some detrital grains (Figure 6.6). Under the SEM the detrital clays grains are no bigger than 50 µm, the grains are sub-angular to sub-rounded and moderately spherical. The clays are illite (Figure 6.5) and is likely being replaced by haematite (Figure 6.5) especially within the Darjaniyon-ki Dhani Sandstones (Figure 6.7).

Figure 6.8

Log: 1
Height: 4614 m
Sample Number: 36
Sandstone name: Sarnoo

Facies: G
Architectural Element: Channel (F1)

Grainsize: Upper very fine sand
Sorting: Moderate
Roundness: Subrounded
Sandstone classification: *haematitic* quartzarenite

Detrital Mineralogy: The detrital mineralogy consists of monocrystalline quartz (43.5%), polycrystalline (26.5%), rigid rock fragments (1%: sedimentary 0.5%, igneous 0.5%) and heavy minerals (0.5%). The monocrystalline quartz is slightly strained. The non-resolvable clay (3%: pseudomatrix 2%, detrital pore filing 1%), is discontinuous around the quartz grains. The sediment rock fragments are made from chert. The igneous fragments contain monocrystalline quartz with muscovite inclusions. The heavy minerals within the zircon and tourmaline. Ductile muscovite mica grains (2%) are pore choking. The grains are slightly aligned within the thin section.

Authigenic Mineralogy: The authigenic mineralogy composes of haematite (14.5%) and quartz overgrowths (1.5%). The haematite is pore-filling and coats multiple quartz grains. The quartz overgrowths are syntaxial and discontinuous around their quartz host grains.

Reservoir Quality: Macroporosity (8%) is composed of primary intergranular porosity (7.5%) and secondary oversized porosity (0.5%). The porosity is partly interconnected.

SEM: Images display quartz grains, cements and clays. There are quartz (silica) grains and overgrowths, muscovite (aluminum) grains. Iron cements are between the quartz grains. Undifferentaiated grains here are iron replacing the silica.

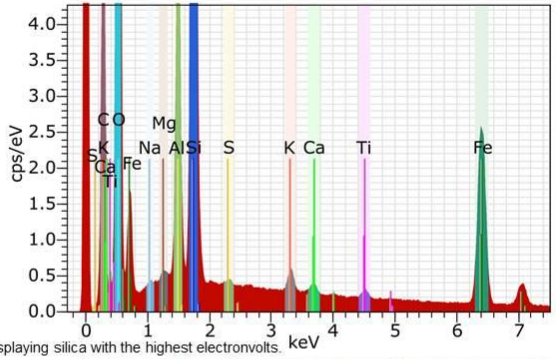

EDAX plot displaying silica with the highest electronvolts.

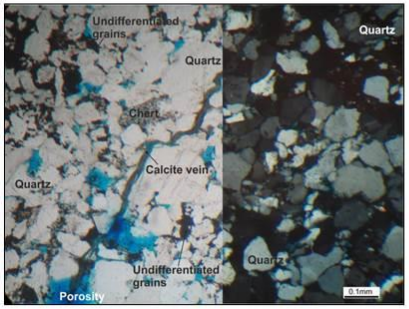

Moderately sorted, subrounded, upper very fine grains. Calcite veins are within grains. Indifferentiated grains and cements are between the quartz grains. Matrix is within between the grains.

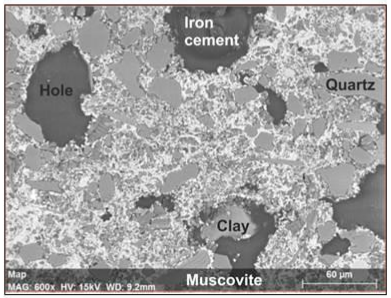

Silica is very abundant. Aluminium and iron cements are abundant between the grains.

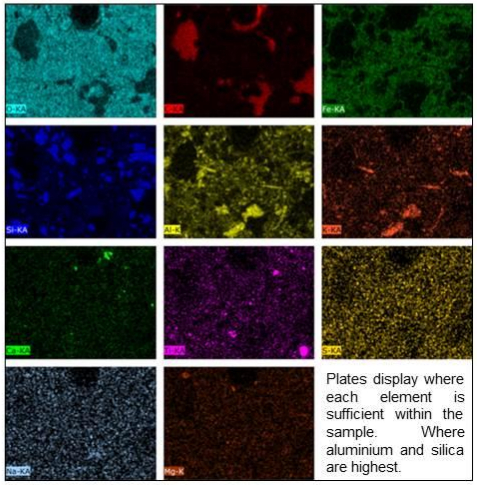

Plates display where each element is sufficient within the sample. Where aluminium and silica are highest.

Figure 6.9

Log: 55
Height: 736 m
Sample Number: 101
Sandstone name: Nosar

Facies: Sxm
Architectural Element: Channel (F1)

Grainsize: Upper medium sand
Sorting: Moderately to well
Roundness: Subrounded
Sandstone classification: Quartzarenite

Detrital Mineralogy: The abundant components of the detrital mineralogy are monocrystalline quartz (42%) and polycrystalline quartz (32%) with minor components of rigid rock fragments (7%: metamorphic 5.5%, sedimentary 1.5%). The monocrystalline grains are slightly-strained to unstrained. The metamorphic grains are composed of sutured, broken and elongated polycrystalline quartz grains. The detrital pore-filing non-resolvable clay (4.5%) are within the pore spaces.

Authigenic Mineralogy: The authigenic mineralogy comprises of cements and clays. Cements include ferroan calcite (2%), quartz overgrowths (1%) and haematite (trace). Clays include kaolinite (4%) and non-resolvable detrital pore-filling clay (1.5%). The quartz overgrowths are syntaxial and are discontinuous around the host quartz grains. The kaolinite, detrital pore-filling clays and calcite cements are filling the pores.

Reservoir Quality: Macroporosity (6%) contains primary intergranular porosity (5.5%) and secondary intragranular porosity (0.5%). Approximately 10% of the pores are interconnected.

SEM: Quartz grains are composed of silica. Between the quartz grains are clays composed of kaolinite booklets (composed of aluminum, calcium and calcite elements).

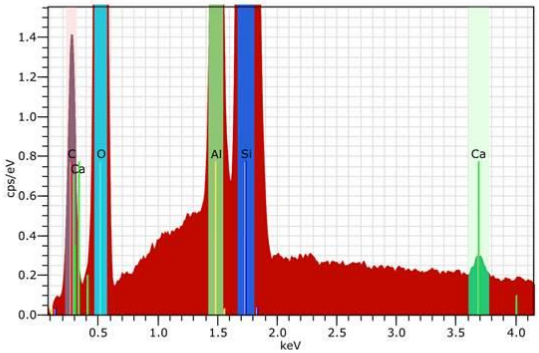

EDAX plot displaying silica with the highest electronvolts.

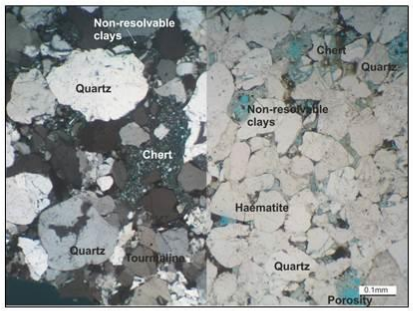

Subrouned, moderately sorted grains, dominated by monocrystalline quartz. Between the grain are non-resolvable clays and haematite cements. Pore space is low.

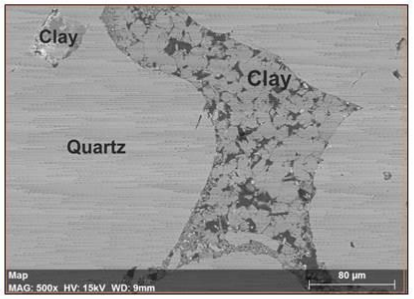

Quartz grains surrounded by kaolinite booklets, limited pore space observed.

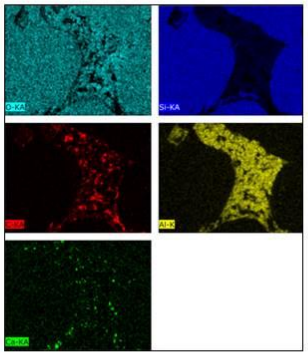

Brighter colours means higher abundance of the element, within the sample. Where silica and aluminium have the most content.

Figure 6.10

Log: 1
Height: 4113 m
Sample Number: 25
Sandstone name: Sarnoo

Facies: Sb
Architectural Element: Channel (F1)

Grainsize: Lower very fine sand
Sorting: Moderately to well
Roundness: Rounded to subrounded
Sandstone classification: Quartzarenite

Detrital Mineralogy: The detrital mineralogy is composed of monocrystalline quartz (44.5%)`, polycrystalline quartz (29%), with minor igneous rigid rock fragments (0.5%) and zircon (trace). The monocrystalline quartz grains are densely packed and have a concave-convex contacts, a limited number have an undulose extinction, which are weakly strained. The polycrystalline grains have long contacts.. The igneous rigid rock fragments are monocrystalline quartz grains with muscovite inclusions. The muscovite mica grains (trace) vary in length but are all elongated thin grains with second order birefringence colours. The non-resolvable clays (1%) are composed of detrital pore-filling clays (0.5%) and pseudomatrix (0.5%) and consist of illite.

Authigenic Mineralogy: The authigenic mineralogy comprises of quartz overgrowths (2%), pore-filling kaolinite (0.5%). The quartz grains are discontinuous around the monocrystalline grains and are syntaxial.

Reservoir Quality: Macroporosity is primary intergranular porosity at 22%, which is high, however the porosity is not interconnected.

SEM: There are multiple quartz grains. There are multiple areas which are clay rich and composed of aluminum, titanium and sulphur. Small areas of calcium and iron cements. Undifferentiated grains are composed of iron which suggests that the iron is replacing the silica.

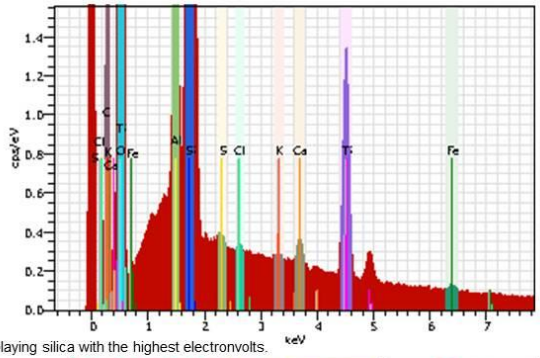

EDAX plot displaying silica with the highest electronvolts.

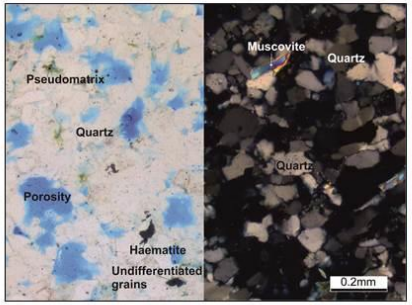

Very fine grained, moderate to well sorted, with subrounded grains. There are multiple types of cements hematite and undifferentiated. There are undifferentiated grains. There is a high amount and multiple types of porosity.

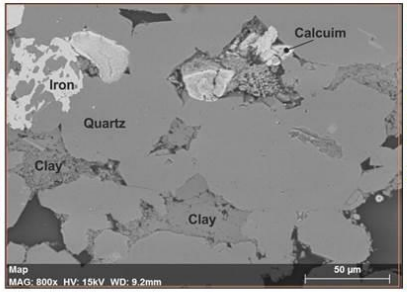

There are unfractured quartz grains. Between the grains there are clays and cements. Clays are composed of aluminium, titanium, sulphur and chlorine. The cements are iron and calcium. There are holes within the sample.

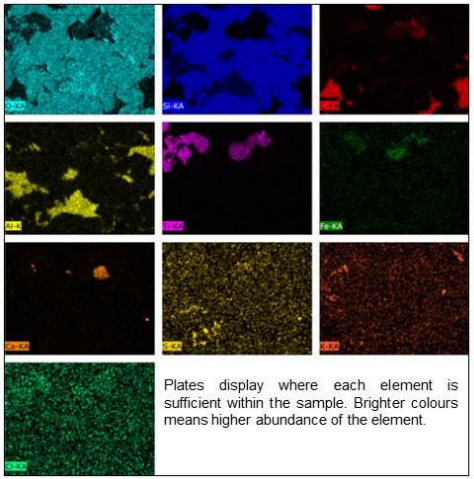

Plates display where each element is sufficient within the sample. Brighter colours means higher abundance of the element.

6.2.3 Authigenic mineralogy

The authigenic cements and clays coat the grains and infill the porosity. The cements are: microcrystalline quartz, quartz overgrowths, haematite, calcite, dolomite and clays.

Microcrystalline quartz occurs in trace amounts within the samples. The microcrystalline quartz is minimal and is only noted under SEM. This cement extends into both primary and secondary pore spaces. It not possible to tell if the microcrystalline quartz has impeded on later cement generations.

Quartz overgrowths are syntaxial and generally discontinuous around their host quartz grains. There are up to 2 mm in thickness. The single-generation overgrowths have not been etched into by other authigenic minerals. The overgrowths occur in both primary and secondary pores spaces. The Sarnoo Sandstone has the highest count at 6% of the sample composition.

Haematite principally coats the detrital quartz grains (Figure 6.11). Within Sample 4 (Figure 6.11), there is an undifferentiated matrix, which is likely to be haematite due to the dark red nature. The haematite also etches and strains the grains a deep red colour. The haematite cements are dominantly within the Darjaniyon-ki Dhani Sandstone only but does occur within the rest of the succession.

Calcite generally occurs within fractures of the coarser quartz grains (Figure 6.9) and is in minor amounts. Occasionally calcite occurs in minor amounts within the pore spaces. Calcite filled veins are throughout the entire formation however, are dominantly noted within the Darjaniyon-ki Dhani Sandstone.

Dolomite is only within the Nosar Sandstone, occurs in minor amounts and is pore-filling. The dolomite is partially poikilotopic.

Asatase is minimal and is of a pale colour. The anatase is noted under SEM as rounded and anhedral.

The clays in the samples are kaolinite and non-resolvable.

Kaolinite booklets that are up to 0.5 µm in length, the booklets are anhedral. The booklets are replacing the muscovite mica. They are filling and choking the pore spaces, particularly within the Sarnoo Sandstone.

Non-resolvable clays are brown in colour and have a fibrous texture and are in minor amounts. The clays under SEM are likely to be illite. The illite is pore-filling, pore-lining and pore-choking.

Figure 6.11

Log: 1
Height: 190 m
Sample Number: 4
Sandstone name: Darjaniyon-ki Dhani

Facies: M
Architectural Element: Gravel bar (F3)

Grainsize: Upper coarse sand
Sorting: Moderate
Roundness: Subrounded
Sandstone classification: Quartzarenite

Detrital Mineralogy: The rigid detrital mineralogy grains are composed of abundant monocrystalline quartz (38.5%) and polycrystalline quartz (27.5%) with minor undifferentiated grains (16%), rigid rock fragments (sedimentary 3%, metamorphic 1%, igneous trace). Some monocrystalline quartz grains are weakly-strained. Polycrystalline quartz grains have sutured grain contacts. Undifferentiated grains are opaque and being replaced by haematite cement. Sedimentary fragments are chert and can be fragmented. Metamorphic fragments contain elongated, sutured polycrystalline quartz and muscovite grains, creating a schistose fabric. Optically non-resolvable clays (1.5%) are pore-filling and likely to be composed of illite and kaolinite.

Authigenic Mineralogy: Significant authigenic minerals contain cements and clays. Cements include haematite (6%), undifferentiated (2.5%) and quartz overgrowths (trace). Haematite is infilling the pores and coating the quartz grains. Undifferentiated cements are likely to be calcite from the pale colours in PPL and low birefringence, which infills the pore spaces. Thin (10 µm) quartz overgrowths are syntaxial and discontinuous around their host grains.

Reservoir Quality: Marcoporosity is very low (3.5%) and composed of primary intergranular porosity and isolated.

SEM: Here, there are multiple quartz grains which can be seen by the silica and titanium content. The matrix is composed of aluminum and magnesium and manganese, which all form to create different types of clays.

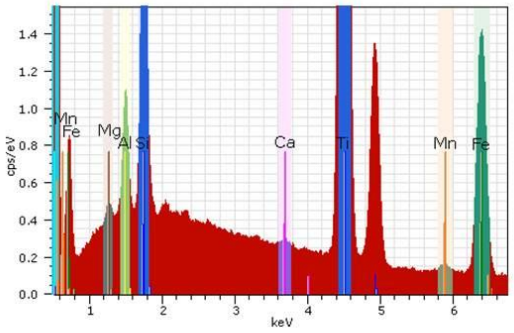

EDAX plot displaying silica with the highest electronvolts.

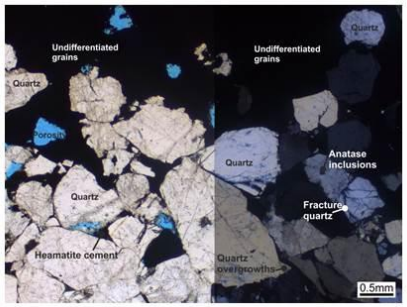

Poorly sorted, angular to subrounded, upper coarse quartz grains up to 20 mm in length, which are heavily fractured in places. Undifferentiated grains fill half the sample.

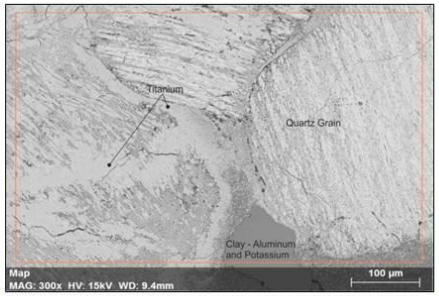

SEM section displays quartz grains (silica, titanium, magnesium, manganese and calcium). Between the grains there are non-resolvable clays, which are composed of oxygen, titanium and aluminium.

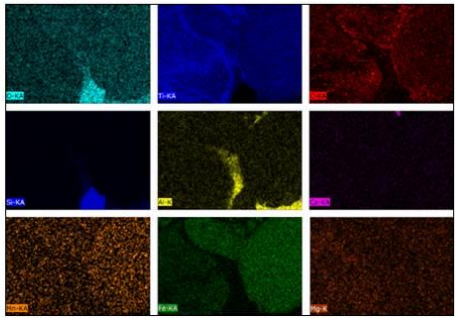

Plates above display the elements within the minerals of the SEM section. We see nine different elements above, compose to make the quartz, grains and the non-resolvable clays. The undifferentiated grains are quartz which have being heavily weathered by iron as seen above.

6.2.4 Pore types

The porosity types are primary intergranular porosity, secondary intragranular porosity and secondary 'oversized' porosity.

Primary intergranular porosity is the void space between the detrital framework grains within the samples (Figures 6.9 to 6.11). It is poorly interconnected within all the sandstone successions. The Darjaniyon-ki Dhani Sandstone and the Nosar Sandstone porosity values do not vary greatly (between 0.5% and 12.5%, Figure 6.10), they average at 5.5% and 4.5%, respectively (Table 6.3). The Sarnoo Sandstone has the highest values, up to 22% (Figure 6.10), with the average at 8.16% (Table 6.3).

Secondary intragranular porosity forms by partial dissolution of grains, likely feldspar, or volcanic rigid rock fragments (Sample 101, Figure 6.9). The sandstone successions have very low secondary intragranular porosity values at approximately 0.5% (Table 6.3).

Secondary 'oversized' porosity forms by the complete dissolution of grains and is connected to other pores for example, Sample 36 (Figure 6.8). The Darjaniyon-ki Dhani Sandstone has the highest secondary values at 1.5% (Table 6.3).

Average porosity values	Primary porosity (%)	Secondary porosity (%)	Secondary 'oversized' porosity (%)
Darjaniyon-ki Dhani Sandstone	**5.5**	**0.6**	**1.5**
Sarnoo Sandstone	**8.2**	**0.5**	**0.5**
Nosar Sandstone	**4.5**	**0.5**	**1.1**

Table 6.3: Average porosity values for each of the sandstone successions.

6.2.5 Composition classification

The composition of the three sandstone successions has been delineated through QFL diagrams (Figures 6.5, 6.7, 6.12 – 6.15). The overall composition of the sandstones varies from sublithic-quartzarenites to pure quartz-arenites (Figure 6.12). Darjaniyon-ki Dhani Sandstone is composed of mainly quartz arenites (60%, Figure 6.12a) however; there are some sublithic-arenites. In-between the detrital grains there are clays (9%) and cements

such as kaolinite booklets (1.4%) and illite clays. Cements include iron (9.9%) and calcite (2.9%). The iron stains and is etching into the detrital quartz grains (Figure 6.7). The spatial location of the sandstones does not affect the composition (Figure 6.13).

The Sarnoo Sandstone is completely composed of quartz-arenites (Figure 6.12b). Between the sub-rounded detrital quartz grains (71.9%) there are kaolinite booklets (1%) and iron (3.2%) and calcite (1.1%) cements. EDX reveals multiple elements within the clays: aluminum, magnesium, potassium, and titanium (Appendix 3), forming kaolinite and potentially gibbsite. Calcite cement occurs between the grains and within the pore spaces (9.2%). It is the most compositionally mature. The spatial location of the sandstone does not affect the composition (Figure 6.13).

The Nosar Sandstone contains the most lithic fragments with a number of samples in the sublithic-arenites zone (Figure 6.12c), the rest of the samples, however, fall into the quartz-arenite zone. There are copious amounts of quartz (66.3%). Kaolinite booklets (1.9%) are pore-filling and are growing outward and replacing the muscovite micas (elements are aluminum, potassium and titanium). Calcite cements (5%) are locally minor. It is the least compositionally mature sandstone succession. The spatial location of the sandstone does not affect the composition (Figure 6.13).

There is no pattern for the grainsize in correspondence with the composition classification of the sandstones (Figure 6.5). Poorly sorted sediments sit within the lower quartz-arenite range whereas the moderately to well sorted sediments are at the top of the quartz-arenite zone or in the sublithic-arenite zone. The sorting is related to the compositional maturity which relates well to the published literature (Dickinson and Suzeck, 1979; Tucker, 2001).

Sx facies (Figure 6.14) is within the quartz-arenite zone and therefore is the cleanest facies as the sediments are generally coarser and have moderate sorting. The rest of the

facies vary from sublithic-arenites to quartz-arenites, therefore it can be suggested that the depositional process does not affect the composition of the sandstones and it is rather the transport processes affecting composition.

The architectural elements measured within the petrographical analysis are the sandy bar element (F1), gravel bar element (F3), point bar element (F5), sheetflood element (F6), and the floodplain element (F7, Section 5.2, Figure 6.15). All the architectural elements range from the sublithic-arenite zone into the quartz-arenite zone. Although this is true the point bar element sits within the quartz-arenite zone only (Figure 6.15). This could be because the sediments within the point bar are deposited via polycyclic reworking (Section 4.1.7), as there is cross-flow migration of the sands and there are small scale ripples upon the point bars.

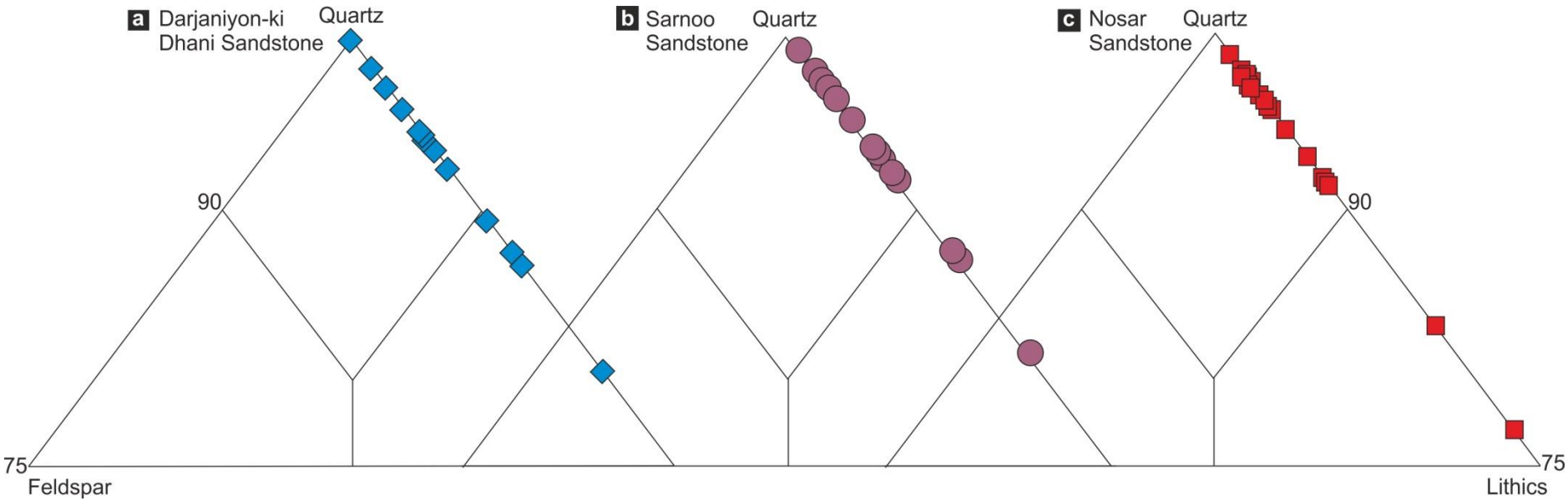

Figure 6.12: QFL diagrams that denote the composition of each sandstone; a) Darjaniyon-ki Dhani Sandstone is within the sublithic-quartzarenite to quartz-arenite ranges; b) Sarnoo Sandstone is within the sublithic-quartzarenite to quartz-arenite ranges, and; c) Nosar Sandstone is within the sublithic-quartzarenite to quartz-arenite ranges.

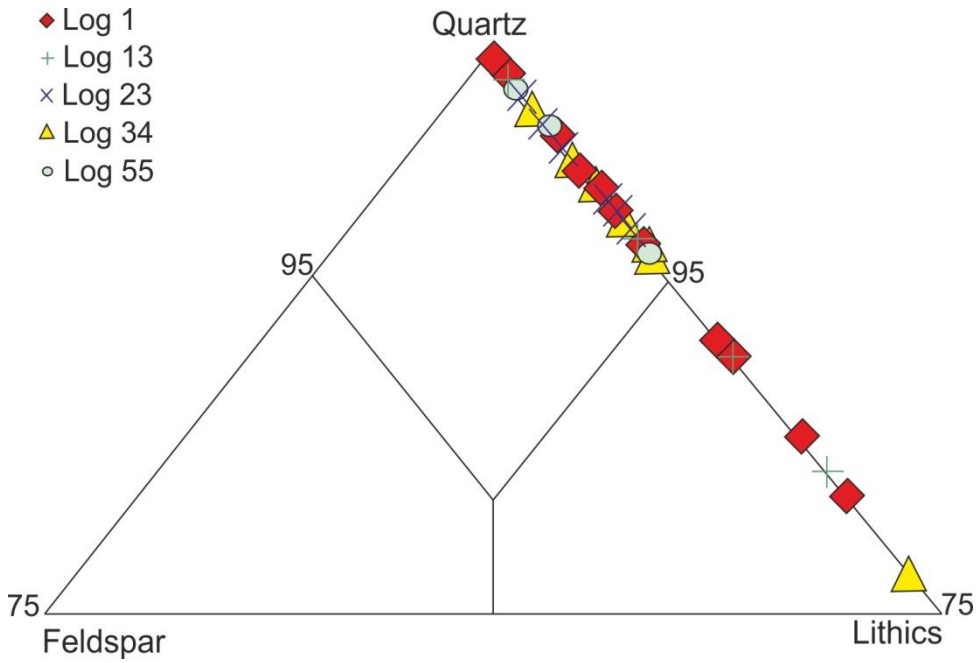

Figure 6.13: QFL diagram displaying the sampled data at each log location of the sampled sandstone successions sublithic-quartzarenite to quartz-arenite ranges. This data suggests that the spatial location does not affect the compositional maturity.

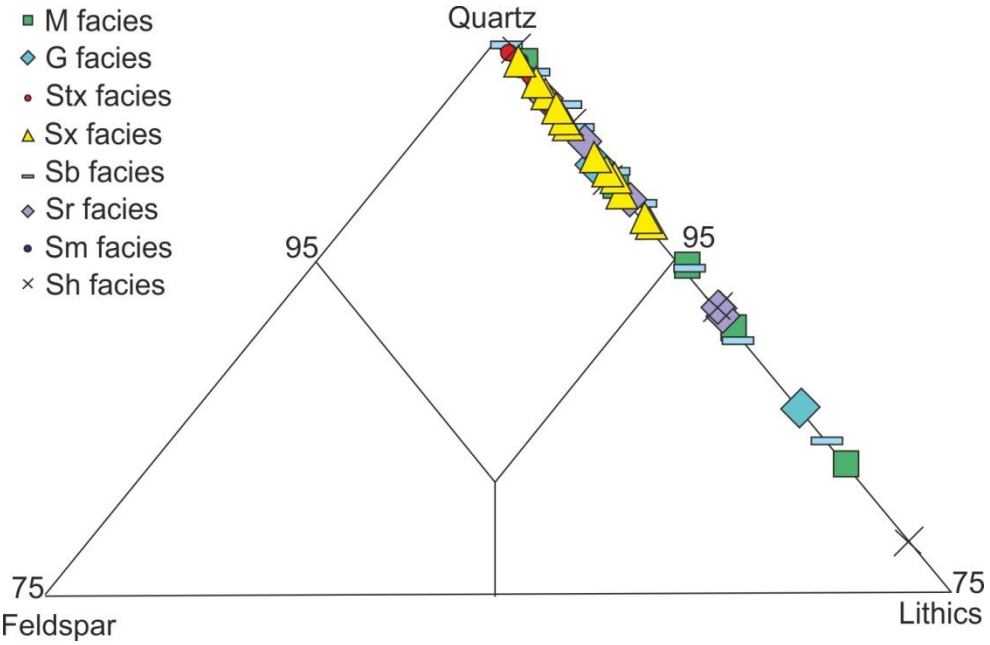

Figure 6.14: QFL diagram displaying the compositional maturity of the separate facies within the sublithic-quartzarenite to quartz-arenite ranges.

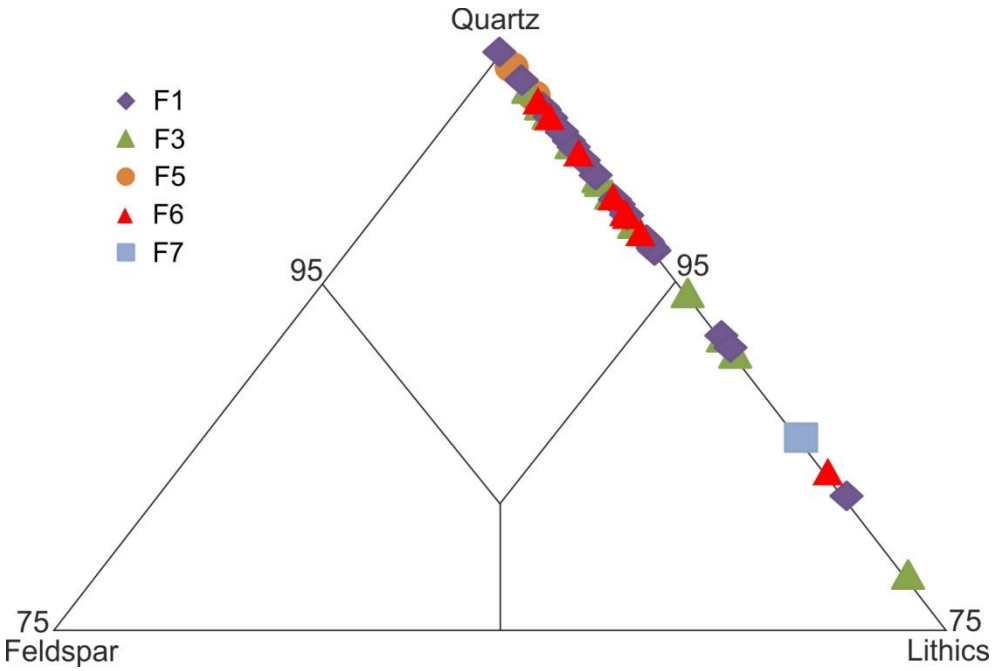

Figure 6.15 QFL diagram displaying the compositional maturity of the separate architectural elements within the sublithic-quartzarenite to quartz-arenite ranges, apart from the F5 element which is within the quartz-arenite zone only; where F1 – channel deposits, F3 – gravel bar deposits, F5 – point bar deposits, F6 – sheetflood deposits and F7 – floodplain deposits (Section 5.2).

6.3 Discussion

Undulose extinction and elongated monocrystalline quartz grains (Section 6.2.2) suggests they are strained and derived from metamorphic rock fragments of low ranks (Section 6.2.2). These are abundant throughout the sandstone successions of the Ghaggar-Hakra Formation. Tourmaline and rutile form within low grade metamorphism (Table 6.1). All these qualities are suggestive of a metamorphic origin (Section 6.2.5) for the detrital grains within the sandstone successions. Apatite, rutile, zircon, tourmaline and igneous rigid rock fragments originate from igneous rocks (Dickinson, 1985), suggesting an igneous origin. However, it is likely that the heavy weathering on the underlying igneous rocks (Karentia Volcanic Formation and Malani Igneous Suite), allowed for the igneous rigid rock fragments and heavy minerals to be entrained within the fluvial system, so they could potentially be intraformational fragments.

The Darjaniyon-ki Dhani Sandstone has high secondary porosity values indicating there has been chemical weathering associated with this arenite succession. There are also more veins of haematite cement throughout, relating to the diagenetic history with alkaline

and oxidized groundwaters. The Sarnoo Sandstone exhibits more quartz overgrowths and microcrystalline quartz than the other sandstone bodies, again potentially related to the diagenetic regime. This sandstone also displays mature sedimentary textures (well sorted, rounded etc.) and high porosity values, attributed to the depositional setting of a high sinuosity, fluvial environment, suggesting it would have the best reservoir quality. The Nosar Sandstone has the highest lithic fragment count and the lowest porosity count attributed to a bedload dominant, low sinuosity fluvial system, however, the grains are moderately sorted and generally quite rounded indicating a high textural maturity (Section 6.1.2). The Darjaniyon-ki Dhani Sandstone and Nosar Sandstone both contain poorly sorted grains suggesting they would have a poor reservoir quality when compared to the Sarnoo Sandstone.

Of the four plate tectonic types – recycled orogens, magnatic arcs, continental blocks and basement uplifts – a recycled orogen is the most likely type of geological source terrane here as the composition of the sandstone succession is dominantly within the quartz-arenite range and there are only trace amounts of feldspar noted (Figures 6.5, 6.7, 6.12 – 6.15). The other three plate types are unlikely contributors to this fluvial system as these would yield significantly different mineral to those recorded from the deposits of the Ghaggar-Hakra Formation.

It is being suggested in this research that the sediment provenance for this sedimentary system is from the ancestral Aravalli-Delhi Mountain Range to the northeast of the field area and it as it was exposed at the time of deposition (6.16). The Aravalli-Delhi Mountain Range is dominated by Precambrian metasediments and rare granites (Roy and Jakhar, 2002; Racey *et al.,* In review). The Aravalli Supergroup contains quartz pebble conglomerates, ‘red beds’ and low grade metamorphic rocks formed from detrital quartz minerals and sedimentary and metamorphic rock fragments (Banerjee and Bhattacharya, 1994) the most dominant components found within the Ghaggar-Hakra Formation. The

majority of the Aravalli sediments were deposited within the continental – marine transition zone, where high energy transport processes produced well sorted, rounded grains (Hart and Plint, 1989). The Cretaceous fluvial system is likely to have eroded into these well sorted and rounded sedimentary rocks leading to recycling of the Aravalli Supergroup. The Aravalli-Delhi Mountain Range also contains metamorphic and igneous rocks containing high amounts of feldspar and rock fragments. The feldspars were likely lost during diagenesis. Igneous rock fragments are more prone to weathering and also can become unstable during diagenesis. The Aravalli-Delhi Mountain Range likely formed within a transitional arc (cf. Banerjee and Bhattacharya, 1994; Dickinson and Suczek, 1979). Thus the sediments within the Ghaggar-Hakra Formation were most probably derived from a recycled orogen.

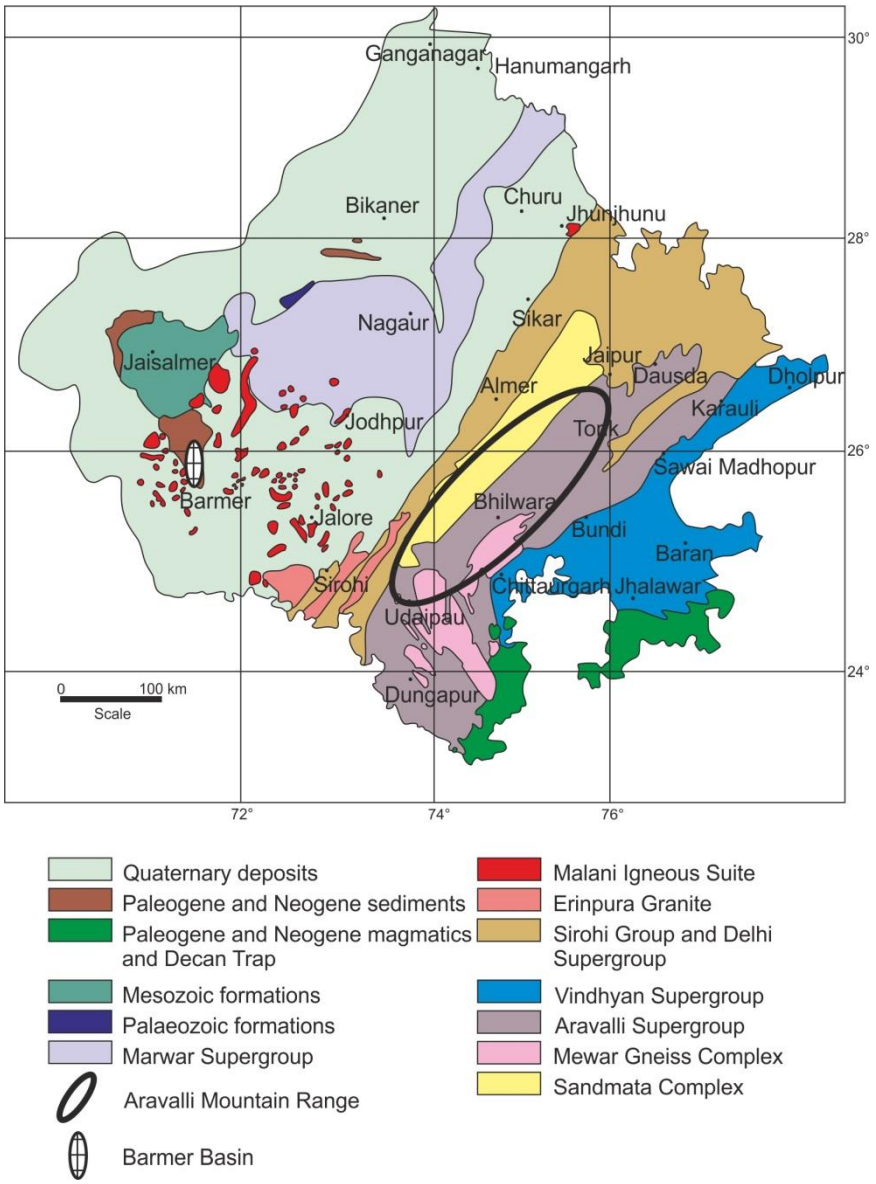

Figure 6.16: Geological map of Rajasthan displaying Aravalli Mountain Range as the potential source. The Barmer Basin is also highlighted to indicate the distance the material has potentially travelled.

6.3.1 Diagenetic history

The diagenetic history (Figure 6.17) of the Ghaggar-Hakra Formation indicates that the formation pore waters matured from acidic to alkaline. Firstly, the mechanical compaction of the grains occurred due to eogenesis. As the burial of the sediments developed there was a notable loss of the intergranular pore space due to compaction. The next process to occur during eogenesis is the dissolution of unstable volcanic grains and feldspars, creating secondary porosity. The dissolution of feldspars happens at depths of between 600 m and 3000 m. This dissolution provides the pore waters with excess silica,

potassium, calcium and magnesium (Burley *et al.,* 1985) allowing for the growth of kaolinite, microcrystalline quartz and then quartz overgrowths as the temperatures and pressure become higher (Fischer *et al.,* 2013). Kaolinite forms between 600 m and 3000 m depth (Beaufort *et al.,* 1998) and is likely to occur before the quartz cementation. Quartz cementation occurs around 2000 – 3000 m depth (Wilkinson and Haszeldine, 2002) and reduces the porosity of the sandstones (this can be up to 40%, Worden and Morad, 2000). It is noted that the microcrystalline quartz and quartz overgrowths extend into both the primary and secondary pore spaces indicating that the precipitation of these cements occurred after the dissolution of the feldspar and unstable igneous fragments. The precipitation of the kaolinite and quartz reduces the acidic nature of the pore waters, leaving them slightly alkaline.

Mesogenesis occurs in the later stages of diagenesis. At this stage the pore waters have become alkaline for two reasons (1) there is further dissolution of unstable igneous fragments and, (2) the authigenic quartz has precipitated. The first cementation of the mesogenesis starts with the formation of illite. It is likely that the illite forms due to the alkaline nature of the pore waters. Illitization of authigenic kaolinite can also occur at temperatures of approximately 120°C to 150°C (Bjorkum and Gjelsvik, 1988). Anhedral poikilotopic dolomite cements also occur at this time and may enclose other authigenic cements. Minor authigenic cements to be precipitated during mesogenesis are the anatase cements.

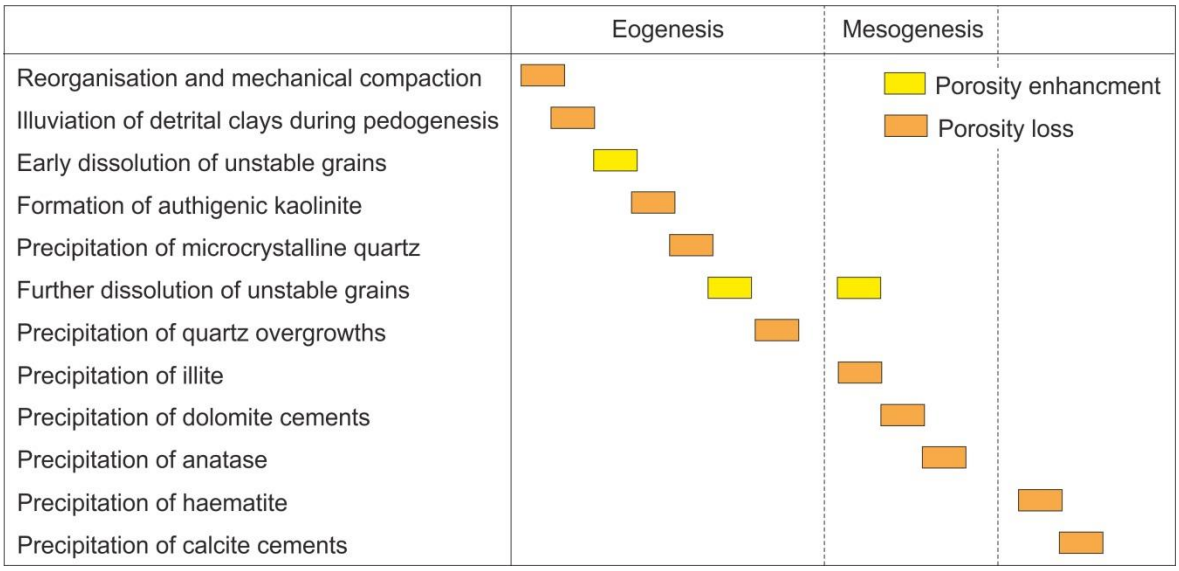

Figure 6.17: Schematic diagenesis diagram based on the precipitation and dissolution of grains, within acidic and alkaline pore waters.

Subsequently, telogenesis is likely to have occurred when the haematite and calcite were cemented. It is interpreted that the haematite cements formed close to or at the surface following uplift, where the sandstones were subjected to meteoric waters of low salinity which tend to be slightly acidic and, more importantly, oxidising. The haematite is likely to have formed through the oxidation of iron-containing minerals, which could be either original detrital or authigenic in origin. There also appears to be a later stage calcite cementation as veins healed by calcite cross cut all other diagenetic phases. This cementation may correspond with the fault network at outcrop. Calcite cement has in-filled the fractures within the monocrystalline quartz grains. This occurs more commonly within the Darjaniyon-ki Dhani Sandstone and within the underlying Karentia Volcanic Formation as coarser grains tend to be easier to fracture (Chuhan *et al.,* 2002). However, there are calcite veins throughout the formation implying that they occurred post-depositionally in relation to the sediments and volcanics. At outcrop scale there are calcite and quartz veins and fractures suggesting that some cementation is a consequence of the rotational faulting during the formation of the Barmer Basin, at Sarnoo (Bladon *et al.,* 2015a). The samples contain no feldspar (Figures 6.7 – 6.11, Appendix 3) which could be because of multiple reasons (1) feldspar underwent dissolution during diagenesis, which would

account for the secondary ‘oversized’ pore spaces; or, (2) chemical weathering (Nesbitt *et al.,* 1997, Section 2.1.1). Here, the loss of feldspar is attributed to dissolution during diagenesis.

6.4 Summary

This research has utilised 50 samples as the basis for petrographical and SEM analysis to determine the provenance of the fluvial system and to quantify the sedimentary textures observed at outcrop scale. The petrographical work implies that the Sarnoo Sandstone would have the best reservoir quality as it has the highest porosity values and is the most texturally and compositionally mature; whereas the Darjaniyon-ki Dhani and Nosar sandstones are texturally and compositionally immature, by comparison. Provenance of the fluvial sediments is most probably the Aravalli-Delhi Mountain Range due to the similarities in the mineral and chemical composition. There is an absence of feldspar in the sediments of the Aravalli-Delhi Mountain Range which are likely to have dissolved during diagenesis and sediment transportation. The volcanic samples are from the Karentia Volcanic Formation and the Malani Igneous Suite, composed of basalts and rhyolites, respectively. They provide the igneous clasts transported by the Cretaceous fluvial system.

7 Chapter Seven: Palaeocurrent Data from the Ghaggar-Hakra Formation

Palaeocurrent analysis is a well-developed approach to determine the palaeoflow patterns responsible for ancient sedimentary systems (Potter and Pettijohn, 1977). Palaeoflow is determined primarily by the orientation of the bedforms and barforms preserved as cross-bedded sets and ripples. Channel erosion can also form flute marks that can be used to determine flow direction. Overall distribution of palaeoflow indicators from genetically related sedimentary successions in fluvial environments show diverse patterns, including uni-, bi- or poly-modal distributions that can prove helpful for establishing the type of a river; palaeodrainage direction, tectonic (allocyclic) influences, palaeotopography and provenance.

This chapter will discuss the literature pertaining to palaeocurrent data, their collection, reorientations and analysis. This chapter will also present the palaeocurrent data for the Ghaggar-Hakra Formation and place these data into the context of the evolving Barmer Basin. Consequently, this chapter is split into two sections, the first section (7.1) reviews the literature pertaining to palaeocurrents including: measurement methods, analysis and how they relate to the tectonic regime. Previous works on the palaeocurrents of the Ghaggar-Hakra Formation are also discussed. The second half of the chapter (7.2 – 7.4) presents the palaeocurrent data and analysis pertaining to this study, and is presented using rose diagrams, moving average maps, vector mean analysis and dispersion. The results of the data are then related to the provenance of the Ghaggar-Hakra fluvial system and its setting within the evolving Barmer Basin and West Indian Rift System.

7.1 Review of Literature

This concise literature review on palaeocurrents covers how data are ranked and analysed through vector mean analysis, dispersion, moving averages. The data obtained can help determine the channel sinuosity and fluvial style (Sections 7.1.3.2 and 2.8.1).

7.1.1 Importance of palaeocurrents

Palaeocurrents are measured from various types of sedimentary structures and from preserved surfaces relating to bedform and barform migration within sedimentary environments. The applicability of the measurements to palaeocurrent analysis is determined by a hierarchy (Table 7.1), commonly ranked from 1 to 6 (Miall, 1974) or 0 to 4 (Allen, 1966); Miall's (1974) six-point system is used within this study.

Rank (Allen 1966)	Rank (Miall 1974)	Source of observations
-	1	System scale variations: multiple fluvial systems
0	2	Amalgamated channel belts
1	3	Individual channels or meander belts
2	4	Point bars and gravel bars
3	5	Large scale sedimentary structures e.g. cross-bedding
4	6	Small scale sedimentary structures e.g. ripples

Table 7.1: Dispersion and hierarchy of different sedimentary structures when measuring palaeoflow (adapted from Allen, 1966; Miall, 1974).

In general, the six different ranks relate to different sedimentological features of the fluvial system giving palaeocurrent orientations relating to different aspects of the flowing system. Larger-scale indicators such as large channels and tributaries give regional directions whereas gravel bars and point bars, and their preserved sets and cosets, record local variations in the flow that are strongly influenced by local factors.

Rank 1 measures the gross scale palaeocurrent direction for the whole channel belt (Table 7.1; Miall, 1974), including channels, point bars and various features in the floodplain. Consequently, it can be considered the most important rank with respect to the regional drainage profile of the fluvial system (Allen, 1966). However, it somewhat ignores the variations of an individual channel and the cross-bedded sets and cosets. As a result, it can be considered as a poor way to account for specific palaeocurrent directions within a fluvial system. This rank also needs to be completed via satellite pictures and is difficult to apply to ancient successions where the whole channel belt may not be seen.

Rank 2 records the palaeocurrent pattern of individual channels and tributaries of the whole channel system (Table 7.1; Miall, 1974) but does not include in-channel variations. The third rank scales down to individual meander belts (Table 7.1; Miall, 1974) where the measurement here is the orientation of the meander migration and not the downstream direction. Rank 4 measures the current direction determined from channel bar forms and the dispersion of palaeocurrent data can be helpful in distinguishing between gravel and point bars (Table 7.1): gravel bars have a lower dispersion than point bars (Long and Young, 1978). Comparisons of these barforms determine the differences between lateral and downstream migration (Allen, 1966).

The fifth rank is the measure of three-dimensional, large-scale sedimentary structures, such as trough cross-bedding preserved as cross-bedded sets and cosets (Table 7.1). The fifth rank of Miall (1974, third of Allen, 1966) is the most useful rank for determining palaeocurrent orientation from preserved sedimentary successions because of its three-dimensional nature and common occurrence within any given sedimentary system. A large number of fifth rank readings can give an average of palaeoflow, measuring both the local variations and an overall (or large-scale) regional picture of the palaeoflow. Rank 6 is the measure of three-dimensional, small-scale structures, such as ripples (Table 7.1; Allen, 1966; Miall, 1974) where very little of the flow is needed to produce these structures (Section 2.4; Allen, 1966).

Rank 5 contains trough and planar cross-bedding where it is orientated in the downstream direction and trough cross-bedding produces a lower value of dispersion than the planar cross-bedding, due to the acute shape of the foreset surfaces (Miall, 1974). However, reliable readings from trough cross-bedding can be difficult to obtain due to the commonly incomplete three-dimensional preservation of trough cross-bedded foresets. Rank 5 is favoured over all the other ranks when measuring palaeocurrent because these structures

present the variations of the individual channels within the fluvial system (Allen, 1966; Miall, 1995).

7.1.2 Analysis

Potter and Pettijohn (1977) and Lindholm (1987) describe various types of statistical palaeocurrent analysis such as dispersion, vector mean analysis and moving average analysis. Further to manual statistical tests software packages such as Matlab can be used to plot and analyse palaeocurrent data.

Vector mean analysis (vm) calculates an average flow direction measured from the sedimentary structures. This can be done per location if more than one sedimentary structure is measured (Table 7.2, Potter and Pettijohn, 1977). Vector mean analysis is calculated by taking the sin and cos values of each azimuth, then calculating the average of each dataset and dividing by each other. The mean is calculated in this way as compass directions in degrees are from 0° to 359°; the vector mean analysis is given by (Equation 7.1, Lindholm, 1987):

$$vm = \frac{\Sigma x \sin \theta n}{\Sigma x \cos \theta n} \qquad \textbf{[7.1]}$$

Where:
Σx = the sum of readings
θn = the azimuth of the palaeocurrent reading

Technique	Advantages	Limitations
Standard deviation	**Displays the variance within the field area**	**Can be time consuming**
Vector mean	**Mean data point for each location**	**Doesn't produce an average for the whole field area; can be time consuming**
Moving averages	**Produces averages throughout the area**	**Average the whole field area, not individual locations**
Software packages	**Time-saving, produces standard deviations; Vector means easily**	**Difficult and does not calculate moving average analysis**

Table 7.2: Advantages and limitations of palaeocurrent analysis techniques.

Dispersion is a measure of the distribution of the palaeocurrent data around the mean, and can be evaluated visually using rose diagrams. It is possible to see the average directional flow patterns of the field areas. The distribution of a dataset of palaeocurrent falls into one of four categories (Potter and Pettijohn, 1977):

- Unimodal, where there is one peak;
- Bipolar, where there are two peaks but at 180° to one another;
- Bimodal, where there are two peaks and / or;
- Polymodal, where there are multiple peaks.

Dispersion analyses determine the variations of palaeocurrents by calculating the standard deviation, and the result can be used to evaluate the sinuosity of a fluvial system (Table 7.2). Dispersion is calculated by square rooting the variance in the data of a locality, given by (Equation 7.2):

$$d = \sqrt{\frac{(x_1 - vm)^2 + (x_2 - vm)^2 + (x_n - vm)^2}{n^{-1}}}$$

[7.2]

Where:
d = dispersion
x_1 = observation number
vm = the vector mean
n = the number of observations

Moving average analysis is completed to highlight large-scale trends and smooth out any local variations (Potter and Pettijohn, 1977; Lindholm, 1987) and areas of anomalies (Table 7.2). Moving average analysis is completed by gridding areas of palaeocurrent data and then the palaeocurrents within that particular gridded square are averaged to get the dominant trend within that square (Equation 7.1, Figure 7.1; Potter and Pettijohn, 1977; Shukla *et al.,* 1999). This type of analysis has been completed on the Brahmaputra River, India (Shukla *et al.,* 1999).

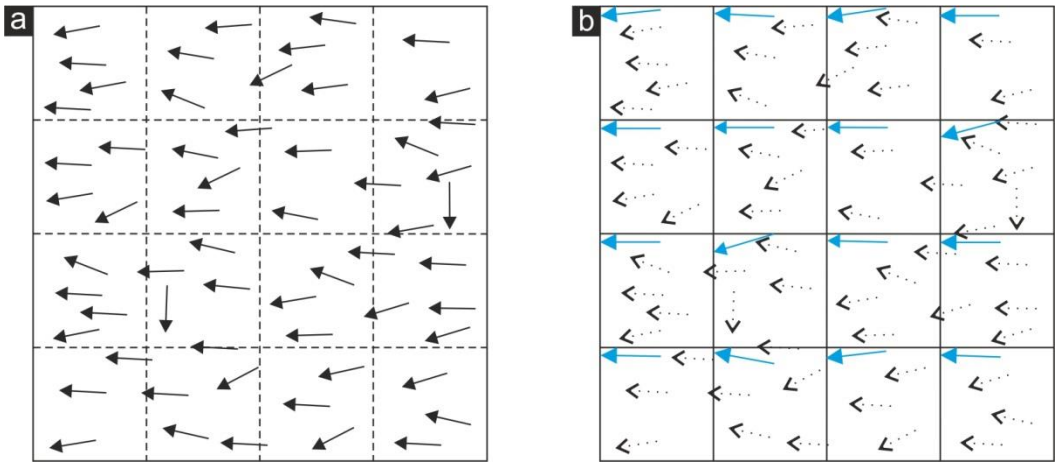

Figure 7.1: Two-dimensional construction of the moving average analysis. The left diagram displays the palaeocurrent directions throughout an area, delineated by the black arrows. The right diagram displays the palaeocurrent diagrams (black dashed lines) and the average palaeoflow in the top left corner in the gridded areas (blue arrows). The calculation involves the averaging of the data using equation 7.1 in each of the gridded squares to form the blue arrows (adapted from Potter and Pettijohn, 1977; Lindholm, 1987).

7.1.3 Palaeocurrents and their relationships to river types

The type of fluvial system observed is determined by two parameters derived from the flow data; the dispersion and channel sinuosity. Channel sinuosity is defined as 'the ratio of channel length to its meander axis' (Figure 7.2; Miall, 1976). A higher dispersion generally means higher channel sinuosity (Miall, 1974; Long and Young, 1978; Ghosh, 2000). Sinuosity itself is a dimensionless number between 0 and 5 where anything below 1 is a low sinuosity river and anything above 1 is a high sinuosity river (Ghosh, 2000). Meander bend cut-off occurs at a sinuosity of 5.24 as demonstrated by LeRoux (1992). Channel sinuosity (P) can be measured in multiple ways and has been determined by Miall (1976), LeRoux (1992) and Ghosh (2000). The Miall (1976) method is an empirical equation taking the maximum angular range and relating it to channel sinuosity, the equation is described as follows (Equation 7.3; Miall, 1976):

$$P = \frac{1}{1} - (\theta/252)^2$$

[7.3]

Where:

θ = maximum angular range of the palaeocurrent data.

This method uses the angular range of the measured palaeocurrent data but the numbers the equation produces are subject to error, especially when used in-conjunction with moving average analysis (Miall, 1976).

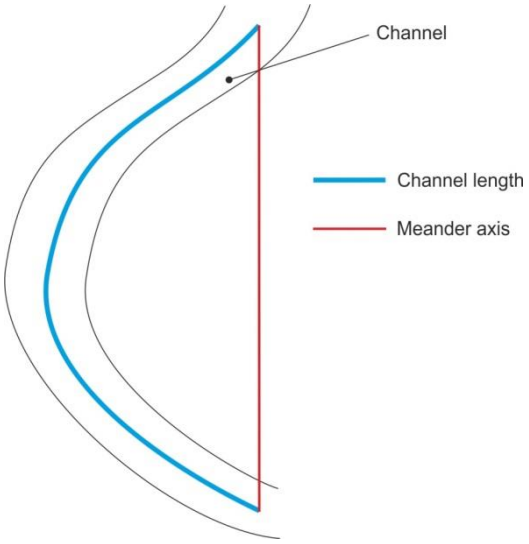

Figure 7.2: The term meander axis relates to the straight line from one point of a meander to the next as indicated by the red line here. The blue line indicates the channel length of the fluvial system.

The LeRoux (1992, 1994) method calculates the channel sinuosity (P) directly from the palaeocurrent data. The data collected at each locality needs to be averaged to be used in the equation using Equation 7.1; LeRoux's (1992) equation is described below (Equation 7.4; LeRoux, 1992):

$$P = \frac{\pi\left(\frac{\emptyset_{ave}}{360}\right)}{\sin\left(\frac{360}{\emptyset_{ave}}\right) - 2}$$

[7.4]

Where:
$\emptyset_{ave}$ = average of the palaeocurrent data

This equation produces a dimensionless number for sinuosity per locality which can be displayed on maps (Section 7.1.2). This determines the sinuous nature of the fluvial system.

Ghosh's (2000) method is determined by fractal modelling of fluvial systems. The patterns that are produced provide a relationship between dispersion and channel sinuosity over a single meander wavelength. This allows for the measured single meander wavelength to be used to predict numbers for whole fluvial systems (Ghosh 2000), however this process needs to be able to measure the channel length data which is not always available in preserved successions. This method is completed by computer modelling.

7.2 Collection of palaeocurrent data from the Ghaggar-Hakra Formation

Palaeocurrent data were collected in the field. The measured data consist of: dip magnitude and dip azimuth of the bedform for palaeocurrent and the dip/strike and dip direction of the planar bedding (Sb facies) that the bedforms are within (in order to correct for tectonic tilt). The heights and foresets of the cross-bedding were measured along with the heights, wavelengths and foresets (where possible) of the ripples to distinguish between ranks of palaeocurrent data (Section 7.1).

The dip magnetude and dip azimuth and the dip/strike data are all measured to restore the sediments to their original placement (Potter and Pettijohn, 1977) as this has to be completed before palaeocurrent analysis can begin. The data were rotated back to their original position by rotating the poles to bedding of the cross-bedded strata around the strike of the planar bedding and through the dip of that bedding (Potter and Pettijohn, 1977). This can be done by hand or by computer programmes. Here, this was completed using Stereonet 9.

Data used for this study were collected from channels, trough and planar cross-bedding, asymmetrical and symmetrical ripples (M, G, Stx, Sx, Sr and Scl facies). The data displayed within this chapter is from the channel structures, trough and planar cross-bedding and asymmetrical ripples only (M, G, Stx, Sx and Sr facies), ranks 3 through 6 from Miall's (1974) hierarchy. The palaeocurrent data were then placed into rose diagrams where the data is presented in ten degree bins so the dispersion can be visually seen, the data here is from ranks 5 and 6 but presented in separate rose diagrams. The data from ranks 3 and 4 have been compared to the rose diagrams displaying ranks 5 and 6 and the moving average analysis maps (Figures 7.3 – 7.10). The vector mean was calculated for each location, these have been averaged together for each sandstone succession (Appendix 4). Moving average analysis (Section 7.1.2) was then applied to each sandstone succession throughout the field area to produce maps and the average palaeocurrent data. The calculation of sinuosity for the sandstone packages has been completed using the LeRoux (1992) method as it uses the averaged palaeocurrent data from each locality and can be combined with the moving average analysis easily.

7.3 Palaeocurrent data and maps

The palaeoflow measured within the field is dominantly from rank 5 and rank 6 features (M, G, Stx, Sx and Sr facies). The facies used for palaeocurrent analysis in the Darjaniyon-ki Dhani Sandstone are M, G and Sx and the individual localities show ranges of directions from south to west (Figure 7.3). The Darjaniyon-ki Dhani Sandstone displays unimodal to bimodal palaeocurrent data (Figure 7.3), indicating a low dispersion as calculated (Table 7.3). This low dispersion is expected as this system is a gravel bedload dominant, low sinuosity system (Figure 5.17). The average palaeoflow for the sandstones from ranks 5 and 6 and is to the south (Figure 7.4).

	Darjaniyon-ki Dhani Sandstone	Sarnoo Sandstone	Nosar Sandstone
Dispersion	**7.732**	**32.43**	**13.5**
Number of data locations:	**5**	**39**	**361**

Table 7.3: Dispersion data displayed for each sandstone succession. The number of data locations refers to the number of locations where palaeocurrent data has been measured.

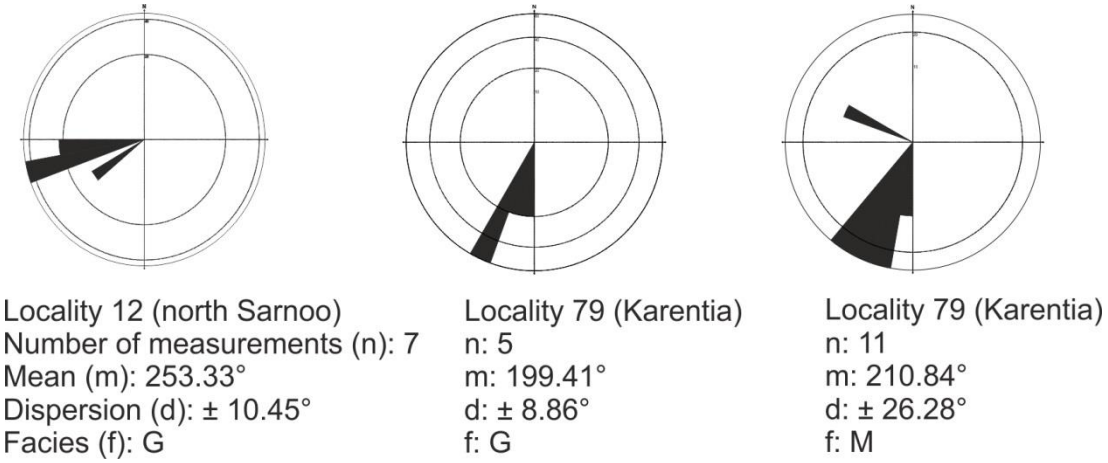

Figure 7.3: Rose diagram data in 10° bins for the Darjaniyon-ki Dhani Sandstone, displaying unimodal data from south to west.

The G, Stx, Sx and Sr facies have palaeocurrent data collected from them within the Sarnoo Sandstone using ranks 5 and 6, and checked against the data from ranks 3 and 4. The data collected shows a range of palaeocurrents from the southwest to the northeast (Figure 7.5) displaying bimodal (Figure 7.5) with high dispersion values due to its sinuous nature (Figure 5.18, Table 7.3). The palaeocurrents have been averaged using the data from ranks 5 and 6 and displays a general palaeoflow to the west (Figure 7.6), matching the second rank data.

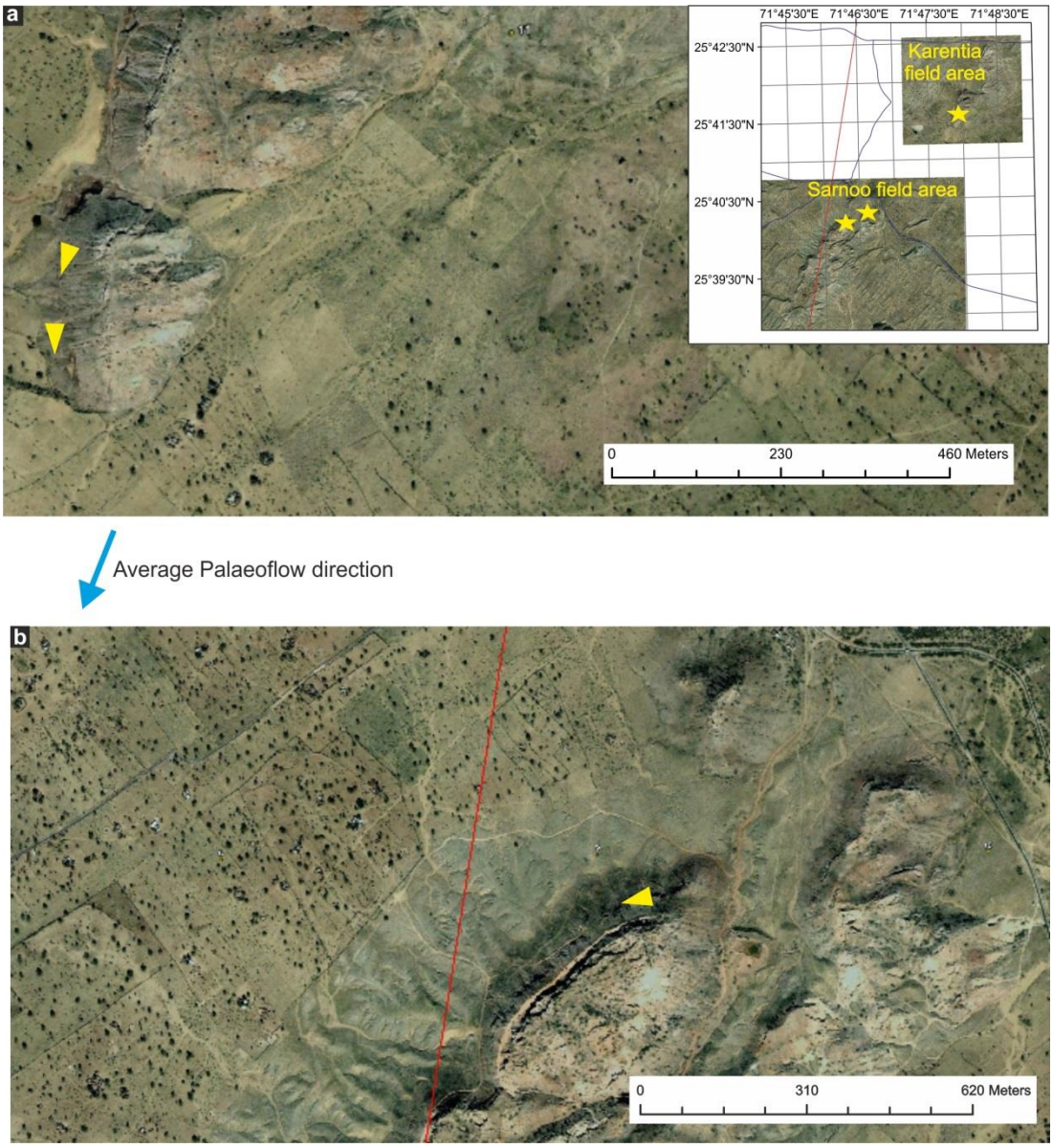

Figure 7.4: Moving average data for the Darjaniyon-ki Dhani Sandstone in (a) southern Karentia and (b) north Sarnoo, with an average flow to the south - southwest.

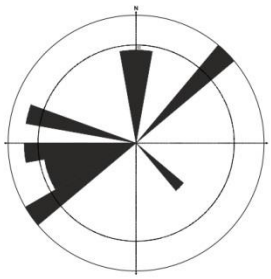

Locality 12 (Sarnoo)
Number of measurements (n): 23
Mean (m): 285.39°
Dispersion (d): ± 61.64°
Facies (f): Sx

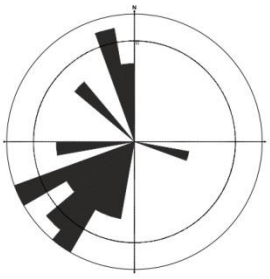

Locality 16 (Sarnoo)
n: 31
m: 249.21°
d: ± 50.95°
f: Sr

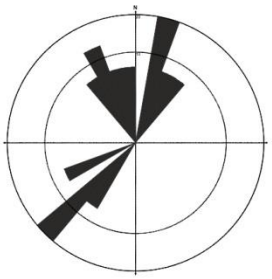

Locality 22 (Sarnoo)
n: 30
m: 328.10°
d: ± 59.30°
f: Sx

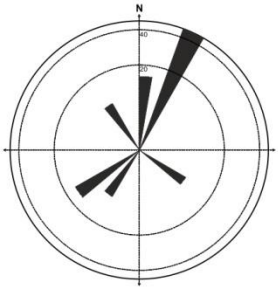

Locality 38 (Sarnoo)
n: 13
m: 9.15°
d: ± 60.03°
f: Sr

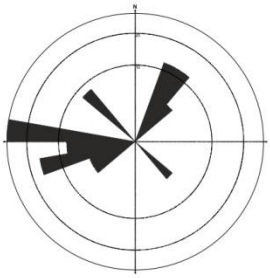

Locality 131 (Darjaniyon-ki Dhani)
n: 25
m: 295.05°
d: ± 56.64°
f: Sx

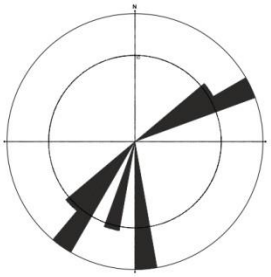

Locality 134 (Sarnoo)
n: 9
m: 171.11°
d: ± 61.41°
f: Sx

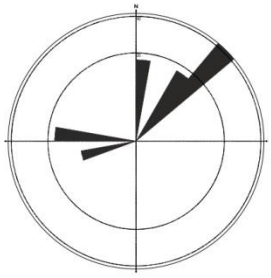

Locality 134 (Sarnoo)
n: 12
m: 17°
d: ± 51.08°
f: Sb

Locality 135 (Sarnoo)
n: 121
m: 260.37°
d: ± 58.75°
f: Sr

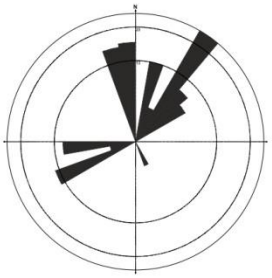

Locality 136 (Sarnoo)
n: 87
m: 215°
d: ± 50.24°
f: Sr

Figure 7.5: Rose diagrams for the Sarnoo Sandstone, with the data presented in 10° bins. The data is bimodal from the southwest to the northeast.

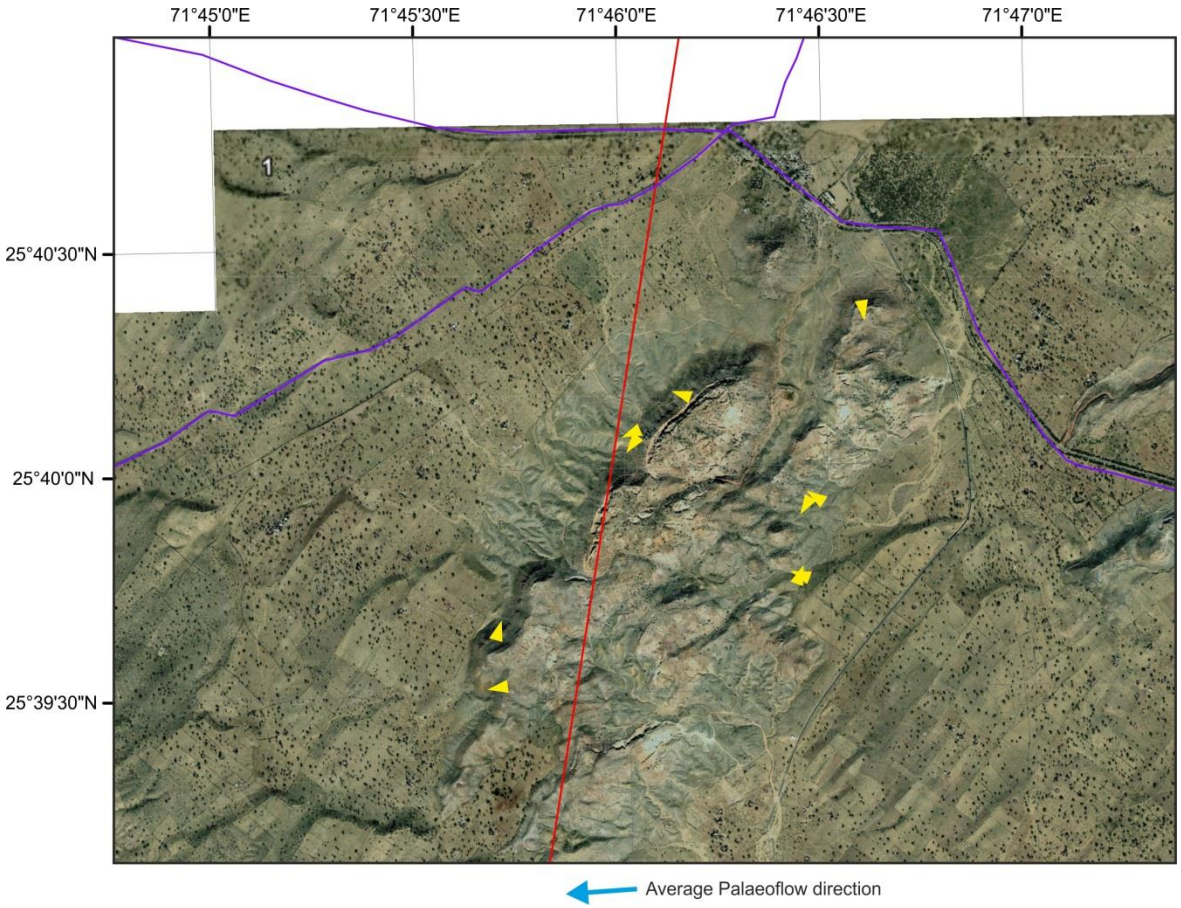

Figure 7.6: Moving average data for the Sarnoo Sandstone, with an average flow to the southwest – west.

The palaeocurrent data collected from the Nosar Sandstone are from facies G, Stx, Sx and Sr using ranks 5 and 6, and checked against the ranks 3 and 4 data. The data display a range of directions from the south to the east (Figure 7.7) displaying bimodal to polymodal palaeocurrent data at all field locations (Figure 7.7) with low dispersion values (Table 7.3) as expected as it is a bedload-dominated, low sinuosity fluvial system (Figure 5.19). The Nosar Sandstone palaeoflow is broadly to the southwest. However the Nosar Sandstone has different average directions within each field site; at the Sarnoo and Karentia field areas the overall average flow is to the southwest (Figures 7.8, 7.9) while the Nosar field area has an overall average flow to the northwest (Figure 7.10).

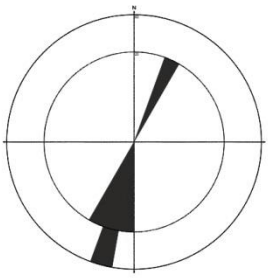

Locality 18 (Sarnoo)
Number of measurements (n): 5
Mean (m): 194.68°
Dispersion (d): ± 51.79°
Facies (f): Sx

Locality 49 (Sarnoo)
n: 26
m: 235.10°
d: ± 49.27°
f: Sx

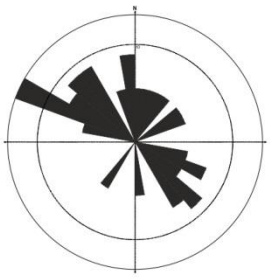

Locality 53 (Sarnoo)
n: 36
m: 342.24°
d: ± 68.66°
f: Sx

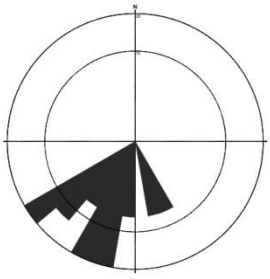

Locality 61 (Sarnoo)
n: 15
m: 208.06°
d: ± 22.30°
f: Sx

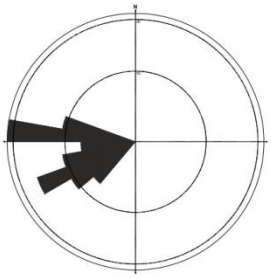

Locality 67 (Sarnoo)
n: 18
m: 260.45°
d: ± 18.51°
f: Sx

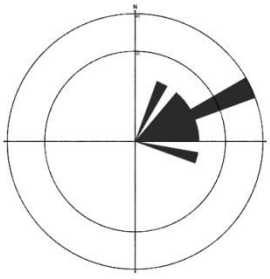

Locality 76 (Sarnoo)_
n: 10
m: 65.62°
d: ± 19.87°
f: Sx

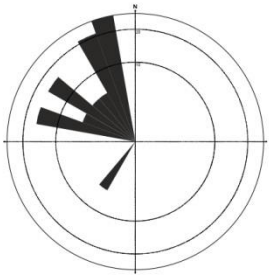

Locality 153 (Sarnoo)
n: 19
m: 318.08°
d: ± 29.64°
f: Sx

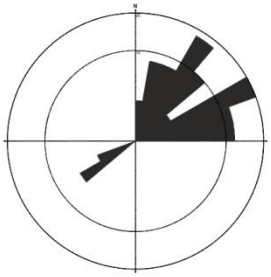

Locality 156 (Sarnoo)
n: 40
m: 52.39°
d: ± 37.69°
f: Sx

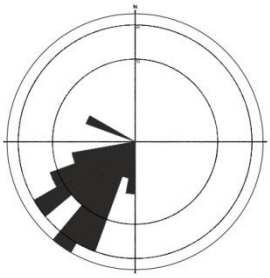

Locality 161 (Sarnoo)
n: 51
m: 225.89°
d: ± 21.30°
f: Sr

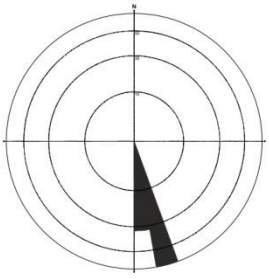

Locality 296 (Sarnoo)
n: 3
m: 170°
d: ± 3.29°
f: Sx

Figure 7.7: Rose diagrams for the Nosar Sandstone, with the data presented in 10° bins. Local vector data varies from unimodal to polymodal with local palaeoflow directions from south through west to northeast.

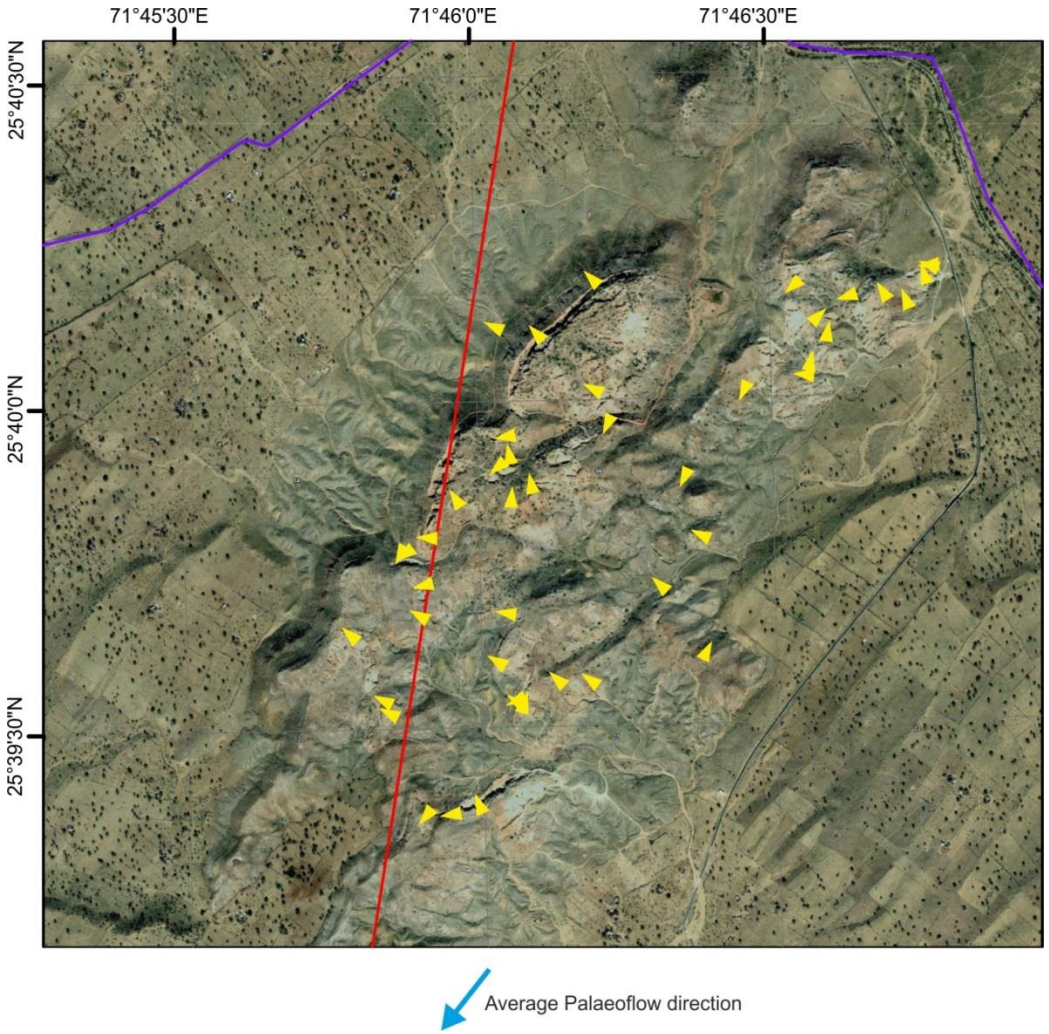

Figure 7.8: Moving average data for the Nosar Sandstone at the Sarnoo field location, with an average flow to the southwest.

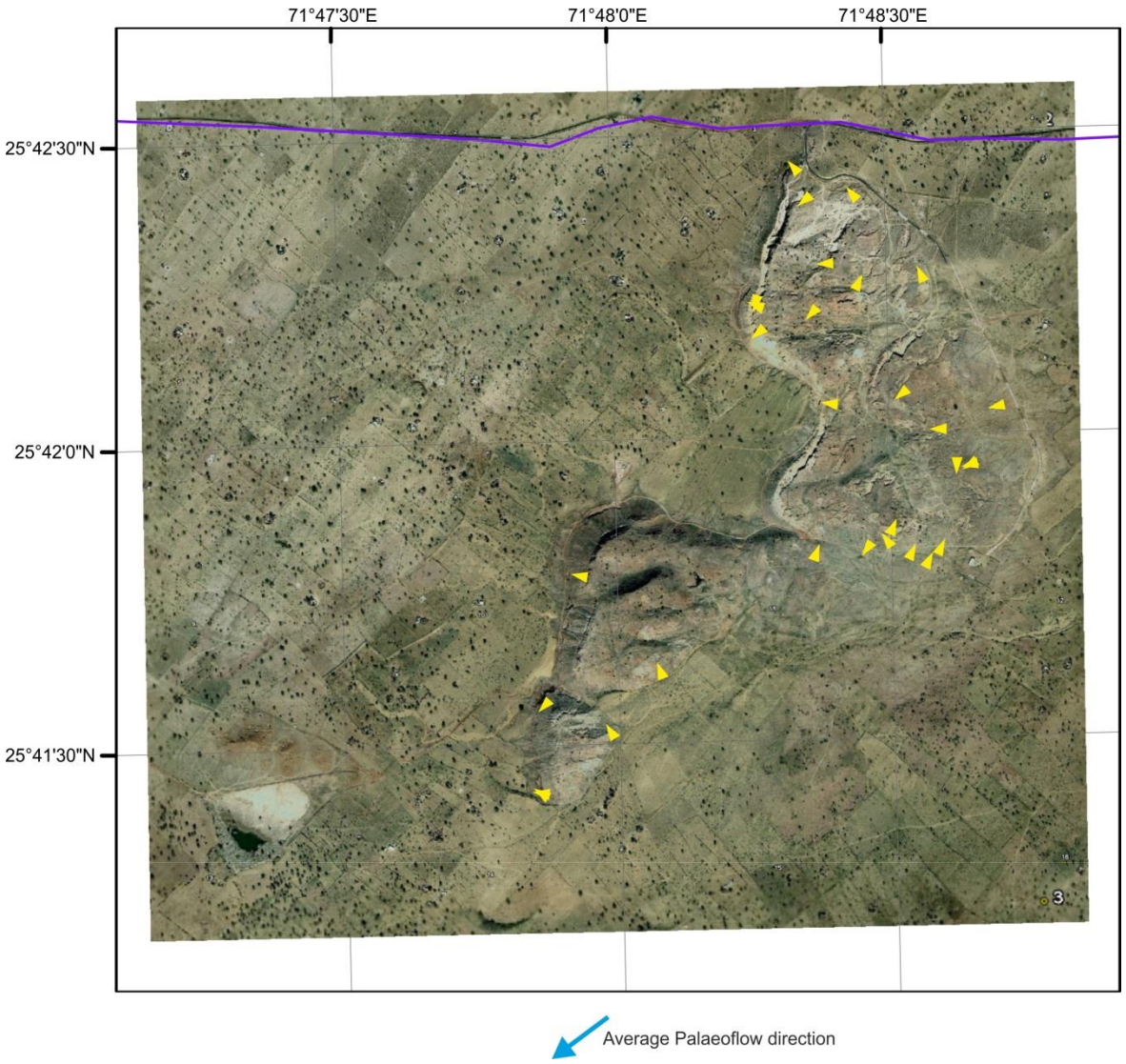

Figure 7.9: Moving average data for the Nosar Sandstone at the Karentia field location, with an average flow to the southwest.

7.3.1 Sinuosity data

The LeRoux (1992) equation has been used to calculate the channel sinuosity. The sinuosity for the Darjaniyon-ki Dhani Sandstone has not been calculated as there is not enough palaeocurrent data for this sandstone due to lack of exposure. The data for the Sarnoo Sandstone produces a high sinuosity system (Table 7.4), as predicted from the dispersion values and the sedimentology. The Nosar Sandstone displays a low sinuous system, as expected from the sedimentology and the dispersion values (Table 7.4), the variations noted within the rose diagrams are likely to be because the palaeocurrent measurements were taken from various parts of the sandy bar (F1), gravel bar (F3) and sheetflood (F6) elements.

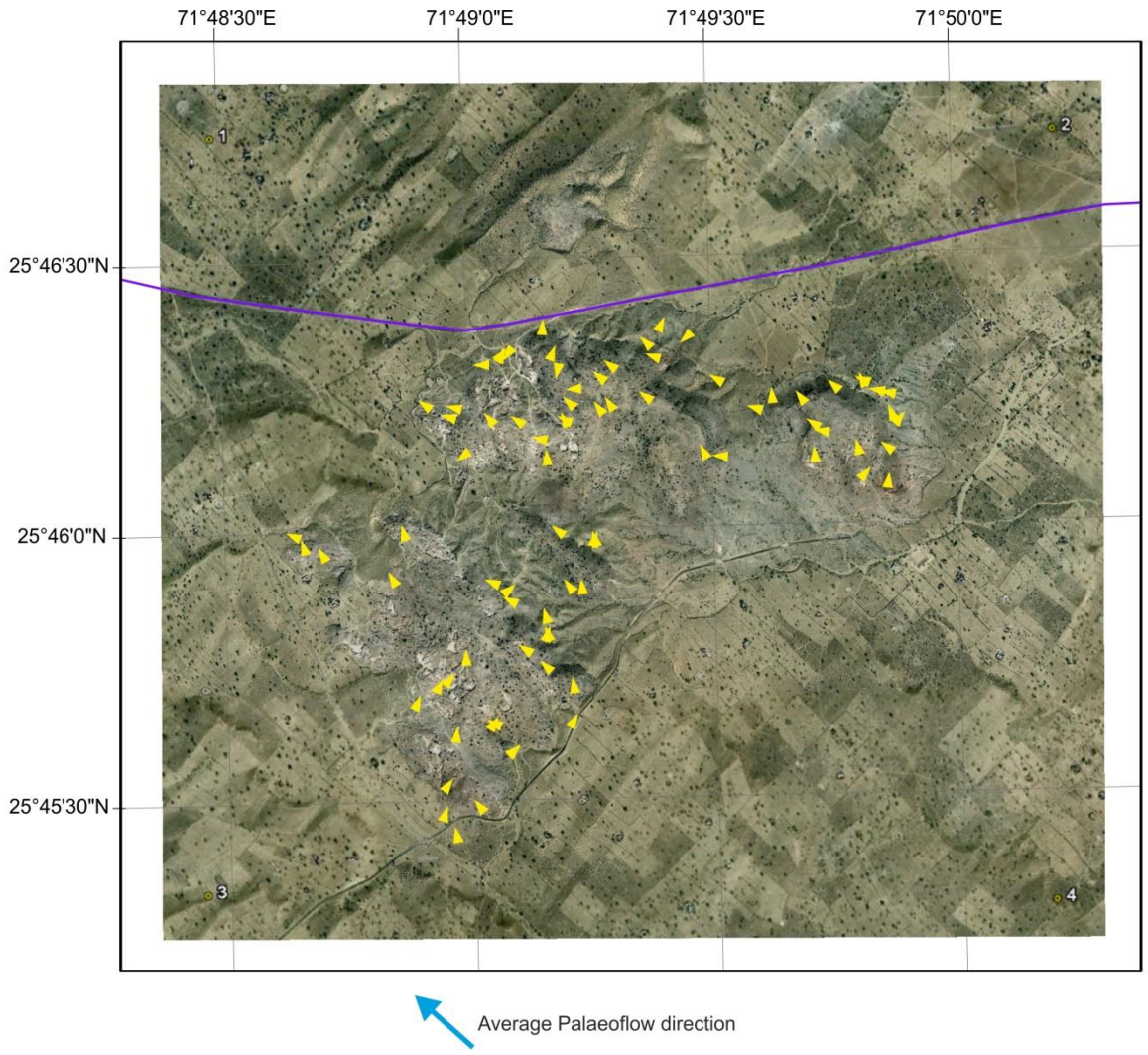

Figure 7.10: Moving average data for the Nosar Sandstone at the Nosar field location, with an average flow to the northwest.

Location	Sinuosity data
Sarnoo Sandstone	
Sarnoo at Sarnoo	**2.69**
Nosar Sandstone	
Nosar at Sarnoo	0.04
Nosar at Karentia	0.045
Nosar at Nosar	0.05

Table 7.4: Averaged sinuosity data for the Sarnoo and the Nosar Sandstone at all locations, using the LeRoux (1992) equation (Equation 7.3).

7.4 Interpretation

From the data presented in this study, the general flow of the Ghaggar-Hakra Formation is to the southwest and this is in agreement with Sisodia and Singh (2000). However, Compton (2009) interprets the Ghaggar-Hakra Formation as a feeder to the Pariwar shelfal system (Figure 7.11), suggesting a northwest palaeoflow to the fluvial system.

Neither of these papers give detailed information on the palaeocurrent dataset upon which the interpretations of the authors are based, as it could be from anywhere within the field area or the subsurface dataset.

The data for the Darjaniyon-ki Dhani Sandstone is unimodal to bimodal because the sparse and indistinct cross-bedded sets and cosets are erratic as expected with a gravel bedload, low sinuous river. The bimodal palaeocurrent data with a high dispersion for the Sarnoo Sandstone is in agreement with the unit's interpretation as it is a mixed load, high sinuosity fluvial system. The bimodal to polymodal flow for the Nosar Sandstone is due to the low sinuosity nature forming the erratic sets and cosets forming transient barforms and bedforms. Based on the information presented here, there are two dominant flows; to the southwest from the Darjaniyon-ki Dhani Sandstone up to the Nosar Sandstone at the Sarnoo and Karentia field areas (Figures 7.4, 7.6, 7.8, 7.9). The second dominant flow is to the northwest as observed within the Nosar Sandstone at the Nosar field area (Figure 7.10).

Although many palaeocurrent readings have been taken is it questionable as to whether the flow of the palaeocurrent is going towards the basin centre as the field area is small. For the Darjaniyon-ki Dhani Sandstone not only does the small size of the field area affect the data collected but, the outcrop extent also minimal. The Darjaniyon-ki Dhani Sandstone has an average palaeoflow to the south (Figures 7.1, 7.6) which differs from the other two sandstone successions; this could be due to multiple reasons. The first reason is this system contains indistinct cross-bedding with a high sediment supply meaning there are few places where measurements could be taken from. The channels of the Darjaniyon-ki Dhani Sandstone could be following the palaeotopography of the Lower Cretaceous Karentia Volcanic Formation or the Precambrian Malani Igneous Suite, (Sunder *et al.,* 2013). The palaeoflow of the Sarnoo Sandstone represents a high sinuosity system, as predicted from the sedimentology (Figure 5.18, Table 7.4); however

as the field area is small the averaged direction of west may not be true. The data for the Nosar Sandstone is likely to be representative of the depositional environment as the Nosar Sandstone outcrops in multiple places and a large amount of data were collected.

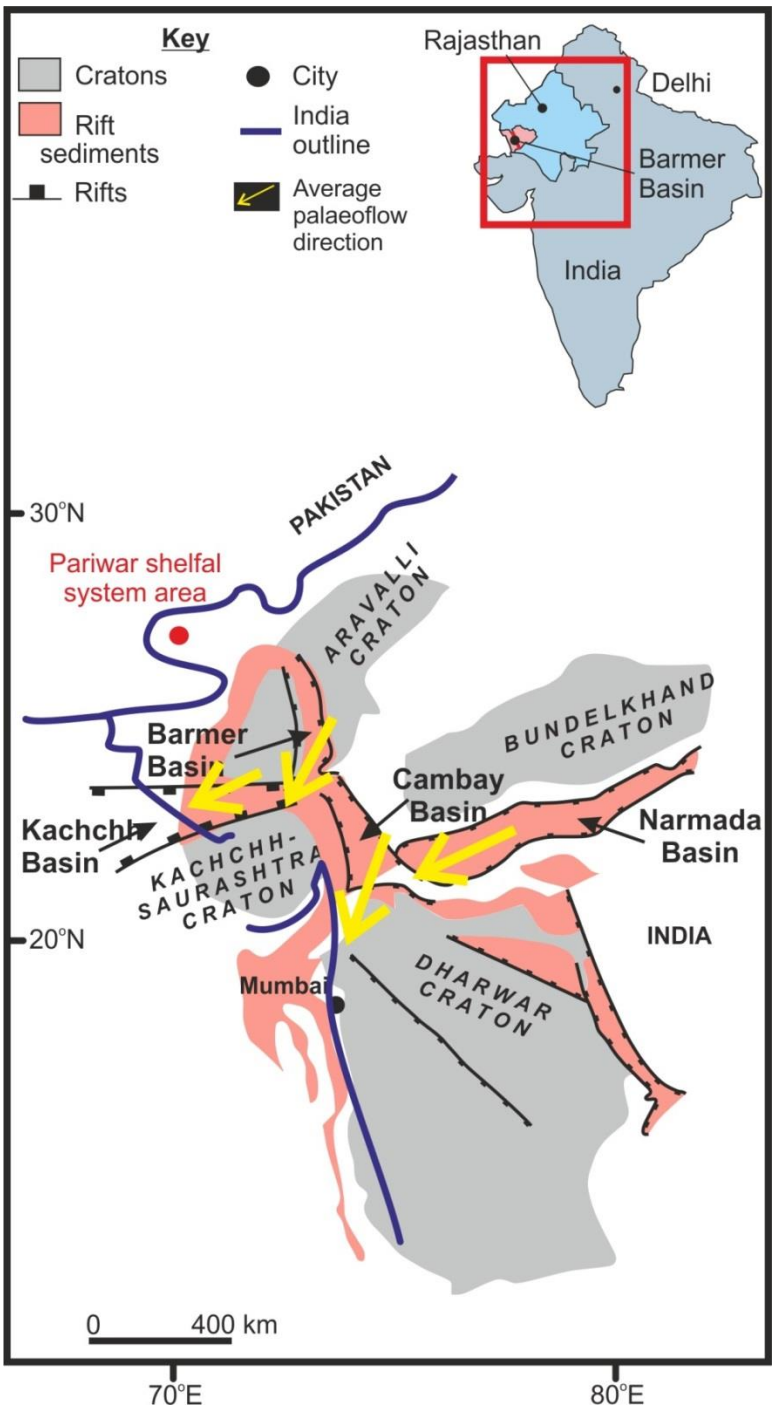

Figure 7.11: Regional palaeoflow of the West Indian Rift System (yellow arrows). The four basins within the West India Rift System all have Lower Cretaceous fluvial systems with an average palaeoflow between south-southwest to southwest, suggesting that all the systems are draining north-western India together (Balakrishnan *et al.,* 2009; Racey *et al.,* In review).

7.5 Discussion

The directions of the palaeocurrent change between each of the sandstone successions, as between the Darjaniyon-ki Dhani and Sarnoo sandstones the palaeoflow changes from south to west, respectively. A change in palaeoflow can occur for multiple reasons: growth in a fault network, uneven palaeotopography or avulsion / rejuvenation of the fluvial system. As stated in Chapter 3 during the Lower Cretaceous Epoch incipient faulting began within the location of the present day eastern Barmer Basin margin (Section 3.2, Figure 3.2c). There is not enough data to tell if the Darjaniyon-ki Dhani Sandstone was affected by the subsidence on incipient growth faults. An assumption is made that the incipient faulting did not affected the variation in palaeoflow between the Darjaniyon-ki Dhani and Sarnoo sandstones because there is no evidence of fluvial rejuvenation. The change in palaeoflow direction is likely to be due to the palaeotopography and channel avulsion within the fluvial system. The palaeoflow changes direction from the Sarnoo to Nosar sandstones from west to southwest, respectively. This can be attributed to three reasons either a change in the palaeotopography, the rejuvenation of the fluvial system (Section 5.4) or fault subsidence on the eastern margin. The Nosar Sandstone has a highly erosive base and rejuvenation of the fluvial system has occurred from a high sinuosity system (Sarnoo Sandstone) into a low sinuosity system (Nosar Sandstone) therefore the most likely reason for the change in fluvial style and palaeoflow direction is fault subsidence on the growing Barmer Basin margin (Section 3.2).

Overall, the limits with the data collected are that some of the surfaces were very uneven which make it difficult to take reliable measurements (Khan and Tewari, 2015). There can be limited space to take measurements making data slightly unreliable, as all palaeocurrent measurements are confined to a few isolated geographical areas, which may not be representative of a system as a whole (Stewart *et al.,* 2001).

Modelling of the Base Cretaceous fault network within the subsurface of the Barmer Basin displays southern depocentres (Figure 7.12) and implies a southerly flow of the subsurface Ghaggar-Hakra Formation directly tying to the palaeocurrent data from the outcrops at the Sarnoo and Karentia field locations. The modelling of the Base Cretaceous fault network also displays a northerly palaeoflow of Cretaceous-aged material to the northwest in the north of the Barmer Basin (Figure 7.12) and also indicated by the Nosar Sandstone at the Nosar field area, potentially feeding Pariwar shelves (Figures 7.11, 7.12, Compton 2009). It is suggested from the subsurface modelling and the palaeoflow data collected at outcrop that the change in the palaeoflow directions from the north to the south of the basin is likely to be controlled by the pre-existing west-striking fault network (Sections 3.2, 3.2.1, Bladon *et al.,* 2015b).

This south-southwest palaeoflow of the southern half of the basin directly ties in with the regional palaeoflow of north-western India (Racey *et al.,* In review) during Lower Cretaceous times. The dominant palaeoflow of the Lower Cretaceous fluvial systems within the Cambay and Narmada basins is west – southwest (Figure 7.11, Racey *et al.,* In Review). By establishing the palaeoflow orientation of the fluvial systems that were depositing during the Lower Cretaceous a regional palaeoflow, regional palaeodrainage and provenance can be inferred (Figures 7.11, 7.12). However, the data range for the Ghaggar-Hakra Formation is sporadic it can only be suggested that the Ghaggar-Hakra links to the Lower Cretaceous fluvial systems of the Cambay and Narmada basin (Racey *et al.,* In review). To help link the palaeoflow of the Ghaggar-Hakra Formation to other fluvial systems during the Lower Cretaceous Epoch, borehole imaging data and palaeocurrent data of the subsurface would be needed as there is no surface expression of the Ghaggar-Hakra within the basin centre.

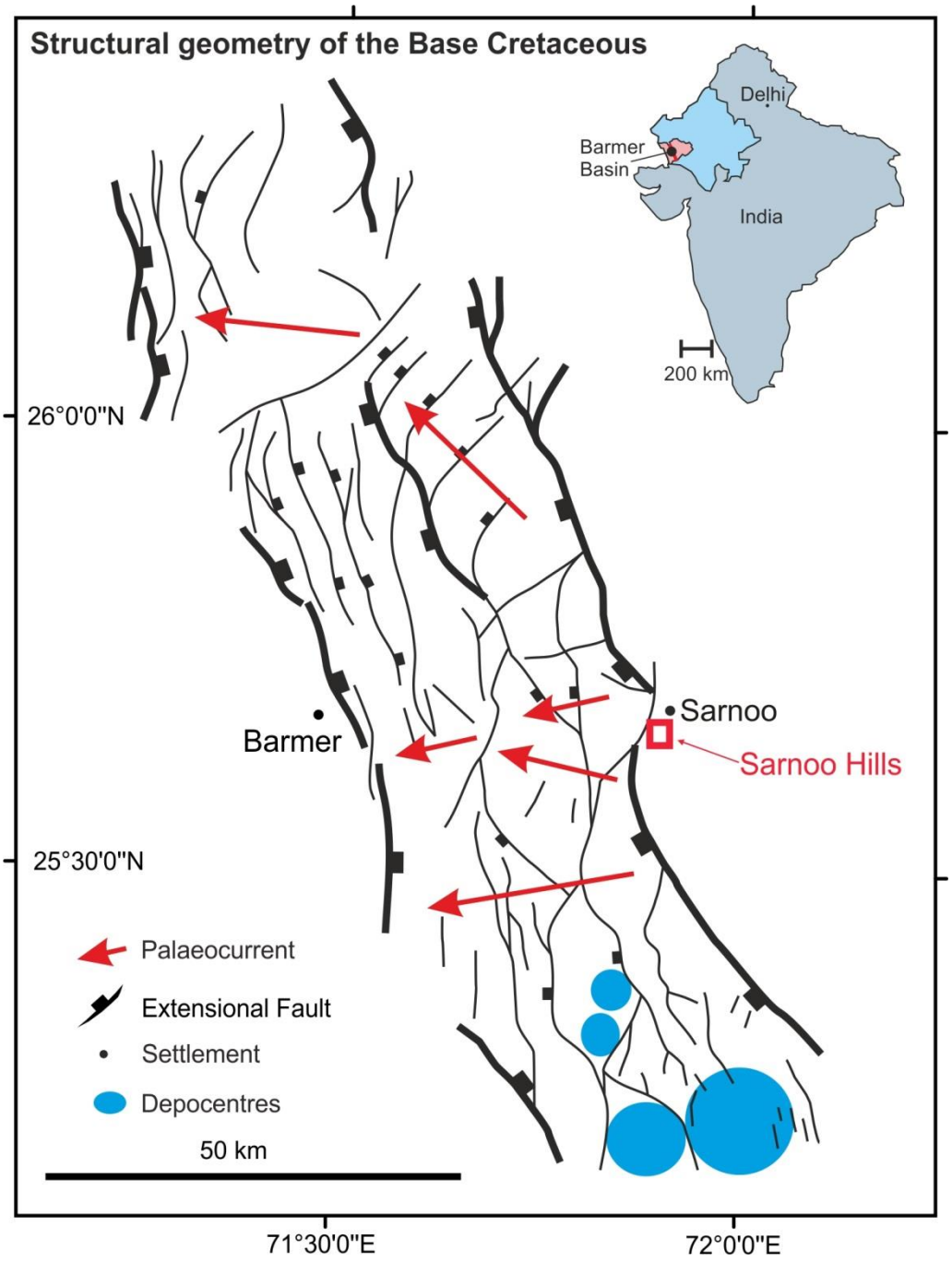

Figure 7.12: Time surface data supplied by Cairn (unpublished), displaying the fault network (black lines) and interpreted palaeocurrent data, overlying (red arrows). The map also displays the southern depocentres in the Barmer Basin (blue circles). Inset: Map of India shows the location of the Barmer Basin. For grid see Figure 1.3.

7.6 Summary

The hierarchical racking system for palaeocurrent analysis takes measurements from entire channel belts to small-scale sedimentary structures (Allen, 1966; Miall, 1974), where the most reliable rank are the large-scale, three-dimensional sedimentary structures such as cross-bedding. Once the palaeocurrent data has been collected there

are numerous analyses conducted, the ones mentioned here are dispersion, vector mean analysis and moving average analysis.

The palaeoflow of the Darjaniyon-ki Dhani Sandstone is to the south and displays a unimodal to bimodal distribution; however there is limited data to support this statement. The Sarnoo Sandstone was deposited by a fluvial system transporting sediment to the west. The rose diagrams are bimodal and there is a high dispersion rate, providing evidence for a mixed load, high sinuosity fluvial system, with a calculated sinuosity of 2.6. The flow of the fluvial system responsible for deposition of the Nosar Sandstone is to the southwest and northwest; this system yields bimodal to polymodal current rose diagrams and is a bedload dominant, low sinuosity fluvial system, with a calculated sinuosity from 0.04 to 0.05. The change in dominant direction between each sandstone succession is due to topographical changes, rejuvenation of the fluvial system or subsidence related to the incipient faulting on the eastern Barmer Basin margin (Section 3.2).

The palaeoflow of the Ghaggar-Hakra Formation is dominantly to the southwest and relates well to the subsurface data of the Barmer Basin and rest of the data observed within the West Indian Rift System as all the Lower Cretaceous fluvial systems drain towards the west (Racey *et al.,* In review, Figures 7.1 – 7.12). The palaeocurrent data from the Nosar field area is to the northwest and probably was diverted by a pre-existing west-striking fault network.

8 Chapter Eight: Interpretations of the Ghaggar-Hakra Formation at outcrop

The Ghaggar-Hakra Formation at outcrop has been previously interpreted as the deposits of a fluvial system (Bower, 2004a, b; Clarke, 2011; Sunder *et al.,* 2013). However, the evolution of the system, the controls upon it and the provenance of the sediments remain unresolved. To address this, the objectives of this research (summarised in Chapter 1) were to:

- Undertake detailed sedimentological analysis of all Ghaggar-Hakra sediments to understand the stratigraphy, nature of the succession and the depositional environment;

- Undertake detailed petrographical analysis and palaeocurrent data analysis to examine the provenance for the fluvial system;

- Produce three-dimensional facies models for the depositional environments of the formation and integrate these models into the post-depositional structure;

- Place the formation in the wider context of the evolving Barmer Basin and the regional West Indian Rift System.

To achieve these objectives this work has integrated multi-disciplinary investigations, from outcrop-based observations and interpretation to laboratory sample analysis (Chapters 4 - 7). The outcrop interpretations were based upon a description and interpretation of facies, architectural elements (Chapters 4 and 5); laboratory sample analysis including petrography (Chapter 6) and palaeocurrent data analysis (Chapter 7).

This chapter discusses these results and relates them back to the original aims of the research to place the evolving Ghaggar-Hakra Formation into the wider context of the evolving Barmer Basin and the West Indian Rift System. The chapter ends by discussing the limitations of the dataset and the petroleum potential of the Ghaggar-Hakra Formation.

8.1 Depositional regime of the Ghaggar-Hakra Formation

The Ghaggar-Hakra Formation is described in Chapters 4 and 5 by facies, facies associations, architectural elements and depositional elements. The evolutionary model is described and interpreted at the end of Chapter 5 (Section 5.4) and by Figure 5.22. Here, a concise summary of the fluvial evolution is presented.

The formation itself contains three separate sandstone successions that are characterised by medium- to coarse-grained, stacked and amalgamated channel sandstones. In between the channel sands are packages of clays- to fine-grained sandstones that are heavily bioturbated, representing cumulative vertisols. The Ghaggar-Hakra also overlies a floodplain succession, containing basaltic dykes of the Karentia Volcanic Formation intruded into the sediments after their deposition (Figure 8.1a), forming baked margins (Figure 8.1b).

The first depositional element DE1 (Figures 5.22, 8.2) starts with an erosive surface and comprises granule-grade conglomerates that are either structureless or contain indistinct cross-beds. Numerous third- to fifth-order bounding surfaces attest to stacked and amalgamated gravel bars (Section 5.2.3, F3), and isolated sandy bars (Section 5.2.1, F1) representing fluvial deposition in a low-sinuosity, fluvial system with a palaeoflow towards the south (Figure 7.4). The detrital mineralogy of sediments is dominantly quartz (60%) with the highest amount of rock fragments (sedimentary 3.3%, and metamorphic 2.9%, Figure 6.11) compared to the other channelized sandstones. The dominant authigenic mineral is haematite cement (Figure 6.11). This depositional element is lithostratigraphically equivalent to the Darjaniyon-ki Dhani Sandstone of Bladon *et al.,* (2015a).

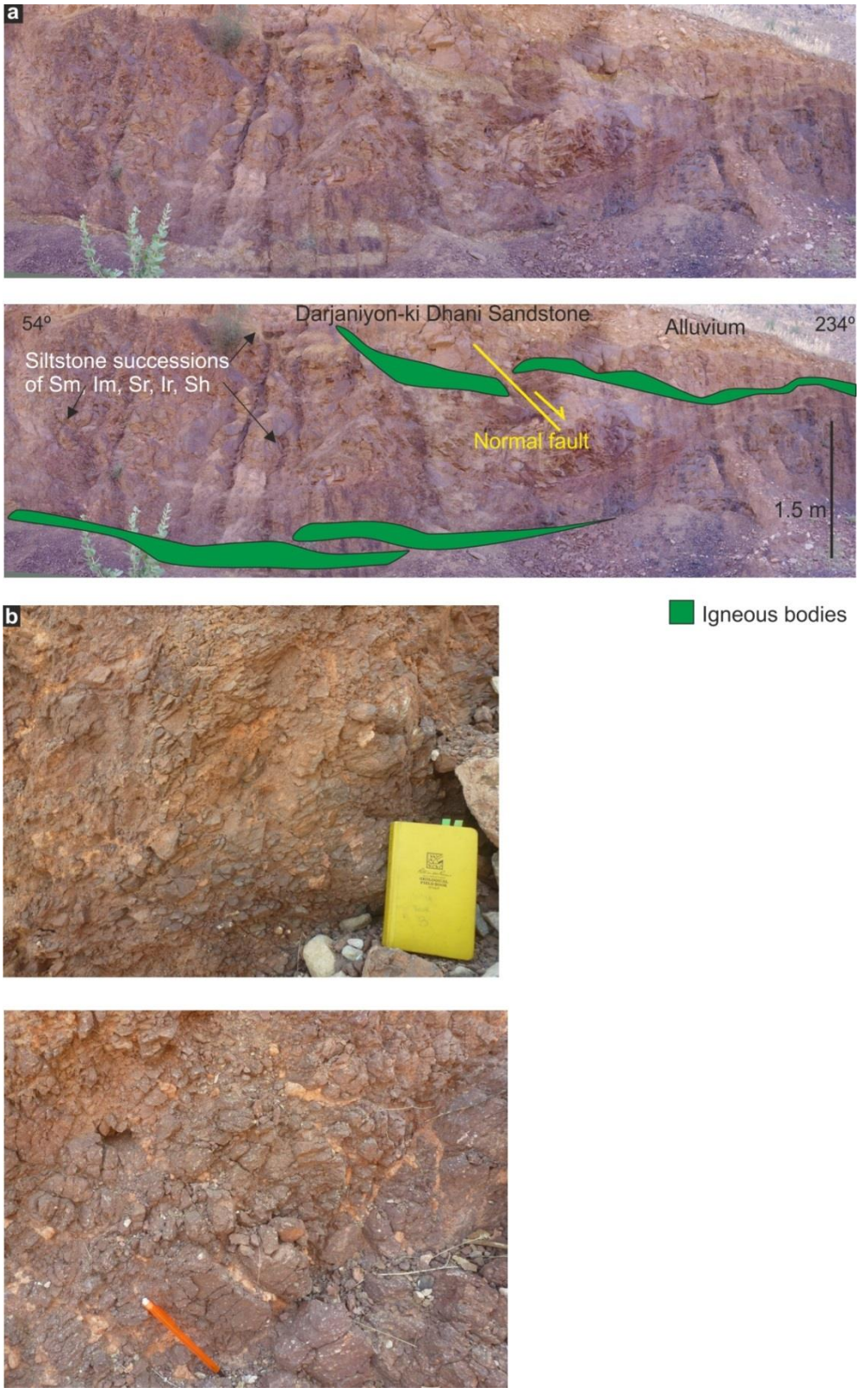

Figure 8.1: The Ghaggar-Hakra floodplain sediments affected by the Karentia Volcanic Formation. (a) Dykes of the Karentia Volcanic Formation intruding into the Ghaggar-Hakra floodplains, the dykes are cross-cuts by faults at the Karentia field locality (UTM 780910, 2845222 and (b) baked margins within the floodplain sediments from the intrusions of dykes from the Sarnoo field locality (UTM 778078, 2842112).

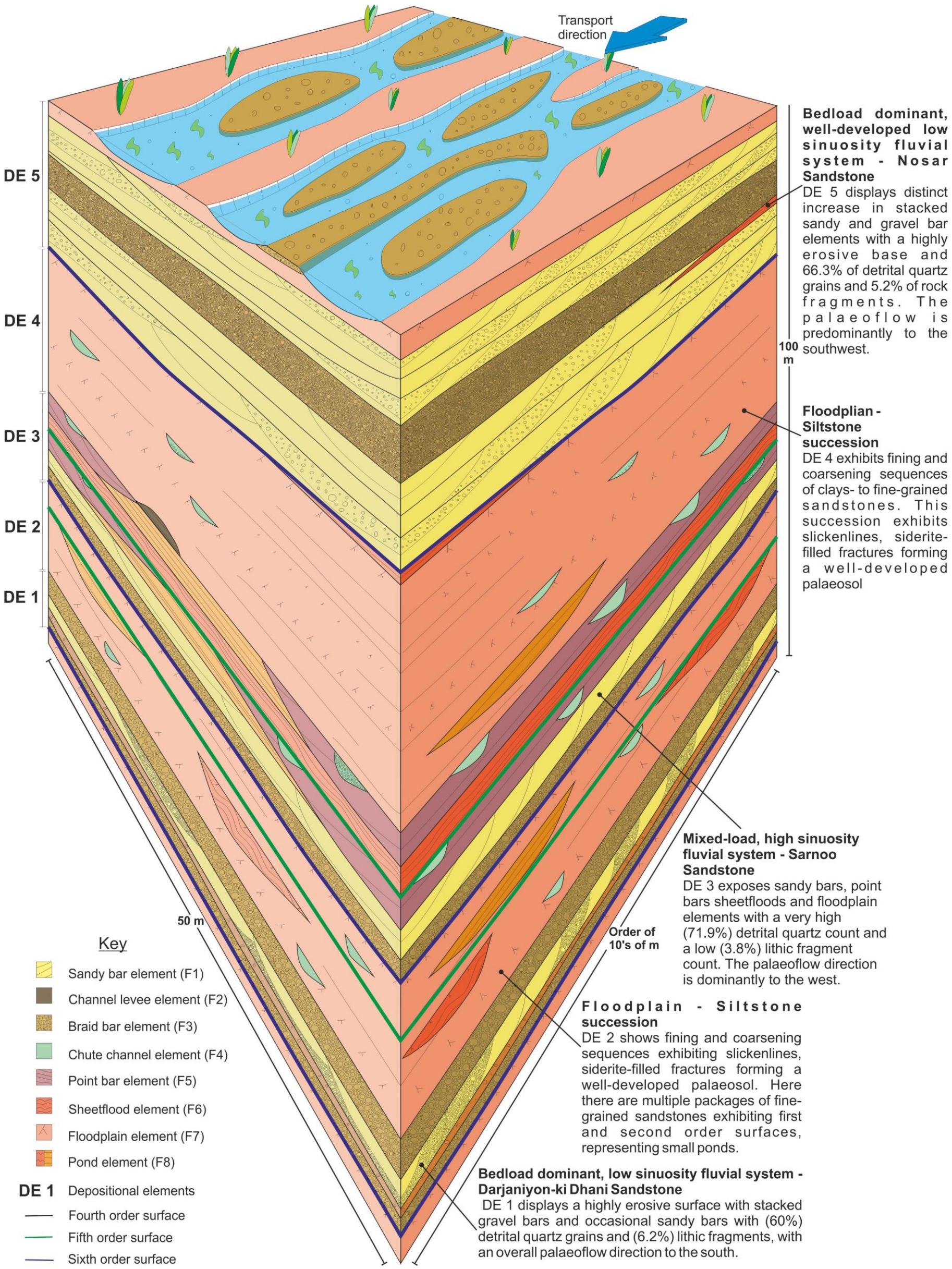

Figure 8.2: Summary diagram of the Ghaggar-Hakra Formation displaying the architectural elements and explaining to key findings of the petrography and the palaeocurrent data.

Above the Darjaniyon-ki Dhani Sandstone, depositional element DE2 comprises clay- to fine-grained red sediments in thin beds to laminae totalling up to 25 m thick succession (Figure 5.22) representing deposition in the floodplain environment. The sediments are fining and coarsening upwards with a haematitic nature and slickenlines forming cumulative well-developed palaeosols (Section 5.2.7, F7). The haematitic nature here indicates vertisols. Within this depositional element, packages of sediment up to 2 m thick and 50 m wide, comprising beds/laminae of sandstone and siltstone arranged into ripple laminated sets containing first and second order surfaces, represent deposition in overbank ponds (Section 5.2.8, F8). The petrography here displays very fine-grained, sub-rounded, highly spherical, detrital quartz grains with high quantities of haematite cements.

The third depositional element DE3 (Figures 5.22, 8.2) comprises a succession up to 20 m thick of fining upwards sandstones. The element contains silt- to coarse-grained sandstones with cross-bedded sets and cosets representing the sandy bars (F1, Section 5.2.1) of a mixed load, high sinuosity depositional system. Fourth to fifth order bounding surfaces mark the channel bases and the bases to associated point bars (F5, Section 5.2.5) and gravel bars (F3, Section 5.2.3). This sandstone succession has the highest quartz volume (71.9%) and the lowest lithic fragment volume (3.8% Section 6.2.5) of the three sandstone bodies studied. The palaeocurrent data for this succession indicates flow towards the west with a high dispersion (32.43, Table 7.3) due to the sinuous nature of the fluvial system. The increased consistency of sets and cosets, compared to the Darjaniyon-ki Dhani Sandstone, suggests stabilisation and maturation of the fluvial system from DE1 to DE3. Lithostratigraphically, this succession is laterally equivalent to the Sarnoo Sandstone.

DE4 displays fining and coarsening upwards successions of clays- to fine-grained sandstones. This succession exhibits slickenlines, siderite-filled fractures forming a well-developed palaeosol. The detrital petrography is composed of quartz grains, with no

feldspar. The authigenic mineralogy comprises dominantly of haematitic cements resulting in no measurable porosity. These sediments represent a well-vegetated floodplain environment. There is a lack of isolated pond successions, when compared to the lower floodplains (Figures 5.22, 8.2), suggesting a lack of flooding from the fluvial system and adding to evidence of a maturing fluvial environment.

The final depositional element (DE5) is at least 25 m thick. The start of this element is marked by a highly erosive sixth order surface. The succession comprises fining upwards successions from granule-grade to fine-grained sandstones with first to fifth order surfaces that relating to sandy bar deposition (F1, Section 5.2.1) and gravel bars (F3, Section 5.2.3). Limited lenticular packages (up to 1 m thick and 2 m wide) of well-developed palaeosols are present. The petrography data demonstrates a decrease in detrital quartz grains (66.3%) and an increase in rock fragments (5.2%). There is a significant increase in non-resolvable clays (11.5%) within this sandstone, likely due to the highly erosive nature of the flows that formed the sandstone succession. The dispersion of the palaeocurrent data is low (13.5, Table 7.3) and towards the southwest. All of the data suggests a well-developed, bedload-dominant, low sinuosity fluvial system, laterally equivalent to the Nosar Sandstone (Figures 5.22, 8.2).

The sedimentary succession from the bedload dominant, low sinuosity fluvial system of the Darjaniyon-ki Dhani Sandstone (DE2, Figures 5.22, 8.2) to the mixed load, high sinuosity system of the Sarnoo Sandstone (DE4, Figures 5.22, 8.2), demonstrates an evolution of the fluvial system. This is evidenced by a general fining of the sediment, an increase in the sediment sorting, roundness and sphericity. Also noted is a reduction in the amount and size of the quartz clasts. There is an increase in consistency of the trough and planar cross-bedded sets and cosets and rippled-scaled sets and cosets. Also there are decreases in the frequency of erosional boundaries within the Sarnoo Sandstone (Figure 5.18) when compared to the Darjaniyon-ki Dhani Sandstone.

The contemporary floodplains appear to evolve during the deposition of the formation; becoming more extensive and laterally continuous, implying the maturation of the fluvial system as a whole. The preserved thicknesses of the floodplain sections are very significant and likely relate to the stability of the fluvial system at the time of deposition. There is a higher amount of ponding within the lower floodplain (DE2, Figures 5.22, 8.2), when compared to the higher floodplain (DE4, Figures 5.22, 8.2). This suggests a higher rate of flooding within the lower floodplain can relate to the stabilisation of the fluvial discharge over time.

The top of the floodplain succession in outcrop is marked by the low sinuosity, fluvial system of the Nosar Sandstone. The sediments formed this erosive channelized environment containing high amounts of lithic fragments (Sections 5.2.1, 5.3.1, 5.3.3) and display a consistently different palaeoflow to the fluvial packages below it (Sections 7.4, 7.5). This may indicate an external influence on the sedimentary system at this point in its evolution.

8.2 Tectonic influences on the Barmer Basin

The tectonic regime that prevailed during the formation of the Barmer Basin created extensional fault networks and the development of relay ramps between fault segments likely influences the drainage patterns of sedimentary regimes (Figure 2.12, Gawthorpe and Hurst, 1993). Relay ramps themselves can be both soft and hard-linked depending on whether the relay structures are breached (Fossen, 2010, Figure 2.12). Breached relay ramps will further influence the drainage patterns of the sedimentary systems.

8.2.1 Current structural interpretations of the eastern Barmer Basin margin

The current structural understanding of the central eastern Barmer Basin margin, where the outcrops of the Ghaggar-Hakra examined in this study are located, have been assessed from outcrop and subsurface data by Bladon *et al.,* (2015a, b). In the central

eastern Barmer Basin margin, pre-Cretaceous, west-striking structures have influenced the growth and development of the Barmer Basin rift. At outcrop, two distinct fault trends have been recognised (Bladon *et al.,* 2015a, b), namely: (1) the pre-existing north-dipping, west-striking faults, and; (2) northwest dipping, southwest-striking faults (Section 3.3.1; Figure 8.3).

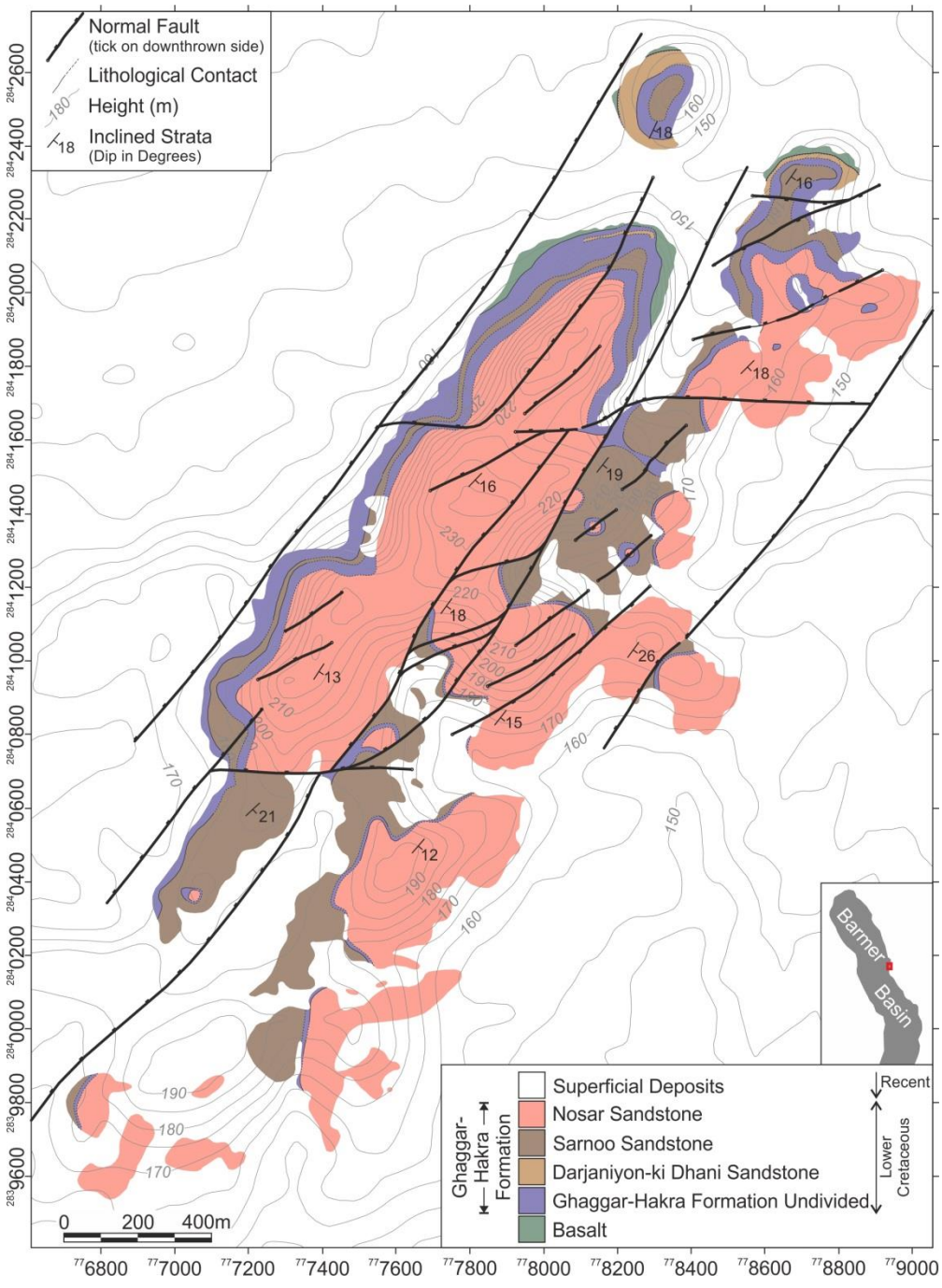

Figure 8.3: Structural geometry of the Sarnoo field area, displaying the pre-existing east-west orientated structures that intersect with the southwest striking, northwest dipping faults (adapted from Bladon *et al.,* 2015a).

The west-striking faults are older and influence the growth of the younger southwest-striking fault network (Bladon *et al.,* 2015b). As extension occurs the west-striking faults are active, as these faults are the most efficient way for extension to occur during the earliest stages of extension (Bladon *et al.,* 2015b). The southwest-striking faults are sub-parallel to the dominant west-striking fault network; hence they are very closely linked and are significantly influenced by the west-striking fault network (Bladon *et al.,* 2015b). Bladon *et al.,* (2015b) state that together they form a zig-zag fault network. This implies that the west-striking fault network played a significant role in the early development of the southwest-striking fault network (Bladon *et al.,* 2015b), as the southwest-striking fault network develops and becomes established within the basin as the extension transfers into this network. Once the southwest-striking network is established, the west-striking network becomes passive (Morley, 1999; Bladon *et al.,* 2015b).

At the larger scale, seismic interpretations of the subsurface, local to the Sarnoo area have identified three areas of distinct structural style that interact during evolution of the Barmer Basin. Bladon *et al.,* (2015a) term these the (1) east-rift margin fault system, (2) mid-rift fault system and (3) the west-rift fault system (Figure 8.4). The east-rift margin fault system comprises predominantly southwest-striking faults dipping northwest along the same trend as those observed at outcrop. The mid-rift fault system comprises faults striking northwest – southeast. The west-rift fault system is a rift-parallel fault system extending southwards, in the west of the Barmer Basin (Figure 8.4).

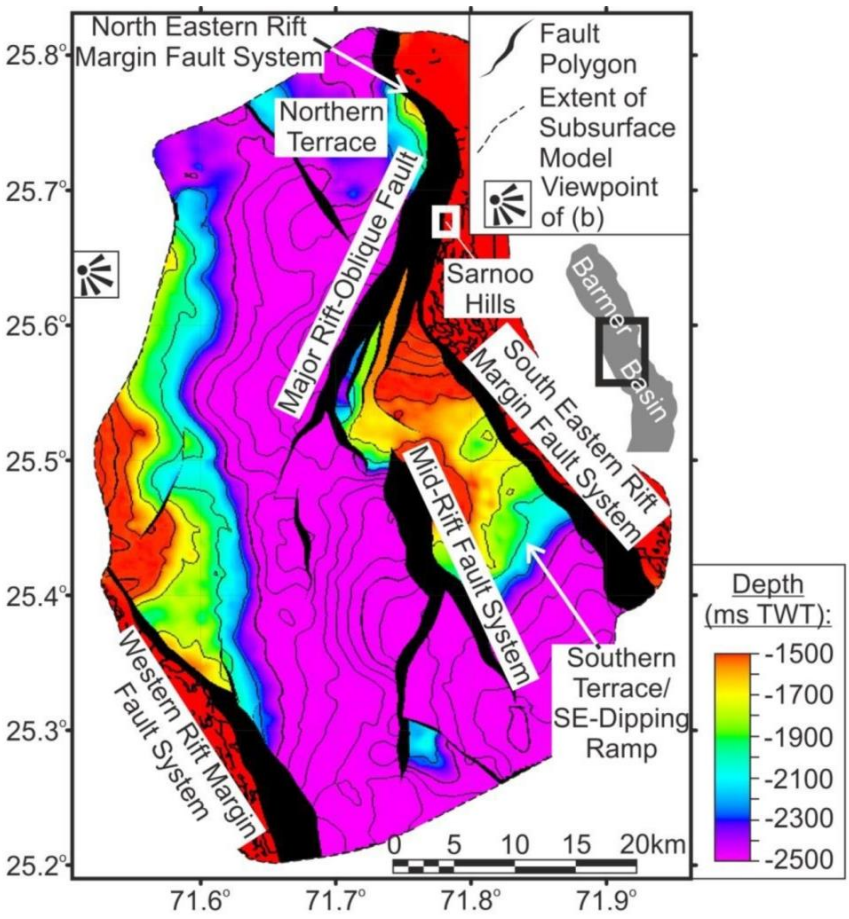

Figure 8.4: Structural interpretation of the subsurface based on seismic data, displaying the linkage of the east-rift and mid-rift systems, with the isolated west-rift system (Bladon *et al.,* 2015b).

The geometry of the basin margin displays a gradual left-stepping of displacement from the east-rift margin fault system into the mid-rift fault system, forming a southeast dipping accommodation ramp and has been termed the 'southern terrace' (Bladon *et al.,* 2015a). This ramp forms an atypical relay ramp structure (Figure 8.5), as within a traditional relay ramp structures the ramp would be expected to dip to the northwest. Bladon *et al.,* (2015b) suggest that the southwest-striking, northwest dipping faults at outcrop and within the subsurface are likely connected and formed during the first (Aptian to Albian) of the two (Paleogene Epoch) phase developments of the eastern basin margin (Bladon *et al.,* 2015b), forming this southern terrace.

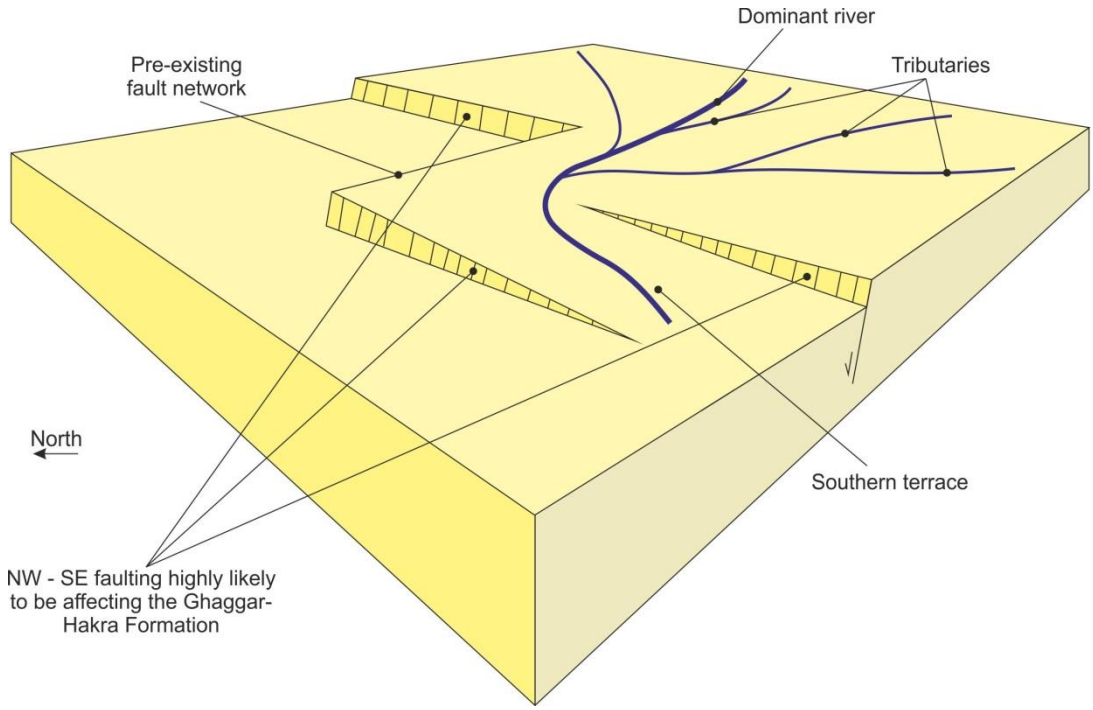

Figure 8.5: Atypical relay ramp, dipping to the southeast (southern terrace) within the subsurface of the eastern Barmer Basin margin (Bladon *et al.,* 2015a, b), based on interpreted seismic data. The fluvial system represents the change in the drainage pattern. Gilbert-type delta sedimentology is expected in the basin.

On traditional relay structures, the sedimentology down a relay ramp within an intracontinental basin can be predicted. The sedimentology here is transitional from fluvial plains, into deltas and then lacustrine environments. However, due to the atypical structural geometries seen on the eastern Barmer Basin margin (Figures 8.4, 8.5), the sedimentology predicted from seismic suggests the sediments are more likely to be proximal rift facies such as coarse-grained alluvial fans and Gilbert-type deltas (Bladon *et al.,* 2015a), rather than the transitional sedimentology.

8.2.2 Linking of the fault network and the sedimentology

The basalts underlying the Ghaggar-Hakra Formation have been dated to the Aptian Stage (120 Ma, Sharma, 2007); suggesting deposition of the Ghaggar-Hakra Formation cannot have occurred prior to this time. Dating from the samples at outcrop of the Ghaggar-Hakra Formation has identified trisaccate pollen types *Microcachrydites spp.* and *Cyclusphaera spp.* from the Early Cretaceous Epoch (Papanikolaou, 2016, pers. Comms.). The dating of the Ghaggar-Hakra Formation and the associated fault network is

poorly constrained, but attributed to the Aptian and Albian Epochs (Bladon *et al.,* 2015a, b).

Based on the sedimentology of the Ghaggar-Hakra there was a maturing channel style from the Darjaniyon-ki Dhani Sandstone (DE1, Figures 5.22, 8.2, Section 5.3.1) into the Sarnoo Sandstone (DE3, Figures 5.22, 8.2, Sections 5.3.2, 5.4, 7.5, 8.1). The floodplains above and below the Sarnoo Sandstone (DE2, 4, Figures 5.22, 8.2) contain well-developed palaeosols indicating tectonic stability (Arguden and Rodolfo, 1986). The lack of flooding within the upper floodplain also suggests an increase in fluvial development and fault stabilisation at the time of Sarnoo Sandstone deposition. It is probable that the channel style within the Ghaggar-Hakra becomes more stacked and amalgamated upwards as a result of fluvial development rather than a growing fault network. All of these pointers suggest that there was a lack of tectonic activity during this time.

The rejuvenation of the fluvial system from the Sarnoo Sandstone to the Nosar Sandstone is marked by the highly erosive base with stacked and amalgamated channels (Figure 5.22, 8.2, Sections 5.3.3). This sudden change in fluvial style (Figures 5.22 8.2, Sections 5.3.2, 5.3.3, 5.3.4, 5.4, 7.5, 8.1) indicates that the southwest-striking fault network began to affect the drainage regime of the fluvial system. As subsidence occurs on the fault network, the gradient of the river changes over time to become steeper, forcing the fluvial system to rejuvenate. Therefore, it can be suggested that the Nosar Sandstone of the Ghaggar-Hakra Formation is the product of syn-rift sedimentation. The timing of this fault network growth is within the Albian / Aptian, further constraints cannot be determined.

8.3 Climatic influences on the Barmer Basin

Climate of an area will influence the discharge of fluvial systems and in turn influence the amount of sediment a fluvial system can carry, affecting the formation of the floodplain.

The depositional packages attributed to the floodplain are cyclic and form thin (maximum 1.5 m thick) fining upwards successions but lacking erosive boundaries (DE2, 4, Figures 5.22, 8.2, Sections 5.2.7, 5.3.4). The facies of the floodplain (F7, Sections 5.2.7, 5.2.8, 5.3.4) results from regular flooding of the fluvial system with sporadic sediment supplies. The lack of erosion and unpredictable sediment deposition resulted in cumulative vertisols (Section 2.2.4). This implies a depositional hiatus' on the floodplain to allow for pedogenesis to occur, but with regular flooding of the fluvial system, so that the floodplain could build up to its preserved 25 – 30 m thickness. When sediment is deposited on the floodplain, it is usually cannibalised by the soil forming processes (Kraus, 1999; Tim Kearsey pers. comms.), as the amount of sediment deposited is no thicker than 1.5 m, hence the floodplain sediments are thick and well-developed.

By understanding palaeosols the drainage of the water table can be determined from the mottling of the soils and the preservation of rhizoliths. From this study, this indicates that the climate at the time of sediment deposition was semi-humid (Section 2.6.4, Simonson and Boersma, 1972; Kraus and Hasiotis, 2006). The cyclic nature of the floodplain deposits suggests high rainfall producing regular flooding of the fluvial system. The mottling and rhizoliths within the floodplains (Section 5.3.4) are very similar to those found by Simonson and Boerma (1972) and Kraus and Hasiotis (2006) and produce imperfectly to poorly drained palaeosols (Section 2.7.4). This type of palaeosol is typically found within semi-humid climates in a subtropical location (Section 3.2, Kraus and Hasiotis, 2006).

The structureless sediments (Section 4.1.5) and indistinct cross-bedding (Section 4.1.3) of the sandstone successions demonstrate variable discharge of the fluvial system, likely due to seasonal change rather than extreme climatic events (Section 3.2). Deposition on the floodplain demonstrates rapid rates of aggradation (Bladon *et al.,* 2015a) and well-developed palaeosols indicating tectonic quiescence within the eastern Barmer Basin

margin at this time (Section 8.2.2). The climate during the time of deposition was semi-humid to arid and the landmass that now comprises Rajasthan was within the Tropic of Capricorn, likely located within the subtropics (Section 3.2, Acharyya and Lahiri, 1991; Torsvik *et al.,* 2005; Ali and Aitchison, 2014; Belda *et al.,* 2014).

8.4 Influences of the evolving West Indian Rift System

Notwithstanding the local tectonics and climate, there are multiple controls on fluvial systems, both intrinsic and extrinsic, that may have contributed to the development of the Ghaggar-Hakra Formation. The extrinsic factors include variations in sediment supply, operating on time-scales of 10^5 – 10^7 years (Leeder, 1993) and base level (Section 2.8.3) operating on time-scales of 10^6 – 10^8 years. The intrinsic controls include discharge (affecting the fluvial system daily, weekly and yearly) and avulsion operating on time-scales of 10^3 – 10^5 years (Section 2.8.5, Leeder, 1993).

8.4.1 Extrinsic controls on the fluvial system

Sediment supply to fluvial systems can be high or low and the grainsize of the sediment can also influence how much sediment is carried within the flow of a fluvial system. Using Schumm's (1972) classification of fluvial systems by the grainsize suggests that coarser sediment of the Darjaniyon-ki Dhani and Nosar sandstones will generally be carried within low sinuosity fluvial systems. In contrast the finer grainsizes seen in the Sarnoo Sandstone are generally carried within high sinuosity systems. The Sarnoo Sandstone also displays fine- to medium-grade sand with continuous trough and planar cross-bedded sets and cosets (Stx, Sx), whereas the Darjaniyon-ki Dhani and Nosar sandstones exhibit massive sandstone (Sm facies) and indistinct cross-beds (M, G, Stx, Sx facies). However, the Sarnoo Sandstone does contain ripple-scale bedforms (Sr, Section 4.1.8), within the sheetflood element (F6, Section 5.2.6), that display supracritical climbing indicating a high sediment yield. This is the only evidence within the Sarnoo Sandstone of a high sediment supply rate and is likely due to the high discharge regime of the sheetflood element

(Section 5.2.6). The subfacies analysis indicates a faster flow and / or a higher sediment supply to the Darjaniyon-ki Dhani Sandstone and the Nosar Sandstone when compared to the Sarnoo Sandstone (Section 4.1). Therefore the evolutionary change throughout the Ghaggar-Hakra Formation is unlikely to be related to the nature of the sediment supply.

Base level (Section 2.7.3) in the study area is lake level as the basin was land-locked during the Cretaceous Period (Gould and Jones, 2013). However, base level of the fluvial system is in the basin centre and not seen in outcrop or within the subsurface and therefore is not guaranteed, nor can the depth of the lake be determined. The abrupt change in the sedimentology could relate to a change in base level. Base level changes are due to external influences (Section 2.8.3), either climate or tectonics. The climate was demonstrably stable throughout the deposition of the Ghaggar-Hakra Formation (Section 8.3). The most likely reason for a change in base level is tectonic subsidence (Section 8.2) affecting the graded profile and therefore the fluvial style, relating back to the active fault regime.

8.4.2 Intrinsic controls on the fluvial system

Avulsion is the most common type of intrinsic control on fluvial systems. There are three types of avulsion which are avulsion by annexation, incision and progradation (Section 2.8.5). These avulsion types of Slingerland and Smith (2004) fit within the stratigraphical transitional avulsion and stratigraphical abrupt avulsion of Jones and Hajek (2007, Section 2.8.5). Avulsion by annexation and incision produce deposits similar to stratigraphically abrupt avulsion where confined, multi-storey channel fills are interleaved with small, sporadic and isolated floodplain deposits (Mohrig *et al.,* 2000; Slingerland and Smith, 2004; Jones and Hajek, 2007). Avulsion by progradation produce deposits similar to stratigraphically transitional avulsion, where the deposits are bounding strata, mudstones, sheet sandstone bodies, ribbon sandstone bodies and large, coarsening upwards channel

sandstone bodies (Slingerland and Smith, 2004). These deposits can have channels successions interbedded with floodplain deposits.

Avulsion within the Ghaggar-Hakra Formation is noted for each of the sandstone successions in turn to determine if avulsion is the controlling factor in their deposition. The Darjaniyon-ki Dhani Sandstone has isolated channels and floodplain deposits with stacked and amalgamated gravel bars (Section 5.3.1). The style of avulsion here falls within the stratigraphically abrupt avulsion style (Section 2.8.5) and was likely the main controlling factor on the location of the preserved deposits within the Darjaniyon-ki Dhani Sandstone. It is clear that the avulsion rate and sediment accumulation rate for this succession are equal (Figure 2.15a). The Sarnoo Sandstone has amalgamated point bar packages indicating laterally migrating channels and point bar (Section 5.3.2) interlayed(?) with thick floodplain deposits. The deposits of the Sarnoo Sandstone were not influenced by avulsion, within the investigated area. The Nosar Sandstone is characterised by stacked and amalgamated channels (Section 5.3.3) interleaved with very little floodplain deposits preserved, indicating that any avulsion here was linked to the subsidence on the fault network and the sediment supply rate (Figure 2.15, Section 2.8.5). However, such avulsion is subsidiary the subsiding tectonic framework of Nosar Sandstone deposition.

8.5 Provenance

To assess provenance the petrography and palaeocurrent pattern needs to be established (Dickinson, 1985; Besra *et al.,* 2000; Garzanti *et al.,* 2008; Tucker, 2001). The textural features observed within the sandstones are grainsize, sorting, roundness, sphericity and all the studied sandstones exhibit mature textures (Sections 6.2.1, 6.3). The detrital mineralogy of the Ghaggar-Hakra Formation is composed of: dominantly quartz grains, with rock fragments of sedimentary, metamorphic and igneous origin, heavy minerals and muscovite mica (Section 6.2.2). The authigenic cements are microcrystalline quartz, quartz overgrowths, haematite, calcite and dolomite cements, kaolinite booklets and clays

(Section 6.2.3). The average palaeoflow pattern palaeocurrents of the Ghaggar-Hakra Formation is dominantly to southwest and west, indicating that the source is to the north or northeast of the field area (Sections 7.3, 7.4). With this information in mind there are two potential source terrains for the Ghaggar-Hakra Formation, which are either the Jodhpur Sandstone or the Aravalli Supergroup (Section 6.3, Figure 6.16).

The Jodhpur Sandstone, part of the Marwar Supergroup was deposited within the Neoproterozoic Era (Kumar and Pandey, 2009) and is to the northeast of the Sarnoo field area. The dominant southwest palaeocurrent pattern inferred for the Ghaggar-Hakra suggests that the Jodhpur Sandstone could be a source rock. The Jodhpur Sandstone is also dominantly composed of detrital quartz grains and very few rock fragments (Kumar *et al.,* 2011) and the textural and compositional maturity of the sandstones considered in the present study may derive from an aeolian setting of the Jodhpur Sandstone (Kumar *et al.,* 2011).

The Aravalli Supergroup is situated in the Aravalli Mountain Range (Figures 1.1, 3.6, 6.16), which formed in the Precambrian (Section 3.1) as a transitional arc (uplifted subduction complexes; Banerjee and Bhattacharya, 1994; Dickinson and Suczek, 1979). This area is to the northeast and east of the field area (Figure 6.16). The Aravalli Supergroup is composed of quartz conglomerates, low grade metamorphic rocks formed from detrital quartz, rock fragments and heavy minerals (Section 6.3, Banerjee and Bhattacharya, 1994). The supergroup is texturally mature and were deposited within a continental to marine transition (Hart and Plint, 1989).

The textural and compositional maturity of the Jodhpur Sandstone here is too high for the Ghaggar-Hakra sediments, as the Jodhpur Sandstones are supermature (Kumar *et al.,* 2011). The terrain of the Jodhpur Sandstone is not a recycled orogen therefore not matching the petrographical data from the Ghaggar-Hakra Formation. However, the lack

of mineralogical studies into the Jodhpur Sandstone makes the Jodhpur Sandstone difficult to judge as the provenance location; whereas the Aravalli Supergroup has mineralogy similar petrographical data to the Ghaggar-Hakra Formation. Moreover, as discussed in Chapter 6, the Ghaggar-Hakra sediments were supplied from a recycled orogen based on the mineralogical composition and relationship with geological terranes (Sections 6.1.3.1, 6.3).

8.6 Evolutionary model for the Ghaggar-Hakra Formation in the context of the evolving Barmer Basin and the West Indian Rift System

From the evidence presented in this study it has been argued that the Ghaggar-Hakra Formation was deposited within the Aptian to Albian epochs. The structural evolution of the eastern basin margin began during this time. However, it is debated as to how or if the Ghaggar-Hakra has been affected by the growing fault network. This section aims to bring together all the points discussed above to analyse the Ghaggar-Hakra story.

The Ghaggar-Hakra sediments interaction with the fault network is complex. As discussed in Section 8.1 the first depositional element (DE1) – the Darjaniyon-ki Dhani Sandstone – is a low sinuosity system with isolated erosive channels and stacked and amalgamated gravel bars. The petrography contains detrital quartz (60%) and lithic fragments (6.2%), with high amounts of authigenic cements and clays and a southerly palaeocurrent. This is the first sandstone succession to be deposited and it is highly unlikely that it is influenced by the fault development (Figure 8.6); therefore, not influencing the drainage area of the Ghaggar-Hakra fluvial system. The genetic controls on this part of the succession are sediment supply and the avulsion rate (Sections 8.4.1 and 8.4.2).

The second sandstone, the Sarnoo Sandstone (DE3) contains stacked and amalgamated channels and point bars with organised sets and cosets. The sandy bars within this sandstone are laterally connected and this sandstone succession is the most texturally and compositionally mature, with the highest amount of quartz grains (71.9%) and the

lowest amount of lithic fragments (3.8%), suggesting a compositionally mature system. The palaeoflow here is to the west, different from the Darjaniyon-ki Dhani Sandstone; however, this system is highly sinuous and there is a high dispersion on the westerly flow. Also between these two sandstone successions there is a decrease in the amount of sediment supplied to the system, as evidenced through the matrix-supported facies (M) and the distinct / indistinct cross-beds (Stx, Sx). During this time it is likely that faults start to develop (Figure 8.7), but not enough to influence the fluvial style.

As discussed earlier the floodplain sediments (DE2 and 4) of the Ghaggar-Hakra system are well-developed vertisols and point to a tectonically stable area (Section 8.2.2). The regular discharge forming cumulative soils indicates a semi-humid climate. The vertisols here suggest long periods of dry weather suggesting a seasonal climate from wetter winters to drier summers, indicating that the discharge of the fluvial system is directly dependant on the climate.

Finally, the Nosar Sandstone (DE5) is highly erosive with stacked and amalgamated channels with inconsistent sets and cosets suggesting turbulent and changing fluvial flows. There is also minimal floodplain preserved unlike the Sarnoo Sandstone. There is an increase in the lithic fragments here (5.2%), a decrease in the detrital quartz (66.3%), making this sandstone the least compositionally mature. The Nosar Sandstone also exhibits a palaeocurrent change to the southwest. This evidence brought together is suggestive of a change to the fluvial system dynamics that is either intrinsic or extrinsic. As discussed (Sections 8.3.1, 8.3.2; Figure 8.8) it highly unlikely to be intrinsic to the fluvial system as these processes would not produce such vast changes in fluvial style.

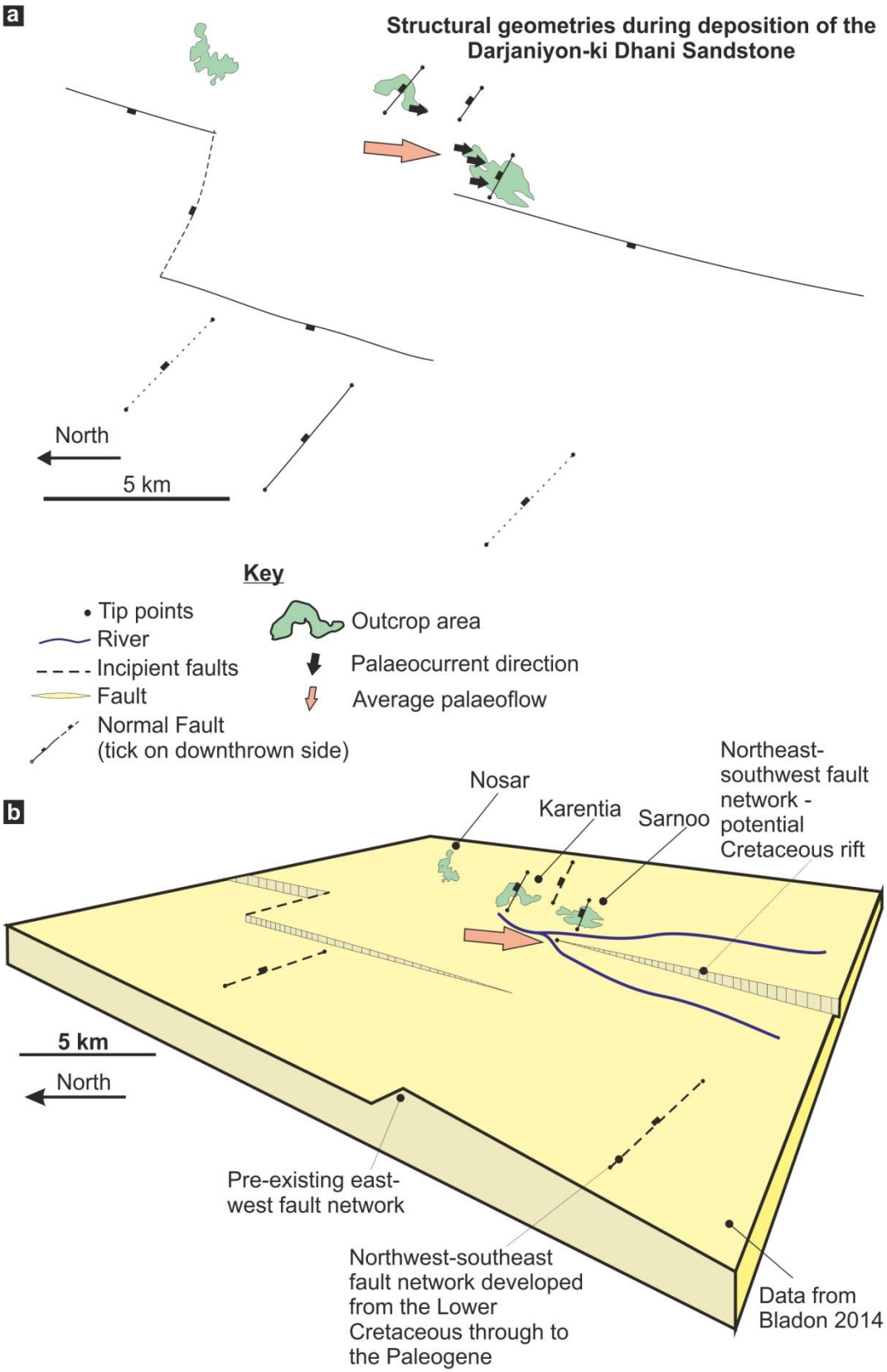

Figure 8.6: (a) Suggested structural geometry in map view of the eastern central margin during the deposition of the Darjaniyon-ki Dhani Sandstone, and; (b) three-dimensional fault block model of the Darjaniyon-ki Dhani Sandstone displaying the interpreted fault network including the pre-existing east-west fault and the incipient northwest-southeast fault network. Also displayed on the diagram are the outcrop locations and the suggested pathway of the fluvial system at the time of deposition; data is from Bladon (2014).

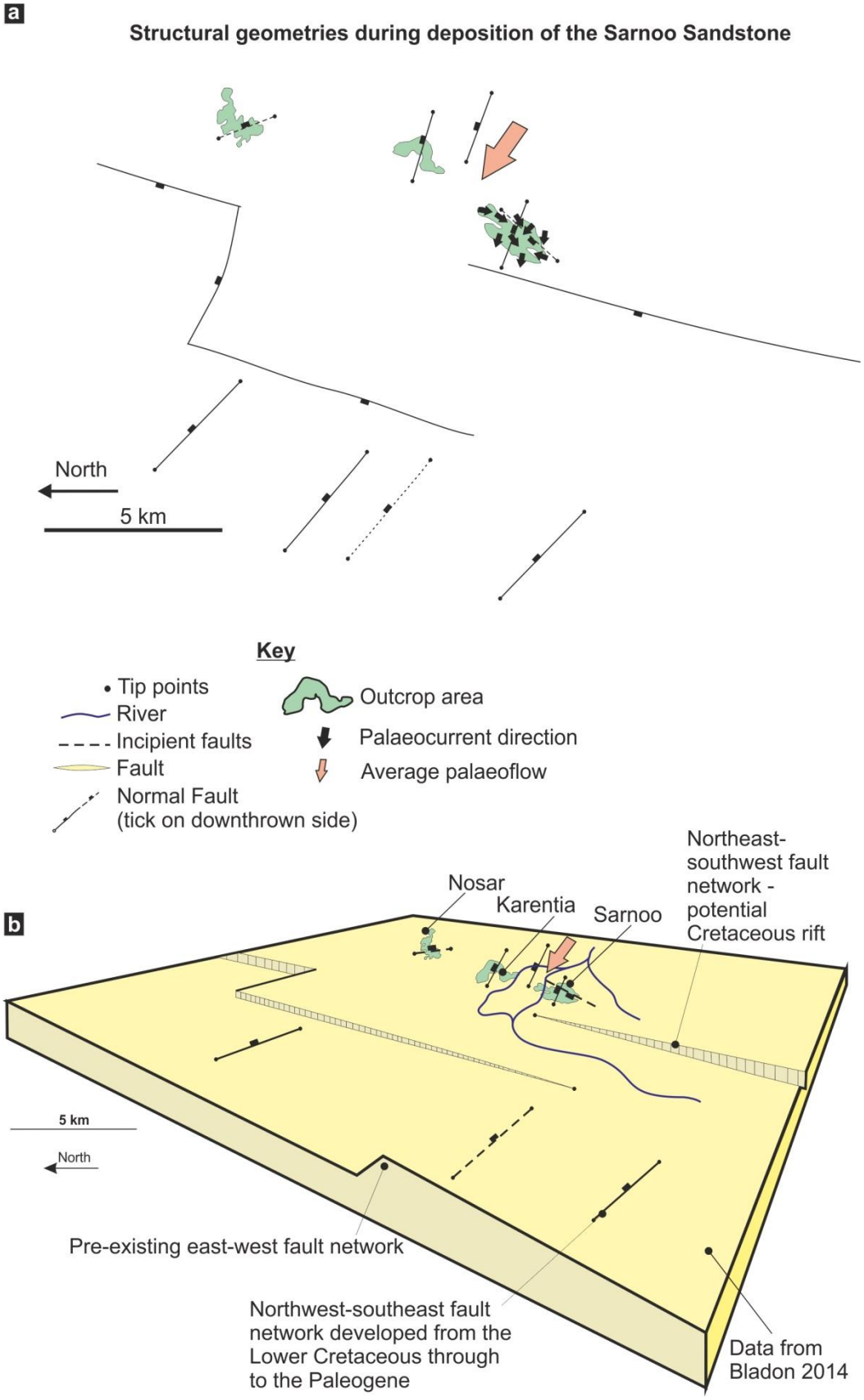

Figure 8.7: (a) Suggested structural geometry in map view of the eastern central margin during the deposition of the Sarnoo Sandstone, and; (b) three-dimensional fault block model of the Sarnoo Sandstone displaying the interpreted fault network including the pre-existing east-west fault and the

incipient northwest-southeast fault network. Also displayed on the diagram are the outcrop locations and the suggested pathway of the fluvial system at the time of deposition; data is from Bladon (2014).

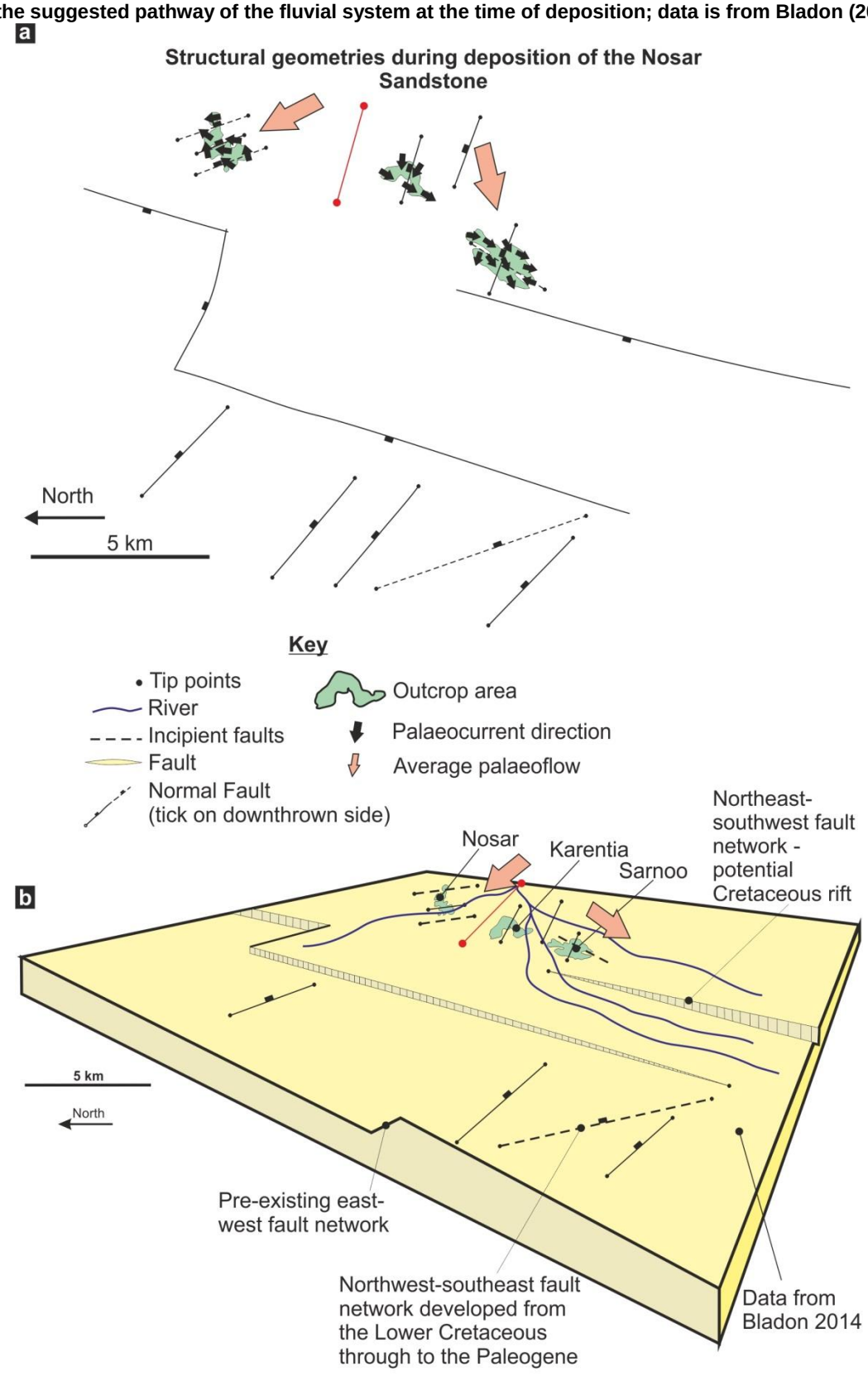

Figure 8.8: (a) Suggested structural geometry in map view of the eastern central margin during the deposition of the Nosar Sandstone, and; (b) three-dimensional fault block model of the Nosar Sandstone displaying the interpreted fault network including the pre-existing east-west fault and the northwest-southeast fault network. Also displayed on the diagram are the outcrop locations and the suggested pathway of the fluvial system at the time of deposition; data is from Bladon (2014). The red

fault indicates the east-west pre-existing fault which is interpreted to have influenced the fluvial drainage.

This change in fluvial style is likely to be due to the extrinsic influences from the growing fault network, climate, base level or interactions of all three. The erosive base of the Nosar Sandstone indicates there is development of the fault network forming the 'southern terrace' between the east-rift system and the mid-rift system (Figure 8.3), ultimately influencing the drainage network of the Ghaggar-Hakra sediments (Figure 8.8). It could be suggested that the formation of this 'southern terrace' could lower the base level (Cretaceous lake) of the fluvial system. The interaction of the fault network and base level is forcing the fluvial system to change hence, a change in channel style from a high sinuosity into a low sinuosity system. There must have been a high sedimentation rate to the Nosar Sandstone as there are stacked channels, indicating that the sediment supply and discharge kept up with the growing subsidence on the fault network.

The discussion of the Ghaggar-Hakra deals with the interaction of the fault network and sediments of the Sarnoo and Karentia field areas and the subsurface. However, in the Nosar field area, the faulting is in a northwest-southeast orientation which is different. These faults are likely to have formed during the Paleogene tectonic events; however, it is likely at the time of deposition for the Nosar Sandstone there were incipient faults there, influencing the fluvial flow. This distinction in palaeocurrent is due to pre-existing west-striking structures diverting the flow of the river into two separate orientations (Figure 8.8).

As debated in Chapter 6 the provenance for all three sandstones evidenced through the petrography and the palaeocurrent data is probably the Aravalli mountain range. It is suggested that the Ghaggar-Hakra fluvial system relates and drains the Aravalli mountain range along with the other Lower Cretaceous fluvial systems of the West Indian Rift System.

8.7 Regional Palaeogeography

The sedimentation of the West Indian Rift System is documented by multiple formations spanning the interval from the Jurassic Period to the Quaternary Period (Figure 3.4). The Ghaggar-Hakra Formation of the Barmer Basin documented here as Lower Cretaceous in age. Other Lower Cretaceous-aged formations are the Nimar Sandstone of the Narmada Basin (Figure 3.5, Kundal and Sanganwar, 1998). The Serau, Dhanduka, (also known as the Songir), the Dhrangadhra formations and the Himatnagar Sandstone of the Cambay Basin are broadly age-equivalent (Figure 3.5, Mohan, 1995; Sunder *et al.,* 2013). These formations are of fluvial origin. The Lower Cretaceous-aged Bhuj Formation of the Katchchh Basin displays coastal to shallow marine sedimentation (Figure 3.5, Sunder *et al.,* 2013). During the Lower Cretaceous the West Indian Rift System was within the Tropic of Capricorn (Figure 3.2c) drifting northwards towards Eurasia, this influenced the climate of these depositional regimes.

The Nimar Sandstone is composed of sub-angular to sub-rounded coarse-grained sandstones (Akhtar and Ahmad, 1991; Kundal and Sanganwar, 1998), with a low textural maturity (Racey *et al.,* In review). The composition of the Nimar Sandstone is dominantly monocrystalline quartz, rock fragments of metamorphic and sedimentary origins (Akhtar and Ahmad, 1991; Racey *et al.,* In review), with detrital micas, rounded feldspar and rounded heavy minerals. The formation has a likely palaeoflow direction to the southwest – west (Akhtar and Ahmad, 1991).

The Serau Formation is composed of moderately to poorly sorted, fine- to coarse-sandstones (Hardas, 1981); to date the palaeocurrents and mineralogical composition have not been documented. The Dhrangadhra Formation comprises moderately sorted, fine- to medium-grained sandstones. The mineralogical composition is composed of dominantly detrital quartz grains, with fractured and corroded feldspar, with tourmaline, zircon, rutile and straurolite heavy minerals (Srivastava *et al.,* 1980). The dominant

palaeocurrent is to the west – southwest (Mukherjee, 1983; Biswas, 1987). Currently there is no information published on the Dhanduka Formation. The Himatnagar Sandstone is composed of moderately sorted, sub-angular fine- to coarse-grained sandstones, with textural immaturity (Desai and Desai, 1989). Petrographically the sandstone comprises of 95% detrital quartz grains, feldspars and heavy minerals (Desai and Desai, 1989), displaying compositional maturity. The palaeocurrent is to the west (Desai and Desai, 1989).

The Ghaggar-Hakra Formation comprises sub-rounded, clay- to pebble-grade sandstones, with a high textural maturity. The mineralogical composition is detrital monocrystalline and polycrystalline quartz, rock fragments of igneous, metamorphic and sedimentary origin, heavy minerals and trace amounts of feldspar (Chapter 6).

The Bhuj Formation is composed of dominantly fine-grained to pebble-grade quartz grains which are well sorted (Bose *et al.,* 1986). Also noted within are few low-grade metamorphic fragments and moderate amounts of feldspar (Racey *et al.,* In review). The palaeocurrent has not been documented for this formation. The fluvial Lower Cretaceous sediments of the Barmer Basin relate well to the fluvial sediments of the other basins within the West Indian Rift System (Srivastava *et al.,* 1980; Mukherjee, 1983; Biswas, 1987; Akhtar and Ahmed, 1991; Racey *et al.,* In Review).

The Nimar Sandstone (Narmada Basin), the Dhrangadhra Formation and the Himatnagar Sandstone (Cambay Basin) match closely in composition to the Ghaggar-Hakra Formation of quartzarenites. The Nimar and Ghaggar-Hakra have recycled orogens (Section 6.3; Akhtar and Ahmad, 1991); however, the provenance of the other formations has not been documented within the literature. The Nimar Sandstone, the Dhrangadhra Formation and the Himatnagar Sandstone display a southwest to west palaeocurrents, suggesting that their provenance is to the northeast – east of the depositional area. Based

on the petrographical and palaeocurrent evidence the suggested source area is the Aravalli Mountain Range (Srivastava *et al.,* 1980; Mukherjee, 1983; Biswas, 1987; Desai and Desai, 1989; Akhtar and Ahmed, 1991; Racey *et al.,* In Review, Sections 6.3, 8.5).

The tectonic regime of the West Indian Rift during the Mesozoic Era is not well documented; however, during the late Jurassic Period India began to migrate northwards (Figure 3.2b) resulting in the reactivation of the Aravalli-Delhi Trend. This influenced the formation of the Katchchh Basin (Biswas, 1987) and incipient faulting in the locations of the Cambay and Barmer basins. During the Early Cretaceous Epoch the Indian Plate began to rotate resulting in the first phase of the Indian – Madagascar rifting (Figure 3.2c), again reactivating the Aravalli-Delhi Trend. This reactivation influenced the fault networks of the Barmer, Cambay and Narmada basins (Bladon *et al.,* 2015b). During the Mesozoic evolution of northwest India, the West Indian Rift System has influenced the sedimentation of the basins (Section 3.2, Desai and Desai, 1989; Bladon *et al.,* 2015a, b). Thus it is suggested that the sedimentation within these basin is syn-rift and not pre-rift as previously suggested.

8.8 Data limitations

Although the outcrops have excellent exposure they are very sparse and limited in extent. This can hinder the data collection from sandstone successions, particularly the palaeocurrent data for the Darjaniyon-ki Dhani Sandstone, making it challenging to interpret. In contrast, the Sarnoo Sandstone and Nosar Sandstone have comparably more outcrop and therefore more data is available from these sandstone successions. Due to the limited outcrops of the whole formation, facies and architectural elements can be difficult to define; however the very detailed datasets have allowed the depositional history to be determined. Although the detail gained from outcrop studies of facies and architectural elements is helpful in understanding the genetic evolution of a sedimentary

system (Cant, 1977), this approach is not easily transferred into the subsurface where the physical limitations of borehole data become important.

Three-dimensional architectural element models and facies models are interpretative, using all the information from all localities of the sandstone successions. Although these models are used to help interpret the subsurface of the Barmer Basin, they are unlikely to help the interpretations of other fluvial systems that are not controlled by an atypical extensional regime like the eastern margin of the Barmer Basin.

Petrography data for the sandstone succession has been collected and measured using PETROG^{TM} software making the data statistically viable. The thin sections from some of the samples were smaller than other sample possibly introducing bias into petrographical data collection.

Research conducted by Bladon *et al.,* (2015a, b) suggests that there is a Mesozoic Barmer Basin that was not mapped at outcrop or within the subsurface and is older than the present day Paleogene Basin. The Mesozoic rift system within northwest India would provide accommodation space for the Ghaggar-Hakra Formation. The Cretaceous basin margins would have being an efficient location for extension and likely superseded by the Paleogene Basin. This suggests that the deposition of the Ghaggar-Hakra Formation is crucial to understanding the Barmer Basin evolution and provides further evidence for the Ghaggar-Hakra Formation representing syn-rift instead of pre-rift sedimentation.

8.9 Hydrocarbon potential?

The reservoir potential for sediments deposited within the Ghaggar-Hakra Formation was thought to be low (Bower, 2004a, b; Compton, 2009). However, the sedimentary architectures could make a good reservoir (Clarke, 2011). The Darjaniyon-ki Dhani Sandstone varies in grainsize from clay- to pebble-grade and is dominated by gravel bars,

channel structures and floodplain material. As the channels are not stacked but the pebble-grade gravel bars are, this indicates that this reservoir would have a low textural maturity. Although there is a high net to gross (Section 5.3.1), the facies and architectural element arrangement within this sandstone can be very compartmentalised; this combined with low porosity values (7.5%, Section 6.2.4) produces a poor quality reservoir. The channels here are also isolated and not influenced by the fault network.

The petrographical work of the Sarnoo Sandstone states that out of the three sandstone successions it is the most texturally and compositionally mature, having high amounts of detrital quartz grains. This sandstone also has the highest porosity values at 9% (Section 6.2.4). At outcrop scale the Sarnoo Sandstone is a laterally migrating high sinuosity fluvial system where the sands of the channel deposits (F1, Section 5.2.1), point bars (Section 5.2.5), channel margins (Section 5.2.2) and chute channels (Section 5.2.4) are stacked and connected laterally and vertically. However, the floodplain sediments are clay- to fine-grained sands and can severely compartmentalise the reservoir vertically, especially within the upper part of the Sarnoo Sandstone, where the proportion of sand to mud becomes 60:40 (Section 5.3.2). The sands here would probably form the best reservoir.

The Nosar Sandstone displays well-connected stacked channels (F1, Section 5.2.1) and gravel bars (F3, Section 5.2.3), with very little floodplain material (F7, Section 5.2.7) preserved. The succession was deposited within the fluvial environment that migrated laterally, forming well-connected channels (Figure 5.19; Clarke, 2011), due to the growing fault network. The petrographical analysis revealed that the detrital grains vary in size from very-fine to upper very coarse-grained sediment; where the dominant detrital minerals are quartz and rock fragments. The dominant authigenic minerals are haematite cements and quartz overgrowths. This sandstone succession has the lowest porosity values (5%, Section 6.2.4) but due to the limited floodplain deposits the sandstone has no

impermeable clay barriers, associated with low sinuosity braided system and the net to gross is 90:10 (Section 5.3.3).

The sedimentary facies and architectural elements within the Ghaggar-Hakra Formation presented within this research, coupled with the extensional regime (Bladon *et al.,* 2015a, b, Section 8.2) where normal fault blocks have been rotated, have the potential to be exploration targets. The grainsize of the Nosar Sandstone is consistent from medium- to upper very coarse-grained and is moderately sorted, unlike the moderately sorted Darjaniyon-ki Dhani Sandstone with a variety of grainsizes. The lack of floodplain deposits within the Nosar Sandstone means it is not compartmentalised like the Sarnoo Sandstone and the channel successions of the Nosar Sandstone are stacked and well-connected and therefore would be the best reservoir out of the three sandstone successions studied.

8.10 Summary

This chapter has brought together the three datasets of this research, namely the facies and architectural element analysis (Chapters 4 and 5), the petrography data (Chapter 6) and the palaeocurrent data (Chapter 7), and discussed them in detail to see how they relate to each other and the evolving Barmer Basin within the West Indian Rift System. The fluvial system here matures up through the succession from a gravel bedload dominant, low sinuosity fluvial system into a mixed load, highly sinuous fluvial system. This is evidenced by the maturation of the sediments, the palaeosol development and the lack of ponding, suggests less flooding of the fluvial channels. The top of this mature floodplain is capped by a highly erosive well-developed bedload dominant, fluvial system, suggesting a tectonic influence, coupled with changing base level to bring about the rejuvenation of the fluvial system.

The eastern Barmer Basin margin has undergone extensional tectonism which occurred throughout the Lower Cretaceous Epoch (Bladon *et al.,* 2015a). Prior to this research the

Ghaggar-Hakra Formation was thought to represent pre-rift sedimentation. However, the development of the fault network caused the fluvial system (Nosar Sandstone) to erode heavily into the underlying floodplain. This increases the lithic fragment count and decreases the detrital quartz count of the Nosar Sandstone when compared to the Sarnoo Sandstone and the change in palaeocurrent pattern also indicates syn-rift sedimentation.

As the climate was stable during the time of deposition it has been eliminated as a cause of the sedimentological changes and the rejuvenation of the fluvial system. The climatic regime of tropical semi-humid to arid conditions has affected the growth of the floodplains and the discharge to the fluvial system. Other suggested controls, discussed within this chapter, include avulsion and sediment supply and they have all been shown to be either less or not important or have been linked to the tectonic regime.

The provenance is in dispute. There are two possible sources which are the Aravalli Supergroup and the Jodhpur Sandstone, both of which contain high contents of detrital quartz grains, but the Jodhpur Sandstone barely contains lithic fragments. They are both positioned to the northeast of the Sarnoo field area (Figure 8.5) therefore the palaeocurrent data cannot eliminate either area. Based on the fact that the Aravalli Supergroup contains rock fragments, as well as detrital quartz grains, it is more likely to be the provenance area. The Lower Cretaceous fluvial systems of the West Indian Rift System all have a provenance in the Aravalli Supergroup as well, and it can be suggested that all the fluvial systems within all the basins of the West Indian Rift System are related.

The main aim of the research was to produce three-dimensional facies models to use within the subsurface, to determine if the Ghaggar-Hakra Formation was a viable reservoir (to be documented and demonstrated in Chapter 9). The main limitation to this data is the size of the field area, impacting the collection of field data for the Darjaniyon-ki Dhani Sandstone succession. From reservoir characterisation of the Ghaggar-Hakra Formation,

it is likely that the Nosar Sandstone is the best reservoir as the channels are stacked and amalgamated with a fairly consistent grainsize of medium- to very coarse-grained, likely influenced by the growing fault network. There is also a lack of floodplain deposits preserved meaning that the reservoir is not compartmentalised.

9 Chapter Nine: Comparison of subsurface core data with outcrop material

The subsurface core data set was obtained from two nearby producing fields named Aishwariya and Saraswati and the data can be used to complement the outcrop derived depositional models (Figure 9.1). Cairn India and Ichron (now RPS Ichron) have kindly provided access to the cores and petrographical thin sections from the following wells: Aishwariya-5, Aishwariya-17, Aishwariya-2Z, Aishwariya-20, Saraswati-4 and Saraswati-2 (Figure 9.1, Bower, 2004a, b; Gould and Jones 2012, 2013).

The Ghaggar-Hakra Formation in the subsurface unconformably overlies either the Karentia Volcanic Formation (Section 3.3.2) or the Lathi Formation (Section 3.3.2) and is itself unconformably overlain by the Mallinath Group (Section 3.3.2). In the subsurface the Ghaggar-Hakra Formation is composed of two members; the fluviatile Pushka Member and the lacustrine Kamyaka Member.

This chapter discusses fourteen facies, four facies associations and the petrography seen in the cores (Section 9.2). Using the facies associations and petrographical data (Section 9.3) three facies assemblages (Section 9.4) are recorded. These assemblages are then compared to the outcrop deposits and used to develop trends which will ultimately aid hydrocarbon exploration in the area.

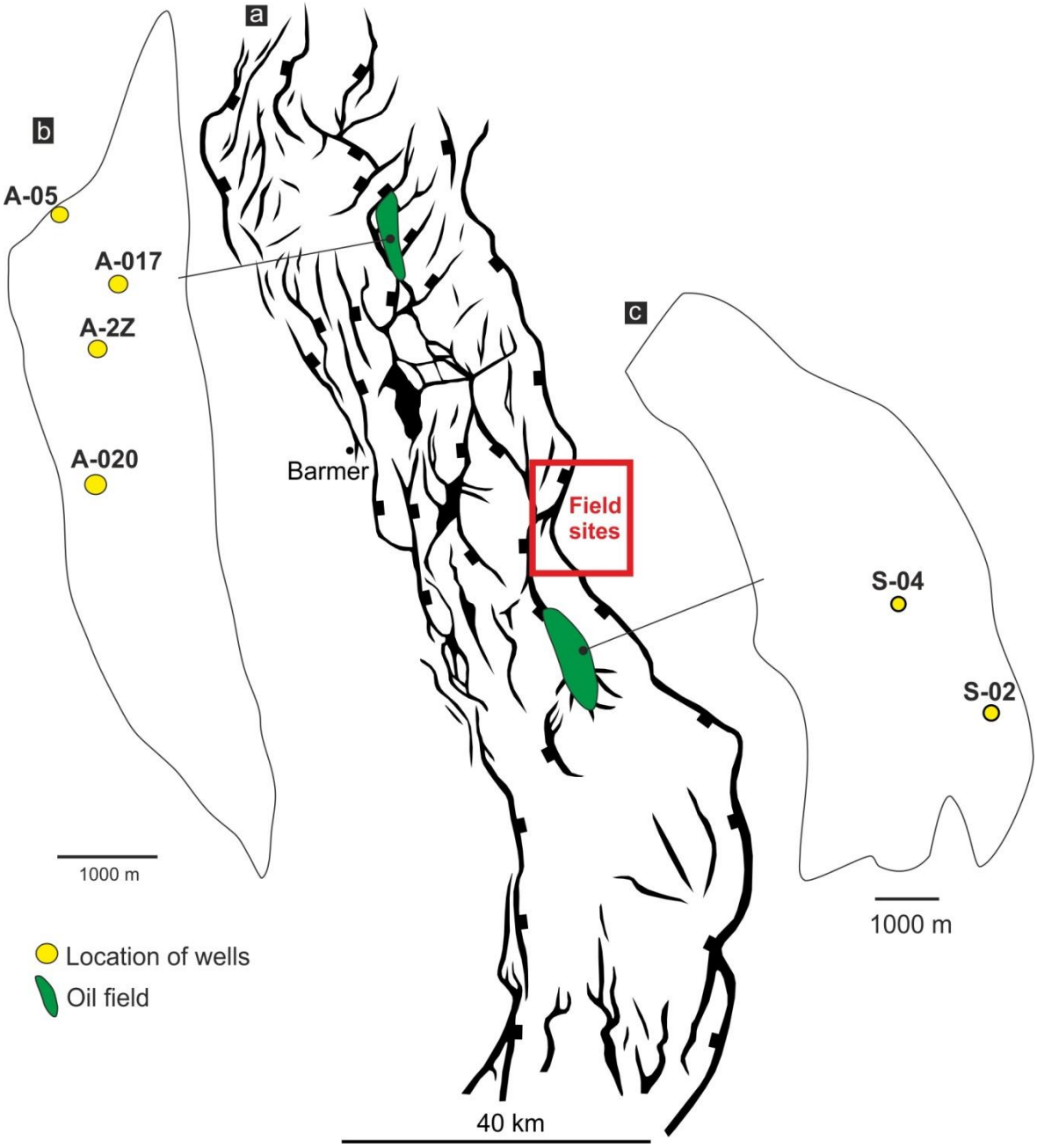

Figure 9.1: (a) Structural geometry of the Barmer Basin from the base Paleocene; (b) The location of the core data from the Aishwariya Field (yellow dots), and; (c) The location of the core data from the Saraswati Fields (yellow dots).

9.1 Facies

The facies noted within the core are extremely similar to those as seen at outcrop allowing for direct correlation between the two datasets. Therefore, the only facies presented with descriptions and interpretations are those that are not seen at outcrop (Tables 9.1, 9.2).

Lithofacies code	Lithofacies	Description	Interpretation	Figure number
G	Grain-supported conglomerates	Pebble grade (31 mm), poorly sorted. Sub-rounded pebbles. Structures – erosional surfaces, grading and cross-beds	Non-confined flow regime – upper flow regime, migration of dune-scale bedforms	9.2
Stx	Trough cross-bedded sandstone	Fine- to coarse-grained, moderately sorted, sub-rounded, clasts (40 mm), trough cross-bedding and erosional surfaces	Migration of sinuous crested dune-scale bedforms in the lower-flow regime	9.3
Sx	Planar cross-bedded sandstone	Fine- to coarse-grained, well sorted, sub-rounded, clasts (15 mm), planar cross-bedding, channel structures, reactivation and erosional surfaces	Migration of straight crested dune-scale bedforms in the lower-flow regime	9.4
Sb	Parallel-bedded sandstone	Very-fine- to coarse-grained, moderately sorted, sub-rounded, clasts (10 mm). Main structures are: parallel bedding, cross-beds, erosional surfaces and silt bands.	Non- or partially-confined flow events within the upper-flow regime	9.5
Sm	Massive sandstone	Fine- to coarse-grained, massive sands	Rapid deposition from suspension	9.6
Sla	Low-angle cross-bedded sandstone	Fine- to coarse-grained sands, moderately sorted, sub-rounded, low angle cross-bedding	Dune-scale bedforms in the lower-flow regime	9.7
Sr	Rippled sandstone	Very fine- to medium-grained, well sorted, sub-rounded and a variety of ripples	Ripple-scale bedforms in the lower-flow regime	9.8
Ss	Soft sediment deformation	Very fine- to fine-grained, well sorted, sub-rounded. Bedding is disrupted	Disrupted bedding due to load and flame structures	9.9
Scl	Cross-laminated sandstone	Fine-grained sands, well sorted, sub-angular with cross-lamination	Ripple-scale bedforms in the lower-flow regime	9.10
M	Matrix-supported conglomerates	<27 cm boulders, matrix-supported	Gravity driven debris flows within a partially / non-confined environment	9.11
Sp	Pedogenic sandstone	Mottled red and white, has a pedogenic nature	Soil formation and associated bioturbation	9.12
She	Haematitic pedogenic sandstone	Mottled red and white, pedogenic nature, glaebules, siderite filled fractures.	Soil formation and associated bioturbation	9.13
Ip	Pedogenic siltstone	Mottled red and white, pedogenic nature, soil slickenlines, fractures and root traces.	Soil formation and associated bioturbation	9.14
Ihe	Heamatitic siltstones	Mottled red and white, has a pedogenic nature, heamatitic	Soil formation and associated bioturbation	9.15

Table 9.1: Facies of the Ghaggar-Hakra Formation in core

Code	Lithofacies	Outcrop	Core	Description	Interpretation
G	Grain-supported conglomerates	✓	✓	Pebble grade (52 mm), poorly sorted. Subrounded pebbles. Erosional surfaces, grading and cross-beds	Non-confined flow regime – upper flow regime, migration of dune-scale bedforms
Stx	Trough cross-bedded sandstone	✓	✓	Fine- to coarse-grained, moderately sorted, sub-rounded, clasts (22 mm), trough cross-bedding and erosional surfaces	Migration of sinuous crested dune-scale bedforms in the lower-flow regime
Sx	Planar cross-bedded sandstone	✓	✓	Fine- to coarse-grained, well sorted, sub-rounded, clasts (50 mm), planar cross-bedding, channel structures, reactivation and erosional surfaces	Migration of straight crested dune-scale bedforms in the lower-flow regime
Sb	Parallel-bedded sandstone	✓	✓	Very-fine- to coarse-grained, moderately sorted, sub-rounded, clasts (22 mm). Main structures are: parallel bedding, erosional surfaces and silt bands.	Non- or partially-confined flow events within the upper-flow regime
Sm	Massive sandstone	✓	✓	Fine- to coarse-grained, massive sands	Rapid deposition from suspension
Sla	Low-angle cross-bedded sandstone	✓	✓	Fine- to coarse-grained sands, moderately sorted, sub-rounded, low angle cross-bedding	Dune-scale bedforms in the lower-flow regime
Sr	Rippled sandstone	✓	✓	Very fine- to medium-grained, well sorted, sub-rounded and a variety of ripples	Ripple-scale bedforms in the lower-flow regime
Ss	Soft sediment deformation		✓	Very fine- to fine-grained, well sorted, sub-rounded. Bedding is disrupted	Disrupted bedding due to load and flame structures
Scl	Cross-laminated sandstone	✓	✓	Fine-grained sands, well sorted, sub-angular with cross-lamination	Ripple-scale bedforms in the lower-flow regime
Sh	Horizontally laminated sandstone	✓		Very fine- to medium-grained sands, moderately sorted, sub-angular to angular grains. Main structures are: horizontal laminations	Low amplitude, long wavelength bedforms in the upper flow regime
Im	Massive siltstone	✓		Massive siltstone	Rapid deposition from suspension
M	Matrix-supported conglomerates	✓	✓	<27 cm boulders, matrix-supported	Gravity driven debris flows within a partially / non-confined environment
Sp	Pedogenic sandstone	✓	✓	Mottled red and white, has a pedogenic nature	Soil formation and associated bioturbation
Ip	Pedogenic siltstone	✓	✓	Mottled red and white, pedogenic nature, slickenlines, fractures and root traces.	Soil formation and associated bioturbation
She	Haematitic pedogenic sandstone		✓	Mottled red and white, pedogenic nature, glaebules, siderite filled fractures.	Soil formation and associated bioturbation
Ihe	Haematitic siltstones	✓	✓	Mottled red and white, has a pedogenic nature, haematitic	Soil formation and associated bioturbation

Table 9.2: Facies comparison between the outcrop and core data.

The facies identified at the outcrop and the in cores relate well together as seen in (Table 9.2). The same outcrop facies types identified within the core data but there are two facies only identified within the core: they are the Ss and She facies. The outcrop dataset contains Sh and Im facies which the core data does not. The facies that are absent from both the outcrop and core relate to the floodplain environment.

The facies that do link (Table 9.2) have very similar characteristics such as grainsize, sorting, roundness, sphericity and where seen the foresets, sets and cosets have similar heights and thicknesses. These facies also have very similar deposition regimes, from Newtonian, non-Newtonian or subaerial regimes.

9.1.1 Fluid flow facies: Soft-sediment deformation: Ss

Description: The soft sediment deformation facies is composed of red with mottled grey patches. The grains are very fine- to fine-grained, well sorted (Figure 9.9), sub-rounded with a high to moderate sphericity. The facies has experienced deformation as the bedding is disrupted. Also noted within the facies are haematite and goethite nodules and haematite cemented fractures. The facies can be oil stained and is found within the Kamyaka Member.

Interpretation: The disrupted bedding is due to heavier material settling and squashing the sediments creating flame and load structures. The disruption of the sediments can also be due to soil formation processes and related to water loss. It is likely that the haematite and goethite nodules and cement filled fractures formed post deposition.

9.1.2 Subaerial facies: Haematitic pedogenic sandstone: She

Description: The haematite pedogenic sandstone facies is dominantly red but is also mottled with grey, brown and white reduction patches (Figure 9.13). The facies is very fine-grained, well sorted, rounded and has a high sphericity. There is a haematitic nature

and there are black nodules which are likely to be glaebules. There are lots of fractures that are filled with siderite. The facies can appear massive in nature.

Interpretation: Red colour is due to haematite cements indicating seasonally dry soils. The grey colouration indicates reducing areas within the sediment from rooting plants or burrowing organisms. The roots, rhizoliths, glaebules and fractures allude to a vegetated surface and soil forming processes (Plint, 1983; Oades, 1993).

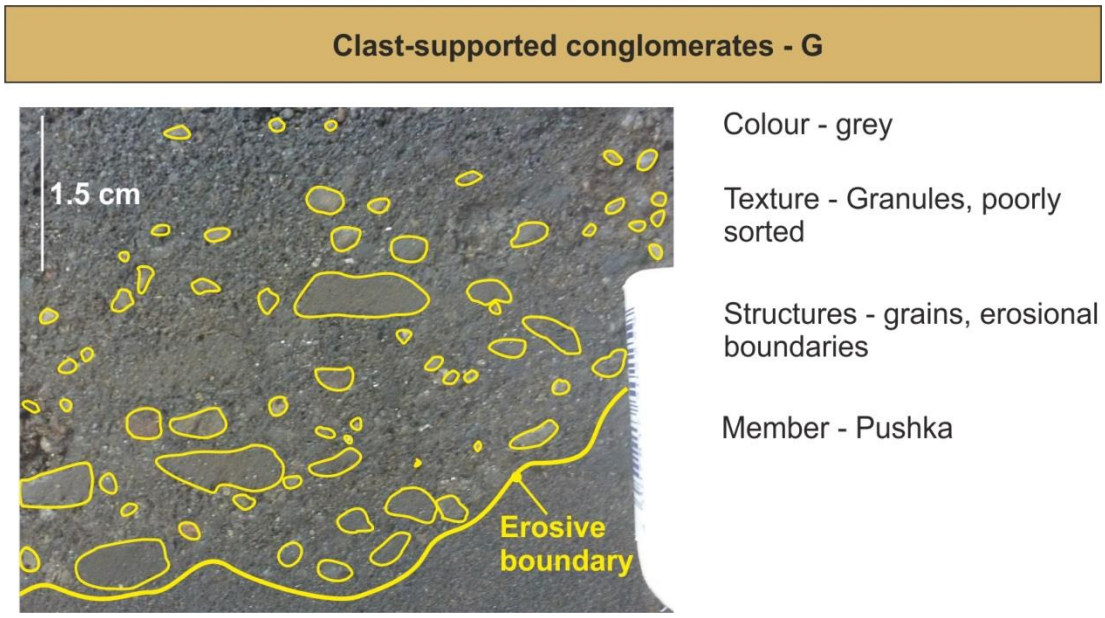

Figure 9.2: Summary of representative texture and structure for the grain-supported conglomerate facies; G, evidence of quartz clasts and rip up clasts which are normally graded with an erosive boundary, from the Aishwariya Field.

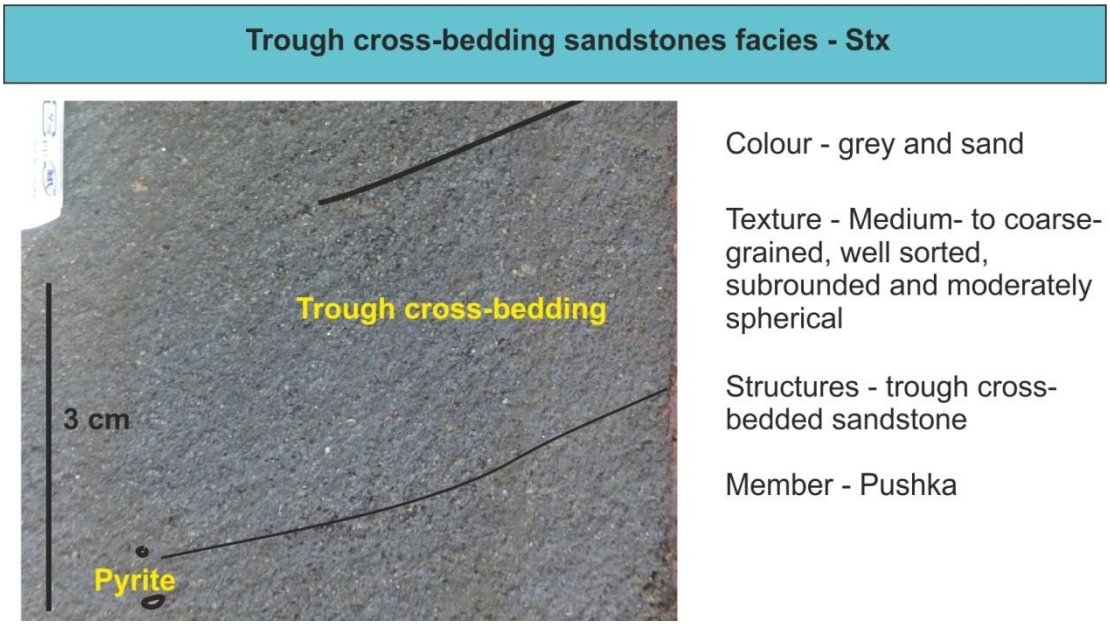

Figure 9.3: Summary of representative texture and structure for the trough cross-bedded sandstone facies; Stx, evidence of quartz clasts and trough cross-beds, from the Aishwariya-20 well.

Figure 9.4: Summary of representative texture and structure for the planar cross-bedded sandstone facies; Sx, with evidence of soft-sediment deformation and planar cross-beds, from the Saraswati-2 well.

Parallel-bedded sandstone facies - Sb

Colour - grey

Texture - Medium- to coarse-grained, moderately sorted, subrounded and moderately spherical

Structures - parallel-beds

Member - Pushka

Figure 9.5: Summary of representative texture and structure for the parallel bedded sandstone facies, Sb; evidence of quartz clasts and parallel bedding, from the Aishwariya-5 well and the Saraswati-2 well.

Massive sandstone facies - Sm

Colour - grey and sand

Texture - Fine- to coarse-grained, moderately sorted, subrounded and moderately spherical

Structures - structureless

Member - Pushka

Figure 9.6: Summary of representative texture and structure for the massive sandstone facies; Sm, is structureless with small (1 mm) quartz clasts, from the Aishwariya-17 and Aishwariya-20 wells and the Saraswati-4 well.

Figure 9.7: Summary of representative texture and structure for the low-angle cross-bedded sandstone facies; Sla, evidence of low-angle cross-beds, from the Aishwariya-20 well.

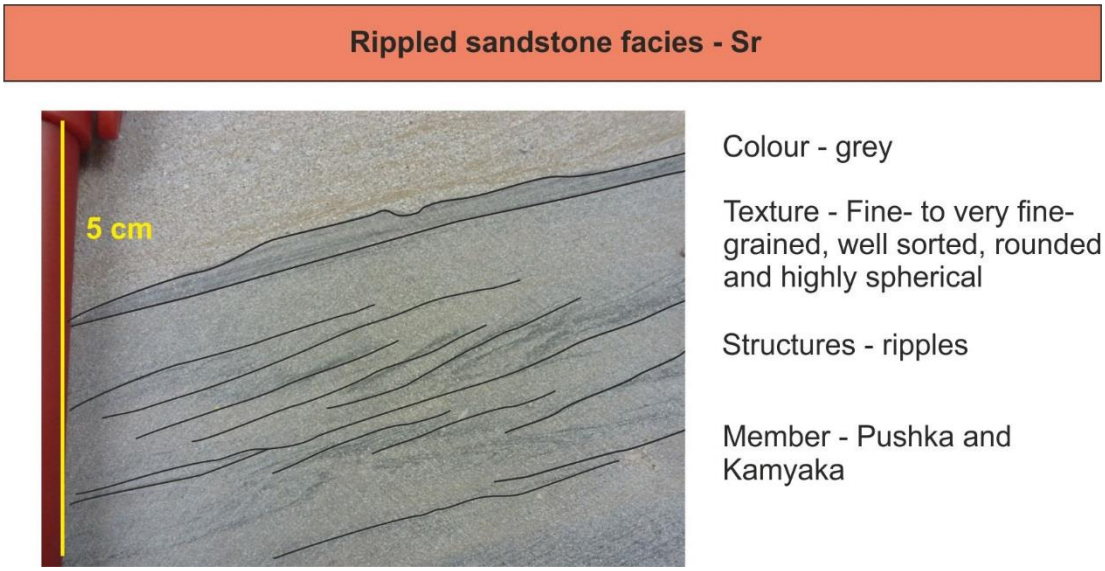

Figure 9.8: Summary of representative texture and structure for the rippled sandstone facies; Sr, displaying evidence of ripple-lamination, from the Aishwariya-5 and Aishwariya-17 wells and the Saraswati-4 well.

Soft-sediment deformation sandstones facies - Ss

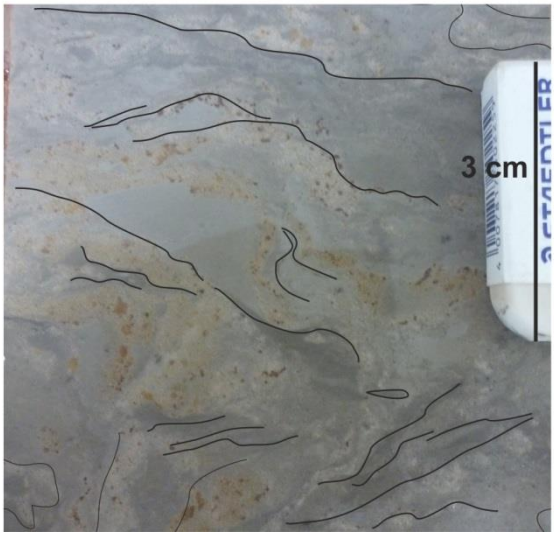

Colour - grey, red and mottled

Texture - fine- to very fine-grained, well sorted, subrounded and moderately spherical

Structures - deformed bedding from organisms and load and flame structures

Member - Pushka and Kamyaka

Figure 9.9: Summary of representative texture and structure for the soft-sediment sandstone facies; Ss, displaying evidence of goethite cement, haematite nodules and bioturbation likely from plants from the Aishwariya-20 well and the Saraswati-2 and Saraswati-4 wells.

Cross-laminated sandstone facies - Scl

Colour - grey and sand

Texture - Fine- to coarse-grained, moderately sorted, subrounded and moderately spherical

Structures - structureless

Member - Pushka and Kamyaka

Figure 9.10: Summary of representative texture and structure for the cross-laminated sandstone facies; Scl, displaying evidence of ripple-lamination, from the Aishwariya-5 and Aishwariya-17 wells and the Saraswati-4 well.

Matrix-supported conglomerates - M

Colour - grey and brown

Texture - granule- to pebble-grade, poorly sorted, rounded and varying spherical

Structures - erosional boundaries

Member - Pushka

Figure 9.11: Summary of representative texture and structure for the matrix-supported conglomerate facies; M, displaying evidence of ripple-lamination, from the Aishwariya Aishwariya-20 well and the Saraswati 4 well.

Pedogenic sandstone - Sp

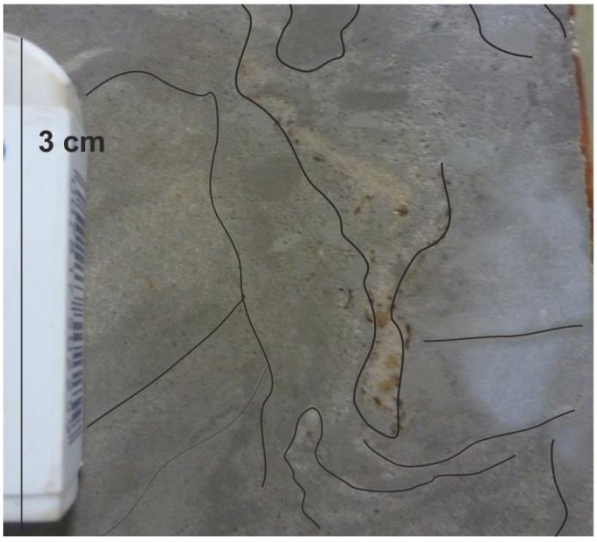

Colour - grey and mottled

Texture - fine- to very fine-grained, well sorted, subrounded and highly spherical

Structures - roots, rithozliths, gleybels, fractures, pedogenic nudules

Member - Pushka and Kamyaka

Figure 9.12: Summary of representative texture and structure for the pedogenic sandstone facies; Sp, displaying evidence of goethite cement, haematite nodules and roots from plants, from the Aishwariya-5, Aishwariya-17, Aishwariya-20 wells and the Saraswati-2 and Saraswati-4 well.

Haematitic pedogenic sandstone - She

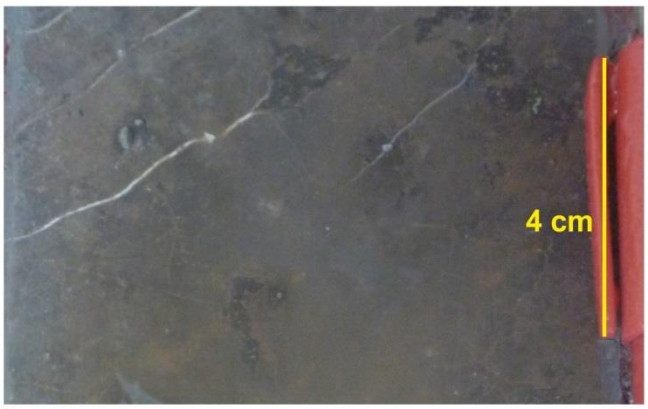

Colour - grey and sand

Texture - Fine- to very fine-grained, well sorted, sub-rounded and highly spherical

Structures - roots, rithozliths, gleybels, fractures, pedogenic nudules

Member - Pushka and Kamyaka

Figure 9.13: Summary of representative texture and structure for the haematite pedogenic sandstone facies; She, evidence of goethite cement and siderite and calcite fractures, from the Aishwariya-20 well and the Saraswati-4 well.

Pedogenic silts and clays - lp

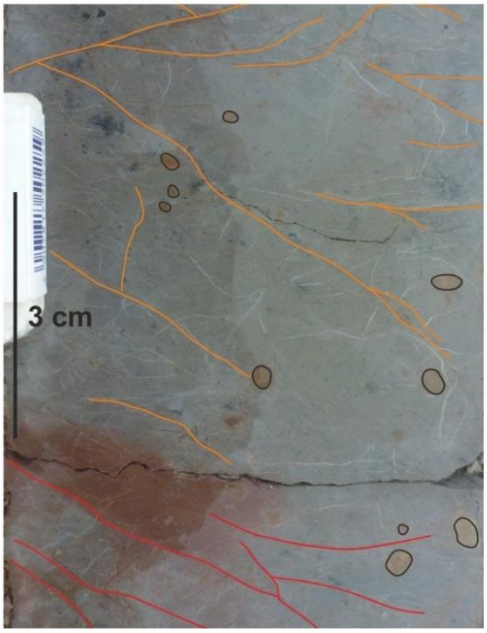

Colour - mottled grey and red

Texture - silts and clay grains

Structures - roots, rithozliths, gleybels, fractures, pedogenic nodules

Member - Pushka and Kamyaka

Figure 9.14: Summary of representative texture and structure for the pedogenic siltstone facies; lp, evidence of goethite and haematite cements filling fractures with haematite nodules, from the Aishwariya-5, Aishwariya-17 Aishwariya-20 and Saraswati-4 well.

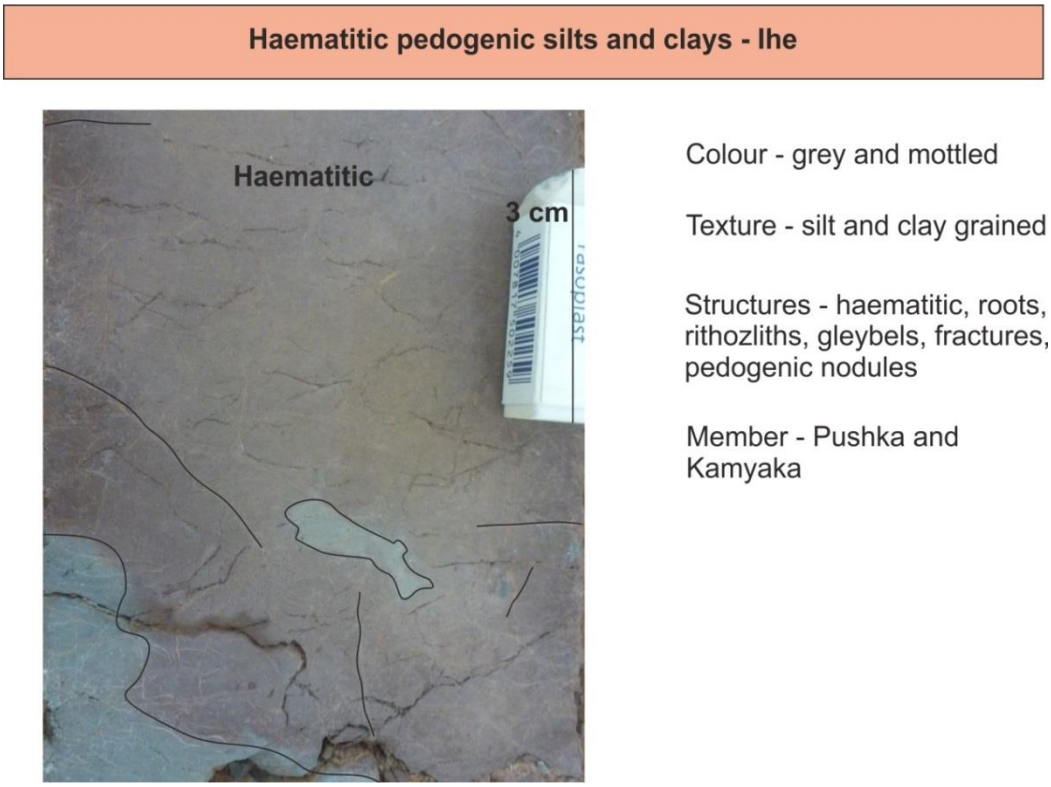

Figure 9.15: Summary of representative texture and structure for the haematite pedogenic siltstone facies; Ihe, evidence of haematite cements, from the Aishwariya-2Z and Saraswati-4 well.

9.2 Facies associations:

The facies associations have been identified based on similar transport and depositional processes occurring together within the sediments. The associations are confined (sandy and gravel bar) and unconfined (floodplain and lake, Table 9.3).

Association	Facies	Facies order	Interpretation
Sandy bar association	**M, G, Stx, Sx, Sb, Sm, Sr**	**M or G, Sx, Sm and Sr is on top**	**The upper and lower flow regime, containing migrating bedforms**
Gravel bar association	**M, G, Stx, Sx**	**M, G, Stx, Sx**	**Migration of bedforms and barforms within the lower flow regime**
Floodplain association	**Sb, Sm, Sp, Ip, She, Ihe**	**Any order**	**Cyclic deposition from unconfined fluid flows, heavily pedogenesis**
Lake association	**Sr, Ss, Scl, Sp, She, Ip, Ihe**	**Any order**	**Shallow water deposition with soft-sediment deformation and pedogenesis**

Table 9.3: Facies associations within the core data

9.2.1 Sandy bar association

Description: The sandy bar association is formed from the M, G, Stx, Sx, Sb, Sm and Sr facies (Figure 9.16). The association is dominated by the G, Sx, Sb and Sm accounting

for 75% of the total facies association; these three facies do not have any particular order but are generally at or near the base. The M facies constitutes 5% of the facies association when noted and is always at the base. Next Stx facies accounts for 5% but can be 0%. When the M and Stx facies are not accounted for the Sx facies takes up the missing 10%. The Sr facies represents 20% and this facies always occur above the G, Sx, Sb and Sm facies.

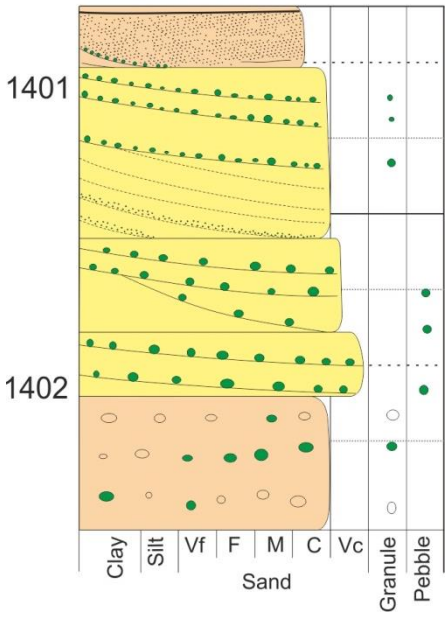

Figure 9.16: Sandy bar association which fines upwards and contains cross-bedded sets and cosets represented by the yellow fill. Massive nature to the channel and is indicated by the biege colour fill.

The sandy bar association contains bars that are stacked and amalgamated channels, this is noted through the sets and cosets of the Stx and Sx facies as the first and second order bounding surfaces terminate against each other where there is a change in facies. Towards the top of the succession the ripple-scaled sets are noted, with a change in facies and the termination of first to fourth order surfaces. The full depositional cycle of the channel association is rarely to observed. This association is dominant within the Pushka Member and in all wells apart from Saraswati 4.

Interpretation: The conglomerates (M, G and Sm facies) were deposited rapidly as they display indistinct cross-bedding; these facies plus the Sb facies were deposited within the

upper flow regime. The Stx and Sx facies exhibit various types of cross-bedding and represent the migration of subaqueous sinuous and planar dune-scale bedforms and barforms within a confined flow (Ghazi and Mountney, 2009). The consistency of the sets and cosets are dependent on the regularity of the fluid flow. The Sr facies forms within a confined flow within the lower flow regime and represent ripple-scale bedforms indicating a waning flow. In aggregate these deposits indicate sandy bar successions that are within the channels.

9.2.2 Gravel bar association

Description: The gravel bar is composed of M, G, Stx, Sx and Sm facies which generally occur in this order (Figure 9.17). The G and Sx facies constitute up to 40% each. The M facies accounts for 10% and along with the G facies occurring at the base of the association. The Stx or Sm facies makes up 10% and is interbedded with the G or Sx facies.

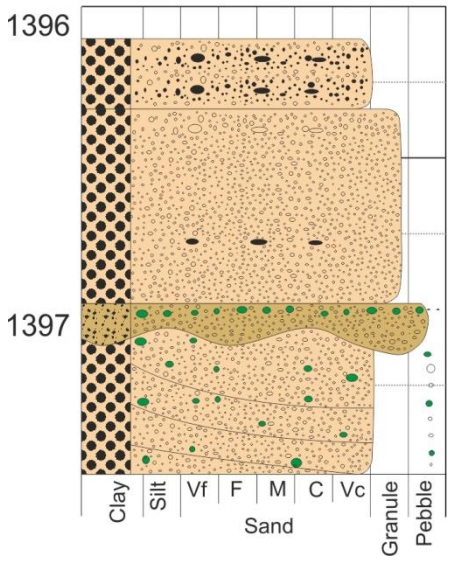

Figure 9.17: Gravel bar association which fines upwards and contains G (brown) and Sm facies (beige) dominantly.

The gravel bar association contains stacked and amalgamated deposits of the M, G, Stx, Sx and Sm facies. Where present the first and second order bounding surfaces Stx and Sx facies terminate against one-another and the sets of the facies are irregular. As these

facies are interbedded terminations of first to fourth order bounding surfaces are common. Full associations are rarely. This association occurs in the Pushka Member and in all wells apart from Saraswati-4.

Interpretation: Various types of cross-bedding within the M, G, Stx and Sx facies represent the migration of dune-scale bedforms and barforms deposited under lower flow regime conditions within a confined fluid flow environment. The sets and cosets relate to variability in flow characteristics making the barforms transient (Bridge, 1993). The internal geometries of the preserved bedforms can be indistinct (Sm facies).

9.2.3 Floodplain association

Description: This association is composed of Sb, Sm, Sp, Ip, She and Ihe facies (Figure 9.18). The order of the association starts with the Sb and Sm facies accounting for 5% and 10%, respectively. The order is then interchangeable between the Sp, She, Ip and the Ihe facies where the Sp / Ip facies account for 45% of the facies association whereas the She / Ihe facies constitutes 40% of the association.

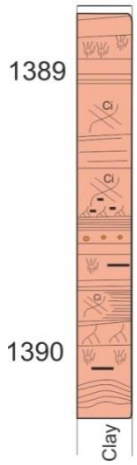

Figure 9.18: Floodplain association dominantly composed of the Sp, She, Ip and Ihe facies.

This association is dominantly mottled and bioturbated, with very few sets and cosets. Where observed they terminate against first and second order surfaces. The change between the facies records the termination of fourth order bounding surfaces, although

this is rare to observe. This association is found within both the Pushka and the Kamyaka members and in all wells.

Interpretation: The association represents cyclic deposits from unconfined fluid flows represented by the planar bedding (Sb) and massive sandstones (Sm), with little erosion suggesting a cumulative soil. Pedogenesis obscures the primary bedding structures (Sp, She, Ip and She facies).

9.2.4 Lake association

Description: The facies within the lake association are: Sr, Ss, Scl, Sp, She, Ip and Ihe facies (Figure 9.19). The coarser-grained facies are at the base of the association such as the Ss (10%) and Scl (10%), these facies exhibit ripples and soft-sediment deformation. The Sp, She, Ip and Ihe facies account for the final 80% of the association and can be modified by bioturbation.

The succession contains first to fourth order bounding surfaces where only the first and second order surface termination is noted throughout the succession. The sets and cosets here are very regular, where the rippled facies (Sr and Scl) are at the bottom of the succession and then noted are the Ss facies interbedded with the subaerial facies (Sp, She, Ip and Ihe). This association is part of the Kamyaka Member in wells: Aishwariya-2Z, Aishwariya-20 and Saraswati-4.

Interpretation: The basal ripple-scale bedforms (Sr, Scl) form under shallow water conditions and are asscaioated with wind movement and pass upwards into the pedogenically modified deposits (Sp, She, Ip and Ihe faces). This indicates subaerial exposure at the lake margin.

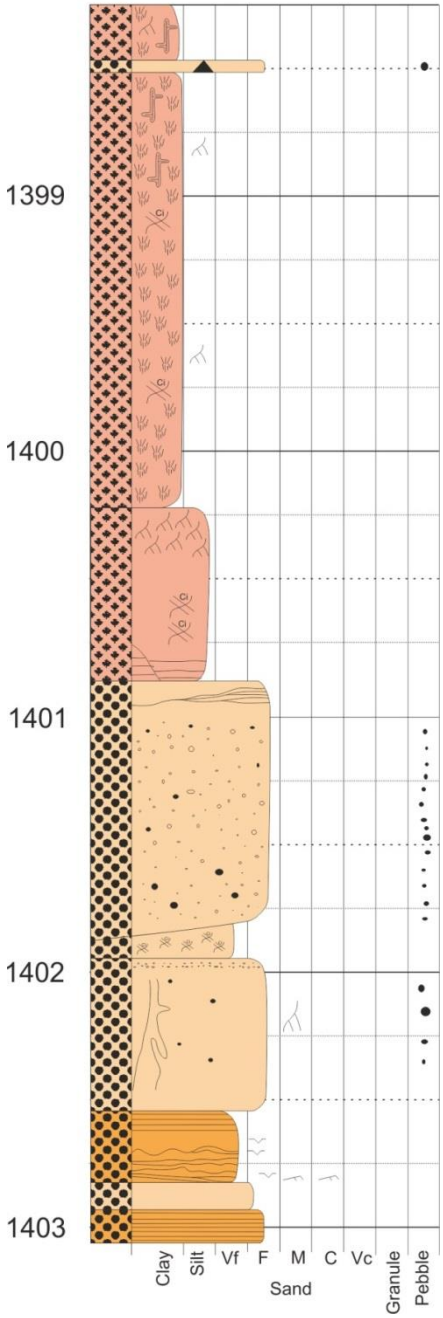

Figure 9.19: Lake association which fines upwards and coasrens upwards containing the Sh (orange), Sm (beige), Sp, She, Ip and Ihe (all pink) facies.

9.3 Petrographical analysis

Petrographical analysis of the core data has been conducted as this can be used to compare the outcrop and core data. The grainsize analysis and modal data of each well was completed by Gould and Jones (2012, 2013), however the QFL diagrams and the comparisons to the outcrop of the Ghaggar-Hakra Formation have been completed as part of this research.

9.3.1 Aishwariya Field

The grainsize within the Pushka Member varies between coarse silt- to lower coarse-grained sand within all the wells of the Aishwariya Field. The Aishwariya-2Z well varies in grainsize between lower very fine- to lower medium-grained sandstones, moderately to well sorted sandstones (Figure 9.20). Aishwariya-5 well grainsize varies between coarse silt- to lower coarse-grained sand with poorly to well sorted grains (Figure 9.21). Aishwariya-17 well varies in grainsize between medium- to coarse-grained sands, with the sorting from poorly to well sorted (Figure 9.22). Aishwariya-20 well grainsize varies between upper coarse silt- to upper medium-grained sand with moderately to well sorted sediments (Figure 9.23).

The data is plotted on a QFL diagram so that the sandstone composition can be determined. This also determines whether the grainsize affects the composition of the sandstones (Figures 6.5, 9.24). It is also noted that the sorting of the samples does not affect the composition (Figures 6.7, 9.25).

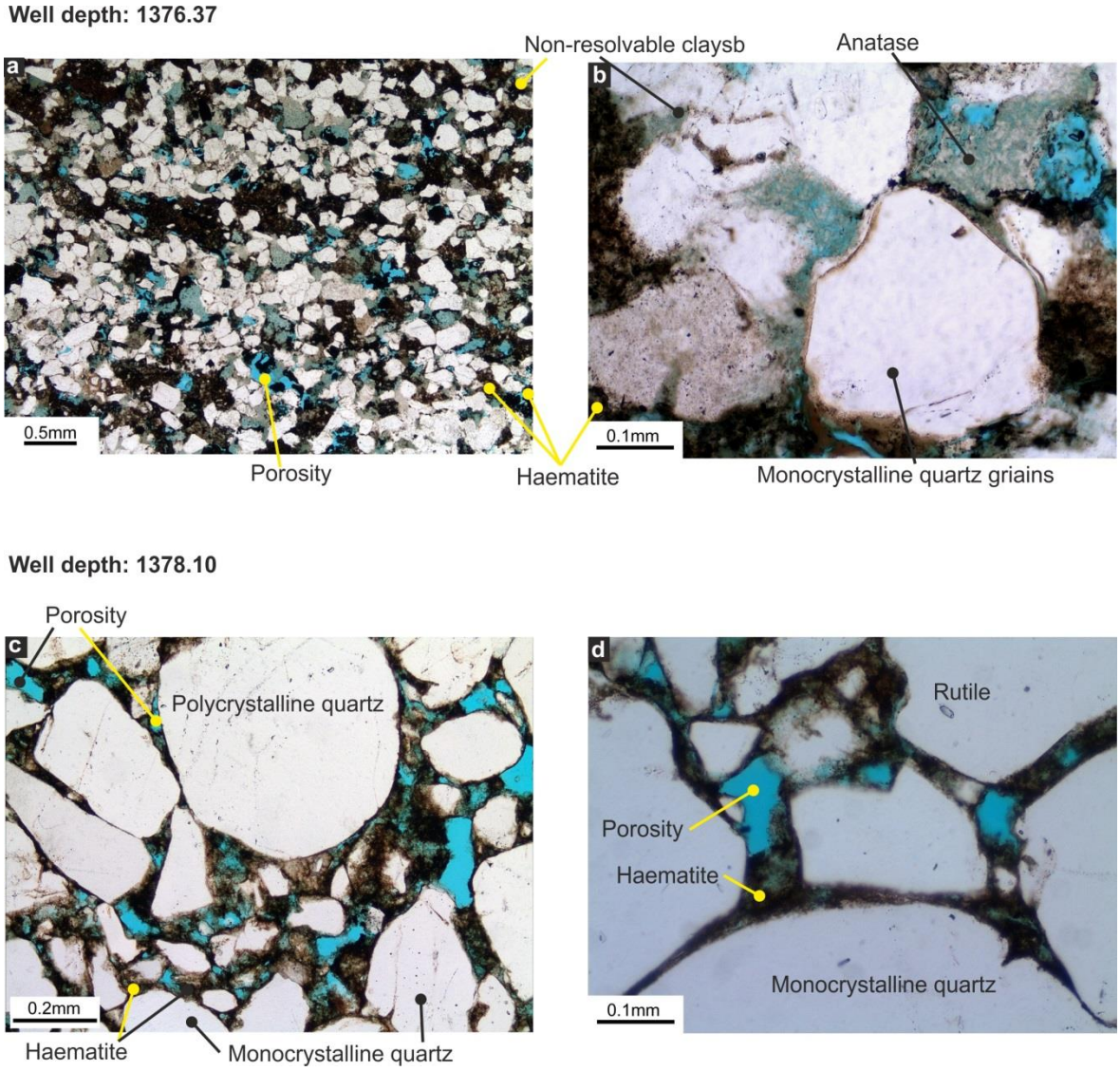

Figure 9:20: Thin section photographs of the Aishwariya 2Z well; (a, b) at a depth of 1376.37 m, displaying strained monocrystalline quartz, pore-filling non-resolvable clays, pore choking anatase cements and pore-filling haematite cements, with very low amounts of primary porosity where (a) is at scale of 0.5 mm and (b) is at a scale of 0.1 mm, and; (c, d) are at a depth of 1378.10 m, displaying strained monocrystalline quartz, sutured polycrystalline, pore filling non-resolvable clays, and pore filling haematite cements, with very low amounts of primary porosity where (c) is at scale of 0.5 mm and (d) is at a scale of 0.1 mm.

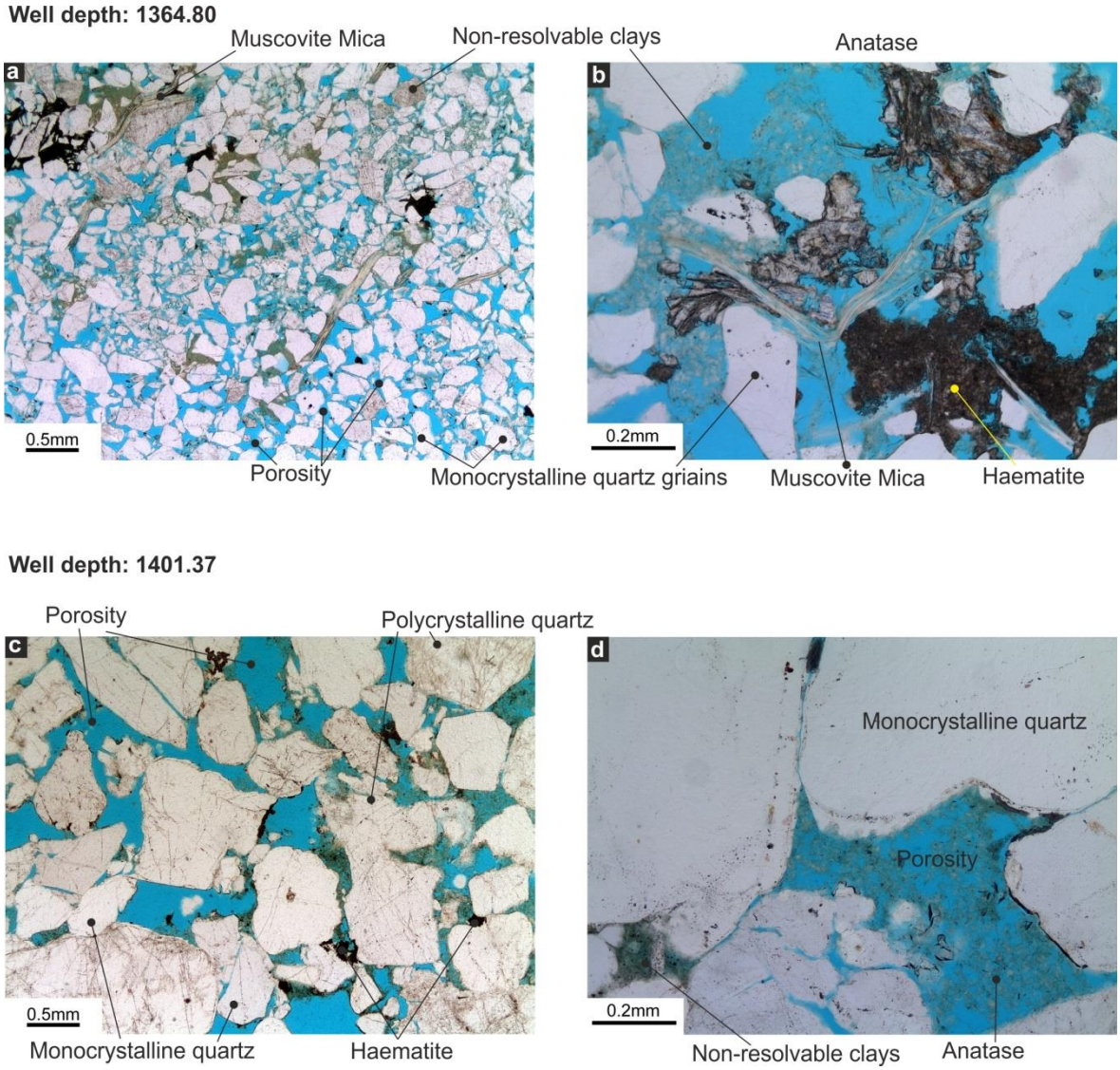

Figure 9:21: Thin section photographs of the Aishwariya 5 well; (a, b) at a depth of 1364.80 m, displaying strained monocrystalline quartz, pore-filling ductile muscovite mica, pore choking anatase cements, pore-filling, detrital grain coating haematite cements, with moderate amounts of primary porosity where (a) is at scale of 0.5 mm and (b) is at a scale of 0.2 mm, and; (c, d) are at a depth of 1401.37 m, displaying strained monocrystalline quartz, sutured polycrystalline quartz, pore filling non-resolvable clays, pore-filling anatase cements and pore filling haematite cements, with moderate amounts of primary porosity where (c) is at scale of 0.5 mm and (d) is at a scale of 0.2 mm.

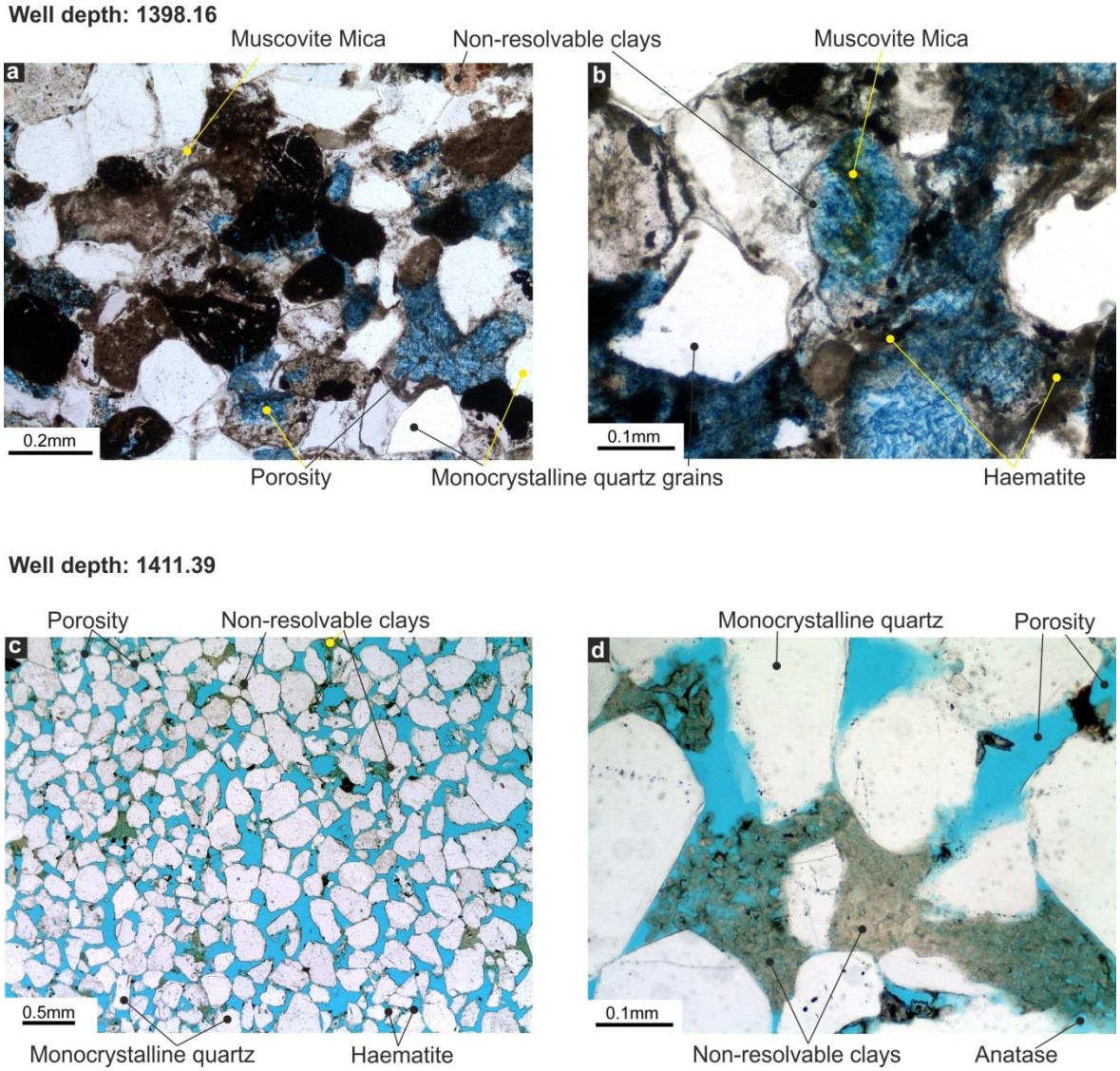

Figure 9:22: Thin section photographs of the Aishwariya 17 well; (a, b) at a depth of 1389.16 m, displaying strained monocrystalline quartz, pore-filling ductile muscovite mica, pore-filling non-resolvable clays, pore-filling, haematite cements, with very low amounts of moderate amounts of primary porosity where (a) is at scale of 0.2 mm and (b) is at a scale of 0.1 mm, and; (c, d) are at a depth of 1411.39 m, displaying strained monocrystalline quartz, pore filling non-resolvable clays, pore-filling anatase cements and pore filling haematite cements, with moderate amounts of primary porosity where (c) is at scale of 0.5 mm and (d) is at a scale of 0.1 mm.

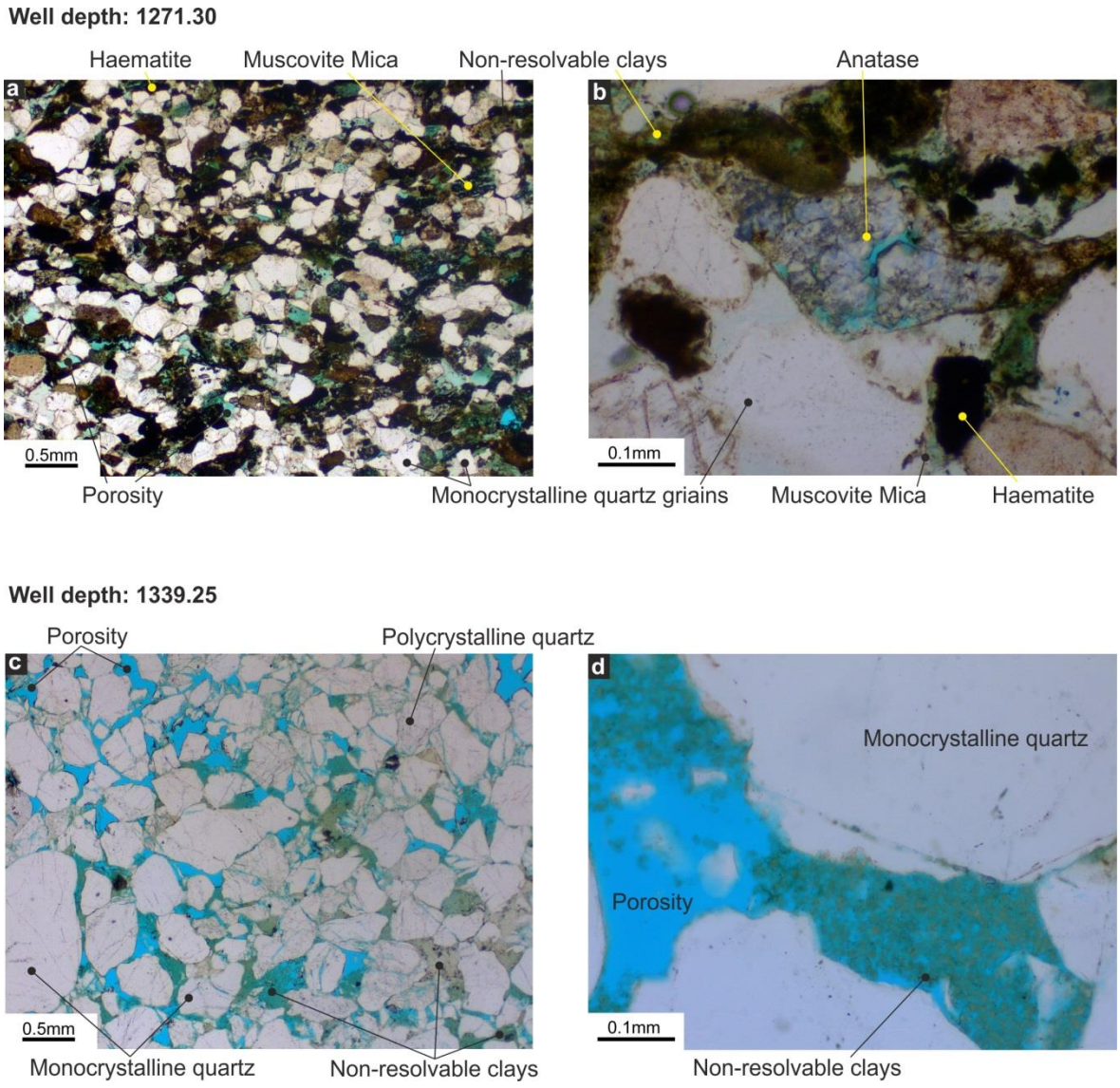

Figure 9:23: Thin section photographs of the Aishwariya 20 well; (a, b) at a depth of 1271.30 m, displaying strained monocrystalline quartz, pore-filling ductile muscovite mica, pore-filling non-resolvable clays, pore-filling anatase cements, pore-filling, haematite cements, with very low amounts of primary porosity where (a) is at scale of 0.5 mm and (b) is at a scale of 0.1 mm, and; (c, d) are at a depth of 1339.25 m, displaying strained monocrystalline quartz, sutured polycrystalline quartz, pore filling non-resolvable clays, with low amounts of primary porosity where (c) is at scale of 0.5 mm and (d) is at a scale of 0.1 mm.

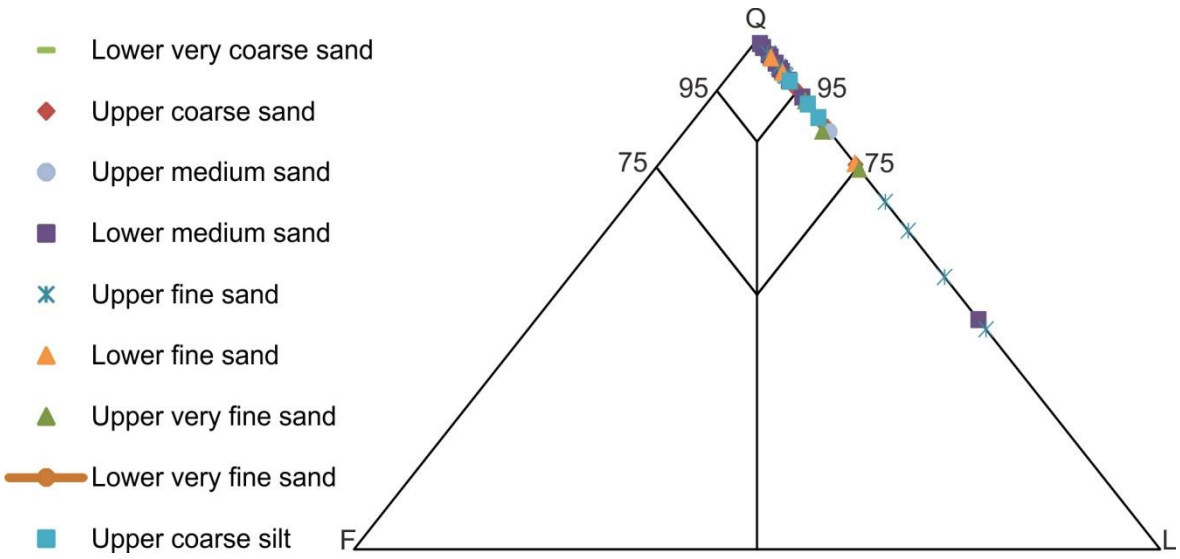

Figure 9.24: QFL plots of the composition of the Aishwariya wells displayed in terms of grainsize, all points are within the quartzarenite to lithic arenite zone.

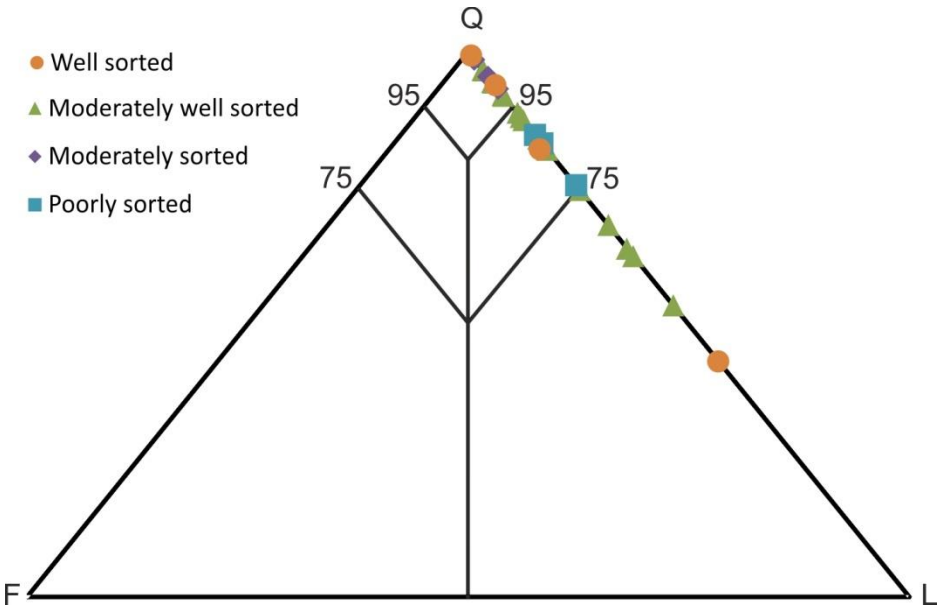

Figure 9.25: QFL plots of the composition of the Aishwariya wells displayed in terms of sorting; all points are within the quartzarenite to lithic arenite zone.

9.3.1.1 Detrital mineralogy, authigenic mineralogy and porosity

There are detrital minerals, authigenic minerals and porosity observed within the Aishwariya Wells.

<u>Detrital mineralogy</u>

The detrital minerals within the Aishwariya Field (Table 9.4) are: quartz, feldspar, rock fragments, heavy minerals, micas and non-resolvable clays. There are strained

monocrystalline quartz grains (46.55%) that are up to very coarse-grained, sub-rounded and rounded, with moderate sphericity. Polycrystalline quartz (5.67%) is coarse-grained, sub-rounded, with a high sphericity. There are small amounts of medium-grained, sub-rounded, moderately spherical feldspar (0.04%). Sedimentary, igneous and metamorphic lithic fragments are also present (3.76%). The sedimentary fragments composed of coarse-grained, rounded moderately spherical chert, whilst the medium-grained, sub-rounded, moderately spherical metamorphic fragments are composed of sutured polycrystalline quartz, exhibiting a schistose fabric. The medium-grained, sub-rounded, moderately spherical igneous rock fragments contain quartz and muscovite mica. The heavy minerals (0.86%) are rutile, tourmaline and zircon, with third order birefringence colours. Ductile sedimentary rock fragments (5.39%) are observed within the pore spaces. Ductile muscovite mica (0.94%) are thin and elongated. The ends of the muscovite are locally altered to kaolinite clays and haematite cements. There are measureable but small amounts of organic fragments (0.16%). The non-resolvable clays (2.98%) are pore-filling and grain coating.

Aishwariya-2Z		Aishwariya-5		Aishwariya-17		Aishwariya-20		Saraswati-2		Outcrop data	Dar	Sar	Nos
DETRITAL MINERALOGY								***DETRITAL MINERALOGY***		***DETRITAL MINERALOGY***			
QUARTZ	55.91	QUARTZ	60.06	QUARTZ	43.62	QUARTZ	49.29	QUARTZ	16.3	QUARTZ	64.5	75.9	81.6
monocrystalline	52.73	monocrystalline	50.81	monocrystalline	39.44	monocrystalline	43.21	monocrystalline	14.1	monocrystalline	44.0	51.9	44.3
polycrystalline	3.18	polycrystalline	9.25	polycrystalline	4.18	polycrystalline	6.07	polycrystalline	2.2	polycrystalline	20.4	24.0	37.2
FELDSPAR	0.00	FELDSPAR	0.06	FELDSPAR	0.06	FELDSPAR	0.02	FELDSPAR	5.0	RIGID ROCK FRAGMENTS	5.5	3.3	3.3
K-feldspar	0.00	K-feldspar	0.00	K-feldspar	0.03	K-feldspar	0.02	plagioclase	4.5	igneous	0.5	1.2	0.8
plagioclase	0.00	plagioclase	0.06	plagioclase	0.03	plagioclase	0	alkali	0.5	metamorphic	2.9	2.3	2.9
RIGID ROCK FRAGMENTS	1.64	RIGID ROCK FRAGMENTS	6.69	RIGID ROCK FRAGMENTS	2.12	RIGID ROCK FRAGMENTS	4.24	AMPHIBOLE	0.1	sedimentary	3.9	1.3	1.5
igneous	1.30	igneous	1.44	igneous	0.76	igneous	1.26	RIGID ROCK FRAGMENTS	21.9	HEAVY MINERALS	0.5	0.7	0.5
metamorphic	0.00	metamorphic	4.88	metamorphic	0.18	metamorphic	0.21	igneous	21.8	heavy mineral types	T, Z, R	T, Z, R	T, Z, R
sedimentary	0.34	sedimentary	0.38	sedimentary	0.29	sedimentary	0.74	(original percentage of igneous fragments)	30.1	UNDIFFERENTIATED	3.4	0.6	0.0
volcanic		volcanic	0.00	volcanic	0.88	volcanic	2.02	metamorphic	0	DUCTILE ROCK FRAGMENTS	0.0	0.0	4.3
HEAVY MINERALS	0.73	HEAVY MINERALS	0.50	HEAVY MINERALS	1.06	HEAVY MINERALS	1.14	sedimentary	0	sedimentary	0.0	0.0	4.3
heavy mineral types	T, Z, R	heavy mineral types	T, Z, R	heavy mineral types	T, Z, R	heavy mineral types	T, Z, R	HEAVY MINERALS	0.4	MICA	0.0	3.5	0.8
BIOCLASTS	0.00	BIOCLASTS	0.00	BIOCLASTS	0.00	BIOCLASTS	0.02	types		muscovite	0.0	3.5	0.8
bioclast types		bioclast types	0.00	bioclast types		bioclast types	FS	MUSCOVITE	0	NON-RESOLVABLE CLAY	10.3	3.2	5.4
DUCTILE ROCK FRAGMENTS	4.09	DUCTILE ROCK FRAGMENTS	1.69	DUCTILE ROCK FRAGMENTS	7.40	DUCTILE ROCK FRAGMENTS	8.38	DUCTILE ROCK FRAGMENTS	11.4	undifferentiated	1.5	#DIV/0!	0.5
degraded igneous	0.43	degraded igneous	0.00	degraded igneous	0.50	degraded igneous	0.07	degraded igneous (original proportion)	9.8	detrital pore-filling	2.7	1.4	5.6
undifferentiated	0.00	undifferentiated	0.00	undifferentiated	0.00	undifferentiated	0		12.8	pseudomatrix	14.4	2.4	#DIV/0!
sedimentary	3.66	sedimentary	1.69	sedimentary	6.91	sedimentary	8.31	sedimentary	1.5	***AUTHIGENIC MINERALOGY***			
MICA	1.09	MICA	1.31	MICA	0.91	MICA	0.43	undifferentiated	0	QUARTZ OVERGROWTHS	1.6	2.3	1.3
muscovite	1.05	muscovite	1.25	muscovite	0.44	muscovite	0.33	ORGANIC FRAGMENTS	2.6	MICROCRYSTALLINE QUARTZ	Trace	Trace	Trace
biotite	0.00	biotite	0.06	biotite	0.47	biotite	0.10	NON-RESOLVABLE CLAY	10.0	CALCITE CEMENT	2.9	1.9	5.0
ORGANIC FRAGMENTS	0.14	ORGANIC FRAGMENTS	0.00	ORGANIC FRAGMENTS	0.44	ORGANIC FRAGMENTS	0.07	detrital	8.3	ferroan	2.9	1.9	5.0
								pseudomatrix	1.7	non-ferroan	0.0	0.0	Trace

NON-RESOLVABLE CLAY	0.84	NON-RESOLVABLE CLAY	0.56	NON-RESOLVABLE CLAY	7.79	NON-RESOLVABLE CLAY	2.71	***AUTHIGENIC MINERALOGY***		DOLOMITE CEMENT	0.7	0.8	1.9
detrital grain-coating	0.61	detrital grain-coating	0.00	detrital grain-coating	0.03	detrital grain-coating	1.90	QUARTZ OVERGROWTH	1.5	ferroan	Trace	0.0	Trace
detrital pore-filling	0.23	detrital pore-filling	0.56	detrital pore-filling	5.94	detrital pore-filling	0.81	MICROCRYSTALLINE QUARTZ	8.2	non-ferroan	0.7	0.8	1.9
pseudomatrix	0.00	pseudomatrix	0.00	pseudomatrix	1.82	pseudomatrix	0	grain coating	0.5	PYRITE CEMENT	Trace	0.0	Trace
AUTHIGENIC MINERALOGY								replacing igneous rigid rock fragments	7.5	ANATASE CEMENT	Trace	0.0	Trace
QUARTZ OVERGROWTHS	5.30	QUARTZ OVERGROWTHS	4.56	QUARTZ OVERGROWTHS	2.29	QUARTZ OVERGROWTHS	5.02	replacing de0ital optically non-resolvable clay	0.1	HAEMATITE	8.6	4.7	0.9
MICROCRYSTALLINE QUARTZ	0.07	MICROCRYSTALLINE QUARTZ	0.00	MICROCRYSTALLINE QUARTZ	0.03	MICROCRYSTALLINE QUARTZ	0	cementing porosity	0.2	pore-filling	8.6	5.3	1.0
CALCITE CEMENT	0.00	CALCITE CEMENT	0.00	CALCITE CEMENT	0.00	CALCITE CEMENT	0	CHALCEDONY	0.1	KAOLINITE	1.4	1.0	1.9
ferroan	0.00	ferroan	0.00	ferroan	1.00	ferroan	0	replacing igneous rigid rock fragments	0.1	pore-filling	1.4	1.0	1.9
non-ferroan	0.00	non-ferroan	0.00	non-ferroan	1.00	non-ferroan	0	CHLORITE	2.8	UNDIFFERENTIATED	1.3	0.5	0.5
DOLOMITE CEMENT	2.45	DOLOMITE CEMENT	0.00	DOLOMITE CEMENT	0.00	DOLOMITE CEMENT	4.71	replacing undifferentiated grain	0.0	NON-RESOLVABLE CLAY	0.0	0.5	1.5
ferroan	2.43	ferroan	0.00	ferroan	7.21	ferroan	4.71	replacing Igneous rigid rock fragments	0.3	pore-filling	0.0	0.5	1.5
non-ferroan	0.00	non-ferroan	0.00	non-ferroan	6.91	non-ferroan	0	cementing porosity	2.2	***POROSITY***			
SIDERITE CEMENT	5.05	SIDERITE CEMENT	3.13	SIDERITE CEMENT	0.29	SIDERITE CEMENT	4.76	replacing degraded igneous ductile rock fragments	0.5	primary intergranular porosity	5.5	8.2	4.5
pore-filling	5.19	pore-filling	3.13	pore-filling	6.88	pore-filling	4.33	CALCITE	4.2	secondary intragranular porosity	0.7	0.5	0.5
replacing detrital clay	0.00	replacing detrital clay	0.00	displacive within detrital clay	4.06	replacing detrital clay	0.31	ferroan	3.2	secondary 'oversized' porosity	1.5	0.5	1.1
occluding secondary porosity	0.09	occluding secondary porosity	0.00	occluding secondary porosity	1.88	occluding secondary porosity	0.12	replacing degraded igneous ductile rock fragments	0.2				
PYRITE CEMENT	0.59	PYRITE CEMENT	0.06	PYRITE CEMENT	0.94	PYRITE CEMENT	0.24	replacing alkali feldspar	0.0				
ANATASE CEMENT	0.23	ANATASE CEMENT	0.00	ANATASE CEMENT	2.24	ANATASE CEMENT	0.88	replacing Igneous rigid rock fragments	0.6				
LIMONITE		LIMONITE		LIMONITE	1.29	LIMONITE	0.12	cementing porosity	1.8				
BARITE		BARITE		BARITE	0.00	BARITE	0.02	replacing undifferentiated grain	0.6				
HAEMATITE	0.80	HAEMATITE	0.00	HAEMATITE	0.00	HAEMATITE	0.12	non-ferroan	1.0				
pore-filling	0.00	pore-filling	0.00	pore-lining	0.38	pore-filling	0.12	cementing porosity	0.5				

replacive	0.80	replacive	0.00	replacive	0.00	replacive	0	replacing undifferentiated grain	0.1
RESIDUAL HYDROCARBONS	0.41	RESIDUAL HYDROCARBONS	0.00	RESIDUAL HYDROCARBONS	0.38	RESIDUAL HYDROCARBONS	0.21	replacing detrital optically non-resolvable clay	0.0
KAOLINITE	6.32	KAOLINITE	7.13	KAOLINITE	0.09	KAOLINITE	8.60	replacing degraded igneous ductile rock fragments	0.3
pore-filling	4.61	pore-filling	5.75	pore-filling	6.94	pore-filling	6.05	DOLOMITE	3.7
replacing unstable grain	1.16	replacing unstable grain	1.31	replacing unstable grain	3.12	replacing unstable grain	2.38	ferroan dolomite	2.0
replacing mica	0.55	replacing mica	0.06	replacing mica	3.41	replacing mica	0.17	cementing porosity	1.0
SMECTITE	0.00	SMECTITE	0.00	SMECTITE	0.41	ILLITE/SMECTITE	0	replacing undifferentiated grain	0.0
ILLITE	0.11	ILLITE	0.00	ILLITE	0.00	ILLITE	0.19	replacing detrital optically non-resolvable clay	0.0
pore-lining	0.00	grain-coating	0.00	pore-lining	0.12	pore-lining	0.05	replacing degraded igneous ductile rock fragments	1.0
replacive	0.07	replacive	0.00	replacive	0.09	replacive	0.14	replacing igneous rigid rock fragment	0
CHLORITE	0.00	CHLORITE	0.00	CHLORITE	0.03	CHLORITE	0	non-ferroan dolomite	0.8
NON-RESOLVABLE CLAY	0.30	NON-RESOLVABLE CLAY	3.19	NON-RESOLVABLE CLAY	0.03	NON-RESOLVABLE CLAY	0.40	replacing igneous rigid rock fragments	0.2
pore-filling	0.26	pore-filling	2.75	pore-filling	1.41	pore-filling	0.14	replacing degraded igneous ductile rock fragments	0.3
pore-lining	0.00	pore-lining	0.00	pore-lining	0.00	pore-lining	0	replacing alkali feldspar	0.0
replacive	0.00	replacive	0.44	replacive	0.03	replacive	0.26	cementing porosity	0.2
MACROPOROSITY								SIDERITE	2.6
primary intergranular porosity	12.23	primary intergranular porosity	10.50	primary intergranular porosity	6.71	primary intergranular porosity	8.05	replacing degraded igneous ductile rock fragments	0.3
secondary intragranular porosity	0.75	secondary intragranular porosity	0.44	secondary intragranular porosity	6.29	secondary intragranular porosity	0.26	replacing undifferentiated grain	0.1
secondary 'oversized' porosity	0.98	secondary 'oversized' porosity	0.13	secondary 'oversized' porosity	0.35	secondary 'oversized' porosity	0.10	replacing detrital optically non-resolvable clay	1.3
fracture porosity		fracture porosity	0.00	fracture porosity	0.06	fracture porosity	0.00	replacing igneous rigid rock fragments	0.1
calculated microporosity	13.95	calculated microporosity	11.06	calculated microporosity	13.41	calculated microporosity	8.40	cementing porosity	0.8
								ANATASE	0.6
								PYRITE	0.3
								HAEMATITE	3.8

replacing degraded igneous ductile rock fragments	0.7
replacing dertital pseudoma0ix	0.8
replacing detrital optically non-resolvable clay	1.8
replacing igneous rigid rock fragments	0.3
GOETHITE	0.1
ILLITE	0.3
KAOLINITE	1.0
replacing undifferentiated detrital grain	0.2
cementing porosity	0.7
NON-RESOLVABLE CLAY	7.3
grain coating and pore filling	2.8
replacive	4.5
MACROPOROSITY	
primary intergranular	1.6
secondary intragranular	0.9
secondary 'oversized' porosty	0.0

Table 9.4: Petrography data for the Aishwariya Field, Saraswati Field and the outcrop (Dar = Darjaniyon-ki Dhani Sandstone, Sar = Sarnoo Sandstone, Nos = Nosar Sandstone), table allows for easy comparison between the three areas. The Saraswati Field appears to have a considerably different mineralogy when compared to the Aishwariya Field and the outcrop.

Authigenic mineralogy

The authigenic minerals are quartz overgrowths, dolomite, siderite, pyrite, anatase and haematite cements, with kaolinite booklets and non-resolvable clays. Syntaxial quartz overgrowths (4.29%) are discontinuous and thin (approximately 3 μm) around the quartz host grain. The growths spread into the primary and secondary intergranular areas. The dolomite cements (1.79%) etch and corrode the detrital grains. Siderite cements (4.88%) infill the pores spaces and fractures. The pyrite cement (0.46%) is within the pore spaces. Cubic anatase (0.84%) is pale and occurs as mineral inclusions within the quartz. Haematite cements (0.23%) etches and stains the grains a deep red colour. The haematite also coats the grains and infills the primary pore spaces. Kaolinite booklets are up to 0.5 mm in length and subhedral (5.53%). The kaolinites are choking the primary pores. The non-resolvable clays under SEM are smectite and illite (0.38%) the clays are pore-filling and grain-coating.

Porosity

There is a moderate amount of porosity from primary intergranular porosity, secondary intragranular porosity and secondary ‘oversized’ porosity. The primary intergranular (9.37%) porosity is from primary deposition. The secondary intergranular (1.94%) porosity and the secondary ‘oversized’ (0.39%) porosity both form when grains dissolve.

9.3.1.2 Petrographical classification

The compositions of the sandstones in these wells vary from quartzarenites to litharenites (Figure 9.26). The Aishwariya-2Z and Aishwariya-5 wells are within the sublithic-quartzarenite zones whereas the Aishwariya-17 and the Aishwariya-20 wells contain samples from the quartzarenite zone into the litharenite zones (Figure 9.26). This suggests that the spatial location of the wells does not affect the sediment composition.

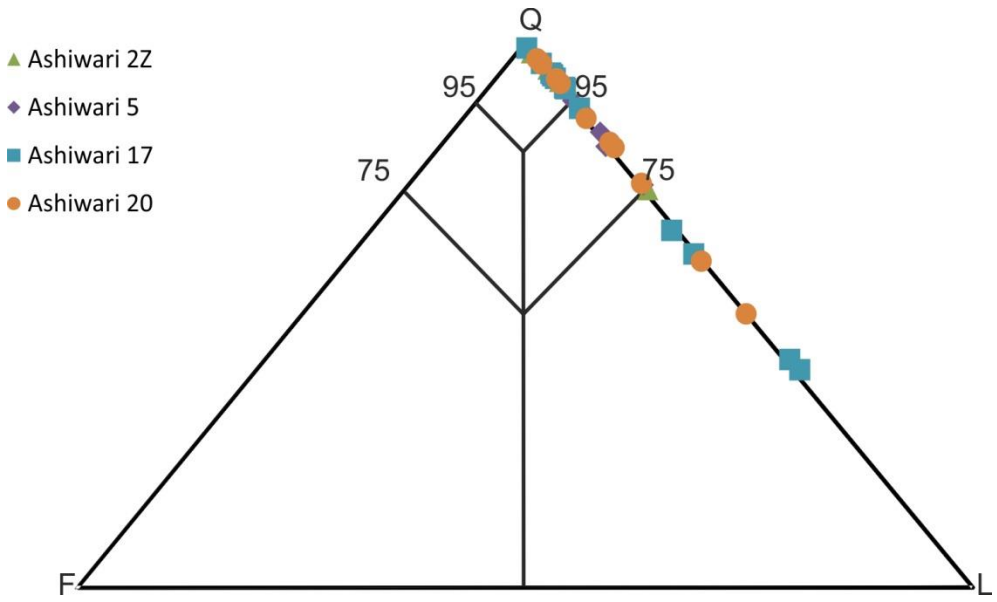

Figure 9.26: QFL plots of the composition of the Aishwariya wells, points are within the quartzarenite to lithic arenite zone.

The grainsize, sorting and facies (Figures 9.24, 9.25, 9.27) are within the quartzarenite zone into the litharenite zones. The deposition processes of the sediments do not affect the composition of the system but rather the transport processes of saltation and rolling affects the texture of the grains (Section 2.1.2). This suggests that the sediment textures do not reflect their distance of transport.

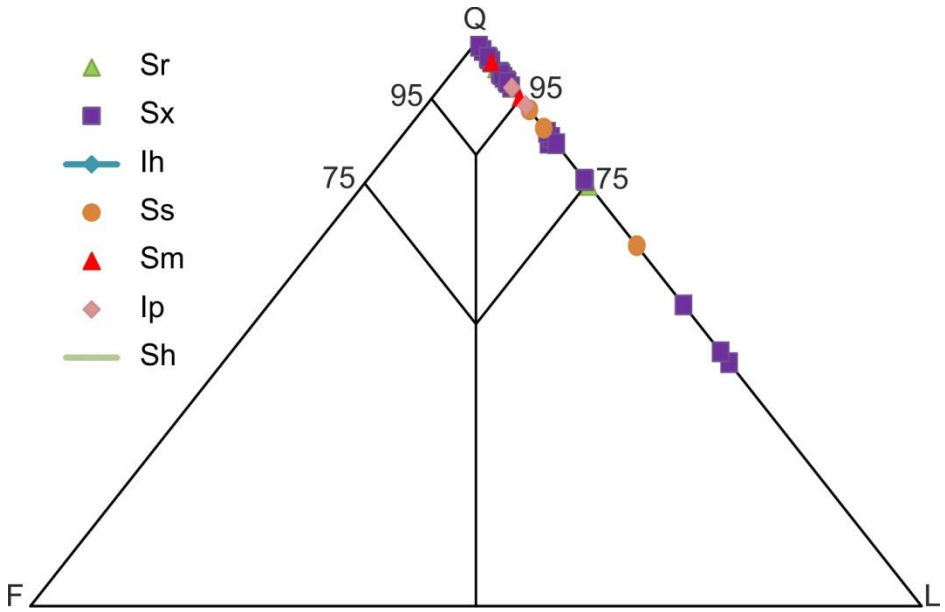

Figure 9.27: QFL plots of the composition of the Aishwariya wells displayed in terms of facies, points are within the quartzarenite to lithic arenite zone.

Within the core data there are three different environments (Figure 9.28) which are: fluvial channels, vegetated lake margins, gravel bars within braided fluvial channels (Section 9.2; Gould and Jones, 2012). Here, it is noted that the fluvial channels have a range from quartz arenite to litharenite, whereas both the lake and braided channel environments are within the quartz arenite to the sublithic arenite zones (Figure 9.28).

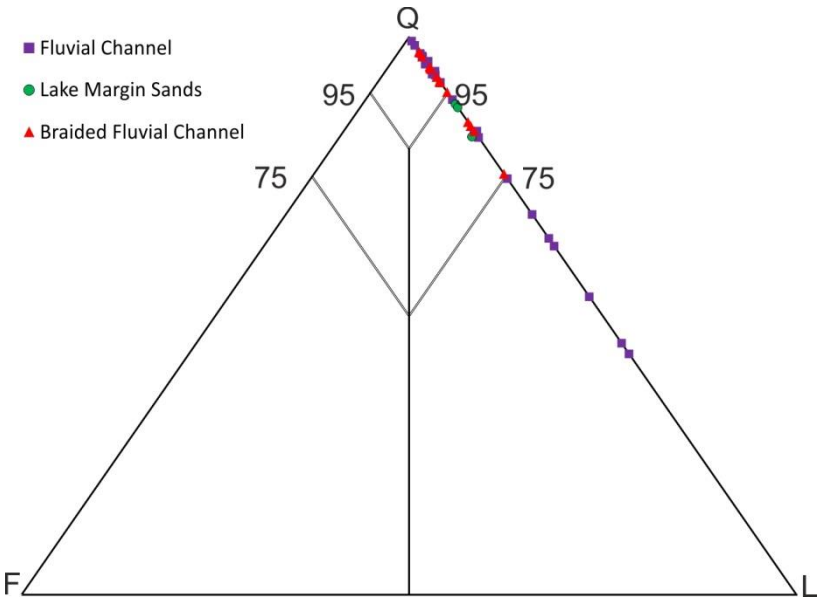

Figure 9.28: QFL plots of the composition of the Aishwariya wells displayed in terms of environment, points are within the quartzarenite to lithic arenite zone.

9.3.2 Saraswati Field

Two wells have been cored and contain the Ghaggar-Hakra Formation (Saraswati-2 and Saraswati-4). However, only one thin section from the Saraswati-2 well at a depth of 1880.80 m has been examined. From this single data point there are some significant differences from the outcrop data, however, it is wise to consider this data as limited.

Mineralogy and porosity

This thin section contains upper fine sands, with moderately to well sorting. The first and more notable point is that there is feldspar within the section (Figures 9.29); however the data point is still within the quartz-arenite field. The detrital mineralogy is composed of quartz, feldspar, rock fragments, heavy minerals, micas, organic fragments and non-

resolvable clays (Table 9.4, Figure 9.30). The fine- to very coarse-grained monocrystalline quartz grains are sub-rounded and highly spherical. The quartz is strained. The coarse-grained polycrystalline quartz grains are sub-rounded with a moderately spherical and subordinate (16.3%) with concave-convex contacts. The medium-grained, sub-angular, moderately spherical igneous fragments (21.9%) are formed from quartz with muscovite mica inclusions. The heavy minerals (0.4%) are rutile, tourmaline and zircon all have third order birefringence colours. The ductile rock fragments (11.4%) are sedimentary and within the pore spaces. The organic fragments (2.6%) are small (1 µm) and within the pore spaces. The non-resolvable clays (10%) infills the pore space and coats the grains.

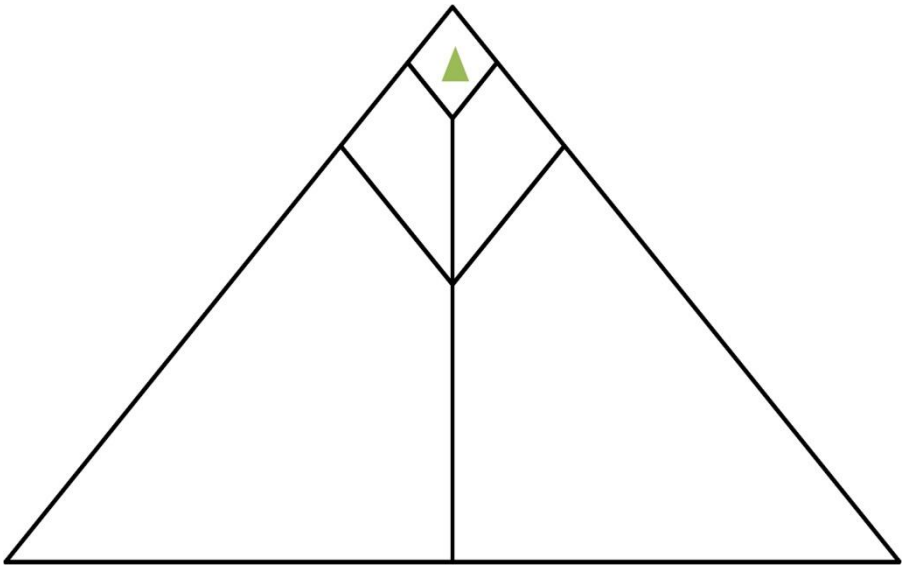

Figure 9.29: QFL plots of the composition of the Sarawati 2 well where the single point is within the quartzarenite zone.

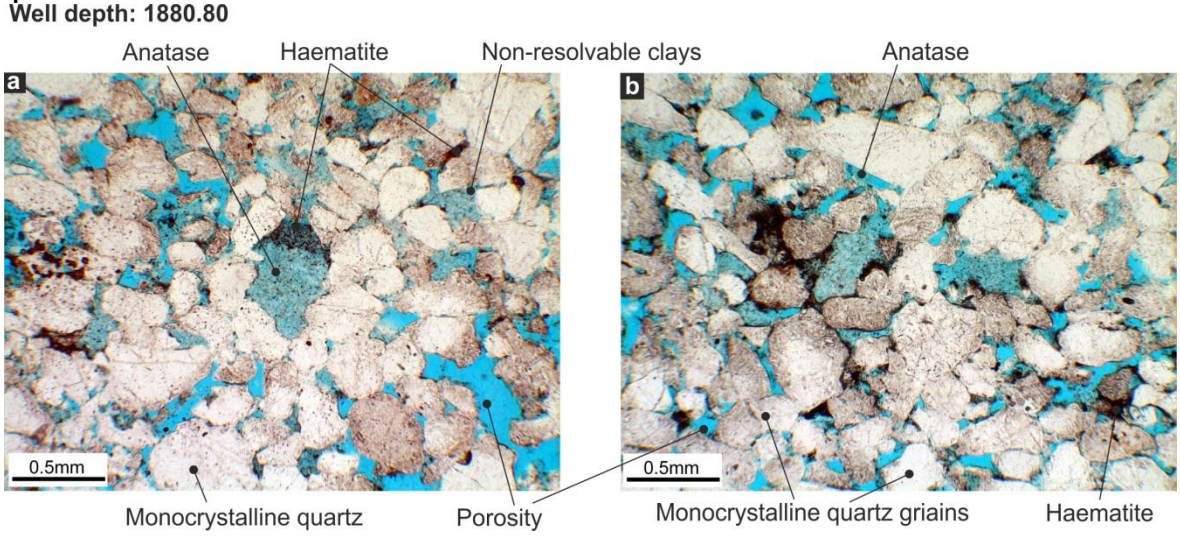

Figure 9:30: Thin section photographs of the Saraswati 2 well; (a, b) at a depth of 1880.80 m, displaying strained monocrystalline quartz, pore-filling non-resolvable clays, pore-choking anatase cements, pore-filling, haematite cements, with low amounts of primary porosity where (a) is at scale of 0.5 mm and (b) is at a scale of 0.5 mm.

The authigenic mineralogy is composed of microcrystalline quartz, chalcedony, chlorite cement, calcite cement and illite clays (Table 9.4, Figure 9.30). The microcrystalline quartz (8.2%) and chalcedony (0.1%) are pore filling. The microcrystalline quartz extends into both primary and second pore spaces. The chlorite cement (2.8%) is infilling the pore space. The calcite cement (4.2%) is infilling the intergranular spaces and fracture filling. The illite (0.3%) is no bigger than 30 µm, the grains are sub-angular and are moderately spherical. The illite is also pore-filling and pore-choking the intergranular spaces.

The isolated porosity is only 1.5%, very low and composed of the primary intergranular porosity only.

9.3.3 Outcrop comparison

Here the outcrop petrography is compared to the Pushka Member within the subsurface (Table 9.4).

The grainsizes and sorting here are broadly similar to those expected from a fluvial depositional system and match the outcrop well. As expected with fluviatile successions the grainsize and sorting profiles for outcrop and core are comparable. However, the principal differences are that the outcrop material lacks silt and the core material lacks very coarse-grained sandstones (Figures 6.5, 6.6, 9.24, 9.25).

Samples from the outcrops and the Aishwariya and Saraswati boreholes have similar mineralogical compositions. However, the Saraswati Field has a unique detrital mineralogy that is different to the outcrop and the Aishwariya Field. The Saraswati Field differences are: (1) the dominant detrital grains are rigid rock fragments; (2) there is measureable feldspar; (3) there are higher amounts of cement, and; (4) the porosity is

lower. On the QFL diagrams all the data points from both the outcrop and the core data of both the Aishwariya and Saraswati fields are within the quartzarenite to sublithic-arenite range and therefore do not differ significantly in composition. Again, there is only one data point from the Saraswati Field affecting the reliability of the interpretations for this field.

9.4 Facies assemblages

The core observations indicate a more basin-centre setting when compared to the outcrop facies associations. By combining sedimentological and petrographical data it is possible to define three distinct facies assemblages.

9.4.1 Low-sinuosity fluvial facies assemblage

The associations represent channel deposition, gravel bars and floodplain environment. The channel association comprises fine- to medium-grained sandstone in planar cross-bedded (Sx) sets and cosets (90 cm high) alternating with medium- to coarse-grained trough cross-bedded sets (50 cm high, Figures 9.28, 9.31). Interbedded with these channels are units of granule-grade conglomerates (G) of the gravel bar association. This association comprises coarse-grained sand to granule-grade conglomerates with indistinct trough cross-bedded sets (Stx, 30 cm high), and granule- to pebble-grade, matrix-supported conglomerates (M) along with units of medium- to very coarse-grained massive sandstones. These associations together are suggestive of a high discharge and avulsion rate. The floodplain association associated with this fluvial system contains clay to fine-grained sand indistinct laminations, some of which have been destroyed due to bioturbation (Sp, Ip), along with mottled patches, roots and siderite nodules. The channel to floodplain ratio is approximately 70:30.

It follows that the contacts in core between separate facies of the channel association, and between facies of the gravel bar association, are likely to represent third order bounding surfaces at outcrop. The contact at the base of the floodplain association is

most likely a forth order surface and again correlates with similar fourth order surfaces visible within the outcrop. By drawing parallels between facies assemblages and bounding surface relationships between the outcrop and subsurface indicates that the Pushka Member in the subsurface represents a low sinuosity fluvial system with channel sizes up to 15 m to 25 m wide and 10 m high. It is likely that the gravel bars are 1.5 m to 4 m long and 20 m wide and are interbedded with the channel facies association. The proportion of floodplain material preserved within the system is likely to be limited to 1 m thick packages that are laterally discontinuous. These three facies associations correlate well with the low sinuosity, fluvial system and associated floodplain deposits of the Nosar Sandstone at outcrop and is equivalent to the Pushka Member.

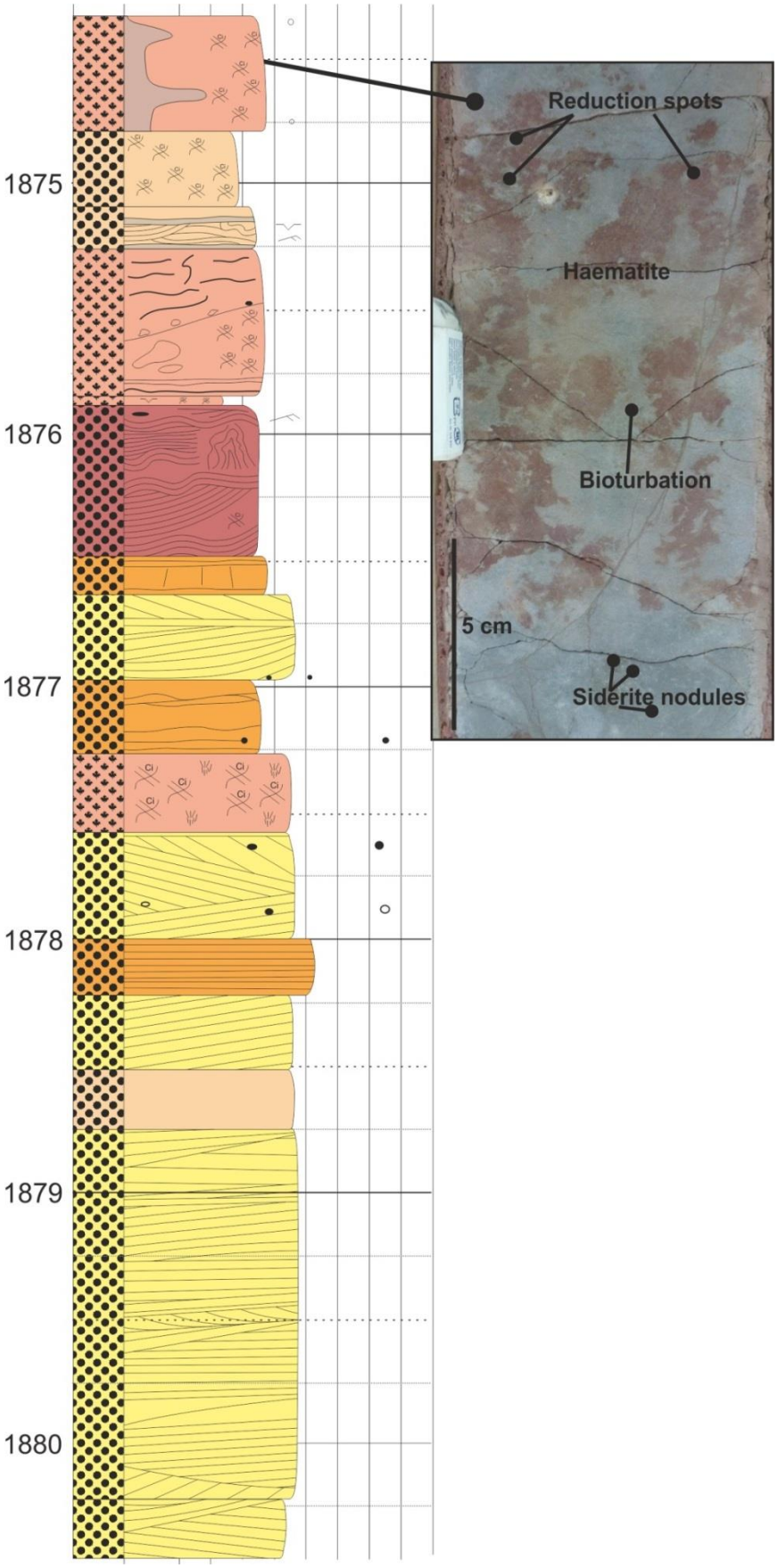
1875
1876
1877
1878
1879
1880
Reduction spots
Haematite
Bioturbation
5 cm
Siderite nodules

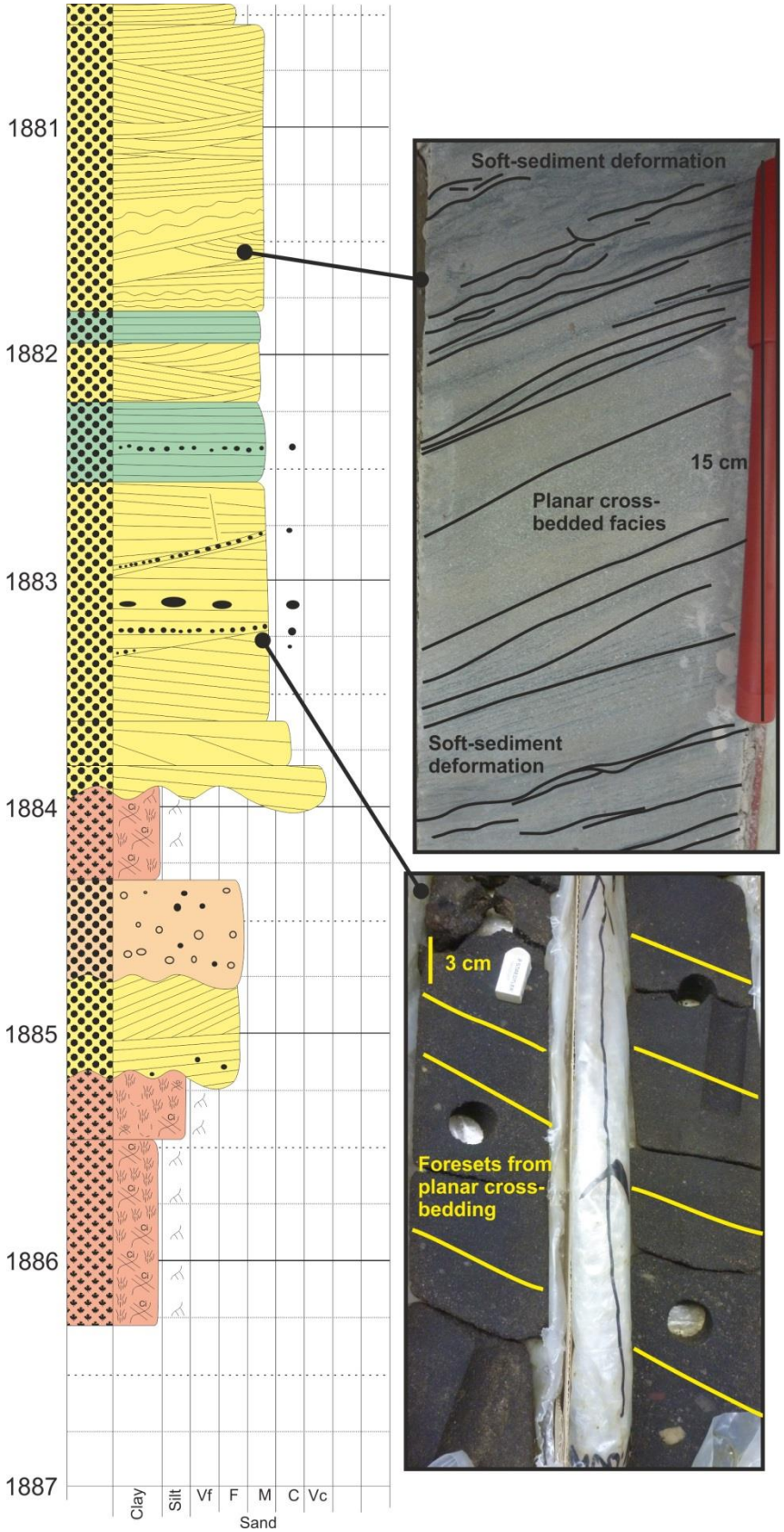

Figure 9.31: Low sinuosity facies assemblage displaying a fining upwards succession, which contains St, Sb, Ip and Ihe facies.

9.4.2 Lake facies assemblage

The second assemblage is composed of fine-grained sandstone with symmetrical and asymmetrical ripples (Sr) with sets (10 cm high) representing barform migration. The ripples are followed by soft-sediment deformation from load and flame structures (Ss) and slumps (Figures 9.28, 9.32). Next, there are very fine- to fine-grained, horizontally laminated sandstones containing little soft-sediment deformation from bioturbation (roots and organisms, She, Ihe). The top of the sedimentary package contains clay- to very fine-grained sands which are massive but can contain siderite nodules (1 – 3 mm, Sp, Ip) and occasional *Lockeia* burrows. This assemblage represents a lacustrine facies association that does not correlate well with the outcrop data. The second facies assemblage evident in core represents the Kamyaka Member (Dolson *et al.,* 2015).

9.4.3 Bedload dominant, low sinuosity fluvial facies assemblage

The third facies assemblage comprises channel and floodplain associations (Figures 9.28, 9.33). The channel bedform association contains medium- to coarse-grained, planar cross-bedded sets (Sx, 20 cm high), interbedded within medium-grained, parallel-bedded (Sb) sandstones. The floodplain association contains very fine- to fine-grained sands with asymmetrical ripple laminations (Sr) and soft-sediment deformation (Ss) due to bioturbation from plant roots. There are also very fine-grained sands with siderite nodules and siderite-filled fractures (Sp, Ip). This facies assemblage forms a bedload dominant, low-sinuosity, fluvial system within the subsurface. The channel to floodplain ratio is approximately 70:30. The association is not correlated directly to the outcrop, but is part of the Pushka Member.

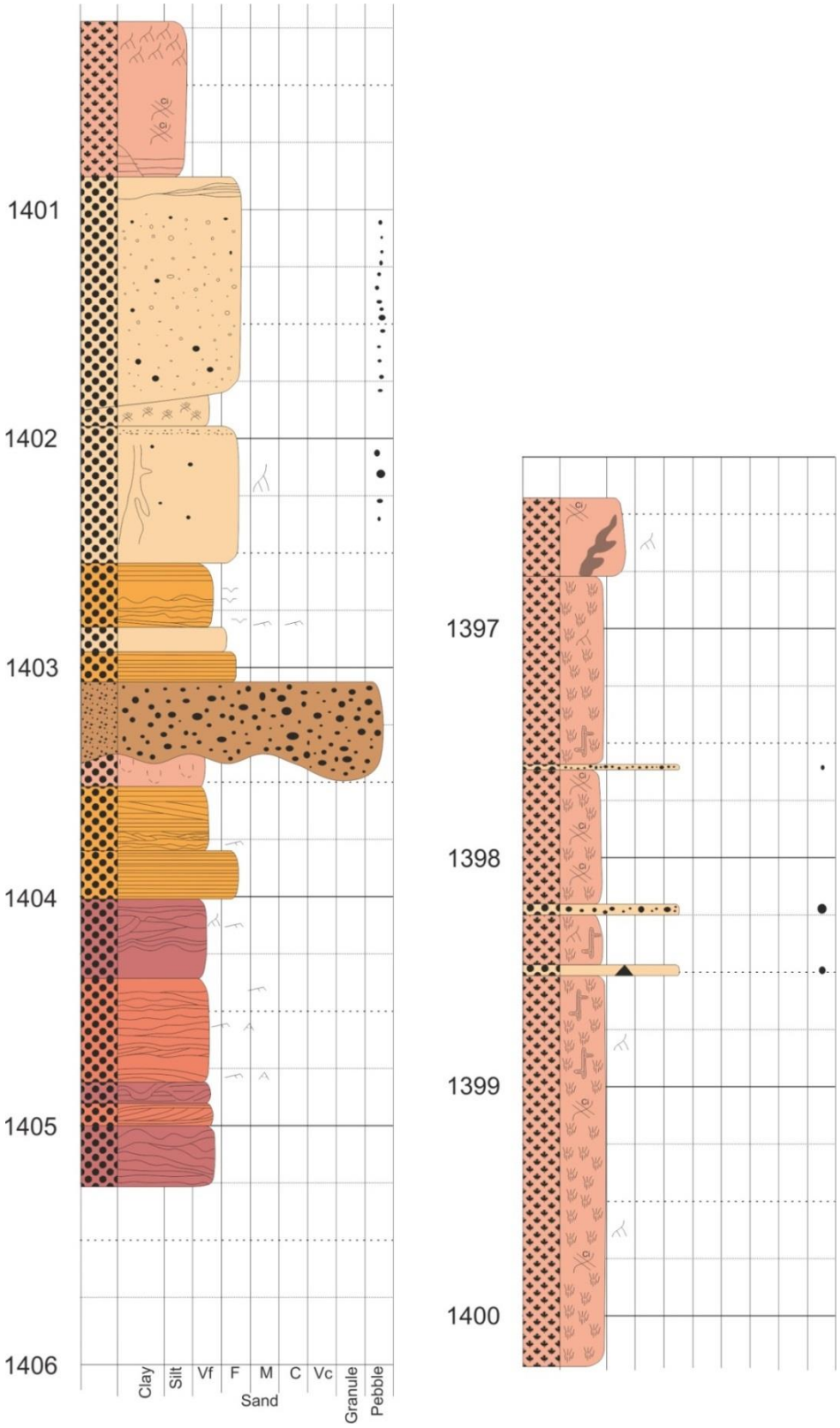

Figure 9.32: The lake facies assemblage containing both fining and coarsening upwards successions, with the dominant facies been Ss, Sr, M, Sh, Sm, Ip and the Ihe facies.

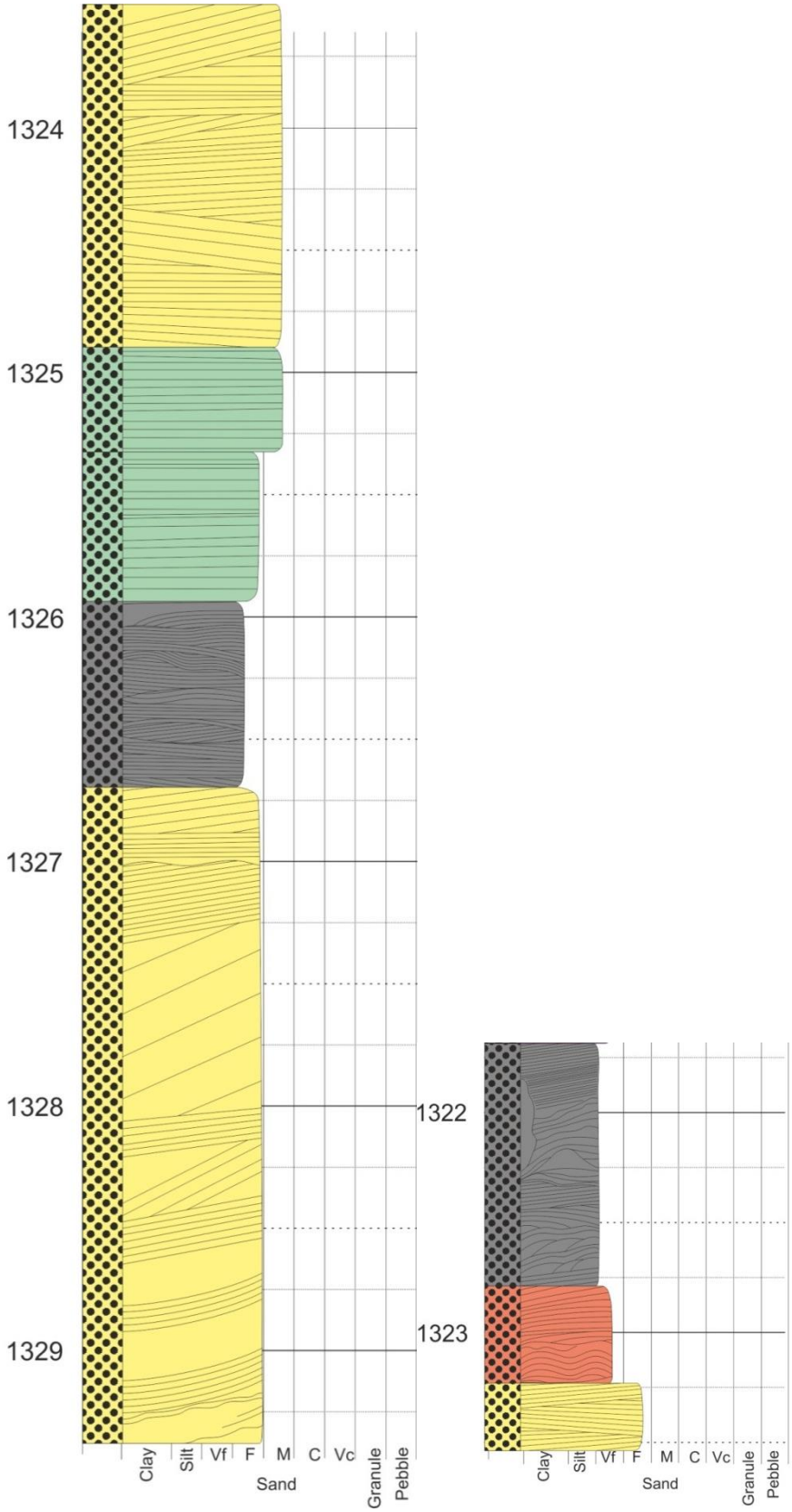

Figure 9.33: The bedload dominant low sinuosity fluvial assemblage which fines upwards and dominantly contains the Sx, Sb and Scl facies.

9.4.4 Outcrop comparisons for predictions within the subsurface

The three-dimensional architectural element models and facies models display the sand to mud ratio, three-dimensional geometry of the bedforms and barforms and the lower, upper and internal boundaries are also defined. Individual architectural elements are not seismically resolvable within the Barmer Basin seismic data (Bladon *et al.,* 2015b; Dolson *et al.,* 2015) therefore by knowing the heights, widths, geometries and textural characteristics of the sediments the reservoir quality can be predicted within the subsurface. The elements that correlate to the facies associations from outcrop to core are displayed in Table 9.5.

9.4.4.1 Channels

The channel architectural element (Section 5.2.1) is at a maximum of 23 m wide and 3 m high, with a concave geometry. The channels are stacked, amalgamated and rarely seen is a full channel succession. The succession contains first- to fifth-order bounding surfaces. By detailing the channels at outcrop, it can be predicted that the channels within the subsurface will appear similar especially those within the low sinuosity fluvial facies assemblage (Section 9.4.1) as these rocks generally resemble the outcrop equivalents, especially in terms of facies (M, G, Stx, Sx, Sb, Sla, Sm and Sr) and first to fifth order bounding surfaces. Good examples of channels that have eroded into one another within the subsurface are seen in the Aishwariya-2Z well.

9.4.4.2 Gravel bars

The gravel bars at outcrop (Section 5.2.3) are at most 75 m wide and 4 m high with a lenticular geometry, internally the gravel bars have first- to third-order bounding surfaces, with the base of the gravel bar being a fifth-order bounding surface. This information can be used within the subsurface as the gravel bars of the low sinuosity, fluvial facies assemblage (Section 9.4.1) and the bedload dominant, low sinuosity, fluvial facies assemblage (Section 9.4.3) appear similar to the outcrop as they contain first to third

order bounding surfaces and similar facies of (M, G, Stx and Sx). Good examples of the gravel bars in the subsurface can be noted in the Aishwariya-5 well.

Core data				
Association / element	Facies	Facies order	Interpretation	Element linked
Sandy bar association	M, G, Stx, Sx, Sb, Sm, Sr	M or G, Sx, Sm then Sr	Within both the upper and lower flow regime, containing migrating bedforms	F1
Gravel bar association	M, G, Stx, Sx	M, G, Stx, Sx	Migration of bedforms and barforms within the lower flow regime and a confined	F3
Floodplain association	Sb, Sm, Sp, Ip, She, Ihe	Any order	Cyclic deposition from unconfined fluid flows, heavily pedogeneic	F7
Lake association	Sr, Ss, Scl, Sp, She, Ip, Ihe	Any order	Shallow water deposition with soft-sediment deposition with is pedogeneic towards the top of the sediment package.	F8
Outcrop data				
Sandy bar element (F1)	M, G, Stx, Sx, Sb, Sm, Sr, Sh, Ip	Fining upwards	To up 23 m wide and 3 m high with first- to fifth-order bounding surfaces. Concave geometry, deposited within channels	Sandy bar
Gravel bar element (F3)	M, G, Sx, Sb, Sm, Sr, Sh	Fining upwards	To up 75 m wide and 5 m high with first- to fifth-order bounding surfaces and a lenticular geometry, representative of a gravel bar	Gravel bar
Floodplain element (F7)	Sb, Sm, Sr, Scl, Sh, Im, Sp, Ip, Ihe	Fining upwards	To up 10 km wide and 25 m high (or 2 m wide and 1 m high) with first- to sixth-order bounding surfaces and a lenticular geometry, pedogenic and bioturbated floodplain sediments	Floodplain
Pond element (F8)	Sm, Sr, Scl, Sh, Im, Sp, Ip, Ihe	Fining upwards	To up 50 m wide and 2 high with first- to second-order bounding surfaces and a lenticular geometry of preserved ponds.	Lake

Table 9.5: Comparisons between the facies associations in the core data to the architectural elements from the outcrop

9.4.4.3 Floodplain

At outcrop, there are two types of floodplain element within Ghaggar-Hakra Formation (Section 5.2.7). The first type is extensive across all the field areas and at least 10 km in length and ≤30 m in height and has a tabular geometry (Section 5.2.7). The base of this succession marks a sixth order bounding surface and the top of this succession is eroded into by channels. However, internally the successions are pedogeneic (Sections 5.2.7, 5.3.4, 5.4.3, 5.4.5, 8.2.3). The second type of floodplain within the sandstone succession is ≤2 m in width and ≤1 m in height, with a lenticular geometry. The lower boundary forms

a fourth order bounding surface and the internal boundaries form first and second order surfaces. These successions are generally eroded into by channels or gravel bars.

The thick (25 m) floodplain succession is not noted within any of the measured wells; the thickest measured floodplain succession is 15 m thick and therefore, it is suggested that a floodplain thickness of 25 m is not represented within the core data. This could be due to a lack of extensive flooding from the fluvial system, lack of accommodation space or the influence of a nearby lacustrine system which interfingers with the channels of the fluvial system. The lenticular floodplains within the sandstone successions are noted in all the measured wells. However, they appear to be slightly thicker (3 m to 8 m), which suggests that the channels of the fluvial systems are more stable than those at outcrop. This would be expected as the fluvial deposits within the wells here are in the distal basin where the fluvial system is likely to be better-developed when compared to the proximal parts of the same fluvial system (Miall, 1996; Nichols, 2009).

9.4.4.4 Lake

The palaeolakes identified at outcrop (Section 5.2.8) are ≤50 m wide, 2 m high and have lenticular geometry, where the base of the pond is a fourth order surface. Internally there are first- and second-order bounding surfaces. At outcrop the ponds are within the floodplain environment and are isolated, whereas within the subsurface the ponds appear significantly bigger in scale and form lacustrine systems. The lacustrine facies associations are at least 9 m thick and represented in wells Aishwariya 2Z, 20 and Saraswati 4. These systems do differ from those noted at outcrop in facies as the facies within the subsurface lake are Sr, Ss, Scl, Sp, She, Ip and Ihe, whereas at outcrop the facies are Sm, Sr, Scl, Sh, Im and Ip. This indicates some differences in the despositional processes within the lake and pond systems.

Predicting the lacustrine extent in the subsurface can be difficult due to the discrepancies between the outcrop and the subsurface. The thickness of these lacustrine systems suggests that the lakes were extensive within the subsurface and should be mappable surfaces within the seismic dataset.

9.4.5 Well analysis

All wells analysed display similar sedimentary packages of fluvial and lacustrine environments. Described below are the wells within each field (Figure 9.1) to determine the nature of the sedimentary packages.

The cored Aishwariya wells display multiple fining upwards successions that start with medium- to very coarse-grained cross-bedded sandstones. Along the base of the cross-bedded sets and cosets there are granule-grade pebbles indicating gravel bars and channel lag. Here, there are under-developed intermittent palaeosols. These deposits occur in the deeper part of the Aishwariya Field boreholes (Figure 9.34). In the shallower parts of the wells within the Aishwariya Field the sediments become finer-grained channels bars, where the cross-bedded sets (90 m) are generally consistent. Above these deposits are finer-grained sediments with a haematitic nature containing rhizoliths, fractures and nodules (Sp, She, Ip and Ihe) indicating well-developed palaeosols in the shallower parts of the wells. These wells dominantly contain the low-sinuosity fluvial facies assemblage. Above the channel assemblage there are fine-grained, strongly bioturbated sands and palaeosols representing the lake assemblage. Aishwariya-5 and Aishwariya-17 wells do not contain any lacustrine facies suggesting that the lacustrine system did not extend into the north of the Aishwariya Field (Figures 9.1, 9.34). This could be due to the faulting within the field.

Within the Saraswati cored wells there are green and grey, clay- to very fine-grained sands with bioturbation, ripple-lamination and soft-sedimentation. There are also siderite

filled fractures, nodules filled with siderite. These deposits represent lacustrine systems. Above this lake assemblage there are gravel bars (M, G) and channel bars (Stx, Sx) that are up to 8 m high, with floodplain deposits that are haematitic with fractures and reduction patches representing the bedload dominant, low sinuosity fluvial facies assemblage.

When comparing the Saraswati wells to the Aishwariya wells and outcrop sediments it is noticeable that they are somewhat different in terms of petrography and facies associations. The measureable feldspar within the Aishwariya Field is likely to be because of the extensive lacustrine deposits where the depositional regime is dominantly through settling out of suspension.

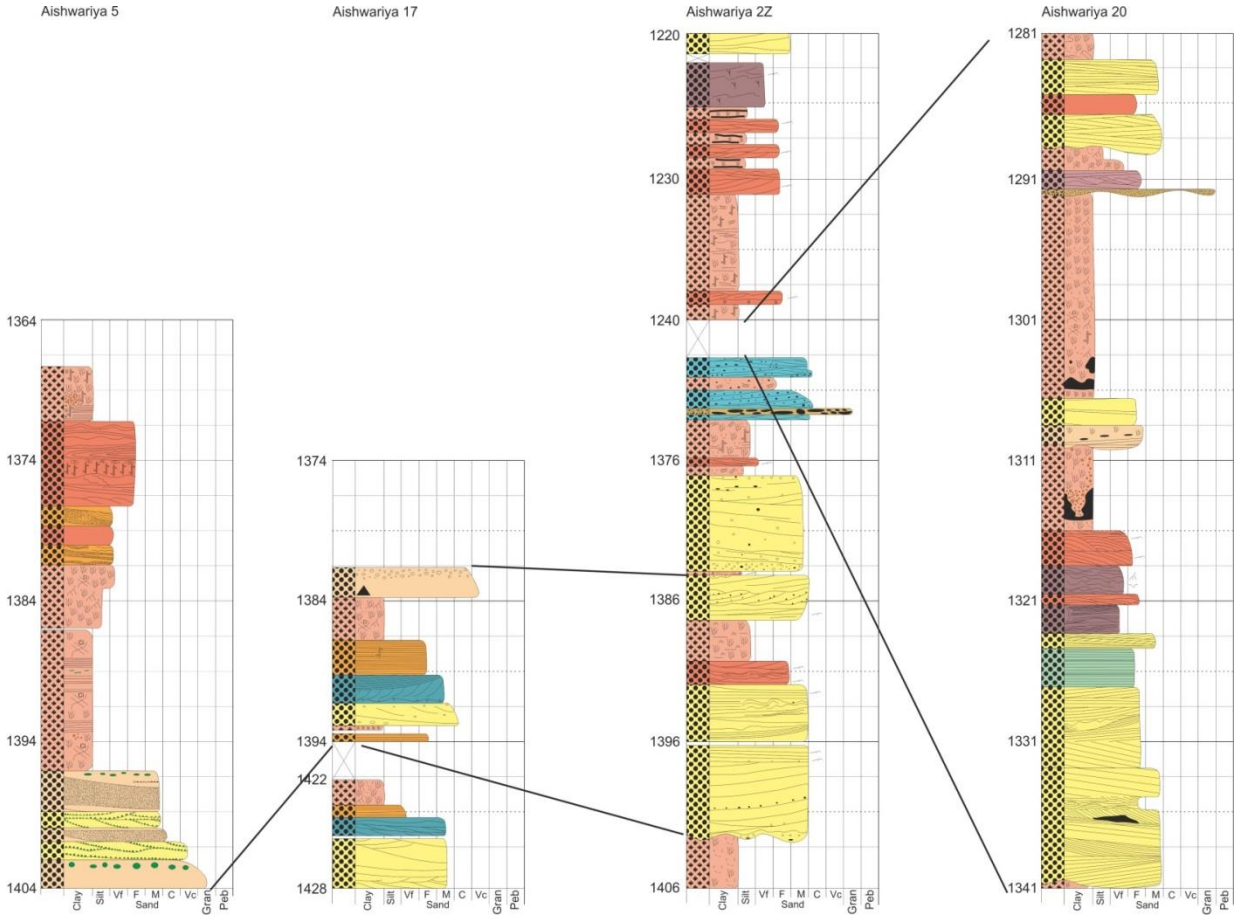

Figure 9.34: Aishwariya well correlations where there are fluvial cycles are noted in Aishwariya Wells 17, 2Z and 20. The lake assemblage is seen in wells in 2Z and 20 to the south of the Aishwariya Field

9.5 Discussion

Comparisons between the outcrop at the basin margin and core data located closer to the basin centre suggest that the Ghaggar-Hakra Formation represents deposition in a dominantly fluvial environment draining from the basin margin into a lacustrine system in the basin centre (Figure 9.35). The lowermost facies assemblage represents the Pushka Member (Dolson *et al.,* 2015) of the Ghaggar-Hakra Formation and comprises three distinct associations that can be correlated with outcrop data. The early stage Cretaceous structural development of the basin margin is likely to have had a strong influence on the fluvial regime especially in later Ghaggar-Hakra times. By drawing comparisons with the channel fill and gravel bar sedimentology with third and fourth order bounding surfaces it is highly likely that the Pushka Member is a low sinuosity, fluvial system comparable to the Nosar Sandstone. The petrographical analysis displays high quartz grains, a lack of feldspar, clays and haematite cements are also common from the outcrop and into the subsurface data. Above this are the lacustrine deposits (Kamyaka Member), overlain by a second low sinuosity, fluvial system, both of which cannot be related to the outcrop deposits. The interbedded nature of fluvial and lacustrine deposits suggests migration of the lacustrine shoreline through time. The change from fluvial to lacustrine depositional environments could be due to the same tectonic activity as seen in the proximal setting (Figure 9.35). The change in environments from lacustrine to fluvial could again be related to the growing fault network and therefore influencing the locations of the lacustrine shoreline and fluvial channels (Figure 9.35), this is the likely reason for the lacustrine system in the Aishwariya Field being contained to the south of the field and not extending northwards. A climatic control on the position of the lacustrine shoreline cannot be ruled out, however it is more likely that the change in the environmental deposition is due to the growing fault network and regional tensions displayed within the West Indian Rift System.

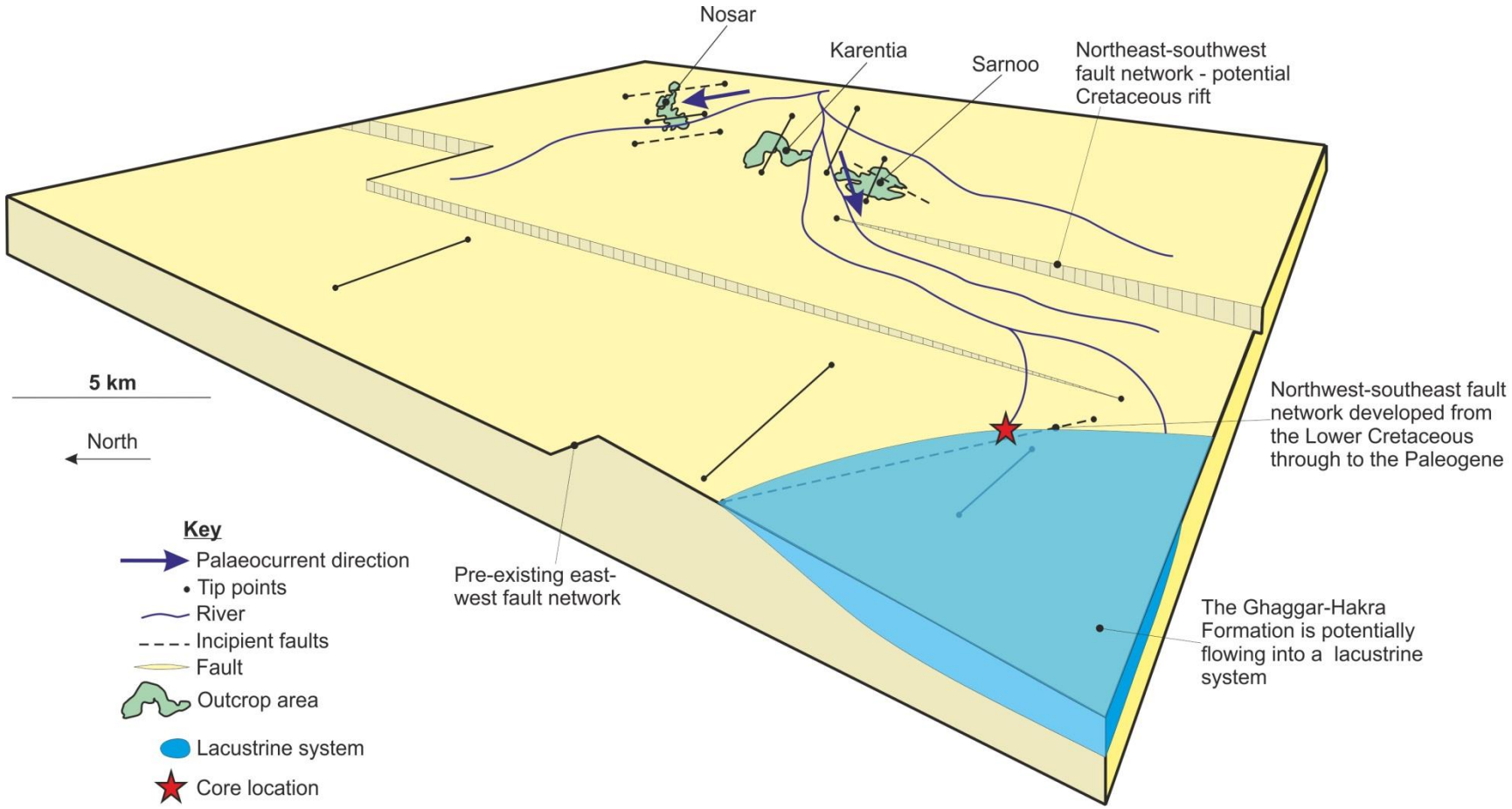

Figure 9:35: Linking the proximal outcrop deposits to the distal core deposits. It is likely that the fluvial system of the Ghaggar-Hakra system at outcrop also deposited material within the Saraswati Field.

As the Kamyaka Member is not extensive throughout the whole of the Barmer Basin like the Pushka Member is, the first assemblage sits underneath the third assemblage in places and both these assemblages are associated with the Pushka Member. The main difference between these two fluvial systems is the volume of quartz clasts deposited within the facies assemblages. There is a reduction in the number and in size of the quartz clasts in the third facies assemblage when compared to the first facies assemblage. Although both of the assemblages represent low sinuosity fluvial systems it is likely that the lower section of the Pushka Member (first facies assemblage Section 9.4.1) is bedload dominant and not as developed as the low sinuosity fluvial system of the third facies assemblage in the Pushka Member (third facies assemblage Section 9.4.3).

Sediments of the Aishwariya and Saraswati fields and the outcrop sediments have all been dated to the Lower Cretaceous (Papanikolaou, 2016 pers. comms.). From the outcrop deposits it is possible to say that the Ghaggar-Hakra was influenced by an evolving extensional regime and likely influenced by the localised climate (Section 8.2). The location of the Saraswati Field is between the soft-linked mid-rift and west-rift systems (Figure 8.4) and therefore likely influenced by the evolving extensional regime (Bladon *et al.,* 2015a, b). As stated, the sediments observed at outcrop and in cores are very similar (Sections 9.1.4, 9.3.3) indicating that the sediments within the Saraswati Field (Figure 9.36) and outcrop are related. The Aishwariya Field is located to the north of the outcrop location and based on the outcrop palaeocurrent data (dominantly to the southwest) it is likely that the sediments in both these fields were supplied through the same wide channel belt, with multiple channels that coalesced upstream (Figure 9.36).

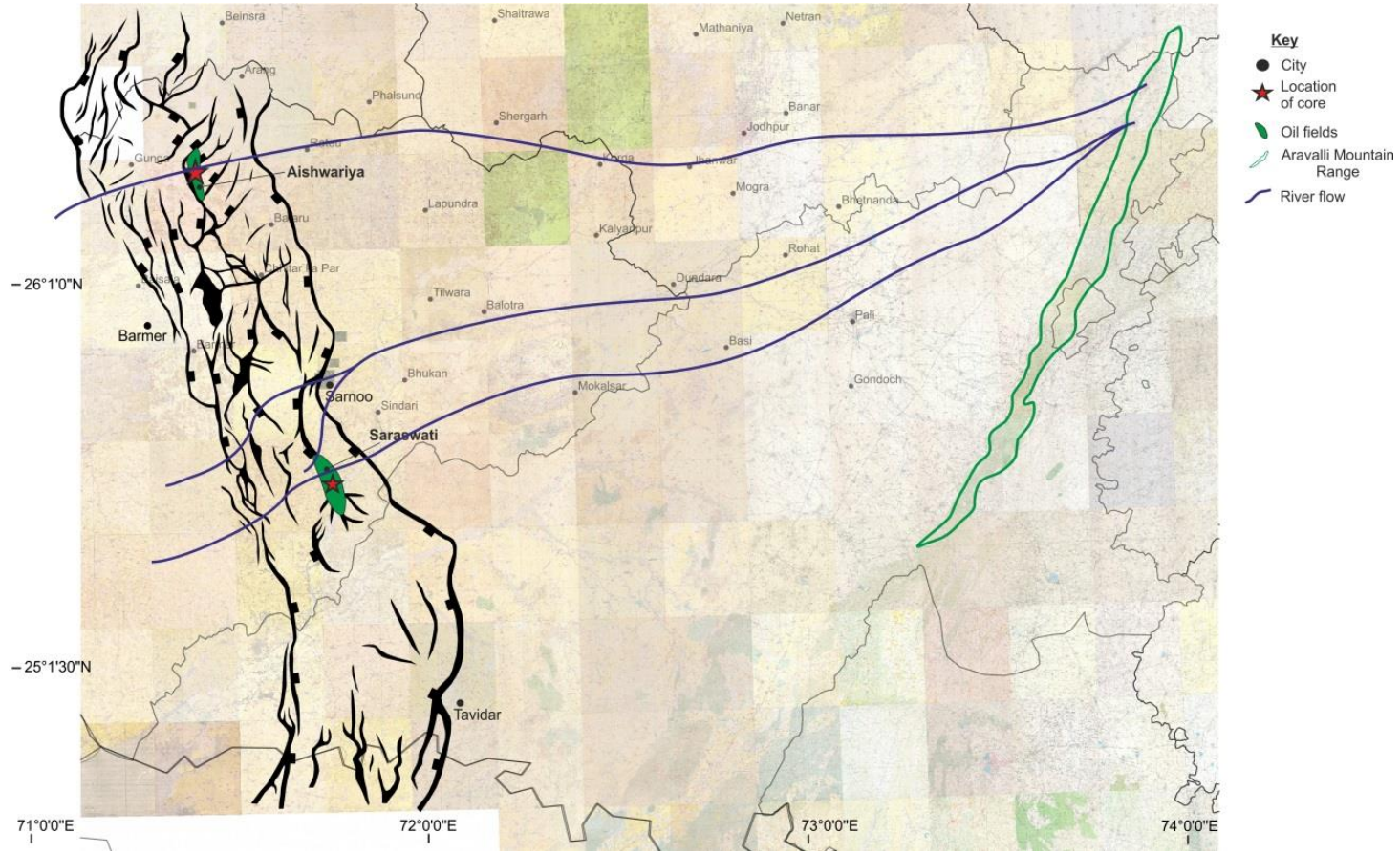

Figure 9:36: Postulated palaeodrainage pattern in the wider study area during the Early Cretaceous times, linking a probable source in the Aravalli Mountain Range with the ultimate deposition sites in the Barmer Basin; it is likely that the outcrop deposits and the Saraswati field link together and the fluvial system split upstream to get the same deposits of the fluvial system from the mountain range deposited so far apart in the basin.

As the core sediments relate closely with those seen the outcrops the three-dimensional architectural elements and facies models can act as analogues to the subsurface. This means, the models can be used to make predictions for reservoir quality, the net to gross ratio and where impermeable barriers might be. The evolutionary model of the formation may also be used to try and interpret the tectonic and climatic affects acting upon the fluvial and lacustrine systems. The models presented in Chapter 5 are more reliable for the Saraswati Field as this field is downstream of the outcrop locations (Figure 9.36).

9.6 Summary

Fourteen different facies within the subsurface core data have been subdivided upon the basis of flow types. There are deposits from Newtonian flows (G, Stx, Sx, Sb, Sla, Sr, Ss, Scl, Sm), non-Newtonian flows (M) and subaerial facies (Sp, Ip, She, Ihe). These different facies can be linked together on the basis of similar transportation and depositional processes into four facies associations: channel association, gravel bar association, floodplain association and the lake association. These facies and facies associations can be related to the outcrop data.

There is a good match in petrographical data between the core and outcrop. They have similar grainsize ranges from silt- to very coarse-grained sands and similar sorting ranges. Observed within the core data are feldspars within the lacustrine system. The compositional data plots within the quartzarenite to sublithic-quartzarenite fields matching the outcrop data.

This analysis produces three facies assemblages named: low sinuosity fluvial facies assemblage, the lake facies assemblage and the bedload-dominant, low sinuosity fluvial facies assemblage. The low sinuosity, fluvial facies assemblage can be directly related to the outcrop observations and enables predictions in the subsurface. The lake facies assemblage is confined to the Kamyaka Member and is not recognised at outcrop. The

pattern of lithostratigraphical evolution and the effects of tectonics and climate can also be discerned in subsurface data (Figure 5.22, Bladon *et al.,* 2015b). The Saraswati Field lies downstream of the outcrop deposits and was probably influenced by the formation of the atypical relay ramp. Coeval sediments from the Aishwariya Field and at outcrop are unlikely to be related downstream but more likely upstream of both locations (Figure 9.36). Finally, the palaeolake margin succession recorded should be mappable on seismic data and it is expected to follow the Cretaceous fault pattern in the Barmer Basin.

The tectonic controls that appear to have influenced lacustrine development in the basin may also have determined the dominant drainage patterns linking the outcrop areas with the basin centre to the west.

10 Chapter Ten: Conclusions

The overall aim of this research is to characterise and interpret the Lower Cretaceous-aged Ghaggar-Hakra Formation in terms of facies, architectural elements, petrography and palaeocurrents. Combined, these analyses have produced three-dimensional models that provide the interpretation for this part of the Barmer Basin succession. The facies, bounding surfaces and three-dimensional models have then been compared to the core data determining the nature to the formation within the basin centre.

Below, each dataset is summarised along with a description of how these are integrated together to form the interpretation of the Ghaggar-Hakra sediments and their application to the subsurface.

10.1 Summary of the sedimentology

The facies, bounding surface analysis and architectural elements of the Ghaggar-Hakra Formation together provide evidence about the nature of the fluvial system. As described in Chapter 4 the facies form facies associations which are related together by the depositional process. The combination of these associations form eight architectural elements which are linked with distinctive types of fluvial systems (Chapter 5). The lowermost fluvial system contains gravel bars, in-channel bars and the floodplain elements (Section 5.2) which in aggregate represent the bedload dominant, low sinuosity fluvial system of the Darjaniyon-ki Dhani Sandstone. Above this is a 25 m thick floodplain containing the floodplain and pond elements. The second fluvial package contains gravel bars, in-channel bars, point bars, channel margins, sheetfloods, chute channels and floodplain elements (Section 5.2), forming a mixed bedload, high sinuosity fluvial system relating to the Sarnoo Sandstone (Figure 5.22). Above this channelised sandstone is the second thick (20 m) floodplain package containing the floodplain elements with sparse ponds. Capping the formation at outcrop, the Nosar sandstone is composed of gravel

bars, in-channel bars, sheetfloods and the floodplain elements (Figure 5.2). This sandstone forms a well-developed, bedload dominant, low sinuosity fluvial system.

The fluvial system represented within the Darjaniyon-ki Dhani Sandstone and the Sarnoo Sandstone matures upwards as attested by an upwards increase in the channelised sediments and the floodplains (Figure 5.22). The Nosar Sandstone is a low sinuosity fluvial system which indicates rejuvenation of the fluvial system over time (Figure 5.22).

10.2 Summary of the petrography

The sediments of the Ghaggar-Hakra Formation do vary in their petrography, but only slightly. The Darjaniyon-ki Dhani Sandstone contains quartz grains, lithic fragments of sedimentary, metamorphic and igneous origin, haematite and calcite cements, kaolinite booklets and non-resolvable clays. The detrital grains here are sub-rounded with poor to moderate sorting. The porosity within this succession is at 5.5%. This data signifies a mature succession. The Sarnoo Sandstone comprises dominantly detrital quartz grains, with few lithic fragments and haematite cements, kaolinite booklets and non-resolvable clays. The detrital grains are rounded and have moderate to well sorting, displaying a texturally mature sandstone package. Porosity here is at 8%. These factors indicate a supermature sandstone succession. Lastly, the Nosar Sandstone contains detrital quartz, rigid rock fragments of sedimentary, igneous and metamorphic origin, haematite cement, kaolinite booklets and non-resolvable clays. The detrital grains are sub-rounded to rounded and the sorting is poor to well. The porosity is at 4.5%. This succession is texturally and compositionally mature.

To summarise, the petrography of the Ghaggar-Hakra Formation is similar within each sandstone body. This is because (1) all the sandstones are within the sublithic-quartzarenite to quartzarenite zones, so are compositionally mature, and; (2) all the packages are texturally mature as well. Of the three sandstone packages the Sarnoo

Sandstone is the most compositionally and texturally mature and has the highest porosity; whereas the Nosar Sandstone is the least compositionally and texturally mature, with the lowest porosity.

From the petrography data that is presented within Chapter 6, it can be suggested that the source for this sediment is the Aravalli Supergroup of the Aravalli Mountain Range which has detrital grains that are very similar to the Ghaggar-Hakra Formation.

10.3 Summary of palaeocurrents

The palaeocurrent data for the formation was collected throughout all the succession, but only certain sedimentary structures have been used as indicated in Chapter 7. The palaeocurrent data has been analysed by a moving average analysis. The Darjaniyon-ki Dhani Sandstone has had a limited amount of data collected as the outcrop availability is sparse. The palaeoflow is south. Sarnoo Sandstone only outcrops in the Sarnoo field area and has a palaeoflow to the west. However, the Sarnoo Sandstone dataset has a high dispersion, typical of a high sinuosity fluvial system. The Nosar Sandstone outcrops extensively and has a dominant palaeoflow to the southwest. The dominant palaeoflow direction changes between the major sandstone successions. Thus the change from southerly flow within the Darjaniyon-ki Dhani Sandstone to westerly transport in the Sarnoo Sandstone is attributed here to the palaeotopography. The change in direction of the palaeoflow from the Sarnoo Sandstone to the Nosar Sandstone is attributed to a changing tectonic regime.

The palaeoflow data observed within the Ghaggar-Hakra Formation suggests that the overall flow was south-westerly, likely flowing towards the west coast of India. The data presented here fits well with the data from Racey *et al.,* (In review) where the Lower Cretaceous fluvial systems of the West Indian Rift System all flow ultimately into the

palaeo-Arabian Sea. It is suggested that all these fluvial systems link and drain north-western India.

10.4 Summary of outcrop evidence

The evolution the Ghaggar-Hakra Formation starts with the deposition of the Darjaniyon-ki Dhani Sandstone succession which contains quartzarenites generalised in gravel and sand bars within a bedload dominant, low sinuous fluvial system. This system was poorly developed and largely confined by the palaeotopography of the Sarnoo field area. This system evolved and mature into the mixed load high sinuosity system of the Sarnoo Sandstone which is composed of fining upwards successions of quartzarenites formed in channel bars and point bars. The floodplain associated with this river system also matures as there is less flooding as evidenced by the lack of ponds within the upper floodplain. The pedogenesis within the upper floodplain is also extensive. This maturation signifies stable tectonic conditions. The overly up Nosar Sandstone is very erosive and composed of quartzarenites-sublithic arenites within gravel bars, channels, sheetfloods and limited floodplain material. The Nosar Sandstone marks rejuvenation of the fluvial system through tectonic instability. This suggests that the Ghaggar-Hakra Formation is syn-rift and not pre-rift as initially thought.

10.5 Application to the subsurface

Based on the outcrop information gathered from the Ghaggar-Hakra Formation, this work takes these interpretations of the outcrop and uses them to interpret the subsurface, based on facies and bounding surface analysis of the core data. In the subsurface the Ghaggar-Hakra Formation contains a low sinuosity fluvial facies assemblage, lake facies assemblage and a bedload dominant, low sinuosity fluvial facies assemblage, where the fluvial facies assemblages can overlie one another and are confined to the Pushka Member. The lake facies assemblage is known as the Kamyaka Member and is limited in

its extent (Figures 9.34 and 9.35). The lacustrine system extent is likely controlled by the development of the atypical relay ramp from the extensional tectonics that interrupted the deposition of the fluvial system at outcrop; however the migration of the lacustrine shoreline maybe due to the climate and this cannot be ruled out.

10.6 Future work

There are three distinct areas in which the understanding of the Ghaggar-Hakra Formation could be further developed. The first future study to be undertaken would be to further identify the palaeosols for the Ghaggar-Hakra Formation to determine the climatic variation in detail at the time of deposition. Secondly, zircon analysis could be completed on the formation to determine the provenance once and for all. Thirdly, Figure 9.36 could be developed into three-dimensions from its current two-dimensional form, which would give a better understanding of the Ghaggar-Hakra Formation within the subsurface of the Barmer Basin and West Indian Rift System. Finally, further study of the Lower Cretaceous fluvial systems within north-western India, could be undertaken with the aim of seeing if these systems all interact and drain the Aravalli Mountain Range.

10.6.1 Palaeosol classification

The palaeosol development has been mentioned and placed into the context of the evolving fluvial system within this research. However, this work would benefit from an in-depth palaeosol reconstruction as this would develop the understanding of the climatic regime within the area. This reconstruction would develop the palaeotopography of the formation and determine how close the fluvial channels were from the palaeosol and exactly how well drained the soils were at the time of deposition. This information would provide extra detail into the climate of the Lower Cretaceous Epoch within the Rajasthan area. This would be completed by using calcrete nodules seen within the core data to determine the water table and relate the soils to the palaeoatmosphere, helping to narrow

down the climatic regime and possibly the depositional environment. Geochemical analysis such as chemostratigraphy and potentially spectral gamma-ray analysis of the palaeosols would offer a more detailed interpretation. These analyses would not only give further detail into the climatic regime and the climatic variations but would also further develop the gamma ray analysis technique at outcrop.

10.6.2 Provenance identification

Heavy minerals can help to constrain the sediment source areas, despite only forming approximately one percent of a sedimentary rock. As such, a potential future research avenue which will help constrain the source locations is to date the zircon ultrastable heavy minerals. A single zircon grain retains the source signature regardless of weathering, sediment transport and deep burial. It is relatively easy to separate the zircon component from sediment through crushing, sieving, and heavy liquid separation. If there are 117, or more, zircon grains per sample, then analysis can continue (Vermeesch, 2004). The separated zircon sample is dated using high precision techniques (Gehrels, 2014), which determine uranium-lead ratios of two decay pathways; the uranium series ^{238}U to ^{206}Pb and or the actinium series ^{235}U to ^{207}Pb). Cathodoluminescence imaging will highlight the best point on the zircon to date as the mineral can represent multiple cycles. There are various mass spectrometers (e.g. TIMS, MC-ICP-MS, etc.) available for U-Pb analysis which has 3% or more precision to be considered to be acceptable for provenance studies.

By dating the zircons within the Ghaggar-Hakra Formation a clear distinction for the provenance of the fluvial system could be made meaning there would no longer be two potential sources: the Neoproterozoic Jodhpur Sandstone or the Paleoproterozoic Aravalli Mountain Range (Goodwin, 1991; Kumar *et al.,* 2011), or it could show a mixing between the two. Given the amount of outcrop available of the Ghaggar-Hakra Formation it is highly likely that only the Nosar Sandstone could be analysed in this way, as this is the

only sandstone where you would be able to collect enough zircons to make the data scientifically viable. This analysis does depend on the availability of zircons in the source rocks at the time of erosion for the fluvial system (Dickinson, 2008) and in the resultant sediment. However, based on the petrography data present in Chapter 6 there should be enough zircons within the Nosar Sandstone for a representative study.

10.6.3 Integration of all subsurface data

Chapter 9 presents the core data and how this data relates to the outcrop data, the discussion at the end of the chapter attempts to bring together the outcrop data and the core data from both the Saraswati and Aishwariya fields. This is done by logs and maps (Figures 9.34, 9.35, 9.36). Understanding of the Mesozoic succession would be significantly enhanced if this two-dimensional map was produced as a model in three-dimensions, using the seismic, well-log and all cored data. This hypothetical three-dimensional model would help predict the flow pathways of the fluvial system. This would then assist in predicting where the hydrocarbon reservoirs would be more likely to occur. A model like this would significantly develop the Mesozoic sections within the subsurface and their further oil potential. Understanding of the Mesozoic sediments in the subsurface would also be significantly improved by more detailed chronostratigrahical investigations of the palaeosols and lake sediments, leading to a detailed analysis of the climatic regime. Chronostratigraphy on the lacustrine sediments may also help to determine if the lake margin was climatically or tectonically controlled.

10.6.4 Linking the Lower Cretaceous fluvial systems together

The Lower Cretaceous Epoch also saw fluvial systems occurring within the other basins in the West Indian Rift System, which were all draining the Aravalli Mountain Range (Biswas, 1987; Racey *et al.,* In review). These fluvial systems have an average palaeoflow to the southwest (Racey *et al.,* In Review), which is very similar to the fluvial systems found in

the Ghaggar-Hakra Formation. These fluvial systems have similar palaeoflow directions and a regional study would be valuable to assess the reservoir potential of each fluvial system. The fluvial systems may also link together upstream from the West Indian Rift System. To investigate this hypothesis, pollen analyse and detailed SEM analyse on the floodplain sediments would be needed to see if the sediments are sourced from the same areas of the Aravalli Mountain Range, this could be completed using zircon analysis (Section 10.6.2). This would indicate whether or not the rivers joined upstream. Also while the fluvial systems of the West Indian Rift System have had some academic attention (Biswas, 1987), it would be of value to know whether the Lower Cretaceous rifting event that caused the rejuvenation of the Ghaggar-Hakra Formation can be identifed throughout each of the contemporaneous fluvial systems, within other basins. This would need very detailed outcrop studies and seismic investigation and would lead to a more confident interpretation of the extensional event affecting the Ghaggar-Hakra Formation being part of a regional event (Indian – Madagascar separation) rather than a local rifting event within the Barmer Basin.

10.7 Cretaceous sedimentation of the Barmer Basin, India

In summary, the Ghaggar-Hakra was deposited within a maturing upwards fluvial system which was rejuvenated as a result of regional tectonic instability. Core data from the equivalent distal setting demonstrates lacustrine and fluvial environments are controlled and constrained by a migrating lacustrine shoreline. Sedimentological correlations can be made between the subsurface and the outcrop successions on the basis of facies and bounding surface analysis, which allow the subsurface succession to be better characterized. These analyses suggest that the migrating shoreline may be controlled by the same tectonic instabilities interpreted from proximal outcrop deposits. Ultimately, this work provides an improved understanding of the effects of regional tectonics upon the depositional systems of the Ghaggar-Hakra Formation preserved at surface and within the

subsurface successions. These successions within the Barmer Basin were deposited during the Lower Cretaceous Epoch and can be related to the West Indian Rift System.

References

Aase N.E., Bjorkum P.A. and Nadeau P.H. (1996) The effect of grain-coating microquartz on preservation of reservoir porosity, *AAPG* Bulletin, 80, issue 10, pp. 1654 – 1673

Acharyya S.K. and Latiri T.C. (1991) Cretaceous palaeogeography of the Indian subcontinent; a review, *Cretaceous Research,* **12,** pp. 3 – 26

Adams A.E., MacKenzie W.S., Guilford C. (1984) Atlas of sedimentary rocks under the microscope, Essex, *Pearson Education Limited*

Akhtar K. and Ahmad A.H.M. (1991) Single-cycle cratonic quartzarenites produced by tropic weathering: the Nimar sandstones (Lower Cretaceous), Narmada Basin, India, *Sedimentary Geology,* **71,** pp. 23 – 32

Ali J.R. and Aitchison J.C. (2014) Greater India's northern margin prior to its collision with Asia, *Basin Research,* **26,** pp. 73 – 84

Allen J.R.L (1983) Studies in fluviatile sedimentation: bars, bar-complexes and sandstone sheets (low-sinuosity braided streams) in the brownstones (L. Devonian), Welsh Borders, *Sedimentary Geology,* **33,** pp. 237 – 293

Allen J.R.L. (1964) Studies in fluviatile sedimentation: implications of pedogenic carbonate units, Lower Old Red Sandstone, Anglo-Welsh outcrop, Geological *Journal*, **9**, pp. 181 - 208

Allen J.R.L. (1965) A Review of the Origin and Characteristics of Recent Alluvial Sediments, *Sedimentology,* **5,** pp. 89 – 191

Allen J.R.L. (1966) On bed forms and palaeocurrents, *Sedimentology*, **6**, pp. 153 – 190

Allen J.R.L. (1968) Current ripples, their relation to patterns of water and sediment motion, Amsterdam, *North Holland Publishing Company*

Allen P.A. and Allen J.R. (2005) Basin Analysis Principles and Applications, (4th Ed.), Oxford, *Blackwell Publishing*

Anderton R. (1985) Clastic facies models and facies analysis, *Geological Society of London, Special Publications,* **18,** pp. 31 – 47

Arguden A.T. and Rodolfo K.S. (1986) Sedimentary facies and tectonic implications of lower Mesozoic alluvial-fan conglomerates of the Newark Basin north-eastern Untied States, *Sedimentary Geology*, **51**, pp. 97 – 118

Baiamonte G. and Ferro V. (1997) The influence of roughness geometry and Shields parameter on flow resistance in gravel-bed channels, *Earth Surface Processes Landforms*, **22**, 759 – 772

Baksi S.K. and Naskar P. (1981) Fossil Plants From Sarnu Hill Formation, Barmer Basin, Rajasthan, *The Palaeobotamist,* **27,** pp. 107 – 111

Balakrishnan T.S., Unnikrishnan P., Murty A.V.S. (2009) The tectonic map of India and contiguous areas, *Journal of the Geological Society of India,* **74,** pp. 158 – 170

Banerjee D.M. and Bhattacharya P. (1994) Petrology and geochemistry of greywackes from the Aravalli Supergroup, Rajasthan, India and the tectonic evolution of a Proterozoic sedimentary basin, *Precambrian research,* **67,** pp. 11 – 35

Banham S.G. and Mountney N.P. (2014) Climatic versus halokinetic control on sedimentation in a dryland fluvial succession: Triassic Moenkopi Formation, Utah, USA, *Sedimentology,* **61,** issue 2, pp. 570 – 608

Batzill M., Morales E.H. and Diebold U. (2006) Influence of nitrogen doping on the defect formation and surface properties of TiO_2 rutile and anatase, *Physical review letters,* **96**, pp. 81 - 85

Beaufort D., Cassagnabere A., Petit S., Lanson B., Berger G., Lacharpagne J.C. and Johansen H. (1998) Kaolinite-to-dickite reaction in sandstone reservoirs, *Clay Minerals,* **33**, pp. 297 – 316

Belda M., Holtanova E., Halenka T. and Kalvova J. (2014) Climate classification revisited: from Koppen to Trewartha, *Climate Research,* **59,** pp. 1 – 13

Besra L., Sengupta D.K. and Roy S.K. (2000) Particle characteristics and their influence on dewatering of kaolin, calcite and quartz suspension, *International Journal Mineral Process,* **59,** pp. 89 – 112

Best J.L., Ashworth P.J., Bristow C.S. and Roden J. (2003) Three-dimensional sedimentary architectural of a large, mid-channel sand braid bar, Jamuna River, Bangladesh, *Journal of Sedimentary Research,* **73**, issue 4, pp. 516 – 530

Biswas S.K. (1982) Rift basins in western margin of India and their hydrocarbon prospects with special reference to Kutch Basin, *AAGP Bulletin,* **66,** pp. 1497 – 1513

Biswas S.K. (1987) Regional tectonic framework, structure and evolution of the western marginal basins of India, *Tectonophysics,* **135,** pp. 307 – 327

Biswas S.K. (1999) A review on the evolution of rift basins in India during Gondwana with special reference to western Indian basins and their hydrocarbon prospects, *Proceedings of the National Indian Science Academy,* **65,** pp. 261-283

Biswas S.K. (2005) A review of structure and tectonics of Kutch basin, western India, with reference to earthquakes, *Current Science,* **88,** pp. 1592 – 1600

Bjorkum P.A. and Gjelsvik N. (1988) An isochemical model for formation of authigenic kaolinite, K-feldspar and illite in sediments, *Journal of Sedimentary Petrology,* **58**, issue 3, pp. 506 – 511

Bladon A.J. (2014) The early-stage structural evolution of the Barmer Basin rift, Rajasthan, northwest India, *PH.D. Thesis*, Keele University, pp. 61 – 100, 207, 217, 231

Bladon A.J., Burley S., Clarke S.M. (2015b) Complex rift geometries resulting from inheritance of pre-existing structures: Insights and regional implications from the Barmer Basin rift, *Journal of Structural Geology,* **71,** pp. 136 – 154

Bladon A.J., Clarke S.M., Burley S., Beaumont H. (2015a) Geology and regional significance of the Sarnoo Hills, eastern rift margin of the Barmer Basin, NW India, *Basin Research,* **27**, issue 5, pp. 636 – 655

Blair T.C. and McPherson J.G. (1994) Alluvial fans and their natural distinctions from rivers based on morphology, hydraulic processes, sediment processes and facies assemblages, *Journal of Sedimentary Research,* **A64**, issue 3, pp. 450 – 489

Blatt H. (1982) Sedimentary petrology, Arizona, *W.H. Freeman and Company*

Blatt H. and Christie J.M., (1963) Undulatory extinction in quartz of igneous and metamorphic rocks and its significance in provenance studies of sedimentary rocks, *Journal of Sedimentary Petrology,* **33,** issue 3, pp. 559 – 579

Bordy E.M., Hancox P.J. and Rubidge B.S. (2004) Fluvial style variations in the Late Triassic-Early Jurassic Elliot Formations, main Karoo Basin, South Africa, *Journal of African Earth Sciences,* **38,** pp. 383 – 400

Bose P.K., Shome S., Bardhan S and Ghosh G. (1986) Facies mosaic in the Ghuneri Member (Jurassic) of the Bhuj Formation, western Kutch, India, *Sedimentary Geology*, **46**, pp. 293 – 309

Bove D.J., Eberl D.D., McCarty D.K. and Meeker G.P. (2002) Characterisation and modelling of illite crystal particles and growth mechanisms in a zoned hydrothermal deposit, Lake City, Colorado, *American Mineralogist,* **87**, pp. 1546 – 1556

Bower S. (2004a) Technical Memorandum: Stratigraphic Framework for the Barmer Basin, Rajasthan, Commissioned on behalf of Cairn India PTY, *Unpublished*

Bower S. (2004b) Integrated field geology report, Rajasthan, India, Barmer Basin, Commissioned on behalf of Cairn India PTY, *Unpublished*

Bridge J.S. (1993) The interaction between channel geometry, water flow, sediment transport and deposition in braided rivers, *Geological Society, London Special Publication,* **75,** pp. 13 – 71

Bridge J.S. and Leeder M.R. (1979) A simulation of model alluvial stratigraphy, *Sedimentology,* **26**, pp. 617 – 644

Bristow C.S., Skelly R.L. and Ethridge F.G. (1999) Crevasse splays from the rapidly aggrading, sand-bed, braided Nibrara River, Nebraska: effect of base-level rise, *Sedimentology*, **46**, pp. 1029 – 1047

Brookfield M.E. (1977) The origin of bounding surfaces in ancient aeolian sandstones, *Sedimentology,* **24,** pp. 303 – 332

Burley S.D. (1984) Patterns of diagenesis in the Sherwood Sandstone Group (Triassic) United Kingdom, *Clay Minerals,* **19**, pp. 403 – 440

Burley S.D., Kantorowicz J.D. and Waugh B. (1985) Clastic diagenesis, *Geological Society of London, Special Publication,* **18,** pp. 189 – 226

Burr D.M., Emery J.P., Lorenz R.D., Geoffrey C.C. and Carling P.A. (2006) Sediment transport by liquid flow: Application to Titan, *Icarus,* **181,** pp. 235 – 242

Cain S.A. and **Mountney N.P.** (2009) Spatial and temporal evolution of a terminal fluvial fan system: the Permian Organ Rock Formation southeast Utah, USA, *Sedimentology*, **56**, pp.1774 – 1800

Cairn (2016) Our business, Rajasthan, [Online], Available at: https://www.cairnindia.com/our-business/rajasthan Date Accessed 23/11/2015

Cant D.J. (1977) Development of a facies model for sandy braided river sedimentation: comparison of the south Saskatchewan River and the Battery Point Sandstone, *Canadian Society or Petroleum Geologists,* Memoir **5,** pp. 627 – 639

Carrigy M.A. and Mellon G.B. (1964) Authigenic clay mineral cements in Cretaceous and Tertiary sandstones of Alberta, *Journal of Sedimentary Research*, **34**, issue 3, pp. 461 – 472

Chan M.A., Parry W.T. and Bowman J.R. (2000) Diagenetic haematite and manganese oxides and fault-related fluid flow in Jurassic Sandstones south-eastern Utah, *AAPG Bulletin*, **84**, issue 9, pp. 1281 – 1310

Chaplin M. (2015) Hydrogen bonding in water, [Online], Available at: http://www1.lsbu.ac.uk/water/water_hydrogen_bonding.html Date Accessed: 4/3/2016

Chapman R.E. (1995) Physics for geologists, London, *UCL Press Limited*

Chuhan F.A., Kjeldstad A., Bjorlykke K. and Hoeg K. (2002) Porosity loss in sand by grain crushing – experimental evidence and relevance to reservoir quality, *Marine and Petroleum Geology*, **19**, issue 1, pp. 39 – 53

Clarke P. and Parnell J. (1999) Facies analysis of a back-tilted lacustrine basin in a strike-slip zone, Lower Devonian, Scotland, *Palaeogeography, Palaeoclimate, Palaeoecology,* **151,** pp. 167 – 190

Clarke S.M. (2011) Outcrop studies in the Barmer Basin, Rajasthan, India, Commissioned on behalf of Cairn India PTY, *Unpublished*

Collier J.S., Sansom V., Ishizuka O., Taylor R.N., Minshull T.A. and Whitmarsh R.B. (2008) Age of Seychelles-India break-up, *Earth and Planetary Sciences Letters,* **272,** pp. 264 – 277

Collinson J., Mountney N., Thompson D. (2006) Sedimentary structures, 3rd Ed., Hertfordshire, *Terra Publishing*

Colombera L., Felletti F., Mountney N.P. and McCaffery W.D. (2012) A database for constraining stochastic simulations of the sedimentary heterogeneity of fluvial reservoirs, *AAPG Bulletin*, **96**, issue 11, pp. 2143 – 2166

Coloumbo F. (1994) Normal and reverse unroofing sequences in syntectonic conglomerates as evidence of progressive basinward deformation, *Geology,* **22,** pp. 235 – 238

Compton P.M. (2009) The geology of the Barmer Basin, Rajasthan, India and the origins of its major oil reservoir, the Fatehgarh Formation, *Petroleum Geoscience*,**15,** pp. 117 – 130

Cox K.G. (1989) The role of mantle plumes in the development of continental drainage patterns, *NATURE,* **342,** pp. 873 – 877

Crawford A.R. and Compton W. (1969) The age of the Vindhyan System of Peninsular India, *Quarterly Journal of the Geological Society,* **125,** pp. 351 – 371

Dawson S. and Smith D.E. (2000) The sedimentology of Middle Holocene tsunami facies in northern Sutherland, Scotland, UK, *Marine Geology,* **170,** pp. 69 – 79

Desai A.G. and Desai S.J. (1989) Himatnagar Sandstones of north Gujarat their depositional environment and tectonic framework, *Ph.D. Thesis*, Maharaja Sayajirao University of Baroda

Dickinson W.R. (2008) Impact of different zircon fertility of grantoid basement rocks in North America on age populations of detrital zircons and implications for granite petrogenesis, *Earth Planetary Science Letters*, **275**, pp. 80 – 92

Dickinson W.R. and Suczek C.A. (1979) Plate tectonics and sandstone compositions, *AAPG Bulletin,* **63,** issue 12, pp. 2164 – 2182

Dickinson W.R., (1985) Interpreting provenance relations from detrital modes of sandstone, *NATO ASI Series,* **148,** pp. 333 – 361

Dickinson W.R., Beard L.S., Robert-Brakenridge G., Erjavec J.L., Ferguson R.C., Inman K.F., Knepp R.A., Lindberg F.A. and Ryberg P.T. (1983) Provenance of North American Phanerozoic sandstones in relation to tectonic setting, *Geological Society of American Bulletin,* **94,** pp. 222 – 235

Dolson J., Burley S.D., Sunder V.R., Kothari V., Naidu B., Whiteley N.P., Farrimond P., Taylor A., Direen N. and Anathakrishnan B. (2015) The discovery of the Barmer Basin, Rajasthan, India, and its Petroleum Geology, *AAPG Bulletin*, **99**, issue 3, pp. 433 – 465

Donselaar M.E. and Overeem I. (2008) Connectivity of fluvial point-bar deposits: An example from the Miocene Huesca fluvial fan, Ebro Basin, Spain, *AAPG Bulletin,* **92,** issue 9, pp. 1109 – 1129

Donselaar M.E., Gozalo M.C. and Moyano S. (2013) Avulsion processes at the terminus of low-gradient semi-arid fluvial systems: Lessons from the Rio Colorado, Altiplano endorheic basin, Bolivia, *Sedimentary Geology,* **283,** pp. 1 – 14

Doyle J.D. and Sweet M.L. (1995) Three-dimensional distribution of lithofacies, bounding surfaces, porosity and permeability in a fluvial sandstone – Gypsy Sandstone of northern Oklahoma, *AAPG Bulletin,* **79,** issue 1, pp. 70 – 96

Eberl D. and Hower D. (1976) Kinetics of illite formation, *Geological Society of American Bulletin*, **87**, pp. 1326 – 1330

Elert G. (2015) *The Physics Hyper-Textbook – Viscosity*, [Online], Available at: http://physics.info/viscosity/ Date Accessed: 12/02/2016

Emery D. and Myers K.J. (1996) Sequence Stratigraphy, Oxford, *Blackwell Publishing company*

Fischer C., Waldmann S., and Eynatten H.V. (2013) Spatial variation in quartz cement type and concentration: An example from the Heidelberg formation (Teufelsmauer outcrops) Upper Cretaceous Subhercynian Basin, Germany, Sedimentary Geology, 291, pp. 48 – 61

Flood Y.S. and Hampson G.J. (2014) Facies and architectural analysis to interpret avulsion style and variability: Upper Cretaceous Blackhawk Formation, Wasatch Plateau, Central Utah, USA, *Journal of Sedimentary Research,* **84,** pp. 743 – 762

Fossen H. (2010) Structural Geology, Cambridge, UK, *Cambridge University Press*

Fraser G.S. and DeCelles P.G. (1992) Geomorphic controls on sediment accumulation at margis of foreland basins, *Basin Research*, **4**, pp. 233 – 252

French M.W. and Worden R.H. (2013) Orientation of microcrystalline quartz in the Fontainebleau Formation, Paris Basin and why it preserves porosity, *Sedimentary Geology,* **284 – 285,** pp. 149 – 158

Gaina C., Muller R.D., Brown B., Ishihara T. and Ivanov S. (2007) Breakup and early seafloor spreading between India and Antarctica, *Geophysical Journal International,* **170,** issue 1, pp. 151 – 169

Garzanti E. and Vezzoli G. (2003) A classification of metamorphic grains in sands based on their composition and grade, *Journal of Sedimentary Research,* **73,** pp. 830 – 837

Garzanti E., Ando S., and Vezzoli (2008) Setting equivalence of detrital minerals and grain-size dependence of sediment composition, *Earth and Planetary Science Letters,* **273,** issue 1, pp. 138 – 151

Garzanti E., Doglioni C., Vezzoli G. and Ando S. (2007) Orogenic belts and organic sediment provenance, *The Journal of geology,* **115**, issue 3, pp. 315 – 334

Garzanti E., Limonta M., Resentini A., Bandopadhyay P.C., Najman Y., Ando S. and Vezzoli G. (2013a) Sediment recycling at convergent plate margins (Indo-Burman Ranges and Andaman-Nicobar Ridge), *Earth-Science Reviews,* **123,** pp. 113 – 132

Garzanti E., Vermeesch P., Ando S., Vezzoli G., Valagussa M., Allen K., Kadi K.A. and Al-Juboury A.I.A. (2013b) Provenance and recycling of Arabian desert sand, *Earth-Science Reviews,* **120,** pp. 1 – 19

Garzanti E., Vermeesch P., Padoan M., Resentini A., Vezzoli G. and Ando S. (2014) Provenance of Passive-Margin Sand (Southern Africa), *The Journal of Geology*, **122**, pp. 17 – 42

Gawthorpe R.L. and Hurst J.M. (1993) Transfer zones in extensional basins: their structural style and influence on drainage development and stratigraphy, *Journal of the Geological Society,* **150,** pp. 1137 – 1152

Gawthorpe R.L. and Leeder M.R. (2000) Tectono-sedimentary evolution of active extensional basins, *Basin Research,* **12,** pp. 195 – 218

Gehrels G. (2014) Detrital Zircon U-Pd Geochronology Applied to Tectonics, *Annual reviews of Earth planetary science*, **42**, pp. 127 – 149

Ghazi S. and Mountney N.P. (2009) Facies and architectural element analysis of a meandering fluvial succession: The Permian Warchha Sandstone, Salt Range, Pakistan, *Sedimentary Geology,* **221,** pp. 99 – 126

Ghinassi M. (2010) Chute channels in the Holocene high-sinuosity river deposits of the Firenze plain, Tuscany, Italy, *Sedimentology*, **58**, issue 3, pp. 618 – 642

Ghosh P. (2000) Estimation of channel sinuosity from paleocurrent data: a method using fractural geometry, *Journal of Sedimentary Research,* **70,** issue 3, pp. 449 – 455

Gombos A.M., Powell W.G. and Norton I.O. (1995) The tectonic evolution of western India and its impact on hydrocarbon occurrences: an overview, *Sedimentary Geology,* **96,** pp. 119 – 129

Gomez J.L., Arche A., Vargas H. and Marzo M. (2009) Fluvial architecture as a response to two-layer lithospheric subsidence during the Permian and Triassic in the Iberian Basin, eastern Spain, *Sedimentary Geology,* **223,** issue 3 – 4, pp. 320 – 333

Goodwin A.M. (1991) Precambrian Geology the dynamic evolution of the continental crust, London, UK, *Academic Press Limited*

Gould T. and Jones S. (2012) Depositional modelling, biostratigraphy and petrographical analysis of well Aishwariya-2Z, Aishwariya Field, Barmer Basin, Rajasthan, India, Ichron Report, Commissioned on behalf of Cairn India, Unpublished, 12/2036/s

Gould T. and Jones S. (2013) Barmer Basin Outcrop Analysis, Ichron Report, Commissioned on behalf of Cairn India, Unpublished, 13/2222/s

Gulliford A.R., Flint S.S. and Hodgson D.M. (2014) Testing applicability of models of distributive fluvial systems or trunk rivers in ephemeral streams: reconstructing 3D fluvial architecture in the Beaufort Group, South Africa, *Journal of Sedimentary Research,* **84,** pp. 1147 – 1169

Gupta S., Underhill J.R., Sharp I.R. and Gawthrope R.L. (1999) Role of fault interactions in controlling synrift sediment dispersal patterns: Miocene, Abu Alaqa Group, Suez Rift, Sinai, Egypt, *Basin Research,* **11**, pp. 167 – 189

Haff P.K. (2007) The landscape Reynolds number and other dimensionless measures of Earth surface processes, *Geomorphology,* **91,** pp. 178 – 185

Hardas M.G. (1981) Textural parameters and depositional processes of the subsurface Serau Formation, Cambay Basin, *Journal of the Palaeontological Society of India*, **25**, pp. 106 – 109

Hart B.S. and Plint A.G. (1989) Gravelly shoreface deposits: a comparison of modern and ancient facies sequences, *Sedimentology,* **36,** issue 4, pp. 551 – 557

Haszeldine R.S., (1983) Fluvial bars reconstructed from a deep, straight channel, Upper Cretaceous coalfield of Northeast England, *Journal of Sedimentary Petrology,* **53,** issue 4 pp. 1233 – 1247

Heller P.L. and Paola C. (1996) Downstream changes in alluvial architecture: an exploration of controls on channel-stacking patterns, *Journal of Sedimentary Research,* **66**, issue 2, pp. 297 – 306

Heydari E. and Moore C.H. (1989) Burial diagenesis and thermochemical sulfate reduction, Smackover Formation, southeastern Mississippi Salt Basin, *Geology*, **17**, pp. 1080 – 1084

Hillier R.D. (2002) Depositional environment and sequence architecture of the Silurian Coralliferous Group, Southern Pembrokeshire, UK, *Geological Journal,* **37,** pp. 247 – 268

Hunter R.E. (1977a) Terminology of cross-stratified sedimentary layers and climbing-ripple structures, *Journal of Sedimentary Petrology,* **47,** issue 2, pp. 697 – 706

Hunter R.E. (1977b) Basic types of stratification in small eolian dunes, *Sedimentology,* **24,** pp. 361 – 387

Hsu K.J. (2004) Physics of sedimentology textbook and reference, Spinger-Verlag Berlin Heidelberg, *New York*

Hus R. and Cathro D. (2010) Barmer-Cambay-Kutch Structural GIS and SEEBASE™, Commissioned on behalf of Cairn India PTY by FrOG Tech, *Unpublished*

Ielpi A. and Ghinazzi M. (2014) Planform architecture, stratigraphic signature and morphodynamics of an exhumed Jurassic meander plain (Scalby Formation, Yorkshire, UK), *Sedimentology,* **61,** issue 7, pp. 1923 – 1960

Jackson R.G. (1976) Depositional model of point bars in the lower Wabash River, *Journal of Sedimentary Petrology,* **46,** issue 3, pp. 579 – 594

Jaeger H.M., Nagel S.R. and Behringer R.P. (1996) Granular solids, liquids and gases, *Reviews of Modern Physics*, **68**, issue 4, pp. 1259 – 1273

Johnson R.H. and Paynter J. (1967) The development of a cutoff on the River Irk at Chadderton, Lancashire, *Geography*, **52**, issue 1, pp. 41 – 49

Jones B.G. and B.R. Rust (1982) Massive sandstone facies in the Hawkesbury Sandstone, a Triassic fluvial deposit near Sydney, Australia, *Journal of Sedimentology Petrology,* **54,** issue 4, pp. 1249 – 1259

Jones C.M. (1977) Effects of varying discharge regimes on bed-from sedimentary structures on modern rivers, *Geology*, **5**, pp. 567 – 570

Jones S. (2013) Depositional modelling, biostratigraphy and petrographical analysis of well Aishwariya-5, Aishwariya Field, Barmer Basin, Rajasthan, India, Ichron Report, Commissioned on behalf of Cairn India, Unpublished, 13/2190/s

Jones H.L. and Hajek E.A. (2007) Characterizing avulsion stratigraphy in ancient alluvial deposits, *Sedimentary Geology,* **202,** pp. 124 – 137

Kennedy J.F. (1969) The formation of ripples, dunes and antidunes, *Annual Reviews of Fluid Mechanics,* **1**, pp. 147 – 168

Khan Z.A. and Tewari R.C. (2015) Paleocurrents, Paleohydraulics, and Palaegeography of Miocene-Pliocene Siwalik Foreland Basin of India, *Hindwari Publishing Corporation,* Article ID 968573, 14 pages

Kneller B. (2003) The influence of flow parameters on turbidite slope channel architecture, *Marine and Petroleum Geology,* **20**, issues 6 – 8, pp. 901 – 910

Kocurek G. (1981) Significance of interdune deposits and bounding surfaces in aeolian dune sands, *Sedimentology,* **28,** pp. 753 – 780

Kraus M.J. (1999) Paleosols in clastic sedimentary rocks: their geologic applications, *Earth reviews,* **47,** pp. 41 – 70

Kraus M.J. and Hasiotis S.T. (2006) Significance of different modes of rhizolith preservation to interpreting paleoenvironmental and paleohyrologicsettings: examples from Paleogene palaeosols, Bighorn Basin, Wyoming, USA, *Journal of Sedimentary Research,* **76,** pp. 633 – 646

Krigstrom A. (1962) Geomorphological studies of Sandur Plains and their braided rivers in Iceland, *Swedish Society for Anthropology and Geography,* **44**, issue 3 – 4, pp. 328 – 346

Kumar S. and Pandey S.K. (2009) Note on the occurrence of Arumberia Banksi and associated fossils from the Jodhpur Sandstone, Marwar Supergroup, western Rajasthan, *Journal of the Palaeontological Society of India*, **54**, issue 2, pp. 171 – 178

Kumar S., Pandey S.K. and Ahmad S. (2011) Occurrence of giant nodules in the Jodhpur Sandstone, Sursagar area, Jodhpur, Rajasthan, *Scientific Correspondence,* **100**, issue 9, pp. 1294 – 1296

Kundal P. and Sanganwar B.N. (1998) Stratigraphy and Palichnology of Nimar Sandstone, Bagh Beds of Jobat Area, Jhabua District, Madhya Pradesh, *Journal Geological Society of India*, **51**, pp. 619 – 634

Lander R.H., Larese R.E. and Bonnell L.M. (2008) Toward more accurate quartz cement models: The importance of euhedral versus noneuhedral growth rates, *AAPG Bulletin,* **92,** issue 11, pp. 1537 – 1563

Lanson B., Beaufort D., Berger G., Bauer A., Cassagnabere A. and Meunier A. (2002) Authigenic kaolin and illite minerals during burial diagenesis of sandstones: a review, *Clay Minerals,* **37**, pp. 1 – 22

Larsen P.H. (1988) Relay structures in a Lower Permian basement-involved extension systems, East Greenland, *Journal of Structural Geology,* **10**, pp. 3 – 8

Leeder M.R. (1993) Tectonic controls upon drainage basin development, river channel migration and alluvial architecture: implications for hydrocarbon reservoir development and characterization, *Geological Society, London, Special Publications,* **73,** pp. 7-22

Leeder M.R. (2011) Sedimentology and Sedimentary Basins: From Turbulence to Tectonics, (2nd Ed.), West Sussex, *John Wiley & Sons Ltd*

Leeder M.R., Harris T. and Kirkby M.J. (1998) Sediment supply and climate change: implications for basin stratigraphy, *Basin Research,* **10,** pp. 7 – 18

Leopold L.B. and Maddock T. (1953) The hydraulic geometry of stream channels and some physiographic implications, *Geological survey professional paper 252,* pp. 1 – 53

LeRoux J.P. (1994) The angular deviation of paleocurrent directions as applied to the calculation of channel sinuosities, *Journal of Sedimentary Research,* **64,** issue 1, pp. 86 – 87

Limonta M. (2012) Short-term erosion pattern in the Alps-Apennines belt constrained by downstream changes of zircons morphology and U-Pb ages from the Po drainage modern sands, *Ph.D. Thesis*, Università degli Studi di Milano Bicocca

Lin C.Y.M. and Venditti J.G. (2013) An empirical model of subcritical bedform migration, *Sedimentology,* **60,** issue 7, pp. 1786 – 1799

Lindholm R. (1987) A practical approach to sedimentology, London, *Allen and Unwin Inc.*

Long D.G.F. and Young G.M. (1978) Dispersion of cross-stratification as a potential tool in the interpretation of Proterozoic Arenites, *Journal of Sedimentary Research,* **48,** issue 3, pp. 857 – 862

Lowe D.R. (1988) Suspended-load fallout rate as an independent variable in the analysis of current structures, *Sedimentology,* **35,** pp. 765 – 776

Lunt I.A., Bridge J.S. and Tye R.S. (2004) A quantitative three-dimensional depositional model or gravelly braided rivers, *Sedimentology,* **51,** pp. 377 – 414

Macedo J. and Bryant R.B. (1987) Morphology, mineralogy and genesis of a hydrosequence of oxides in Brazil, *Soil Science of America Journal*, **51**, pp. 690 – 700

Mahashwari A. Sial A.N. and Mathur S.C. (2000) Carbon isotope fluctuations through the Neoproterozoic-lower Cambrian Birmania Basin, Rajasthan, India, *Carbonates and Evaporites,* **17,** issue 1, pp. 53 – 59

Mahashwari A., Sial A.N. and Mathur S.C. (2007) Carbon-13 stratigraphy of the Birmania Basin, Rajasthan, India: implications for the Vendian – Cambrian transition, In: Vickers-rich, P. & Komarower, P. (eds) The Rise and Fall of the Ediacaran Biota, *Geological Society, London, Special Publications*, **286**, 439–441.

Makaske B. (2001) Anastomosing rivers: a review of their classification, origin and sedimentary products, *Earth Science Reviews,* **53,** pp. 149 – 196

Martin C.A.L. and Turner B.R. (1998) Origins of massive-type sandstones in braided river systems, *Earth-Science Reviews,* **44,** pp. 15 – 38

Mather A., Stokes M., Pirrie D. and Hartley R. (2008) Generation, transport and preservation of armoured mudballs in an ephemeral gully system, *Geomorphology,* **100,** pp. 104 – 119

Mazumder R. (2003) Sediment transport, aqueous bedform stability and morphodynamics under unidirectional current: a brief overview, *Journal of African Earth Sciences,* **36,** pp. 1 – 14

McAulay G.E., Burley S.D. and Johnes L.H. (1993) Silicate mineral authigenesis in the Hutton and NW Hutton fields: implications for sub-surface porosity development, *Petroleum Geology Conference Series,* **4**, pp. 1377 – 1394

Mckee E.D. and Weir G.W. (1953) Terminology for stratigraphy and cross-stratification in sedimentary rocks, *Bulletin of the Geological Society of America,* **64,** pp. 381 – 390

Merritt E. (1984) The identification of four stages during micro-rill development, *Earth Surface Processes and* Landforms, **9**, pp. 493 – 496

Miall A.D. (1974) Palaeocurrent analysis of alluvial sediments: a discussion of directional variance and vector magnitude, *Journal of Sedimentary Petrology,* **44,** issue 4, pp. 1174 – 1185

Miall A.D. (1976) Palaeocurrent and palaeohydrologic analysis of some vertical profiles through a Cretaceous braided stream deposit, Banks Island, Arctic Canada, *Sedimentology*, **23**, pp. 459 – 483

Miall A.D. (1977) Lithofacies types and vertical profile models in braided river deposits: a summary, *International Association of Sedimentology, Special Publications, Fluvial Sedimentology,* **Memoir 5,** pp. 597 – 604

Miall A.D. (1985) Architectural-element analysis: A new method of facies analysis applied to fluvial deposits, *Earth Science Review,* **22,** pp. 261 – 308

Miall A.D. (1988) Architectural elements and bounding surfaces in fluvial deposits: anatomy of the Kayenta Formation (Lower Jurassic), southwest Colorado, *Sedimentary Geology,* **55,** pp. 233 – 262

Miall A.D. (1995) Discussion, Description and interpretation of fluvial deposits: a critical perspective, *Sedimentology*, **42**, pp. 379 – 389

Miall A.D. (1996) The Geology of Fluvial Deposits, Springer, *Berlin*

Miller M.C., McCave I.N. and Komar P.D. (1977) Threshold of sediment motion under unidirectional currents, *Sedimentology*, **24**, pp. 507 – 527

Meillie S. and Garboczi E.J., (2001) Linear elastic properties of 2D and 3D models of porous materials made from elongated objects, *Modelling and simulation in material science and engineering,* **9,** pp. 371 – 390

Mishra *et al.* (1993) In: Sunder V.R., Raine R., Taylor A., Whiteley N.J., Burley A. and Kothari V. (2012) The Mesozoic to Cenozoic stratigraphy of the Barmer Basin, Rajasthan, India, *Unpublished*

Mohan M. (1995) Cambay Basin – A promise of oil and gas potential, *Journal of The Palaeontological Society of India*, **40**, pp. 41 – 47

Mohrig D., Heller P.L., Paola C. and Lyons W.J. (2000) Interpreting avulsion process from ancient alluvial sequences: Guadalope-Matarranya system (northern Spain) and Wasatch Formation (western Colorado), *GSA Bulletin,* **112,** issue 12, pp. 1787 – 1803

Morley C.K. (1999) How successful are analogue models in addressing the influence of pre-existing fabrics on the rift structure? *Journal of Structural Geology*, **21**, pp. 1267 – 1274

Mukherjee M.K. (1983) Petroleum prospects of Cretaceous sediments of the Cambay Basin, Gujarat, India, *Journal of Petroleum Geology,* **5**, pp. 275 – 286

Nesbitt P. and Bhadra S. (2013) Structural framework for the emplacement of the Bolangir anorthosite massif in the Eastern Ghats Granulite Belt, India: implications for the post-Rodinia pre-Gondwana tectonics, *Mineralogy and Petrology,* **107,** issue 5, pp. 861 – 880

Nichols G. (2009) Sedimentology and Stratigraphy, (2nd Ed.), West Sussex, *John Wiley & Sons Ltd*

North C.P. and Taylor K.S. (1996) Ephemeral-Fluvial Deposits: Integrated Outcrop and Simulation Studies Reveal Complexity, *AAPG Bulletin,* **80,** issue 6, pp. 811 – 830

Nyman S.L., Gani M.R., Bhattacharya J.P., and Lee K (2014) Origin and distribution of calcite concretions in Cretaceous Wall Creek Member, Wyoming: Reservoir-quality implication for shallow-marine deltaic strata, *Cretaceous Research,* **48,** pp. 139 – 152

Oades J.M. (1993) The role of biology in the formation, stabilization and degradation of soil structure, *Geoderma,* **56**, pp. 377 – 400

Ouchi S. (1985) Response of alluvial river to slow active tectonic movement, *Geological Soceity of American Bulletin,* **96,** pp. 504 – 515

Parker G. (1976) On the cause and characteristics scales of meandering and braiding in river, *Journal of Fluid Mechanics,* **76**, issue 3, pp. 457 – 480

Peacock D.C.P. and Sanderson D.J. (1994) Geometry and development of relay ramp in normal fault systems, *AAPG Bulletin*, **78,** issue 2, pp. 147 – 165

Péron S., Bourquin S., Flutean F. and Guillocheau F. (2005) Paleoenvironmental reconstructions and climate simulations of the Early Triassic: Impact of the water and sediment supply on the preservation of fluvial systems, *Geodinamica,* **18**, issue 6, pp. 431 – 446

Pettijohn F.J. (1955) Classification of sandstones, *The Journal of Geology*, **62**, issue 4, pp. 360 – 365

Plint A.G. (1983) Sandy fluvial point-bar sediments from the Middle Eocene of Dorset, England, *Modern and ancient fluvial systems, Special Publication 6 of the ISA,* **6,** pp. 355 – 368

Poppe L.J., Commeau J.A. and Pense G.M. (1989) Effect of chlorine in clay-mineral specimens prepared on silver metal-membrane mounts for x-ray powder diffraction analysis, *Clays and clay minerals*, **37**, issue 4, pp. 381 – 384

Postma G. (1986) Classification for Sediment gravity-flow deposits based on flow conditions during sedimentation, *Geology,* **14**, pp. 291 – 294

Potter P.E. (1997) Petrology and chemistry of modern big river sands, *Journal of geology,* **86,** pp. 423 – 449

Potter P.E. and Pettijohn F.J. (1977) Paleocurrents and basin analysis, 2nd Ed. New York, USA, *Springer-Verlag*

Racey A., Fisher J and Bailey H (In review) The value of fieldwork in making connections between onshore outcrops and offshore models: an example from India, In Review

Rahn P.H. (1966) Sheetfloods, streamfloods and the formation of pediments, *Annals of the Association of American Geographers,* **57,** issue 3 pp. 593 – 604

Reeves C. (2014) The position of Madagascar within Gondwana and its movements during Gondwana dispersal, *Journal of African Earth Sciences,* **94,** pp. 45 – 57

Rohrman M. (2007) Prospectivity of volcanic basins: Trap delineation and acreage de-risking, *AAPG Bulletin,* **91,** issue 6, pp. 915 – 939

Roy A.B. and Jokhar S.R. (2002) Geology of Rajasthan (Northwest India) Precambrian to recent, *Pawan Kumar, Scientific Publishers, India,* Jodphur, India

Schumm S.A. (1972) Fluvial paleochannels, *The Society of Economic Paleontologists and Mineralogists (SEPM) Recognition of Ancient Sedimentary Environments,* pp. 98 - 107

Schumm S.A. (1981) Evolution and response of the Fluvial System, sedimentologic implications, *The Society of Economic Paleologists and Mineralogists (SEPM), Special Publications,* **31**, pp. 19 – 29

Schumm S.A. (1993) River response to baselevel change: Implications for sequence stratigraphy, *The Journal of Geology*, **101**, issue 2, pp. 279 – 294

Schumm S.A. and Khan (1972) experimental study of channel patterns, *Geological Society of America Bulletin,* **85,** pp. 1755 – 1770

Sharma K.K. (2007) K-T magnetism and basin tectonics in western Rajasthan, India: Results from extensional tectonics and not from Reunion plume activity, in Foulger G.R. and Jurdy D.M. Eds. Plates, plumes and planetary processes: *Geological Society of America Special Paper*, **430**, pp. 775 – 784

Shaw E.M., Beven K.J., Chappell N.A. and Lamb R. (2011) Hydrology in practice, 4th Ed. Wiltshire, *CPI Antony Rowe*

Sheth H.C. (2005) Were the Deccan Flood Basalts derived in part from ancient oceanic crust within the Indian continental lithosphere, *Gondwana Research,* **8,** issue 2, pp. 109 – 127

Sheth H.C. (2007) Plume-related regional prevolcanic uplift in the Deccan Traps: Absence of evidence, evidence of absence, *The Geological Society of America Special Paper,* **430,** pp. 785 – 813

Shukla U.K., Singh I.B., Srivastava P., and Singh D.S., (1999) Paleocurrent patterns in braid-bar and point-bar deposits: examples from the Ganga River, India, *Journal of Sedimentary Research,* **69,** issue 5, pp. 992 – 1002

Simons D.B., Richardson E.V., and Nordin C.F. (1960) Sedimentary structures generated by flow in alluvial channels, *The Society of Economic Paleonologists and Mineralogists (SEPM),* **SP12,** pp. 34 – 52

Simonson G.H. and Boersma L. (1972) Soil morphology and water table relations: II. Correlation between annual water table fluctuations and profile features, *Soil Science Society of America*, **34**, pp. 649 – 653

Singh, N.P. (2006) Mesozoic Lithostratigraphy of the Jaisalmer Basin, Rajasthan. *Journal of the Palaeontological Society of India*, **51,** issue 2, pp. 1 - 25

Sisodia M.S. and Singh U.K. (2000) Depositional environment and hydrocarbon prospects of the Barmer Basin, Rajasthan, India, *North American Free Trade Association,* **9,** pp. 309 – 326

Slingerland R. and Smith N.D. (2004) River avulsions and their deposits, *Annual Review of Earth and Planetary Sciences,* **32,** pp. 257 – 285

Smith N.D. (1971) Transverse bars and braiding in the Lower Platte River, Nebraska, *Geological Society of American Bulletin,* **82**, pp. 3407 – 3420

Srivastava D.C., Rao, P.V. and Hardas M.G. (1980) Depositional environment of Mesozoic sediments of Saurashtra revealed by textural parameters, *Journal of the Palaeontological Society of India*, **23**, pp. 136 – 139

Stewart L.K., Woolfe K.J. and Zwartz D.P. (2001) A new tool for the integration, graphical presentation and comparison of files containing palaeocurrent data, *Computers and Geosciences,* **27,** pp. 351 – 355

Sunder V.R., Raine R., Taylor A., Whiteley N.J., Burley A. and Kothari V. (2013) The Mesozoic to Cenozoic stratigraphy of the Barmer Basin, Rajasthan, India, *Internal Cairn Report*

Svendsen J., Stollhofen H., Krapf C.B.E. and Stanistreet I.G. (2003) Mass and hyperconcentrated flow deposits record dune damming and catastrophic breakthrough of ephemeral rivers, Skeleton Coast Erg, Namibia, *Sedimentary Geology*, **160**, pp. 7 – 31

Tabaei M. and Singh R.Y. (2002) Paleoenvironment and paleoecoligical significance of microforaminiferal linings in the Akli Lignite, Barmer Basin, Rajasthan, India, *Iranian International Journal of Science,* **3,** issue 2, pp. 263 – 277

Taylor A., Raine R., Sunder V.R., Premand and Mishra (2010) Barmer Basin Outcrop Work Summary, Commissioned on behalf of Cairn India PTY, *Unpublished*

Tjerry S. and Fredose J. (2005) Calculation of dune morphology, *Journal of geophysical research: Earth Surface*, **110**, issue F4, DOI: http://dx.doi.org/10.1029/2004JF000171

Torri D. and Poesen J. (1988) Incipient motion conditions for single rock fragments in simulated rill flow, *Earth Surface Processes and Landforms,* **13**, pp. 225 – 237

Torsvik T.H., Pandit M.K., Redfield T.F., Ashwal L.D. and Webb S.J. (2005) Remagnetization of Mesozoic limestones from the Jaisalmer Basin NW India, *Geophysics Journal International,* **161,** pp. 57 – 64

Tripath S.K.M., Kumar M. and Srivastava D. (2009) Palynology of Lower Palaeogene (Thanetian-Ypresian) costal deposits from the Barmer Basin (Akli Formation, Western Rajasthan, India): Palaeoenvironmental and palaeoclimatic implications, *Geological Acta,* **7,** issue 1 – 2, pp. 147 – 160

Tucker M.E. (2001) Sedimentary Petrology Analysis, (3rd Ed.), Oxford, UK, *Blackwell Science*

Tunbridge I.P. (1981) Sandy high-energy flood sedimentation – some criteria for recognition, with an example from the Devonian of S.W. England, *Sedimentary Geology,* **28,** pp. 79 – 95

Vagle T., Hurst A. and Dypvik H. (1994) Origin of quartz cement in some sandstones from the Jurassic of the Inner Moray Firth (UK), *Sedimentology,* **41,** pp. 363 – 377

Vazquez-Urbez M. and Oscar M.C. (2013) Intrinsic and extrinsic controls of spatial and temporal variations in modern fluvial tufa sedimentation: A thirteen-year record from a seim-arid environment, *Sedimentology*, **61**, pp. 90 – 132

Vemeesch P. (2204) How many grains are needed for a provenance study? *Earth and Planetary Science Letters*, **224(3-4)**, pp. 441 – 451

Vine J.D. and Tourtelot E.B. (1970) Preliminary geochemical and petrographical analysis of lower Eocene fluvial sandstones in the Rocky Mountain Region, *Book/Publication*

Symposium on Wyoming Sandstones: Their Economic Importance—Past, Present & Future; **22nd Annual Field Conference Guidebook**

Walker R.G. and James N.P., (1992) Facies models: responses to sea-level change. Ontario, Canada, *Geological Association of Canada*

Wassgren C. (2015) An introduction to granular physics, [Online] http://jfi.uchicago.edu/granular/introduction.html Date Accessed: 5/10/15

Weltje G.J. and Eynatten H.V. (2004) Quantitative provenance analysis of sediments: review and outlook, *Sedimentary Geology,* **171,** pp. 1 – 11

Wilkinson M. and Haszeldine R.S. (2002) Fibrous illite in oilfield sandstones - a nucleation kinetic theory of growth, *Terra Nova*, **14**, issue 1, pp. 56 – 60

Winker W. (1984) Palaeocurrents and petrography of the Gurnigel-Schlieren flysch: a basin analysis, *Sedimentary Geology,* **40,** pp. 169 – 189

Wong W., Chan K., Yeung and Lau K.S. (2003) Surface structuring of poly(ethylene terephthalate) by UV excimer laser, *Journal of materials processing technology*, **132**, issues 1 – 3, pp. 114 – 118

Worden R.H. and Morda S. (2000) Quartz cementation in oil field sandstones: a review of the key controversies, *Special Publication Number 29 of the International Association of Sedimentologists,* **29**, pp. 1 – 20

Worden R.H., French M.W. and Mariani E. (2012) Amorphous silica nanofilms result in growth of misoriented microcrystalline quartz cement maintaining porosity in deeply buried sandstones, *Geology*, **40**, issue 2, pp. 179 – 182

Wright V.P. and Marriott S.B. (1993) The sequence stratigraphy of fluvial depositional systems: the role of floodplain sediment storage, *Sedimentary Geology,* **86,** pp. 203 – 210

Wright V.P. and Marriott S.B. (1996) A quantitative approach to soil occurrence in alluvial deposits and its application to the Old Red Sandstone of Britain, *Journal of the Geological Society,* **153,** pp. 907 – 913

Zalawadia H. and Powde C. (2013) Case study on handling paraffinic and viscous crude of Mangala Oil Field of Rajasthan-India, *Society of Petroleum Engineers*, north Africa Technical Conference and Exhibition, 15 – 17 April, Cairo, Egypt

Appendix 1: Field Logs

Key for logs and three-dimensional diagrams

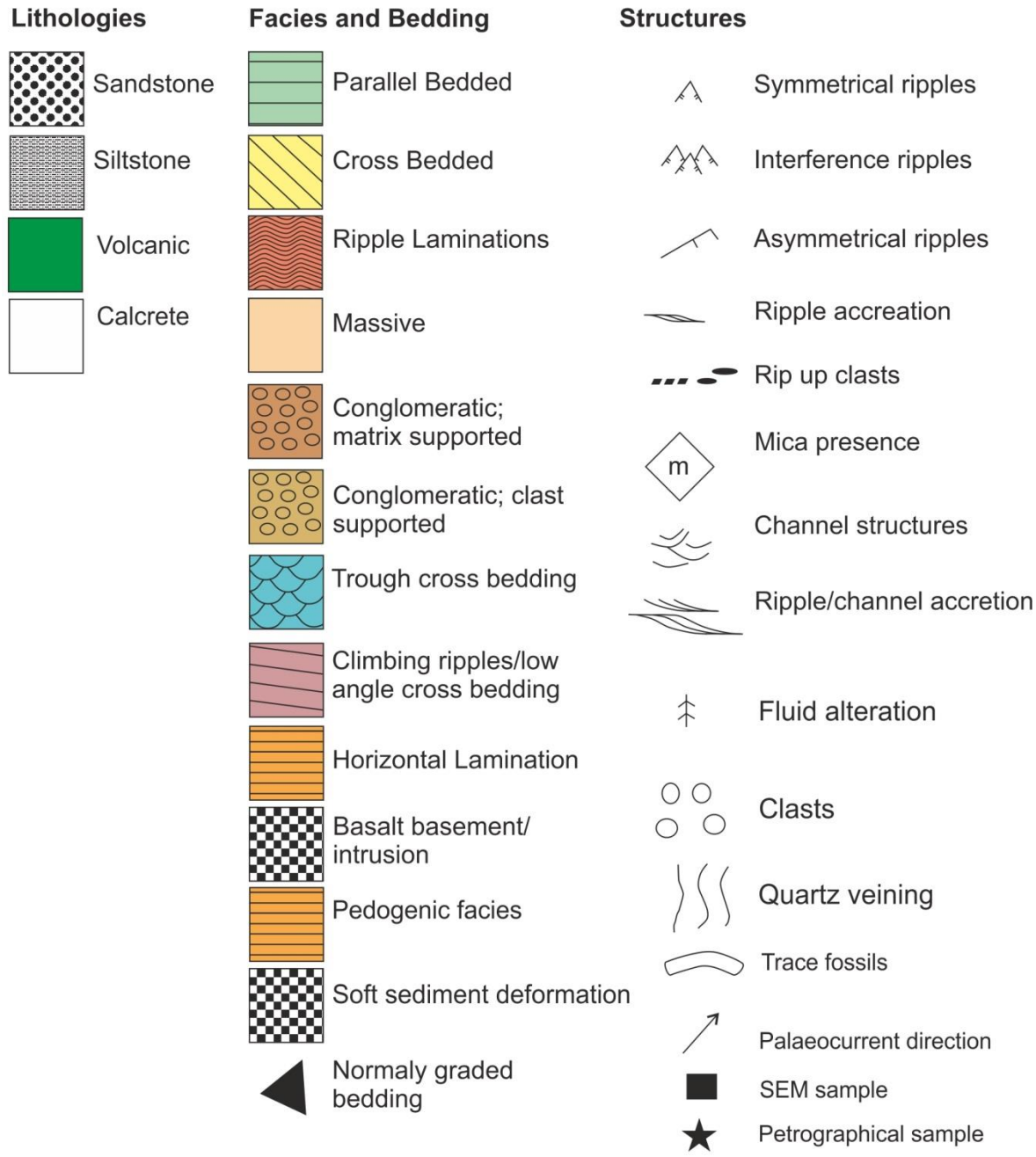

Unless otherwise stated all logs are in metres

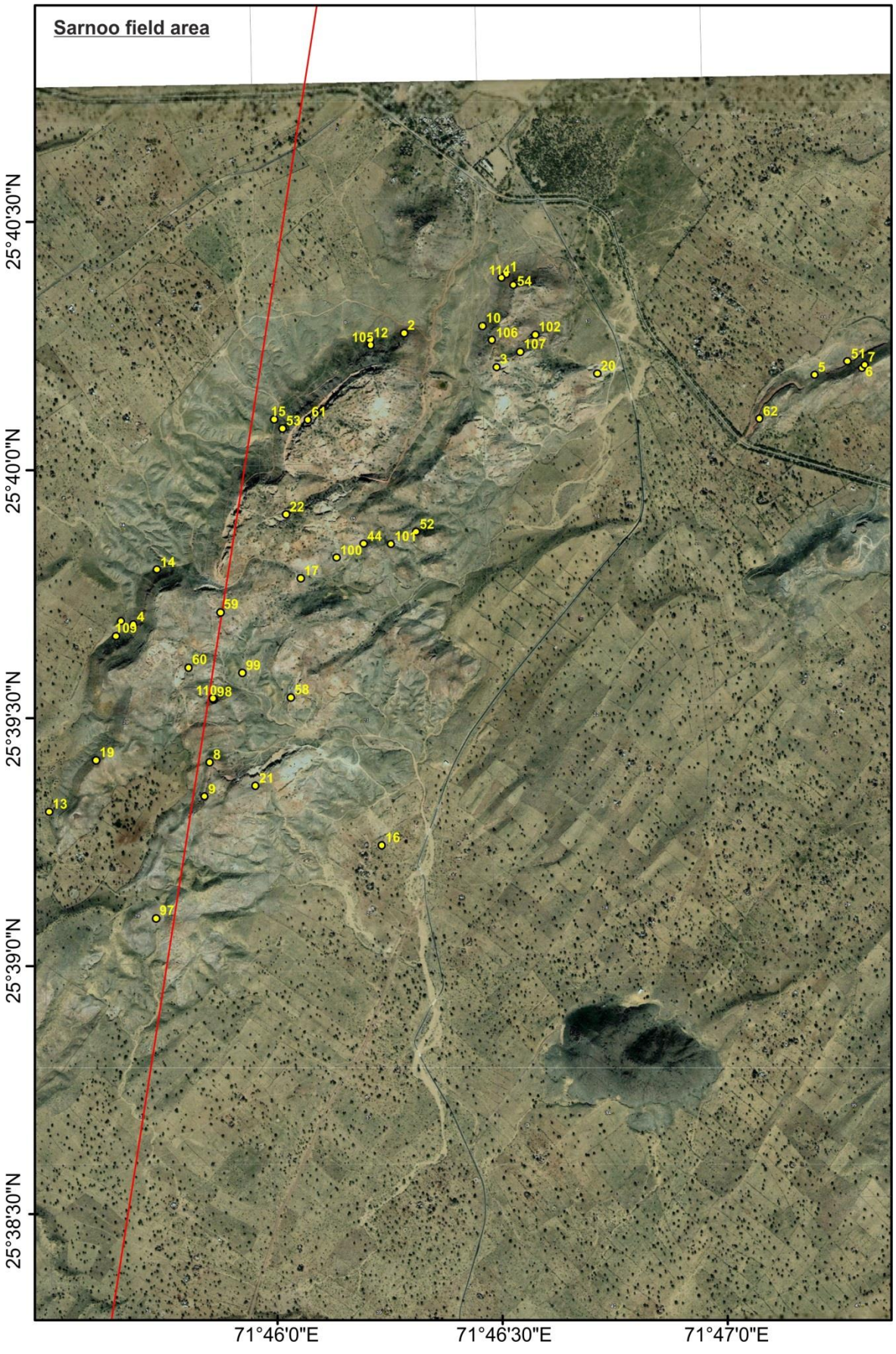
Sarnoo field area
25°40'30"N
25°40'0"N
25°39'30"N
25°39'0"N
25°38'30"N
71°46'0"E
71°46'30"E
71°47'0"E
1
54
10
106
102
107
105
12
2
3
20
5
51
7
6
62
15
53
61
22
52
44
101
100
14
17
59
4
109
60
99
110
98
58
19
8
21
9
13
16
97

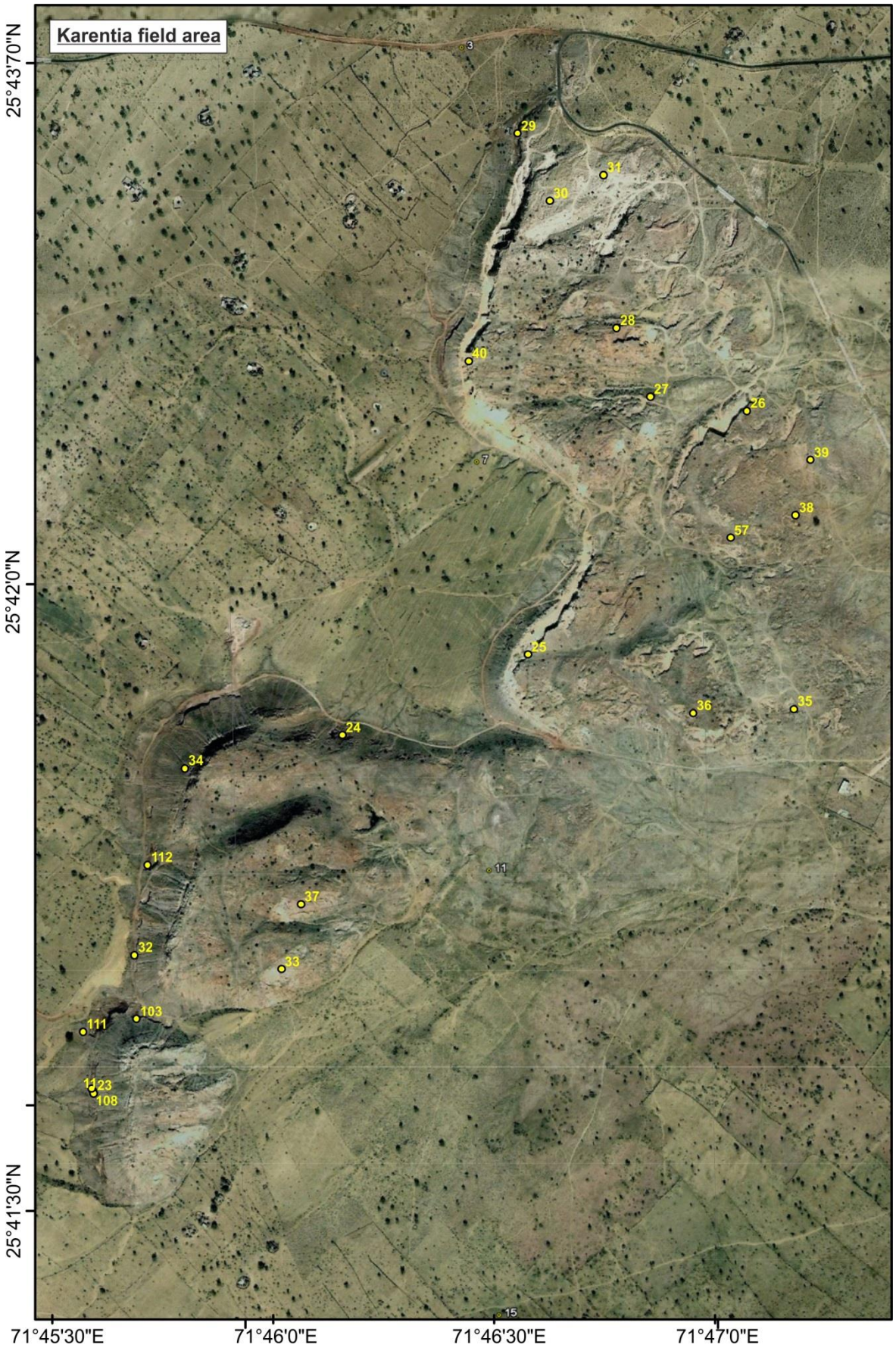
Karentia field area
25°43'70"N
25°42'0"N
25°41'30"N
71°45'30"E
71°46'0"E
71°46'30"E
71°47'0"E
3
29
31
30
28
40
27
26
7
39
38
57
25
36
35
24
34
112
11
37
32
33
103
111
123
108
15

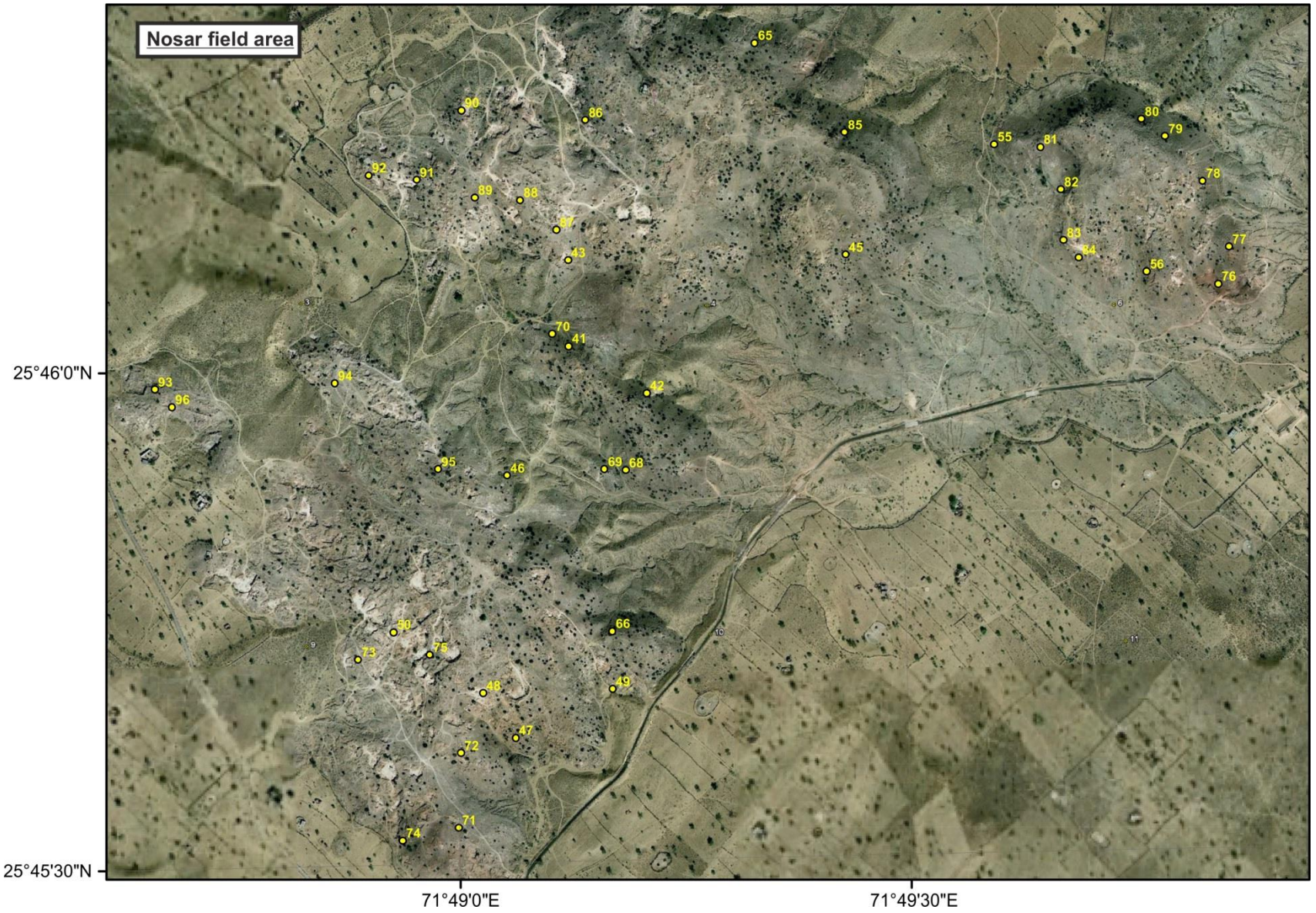
Nosar field area
65
90
86
85
80
79
55
81
92
91
89
88
82
78
87
83
77
43
45
84
56
76
70
41
25°46'0"N
93
94
42
96
95
46
69
68
66
50
73
75
48
49
47
72
71
74
25°45'30"N
71°49'0"E
71°49'30"E

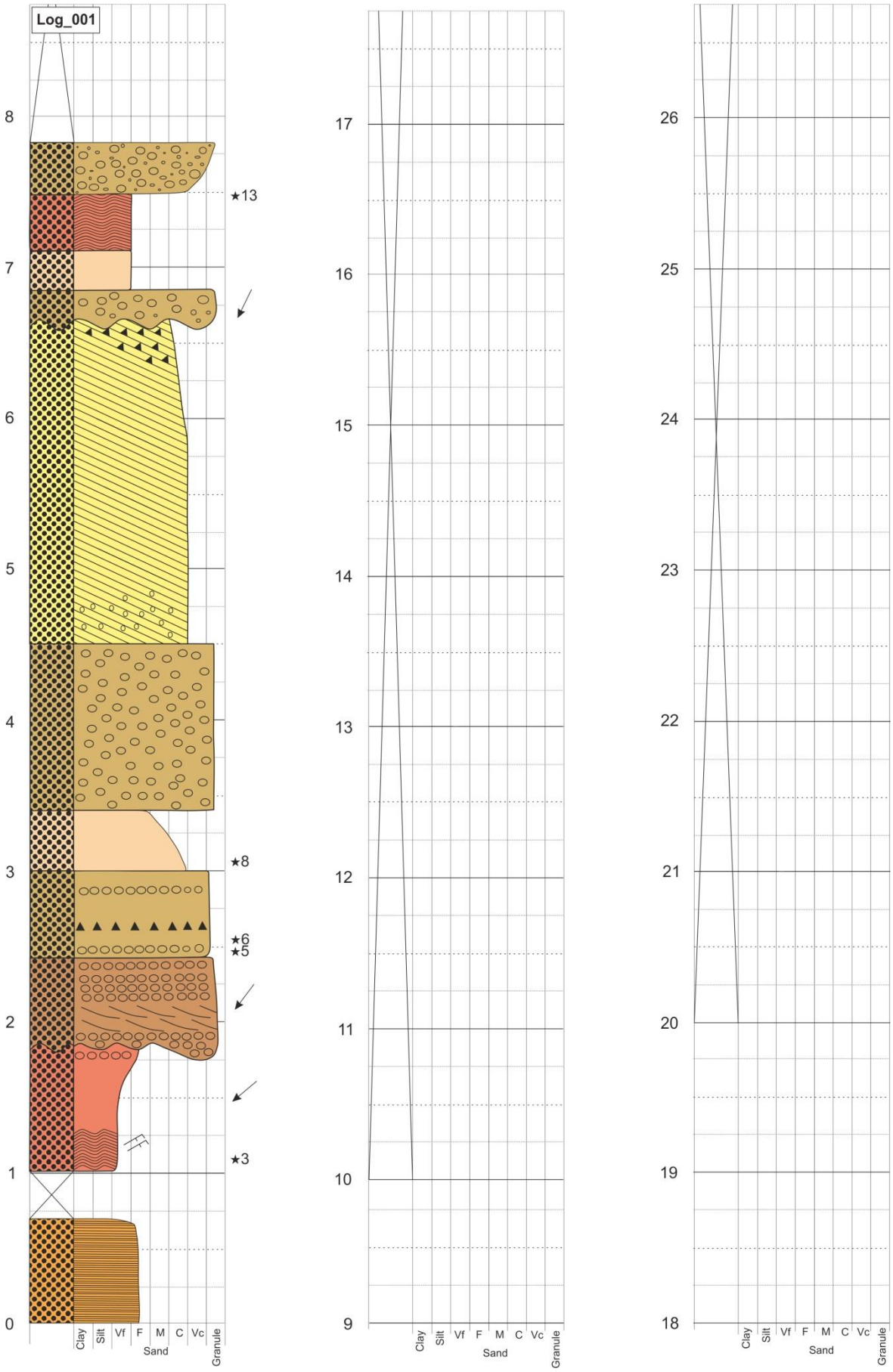
Log_001
8
7
6
5
4
3
2
1
0
★13
★8
★6
★5
★3
Clay
Silt
Vf
F
M
C
Vc
Sand
Granule
17
16
15
14
13
12
11
10
9
26
25
24
23
22
21
20
19
18

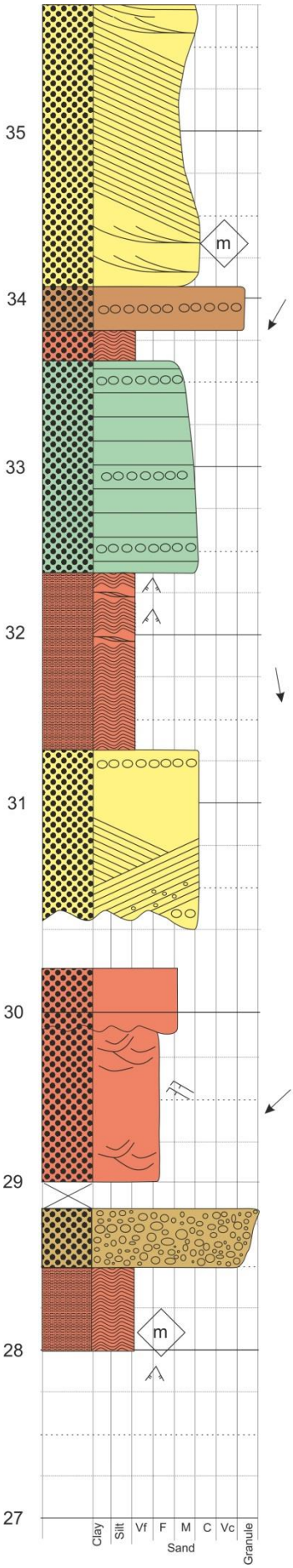
35
34
33
32
31
30
29
28
27
m
m
Clay
Silt
Vf
F
M
C
Vc
Granule
Sand

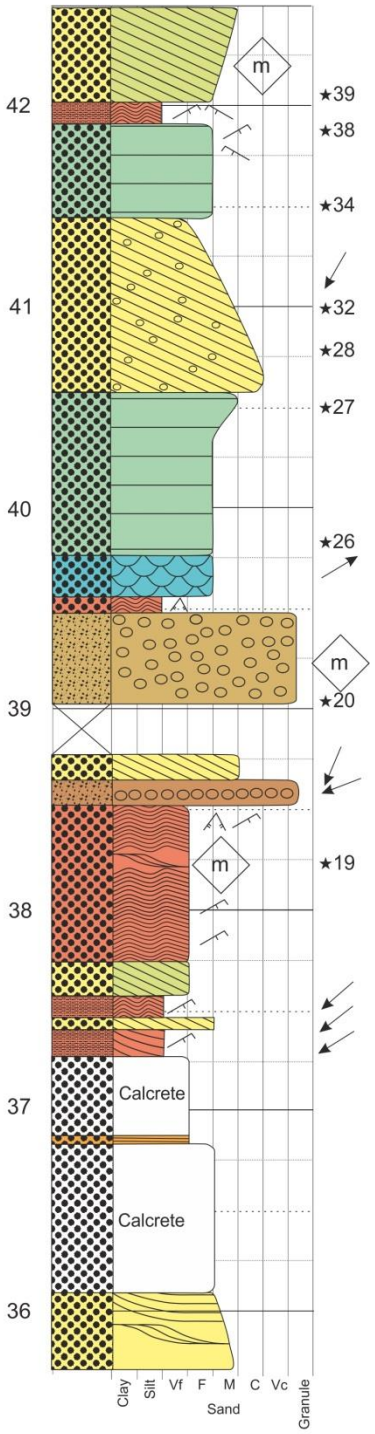
42
41
40
39
38
37
36
m
m
m
★39
★38
★34
★32
★28
★27
★26
★20
★19
Calcrete
Calcrete
Clay
Silt
Vf
F
M
C
Vc
Granule
Sand

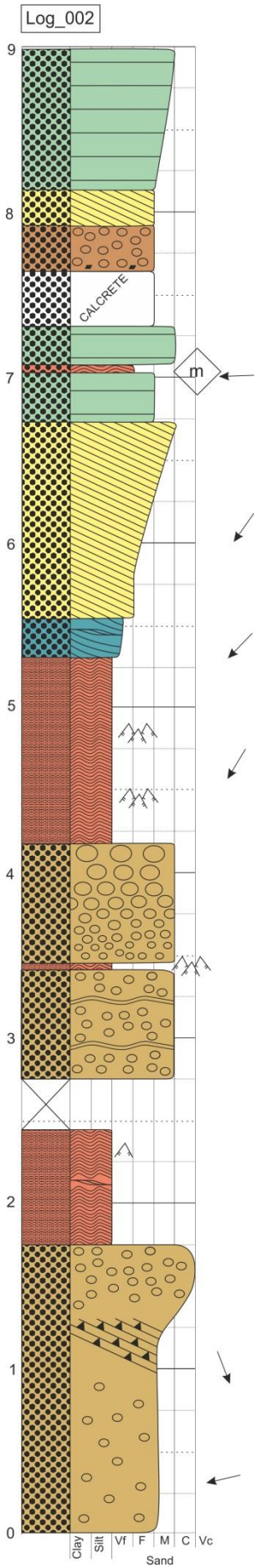
Log_002
9
8
7
6
5
4
3
2
1
0
CALCRETE
m
Clay
Silt
Vf
F
M
C
Vc
Sand

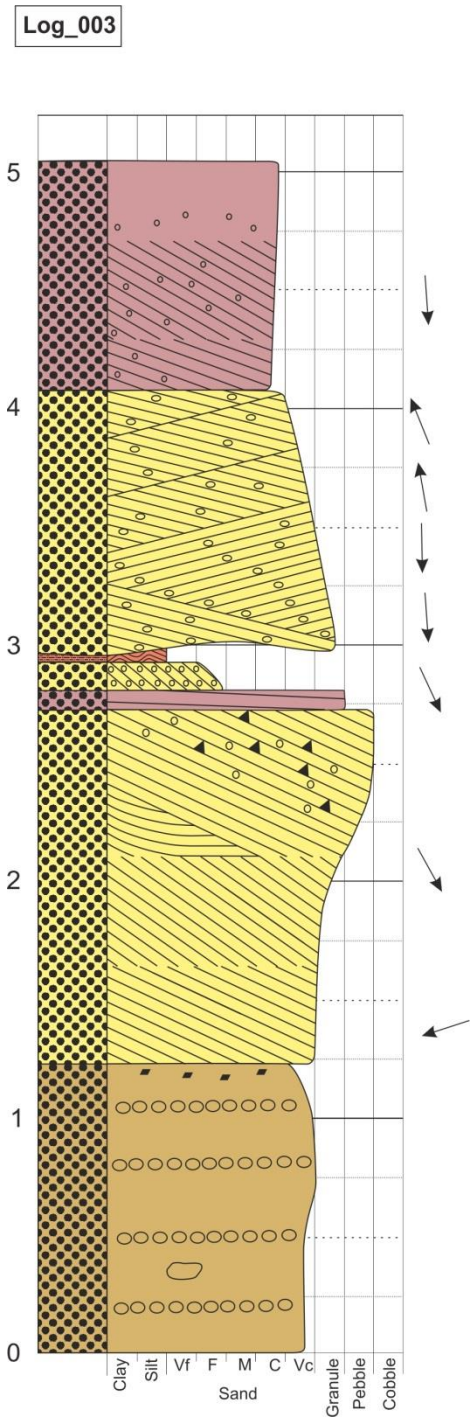
Log_003
5
4
3
2
1
0
Clay
Silt
Vf
F
M
C
Vc
Sand
Granule
Pebble
Cobble

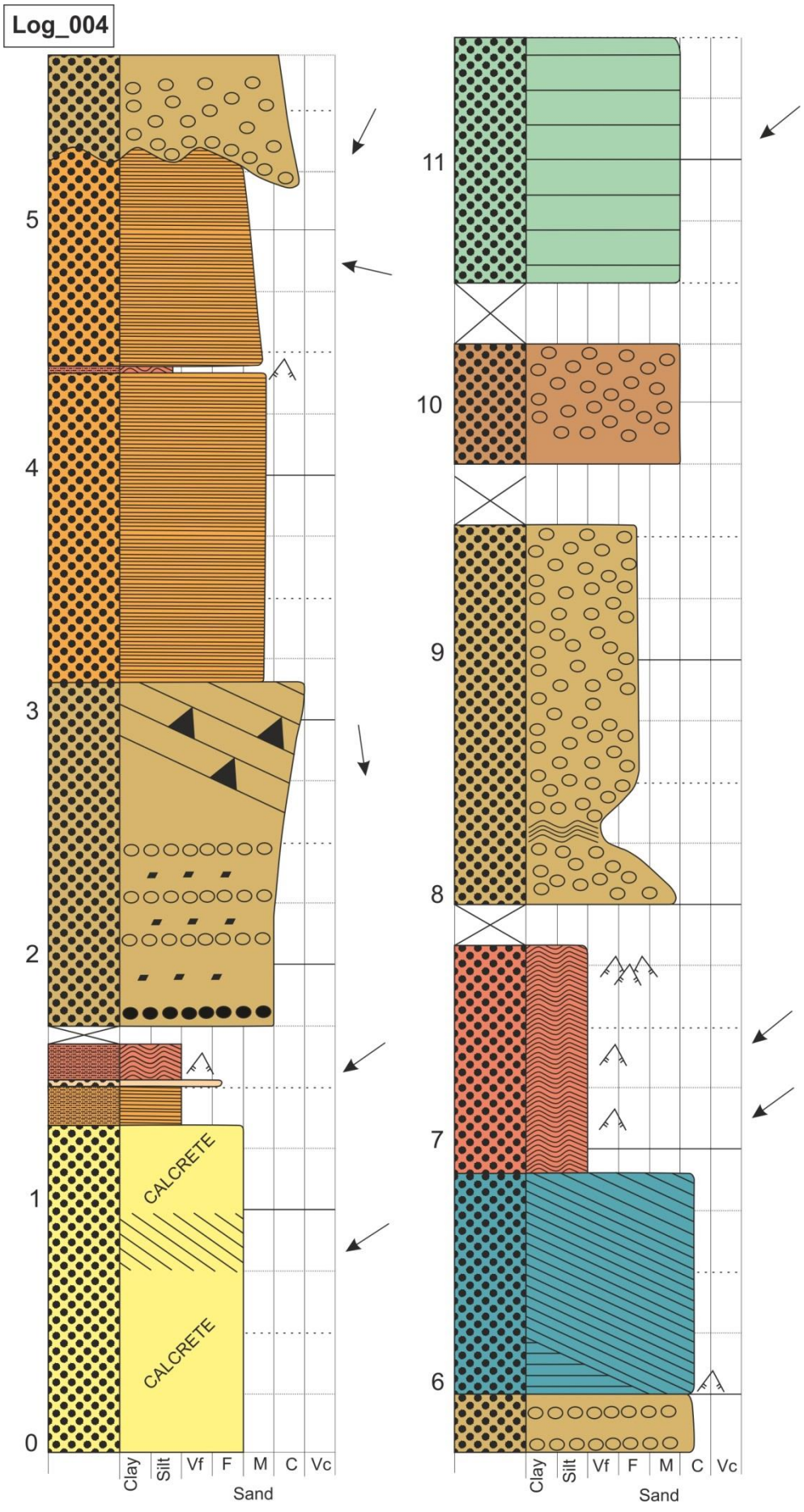
Log_004
0
1
2
3
4
5
6
7
8
9
10
11
CALCRETE
CALCRETE
Clay
Silt
Vf
F
M
C
Vc
Sand
Clay
Silt
Vf
F
M
C
Vc
Sand

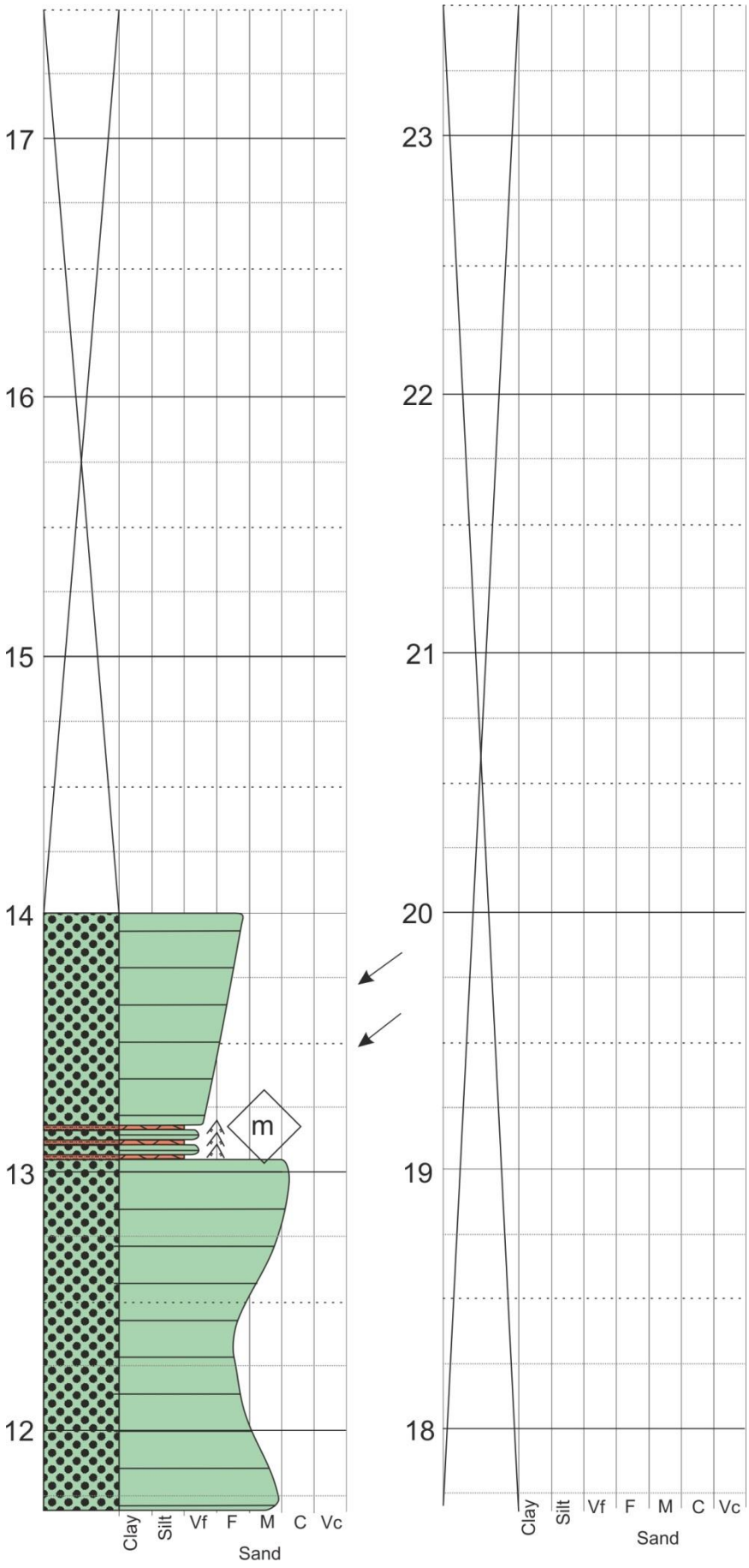
17
16
15
14
13
12
m
Clay
Silt
Vf
F
M
C
Vc
Sand
23
22
21
20
19
18
Clay
Silt
Vf
F
M
C
Vc
Sand

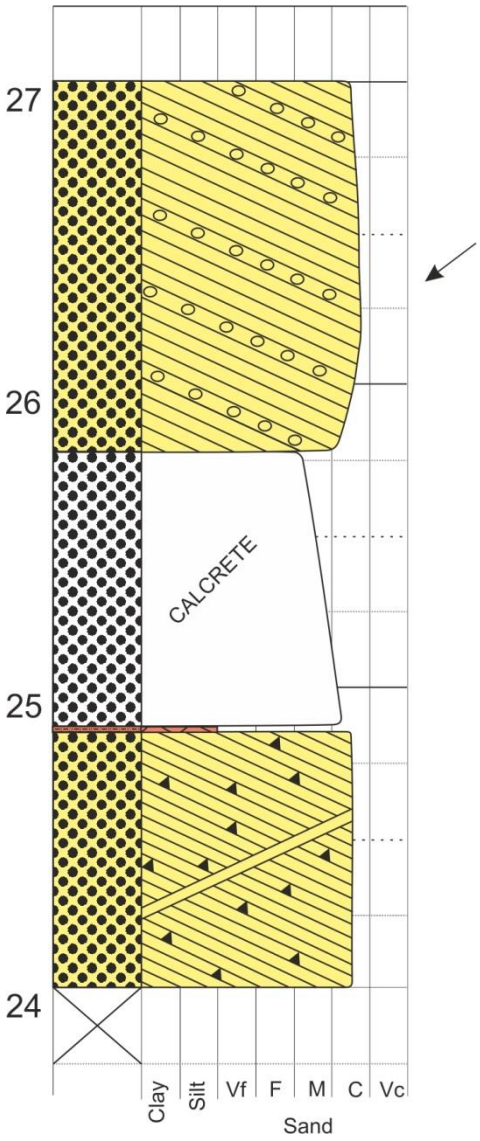
27
26
25
24
CALCRETE
Clay
Silt
Vf
F
M
C
Vc
Sand

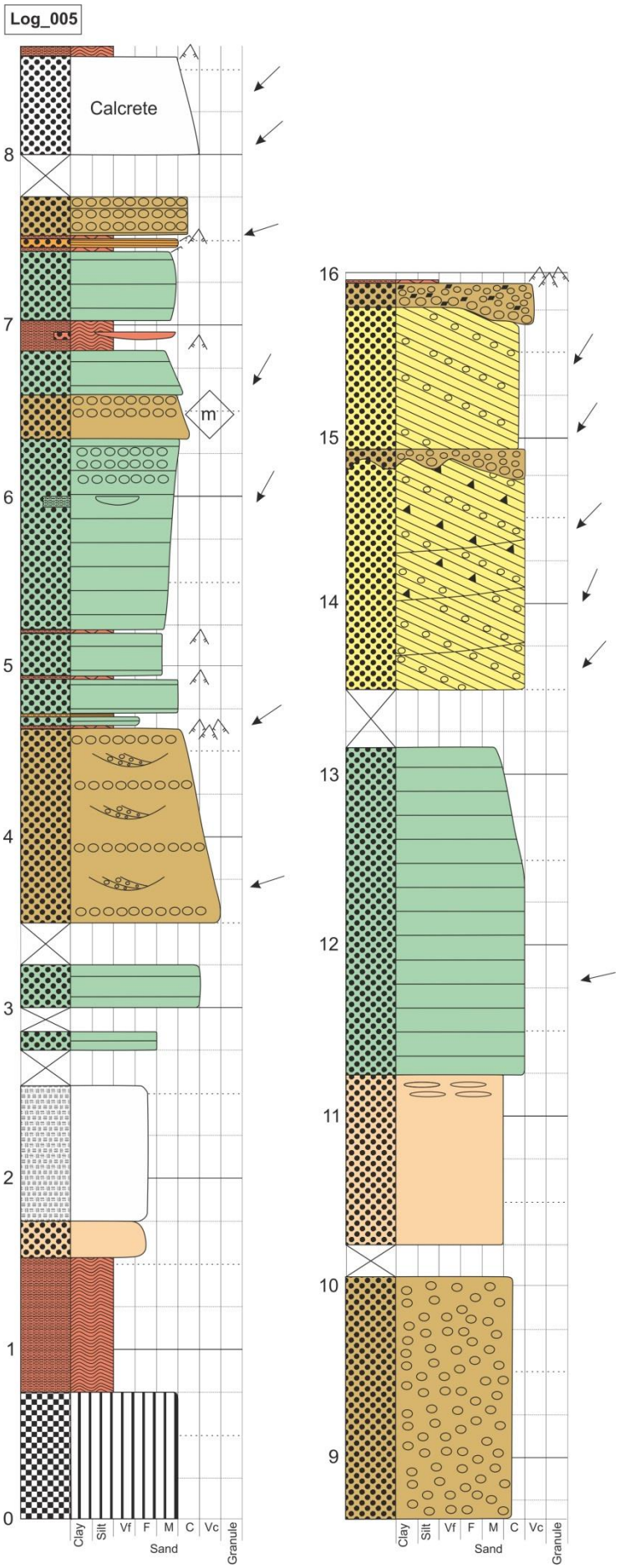
Log_005
Calcrete
m
0
1
2
3
4
5
6
7
8
9
10
11
12
13
14
15
16
Clay
Silt
Vf
F
M
C
Vc
Granule
Sand

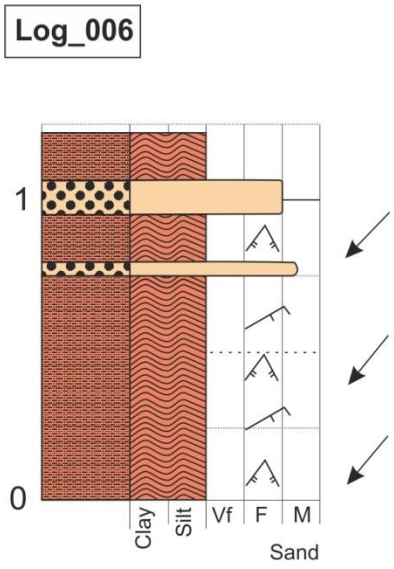
Log_006
1
0
Clay
Silt
Vf
F
M
Sand

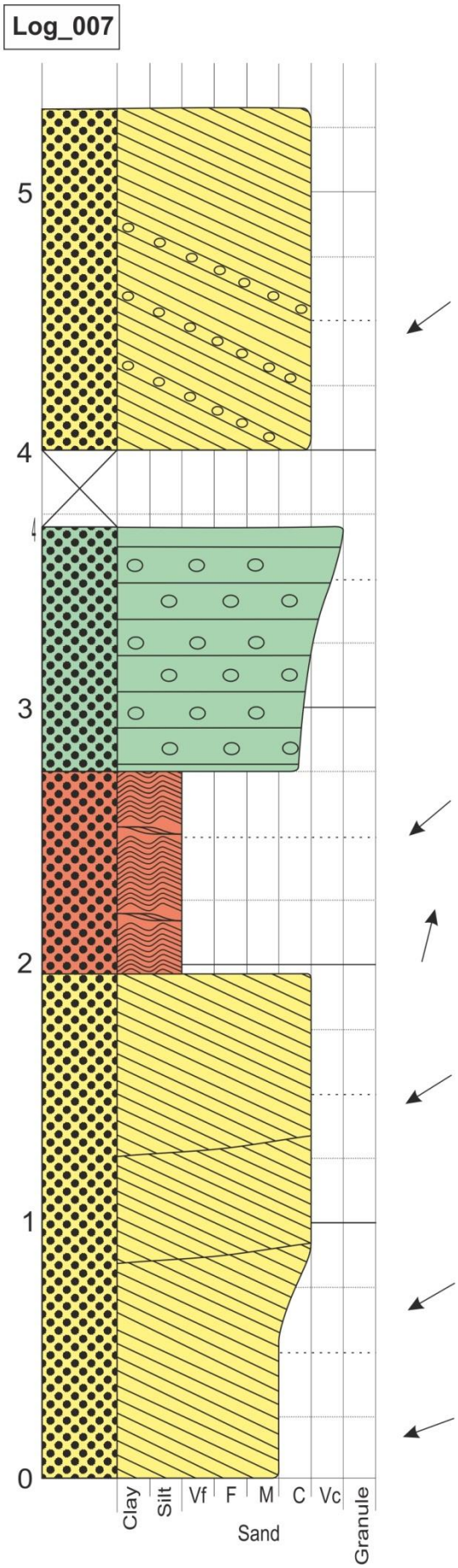
Log_007
5
4
3
2
1
0
Clay
Silt
Vf
F
M
C
Vc
Granule
Sand

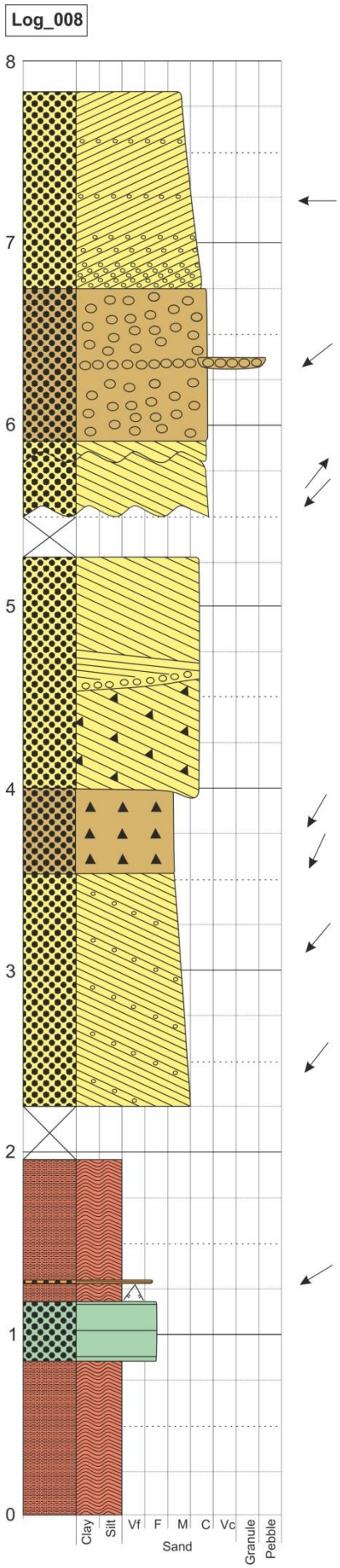
Log_008
8
7
6
5
4
3
2
1
0
Clay
Silt
Vf
F
M
C
Vc
Granule
Pebble
Sand

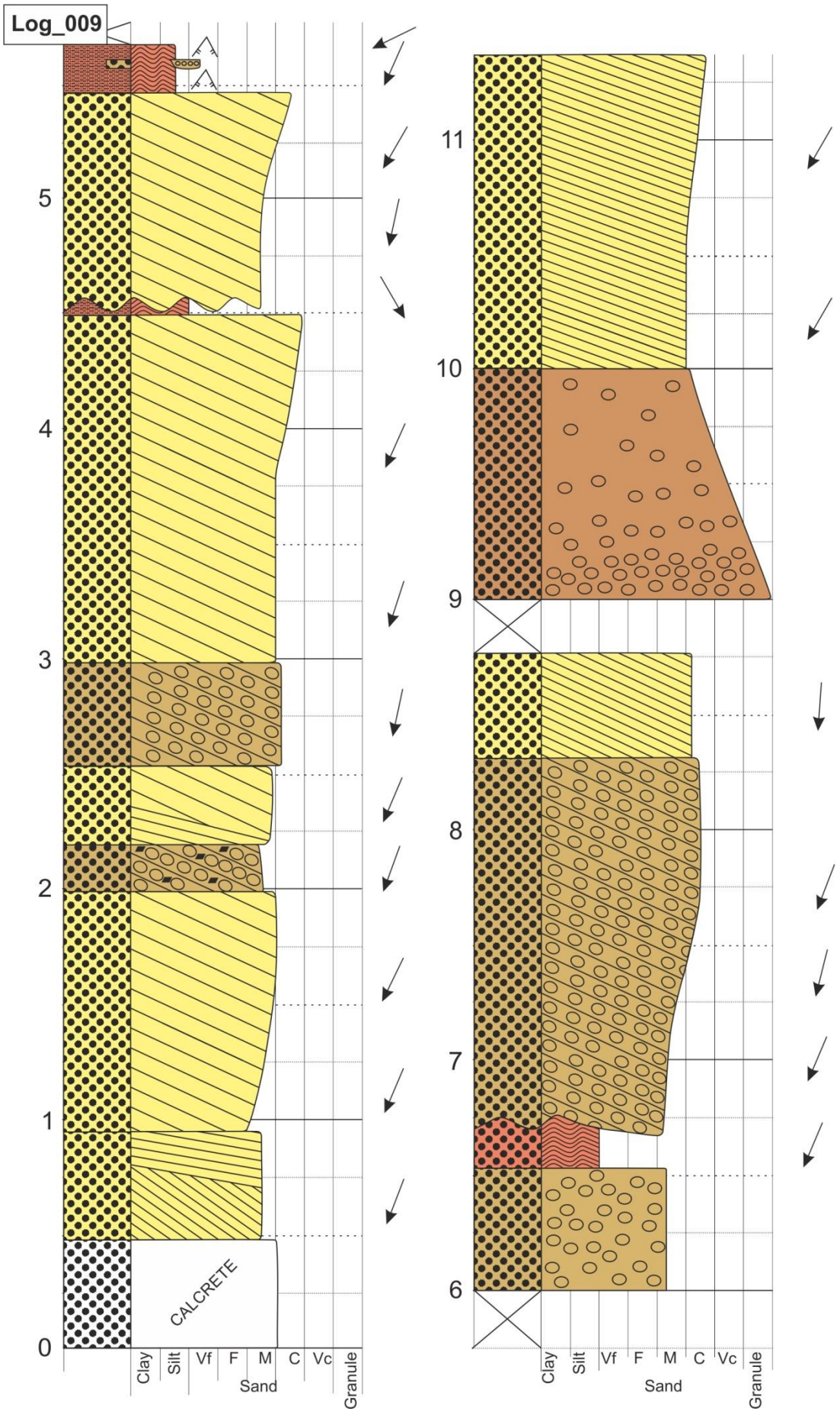
Log_009
0
1
2
3
4
5
6
7
8
9
10
11
CALCRETE
Clay
Silt
Vf
F
M
C
Vc
Granule
Sand

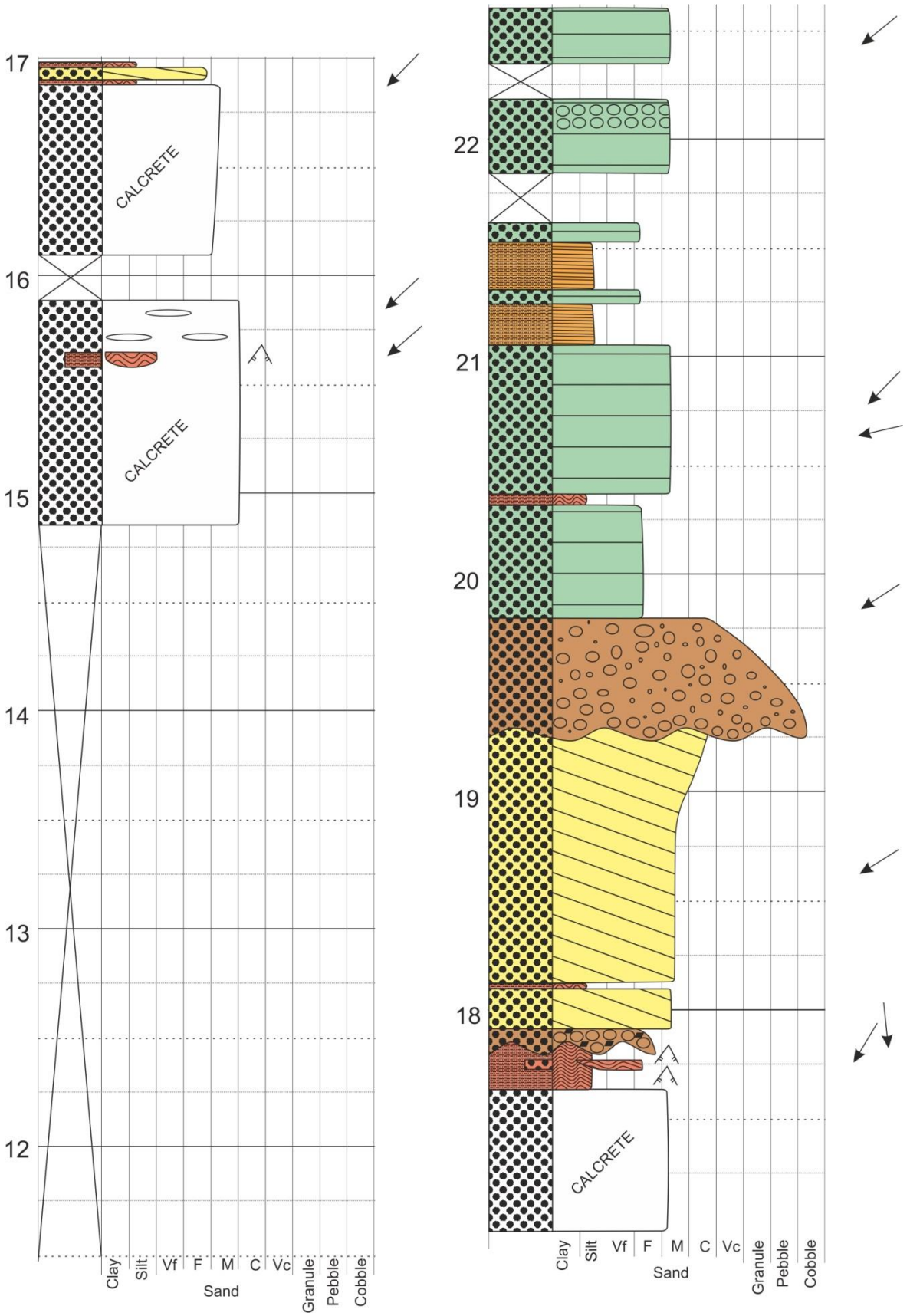
17
16
15
14
13
12
CALCRETE
CALCRETE
Clay
Silt
Vf
F
M
C
Vc
Sand
Granule
Pebble
Cobble
22
21
20
19
18
CALCRETE
Clay
Silt
Vf
F
M
C
Vc
Sand
Granule
Pebble
Cobble

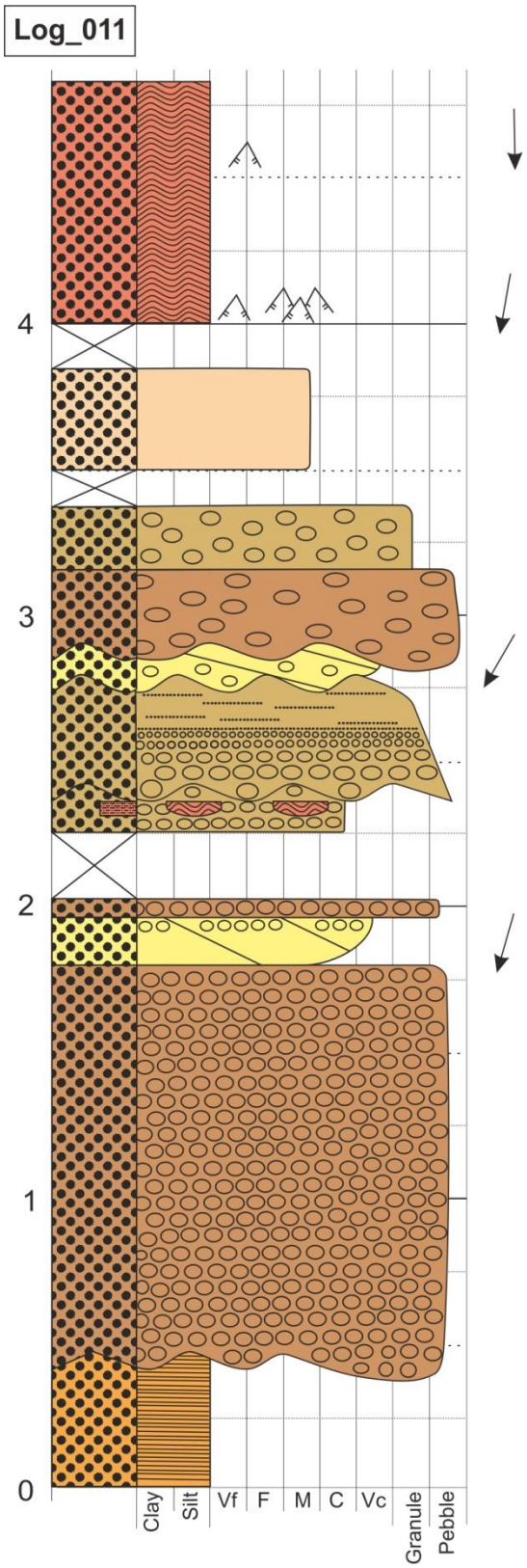
Log_011
4
3
2
1
0
Clay
Silt
Vf
F
M
C
Vc
Granule
Pebble

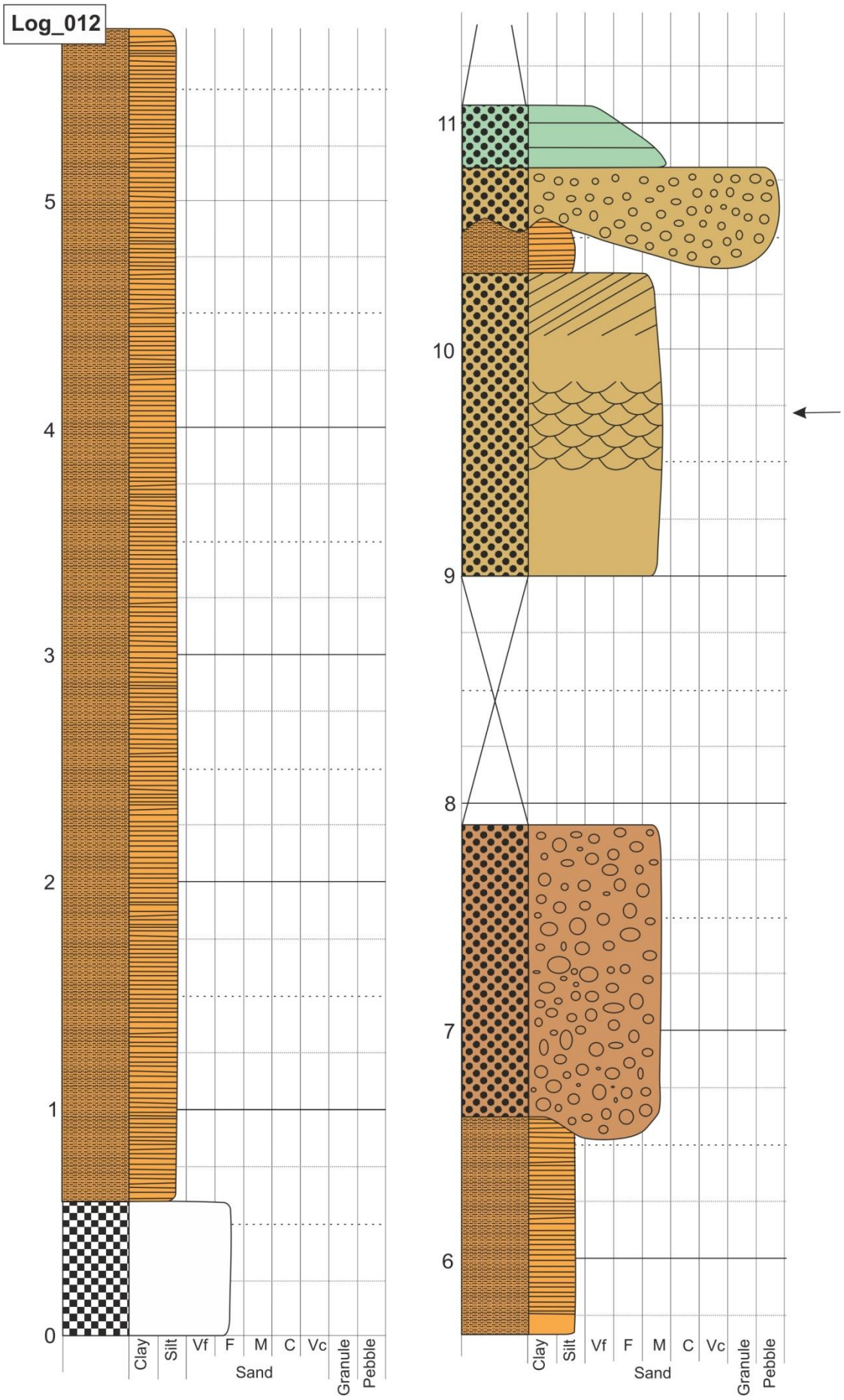
Log_012
0
1
2
3
4
5
6
7
8
9
10
11
Clay
Silt
Vf
F
M
C
Vc
Sand
Granule
Pebble

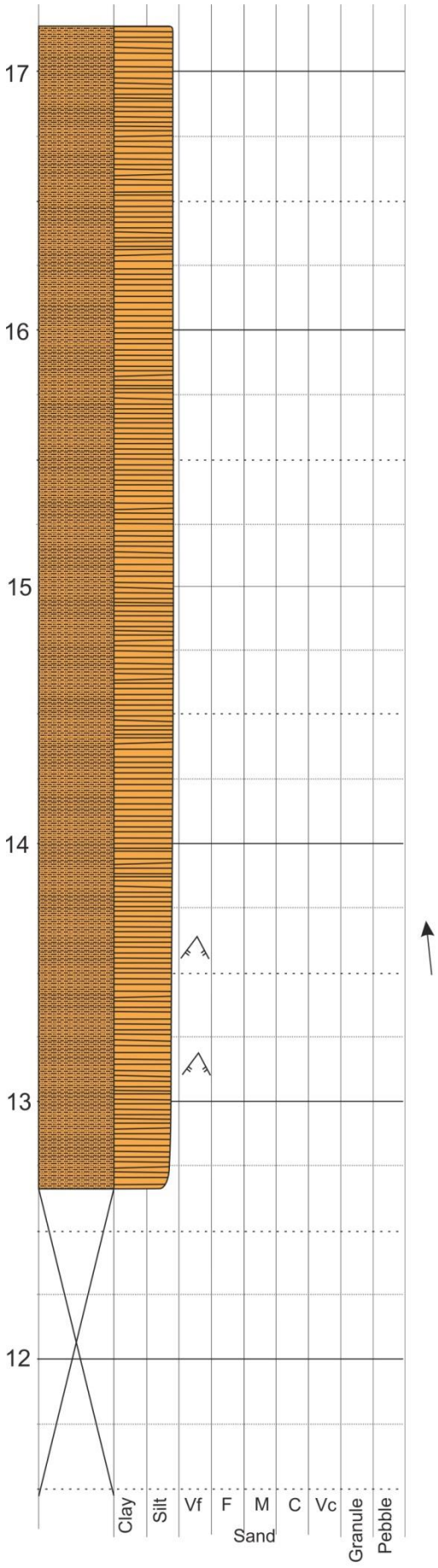
17
16
15
14
13
12
Clay
Silt
Vf
F
M
C
Vc
Sand
Granule
Pebble

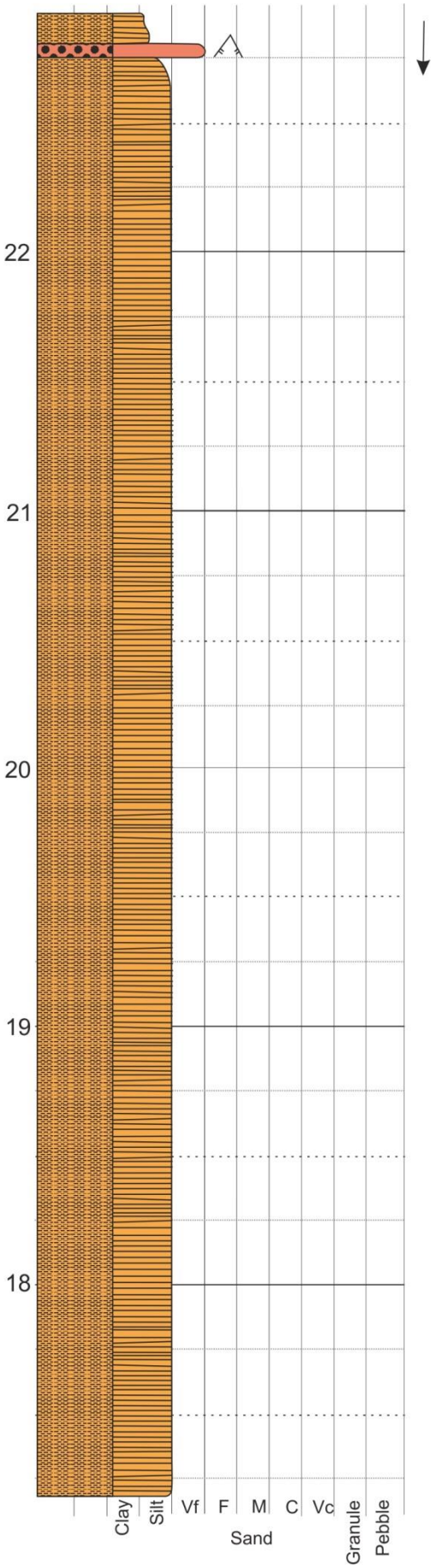
22
21
20
19
18
Clay
Silt
Vf
F
M
C
Vc
Sand
Granule
Pebble

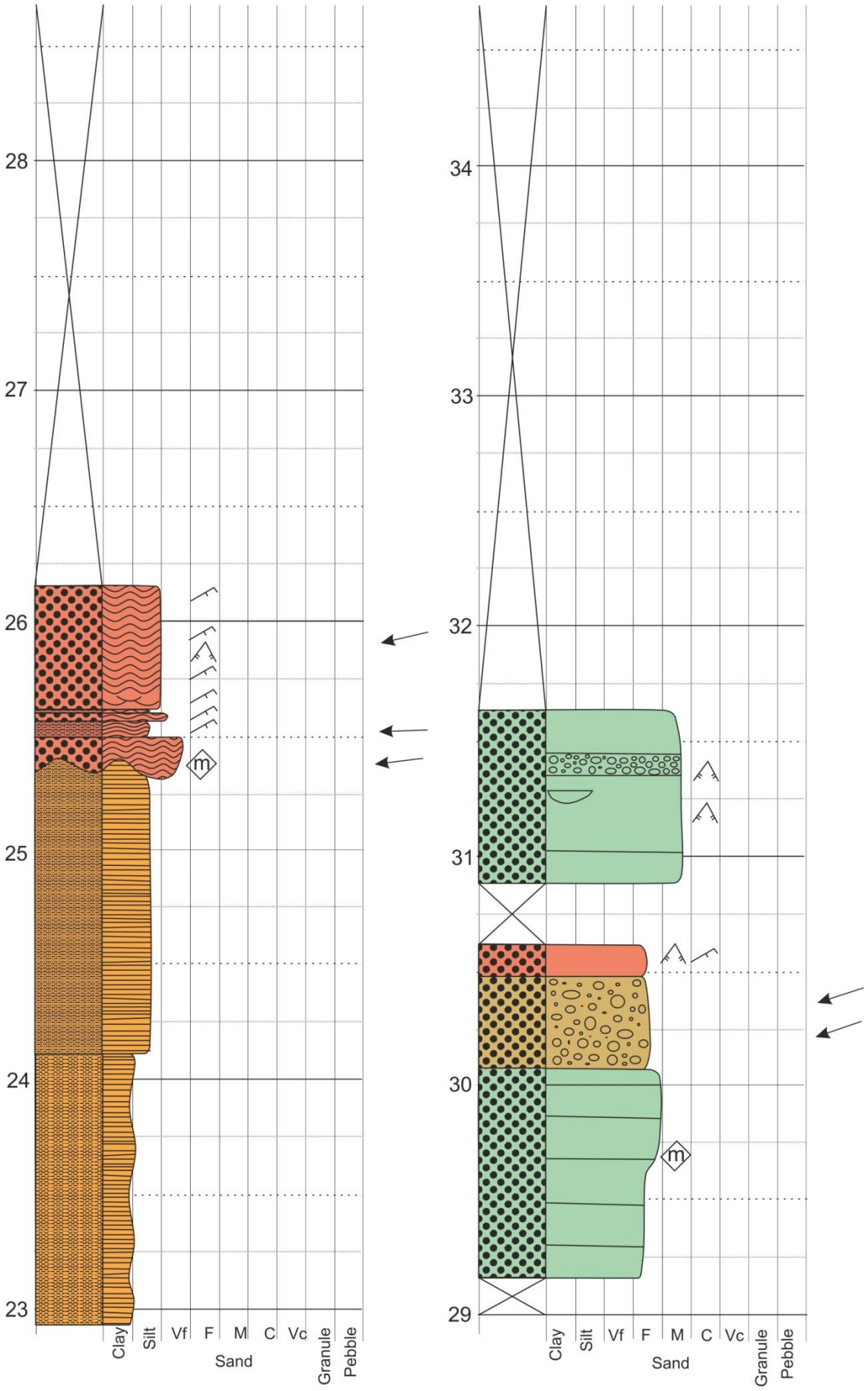
28
27
26
25
24
23
m
Clay
Silt
Vf
F
M
C
Vc
Granule
Pebble
Sand
34
33
32
31
30
29
m
Clay
Silt
Vf
F
M
C
Vc
Granule
Pebble
Sand

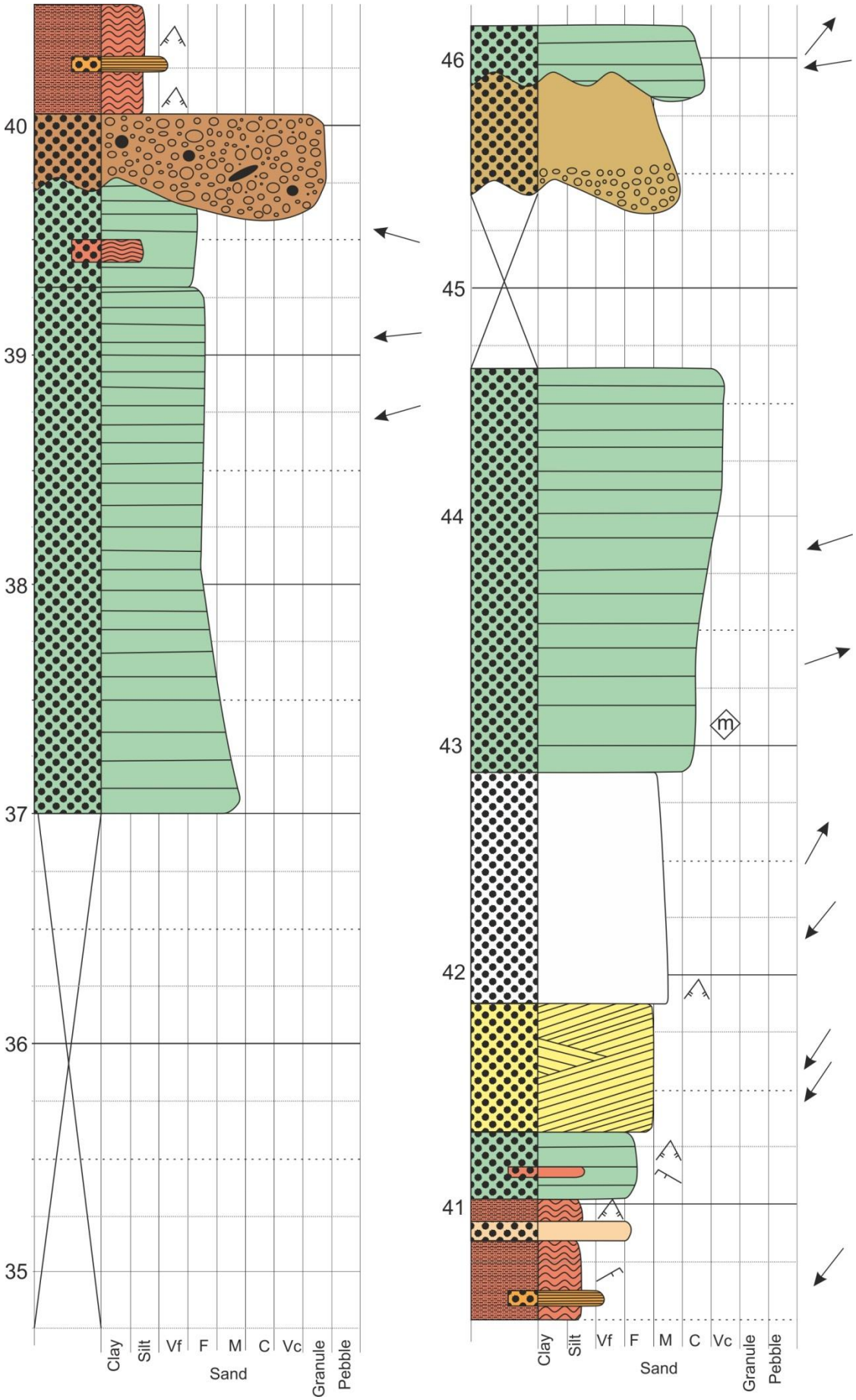
40
39
38
37
36
35
46
45
44
43
42
41
m
Clay
Silt
Vf
F
M
C
Vc
Granule
Pebble
Sand

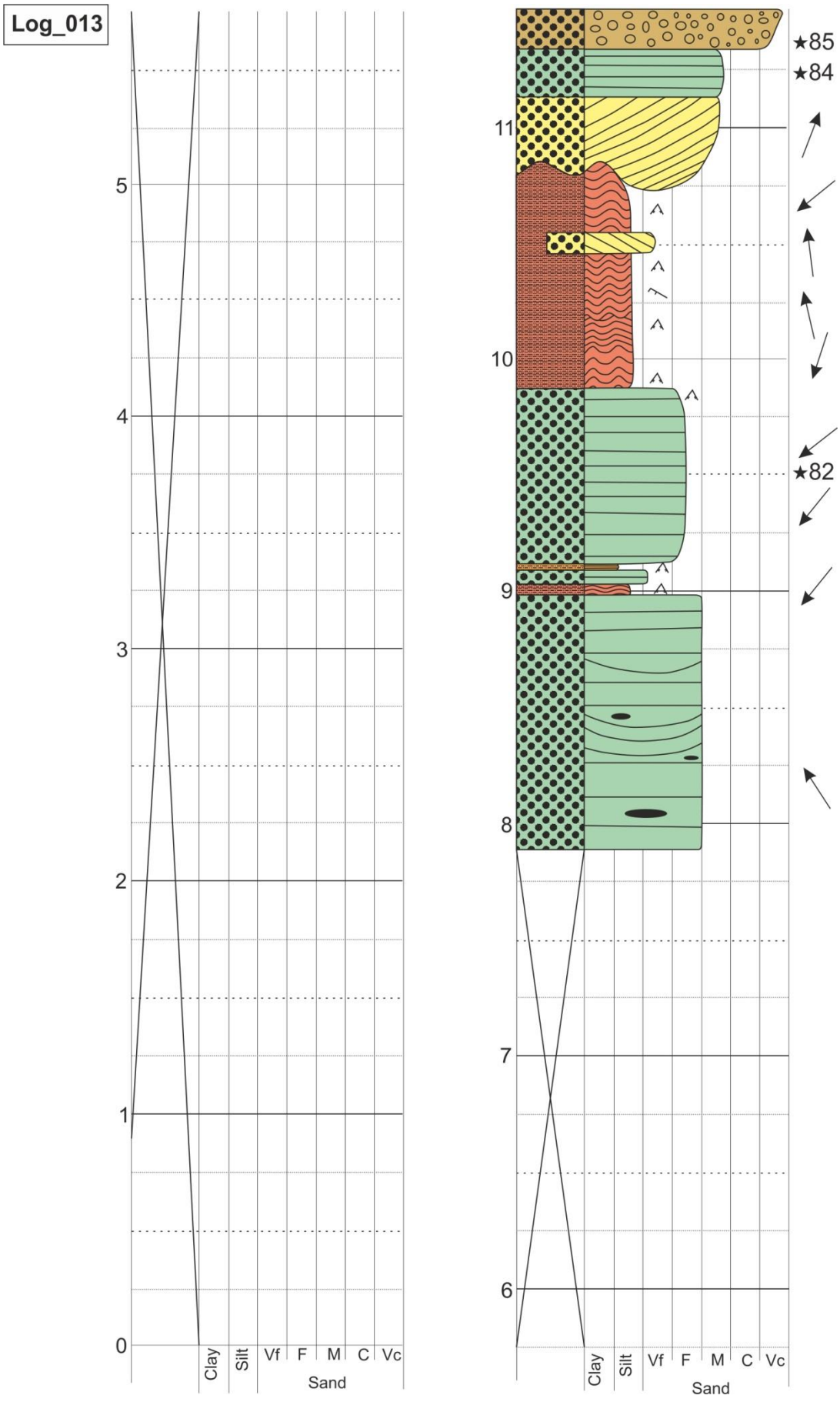
Log_013
0
1
2
3
4
5
6
7
8
9
10
11
★85
★84
★82
Clay
Silt
Vf
F
M
C
Vc
Sand

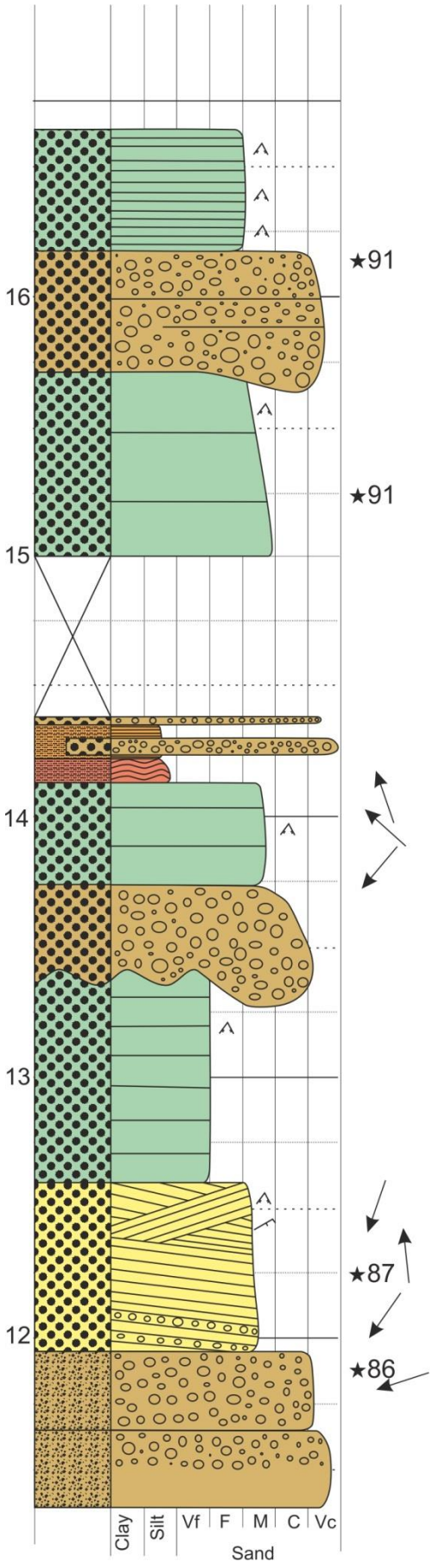
16
15
14
13
12
★91
★91
★87
★86
Clay
Silt
Vf
F
M
C
Vc
Sand

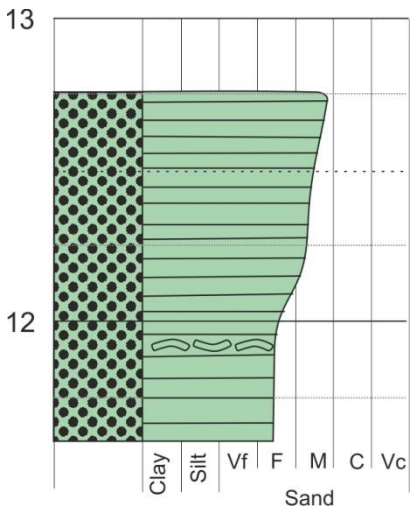
13
12
Clay
Silt
Vf
F
M
C
Vc
Sand

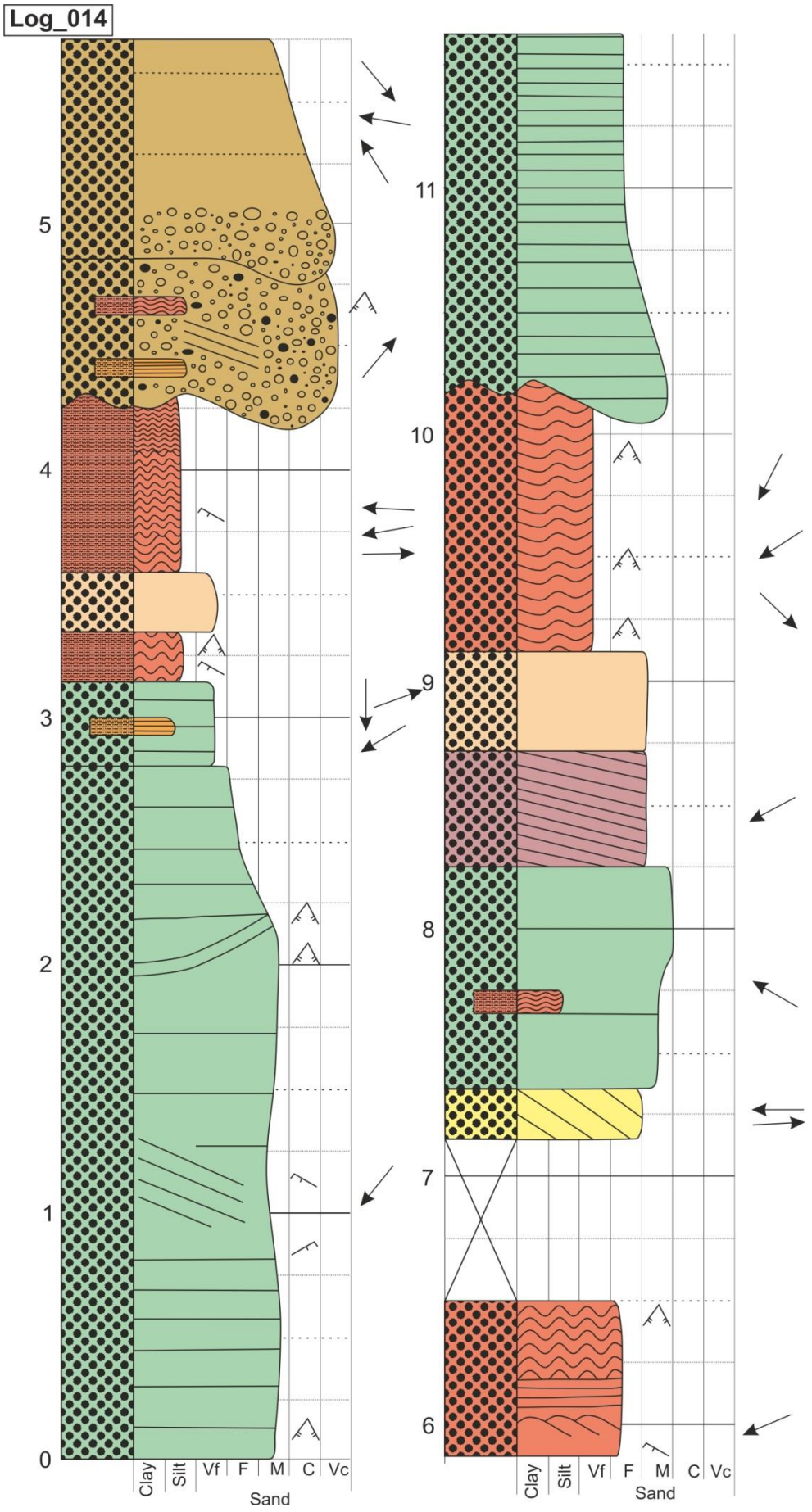
Log_014
0
1
2
3
4
5
6
7
8
9
10
11
Clay
Silt
Vf
F
M
C
Vc
Sand
Clay
Silt
Vf
F
M
C
Vc
Sand

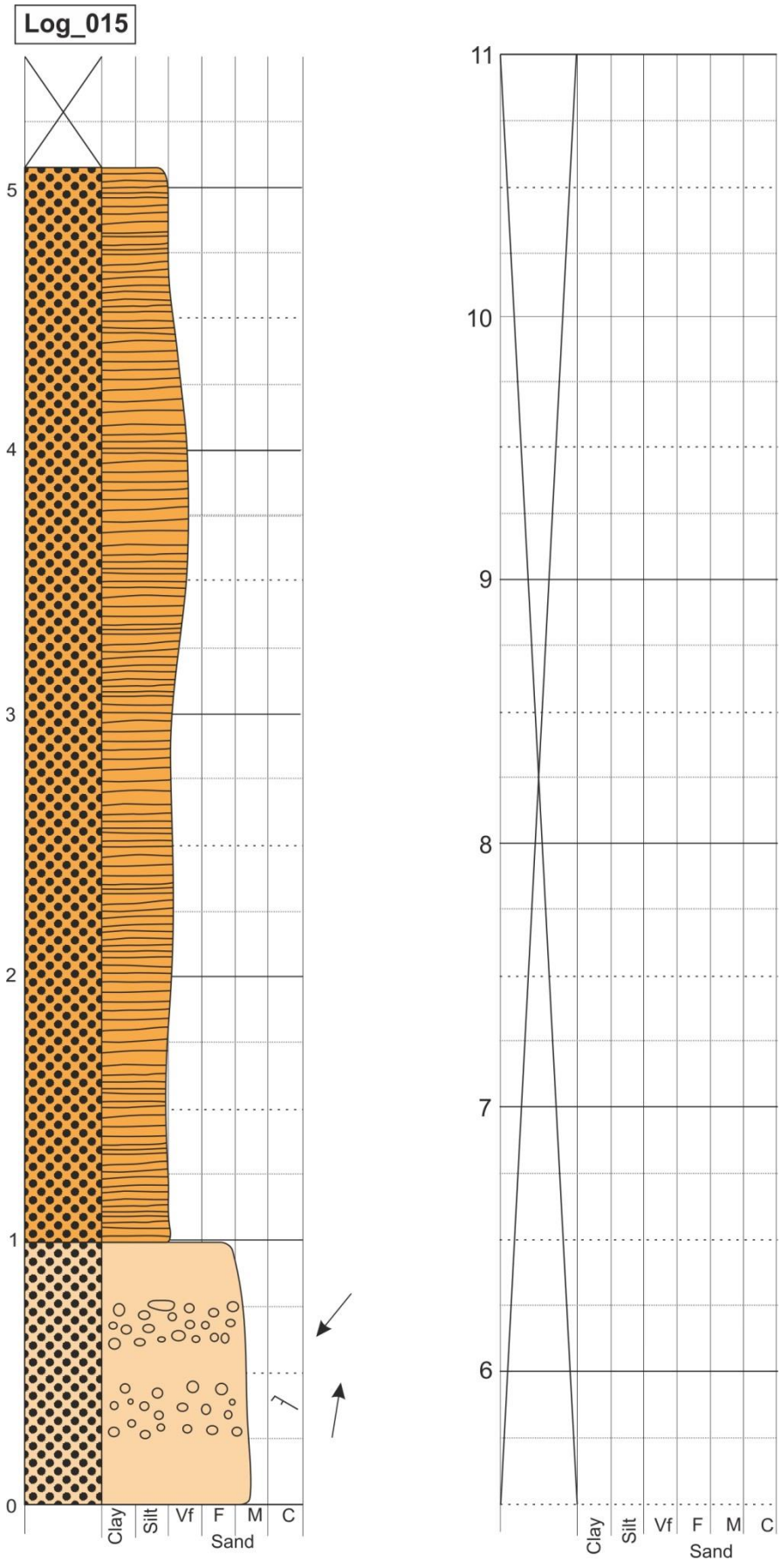
Log_015
5
4
3
2
1
0
Clay
Silt
Vf
F
M
C
Sand
11
10
9
8
7
6
Clay
Silt
Vf
F
M
C
Sand

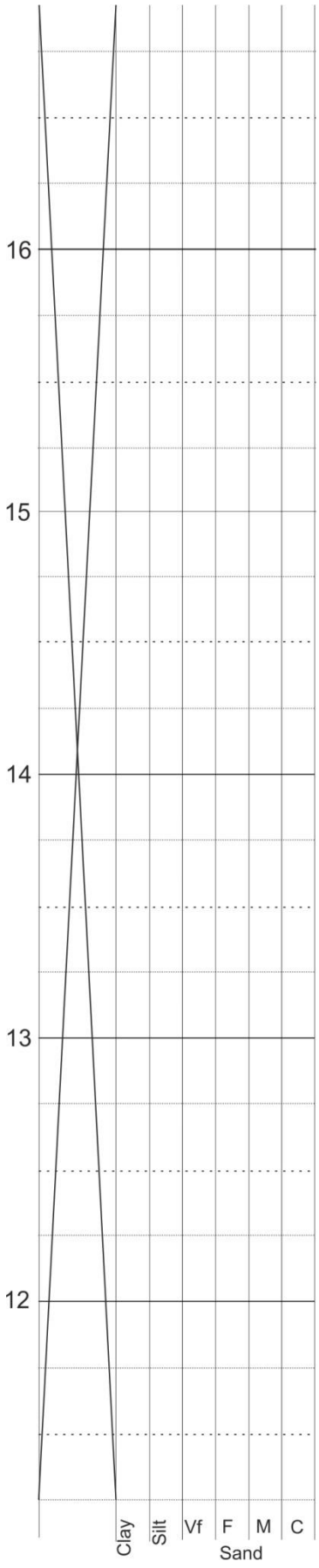
16
15
14
13
12
Clay
Silt
Vf
F
M
C
Sand

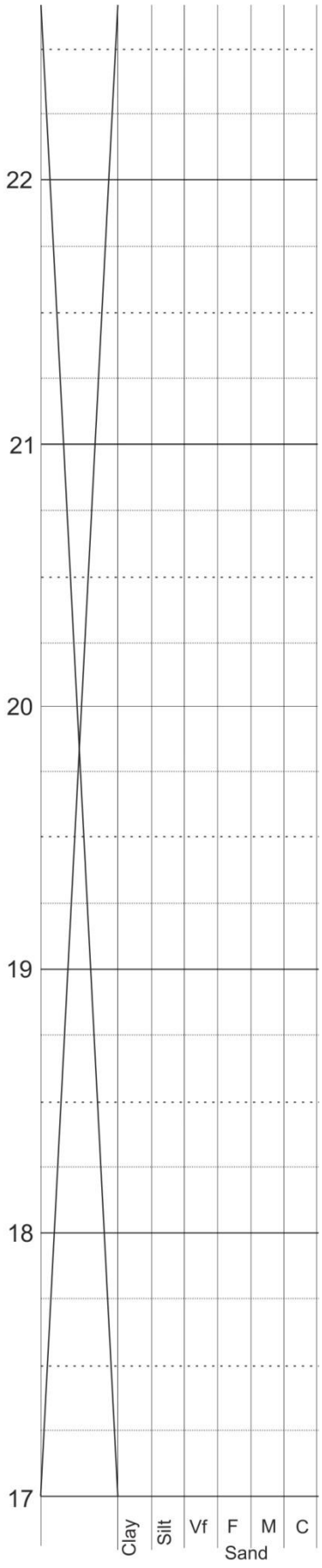
22
21
20
19
18
17
Clay
Silt
Vf
F
M
C
Sand

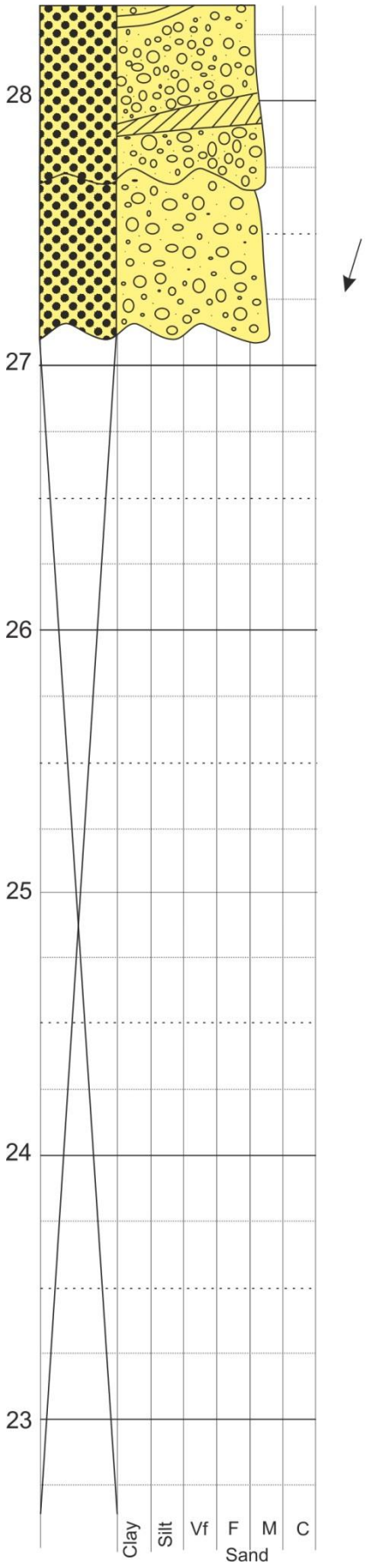
28
27
26
25
24
23
Clay
Silt
Vf
F
M
C
Sand

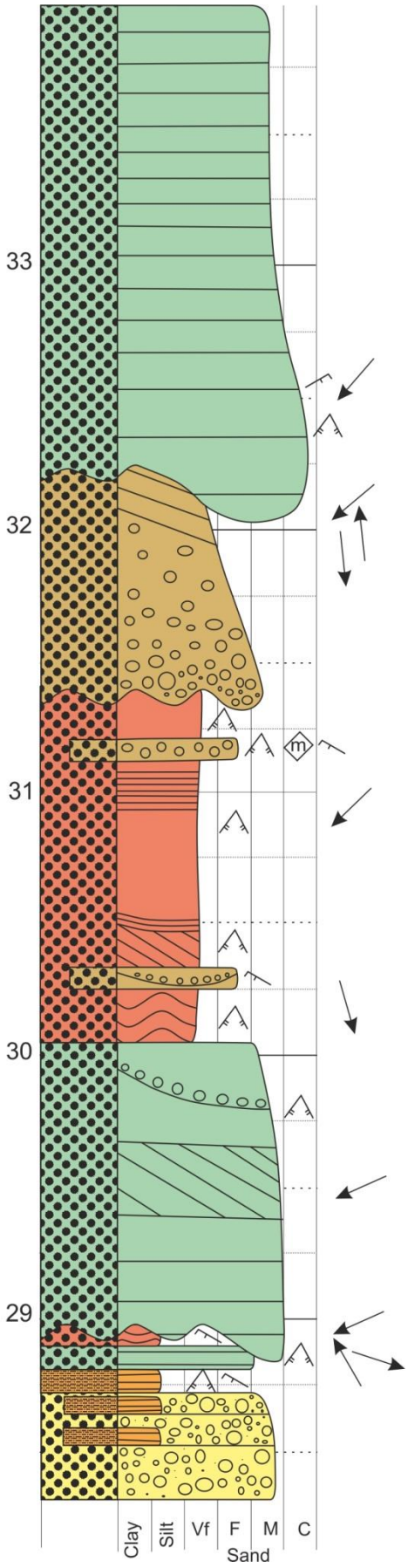
33
32
31
30
29
m
Clay
Silt
Vf
F
M
C
Sand

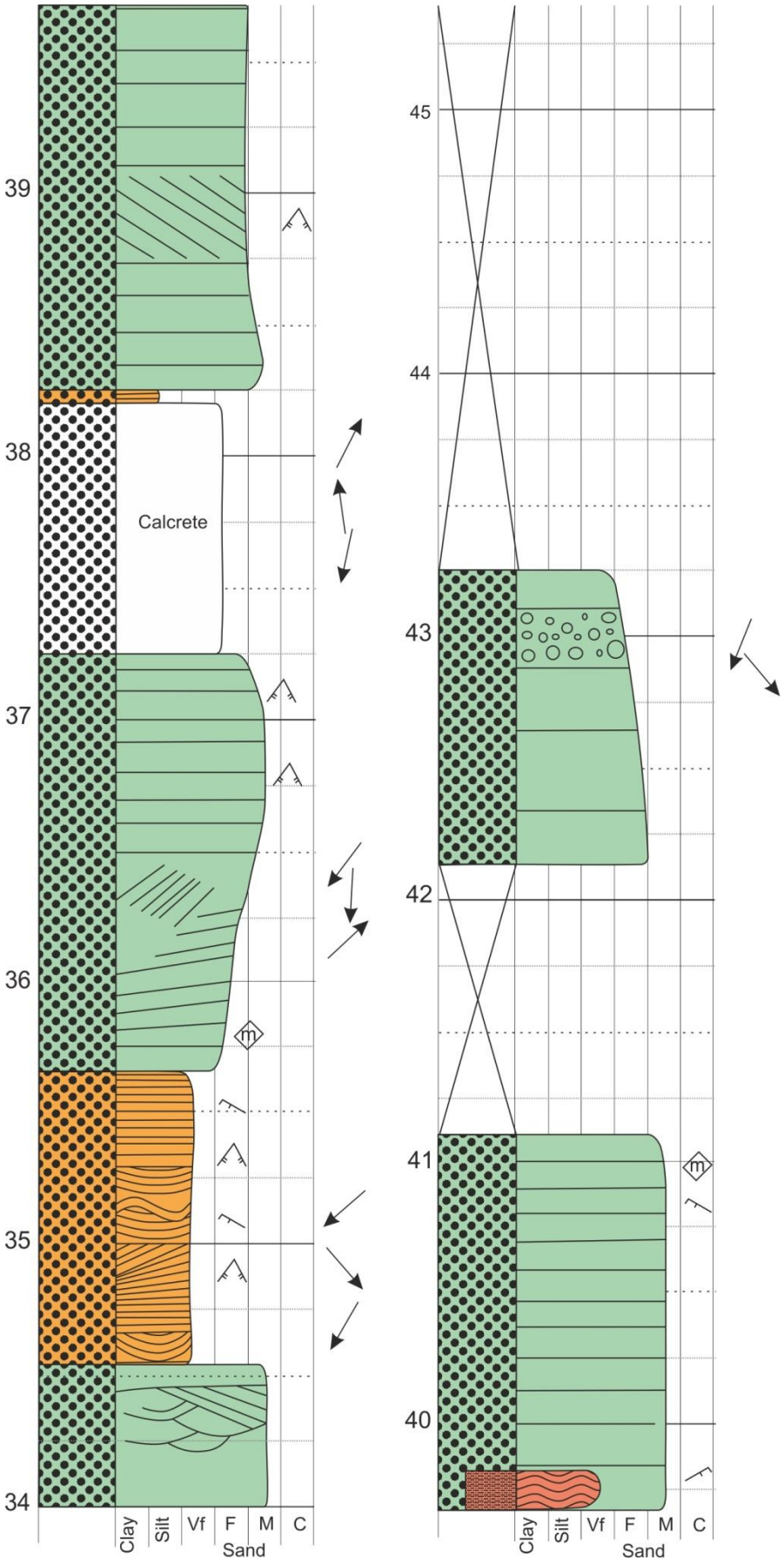
39
38
Calcrete
37
36
35
34
45
44
43
42
41
40
Clay
Silt
Vf
F
M
C
Sand

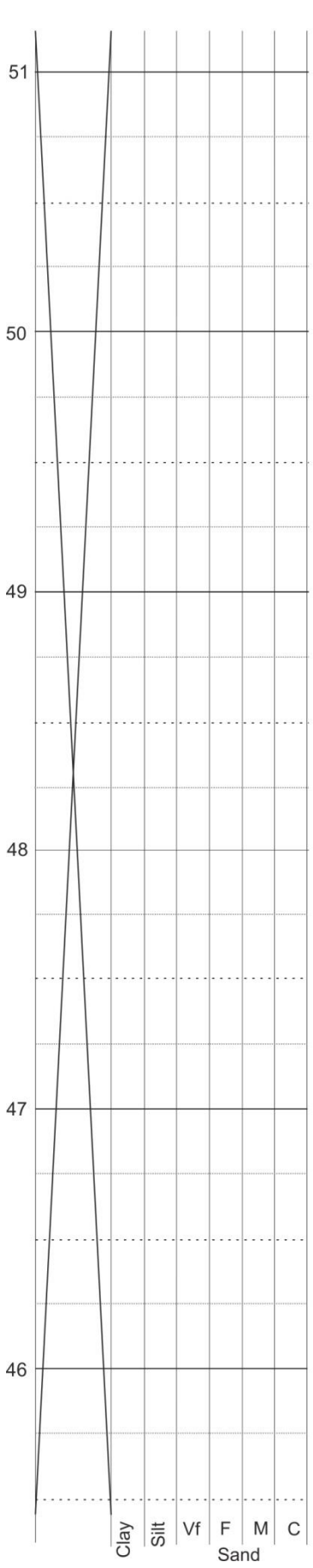
51
50
49
48
47
46
Clay
Silt
Vf
F
M
C
Sand

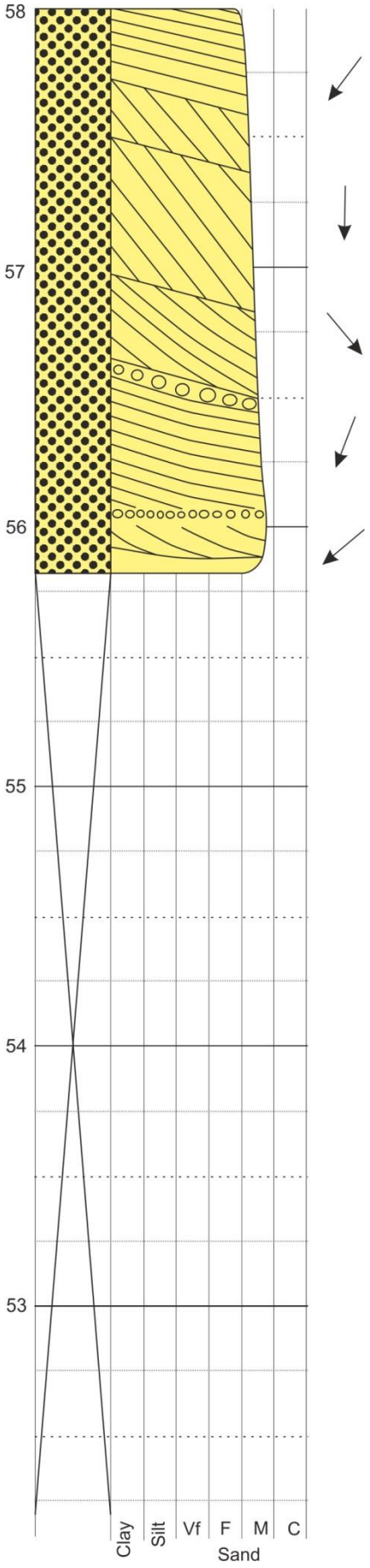
58
57
56
55
54
53
Clay
Silt
Vf
F
M
C
Sand

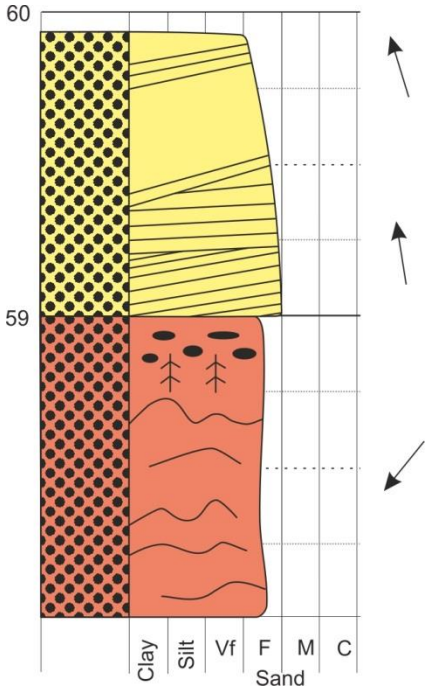
60
59
Clay
Silt
Vf
F
M
C
Sand

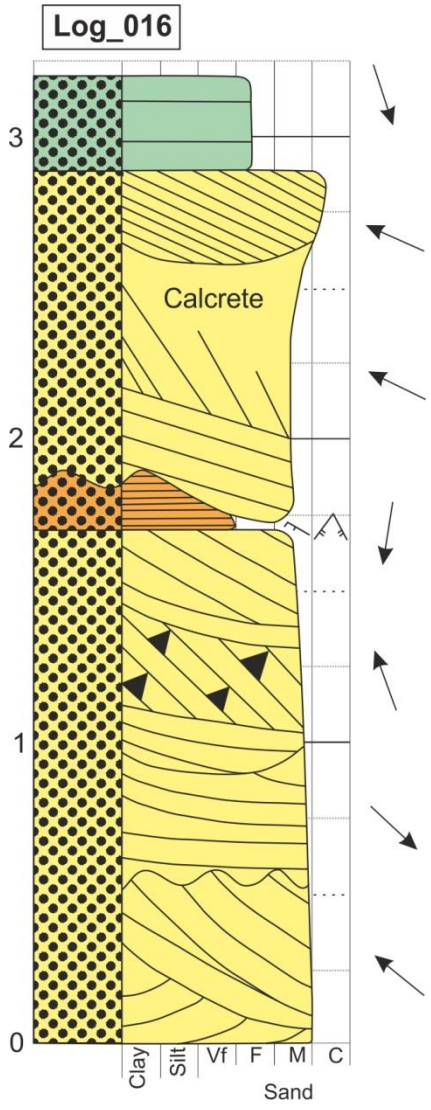
Log_016
3
2
1
0
Calcrete
Clay
Silt
Vf
F
M
C
Sand

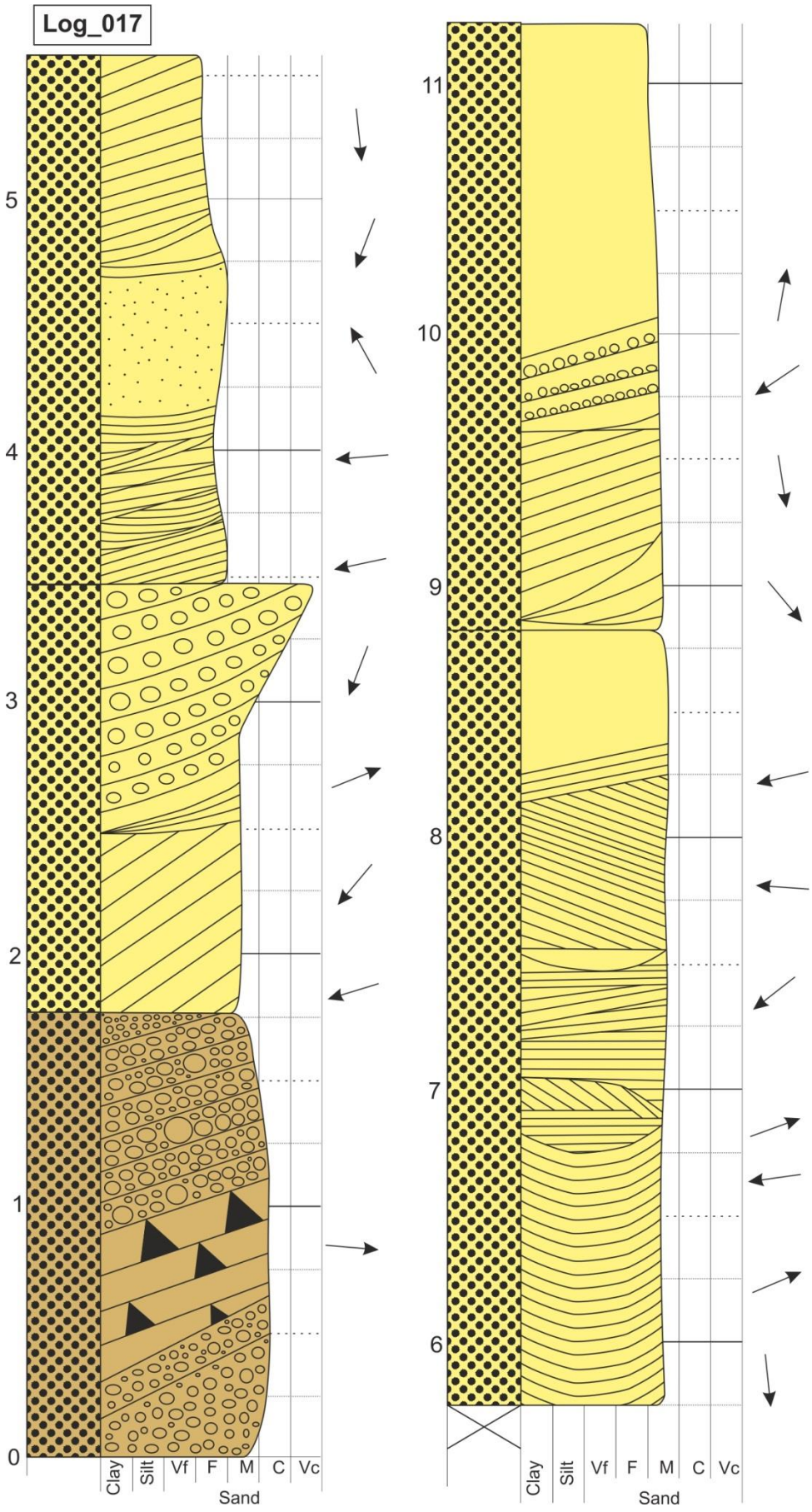
Log_017
0
1
2
3
4
5
6
7
8
9
10
11
Clay
Silt
Vf
F
M
C
Vc
Sand
Clay
Silt
Vf
F
M
C
Vc
Sand

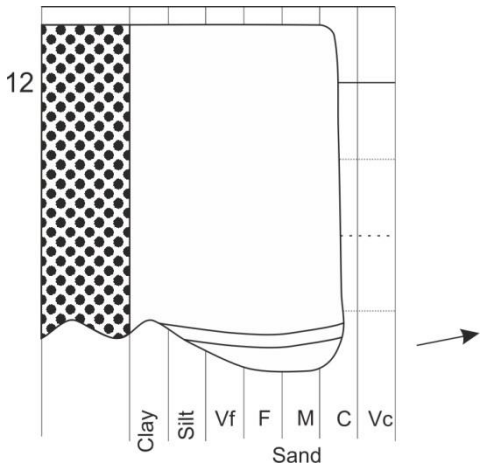
12
Clay
Silt
Vf
F
M
C
Vc
Sand

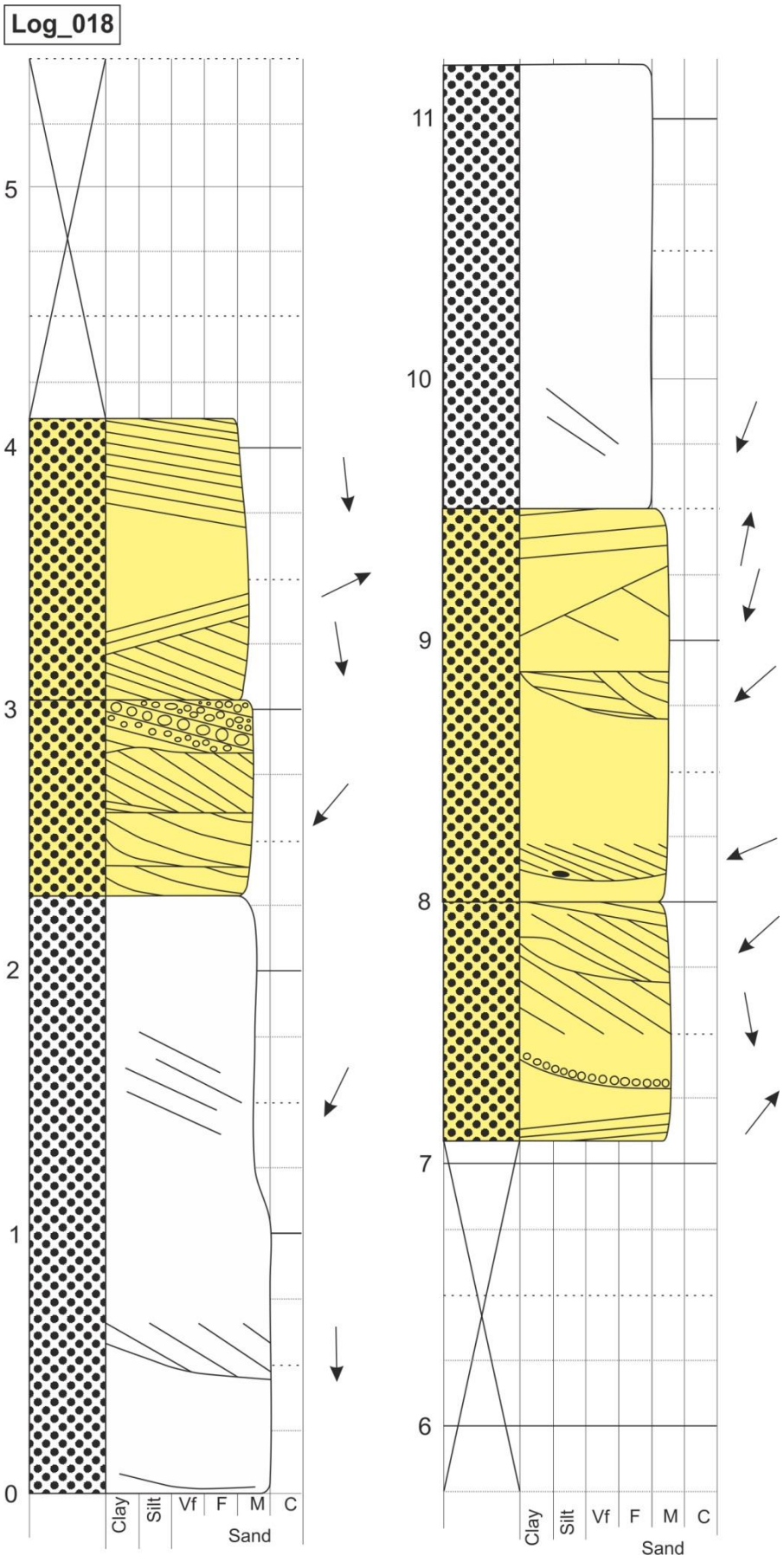
Log_018
0
1
2
3
4
5
6
7
8
9
10
11
Clay
Silt
Vf
F
M
C
Sand
Clay
Silt
Vf
F
M
C
Sand

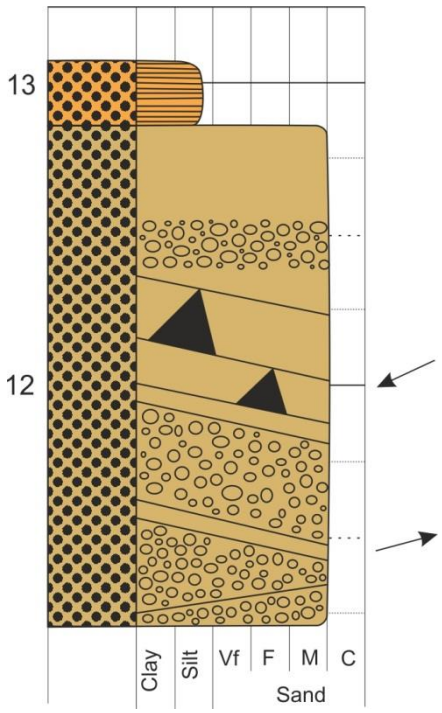
13
12
Clay
Silt
Vf
F
M
C
Sand

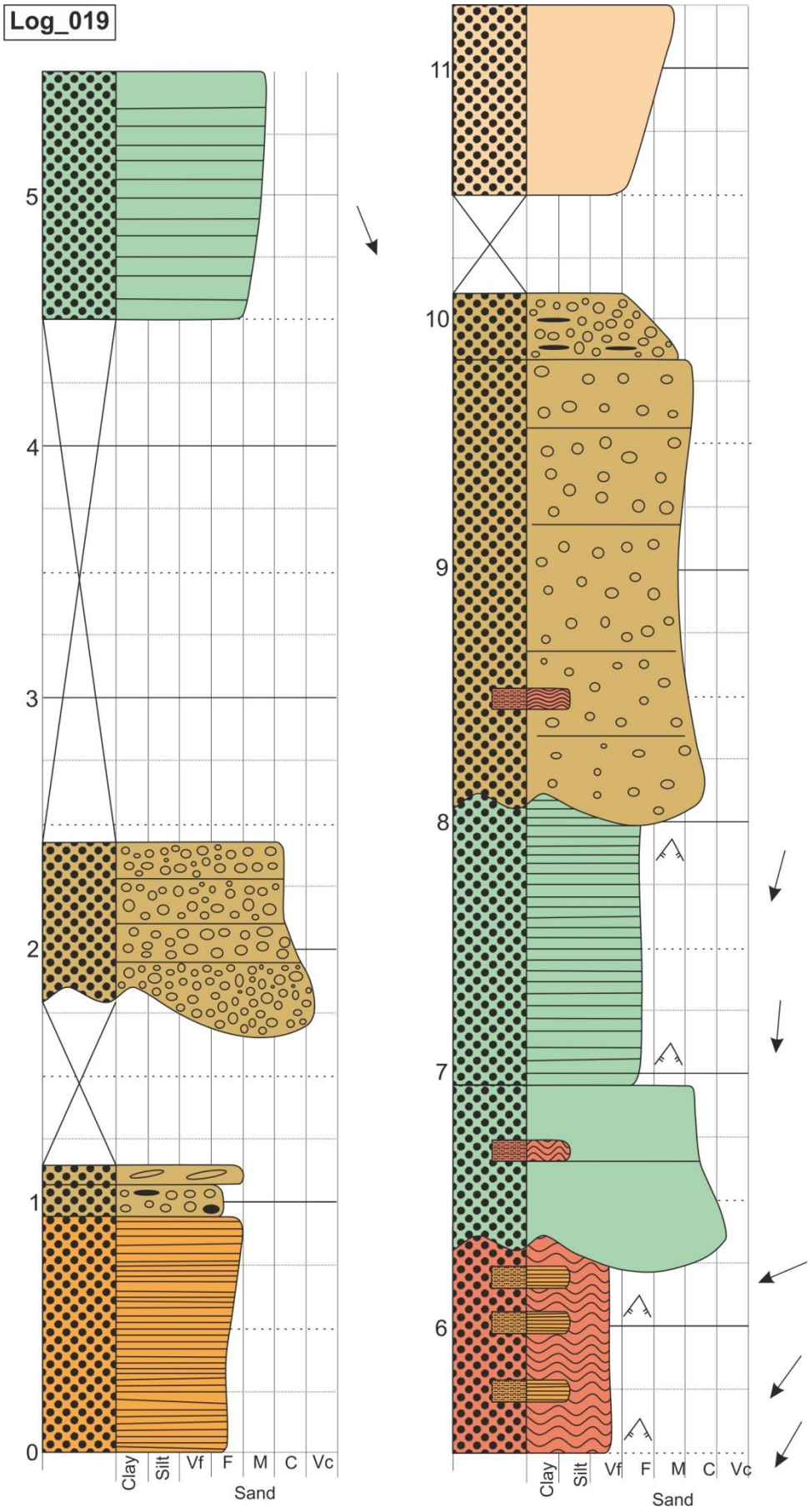
Log_019
0
1
2
3
4
5
6
7
8
9
10
11
Clay
Silt
Vf
F
M
C
Vc
Sand

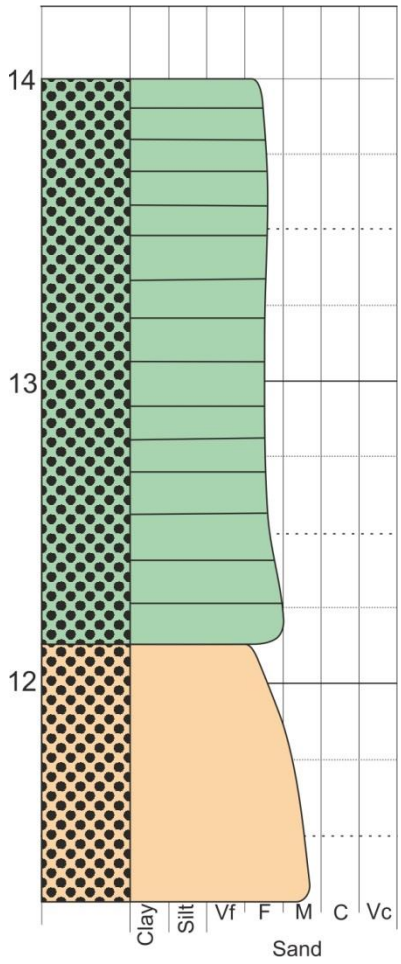
14
13
12
Clay
Silt
Vf
F
M
C
Vc
Sand

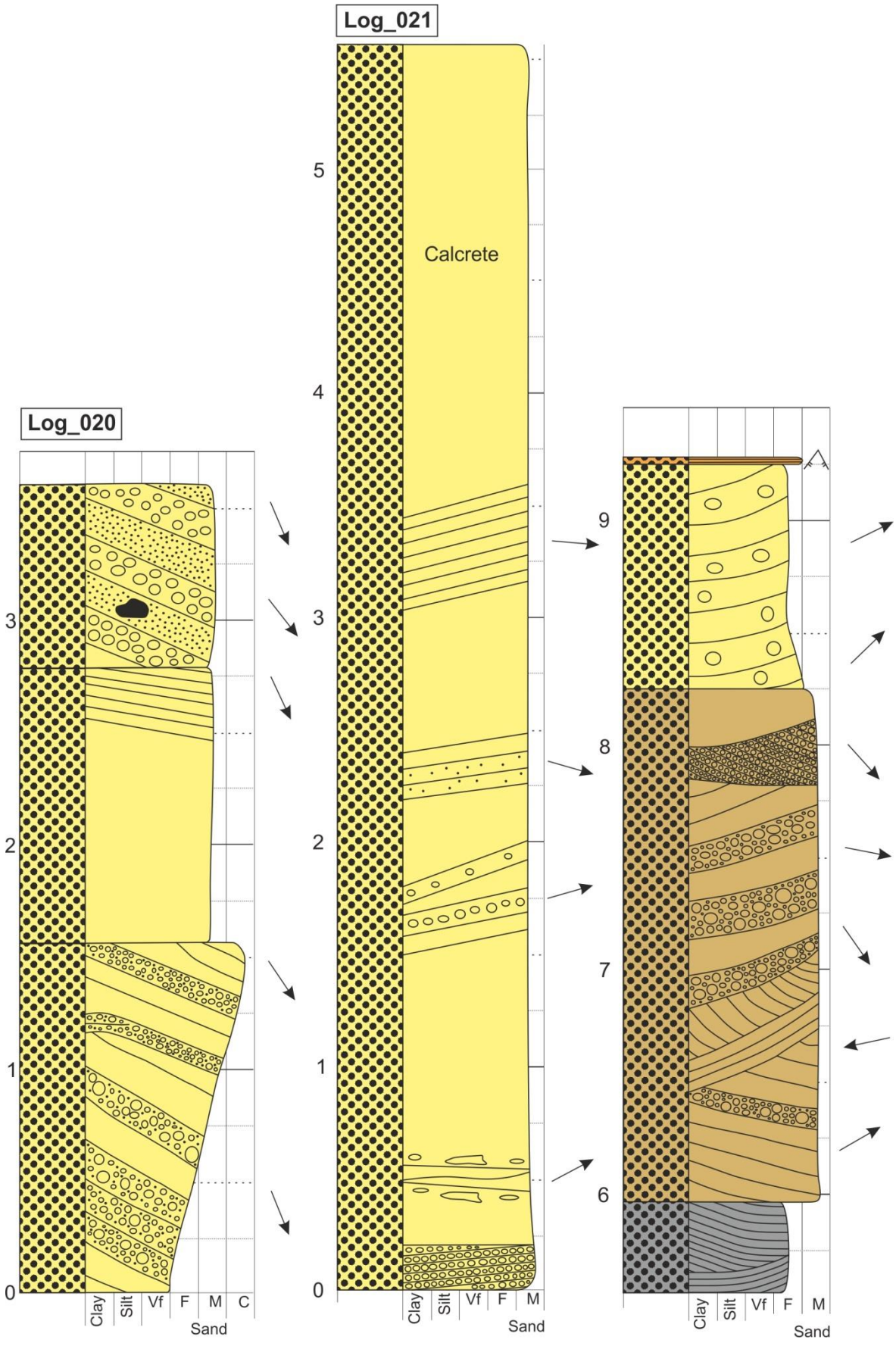
Log_020
Log_021
Calcrete
0
1
2
3
4
5
6
7
8
9
Clay
Silt
Vf
F
M
C
Sand

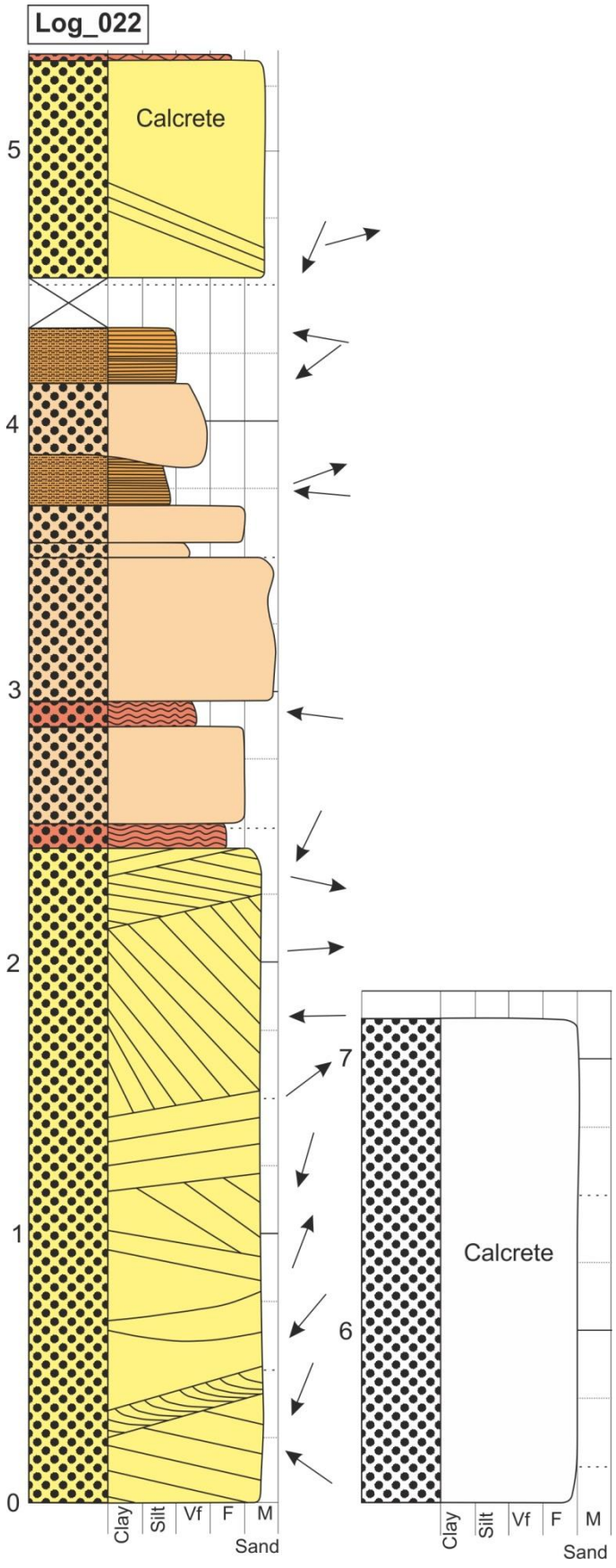
Log_022
Calcrete
5
4
3
2
1
0
Clay
Silt
Vf
F
M
Sand
7
6
Calcrete
Clay
Silt
Vf
F
M
Sand

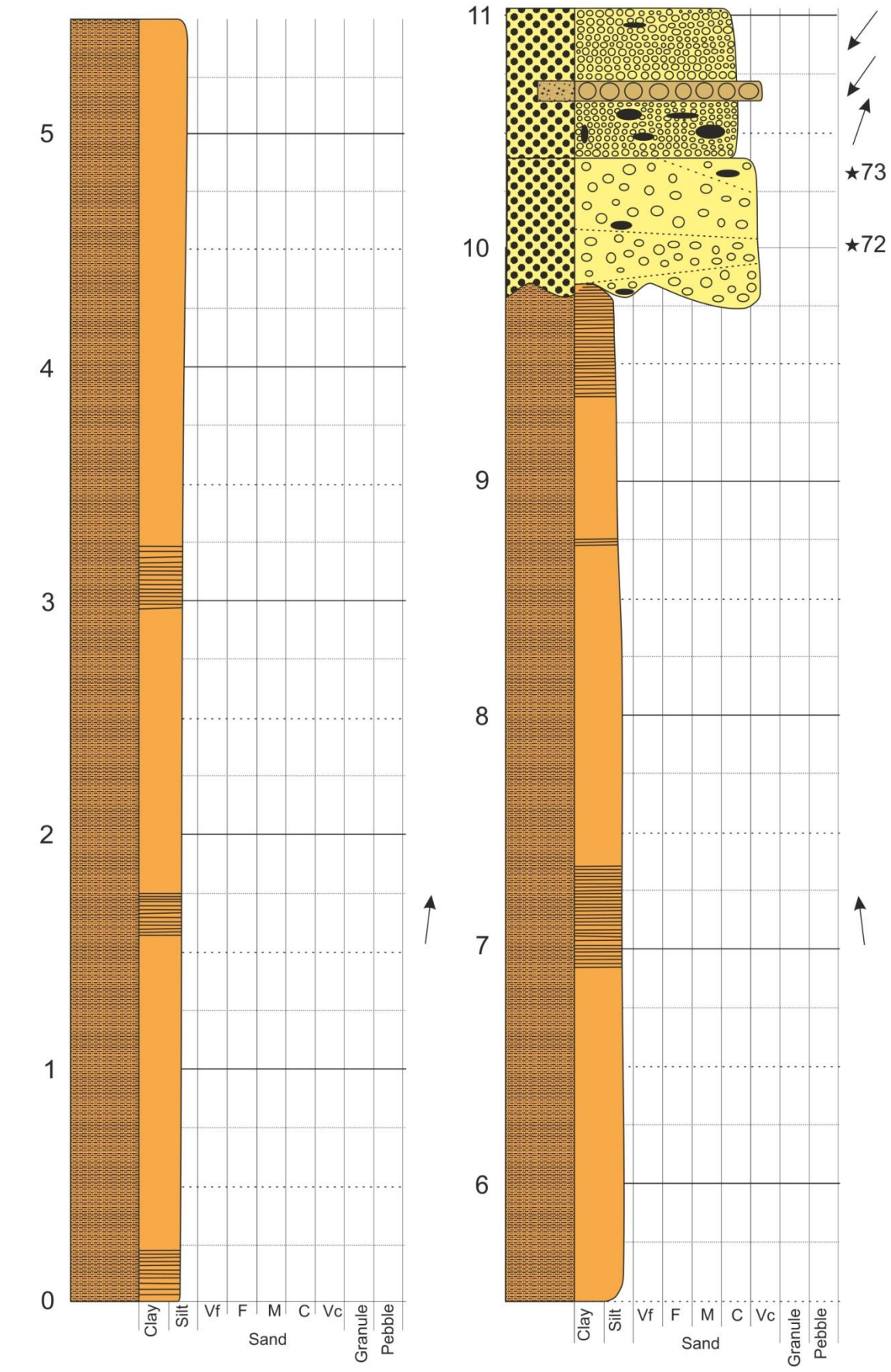
Log_023
0
1
2
3
4
5
6
7
8
9
10
11
★73
★72
Clay
Silt
Vf
F
M
C
Vc
Sand
Granule
Pebble

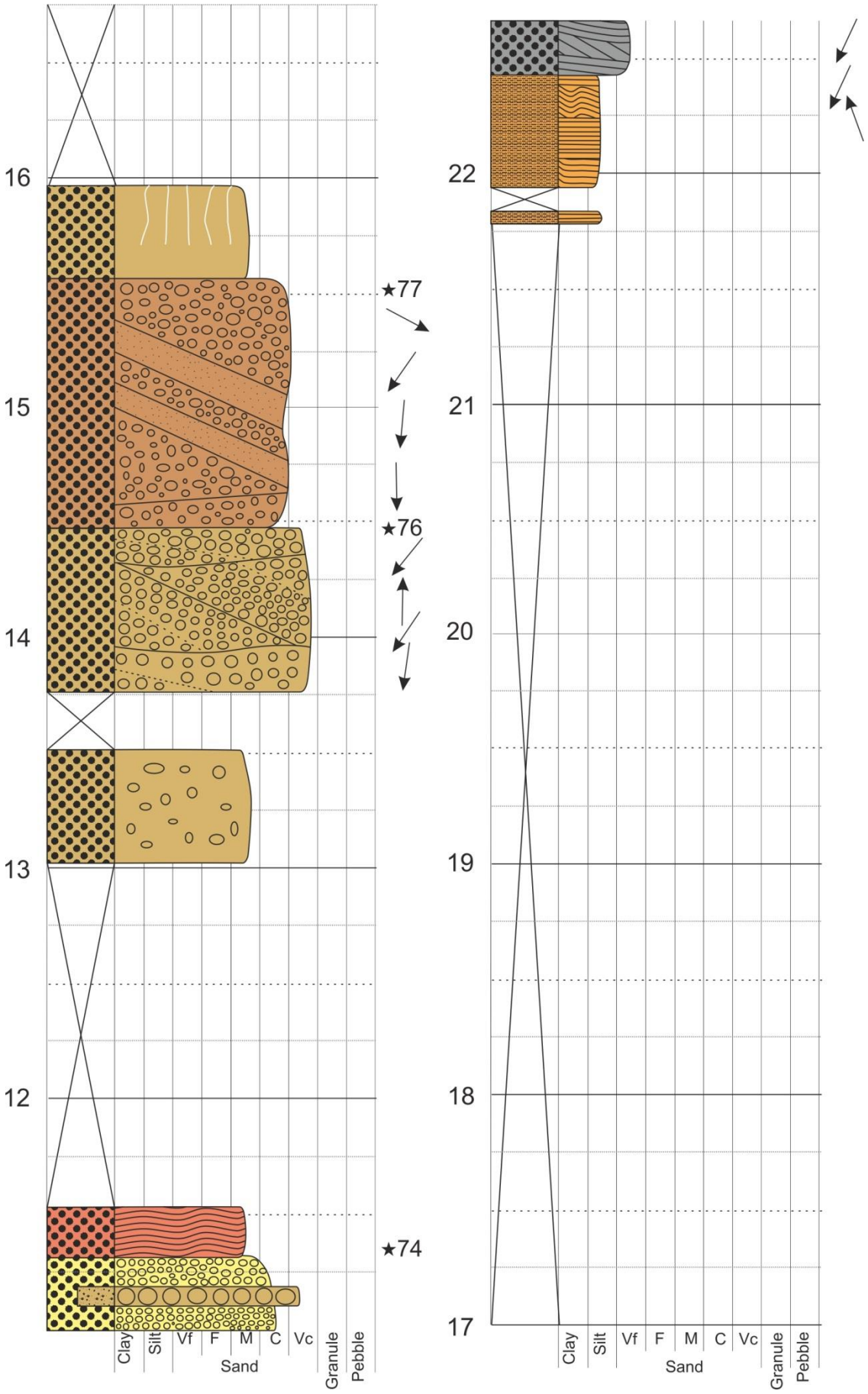
16
15
14
13
12
★77
★76
★74
Clay
Silt
Vf
F
M
C
Vc
Sand
Granule
Pebble
22
21
20
19
18
17
Clay
Silt
Vf
F
M
C
Vc
Sand
Granule
Pebble

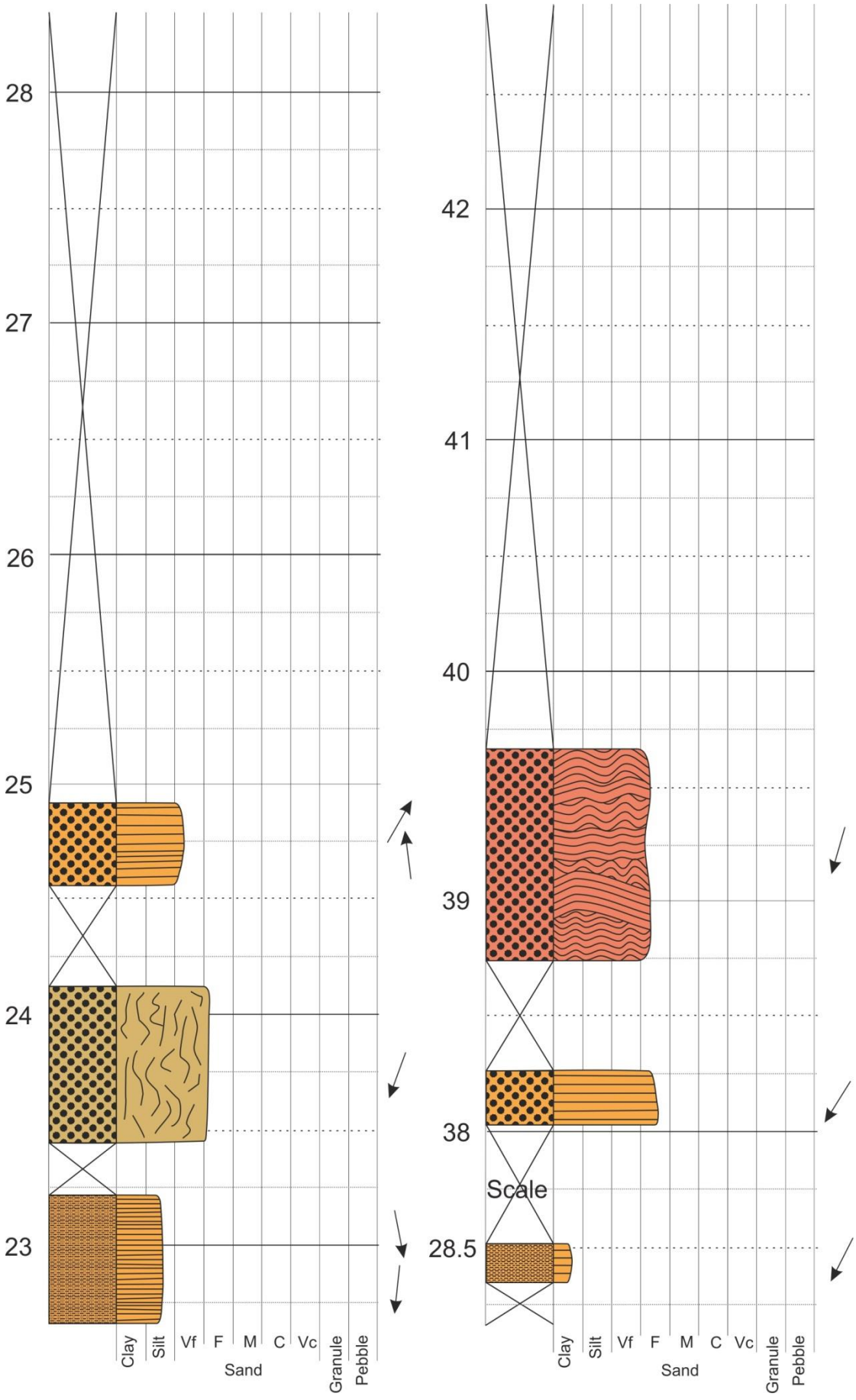
28
27
26
25
24
23
42
41
40
39
38
28.5
Scale
Clay
Silt
Vf
F
M
C
Vc
Sand
Granule
Pebble

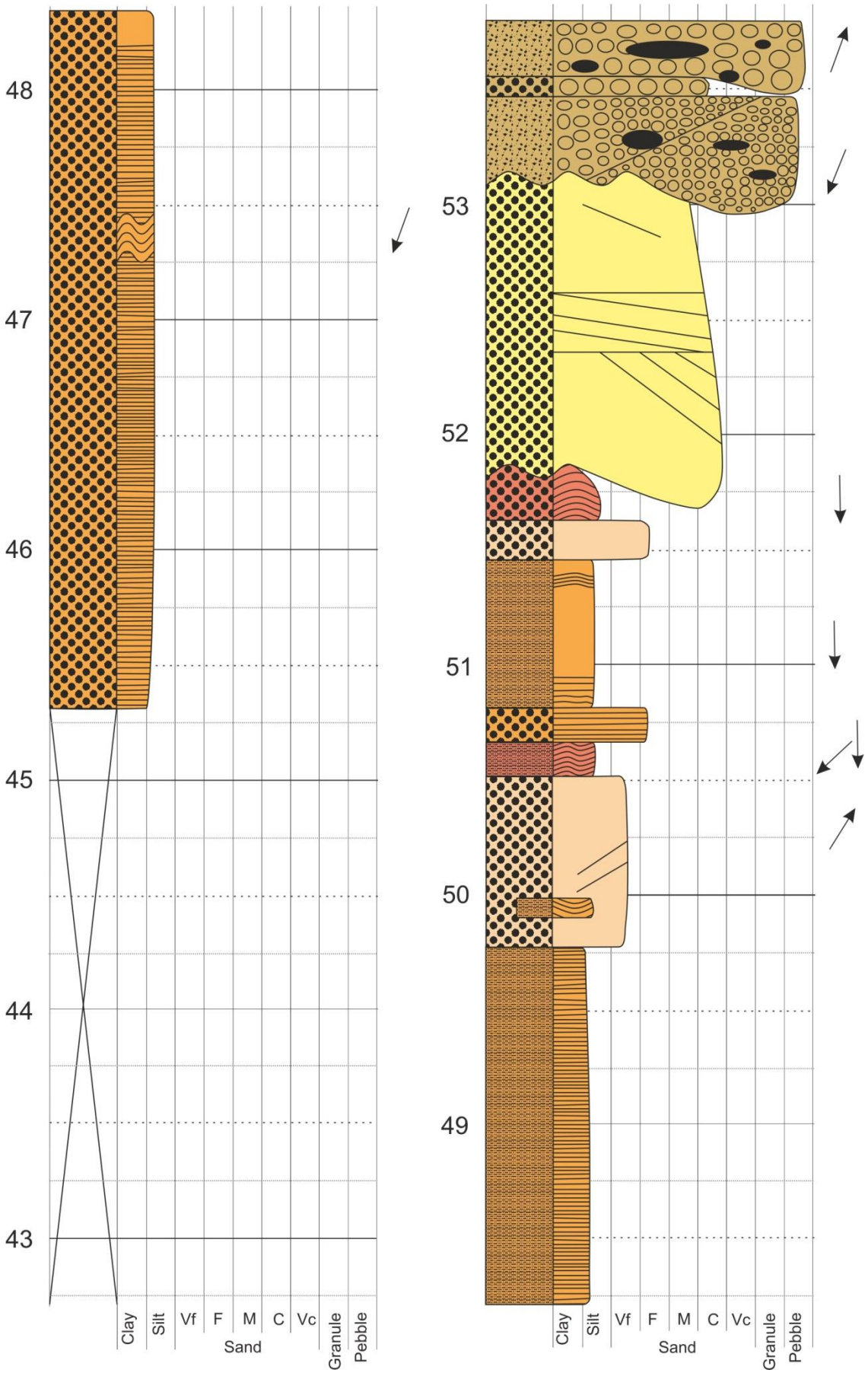
48
47
46
45
44
43
53
52
51
50
49
Clay
Silt
Vf
F
M
C
Vc
Sand
Granule
Pebble

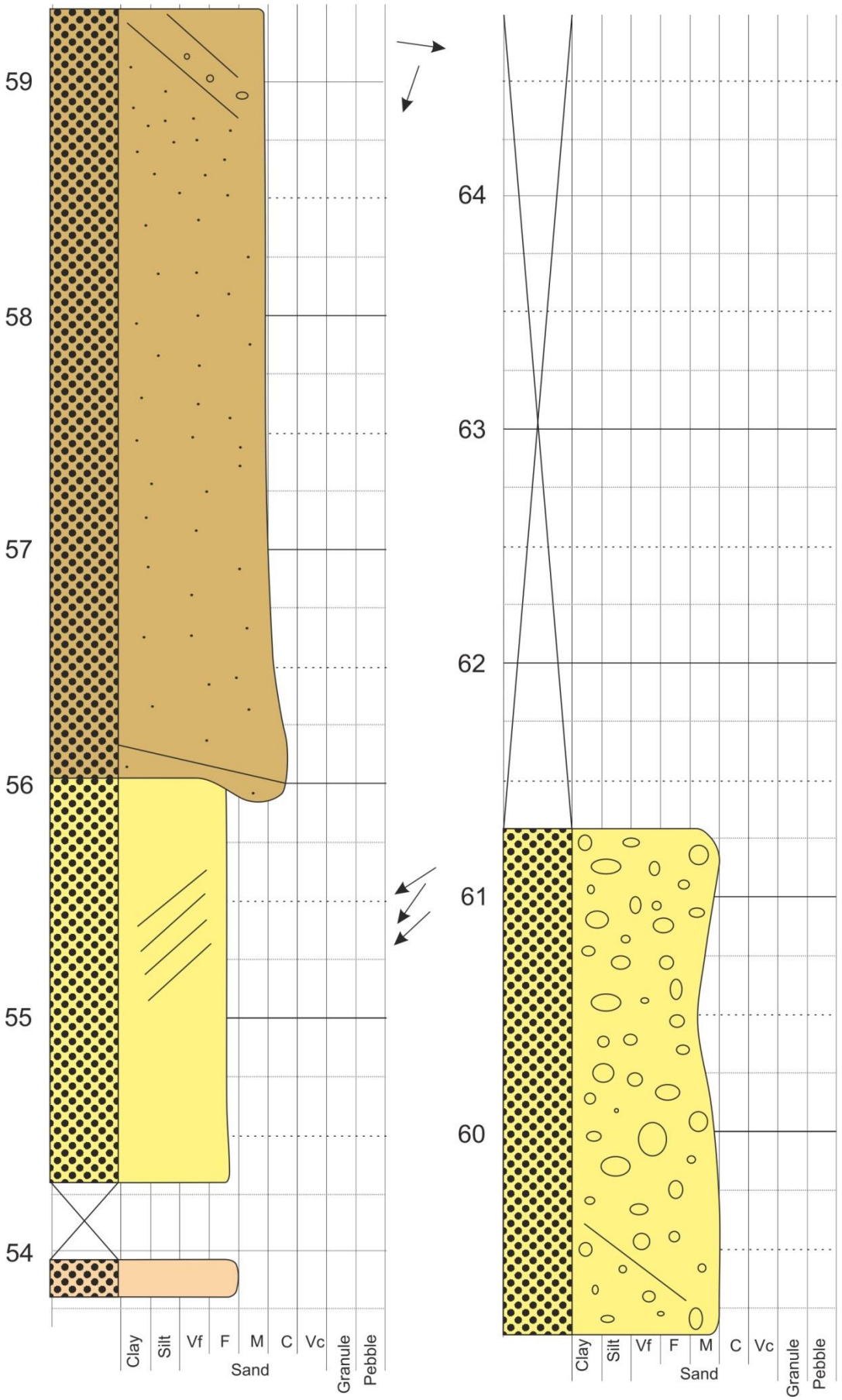
59
58
57
56
55
54
64
63
62
61
60
Clay
Silt
Vf
F
M
C
Vc
Sand
Granule
Pebble

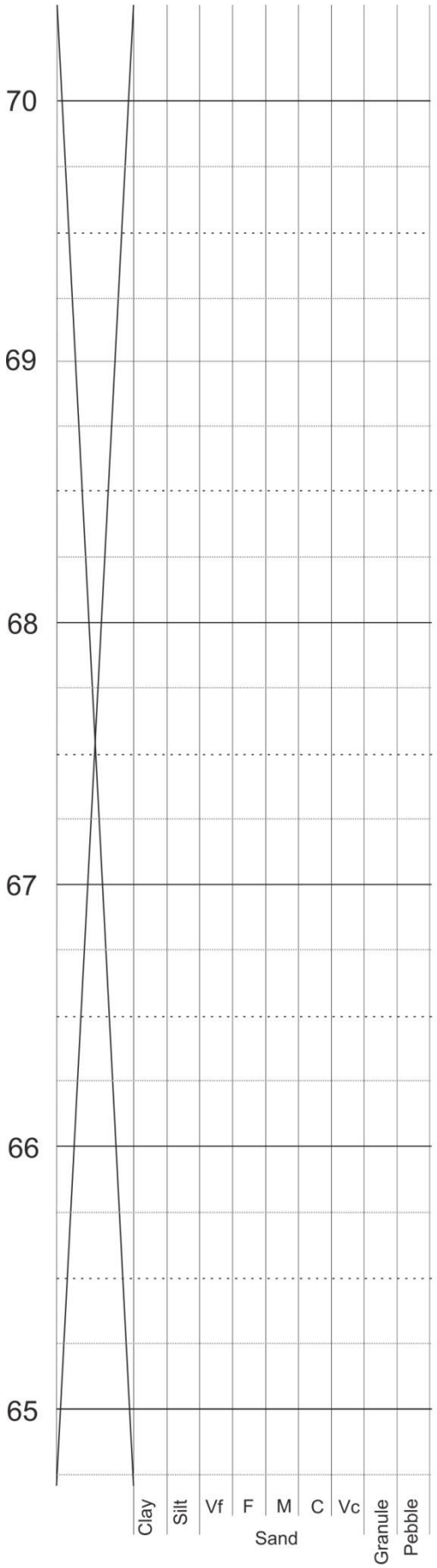
70
69
68
67
66
65
Clay
Silt
Vf
F
M
C
Vc
Sand
Granule
Pebble

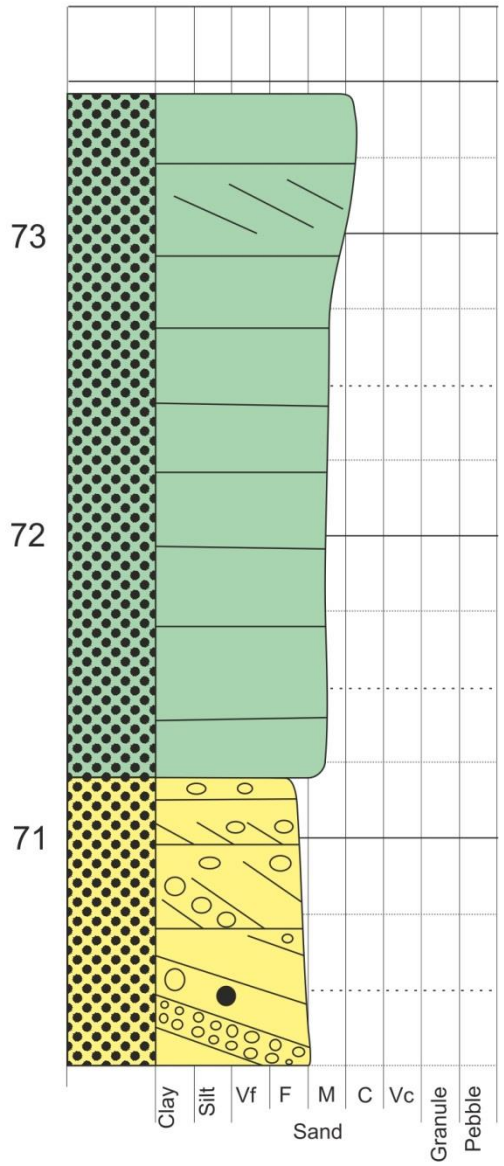
73
72
71
Clay
Silt
Vf
F
M
C
Vc
Sand
Granule
Pebble

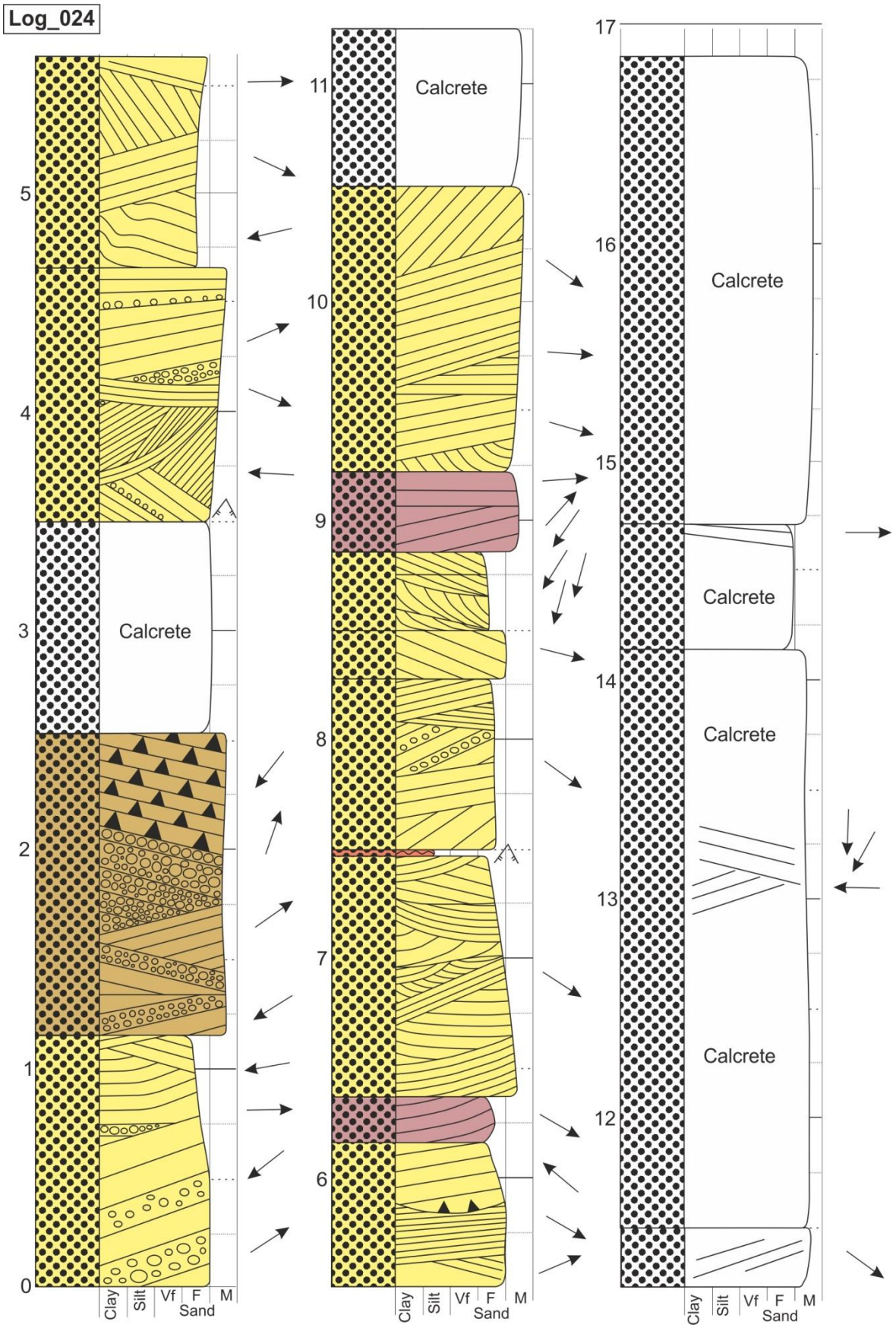
Log_024
Calcrete
Calcrete
Calcrete
Calcrete
Calcrete
0
1
2
3
4
5
6
7
8
9
10
11
12
13
14
15
16
17
Clay
Silt
Vf
F
M
Sand

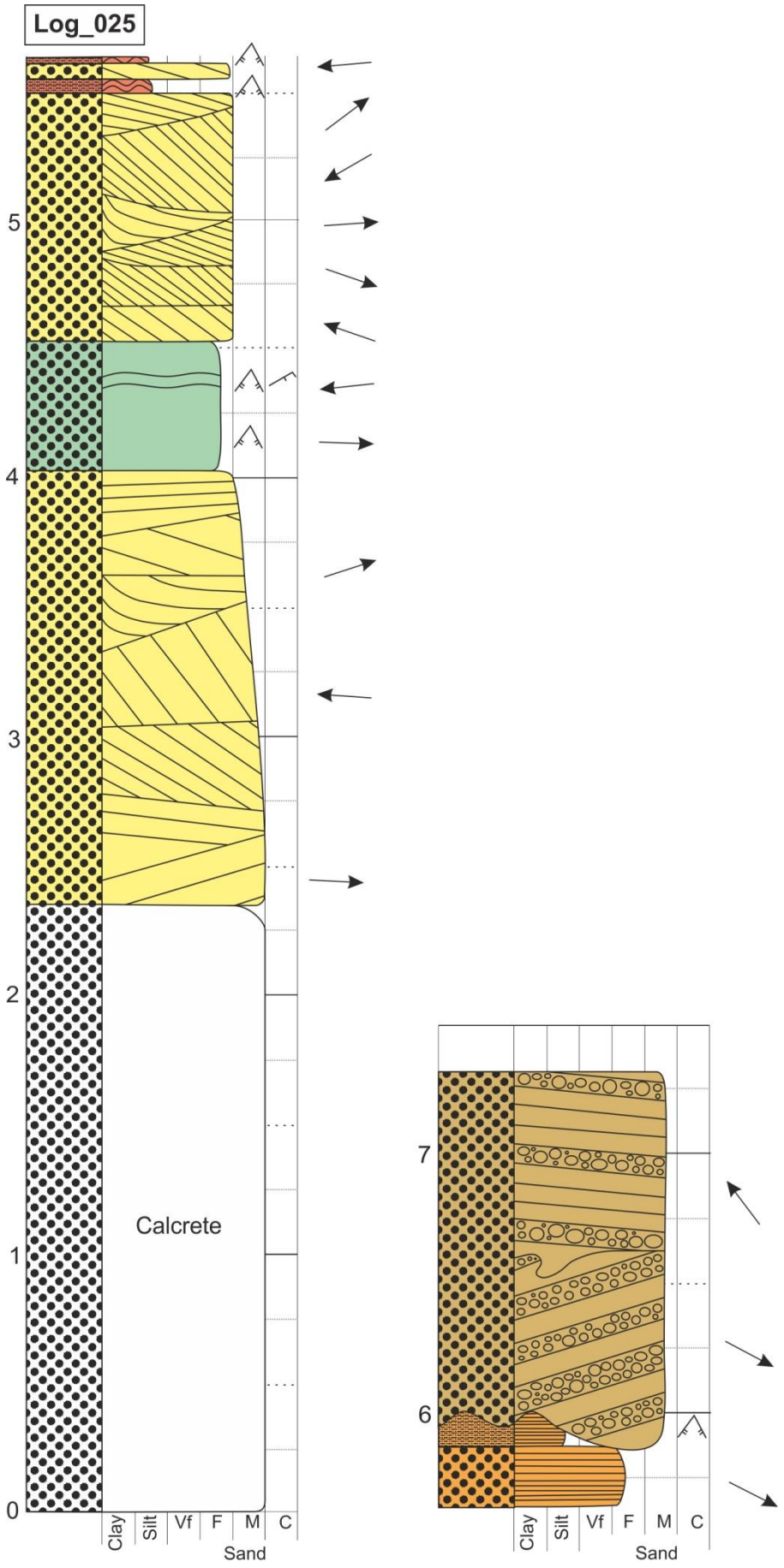
Log_025
5
4
3
2
1
0
Calcrete
Clay
Silt
Vf
F
M
C
Sand
7
6
Clay
Silt
Vf
F
M
C
Sand

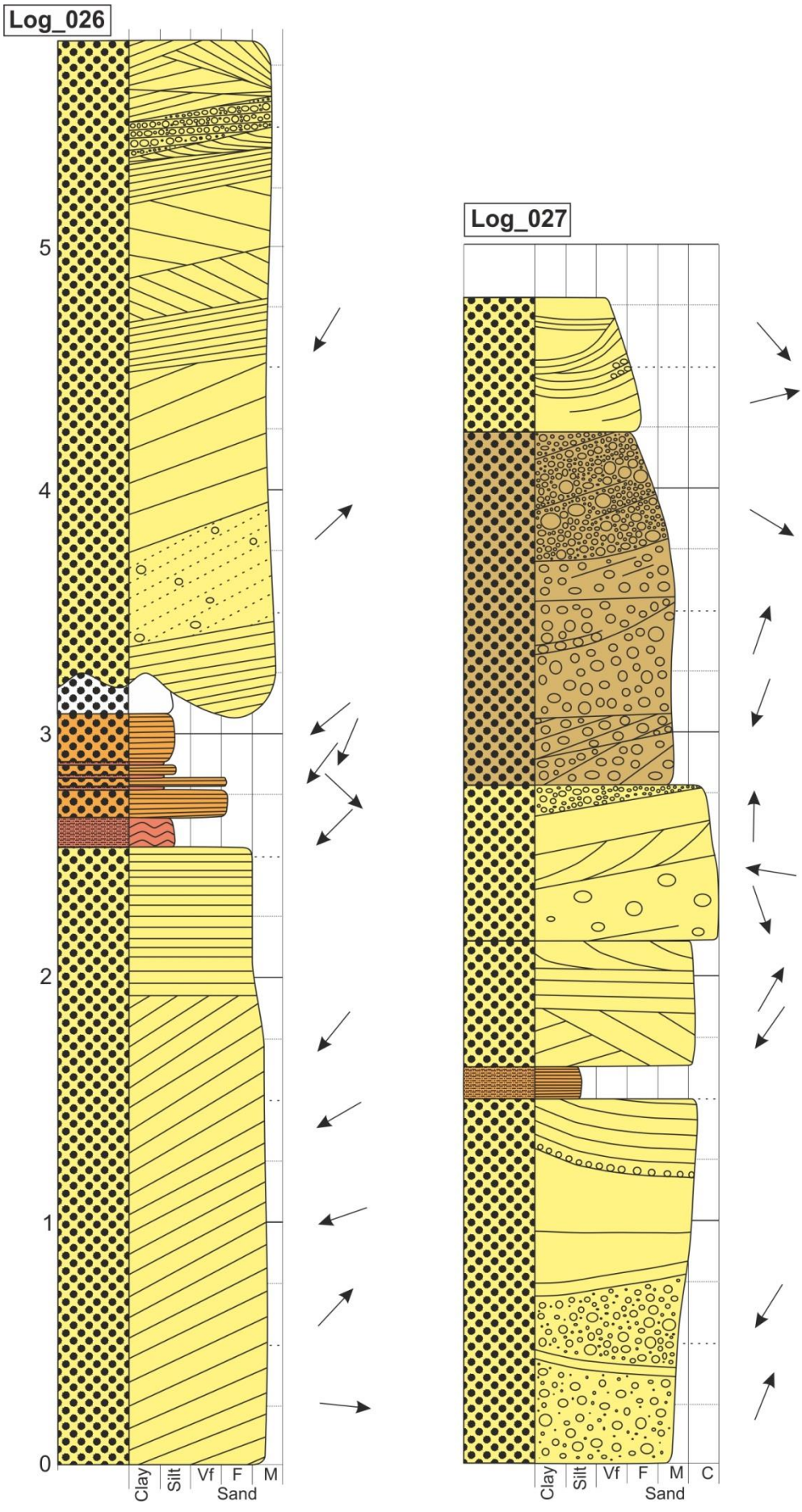
Log_026
5
4
3
2
1
0
Clay
Silt
Vf
F
M
Sand
Log_027
Clay
Silt
Vf
F
M
C
Sand

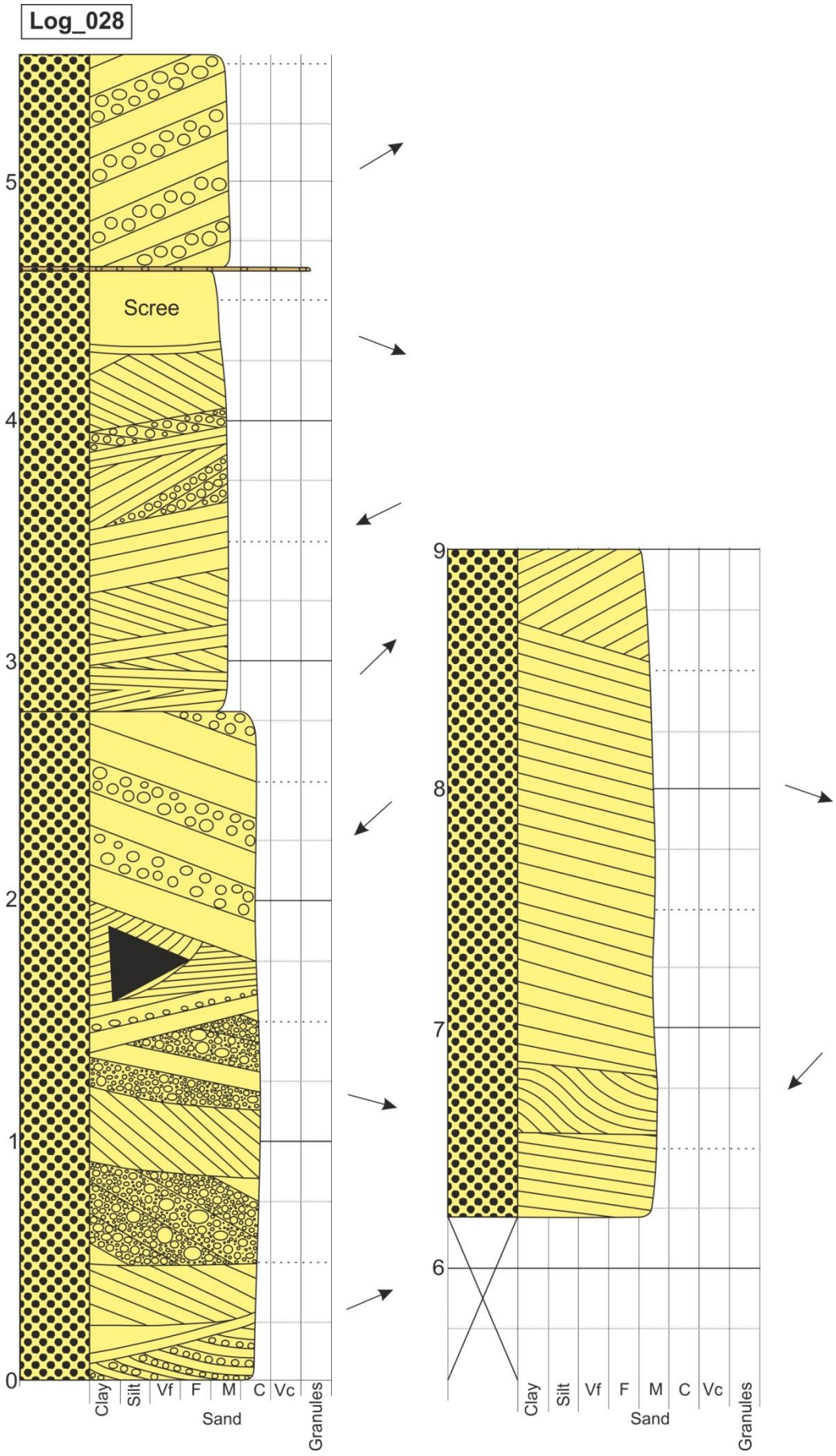
Log_028
Scree
5
4
3
2
1
0
9
8
7
6
Clay
Silt
Vf
F
M
C
Vc
Sand
Granules

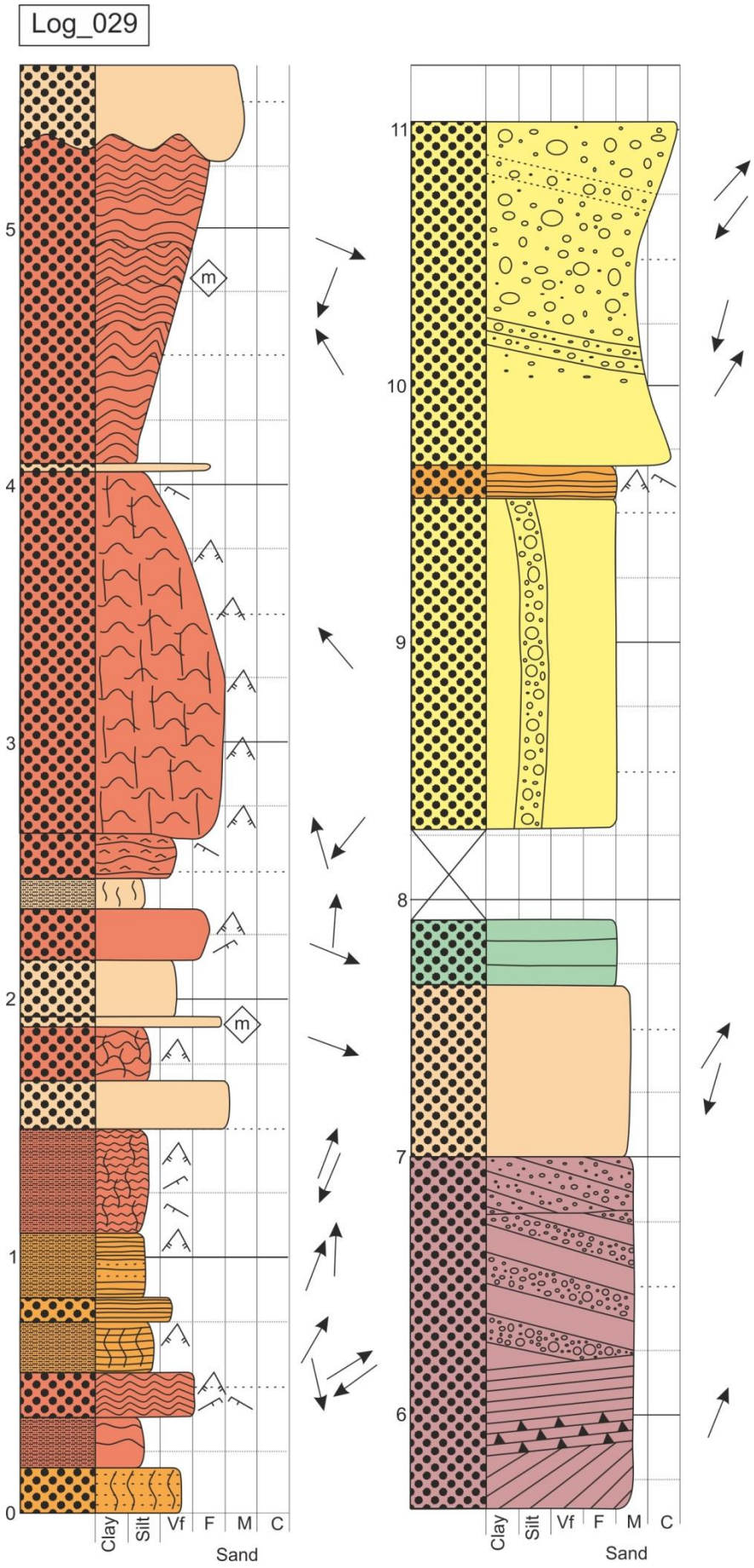
Log_029
0
1
2
3
4
5
6
7
8
9
10
11
m
m
Clay
Silt
Vf
F
M
C
Sand
Clay
Silt
Vf
F
M
C
Sand

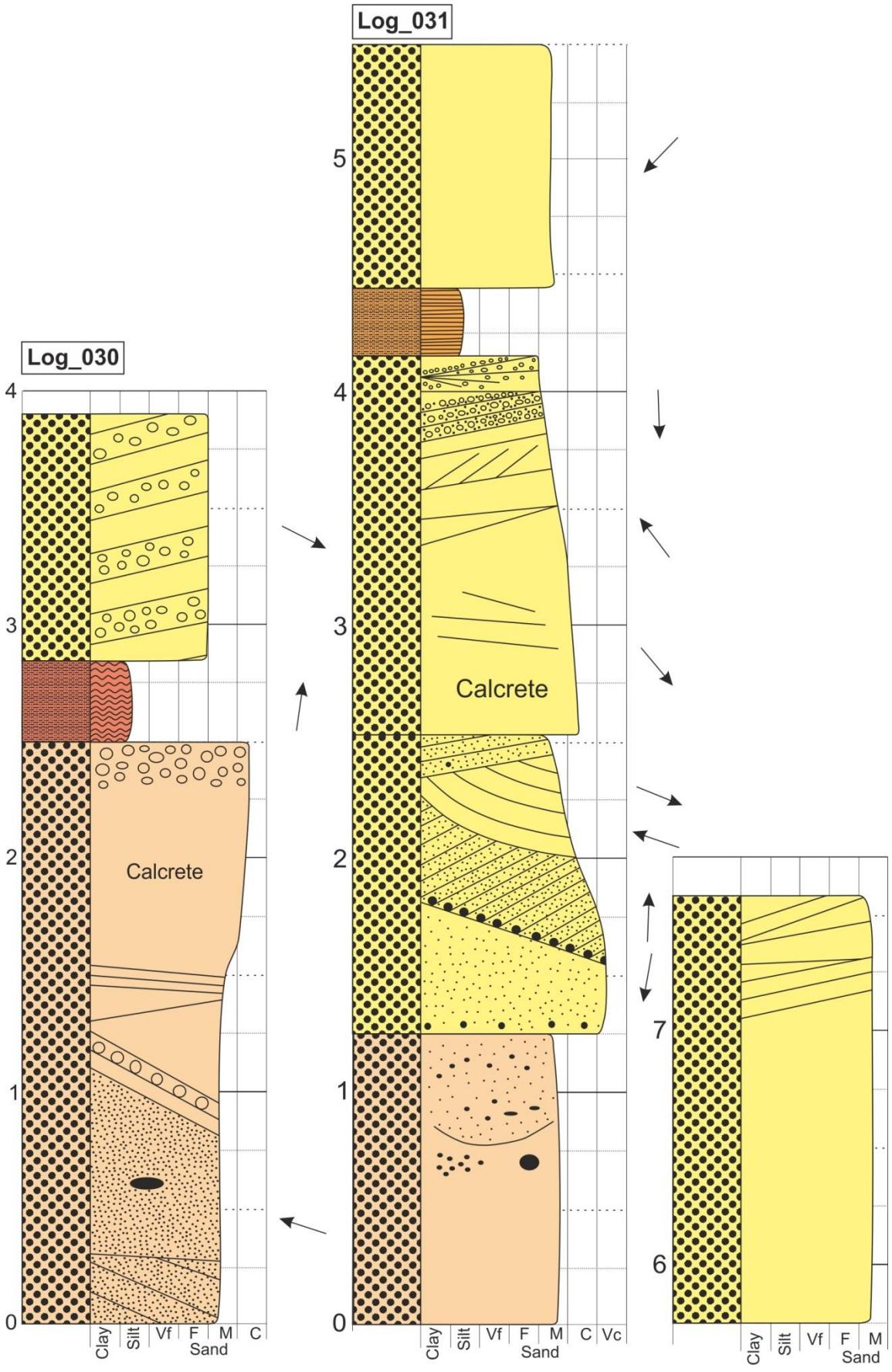
Log_031
Log_030
Calcrete
Calcrete
Clay
Silt
Vf
F
M
C
Vc
Sand
0
1
2
3
4
5
6
7

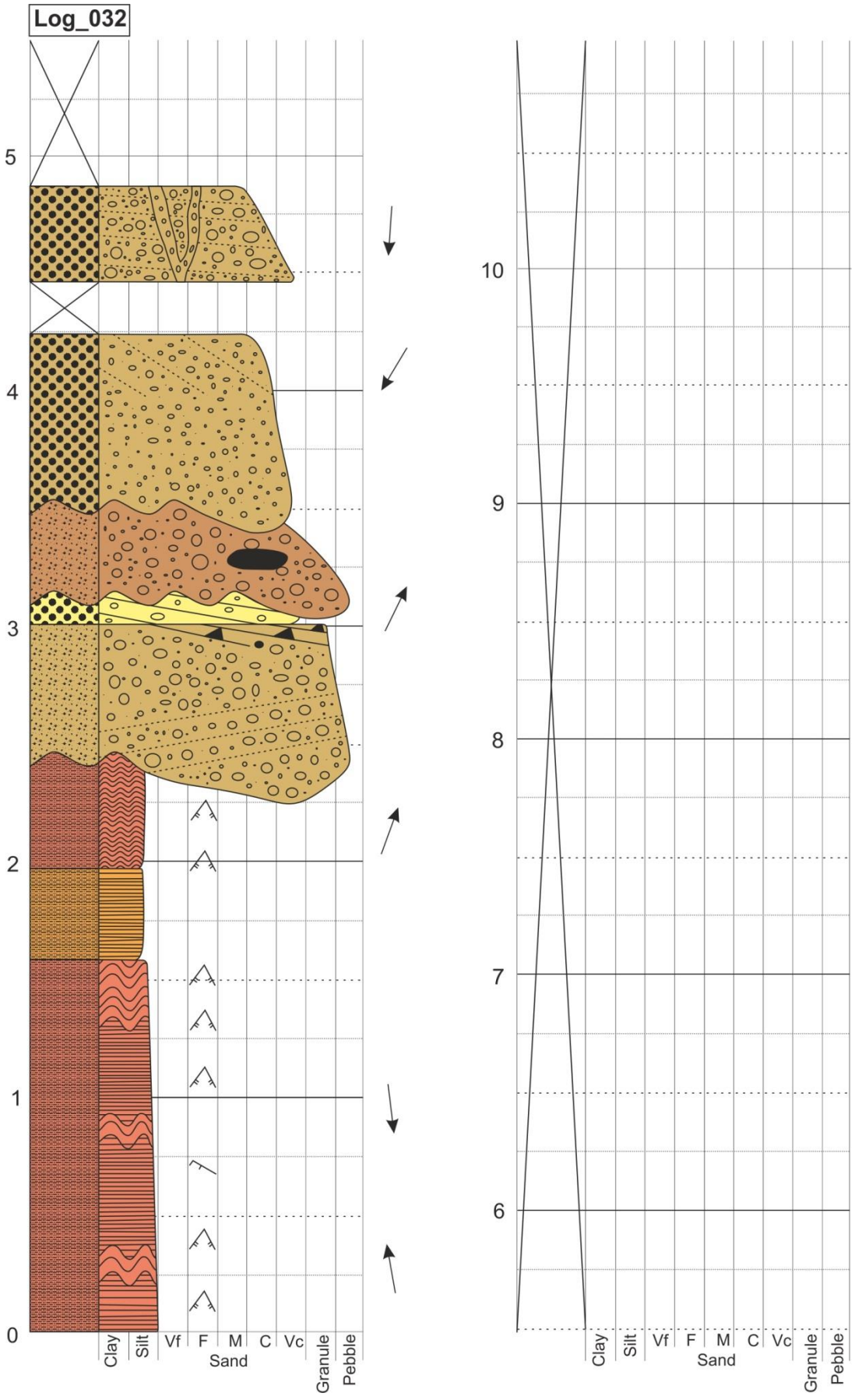
Log_032
5
4
3
2
1
0
10
9
8
7
6
Clay
Silt
Vf
F
M
C
Vc
Sand
Granule
Pebble

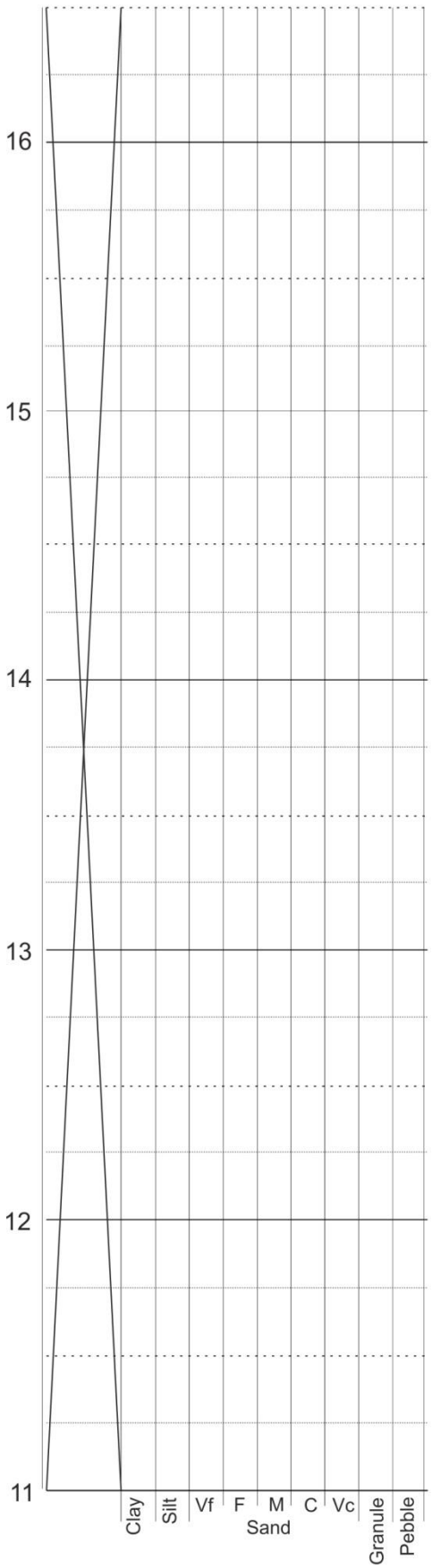
16
15
14
13
12
11
Clay
Silt
Vf
F
M
C
Vc
Sand
Granule
Pebble

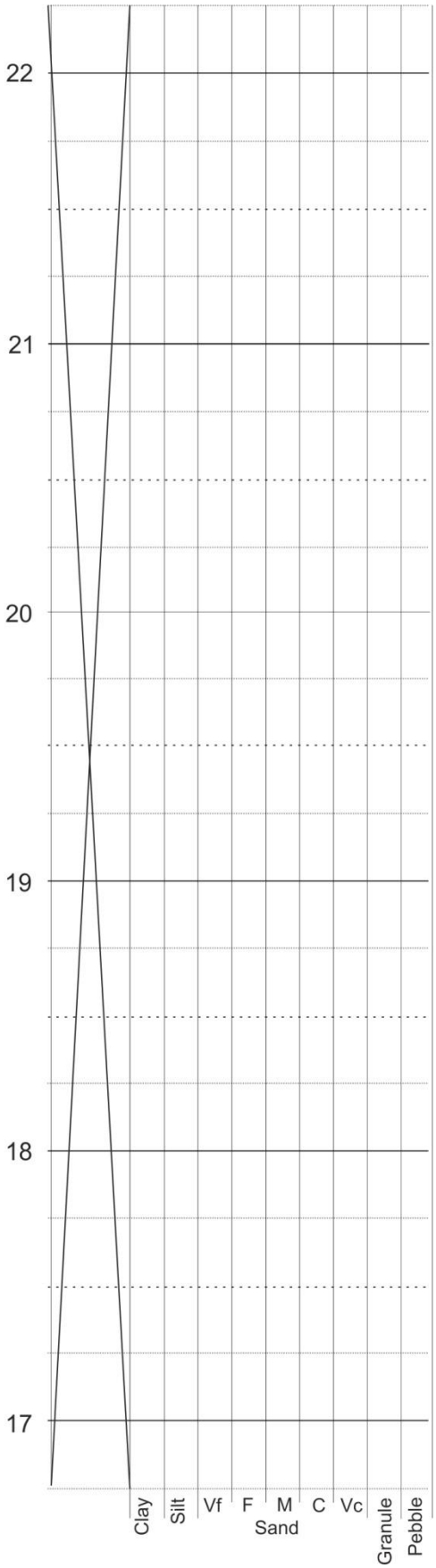
22
21
20
19
18
17
Clay
Silt
Vf
F
M
C
Vc
Sand
Granule
Pebble

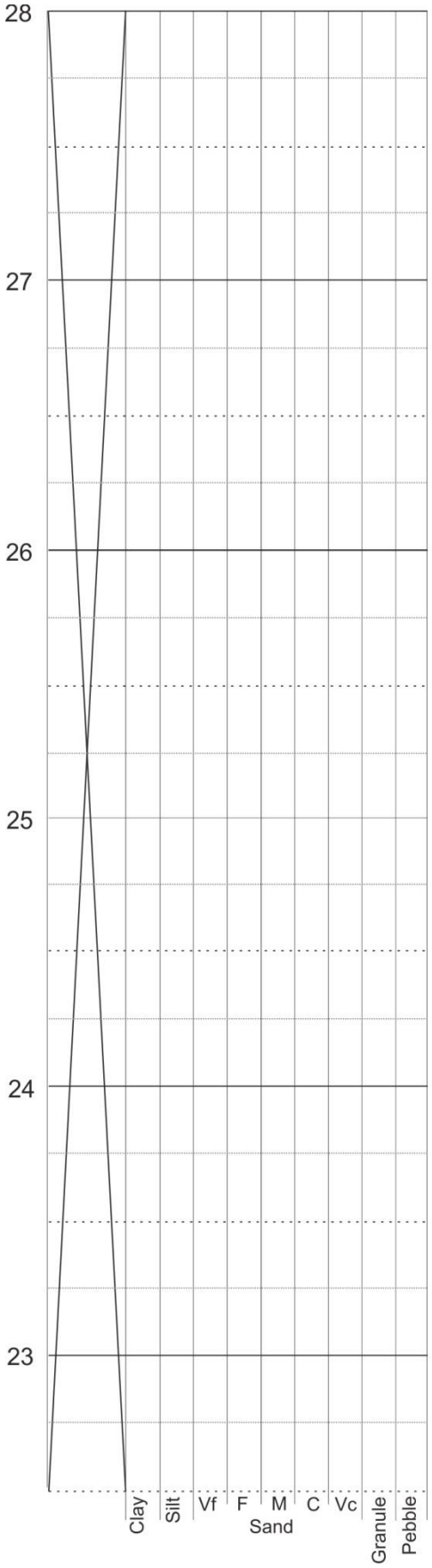
28
27
26
25
24
23
Clay
Silt
Vf
F
M
C
Vc
Sand
Granule
Pebble

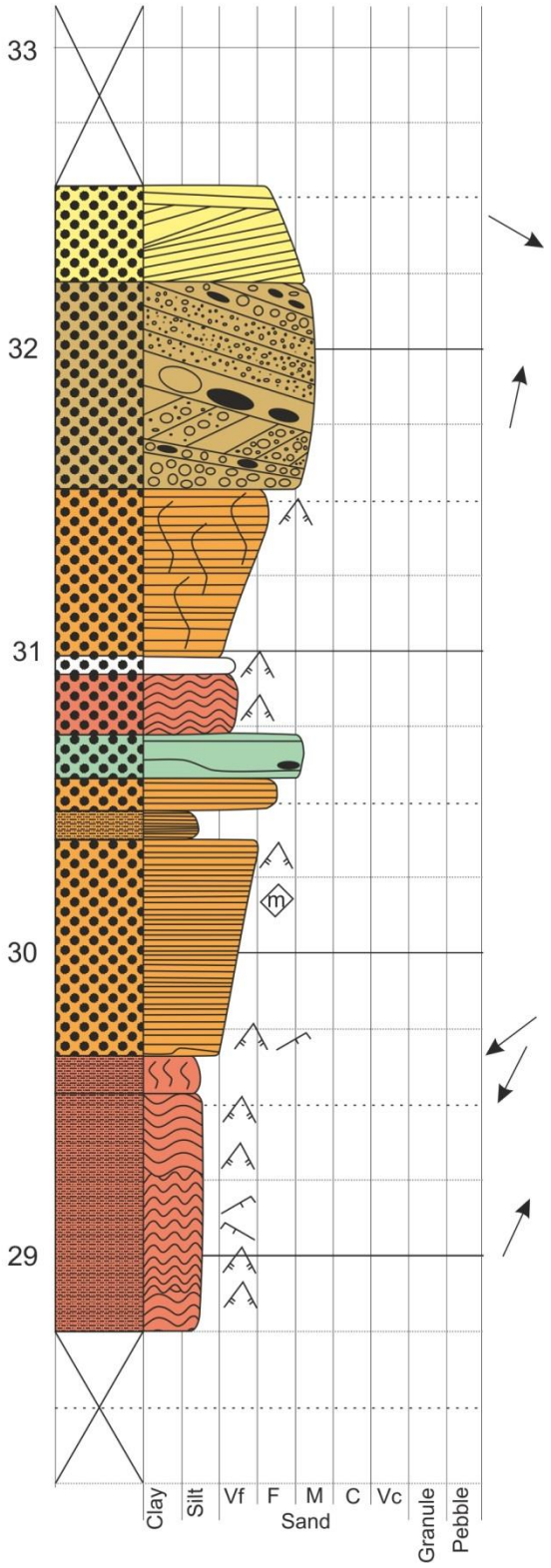
33
32
31
30
29
m
Clay
Silt
Vf
F
M
C
Vc
Sand
Granule
Pebble

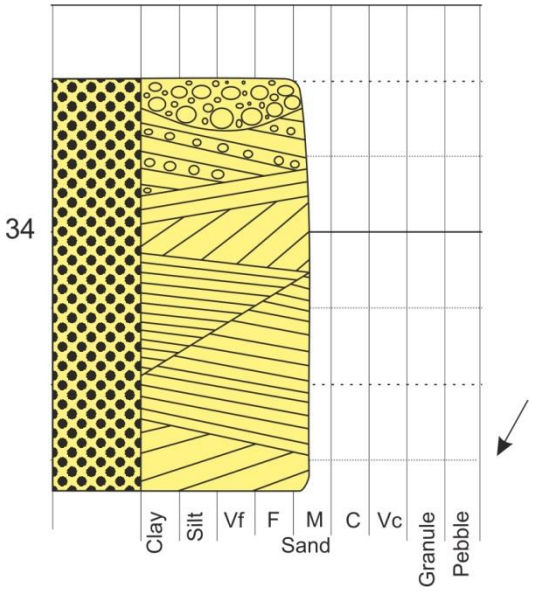
34
Clay
Silt
Vf
F
M
C
Vc
Granule
Pebble
Sand

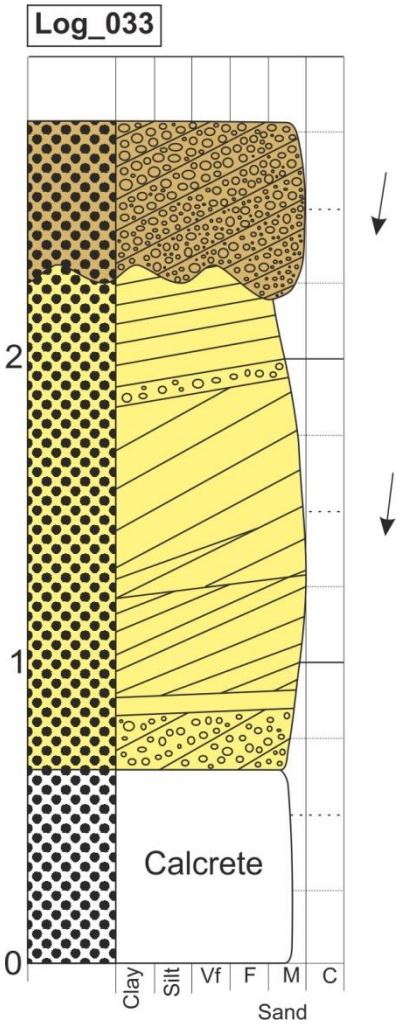
Log_033
2
1
0
Calcrete
Clay
Silt
Vf
F
M
C
Sand

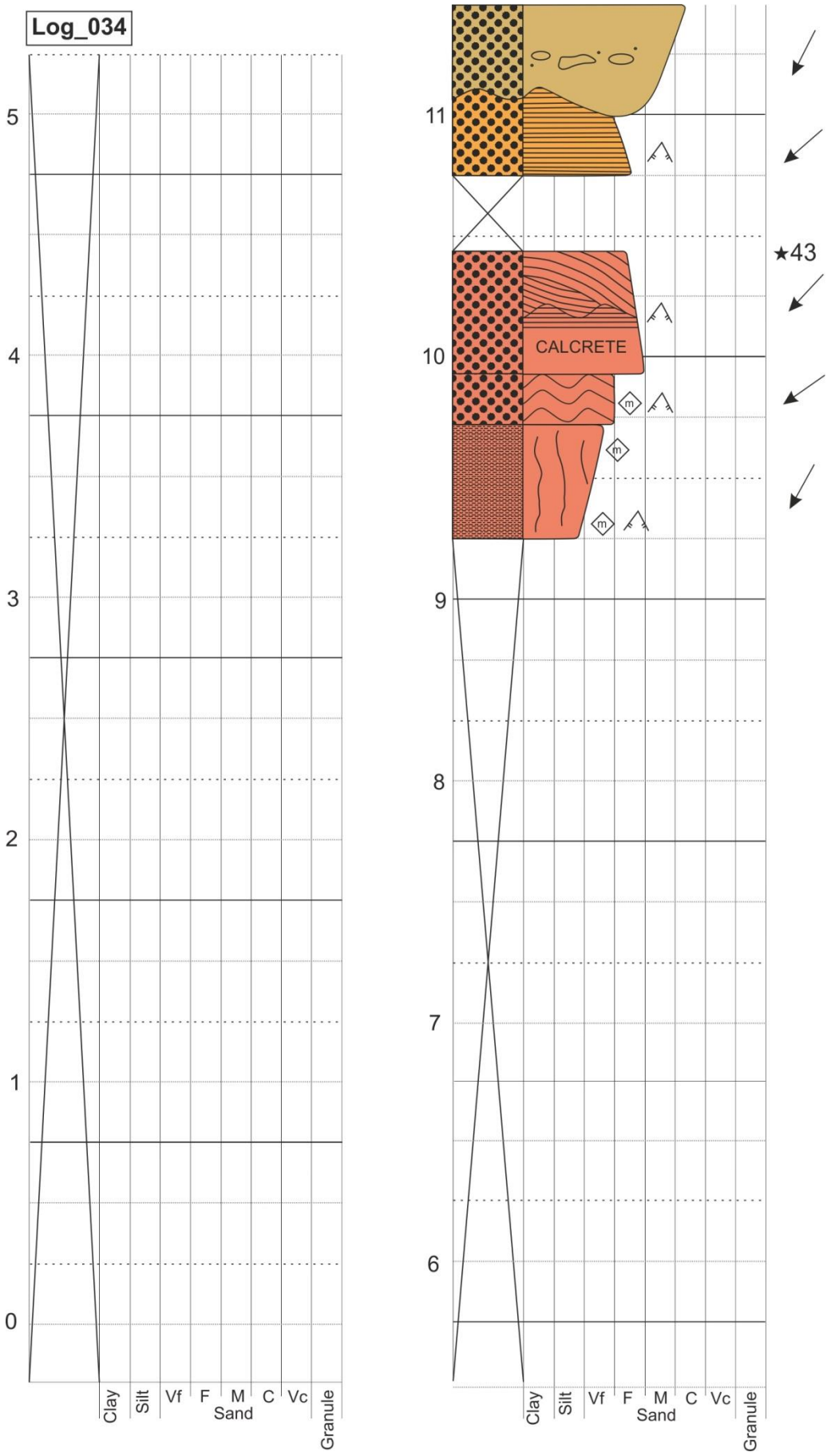
Log_034
5
4
3
2
1
0
11
10
9
8
7
6
★43
CALCRETE
m
m
m
Clay
Silt
Vf
F
M
C
Vc
Sand
Granule
Clay
Silt
Vf
F
M
C
Vc
Sand
Granule

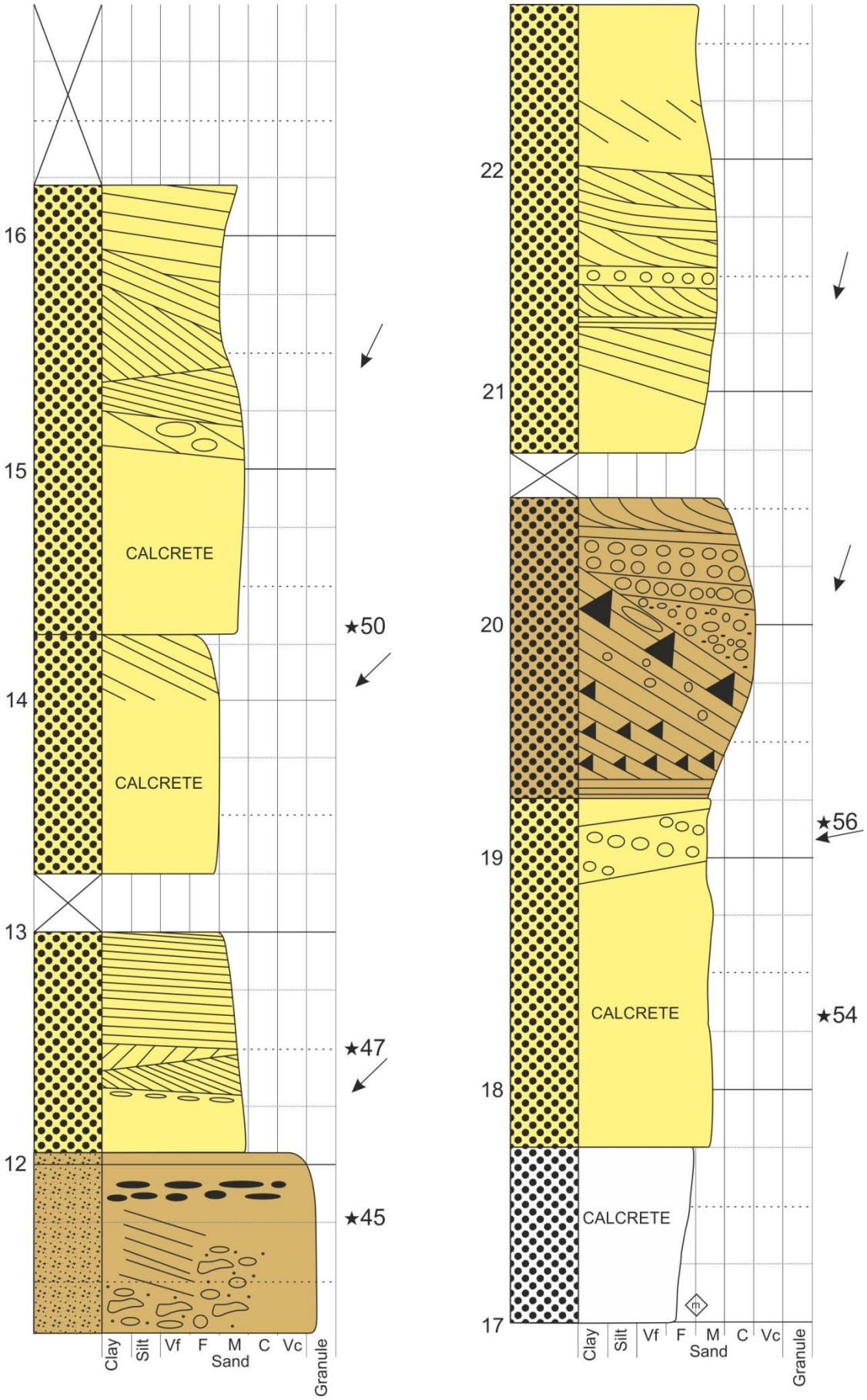
16
15
14
13
12
CALCRETE
CALCRETE
★50
★47
★45
Clay
Silt
Vf
F
M
C
Vc
Sand
Granule
22
21
20
19
18
17
CALCRETE
CALCRETE
★56
★54
m
Clay
Silt
Vf
F
M
C
Vc
Sand
Granule

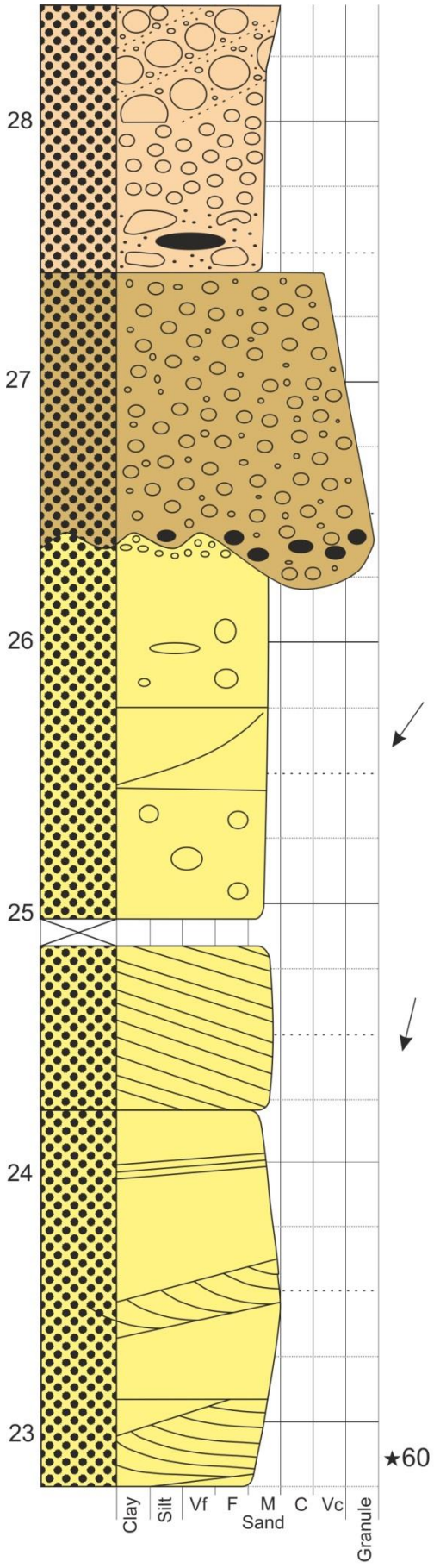
28
27
26
25
24
23
★60
Clay
Silt
Vf
F
M
C
Vc
Sand
Granule

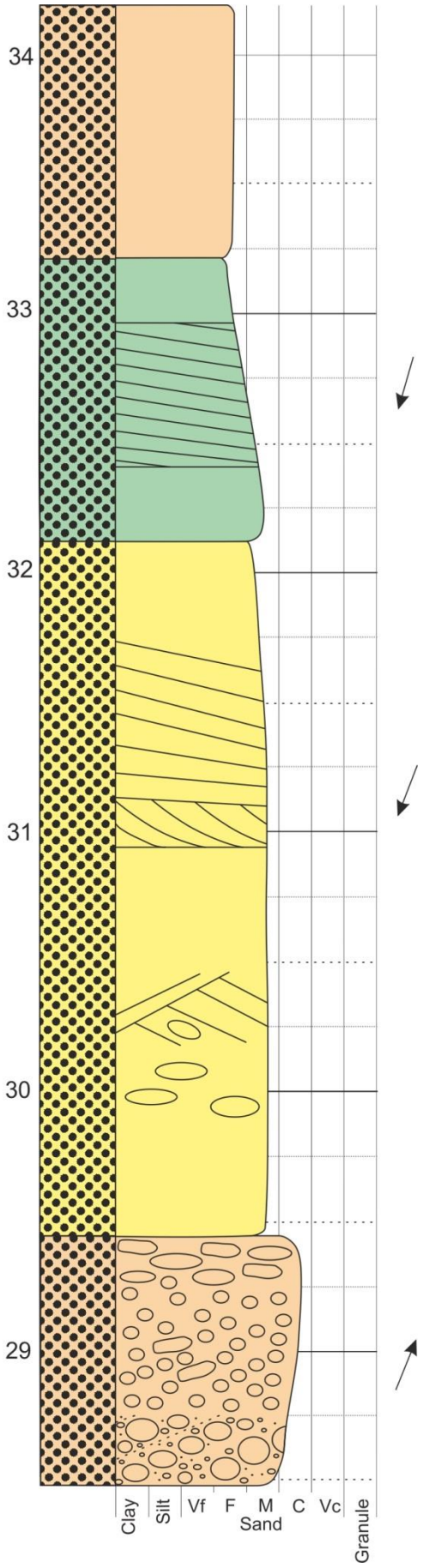
34
33
32
31
30
29
Clay
Silt
Vf
F
M
C
Vc
Sand
Granule

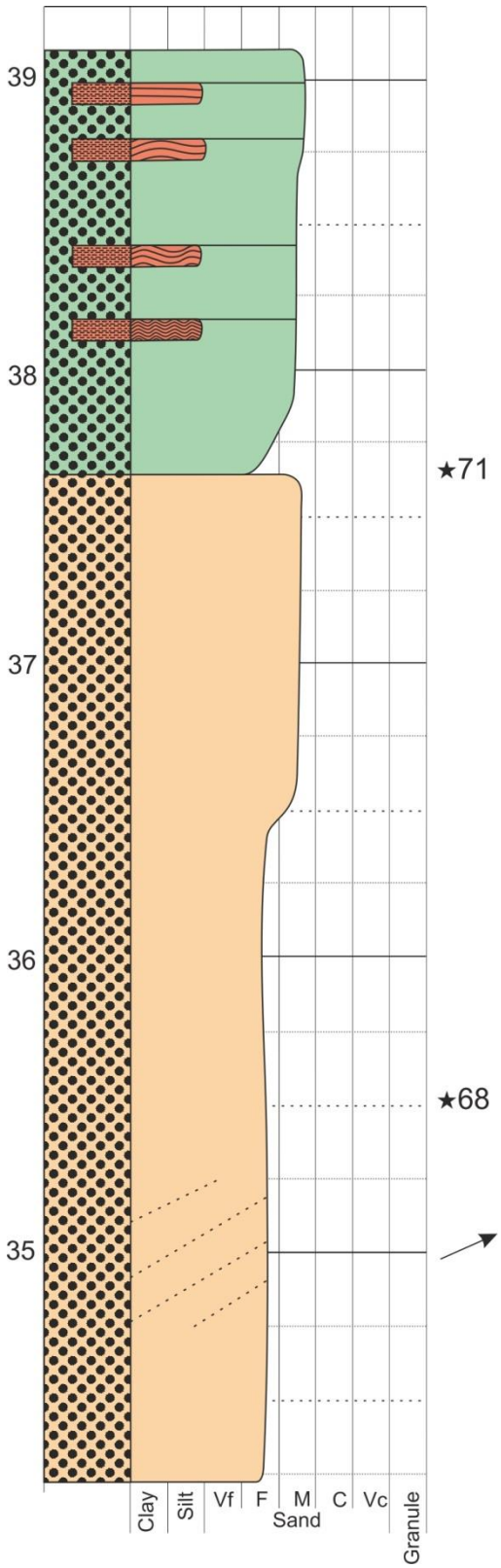
39
38
37
36
35
★71
★68
Clay
Silt
Vf
F
M
C
Vc
Granule
Sand

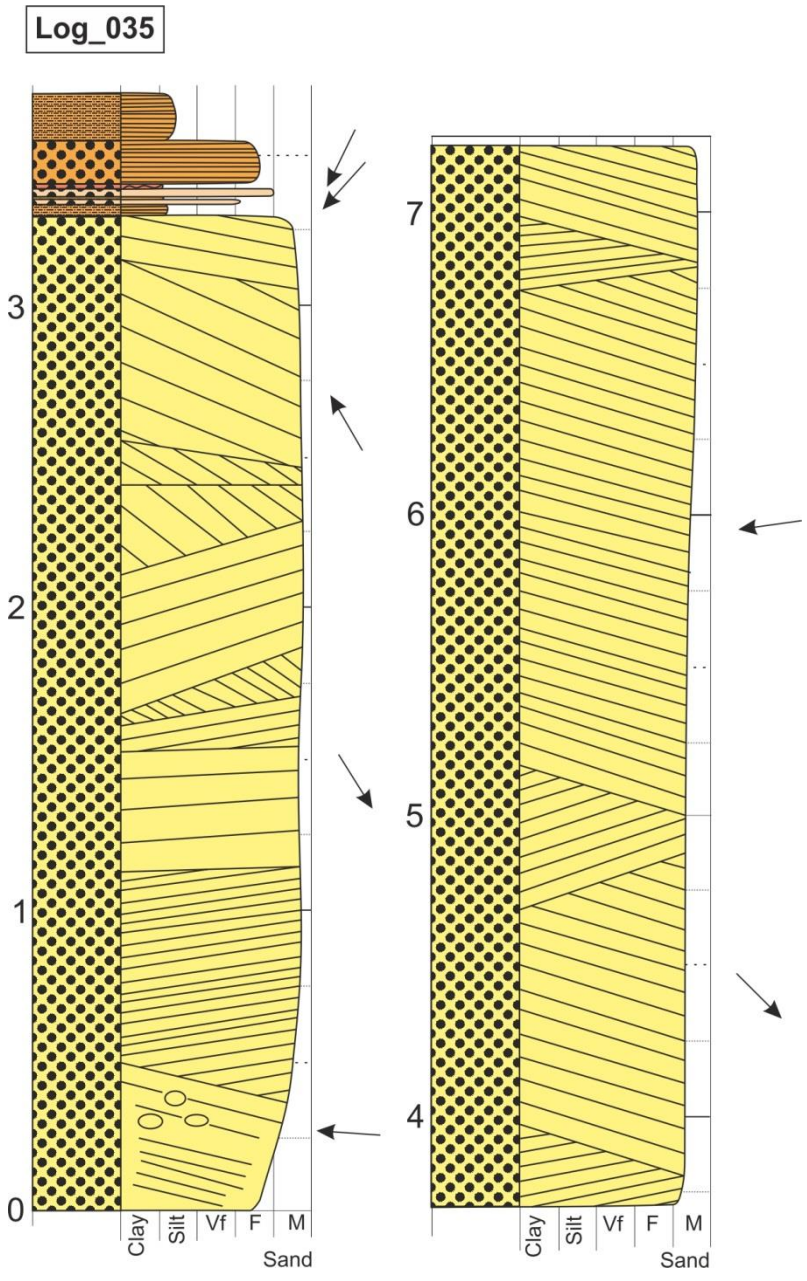
Log_035
0
1
2
3
4
5
6
7
Clay
Silt
Vf
F
M
Sand
Clay
Silt
Vf
F
M
Sand

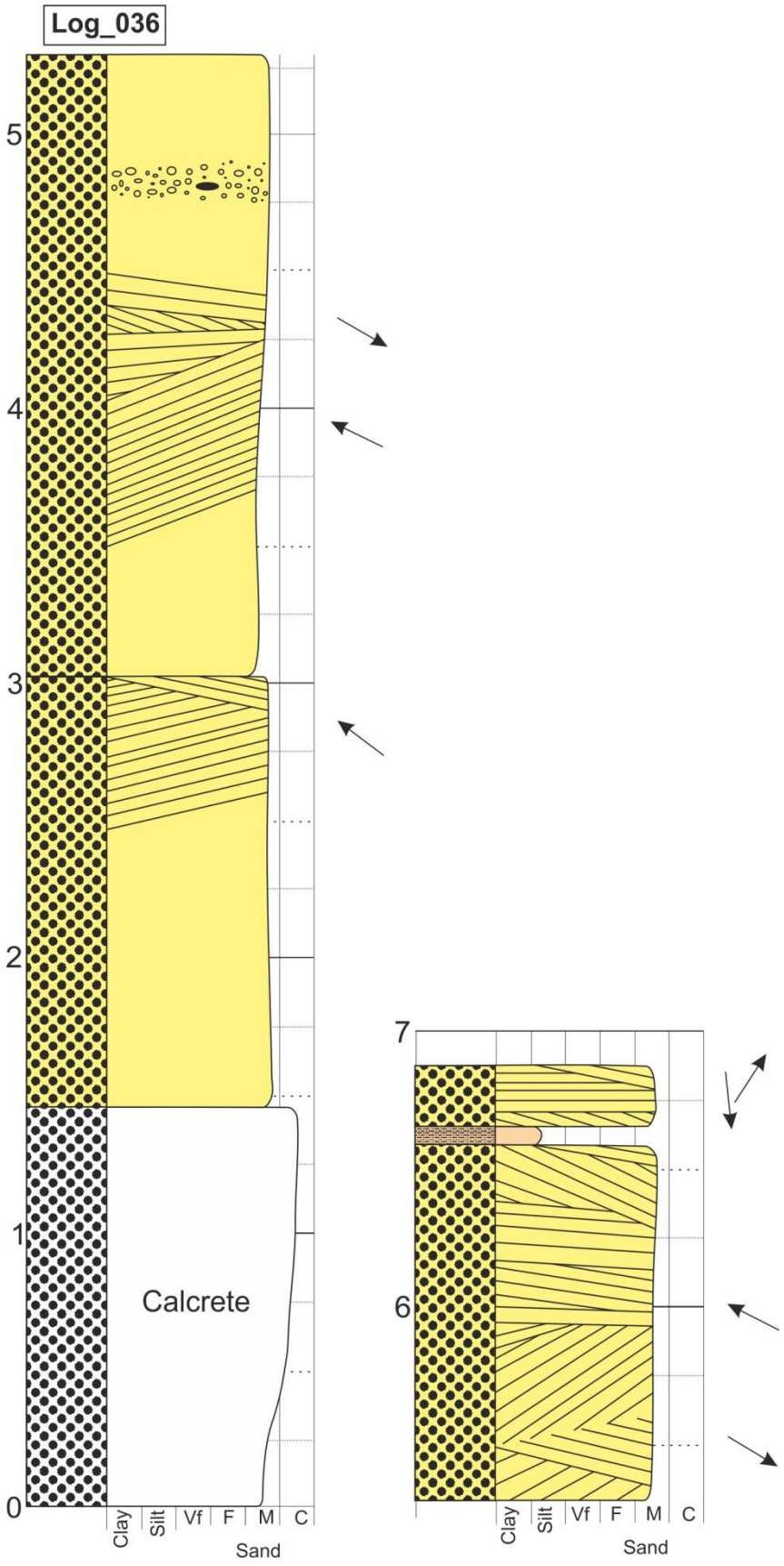
Log_036
5
4
3
2
1
0
Calcrete
Clay
Silt
Vf
F
M
C
Sand
7
6
Clay
Silt
Vf
F
M
C
Sand

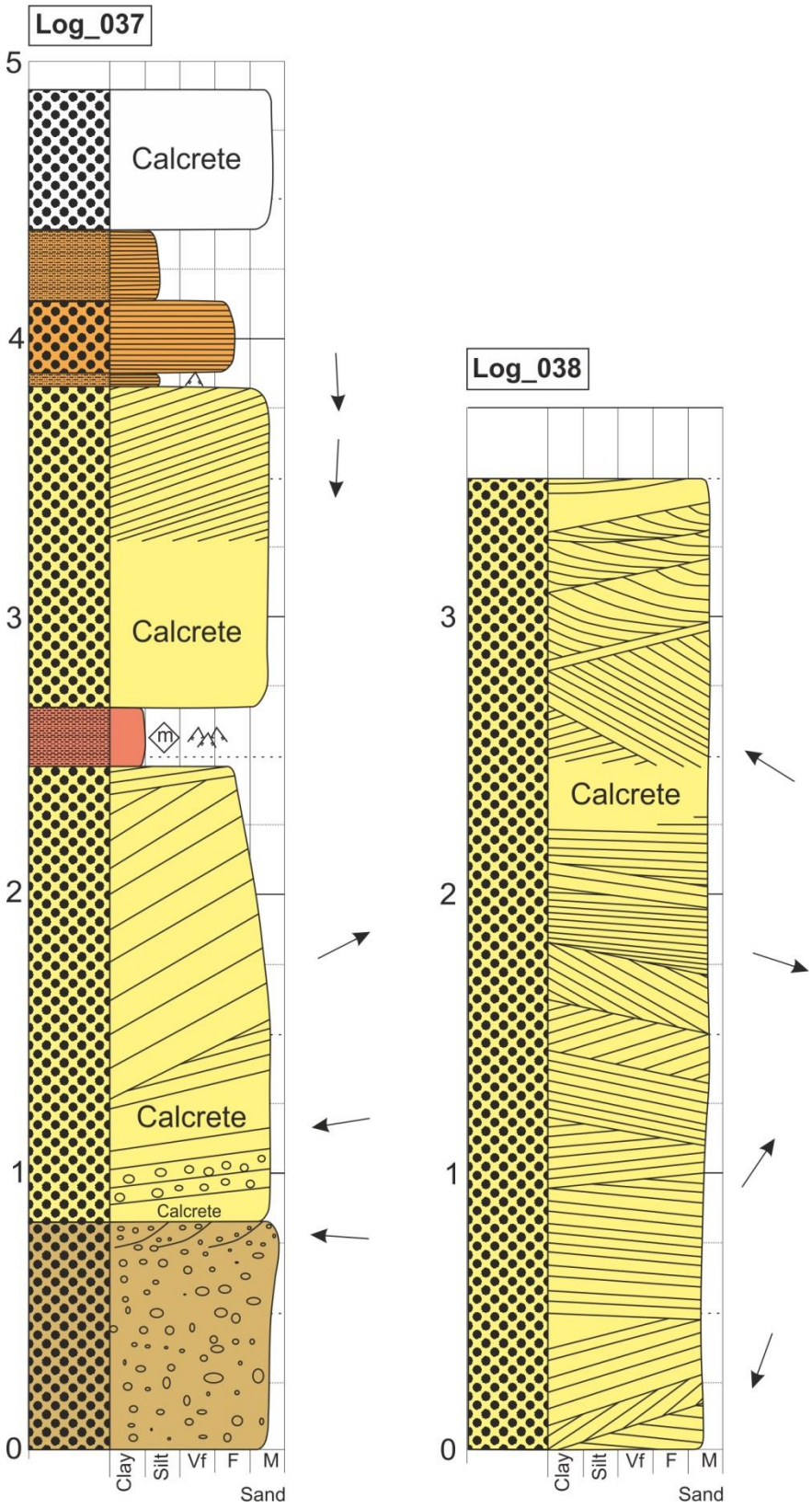
Log_037
5
4
3
2
1
0
Calcrete
Calcrete
m
Calcrete
Calcrete
Clay
Silt
Vf
F
M
Sand
Log_038
3
2
1
0
Calcrete
Clay
Silt
Vf
F
M
Sand

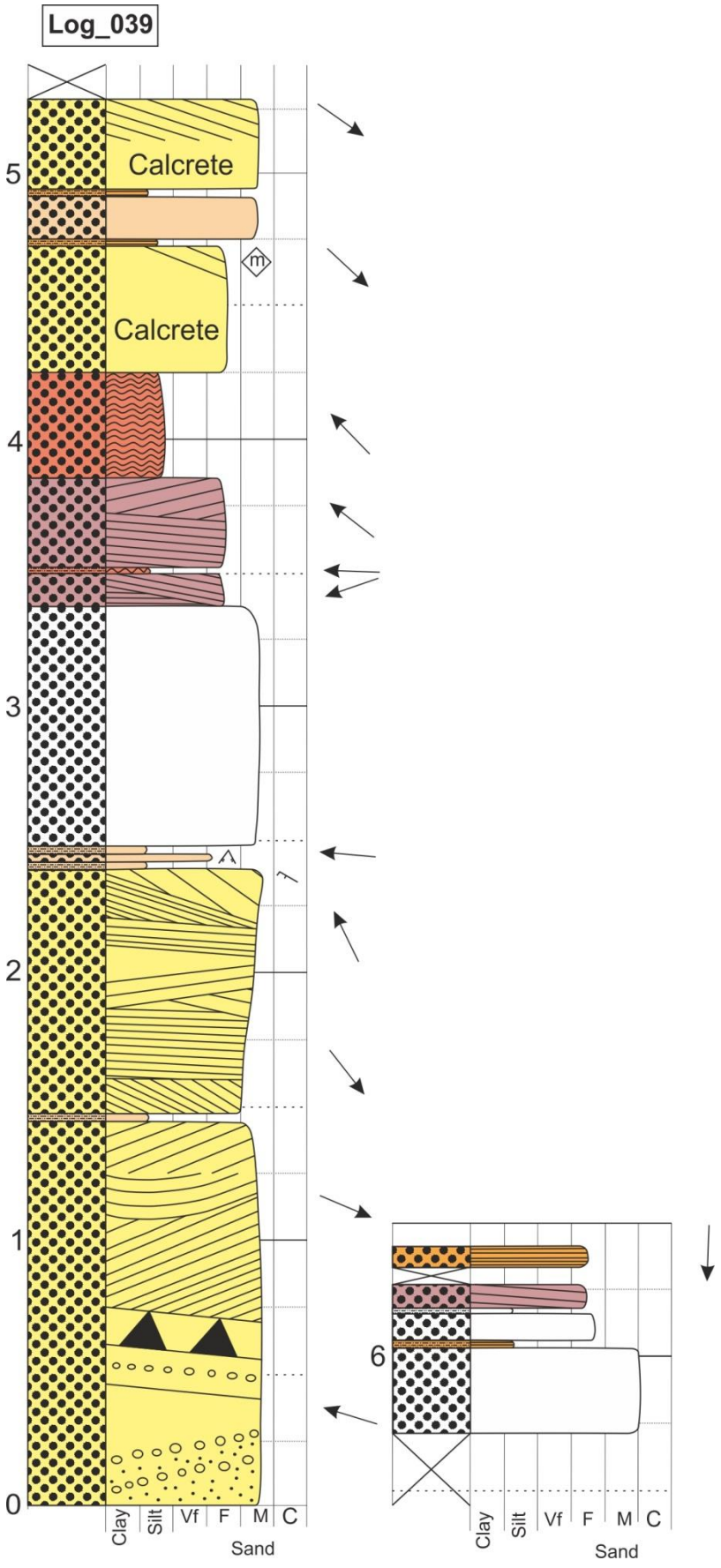
Log_039
Calcrete
Calcrete
m
5
4
3
2
1
0
6
Clay
Silt
Vf
F
M
C
Sand
Clay
Silt
Vf
F
M
C
Sand

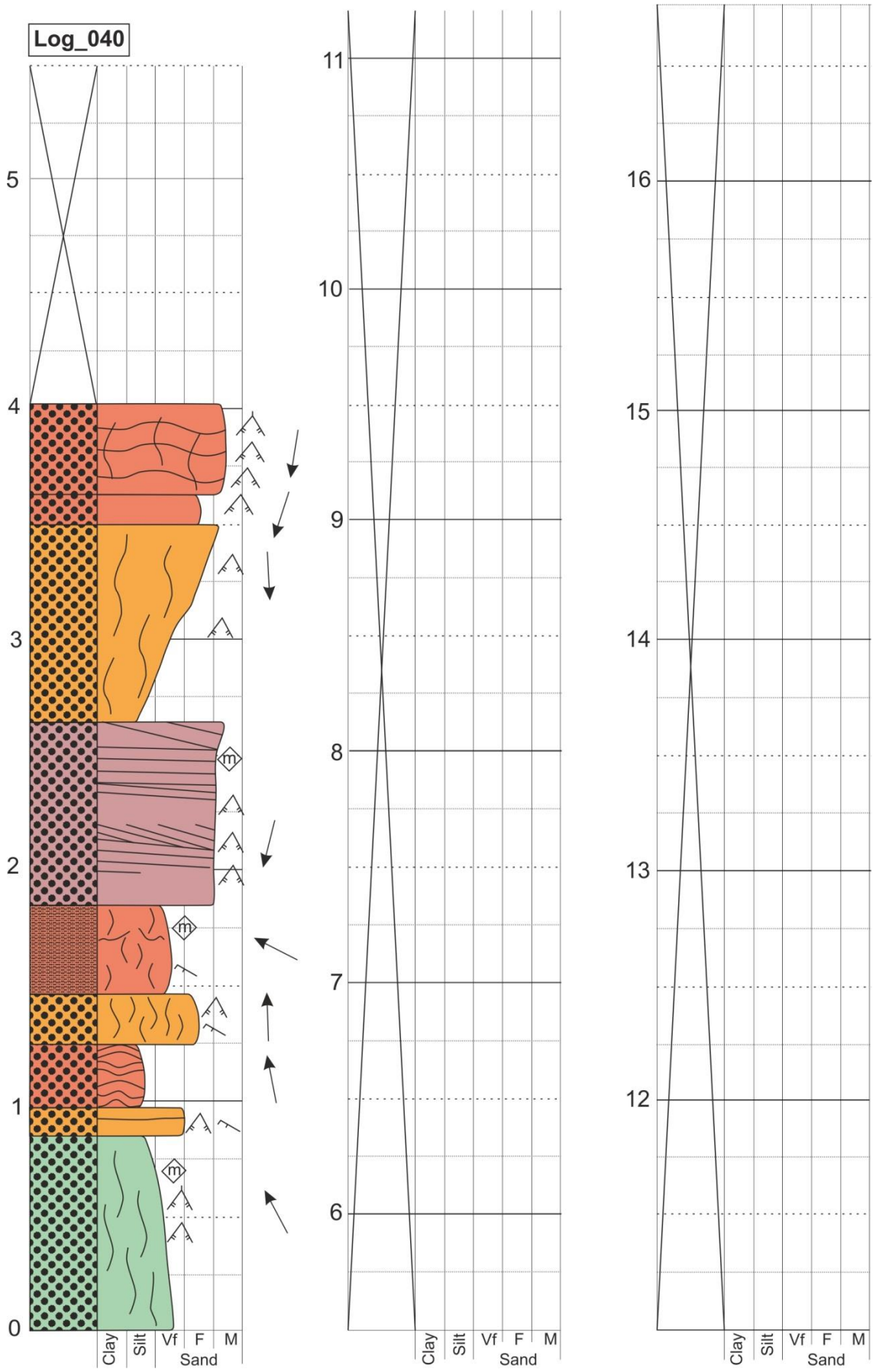
Log_040
0
1
2
3
4
5
6
7
8
9
10
11
12
13
14
15
16
m
Clay
Silt
Vf
F
M
Sand

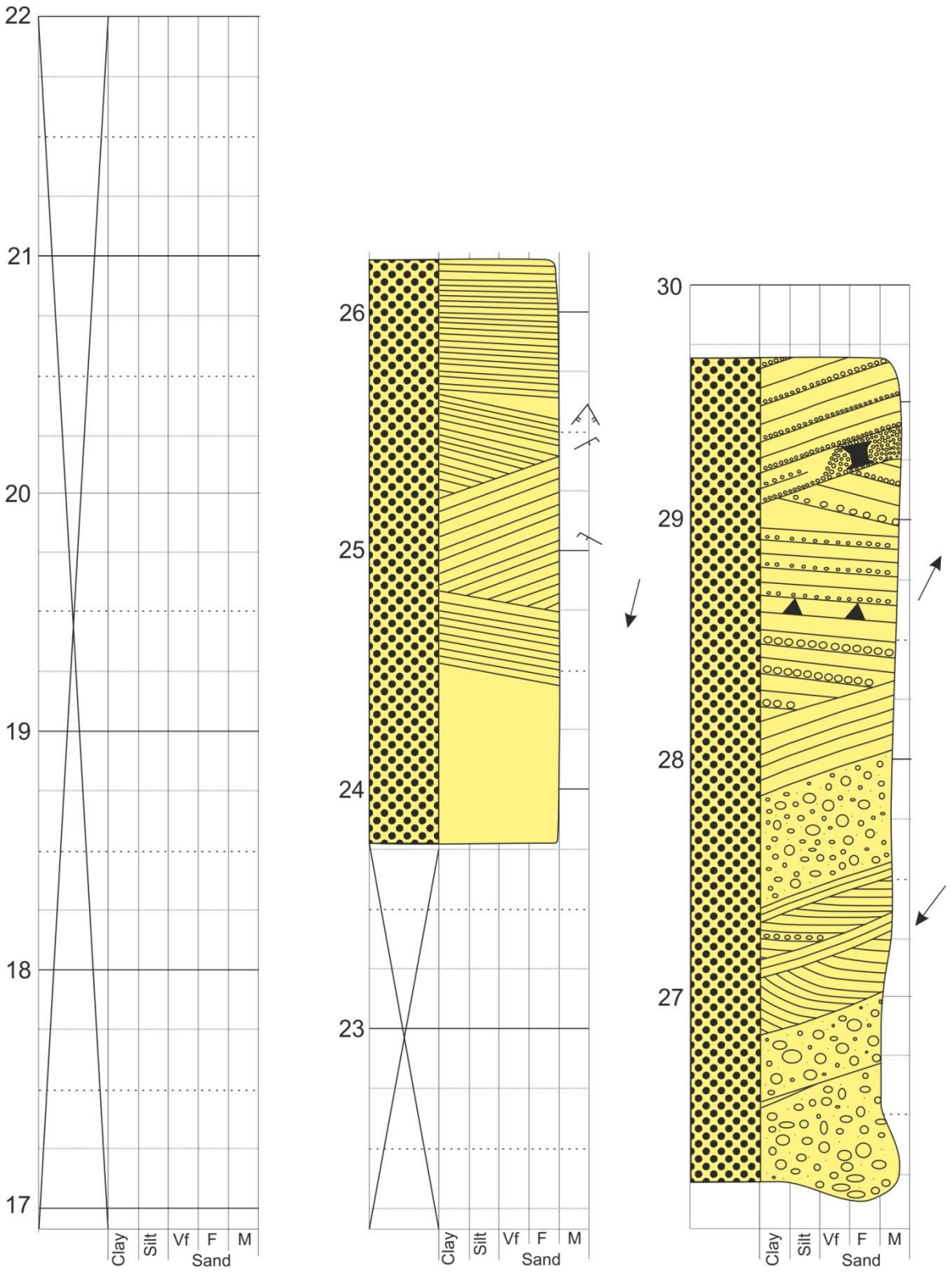
22
21
20
19
18
17
Clay
Silt
Vf
F
M
Sand
26
25
24
23
Clay
Silt
Vf
F
M
Sand
30
29
28
27
Clay
Silt
Vf
F
M
Sand

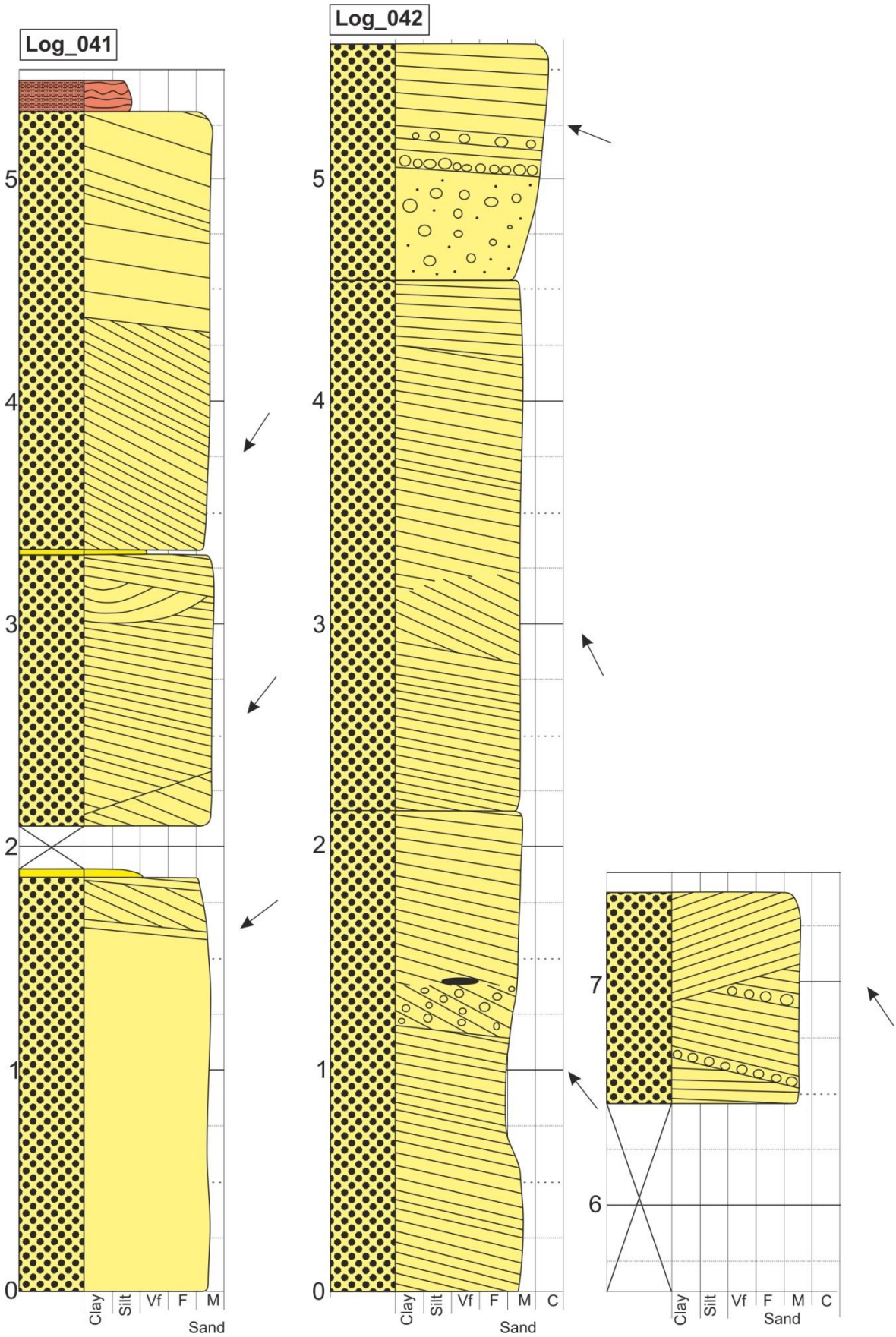
Log_041
Log_042
5
4
3
2
1
0
7
6
Clay
Silt
Vf
F
M
C
Sand

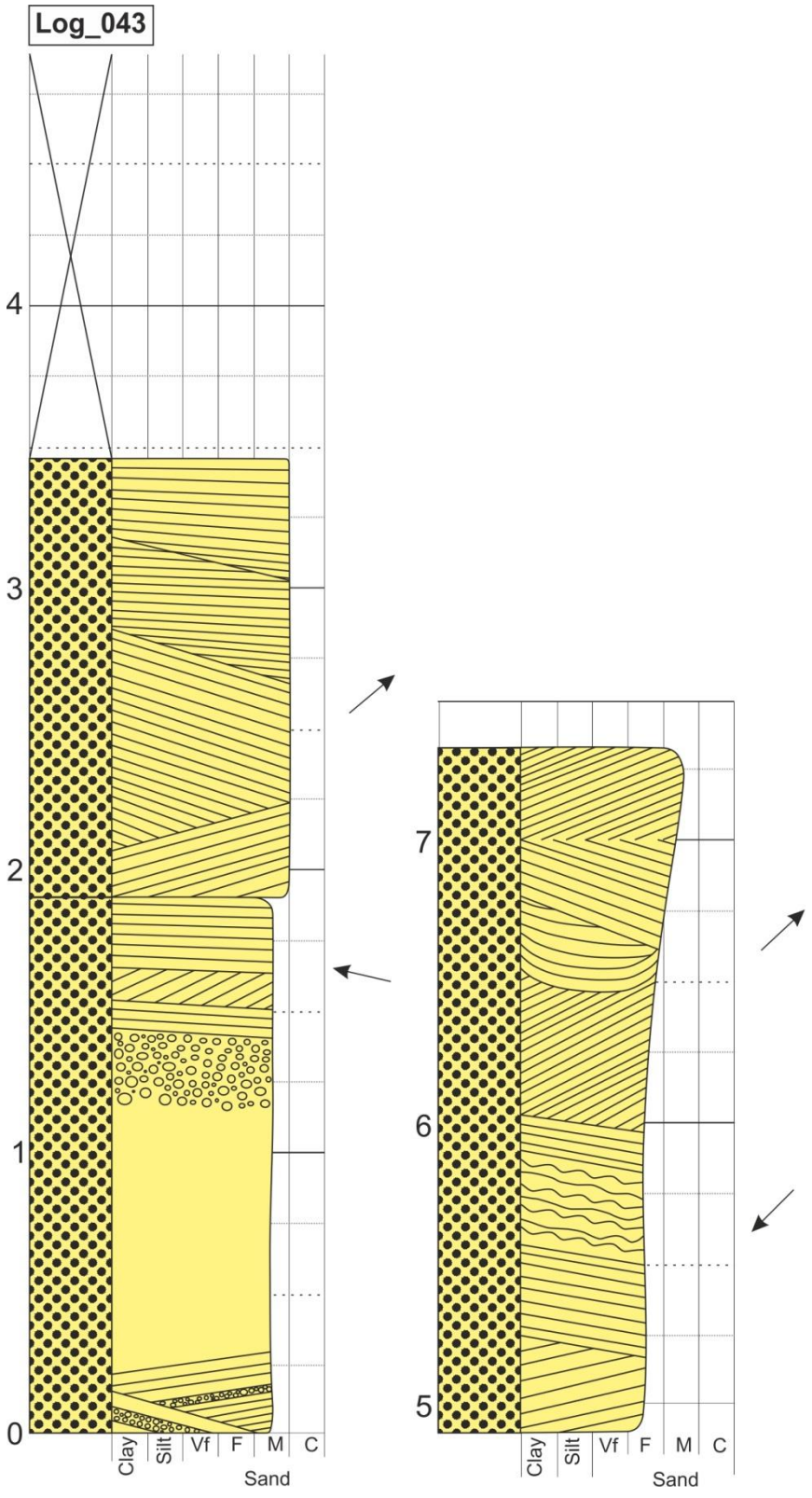
Log_043
4
3
2
1
0
Clay
Silt
Vf
F
M
C
Sand
7
6
5
Clay
Silt
Vf
F
M
C
Sand

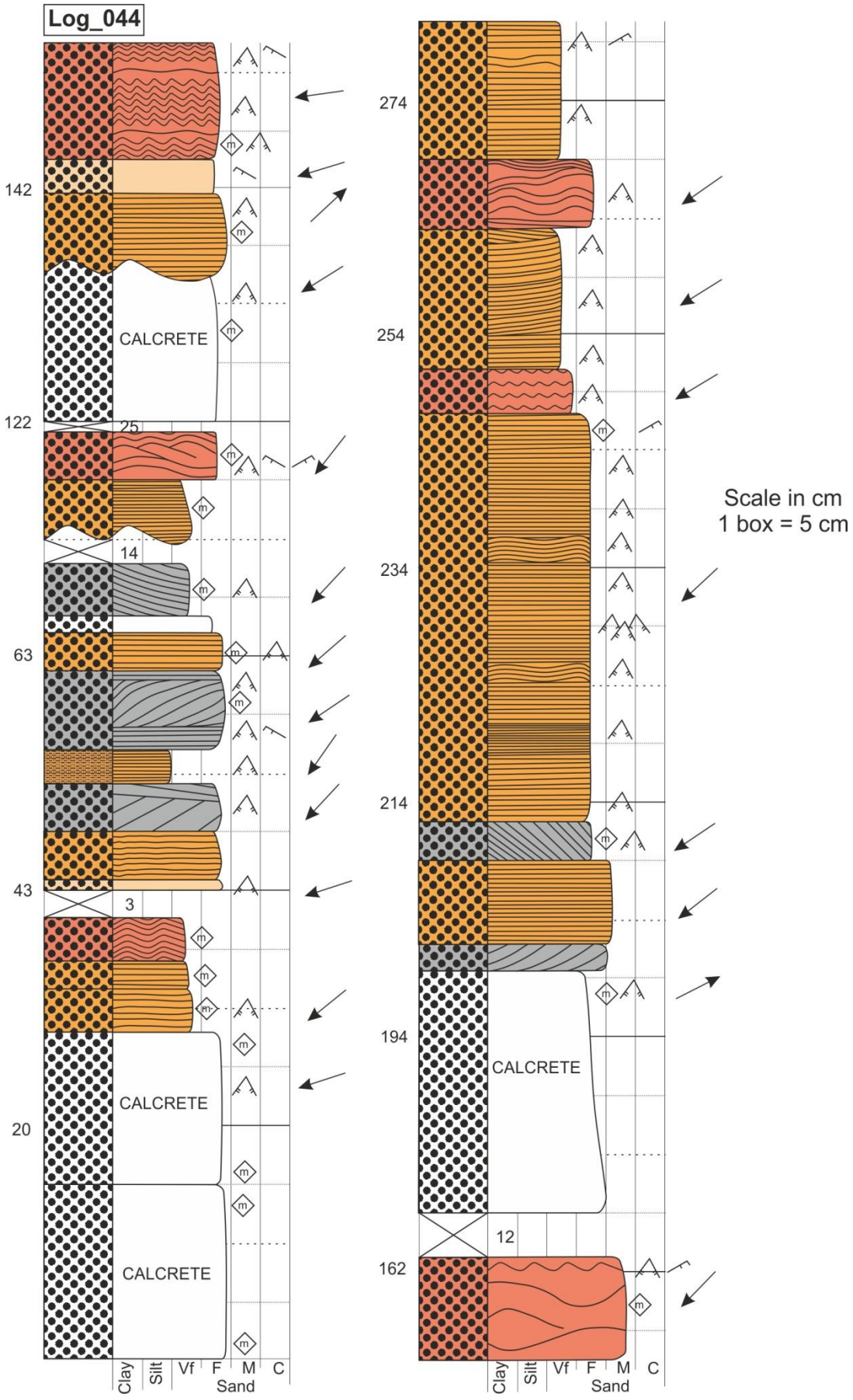
Log_044
142
122
63
43
20
274
254
234
214
194
162
CALCRETE
CALCRETE
CALCRETE
CALCRETE
25
14
3
12
Clay
Silt
Vf
F
M
C
Sand
Scale in cm
1 box = 5 cm

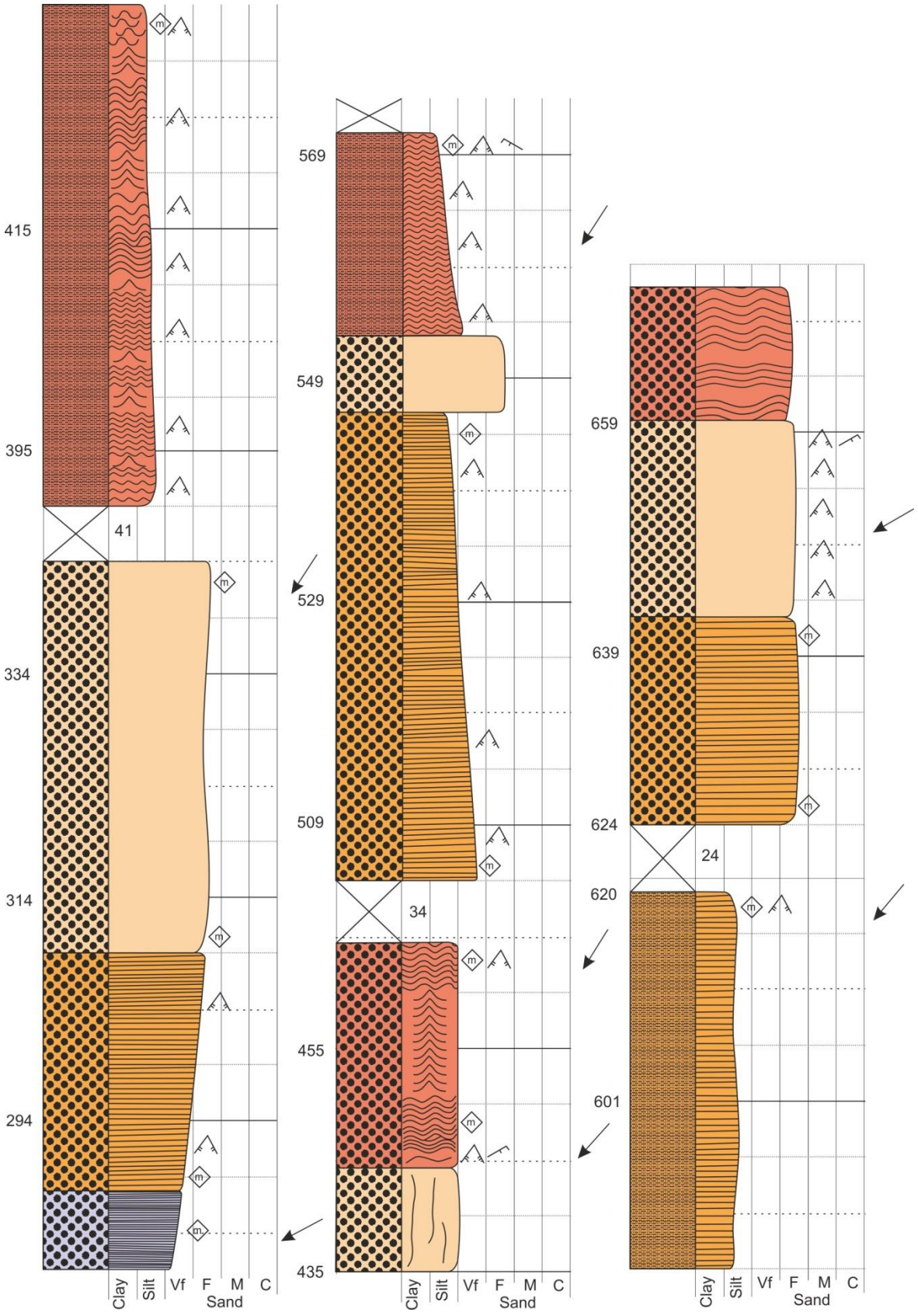
415
395
41
334
314
294
529
509
34
455
435
569
549
659
639
624
24
620
601
Clay
Silt
Vf
F
M
C
Sand

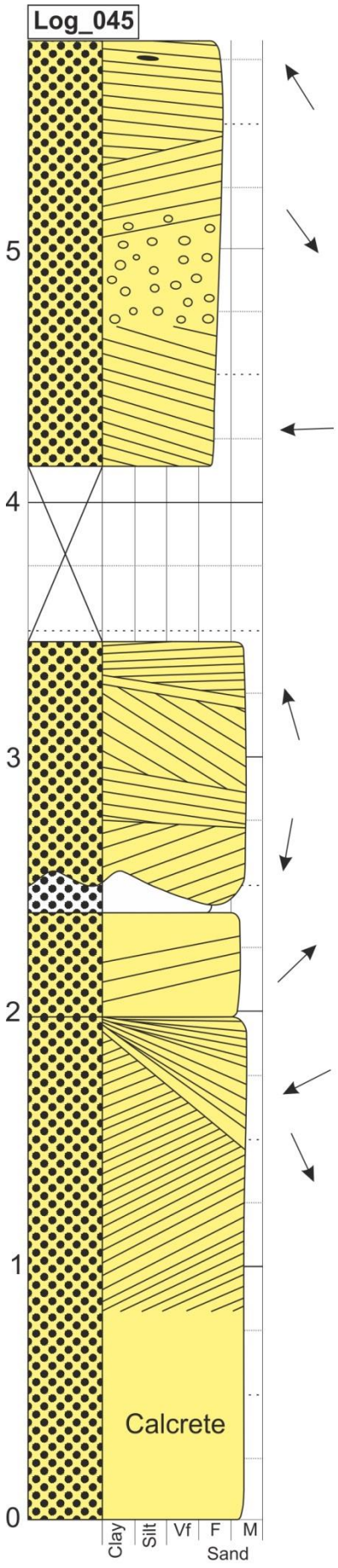
Log_045
5
4
3
2
1
0
Calcrete
Clay
Silt
Vf
F
M
Sand

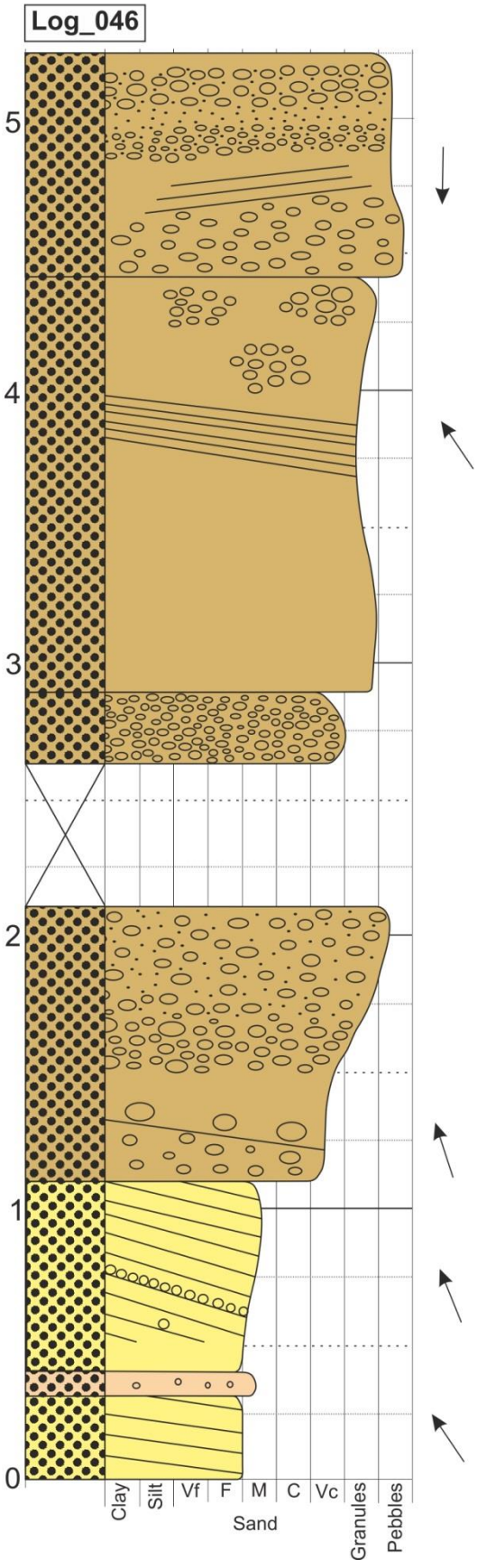
Log_046
5
4
3
2
1
0
Clay
Silt
Vf
F
M
C
Vc
Sand
Granules
Pebbles

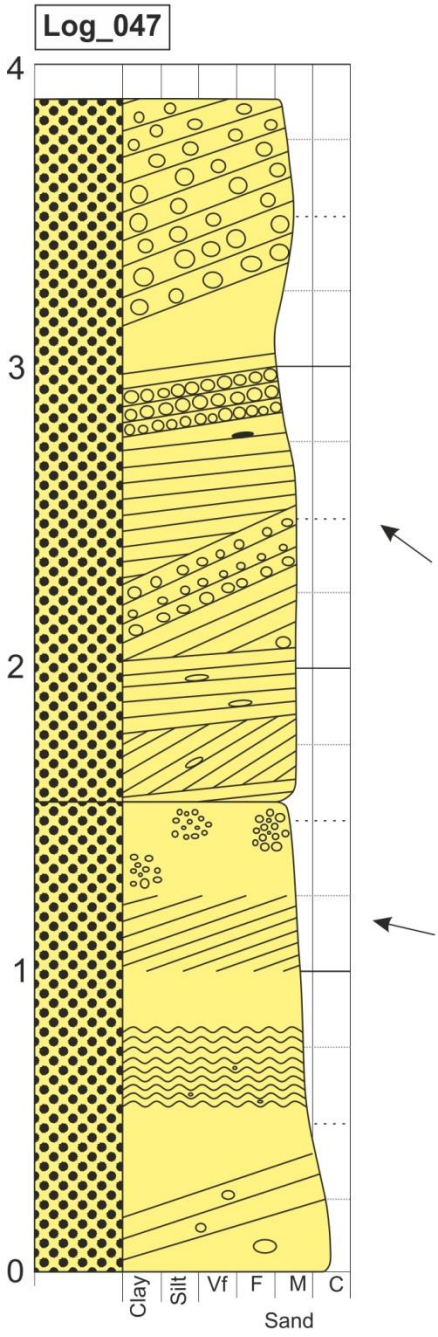
Log_047
4
3
2
1
0
Clay
Silt
Vf
F
M
C
Sand

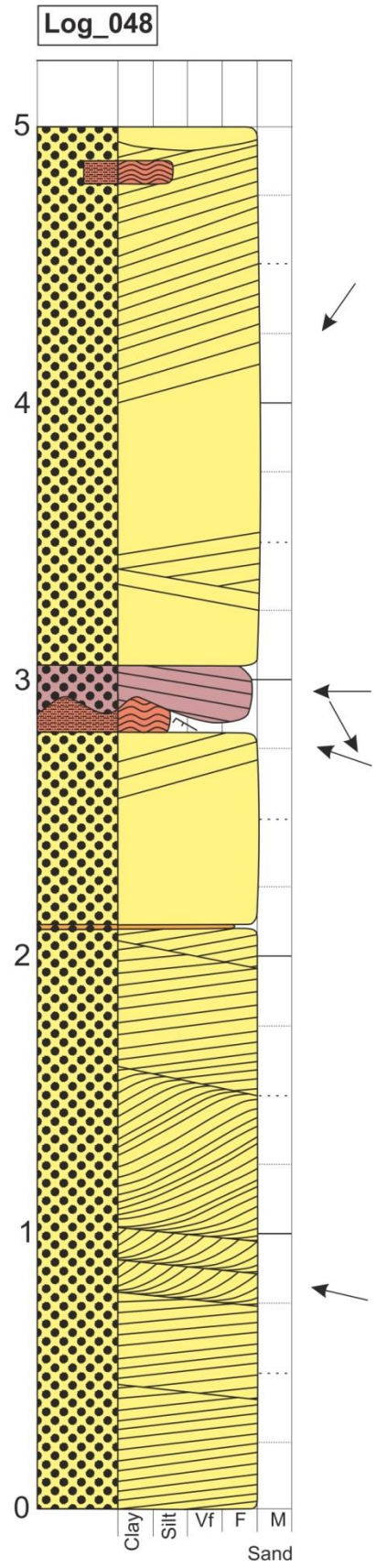
Log_048
5
4
3
2
1
0
Clay
Silt
Vf
F
M
Sand

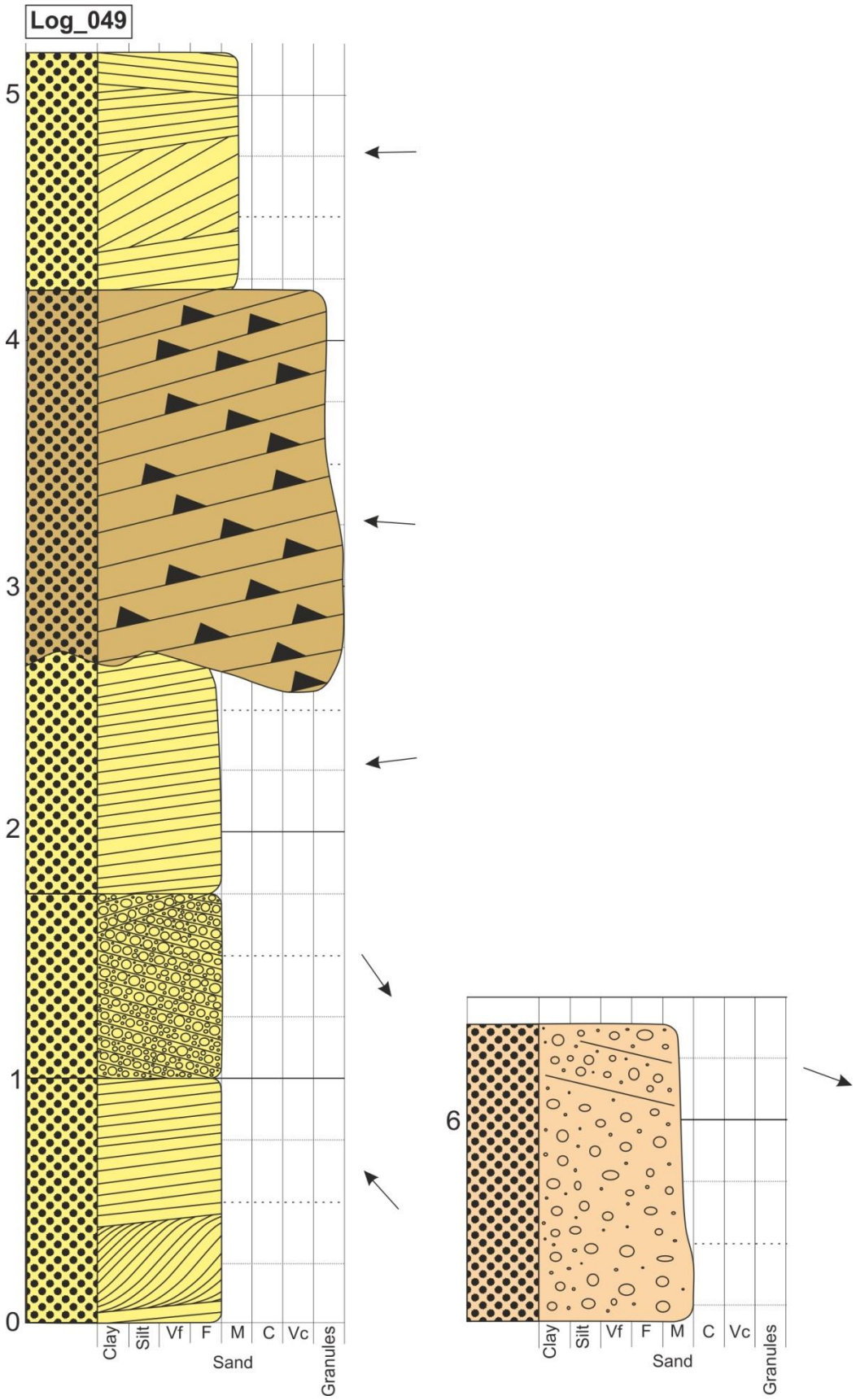
Log_049
5
4
3
2
1
0
6
Clay
Silt
Vf
F
M
C
Vc
Granules
Sand

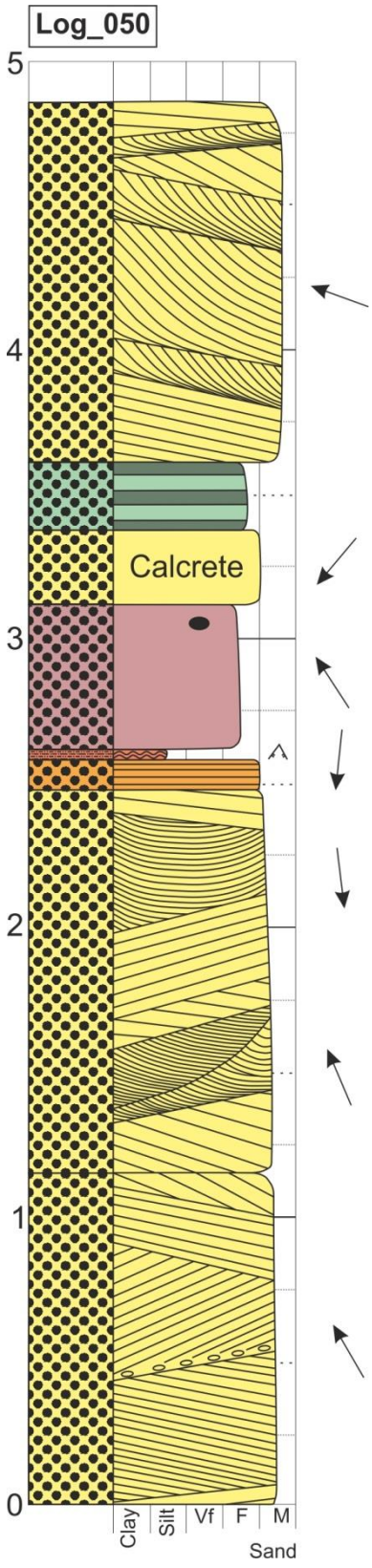
Log_050
5
4
3
2
1
0
Calcrete
Clay
Silt
Vf
F
M
Sand

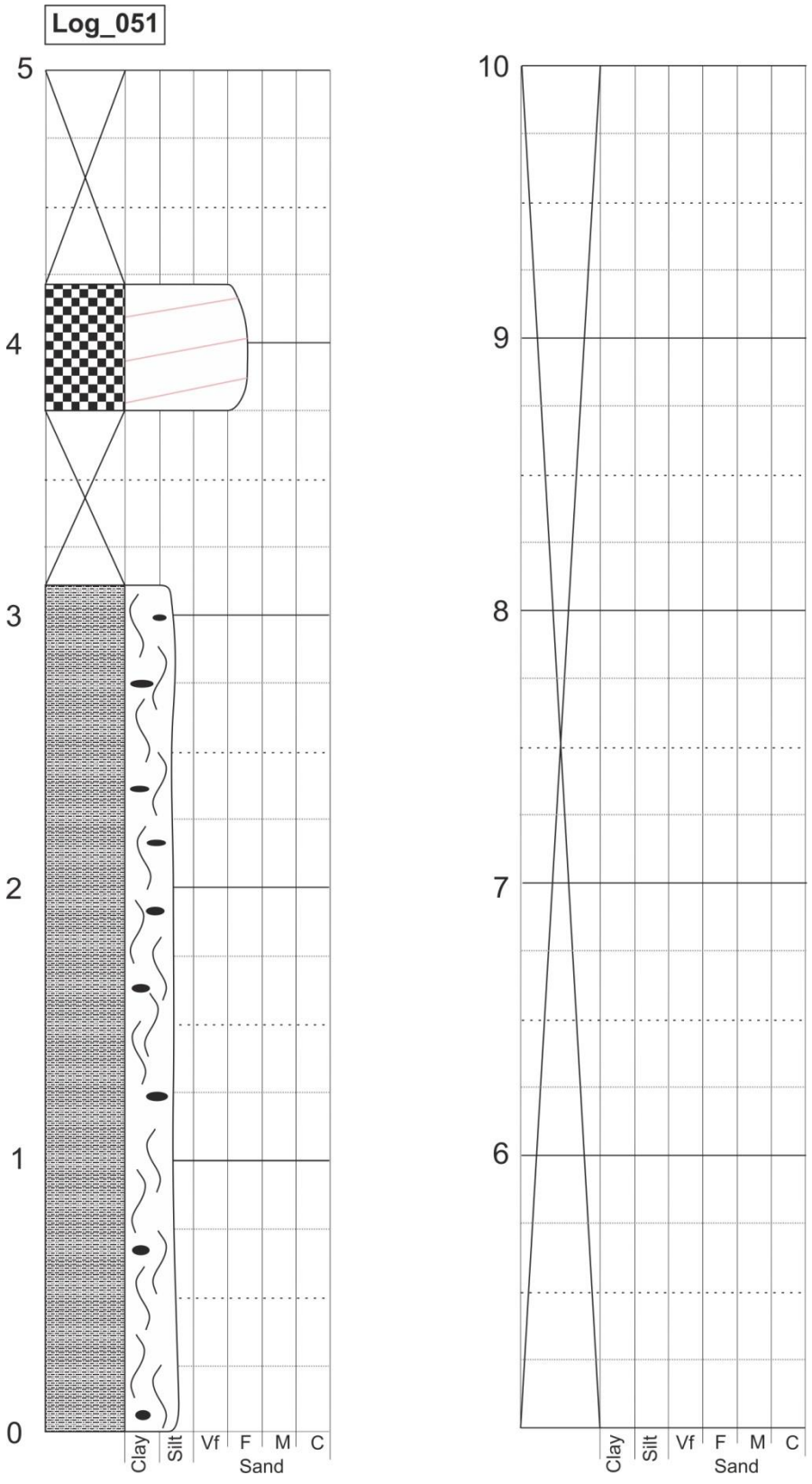
Log_051
5
4
3
2
1
0
10
9
8
7
6
Clay
Silt
Vf
F
M
C
Sand

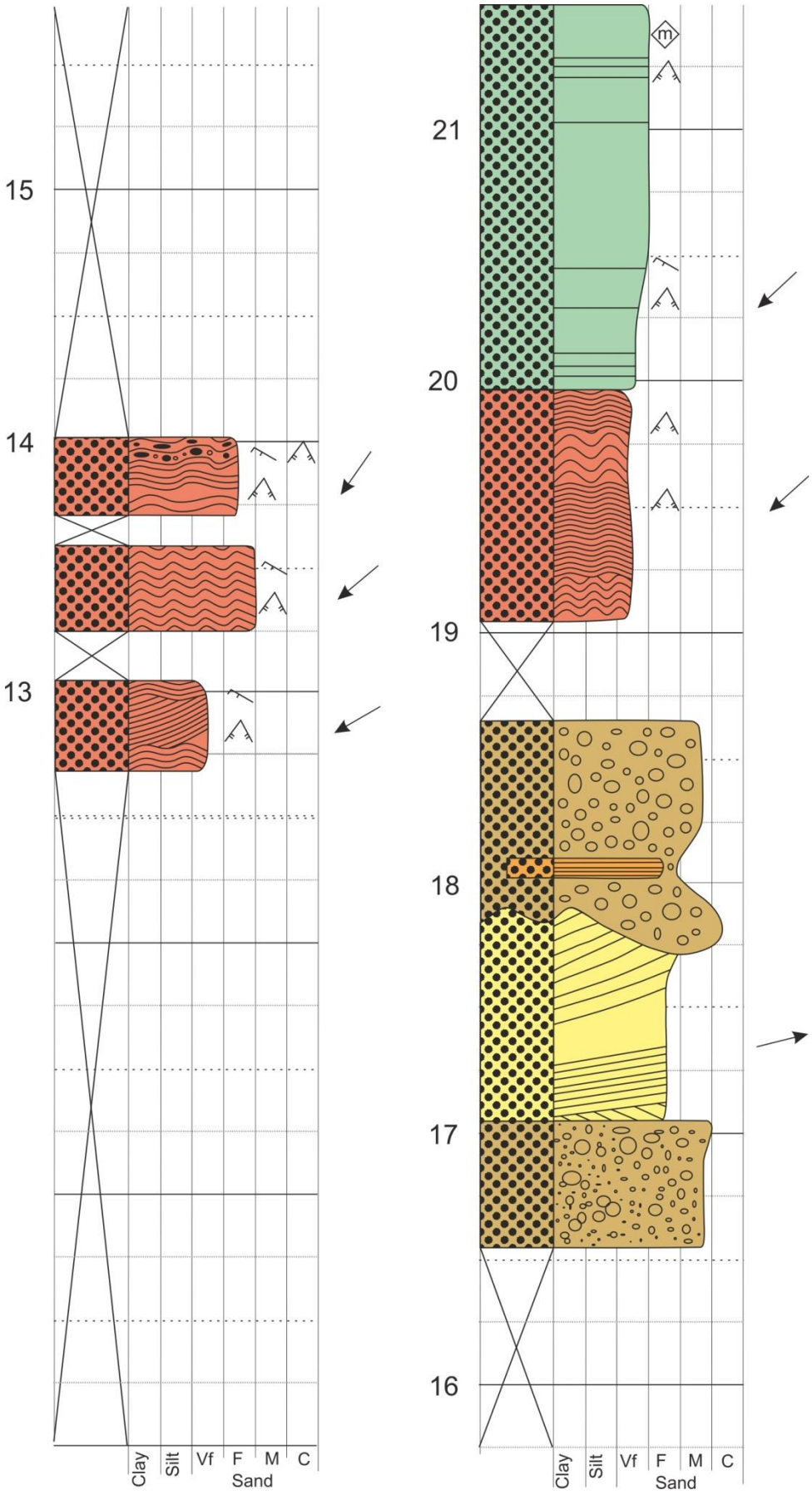
15
14
13
Clay
Silt
Vf
F
M
C
Sand
21
20
19
18
17
16
m
Clay
Silt
Vf
F
M
C
Sand

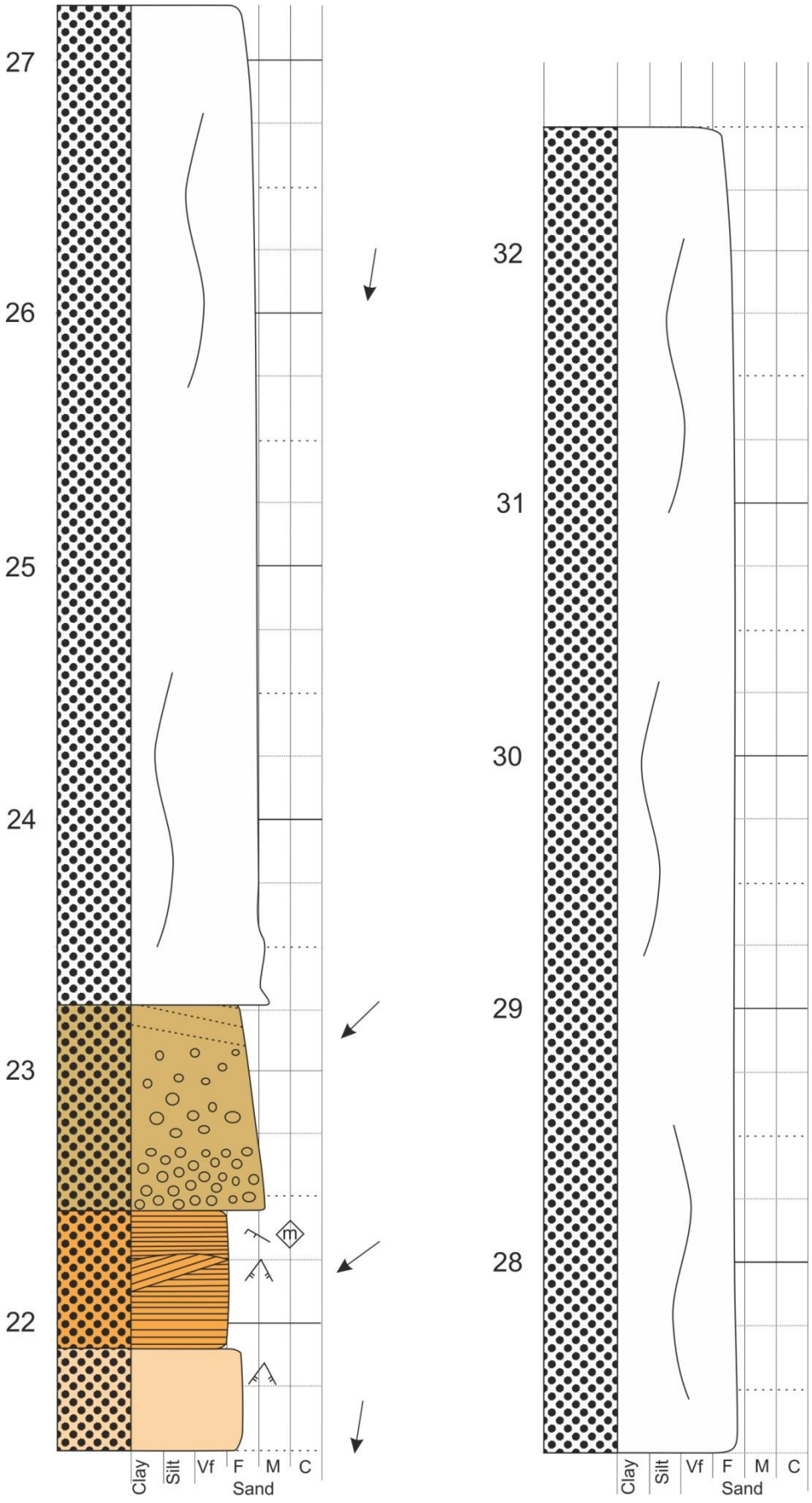
27
26
25
24
23
22
m
Clay
Silt
Vf
F
M
C
Sand
32
31
30
29
28
Clay
Silt
Vf
F
M
C
Sand

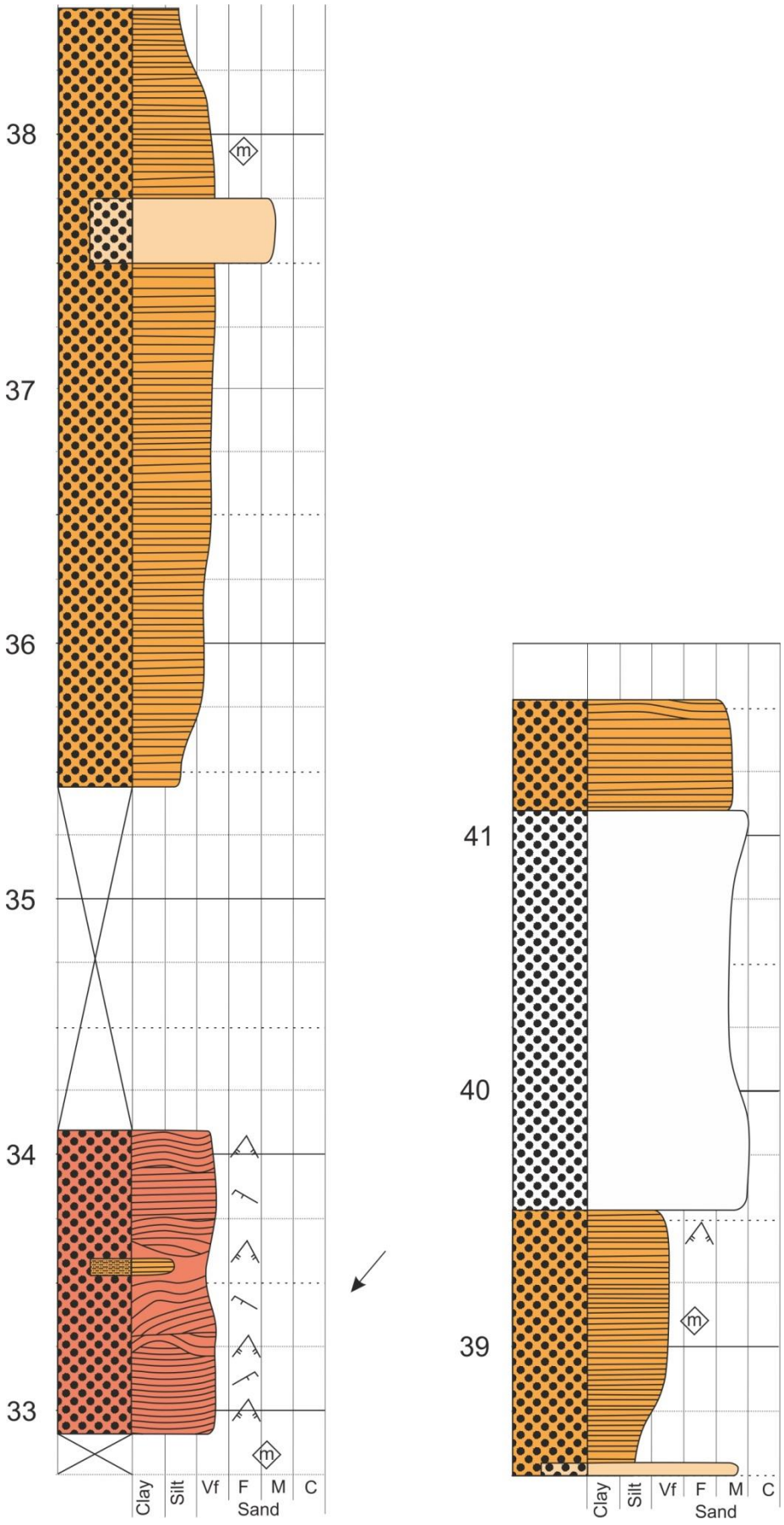
38
37
36
35
34
33
m
m
Clay
Silt
Vf
F
M
C
Sand
41
40
39
m
Clay
Silt
Vf
F
M
C
Sand

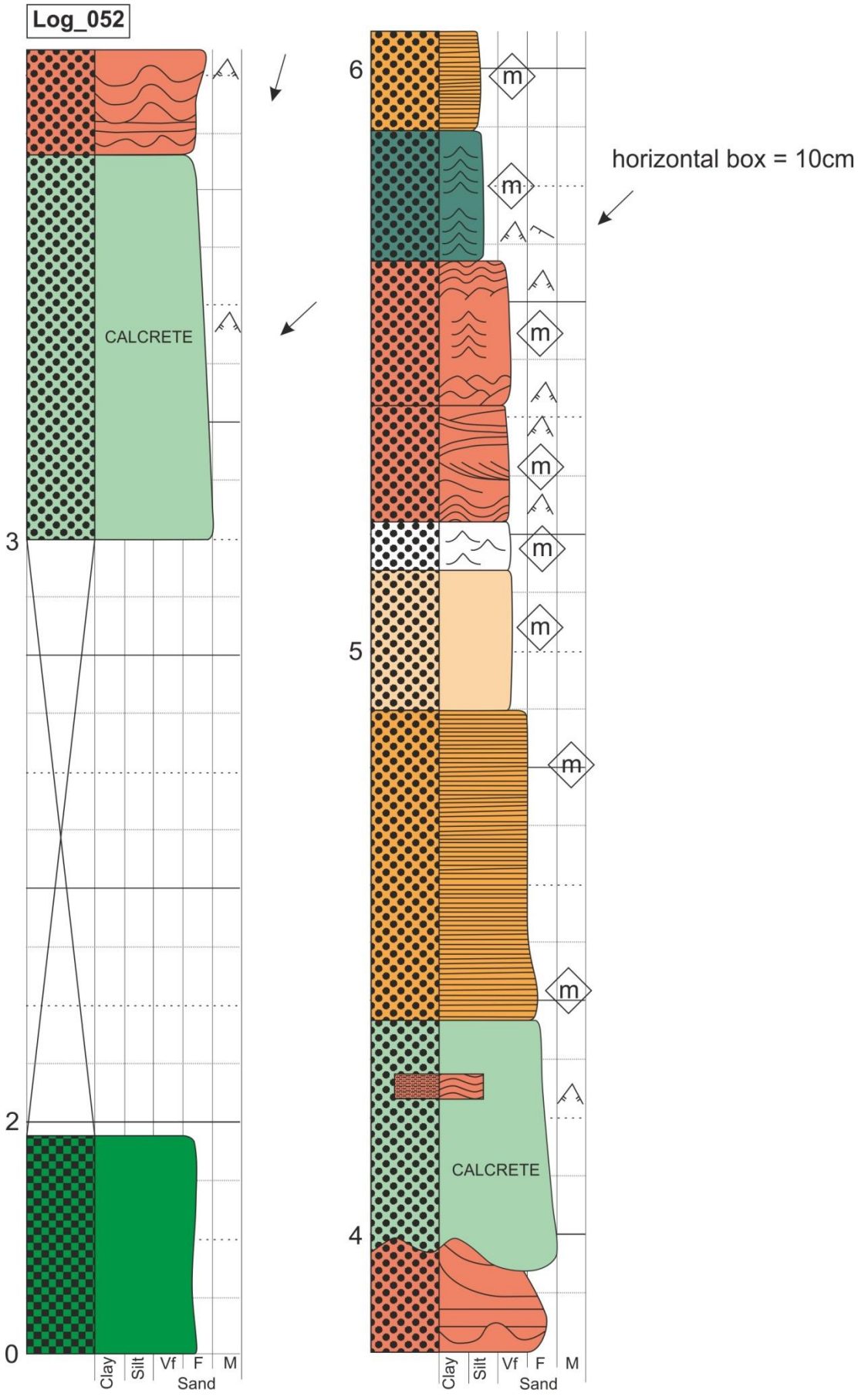
Log_052
CALCRETE
CALCRETE
horizontal box = 10cm
m
0
2
3
4
5
6
Clay
Silt
Vf
F
M
Sand

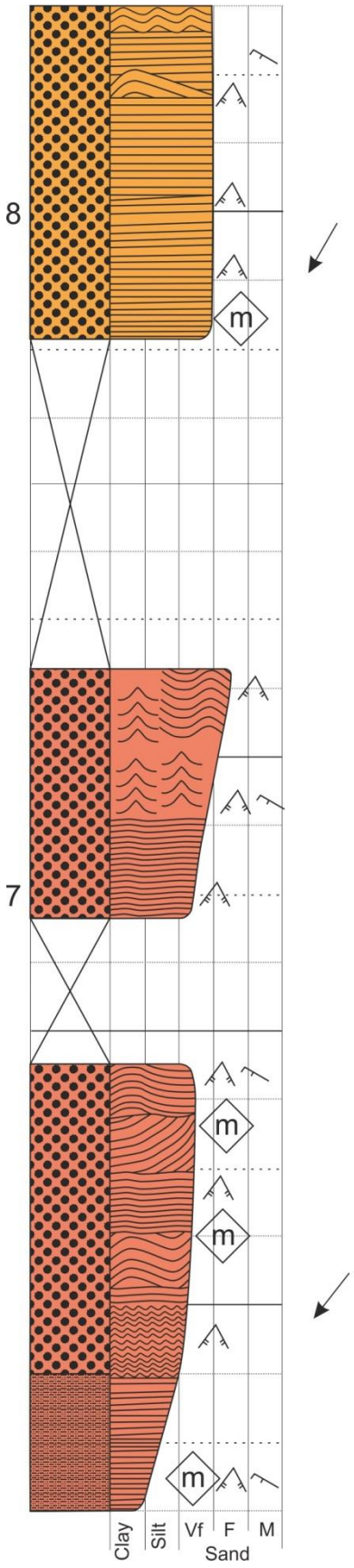
8
m
7
m
m
m
Clay
Silt
Vf
F
M
Sand

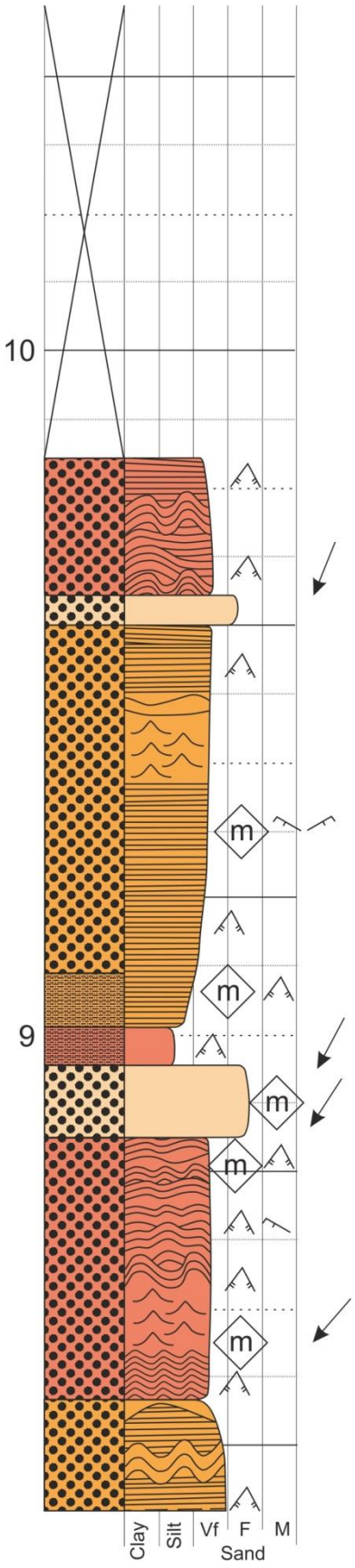
10
m
m
9
m
m
m
Clay
Silt
Vf
F
M
Sand

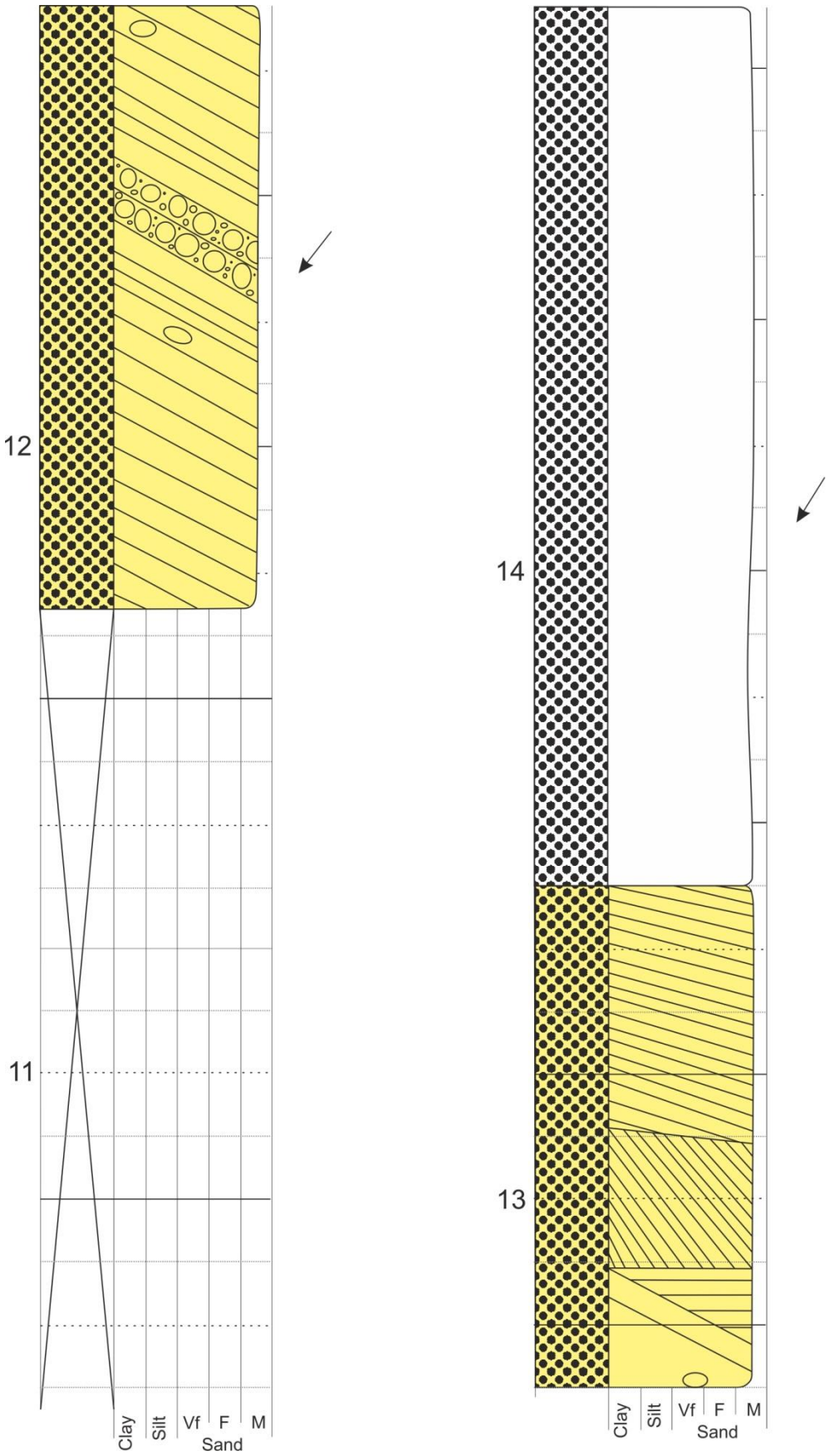
12
11
Clay
Silt
Vf
F
M
Sand
14
13
Clay
Silt
Vf
F
M
Sand

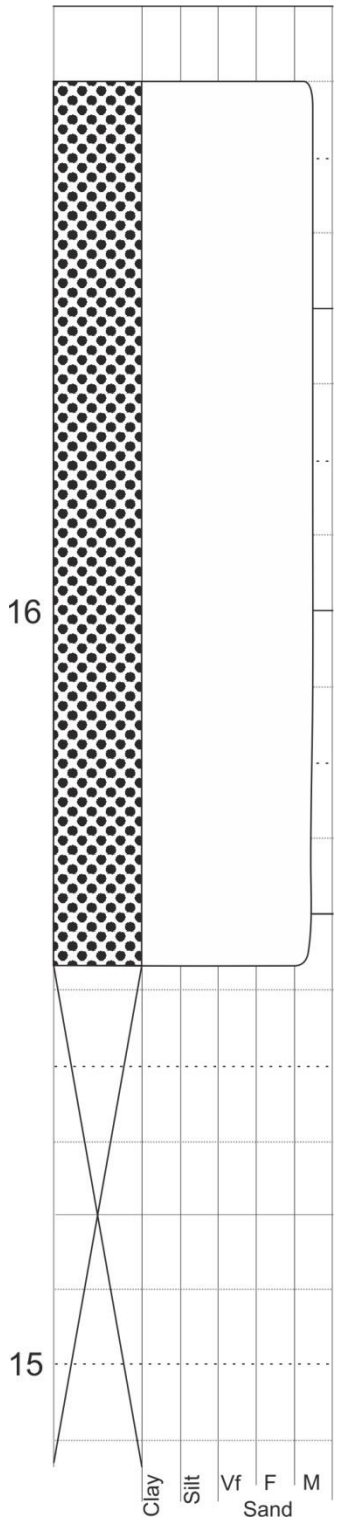
16
15
Clay
Silt
Vf
F
M
Sand

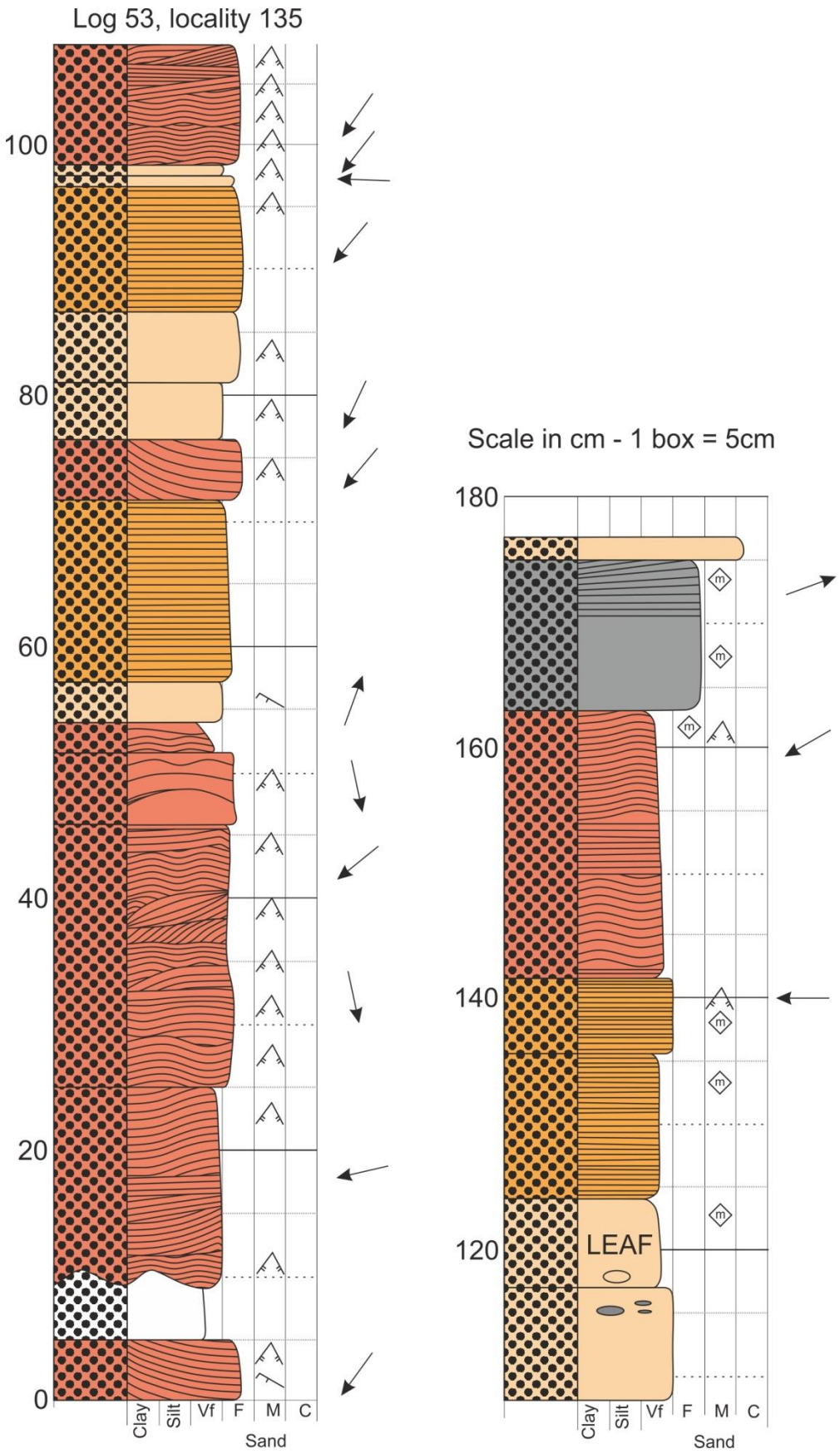
Log 53, locality 135
100
80
60
40
20
0
Clay
Silt
Vf
F
M
C
Sand
Scale in cm - 1 box = 5cm
180
160
140
120
LEAF
m
Clay
Silt
Vf
F
M
C
Sand

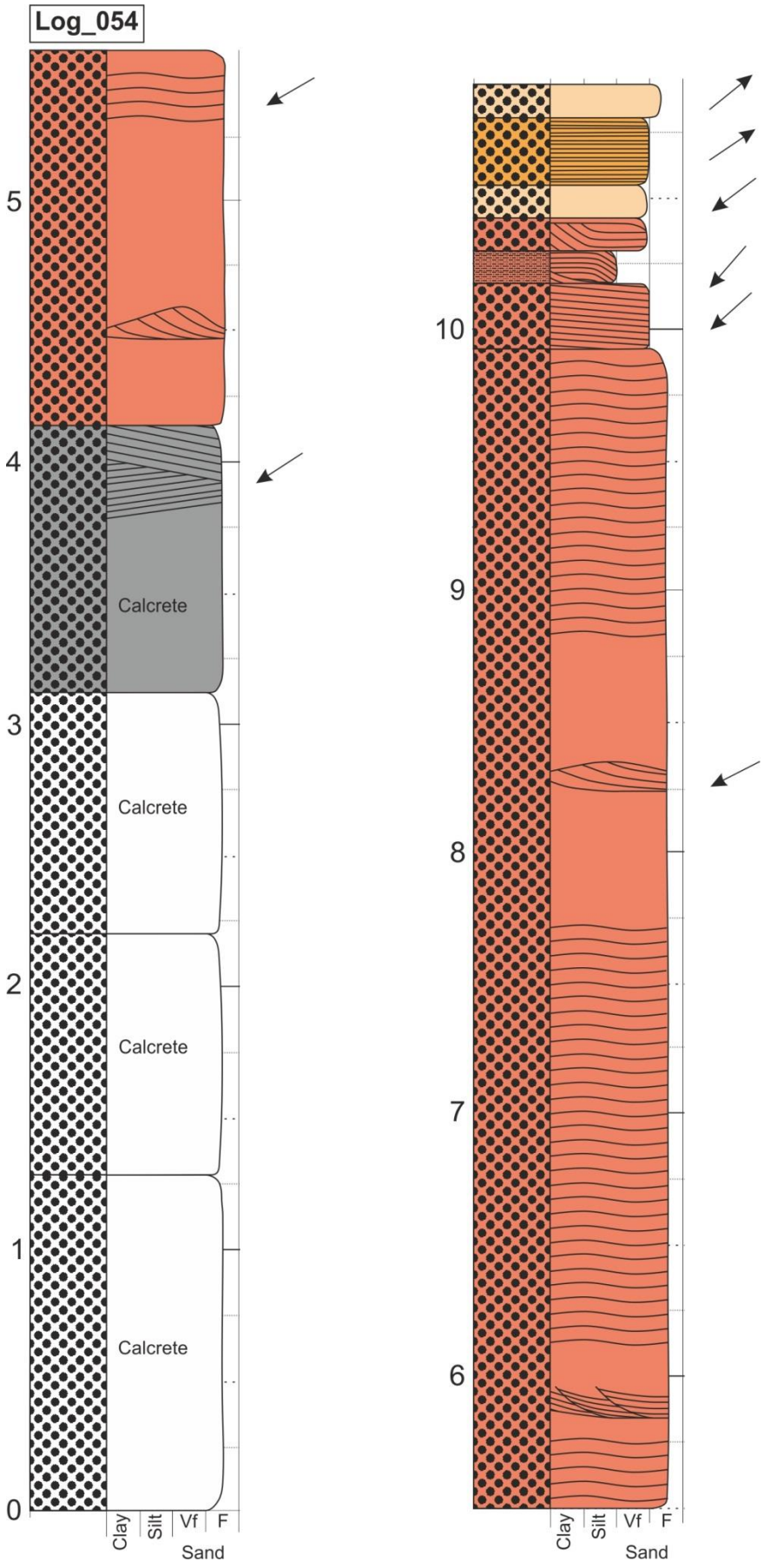
Log_054
5
4
3
2
1
0
Calcrete
Calcrete
Calcrete
Calcrete
Clay
Silt
Vf
F
Sand
10
9
8
7
6
Clay
Silt
Vf
F
Sand

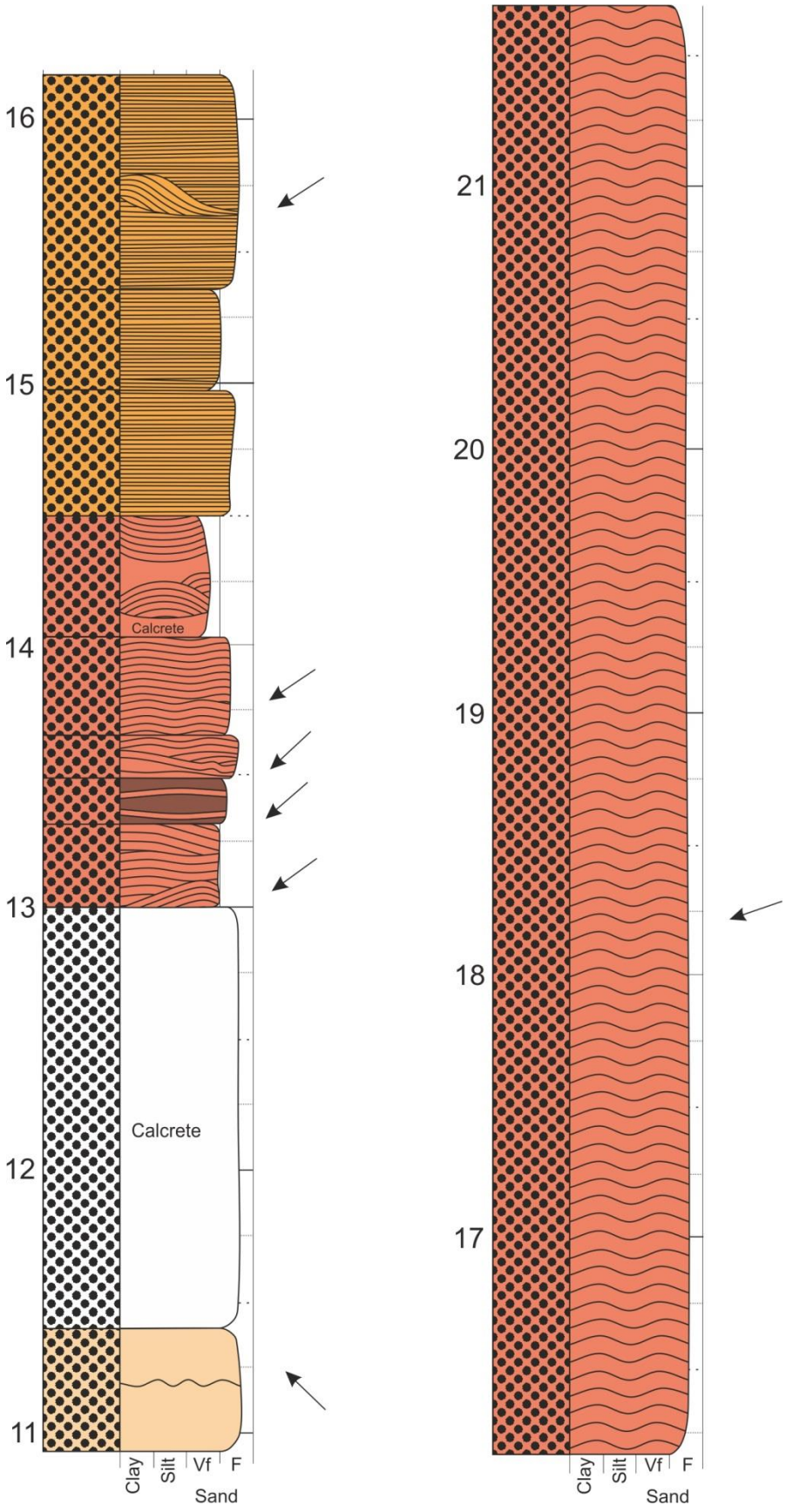
16
15
14
13
12
11
Calcrete
Calcrete
Clay
Silt
Vf
F
Sand
21
20
19
18
17
Clay
Silt
Vf
F
Sand

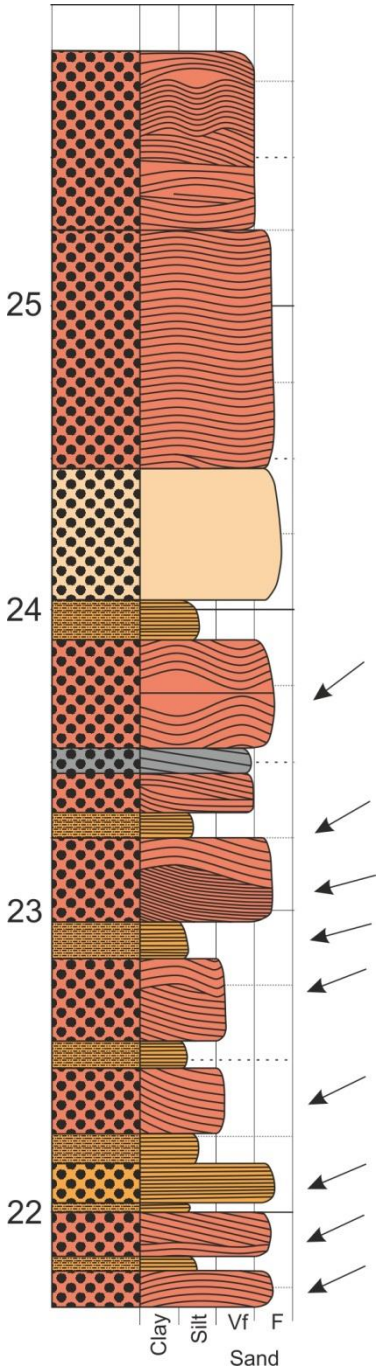
25
24
23
22
Clay
Silt
Vf
F
Sand

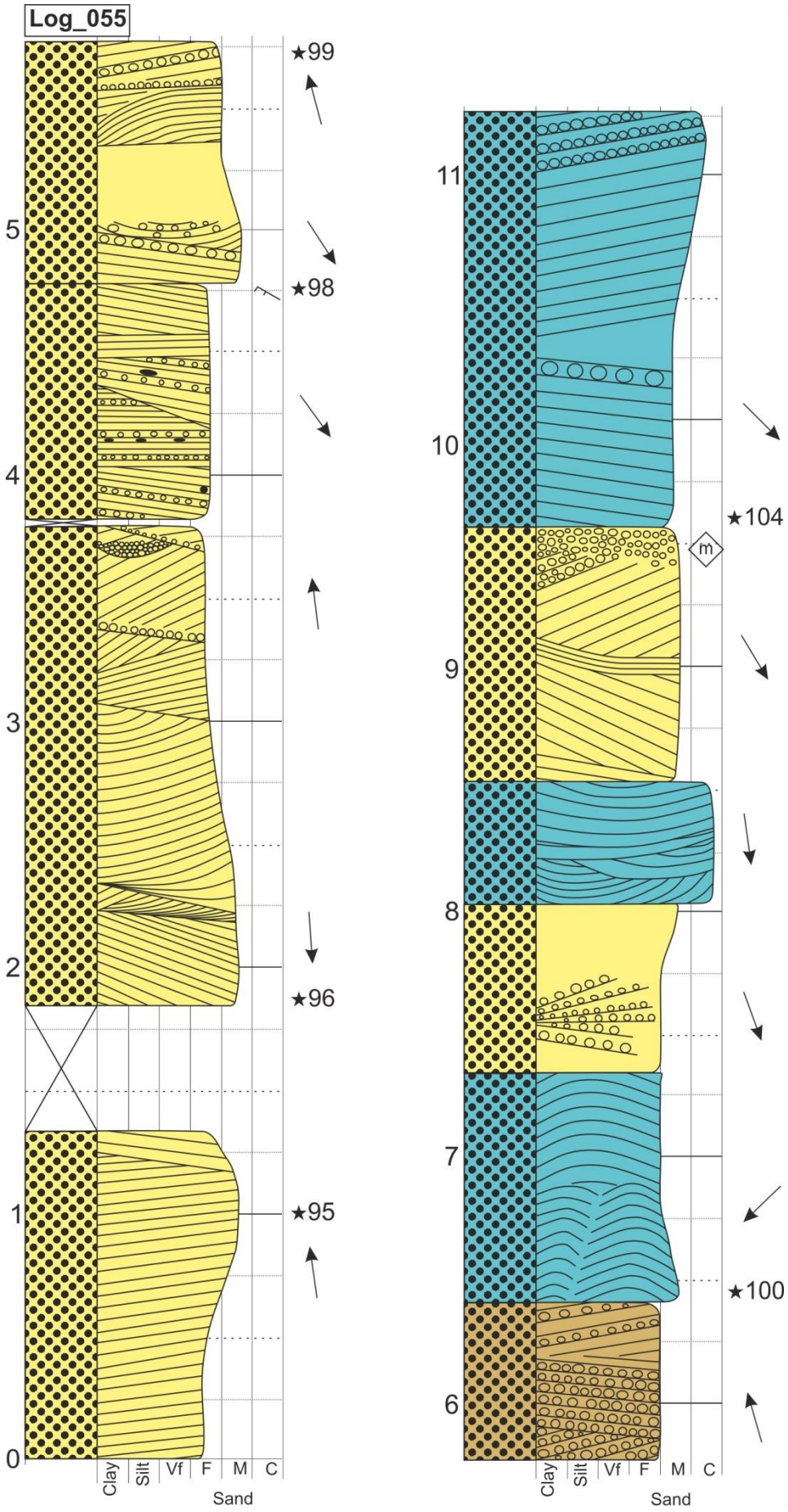
Log_055
★99
★98
★96
★95
★104
★100
m
0
1
2
3
4
5
6
7
8
9
10
11
Clay
Silt
Vf
F
M
C
Sand

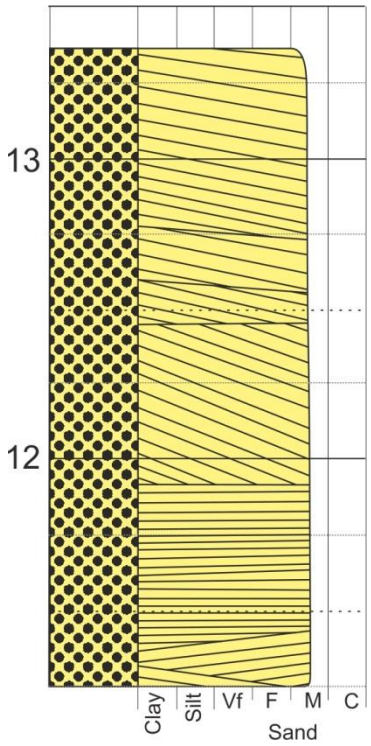
13
12
Clay
Silt
Vf
F
M
C
Sand

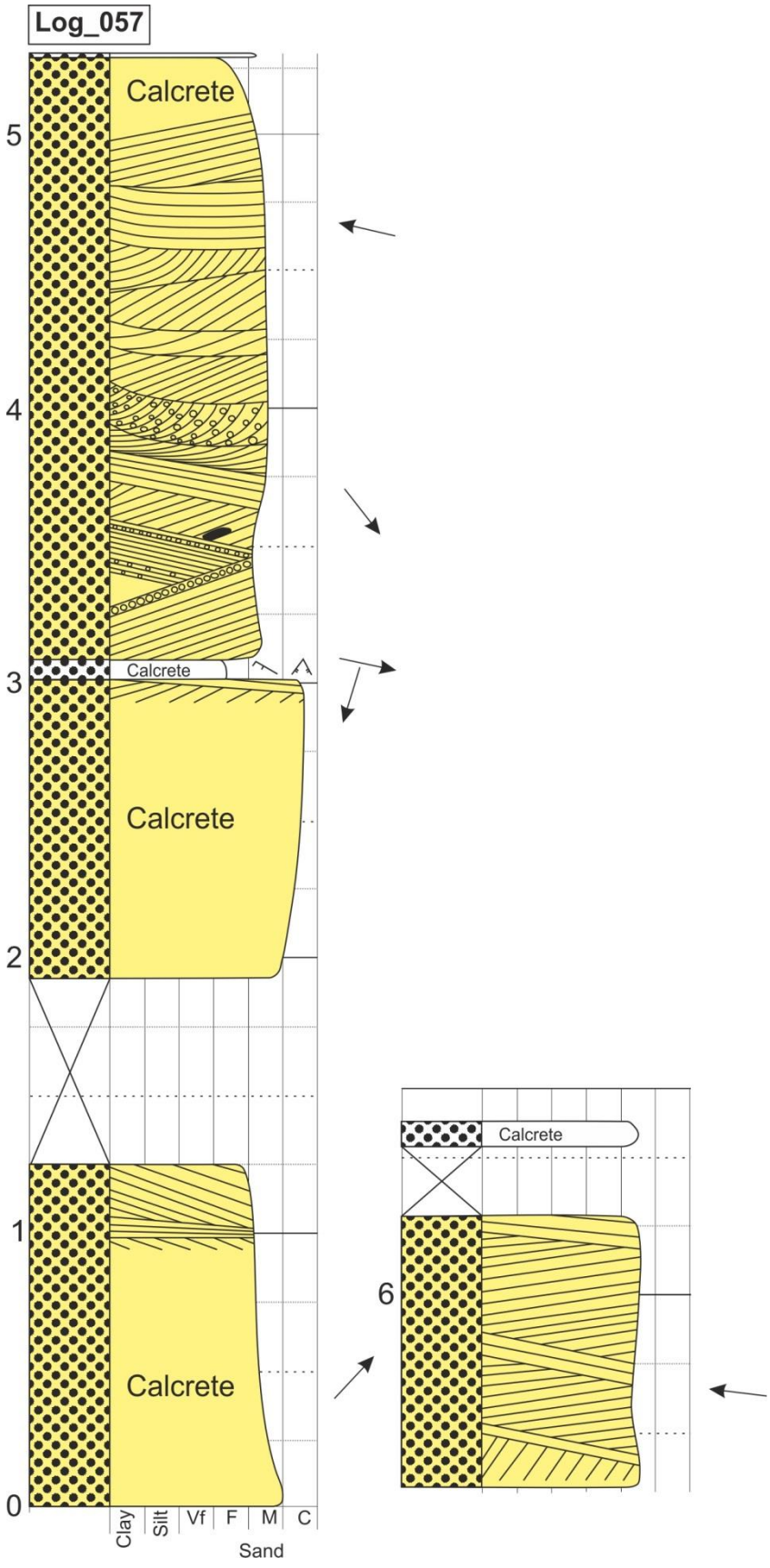
Log_057
Calcrete
5
4
Calcrete
3
Calcrete
2
1
Calcrete
0
Clay
Silt
Vf
F
M
C
Sand
Calcrete
6

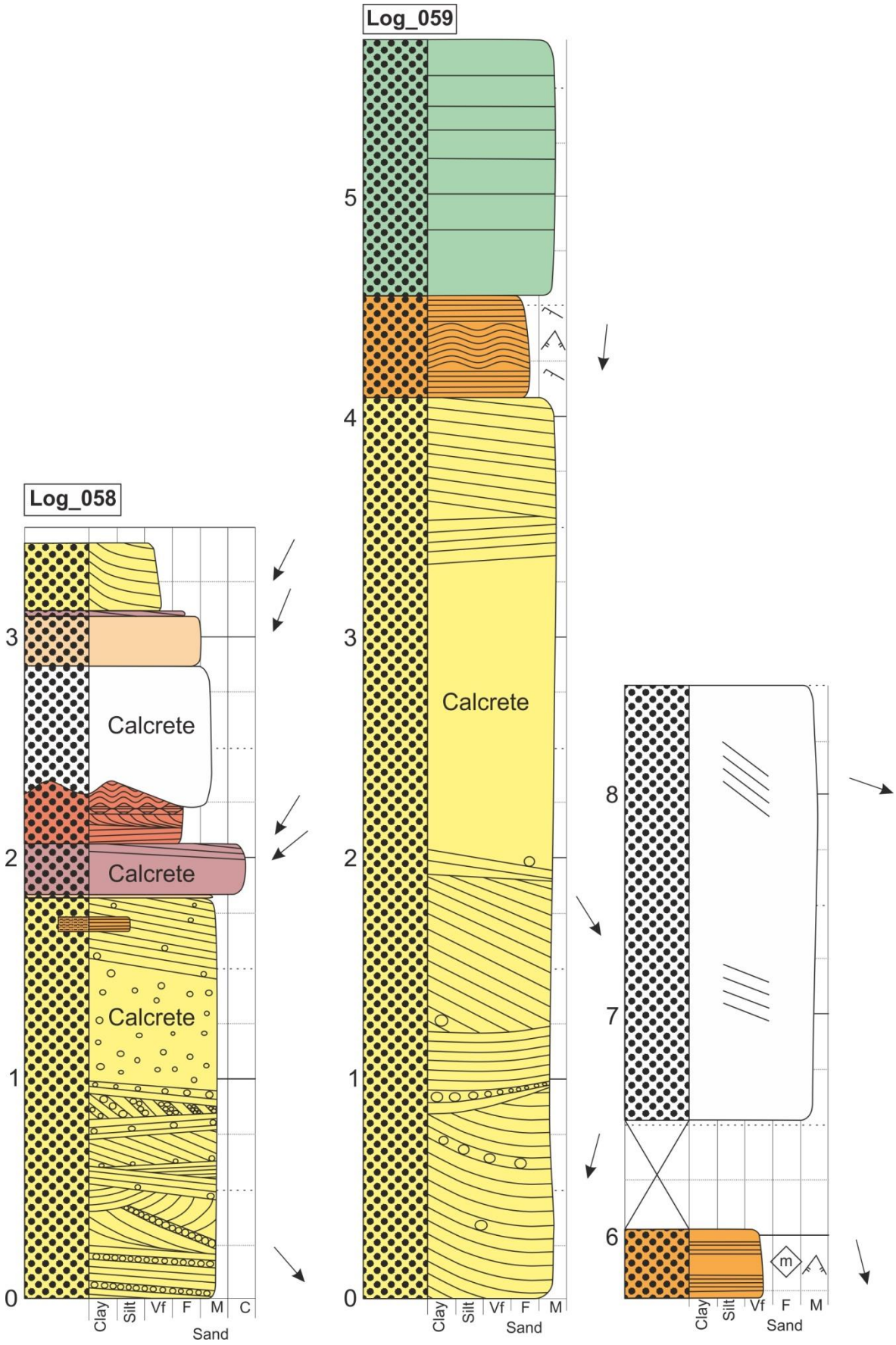
Log_059
Log_058
Calcrete
Calcrete
Calcrete
Calcrete
m
Clay
Silt
Vf
F
M
C
Sand

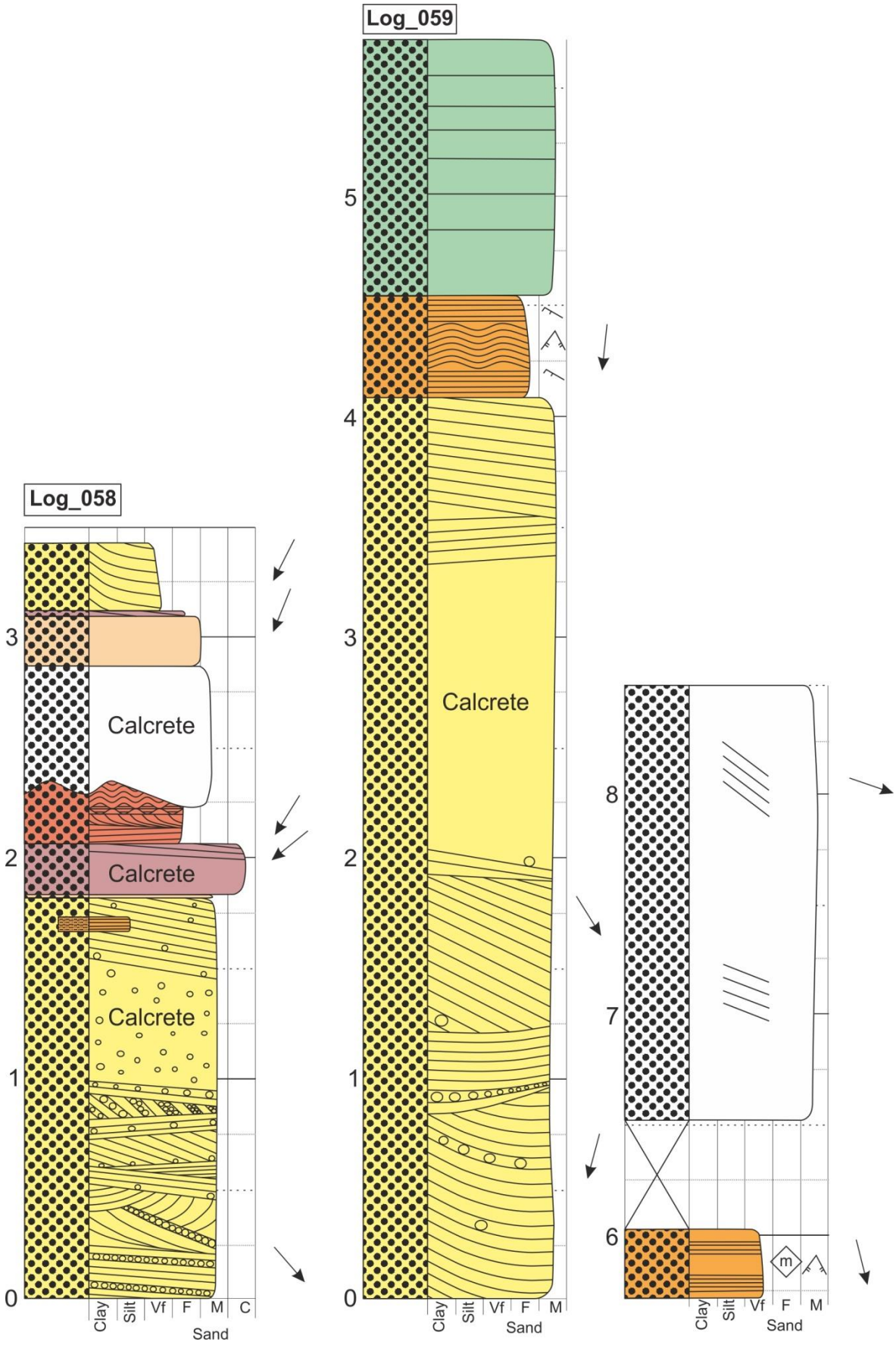
Log_059
Log_058
Calcrete
Calcrete
Calcrete
Calcrete
m
0
1
2
3
4
5
6
7
8
Clay
Silt
Vf
F
M
C
Sand

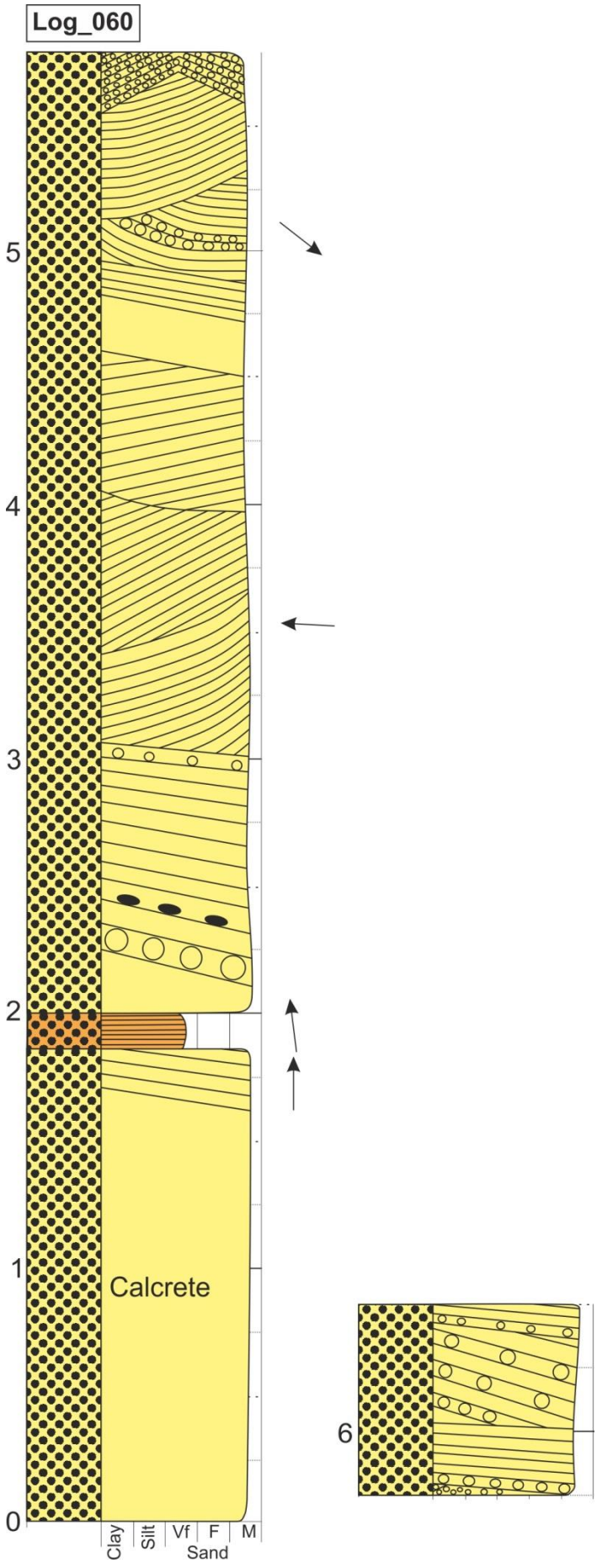
Log_060
5
4
3
2
1
0
Calcrete
6
Clay
Silt
Vf
F
M
Sand

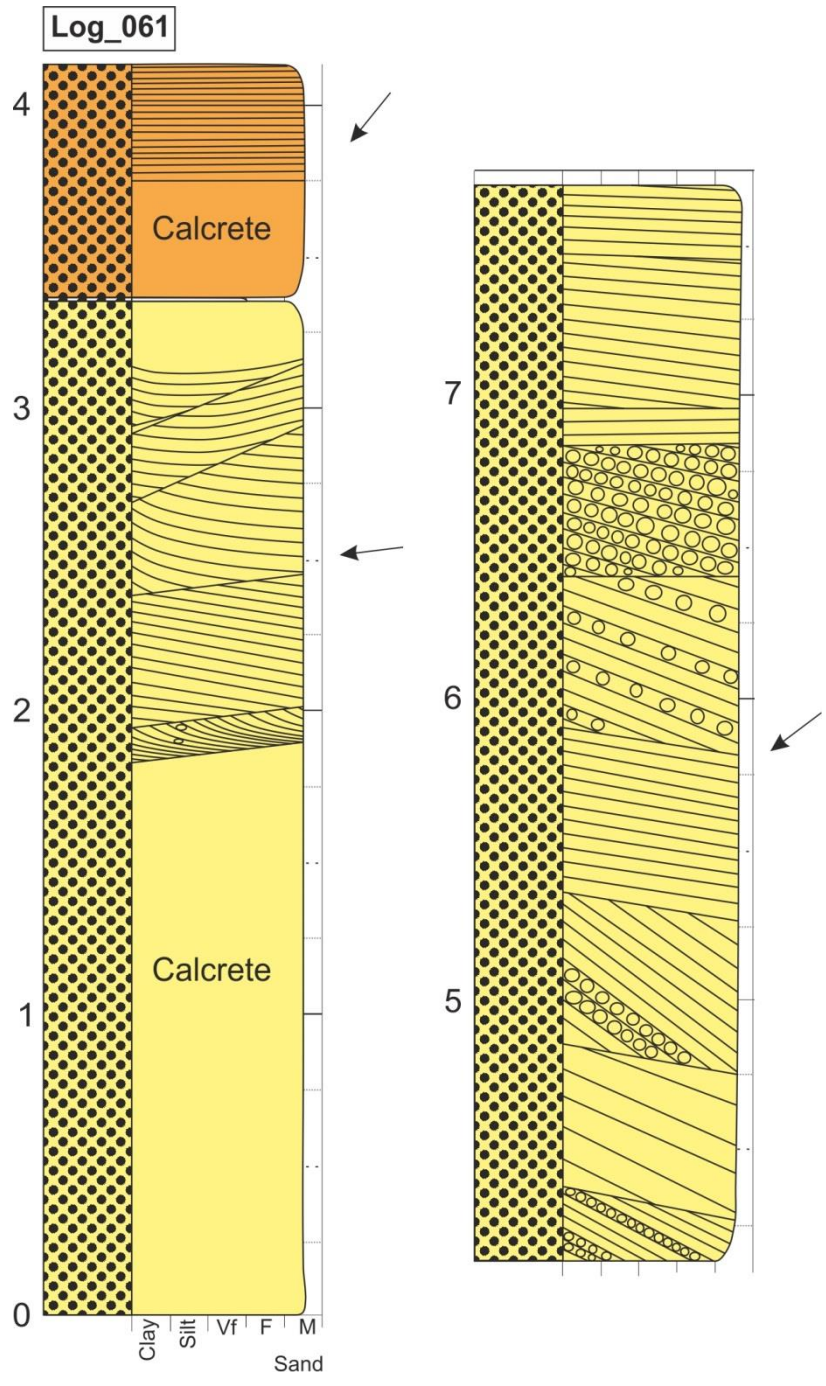
Log_061
4
3
2
1
0
Calcrete
Calcrete
Clay
Silt
Vf
F
M
Sand
7
6
5

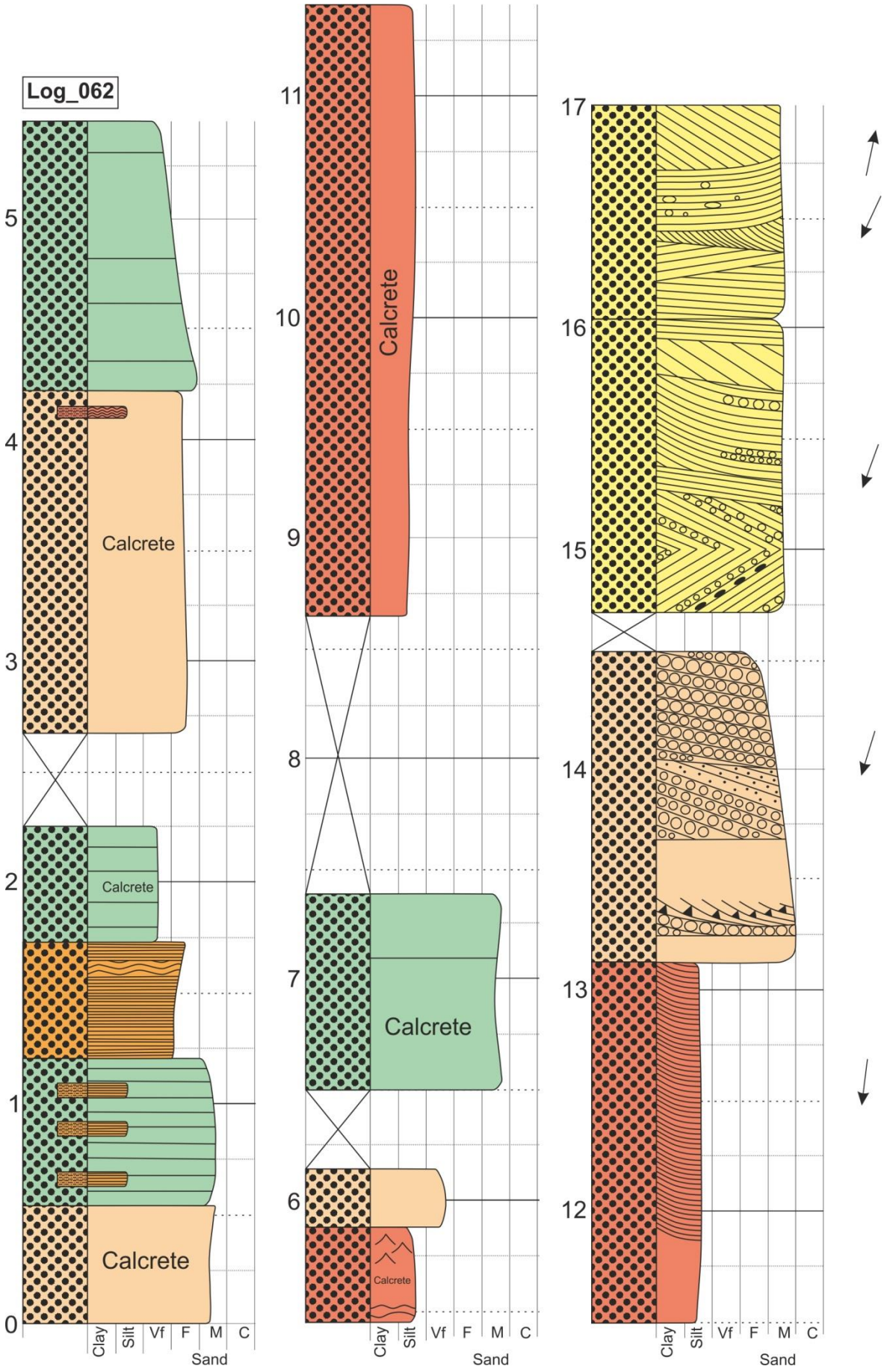
Log_062
0
1
2
3
4
5
6
7
8
9
10
11
12
13
14
15
16
17
Calcrete
Calcrete
Calcrete
Calcrete
Calcrete
Clay
Silt
Vf
F
M
C
Sand

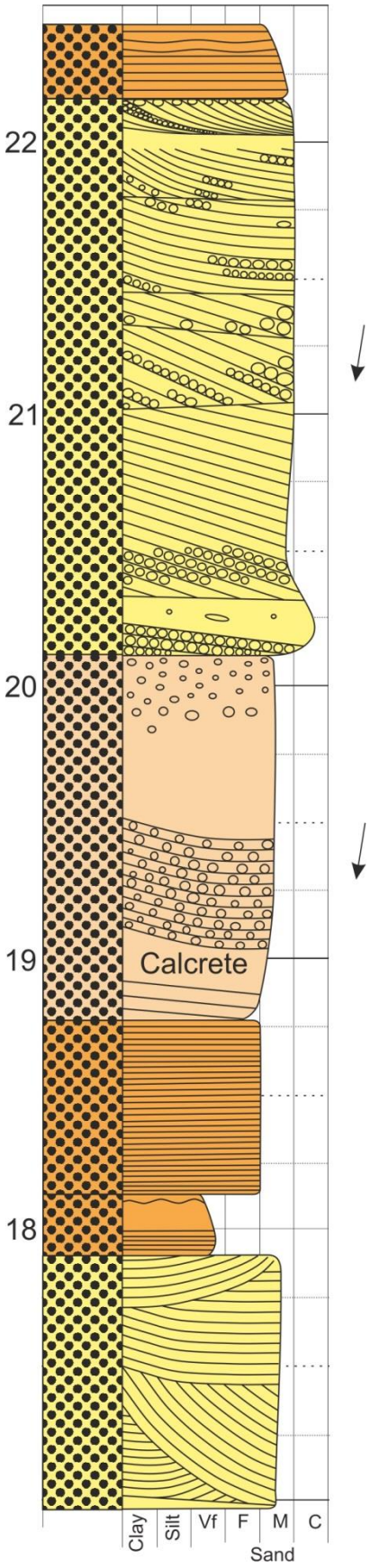
22
21
20
19
18
Calcrete
Clay
Silt
Vf
F
M
C
Sand

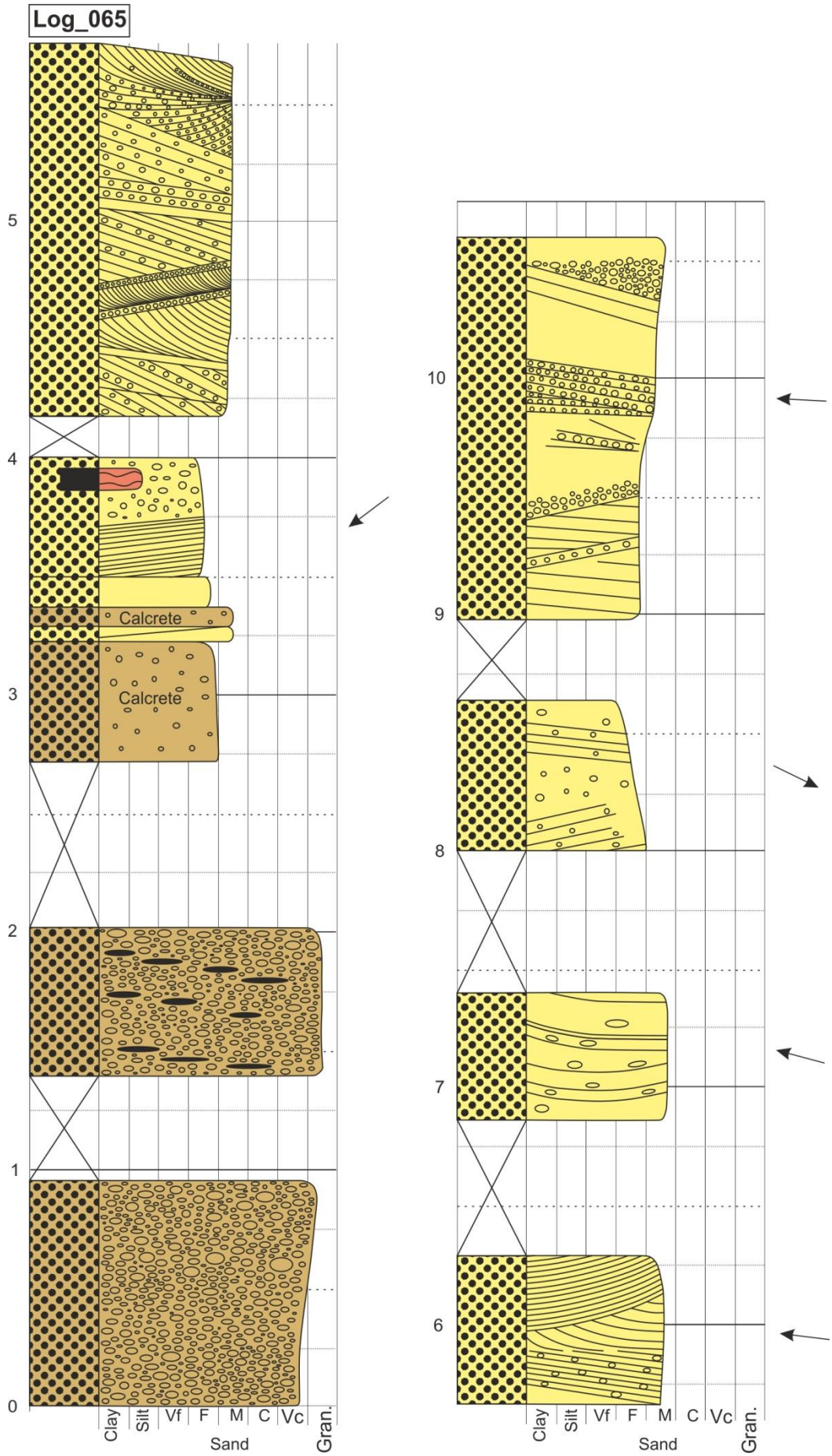
Log_065
Calcrete
Calcrete
0
1
2
3
4
5
6
7
8
9
10
Clay
Silt
Vf
F
M
C
Vc
Gran.
Sand

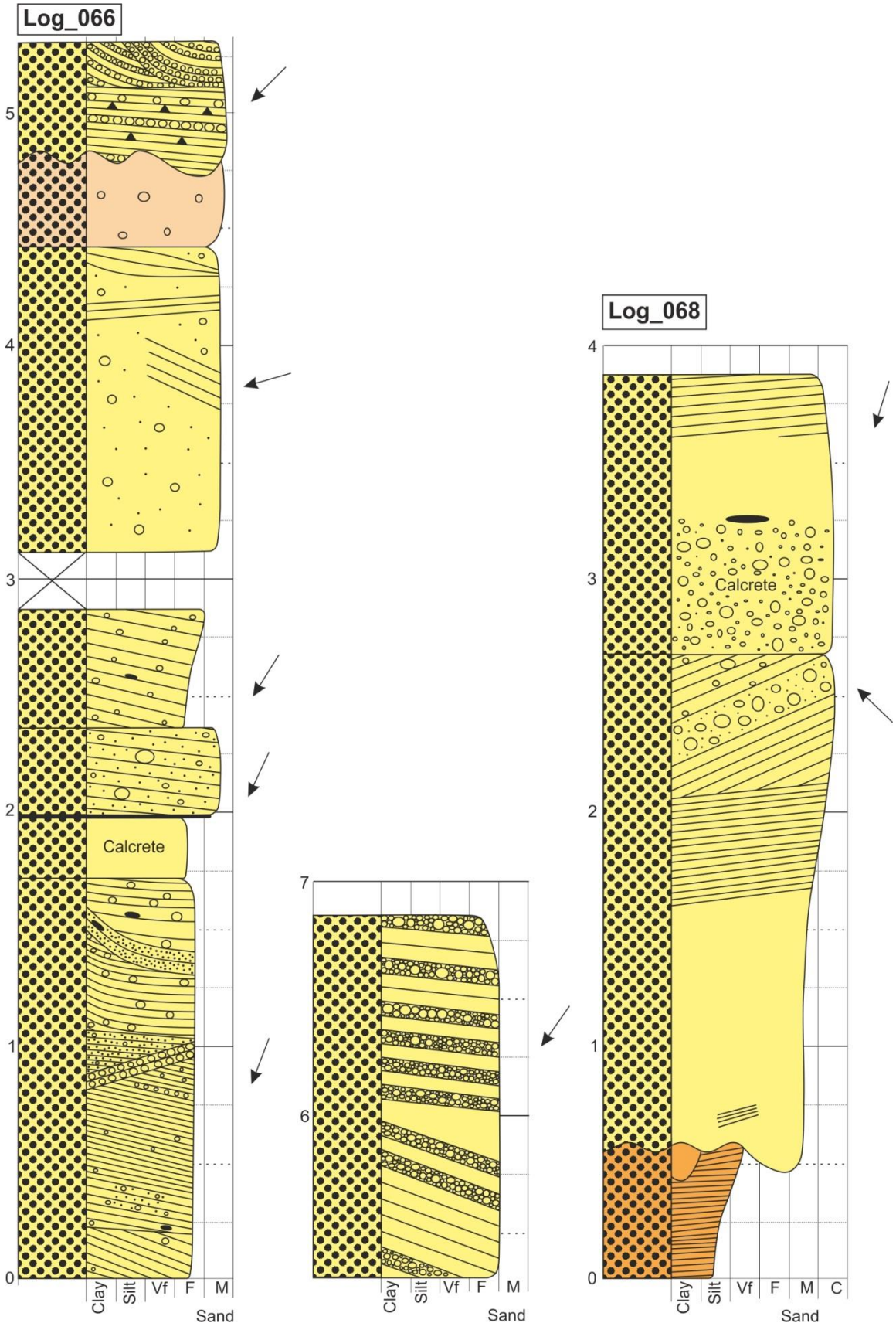
Log_066
5
4
3
2
1
0
Calcrete
Clay
Silt
Vf
F
M
Sand
7
6
Clay
Silt
Vf
F
M
Sand
Log_068
4
3
2
1
0
Calcrete
Clay
Silt
Vf
F
M
C
Sand

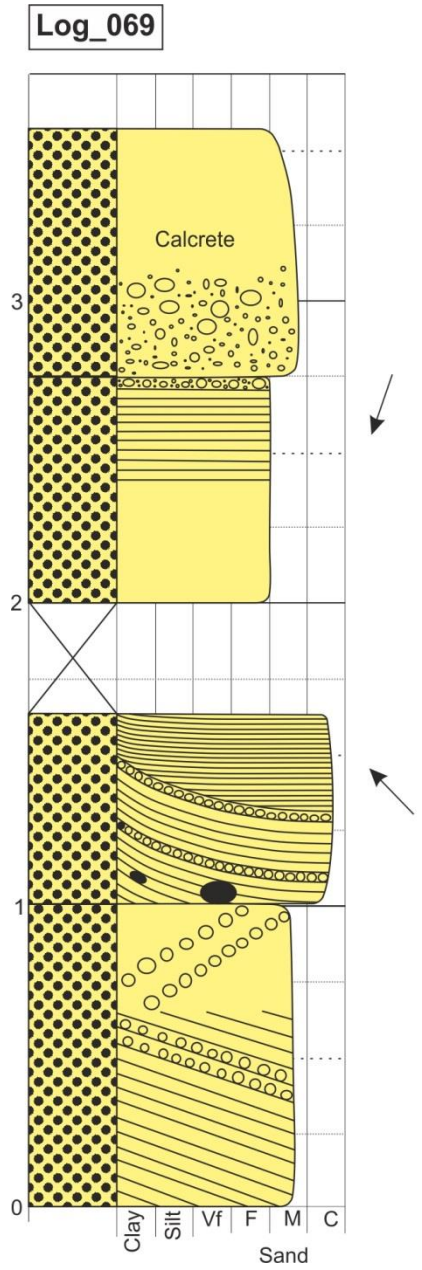
Log_069
Calcrete
3
2
1
0
Clay
Silt
Vf
F
M
C
Sand

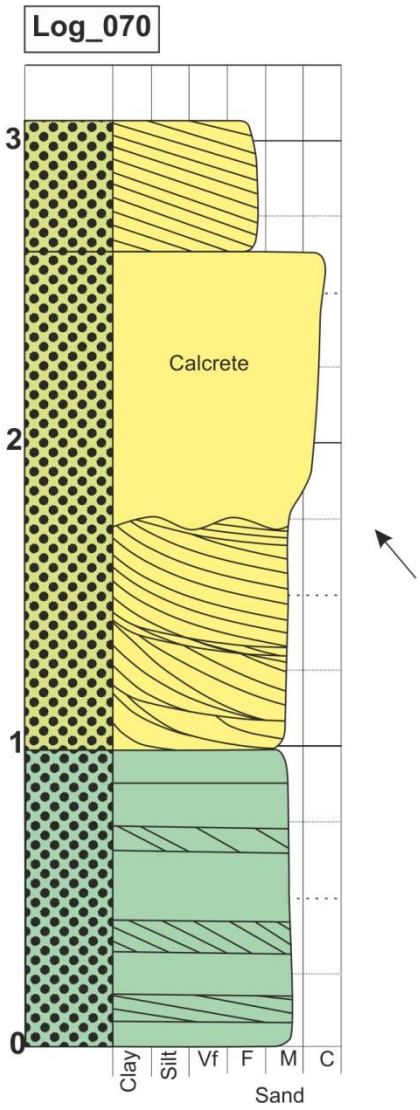
Log_070
3
Calcrete
2
1
0
Clay
Silt
Vf
F
M
C
Sand

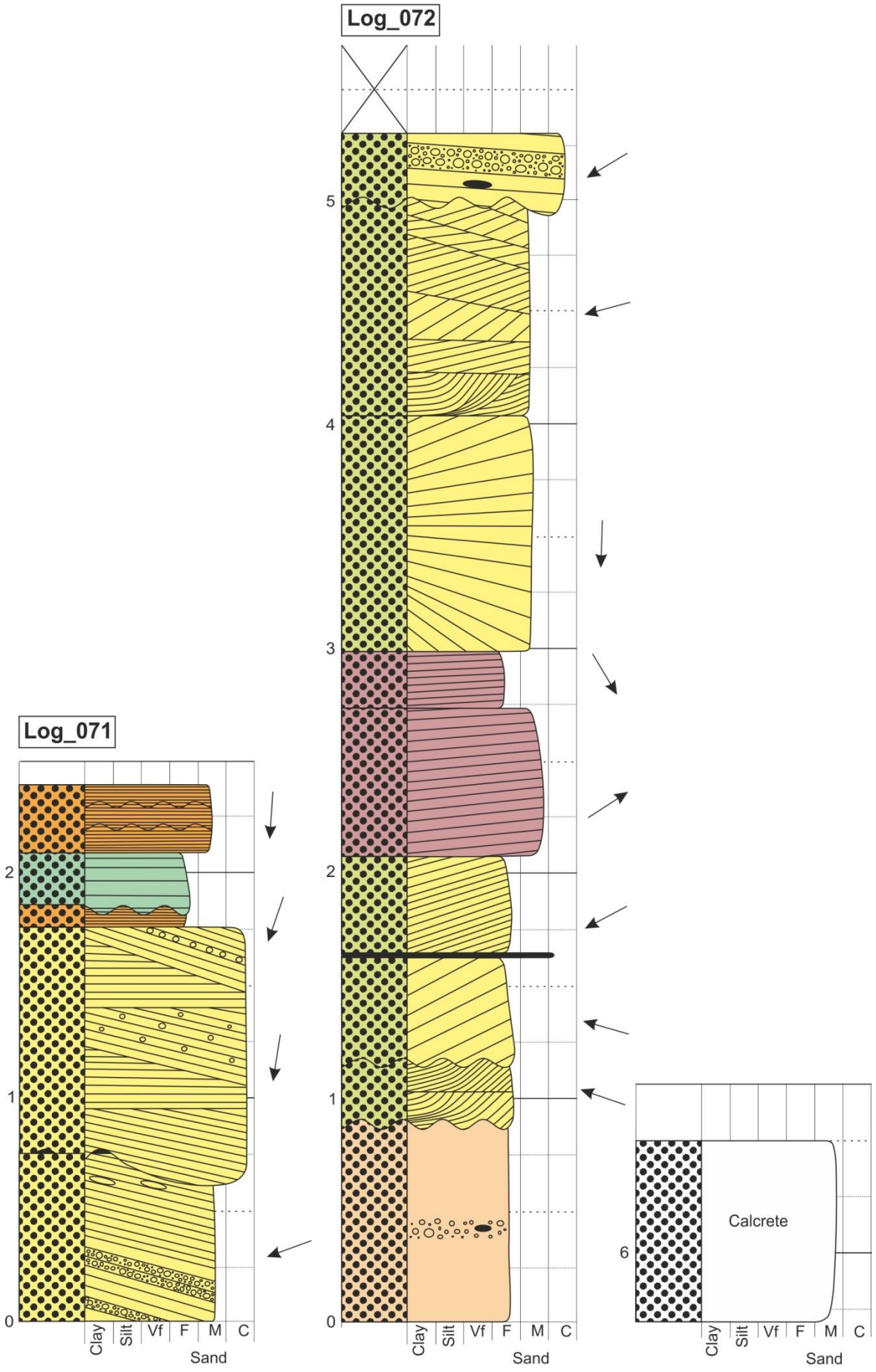
Log_072
Log_071
Calcrete
0
1
2
3
4
5
6
Clay
Silt
Vf
F
M
C
Sand

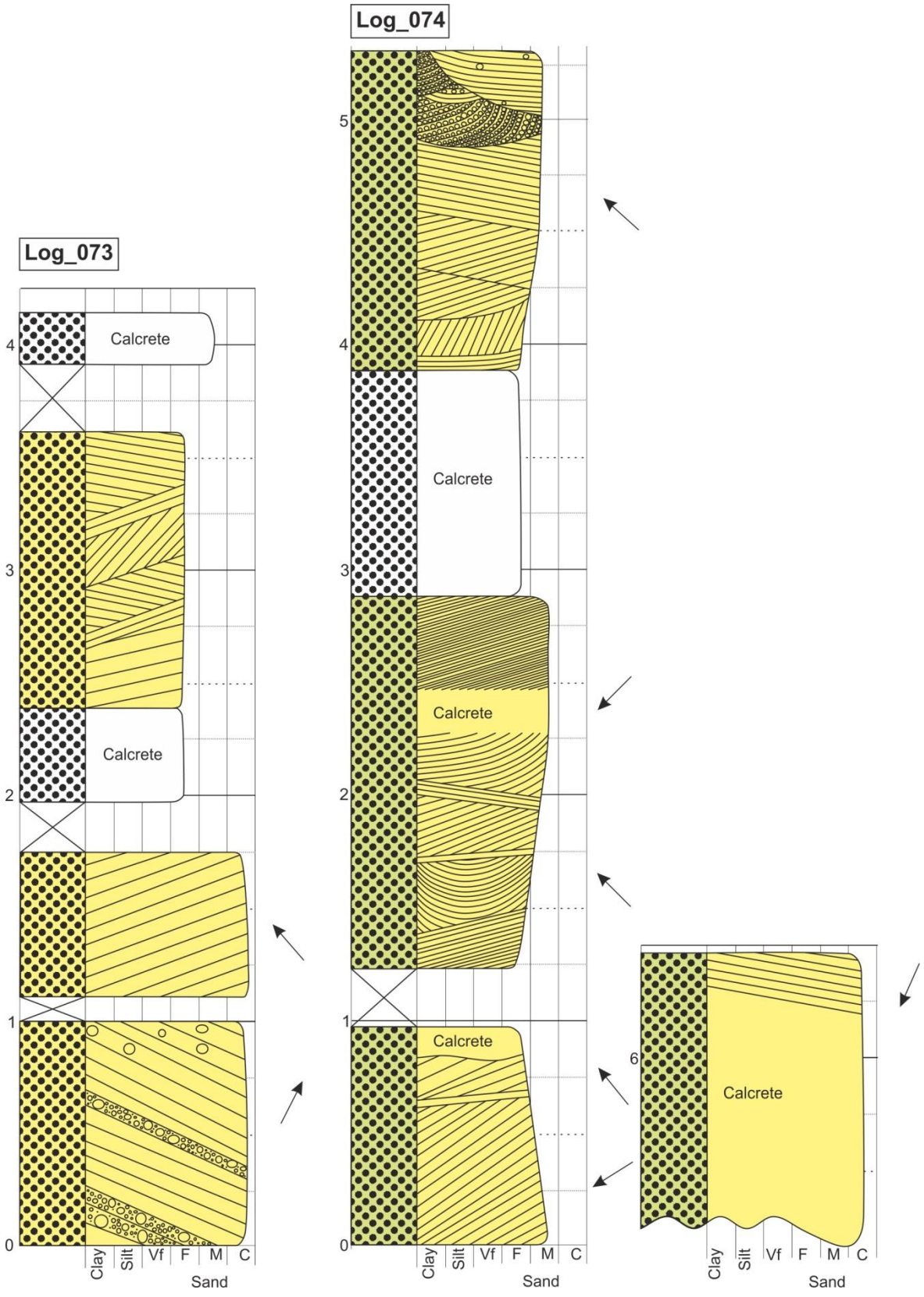
Log_073
Calcrete
Calcrete
4
3
2
1
0
Clay
Silt
Vf
F
M
C
Sand
Log_074
Calcrete
Calcrete
Calcrete
5
4
3
2
1
0
Clay
Silt
Vf
F
M
C
Sand
Calcrete
6
Clay
Silt
Vf
F
M
C
Sand

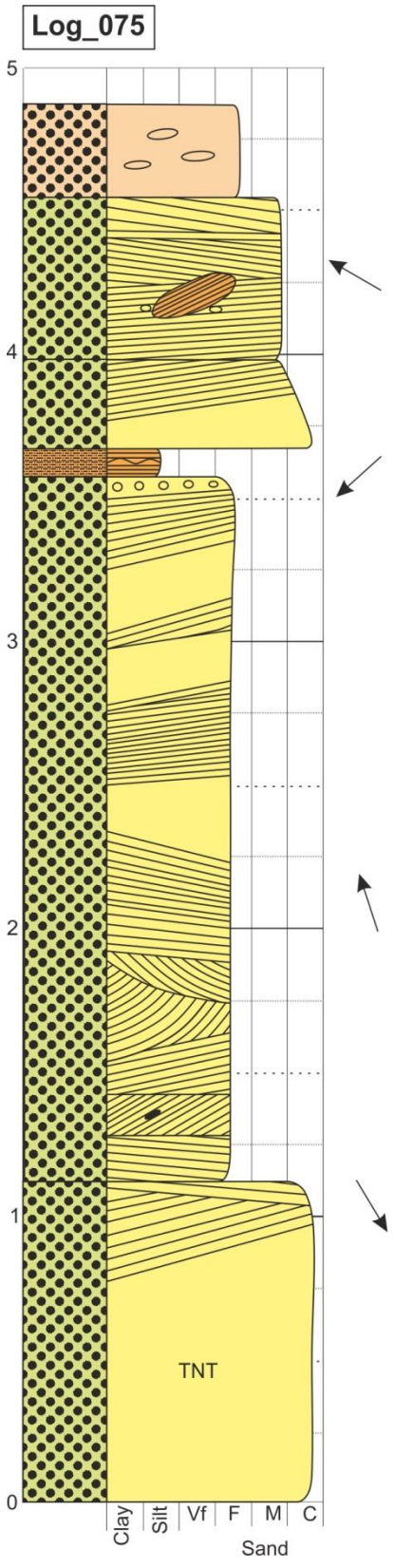
Log_075
5
4
3
2
1
0
TNT
Clay
Silt
Vf
F
M
C
Sand

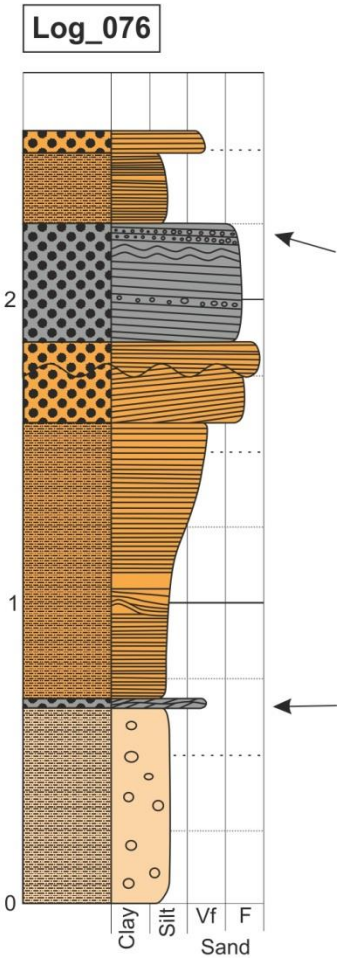
Log_076
2
1
0
Clay
Silt
Vf
F
Sand

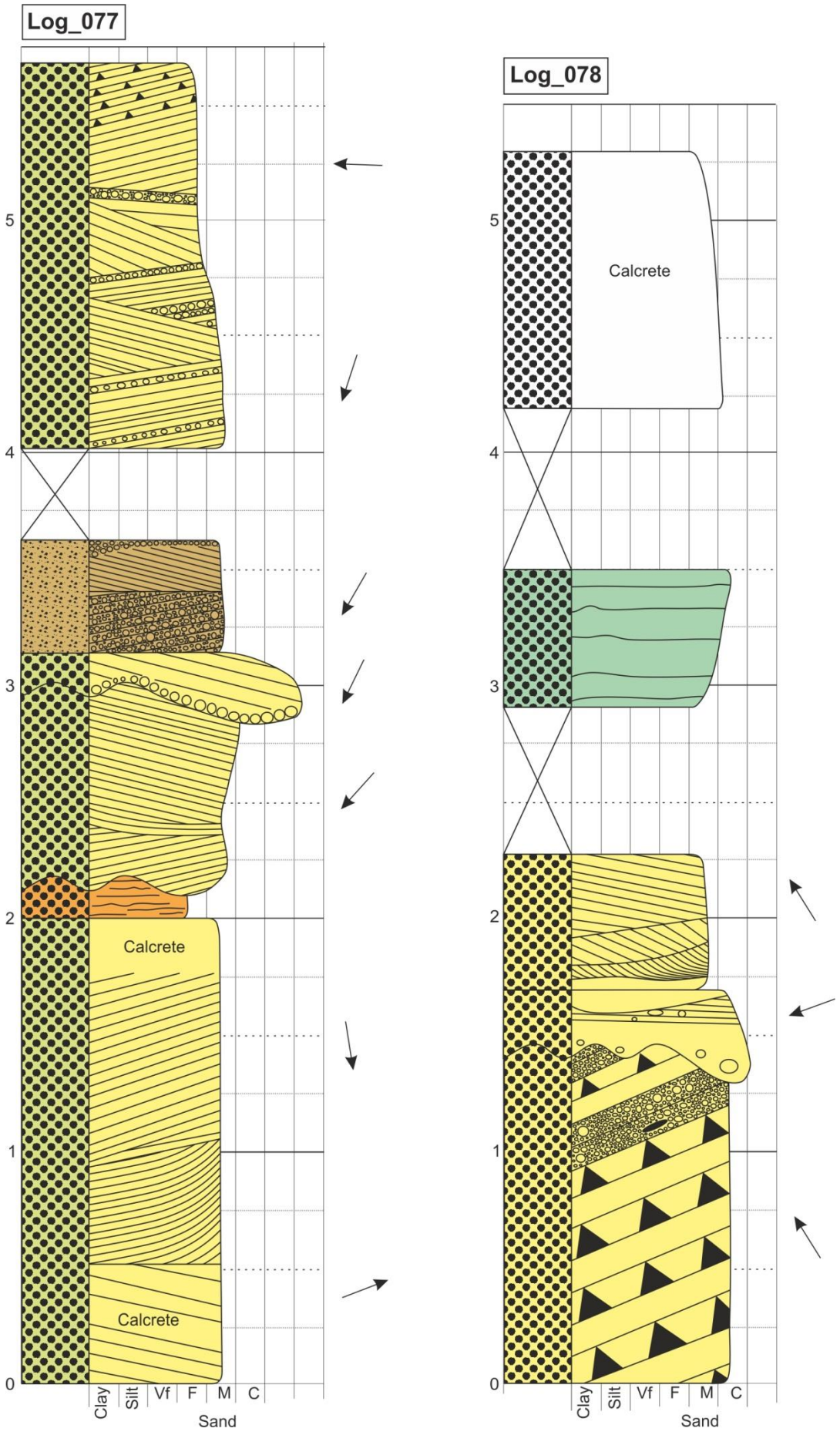
Log_077
5
4
3
2
1
0
Calcrete
Calcrete
Clay
Silt
Vf
F
M
C
Sand
Log_078
5
4
3
2
1
0
Calcrete
Clay
Silt
Vf
F
M
C
Sand

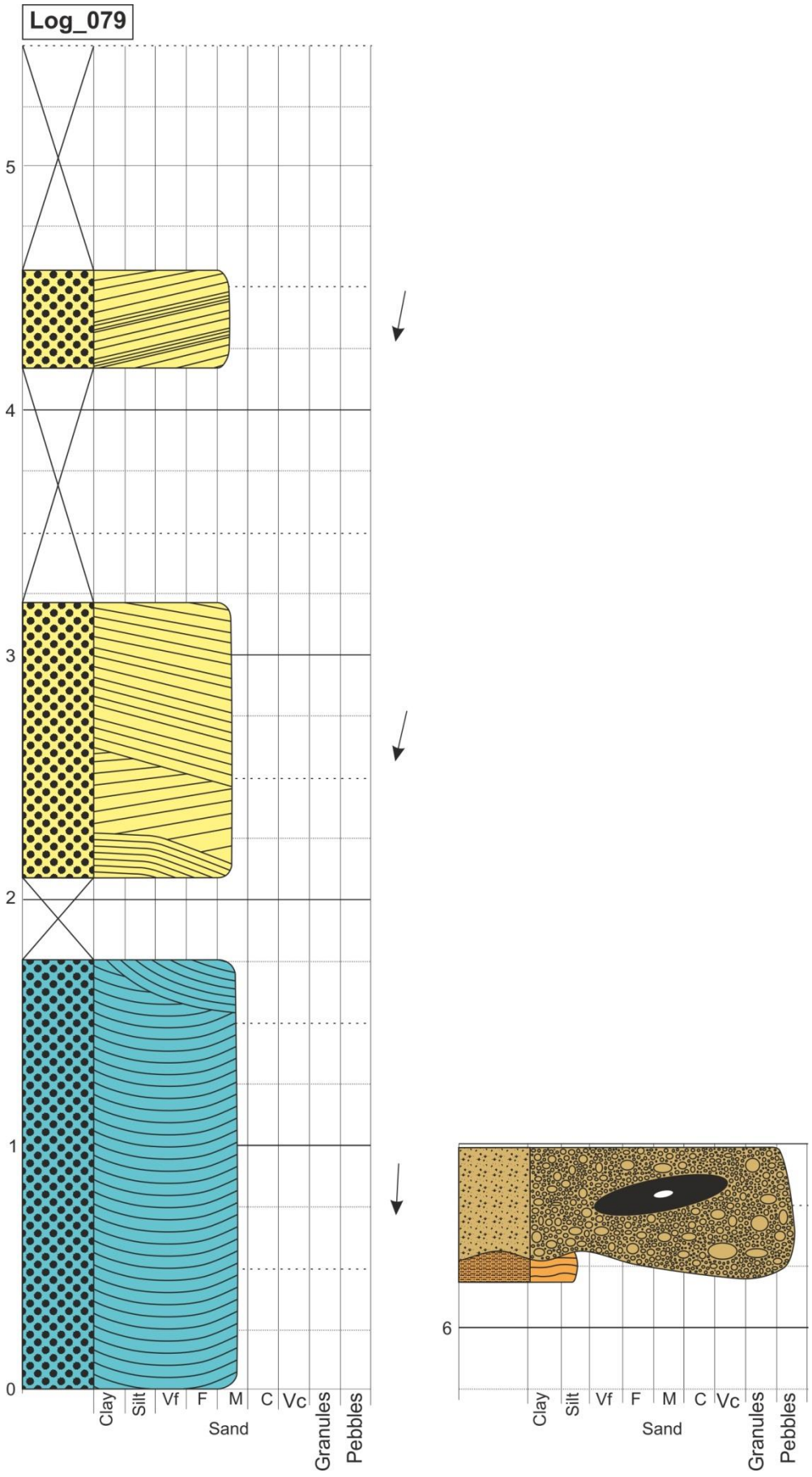
Log_079
5
4
3
2
1
0
6
Clay
Silt
Vf
F
M
C
Vc
Sand
Granules
Pebbles

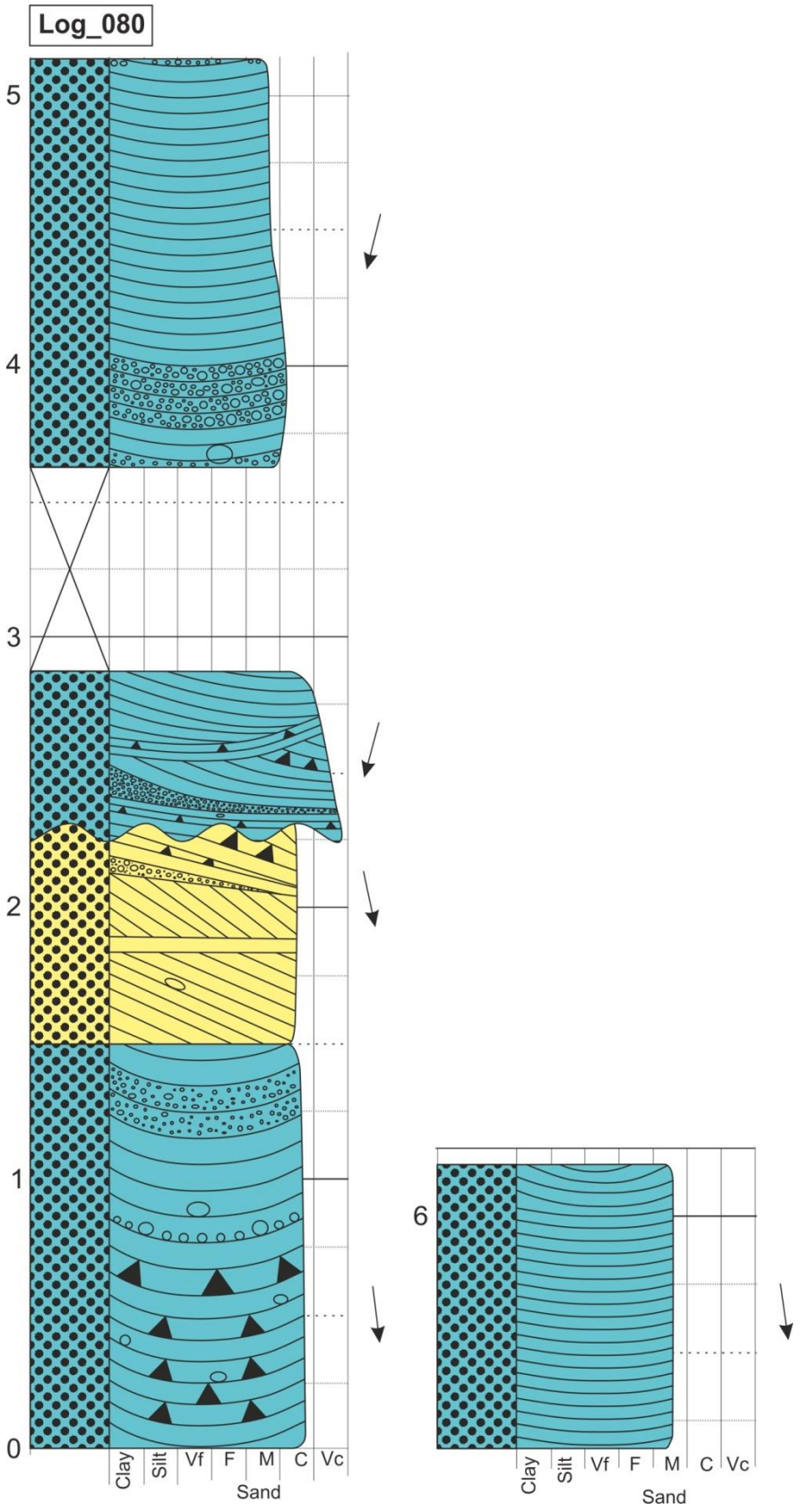
Log_080
5
4
3
2
1
0
Clay
Silt
Vf
F
M
C
Vc
Sand
6
Clay
Silt
Vf
F
M
C
Vc
Sand

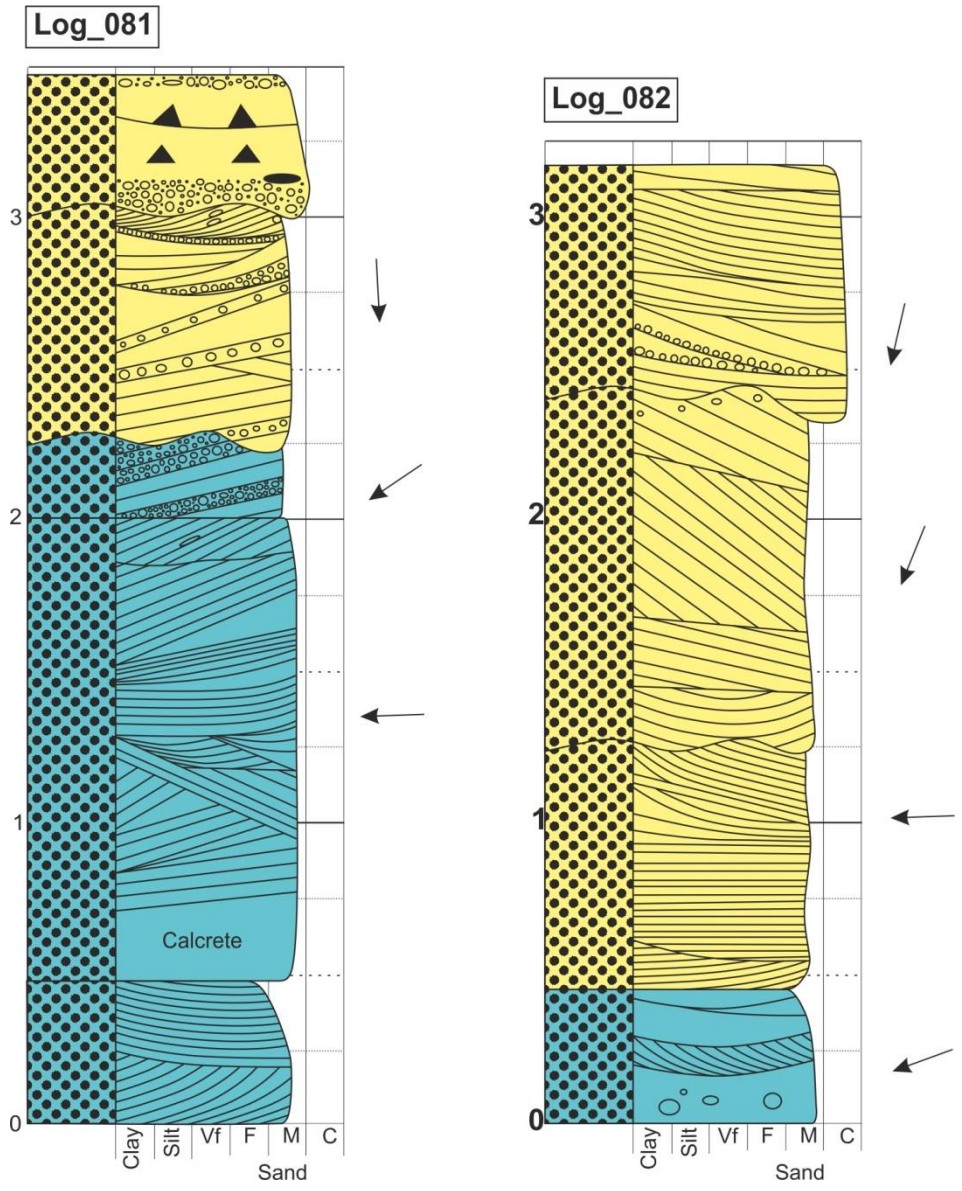
Log_081
Log_082
3
2
1
0
Calcrete
Clay
Silt
Vf
F
M
C
Sand

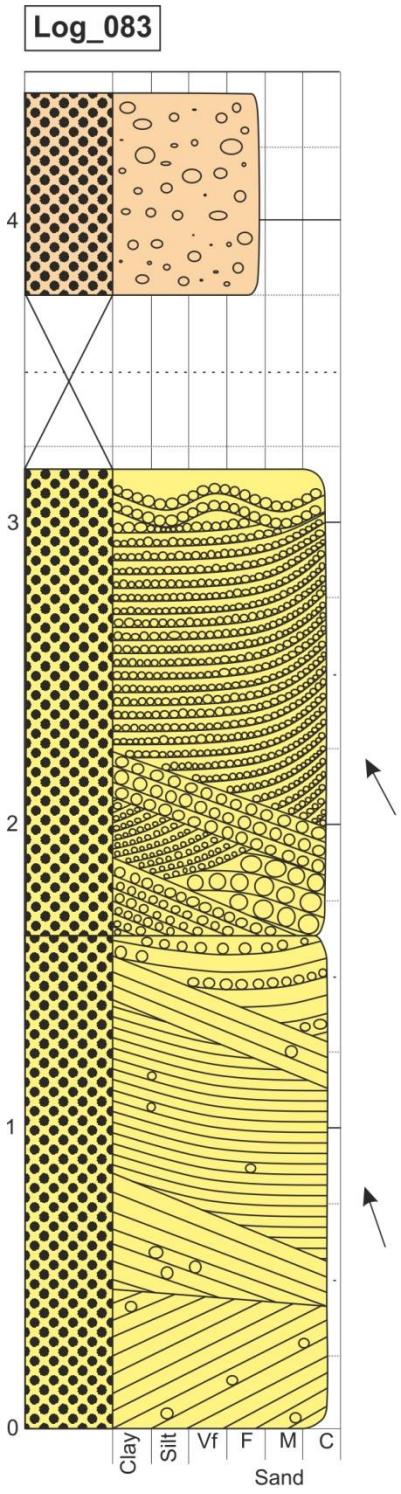
Log_083
4
3
2
1
0
Clay
Silt
Vf
F
M
C
Sand

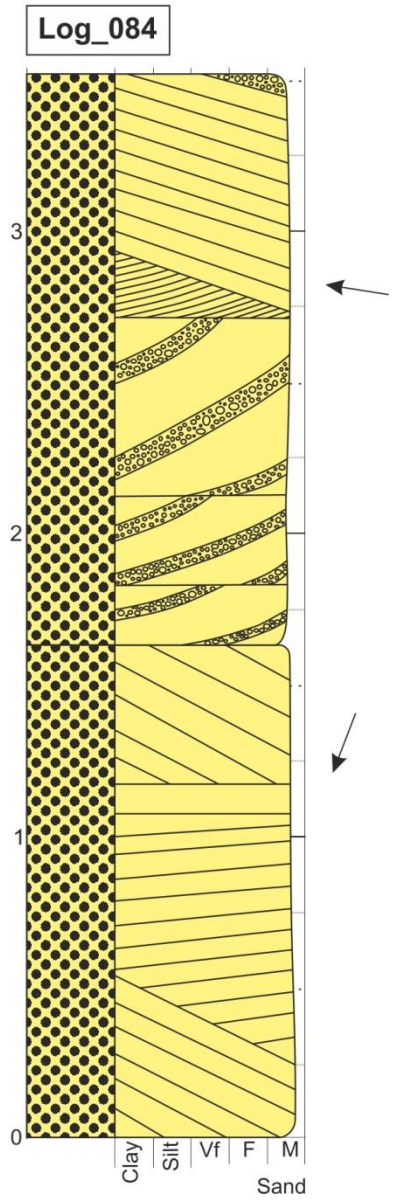
Log_084
3
2
1
0
Clay
Silt
Vf
F
M
Sand

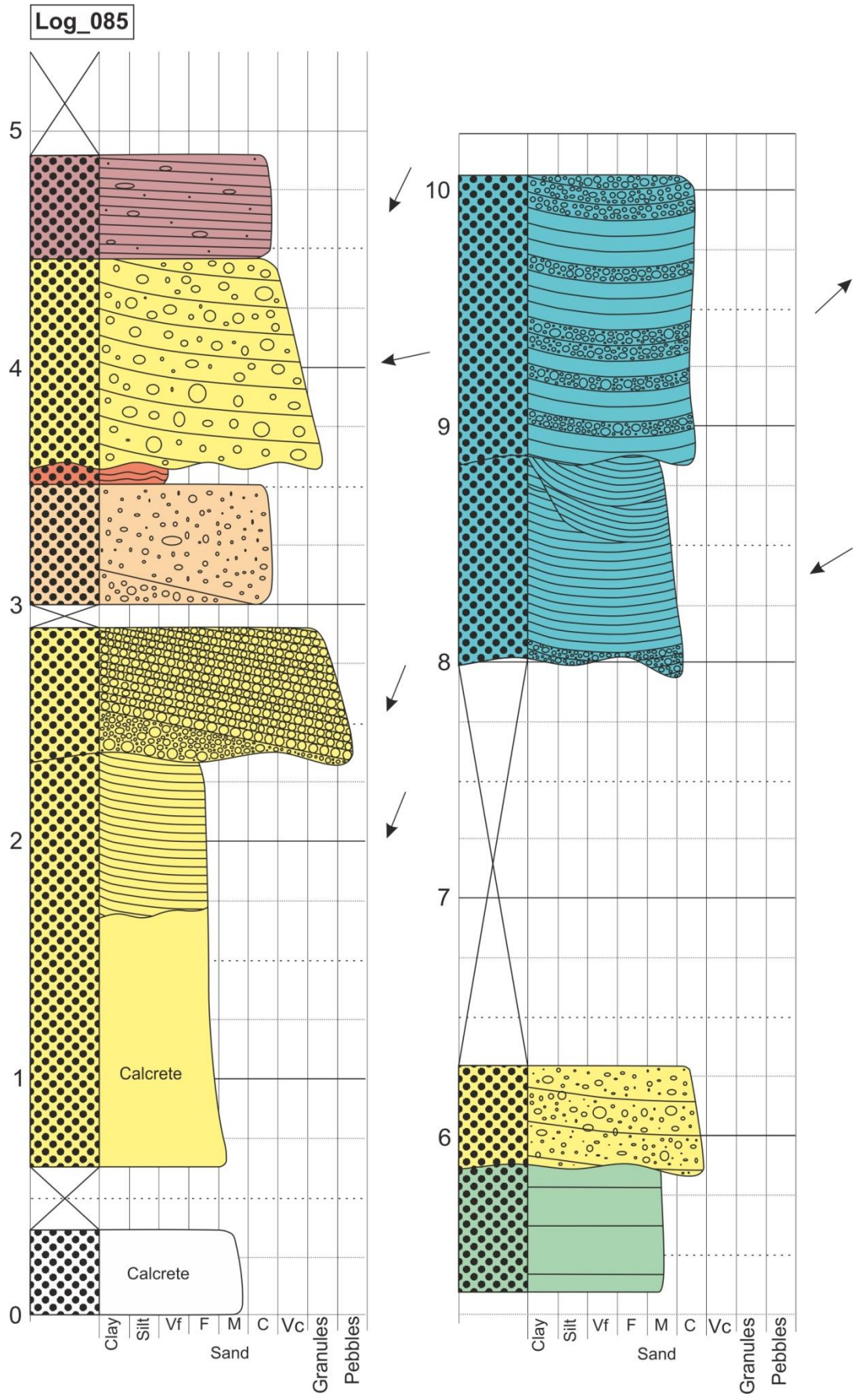
Log_085
5
4
3
2
1
0
Calcrete
Calcrete
10
9
8
7
6
Clay
Silt
Vf
F
M
C
Vc
Sand
Granules
Pebbles

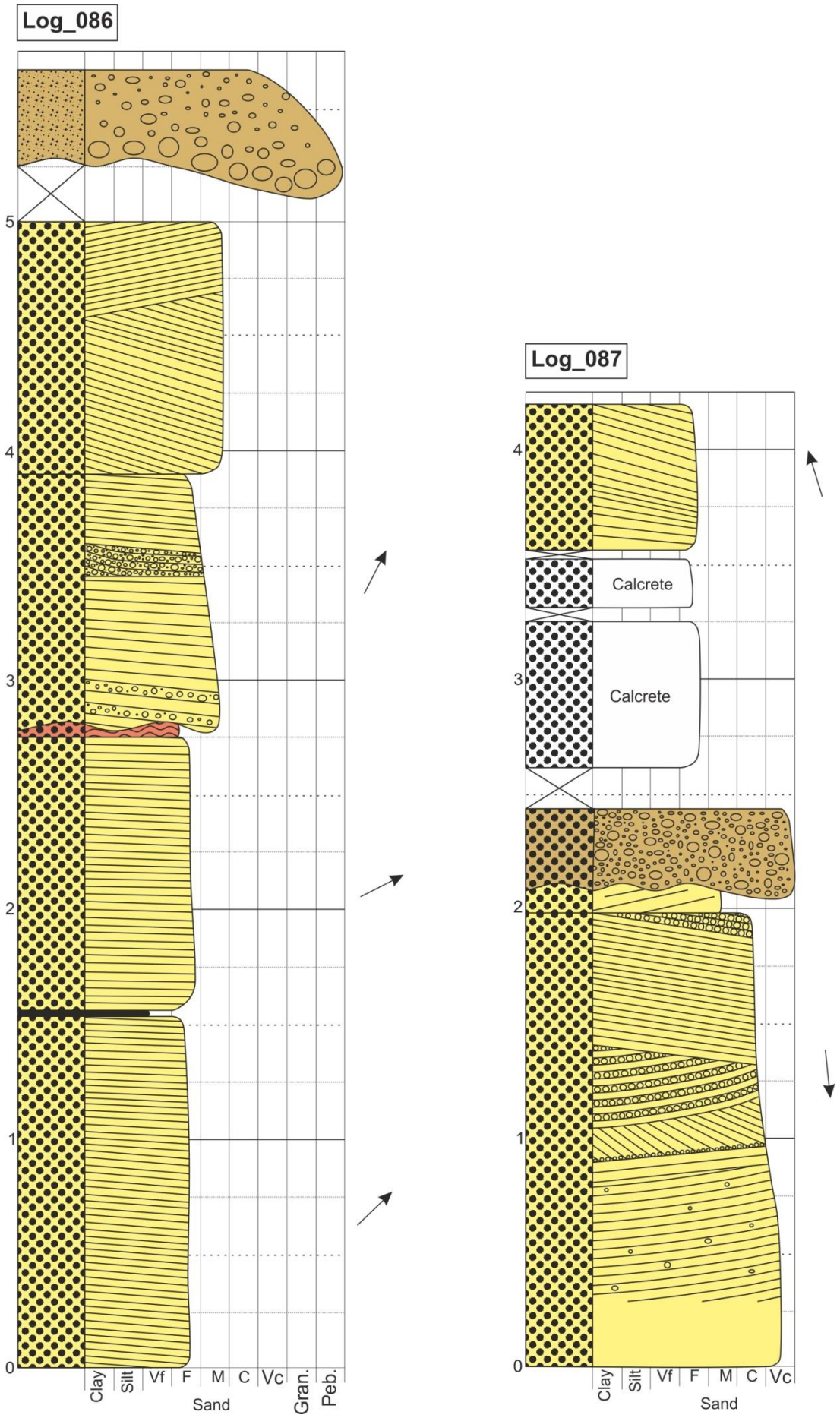
Log_086
5
4
3
2
1
0
Clay
Silt
Vf
F
M
C
Vc
Gran.
Peb.
Sand
Log_087
Calcrete
Calcrete
4
3
2
1
0
Clay
Silt
Vf
F
M
C
Vc
Sand

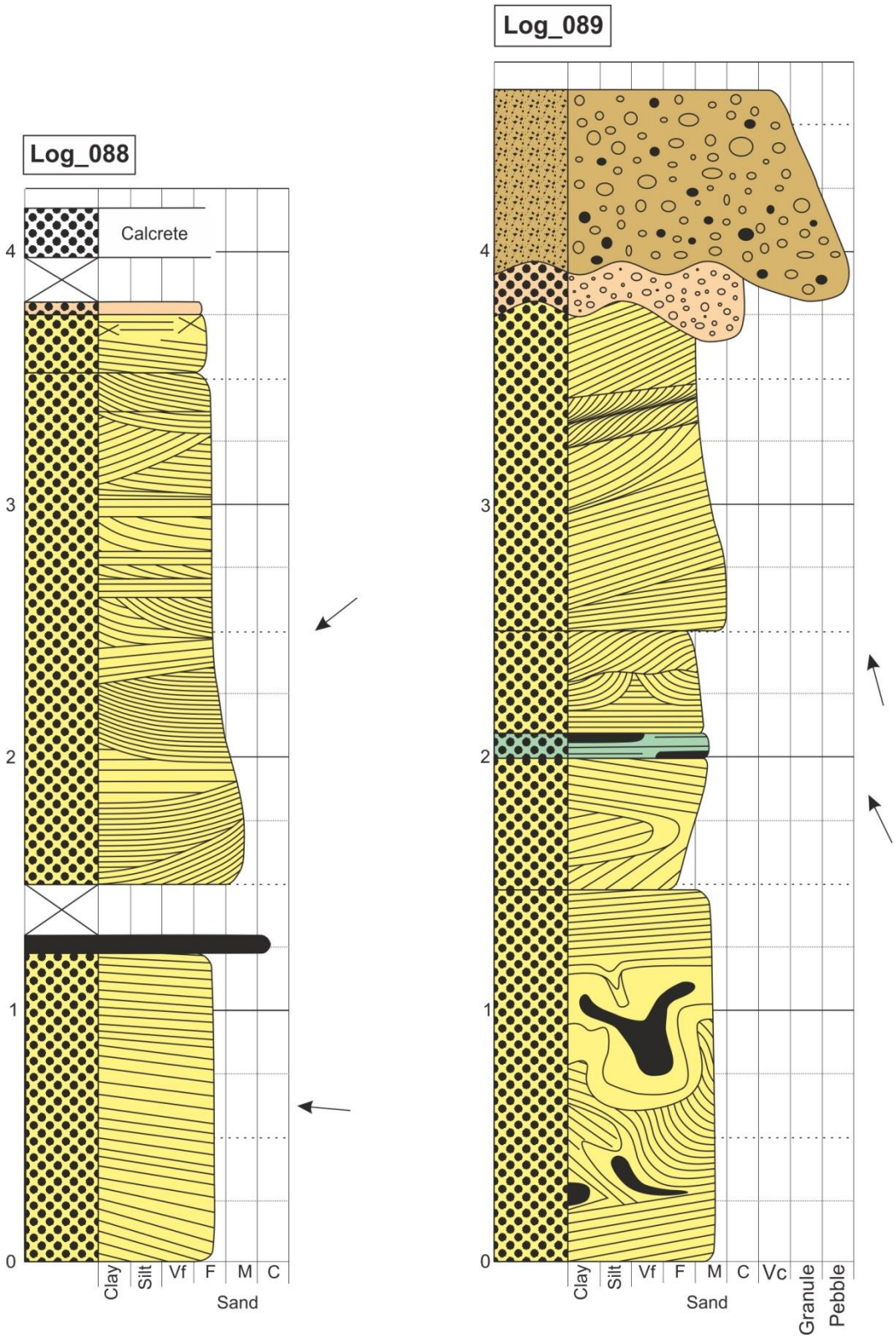
Log_088
Calcrete
4
3
2
1
0
Clay
Silt
Vf
F
M
C
Sand
Log_089
4
3
2
1
0
Clay
Silt
Vf
F
M
C
Vc
Granule
Pebble
Sand

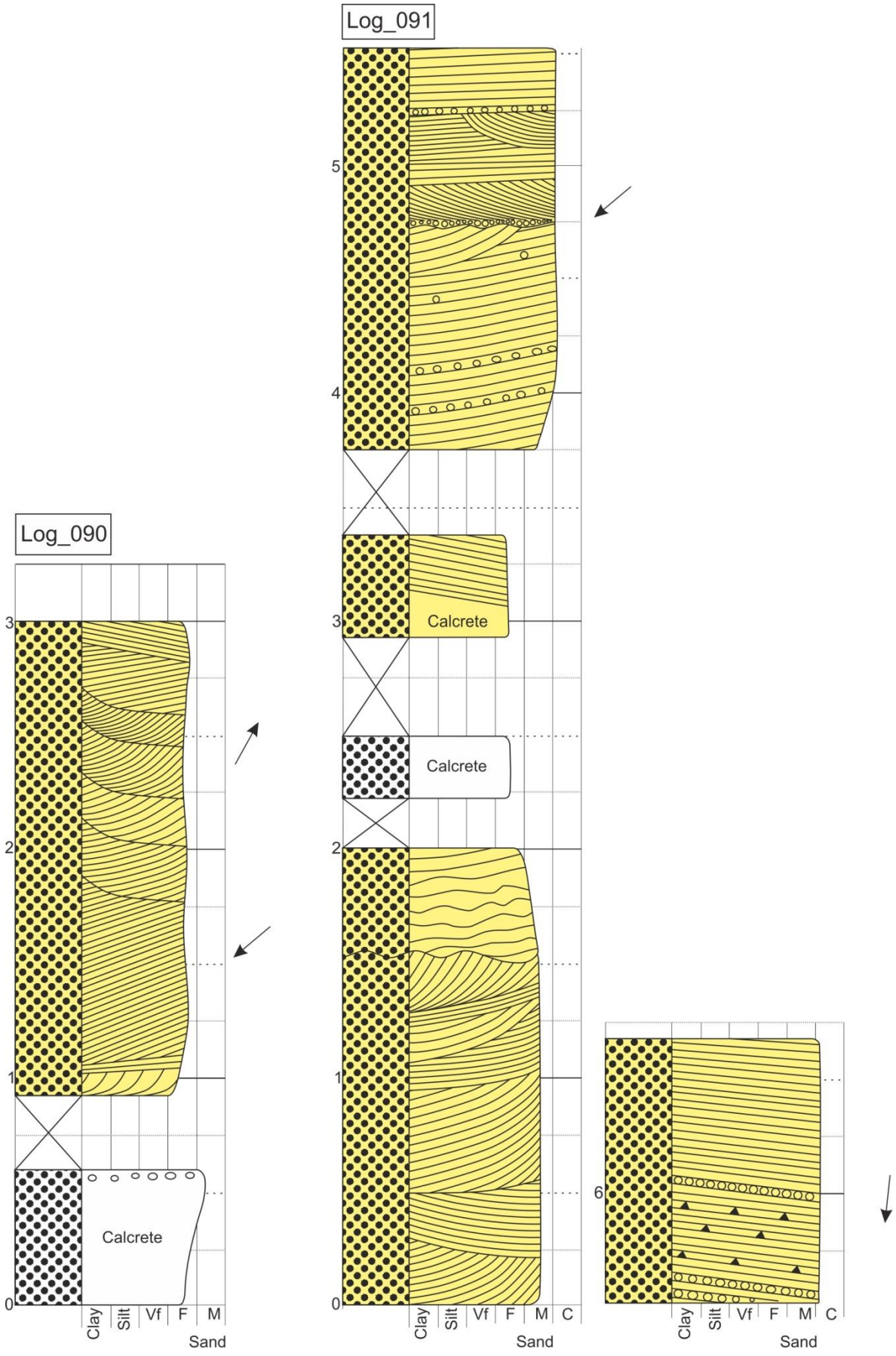
Log_091
Log_090
Calcrete
Calcrete
Calcrete
0
1
2
3
4
5
6
Clay
Silt
Vf
F
M
C
Sand

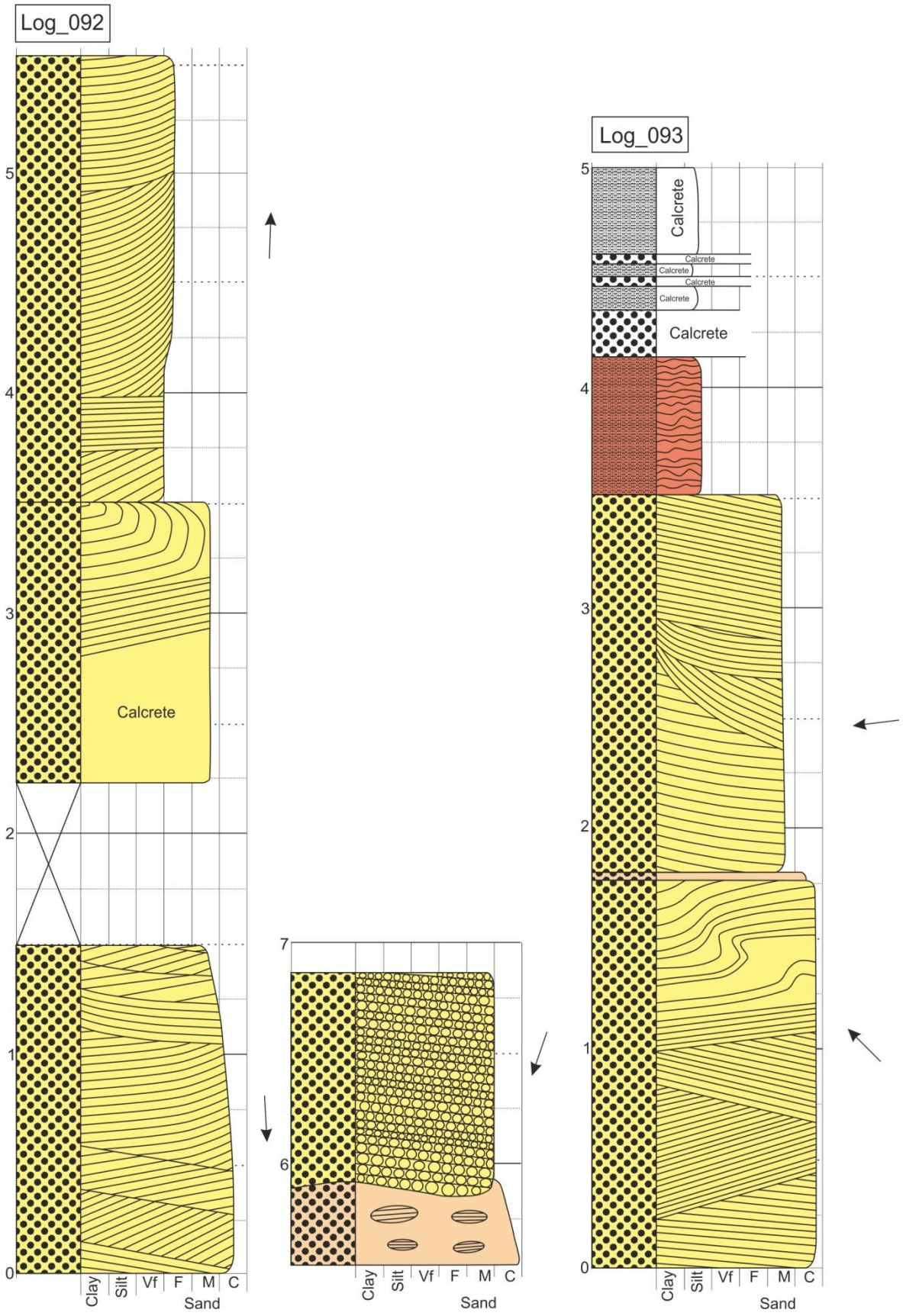
Log_092
Log_093
Calcrete
Calcrete
Calcrete
Calcrete
Calcrete
Calcrete
Clay
Silt
Vf
F
M
C
Sand
0
1
2
3
4
5
6
7

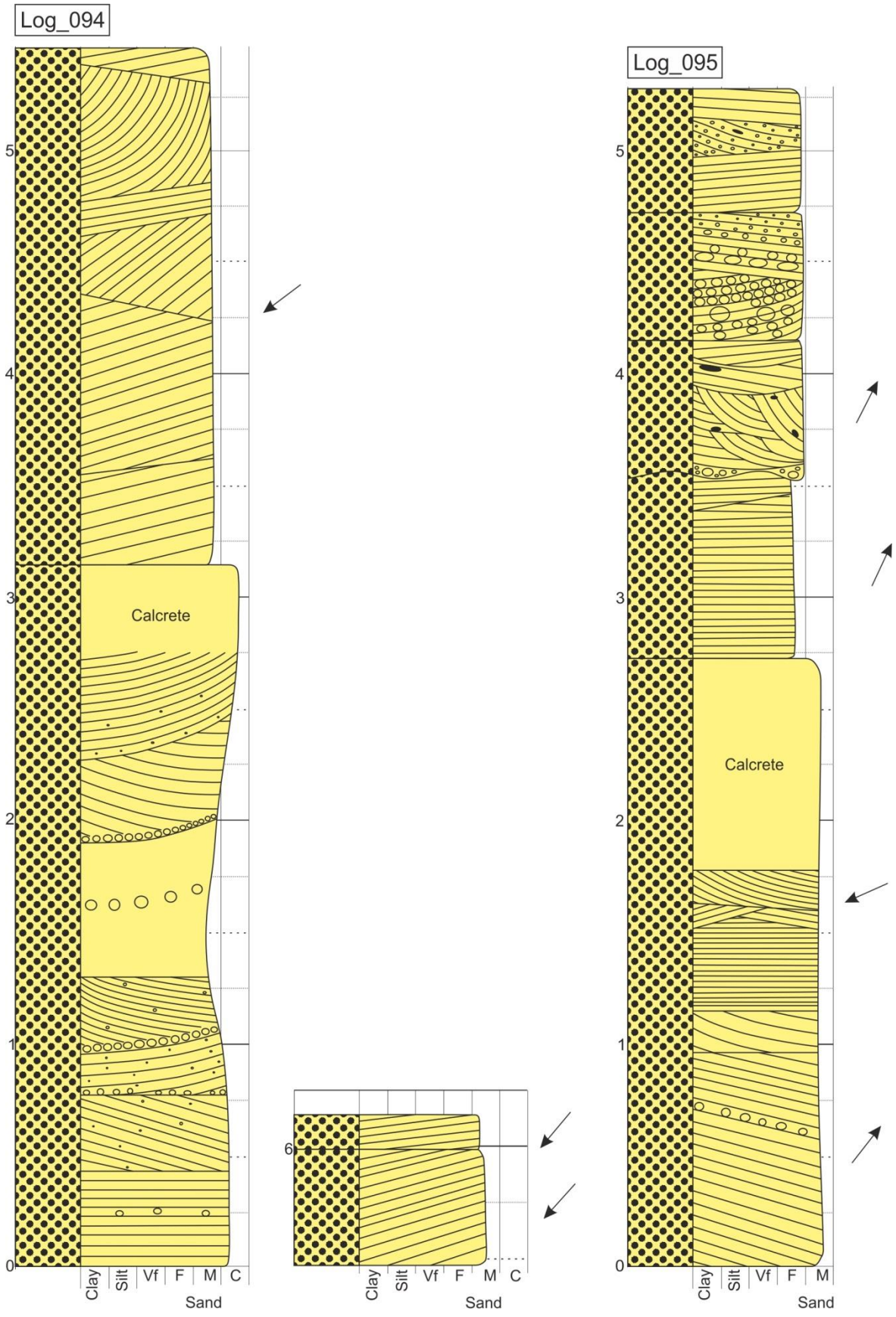
Log_094
Log_095
Calcrete
Calcrete
0
1
2
3
4
5
6
Clay
Silt
Vf
F
M
C
Sand

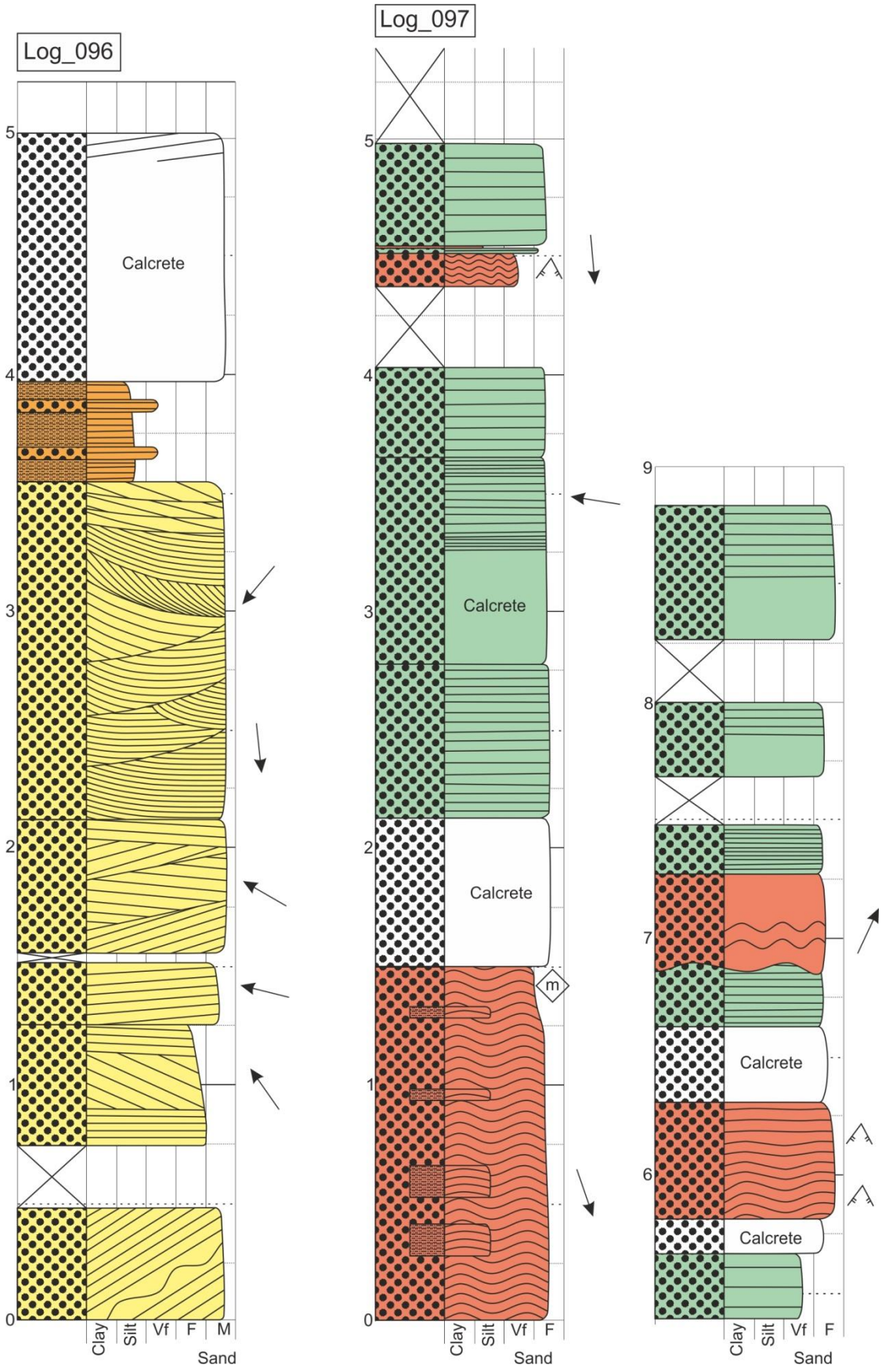
Log_096
Calcrete
5
4
3
2
1
0
Clay
Silt
Vf
F
M
Sand
Log_097
Calcrete
Calcrete
m
5
4
3
2
1
0
Clay
Silt
Vf
F
Sand
9
8
7
6
Calcrete
Calcrete
Clay
Silt
Vf
F
Sand

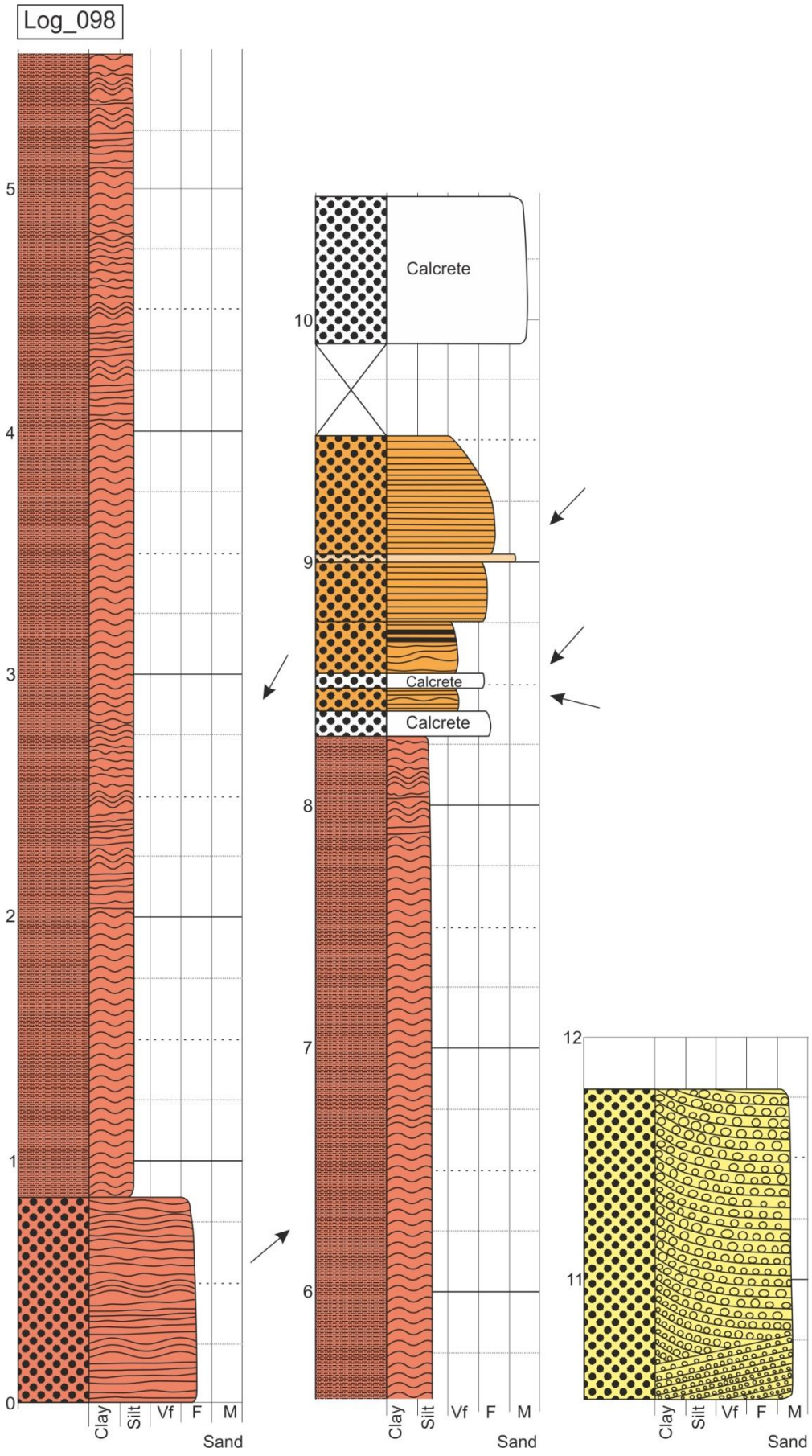
Log_098
5
4
3
2
1
0
Clay
Silt
Vf
F
M
Sand
Calcrete
10
9
Calcrete
Calcrete
8
7
6
Clay
Silt
Vf
F
M
Sand
12
11
Clay
Silt
Vf
F
M
Sand

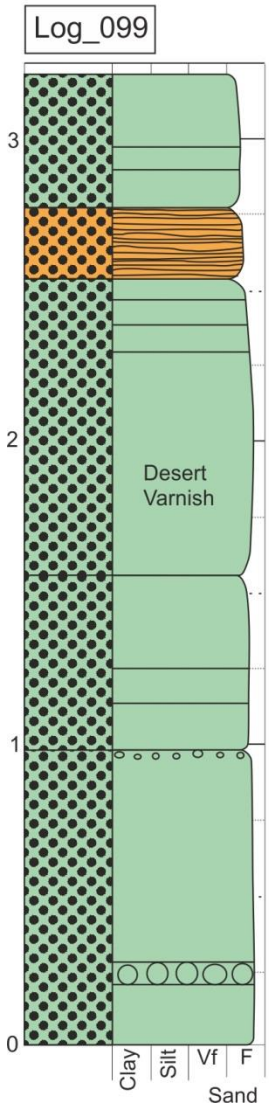
Log_099
3
2
1
0
Desert
Varnish
Clay
Silt
Vf
F
Sand

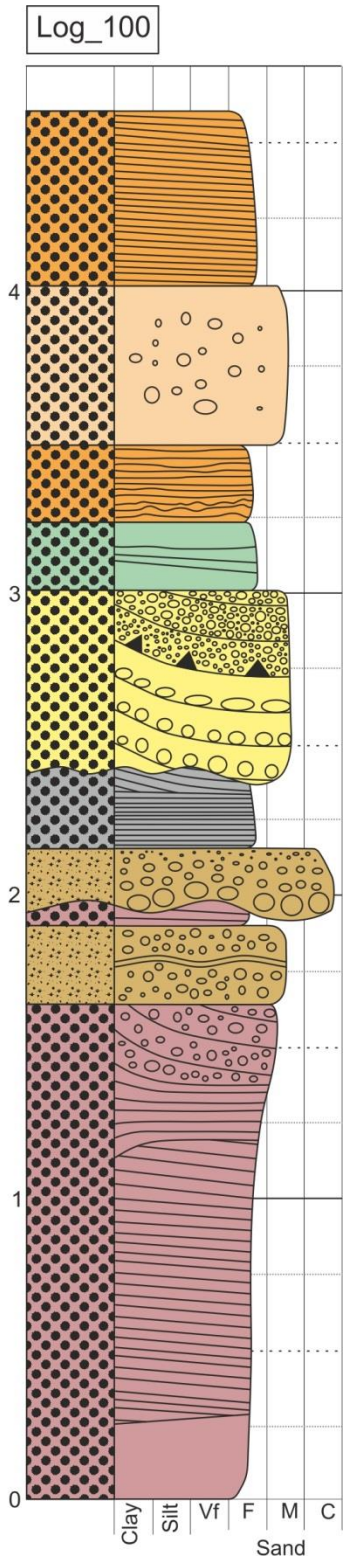
Log_100
4
3
2
1
0
Clay
Silt
Vf
F
M
C
Sand

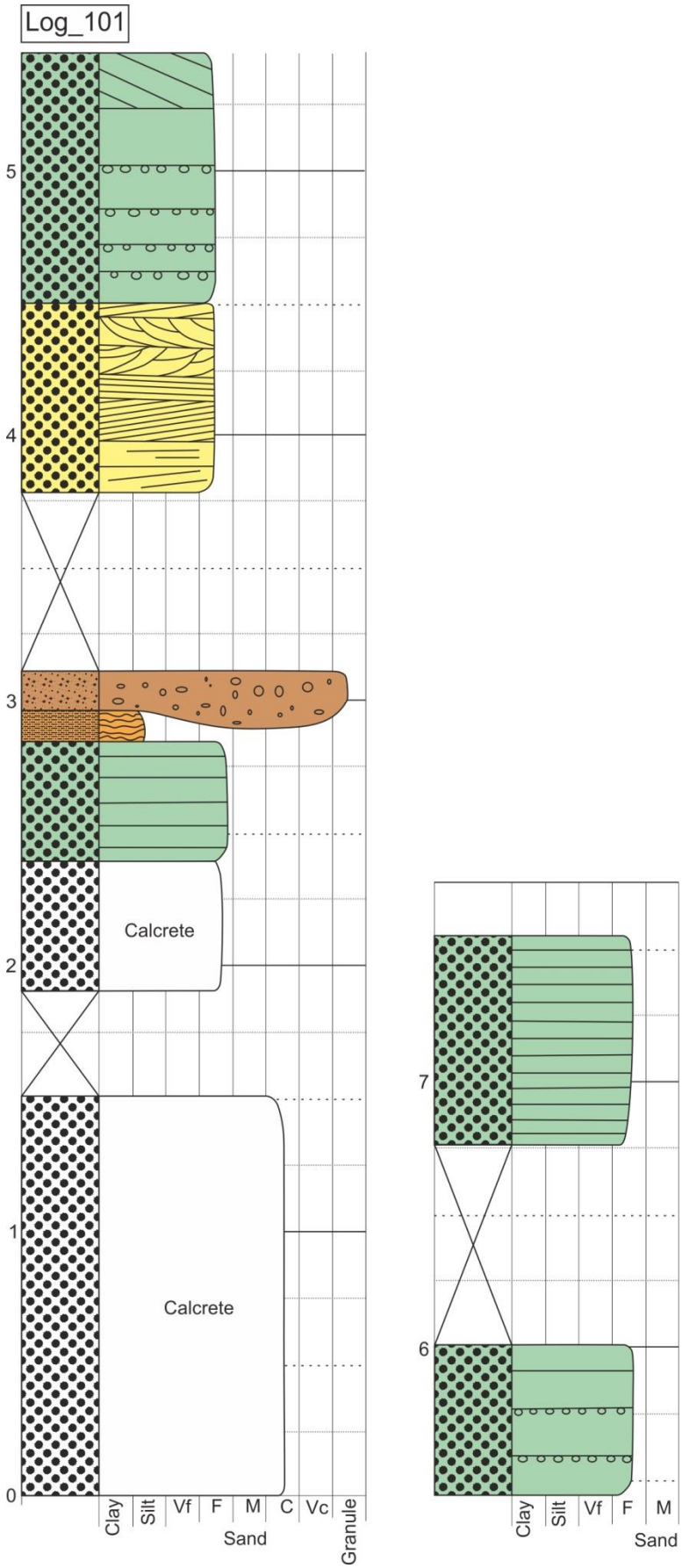
Log_101
5
4
3
2
1
0
Calcrete
Calcrete
7
6
Clay
Silt
Vf
F
M
C
Vc
Granule
Sand
Clay
Silt
Vf
F
M
Sand

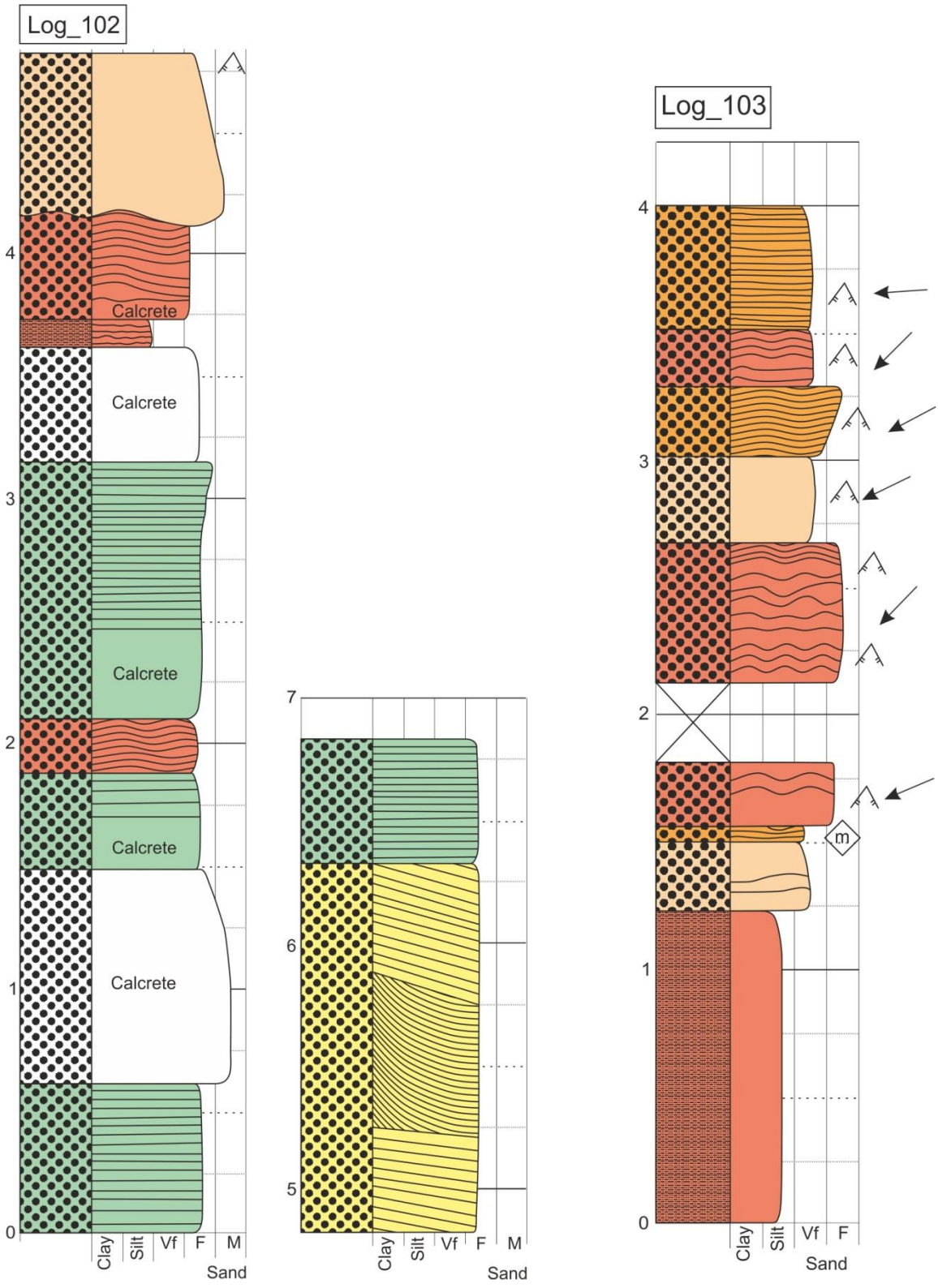
Log_102
Calcrete
Calcrete
Calcrete
Calcrete
Calcrete
0
1
2
3
4
Clay
Silt
Vf
F
M
Sand
5
6
7
Log_103
m

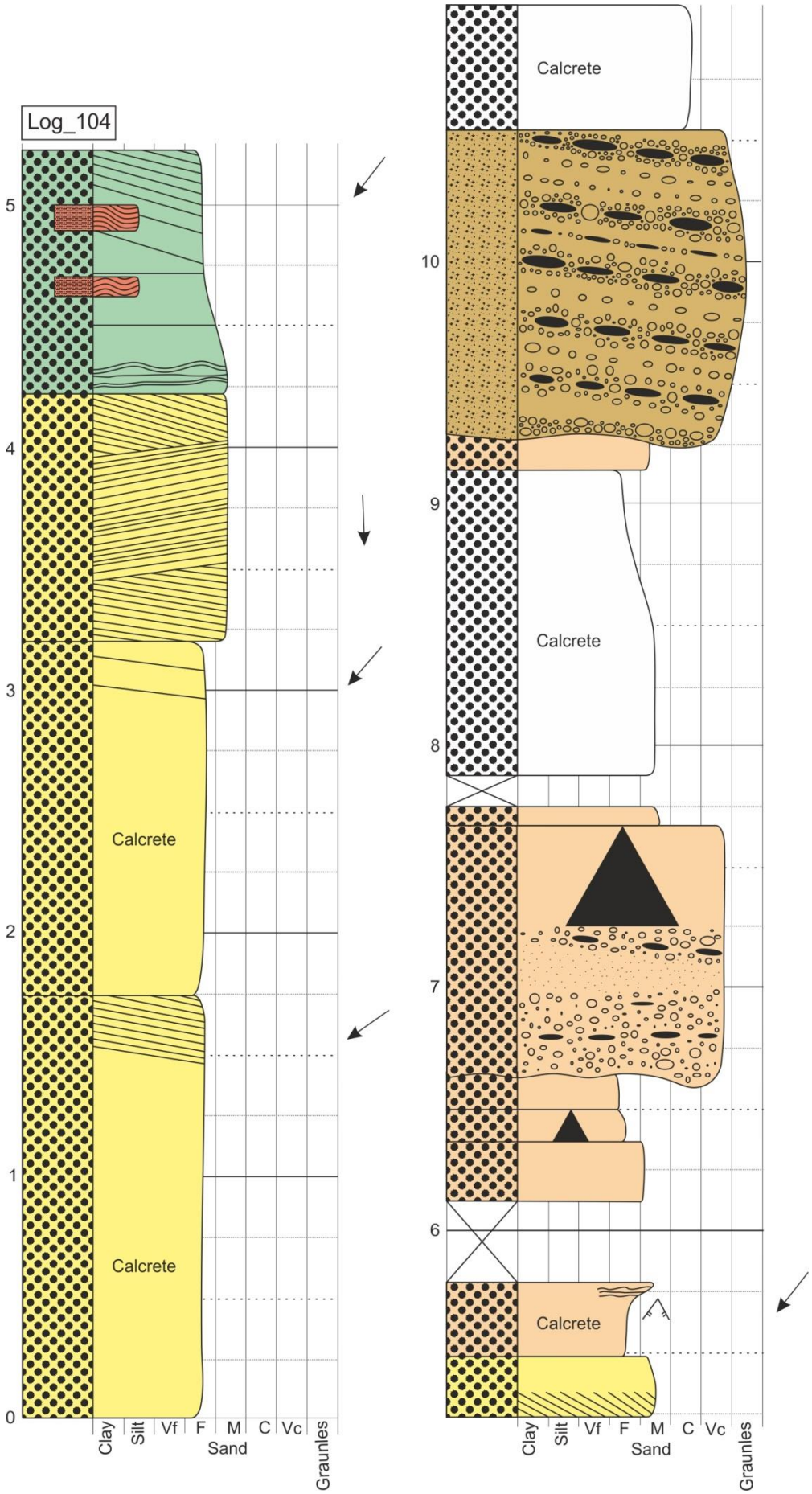
Log_104
5
4
3
2
1
0
Calcrete
Calcrete
Clay
Silt
Vf
F
M
C
Vc
Sand
Graunles
Calcrete
10
9
Calcrete
8
7
6
Calcrete
Clay
Silt
Vf
F
M
C
Vc
Sand
Graunles

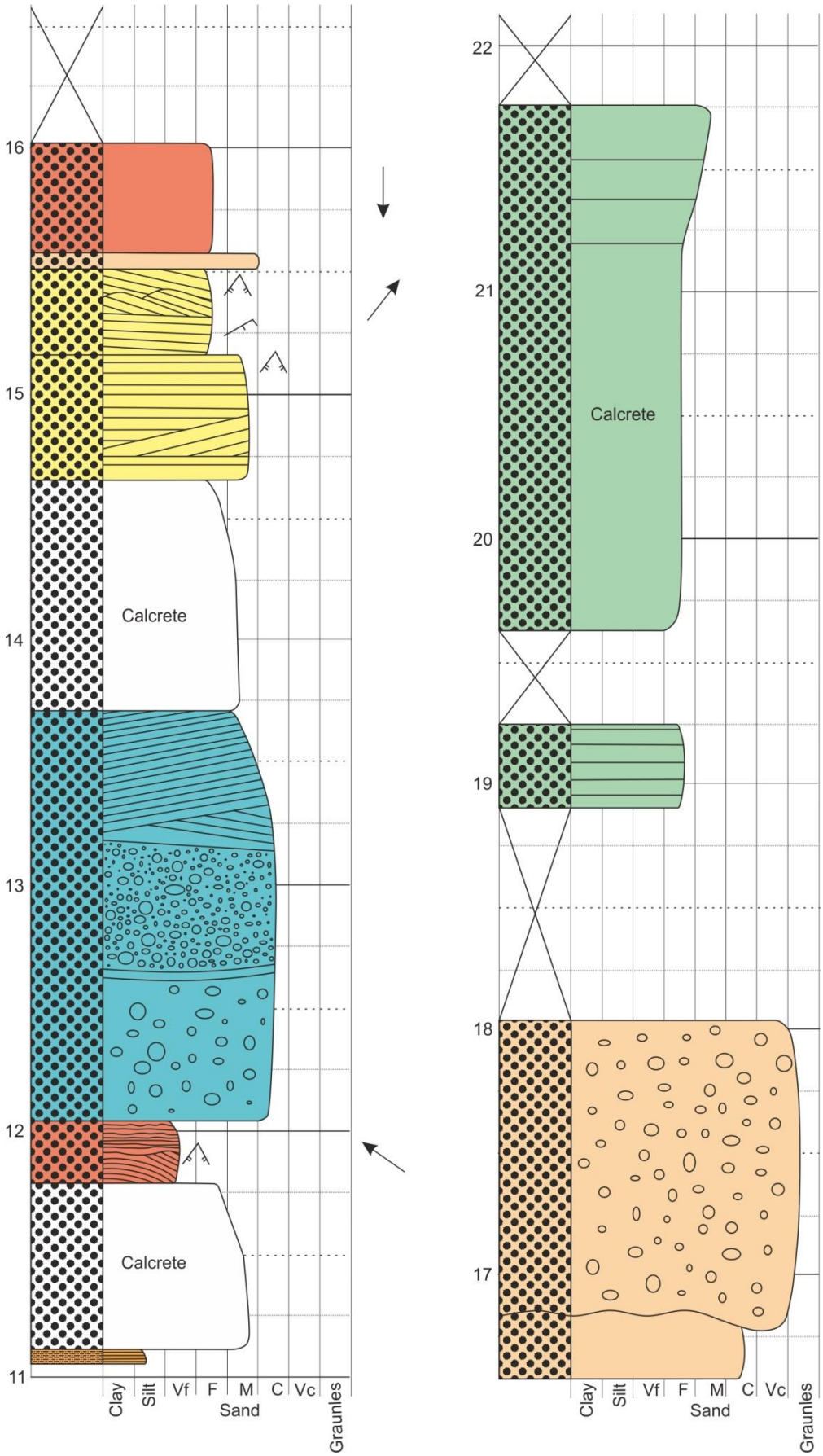
16
15
14
13
12
11
Calcrete
Calcrete
22
21
20
19
18
17
Calcrete
Clay
Silt
Vf
F
M
C
Vc
Sand
Graunles
Clay
Silt
Vf
F
M
C
Vc
Sand
Graunles

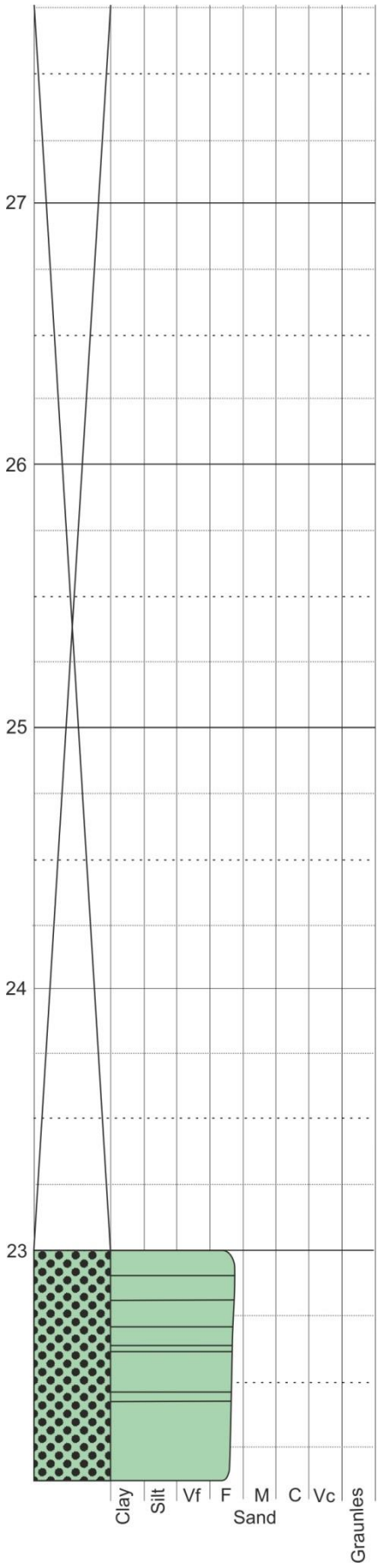
27
26
25
24
23
Clay
Silt
Vf
F
M
C
Vc
Sand
Graunles

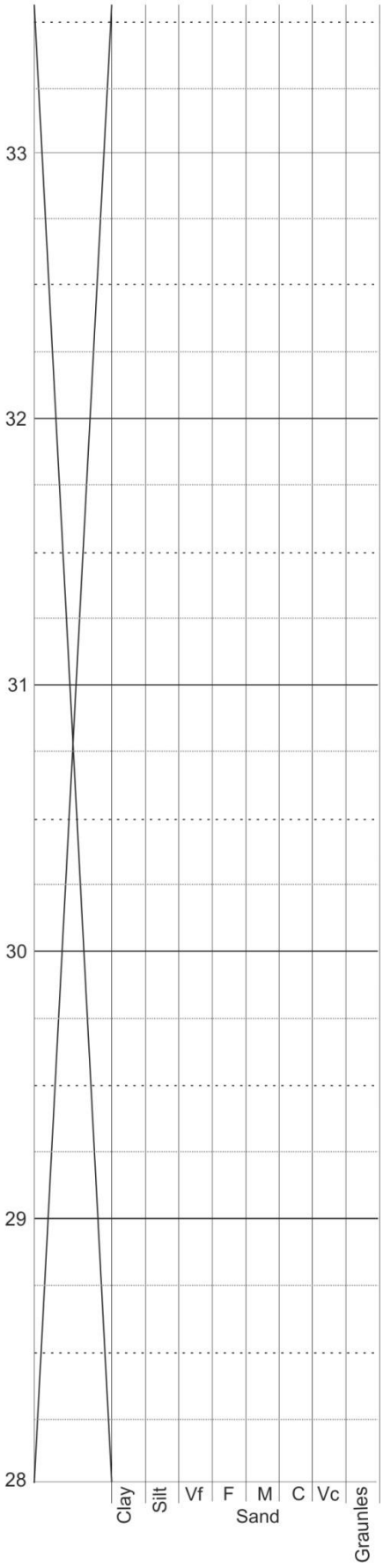
33
32
31
30
29
28
Clay
Silt
Vf
F
M
C
Vc
Sand
Graunles

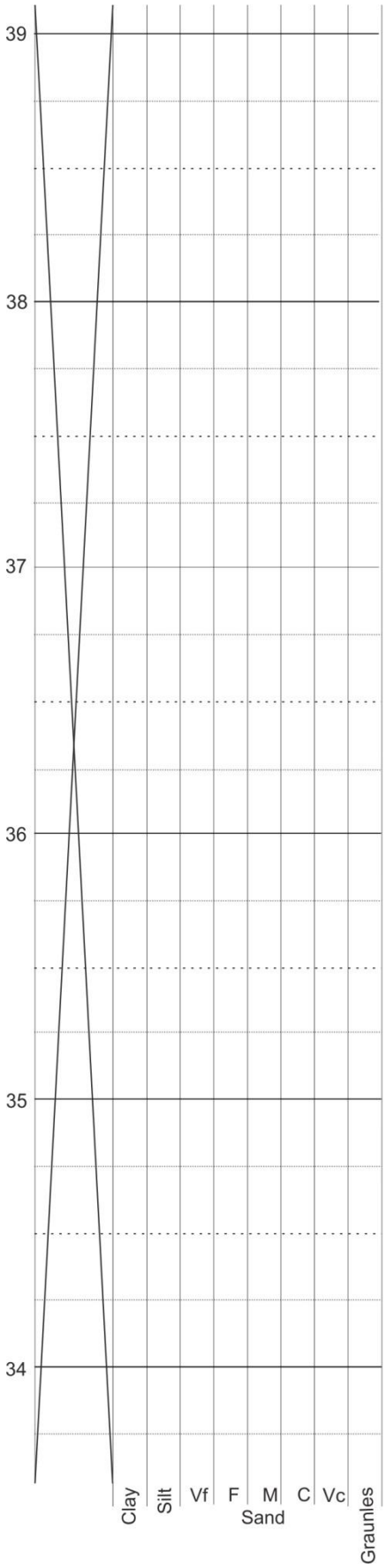
39
38
37
36
35
34
Clay
Silt
Vf
F
M
C
Vc
Sand
Graunles

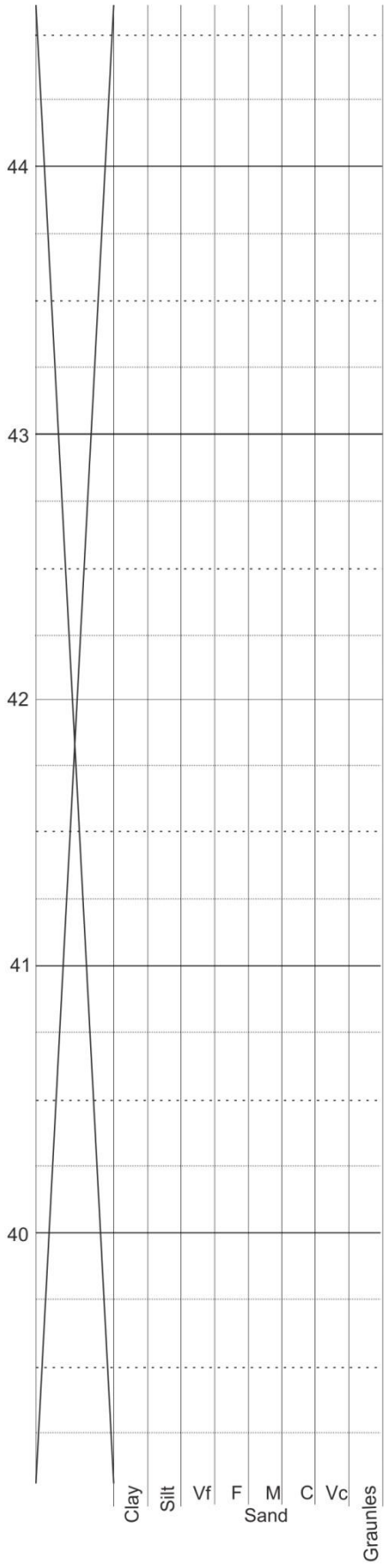
44
43
42
41
40
Clay
Silt
Vf
F
M
C
Vc
Sand
Graunles

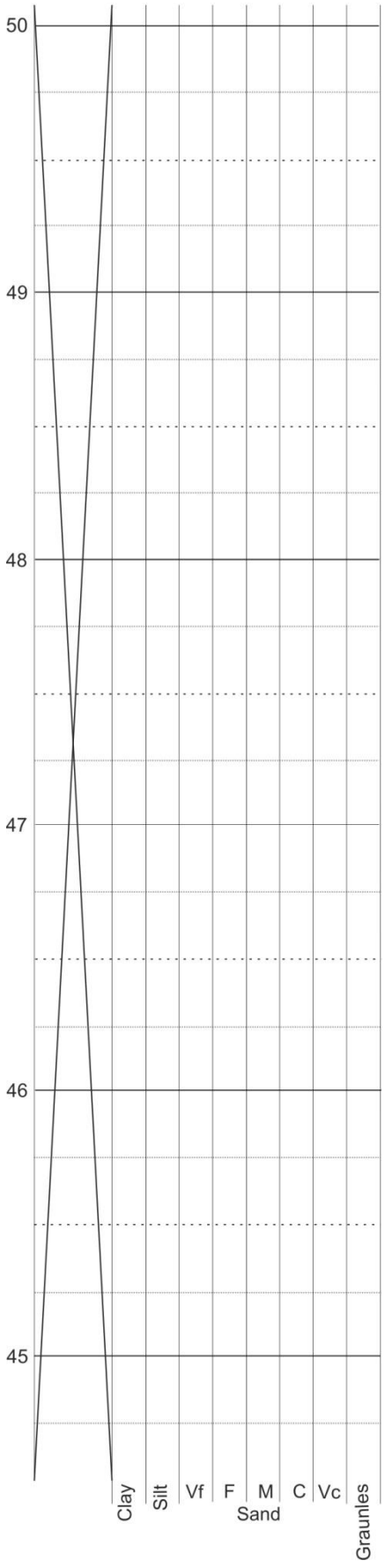
50
49
48
47
46
45
Clay
Silt
Vf
F
M
C
Vc
Sand
Graunles

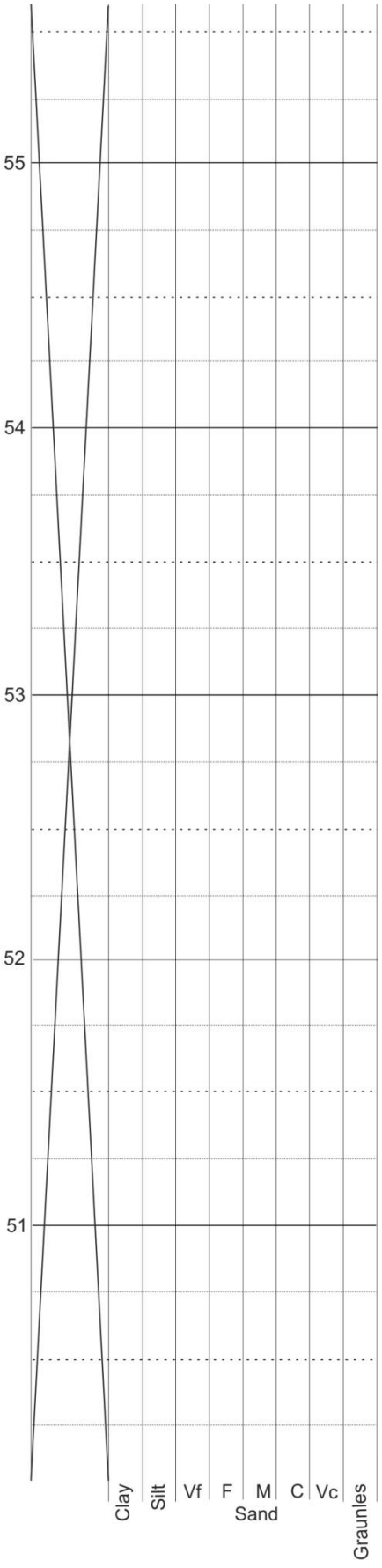
55
54
53
52
51
Clay
Silt
Vf
F
M
C
Vc
Sand
Graunles

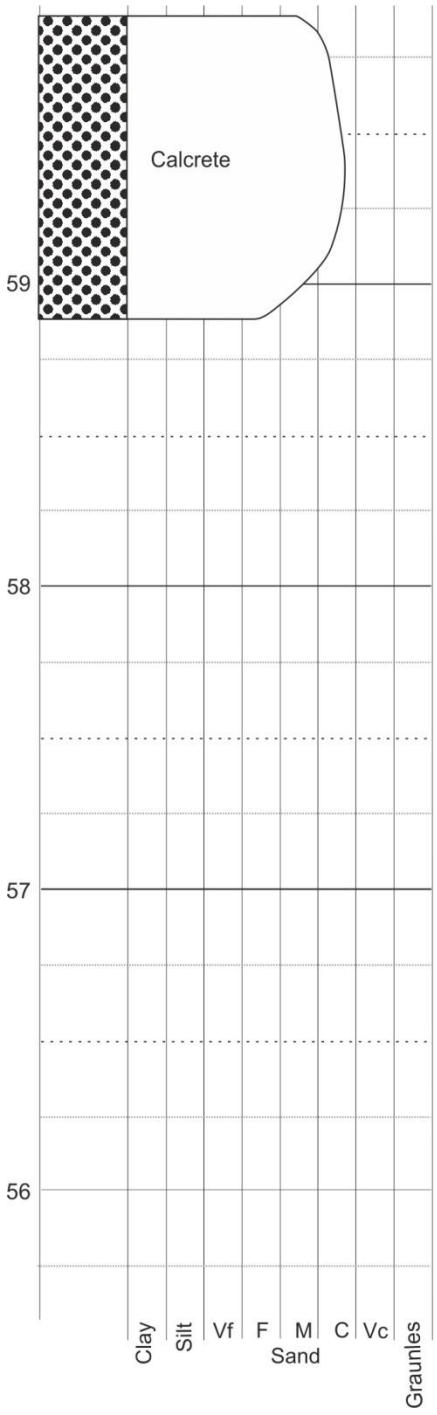
Calcrete
59
58
57
56
Clay
Silt
Vf
F
M
C
Vc
Sand
Graunles

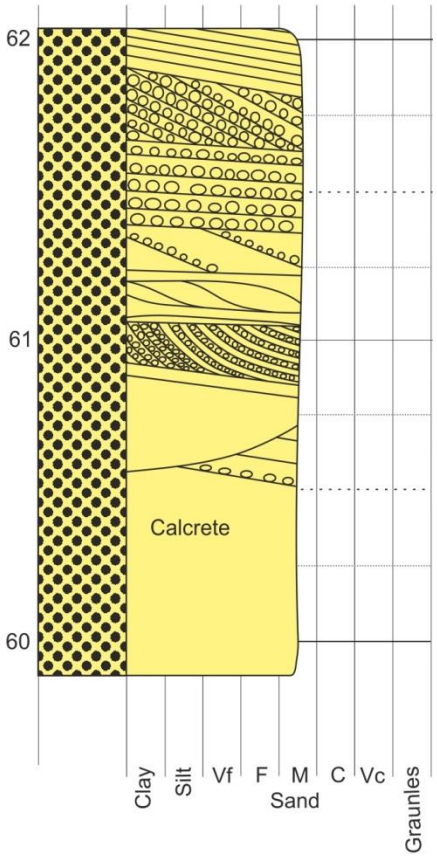
62
61
60
Calcrete
Clay
Silt
Vf
F
M
C
Vc
Sand
Graunles

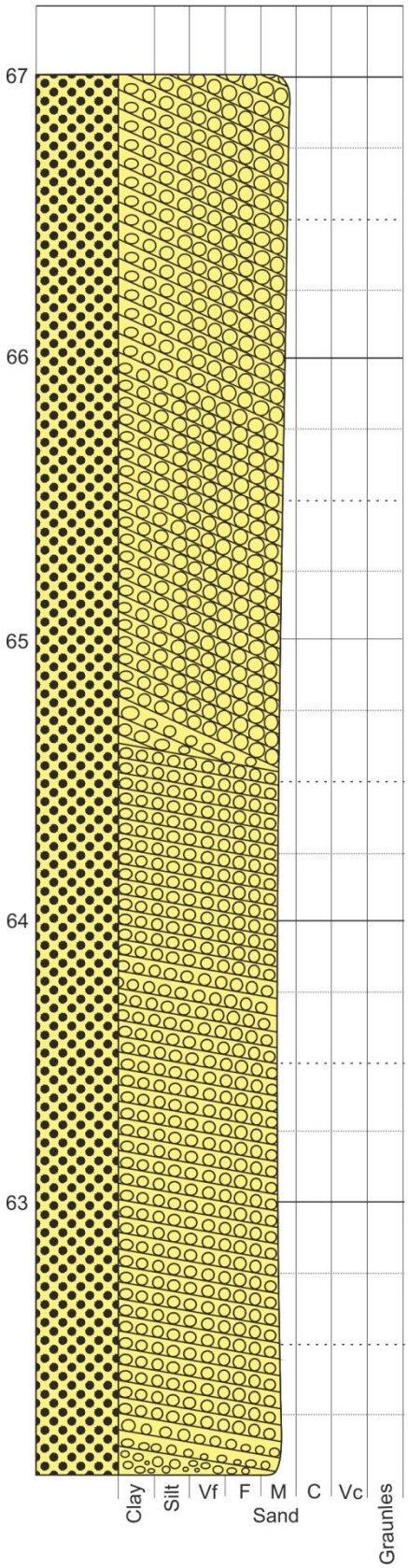
67
66
65
64
63
Clay
Silt
Vf
F
M
C
Vc
Sand
Graunles

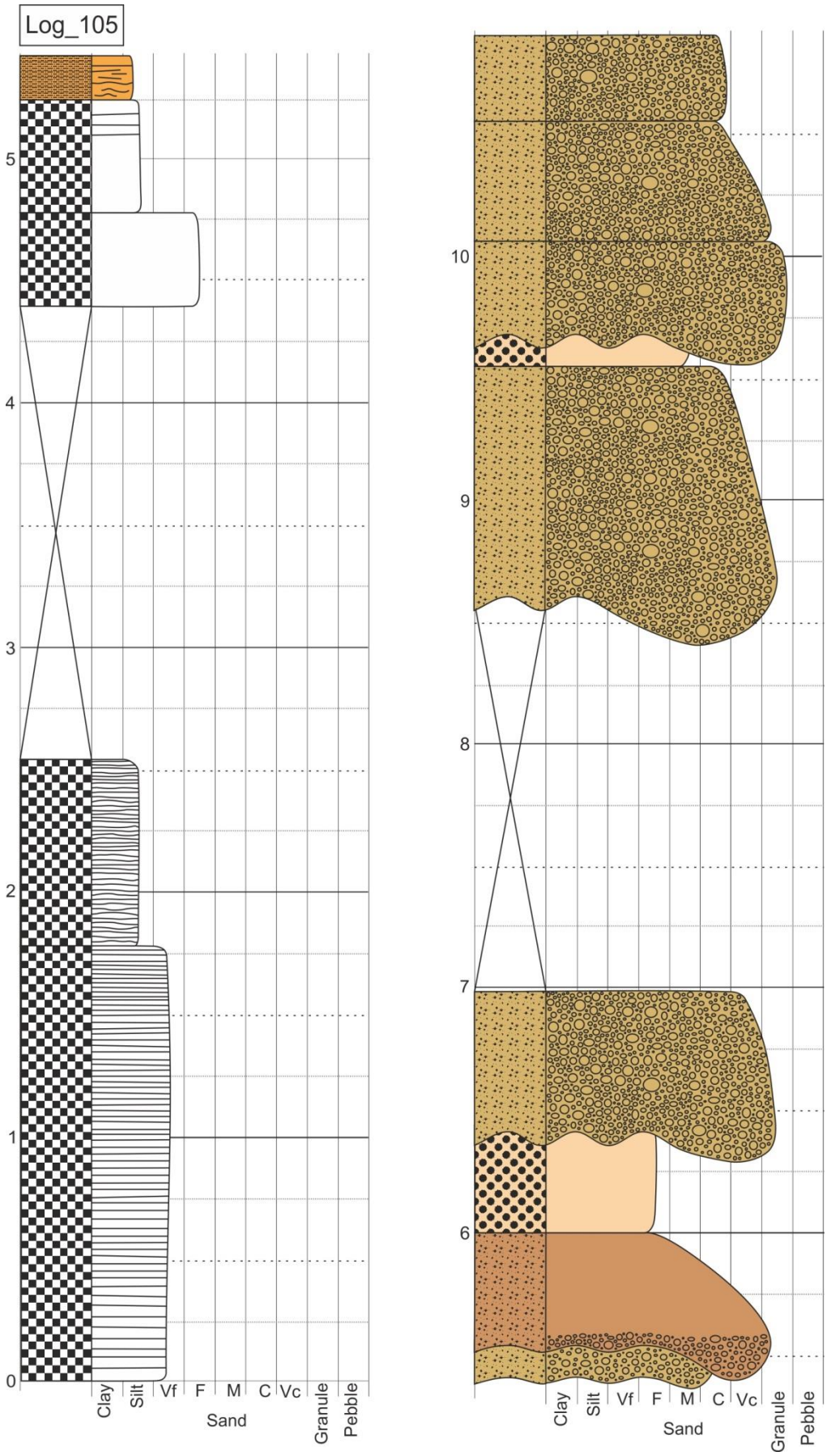
Log_105
0
1
2
3
4
5
6
7
8
9
10
Clay
Silt
Vf
F
M
C
Vc
Sand
Granule
Pebble

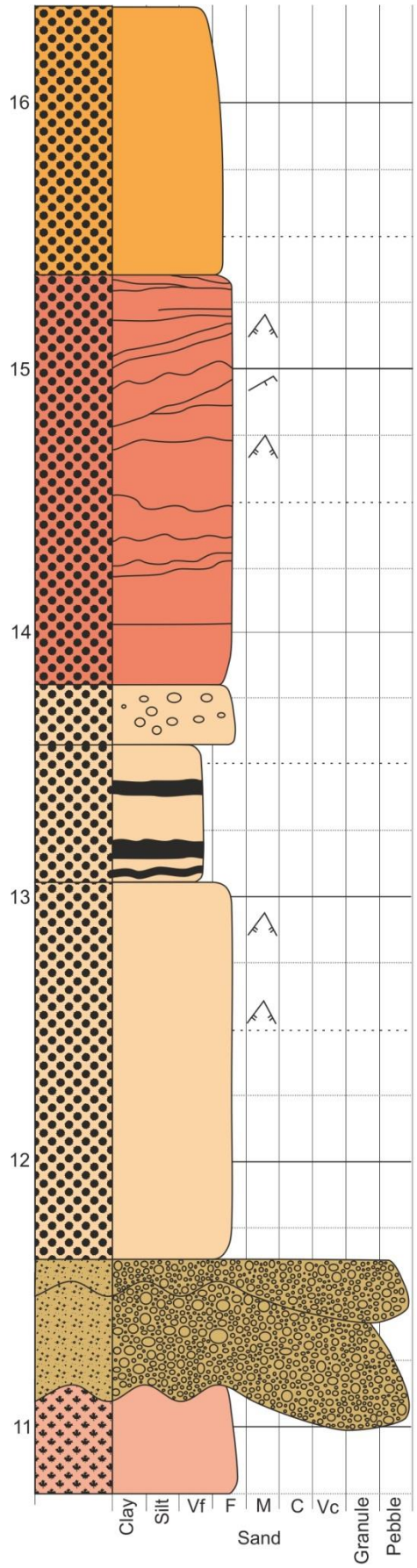
16
15
14
13
12
11
Clay
Silt
Vf
F
M
C
Vc
Granule
Pebble
Sand

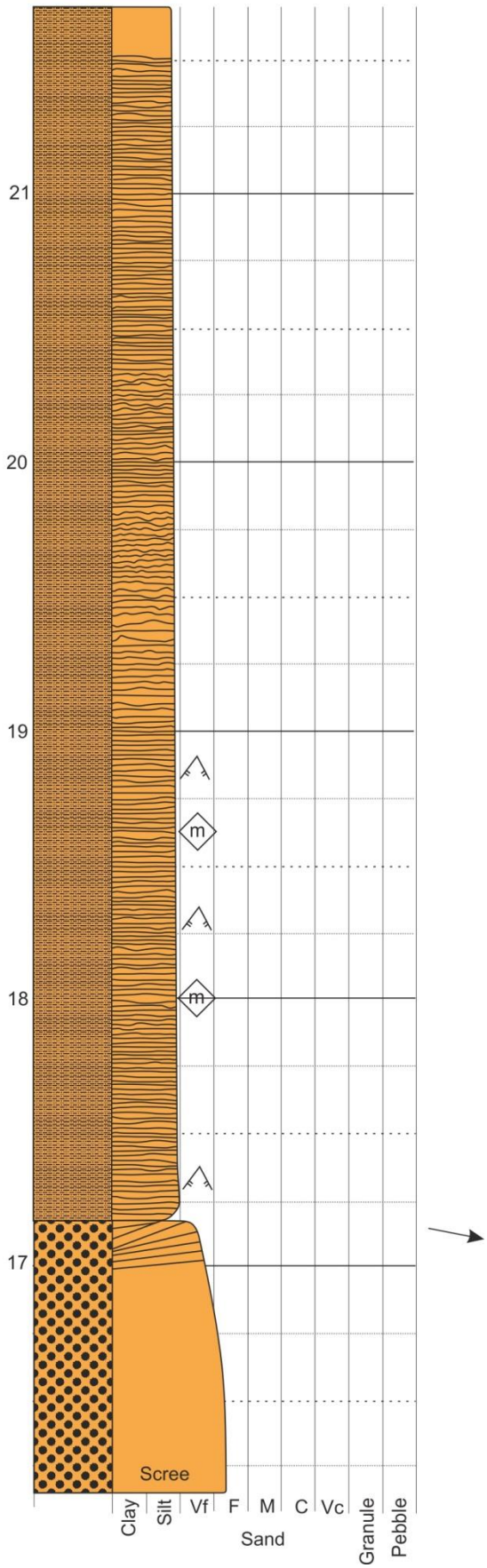
21
20
19
18
17
m
m
Scree
Clay
Silt
Vf
F
M
C
Vc
Granule
Pebble
Sand

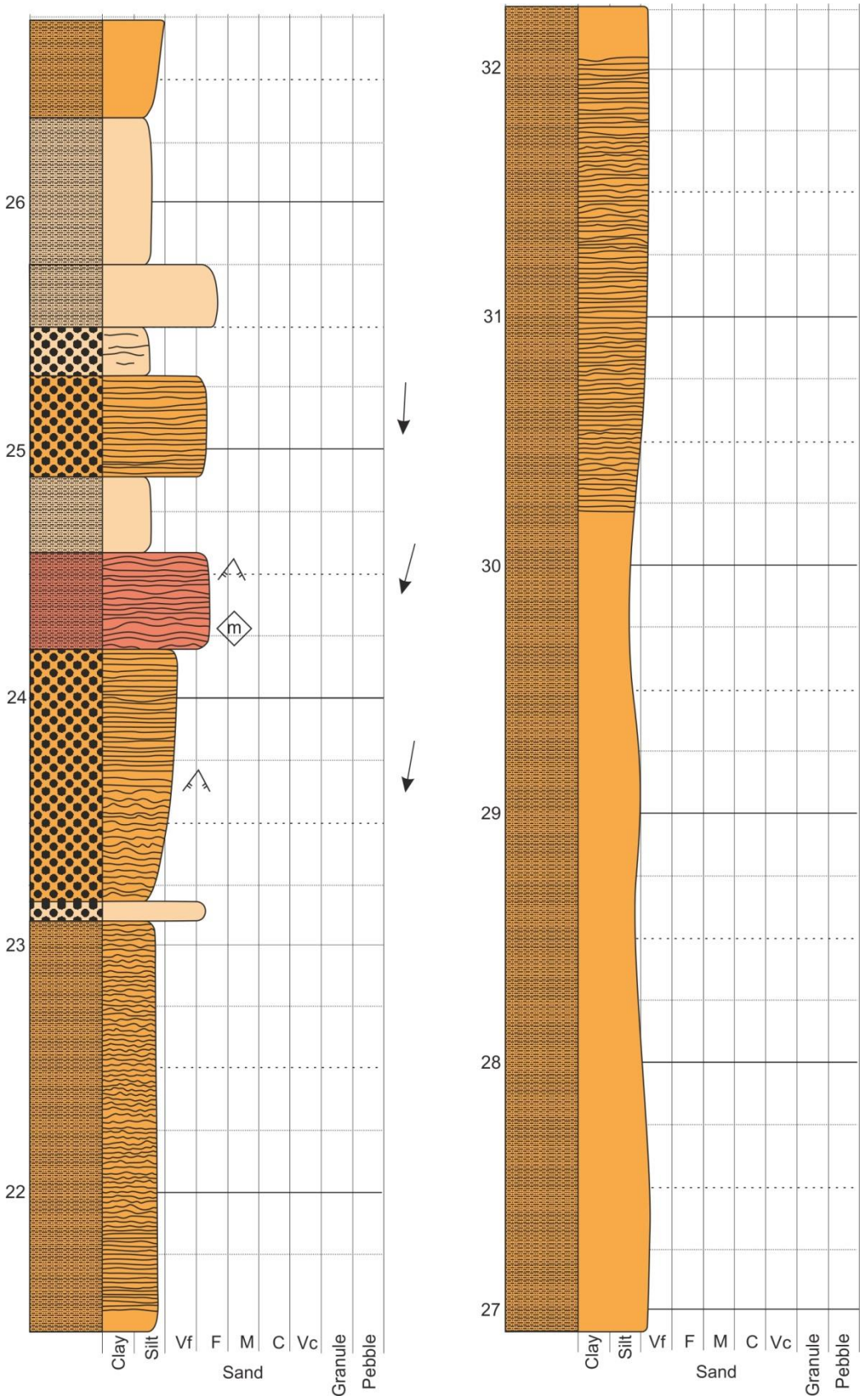
26
25
24
23
22
m
Clay
Silt
Vf
F
M
C
Vc
Granule
Pebble
Sand
32
31
30
29
28
27
Clay
Silt
Vf
F
M
C
Vc
Granule
Pebble
Sand

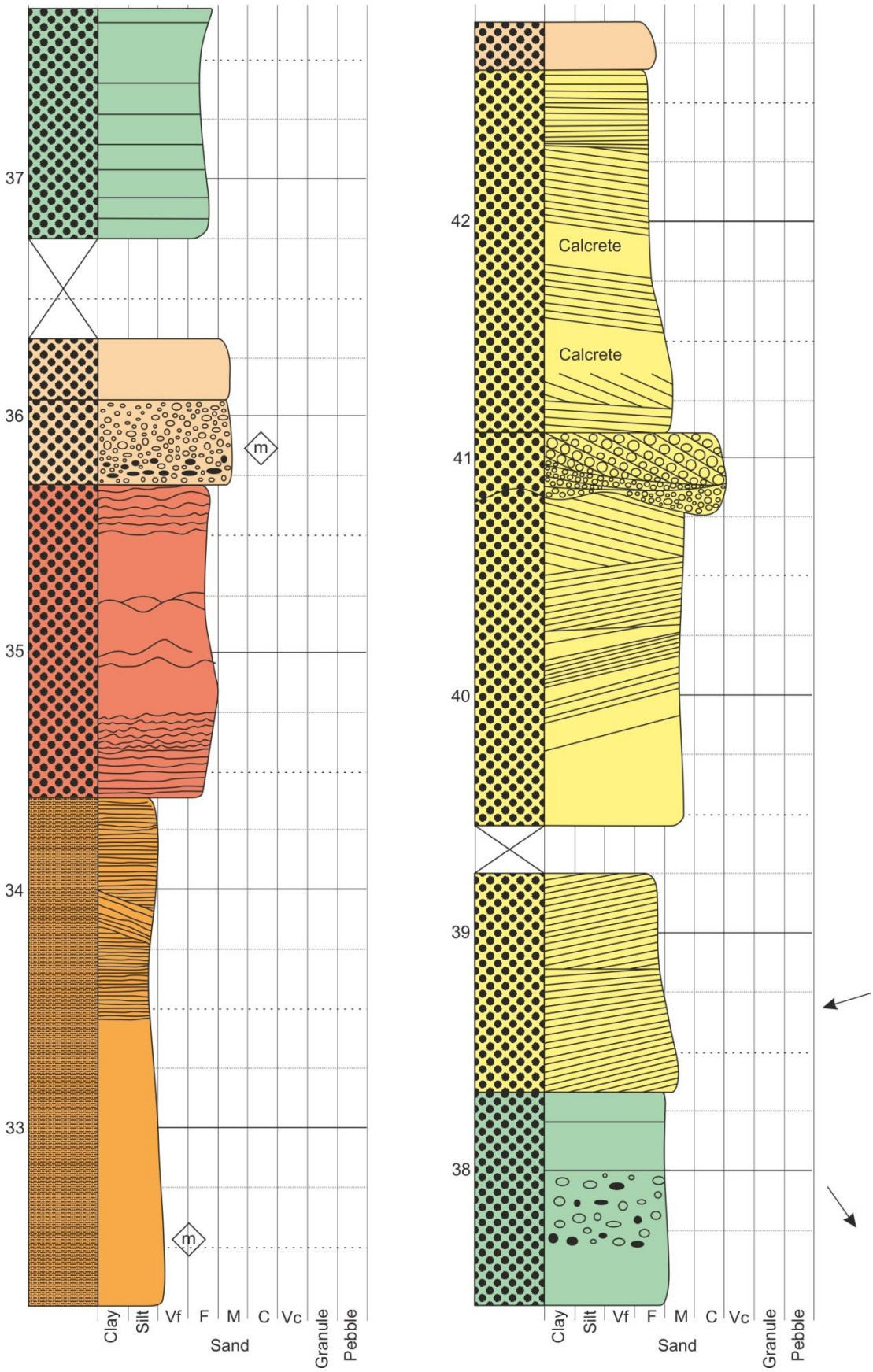
37
36
35
34
33
m
m
Clay
Silt
Vf
F
M
C
Vc
Granule
Pebble
Sand
42
41
40
39
38
Calcrete
Calcrete
Clay
Silt
Vf
F
M
C
Vc
Granule
Pebble
Sand

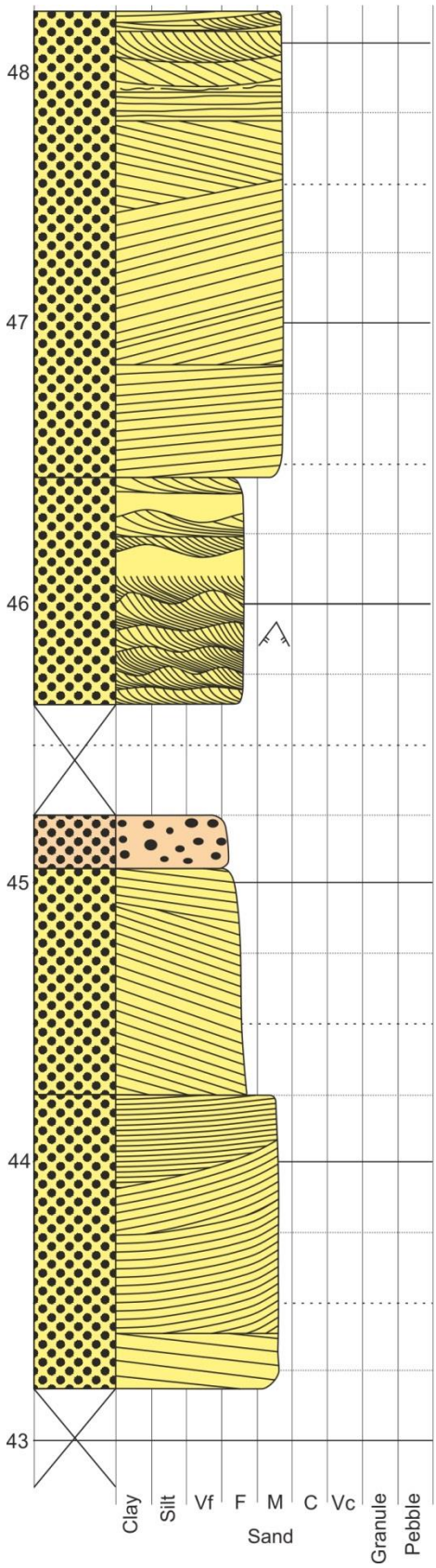
48
47
46
45
44
43
Clay
Silt
Vf
F
M
C
Vc
Granule
Pebble
Sand

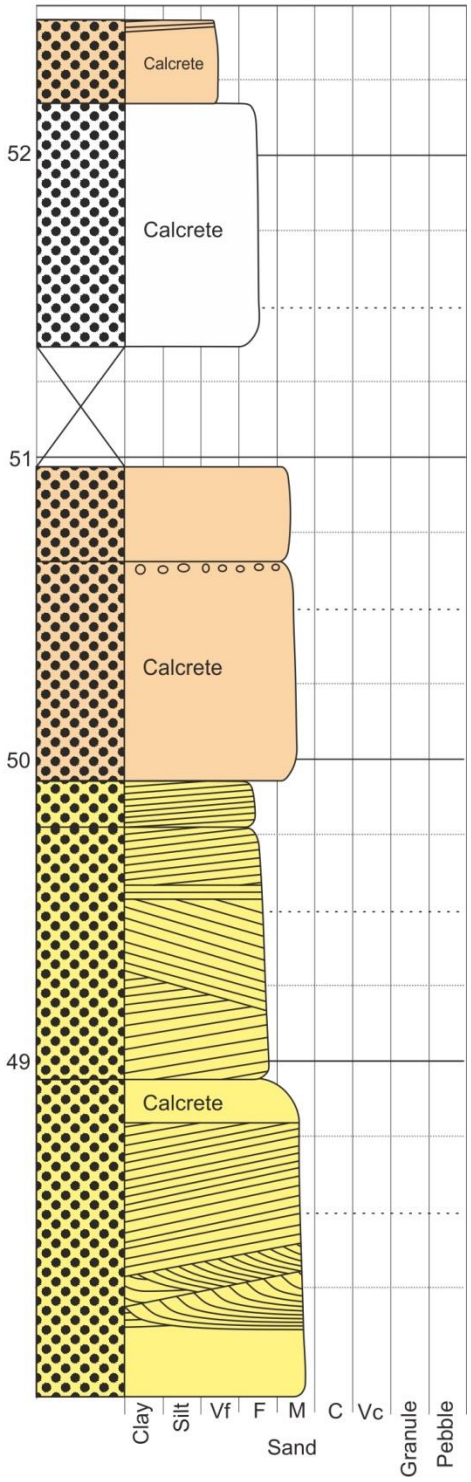
Calcrete
52
Calcrete
51
Calcrete
50
49
Calcrete
Clay
Silt
Vf
F
M
C
Vc
Granule
Pebble
Sand

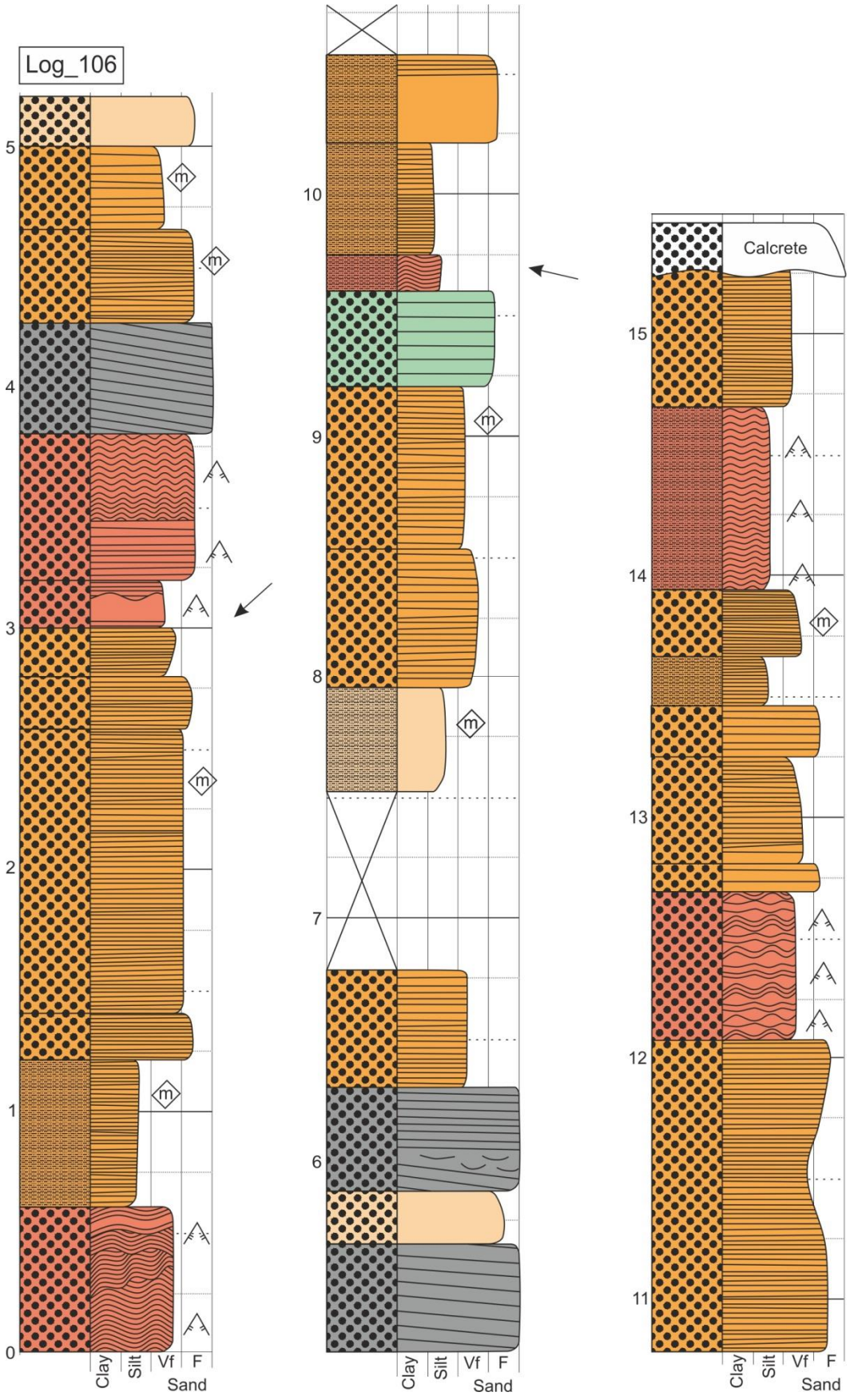
Log_106
Calcrete
Clay
Silt
Vf
F
Sand

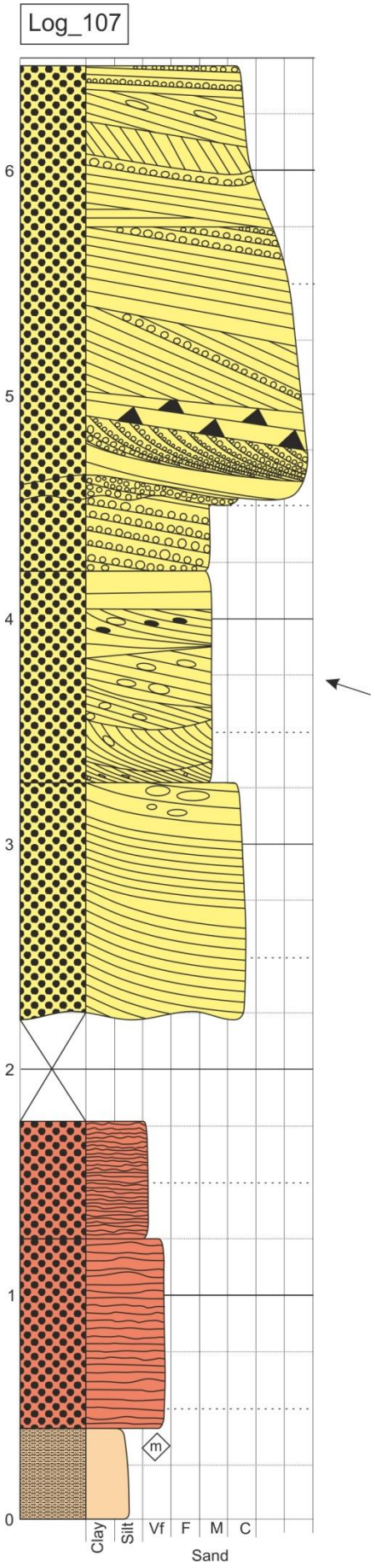
Log_107
6
5
4
3
2
1
0
m
Clay
Silt
Vf
F
M
C
Sand

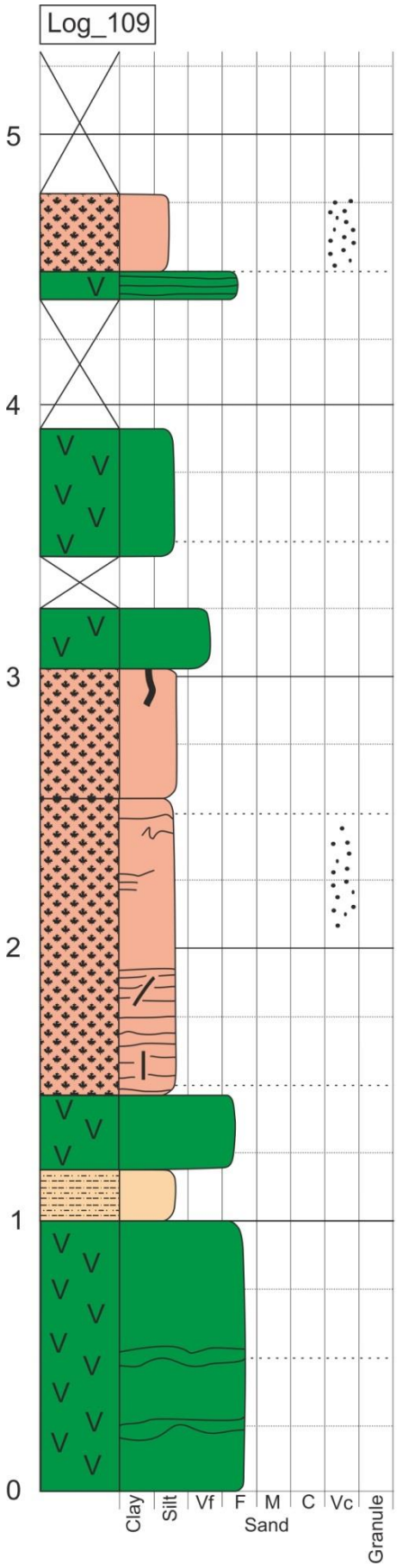
Log_109
5
4
3
2
1
0
Clay
Silt
Vf
F
M
C
Vc
Granule
Sand

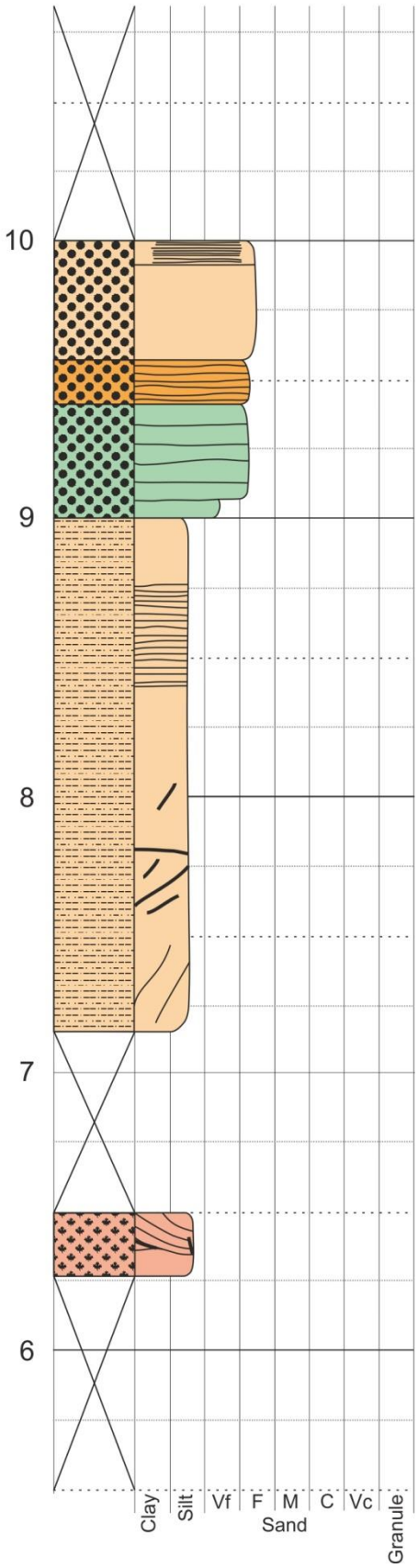
10
9
8
7
6
Clay
Silt
Vf
F
M
C
Vc
Granule
Sand

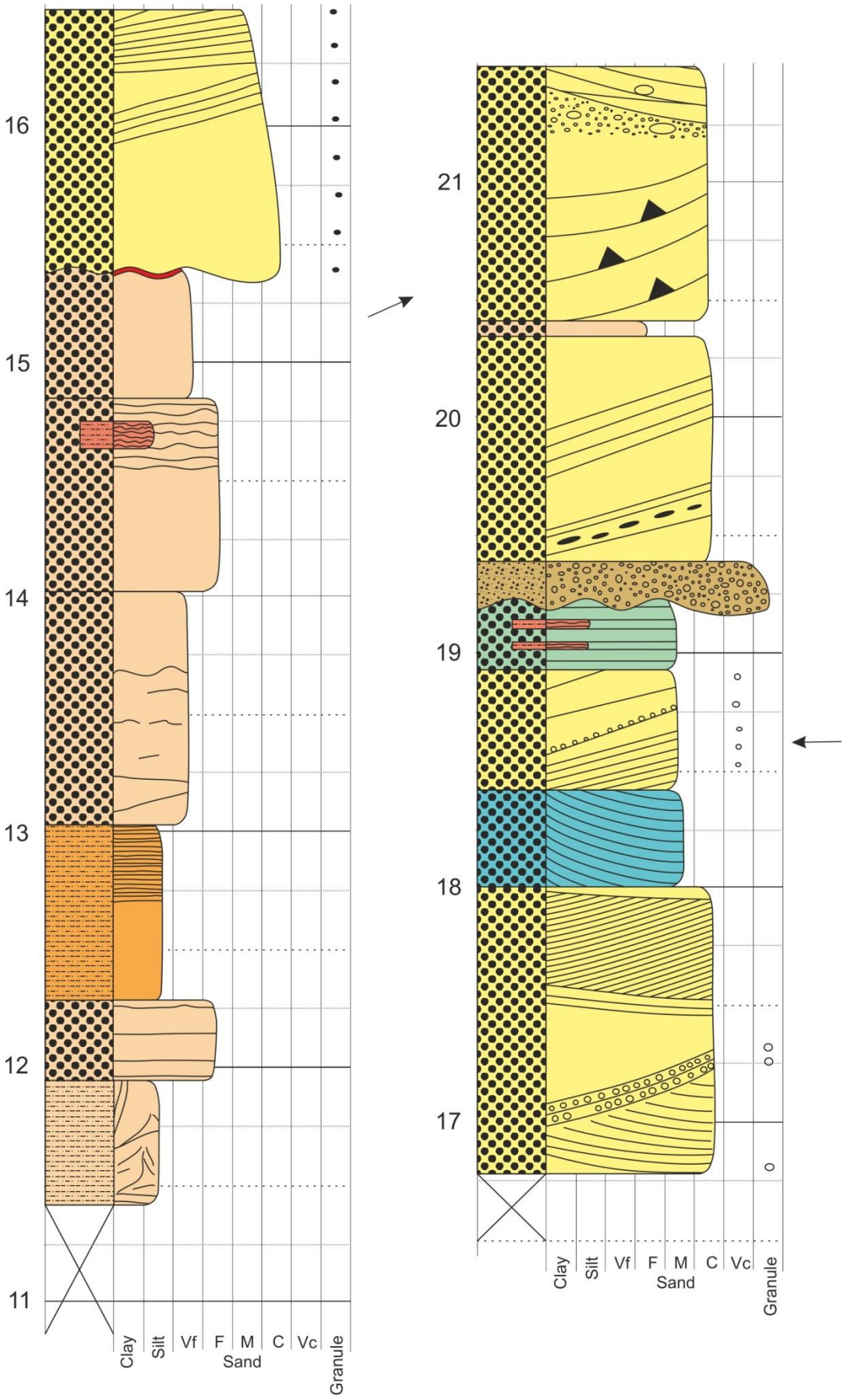
16
15
14
13
12
11
21
20
19
18
17
Clay
Silt
Vf
F
M
C
Vc
Sand
Granule

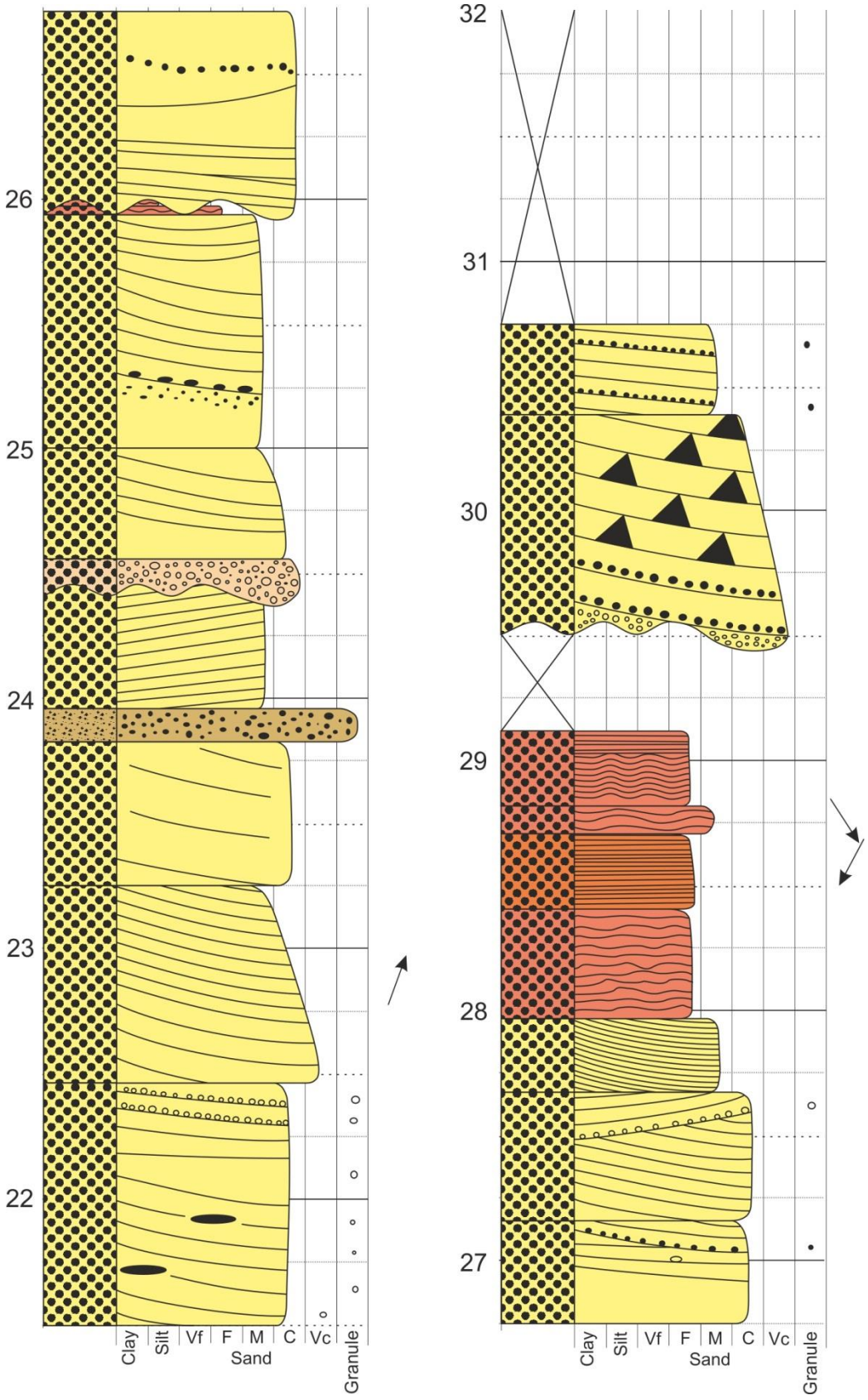
26
25
24
23
22
32
31
30
29
28
27
Clay
Silt
Vf
F
M
C
Vc
Sand
Granule

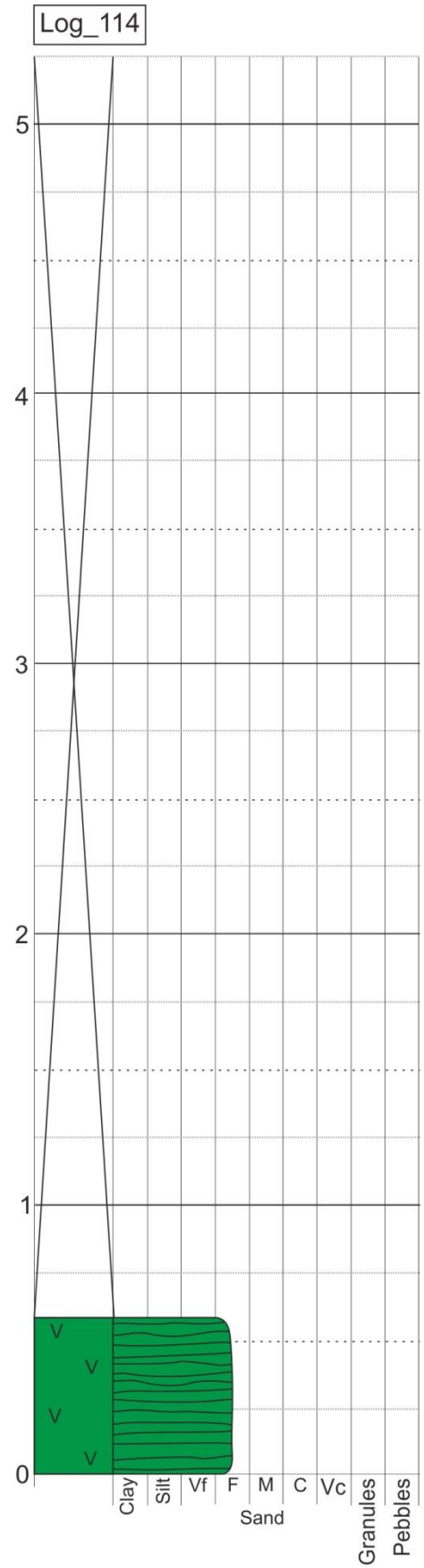
Log_114
5
4
3
2
1
0
V
V
V
V
Clay
Silt
Vf
F
M
C
Vc
Sand
Granules
Pebbles

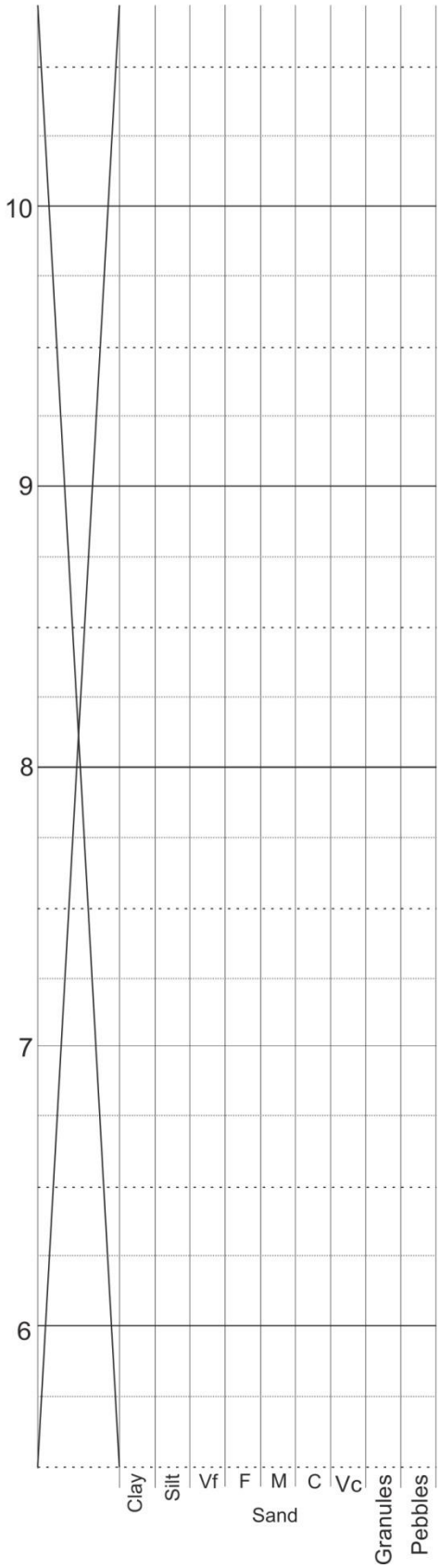
10
9
8
7
6
Clay
Silt
Vf
F
M
C
Vc
Sand
Granules
Pebbles

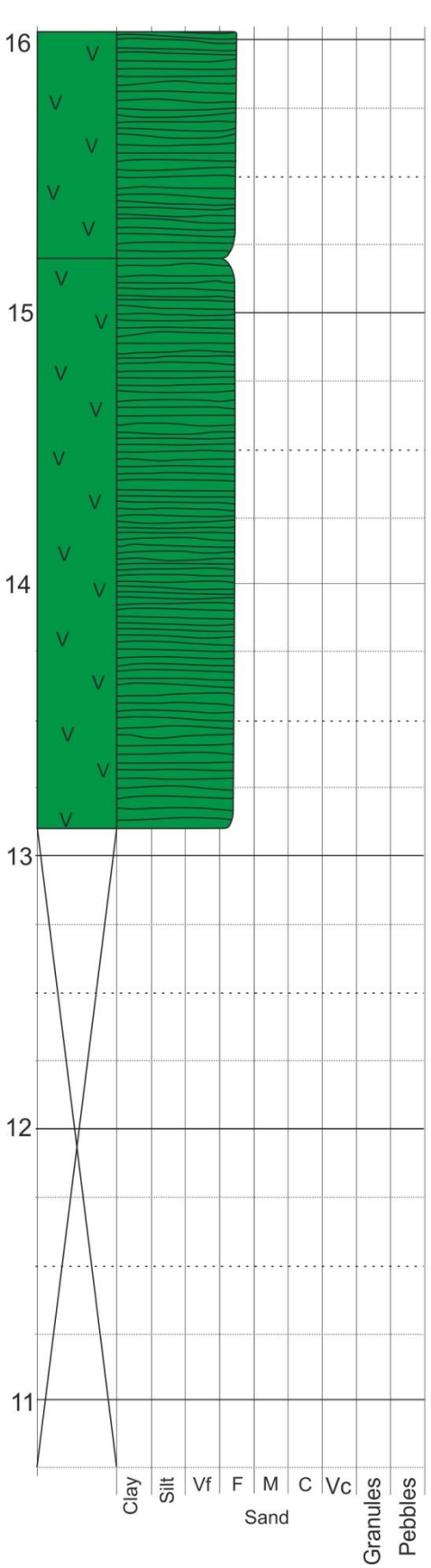
16
15
14
13
12
11
Clay
Silt
Vf
F
M
C
Vc
Sand
Granules
Pebbles

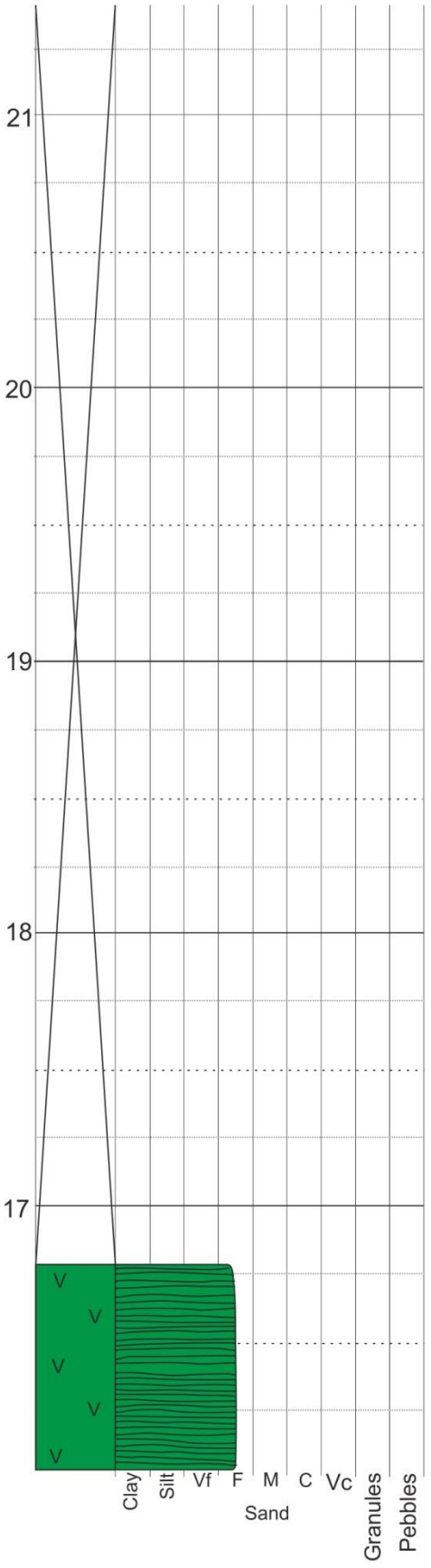
21
20
19
18
17
Clay
Silt
Vf
F
M
C
Vc
Sand
Granules
Pebbles

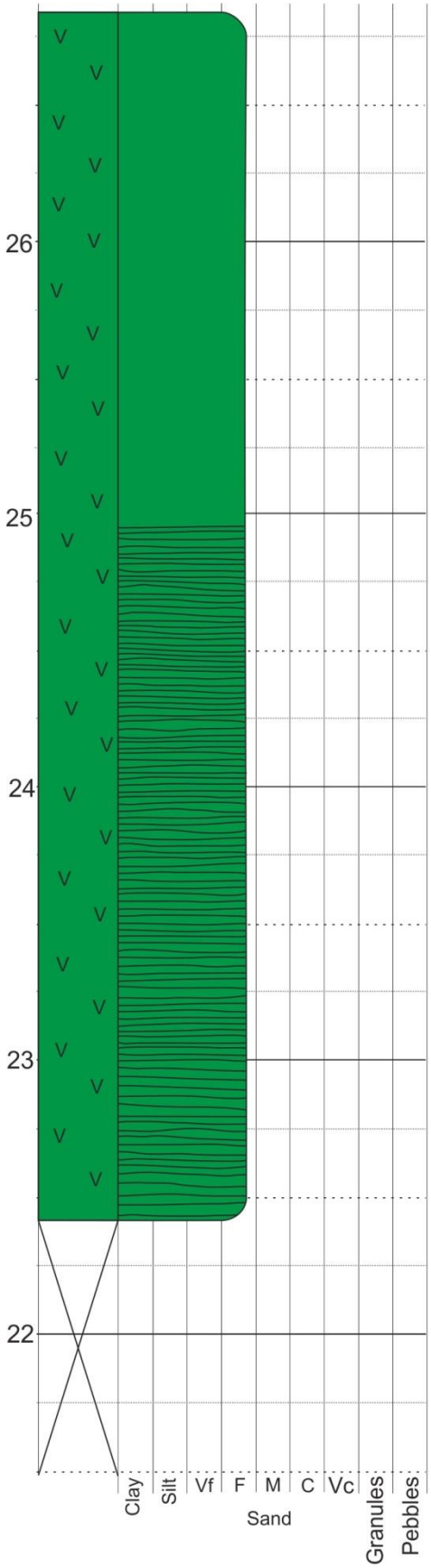
26
25
24
23
22
Clay
Silt
Vf
F
M
C
Vc
Sand
Granules
Pebbles

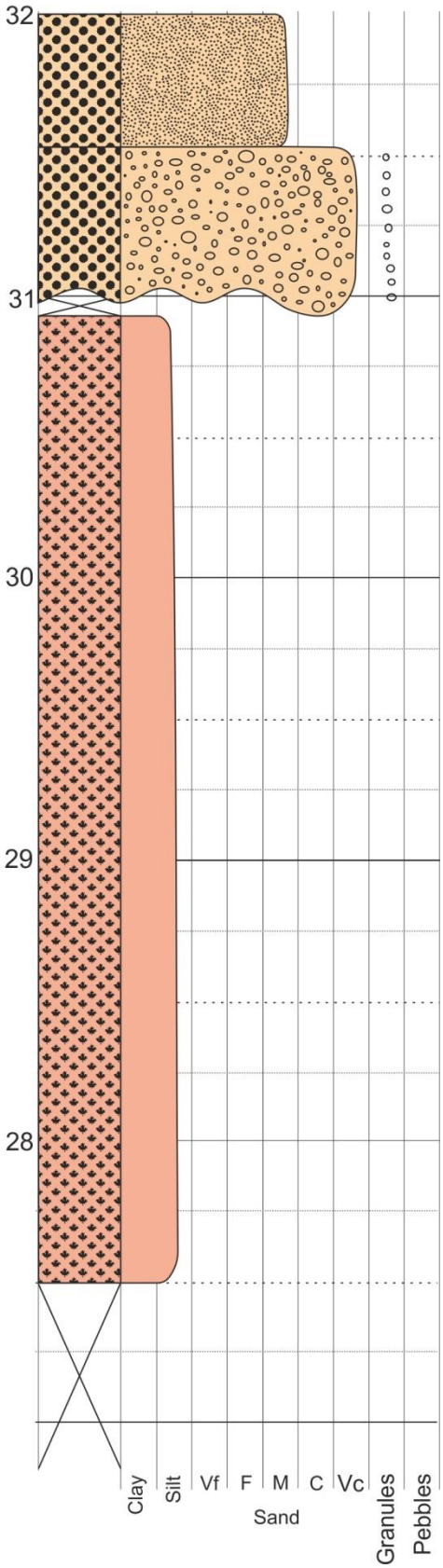
32
31
30
29
28
Clay
Silt
Vf
F
M
C
Vc
Sand
Granules
Pebbles

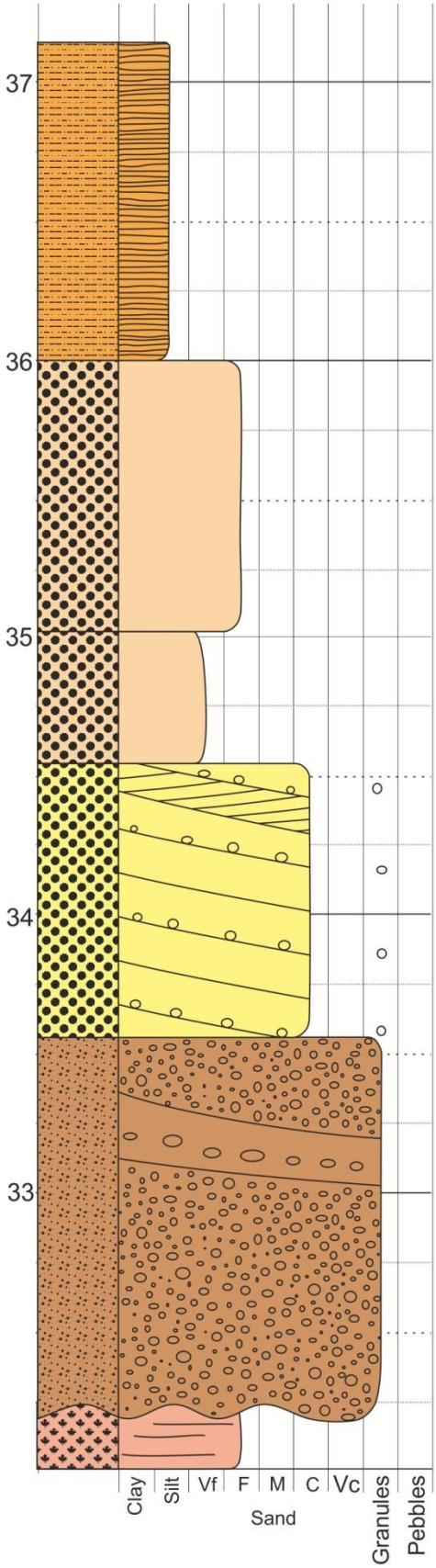
37
36
35
34
33
Clay
Silt
Vf
F
M
C
Vc
Sand
Granules
Pebbles

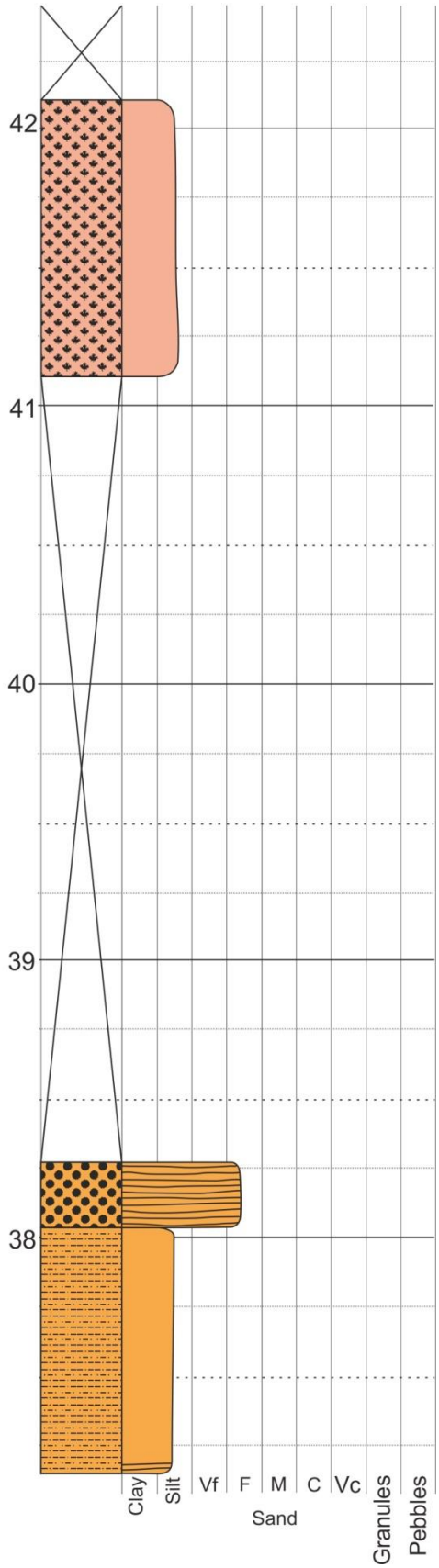
42
41
40
39
38
Clay
Silt
Vf
F
M
C
Vc
Sand
Granules
Pebbles

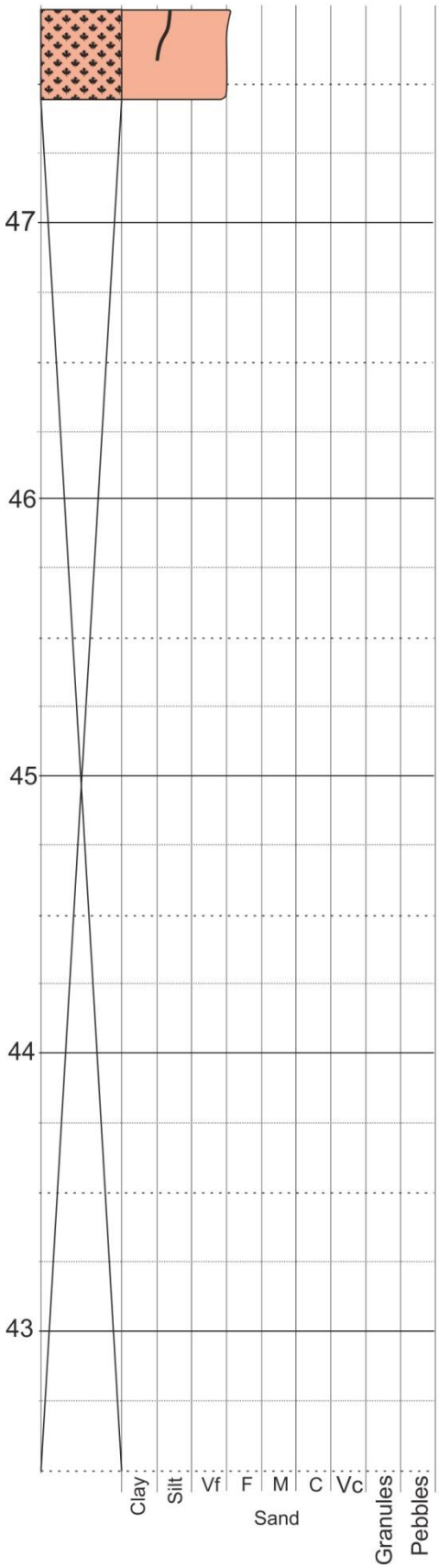
47
46
45
44
43
Clay
Silt
Vf
F
M
C
Vc
Granules
Pebbles
Sand

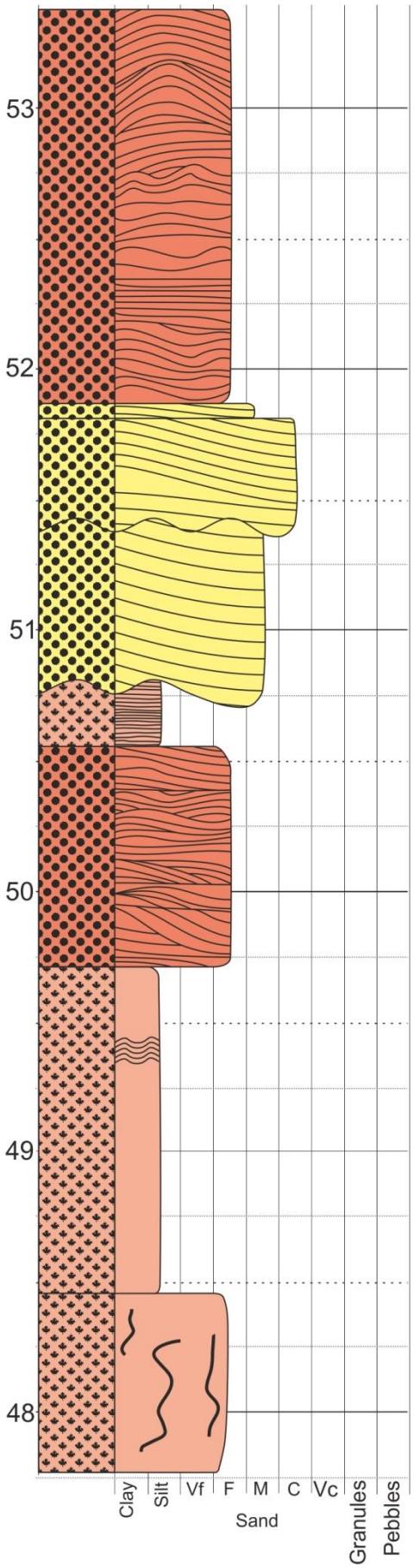
53
52
51
50
49
48
Clay
Silt
Vf
F
M
C
Vc
Granules
Pebbles
Sand

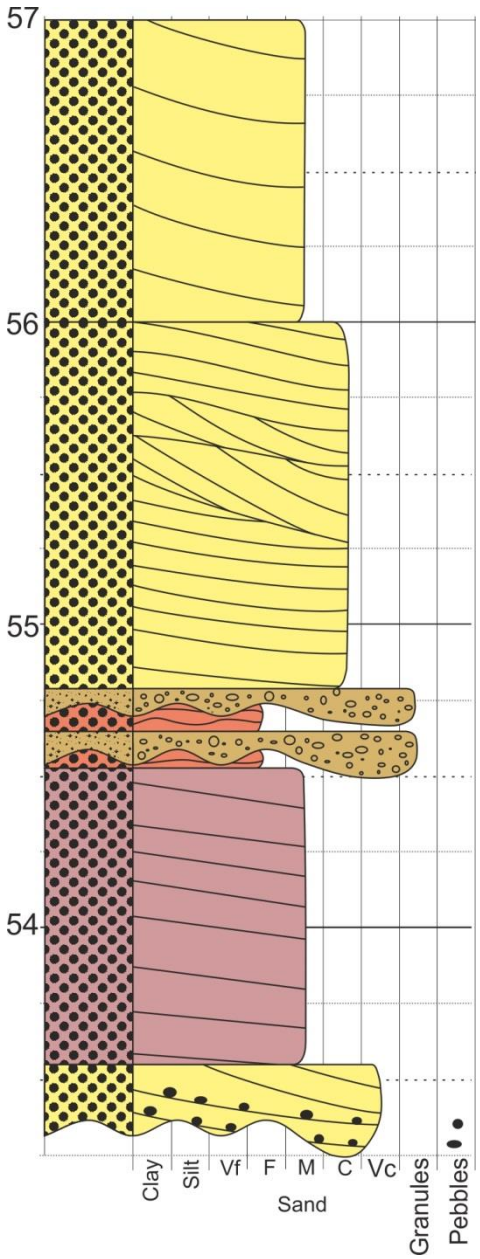
57
56
55
54
Clay
Silt
Vf
F
M
C
Vc
Sand
Granules
Pebbles

Appendix 2: Bedding field data

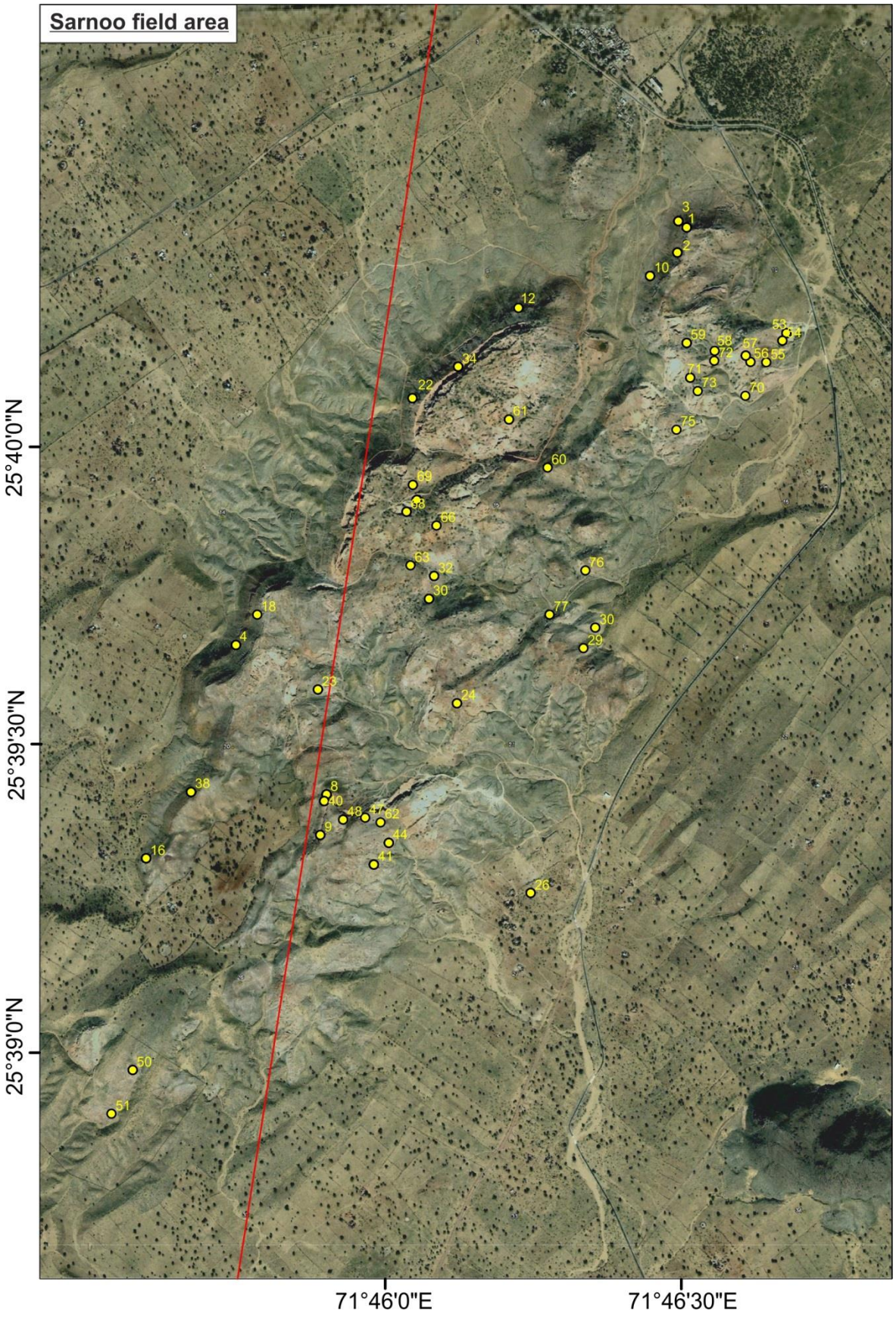
Sarnoo field area
25°40'0"N
25°39'30"N
25°39'0"N
71°46'0"E
71°46'30"E
3
1
2
10
12
59
58
57
54
53
72
56
55
71
73
70
34
22
61
75
60
69
68
66
63
32
30
76
77
30
29
18
4
23
24
38
8
40
48
47
62
9
44
41
16
26
50
51

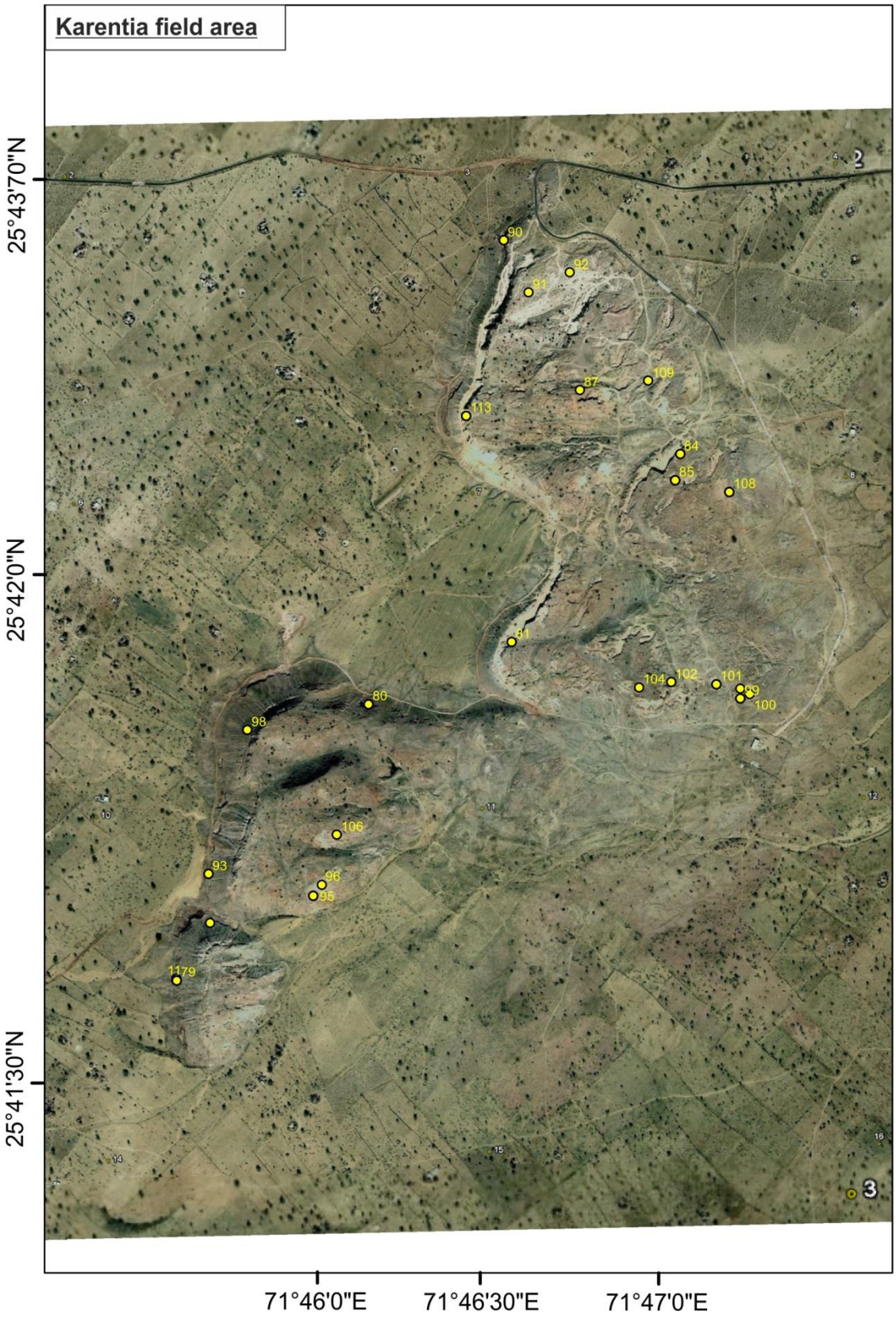
Karentia field area
25°43'70"N
25°42'0"N
25°41'30"N
71°46'0"E
71°46'30"E
71°47'0"E
90
92
91
87
109
113
84
85
108
81
104
102
101
99
100
80
98
106
93
96
95
1179
2
3

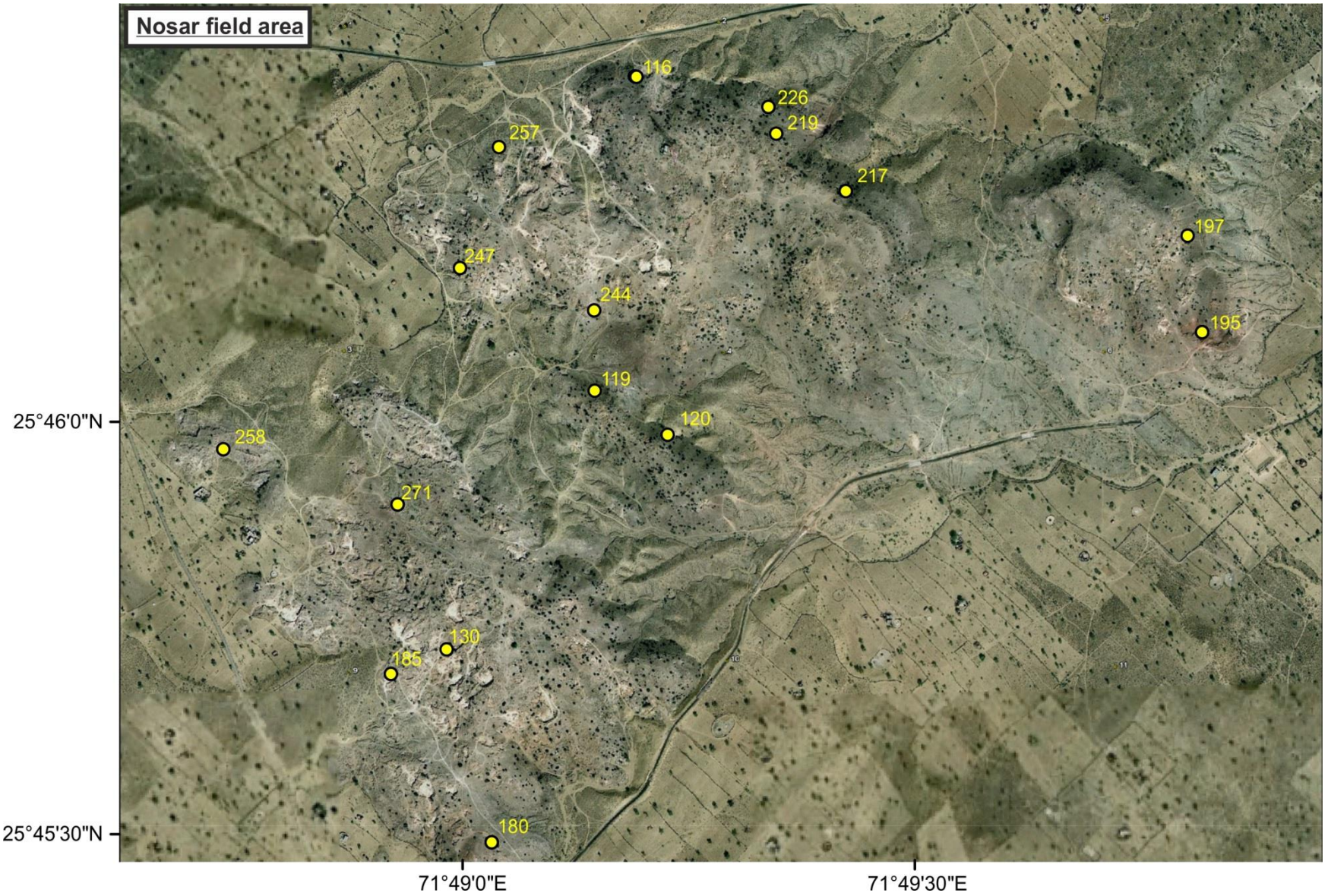
Nosar field area
116
226
219
257
217
197
247
244
195
119
120
258
271
130
185
180
25°46'0"N
25°45'30"N
71°49'0"E
71°49'30"E

Location	Northing	Easting	Log	Unit	Panel	Dip	Strike	Dip Direction
1	0778635	2842366	1	8		39	222	SE
	0778635	2842366		18		28	255	SSE
	0778635	2842366		21		20	226	SSE
	0778635	2842366		22		14	241	SSE
	0778635	2842366		34		15	222	SE
	0778635	2842366		40		10	220	SE
	0778635	2842366		40		10	222	SE
	0778635	2842366		42		22	208	E
	0778635	2842366		44		17	230	E
2	0778635	2842386	2	3		14	266	SSE
	0778635	2842386		4		7	227	SE
	0778635	2842386		6		16	234	SE
	0778635	2842386		8		14	246	SSE
	0778635	2842386		9		8	224	SE
	0778635	2842386		11		8	237	SE
	0778635	2842386		15		10	221	SE
	0778635	2842386		15		10	241	SSE
3	0778635	2842386	3	1		20	261	S
	0778635	2842386		3		17	251	SSE
	0778635	2842386		5		21	262	S
	0778635	2842386		6		21	234	SSE
4	0777247	2841038	4	5		20	219	SE
	0777247	2841038		14		19	248	SE
	0777247	2841038		14		17	230	SE
	0777247	2841038		14		22	224	SE
	0777247	2841038		16		20	216	SE
	0777247	2841038		18		18	220	SE
	0777247	2841038		20		16	221	SE
	0777247	2841038		20		8	215	SE
5	0779784	2842013	5	5		30	249	SE
	0779784	2842013		6		40	228	SE
	0779784	2842013		7		39	233	SE
	0779784	2842013		9		48	245	SE
	0779784	2842013		10		38	244	SE
	0779784	2842013		11		44	234	SE
	0779784	2842013		13		36	251	SE
	0779784	2842013		15		49	239	SE
	0779784	2842013		16		41	231	SE
	0779784	2842013		17		40	235	SE
	0779784	2842013		19		38	232	SE
	0779784	2842013		21		44	231	SE

	0779784	2842013		26		41	234	SE
	0779784	2842013		28		40	240	SE
	0779784	2842013		28		42	234	SE
	0779784	2842013		29		34	234	SSE
	0779784	2842013		31		44	236	SE
7	0779969	2842050	7	1		41	246	SSE
	0779969	2842050		3		54	268	S
	0779969	2842050		4		48	257	SSE
8	0777531	2840569	8	1		16	222	SE
	0777531	2840569		2		13	240	SE
	0777531	2840569		4		17	259	SE
	0777531	2840569		7		18	220	SE
	0777531	2840569		8		17	120	SE
9	0777512	2840442	9	3		12	215	SE
	0777512	2840442		7		20	238	SE
	0777512	2840442		11		9	206	SE
	0777512	2840442		13		38	206	SE
	0777512	2840442		15		16	229	SE
	0777512	2840442		16		16	232	SE
10	0778546	2842195	10	14		17	271	S
	0778546	2842195		18		18	262	S
	0778546	2842195		20		21	242	SE
	0778546	2842195		22		18	261	SSE
	0778546	2842195		24		12	243	SSE
	0778546	2842195		26		18	226	SE
	0778546	2842195		29		18	229	SE
	0778546	2842195		31		29	229	SE
11	0780744	2844534	11	12		13	183	E
	0780744	2844534		14		10	358	E
12	0778128	2842140	12	7		10	196	SW
	0778128	2842140		8		7	270	S
	0778128	2842140		9		6	267	SEE
	0778128	2842140		18		32	210	SE
	0778128	2842140				28	219	SE
	0778128	2842140				22	232	SE
	0778128	2842140		20		14	199	ESE
	0778128	2842140		21		18	208	SE
	0778128	2842140		22		12	224	SE
	0778128	2842140				11	210	SE
	0778128	2842140				11	210	SE
	0778128	2842140		28		21	209	SE
	0778128	2842140		29		7	251	SSE
	0778128	2842140		30		12	214	SE
	0778128	2842140		31		8	231	SE
	0778128	2842140				9	221	SE

	0778128	2842140				11	251	SE
	0778128	2842140				4	231	SE
	0778128	2842140				8	219	SE
	0778128	2842140			1	22	257	SSE
	0778128	2842140				20	261	SSE
	0778128	2842140				34	239	SE
	0778128	2842140				34	234	SE
	0778128	2842140				21	232	SE
	0778128	2842140				21	236	SE
	0778128	2842140				17	251	SE
	0778128	2842140				28	247	SE
	0778128	2842140				28	248	SE
	0778889	2841926				20	260	SSE
	0778889	2841926				23	248	SE
16	0776966	2840369	13	1		8	260	S
	0776966	2840369				9	256	SSE
	0776966	2840369		5		12	153	SSE
	0776966	2840369		7		19	190	ESE
	0776966	2840369				15	193	ESE
	0776966	2840369		10		4	195	ESE
	0776966	2840369				11	199	ESE
	0776966	2840369		11		16	212	SE
	0776966	2840369				16	217	SE
	0776966	2840369		12		9	209	ESE
	0776966	2840369				14	207	ESE
	0776966	2840369				7	221	SE
	0776966	2840369		14		12	199	ESE
	0776966	2840369				19	200	ESE
	0776966	2840369		18		17	202	ESE
	0776966	2840369				19	214	SE
	0776966	2840369		20		8	231	SE
	0776966	2840369				8	229	SE
	0776966	2840369				12	229	SE
	0777334	2841287		1		8	221	SE
	0777334	2841287				9	210	SE
	0777334	2841287				11	229	SE
	0777334	2841287		2		9	215	SE
	0777334	2841287				12	198	E
	0777334	2841287		6		4	238	SE
	0777334	2841287		8		12	259	E
	0777334	2841287				8	236	SE
	0777334	2841287		9		9	242	ESE
	0777334	2841287				6	239	ESE
	0777334	2841287		10		1	246	ESE
	0777334	2841287		11		2	218	SE

	0777334	2841287		15		3	220	SE
	0777334	2841287				3	233	SE
	0777334	2841287				4	216	SE
18	0777314	2841133			2	9	193	E
22	0777771	2841846	15	1		9	203	SE
	0777771	2841846		4		9	247	SE
	0777771	2841846		5		12	199	SE
	0777771	2841846		9		8	215	SE
	0777771	2841846				9	207	SE
	0777771	2841846		10		3	210	SE
	0777771	2841846		11		8	232	SE
	0777771	2841846		12		12	219	SE
	0777771	2841846				8	220	SE
	0777771	2841846				12	219	SE
	0777771	2841846				12	207	SE
	0777771	2841846				7	234	SE
	0777771	2841846				6	228	SE
	0777771	2841846		14		8	201	SE
	0777771	2841846				6	211	SE
	0777771	2841846				4	218	SE
	0777771	2841846				6	210	SE
	0777771	2841846				8	204	SE
	0777771	2841846		17		8	229	SE
	0777771	2841846				10	214	SE
	0777771	2841846				10	202	SE
	0777771	2841846				8	208	SE
	0777771	2841846				12	202	SE
	0777771	2841846				8	226	SE
	0777771	2841846		18		12	225	SE
	0777771	2841846				11	239	SE
	0777771	2841846		19		8	227	SE
	0777771	2841846				9	222	SE
	0777771	2841846				6	207	SE
	0777771	2841846		21		8	192	E
23	0777504	2840898			3	9	230	SE
	0777504	2840898				9	199	SE
	0777504	2840898				8	240	SE
	0777504	2840898				4	214	SE
24	0777941	2840855				7	237	SE
	0777941	2840855				29	239	SE
	0777941	2840855				15	270	E
	0777941	2840855				24	237	SE
26	0778172	2840260	16	1		11	191	E
	0778172	2840260		2		8	209	SE
	0778172	2840260		4		19	230	SE

	0778172	2840260				10	211	SE
	0778363	2840950				46	227	SE
29	0778338	2841028				41	225	SE
30	0778374	2841092				21	193	E
	0778374	2841092				18	208	SE
30	0777853	2841183				40	256	SSE
	0777853	2841183				9	224	SE
	0777853	2841183				18	231	SE
	0777853	2841183				13	219	SE
	0777853	2841183				18	260	SSE
	0777853	2841183				18	238	SE
	0777853	2841183				20	262	SSE
	0777853	2841183				20	259	SSE
	0777853	2841183				10	241	SE
32	0777869	2841254				16	209	SE
	0777869	2841254				12	205	SE
	0777869	2841254				19	221	SE
	0777869	2841254				12	239	SE
	0777869	2841254				10	254	SSE
	0777869	2841254				14	251	SSE
34	0777944	2841910				15	253	SSE
	0777944	2841910				12	271	S
	0777944	2841910				8	248	SSE
	0777944	2841910				40	206	SE
	0777944	2841910				10	214	SE
	0777944	2841910				8	194	E
36	0777447	2849376	18	1		20	203	SE
	0777447	2849376				14	190	E
	0777447	2849376		2		22	178	E
	0777447	2849376		3		15	188	E
	0777447	2849376		4		5	182	E
38	0777107	2840577	19	1		17	196	SE
	0777107	2840577		4		8	202	SE
	0777107	2840577				23	201	SE
	0777107	2840577		5		8	195	E
	0777107	2840577				20	202	SE
	0777107	2840577		6		21	246	SE
	0777107	2840577				18	226	SE
	0777107	2840577				36	203	SE
	0777107	2840577		8		10	209	SE
	0777107	2840577				11	211	SE
	0777107	2840577		9		20	242	SE
	0777107	2840577				10	253	SSE
	0777107	2840577		12		16	194	E
	0777107	2840577				10	192	E

	0777107	2840577				20	204	SE
	0777107	2840577				21	218	SE
40	0777524	2840549				21	194	E
	0777524	2840549				18	226	SE
	0777524	2840549				19	209	SE
	0777524	2840549				15	206	SE
	0777524	2840549				12	221	SE
	0777524	2840549				12	220	SE
	0777524	2840549				22	206	SE
	0777524	2840549				18	146	SW
41	0777680	2840349				7	252	SSE
	0777680	2840349				2	272	SSE
	0777680	2840349				17	216	SE
	0777680	2840349				19	245	SE
	0777680	2840349				12	200	SE
	0777680	2840349				11	231	SE
	0777680	2840349				16	221	SE
	0777680	2840349				17	191	ESE
	0777680	2840349				9	209	SE
44	0777727	2840417				11	240	SSE
	0777727	2840417				21	228	SE
	0777727	2840417				19	180	E
	0777727	2840417				18	229	SE
	0777727	2840417				20	231	SE
	0777727	2840417				12	228	SE
45	0777732	2840526				12	187	SSE
	0777732	2840526				11	170	ENE
47	0777653	2840496				13.5	238	SE
48	0777584	2840490				22	254	SSE
	0777584	2840490				8	251	SSE
49A	0776781	2839852				16	229	SE
	0776781	2839852				22	269	S
49C	0776740	2839776				16	210	SE
	0776740	2839776				24	223	SE
	0776740	2839776				9	207	SE
	0776740	2839776				8	193	E
50	0776923	2839705				14	211	SE
	0776923	2839705				10	174	E
	0776923	2839705				16	251	SSE
	0776923	2839705				10	216	SE
	0776923	2839705				11	231	SE
51	0776857	2839568				12	251	SE
53	0778974	2842016	20			28	241	SE
	0778974	2842016				22	241	SE
	0778974	2842016				26	236	SE

	0778974	2842016				18	221	SE
	0778974	2842016				17	244	SE
54	0778962	2841992				12	252	SSE
	0778962	2841992				18	208	SE
	0778962	2841992				18	243	SSE
	0778962	2841992				16	258	SSE
55	0778911	2841924				22	253	SSE
56	0778862	2841925				12	239	SE
	0778862	2841925				24	234	SE
57	0778847	2841945				9	219	SE
	0778847	2841945				24	255	SE
	0778847	2841945				19	229	SE
	0778847	2841945				24	261	S
	0778847	2841945				12	221	SE
58	0778749	2841960				22	221	
59	0778661	2841985				22	223	
	0778661	2841985				25	241	
	0778661	2841985				32	222	
	0778661	2841985				20	255	
	0778661	2841985				37	238	
	0778661	2841985				29	238	
	0778661	2841985				20	242	
	0778661	2841985				11	269	
	0778661	2841985				24	235	
	0778661	2841985				19	210	
60	0778225	2841594				24	210	
61	0778104	2841745			5	18	185	E
	0778104	2841745				6	210	SE
	0778104	2841745				3	270	SE
62	0777701	2840482	21			12	254	SE
63	0777795	2841287				12	251	SE
66	0777876	2841412				10	164	ENE
	0777876	2841412				10	221	SE
67	0777815	2841493				8	235	SE
	0777815	2841493				8	213	SE
	0777815	2841493				10	220	SE
	0777815	2841493				21	237	SE
	0777815	2841493				14	214	SE
	0777815	2841493				3	196	E
68	0777782	2841455				12	187	E
	0777782	2841455				13	174	E
	0777782	2841455				12	241	SE
	0777782	2841455				12	247	SE
	0777782	2841455				6	264	S
69	0777802	2841540				10	200	SE

	0777802	2841540				10	232	SE
70	0778845	2841819				28	241	SE
71	0778672	2841876				38	239	SE
	0778672	2841876				27	219	SE
	0778672	2841876				30	232	SE
72	0778748	2841929				19	249	SSE
73	0778696	2841834				26	228	SE
75	0778629	2841713				19	239	SE
77	0778231	2841133				10	184	E
	0778231	2841133				12	246	SSE
76	0778343	2841271				28	200	SE
79	0780745	2844530	23	3		13	215	SE
	0780745	2844530		5		8	199	E
	0780745	2844530				14	201	E
	0780745	2844530		8		13	232	SE
	0780745	2844530		13		2	189	E
	0780745	2844530		14		8	214	SE
	0780745	2844530		15		11	230	SE
	0780745	2844530		16		45	217	SE
	0780745	2844530		17		19	238	SE
	0780745	2844530		18		18	254	SE
	0780745	2844530		19		12	211	SE
	0780745	2844530		20		13	220	SE
	0780745	2844530		23		22	200	SE
	0780745	2844530		26		11	224	SE
	0780745	2844530				4	209	SE
	0780745	2844530		31		20	232	SE
	0780745	2844530		32		33	237	SSE
	0780745	2844530		33		11	212	SE
	0780745	2844530		34		24	223	SE
	0780745	2844530				24	215	SE
	0780745	2844530				21	205	SE
	0780745	2844530				28	215	SE
	0780745	2844530				18	218	SE
80	0781186	2845165	24	1		22	231	SE
	0781186	2845165		2		15	230	SE
	0781186	2845165				10	233	SE
	0781186	2845165		3		18	229	SE
	0781186	2845165		4		12	254	SSE
	0781186	2845165				15	250	SSE
	0781186	2845165		7		18	206	SE
	0781186	2845165				25	200	ESE
	0781186	2845165		11		24	221	SE
	0781186	2845165		12		22	232	SE
	0781186	2845165				22	221	SE

	0781186	2845165				34	221	SE
	0781186	2845165		13		33	195	E
	0781186	2845165				31	220	SE
	0781186	2845165				24	221	SE
	0781186	2845165		14		12	192	E
	0781186	2845165		15		21	200	E
	0781186	2845165		16		2	191	E
81	0781515	2845308		2		7	208	E
	0781515	2845308		4		2	248	SE
	0781515	2845308		8		10	207	E
	0781558	2845206				10	241	SE
	0781558	2845206				38	232	SE
	0781558	2845206				12	226	SE
	0781558	2845206				18	227	SE
84	0781903	2845740	26	2		4	197	E
	0781903	2845740		3		10	214	SE
	0781903	2845740		4		4	209	ESE
	0781903	2845740		7		10	207	SE
85	0781891	2845680	27	1		3	249	SE
	0781891	2845680		4		10	234	SE
	0781891	2845680				14	189	E
	0781891	2845680				13	203	SE
	0781891	2845680				22	229	SE
	0781891	2845680				23	248	SSE
	0781891	2845680		5		16	239	SE
	0781891	2845680				18	237	SE
	0781891	2845680				20	242	SE
87	0781672	2845887	28	1		12	251	SSE
	0781586	2845934				23	229	SE
	0781586	2845934				18	231	SE
90	0781497	2846232	29	6		8	232	SE
	0781497	2846232		15		4	186	E
	0781497	2846232		16		7	211	ESE
	0781497	2846232		23		8	199	E
	0781497	2846232		24		10	180	E
91	0781554	2846112	30			3.5	245.5	SE
92	0781649	2846158	31	2		7	221	SE
93	0780818	2844775	32	11		11	246	SE
	0780818	2844775				10	248	SE
	0780818	2844775		17		20	228	SE
	0780818	2844775				11	215	SE
	0780818	2844775		18		22	230	SE
95	0781059	2844725				28	242	SE
	0781059	2844725				26	242	SE
	0781059	2844725				28	233	SE

	0781059	2844725				32	237	SE
	0781059	2844725				32	238	SE
	0781059	2844725				27	245	SE
96	0781078	2844750	33	1		24	211	ESE
98	0780907	2845106	34	4		23	216	SE
	0780907	2845106		8		10	210	SE
	0780907	2845106		10		11	220	SE
	0780907	2845106		11		11	238	SE
	0780907	2845106		18		14	258	SSE
	0780907	2845106				8	242	SE
	0780907	2845106				10	235	SE
	0780907	2845106		19		5	248	SSE
	0780907	2845106				8	243	SE
	0780907	2845106		20		10	228	SE
	0780907	2845106				10	241	SE
	0780907	2845106				11	246	SE
99	0782041	2845178				13	254	SE
	0782041	2845178				11	191	E
	0782041	2845178				8	226	SE
	0782041	2845201				11	261	S
100	0782063	2845188				10	185	E
101	0781986	2845211	35	1		4	234	SE
	0781986	2845211				8	250	SE
	0781986	2845211				7	258	SE
	0781986	2845211				24	208	SE
102	0781882	2845216				10	217	SE
	0781882	2845216				20	218	SE
104	0781808	2845204	36	6		15	187	E
106	0781113	2844865	37	1		10	198	E
	0781113	2844865		2		18	242	SE
	0781113	2844865		5		2	210	SE
108	0782016	2845653	38	2		12	140	NE
	0782016	2845653		3		14	153	NE
	0782016	2845653				9	142	NE
	0782016	2845653		6		11	155	NE
	0782016	2845653		7		19	156	NE
	0782016	2845653		10		18	158	NE
	0782016	2845653				8	175	E
	0782016	2845653				13	146	NE
	0782016	2845653				13	143	NE
109	0781829	2845909				12	231	SE
	0781829	2845909				24	227	SE
113	0781410	2845828	40	4		12	172	E
	0781410	2845828		7		10	224	SE
	0781410	2845828		10		6	220	SE

	0781410	2845828				10	222	SE
	0781410	2845828				6	210	SE
	0781410	2845828				5	206	ESE
	0781410	2845828				2	210	SE
	0781410	2845828		11		12	196	E
116D	0782802	2853524				4	187	E
116F	0782805	2853523				7	168	ENE
	0782805	2853523				6	104	N
119	0782722	2852901				5	341	SW
120	0782867	2852814				10	174	
121	0782721	2853061				6	178	
	0782721	2853061				5	176	
123	0778103	2841383	44	2		18	235	
	0778103	2841383		5		10	215	
	0778103	2841383		8		9	235	
	0778103	2841383		9		7	257	
	0778103	2841383		10		16	233	
	0778103	2841383				15	246	
	0778103	2841383		11		14	224	
	0778103	2841383				18	239	
	0778103	2841383		14		16	211	
	0778103	2841383		17		16	240	
	0778103	2841383		18		18	238	
	0778103	2841383		19		18	234	
	0778103	2841383		21		23	257	
	0778103	2841383		22		21	257	
	0778103	2841383		23		26	240	
	0778103	2841383		24		15	221	
	0778103	2841383		25		19	236	
	0778103	2841383		26		24	228	
	0778103	2841383		28		34	232	
	0778103	2841383				31	230	
	0778103	2841383		30		36	243	
	0778103	2841383				20	224	
	0778103	2841383				20	244	
	0778103	2841383				21	238	
	0778103	2841383		31		24	209	
	0778103	2841383				34	228	
	0778103	2841383		32		25	215	
	0778103	2841383		37		25	216	
	0778103	2841383		41		35	205	
131	0779904	2842062	51	5		9	223	
	0779904	2842062		7		46	238	
	0779904	2842062		8		41	244	
	0779904	2842062		10		32	220	

	0779904	2842062				42	228	
	0779904	2842062				37	254	
	0779904	2842062		11		40	238	
	0779904	2842062		12		24	224	
	0779904	2842062				42	231	
	0779904	2842062				38	224	
	0779904	2842062				39	235	
	0779904	2842062		13		37	238	
	0779904	2842062		14		38	221	
	0779904	2842062				37	217	
	0779904	2842062		15		33	234	
	0779904	2842062		16		41	239	
134	0778299	2841427	52	2		24	212	
	0778299	2841427		3		23	200	
	0778299	2841427		4		24	198	
	0778299	2841427		5		28	218	
	0778299	2841427		6		20	223	
	0778299	2841427		7		25	221	
	0778299	2841427		10		26	210	
	0778299	2841427		13		29	235	
	0778299	2841427		16		32	212	
	0778299	2841427		17		35	220	
	0778299	2841427		19		21	198	
	0778299	2841427		22		38	227	
135	0777801	2841812	53	5		12	251	
	0777801	2841812		9		12	231	
	0777801	2841812		22		9	218	
	0777801	2841812				3	221	
136	0778661	2842347	54	2		11	233	
	0778661	2842347		4		10	229	
	0778661	2842347		8		9	236	
	0778661	2842347		12		19	224	
	0778661	2842347		17		10	230	
	0778661	2842347		18		18	236	
	0778661	2842347		19		13	234	
	0778661	2842347				20	229	
	0778661	2842347		20		16	229	
	0778661	2842347		22		18	232	
	0778661	2842347		37		11	241	
	0778661	2842347		38		10	256	
144	0781870	2845443				2	194	
153	0777565	2841047				10	210	
	0777565	2841047				19	195	
154	0777570	2841128		2		10	214	
	0777570	2841128		3		22	209	

	0777570	2841128				15	222	
	0777570	2841128				16	197	
	0777570	2841128				18	197	
	0777570	2841128		4		12	214	
156	0777514	2841213				8	255	
158	0777374	2840994				15	228	
	0777374	2840994				11	226	
	0777374	2840994				16	224	
159	0777452	2840922	60	1		3	240	
	0778156	2842034				14	267	
	0777896	2841845		2		8	221	
164	0779578	2841849	62	2		30	017	
	0779578	2841849				33	020	
	0779578	2841849				33	010	
	0779578	2841849				33	011	
	0779578	2841849		4		24	015	
	0779578	2841849				32	008	
	0779578	2841849				32	019	
	0779578	2841849		6		25	011	
	0779578	2841849				30	009	
	0779578	2841849				37	007	
	0779578	2841849				38	004	
	0779578	2841849				37	022	
	0779578	2841849		9		29	026	
	0779578	2841849				31	026	
	0779578	2841849				28	014	
	0779578	2841849		11		38	028	
	0779578	2841849		13		27	019	
	0779578	2841849		14		36	036	
	0779578	2841849		17		26	024	
165	0783067	2853464	65	3		7	224	SE
	0783067	2853464		4		7	191	E
176	0782659	2852890				10	350	W
177	0782691	2852924	70	1		20	302	WSW
	0782691	2852924				32	304	WSW
	0782691	2852924				21	309	WSW
180	0782518	2852007	71	3		18	279	S
	0782518	2852007		4		20	276	S
	0782518	2852007				16	280	SSW
	0782318	2852340				6	302	SW
	0782318	2852340				12	300	SW
191	0782429	2852389	75	4		10	329	SW
195	0783927	2853017	76	6		11	223	SE
	0783927	2853017				10	209	SE
	0783927	2853017		7		6	223	SE

198	0783898	2853208	78	4		16	333	SW
211	0783220	2853297	84	8		18	303	
	0783220	2853297				21	301	
221	0783082	2853411				18	298	SW
248	0782455	2853144				28	311	SW
	0782455	2853144				30	314	SW
249	0782532	2853384				20	350	WSW
267	0782656	2852481				20	332	SW
270	0782331	2852676				18	353	WSW
	0782331	2852676				8	344	SW
	0782331	2852676				10	347	WSW
273	0781986	2852786	96	3		8	321	SW
	0781986	2852786		4		2	306	SW
284	0777345	2840014				30	189	E
	0777345	2840014				25	164	E
	0777345	2840014				34	172	E
	0777345	2840014				32	173	E
288	0777339	2839915				12	207	E
	0777339	2839915				25	200	E
	0777329	2839985				36	350	E
290	0777331	2839988	97	1		40	341	E
	0777331	2839988		3		18	353	E
	0777331	2839988				20	341	E
	0777331	2839988		4		18	350	E
	0777331	2839988				37	356	E
	0777331	2839988				36	358	E
	0777331	2839988		5		14	360	E
	0777331	2839988				15	2	E
	0777331	2839988		8		26	176	E
	0777331	2839988		10		26	176	E
	0777331	2839988				22	355	E
	0777331	2839988				21	357	E
	0777331	2839988				13	6	E
	0777331	2839988				24	17	E
	0777331	2839988		11		25	356	E
	0777331	2839988		13		39	187	E
	0777331	2839988				37	198	E
	0777331	2839988		14		38	195	E
	0777331	2839988		15		36	184	E
	0777331	2839988		17		31	352	E
	0777331	2839988		18		31	360	E
	0777331	2839988				35	1	E
	0777331	2839988		20		25	25	SE
	0777331	2839988				36	25	SE
291	0777290	2840142				20	42	SE

292	0777447	2840496				20	227	SE
	0777447	2840496				20	221	SE
293	0777483	2840686				12	209	SE
	0777483	2840686				12	211	SE
	0777483	2840686				12	211	SE
	0777483	2840686				5	232	SE
294	0777444	2840738				21	186	E
300	0777545	2840803	98	1		10	235	SE
	0777545	2840803				15	197	ESE
	0777545	2840803				12	227	SE
	0777545	2840803		3		8	218	SE
	0777545	2840803		5		12	229	SE
	0777545	2840803		7		11	207	SE
	0777545	2840803		9		13	223	SE
	0777545	2840803		10		20	215	SE
302	0777652	2840902	99	1		8	217	SE
	0777652	2840902				20	212	SE
	0777652	2840902		2		13	196	ESE
	0777652	2840902				8	199	ESE
	0777652	2840902		3		6	228	SE
	0777652	2840902				12	214	SE
	0777652	2840902		5		14	214	SE
306	0777906	2841054				14	227	SE
308	0777973	2841028				25	231	SE
	0777973	2841028				17	243	SE
311	0777972	2841218				28	244	SE
	0777972	2841218				28	250	SE
	0777972	2841218				16	244	SE
	0777972	2841218				22	258	SE
312	0777950	2841272				13	233	SE
	0777950	2841272				10	239	SE
	0777950	2841272				13	204	ESE
313	0778003	2841331	100	3		15	210	SE
	0778003	2841331		5		25	223	SE
	0778003	2841331				18	217	SE
	0778003	2841331		6		25	214	SE
	0778003	2841331				20	210	SE
	0778003	2841331		7		20	192	ESE
	0778003	2841331		9		29	201	ESE
	0778003	2841331		10		28	223	SE
	0778003	2841331				17	218	SE
314	0778194	2841334				18	204	ESE
	0778194	2841334				28	205	ESE
	0778194	2841334				23	174	E
	0778194	2841334				20	200	ESE

315	0778304	2841300				37	210	SE
	0778304	2841300				30	195	E
317	0778205	2841382	101	2		24	194	ESE
	0778205	2841382		3		19	207	SE
	0778205	2841382				19	203	SE
	0778205	2841382				23	203	SE
	0778205	2841382		6		17	204	SE
	0778205	2841382				25	202	SE
	0778205	2841382		7		15	212	SE
	0778205	2841382				18	207	SE
	0778205	2841382				21	204	SE
	0778205	2841382				18	205	SE
	0778205	2841382		8		18	225	SE
	0778205	2841382				19	194	ESE
	0778205	2841382				20	206	SE
	0778205	2841382		9		25	194	ESE
	0778205	2841382				21	213	SE
	0778205	2841382				31	210	SE
320	0778136	2841939				10	222	SE
322	0778207	2841583				25	200	SE
323	0778315	2841630				20	214	SE
	0778315	2841630				20	214	SE
	0778315	2841630				28	198	E
324	0778344	2841658				18	202	SE
325	0778412	2841788				31	207	SE
	0778412	2841788				20	204	SE
331	0778591	2842109				25	221	SE
	0778591	2842109				18	232	SE
334	0778743	2842162	102	1		20	215	SE
	0778743	2842162		2		18	225	SE
	0778743	2842162				18	229	SE
	0778743	2842162		5		24	216	SE
	0778743	2842162				18	224	SE
	0778743	2842162				18	235	SE
	0778743	2842162				18	241	SE
	0778743	2842162		6		14	213	SE
	0778743	2842162				14	223	SE
	0778743	2842162				20	215	SE
	0778743	2842162		9		21	239	SE
	0778743	2842162		10		17	236	SE
	0778743	2842162				15	220	SE
	0778743	2842162				13	210	SE
	0778743	2842162		11		15	259	SSE
335	0781872	2845447				15	208	SE
337	0781689	2845678				10	194	ESE

338	0781670	2845628				18	250	SSE
342	0781521	2845710				10	223	SE
343	0781416	2845758				16	171	E
344	0781632	2845503			51	15	226	SE
346	0781699	2845435				6	206	SE
347	0781690	2845361				9	207	ESE
349	0781608	2845285				6	211	SE
352	0780979	2845092				14	220	SE
353	0780957	2844965				18	240	SE
354	0781021	2844975				24	245	SE
355	0781069	2844989				22	277	S
	0781069	2844989				24	274	S
356	0780821	2844662	103	4		6	221	SE
	0780821	2844662		5		10	233	SE
	0780821	2844662		6		18	213	SE
359	0780867	2844534				27	210	SE
361	0780859	2844388				40	199	ESE
362	0780797	2844366				23	250	SE
364	0777201	2841094	104	4		18	228	SE
	0777201	2841094		6		12	277	S
	0777201	2841094		14		9	210	SE
	0777201	2841094		17		12	241	SSE
	0777201	2841094		19		8	187	E
	0777201	2841094		20		8	211	SE
	0777201	2841094		24		15	217	SE
	0777201	2841094				10	190	E
	0777201	2841094		27		15	207	ESE
	0777201	2841094		28		5	215	SE
	0777201	2841094				10	183	E
	0777201	2841094		29		20	228	SE
	0777201	2841094				19	205	SE
	0777201	2841094				12	236	SE
	0777201	2841094		30		10	207	SE
365	0778129	2842137	105	6		13	240	SE
	0778129	2842137		29		21	297	SSW
	0778129	2842137		31		18	270	S
	0778129	2842137		45		26	232	SE
	0778129	2842137		51		15	210	SE
	0778129	2842137		53		12	237	SE
	0778129	2842137		57		18	220	SE
	0778133	2842095			54	19	240	SE
367	0778582	2842142	106	14		22	240	SSE
	0778582	2842142		33		14	216	SE
368	0778687	2842098	107	5		18	258	SSE
370	0777181	2841039	109	16		42	262	NNW

	0777181	2841039		17		26	309	NE
	0777181	2841039		24		3	193	SE
	0777181	2841039		25		20	200	SE
	0777181	2841039		50		12	206	SE

Appendix 3: Thin sections

Log: 1
Height: 1.10m
Sample Number: 3
Sandstone name: Darjaniyon-ki Dhani

Facies: Srm
Architectural Element: Channel (F1)

Grainsize: Upper coarse sand
Sorting: Moderate
Roundness: Sub-rounded to sub-angular
Sandstone classification: Quartz wacke

Detrital Mineralogy: The rigid detrital mineralogy is dominantly composed of quartz (monocrystalline 38% and polycrystalline 23%). Subordinate minerals are sedimentary rigid rock fragments (7.5%), metamorphic rigid rock fragments (5%), undifferentiated grains (trace) and muscovite mica (trace). The monocrystalline quartz grains are unstrained to weakly-strained. Sedimentary fragments are composed of chert. whilst the metamorphic fragments are composed of sutured polycrystalline quartz, exhibiting a schistose fabric. Ductile grains of muscovite mica are buckled between the rigid detrital grains. Optically non-resolvable clays (15.5%) locally coats grain and infills intergranular pores. The undifferentiated grains are replaced by the haematite.

Authigenic Mineralogy: The authigenic mineralogy comprises cements and clays. Cements include: haematite (1%), quartz overgrowths (0.5%), non-ferroan dolomite (0.5%), anatase (trace) and calcite (trace). The haematite locally coats quartz grains and infills pore space. Syntaxial quartz overgrowths are thin (2 – 3µm) and discontinuous around their host grains. The dolomite and calcite cements partially occlude intergranular primary porosity. Authigenic clays includes kaolinite (1%), which infills the pore spaces.

Reservoir Quality: Macroporosity is low (8%), consisting of primary intergranular porosity (7.5%) and secondary intergranular porosity (0.5%). The primary porosity well interconnected. Secondary porosity occurs after unstable grain dissolution and can be connected to primary pores.

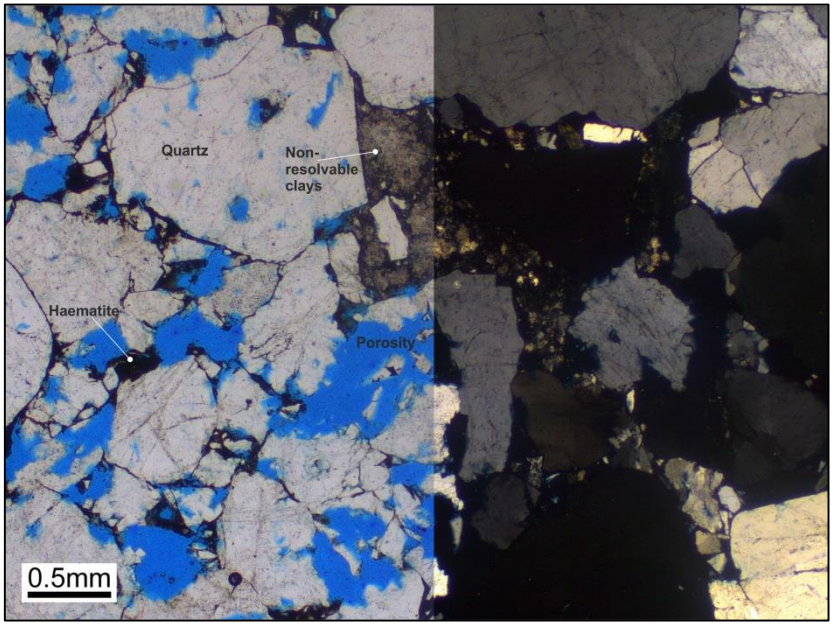

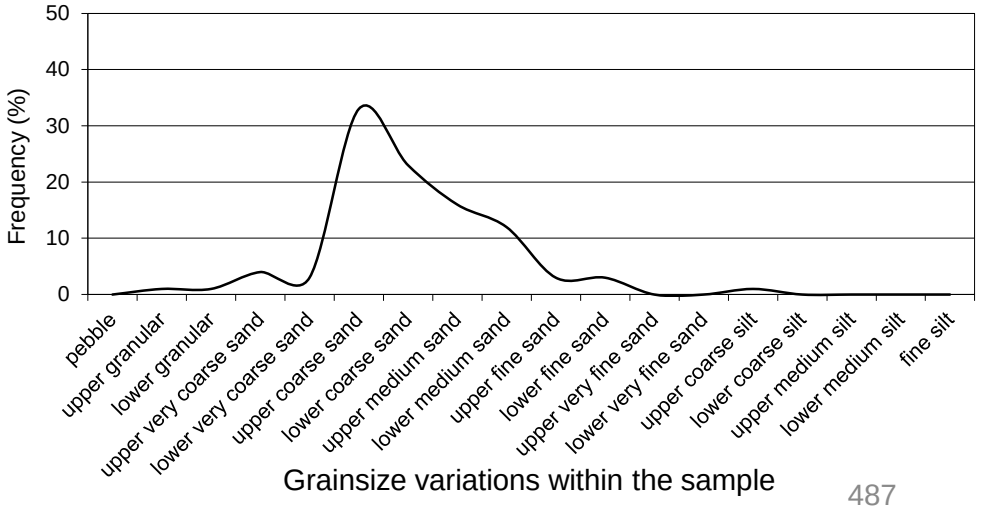

Log: 1
Height: 2.49m
Sample Number: 5
Sandstone name: Darjaniyon-ki Dhani

Facies: G
Architectural Element: Gravel bar (F3)

Grainsize: Upper medium sand
Sorting: Moderate
Roundness: Sub-rounded
Sandstone classification: Sublithic arenite

Detrital Mineralogy: The rigid detrital mineralogy comprises abundant monocrystalline quartz (37%) and subordinate polycrystalline quartz (29%). Subordinate rigid detrital minerals are: sedimentary rigid rock fragments (7%) and metamorphic rigid rock fragments (2.5%), undifferentiated grains (1.5%) and rutile (trace). The majority of the monocrystalline quartz is very weakly-strained. The quartz grains contain rare rutile inclusions. Sedimentary fragments are composed of chert. Metamorphic fragments are composed of highly-sutured polycrystalline quartz, exhibiting a schistose fabric. The undifferentiated minerals are partially replaced by haematite. Optically non-resolvable clays (1%) locally coats the grains and fills the intergranular areas.

Authigenic Mineralogy: Authigenic minerals consist of cements and clays. The cements are: haematite (9.5%), quartz overgrowths (1.5%) and ferroan calcite (trace) and the only clay is kaolinite (4%). The haematite locally fills pores and coats the detrital grains. Syntaxial quartz overgrowths are discontinuous around their host grains. Trace amounts of calcite is replacing the non-resolvable clays. Kaolinite booklets locally choke primary pores.

Reservoir Quality: The macroporosity consists of primary intergranular porosity only and is low (7%). The limited porosity is primarily due to compaction and haematitic and kaolinite cements. There is secondary porosity which has formed due to fracturing within the rock.

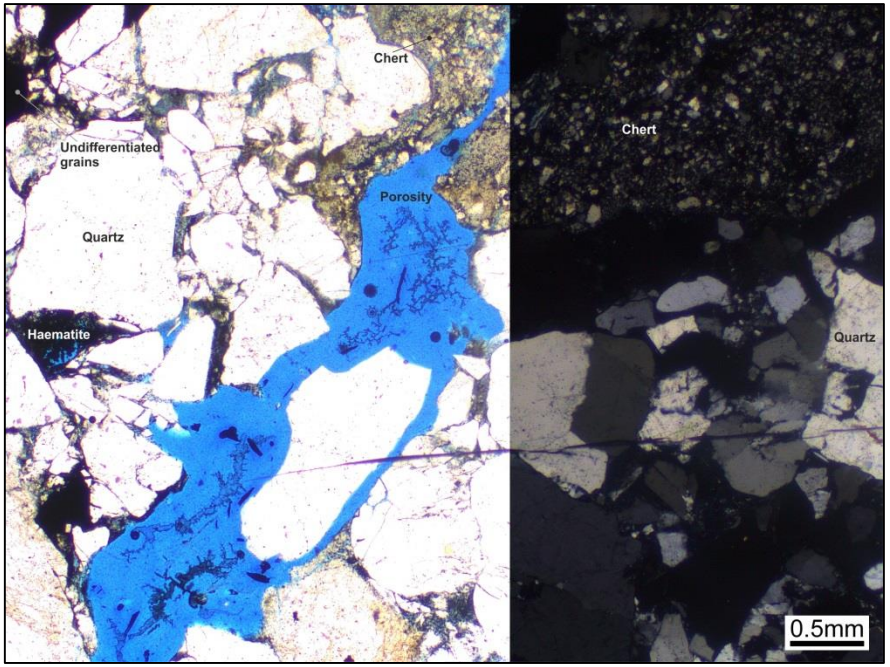

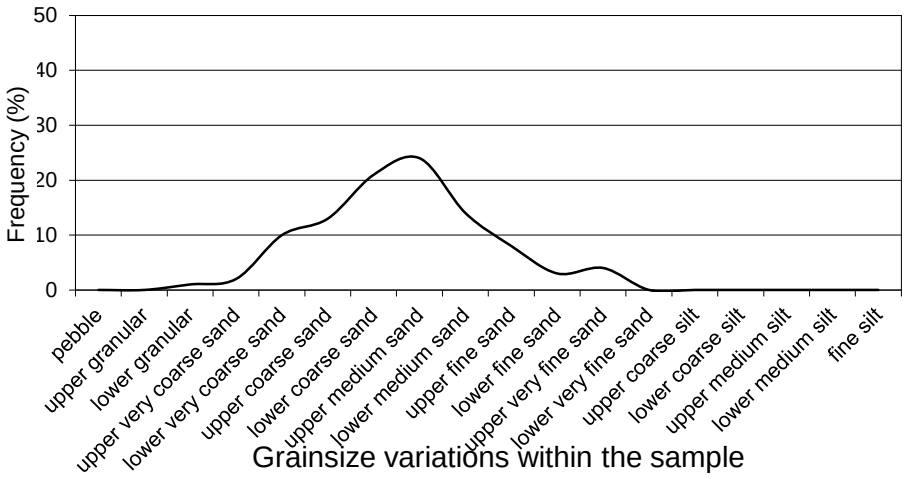

Log: 1
Height: 2.57m
Sample Number: 6
Sandstone name: Darjaniyon-ki Dhani

Facies: M
Architectural Element: Gravel bar (F3)

Grainsize: Lower medium sand
Sorting: Moderate
Roundness: Sub-rounded
Sandstone classification: *Haematite* Sublithic arenite

Detrital Mineralogy: The principle rigid detrital mineralogy comprises monocrystalline quartz (54.5%) with subordinate polycrystalline quartz (14%), rigid rock fragments (sedimentary 9.5% and igneous 0.5%) and zircon (0.5%). Monocrystalline quartz grains are euhedral and exhibit no straining, whilst polycrystalline quartz grains have mildly sutured contacts. The sedimentary fragments are formed from chert that contain monocrystalline quartz. The igneous rock fragments contain quartz and muscovite grains. Zircon grains are highly spherical and have a high birefringence. Optically non-resolvable clays (3.5%) locally coat the grains and choke and fill the primary pore spaces.

Authigenic Mineralogy: The authigenic mineralogy contains cements and clays. Cements include: haematite (12.5%), quartz overgrowths (1%), non-ferroan dolomite (1%). Clays include kaolinite (2%). The haematite is infilling pore spaces and coating quartz grains. Syntaxial quartz overgrowths are thin (1-2µm) and discontinuous around the host quartz grains. The non-ferroan dolomite cement which is replacing the quartz grains. Kaolinite forms booklets and is infilling the pore spaces locally.

Reservoir Quality: Macroporosity is very (1%) and comprise primary intergranular pores which are isolated. The haematite cement has in-filled the pore spaces.

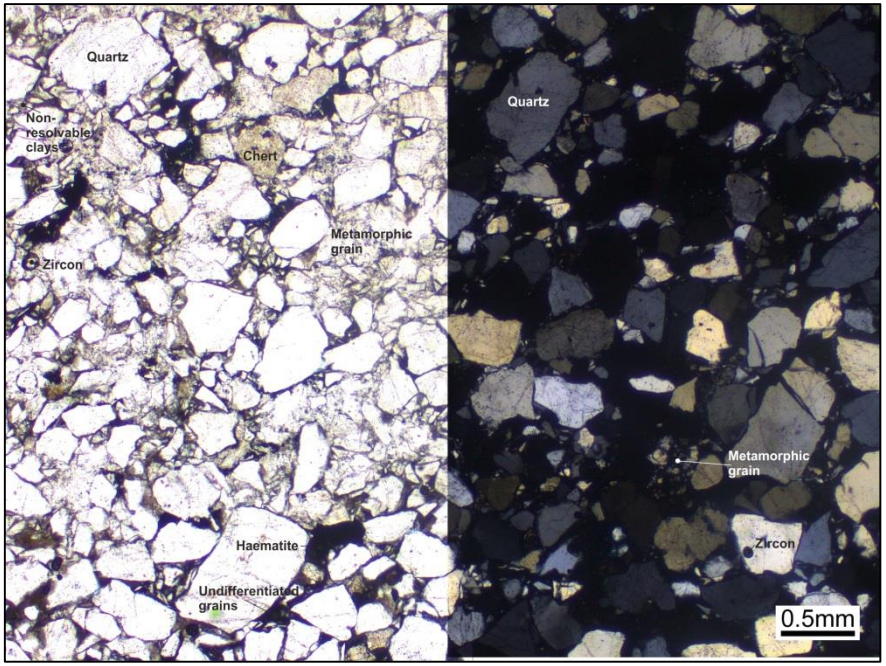

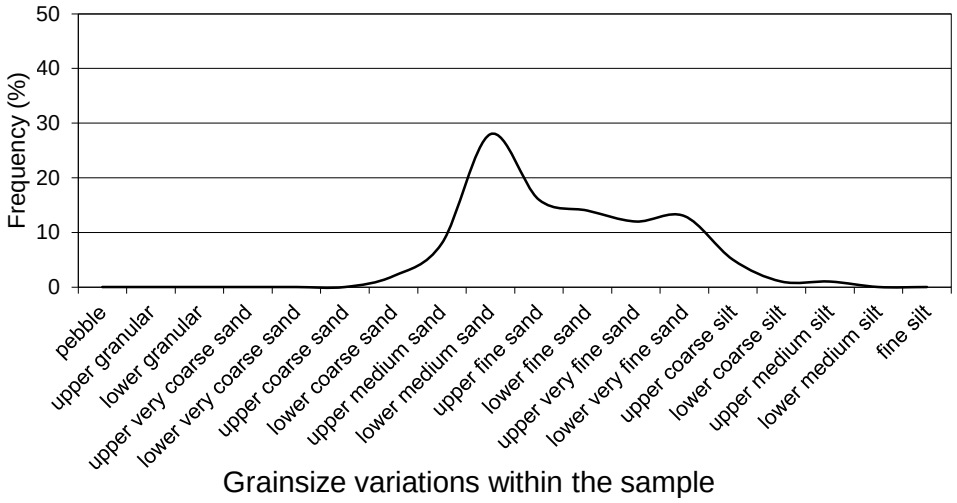

Log: 1
Height: 3.05m
Sample Number: 8
Sandstone name: Darjaniyon-ki Dhani

Facies: G
Architectural Element: Gravel bar (F3)

Grainsize: Upper medium sand
Sorting: Poor
Roundness: Rounded to Sub-rounded
Sandstone classification: Sublithic arenite

Detrital Mineralogy: The rigid detrital mineralogy comprises abundant amounts of polycrystalline quartz grains (51.5%). Subordinate rigid grains comprise monocrystalline quartz (28.5%), rigid rock fragments (metamorphic 8%; sedimentary 1.5%). Monocrystalline quartz grains are weakly-strained and locally exhibit an undulose extinction. Polycrystalline quartz grains have concave-convex contacts within the grain and contain small rutile inclusions (2µm). The metamorphic fragments contain fragmented, elongated, sutured polycrystalline quartz grains which have a preferred orientation. The rigid sedimentary fragments are composed of chert. Ductile muscovite mica grains are partially altered to kaolinite clays and haematite cements. Optically non-resolvable clays (0.5%) locally coat grains and fill pores.

Authigenic Mineralogy: Authigenic mineral components composes of cements and clays. Cements include: haematite (2.5%), quartz overgrowths (1.5%), ferroan calcite (trace) and anatase (trace), whilst the authigenic clays consist of kaolinite (0.5%). Haematite cements locally coat the detrital grains. Syntaxial quartz overgrowths are discontinuous around the quartz grains. Calcite cement are within intergranular areas. The anatase occurs as inclusions within the monocrystalline quartz. The kaolinite locally infills pores. The trace amounts of calcite cement appears to be replacing the kaolinite and quartz grains.

Reservoir Quality: The macroporosity is low (5.5%), with both primary intergranular porosity (4.5%) and secondary intergranular porosity (1%). The limited porosity is not interconnected and chocked by kaolinite and partially occluded by calcite cements.

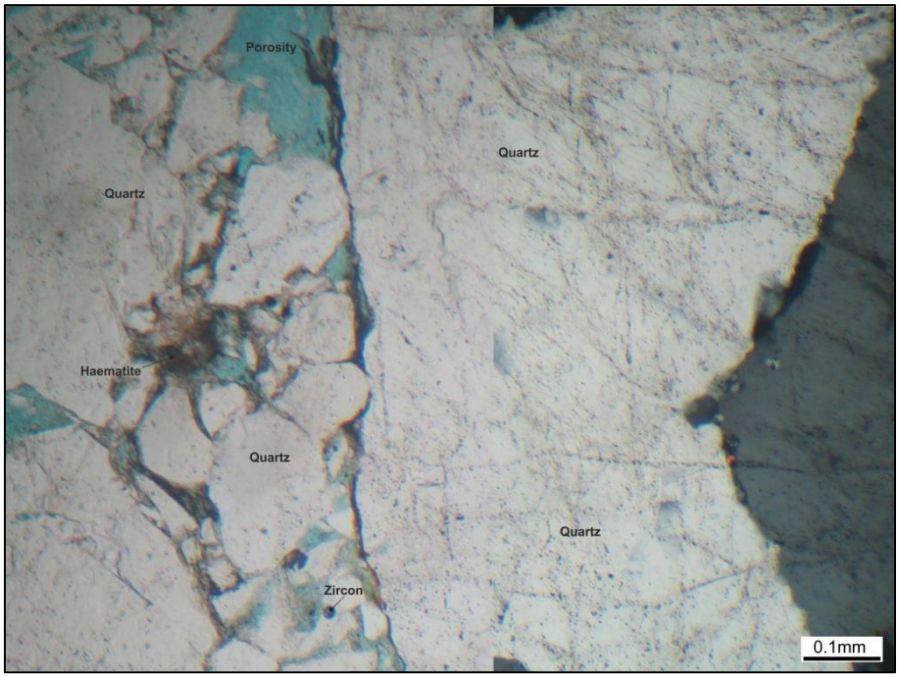

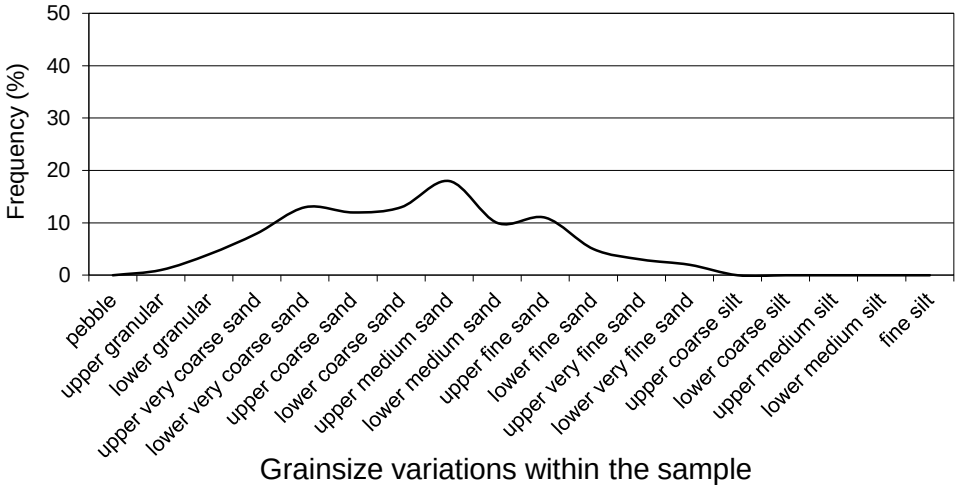

Grainsize variations within the sample

Log: 1
Height: 7.47m
Sample Number: 13
Sandstone name: Darjaniyon-ki Dhani

Facies: M
Architectural Element: Channel (F1)

Grainsize: Upper fine sand
Sorting: Poor
Roundness: Sub-rounded to sub-angular
Sandstone classification: *Haematitic* Sublithic arenite

Detrital Mineralogy: Rigid detrital mineralogy comprises abundant monocrystalline quartz grains (38.5%), with subordinate polycrystalline quartz (17%), metamorphic rigid rock fragments (0.5%), undifferentiated grains (0.5%) and muscovite (trace). Some of the monocrystalline quartz have suffered corrosion as the grains are embayed. They are weakly-strained. The polycrystalline quartz grains are fractured. Undifferentiated grains are replaced by haematite. Ductile muscovite mica is buckled between the rigid grains and is locally altered to kaolinite. Optically non-resolvable clays (13.5%) constitutes pseudomatrix (13%) and pore-filling clays (0.5%). The clays coat grains and choke pore spaces. The pseudomatrix is likely to comprise compacted ductile grains and clay, associated with calcite and / or haematite.

Authigenic Mineralogy: Authigenic mineralogy comprises cements which include: haematite (20%) and quartz overgrowths (3%). Authigenic clays comprise only kaolinite (0.5%). Haematite cements are coating the grains and infilling the primary pore spaces; some grains have being completely replaced by the haematite cement. Syntaxial quartz overgrowths are discontinuous and thin (approximately 3µm) around the quartz host grain. The kaolinite booklets are choking the primary pores.

Reservoir Quality: Macroporosity constitutes primary intergranular porosity which is low (6.5%). There is porosity within the grains due to fractures, but this occurs rarely. The primary porosity is largely isolated.

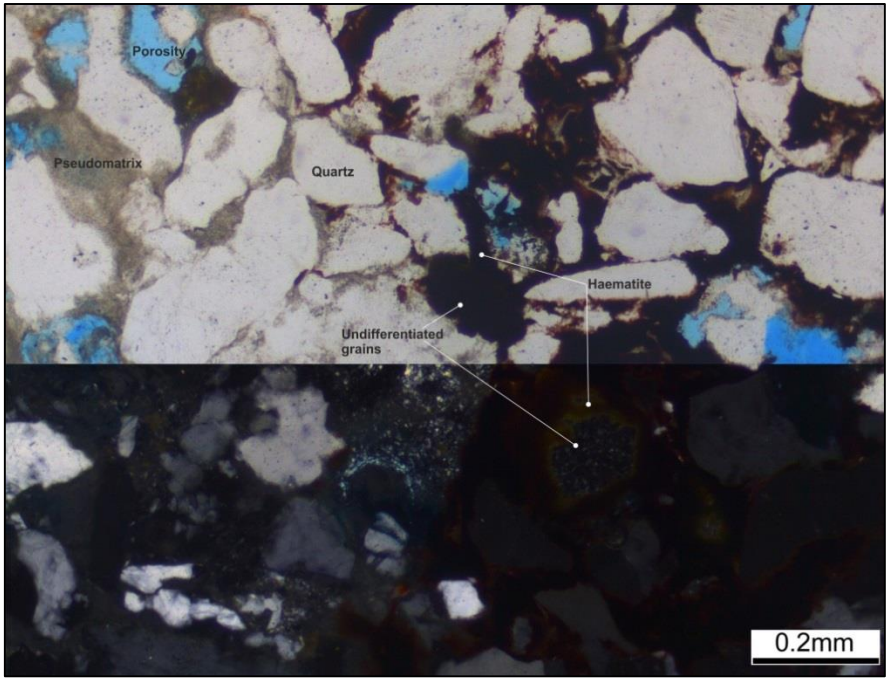

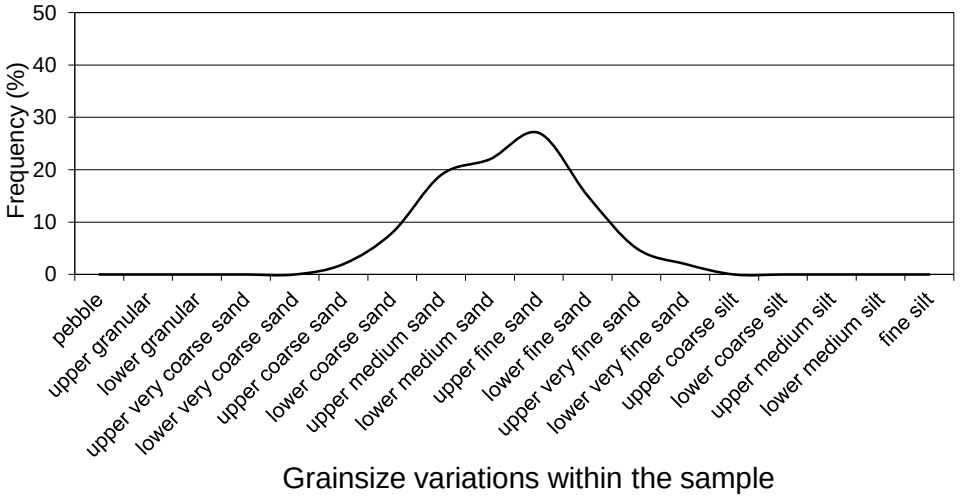

Grainsize variations within the sample

Log: 1
Height: 3.821m
Sample Number: 19
Sandstone name: Sarnoo

Facies: G
Architectural Element: Channel (F1)

Grainsize: Lower medium sand
Sorting: Moderate
Roundness: Sub-rounded to sub-angular
Sandstone classification: Sublithic arenite

Detrital Mineralogy: The rigid detrital minerals comprise quartz (monocrystalline 52%, polycrystalline 26.5%), rigid rock fragments (metamorphic 4%, sedimentary 0.5%), heavy minerals (trace) and muscovite (trace). Some of the monocrystalline quartz grains exhibit undulose extinction and have suffered corrosion. The metamorphic fragments are formed from sutured polycrystalline quartz grains displaying a schistose fabric, whilst the sedimentary fragments are composed of chert. The heavy minerals include rutile and zircon. Muscovite mica grains are compacted within the primary pores between the rigid grains. Optically non-resolvable clay (3.5%) is composed of detrital pore-filling clays (2.5%) and pseudomatrix (1%) both of which coats the grains locally and chokes the primary pores. It is likely that the clays are haematitic in composition.

Authigenic Mineralogy: Authigenic minerals comprise cements including: haematite (10%) and quartz overgrowths (3%). The haematite commonly fills pores. Syntaxial quartz overgrowths are discontinuous and thin (1-2µm) around the host quartz grain.

Reservoir Quality: The macroporosity is negligible (0.5%) and constitutes isolated secondary intergranular pores only. There is a trace of primary intergranular porosity.

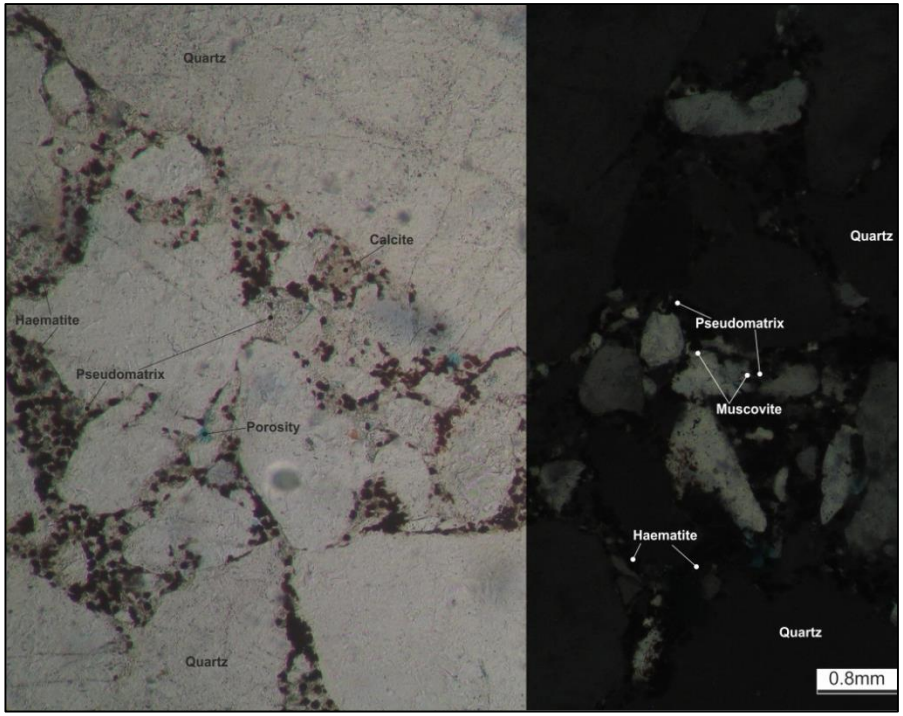

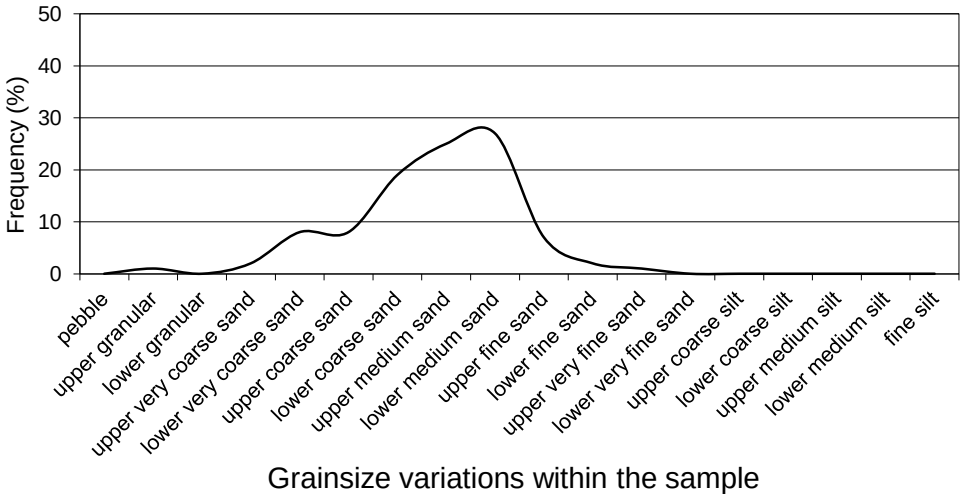

Grainsize variations within the sample

Log: 1
Height: 3.900m
Sample Number: 20
Sandstone name: Sarnoo

Facies: G
Architectural Element: Channel (F1)

Grainsize: Upper coarse sand
Sorting: Poorly
Roundness: Rounded to Sub-rounded
Sandstone classification: Quartzarenite

Detrital Mineralogy: The rigid detrital mineralogy comprises dominantly monocrystalline quartz (35%), with highly subordinate amounts of polycrystalline quartz (26%) and rigid rock fragments (5.5%: metamorphic – 3.5%, sedimentary 1.5% and igneous 0.5%). Quartz grains are unstrained to slightly strained. Rarely polycrystalline quartz grains are sutured and form the metamorphic rigid rock fragments, with a schistose fabric. The sedimentary fragments are chert, whilst the igneous fragments are formed of muscovite mica and quartz. Ductile muscovite mica grains are compacted within the primary pores and the terminations are locally replaced by kaolinite. Optically non-resolvable clays (15%) comprise pseudomatrix (13%) and pore-filling clays (2%). They are likely to be composed of haematite.

Authigenic Mineralogy: Authigenic mineralogy comprise cements and clays. Cements include: haematite (3.5%) and quartz overgrowths (0.5%). The clays constitute kaolinite (3%) and pore-filling non-resolvable clays (0.5%). The haematite coats the quartz grains and in-fills the pore spaces. Syntaxial quartz overgrowths are thin (1-2µm) and discontinuous around the host quartz grains. Kaolinite and non-resolvable clays locally infill the primary pore space.

Reservoir Quality: The macroporosity is moderate (11%) is composed of primary intergranular porosity only. The porosity is interconnected.

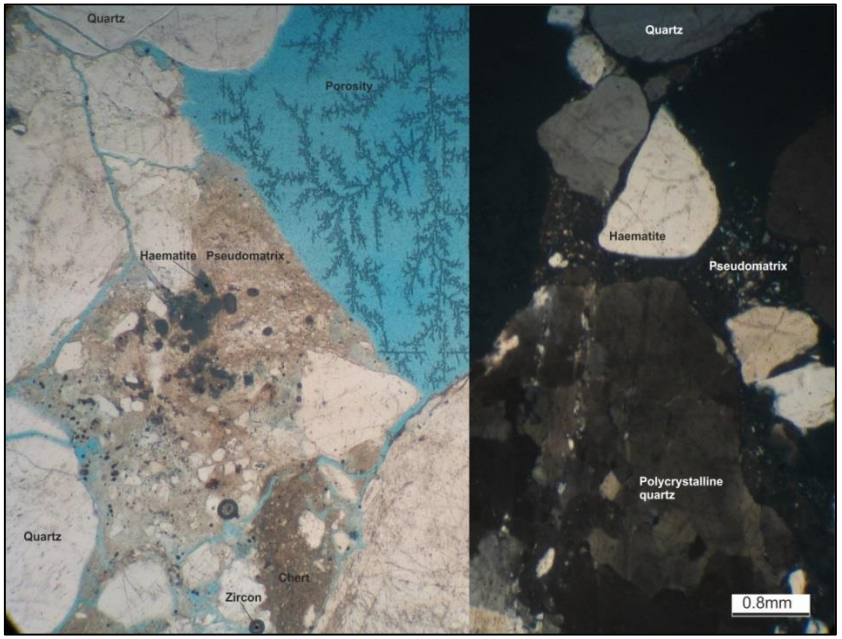

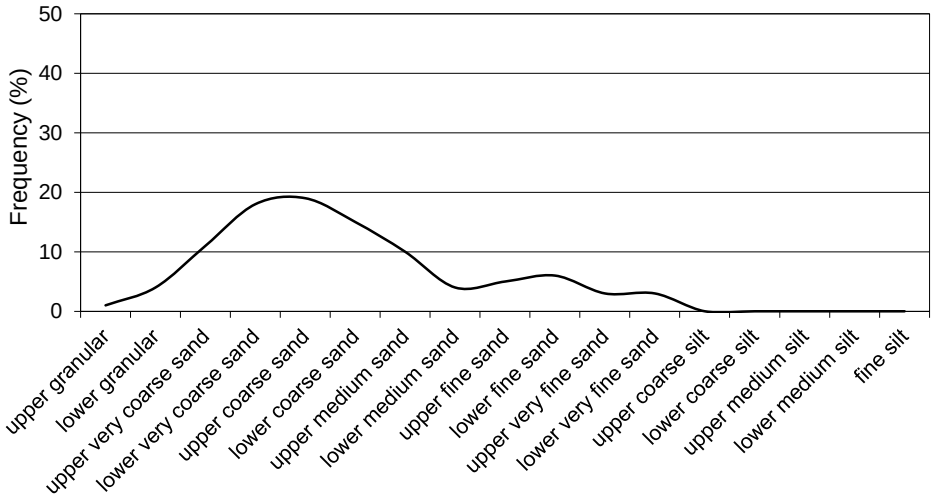

Grainsize variations within the sample

Log: 1
Height: 4.147m
Sample Number: 26
Sandstone name: Sarnoo

Facies: Sb
Architectural Element: Point bar (F5)

Grainsize: Upper very fine sand
Sorting: Moderate to well
Roundness: Rounded
Sandstone classification: Quartzarenite

Detrital Mineralogy: Rigid detrital mineralogy is composed of abundant monocrystalline quartz (40.5%) and polycrystalline quartz (36.5%), sedimentary rigid rock fragments (0.5%) and heavy minerals (trace). The monocrystalline grains are weakly-strained. The polycrystalline quartz has concave-convex contacts. Muscovite mica booklets have been expanded into primary porosity. Sedimentary fragments are composed of chert. Heavy minerals comprise tourmaline. Optically non-resolvable clay (8%) constitutes pseudomatrix (5.5%) and detrital pore-filling clays (2.5%) which coat rigid grains. It is probably composed of illite and calcite. The thin section has an alignment as the grains are slightly elongated.

Authigenic Mineralogy: The authigenic mineralogy is composed of cements and clay. The cements include: quartz overgrowths (3%), haematite (1.5%), non-ferroan dolomite (1%). Authigenic clays are: kaolinite (1%). Syntaxial quartz overgrowths are thin (1-2µm) and discontinuous around the monocrystalline quartz host grains. The haematite partially replaces the detrital quartz grains. The non-ferroan dolomite occludes pore space. Kaolinite clays are patchy within the primary pore space.

Reservoir Quality: The macroporosity is low (7%) and comprises only primary intergranular porosity, which is poorly interconnected.

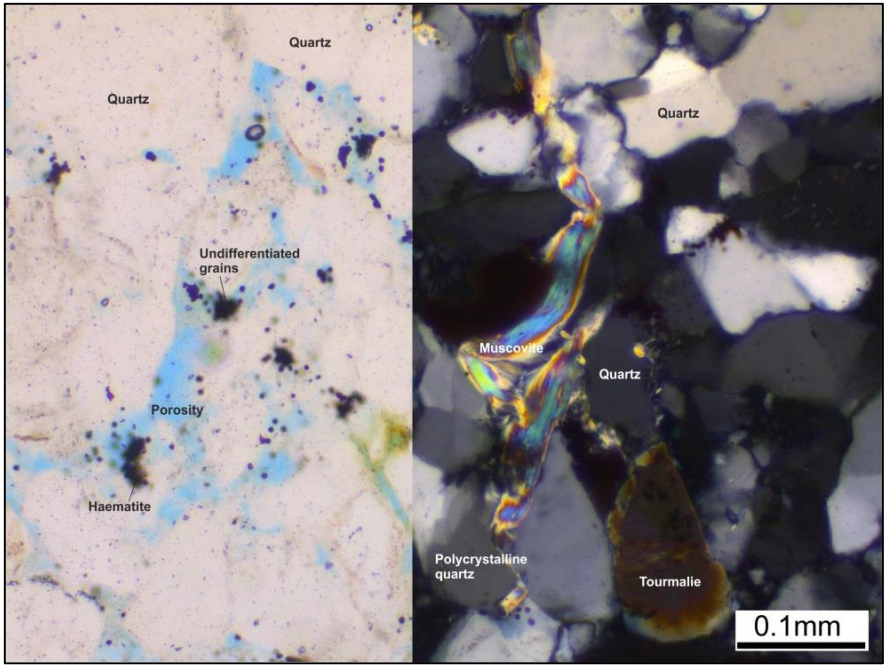

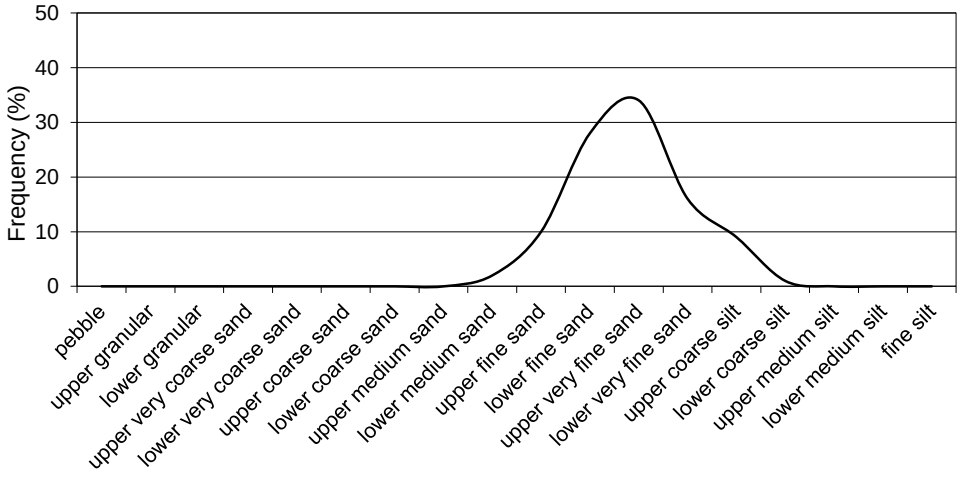

Grainsize variations within the sample

Log: 1
Height: 4.172m
Sample Number: 27
Sandstone name: Sarnoo

Facies: G
Architectural Element: Point bar (F5)

Grainsize: Lower fine sand
Sorting: Moderate to well
Roundness: Rounded to Sub-rounded
Sandstone classification: Quartzarenite

Detrital Mineralogy: The main components of the rigid detrital mineralogy is monocrystalline quartz (45%) and polycrystalline quartz (38.5%), with minor components of rigid rock fragments (2.5%: sedimentary – 1.5%, metamorphic – 0.5%, igneous – 0.5%) and zircon (trace). A few of the monocrystalline quartz grains are weakly-strained. Polycrystalline quartz has concave-convex contacts. Sedimentary fragments are formed of chert. Metamorphic fragments are formed from polycrystalline grains with a weak schistose fabric. Igneous fragments are formed from quartz and muscovite mica and are inter-grown. Trace muscovite occurs as thin elongated grains which vary in length. Optically non-resolvable clays (5%) are formed from pseudomatrix (3%) and detrital pore-filling clays (2%). The non-resolvable clays are likely to be formed from illite.

Authigenic Mineralogy: The authigenic mineralogy is composed of cements, including: quartz overgrowths (1%), dolomite cement (1%) and haematite (trace). Syntaxial quartz overgrowths are discontinuous and thin (1-4µm) around the quartz host grain. The dolomite exhibits first order birefringence and is replacing the quartz or is in-filling the pore spaces. There are no authigenic clays within this sample.

Reservoir Quality: The macroporosity is low (7%) and consists of primary intergranular porosity. The porosity is isolated.

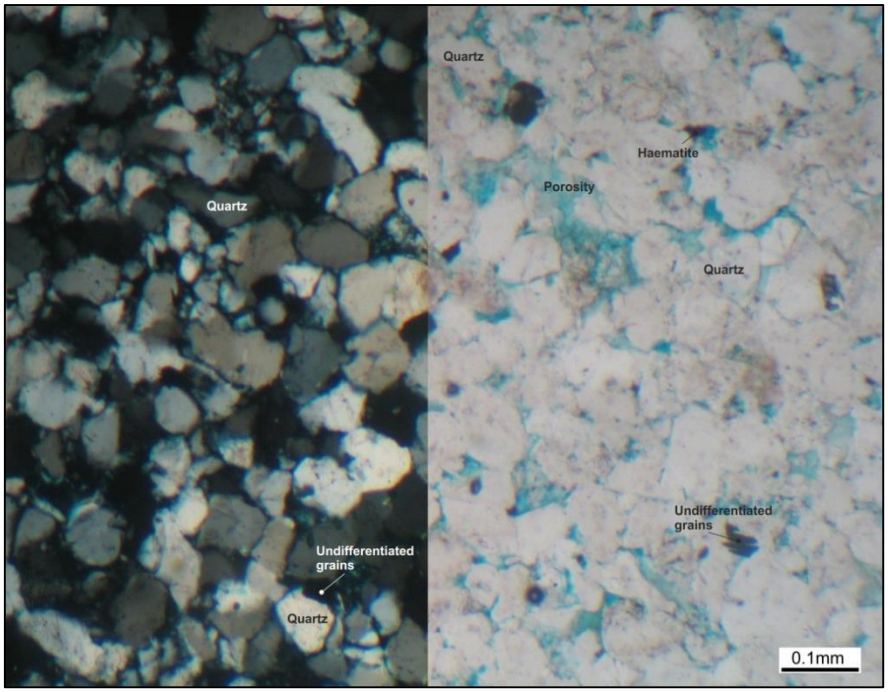

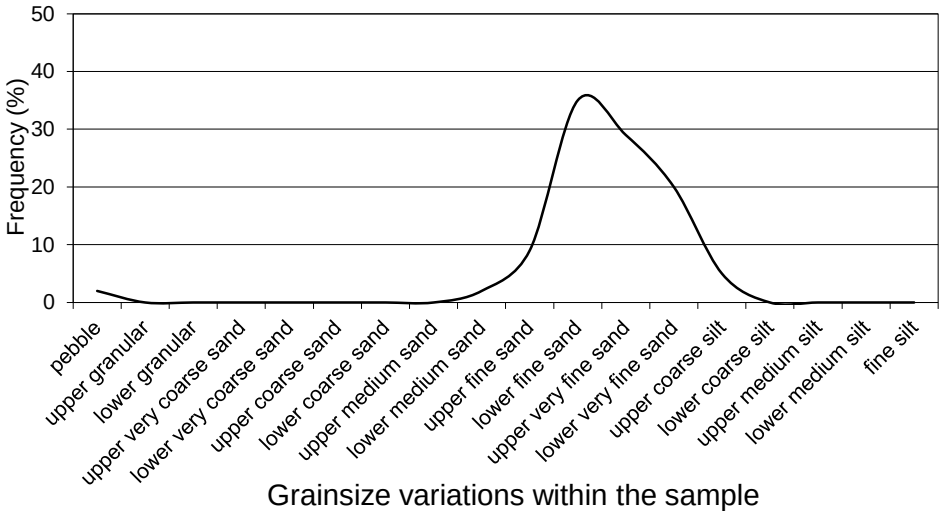

Grainsize variations within the sample

Log: 1
Height: 4.197m
Sample Number: 28
Sandstone name: Sarnoo

Facies: M
Architectural Element: Channel (F1)

Grainsize: Lower fine sand
Sorting: Moderate well
Roundness: Rounded - Sub-rounded
Sandstone classification: Quartzarenite

Detrital Mineralogy: Rigid grains comprise subequal amounts of monocrystalline quartz and polycrystalline quartz (41%), rigid rock fragments (3%: sedimentary – 1.5%, metamorphic 1%, igneous – 0.5%) and heavy minerals (trace). Monocrystalline quartz is moderately-strained. The polycrystalline quartz grains have concave-convex contacts. The sedimentary fragments comprise chert. Metamorphic fragments consist of fragmented, sutured quartz, with a schistose fabric. Igneous fragments contain quartz and muscovite, with rutile inclusions. Optically non-resolvable clays (0.5%) consists of pseudomatrix which coats monocrystalline quartz grains. It is likely that the matrix is composed of illite.

Authigenic Mineralogy: The authigenic mineralogy comprises of cements and clays. The cements include: quartz overgrowths (0.5%), ferroan dolomite (trace) and anatase (trace). Syntaxial quartz overgrowths are discontinuous and thin (1µm) around their host quartz grains. The ferroan dolomite corrodes quartz grains. Cubic anatase occurs as mineral inclusions within the quartz. Kaolinite booklets are choking the pores spaces.

Reservoir Quality: The macroporosity is moderate (14%), formed of primary intergranular porosity. The porosity is poorly interconnected.

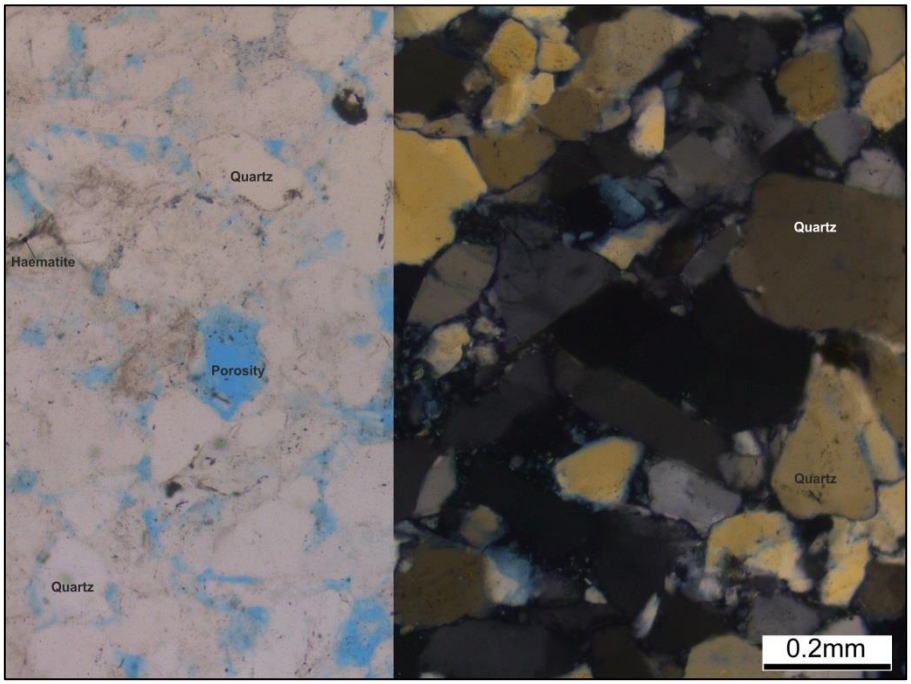

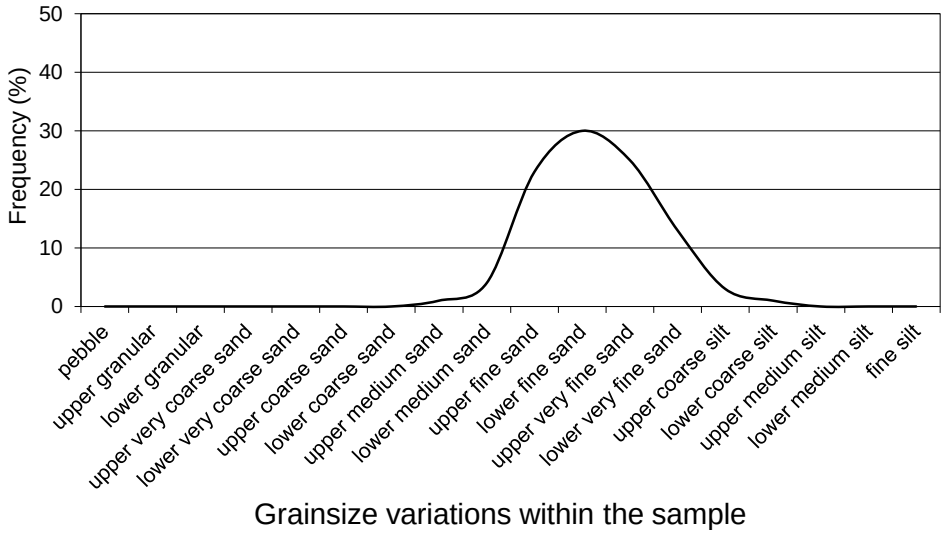

Grainsize variations within the sample

Log: 1
Height: 4.492m
Sample Number: 32
Sandstone name: Sarnoo

Facies: Sxm
Architectural Element: Channel (F1)

Grainsize: Upper medium sand
Sorting: Well
Roundness: Sub-rounded - sub-angular
Sandstone classification: Quartzarenite

Detrital Mineralogy: The rigid detrital mineralogy comprises abundant monocrystalline quartz (58.5%), polycrystalline quartz (22%), sedimentary rigid rock fragments (0.5%) and heavy minerals (trace). Monocrystalline quartz are strained. The contacts between the grains are concave-convex. Ductile muscovite mica (2%) grains are elongated and thin (1-2µm) and some grains occur within the quartz grains and others have expanded into the pore space. The heavy minerals are tourmaline and rutile. Sedimentary fragments are chert. The sample has a slight schistose fabric. Optically non-resolvable clays (2.%) and composed of pseudomatrix (2%) and detrital pore-filling clays (0.5%). Clays locally coat the grains and infill porosity. It is likely that the non-resolvable clays are composed of gibbsite.

Authigenic Mineralogy: Authigenic mineralogy comprises cements which include: haematite (1%) and anatase (trace). Haematite occurs in sporadic layers thoughout, which are aligned. The cubic anatase crystals are associated quartz. There are no authigenic clays.

Reservoir Quality: Primary intergranular porosity is the only constituent of the macroporosity and is of a moderate volume (14%), of which approximately half of the porosity is interconnected.

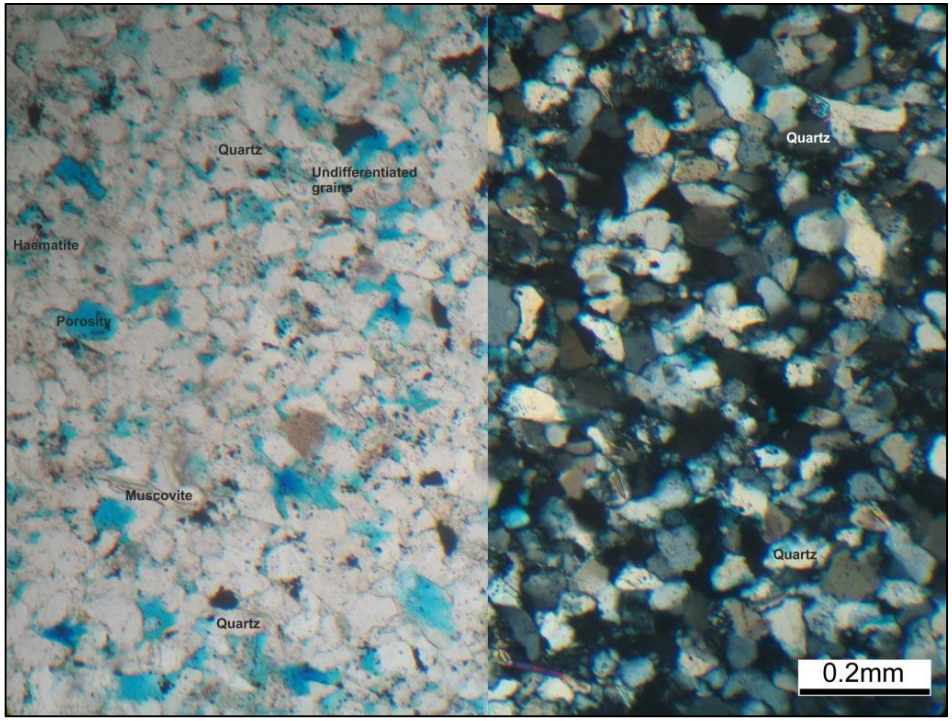

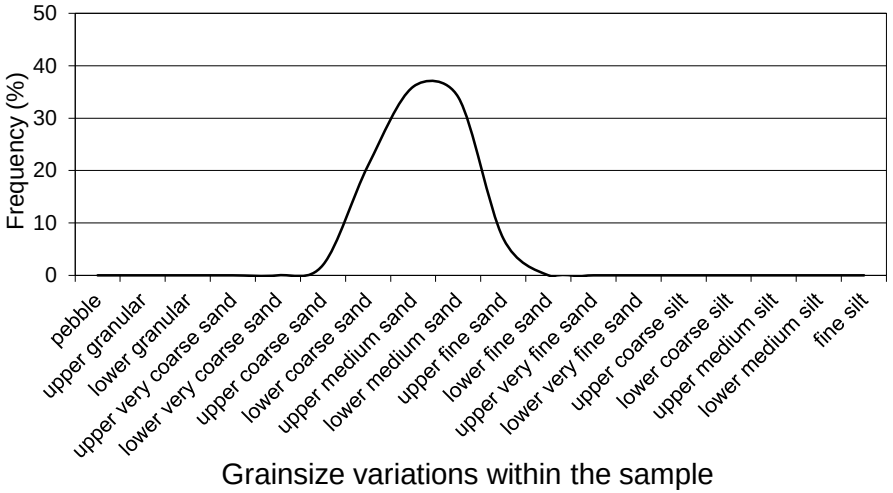

Grainsize variations within the sample

Log: 1
Height: 41.97m
Sample Number: 34
Sandstone name: Sarnoo

Facies: Sxm
Architectural Element: Channel (F1)

Grainsize: Lower fine sand
Sorting: Moderate well
Roundness: Sub-rounded
Sandstone classification: Quartzarenite

Detrital Mineralogy: Detrital mineralogy constitutes abundant monocrystalline quartz (44%), polycrystalline quartz (32.5%) and minor constituents of muscovite mica (3%), igneous rigid rock fragments (2.5%), undifferentiated grains (1%) and heavy minerals (trace). The quartz grains are weakly strained. Ductile muscovite micas are pore filling and being locally replaced by kaolinite at its terminations. The igneous fragments are quartz and muscovite grains that are intergrown. Undifferentiated grains are undistinguishable due to being replaced by haematite. The heavy minerals are tourmaline and zircons. Optically non-resolvable clays (4%), composed from detrital pore filling clays (3%) pseudomatrix (0.5%) which are coating the grains within the pores.

Authigenic Mineralogy: Authigenic mineralogy comprises of cements and clays, the cements include: quartz overgrowths (2%), haematite (1.5%) and clays include: kaolinite (trace). Syntaxial quartz overgrowths are discontinuous and thin (2µm) around their monocrystalline quartz host grain.

Reservoir Quality: The macroporosity is low (9.5%), contains the intergranular porosity only, which is not interconnected.

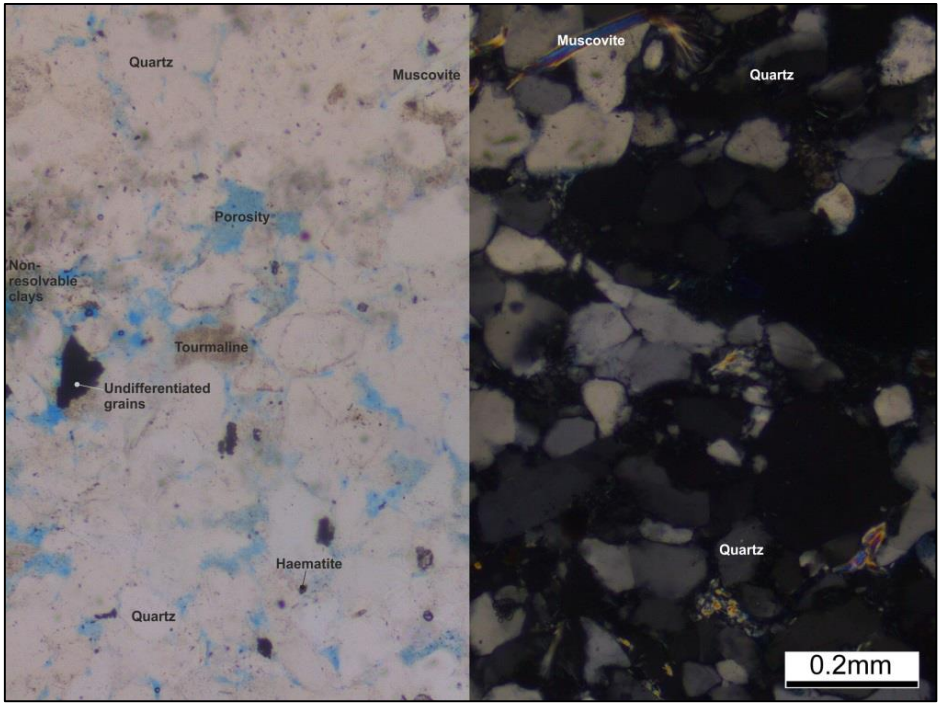

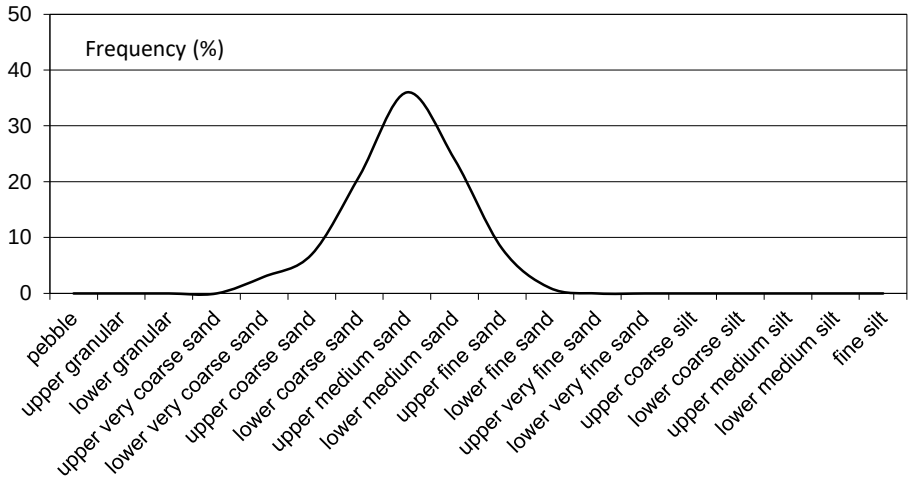

Grainsize variations within the sample

Log: 1
Height: 47.94m
Sample Number: 38
Sandstone name: Sarnoo

Facies: Sbvf
Architectural Element: Sheetflood (F6)

Grainsize: Upper very fine sand
Sorting: Moderate to well
Roundness: Sub-rounded to sub-angular
Sandstone classification: *haematitic* quartzarenite

Detrital Mineralogy: Main components of the detrital mineralogy are the monocrystalline (44.5%), polycrystalline (29%) quartz, the minor components are rigid rock fragments, sedimentary (2%), igneous (1.5%), muscovite mica (1.5%), undifferentiated grains (0.5%) and heavy minerals (trace). The monocrystalline quartz is slightly strained. Sedimentary fragments are composed of chert, whilst igneous fragments are composed of monocrystalline quartz and muscovite grains. Ductile muscovite mica is elongated and thin. Undifferentiated grains are undistinguishable as they are cemented by haematite. Heavy minerals are tourmaline and zircon. The grains are aligned as the sample has a weak schistose fabric. The optically non-resolvable clay (0.5%) is pore-filling and coats the quartz grains.

Authigenic Mineralogy: Authigenic mineralogy composes of cements and clays, the cements are: haematite (8.5%), quartz overgrowths (1%), undifferentiated cement (0.5%); the authigenic clay is kaolinite (0.5%). Haematite cement fills and chokes the pores, and coats the quartz grains. Syntaxial quartz overgrowths are up to 3µm in thickness and discontinuous around their host grains. Undifferentiated cements coat the quartz grains and is likely to be haematite. Kaolinite booklets choke and fill the pores.

Reservoir Quality: The macroporosity is moderate (10%) and consists of the primary intergranular porosity and is interconnected.

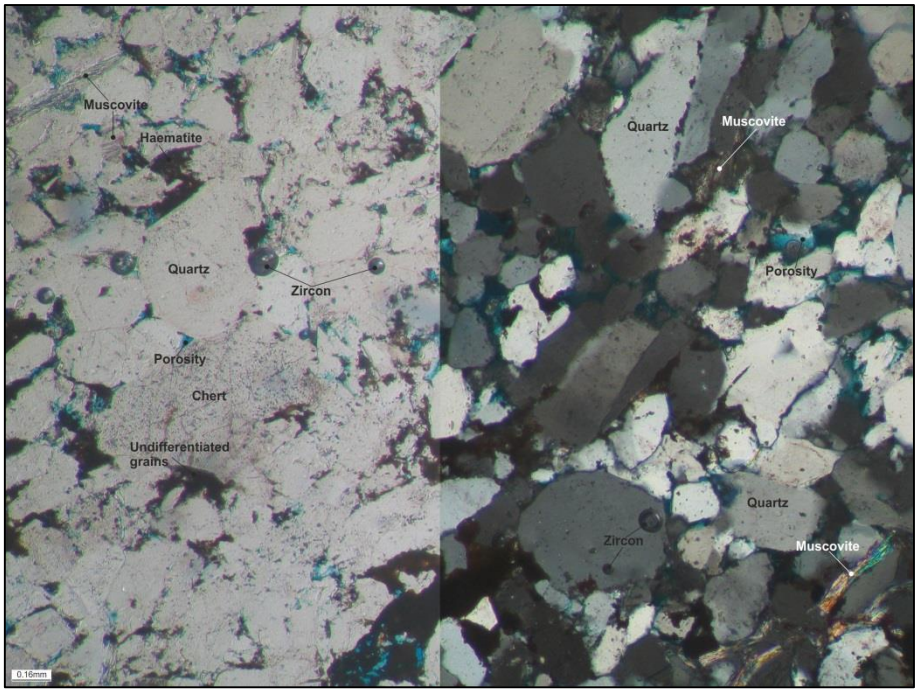

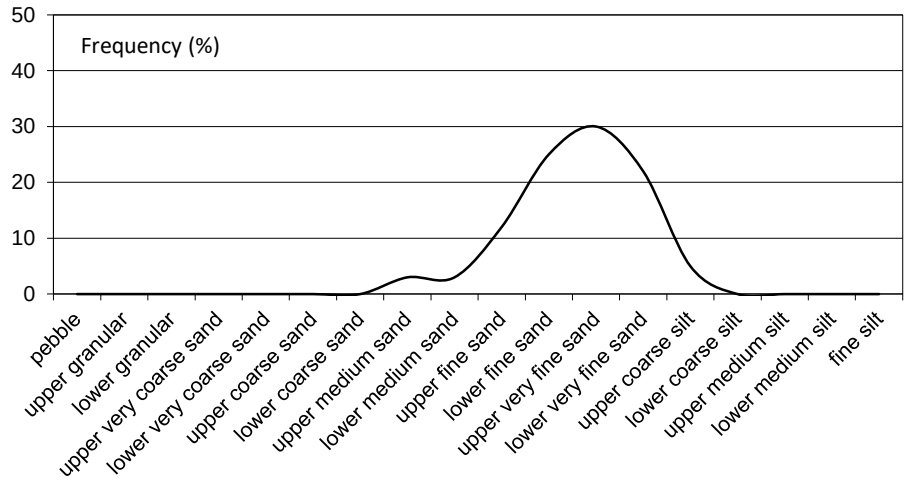

Grainsize variations within the sample

Log: 1
Height: 48.09m
Sample Number: 39
Sandstone name: Sarnoo

Facies: Sbmf
Architectural Element: Sheetflood (F6)

Grainsize: Upper very fine sand
Sorting: Moderate to well
Roundness: Sub-rounded to sub-angular
Sandstone classification: Quartzarenite

Detrital Mineralogy: Detrital mineralogy has abundant monocrystalline quartz (47%) and polycrystalline quartz (24%), the minor detrital grains are muscovite mica (2.5%), heavy minerals (1%) and rigid rock fragments: sedimentary (1%), metamorphic (0.5%), igneous (0.5%). Monocrystalline quartz is unstrained to weakly strained. Ductile muscovite mica grains vary in length and are within the pores spaces. Sediment fragments are formed from chert. Metamorphic fragments contain sutured polycrystalline quartz which has a schistose fabric. Igneous fragments are composed of quartz and muscovite grains which are intergrown. The heavy minerals within the sample are zircon. There is a weak fabric throughout the thin section. Optically non-resolvable clay (2.5%), is composed of detrital pore filling clay (1.5%) and pseudomatrix (1%), which is pore filling.

Authigenic Mineralogy: Authigenic mineralogy is composed of cement and clay the cements include: undifferentiated (6.5%), quartz overgrowths (1.5%) and the clays include: kaolinite (0.5%). Undifferentiated cements is likely to be haematite. Syntaxial quartz overgrowths are discontinuous around their quartz host grains. Kaolinite booklets are pore filling.

Reservoir Quality: The macroporosity is moderate (12.5%) is composed of primary intergranular porosity and the pores are interconnected.

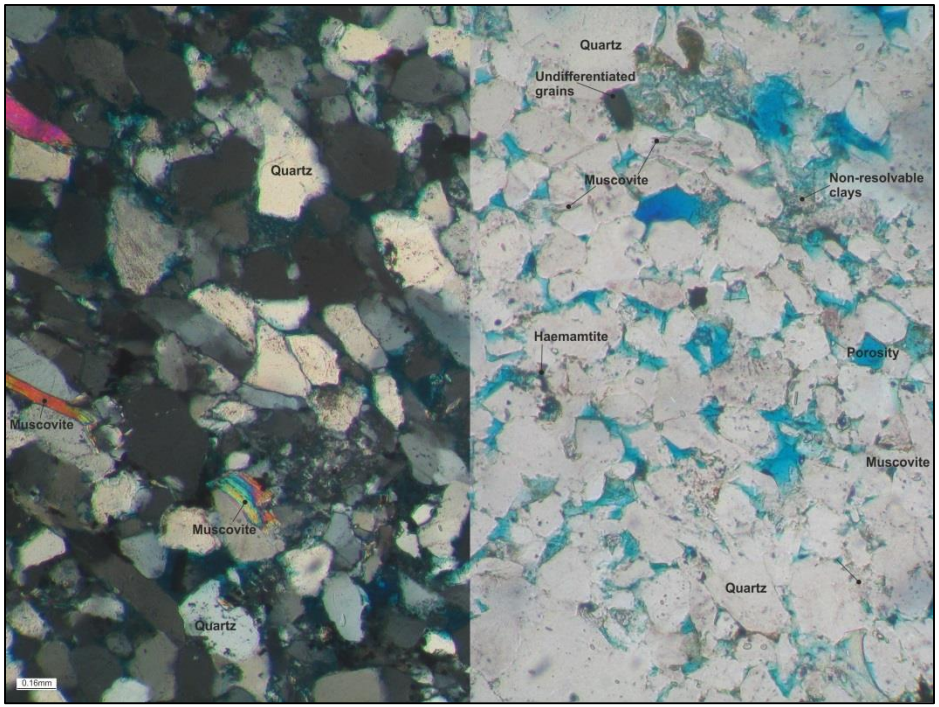

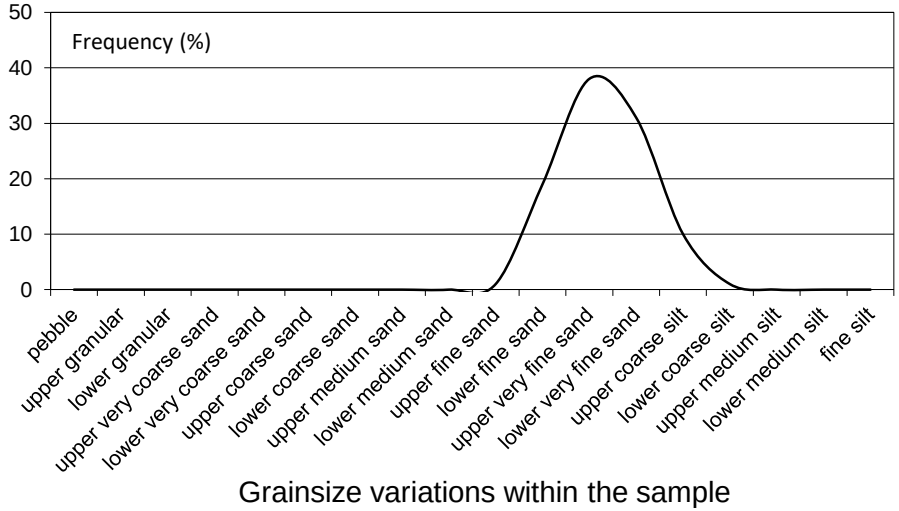

Grainsize variations within the sample

Log: 34
Height: 10.45m
Sample Number: 43
Sandstone name: Nosar

Facies: Shg
Architectural Element: Gravel bar (F3)

Grainsize: Upper very fine sand
Sorting: Moderately to well
Roundness: Sub-rounded to sub-angular
Sandstone classification: Sublithic arenite

Detrital Mineralogy: The abundant detrital grains are monocrystalline quartz (33%) and polycrystalline quartz (30%) grains the minor components to the detrital mineralogy include: sedimentary rigid rock fragments (15%), metamorphic rigid rock fragments (2%) muscovite mica (2%) and heavy minerals (trace). Monocrystalline grains are weakly strained. Sediment fragments are composed of chert, whilst the metamorphic fragments are formed from sutured polycrystalline quartz, with a schistose fabric. Ductile muscovite mica is within the pore spaces. The heavy mineral is tourmaline. Optically non-resolvable clays (10%) are pore filling. The entire sample has a weak alignment.

Authigenic Mineralogy: Authigenic mineralogy contains cements: quartz overgrowths (3%), haematite (2%) and undifferentiated grains (0.5%). Syntaxial quartz overgrowths are discontinuous around the quartz host grains. Haematite cement coats the grains and infills pore spaces. Undifferentiated cements are likely to be haematite.

Reservoir Quality: The macroporosity is very low (2%) is only composed of primary intergranular porosity and is not interconnected.

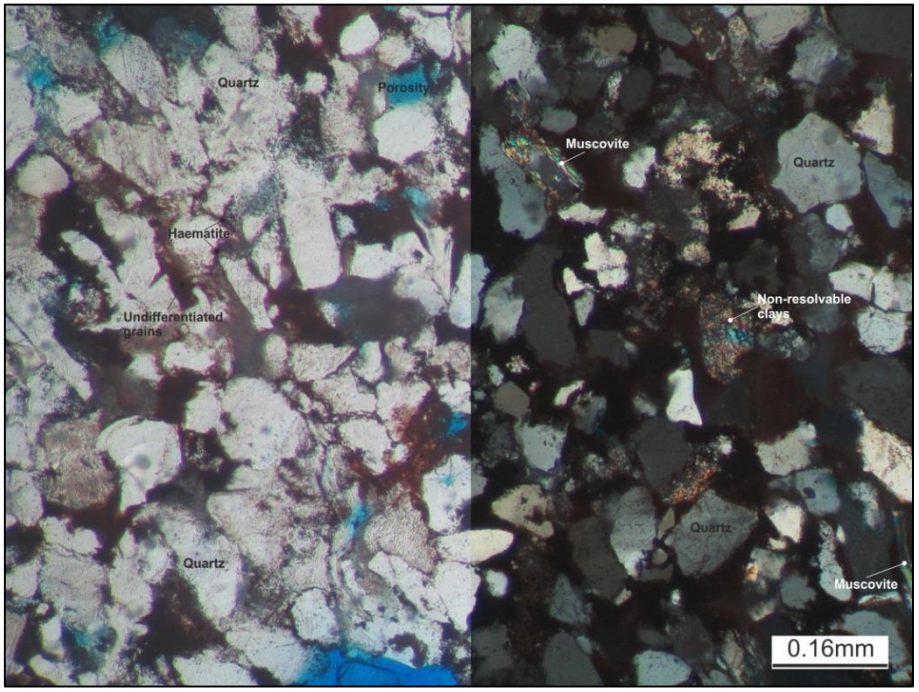

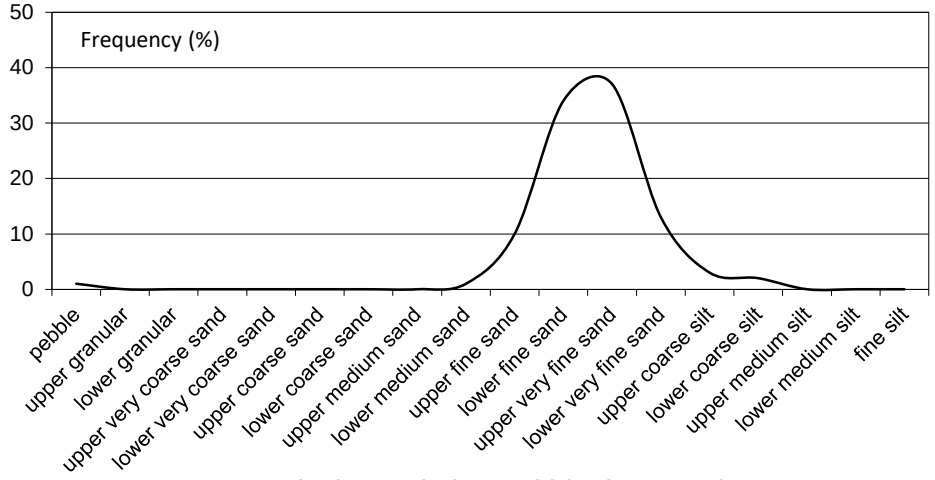

Grainsize variations within the sample

Log: 34
Height: 11.79m
Sample Number: 45
Sandstone name: Nosar

Facies: G
Architectural Element: Gravel bar (F3)

Grainsize: Lower coarse sand
Sorting: Moderate
Roundness:
Sandstone classification: Quartzarenite

Detrital Mineralogy: Detrital mineralogy contains abundant monocrystalline quartz (42%) and polycrystalline quartz (41.5%), with significant amounts of metamorphic rigid rock fragments (7%), minor constitutes igneous rigid rock fragments (1%), undifferentiated grains (trace) and heavy minerals (trace). Monocrystalline quartz is slightly strained and others have rutile inclusions. Some of the quartz grains are embayed due to corrosion. Metamorphic fragments have a schistose fabric. Igneous fragments Undifferentiated grains are undistinguishable and they have being replaced by haematite. The heavy minerals are composed from tourmaline and rutile. Optically non-resolvable clays (4%) is composed from detrital pore-filling clays (4%). The clays fills the pores and coats a few of the quartz grains.

Authigenic Mineralogy: Authigenic mineralogy is composed of cements and clays, cements include: quartz overgrowths (2%), and undifferentiated cement (0.5%), ferroan calcite (trace), haematite (trace), anatase (trace); clays include: kaolinite (0.5%) . Syntaxial quartz overgrowths are thin (3µm) and discontinuous around their quartz host grains. Undifferentiated cements are undistinguishable but likely to be haematite due to the red colour, the cement coats the detrital grains. The ferroan calcite is within the pore spaces. The haematite coats the detrital grains. Cubic anatase crystals are within the quartz grains.

Reservoir Quality: The macroporosity is low (2.5%), is composed of primary intergranular porosity.

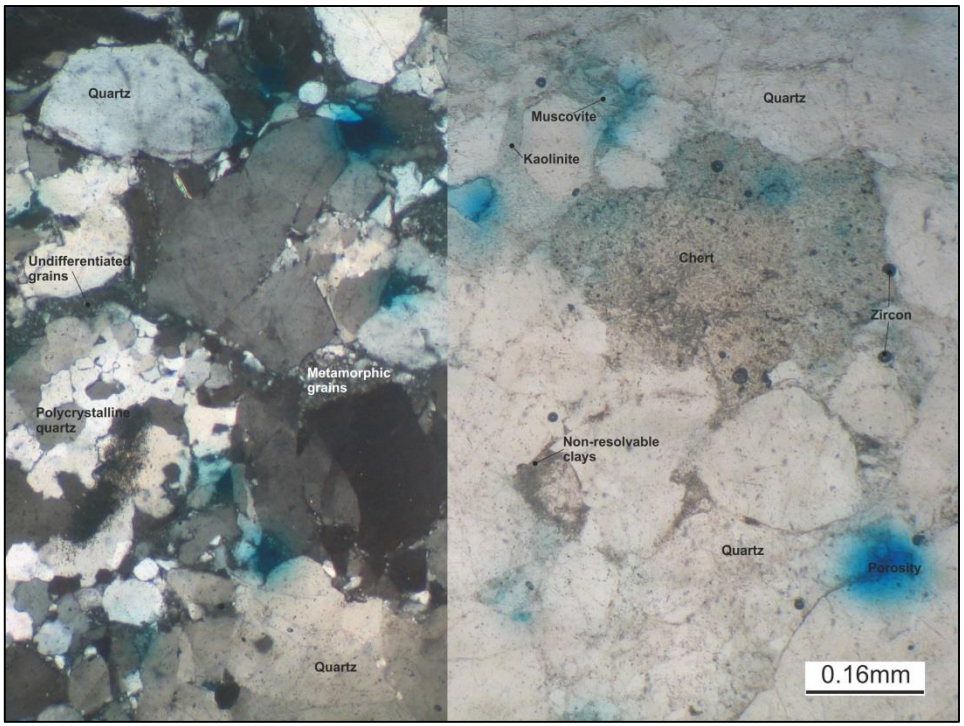

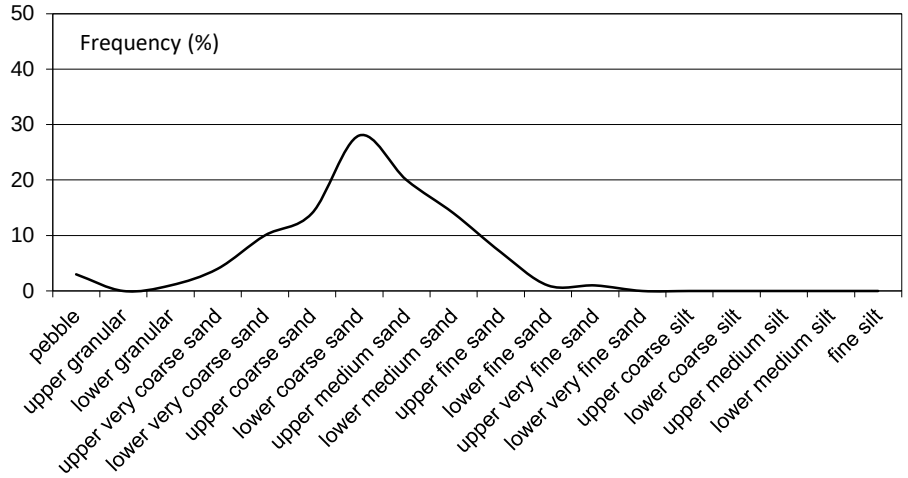

Grainsize variations within the sample

Log: 43
Height: 12.50m
Sample Number: 47
Sandstone name: Nosar

Facies: Sxm
Architectural Element: Channel (F1)

Grainsize: Lower medium sand
Sorting: Well
Roundness:
Sandstone classification: sublithic arenite

Detrital Mineralogy: Detrital mineralogy contains abundant polycrystalline quartz (48%) and monocrystalline quartz (38%) with minor sedimentary rigid rock fragments (2%), metamorphic rigid rock fragments (1%), heavy minerals (0.5%) and trace muscovite. The grains are not strained. Sedimentary fragments are composed from chert. Metamorphic fragments are formed from sutured polycrystalline quartz, containing a schistose fabric. The heavy minerals within are rutile and tourmaline. Rutile grains are inclusions within the monocrystalline grains. Ductile muscovite mica chokes the pores. Optically non-resolvable clays (2.5%) are pore-filling clays.

Authigenic Mineralogy: Authigenic cements are: quartz overgrowths (1%), anatase (trace) and the authigenic clays are kaolinite (0.5%). Syntaxial quartz overgrowths are discontinuous around their host monocrystalline quartz grains. Anatase crystals are within the monocrystalline crystals. Kaolinite booklets are choking the porosity.

Reservoir Quality: Macroporosity is low (6.5%) and composed from the primary intergranular porosity (6%) and secondary oversized porosity (0.5%), approximately 25% of the porosity is interconnected.

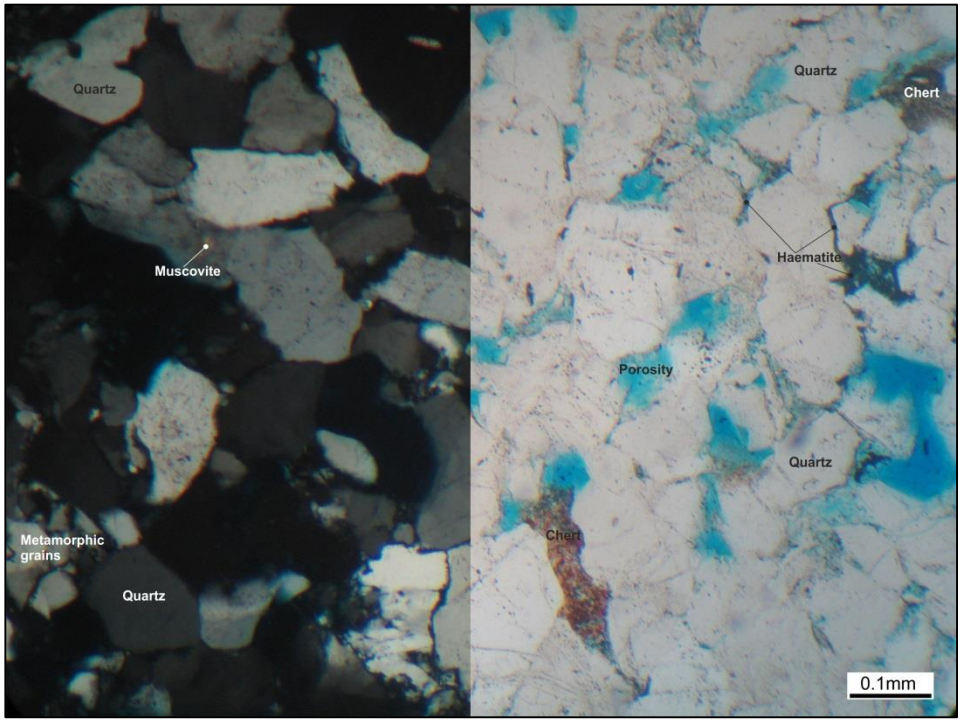

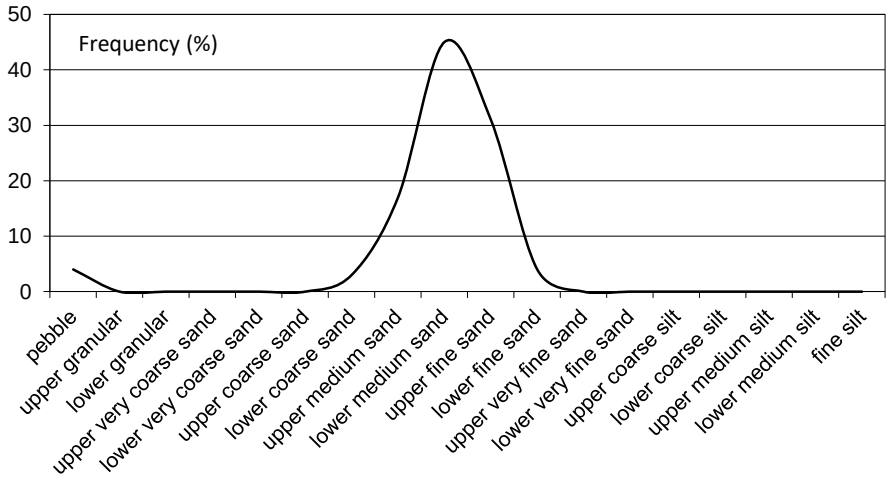

Grainsize variations within the sample

Log: 34
Height: 14.34m
Sample Number: 50
Sandstone name: Nosar

Facies: Sxm
Architectural Element: Channel (F1)

Grainsize: Upper medium sand
Sorting: Moderate to well
Roundness: Sub-rounded to sub-angular
Sandstone classification: Quartzarenite

Detrital Mineralogy: Detrital mineralogy is composed of abundant monocrystalline quartz (43%), polycrystalline quartz (41%) and minor detrital grains are composed of rigid rock fragments: metamorphic (5%), sedimentary (1%) and igneous (0.5%) and heavy minerals (trace). Monocrystalline quartz is unstrained to slightly strained. Metamorphic grains are sutured quartz fragments, which have a schistose texture. Sedimentary fragments are made from chert, whilst igneous fragments are formed from quartz and muscovite grains. Heavy minerals are zircon and rutile; rutile grains are more common within the haematite cemented areas. Optically non-resolvable clay (6%) is pore filling.

Authigenic Mineralogy: Authigenic cements are: haematite (trace) and authigenic clays are kaolinite (0.5%). Haematite has coated the quartz grains. Kaolinite is choking the pores and forming around the edges quartz grains.

Reservoir Quality: Macroporosity is low (3%) contains primary intergranular porosity. The porosity is approximately 25-30% interconnected.

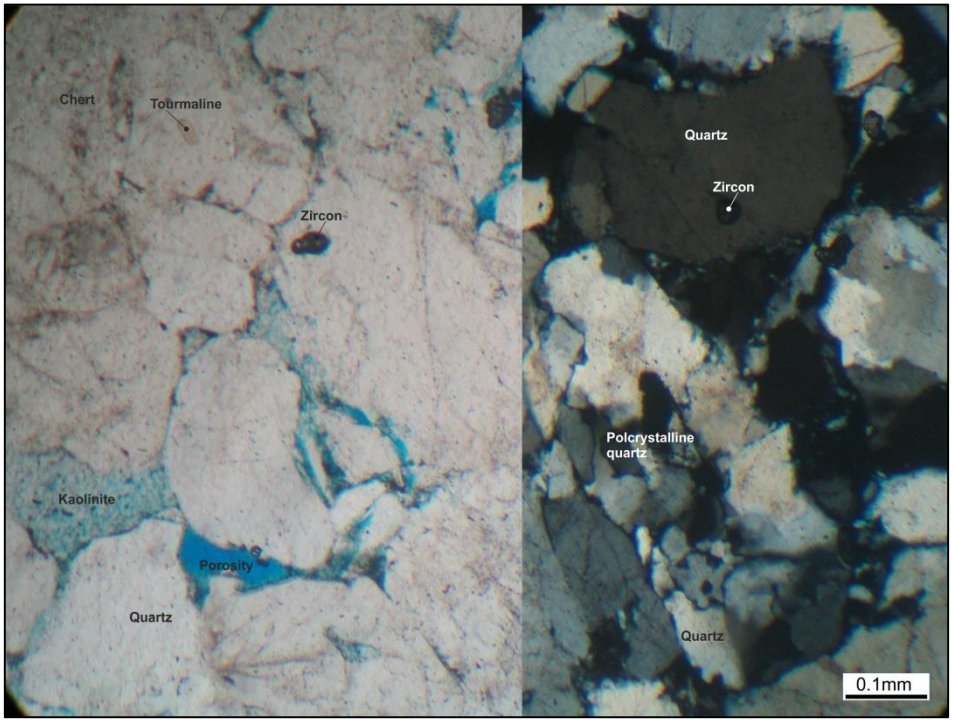

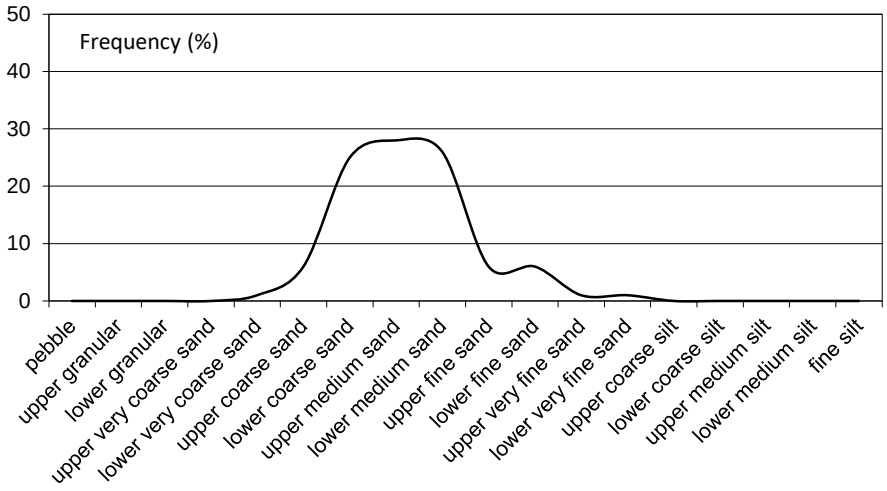

Grainsize variations within the sample

Log: 34
Height: 18.32m
Sample Number: 54
Sandstone name: Nosar

Facies: Sxm
Architectural Element: Gravel bar (F3)

Grainsize: Lower coarse sand
Sorting: Poorly
Roundness: Sub-rounded to sub-angular
Sandstone classification: Quartzarenite

Detrital Mineralogy: Detrital minerals are: monocrystalline (47%), polycrystalline (38%), metamorphic rigid rock fragments (3.5%), igneous rigid rock fragments (1%), heavy minerals (0.5%) and undifferentiated non-resolvable clay (0.5%). The monocrystalline quartz is strained as there is an undulose extinction. The metamorphic fragments contain sutured and elongated polycrystalline quartz. The igneous fragments are monocrystalline quartz with muscovite mica inclusions. The heavy minerals include rutile and tourmaline. The non-resolvable clay coats the quartz grains. There is a slight alignment to the grains within the sample.

Authigenic Mineralogy: Authigenic minerals are composed cements and clays, cements include: quartz overgrowths (1%) and ferroan calcite (trace); clays include kaolinite (2%) . Syntaxial quartz overgrowths are thin (2µm) and discontinuous around their host grains. Ferroan calcite fills the fractures within the quartz grains and is pore filling. Kaolinite is pore filling.

Reservoir Quality: Macroporosity is moderate (6.5%) and contains primary intergranular porosity (4.5%), secondary oversized porosity (1.5%) and secondary intragranular porosity (0.5%). The porosity is not interconnected.

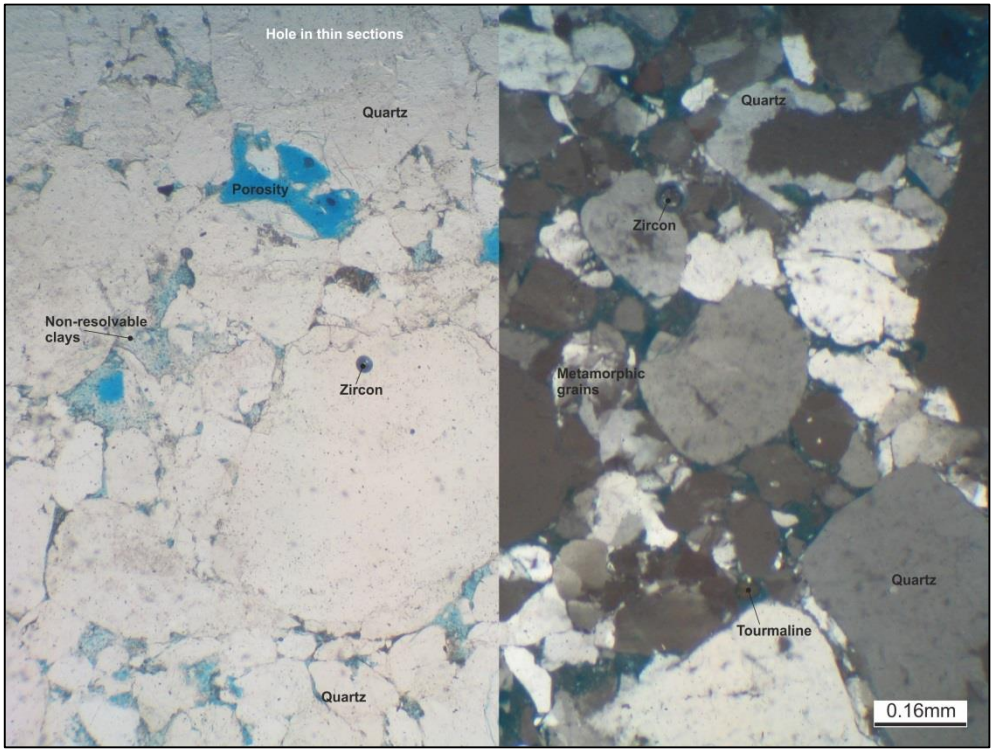

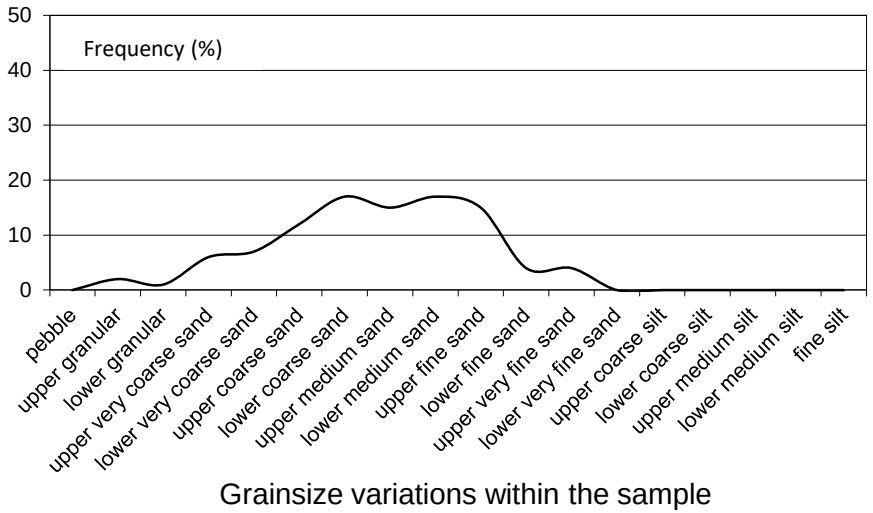

Grainsize variations within the sample

Log: 34
Height: 19.14m
Sample Number: 56
Sandstone name: Nosar

Facies: G
Architectural Element: Gravel bar (F3)

Grainsize: Lower medium sand
Sorting: Moderately
Roundness: Sub-rounded
Sandstone classification: Quartzarenite

Detrital Mineralogy: Detrital mineralogy contains abundant monocrystalline quartz (45%), polycrystalline quartz (42.5%) and minor constituents contain rigid rock fragments sedimentary (1.5%), metamorphic (0.5%) and sedimentary ductile rock fragments (0.5%). Coarser monocrystalline quartz are strained whereas the finer monocrystalline quartz are unstrained. Rigid sedimentary fragments are made from chert, whilst metamorphic fragments contain sutured slightly elongated quartz, a schistose fabric. Ductile sedimentary grains are formed from muscovite mica and are within the pore spaces. Optically non-resolvable clays (3%) are infilling the pores and coating the quartz grains.

Authigenic Mineralogy: Authigenic mineralogy contains authigenic cements and clays. The cements are: quartz overgrowths (0.5%) ferron calcite (trace) and haematite (trace) and the authigenic clays are kaolinite (1.5%). Syntaxial quartz overgrowths are thin (4µm) and discontinuous around the host quartz grains. Ferroan calcite has formed in the fractures of the quartz in the pores in-between the grains. Haematite cements forms around the quartz grains. Kaolinite booklets are pore filling.

Reservoir Quality: Macroporosity is low (5%) and contains primary intergranular porosity only, which is 30% interconnected.

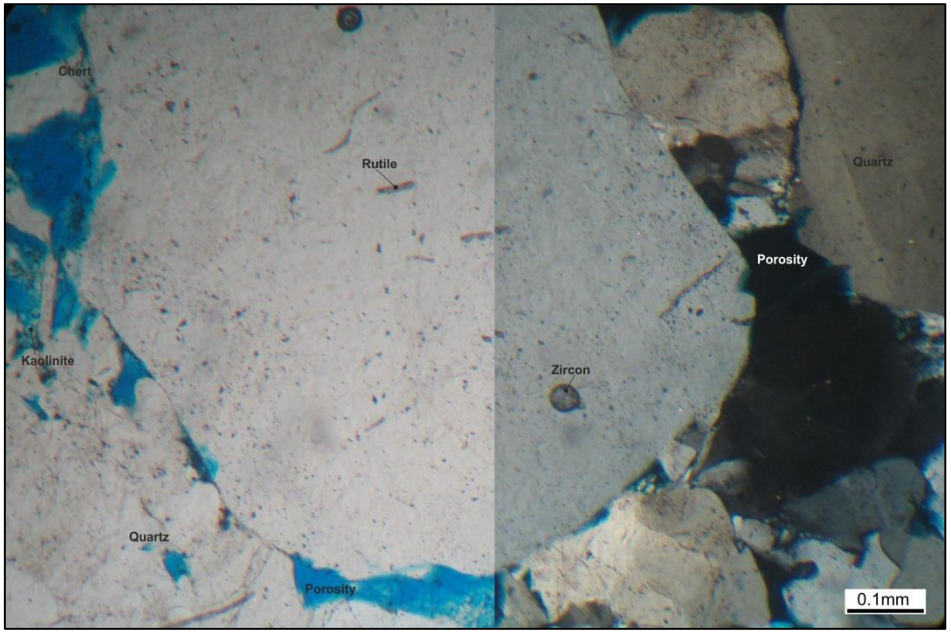

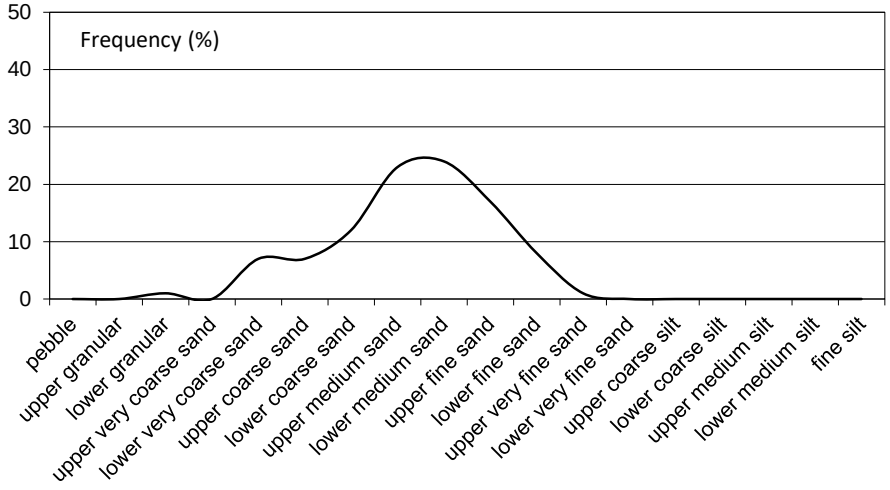

Grainsize variations within the sample

Log: 34
Height: 22.82m
Sample Number: 60
Sandstone name: Nosar

Facies: Sxm
Architectural Element:

Grainsize: Lower fine sand
Sorting: Moderately to well
Roundness: Sub-rounded to sub-angular
Sandstone classification: Quartzarenite

Detrital Mineralogy: Detrital mineralogy contains abundant monocrystalline quartz (48%), polycrystalline quartz (41.5%) and minor igneous rigid rock fragments (1%), ductile sedimentary rock fragments (0.5%) muscovite mica (0.5%) and heavy minerals (trace). Monocrystalline quartz is slightly strained. Igneous fragments contains quartz and muscovite mica intergrown. Ductile sedimentary grains are muscovite mica grains 5µm wide. Heavy minerals include tourmaline. The grains within the sample are partially aligned, has a schistose fabric. Optically non-resolvable clays (2%) are pore-filing and grain coating in places.

Authigenic Mineralogy: Authigenic mineralogy contains cements and clays, cements include: quartz overgrowths (0.5%) and trace calcite and haematite cements and clays include kaolinite (4.5%). Syntaxial quartz overgrowths are thin (2-3µm) and discontinuous around their host quartz grains. Calcite cements are within fractures. Haematite coats the some of the quartz grains. Kaolinite booklets are pore-filling.

Reservoir Quality: The macroporosity (1.5%)is primary intergranular porosity only. The porosity is not connected.

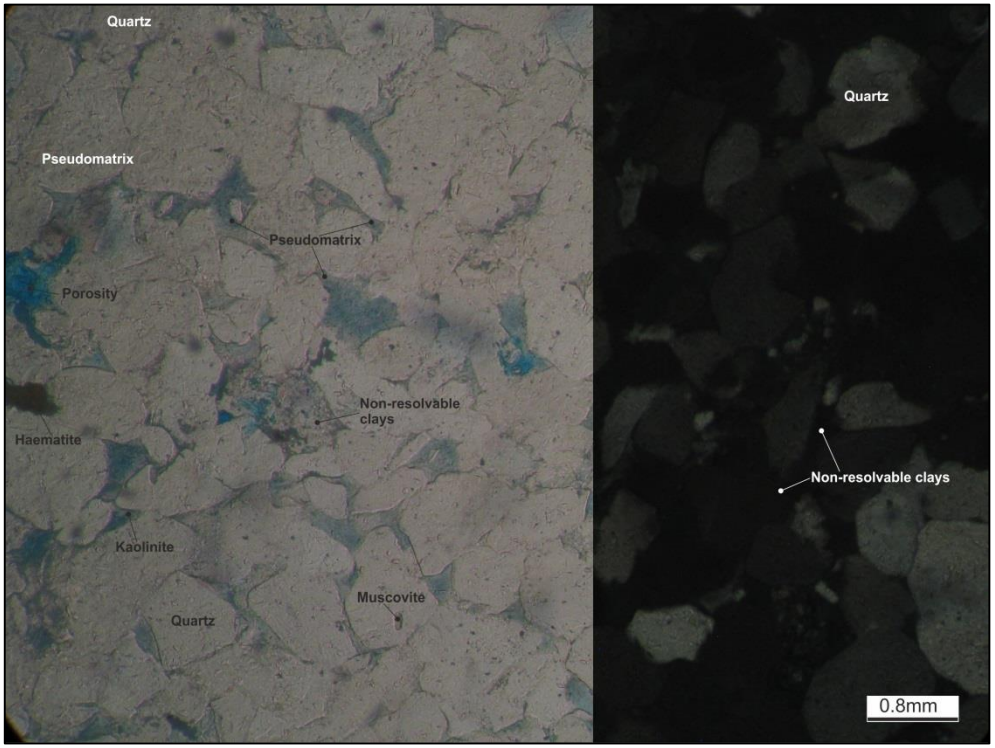

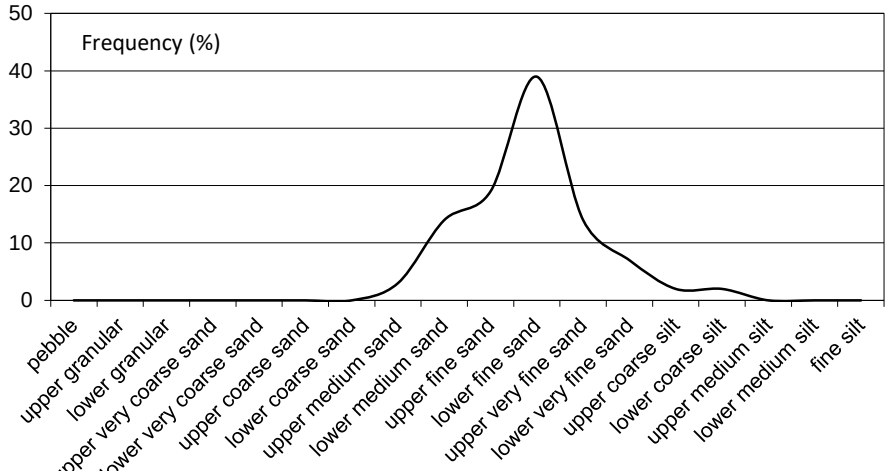

Grainsize variations within the sample

Log: 34
Height: 35.58m
Sample Number: 68
Sandstone name: Nosar

Facies: Smm
Architectural Element: Sheetflood (F6)

Grainsize: Upper medium sand
Sorting: Moderately to well
Roundness: Sub-rounded
Sandstone classification: Quartzarenite

Detrital Mineralogy: The detrital mineralogy contains monocrystalline quartz (47.5%), polycrystalline quartz (38.5%), detrital pore-filling non-resolvable clay (3%), sedimentary rigid rock fragments (1.5%) and igneous rigid rock fragments (1%) and traces of heavy minerals. The monocrystalline quartz is strained as they display an undulose extinction. A few of the monocrystalline quartz grains have been corroded. The sedimentary rock fragments are formed from chert. The igneous fragments are formed from quartz with intergrown muscovite. The heavy minerals are composed of rutile.

Authigenic Mineralogy: The authigenic mineralogy contains quartz overgrowths (1.5%) and kaolinite (1%). The syntiaxal quartz overgrowths are discontinuous The kaolinite is pore filling and chokes the pores.

Reservoir Quality: The macroporosity (6%) contains primary intergranular porosity. The pores are approximately 40% interconnected.

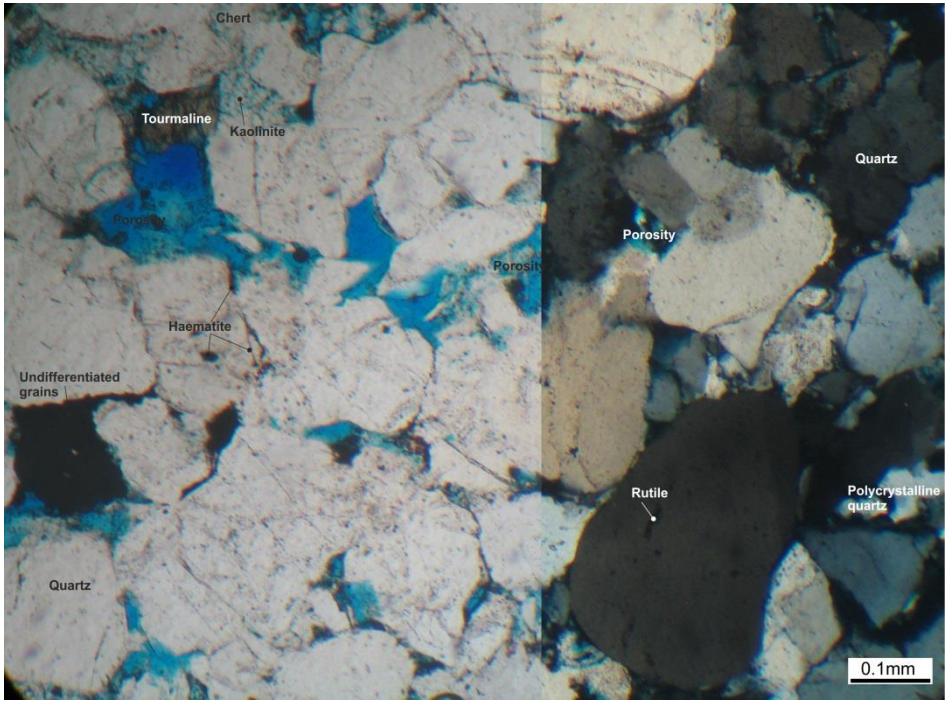

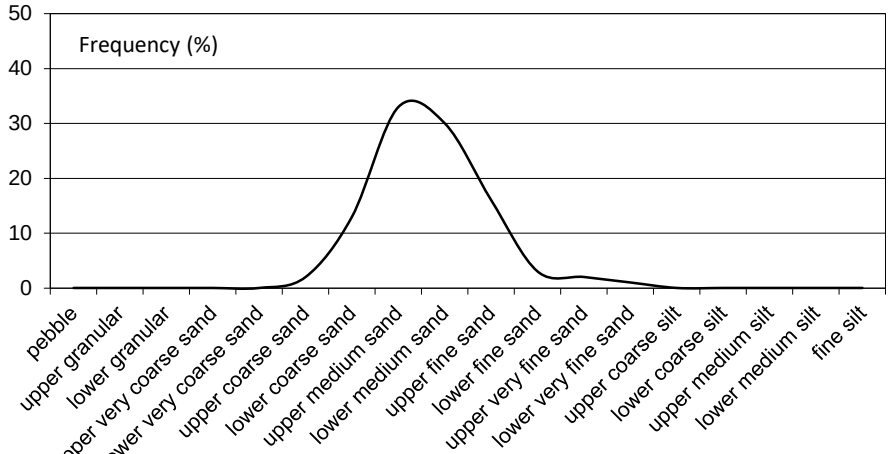

Grainsize variations within the sample

Log: 34
Height: 37.58m
Sample Number: 71
Sandstone name: Nosar

Facies: Sb
Architectural Element: Sheetflood (F6)

Grainsize: Lower coarse sand
Sorting: Moderately to well
Roundness: Rouned to Sub-rounded
Sandstone classification: Quartzarenite

Detrital Mineralogy: Detrital mineralogy has abundant polycrystalline quartz (45%), monocrystalline quartz (41%) and minor grains include rigid rock fragments sedimentary (3%), igneous (0.5%) and heavy minerals (trace). Approximately 30% of the monocrystalline quartz is strained. Sedimentary fragments are formed from chert, whilst igneous fragments are composed of unstrained monocrystalline quartz with muscovite inclusions. Heavy minerals include zircon and tourmaline. Optically non-resolvable clays (1.5%) are within the pore spaces.

Authigenic Mineralogy: Authigenic cements are quartz overgrowths (1%), non-ferroan dolomite (0.5%) haematite (0.5%) and the authigenic clays are kaolinite (trace). Syntaxial quartz overgrowths are thin (3µm) and discontinuous around their host grain. Non-ferroan dolomite cements are within the pore spaces and haematite cement coats the grains.

Reservoir Quality: Macroporosity is low (7%) is only composed of the primary intergranular porosity. The pores are not interconnected.

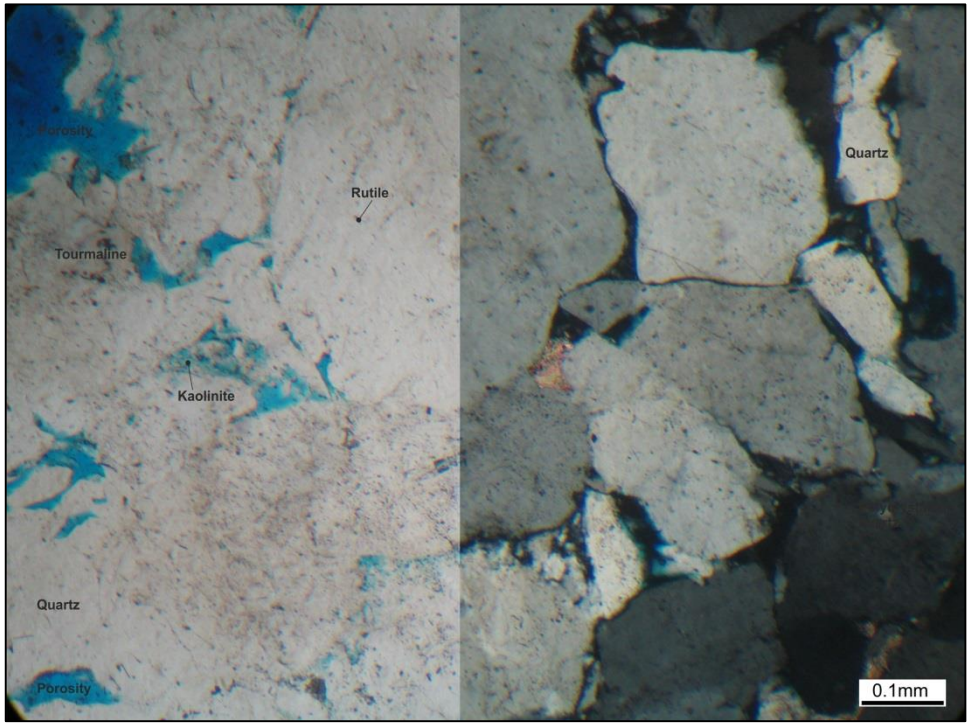

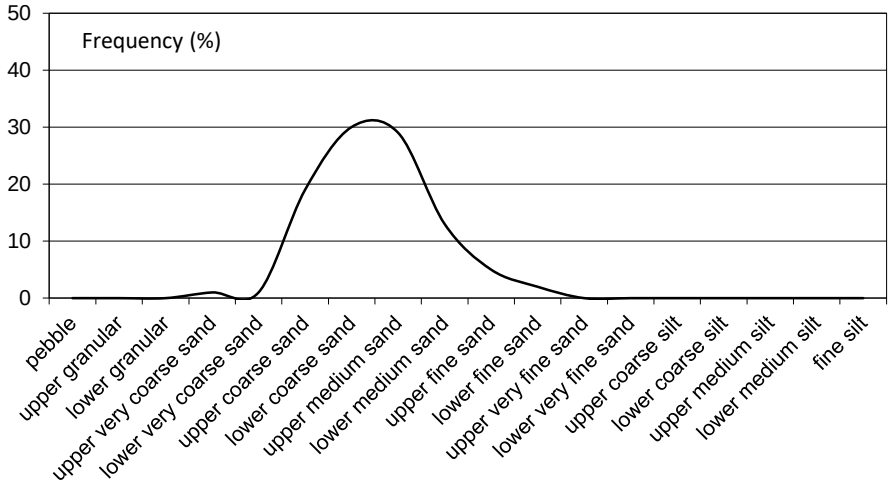

Grainsize variations within the sample

Log: 55
Height: 1.00m
Sample Number: 72
Sandstone name: Darjaniyon-ki Dhani

Facies: Sx
Architectural Element: Gravel Bar (F3)

Grainsize: Lower medium sand
Sorting: Well
Roundness: Sub-rounded to sub-angular
Sandstone classification: Quartzarenite

Detrital Mineralogy: Detrital mineralogy has abundant monocrystalline quartz (49%), polycrystalline quartz (10%) with subordinate rigid rock fragments sedimentary (2%), metamorphic (0.5%) and heavy minerals (0.5%). Heavily broken monocrystalline quartz is slightly strained (25% of the quartz grains). Sedimentary grains are made from chert. Metamorphic fragments are formed from quartz with muscovite and chlorite, which are sutured and have a schistose fabric. The heavy minerals are rutile (which are inclusions in the quartz). Optically non-resolvable clays (15%) are pore-filling and coat 10% of the quartz grains.

Authigenic Mineralogy: Authigenic mineralogy contains cements and clays, cements include: ferroan calcite (3%), haematite (3%), undifferentiated (1%), quartz overgrowths (1%) and non-ferroan dolomite (0.5%). Calcite and non-ferroan dolomite cement has coated and is within the fractures of the detrital grains. Haematite cement is within the pore space. Undifferentiated cements is undistinguishable but likely to be haematite. Syntaxial quartz overgrowths are thin (1-5µm) and discontinuous around their host grains.

Reservoir Quality: Macroporosity is low (6%) is composed of primary intergranular and not interconnected.

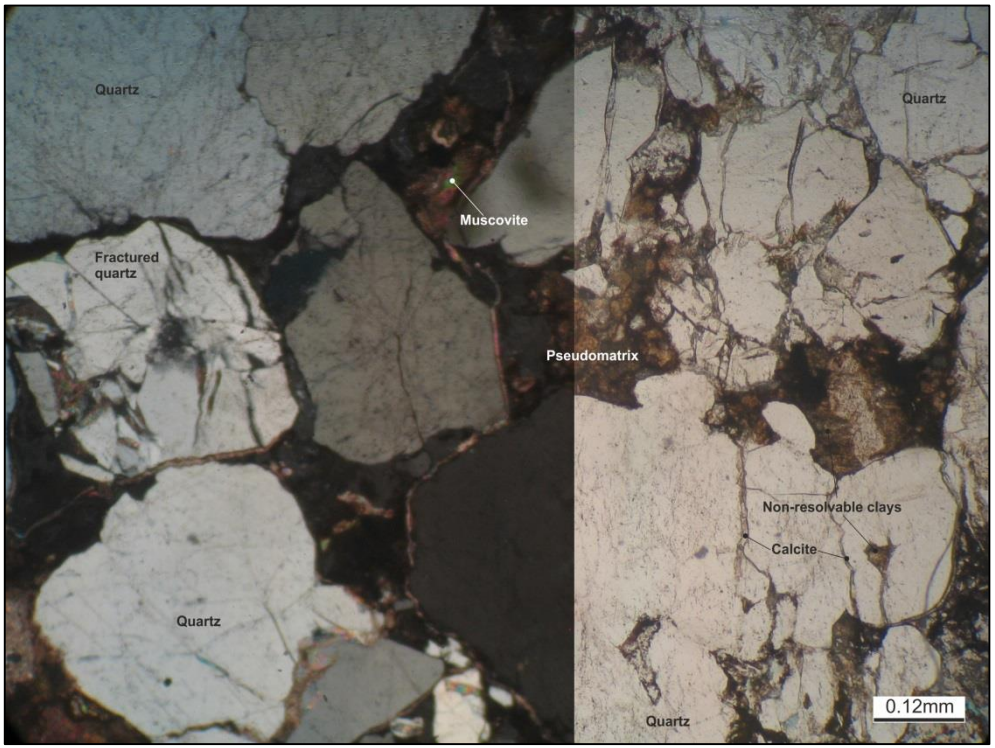

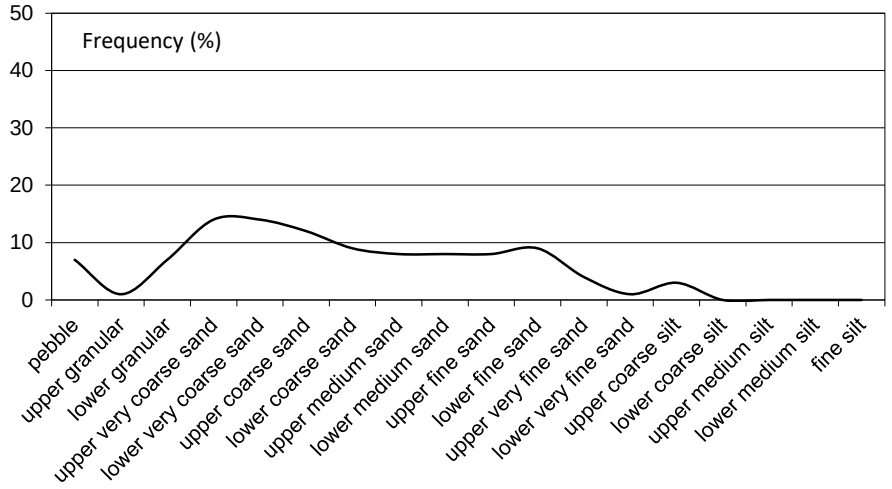

Grainsize variations within the sample

Log: 23
Height: 10.39m
Sample Number: 73
Sandstone name: Darjaniyon-ki Dhani

Facies: G
Architectural Element: Gravel Bar (F3)

Grainsize: Lower coarse sand
Sorting: Poorly
Roundness: Sub-rounded to sub-angular
Sandstone classification: Quartz wacke

Detrital Mineralogy: Detrital mineralogy consists of abundant monocrystalline quartz (49%), polycrystalline quartz (10%) and minor minerals include: rigid rock fragments (2.5%: sedimentary 2%, metamorphic 0.5%), undifferentiated grains (1.5%) and trace tourmaline. Monocrystalline grains are unstrained. Sedimentary fragments are composed of chert, whilst metamorphic fragments are composed of sutured quartz grains with rutile and calcite inclusions, with a schistose fabric. Undifferentiated grains are undistinguishable as they have being replaced by haematite. Optically non-resolvable clay (15%) is composed of pseudomatrix (14%), detrital pore filling clays (1%) which infill the pores and coats the quartz grains.

Authigenic Mineralogy: Authigenic cements include: calcite (7.5%), haematite (2.5%) and quartz overgrowths (2%). Syntaxial quartz overgrowths are thin and discontinuous around their host grains. Calcite and haematite cements are coating the grains.

Reservoir Quality: Macroporosity is moderate (10%) and comprises of primary intergranular porosity (8%), secondary oversized porosity (1.5%) and secondary intragranular porosity (0.5%). The porosity is largely connected.

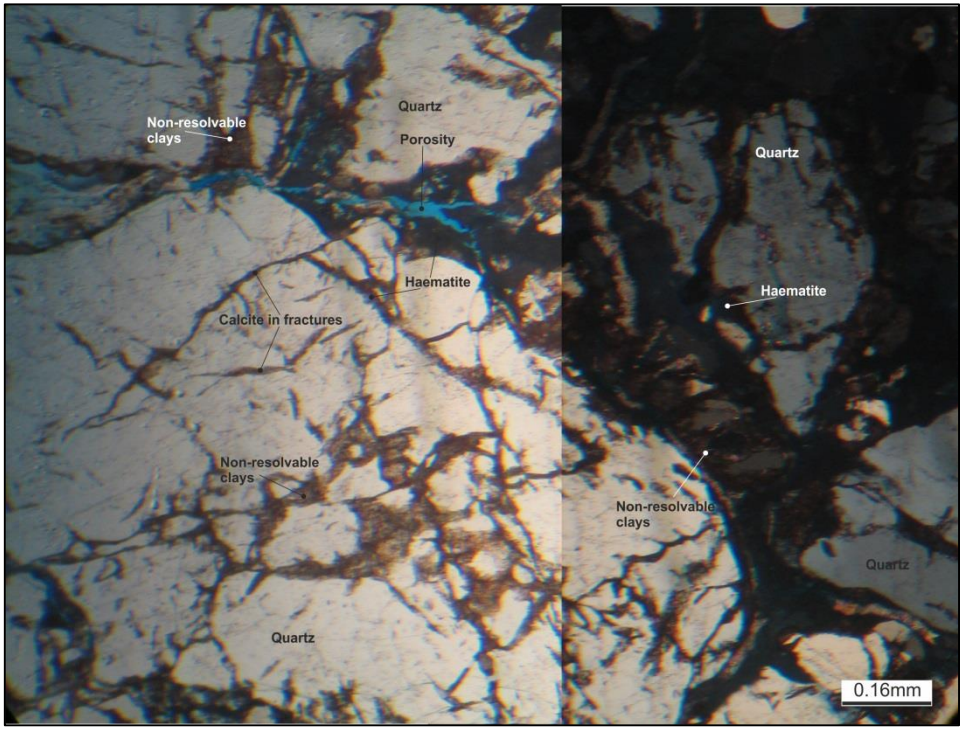

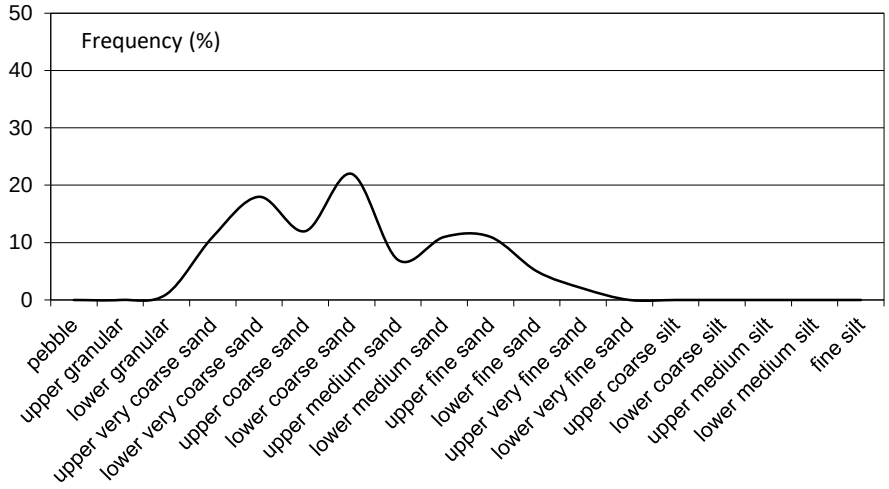

Grainsize variations within the sample

Log: 23
Height: 11.38m
Sample Number: 74
Sandstone name: Sarnoo

Facies: G
Architectural Element: Channel (F1)

Grainsize: Upper very fine sand
Sorting: Moderate
Roundness:
Sandstone classification: *haematitic* quartzarenite

Detrital Mineralogy: Detrital mineralogy composes of abundant monocrystalline quartz (45%), polycrystalline quartz (12.5%), with minor contains sedimentary rigid rock fragments (4%), undifferentiated grains (1%) and trace rutile. Grains are not strained and have concave to convex contact. Sedimentary fragments formed in chert. Undifferentiated grains are undistinguishable as they are being replaced by haematite. Optically non-resolvable clays are pseudomatrix (9%) and detrital pore-filling clay (2%) which fills the pore and coats the grains. The optically non-resolvable clay are composed of illite and coats the grains.

Authigenic Mineralogy: Authigenic mineralogy contains cements: haematite (9.5%), ferroan calcite (2%), quartz overgrowths (1.5%), undifferentiated (0.5%), anatase (trace) and authigenic clays – kaolinite (0.5%). Haematite and ferroan calcite cements are coating the grains and within the pore space. Syntaxial quartz overgrowths are thin (0.5µm) and discontinuous around their host grains. Undifferentiated cements choke the pores and coats detrital grains. Anatase crystals grow within the quartz grains. Kaolinite booklets choke the pore spaces.

Reservoir Quality: Macroporosity is moderate (12.5%) and is only composed of the primary intergranular porosity, porosity is not connected.

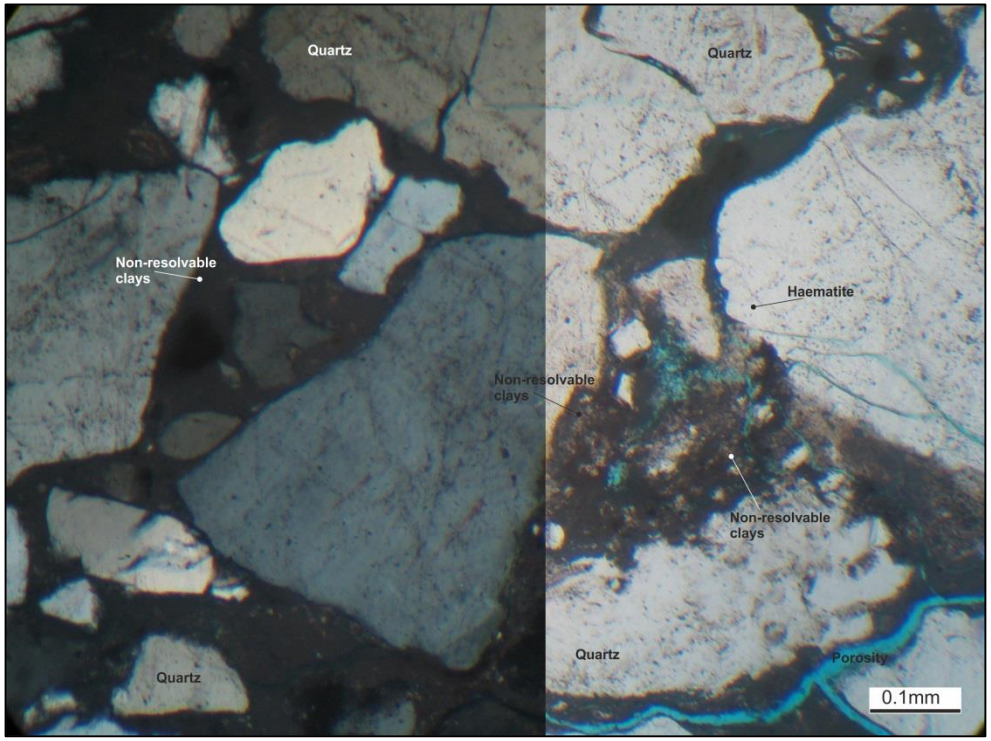

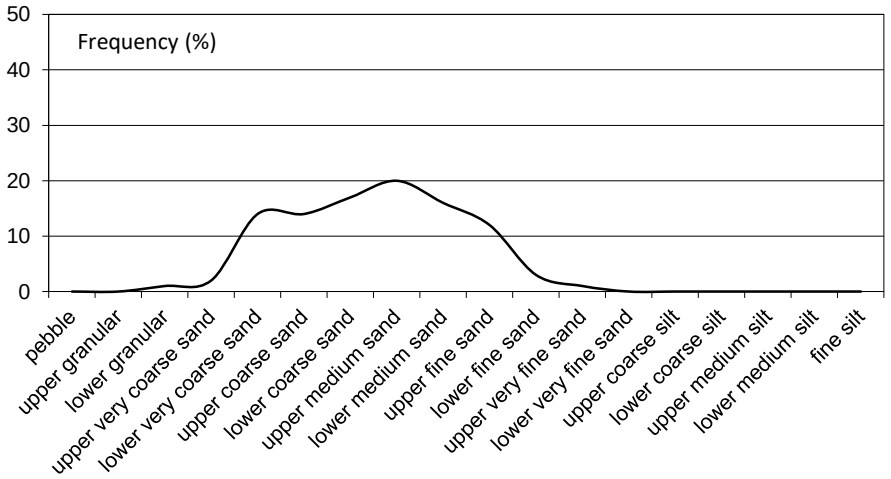

Grainsize variations within the sample

Log: 23
Height: 14.45m
Sample Number: 76
Sandstone name: Darjaniyon-ki Dhani

Facies: Gc
Architectural Element: Gravel Bar (F3)

Grainsize: Lower coarse sand
Sorting: Moderately
Roundness: Sub-rounded to sub-angular
Sandstone classification: *haematite* Quartzarenite

Detrital Mineralogy: Detrital mineralogy contains abundant monocrystalline quartz (64.5%), polycrystalline quartz (6%), with minor minerals containing: metamorphic rigid rock fragments (2%). Quartz grains are not strained and have rutile inclusions within them. Metamorphic grains are composed of sutured, broken quartz grains, which have a schistose fabric. Non-resolvable clays (4%) containing pseudomatrix (3%) and detrital pore filling clays (1%) which is within the pore spaces. It is likely that the pseudomatrix and pore filling clays are formed from illite.

Authigenic Mineralogy: Authigenic cements contain: haematite (18%), quartz overgrowths (3.5%) and ferroan calcite (1.5%). Haematite and ferroan calcite cements are coating the quartz grains. The quartz overgrowths are syntaxial and discontinuous around the host quartz grains.

Reservoir Quality: Macroporosity is negligible (0.5%) and composed of primary intergranular porosity (0.5%) only and is not interconnected.

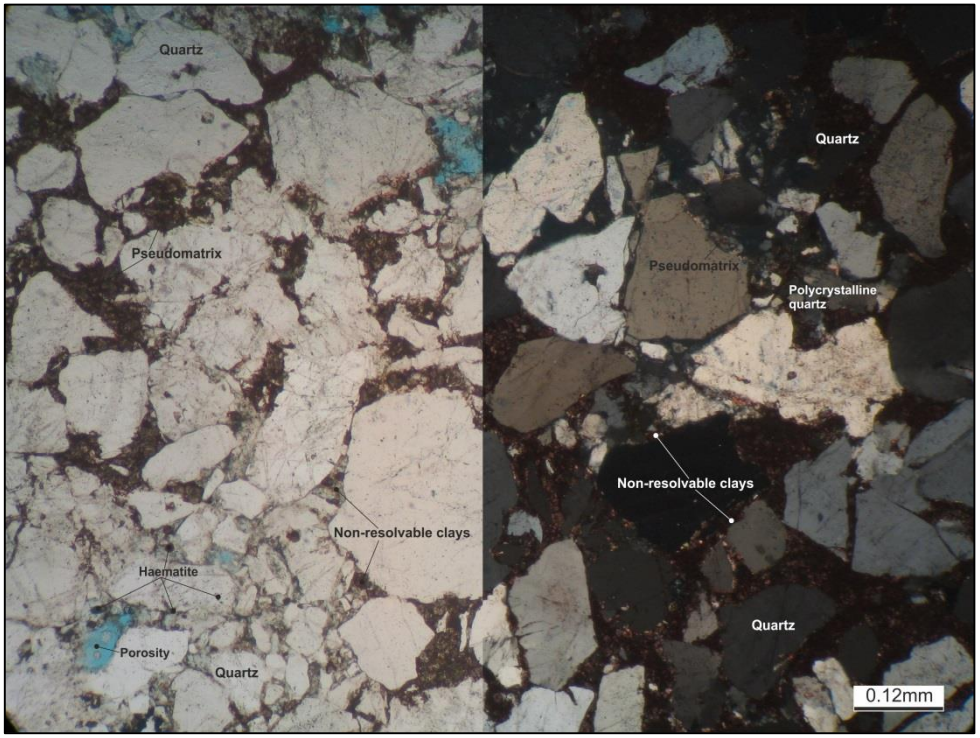

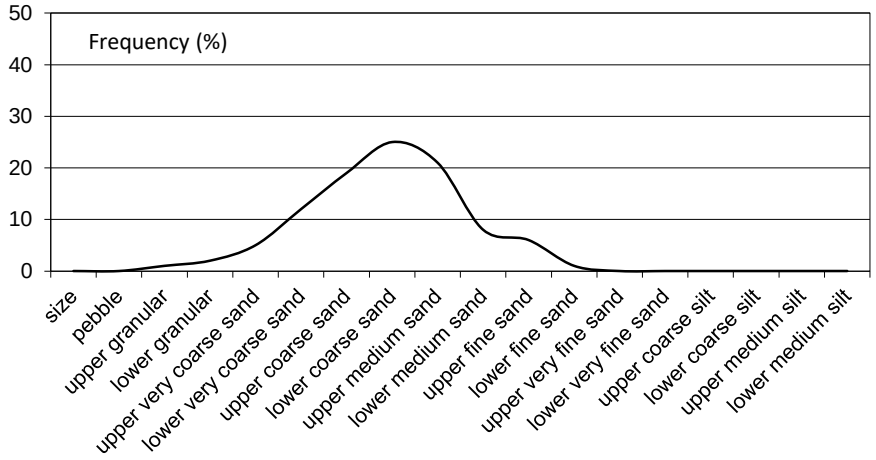

Grainsize variations within the sample

Log: 23
Height: 15.56m
Sample Number: 77
Sandstone name: Darjaniyon-ki Dhani

Facies: G
Architectural Element: Gravel Bar (F3)

Grainsize: Upper medium sand
Sorting: Moderately to well
Roundness: Sub-rounded to sub-angular
Sandstone classification: Quartzarenite

Detrital Mineralogy: Detrital mineralogy contains abundant monocrystalline quartz (55.5%), with significant polycrystalline quartz (5.5%) and minor sedimentary rigid rock fragments (0.5%) and heavy minerals (0.5%). The grains are not strained, but fractured. Quartz grains have rutile within them. Sedimentary fragments are composed of chert. Heavy minerals are formed from zircon and rutile. Optically non-resolvable clay (9.5%) formed of pseudomatrix (9%) and detrital pore filling (0.5%) form within the pores.

Authigenic Mineralogy: Authigenic cements include: haematite (21%), quartz overgrowths (2%) and ferroan calcite (0.5%). Haematite and ferron calcite cements are coating the quartz grains and within the porosity. Syntaxial quartz overgrowths are thin (0.5µm) and discontinuous around their host grains.

Reservoir Quality: Macroporosity is very low (3.5%) is composed of primary intergranular porosity however, it is not interconnected.

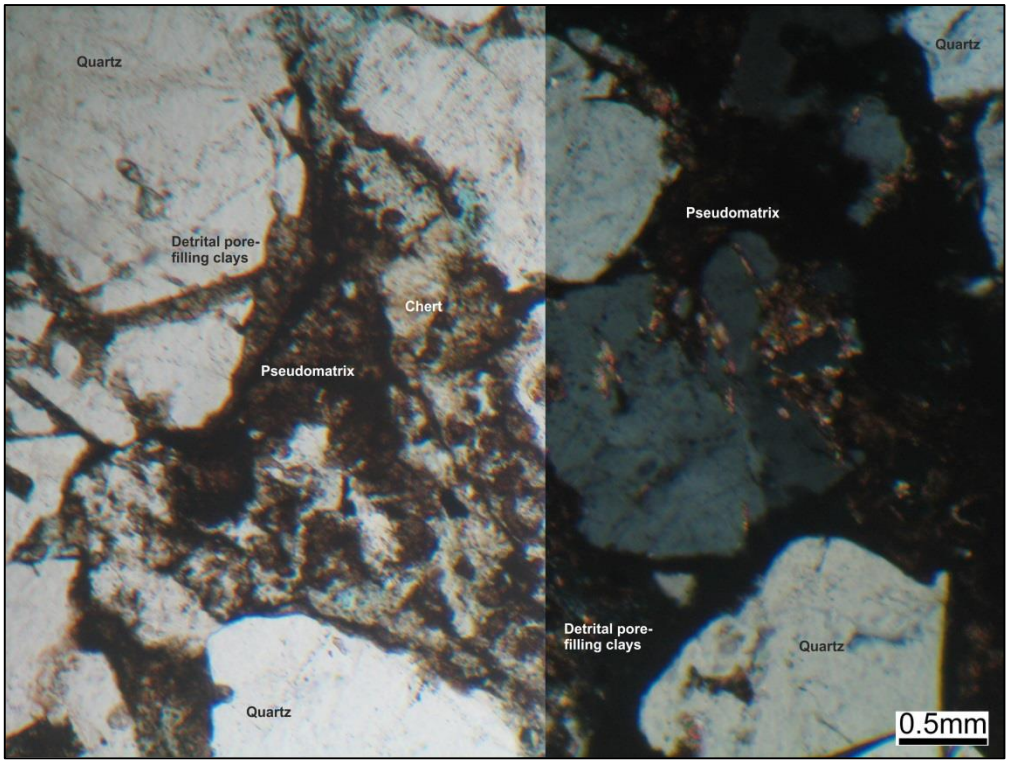

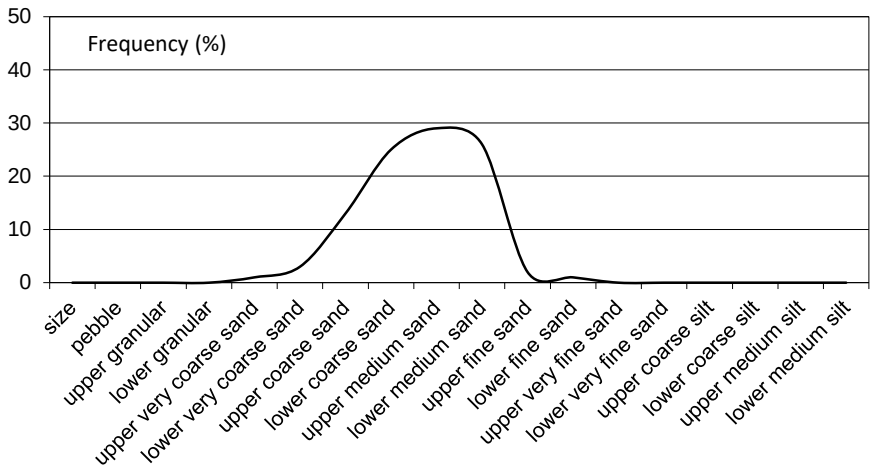

Grainsize variations within the sample

Log: 13
Height: 20.99m
Sample Number: 82
Sandstone name: Sarnoo

Facies: Sbmf
Architectural Element: Sheetflood (F6)

Grainsize: Lower coarse sand
Sorting: Moderately to well
Roundness: Sub-rounded to sub-angular
Sandstone classification: Quartzarenite

Detrital Mineralogy: Detrital mineralogy has abundant monocrystalline quartz (57%), polycrystalline quartz (12.5%), muscovite mica (5%), heavy minerals (1%) and undifferentiated grains (0.5%). Grains have concave to convex contacts and are very weakly strained. Ductile muscovite mica grains are thin (5 – 15µm). Heavy minerals are zircon and tourmaline. Undifferentiated grains are undistinguishable as they are being replaced by haematite. Optically non-resolvable clays (4%) which contains pseudomatrix (3%) and detrital pore-filling clays (1%) which fill the pores and coats approximately 10% of the grains.

Authigenic Mineralogy: The major components of the authigenic cements are: haematite (13.5%), ferron calcite (2.5%) and quartz overgrowths (2%), authigenic clays are kaolinite (trace). Haematite cement is contained within the pores and coats the grains. Ferron calcite is within the pore spaces. Syntaxial quartz overgrowths are thin (0.5µ) and discontinuous around their host grains. Kaolinite booklets are choking and infilling the pore spaces.

Reservoir Quality: Macroporosity is very low (2%) is composed of the primary intergranular porosity and they are not interconnected.

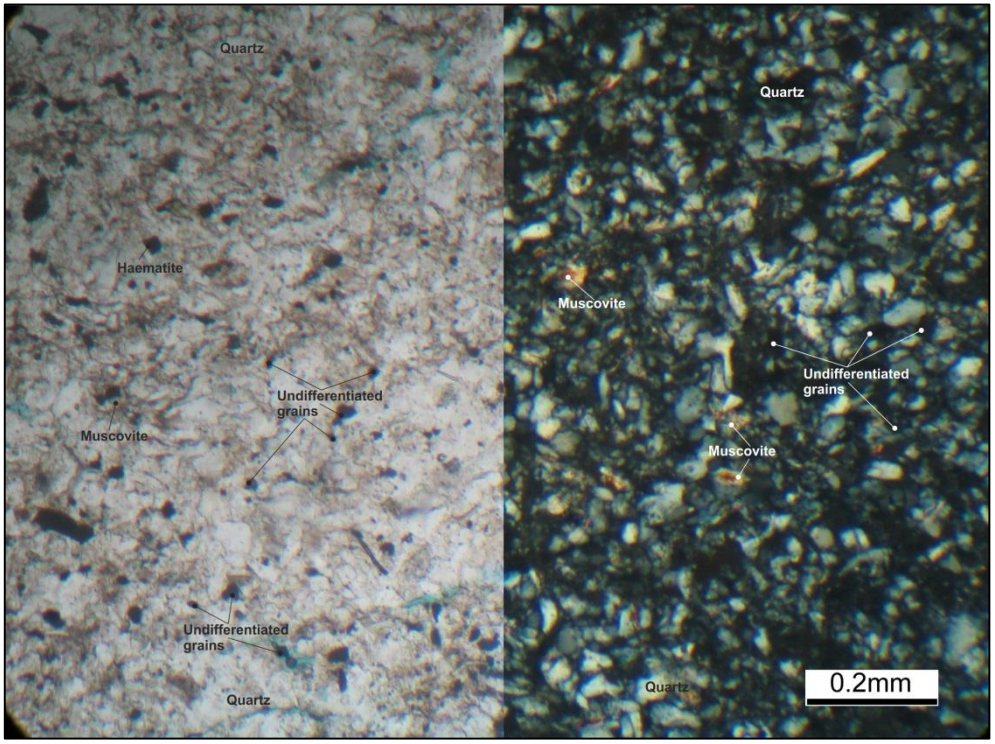

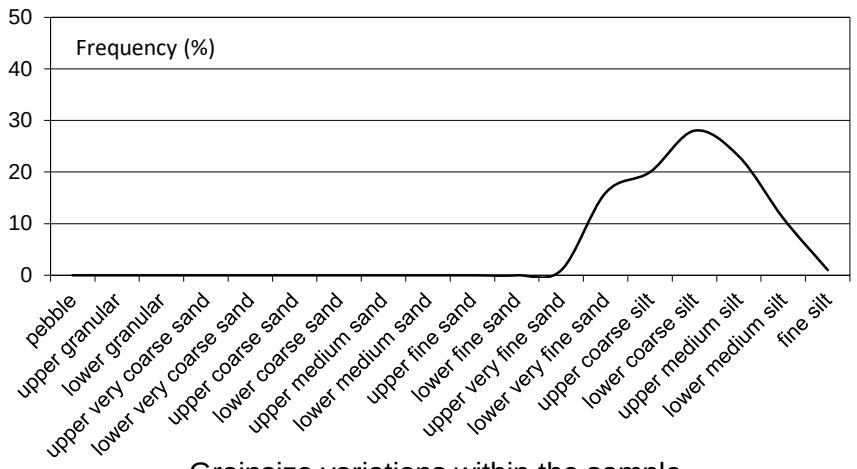

Grainsize variations within the sample

Log: 13
Height: 23.12m
Sample Number: 84
Sandstone name: Sarnoo

Facies: Sbmf
Architectural Element: Sheetflood (F6)

Grainsize: Upper coarse sand
Sorting: Moderately
Roundness: Rounded to Sub-rounded
Sandstone classification: Quartzarenite

Detrital Mineralogy: Detrital mineralogy is composed of abundant monocrystalline quartz (43.5%), polycrystalline quartz (35.5%), with minor constituents of rigid rock fragments metamorphic (5%), igneous (1%), and undifferentiated grains (0.5%). Monocrystalline quartz grains are slightly strained. Metamorphic fragments are composed of sutured quartz grains, with a schistose fabric; as igneous fragments are composed of intergrown monocrystalline quartz and muscovite mica. Undifferentiated grains are not detectable as they are being replaced by haematite. Optically non-resolvable clays (1%) contain pseudomatrix only, which is likely to be composed of illite and is within the pores spaces.

Authigenic Mineralogy: Authigenic mineralogy contains cements only: quartz overgrowths (3.5%), haematite (3.5%), ferroan calcite (0.5%) and undifferentiated (0.5%). Syntaxial quartz overgrowths are thin (0.5µm) discontinuous around their host grains. Haematite, calcite and undifferentiated cements are coating the quartz grains and within the pores. The undifferentiated cement is likely to be haematite.

Reservoir Quality: The macroporosity is very low (5.5%) constitutes the primary intergranular porosity only. Approximately 75% of the porosity is interconnected.

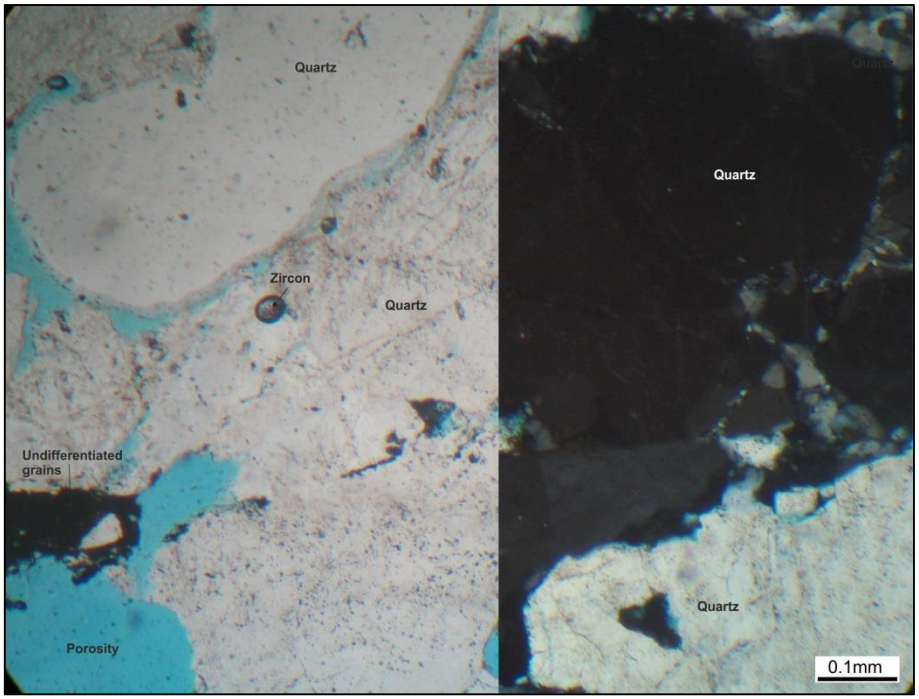

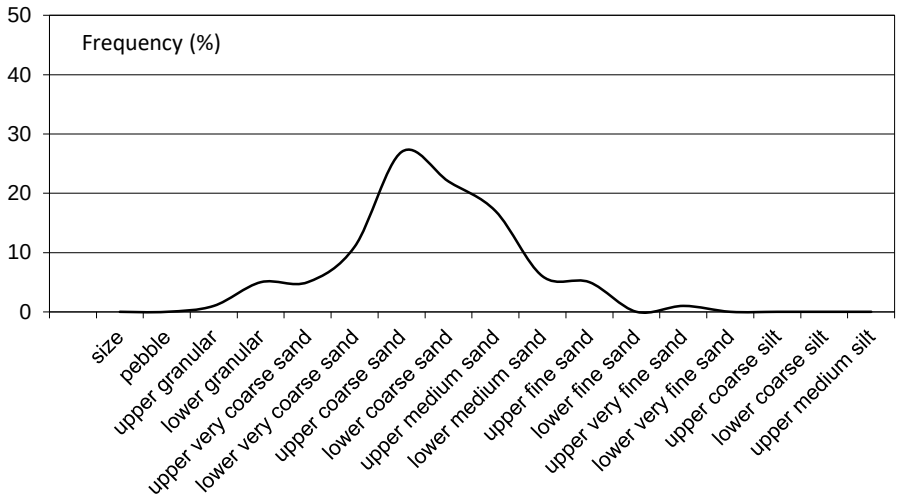

Grainsize variations within the sample

Log: 13
Height: 23.50m
Sample Number: 85
Sandstone name: Sarnoo

Facies: G
Architectural Element: Channel (F1)

Grainsize: Lower coarse sand
Sorting: Poorly
Roundness: Sub-rounded to sub-angular
Sandstone classification: Sublithic arenite

Detrital Mineralogy: The detrital grains comprise of monocrystalline quartz (66.5%), polycrystalline quartz (10.5%) and small amounts of rigid rock fragments metamorphic (6.5%), sedimentary (3.5%), igneous (1%) and trace amounts of heavy minerals. Some of the monocrystalline quartz are weakly strained. Metamorphic grains are sutured quartz grains, with a schistose fabric. Sedimentary fragments are made from chert and the igneous fragments are composed of monocrystalline quartz with muscovite mica inclusions. The heavy minerals contains tourmaline. Non-resolvable clays are composed from pseudomatrix (0.5%) which coats the grains.

Authigenic Mineralogy: Authigenic mineralogy contains authigenic cements: quartz overgrowths (4.5%), haematite (2.5%) and calcite (2%). Thin (3-6µm) quartz overgrowths are syntaxial and discontinuous around their host grains. Haematite and calcite cements are within the pores and coats the grains of the quartz.

Reservoir Quality: Macroporosity is very low (2.5%) constitutes the primary intergranular porosity and is not interconnected.

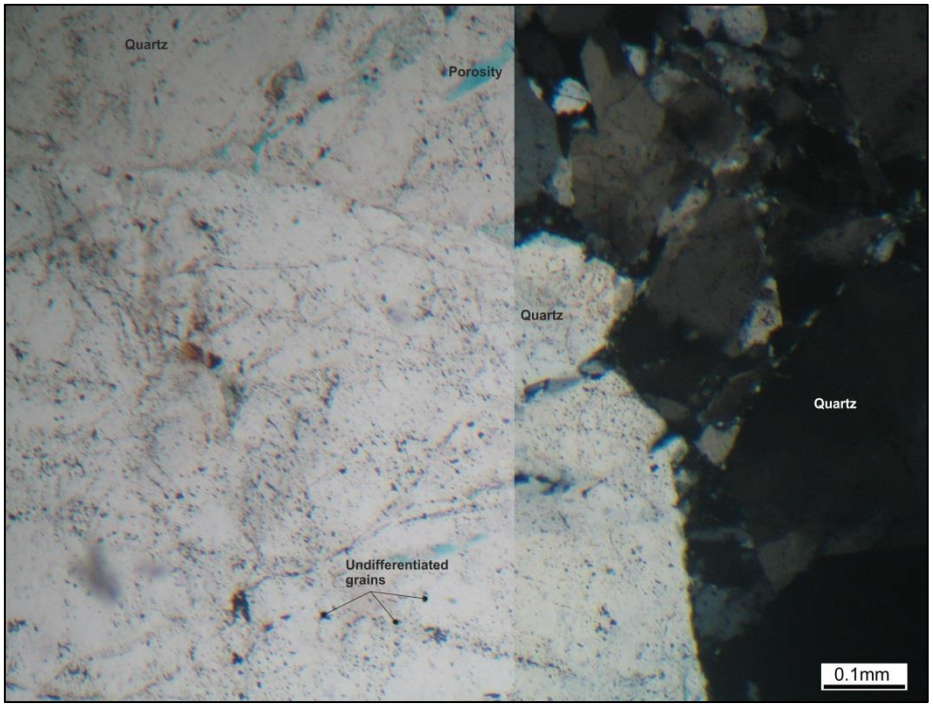

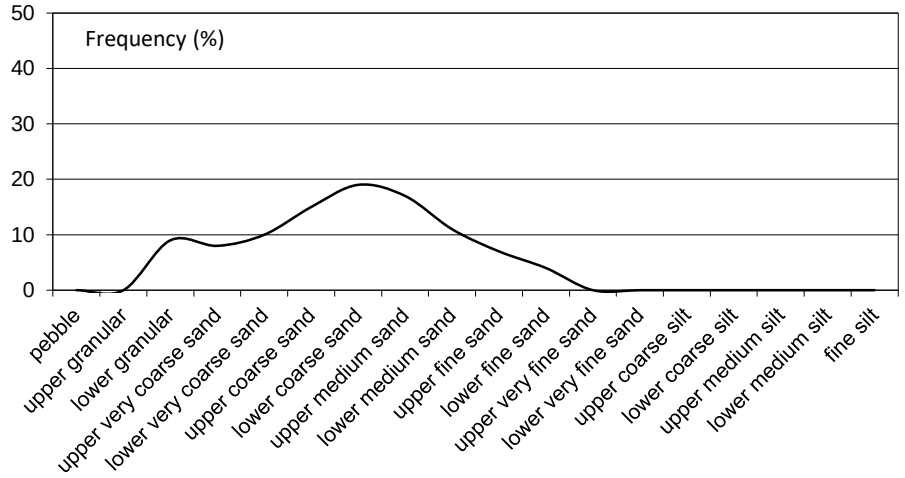

Grainsize variations within the sample

Log: 13
Height: 23.87m
Sample Number: 86
Sandstone name: Sarnoo

Facies: Sxm
Architectural Element: Channel (F1)

Grainsize: Lower fine sand
Sorting: Moderately
Roundness: Sub-rounded to sub-angular
Sandstone classification: Quartzarenite

Detrital Mineralogy: Primary detrital minerals are: monocrystalline quartz (70.5%), polycrystalline quartz (14.5%) and the minor detrital minerals are: rigid rock fragments sedimentary (2%), metamorphic (0.5%) and heavy minerals (trace). Approximately 15% of the monocrystalline quartz is slightly strained. Sedimentary fragments are composed of chert and the metamorphic fragments are composed of broken and sutured polycrystalline quartz grains, which has a schistose fabric. Heavy minerals are tourmaline and zircon. The non-resolvable clays (1.5%) are pseudomatrix (1%) and pore filling clays (0.5%) are likely to be composed of illite. The clays are pore-filling and grain coating.

Authigenic Mineralogy: Authigenic cements are: quartz overgrowths (3%), calcite (2%) and haematite (1%) and the authigenic clays are kaolinite. Thin (6µm), syntaxial quartz overgrowths are discontinuous around their host grains. Calcite and haematite are pore filling and coat approximately 40% of the quartz grains. Kaolinite booklets are choking the pore spaces.

Reservoir Quality: Macroporosity is low (5%) is composed of primary intergranular porosity and is not interconnected.

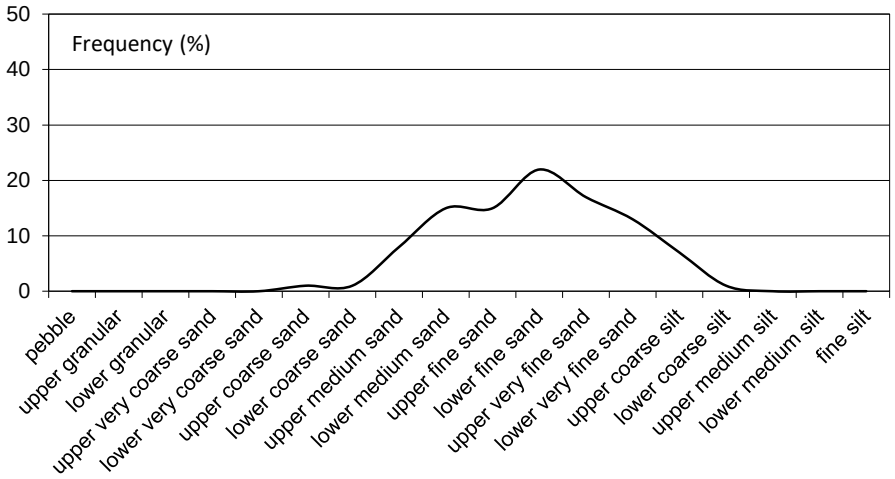

Grainsize variations within the sample

Log: 13
Height: 24.50m
Sample Number: 87
Sandstone name: Sarnoo

Facies: Sbmf
Architectural Element: Channel (F1)

Grainsize: Lower fine sand
Sorting: Moderately to well
Roundness: Sub-rounded to sub-angular
Sandstone classification: Quartzarenite

Detrital Mineralogy: Detrital minerals constitutes abundant amounts of monocrystalline quartz (68%), polycrystalline quartz (14.5%), with minor amounts of muscovite mica (2%), sedimentary rigid rock fragments (0.5%) and heavy minerals (0.5%). Grains have concave to convex contacts and are not strained. Ductile muscovite mica here are thin (5 – 15µm). Sedimentary fragments are chert. Heavy minerals are zircon.

Authigenic Mineralogy: The authigenic cements comprise of: haematite (6.5%), ferroan calcite (1.5%) and quartz overgrowths (1.5%). Haematite and calcite cements are within the pore spaces and coats approximately 10% of the quartz grains. Thin quartz overgrowths are syntaxial and discontinuous around their host grains.

Reservoir Quality: Macroporosity is low (5%) and formed from primary intergranular porosity which is not interconnected.

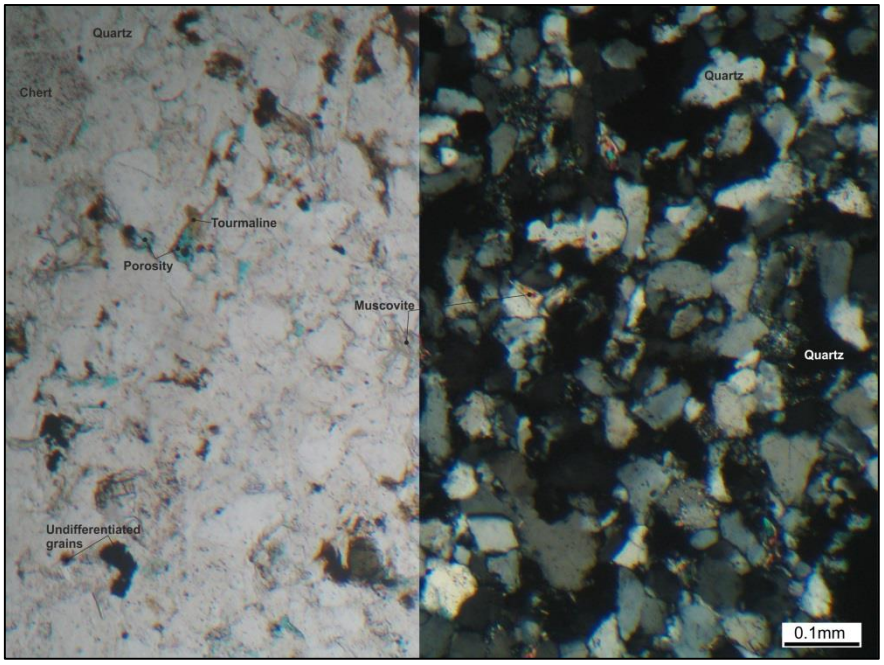

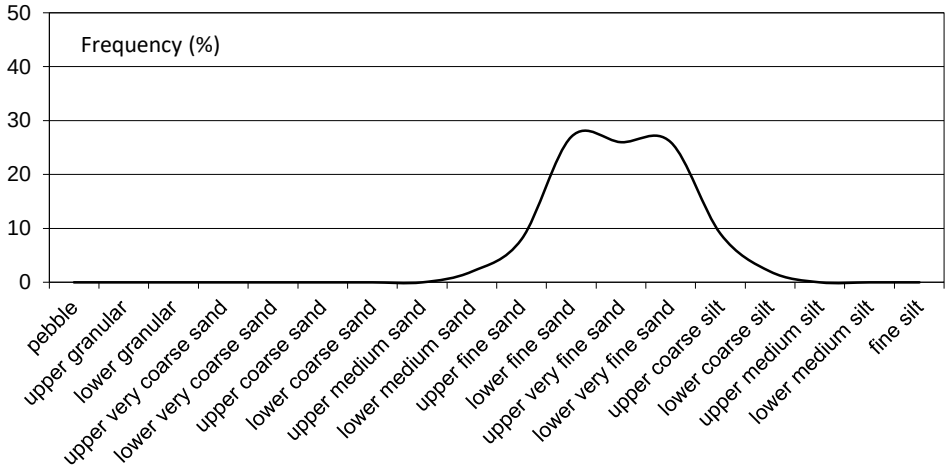

Grainsize variations within the sample

Log: 13
Height: 27.33m
Sample Number: 91
Sandstone name: Sarnoo

Facies: Sbmf
Architectural Element: Channel (F1)

Grainsize: Lower fine sand
Sorting: Moderately to well
Roundness: Sub-rounded to sub-angular
Sandstone classification: Quartzarenite

Detrital Mineralogy: The primary detrital minerals are: monocrystalline quartz (64%), polycrystalline quartz (14%), the smaller components are: muscovite mica (2.5%) rigid rock fragments igneous (1.5%), sedimentary (1%), metamorphic (0.5%), and heavy minerals (0.5%). Approximately 5% of the monocrystalline quartz is mildly strained. Muscovite micas occur in layers within the quartz grains. Igneous monocrystalline quartz have muscovite mica inclusions within. Sedimentary fragments are formed from chert. Metamorphic grains are formed from sutured quartz with a schistose fabric. Heavy minerals are formed from tourmaline and zircon.

Authigenic Mineralogy: The authigenic mineralogy contains cements and clays, cements include: quartz overgrowths (6%), calcite cement (2.5%), haematite (2%), non-ferroan dolomite (0.5%) and the clays include: kaolinite (1%). Thin (6µm), syntaxial quartz overgrowths are discontinuous around their host grain. The calcite, haematite cements are pore filing. The calcite and haematite cements coats the detrital grains. Kaolinite booklets chokes the pore spaces.

Reservoir Quality: Primary intergranular porosity (4%), comprises the macroporosity, is not interconnected.

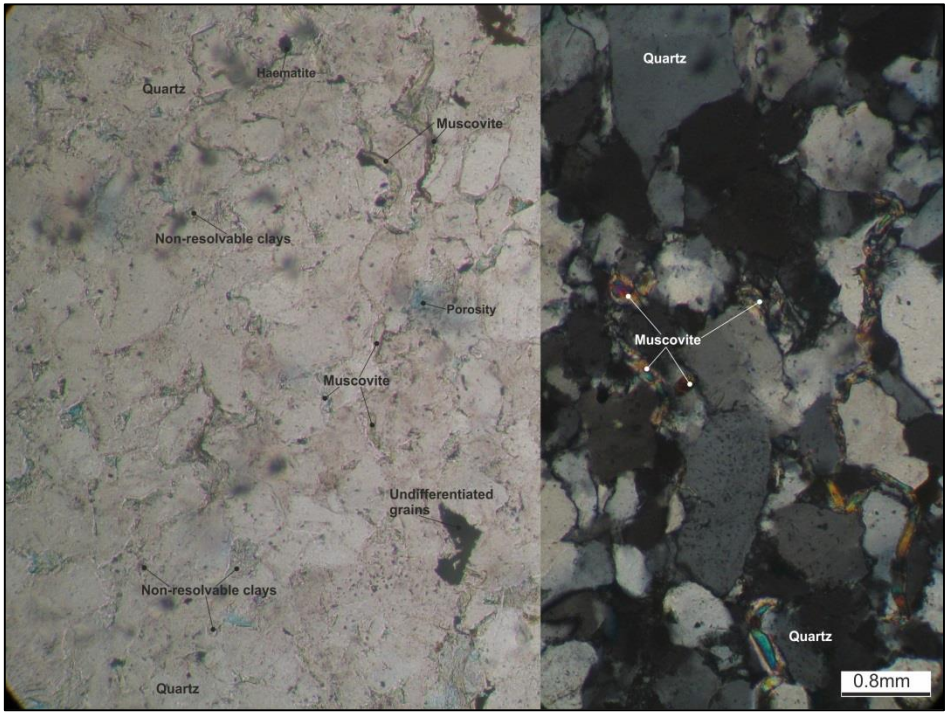

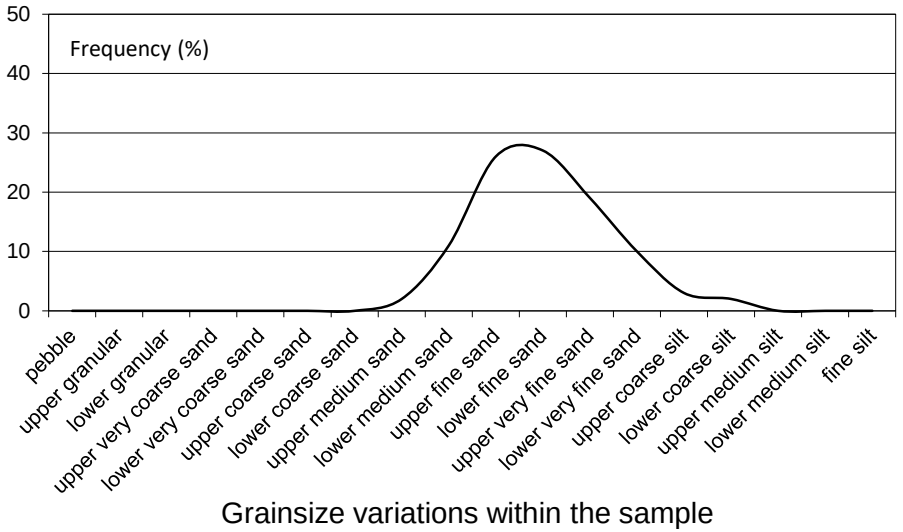

Grainsize variations within the sample

Log: 23
Height: 28.03m
Sample Number: 93
Sandstone name: Sarnoo

Facies: G
Architectural Element: Channel (F1)

Grainsize: Lower medium sand
Sorting: Moderate to well
Roundness: sub-angular
Sandstone classification: Sublithic arenite

Detrital Mineralogy: Detrital mineralogy contains abundant: monocrystalline quartz (63%), polycrystalline quartz (10.5%), and minor rigid rock fragments igneous (3.5%), metamorphic (3.5%), sedimentary (1.5%), muscovite mica (2.5%) and heavy minerals (trace). Quartz grains are unstrained to slightly strained. Igneous fragments are composed of quartz grains with muscovite inclusions. Metamorphic fragments are sutured and heavy broken quartz clasts, which have an schistose fabric, while the sedimentary fragments are composed of chert. Ductile muscovite mica has long contacts to the quartz grains. There are distinct layers within the sample which hold finer and coarser clasts. Optically non-resolvable clay (1%) is pore filling.

Authigenic Mineralogy: The authigenic cements include: haematite (5.5%), quartz overgrowths (4%), ferroan calcite (2%) and the authigenic clays include: kaolinite (0.5%). Haematite and ferroan calcite cements are pore filling. Ferroan calcite coats approximately 30% of the quartz grains. Syntaxial, thin (7-8µm) quartz overgrowths are discontinuous around their host. Kaolinite booklets are pore filling.

Reservoir Quality: The primary intergranular porosity is very low (2.5%) is the only constitute of the macroporosity which is not interconnected.

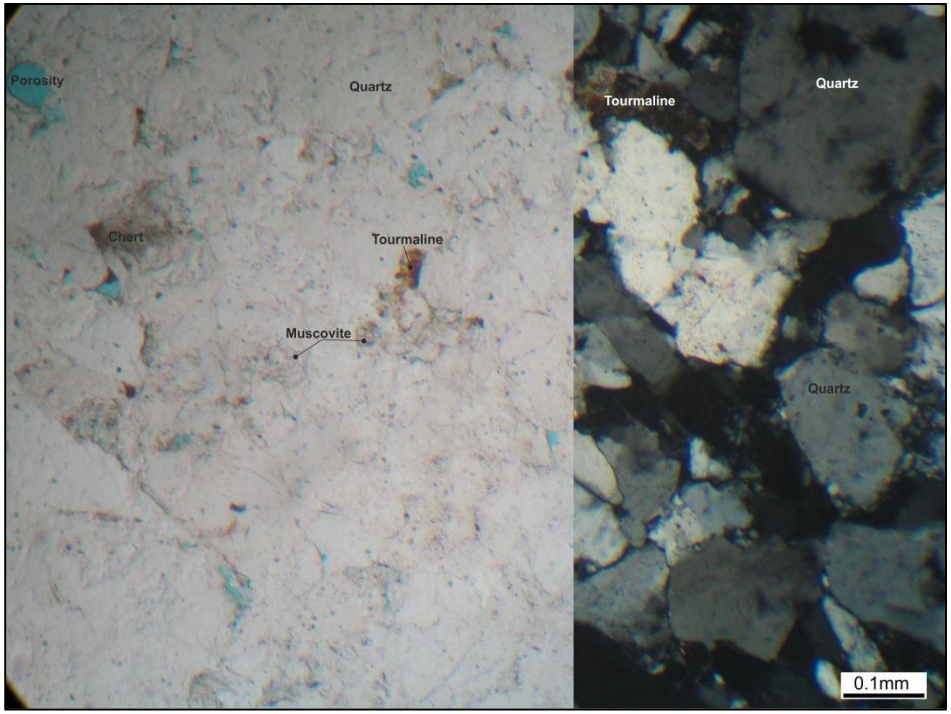

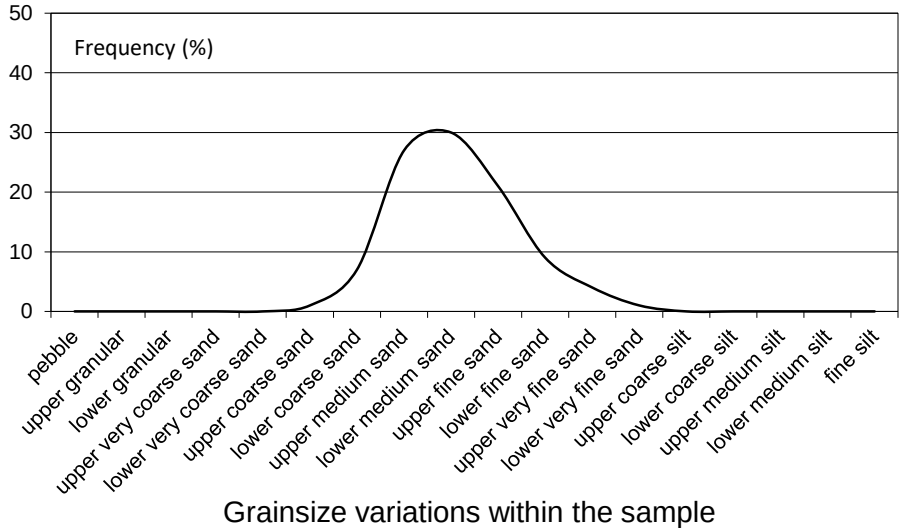

Grainsize variations within the sample

Log: 55
Height: 1.00m
Sample Number: 95
Sandstone name: Nosar

Facies: Sx
Architectural Element: Channel (F1)

Grainsize: Lower medium sand
Sorting: Well
Roundness: sub-angular
Sandstone classification: Quartzarenite

Detrital Mineralogy: Detrital mineralogy has abundant monocrystalline quartz (46.5%), polycrystalline quartz (30%) and minor constituents which are rigid rock fragments sedimentary (0.5%), igneous (0.5%) and heavy minerals (0.5%). Approximately 20% of the monocrystalline quartz are weakly strained. Sedimentary fragments are made from chert and the igneous fragments are composed of monocrystalline quartz with muscovite mica inclusions. The heavy minerals are made from rutile and tourmaline. Optically non-resolvable clays (12%) is pore filling and coats the quartz grains.

Authigenic Mineralogy: The authigenic cements are: calcite (5%), quartz overgrowths (1.5%), haematite (0.5%) and the authigenic clays are: kaolinite (0.5%). Calcite and haematite cements are coating the detrital grains and within the porosity. Thin (8µm) quartz overgrowths are syntaxial and discontinuous around their host grains. Kaolinite booklets are within the porosity.

Reservoir Quality: Macroporosity is very low (2.5%) is composed of primary intergranular porosity (2%) and secondary oversized porosity (0.5%). The porosity is not interconnected.

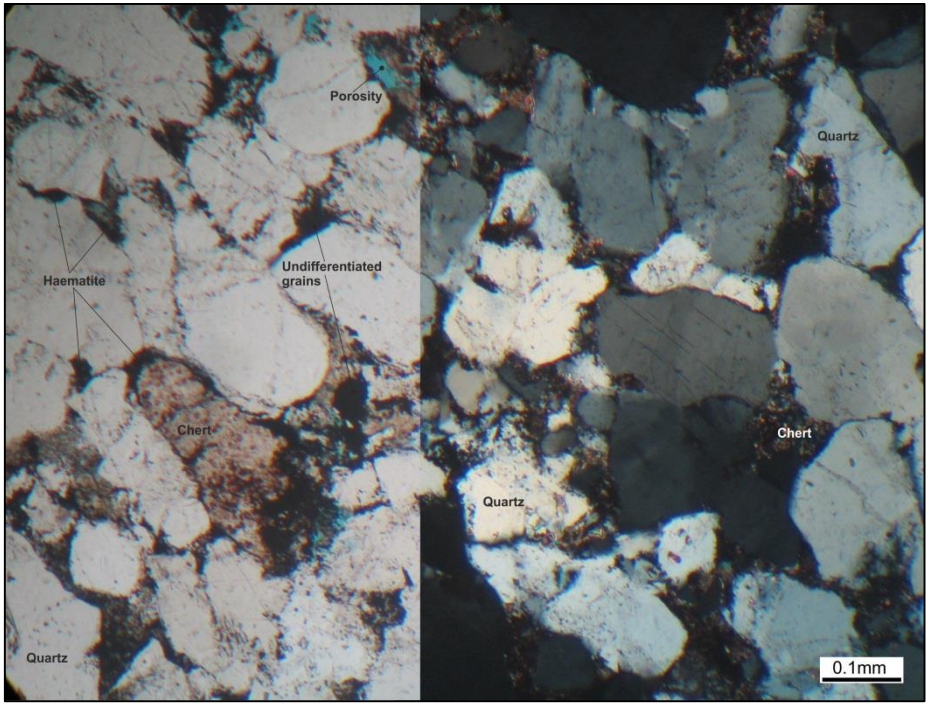

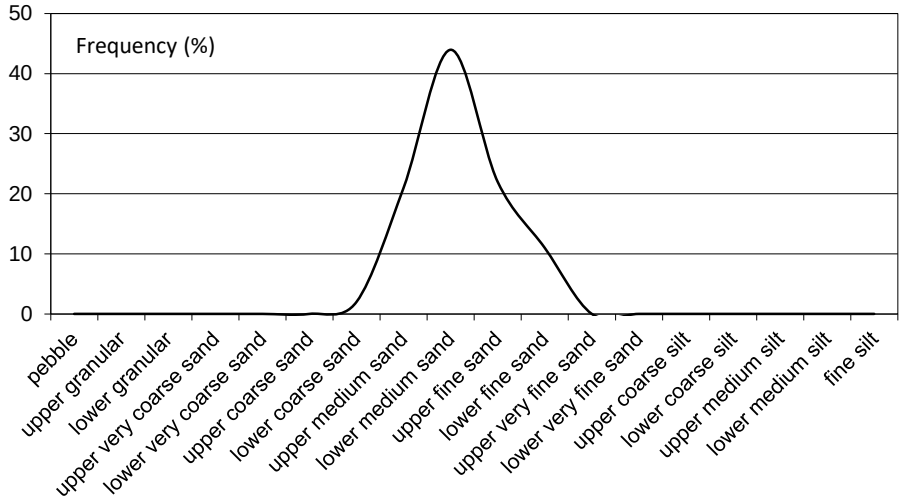

Grainsize variations within the sample

Log: 55
Height: 1.84m
Sample Number: 96
Sandstone name: Nosar

Facies: Sxm
Architectural Element: Channel (F1)

Grainsize: Upper medium sand
Sorting: Poorly
Roundness: Sub-rounded
Sandstone classification: Quartzarenite

Detrital Mineralogy: The detrital mineralogy contains abundant monocrystalline quartz (51%) and polycrystalline quartz (29%), with minor components are: rigid rock fragments sedimentary (1.5%), metamorphic (0.5%), igneous (0.5%), muscovite mica 0.5% and heavy minerals (trace). Monocrystalline quartz is slightly strained. The sedimentary fragments are made from chert. Metamorphic fragments are composed of sutured quartz, with a slatey texture and igneous fragments containing quartz and muscovite mica inclusions. The heavy minerals are tourmaline. Non-resolvable clays (8.5%) are pore filling and coats the grains.

Authigenic Mineralogy: Authigenic cements contain: non-ferroan dolomite (0.5%) quartz overgrowths (0.5%) and trace haematite; authigenic clays are kaolinite (1.5%). Non-ferroan dolomite and haematite cements have in-filled the pores. Syntaxial and thin quartz overgrowths are discontinuous around their quartz overgrowths. Haematite cements have coats the quartz grains. Kaolinite booklets infill the pore spaces.

Reservoir Quality: Macroporosity (6%) contains both primary intergranular porosity (4.5%) and secondary oversized porosity (1.5%) which are not interconnected.

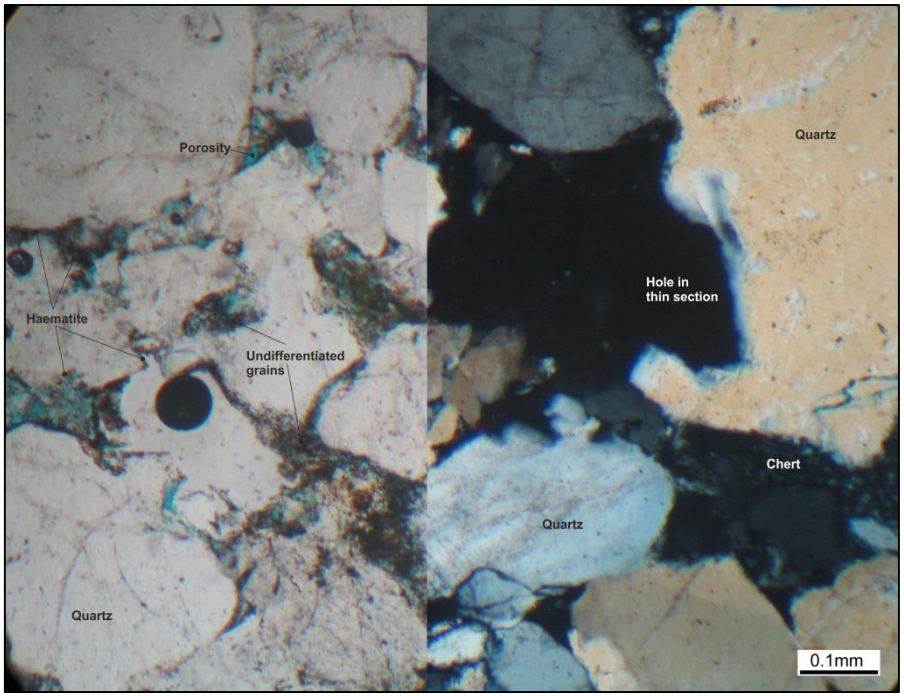

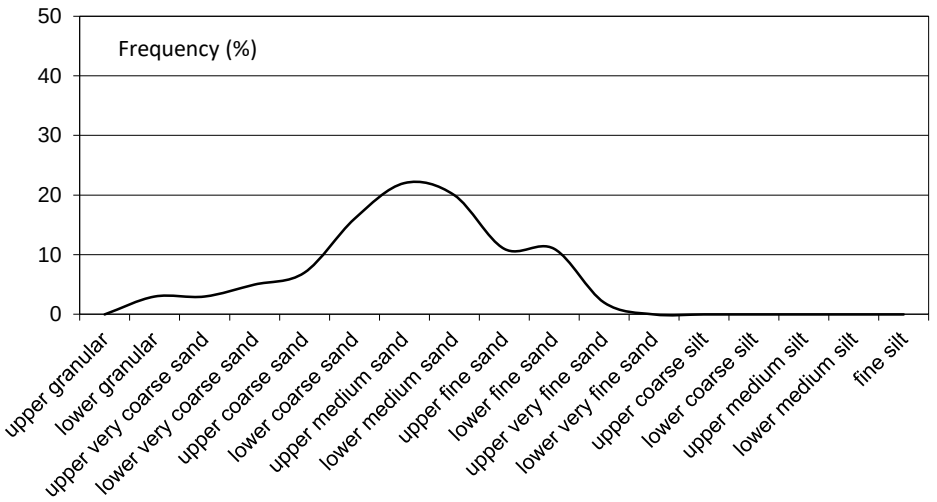

Grainsize variations within the sample

Log: 55
Height: 4.75m
Sample Number: 98
Sandstone name: Nosar

Facies: Sxm
Architectural Element: Channel (F1)

Grainsize: Upper medium sand
Sorting: Moderately
Roundness: Rounded to sub-rounded
Sandstone classification: Quartzarenite

Detrital Mineralogy: The detrital mineralogy constitutes abundant monocrystalline quartz (50%), polycrystalline quartz (31%), and sedimentary rigid rock fragment (1%). The monocrystalline quartz is slightly strained. Some of the monocrystalline quartz is fractured and the fractures are filled with calcite. The sedimentary fragments are formed from chert. There are trace amounts of metamorphic fragments within the sample which are composed of sutured quartz grains. Non-resolvable clays (2.5%) and is within the pores.

Authigenic Mineralogy: The authigenic cements: non-ferroan dolomite (4.5%) and haematite (0.5%) and authigenic clays kaolinite (2.5%). Non-ferron dolomite is pore-filling. Haematite cement is both pore filling and coat graining. Kaolinite booklets are pore-filling.

Reservoir Quality: The macroporosity is low (6.5%) contains primary intergranular porosity (6.5%) and secondary oversized porosity (1.5%). The porosity is interconnected.

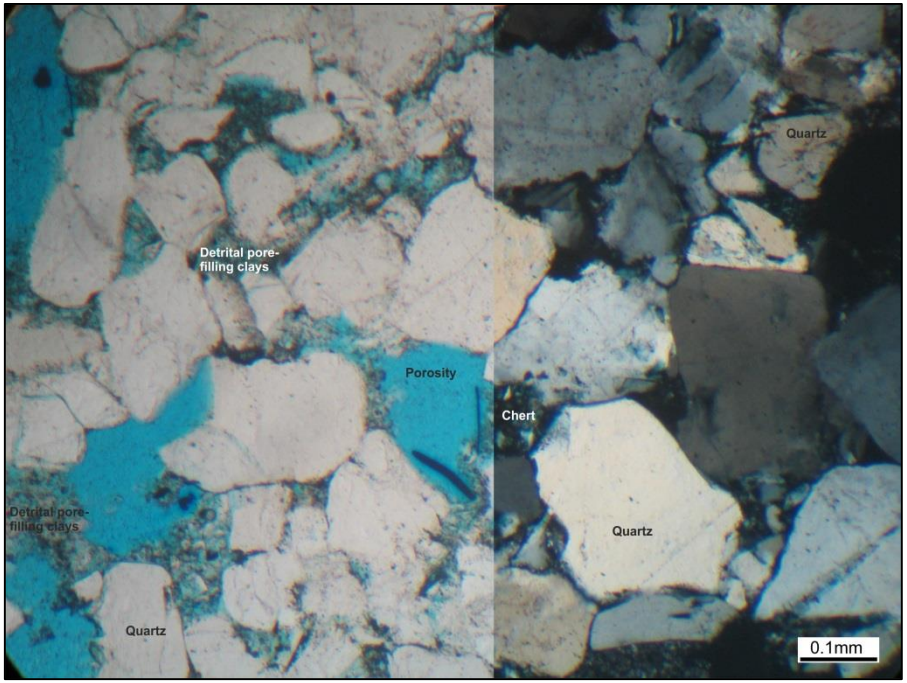

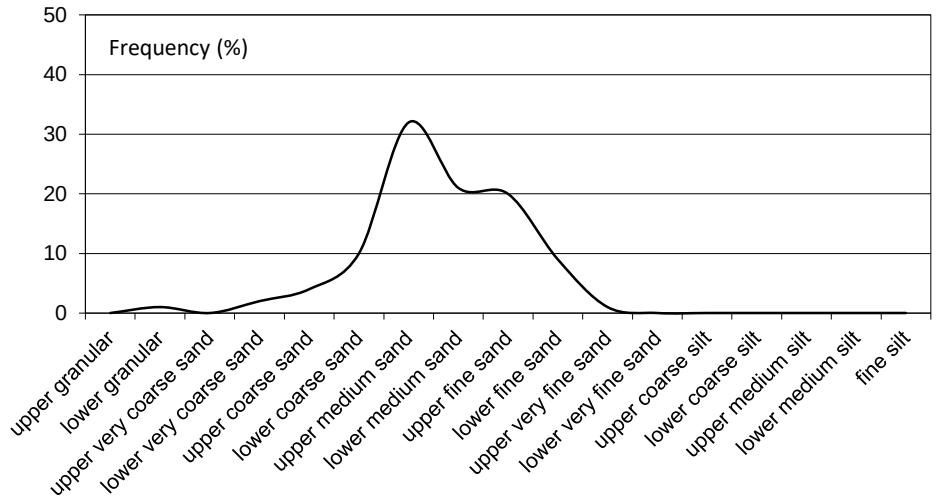

Grainsize variations within the sample

Log: 55
Height: 5.74m
Sample Number: 99
Sandstone name: Nosar

Facies: Sxf
Architectural Element: Channel (F1)

Grainsize: Lower medium sand
Sorting: Moderate to well
Roundness: Sub-angular
Sandstone classification: Quartzarenite

Detrital Mineralogy: The main compositional minerals are: polycrystalline quartz (42%), monocrystalline quartz (40.5%), with the minor components which are: rigid rock fragments sedimentary (2.5%), and heavy minerals (0.5%). Grains are not strained. The sedimentary fragments are composed of chert. Heavy minerals are rutile and tourmaline. Non-resolvable clays (6.5%) fill the pore spaces.

Authigenic Mineralogy: The authigenic cements are: non-ferroan dolomite (2%), haematite (1.5%) and the authigenic clays are: kaolinite (0.5%). All authigenic minerals coat the grains. Haematite cements are also within the pore spaces.

Reservoir Quality: The macroporosity (4%) and comprises of primary intergranular porosity. The porosity is not connected.

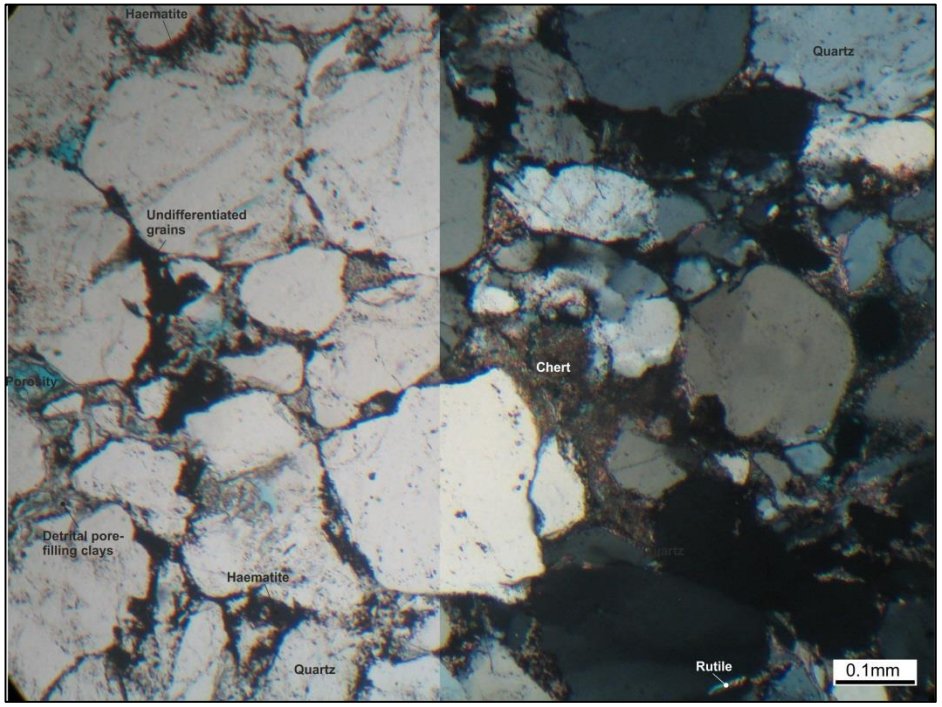

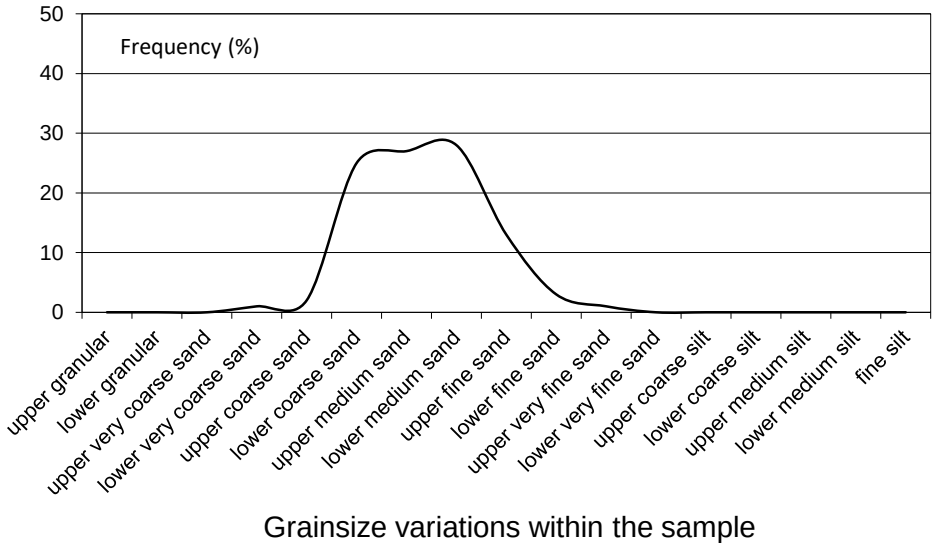

Grainsize variations within the sample

Log: 55
Height: 6.42m
Sample Number: 100
Sandstone name: Nosar

Facies: Stxf
Architectural Element: Channel (F1)

Grainsize: Upper fine sand
Sorting: Moderately to well
Roundness: Sub-angular
Sandstone classification: Quartzarenite

Detrital Mineralogy: The detrital mineralogy comprises abundant amounts of: monocrystalline quartz (41%), polycrystalline quartz (37%) with minor constituents of sedimentary rigid rock fragments (0.5%) and muscovite mice (0.5%). The grains are unstrained, with little corrosion. The sedimentary fragments are formed from chert. The non-resolvable detrital clays (12%) are pore filling and coats a few of the grains.

Authigenic Mineralogy: The authigenic mineralogy contains cements and clays, cements include: non-ferroan dolomite cement (1%) and quartz overgrowths (1%) and the clays include: kaolinite (5%). Non-ferroan dolomite cements are pore-filling and coats the grains. Thin (4-6µm) quartz overgrowths are discontinuous around their host grains and syntaxial. Kaolinite clays are choking the pore spaces.

Reservoir Quality: The macroporosity (2%) contains primary intergranular porosity. The porosity is not interconnected.

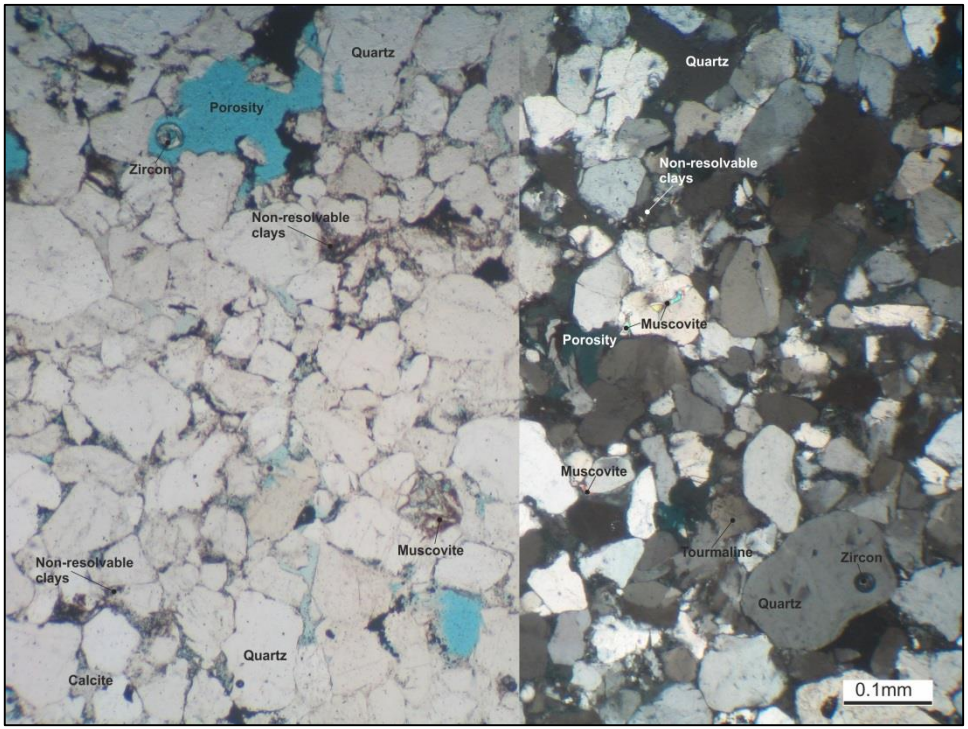

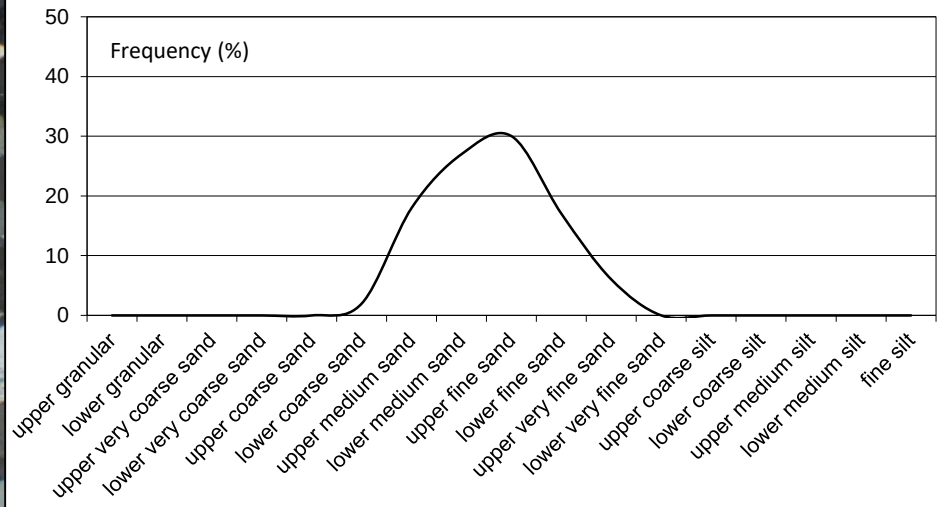

Grainsize variations within the sample

Log: 55
Height: 9.59m
Sample Number: 104
Sandstone name: Nosar

Facies: Stxc
Architectural Element: Channel (F1)

Grainsize: Lower medium sand
Sorting: Moderately to well
Roundness: Sub-rounded to sub-angular
Sandstone classification: Quartzarenite

Detrital Mineralogy: The main components of the detrital mineralogy comprises abundant monocrystalline quartz (59%), polycrystalline quartz (21%), with minor grains of rigid rock fragments sedimentary (1%), metamorphic (0.5%), igneous (0.5%) and the heavy minerals. The grains are slightly strained to unstrained. Sedimentary fragments are formed from chert. Metamorphic fragments are sutured grains, with a schistose fabric. The igneous fragments are quartz grains with muscovite inclusions. Heavy minerals include tourmaline. Detrital pore-filing non-resolvable clay (13%) fills pores and coats grains.

Authigenic Mineralogy: Authigenic mineralogy contains non-ferroan dolomite cement (3%), and traces of haematite cement and kaolinite clay (2%). All cements are within the pores. Haematite coats the detrital grains. Kaolinite booklets are within the pore spaces.

Reservoir Quality: Traces amounts of primary intergranular porosity.

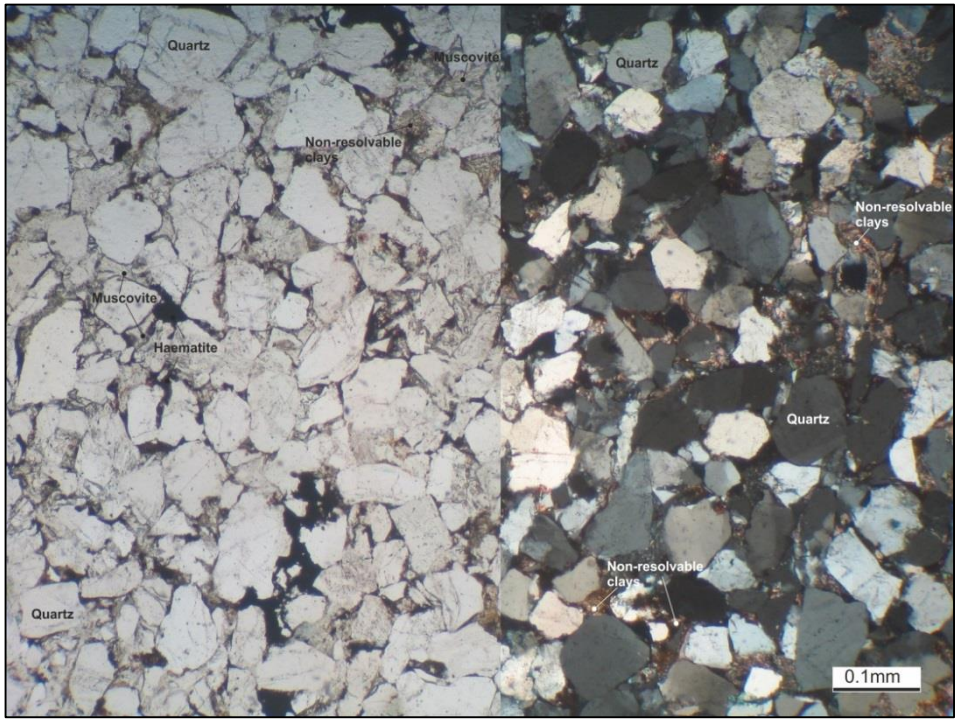

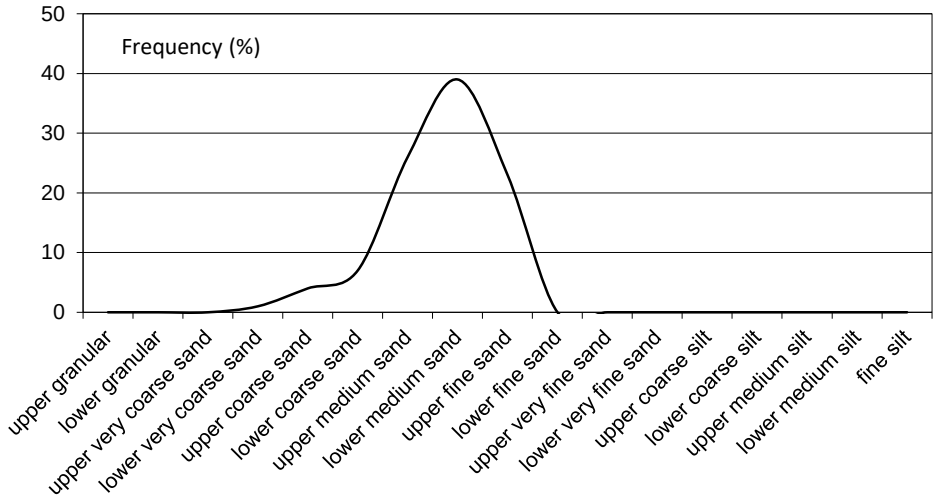

Grainsize variations within the sample

Location: 0738893 2849654
Sample Number: AJB_S_47
Crystal size: Fine

Crystallinity: Holocrystalline
Texture: Non-foliated, porphyritic

Detrital Mineralogy: Detrital mineralogy comprises abundant plagioclase feldspar (59.0%) and clinopyroxene (18.5%), with subordinate undifferentiated crystals (6.0%). Plagioclase feldspar crystals are euhedral in shape, display polysynthetic twinning and most commonly constitute the groundmass. Large (1 mm), euhedral crystals of plagioclase also locally occur as phenocrysts, which are commonly pristine. Clinopyroxene (18.5%) occurs as subhedral to euhedral crystals, which commonly form the groundmass along with plagioclase feldspar. Clinopyroxene also locally occurs as phenocrysts. Undifferentiated grains (6.0%) are commonly associated with plagioclase feldspar and clinopyroxene crystals.

Authigenic Mineralogy: Authigenic minerals comprising authigenic cements (14.5%) and clays (2.0%) are abundant. Cements comprise ferroan calcite (8.5%) and haematite (6.0%). Ferroan calcite commonly heals veins that cross-cut the sample. Haematite locally replaces plagioclase feldspar and forms part of the groundmass. It is most likely, that haematite represents weathering of the sample. Chlorite (2.0%) occurs in an acicular habit, forming part of the groundmass

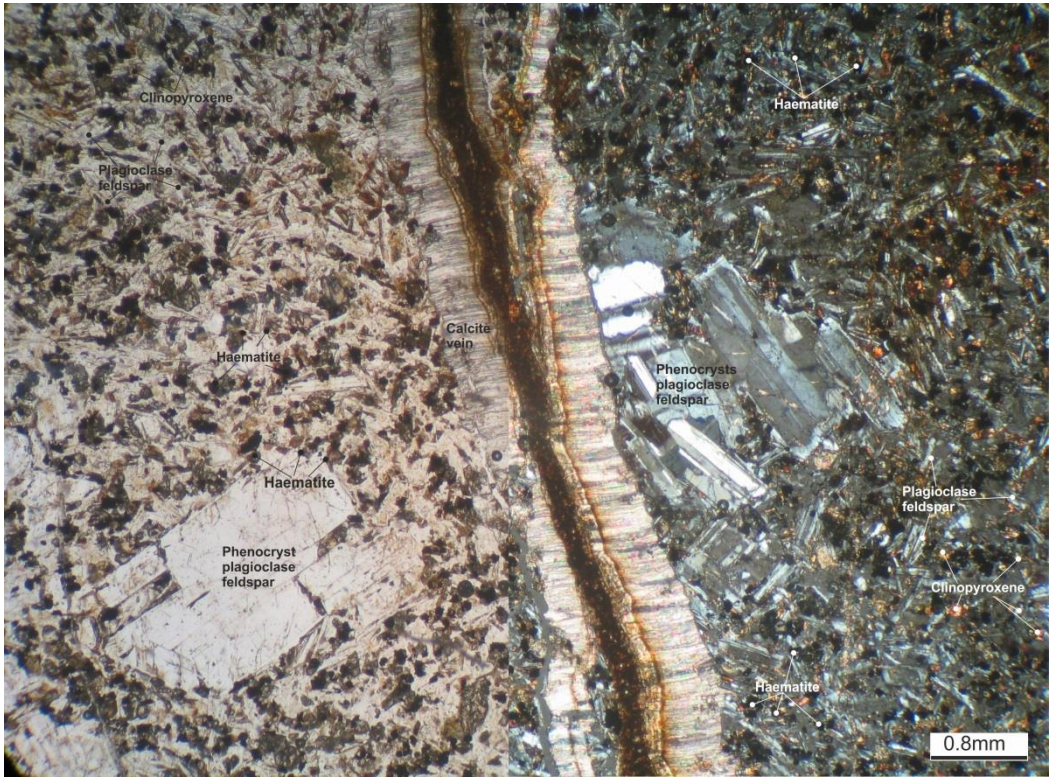

Location: 0736088 2852264
Sample Number: AJB_S_48
Crystal size: Medium

Crystallinity: Holocrystalline
Texture: Non-foliated, porphyritic

Detrital Mineralogy: The detrital mineralogy is composed of: plagioclase feldspar (49%), undifferentiated grains (14.5%), polycrystalline quartz (8.5%), clinopyroxene (3%), monocrystalline quartz (1%) and apatite (1%). The plagioclase feldspar and undifferentiated grains form part of the groundmass. The quartz (monocrystalline and polycrystalline) form phenocrysts and are likely to be in-filled vesicles (amygdales) around the edges of the quartz grains is epidote and altered epidote, the quartz is replacing the epiodote which is breaking down. The apatite is forming within a few of the quartz grains. The quartz grains are unstrained.

Authigenic Mineralogy: The authigenic mineralogy contains ferroan-calcite (9.5%), haematite (7%), epidote (5%), feldspar overgrowths (1%) and chlorite (0.5%). The calcite forms veins within sample, of which there are multiple and all form in the same orientation. The haematite is slowly replacing the plagioclase feldspar. The plagioclase feldspar overgrowths are syntaxial and discontinuous around the plagioclase feldspar host grains; rapakivi overgrowths are also noted. The chlorite within the section forms within the groundmass.

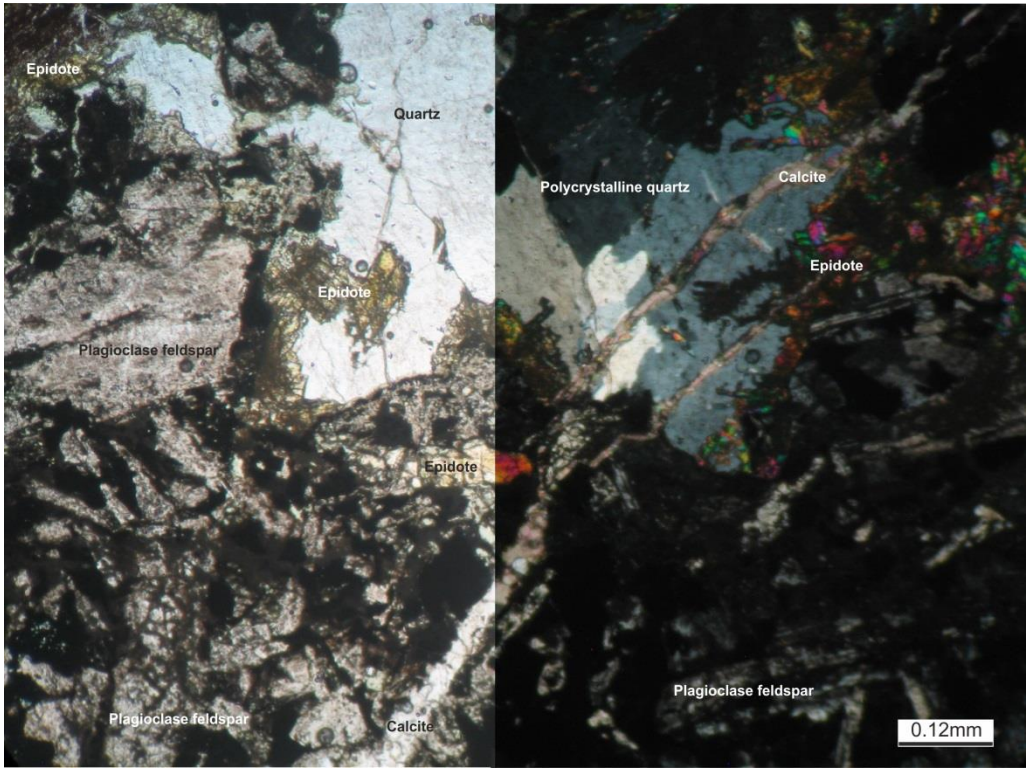

Appendix 3.b: SEM data

Log: 1
Height: 1.90 m
Sample Number: 4
Sandstone name: Darjaniyon-ki Dhani

Facies: M
Architectural Element: Gravel bar (F3)

Grainsize: Upper coarse sand
Sorting: Moderate
Roundness: Sub-rounded
Sandstone classification: Quartzarenite

Detrital Mineralogy: The rigid detrital mineralogy grains are composed of abundant monocrystalline quartz (38.5%) and polycrystalline quartz (27.5%) with minor undifferentiated grains (16%), rigid rock fragments (sedimentary 3%, metamorphic 1%, igneous trace). Some monocrystalline quartz grains are weakly-strained. Polycrystalline quartz grains have sutured grain contacts. Undifferentiated grains are opaque and being replaced by haematite cement. Sedimentary fragments are chert and can be fragmented. Metamorphic fragments contain elongated, sutured polycrystalline quartz and muscovite grains, creating a schistose fabric. Optically non-resolvable clays (1.5%) are pore-filling and likely to be composed of illite and kaolinite.

Authigenic Mineralogy: Significant authigenic minerals contain cements and clays. Cements include haematite (6%), undifferentiated (2.5%) and quartz overgrowths (trace). Haematite is infilling the pores and coating the quartz grains. Undifferentiated cements are likely to be calcite from the pale colours in PPL and low birefringence, which infills the pore spaces. Thin (10 µm) quartz overgrowths are syntaxial and discontinuous around their host grains.

Reservoir Quality: Macroporosity is very low (3.5%) and composed of primary intergranular porosity and isolated.

SEM: Here, there are multiple quartz grains which can be seen by the silica and titanium content. The matrix is composed of aluminum and magnesium and manganese, which all form to create different types of clays.

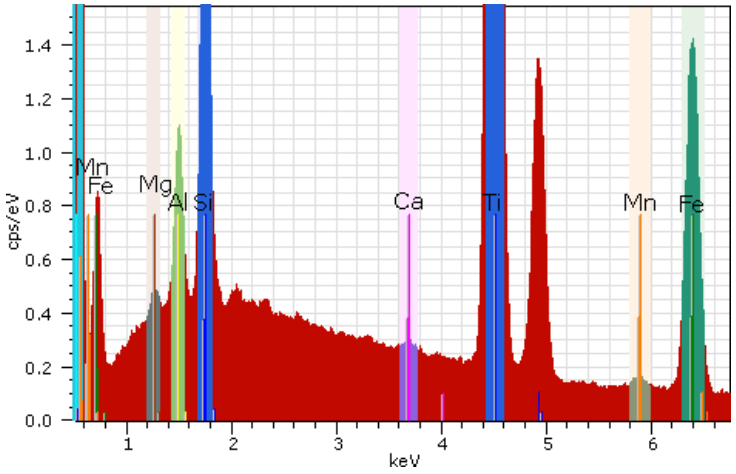

EDAX plot displaying silica with the highest electronvolts.

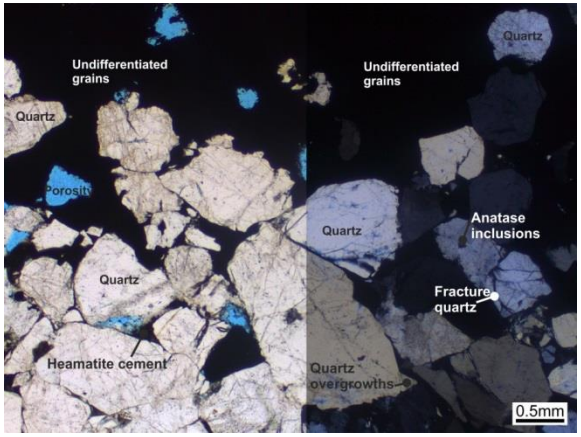

Poorly sorted, angular to Sub-rounded, upper coarse quartz grains up to 20 mm in length, which are heavily fractured in places. Undifferentiated grains fill half the sample.

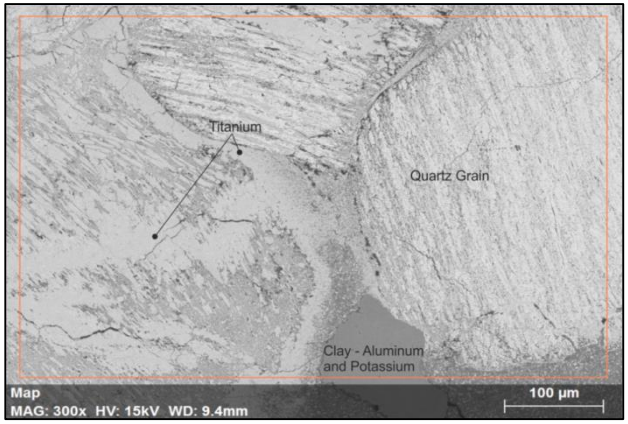

SEM section displays quartz grains (silica, titanium, magnesium, manganese and calcium). Between the grains there are non-resolvable clays, which are composed of oxygen, titanium and aluminium.

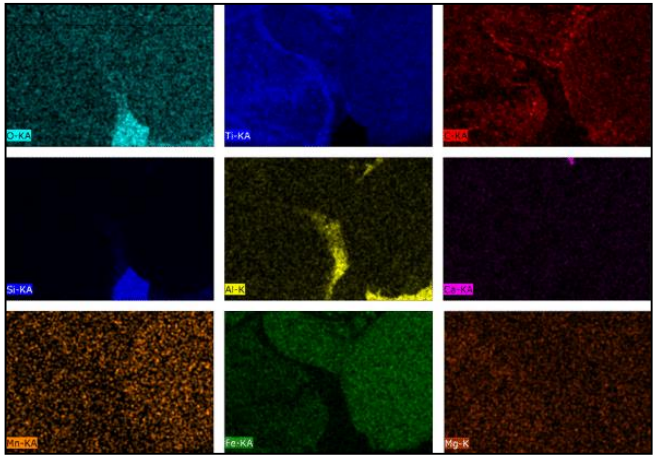

Plates above display the elements within the minerals of the SEM section. We see nine different elements above, compose to make the quartz, grains and the non-resolvable clays. The undifferentiated grains are quartz which have being heavily weathered by iron as seen above.

Log: 1
Height: 4.21 m
Sample Number: 9
Sandstone name: Darjaniyon-ki Dhani

Facies: M
Architectural Element: Gravel bar (F3)

Grainsize: Lower coarse sand
Sorting: Moderate
Roundness: Sub-rounded to subanguar
Sandstone classification: Quartzarenite

Detrital Mineralogy: The rigid detrital mineralogy comprises of abundant monocrystalline quartz (42%) and polycrystalline quartz (40%) with minor rigid rock fragments (metamorphic 5%, sedimentary 0.5%), and heavy minerals (trace). Smaller monocrystalline quartz grains are weakly-strained whereas the larger monocrystalline quartz grains are unstrained. Some grains are heavily fragmented. Polycrystalline quartz grains exhibit a concave-convex contact and some contacts are slightly sutured. Metamorphic fragments are sutured, elongated quartz grains with a schistose fabric. Sedimentary fragments are composed of chert. Ductile muscovite mica (trace) occurs within the polycrystalline quartz grains. Heavy minerals include tourmaline as inclusions within the quartz grains.

Authigenic Mineralogy: Authigenic mineralogy includes cements and clays. The cements include: quartz overgrowths (1.5%) and haematite (1%). Syntaxial quartz overgrowths are discontinuous around the quartz host grain. Haematite chokes and in-fills the pores and forms from the edges of the pores inwards. There are no optically observable clays.

Reservoir Quality: There is a moderate macroporosity (10%) and only composed of primary intergranular porosity. Approximately 30% of the porosity is interconnected.

SEM: The quartz grains are sub-angular to sub-rounded, with quartz overgrowths (10 µm). Other grains are zircon. In-between the rigid detrital grains are muscovite micas.

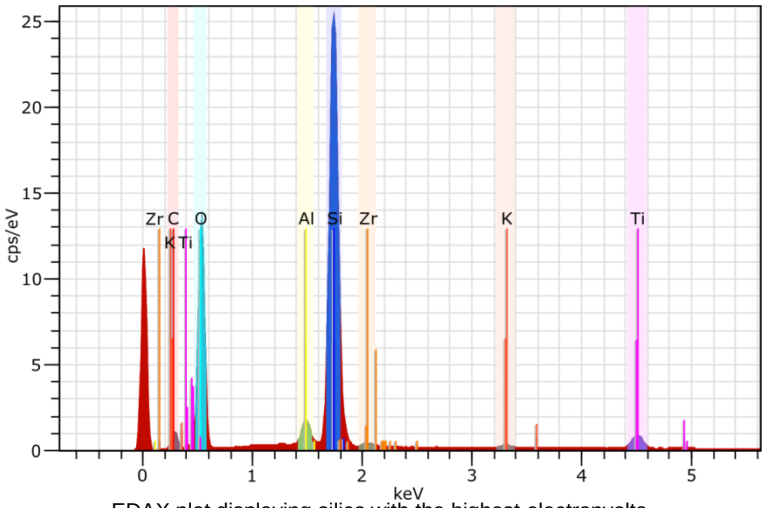

EDAX plot displaying silica with the highest electronvolts.

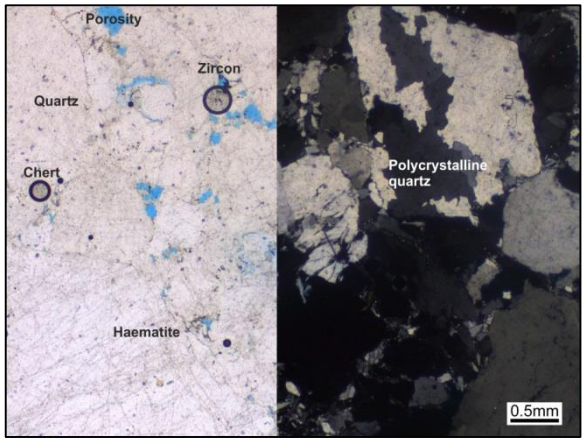

Lower coarse, moderately, Sub-rounded quartz grains, with zircon and chert (sedimentary rigid rock fragments). Between the grains are haematite cements and clays.

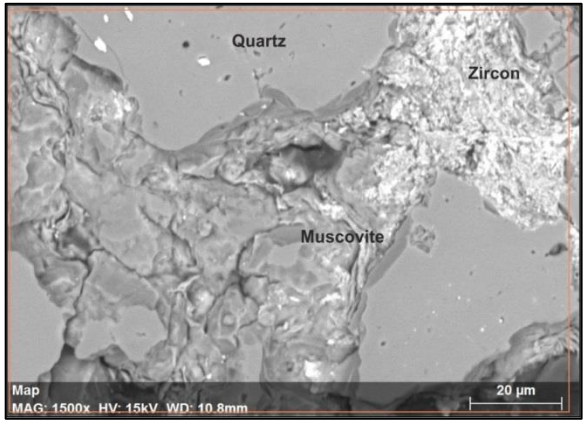

Grains include quartz and zircon. Matrix includes muscovite booklets.

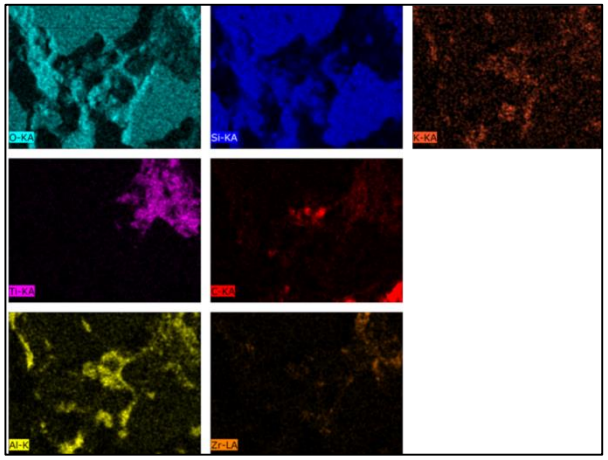

Brighter colours means higher abundance of the element, within the sample. Where silica and aluminium have the most content.

Log: 1
Height: 7.84 m
Sample Number: 14
Sandstone name: Darjaniyon-ki Dhani

Facies: Sm
Architectural Element: Floodplain (F7)

Grainsize: Lower medium sand
Sorting: Moderate
Roundness: Sub-rounded to sub-angular
Sandstone classification: Quartz wacke

Detrital Mineralogy: The rigid detrital mineralogy contains abundant monocrystalline quartz grains (38.5%) with minor polycrystalline quartz grains (11.5%). A few of the monocrystalline grains are slightly-strained. Polycrystalline quartz grains have long contacts within. Optically non-resolvable clays are composed of pseudomatrix (37.5%) and pore-filling clays (4%). The clays fill the pores and coat the grains and are likely to be composed of illite.

Authigenic Mineralogy: The authigenic mineralogy comprises of cements and clays. Cements include haematite (20%), quartz overgrowths (3%). Clays include kaolinite (0.5%) only. The haematite is patchy throughout the thin section and where it occurs it coats the grains and in-fills the pore space. The quartz overgrowths occur on the quartz grains and are discontinuous and syntaxial.

Reservoir Quality: Macroporosity is very low (1.5%), this is primary intergranular porosity.

SEM: The main quartz grain are dominantly composed of silica and oxygen. The matrix within the sample is composed of aluminum, potassium and iron, which make up the non-resolvable clays under the microscope.

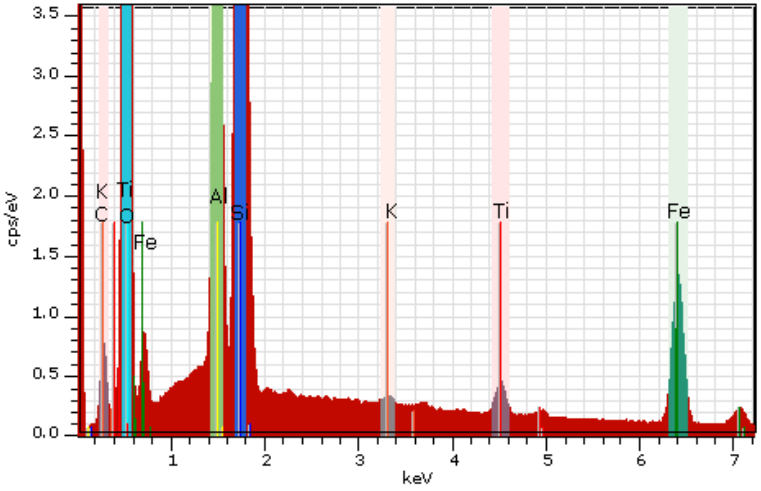

EDAX plot displaying silica with the highest electronvolts.

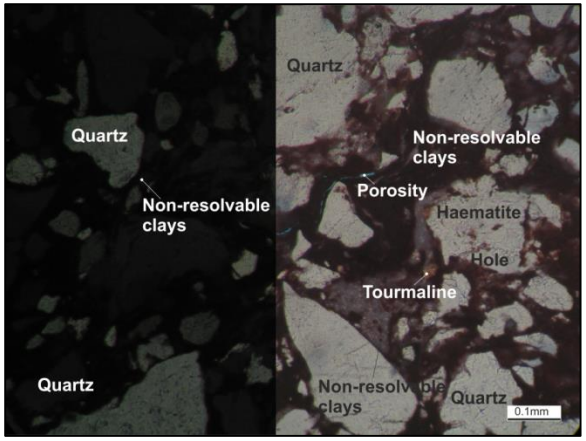

Lower medium quartz grains which are moderately sorted, from sub-angular to Sub-rounded. Non-resolvable clays are between the quartz grains. Porosity is low.

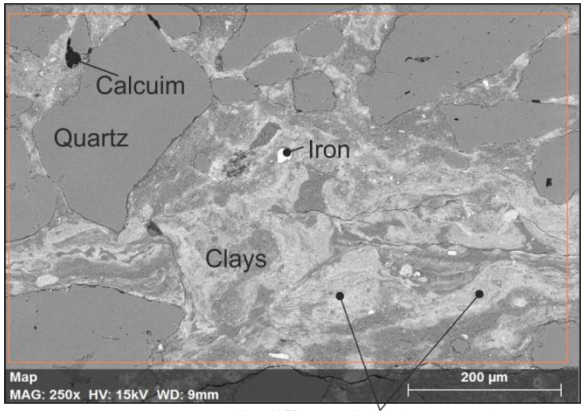

Undifferentiated cements

Quartz grains are Sub-rounded and composed of silica. There are clays and non-resolvable clays which are composed of aluminium, iron and potassium, likely illite.

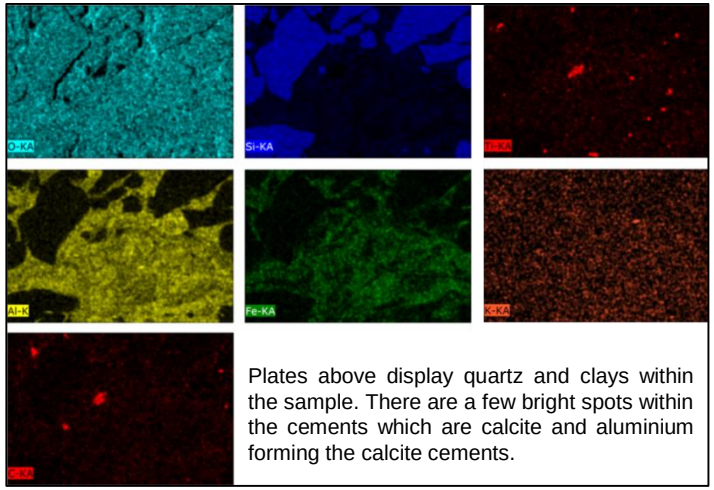

Plates above display quartz and clays within the sample. There are a few bright spots within the cements which are calcite and aluminium forming the calcite cements.

Log: 1
Height: 39.75 m
Sample Number: 25
Sandstone name: Sarnoo

Facies: Sb
Architectural Element: Channel (F1)

Grainsize: Lower very fine sand
Sorting: Moderately to well
Roundness: Rounded to Sub-rounded
Sandstone classification: Quartzarenite

Detrital Mineralogy: The detrital mineralogy is composed of monocrystalline quartz (44.5%)`, polycrystalline quartz (29%), with minor igneous rigid rock fragments (0.5%) and zircon (trace). The monocrystalline quartz grains are densely packed and have a concave-convex contacts, a limited number have an undulose extinction, which are weakly strained. The polycrystalline grains have long contacts.. The igneous rigid rock fragments are monocrystalline quartz grains with muscovite inclusions. The muscovite mica grains (trace) vary in length but are all elongated thin grains with second order birefringence colours. The non-resolvable clays (1%) are composed of detrital pore-filling clays (0.5%) and pseudomatrix (0.5%) and consist of illite.

Authigenic Mineralogy: The authigenic mineralogy comprises of quartz overgrowths (2%), pore-filling kaolinite (0.5%). The quartz grains are discontinuous around the monocrystalline grains and are syntaxial.

Reservoir Quality: Macroporosity is primary intergranular porosity at 22%, which is high, however the porosity is not interconnected.

SEM: There are multiple quartz grains. There are multiple areas which are clay rich and composed of aluminum, titanium and sulphur. Small areas of calcium and iron cements. Undifferentiated grains are composed of iron which suggests that the iron is replacing the silica.

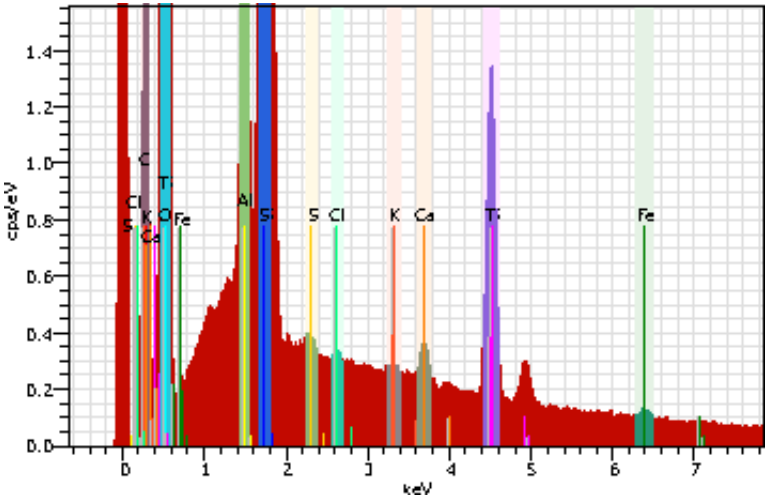

EDAX plot displaying silica with the highest electronvolts.

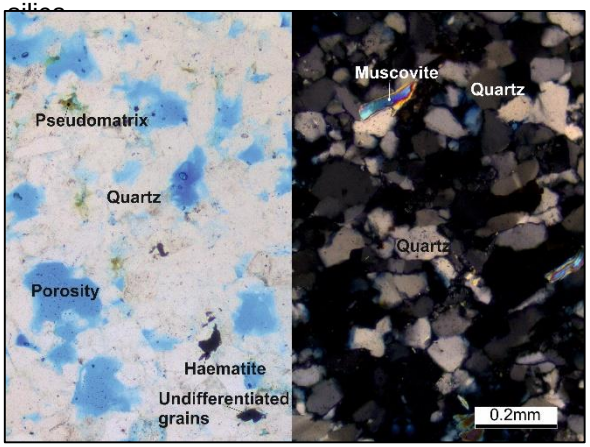

Very fine grained, moderate to well sorted, with Sub-rounded grains. There are multiple types of cements hematite and undifferentiated. There are undifferentiated grains. There is a high amount and multiple types of porosity.

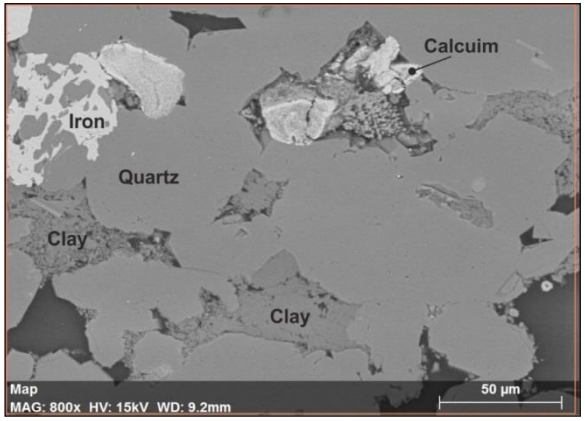

There are unfractured quartz grains. Between the grains there are clays and cements. Clays are composed of aluminium, titanium, sulphur and chlorine. The cements are iron and calcium. There are holes within the sample.

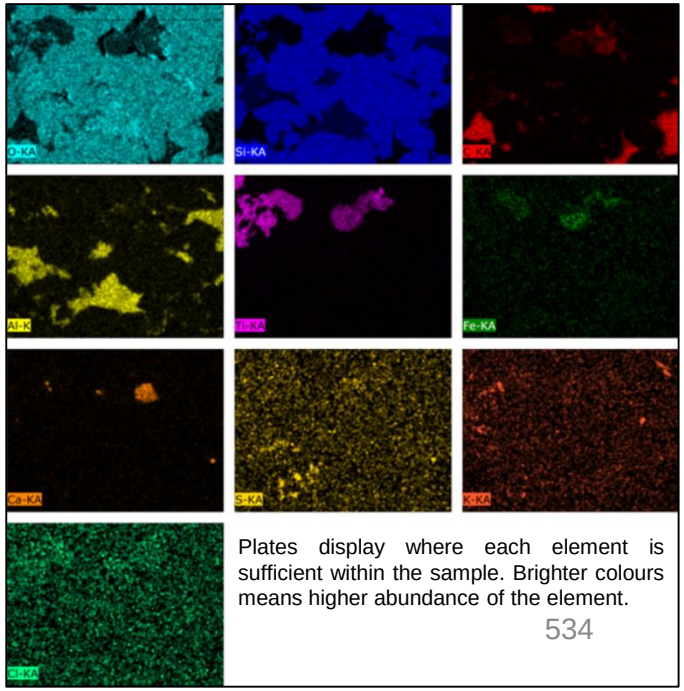

Plates display where each element is sufficient within the sample. Brighter colours means higher abundance of the element.

Log: 1
Height: 41.76 m
Sample Number: 36
Sandstone name: Sarnoo

Facies: Sb
Architectural Element: Channel (F1)

Grainsize: Upper very fine sand
Sorting: Moderate
Roundness: Sub-rounded
Sandstone classification: *haematitic* quartzarenite

Detrital Mineralogy: The detrital mineralogy consists of monocrystalline quartz (43.5%), polycrystalline (26.5%), rigid rock fragments (1%: sedimentary 0.5%, igneous 0.5%) and heavy minerals (0.5%). The monocrystalline quartz is slightly strained. The non-resolvable clay (3%: pseudomatrix 2%, detrital pore filing 1%), is discontinuous around the quartz grains. The sediment rock fragments are made from chert. The igneous fragments contain monocrystalline quartz with muscovite inclusions. The heavy minerals within the zircon and tourmaline. Ductile muscovite mica grains (2%) are pore choking. The grains are slightly aligned within the thin section.

Authigenic Mineralogy: The authigenic mineralogy composes of haematite (14.5%) and quartz overgrowths (1.5%). The haematite is pore-filling and coats multiple quartz grains. The quartz overgrowths are syntaxial and discontinuous around their quartz host grains.

Reservoir Quality: Macroporosity (8%) is composed of primary intergranular porosity (7.5%) and secondary oversized porosity (0.5%). The porosity is partly interconnected.

SEM: Images display quartz grains, cements and clays. There are quartz (silica) grains and overgrowths, muscovite (aluminum) grains. Iron cements are between the quartz grains. Undifferentaiated grains here are iron replacing the silica.

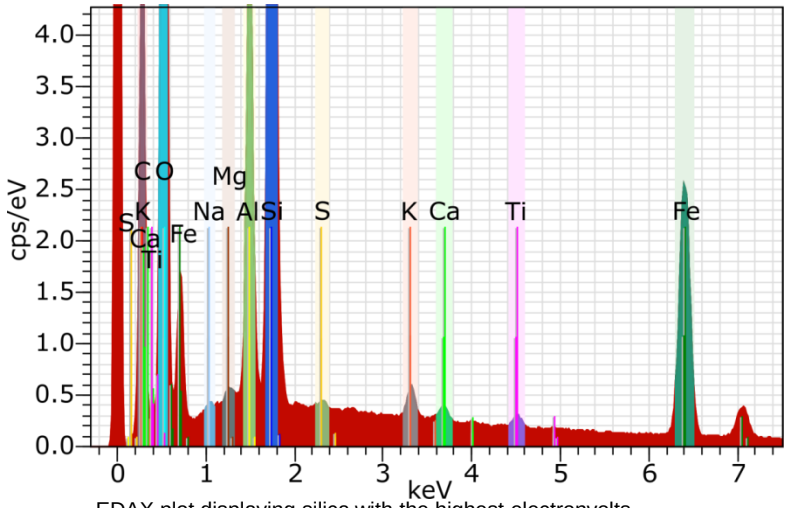

EDAX plot displaying silica with the highest electronvolts.

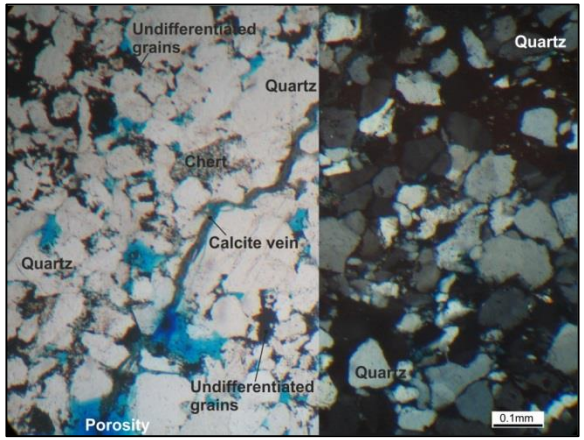

Moderately sorted, Sub-rounded, upper very fine grains. Calcite veins are within grains. Indifferentiated grains and cements are between the quartz grains. Matrix is within between the grains.

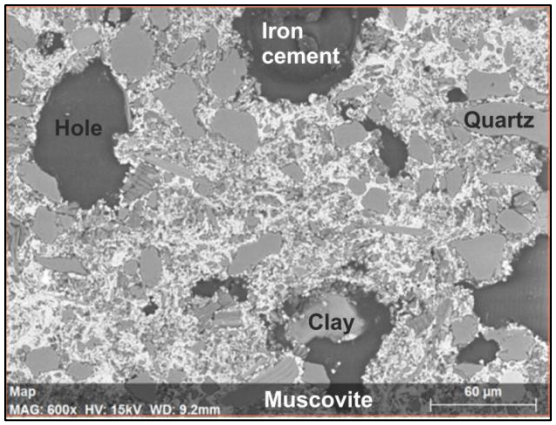

Silica is very abundant. Aluminium and iron cements are abundant between the grains.

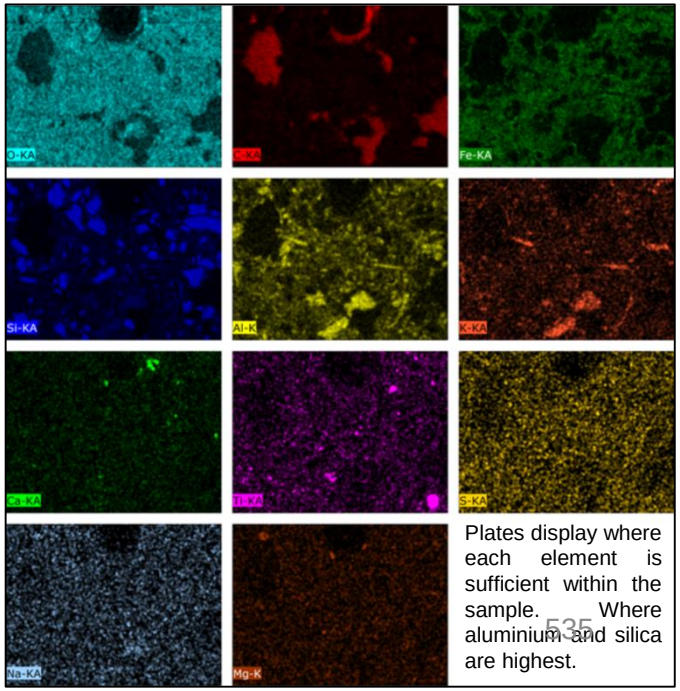

Plates display where each element is sufficient within the sample. Where aluminium and silica are highest.

Log: 13
Height: 8.00 m
Sample Number: 80
Sandstone name: Sarnoo

Facies: Sbfm
Architectural Element: Point bar (F5)

Grainsize: Lower coarse sand
Sorting: Moderately to well
Roundness: Sub-rounded to sub-angular
Sandstone classification: Sublithic arenite

Detrital Mineralogy: The main components of the detrital mineralogy are monocrystalline quartz (57.5%), polycrystalline (13%), and metamorphic rigid rock fragments (1%). The quartz grains are not strained. Some of the monocrystalline quartz grains corroded. The quartz and muscovite grains are interlayered. The metamorphic grains are slightly sutured quartz grains with muscovite within. The muscovite mica (1.5%) is pore-filling and coat a few of the grains. The non-resolvable clays (1.5%) are composed of pseudomatrix (1%) and pore-filling clays (0.%).

Authigenic Mineralogy: Major components of the authigenic mineralogy are cements haematite (3%), calcite (2.5%) and quartz overgrowths (1%). The haematite is within the pores. The calcite cement is coating the quartz grains. The quartz overgrowths are syntaxial and discontinuous around the host quartz grains. No clays are observed.

Reservoir Quality: The macroporosity (5.5%) is composed of only the primary intergranular porosity. The porosity is not interconnected.

SEM: Dominantly quartz grains which appear anhedral, dominated by silica and aluminum. There are calcite cements within. There are pore spaces visible, which have pore filling clays within, as seen on the plates.

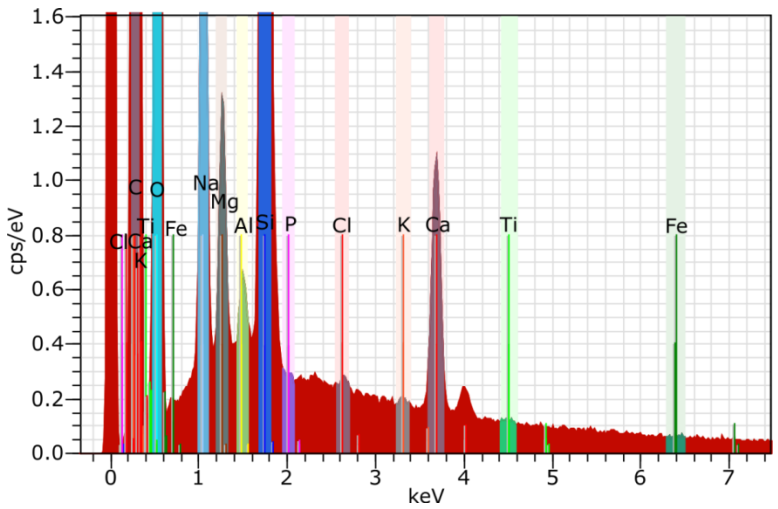

EDAX plot displaying silica with the highest electronvolts.

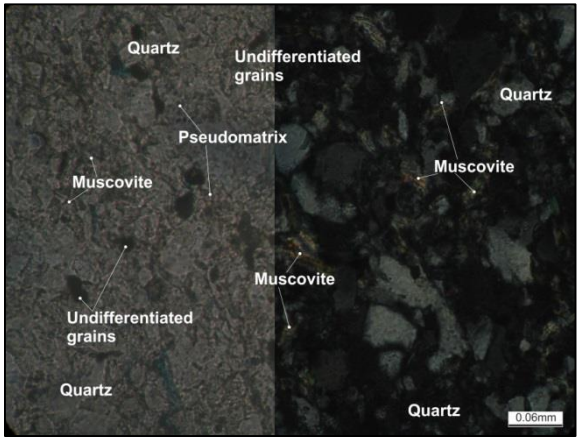

Lower coarse with moderately sorted, Sub-rounded monocrystalline quartz grains. Between the grains there are muscovite booklets and pseudomatrix. The porosity is low.

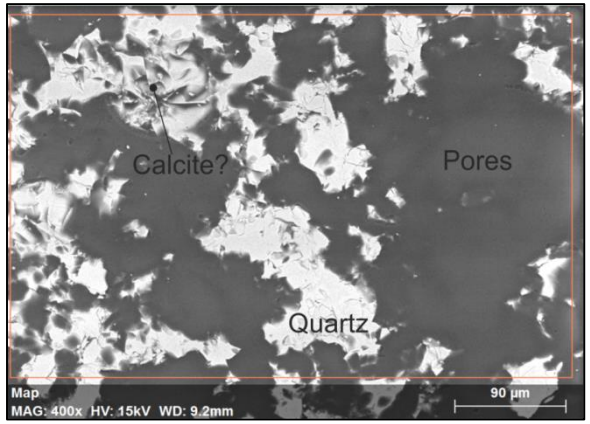

Quartz grains are Sub-rounded to sub-angular. Within the pores there are elements which are aluminium, titanium, potassium and chlorine

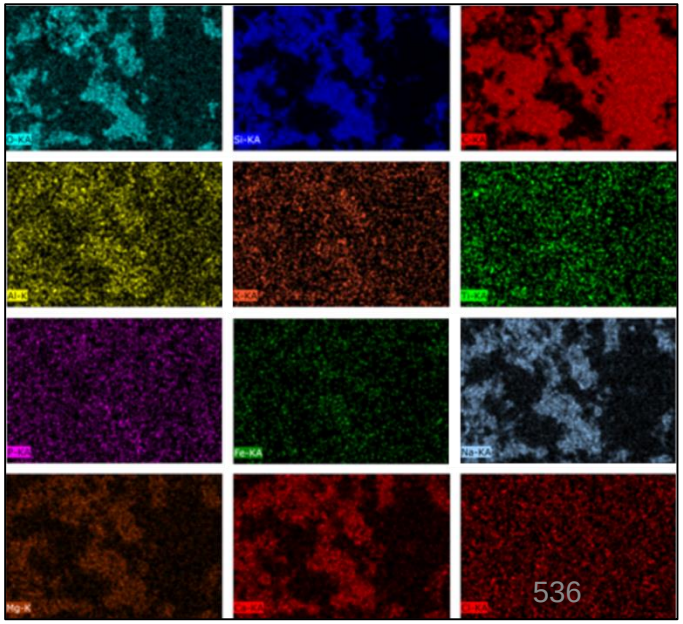

Brighter colours means higher abundance of the element, within the sample. Where silica, calcium, potassium, aluminium and titanium have the most content.

Log: 34
Height: 10.81 m
Sample Number: 44
Sandstone name: Nosar

Facies: G
Architectural Element: Channel (F1)

Grainsize: Lower coarse sand
Sorting: Poorly
Roundness: Sub-rounded to sub-angular
Sandstone classification: Quartz wacke

Detrital Mineralogy: The detrital mineralogy consists of monocrystalline quartz (42%) polycrystalline quartz (40.5%), and sedimentary rigid rock fragments (1%). The monocrystalline quartz is slightly strained and in the unstrained grains there are some rutile inclusions. The polycrystalline grains have concave-convex contacts. The sedimentary rigid rock grains are composed from chert. The muscovite grains (0.5%) are smaller in this sample then in the other samples. The detrital pore-filling clays (2%) has coated the quartz grains and filled the porosity.

Authigenic Mineralogy: The authigenic mineralogy contains quartz overgrowths (2%) and kaolinite (1%). The quartz overgrowths are syntaxial and discontinuous around the quartz host grains

Reservoir Quality: The macroporosity (10.5%) consists of primary intergranular porosity (9.5%), secondary oversized porosity (1%). The pores are approximately 40% interconnected.

SEM: Dominant grains are composed of silica and oxygen. Matrix is composed of aluminum, potassium, very minor amount of titanium and iron, accounting for the non-resolvable clays under the microscope.

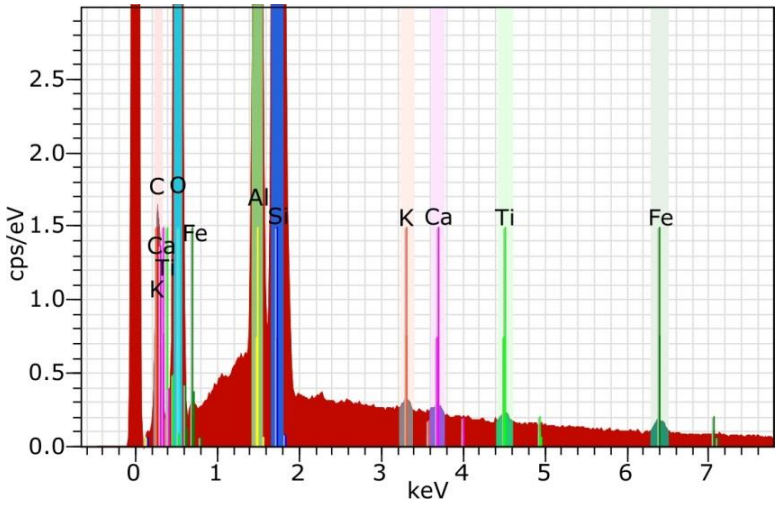

EDAX plot displaying silica with the highest electronvolts.

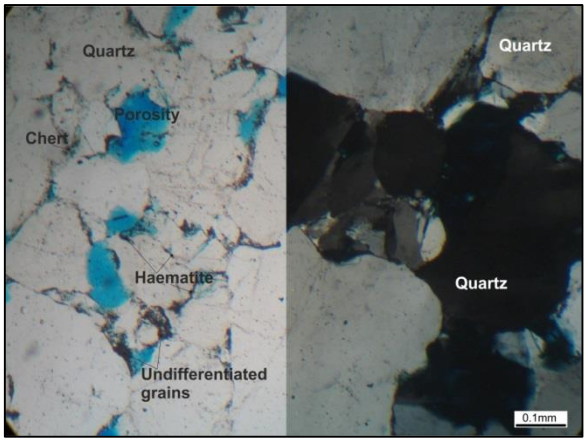

Poorly sorted, Sub-rounded, lower coarse grains. Undifferentiated grains and haematite cements are present. Pore are evident.

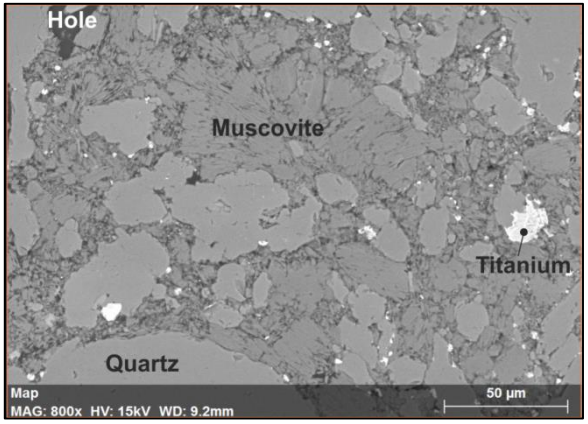

Quartz grains are present with overgrowths. Muscovite occurs in booklets and composed of aluminium, titanium and potassium. Calcium cement is noted. Pores are noted in SEM.

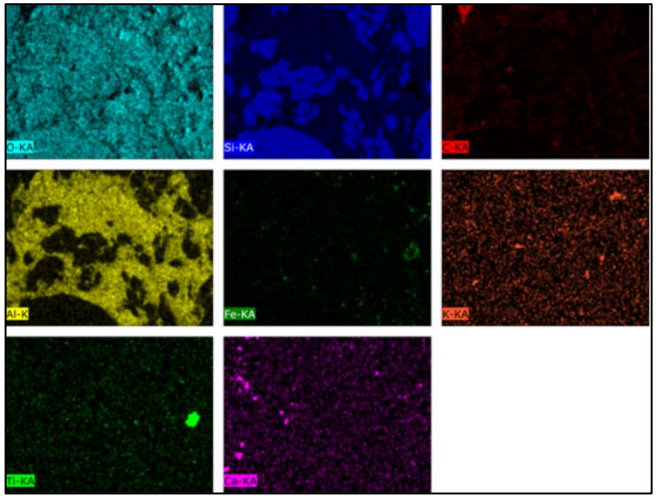

Brighter colours means higher abundance of the element, within the sample. Where aluminium is highest.

Log: 34
Height: 14.00 m
Sample Number: 49
Sandstone name: Nosar

Facies: Sxf
Architectural Element: Gravel bar (F2)

Grainsize: Upper fine sand
Sorting: Moderate
Roundness: Sub-rounded to sub-angular
Sandstone classification: Sublithic arenite

Detrital Mineralogy: The detrital mineralogy comprises of abundant polycrystalline quartz (41.5%) and monocrystalline quartz (40.5%), with subordinate amounts of metamorphic rigid rock fragments (3%), sedimentary rigid rock fragments (2.5%) igneous rigid rock fragments (1%), heavy minerals (trace), undifferentiated grains (trace) and ductile grains (trace). Monocrystalline grains are weakly-strained and display sutured contacts at times. Metamorphic grains comprise polycrystalline quartz grains exhibiting a schistose fabric. Sedimentary grains are formed of chert, whilst igneous fragments are composed of quartz and muscovite grains. Heavy minerals include tourmaline, zircon and rutile. Ductile grains comprise of muscovite mica which is buckled between the rigid grains, locally the terminations are being replaced by kaolinite. The micas are within the primary pore spaces. Optically non-resolvable clay (3%), coats grains and fills primary pore spaces. The undifferentiated grains are being replaced by haematite.

Authigenic Mineralogy: Authigenic mineralogy comprises of authigenic cements and clays. Cements include quartz overgrowths (1.5%), haematite (0.5%) and anatase (trace), whilst clays comprise kaolinite (1.5%). Syntaxial quartz grains are thin (1-3 µm) discontinuous around their host grains, primarily monocrystalline quartz. The haematite locally coats and replaces grains. Cubic anatase crystals locally occlude intergranular areas. Kaolinite booklets locally choke the primary and secondary pores.

Reservoir Quality: The macroporosity is minor (5%) composed of primary intergranular porosity. The porosity is isolated.

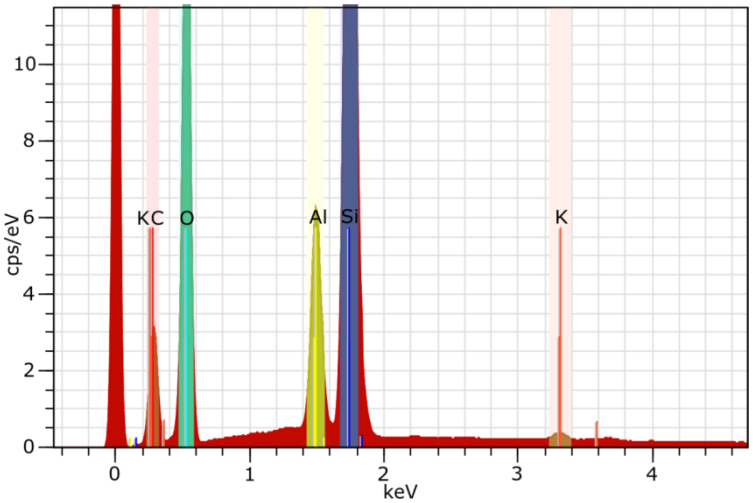

EDAX plot displaying silica with the highest electronvolts.

SEM: Dominantly quartz grains which appear subhedral, commonly with quartz overgrowths at 5 µm. Muscovite booklets are infilling the pores holes. Pore space is noted.

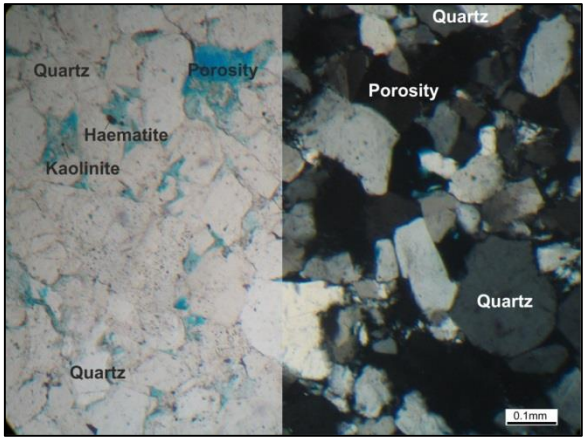

Moderately sorted, Sub-rounded, upper fine monocrystalline quartz grains. Haematite cements are dominant. Kaolinite clays are pore-filling. Porosity is low.

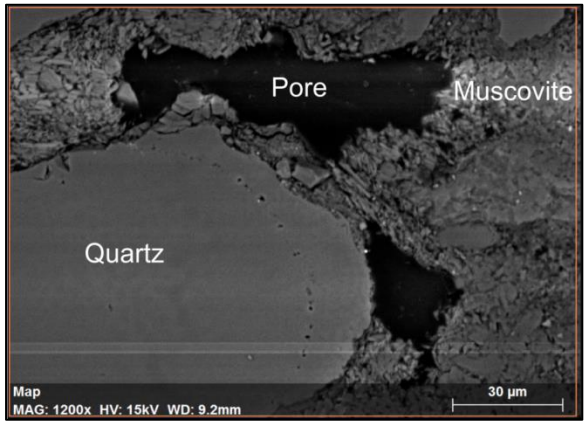

Quartz grains with quartz overgrowths (15 µm) upon. Muscovite booklets in filling the pore spaces. Pores visible.

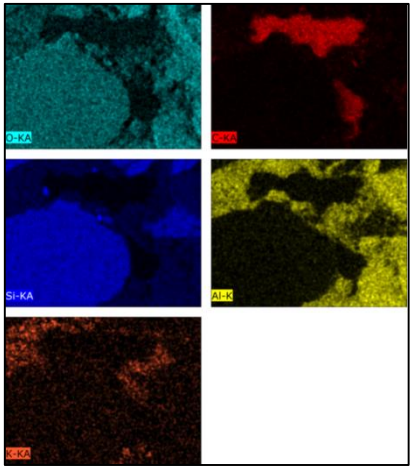

Brighter colours means higher abundance of the element, within the sample. Where silica and aluminium have the most content.

Log: 55
Height: 7.36 m
Sample Number: 101
Sandstone name: Nosar

Facies: Sxm
Architectural Element: Channel (F1)

Grainsize: Upper medium sand
Sorting: Moderately to well
Roundness: Sub-rounded
Sandstone classification: Quartzarenite

Detrital Mineralogy: The abundant components of the detrital mineralogy are monocrystalline quartz (42%) and polycrystalline quartz (32%) with minor components of rigid rock fragments (7%: metamorphic 5.5%, sedimentary 1.5%). The monocrystalline grains are slightly-strained to unstrained. The metamorphic grains are composed of sutured, broken and elongated polycrystalline quartz grains. The detrital pore-filing non-resolvable clay (4.5%) are within the pore spaces.

Authigenic Mineralogy: The authigenic mineralogy comprises of cements and clays. Cements include ferroan calcite (2%), quartz overgrowths (1%) and haematite (trace). Clays include kaolinite (4%) and non-resolvable detrital pore-filling clay (1.5%). The quartz overgrowths are syntaxial and are discontinuous around the host quartz grains. The kaolinite, detrital pore-filling clays and calcite cements are filling the pores.

Reservoir Quality: Macroporosity (6%) contains primary intergranular porosity (5.5%) and secondary intragranular porosity (0.5%). Approximately 10% of the pores are interconnected.

SEM: Quartz grains are composed of silica. Between the quartz grains are clays composed of kaolinite booklets (composed of aluminum, calcium and calcite elements).

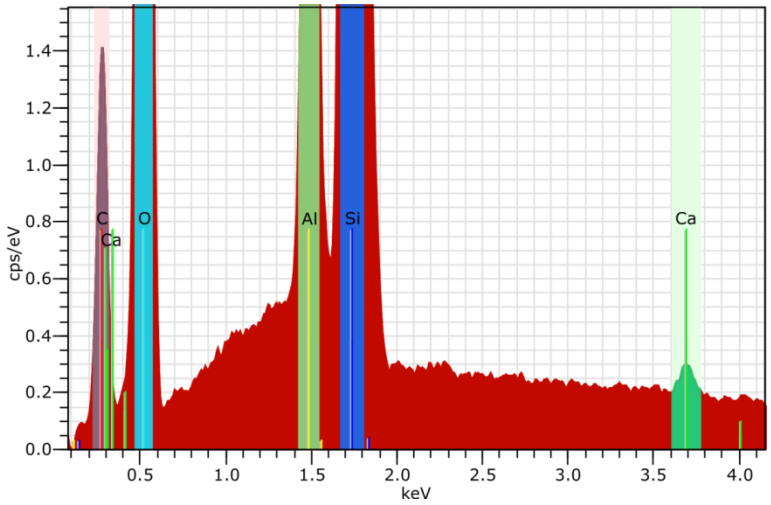

EDAX plot displaying silica with the highest electronvolts.

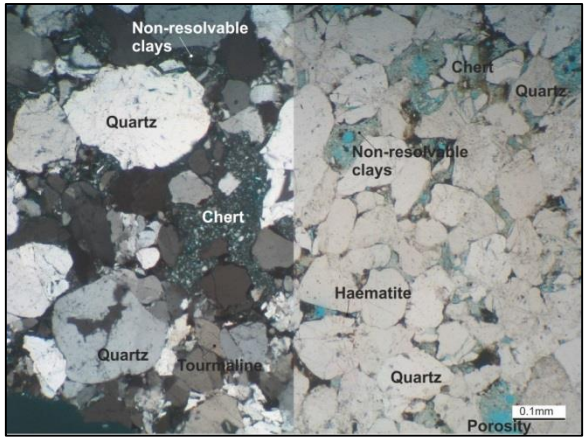

Subrouned, moderately sorted grains, dominated by monocrystalline quartz. Between the grain are non-resolvable clays and haematite cements. Pore space is low.

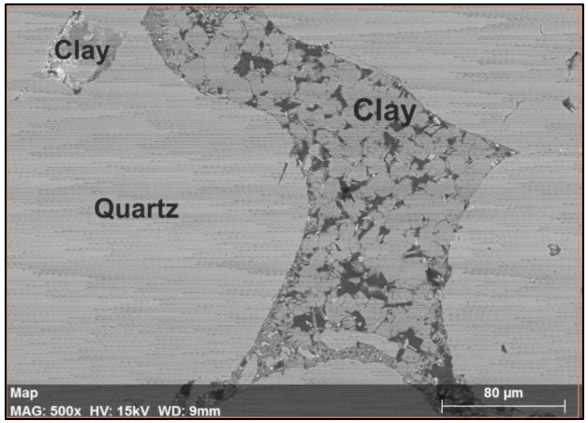

Quartz grains surrounded by kaolinite booklets, limited pore space observed.

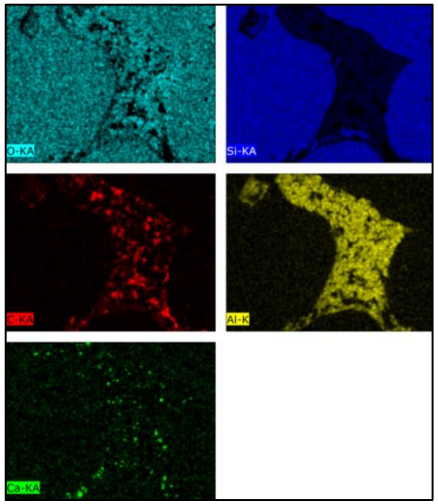

Brighter colours means higher abundance of the element, within the sample. Where silica and aluminium have the most content.

Location: 0779950 2842100
Sample Number: AB49
Crystal size: Very fine

Crystallinity: Hypocrystalline?
Texture: Non-foliated

Due to the grain size the mineralogy was not point counted. Therefore we have a brief thin section description only.

As the grainsize is so fine it is likely that the groundmass is a devitrified glass which is now composed of plagioclase feldspar and augite. There are augite and ploycrystalline quartz phenocrysts, where at the centre there are undifferentiated grains (probably haematite – sample 4). Within the phenocrysts there are apatite crystals. The calcite veins are thinner than the previous samples and are altered by haematite. The haematite is replacing the glassy / plagioclase groundmass.

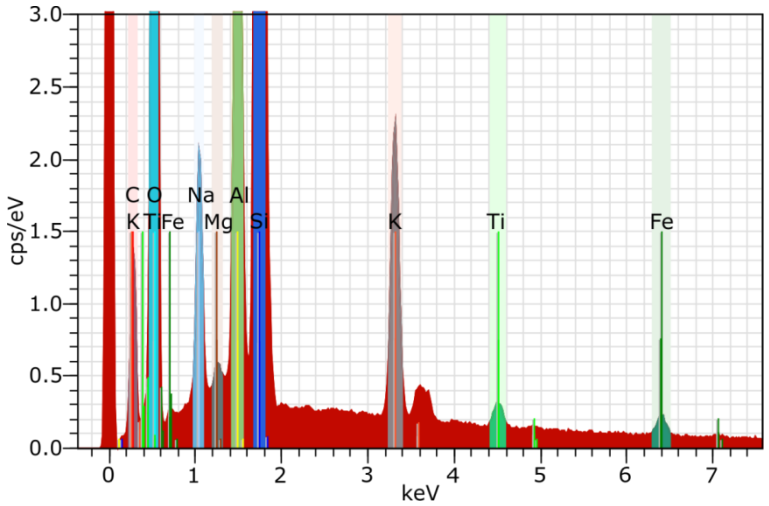

EDAX plot displaying silica with the highest electronvolts.

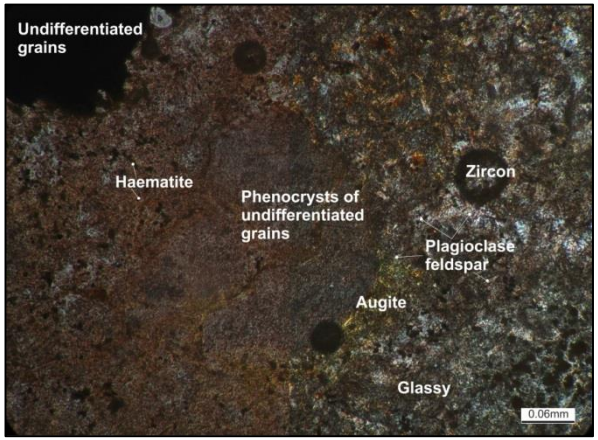

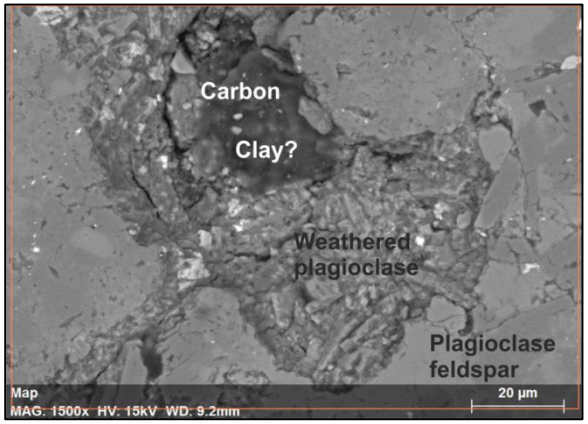

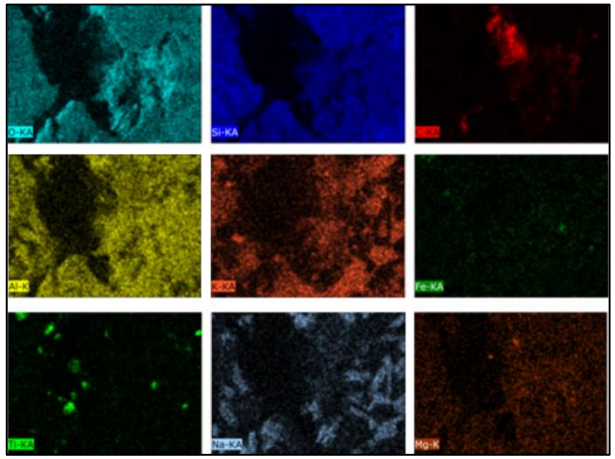

Brighter colours means higher abundance of the element, within the sample. Where silica, aluminium, potassium and sodium have the most content.

Location: 0779888 2842039
Sample Number: AB50
Crystal size: Medium

Crystallinity: Holocrystalline
Texture: Non-foliated, porphyritic

Detrital Mineralogy: The detrital mineralogy comprises of abundant plagioclase feldspar (68.5%) with subordinate clinopyroxene (10.5%) and undifferentiated grains (10%). The plagioclase feldspars and clinopyroxene form the phenocrysts in the sample. The undifferentiated grains in thin section analysis are haematite under the SEM and EDAX plots. All three detrital minerals form the groundmass.

Authigenic Mineralogy: The authigenic mineralogy constitutes cements only. There are subordinate amounts of haematite (8.5%) within minor amounts are ferroan calcite (1.5%), feldspar overgrowths (0.5%) and chlorite (0.5%). The haematite is replacing the plagioclase feldspar. The calcite forms the veins in the sample which are randomly orientated. The feldspar overgrowths are syntaxial and discontinuous around the host grain.

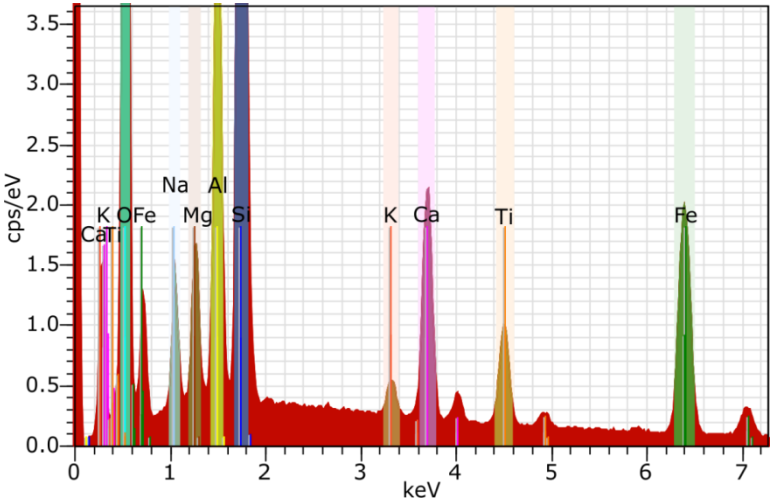

EDAX plot displaying silica with the highest electronvolts.

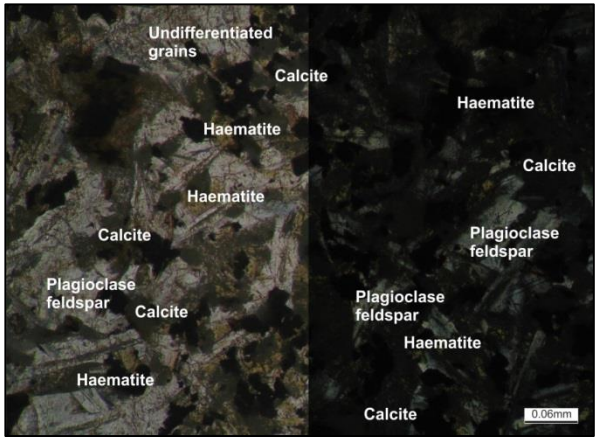

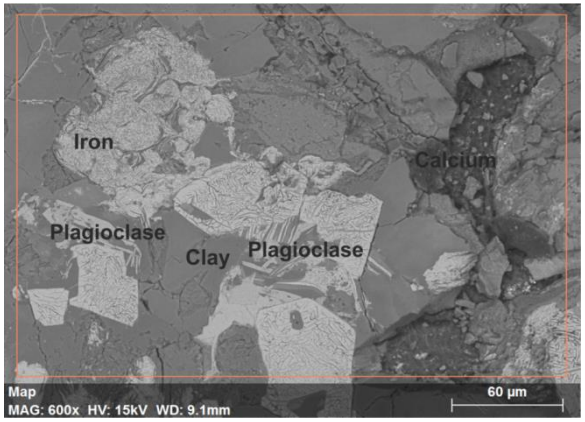

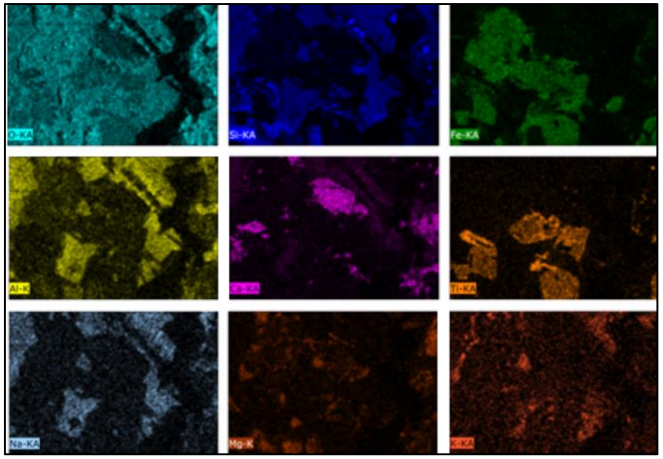

Brighter colours means higher abundance of the element, within the sample. Where iron, aluminium, titanium and sodium have the most content.

	Darjaniyon-ki Dhani Sandstone			Sarnoo Sandstone			Nosar Sandstone		
	Average	St. De.	St. Er.	Average	St. De.	St. Er.	Average	St. De.	St. Er.
Deitrital Mineralogy									
Quartz	64.46	9.18	2.54	75.89	5.94	1.36	81.64	6.11	1.44
Rigid rock fragmenets									
igneous	0.50			1.17	0.96	0.28	0.75	0.26	0.08
metamorphic	2.94	2.54	0.85	2.25	2.14	0.62	2.85	2.36	0.75
sedimentary	3.85	3.13	0.99	1.35	0.85	0.24	1.54	0.78	0.22
Heavy Minerals	0.50			0.70	0.27	0.12	0.50		
Undifferentiated	3.43	5.56	2.10	0.63	0.25	0.13	4.25	7.17	3.59
Muscovite Mica							0.80	0.67	0.30
Non-resolvable clay	10.31	11.32	3.14	3.24	3.62	0.88	5.33	4.07	0.96
Undifferentiated	1.50			1.36	0.89	0.24	5.65	3.96	0.96
Detrital pore-filling	2.67	4.20	1.21						
Pseudomatrix	14.36	10.99	4.15	2.40	3.22	0.83			
Authigenic Mineralogy									
Quartz Overgrowths	1.62	0.87	0.24	2.28	1.52	0.36	1.29	0.70	0.19
Calcite cement	2.90	2.72	1.22	1.94	0.68	0.24	5.00		
Dolomite cement	0.67	0.29	0.17	0.83	0.29	0.17	1.93	1.46	0.55
Haematite	8.62	7.23	2.00	4.69	4.43	1.04	0.92	0.66	0.27
pore-filling	8.62	7.23	2.00	5.28	4.35	1.09	1.00	0.65	0.24
Kaolinite	1.42	1.39	0.57	1.00	0.91	0.35	1.90	1.49	0.38
Undifferentiated	1.33	1.04	0.60	0.50			0.50		
Non-resolvable clay							1.50		
Marcoporosity									
Primary intergranular porosity	5.54	3.57	0.99	8.17	5.22	1.23	4.50	2.17	0.53
Secondary intragranular porosity	0.67	0.29	0.17	0.50			0.50		
Secondary 'oversized' porosity	1.50			0.50			1.08	0.49	0.20

Appendix 4: Palaeocurrent field data

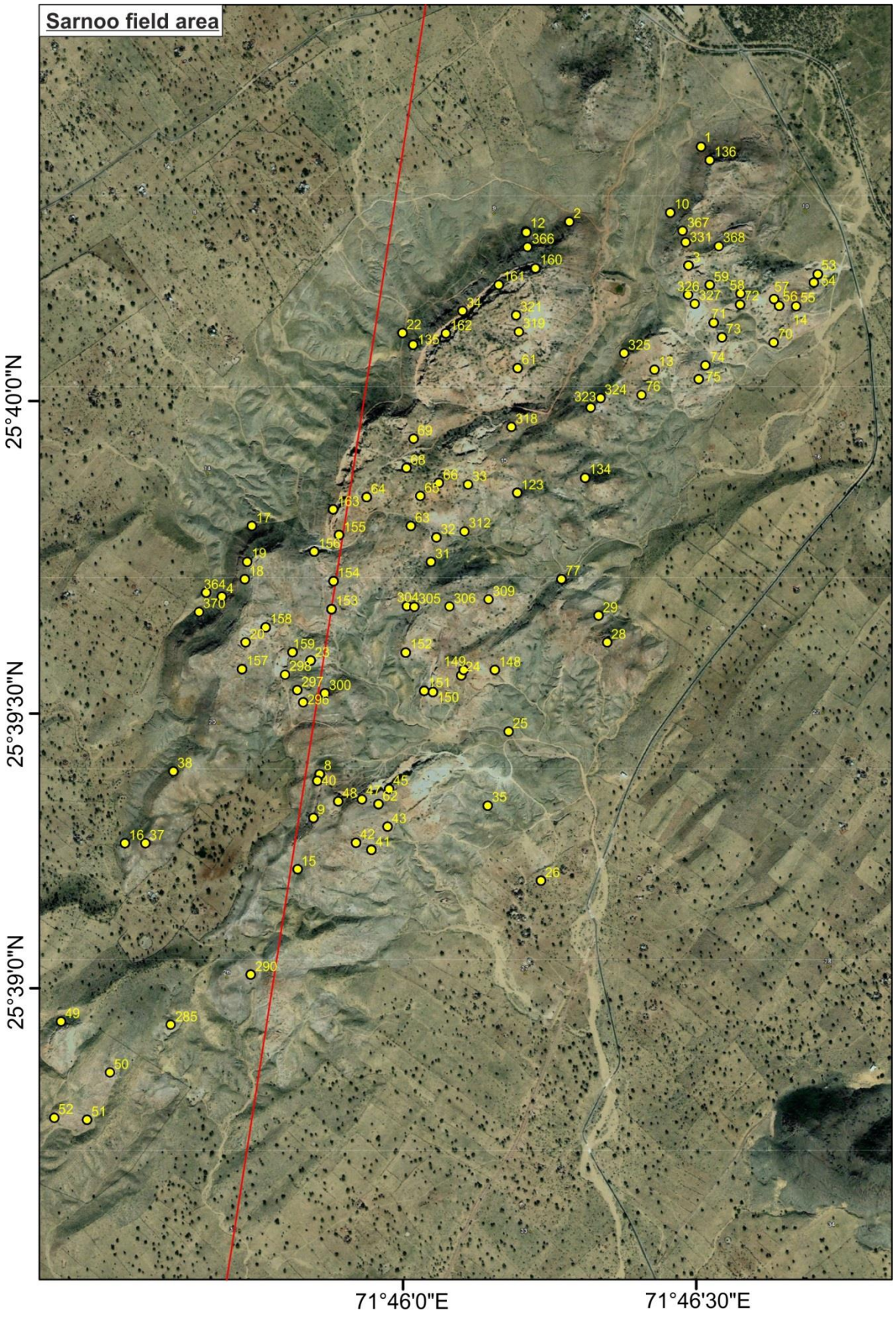
Sarnoo field area
25°40'0"N
25°39'30"N
25°39'0"N
71°46'0"E
71°46'30"E

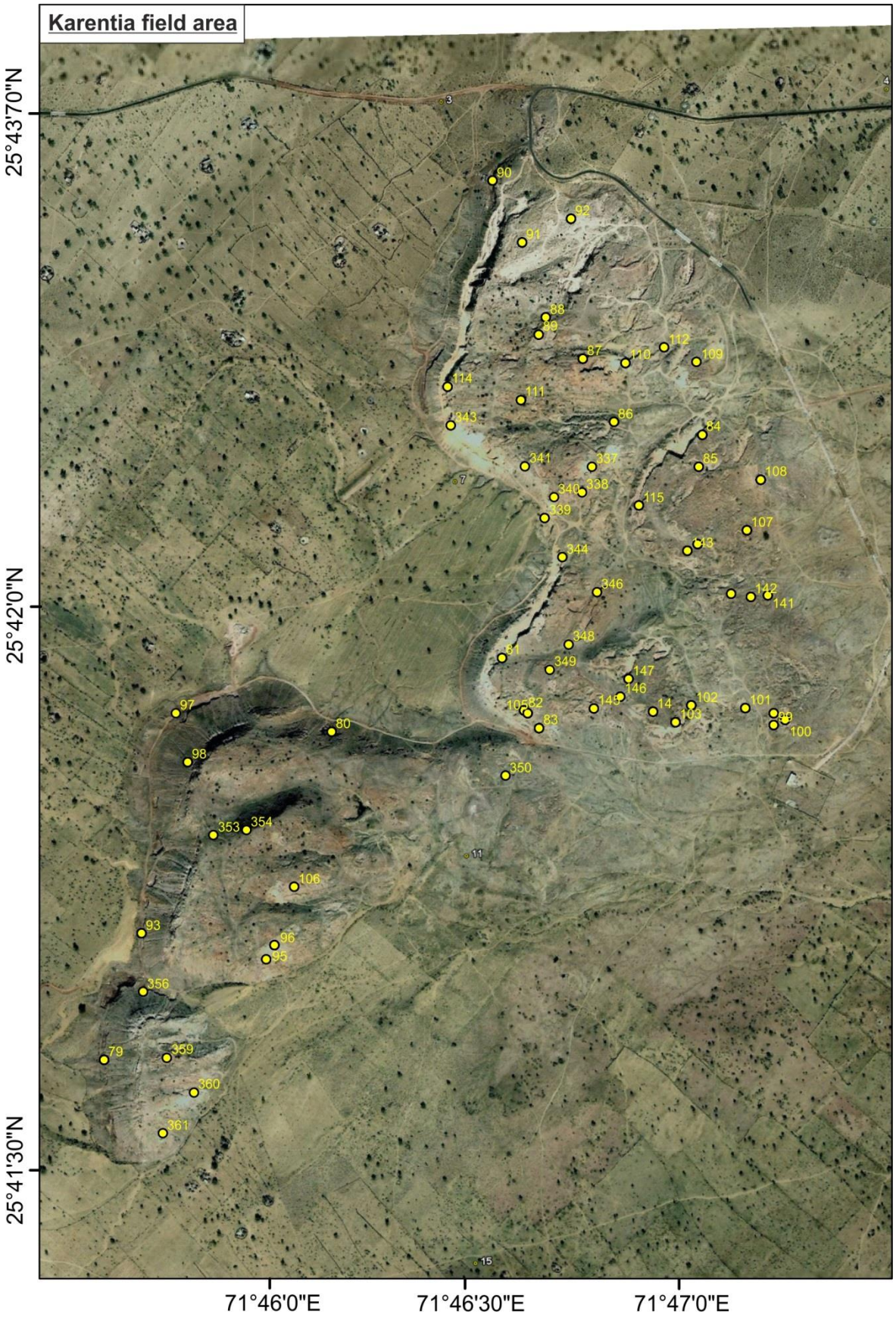
Karentia field area
25°43'70"N
25°42'0"N
25°41'30"N
71°46'0"E
71°46'30"E
71°47'0"E
90
92
91
88
89
87
110
112
109
114
111
343
86
84
341
337
85
108
340
338
115
339
107
113
344
346
142
141
348
81
349
147
146
105
82
149
14
102
101
103
83
100
97
80
98
350
353
354
11
106
93
96
95
356
79
359
360
361
15

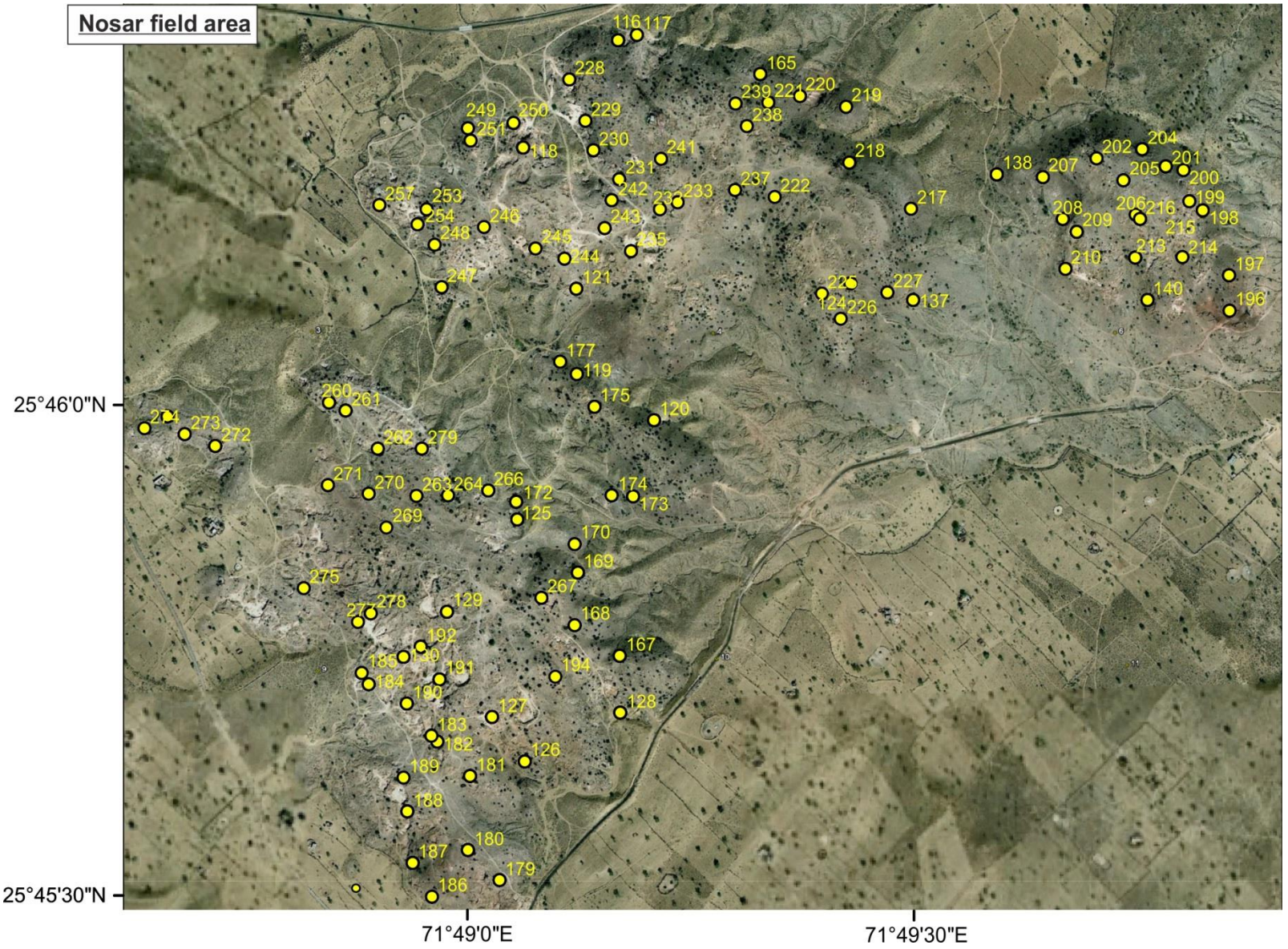
Nosar field area
25°46'0"N
25°45'30"N
71°49'0"E
71°49'30"E

Location	Northing	Easting	Log	Panel	Direction	Bi-directional	Dip	Sedimentary Structure
HZB_001	0778635	2842386	1		220			Cross Bedding
	0778635	2842386			207			Cross Bedding
	0778635	2842386			206			Cross Bedding
	0778635	2842386			43	223		Ripples
	0778635	2842386			100			Cross Bedding
	0778635	2842386			60	240		Ripples
	0778635	2842386			62	242		Ripples
	0778635	2842386			210			Cross Bedding
	0778635	2842386			228			Cross Bedding
	0778635	2842386			212			Cross Bedding
	0778635	2842386			218			Cross Bedding
	0778635	2842386			221			Cross Bedding
	0778635	2842386			251			Cross Bedding
	0778635	2842386			33	213		Ripples
	0778635	2842386			31			Cross Bedding
	0778635	2842386			210			Cross Bedding
HZB_002	0778254	2842168	2		252			Cross Bedding
	0778254	2842168			161			Cross Bedding
	0778254	2842168			221			Cross Bedding
	0778254	2842168			51	231		Ripples
	0778254	2842168			226			Cross Bedding
	0778254	2842168			231			Cross Bedding
	0778254	2842168			215			Cross Bedding
	0778254	2842168			272	92		Ripples
HZB_003	0778599	2842041	3		197			Cross Bedding
	0778599	2842041			199			Cross Bedding
	0778599	2842041			165			Cross Bedding
	0778599	2842041			170			Cross Bedding
	0778599	2842041			173			Cross Bedding
	0778599	2842041			176			Cross Bedding
	0778599	2842041			347			Cross Bedding
	0778599	2842041			169			Cross Bedding
	0778599	2842041			350			Cross Bedding
	0778599	2842041			170			Cross Bedding
	0778599	2842041			345			Cross Bedding
	0778599	2842041			168			Cross Bedding
	0778599	2842041	3		176			Cross Bedding
HZB_004	0777247	2841083			213			Cross Bedding
	0777247	2841083			215	35		Ripples
	0777247	2841083			198			Cross Bedding
	0777247	2841083			293			Cross Bedding
	0777247	2841083			207			Cross Bedding
	0777247	2841083			216	36		Ripples

	0777247	2841083			219	39		Ripples
	0777247	2841083			219			Cross Bedding
	0777247	2841083			220			Cross Bedding
	0777247	2841083			219			Cross Bedding
	0777247	2841083			218			Cross Bedding
	0777247	2841083			216			Cross Bedding
	0777247	2841083			217			Cross Bedding
HZB_005	0779783	2842013	5		252			Cross Bedding
	0779783	2842013			236	56		Ripples
	0779783	2842013			209	29		Ripples
	0779783	2842013			210	30		Ripples
	0779783	2842013			222	42		Ripples
	0779783	2842013			232			Cross Bedding
	0779783	2842013			229			Cross Bedding
	0779783	2842013			226	46		Ripples
	0779783	2842013			257	77		Ripples
	0779783	2842013			231			Cross Bedding
	0779783	2842013			204			Cross Bedding
	0779783	2842013			235			Cross Bedding
	0779783	2842013			224			Cross Bedding
	0779783	2842013			222			Cross Bedding
HZB_006	0779959	2842038	6		230	50		Ripples
	0779959	2842038			231			Cross Bedding
	0779959	2842038			2226	46		Ripples
HZB_007	0779969	2842050	7		250			Cross Bedding
	0779969	2842050			240			Cross Bedding
	0779969	2842050			242			Cross Bedding
	0779969	2842050			14			Cross Bedding
	0779969	2842050			230			Cross Bedding
	0779969	2842050			236			Cross Bedding
HZB_008	0777531	2840569	8		239	59		Ripples
	0777531	2840569			232	52		Ripples
	0777531	2840569			230	50		Ripples
	0777531	2840569			215			Cross Bedding
	0777531	2840569			220			Cross Bedding
	0777531	2840569			218			Cross Bedding
	0777531	2840569			224			Cross Bedding
	0777531	2840569			38			Cross Bedding
	0777531	2840569			226			Cross Bedding
	0777531	2840569			232			Cross Bedding
	0777531	2840569			270			Cross Bedding
	0777531	2840569			149			Cross Bedding
	0777531	2840569			157			Cross Bedding
HZB_009	0777512	2840442	9		201			Cross Bedding
	0777512	2840442			203			Cross Bedding

	0777512	2840442			206			Cross Bedding
	0777512	2840442			200			Cross Bedding
	0777512	2840442			203			Cross Bedding
	0777512	2840442			192			Cross Bedding
	0777512	2840442			198			Cross Bedding
	0777512	2840442			206			Cross Bedding
	0777512	2840442			150			Cross Bedding
	0777512	2840442			192			Cross Bedding
	0777512	2840442			174			Cross Bedding
	0777512	2840442			210			Cross Bedding
	0777512	2840442			206	26		Ripples
	0777512	2840442			244			Cross Bedding
	0777512	2840442			203			Cross Bedding
	0777512	2840442			203			Cross Bedding
	0777512	2840442			194			Cross Bedding
	0777512	2840442			201			Cross Bedding
	0777512	2840442			184			Cross Bedding
	0777512	2840442			200			Cross Bedding
HZB_010	0778546	2842195	10		213			Cross Bedding
	0778546	2842195			216			Cross Bedding
	0778546	2842195			206			Cross Bedding
	0778546	2842195			229	49		Ripples
	0778546	2842195			227			Cross Bedding
	0778546	2842195			224			Cross Bedding
	0778546	2842195			211	31		Ripples
	0778546	2842195			174	354		Ripples
	0778546	2842195			228			Cross Bedding
	0778546	2842195			227			Cross Bedding
	0778546	2842195			228			Cross Bedding
	0778546	2842195			257	37		Ripples
	0778546	2842195			224	44		Ripples
	0778546	2842195			231	51		Ripples
HZB_011	0780744	2844534	11		196			Cross Bedding
	0780744	2844534			210			Cross Bedding
	0780744	2844534			190	10		Ripples
	0780744	2844534			181	1		Ripples
	0780744	2844534			22			Cross Bedding
	0780744	2844534			193			Cross Bedding
	0780744	2844534			195	15		Ripples
	0780744	2844534			158	338		Ripples
HZB_012	0778128	2842140	12		269		2	Cross Bedding
	0778128	2842140			354	174		Ripples
	0778128	2842140			181	1		Ripples
	0778128	2842140			282	82		Ripples
	0778128	2842140			263			Asymmetric

	0778128	2842140			268			Asymmetric
	0778128	2842140			253			Asymmetric
	0778128	2842140			251			Asymmetric
	0778128	2842140			252			Asymmetric
	0778128	2842140			254			Asymmetric
	0778128	2842140			264	84		Ripples
	0778128	2842140			286	106		Ripples
	0778128	2842140			244	64		Ripples
	0778128	2842140			232	52		Ripples
	0778128	2842140			232			Asymmetric
	0778128	2842140			227	47		Ripples
	0778128	2842140			226	46		Ripples
	0778128	2842140			29			Asymmetric
	0778128	2842140			231	51		Ripples
	0778128	2842140			71		2	Cross Bedding
	0778128	2842140			252		7	Cross Bedding
	0778128	2842140			39			Asymmetric Ripple
	0778128	2842140			261	81		Ripples
HZB_013	0778500	2841740		1	151			Trough Cross Bedding
	0778500	2841740			207		24	Cross Bedding
	0778500	2841740			310		21	Cross Bedding
HZB_014	0778889	2841926			251			Asymmetric
	0778889	2841926			68		3	Cross Bedding
	0778889	2841926			252		3	Cross Bedding
	0778889	2841926			7	187		Ripples
HZB_015	0777466	2840293			109		9	Cross Bedding
	0777466	2840293			193		10	Cross Bedding
	0777466	2840293			172		22	Cross Bedding
	0777466	2840293			201		17	Cross Bedding
	0777466	2840293			6	186		Ripples
HZB_016	0776966	2840369	13		327	147		Channel
	0776966	2840369			231	51		Ripples
	0776966	2840369			271	91		Ripples
	0776966	2840369			242	62		Ripples
	0776966	2840369			231	51		Ripples
	0776966	2840369			198	18		Ripples
	0776966	2840369			347			Asymmetric
	0776966	2840369			344	164		Ripples
	0776966	2840369			241	61		Ripples
	0776966	2840369			21		6	Cross Bedding
	0776966	2840369			209		12	Cross Bedding
	0776966	2840369			219		20	Cross Bedding
	0776966	2840369			36		1	Cross Bedding

	0776966	2840369			237		2	Cross Bedding
	0776966	2840369			354	174		Ripples
	0776966	2840369			217	37		Ripples
	0776966	2840369			18	209		Cross Bedding
	0776966	2840369			4	24		Cross Bedding
	0776966	2840369			11	209		Cross Bedding
	0776966	2840369			207	27		Ripples
	0776966	2840369			341	161		Ripples
	0776966	2840369			242	62		Ripples
	0776966	2840369			313	131		Ripples
	0776966	2840369			251	31		Ripples
	0776966	2840369			220	40		Ripples
HZB_017	0777334	2841287	14		219	39		Ripples
	0777334	2841287			242		0	Cross Bedding
	0777334	2841287			207			Asymmetric
	0777334	2841287			70			Asymmetric
	0777334	2841287			271	91		Ripples
	0777334	2841287			264	84		Ripples
	0777334	2841287			211	41		Ripples
	0777334	2841287			180	360		Channel
	0777334	2841287			273	93		Ripples
	0777334	2841287			260	80		Ripples
	0777334	2841287			89			Asymmetric
	0777334	2841287			40		18	Asymmetric
	0777334	2841287			338		10	Cross Bedding
	0777334	2841287			140		12	Asymmetric
	0777334	2841287			280	60		Ripples
	0777334	2841287			247	27		Ripples
	0777334	2841287			87			Asymmetric
	0777334	2841287			280	100		Ripples
	0777334	2841287			260	80		Ripples
	0777334	2841287			330			Cross bedding
	0777334	2841287			242		2	Low angle cross bedding
	0777334	2841287			213	33		Ripples
	0777334	2841287			213		34	Asymmetric
	0777334	2841287			207	27		Ripples
	0777334	2841287			136	316		Ripples
HZB_018	0777314	2841133		2	202	22		Ripples
	0777314	2841133			210		16	Cross Bedding
	0777314	2841133			184		12	Cross Bedding
	0777314	2841133			201		17	Cross Bedding
	0777314	2841133			201		5	Cross Bedding
	0777314	2841133			23		3	Cross Bedding
HZB_019	0777320	2841184			354	174		Ripples

	0777320	2841184			350	170		Ripples
	0777320	2841184			355	175		Ripples
	0777320	2841184			315	135		Ripples
HZB_020	0777316	2840950			203	23		Ripples
	0777316	2840950			330		8	Asymmetric
HZB_022	0777771	2841846	15		9		10	Asymmetric
	0777771	2841846			219	39		Ripples
	0777771	2841846			197	17		Ripples
	0777771	2841846			325	145		Ripples
	0777771	2841846			108		14	Asymmetric
	0777771	2841846			336	151		Ripples
	0777771	2841846			246	64		Ripples
	0777771	2841846			216		24	Asymmetric
	0777771	2841846			164		12	Cross Bedding
	0777771	2841846			224	44		Ripples
	0777771	2841846			191	11		Ripples
	0777771	2841846			178		21	Asymmetric
	0777771	2841846			354	174		Ripples
	0777771	2841846			226	46		Ripples
	0777771	2841846			191	11		Ripples
	0777771	2841846			214		19	Asymmetric
	0777771	2841846			211		14	Cross Bedding
	0777771	2841846			209	29		Ripples
	0777771	2841846			229			Asymmetric
	0777771	2841846			211	31		Ripples
	0777771	2841846			139		9	Cross Bedding
	0777771	2841846			47	227		Ripples
	0777771	2841846			183			Asymmetric
	0777771	2841846			217	37		Ripples
	0777771	2841846			193		2	Cross Bedding
	0777771	2841846			190		16	Cross Bedding
	0777771	2841846			29		6	Cross Bedding
	0777771	2841846			350	170		Ripples
	0777771	2841846			334	154		Ripples
	0777771	2841846			199	19		Ripples
	0777771	2841846			208		16	Cross Bedding
	0777771	2841846			206			Asymmetric
	0777771	2841846			140			Asymmetric
	0777771	2841846			196			Asymmetric
	0777771	2841846			240		12	Cross Bedding
	0777771	2841846			211		15	Cross Bedding
	0777771	2841846			140		20	Cross Bedding
	0777771	2841846			190		4	Cross Bedding
	0777771	2841846			181		10	Cross Bedding
	0777771	2841846			217		6	Cross Bedding

	0777771	2841846			219		32	Asymmetric
	0777771	2841846			347		13	Cross Bedding
	0777771	2841846			351		11	Cross Bedding
HZB_023	0777504	2840898		3	96		9	Cross Bedding
	0777504	2840898			307	127		Ripples
	0777504	2840898			199	19		Ripples
	0777504	2840898			78		8	Cross Bedding
	0777504	2840898			292		38	Cross Bedding
	0777504	2840898			113		24	Cross Bedding
	0777504	2840898			203		12	Cross Bedding
	0777504	2840898			203		10	Cross Bedding
	0777504	2840898			206		5	Cross Bedding
	0777504	2840898			236		-2	Cross Bedding
	0777504	2840898			261		3	Cross Bedding
	0777504	2840898			90		19	Cross Bedding
	0777504	2840898			249		6	Cross Bedding
HZB_024	0777941	2840855			253		11	Cross Bedding
	0777941	2840855			111		24	Cross Bedding
	0777941	2840855			183		19	Cross Bedding
	0777941	2840855			187		4	Cross Bedding
	0777941	2840855			159		30	Cross Bedding
	0777941	2840855			110		14	Cross Bedding
	0777941	2840855			60		6	Cross Bedding
	0777941	2840855			239		8	Cross Bedding
	0777941	2840855			89		3	Cross Bedding
	0777941	2840855			102		9	Cross Bedding
HZB_025	0778078	2840692			201		1	Cross Bedding
	0778078	2840692			216		12	Cross Bedding
	0778078	2840692			191		11	Cross Bedding
HZB_026	0778172	2840260			309		8	Cross Bedding
	0778172	2840260			130		20	Cross Bedding
	0778172	2840260			340		2	Cross Bedding
	0778172	2840260			130		19	Cross Bedding
	0778172	2840260			189		3	Cross Bedding
	0778172	2840260			308		12	Asymmetric Ripples
	0778172	2840260			295		13	Asymmetric Ripples
	0778172	2840260			291	111		Ripples
	0778172	2840260			297		2	Cross Bedding
	0778172	2840260			168		21	Cross Bedding
	0778172	2840260			139		29	Cross Bedding
HZB_028	0778363	2840950			225		20	Cross Bedding
	0778363	2840950			225		11	Cross Bedding
	0778363	2840950			39		10	Cross Bedding

	0778363	2840950			45		78	Cross Bedding
	0778363	2840950			38		7	Cross Bedding
	0778363	2840950			120	300		Channel
HZB_029	0778338	2841028			137		16	Cross Bedding
	0778338	2841028			137		28	Cross Bedding
	0778338	2841028			122		19	Cross Bedding
	0778338	2841028			193	13		Ripples
	0778338	2841028			156		18	Cross Bedding
	0778338	2841028			151		9	Cross Bedding
	0778338	2841028			87	267		Channel
	0778338	2841028			56		9	Cross Bedding
	0778338	2841028			130	310		Ripples
	0778338	2841028			94	274		Ripples
	0778338	2841028			195		9	Cross Bedding
	0778338	2841028			152		38	Asymmetric Ripple
	0778338	2841028			191		11	Cross Bedding
	0778338	2841028			187		3	Cross Bedding
HZB_031	0777853	2841183			95		9	Cross Bedding
	0777853	2841183			257		3	Cross Bedding
	0777853	2841183			230		5	Cross Bedding
	0777853	2841183			68		2	Cross Bedding
	0777853	2841183			219		7	Cross Bedding
	0777853	2841183			258		9	Cross Bedding
	0777853	2841183			265		3	Cross Bedding
	0777853	2841183			329	139		Ripples
	0777853	2841183			211	31		Ripples
	0777853	2841183			174		13	Cross Bedding
	0777853	2841183			174		12	Cross Bedding
	0777853	2841183			77		7	Cross Bedding
	0777853	2841183			262		7	Cross Bedding
	0777853	2841183			70		6	Cross Bedding
	0777853	2841183			238		13	Cross Bedding
	0777853	2841183			274		9	Cross Bedding
	0777853	2841183			257		2	Cross Bedding
	0777853	2841183			140		-2	Cross Bedding
	0777853	2841183			187		15	Cross Bedding
	0777853	2841183			236		8	Cross Bedding
	0777853	2841183			187		1	Cross Bedding
	0777853	2841183			10		10	Cross Bedding
	0777853	2841183			79		12	Cross Bedding
HZB_032	0777869	2841254			174		21	Cross Bedding
	0777869	2841254			164		15	Cross Bedding
	0777869	2841254			161		20	Cross Bedding
	0777869	2841254			169		20	Cross Bedding

	0777869	2841254			168		18	Cross Bedding
	0777869	2841254			131		19	Cross Bedding
	0777869	2841254			341		1	Cross Bedding
	0777869	2841254			161		12	Cross Bedding
	0777869	2841254			139		11	Cross Bedding
	0777869	2841254			123		3	Cross Bedding
	0777869	2841254			123		20	Cross Bedding
	0777869	2841254			124		22	Cross Bedding
	0777869	2841254			124		21	Cross Bedding
	0777869	2841254			147		19	Cross Bedding
	0777869	2841254			126		3	Cross Bedding
	0777869	2841254			291		3	Cross Bedding
	0777869	2841254			276		9	Cross Bedding
	0777869	2841254			116		8	Cross Bedding
	0777869	2841254			116		0	Cross Bedding
	0777869	2841254			330		2	Cross Bedding
	0777869	2841254			141		8	Cross Bedding
	0777869	2841254			229		14	Cross Bedding
	0777869	2841254			142		10	Cross Bedding
	0777869	2841254			324		1	Cross Bedding
	0777869	2841254			40		1	Cross Bedding
	0777869	2841254			129		20	Cross Bedding
	0777869	2841254			251		14	Cross Bedding
HZB_033	0777960	2841407			319	139		Channel
HZB_034	0777944	2841910			2		2	Cross Bedding
	0777944	2841910			186		9	Cross Bedding
	0777944	2841910			171		8	Cross Bedding
	0777944	2841910			153		12	Cross Bedding
	0777944	2841910			181		24	Cross Bedding
	0777944	2841910			198		12	Cross Bedding
HZB_035	0778017	2840478			209		7	Cross Bedding
	0778017	2840478			309		9	Cross Bedding
	0778017	2840478			156		1	Cross Bedding
	0778017	2840478			311		6	Cross Bedding
	0778017	2840478			101		12	Cross Bedding
	0778017	2840478			104		0	Cross Bedding
HZB_036	0777447	2849376	18		179		14	Cross Bedding
	0777447	2849376			179		13	Cross Bedding
	0777447	2849376			206		23	Cross Bedding
	0777447	2849376			229		20	Cross Bedding
	0777447	2849376			217		8	Cross Bedding
	0777447	2849376			230		16	Cross Bedding
	0777447	2849376			212		11	Cross Bedding
	0777447	2849376			213		-1	Cross Bedding
	0777447	2849376			222		12	Cross Bedding

	0777447	2849376			196		12	Cross Bedding
	0777447	2849376			64		6	Cross Bedding
	0777447	2849376			198		8	Cross Bedding
	0777447	2849376			38		6	Cross Bedding
	0777447	2849376			171		25	Cross Bedding
	0777447	2849376			168		20	Cross Bedding
	0777447	2849376			226		23	Cross Bedding
	0777447	2849376			230		0	Cross Bedding
	0777447	2849376			229		3	Cross Bedding
	0777447	2849376			247		1	Cross Bedding
	0777447	2849376			229		5	Cross Bedding
	0777447	2849376			195		3	Cross Bedding
	0777447	2849376			11		10	Cross Bedding
	0777447	2849376			209		17	Cross Bedding
	0777447	2849376			75		11	Cross Bedding
	0777447	2849376			240		3	Cross Bedding
	0777447	2849376			250		8	Cross Bedding
	0777447	2849376			249		20	Cross Bedding
	0777447	2849376			94		26	Cross Bedding
	0777447	2849376			111		3	Cross Bedding
	0777447	2849376			109		34	Cross Bedding
	0777447	2849376			190		10	Cross Bedding
	0777447	2849376			231		11	Cross Bedding
	0777447	2849376			91		17	Cross Bedding
	0777447	2849376			69		5	Cross Bedding
	0777447	2849376			198		22	Cross Bedding
	0777447	2849376			190		10	Cross Bedding
	0777447	2849376			168		13	Cross Bedding
	0777447	2849376			175		20	Cross Bedding
	0777447	2849376			199		1	Cross Bedding
	0777447	2849376			203		2	Cross Bedding
	0777447	2849376			222		18	Cross Bedding
	0777447	2849376			215		12	Cross Bedding
	0777447	2849376			210		20	Cross Bedding
	0777447	2849376			202		13	Cross Bedding
HZB_037	0777026	2840369			325	145		Ripples
	0777026	2840369			343	163		Ripples
	0777026	2840369			11	191		Ripples
	0777026	2840369			354	174		Ripples
HZB_038	0777107	2840577	19		28	148		Ripples
	0777107	2840577			40	210		Ripples
	0777107	2840577			26	206		Ripples
	0777107	2840577			57	237		Ripples
	0777107	2840577			5	185		Ripples
	0777107	2840577			25	205		Ripples

HZB_040	0777524	2840549			152		30	Cross Bedding
	0777524	2840549			194		15	Cross Bedding
	0777524	2840549			150		15	Cross Bedding
	0777524	2840549			218		5	Cross Bedding
	0777524	2840549			186		17	Cross Bedding
	0777524	2840549			186		5	Cross Bedding
	0777524	2840549			41		2	Cross Bedding
	0777524	2840549			213		9	Cross Bedding
	0777524	2840549			208		24	Cross Bedding
	0777524	2840549			197		22	Cross Bedding
	0777524	2840549			154		24	Cross Bedding
	0777524	2840549			143		15	Cross Bedding
	0777524	2840549			146		24	Cross Bedding
	0777524	2840549			258		3	Cross Bedding
	0777524	2840549			320		1	Cross Bedding
HZB_041	0777680	2840349			259		8	Cross Bedding
	0777680	2840349			246		12	Cross Bedding
	0777680	2840349			277		6	Cross Bedding
	0777680	2840349			303		11	Cross Bedding
	0777680	2840349			202		2	Cross Bedding
	0777680	2840349			93		21	Cross Bedding
	0777680	2840349			273		1	Cross Bedding
	0777680	2840349			286		0	Cross Bedding
	0777680	2840349			231		7	Cross Bedding
	0777680	2840349			290		3	Cross Bedding
	0777680	2840349			198		7	Cross Bedding
	0777680	2840349			54		12	Cross Bedding
	0777680	2840349			213		7	Cross Bedding
	0777680	2840349			231		11	Cross Bedding
	0777680	2840349			284		5	Cross Bedding
	0777680	2840349			109		19	Cross Bedding
	0777680	2840349			290		1	Cross Bedding
	0777680	2840349			176		9	Cross Bedding
	0777680	2840349			137		1	Cross Bedding
	0777680	2840349			15		18	Cross Bedding
HZB_042	0777636	2840370			160		10	Cross Bedding
	0777636	2840370			108		17	Cross Bedding
	0777636	2840370			71		4	Cross Bedding
	0777636	2840370			198		7	Cross Bedding
	0777636	2840370			200		3	Cross Bedding
HZB_042b	0777636	2840370			148		19	Cross Bedding
	0777636	2840370			88		6	Cross Bedding
	0777636	2840370			193		8	Cross Bedding
	0777636	2840370			171		30	Cross Bedding
	0777636	2840370			180		17	Cross Bedding

	0777636	2840370			229		2	Cross Bedding
	0777636	2840370			221		15	Cross Bedding
HZB_043	0777727	2840417			169		14	Cross Bedding
	0777727	2840417			210		21	Cross Bedding
	0777727	2840417			230		10	Cross Bedding
	0777727	2840417			229		6	Cross Bedding
	0777727	2840417			233		10	Cross Bedding
	0777727	2840417			231		2	Cross Bedding
	0777727	2840417			293		20	Cross Bedding
HZB_045	0777732	2840526			187		7	Cross Bedding
	0777732	2840526			218		11	Cross Bedding
	0777732	2840526			239		22	Cross Bedding
	0777732	2840526			99	279		Channel
	0777732	2840526			159		18	Cross Bedding
	0777732	2840526			97	277		Channel
	0777732	2840526			47	227		Channel
HZB_046	0777740	2840518			229		1	Cross Bedding
	0777740	2840518			196		11	Cross Bedding
	0777740	2840518			194		11	Cross Bedding
	0777740	2840518			147	327		Ripples
	0777740	2840518			246		8	Cross Bedding
	0777740	2840518			230		11	Cross Bedding
	0777740	2840518			136		27	Cross Bedding
	0777740	2840518			336		2	Cross Bedding
	0777740	2840518			281		7	Cross Bedding
	0777740	2840518			90		14	Cross Bedding
	0777740	2840518			184		1	Cross Bedding
	0777740	2840518			132		8	Cross Bedding
	0777740	2840518			134		10	Cross Bedding
HZB_047	0777653	2840496			107		11	Cross Bedding
	0777653	2840496			78		15	Cross Bedding
HZB_048	0777584	2840490			106		10	Cross Bedding
	0777584	2840490			87		0	Cross Bedding
	0777584	2840490			62		3	Cross Bedding
	0777584	2840490			101		19	Cross Bedding
	0777584	2840490			70		8	Cross Bedding
HZB_049	0776781	2839852			200		22	Cross Bedding
	0776781	2839852			6		1	Cross Bedding
	0776781	2839852			85		17	Cross Bedding
	0776781	2839852			95		13	Cross Bedding
	0776781	2839852			131		17	Cross Bedding
	0776781	2839852			247		1	Cross Bedding
HZB_049c	0776779	2839722			280		1	Cross Bedding
	0776779	2839722			160		10	Cross Bedding
	0776779	2839722			160		17	Cross Bedding

HZB_049b	0776740	2839776			58		6	Cross Bedding
	0776740	2839776			87		2	Cross Bedding
	0776740	2839776			247		8	Cross Bedding
	0776740	2839776			91		6	Cross Bedding
	0776740	2839776			241		8	Cross Bedding
	0776740	2839776			60		11	Cross Bedding
	0776740	2839776			62		21	Cross Bedding
	0776740	2839776			74		2	Cross Bedding
	0776740	2839776			279		1	Cross Bedding
	0776740	2839776			86		21	Cross Bedding
	0776740	2839776			192		22	Cross Bedding
	0776740	2839776			84		1	Cross Bedding
	0776740	2839776			31		5	Cross Bedding
	0776740	2839776			211		15	Cross Bedding
	0776740	2839776			223		3	Cross Bedding
	0776740	2839776			220		21	Cross Bedding
	0776740	2839776			191		11	Cross Bedding
	0776740	2839776			170		10	Cross Bedding
	0776740	2839776			256		11	Cross Bedding
	0776740	2839776			222		2	Cross Bedding
	0776740	2839776			251		12	Cross Bedding
	0776740	2839776			224		28	Cross Bedding
	0776740	2839776			206		21	Cross Bedding
	0776740	2839776			199		22	Cross Bedding
	0776740	2839776			206		21	Cross Bedding
	0776740	2839776			176		8	Cross Bedding
HZB_050	0776923	2839705			194		21	Cross Bedding
HZB_051	0776857	2839568			1		3	Cross Bedding
	0776857	2839568			174		12	Cross Bedding
	0776857	2839568			324		1	Cross Bedding
	0776857	2839568			181		22	Cross Bedding
	0776857	2839568			234		17	Cross Bedding
	0776857	2839568			343		-10	Cross Bedding
	0776857	2839568			162		3	Cross Bedding
HZB_052	0776762	2839574			141		21	Cross Bedding
	0776762	2839574			112		9	Cross Bedding
HZB_053	0778974	2842016			176		30	Cross Bedding
	0778974	2842016			137		32	Cross Bedding
	0778974	2842016			199		1	Cross Bedding
	0778974	2842016			180		18	Cross Bedding
	0778974	2842016			92	272		Ripples
	0778974	2842016			134		26	Cross Bedding
	0778974	2842016			178		10	Cross Bedding
	0778974	2842016			142		30	Cross Bedding
	0778974	2842016			111		17	Cross Bedding

	0778974	2842016			114		24	Cross Bedding
	0778974	2842016			183		11	Cross Bedding
	0778974	2842016	20		112		19	Cross Bedding
	0778974	2842016			123		3	Cross Bedding
	0778974	2842016			104		17	Cross Bedding
	0778974	2842016			107		10	Cross Bedding
	0778974	2842016			126		19	Cross Bedding
	0778974	2842016			142		17	Cross Bedding
	0778974	2842016			145		17	Cross Bedding
	0778974	2842016			135		32	Cross Bedding
	0778974	2842016			131		14	Cross Bedding
	0778974	2842016			146		32	Cross Bedding
	0778974	2842016			59		11	Cross Bedding
	0778974	2842016			32		9	Cross Bedding
	0778974	2842016			125		21	Cross Bedding
	0778974	2842016			119		1	Cross Bedding
	0778974	2842016			114		12	Cross Bedding
	0778974	2842016			144		12	Cross Bedding
	0778974	2842016			296		8	Cross Bedding
	0778974	2842016			111		18	Cross Bedding
	0778974	2842016			161		10	Cross Bedding
	0778974	2842016			218		16	Cross Bedding
	0778974	2842016			176		6	Cross Bedding
	0778974	2842016			346	166		Ripples
	0778974	2842016			140		18	Cross Bedding
	0778974	2842016			196		12	Cross Bedding
	0778974	2842016			130		18	Cross Bedding
	0778974	2842016			114		10	Cross Bedding
	0778974	2842016			55		2	Cross Bedding
HZB_054	0778962	2841992			232		8	Cross Bedding
	0778962	2841992			190		8	Cross Bedding
	0778962	2841992			210		8	Cross Bedding
	0778962	2841992			228		20	Cross Bedding
HZB_055	0778911	2841924			326		22	Cross Bedding
	0778911	2841924			281		1	Cross Bedding
HZB_056	0778862	2841925			178		9	Cross Bedding
	0778862	2841925			164		12	Cross Bedding
	0778862	2841925			147		9	Cross Bedding
	0778862	2841925			176		12	Cross Bedding
	0778862	2841925			267		4	Cross Bedding
	0778862	2841925			202		20	Cross Bedding
	0778862	2841925			101		11	Cross Bedding
	0778862	2841925			163		22	Cross Bedding
	0778862	2841925			116		12	Cross Bedding
	0778862	2841925			347		21	Asymmetric

	0778862	2841925			160		24	Cross Bedding
	0778862	2841925			36		3	Cross Bedding
	0778862	2841925			226		26	Cross Bedding
	0778862	2841925			231		9	Cross Bedding
	0778862	2841925			64		1	Cross Bedding
	0778862	2841925			230		12	Cross Bedding
	0778862	2841925			218		19	Cross Bedding
	0778862	2841925			221		1	Cross Bedding
	0778862	2841925			178		1	Cross Bedding
	0778862	2841925			226		9	Cross Bedding
	0778862	2841925			172		40	Cross Bedding
HZB_057	0778847	2841945			247		2	Cross Bedding
	0778847	2841945			204		9	Cross Bedding
	0778847	2841945			147		22	Cross Bedding
	0778847	2841945			338		8	Cross Bedding
	0778847	2841945			181		12	Cross Bedding
	0778847	2841945			34		10	Cross Bedding
	0778847	2841945			214		24	Cross Bedding
HZB_058	0778749	2841960			34		12	Asymmetric
	0778749	2841960			191		9	Cross Bedding
	0778749	2841960			187		7	Cross Bedding
HZB_059	0778661	2841985			298		4	Cross Bedding
	0778661	2841985			312		1	Cross Bedding
	0778661	2841985			129		31	Cross Bedding
	0778661	2841985			139		39	Cross Bedding
	0778661	2841985			72		11	Cross Bedding
	0778661	2841985			117		12	Cross Bedding
	0778661	2841985			264		17	Cross Bedding
	0778661	2841985			164		19	Cross Bedding
	0778661	2841985			95		1	Cross Bedding
HZB_061	0778104	2841745		5	208		3	Cross Bedding
	0778104	2841745			201		20	Cross Bedding
	0778104	2841745			200		4	Cross Bedding
	0778104	2841745			178		3	Cross Bedding
	0778104	2841745			203		19	Cross Bedding
	0778104	2841745			30		2	Cross Bedding
	0778104	2841745			33		2	Cross Bedding
	0778104	2841745			206		13	Cross Bedding
	0778104	2841745			70	250		Ripples
	0778104	2841745			286	106		Ripples
	0778104	2841745			212	32		Ripples
	0778104	2841745			355		11	Cross Bedding
	0778104	2841745			160		10	Cross Bedding
	0778104	2841745			227		20	Cross Bedding
	0778104	2841745			211		8	Cross Bedding

	0778104	2841745			240		14	Cross Bedding
	0778104	2841745			229		2	Cross Bedding
	0778104	2841745			37		26	Cross Bedding
	0778104	2841745			168		8	Cross Bedding
	0778104	2841745			190		10	Cross Bedding
	0778104	2841745			236		18	Cross Bedding
	0778104	2841745			320		9	Cross Bedding
	0778104	2841745			58		2	Cross Bedding
	0778104	2841745			217		1	Cross Bedding
	0778104	2841745			349		2	Cross Bedding
HZB_062	0777701	2840482	21		63		10	Cross Bedding
	0777701	2840482			83		19	Cross Bedding
	0777701	2840482			88		20	Cross Bedding
	0777701	2840482			104		22	Cross Bedding
	0777701	2840482			110		17	Cross Bedding
	0777701	2840482			95		18	Cross Bedding
	0777701	2840482			60		11	Cross Bedding
	0777701	2840482			254		8	Cross Bedding
	0777701	2840482			271		6	Cross Bedding
	0777701	2840482			148		12	Cross Bedding
	0777701	2840482			101		2	Cross Bedding
	0777701	2840482			101		18	Cross Bedding
	0777701	2840482			141		16	Cross Bedding
	0777701	2840482			110		26	Cross Bedding
	0777701	2840482			133		23	Cross Bedding
	0777701	2840482			64		33	Asymmetric
	0777701	2840482			46	226		Ripples
HZB_063	0777795	2841287			139		11	Cross Bedding
	0777795	2841287			186		19	Cross Bedding
	0777795	2841287			250		1	Cross Bedding
	0777795	2841287			83		5	Cross Bedding
	0777795	2841287			246		14	Cross Bedding
	0777795	2841287			99		10	Cross Bedding
	0777795	2841287			275		3	Cross Bedding
	0777795	2841287			76		16	Cross Bedding
	0777795	2841287			93		18	Cross Bedding
	0777795	2841287			83		20	Cross Bedding
HZB_064	0777666	2841371			259		10	Cross Bedding
	0777666	2841371			238		18	Cross Bedding
	0777666	2841371			62		2	Cross Bedding
	0777666	2841371			245		10	Cross Bedding
	0777666	2841371			225		19	Cross Bedding
	0777666	2841371			242		18	Cross Bedding
	0777666	2841371			11		3	Cross Bedding
	0777666	2841371			107		9	Cross Bedding

	0777666	2841371			158		3	Cross Bedding
	0777666	2841371			107		3	Cross Bedding
	0777666	2841371			138		10	Cross Bedding
	0777666	2841371			290		17	Cross Bedding
	0777666	2841371			289		11	Cross Bedding
	0777666	2841371			6		8	Cross Bedding
	0777666	2841371			292		3	Cross Bedding
	0777822	2841374			311		14	Cross Bedding
HZB_065	0777822	2841374			161		6	Cross Bedding
	0777822	2841374			283		5	Cross Bedding
	0777822	2841374			192		7	Cross Bedding
HZB_065b	0777846	2841390			248		10	Cross Bedding
	0777846	2841390			32		1	Cross Bedding
	0777846	2841390			206		8	Cross Bedding
	0777846	2841390			287		8	Cross Bedding
	0777846	2841390			283		11	Cross Bedding
	0777846	2841390			211		8	Cross Bedding
	0777846	2841390			273		1	Cross Bedding
HZB__066	0777876	2841412			96		4	Cross Bedding
	0777876	2841412			220		5	Cross Bedding
	0777876	2841412			224		12	Cross Bedding
	0777876	2841412			222		16	Cross Bedding
	0777876	2841412			261		7	Cross Bedding
	0777876	2841412			107		10	Cross Bedding
	0777876	2841412			278		12	Cross Bedding
	0777876	2841412			106		2	Cross Bedding
	0777876	2841412			189		2	Cross Bedding
HZB_067	0777815	2841493	22		305		2	Cross Bedding
	0777815	2841493			193		5	Cross Bedding
	0777815	2841493			192		13	Cross Bedding
	0777815	2841493			192		5	Cross Bedding
	0777815	2841493			220		9	Cross Bedding
	0777815	2841493			29		9	Cross Bedding
	0777815	2841493			194		18	Cross Bedding
	0777815	2841493			67		21	Cross Bedding
	0777815	2841493			60		1	Cross Bedding
	0777815	2841493			269		7	Cross Bedding
	0777815	2841493			84		12	Cross Bedding
	0777815	2841493			301		3	Cross Bedding
	0777815	2841493			102		15	Cross Bedding
	0777815	2841493			86	226		Ripples
	0777815	2841493			286		24	Asymmetric
	0777815	2841493			97	277		Ripples
	0777815	2841493			97		27	Ripples
	0777815	2841493			217		8	Cross Bedding

	0777815	2841493			70		30	Asymmetric
	0777815	2841493			78	278		Ripples
	0777815	2841493			270		41	Asymmetric
	0777815	2841493			104	284		Ripples
	0777815	2841493			96	276		Ripples
	0777815	2841493			53	233		Ripples
	0777815	2841493			292		12	Cross Bedding
	0777815	2841493			291		2	Cross Bedding
	0777815	2841493			76		31	Asymmetric
	0777815	2841493			65	245		Ripples
	0777815	2841493			67	247		Ripples
HZB_068	0777782	2841455			253		2	Cross Bedding
	0777782	2841455			70		2	Cross Bedding
	0777782	2841455			264		20	Cross Bedding
	0777782	2841455			50		9	Cross Bedding
	0777782	2841455			199	19		Ripples
	0777782	2841455			344		15	Cross Bedding
HZB_069	0777802	2841540			129		29	Cross Bedding
	0777802	2841540			314		1	Cross Bedding
	0777802	2841540			30		7	Cross Bedding
	0777802	2841540			23		2	Cross Bedding
	0777802	2841540			32		12	Cross Bedding
	0777802	2841540			203		5	Cross Bedding
HZB_069b	0777885	2841576			217		14	Cross Bedding
	0777885	2841576			221		12	Cross Bedding
	0777885	2841576			236		30	Cross Bedding
HZB_070	0778845	2841819			118		24	Cross Bedding
	0778845	2841819			100		12	Cross Bedding
	0778845	2841819			139		17	Cross Bedding
HZB_071	0778672	2841876			228		6	Cross Bedding
	0778672	2841876			177		15	Cross Bedding
	0778672	2841876			119		20	Cross Bedding
	0778672	2841876			124		12	Cross Bedding
	0778672	2841876			200		14	Cross Bedding
	0778672	2841876			355		2	Cross Bedding
	0778672	2841876			154		21	Cross Bedding
	0778672	2841876			342		3	Cross Bedding
	0778672	2841876			167		19	Cross Bedding
HZB_072	0778748	2841929		6	10	190		Ripples
	0778748	2841929			71		20	Asymmetric
	0778748	2841929			181		8	Cross Bedding
	0778748	2841929			202		21	Cross Bedding
	0778748	2841929			199		1	Cross Bedding
	0778748	2841929			15		15	Cross Bedding
	0778748	2841929			194		47	Cross Bedding

	0778748	2841929			210		18	Cross Bedding
	0778748	2841929			148		34	Cross Bedding
	0778748	2841929			195		13	Cross Bedding
	0778748	2841929			190		18	Cross Bedding
HZB_073	0778696	2841834			177		21	Cross Bedding
	0778696	2841834			179		23	Cross Bedding
	0778696	2841834			344		-8	Cross Bedding
	0778696	2841834			202		21	Cross Bedding
	0778696	2841834			8		1	Cross Bedding
	0778696	2841834			281		12	Cross Bedding
	0778696	2841834			22		-1	Cross Bedding
	0778696	2841834			161		38	Cross Bedding
	0778696	2841834			141		19	Cross Bedding
	0778696	2841834			154		38	Cross Bedding
	0778696	2841834			158		26	Cross Bedding
	0778696	2841834			140		19	Cross Bedding
	0778696	2841834			149		22	Cross Bedding
	0778696	2841834			147		11	Cross Bedding
	0778696	2841834			191		20	Cross Bedding
	0778696	2841834			139		21	Cross Bedding
	0778696	2841834			139		20	Cross Bedding
	0778696	2841834			149		22	Cross Bedding
	0778696	2841834			337		-2	Cross Bedding
HZB_074	0778648	2841752			93		2	Cross Bedding
	0778648	2841752			273		21	Cross Bedding
	0778648	2841752			292		1	Cross Bedding
	0778648	2841752			166		19	Cross Bedding
	0778648	2841752			250		1	Cross Bedding
HZB_075	0778629	2841713			195		32	Cross Bedding
	0778629	2841713			84		13	Cross Bedding
	0778629	2841713			230		2	Cross Bedding
	0778629	2841713			185		3	Cross Bedding
	0778629	2841713			80		18	Cross Bedding
	0778629	2841713			99		21	Cross Bedding
	0778629	2841713			121		21	Cross Bedding
HZB_076	0778463	2841667			171		21	Cross Bedding
HZB_077	0778231	2841133			176		6	Cross Bedding
	0778231	2841133			200		17	Asymmetric
	0778231	2841133			27		6	Cross Bedding
	0778231	2841133			81	261		Ripple
	0778231	2841133			87		11	Cross Bedding
	0778231	2841133			189		12	Cross Bedding
	0778231	2841133			59		4	Cross Bedding
	0778231	2841133			38		22	Cross Bedding
	0778231	2841133			292		-2	Cross Bedding

	0778231	2841133			68		13	Cross Bedding
	0778231	2841133			232		17	Cross Bedding
	0778231	2841133			258		2	Cross Bedding
	0778231	2841133			63		10	Cross Bedding
	0778231	2841133			252		2	Cross Bedding
	0778231	2841133			72		15	Cross Bedding
	0778231	2841133			62		12	Cross Bedding
	0778231	2841133			51		-1	Cross Bedding
	0778231	2841133			55		7	Cross Bedding
	0778231	2841133			60		4	Cross Bedding
	0778231	2841133			65		12	Cross Bedding
	0778231	2841133			102		20	Cross Bedding
HZB_079	0780745	2844530	23		7	187		Ripples
	0780745	2844530			356	176		Ripples
	0780745	2844530			347	167		Ripples
	0780745	2844530			21		11	Cross Bedding
	0780745	2844530			205		8	Cross Bedding
	0780745	2844530			193		12	Cross Bedding
	0780745	2844530			209		12	Cross Bedding
	0780745	2844530			188		9	Cross Bedding
	0780745	2844530			214		18	Cross Bedding
	0780745	2844530			1		12	Cross Bedding
	0780745	2844530			55		13	Cross Bedding
	0780745	2844530			189		10	Cross Bedding
	0780745	2844530			198		20	Cross Bedding
	0780745	2844530			197		20	Cross Bedding
	0780745	2844530			200		18	Cross Bedding
	0780745	2844530			219		10	Cross Bedding
	0780745	2844530			210		8	Cross Bedding
	0780745	2844530			221		12	Cross Bedding
	0780745	2844530			118		11	Cross Bedding
	0780745	2844530			212		14	Cross Bedding
	0780745	2844530			218		23	Cross Bedding
	0780745	2844530			211		12	Cross Bedding
	0780745	2844530			340	160		Ripples
	0780745	2844530			58	238		Ripples
	0780745	2844530			25	205		Ripples
	0780745	2844530			342	162		Ripples
	0780745	2844530			190		2	Cross Bedding
	0780745	2844530			187		6	Cross Bedding
	0780745	2844530			203		8	Cross Bedding
	0780745	2844530			204		20	Cross Bedding
	0780745	2844530			200		31	Asymmetric
	0780745	2844530			159	339		Ripples
	0780745	2844530			191	11		Ripples

	0780745	2844530			17	197		Ripples
	0780745	2844530			10	190		Ripples
	0780745	2844530			25	205		Ripples
	0780745	2844530			38	218		Ripples
	0780745	2844530			357	177		Ripples
	0780745	2844530			30	210		Ripples
	0780745	2844530			17	197		Ripples
	0780745	2844530			238		21	Cross Bedding
	0780745	2844530			335	155		Ripples
	0780745	2844530			11		21	Asymmetric
	0780745	2844530			28	208		Ripples
	0780745	2844530			36	216		Ripples
	0780745	2844530			21	201		Ripples
	0780745	2844530			6	186		Ripples
	0780745	2844530			206		14	Asymmetric
	0780745	2844530			3	183		Ripples
	0780745	2844530			28	208		Ripples
	0780745	2844530			18	198		Ripples
	0780745	2844530			17	197		Ripples
	0780745	2844530			21	201		Ripples
	0780745	2844530			34	214		Ripples
	0780745	2844530			12	192		Ripples
	0780745	2844530			184		4	Asymmetric
	0780745	2844530			359	179		Ripples
	0780745	2844530			30	210		Ripples
	0780745	2844530			39	219		Ripples
	0780745	2844530			32		10	Cross Bedding
	0780745	2844530			37	227		Ripples
	0780745	2844530			37	227		Ripples
	0780745	2844530			1	181		Ripples
	0780745	2844530			28	208		Ripples
	0780745	2844530			20	200		Ripples
	0780745	2844530			159	179		Ripples
	0780745	2844530			54	234		Ripples
	0780745	2844530			17	197		Ripples
	0780745	2844530			241		19	Cross Bedding
	0780745	2844530			216		15	Cross Bedding
	0780745	2844530			47		3	Cross Bedding
	0780745	2844530			199		21	Cross Bedding
	0780745	2844530			9		9	Cross Bedding
	0780745	2844530			2	202		Ripples
	0780745	2844530			20		14	Cross Bedding
	0780745	2844530			192		22	Cross Bedding
	0780745	2844530			169		10	Cross Bedding
	0780745	2844530			227		7	Cross Bedding

	0780745	2844530			215		24	Cross Bedding
	0780745	2844530			234		32	Cross Bedding
	0780745	2844530			232		2	Cross Bedding
	0780745	2844530			230		4	Cross Bedding
	0780745	2844530			26	206		Ripples
	0780745	2844530			7	187		Ripples
	0780745	2844530			22	202		Ripples
	0780745	2844530			98		3	Cross Bedding
	0780745	2844530			206		25	Asymmetric
	0780745	2844530			19	199		Ripples
	0780745	2844530			18	198		Ripples
HZB_080	0781186	2845165	23		55		8	Cross Bedding
	0781186	2845165			232		20	Cross Bedding
	0781186	2845165			59		8	Cross Bedding
	0781186	2845165			260		4	Cross Bedding
	0781186	2845165			89		20	Cross Bedding
	0781186	2845165			53		19	Cross Bedding
	0781186	2845165			234		8	Cross Bedding
	0781186	2845165			244		6	Cross Bedding
	0781186	2845165			62		15	Cross Bedding
	0781186	2845165			230		9	Cross Bedding
	0781186	2845165			238		12	Cross Bedding
	0781186	2845165			225		10	Cross Bedding
	0781186	2845165			228		11	Cross Bedding
	0781186	2845165			221		2	Cross Bedding
	0781186	2845165			302		3	Cross Bedding
	0781186	2845165			52		9	Cross Bedding
	0781186	2845165			61		14	Cross Bedding
	0781186	2845165			250		11	Cross Bedding
	0781186	2845165			211		12	Cross Bedding
	0781186	2845165			236		12	Cross Bedding
	0781186	2845165			240		8	Cross Bedding
	0781186	2845165			19		1	Cross Bedding
	0781186	2845165			227		6	Cross Bedding
	0781186	2845165			51		3	Cross Bedding
	0781186	2845165			53		9	Cross Bedding
	0781186	2845165			238		10	Cross Bedding
	0781186	2845165			273		3	Cross Bedding
	0781186	2845165			67		17	Cross Bedding
	0781186	2845165			103		4	Cross Bedding
	0781186	2845165			99		8	Cross Bedding
	0781186	2845165			113		10	Cross Bedding
	0781186	2845165			113		16	Cross Bedding
	0781186	2845165			116	296		Ripple
	0781186	2845165			257		22	Cross Bedding

	0781186	2845165			119		18	Cross Bedding
	0781186	2845165			228		4	Cross Bedding
	0781186	2845165			91		12	Cross Bedding
	0781186	2845165			116		14	Cross Bedding
	0781186	2845165			67		11	Cross Bedding
	0781186	2845165			107		21	Cross Bedding
	0781186	2845165			252		18	Cross Bedding
	0781186	2845165			103		22	Cross Bedding
	0781186	2845165			130	310		Ripple
	0781186	2845165			301		1	Asymmetric
	0781186	2845165			300		-4	Cross Bedding
	0781186	2845165			110		26	Cross Bedding
	0781186	2845165			94		19	Cross Bedding
	0781186	2845165			120		18	Low Angle Cross Bedding
	0781186	2845165			114		16	Cross Bedding
	0781186	2845165			131		21	Cross Bedding
	0781186	2845165			121		20	Cross Bedding
	0781186	2845165			121		28	Cross Bedding
	0781186	2845165			84		30	Cross Bedding
	0781186	2845165			132		47	Cross Bedding
	0781186	2845165			122		3	Cross Bedding
	0781186	2845165			132		4	Cross Bedding
	0781186	2845165			111		34	Cross Bedding
	0781186	2845165			91		24	Cross Bedding
	0781186	2845165			124		18	Cross Bedding
	0781186	2845165			123		21	Cross Bedding
	0781186	2845165			123		17	Cross Bedding
	0781186	2845165			110		24	Cross Bedding
	0781186	2845165			107		34	Cross Bedding
	0781186	2845165			111		18	Cross Bedding
	0781186	2845165			111		32	Cross Bedding
	0781186	2845165			106		18	Cross Bedding
	0781186	2845165			201		13	Cross Bedding
	0781186	2845165			192		22	Cross Bedding
	0781186	2845165			198		13	Cross Bedding
	0781186	2845165			193		33	Cross Bedding
	0781186	2845165			199		19	Cross Bedding
	0781186	2845165			189		17	Cross Bedding
	0781186	2845165			190		8	Cross Bedding
	0781186	2845165			21		12	Cross Bedding
	0781186	2845165			210		20	Cross Bedding
	0781186	2845165			208		18	Cross Bedding
	0781186	2845165			217		22	Cross Bedding
	0781186	2845165			95		30	Low Angle

								Cross Bedding
	0781186	2845165			96		11	Low Angle Cross Bedding
	0781186	2845165			74		22	Low Angle Cross Bedding
	0781186	2845165			97		23	Low Angle Cross Bedding
	0781186	2845165			42		8	Low Angle Cross Bedding
	0781186	2845165			238		22	Low Angle Cross Bedding
	0781186	2845165			214		12	Low Angle Cross Bedding
	0781186	2845165			216		11	Low Angle Cross Bedding
	0781186	2845165			71		18	Low Angle Cross Bedding
	0781186	2845165			107		2	Cross Bedding
	0781186	2845165			99		32	Cross Bedding
	0781186	2845165			93		21	Cross Bedding
	0781186	2845165			96		12	Cross Bedding
	0781186	2845165			103		36	Cross Bedding
	0781186	2845165			116		25	Cross Bedding
	0781186	2845165			116		36	Cross Bedding
	0781186	2845165			111		11	Cross Bedding
	0781186	2845165			182		20	Cross Bedding
	0781186	2845165			123		25	Cross Bedding
	0781186	2845165			271		3	Cross Bedding
	0781186	2845165			188		20	Cross Bedding
	0781186	2845165			184		17	Cross Bedding
	0781186	2845165			209		19	Cross Bedding
	0781186	2845165			74		17	Cross Bedding
	0781186	2845165			74		21	Cross Bedding
	0781186	2845165			90		-2	Cross Bedding
HZB_081	0781515	2845308	24		97		12	Cross Bedding
	0781515	2845308			286		7	Cross Bedding
	0781515	2845308			72		2	Cross Bedding
	0781515	2845308			93		13	Cross Bedding
	0781515	2845308			278		27	Cross Bedding
	0781515	2845308			87		8	Cross Bedding
	0781515	2845308			269		21	Cross Bedding
	0781515	2845308			259		19	Cross Bedding
	0781515	2845308			79		3	Cross Bedding
	0781515	2845308			96		12	Cross Bedding
	0781515	2845308			278		9	Cross Bedding
	0781515	2845308			90	270		Ripples
	0781515	2845308			264		13	Asymmetric

	0781515	2845308			95	275		Ripples
	0781515	2845308			294		10	Cross Bedding
	0781515	2845308			115		2	Cross Bedding
	0781515	2845308			290		15	Cross Bedding
	0781515	2845308			289		1	Cross Bedding
	0781515	2845308			110		7	Cross Bedding
	0781515	2845308			286		20	Cross Bedding
	0781515	2845308			96		0	Cross Bedding
	0781515	2845308			278		1	Cross Bedding
	0781515	2845308			234		19	Cross Bedding
	0781515	2845308			226		13	Cross Bedding
	0781515	2845308			48		14	Cross Bedding
	0781515	2845308			29		14	Cross Bedding
	0781515	2845308			71		13	Cross Bedding
	0781515	2845308			102		2	Cross Bedding
	0781515	2845308			61		8	Cross Bedding
	0781515	2845308			47		7	Cross Bedding
	0781515	2845308			291		11	Cross Bedding
	0781515	2845308			60		6	Cross Bedding
	0781515	2845308			251		6	Cross Bedding
	0781515	2845308			298		10	Cross Bedding
	0781515	2845308			243		10	Cross Bedding
	0781515	2845308			265		20	Cross Bedding
	0781515	2845308			155	335		Ripples
	0781515	2845308			145	325		Ripples
	0781515	2845308			110		32	Asymmetric
	0781515	2845308			134		48	Asymmetric
	0781515	2845308			73	253		Ripples
	0781515	2845308			84	264		Ripples
	0781515	2845308			21	201		Ripples
	0781515	2845308			62	242		Ripples
	0781515	2845308			127	307		Ripples
	0781515	2845308			123		0	Cross Bedding
	0781515	2845308			328		3	Cross Bedding
	0781515	2845308			326		5	Cross Bedding
	0781515	2845308			122		2	Cross Bedding
	0781515	2845308			129		4	Cross Bedding
	0781515	2845308			125		2	Cross Bedding
	0781515	2845308			102		2	Cross Bedding
	0781515	2845308			98		2	Cross Bedding
HZB_082	0781558	2845206			269	69		Ripples
	0781558	2845206			248	68		Ripples
	0781558	2845206			114		3	Cross Bedding
	0781558	2845206			308		19	Cross Bedding
	0781558	2845206			268		10	Cross Bedding

	0781558	2845206			301		8	Cross Bedding
	0781558	2845206			144		19	Cross Bedding
	0781558	2845206			117		7	Cross Bedding
	0781558	2845206			71	251		Ripples
	0781558	2845206			109		11	Cross Bedding
	0781558	2845206			324		17	Cross Bedding
	0781558	2845206			302		10	Cross Bedding
	0781558	2845206			133		2	Cross Bedding
	0781558	2845206			218			Trough Cross Bedding
	0781558	2845206			318		0	Cross Bedding
	0781558	2845206			108		14	Cross Bedding
	0781558	2845206			142		14	Cross Bedding
	0781558	2845206			131		24	Cross Bedding
	0781558	2845206			74		26	Cross Bedding
	0781558	2845206			116		15	Cross Bedding
	0781558	2845206			76		9	Cross Bedding
	0781558	2845206			129		14	Cross Bedding
HZB_083a	0781587	2845172			273		10	Cross Bedding
	0781587	2845172			174		8	Cross Bedding
	0781587	2845172			135		1	Cross Bedding
	0781587	2845172			176		-1	Cross Bedding
	0781587	2845172			338		8	Cross Bedding
	0781587	2845172			146		17	Cross Bedding
	0781587	2845172			309		7	Cross Bedding
	0781587	2845172			222		34	Cross Bedding
	0781587	2845172			127		17	Cross Bedding
	0781587	2845172			120		11	Cross Bedding
HZB_084	0781903	2845740	24		94		5	Cross Bedding
	0781903	2845740			101		5	Cross Bedding
	0781903	2845740			102		2	Cross Bedding
	0781903	2845740			99		4	Cross Bedding
	0781903	2845740			82		0	Cross Bedding
	0781903	2845740			86		8	Cross Bedding
	0781903	2845740			94		0	Cross Bedding
	0781903	2845740			109		2	Cross Bedding
	0781903	2845740			244		1	Cross Bedding
	0781903	2845740			40		3	Cross Bedding
	0781903	2845740			40		13	Cross Bedding
	0781903	2845740			46		12	Cross Bedding
	0781903	2845740			58		14	Cross Bedding
	0781903	2845740			38		2	Cross Bedding
	0781903	2845740			116		3	Cross Bedding
	0781903	2845740			38		4	Cross Bedding
	0781903	2845740			41		12	Cross Bedding

	0781903	2845740			48		9	Cross Bedding
	0781903	2845740			46		13	Cross Bedding
	0781903	2845740			230		12	Cross Bedding
	0781903	2845740			209		8	Cross Bedding
	0781903	2845740			258		17	Cross Bedding
	0781903	2845740			71	251		Ripples
	0781903	2845740			30	210		Ripples
	0781903	2845740			239		11	Cross Bedding
	0781903	2845740			133		34	Asymmetric
	0781903	2845740			20	200		Ripples
	0781903	2845740			31	213		Ripples
	0781903	2845740			65	245		Ripples
	0781903	2845740			27	207		Ripples
	0781903	2845740			23	203		Ripples
	0781903	2845740			51	231		Ripples
	0781903	2845740			63		8	Cross Bedding
	0781903	2845740			74		1	Cross Bedding
	0781903	2845740			25		5	Cross Bedding
	0781903	2845740			47		17	Cross Bedding
	0781903	2845740			194		17	Cross Bedding
	0781903	2845740			213		12	Cross Bedding
	0781903	2845740			25		3	Cross Bedding
	0781903	2845740			31		10	Cross Bedding
	0781903	2845740			71		21	Cross Bedding
	0781903	2845740			39		16	Cross Bedding
	0781903	2845740			226		3	Cross Bedding
HZB_086	0781732	2845765	25		23		12	Cross Bedding
	0781732	2845765			212		3	Cross Bedding
	0781732	2845765			27		7	Cross Bedding
	0781732	2845765			39		12	Cross Bedding
	0781732	2845765			39		10	Cross Bedding
	0781732	2845765			215		12	Cross Bedding
	0781732	2845765			30		9	Cross Bedding
	0781732	2845765			29		11	Cross Bedding
	0781732	2845765			197		13	Cross Bedding
	0781732	2845765			208		10	Cross Bedding
	0781732	2845765			202		21	Cross Bedding
	0781732	2845765			271		12	Cross Bedding
	0781732	2845765			119		12	Cross Bedding
	0781732	2845765			289		18	Cross Bedding
	0781732	2845765			119		19	Cross Bedding
	0781732	2845765			279		1	Cross Bedding
	0781732	2845765			1		18	Cross Bedding
	0781732	2845765			290		1	Cross Bedding
	0781732	2845765			187		20	Cross Bedding

	0781732	2845765			200		4	Cross Bedding
	0781732	2845765			195		0	Cross Bedding
	0781732	2845765			194		7	Cross Bedding
	0781732	2845765			203		10	Cross Bedding
	0781732	2845765			29		10	Cross Bedding
	0781732	2845765			139		2	Cross Bedding
	0781732	2845765			114		1	Cross Bedding
	0781732	2845765			82		12	Cross Bedding
	0781732	2845765			209		22	Cross Bedding
	0781732	2845765			63			Trough Cross Bedding
	0781732	2845765			130		3	Cross Bedding
	0781732	2845765			82		1	Cross Bedding
	0781732	2845765			83		9	Cross Bedding
	0781732	2845765			140		17	Cross Bedding
	0781732	2845765			148		4	Cross Bedding
HZB_087	0781672	2845887	26		62		6	Cross Bedding
	0781672	2845887			226		2	Cross Bedding
	0781672	2845887			227		11	Cross Bedding
	0781672	2845887			227		10	Cross Bedding
	0781672	2845887			240		10	Cross Bedding
	0781672	2845887			222		16	Cross Bedding
	0781672	2845887			231		1	Cross Bedding
	0781672	2845887			35		4	Cross Bedding
	0781672	2845887			47		-3	Cross Bedding
	0781672	2845887			35		0	Cross Bedding
	0781672	2845887			211		18	Cross Bedding
	0781672	2845887			251		11	Cross Bedding
	0781672	2845887			42		-1	Cross Bedding
	0781672	2845887			191		10	Cross Bedding
	0781672	2845887			207		2	Cross Bedding
	0781672	2845887			21		9	Cross Bedding
	0781672	2845887			49		6	Cross Bedding
	0781672	2845887			224		9	Cross Bedding
	0781672	2845887			264		10	Cross Bedding
	0781672	2845887			23		8	Cross Bedding
	0781672	2845887			222		4	Cross Bedding
	0781672	2845887			47		3	Cross Bedding
	0781672	2845887			42		2	Cross Bedding
	0781672	2845887			105		10	Cross Bedding
	0781672	2845887			259		12	Cross Bedding
	0781672	2845887			42		1	Cross Bedding
	0781672	2845887			225		11	Cross Bedding
	0781672	2845887			46		9	Cross Bedding
	0781672	2845887			41		0	Cross Bedding

	0781672	2845887			43		0	Cross Bedding
	0781672	2845887			231		24	Cross Bedding
	0781672	2845887			214		20	Cross Bedding
	0781672	2845887			33		-2	Cross Bedding
	0781672	2845887			216		22	Cross Bedding
	0781672	2845887			271		11	Cross Bedding
	0781672	2845887			289		2	Cross Bedding
	0781672	2845887			115		14	Cross Bedding
	0781672	2845887			120		13	Cross Bedding
	0781672	2845887			207		4	Cross Bedding
	0781672	2845887			228		14	Cross Bedding
	0781672	2845887			229		14	Cross Bedding
	0781672	2845887			235		12	Cross Bedding
	0781672	2845887			255		12	Cross Bedding
	0781672	2845887			49		4	Cross Bedding
	0781672	2845887			104		12	Cross Bedding
	0781672	2845887			290		14	Cross Bedding
	0781672	2845887			108		2	Cross Bedding
	0781672	2845887			288		12	Cross Bedding
	0781672	2845887			229		10	Cross Bedding
	0781672	2845887			62		2	Cross Bedding
	0781672	2845887			55		6	Cross Bedding
	0781672	2845887			247		8	Cross Bedding
	0781672	2845887			250		9	Cross Bedding
	0781672	2845887			247		10	Cross Bedding
	0781672	2845887			60		10	Cross Bedding
	0781672	2845887			35		2	Cross Bedding
	0781672	2845887			61		1	Cross Bedding
	0781672	2845887			52		8	Cross Bedding
	0781672	2845887			76		7	Cross Bedding
	0781672	2845887			75		8	Cross Bedding
	0781672	2845887			218		3	Cross Bedding
	0781672	2845887			209		7	Cross Bedding
	0781672	2845887			218		17	Cross Bedding
	0781672	2845887			250		20	Cross Bedding
	0781672	2845887			224		14	Cross Bedding
	0781672	2845887			139		34	Cross Bedding
	0781672	2845887			138		4	Cross Bedding
	0781672	2845887			128		6	Cross Bedding
	0781672	2845887			122		10	Cross Bedding
HZB_088	0781600	2845967			199		14	Cross Bedding
	0781600	2845967			297		9	Cross Bedding
	0781600	2845967			199		8	Cross Bedding
	0781600	2845967			50		2	Cross Bedding
	0781600	2845967			47		11	Cross Bedding

	0781600	2845967			75		19	Cross Bedding
	0781600	2845967			245		2	Cross Bedding
	0781600	2845967			91		11	Cross Bedding
	0781600	2845967			273		20	Cross Bedding
	0781600	2845967			86		16	Cross Bedding
	0781600	2845967			43		10	Cross Bedding
	0781600	2845967			34		5	Cross Bedding
	0781600	2845967			45		2	Cross Bedding
	0781600	2845967			68		20	Cross Bedding
	0781600	2845967			250		11	Cross Bedding
	0781600	2845967			30		8	Cross Bedding
	0781600	2845967			335		16	Cross Bedding
	0781600	2845967			156		4	Cross Bedding
	0781600	2845967			118		23	Cross Bedding
HZB_089	0781586	2845934			155		3	Cross Bedding
	0781586	2845934			160		24	Cross Bedding
	0781586	2845934			108		2	Cross Bedding
	0781586	2845934			60		3	Cross Bedding
	0781586	2845934			59		2	Cross Bedding
	0781586	2845934			30		7	Cross Bedding
	0781586	2845934			105		11	Cross Bedding
	0781586	2845934			145		10	Cross Bedding
	0781586	2845934			173		8	Cross Bedding
	0781586	2845934			41		22	Cross Bedding
	0781586	2845934			216		4	Cross Bedding
	0781586	2845934			44		11	Cross Bedding
HZB_090	0781497	2846232	27		241		14	Asymmetric
	0781497	2846232			58		15	Asymmetric
	0781497	2846232			192	12		Ripples
	0781497	2846232			187	7		Ripples
	0781497	2846232			195	15		Ripples
	0781497	2846232			199	19		Ripples
	0781497	2846232			26	206		Ripples
	0781497	2846232			35	215		Ripples
	0781497	2846232			25	205		Ripples
	0781497	2846232			33	213		Ripples
	0781497	2846232			2	182		Ripples
	0781497	2846232			203		27	Asymmetric
	0781497	2846232			21		28	Asymmetric
	0781497	2846232			20	200		Ripples
	0781497	2846232			24	204		Ripples
	0781497	2846232			21	201		Ripples
	0781497	2846232			333	153		Ripples
	0781497	2846232			341	169		Ripples
	0781497	2846232			347	167		Ripples

	0781497	2846232			355	175		Ripples
	0781497	2846232			333	153		Ripples
	0781497	2846232			349	169		Ripples
	0781497	2846232			349	169		Ripples
	0781497	2846232			4	184		Ripples
	0781497	2846232			350		14	Asymmetric
	0781497	2846232			321		34	Asymmetric
	0781497	2846232			219		22	Asymmetric
	0781497	2846232			354	174		Ripples
	0781497	2846232			349	169		Ripples
	0781497	2846232			330	170		Ripples
	0781497	2846232			335	155		Ripples
	0781497	2846232			356	176		Ripples
	0781497	2846232			354	174		Ripples
	0781497	2846232			312	132		Ripples
	0781497	2846232			295	115		Ripples
	0781497	2846232			289	109		Ripples
	0781497	2846232			324	144		Ripples
	0781497	2846232			344	166		Ripples
	0781497	2846232			349	169		Ripples
	0781497	2846232			343	163		Ripples
	0781497	2846232			201		21	Asymmetric
	0781497	2846232			137		31	Asymmetric
	0781497	2846232			326	146		Ripples
	0781497	2846232			138		21	Asymmetric
	0781497	2846232			22	202		Ripples
	0781497	2846232			27		0	Cross Bedding
	0781497	2846232			32		1	Cross Bedding
	0781497	2846232			38		0	Cross Bedding
	0781497	2846232			210		15	Cross Bedding
	0781497	2846232			216		15	Cross Bedding
	0781497	2846232			194		2	Cross Bedding
	0781497	2846232			37	217		Ripples
	0781497	2846232			38	218		Ripples
	0781497	2846232			23	203		Ripples
	0781497	2846232			195		46	Asymmetric
	0781497	2846232			215		25	Cross Bedding
	0781497	2846232			210		20	Cross Bedding
	0781497	2846232			228		14	Cross Bedding
	0781497	2846232			42		6	Cross Bedding
HZB_091	0781554	2846112	28		300		10	Cross Bedding
	0781554	2846112			305		0	Cross Bedding
	0781554	2846112			293		14	Cross Bedding
	0781554	2846112			298		17	Cross Bedding
	0781554	2846112			297		9	Cross Bedding

	0781554	2846112			6	186		Ripples
	0781554	2846112			10	190		Ripples
	0781554	2846112			137			Cross Bedding
	0781554	2846112			114		5	Cross Bedding
	0781554	2846112			109		4	Cross Bedding
	0781554	2846112			112		6	Cross Bedding
	0781554	2846112			314		14	Cross Bedding
	0781554	2846112			311		5	Cross Bedding
	0781554	2846112			355		10	Cross Bedding
	0781554	2846112			290		12	Cross Bedding
	0781554	2846112			288		7	Cross Bedding
	0781554	2846112			124		9	Cross Bedding
	0781554	2846112			99		8	Cross Bedding
	0781554	2846112			189		20	Cross Bedding
	0781554	2846112			8		14	Cross Bedding
	0781554	2846112			118		12	Cross Bedding
	0781554	2846112			324		14	Cross Bedding
	0781554	2846112			37		12	Cross Bedding
	0781554	2846112			185		20	Cross Bedding
	0781554	2846112			13		5	Cross Bedding
	0781554	2846112			196		2	Cross Bedding
	0781554	2846112			4		10	Cross Bedding
	0781554	2846112			127		18	Cross Bedding
	0781554	2846112			34		2	Cross Bedding
	0781554	2846112			130		7	Cross Bedding
	0781554	2846112			110		1	Cross Bedding
	0781554	2846112			15		5	Cross Bedding
	0781554	2846112			12		10	Cross Bedding
	0781554	2846112			15		12	Cross Bedding
HZB_092	0781649	2846158	31		186		7	Cross Bedding
	0781649	2846158			2		3	Cross Bedding
	0781649	2846158			3		0	Cross Bedding
	0781649	2846158			285		8	Cross Bedding
	0781649	2846158			192		8	Cross Bedding
	0781649	2846158			192		10	Cross Bedding
	0781649	2846158			294		-5	Cross Bedding
	0781649	2846158			119		20	Cross Bedding
	0781649	2846158			115		3	Cross Bedding
	0781649	2846158			114		18	Cross Bedding
	0781649	2846158			124		1	Cross Bedding
	0781649	2846158			321		12	Cross Bedding
	0781649	2846158			156		13	Cross Bedding
	0781649	2846158			223		15	Cross Bedding
	0781649	2846158			322		0	Cross Bedding
	0781649	2846158			327		1	Cross Bedding

	0781649	2846158			178		10	Cross Bedding
	0781649	2846158			220		2	Cross Bedding
	0781649	2846158			221		3	Cross Bedding
	0781649	2846158			228		5	Cross Bedding
	0781649	2846158			228		1	Cross Bedding
	0781649	2846158			224		2	Cross Bedding
HZB_093	0780818	2844775	32		351	171		Ripples
	0780818	2844775			355	175		Ripples
	0780818	2844775			157		30	Asmmetric
	0780818	2844775			345	165		Ripples
	0780818	2844775			350	170		Ripples
	0780818	2844775			186		18	Asmmetric
	0780818	2844775			42	222		Ripples
	0780818	2844775			23	203		Ripples
	0780818	2844775			11	191		Ripples
	0780818	2844775			14	194		Ripples
	0780818	2844775			10	190		Ripples
	0780818	2844775			26		9	Cross Bedding
	0780818	2844775			208		20	Cross Bedding
	0780818	2844775			212		2	Cross Bedding
	0780818	2844775			215		4	Cross Bedding
	0780818	2844775			198		15	Cross Bedding
	0780818	2844775			198		10	Cross Bedding
	0780818	2844775			193		15	Cross Bedding
	0780818	2844775			190		7	Cross Bedding
	0780818	2844775			18	198		Ripples
	0780818	2844775			347	167		Ripples
	0780818	2844775			31		20	Asmmetric
	0780818	2844775			120		15	Asmmetric
	0780818	2844775			358	178		Ripples
	0780818	2844775			360	180		Ripples
	0780818	2844775			353	173		Ripples
	0780818	2844775			24	204		Ripples
	0780818	2844775			24	204		Ripples
	0780818	2844775			10	190		Ripples
	0780818	2844775			33		20	Asmmetric
	0780818	2844775			39	219		Ripples
	0780818	2844775			25	205		Ripples
	0780818	2844775			31	131		Ripples
	0780818	2844775			19	199		Ripples
	0780818	2844775			23	203		Ripples
	0780818	2844775			30	210		Ripples
	0780818	2844775			45	225		Ripples
	0780818	2844775			1	181		Ripples
	0780818	2844775			125		37	Asmmetric

	0780818	2844775			32	212		Ripples
	0780818	2844775			45	225		Ripples
	0780818	2844775			35	215		Ripples
	0780818	2844775			12	192		Ripples
	0780818	2844775			8	188		Ripples
	0780818	2844775			233	153		Ripples
	0780818	2844775			354	174		Ripples
	0780818	2844775			203		10	Cross Bedding
	0780818	2844775			5		30	Cross Bedding
	0780818	2844775			215		18	Cross Bedding
	0780818	2844775			205		18	Cross Bedding
	0780818	2844775			208		18	Cross Bedding
	0780818	2844775			30		0	Cross Bedding
	0780818	2844775			34		3	Cross Bedding
	0780818	2844775			37		11	Cross Bedding
	0780818	2844775			39		1	Cross Bedding
	0780818	2844775			22		12	Cross Bedding
	0780818	2844775			220		24	Cross Bedding
	0780818	2844775			208		21	Cross Bedding
	0780818	2844775			22		-3	Cross Bedding
	0780818	2844775			194		14	Cross Bedding
	0780818	2844775			51		4	Cross Bedding
	0780818	2844775			28		2	Cross Bedding
	0780818	2844775			215		2	Cross Bedding
HZB_095	0781059	2844725			103		20	Cross Bedding
	0781059	2844725			147		2	Cross Bedding
	0781059	2844725			101		23	Cross Bedding
HZB_096a	0781078	2844750	31		197		20	Cross Bedding
	0781078	2844750			204		10	Cross Bedding
	0781078	2844750			196		25	Cross Bedding
	0781078	2844750			202		4	Cross Bedding
	0781078	2844750			199		25	Cross Bedding
	0781078	2844750			193		18	Cross Bedding
	0781078	2844750			195		8	Cross Bedding
	0781078	2844750			209		7	Cross Bedding
	0781078	2844750			197			Cross Bedding
HZB_096b	0781075	2844752			177		13	Cross Bedding
	0781075	2844752			191		21	Cross Bedding
	0781075	2844752			197		22	Cross Bedding
	0781075	2844752			183		20	Cross Bedding
	0781075	2844752			193		21	Cross Bedding
	0781075	2844752			200		18	Cross Bedding
	0781075	2844752			200		10	Cross Bedding
	0781075	2844752			213		2	Cross Bedding
	0781075	2844752			199		19	Cross Bedding

	0781075	2844752			245		0	Cross Bedding
	0781075	2844752			107		23	Cross Bedding
	0781075	2844752			105		32	Cross Bedding
	0781075	2844752			95		34	Cross Bedding
	0781075	2844752			93		79	Cross Bedding
	0781075	2844752			285		7	Cross Bedding
	0781075	2844752			287		0	Cross Bedding
	0781075	2844752			283		1	Cross Bedding
	0781075	2844752			110		10	Cross Bedding
	0781075	2844752			110		2	Cross Bedding
	0781075	2844752			245		4	Cross Bedding
	0781075	2844752			100		5	Cross Bedding
	0781075	2844752			103		115	Cross Bedding
	0781075	2844752			13		8	Cross Bedding
	0781075	2844752			286		13	Cross Bedding
	0781075	2844752			112		8	Cross Bedding
	0781075	2844752			125		12	Cross Bedding
	0781075	2844752			296		5	Cross Bedding
	0781075	2844752			309		5	Cross Bedding
HZB_097a	0780884	2845201		9a	356	186		Ripples
HZB_097b	0780939	2845224		9b	64	244		Ripples
	0780939	2845224			352	182		Ripples
	0780939	2845224			352	182		Ripples
	0780939	2845224			62		21	Asymmetric
	0780939	2845224			246	84		Ripples
	0780939	2845224			121		30	Asymmetric
	0780939	2845224			53	233		Ripples
	0780939	2845224			273		23	Asymmetric
	0780939	2845224			68	248		Ripples
HZB_098	0780907	2845106	34		20	209		Ripples
	0780907	2845106			17	197		Ripples
	0780907	2845106			65	245		Ripples
	0780907	2845106			345	165		Ripples
	0780907	2845106			8	188		Ripples
	0780907	2845106			46	226		Ripples
	0780907	2845106			50	230		Ripples
	0780907	2845106			14		12	Asymmertic
	0780907	2845106			214		51	Asymmertic
	0780907	2845106			48		5	Asymmertic
	0780907	2845106			338	158		Ripples
	0780907	2845106			76	256		Ripples
	0780907	2845106			49	229		Ripples
	0780907	2845106			207		11	Cross Bedding
	0780907	2845106			219		10	Cross Bedding
	0780907	2845106			208		15	Cross Bedding

	0780907	2845106			360		-7	Cross Bedding
	0780907	2845106			205		21	Cross Bedding
	0780907	2845106			293		2	Cross Bedding
	0780907	2845106			208		11	Cross Bedding
	0780907	2845106			218		28	Cross Bedding
	0780907	2845106			209		21	Cross Bedding
	0780907	2845106			209		4	Cross Bedding
	0780907	2845106			20		2	Cross Bedding
	0780907	2845106			200		10	Cross Bedding
	0780907	2845106			199		8	Cross Bedding
	0780907	2845106			214		9	Cross Bedding
	0780907	2845106			97		11	Cross Bedding
	0780907	2845106			259		4	Cross Bedding
	0780907	2845106			101		12	Cross Bedding
	0780907	2845106			198		1	Cross Bedding
	0780907	2845106			196		21	Cross Bedding
	0780907	2845106			190		22	Cross Bedding
	0780907	2845106			190		24	Cross Bedding
	0780907	2845106			211		19	Cross Bedding
	0780907	2845106			199		4	Cross Bedding
	0780907	2845106			192		3	Cross Bedding
	0780907	2845106			208		8	Cross Bedding
	0780907	2845106			219		21	Cross Bedding
	0780907	2845106			198		8	Cross Bedding
	0780907	2845106			210		14	Cross Bedding
	0780907	2845106			207		14	Cross Bedding
	0780907	2845106			207		11	Cross Bedding
	0780907	2845106			207		12	Cross Bedding
	0780907	2845106			207		18	Cross Bedding
	0780907	2845106			202		25	Cross Bedding
	0780907	2845106			205		8	Cross Bedding
	0780907	2845106			200		24	Cross Bedding
	0780907	2845106			250		20	Cross Bedding
	0780907	2845106			260		10	Cross Bedding
	0780907	2845106			271		4	Cross Bedding
	0780907	2845106			272		11	Cross Bedding
	0780907	2845106			263		10	Cross Bedding
	0780907	2845106			204		12	Cross Bedding
	0780907	2845106			242		2	Cross Bedding
	0780907	2845106			57		17	Cross Bedding
	0780907	2845106			215		10	Cross Bedding
	0780907	2845106			215		10	Cross Bedding
	0780907	2845106			36		10	Cross Bedding
	0780907	2845106			22		21	Cross Bedding
	0780907	2845106			8		22	Cross Bedding

	0780907	2845106			198		23	Cross Bedding
	0780907	2845106			19		0	Cross Bedding
	0780907	2845106			202		10	Cross Bedding
	0780907	2845106			208		12	Cross Bedding
	0780907	2845106			194		6	Cross Bedding
	0780907	2845106			206		9	Cross Bedding
	0780907	2845106			200		15	Cross Bedding
	0780907	2845106			200		22	Cross Bedding
	0780907	2845106			192		19	Cross Bedding
	0780907	2845106			75		6	Cross Bedding
	0780907	2845106			76		12	Cross Bedding
	0780907	2845106			78		2	Cross Bedding
HZB_099a	0782041	2845178			44		11	Cross Bedding
	0782041	2845178			26		3	Cross Bedding
	0782041	2845178			200		11	Cross Bedding
	0782041	2845178			30		16	Cross Bedding
	0782041	2845178			30		11	Cross Bedding
	0782041	2845178			215		5	Cross Bedding
	0782041	2845178			35		10	Cross Bedding
	0782041	2845178			31		10	Cross Bedding
	0782041	2845178			29		10	Cross Bedding
	0782041	2845178			31		11	Cross Bedding
	0782041	2845178			30		3	Cross Bedding
	0782041	2845178			324		8	Cross Bedding
	0782041	2845178			71		1	Cross Bedding
	0782041	2845178			322		2	Cross Bedding
	0782041	2845178			327		11	Cross Bedding
	0782041	2845178			148		10	Cross Bedding
	0782041	2845178			19		2	Cross Bedding
	0782041	2845178			25		19	Cross Bedding
	0782041	2845178			312		12	Cross Bedding
	0782041	2845178			209		8	Cross Bedding
	0782041	2845178			261		8	Cross Bedding
	0782041	2845178			81		2	Cross Bedding
	0782041	2845178			230		12	Cross Bedding
HZB_099b	0782041	2845201			300		1	Cross Bedding
	0782041	2845201			301		8	Cross Bedding
	0782041	2845201			271		8	Cross Bedding
	0782041	2845201			92		2	Cross Bedding
	0782041	2845201			118		23	Cross Bedding
	0782041	2845201			293		11	Cross Bedding
	0782041	2845201			293		8	Cross Bedding
	0782041	2845201			24		15	Cross Bedding
	0782041	2845201			27		0	Cross Bedding
	0782041	2845201			27		8	Cross Bedding

	0782041	2845201			29		9	Cross Bedding
	0782041	2845201			26		12	Cross Bedding
	0782041	2845201			24		11	Cross Bedding
	0782041	2845201			160		10	Cross Bedding
	0782041	2845201			221		19	Cross Bedding
	0782041	2845201			142		10	Cross Bedding
	0782041	2845201			198		3	Cross Bedding
	0782041	2845201			40		10	Cross Bedding
	0782041	2845201			209		11	Cross Bedding
HZB_100	0782063	2845188			300		13	Cross Bedding
	0782063	2845188			81		2	Cross Bedding
	0782063	2845188			300		1	Cross Bedding
	0782063	2845188			299		10	Cross Bedding
	0782063	2845188			312		19	Cross Bedding
	0782063	2845188			319		6	Cross Bedding
	0782063	2845188			4		18	Cross Bedding
	0782063	2845188			354		21	Cross Bedding
	0782063	2845188			355	185		Ripples
	0782063	2845188			355		30	Asyemmetric
	0782063	2845188			334	154		Ripples
	0782063	2845188			3		9	Cross Bedding
	0782063	2845188			23		13	Cross Bedding
	0782063	2845188			4		24	Cross Bedding
	0782063	2845188			355		8	Cross Bedding
	0782063	2845188			216		-2	Cross Bedding
	0782063	2845188			208		10	Cross Bedding
	0782063	2845188			210		1	Cross Bedding
	0782063	2845188			310		13	Cross Bedding
	0782063	2845188			216		9	Cross Bedding
	0782063	2845188			39		11	Cross Bedding
	0782063	2845188			30		2	Cross Bedding
	0782063	2845188			359		9	Cross Bedding
	0782063	2845188			30		19	Cross Bedding
	0782063	2845188			359		22	Cross Bedding
HZB_101	0781986	2845211	33		39		3	Cross Bedding
	0781986	2845211			274		11	Cross Bedding
	0781986	2845211			176		12	Cross Bedding
	0781986	2845211			281		3	Cross Bedding
	0781986	2845211			133		3	Cross Bedding
	0781986	2845211			138		13	Cross Bedding
	0781986	2845211			132		8	Cross Bedding
	0781986	2845211			130		1	Cross Bedding
	0781986	2845211			176		20	Cross Bedding
	0781986	2845211			173		2	Cross Bedding
	0781986	2845211			163		10	Cross Bedding

	0781986	2845211			130		5	Cross Bedding
	0781986	2845211			312	132		Ripples
	0781986	2845211			351	181		Ripples
	0781986	2845211			302		21	Asymmetric
	0781986	2845211			222	42		Ripples
	0781986	2845211			26	206		Ripples
	0781986	2845211			169	349		Ripples
	0781986	2845211			6		20	Asymmetric
	0781986	2845211			278		2	Cross Bedding
	0781986	2845211			126		5	Cross Bedding
	0781986	2845211			299		2	Cross Bedding
	0781986	2845211			129		4	Cross Bedding
	0781986	2845211			307		3	Cross Bedding
	0781986	2845211			157		3	Cross Bedding
	0781986	2845211			297		17	Cross Bedding
	0781986	2845211			281		3	Cross Bedding
	0781986	2845211			256		2	Cross Bedding
	0781986	2845211			130		12	Cross Bedding
HZB_102	0781882	2845216			238		10	Cross Bedding
	0781882	2845216			25		8	Cross Bedding
	0781882	2845216			168		2	Cross Bedding
	0781882	2845216			187		8	Cross Bedding
	0781882	2845216			356		3	Cross Bedding
	0781882	2845216			206			Cross Bedding
	0781882	2845216			325		12	Cross Bedding
	0781882	2845216			289		15	Cross Bedding
	0781882	2845216			298		16	Cross Bedding
	0781882	2845216			200		9	Cross Bedding
	0781882	2845216			286		10	Cross Bedding
	0781882	2845216			113		3	Cross Bedding
	0781882	2845216			214		3	Cross Bedding
	0781882	2845216			238		10	Cross Bedding
	0781882	2845216			209		15	Cross Bedding
	0781882	2845216			203		1	Cross Bedding
	0781882	2845216			186		0	Cross Bedding
	0781882	2845216			100		20	Cross Bedding
	0781882	2845216			38		10	Cross Bedding
	0781882	2845216			34		8	Cross Bedding
	0781882	2845216			1		6	Cross Bedding
	0781882	2845216			20		0	Cross Bedding
	0781882	2845216			6		0	Cross Bedding
	0781882	2845216			148		3	Cross Bedding
	0781882	2845216			318		15	Cross Bedding
	0781882	2845216			297		9	Cross Bedding
	0781882	2845216			113		1	Cross Bedding

	0781882	2845216			112		13	Cross Bedding
	0781882	2845216			112		5	Cross Bedding
	0781882	2845216			113		6	Cross Bedding
	0781882	2845216			292		1	Cross Bedding
	0781882	2845216			112		7	Cross Bedding
	0781882	2845216			111		3	Cross Bedding
	0781882	2845216			290		5	Cross Bedding
	0781882	2845216			115		7	Cross Bedding
	0781882	2845216			115		19	Cross Bedding
	0781882	2845216			114		3	Cross Bedding
	0781882	2845216			292		3	Cross Bedding
	0781882	2845216			289		5	Cross Bedding
HZB_103	0781851	2845183			147		3	Cross Bedding
	0781851	2845183			292		2	Cross Bedding
	0781851	2845183			138		9	Cross Bedding
	0781851	2845183			238		11	Cross Bedding
	0781851	2845183			40		1	Cross Bedding
	0781851	2845183			284		2	Cross Bedding
	0781851	2845183			282		12	Cross Bedding
	0781851	2845183			97		5	Cross Bedding
	0781851	2845183			305		2	Cross Bedding
	0781851	2845183			127		8	Cross Bedding
	0781851	2845183			297		13	Cross Bedding
	0781851	2845183			111		1	Cross Bedding
	0781851	2845183			289		9	Cross Bedding
	0781851	2845183			100		8	Cross Bedding
	0781851	2845183			106		3	Cross Bedding
	0781851	2845183			281		21	Cross Bedding
	0781851	2845183			122		10	Cross Bedding
	0781851	2845183			295		8	Cross Bedding
	0781851	2845183			111		13	Cross Bedding
	0781851	2845183			276		13	Cross Bedding
	0781851	2845183			134		1	Cross Bedding
	0781851	2845183			314		1	Cross Bedding
	0781851	2845183			327		2	Cross Bedding
	0781851	2845183			150		13	Cross Bedding
	0781851	2845183			324		4	Cross Bedding
	0781851	2845183			345		8	Cross Bedding
	0781851	2845183			162		9	Cross Bedding
	0781851	2845183			165		11	Cross Bedding
	0781851	2845183			58		18	Cross Bedding
HZB_104	0781808	2845204	36		308		1	Cross Bedding
	0781808	2845204			306		0	Cross Bedding
	0781808	2845204			138		10	Cross Bedding
	0781808	2845204			298		8	Cross Bedding

	0781808	2845204			294		0	Cross Bedding
	0781808	2845204			298		14	Cross Bedding
	0781808	2845204			115		14	Cross Bedding
	0781808	2845204			119		18	Cross Bedding
	0781808	2845204			126		8	Cross Bedding
	0781808	2845204			321		10	Cross Bedding
	0781808	2845204			133		11	Cross Bedding
	0781808	2845204			293		20	Cross Bedding
	0781808	2845204			305		12	Cross Bedding
	0781808	2845204			294		10	Cross Bedding
	0781808	2845204			90		6	Cross Bedding
	0781808	2845204			125		8	Cross Bedding
	0781808	2845204			135		30	Cross Bedding
	0781808	2845204			124		8	Cross Bedding
	0781808	2845204			178		9	Cross Bedding
	0781808	2845204			182		9	Cross Bedding
	0781808	2845204			183		2	Cross Bedding
	0781808	2845204			196		15	Cross Bedding
	0781808	2845204			52		11	Cross Bedding
	0781808	2845204			192		2	Cross Bedding
	0781808	2845204			210		8	Cross Bedding
	0781808	2845204			32		21	Cross Bedding
	0781808	2845204			3		1	Cross Bedding
	0781808	2845204			41		11	Cross Bedding
	0781808	2845204			42		3	Cross Bedding
	0781808	2845204			206		7	Cross Bedding
	0781808	2845204			38		7	Cross Bedding
	0781808	2845204			217		19	Cross Bedding
	0781808	2845204			21		8	Cross Bedding
	0781808	2845204			213		20	Cross Bedding
	0781808	2845204			31		8	Cross Bedding
	0781808	2845204			27		6	Cross Bedding
	0781808	2845204			215		8	Cross Bedding
	0781808	2845204			332		6	Cross Bedding
	0781808	2845204			220		11	Cross Bedding
	0781808	2845204			153		10	Cross Bedding
	0781808	2845204			166		15	Cross Bedding
	0781808	2845204			218		9	Cross Bedding
	0781808	2845204			50		7	Cross Bedding
	0781808	2845204			76		5	Cross Bedding
	0781808	2845204			32		7	Cross Bedding
	0781808	2845204			26		0	Cross Bedding
	0781808	2845204			197		14	Cross Bedding
	0781808	2845204			197		17	Cross Bedding
	0781808	2845204			188		17	Cross Bedding

	0781808	2845204			299		8	Cross Bedding
	0781808	2845204			121		9	Cross Bedding
	0781808	2845204			128		2	Cross Bedding
	0781808	2845204			326		10	Cross Bedding
	0781808	2845204			345		5	Cross Bedding
	0781808	2845204			348		2	Cross Bedding
	0781808	2845204			341		11	Cross Bedding
	0781808	2845204			349		5	Cross Bedding
	0781808	2845204			348		5	Cross Bedding
	0781808	2845204			176		0	Cross Bedding
	0781808	2845204			359		10	Cross Bedding
	0781808	2845204			336		18	Cross Bedding
	0781808	2845204			340		26	Cross Bedding
	0781808	2845204			337		8	Cross Bedding
	0781808	2845204			337		9	Cross Bedding
	0781808	2845204			336		18	Cross Bedding
	0781808	2845204			340		26	Cross Bedding
	0781808	2845204			2		11	Cross Bedding
	0781808	2845204			154		13	Cross Bedding
HZB_105	0781565	2845201			339		14	Cross Bedding
	0781565	2845201			123		10	Cross Bedding
	0781565	2845201			330		-1	Cross Bedding
	0781565	2845201			310		10	Cross Bedding
	0781565	2845201			280		3	Cross Bedding
	0781565	2845201			295		9	Cross Bedding
	0781565	2845201			135		15	Cross Bedding
	0781565	2845201			300		17	Cross Bedding
	0781565	2845201			301		5	Cross Bedding
	0781565	2845201			119		7	Cross Bedding
	0781565	2845201			85		12	Cross Bedding
	0781565	2845201			75		22	Cross Bedding
	0781565	2845201			337		13	Cross Bedding
	0781565	2845201			150		11	Cross Bedding
	0781565	2845201			160		15	Cross Bedding
	0781565	2845201			232			Cross Bedding
	0781565	2845201			230		7	Cross Bedding
	0781565	2845201			50		13	Cross Bedding
	0781565	2845201			53		3	Cross Bedding
	0781565	2845201			226		11	Cross Bedding
	0781565	2845201			57		15	Cross Bedding
	0781565	2845201			80		12	Cross Bedding
	0781565	2845201			40		6	Cross Bedding
	0781565	2845201			84		5	Cross Bedding
	0781565	2845201			75		7	Cross Bedding
	0781565	2845201			228	48		RUC

	0781565	2845201			278	98		RUC
	0781565	2845201			118		15	Cross Bedding
	0781565	2845201			118		25	Cross Bedding
	0781565	2845201			128		16	Cross Bedding
	0781565	2845201			120		7	Cross Bedding
	0781565	2845201			136		21	Cross Bedding
	0781565	2845201			132		14	Cross Bedding
	0781565	2845201			314		5	Cross Bedding
	0781565	2845201			277		7	Cross Bedding
	0781565	2845201			113		12	Cross Bedding
	0781565	2845201			60		11	Cross Bedding
	0781565	2845201			241		0	Cross Bedding
	0781565	2845201			65		11	Cross Bedding
	0781565	2845201			68		12	Cross Bedding
	0781565	2845201			85		6	Cross Bedding
	0781565	2845201			253		1	Cross Bedding
HZB_106	0781113	2844865	37		274		4	Cross Bedding
	0781113	2844865			263		15	Cross Bedding
	0781113	2844865			271		3	Cross Bedding
	0781113	2844865			73		10	Cross Bedding
	0781113	2844865			251		7	Cross Bedding
	0781113	2844865			180		32	Cross Bedding
	0781113	2844865			185		34	Cross Bedding
	0781113	2844865			185		30	Cross Bedding
	0781113	2844865			183	3		Ripples
HZB_107	0781989	2845555	38		11		15	Cross Bedding
	0781989	2845555			187		5	Cross Bedding
	0781989	2845555			175		0	Cross Bedding
	0781989	2845555			356		20	Cross Bedding
	0781989	2845555			18		14	Cross Bedding
	0781989	2845555			29		20	Cross Bedding
	0781989	2845555			208		-1	Cross Bedding
	0781989	2845555			210		-2	Cross Bedding
	0781989	2845555			55		16	Cross Bedding
	0781989	2845555			42		11	Cross Bedding
	0781989	2845555			224		43	Cross Bedding
	0781989	2845555			63		11	Cross Bedding
	0781989	2845555			59		18	Cross Bedding
	0781989	2845555			65		10	Cross Bedding
	0781989	2845555			64		-3	Cross Bedding
	0781989	2845555			68		5	Cross Bedding
	0781989	2845555			9		2	Cross Bedding
	0781989	2845555			183		5	Cross Bedding
	0781989	2845555			33		20	Cross Bedding
	0781989	2845555			25		20	Cross Bedding

	0781989	2845555			198		-10	Cross Bedding
	0781989	2845555			23		22	Cross Bedding
	0781989	2845555			203		6	Cross Bedding
	0781989	2845555			25		15	Cross Bedding
	0781989	2845555			198		-4	Cross Bedding
	0781989	2845555			18		10	Cross Bedding
	0781989	2845555			199		20	Cross Bedding
	0781989	2845555			6		8	Cross Bedding
	0781989	2845555			21		12	Cross Bedding
	0781989	2845555			20		2	Cross Bedding
	0781989	2845555			210		2	Cross Bedding
	0781989	2845555			34		5	Cross Bedding
	0781989	2845555			104		10	Cross Bedding
	0781989	2845555			111		7	Cross Bedding
	0781989	2845555			289		18	Cross Bedding
	0781989	2845555			287		1	Cross Bedding
	0781989	2845555			204		17	Cross Bedding
	0781989	2845555			38		21	Cross Bedding
	0781989	2845555			34		17	Cross Bedding
	0781989	2845555			21		7	Cross Bedding
	0781989	2845555			36		19	Cross Bedding
	0781989	2845555			36		19	Cross Bedding
	0781989	2845555			22		11	Cross Bedding
	0781989	2845555			25		10	Cross Bedding
	0781989	2845555			106		6	Cross Bedding
	0781989	2845555			342		21	Cross Bedding
	0781989	2845555			19		6	Cross Bedding
	0781989	2845555			33		1	Cross Bedding
	0781989	2845555			22		4	Cross Bedding
	0781989	2845555			40		10	Cross Bedding
	0781989	2845555			29		10	Cross Bedding
	0781989	2845555			211		3	Cross Bedding
	0781989	2845555			30		11	Cross Bedding
	0781989	2845555			32		14	Cross Bedding
	0781989	2845555			205		18	Cross Bedding
	0781989	2845555			110		10	Cross Bedding
	0781989	2845555			347		11	Cross Bedding
	0781989	2845555			30		17	Cross Bedding
	0781989	2845555			199		4	Cross Bedding
	0781989	2845555			36		19	Cross Bedding
	0781989	2845555			47		11	Cross Bedding
	0781989	2845555			30		24	Cross Bedding
	0781989	2845555			38		15	Cross Bedding
	0781989	2845555			213		1	Cross Bedding
	0781989	2845555			220		8	Cross Bedding

	0781989	2845555			104		2	Cross Bedding
	0781989	2845555			284		4	Cross Bedding
	0781989	2845555			160		3	Cross Bedding
	0781989	2845555			31		19	Cross Bedding
	0781989	2845555			20		19	Cross Bedding
	0781989	2845555			34		15	Cross Bedding
	0781989	2845555			41		9	Cross Bedding
	0781989	2845555			222		2	Cross Bedding
	0781989	2845555			296		9	Cross Bedding
	0781989	2845555			294		6	Cross Bedding
	0781989	2845555			114		21	Cross Bedding
	0781989	2845555			109		10	Cross Bedding
	0781989	2845555			104		11	Cross Bedding
	0781989	2845555			307		6	Cross Bedding
	0781989	2845555			109		25	Cross Bedding
	0781989	2845555			46		12	Cross Bedding
	0781989	2845555			298		4	Cross Bedding
	0781989	2845555			281		3	Cross Bedding
	0781989	2845555			205		3	Cross Bedding
	0781989	2845555			288		10	Cross Bedding
	0781989	2845555			275		7	Cross Bedding
	0781989	2845555			77		2	Cross Bedding
	0781989	2845555			38		9	Cross Bedding
	0781989	2845555			108		16	Cross Bedding
	0781989	2845555			294		7	Cross Bedding
	0781989	2845555			115		9	Cross Bedding
	0781989	2845555			109		5	Cross Bedding
	0781989	2845555			297		15	Cross Bedding
	0781989	2845555			291		10	Cross Bedding
	0781989	2845555			293		11	Cross Bedding
	0781989	2845555			116		8	Cross Bedding
	0781989	2845555			112		19	Cross Bedding
	0781989	2845555			105		2	Cross Bedding
	0781989	2845555			100		12	Cross Bedding
	0781989	2845555			295		19	Cross Bedding
	0781989	2845555			104		11	Cross Bedding
HZB_108	0782016	2845653	39		311		3	Cross Bedding
	0782016	2845653			112		7	Cross Bedding
	0782016	2845653			110		6	Cross Bedding
	0782016	2845653			114		1	Cross Bedding
	0782016	2845653			289		3	Cross Bedding
	0782016	2845653			293		11	Cross Bedding
	0782016	2845653			119		6	Cross Bedding
	0782016	2845653			310		2	Cross Bedding
	0782016	2845653			336		17	Cross Bedding

	0782016	2845653			149		3	Cross Bedding
	0782016	2845653			347		7	Cross Bedding
	0782016	2845653			334		8	Cross Bedding
	0782016	2845653			347		20	Cross Bedding
	0782016	2845653			140		6	Cross Bedding
	0782016	2845653			321		2	Cross Bedding
	0782016	2845653			346		10	Cross Bedding
	0782016	2845653			331		16	Cross Bedding
	0782016	2845653			143		37	Ripples
	0782016	2845653			316	136		Asymmetric
	0782016	2845653			290	110		Ripples
	0782016	2845653			264	44		Ripples
	0782016	2845653			96		25	Asymmetric
	0782016	2845653			259		-9	Low Angle Cross Bedding
	0782016	2845653			109		26	Low Angle Cross Bedding
	0782016	2845653			271	91		Ripples
	0782016	2845653			270	90		Ripples
	0782016	2845653			275	95		Ripples
	0782016	2845653			306		-4	Cross Bedding
	0782016	2845653			310		2	Cross Bedding
	0782016	2845653			326	146		Ripples
	0782016	2845653			323	143		Ripples
	0782016	2845653			301	121		Ripples
	0782016	2845653			305		20	Asymmetric
	0782016	2845653			133		9	Cross Bedding
	0782016	2845653			123	11		Cross Bedding
	0782016	2845653			128	12		Cross Bedding
	0782016	2845653			182	3		Low Angle Cross Bedding
HZB_109	0781892	2845881			307		15	Cross Bedding
	0781892	2845881			143		5	Cross Bedding
	0781892	2845881			358			Cross Bedding
	0781892	2845881			346		2	Cross Bedding
HZB_109b	0781880	2845865			133		12	Cross Bedding
	0781880	2845865			17		12	Cross Bedding
	0781880	2845865			19		10	Cross Bedding
	0781880	2845865			51		12	Cross Bedding
	0781880	2845865			67		12	Cross Bedding
	0781880	2845865			238		11	Cross Bedding
	0781880	2845865			20		1	Cross Bedding
	0781880	2845865			57		12	Cross Bedding
	0781880	2845865			69		9	Cross Bedding
	0781880	2845865			18		1	Cross Bedding

	0781880	2845865			58		3	Cross Bedding
	0781880	2845865			235		10	Cross Bedding
	0781880	2845865			5		19	Cross Bedding
	0781880	2845865			84		11	Cross Bedding
	0781880	2845865			230		2	Cross Bedding
	0781880	2845865			25		12	Cross Bedding
	0781880	2845865			224		4	Cross Bedding
	0781880	2845865			38		11	Cross Bedding
HZB_110	0781754	2845879			125		25	Cross Bedding
	0781754	2845879			120		5	Cross Bedding
	0781754	2845879			114		21	Cross Bedding
	0781754	2845879			118		20	Cross Bedding
	0781754	2845879			110		18	Cross Bedding
	0781754	2845879			121		1	Cross Bedding
	0781754	2845879			116		2	Cross Bedding
	0781754	2845879			120		25	Cross Bedding
	0781754	2845879			123		29	Cross Bedding
	0781754	2845879			120		2	Cross Bedding
	0781754	2845879			115		24	Cross Bedding
	0781754	2845879			121		19	Cross Bedding
	0781754	2845879			115		25	Cross Bedding
	0781754	2845879			121		23	Cross Bedding
	0781754	2845879			129		2	Cross Bedding
	0781754	2845879			110		25	Cross Bedding
	0781754	2845879			138		21	Cross Bedding
	0781754	2845879			161		34	Cross Bedding
	0781754	2845879			157		17	Cross Bedding
	0781754	2845879			178		14	Cross Bedding
	0781754	2845879			189		7	Cross Bedding
	0781754	2845879			150		6	Cross Bedding
	0781754	2845879			134		10	Cross Bedding
HZB_111a	0781552	2845807			193			Cross Bedding
	0781552	2845807			203		13	Cross Bedding
	0781552	2845807			33		5	Cross Bedding
	0781552	2845807			200		12	Cross Bedding
	0781552	2845807			8		3	Cross Bedding
	0781552	2845807			196		9	Cross Bedding
	0781552	2845807			201		2	Cross Bedding
	0781552	2845807			200		2	Cross Bedding
	0781552	2845807			193		19	Cross Bedding
	0781552	2845807			191		8	Cross Bedding
	0781552	2845807			189		9	Cross Bedding
	0781552	2845807			176		10	Cross Bedding
	0781552	2845807			177		2	Cross Bedding
	0781552	2845807			221			Cross Bedding

	0781552	2845807			235		2	Cross Bedding
	0781552	2845807			228		10	Cross Bedding
	0781552	2845807			206		4	Cross Bedding
	0781552	2845807			208		2	Cross Bedding
	0781552	2845807			205		5	Cross Bedding
HZB_111b	0781547	2845798			195		22	Cross Bedding
	0781547	2845798			11		1	Cross Bedding
	0781547	2845798			197		19	Cross Bedding
	0781547	2845798			197		3	Cross Bedding
	0781547	2845798			193		15	Cross Bedding
	0781547	2845798			198		16	Cross Bedding
	0781547	2845798			194		14	Cross Bedding
	0781547	2845798			203		10	Cross Bedding
	0781547	2845798			170		11	Cross Bedding
	0781547	2845798			175		9	Cross Bedding
	0781547	2845798			179		11	Cross Bedding
	0781547	2845798			173		0	Cross Bedding
	0781547	2845798			189		14	Cross Bedding
HZB_112	0781829	2845909			213		21	Cross Bedding
	0781829	2845909			209		19	Cross Bedding
	0781829	2845909			26		3	Cross Bedding
	0781829	2845909			208		17	Cross Bedding
	0781829	2845909			220		4	Cross Bedding
	0781829	2845909			281		8	Cross Bedding
	0781829	2845909			284		7	Cross Bedding
	0781829	2845909			284		8	Cross Bedding
	0781829	2845909			45		2	Cross Bedding
	0781829	2845909			51		9	Cross Bedding
	0781829	2845909			67	247		Ripples
	0781829	2845909			50	230		Ripples
HZB_113	0781410	2845828	40		344	164		Ripples
	0781410	2845828			329	19		Ripples
	0781410	2845828			339	159		Ripples
	0781410	2845828			341	161		Ripples
	0781410	2845828			307	127		Ripples
	0781410	2845828			242	162		Ripples
	0781410	2845828			360	180		Ripples
	0781410	2845828			351	171		Ripples
	0781410	2845828			336		40	Asymmetric
	0781410	2845828			7	187		Ripples
	0781410	2845828			7	187		Ripples
	0781410	2845828			358	178		Ripples
	0781410	2845828			4	184		Ripples
	0781410	2845828			343	163		Ripples
	0781410	2845828			355	175		Ripples

	0781410	2845828			194		31	Asymmetric
	0781410	2845828			8		4	Ripples
	0781410	2845828			14	194		Ripples
	0781410	2845828			15	195		Ripples
	0781410	2845828			182		17	Low Angle Cross Beddig
	0781410	2845828			175		19	Low Angle Cross Beddig
	0781410	2845828			157		5	Low Angle Cross Beddig
	0781410	2845828			39	159		Ripples
	0781410	2845828			159		35	Asymmetric
	0781410	2845828			155		37	Asymmetric
	0781410	2845828			25	205		Ripples
	0781410	2845828			5	185		Ripples
	0781410	2845828			325	145		Ripples
	0781410	2845828			345	165		Ripples
	0781410	2845828			5	185		Ripples
	0781410	2845828			19	199		Ripples
	0781410	2845828			26	206		Ripples
	0781410	2845828			22	202		Ripples
	0781410	2845828			5	185		Ripples
	0781410	2845828			1	181		Ripples
	0781410	2845828			20	200		Ripples
	0781410	2845828			8	188		Ripples
	0781410	2845828			185		10	Cross Bedding
	0781410	2845828			198		19	Cross Bedding
	0781410	2845828			33		32	Ripples
	0781410	2845828			16		-1	Cross Bedding
	0781410	2845828			16		20	Cross Bedding
	0781410	2845828			352		40	Ripples
	0781410	2845828			21	201		Asymmetric
	0781410	2845828			213		34	Cross Bedding
	0781410	2845828			214		28	Cross Bedding
	0781410	2845828			33		6	Cross Bedding
	0781410	2845828			30		3	Cross Bedding
	0781410	2845828			228		2	Cross Bedding
	0781410	2845828			221		10	Cross Bedding
	0781410	2845828			52		6	Cross Bedding
	0781410	2845828			14		2	Cross Bedding
	0781410	2845828			40		12	Cross Bedding
	0781410	2845828			230		8	Cross Bedding
	0781410	2845828			233		18	Cross Bedding
	0781410	2845828			217		8	Cross Bedding
	0781410	2845828			199		18	Cross Bedding

	0781410	2845828			213		14	Cross Bedding
	0781410	2845828			23		15	Cross Bedding
	0781410	2845828			22		1	Cross Bedding
	0781410	2845828			20		0	Cross Bedding
	0781410	2845828			17		2	Cross Bedding
	0781410	2845828			22		3	Cross Bedding
	0781410	2845828			31		5	Cross Bedding
	0781410	2845828			217		25	Cross Bedding
	0781410	2845828			210		30	Cross Bedding
	0781410	2845828			212		10	Cross Bedding
HZB_114	0781410	2845833			180			Cross Bedding
	0781410	2845833			176			Cross Bedding
	0781410	2845833			336			Cross Bedding
	0781410	2845833			175			Cross Bedding
	0781410	2845833			191			Cross Bedding
	0781410	2845833			200			Cross Bedding
	0781410	2845833			206			Cross Bedding
	0781410	2845833			218		7	Cross Bedding
	0781410	2845833			206		16	Cross Bedding
	0781410	2845833						Cross Bedding
HZB_115	0781780	2845603			313	133		Ripples
	0781780	2845603			300			Asymmetric
	0781780	2845603			120		2	Cross Bedding
	0781780	2845603			127		11	Cross Bedding
	0781780	2845603			117		17	Cross Bedding
	0781780	2845603			16		7	Cross Bedding
	0781780	2845603			37		13	Cross Bedding
	0781780	2845603			40		8	Cross Bedding
	0781780	2845603			215			Cross Bedding
	0781780	2845603			222		1	Cross Bedding
	0781780	2845603			22		11	Cross Bedding
	0781780	2845603			23		9	Cross Bedding
	0781780	2845603			21		9	Cross Bedding
	0781780	2845603			197		5	Cross Bedding
	0781780	2845603			25		15	Cross Bedding
	0781780	2845603			27		10	Cross Bedding
	0781780	2845603			25		10	Cross Bedding
	0781780	2845603			30		12	Cross Bedding
	0781780	2845603			62		6	Cross Bedding
	0781780	2845603			62		18	Cross Bedding
	0781780	2845603			47		17	Cross Bedding
	0781780	2845603			43		17	Cross Bedding
HZB_85b	0781896	2845678			286		6	Cross Bedding
	0781896	2845678			111		15	Cross Bedding
	0781896	2845678			291			Cross Bedding

	0781896	2845678			267		3	Cross Bedding
	0781896	2845678			267		20	Cross Bedding
	0781896	2845678			107		9	Cross Bedding
	0781896	2845678			289		6	Cross Bedding
	0781896	2845678			244		30	Asymmetric
	0781896	2845678			118	298		Ripples
HZB_116c	0782800	2853527			328		19	Cross Bedding
	0782800	2853527			325		4	Cross Bedding
	0782800	2853527			330		15	Cross Bedding
	0782800	2853527			144		8	Cross Bedding
	0782800	2853527			321		25	Cross Bedding
	0782800	2853527			331		14	Cross Bedding
	0782800	2853527			145		8	Cross Bedding
	0782800	2853527			152		11	Cross Bedding
	0782800	2853527			324		3	Cross Bedding
	0782800	2853527			329		1	Cross Bedding
	0782800	2853527			139		1	Cross Bedding
	0782800	2853527			320		17	Cross Bedding
	0782800	2853527			319		1	Cross Bedding
	0782800	2853527			325		1	Cross Bedding
	0782800	2853527			133		3	Cross Bedding
	0782800	2853527			155		4	Cross Bedding
	0782800	2853527			324		1	Cross Bedding
	0782800	2853527			334		17	Cross Bedding
	0782800	2853527			328		11	Cross Bedding
	0782800	2853527			330		21	Cross Bedding
	0782800	2853527			334		23	Cross Bedding
	0782800	2853527			343		8	Cross Bedding
	0782800	2853527			328		11	Cross Bedding
	0782800	2853527			341		17	Cross Bedding
	0782800	2853527			308		15	Cross Bedding
	0782800	2853527			23		20	Cross Bedding
	0782800	2853527			293		1	Cross Bedding
	0782800	2853527			189		1	Cross Bedding
	0782800	2853527			330		15	Cross Bedding
	0782800	2853527			355		22	Cross Bedding
	0782800	2853527			330		3	Cross Bedding
	0782800	2853527			350		21	Cross Bedding
	0782800	2853527			328		18	Cross Bedding
	0782800	2853527			339		5	Cross Bedding
	0782800	2853527			341		20	Cross Bedding
	0782800	2853527			337		21	Cross Bedding
	0782800	2853527			144		1	Cross Bedding
	0782800	2853527			337		22	Cross Bedding
	0782800	2853527			323		31	Cross Bedding

	0782800	2853527			320		11	Cross Bedding
	0782800	2853527			320		32	Cross Bedding
	0782800	2853527			142		5	Cross Bedding
	0782800	2853527			310		3	Cross Bedding
	0782800	2853527			353		13	Cross Bedding
	0782800	2853527			170		2	Cross Bedding
	0782800	2853527			353		21	Cross Bedding
	0782800	2853527			354		3	Cross Bedding
	0782800	2853527			354		24	Cross Bedding
	0782800	2853527			169		7	Cross Bedding
	0782800	2853527			344		19	Cross Bedding
	0782800	2853527			163		1	Cross Bedding
	0782800	2853527			293			Cross Bedding
	0782800	2853527			172		17	Cross Bedding
	0782800	2853527			351		8	Cross Bedding
	0782800	2853527			347		12	Cross Bedding
	0782800	2853527			346		21	Cross Bedding
	0782800	2853527			321		16	Cross Bedding
	0782800	2853527			324		13	Cross Bedding
	0782800	2853527			345		9	Cross Bedding
	0782800	2853527			329			Cross Bedding
	0782800	2853527			318		13	Cross Bedding
	0782800	2853527			333		9	Cross Bedding
	0782800	2853527			351		20	Cross Bedding
	0782800	2853527			181	1		Ripples
	0782800	2853527			181		15	Asymmetric
HZB_116d	0782816	2853526			237		15	Cross Bedding
	0782816	2853526			60		1	Cross Bedding
	0782816	2853526			260		9	Cross Bedding
	0782816	2853526			265		18	Cross Bedding
	0782816	2853526			255		20	Cross Bedding
	0782816	2853526			321		16	Cross Bedding
	0782816	2853526			55	235		Ripples
	0782816	2853526			120	300		Ripples
	0782816	2853526			111		2	Cross Bedding
	0782816	2853526			221		19	Cross Bedding
	0782816	2853526			221		18	Cross Bedding
	0782816	2853526			219		17	Cross Bedding
	0782816	2853526			207		11	Cross Bedding
	0782816	2853526			278		21	Cross Bedding
	0782816	2853526			284		2	Cross Bedding
	0782816	2853526			290		22	Cross Bedding
	0782816	2853526			286		3	Cross Bedding
	0782816	2853526			287		10	Cross Bedding
	0782816	2853526			225		4	Cross Bedding

	0782816	2853526			228		7	Cross Bedding
	0782816	2853526			44		12	Cross Bedding
	0782816	2853526			218		20	Cross Bedding
	0782816	2853526			324		11	Cross Bedding
	0782816	2853526			227		1	Cross Bedding
	0782816	2853526			266		22	Cross Bedding
	0782816	2853526			320		11	Cross Bedding
	0782816	2853526			322		20	Cross Bedding
	0782816	2853526			323		4	Cross Bedding
	0782816	2853526			335		18	Cross Bedding
	0782816	2853526			331		8	Cross Bedding
	0782816	2853526			332		22	Cross Bedding
HZB_116f	0782805	2853523			283		18	Cross Bedding
	0782805	2853523			283		1	Cross Bedding
	0782805	2853523			260		15	Cross Bedding
	0782805	2853523			272		11	Cross Bedding
	0782805	2853523			265		11	Cross Bedding
	0782805	2853523			273		1	Cross Bedding
	0782805	2853523			295		27	Cross Bedding
	0782805	2853523			261		29	Cross Bedding
	0782805	2853523			277		31	Cross Bedding
	0782805	2853523			255		11	Cross Bedding
	0782805	2853523			276		20	Cross Bedding
	0782805	2853523			293		2	Cross Bedding
	0782805	2853523			291		11	Cross Bedding
	0782805	2853523			271		1	Cross Bedding
	0782805	2853523			283		20	Cross Bedding
	0782805	2853523			258		19	Cross Bedding
	0782805	2853523			321		21	Cross Bedding
	0782805	2853523			273		21	Cross Bedding
	0782805	2853523			82		1	Cross Bedding
	0782805	2853523			315		21	Cross Bedding
	0782805	2853523			215		15	Cross Bedding
	0782805	2853523			209		9	Cross Bedding
	0782805	2853523			206		11	Cross Bedding
	0782805	2853523			236		20	Cross Bedding
	0782805	2853523			244		15	Cross Bedding
	0782805	2853523			35		10	Cross Bedding
	0782805	2853523			247		12	Cross Bedding
	0782805	2853523			62		15	Cross Bedding
	0782805	2853523			252		13	Cross Bedding
	0782805	2853523			70		5	Cross Bedding
	0782805	2853523			338		14	Cross Bedding
	0782805	2853523			247		9	Cross Bedding
	0782805	2853523			220		17	Cross Bedding

	0782805	2853523			191		9	Cross Bedding
	0782805	2853523			191		2	Cross Bedding
	0782805	2853523			193		6	Cross Bedding
	0782805	2853523			231		12	Cross Bedding
	0782805	2853523			232		8	Cross Bedding
	0782805	2853523			231		12	Cross Bedding
	0782805	2853523			49		11	Cross Bedding
	0782805	2853523			52		10	Cross Bedding
	0782805	2853523			27		3	Cross Bedding
	0782805	2853523			27		11	Cross Bedding
	0782805	2853523			262		2	Cross Bedding
	0782805	2853523			257		14	Cross Bedding
	0782805	2853523			202		12	Cross Bedding
	0782805	2853523			28		1	Cross Bedding
	0782805	2853523			339		35	Cross Bedding
	0782805	2853523			61		0	Cross Bedding
	0782805	2853523			61		21	Cross Bedding
	0782805	2853523			222		14	Cross Bedding
	0782805	2853523			247		0	Cross Bedding
	0782805	2853523			254		20	Cross Bedding
	0782805	2853523			248		15	Cross Bedding
	0782805	2853523			45		14	Cross Bedding
	0782805	2853523			242		1	Cross Bedding
	0782805	2853523			248		8	Cross Bedding
	0782805	2853523			42		2	Cross Bedding
	0782805	2853523			48		0	Cross Bedding
	0782805	2853523			227		1	Cross Bedding
	0782805	2853523			218		6	Cross Bedding
	0782805	2853523			45		8	Cross Bedding
	0782805	2853523			220		16	Cross Bedding
	0782805	2853523			222		1	Cross Bedding
	0782805	2853523			221		10	Cross Bedding
	0782805	2853523			42		15	Cross Bedding
	0782805	2853523			222		3	Cross Bedding
	0782805	2853523			232		18	Cross Bedding
HZB_117	0782835	2853538			335		22	Cross Bedding
	0782835	2853538			336		22	Cross Bedding
	0782835	2853538			327		8	Cross Bedding
	0782835	2853538			25		24	Cross Bedding
	0782835	2853538			181		3	Cross Bedding
	0782835	2853538			22		18	Cross Bedding
	0782835	2853538			202		14	Cross Bedding
	0782835	2853538			199		1	Cross Bedding
	0782835	2853538			44		11	Cross Bedding
	0782835	2853538			225		12	Cross Bedding

	0782835	2853538			263		22	Cross Bedding
	0782835	2853538			62		1	Cross Bedding
	0782835	2853538			243		13	Cross Bedding
	0782835	2853538			228		8	Cross Bedding
	0782835	2853538			237		3	Cross Bedding
	0782835	2853538			240		26	Cross Bedding
	0782835	2853538			229		11	Cross Bedding
	0782835	2853538			301		9	Cross Bedding
	0782835	2853538			330		28	Cross Bedding
	0782835	2853538			299		24	Cross Bedding
	0782835	2853538			300		8	Cross Bedding
	0782835	2853538			306		10	Cross Bedding
HZB_118	0782621	2853326			252			Cross Bedding
	0782621	2853326			67			Cross Bedding
	0782621	2853326			92			Cross Bedding
	0782621	2853326			268			Cross Bedding
	0782621	2853326			265			Cross Bedding
	0782621	2853326			85			Cross Bedding
	0782621	2853326			267			Cross Bedding
	0782621	2853326			276			Cross Bedding
	0782621	2853326			238		21	Cross Bedding
	0782621	2853326			233		23	Cross Bedding
	0782621	2853326			255		20	Cross Bedding
	0782621	2853326			269			Cross Bedding
	0782621	2853326			239		20	Cross Bedding
	0782621	2853326			248		23	Cross Bedding
	0782621	2853326			228		3	Cross Bedding
	0782621	2853326			83		1	Cross Bedding
	0782621	2853326			259		20	Cross Bedding
	0782621	2853326			262		3	Cross Bedding
	0782621	2853326			261		11	Cross Bedding
	0782621	2853326			260		15	Cross Bedding
	0782621	2853326			246		8	Cross Bedding
	0782621	2853326			255		10	Cross Bedding
	0782621	2853326			247		5	Cross Bedding
	0782621	2853326			20		20	Cross Bedding
	0782621	2853326			70		0	Cross Bedding
	0782621	2853326			258		16	Cross Bedding
HZB_119	0782722	2852901	41		247		24	Cross Bedding
	0782722	2852901			239		21	Cross Bedding
	0782722	2852901			244		36	Cross Bedding
	0782722	2852901			245		5	Cross Bedding
	0782722	2852901			220		1	Cross Bedding
	0782722	2852901			56		20	Cross Bedding
	0782722	2852901			219		19	Cross Bedding

	0782722	2852901			216		21	Cross Bedding
	0782722	2852901			45		1	Cross Bedding
	0782722	2852901			222		10	Cross Bedding
	0782722	2852901			245		15	Cross Bedding
	0782722	2852901			265		3	Cross Bedding
	0782722	2852901			216		1	Cross Bedding
	0782722	2852901			216		12	Cross Bedding
	0782722	2852901			218		12	Cross Bedding
	0782722	2852901			208		10	Cross Bedding
HZB_120	0782867	2852814	42		299		10	Cross Bedding
	0782867	2852814			301		8	Cross Bedding
	0782867	2852814			316		1	Cross Bedding
	0782867	2852814			8		5	Cross Bedding
	0782867	2852814			5		37	Cross Bedding
	0782867	2852814			356		13	Cross Bedding
	0782867	2852814			349		8	Cross Bedding
	0782867	2852814			351		10	Cross Bedding
	0782867	2852814			313		14	Cross Bedding
	0782867	2852814			325		8	Cross Bedding
	0782867	2852814			315		16	Cross Bedding
	0782867	2852814			307		8	Cross Bedding
	0782867	2852814			313		24	Cross Bedding
	0782867	2852814			307		12	Cross Bedding
	0782867	2852814			316		12	Cross Bedding
	0782867	2852814			303		11	Cross Bedding
	0782867	2852814			284		7	Cross Bedding
	0782867	2852814			290		12	Cross Bedding
	0782867	2852814			334		11	Cross Bedding
	0782867	2852814			321		3	Cross Bedding
	0782867	2852814			325		3	Cross Bedding
HZB_121	0782721	2853061	43		283		4	Cross Bedding
	0782721	2853061			251		10	Cross Bedding
	0782721	2853061			66		3	Cross Bedding
	0782721	2853061			55		3	Cross Bedding
	0782721	2853061			45		2	Cross Bedding
	0782721	2853061			42		9	Cross Bedding
	0782721	2853061			42		1	Cross Bedding
	0782721	2853061			243		11	Cross Bedding
	0782721	2853061			55		11	Cross Bedding
	0782721	2853061			211		2	Cross Bedding
	0782721	2853061			210		2	Cross Bedding
	0782721	2853061			226		11	Cross Bedding
	0782721	2853061			222		13	Cross Bedding
	0782721	2853061			48		9	Cross Bedding
	0782721	2853061			33		10	Cross Bedding

	0782721	2853061			50		5	Cross Bedding
	0782721	2853061			237		5	Cross Bedding
	0782721	2853061			232		15	Cross Bedding
HZB_122	0782584	2853370			359		12	Cross Bedding
	0782584	2853370			357		8	Cross Bedding
	0782584	2853370			354		6	Cross Bedding
	0782584	2853370			355		5	Cross Bedding
	0782584	2853370			318		28	Cross Bedding
	0782584	2853370			360		1	Cross Bedding
	0782584	2853370			340		3	Cross Bedding
	0782584	2853370			350		10	Cross Bedding
	0782584	2853370			347		10	Cross Bedding
	0782584	2853370			330		24	Cross Bedding
	0782584	2853370			197		3	Cross Bedding
	0782584	2853370			81		12	Cross Bedding
	0782584	2853370			358		2	Cross Bedding
	0782584	2853370			168		7	Cross Bedding
	0782584	2853370			78		20	Cross Bedding
	0782584	2853370			216		14	Cross Bedding
	0782584	2853370			262		14	Cross Bedding
	0782584	2853370			264		29	Cross Bedding
	0782584	2853370			263		22	Cross Bedding
	0782584	2853370			261		20	Cross Bedding
	0782584	2853370			260		15	Cross Bedding
	0782584	2853370			217		18	Cross Bedding
	0782584	2853370			215		8	Cross Bedding
	0782584	2853370			220		16	Cross Bedding
HZB_123	0778103	2841383	44		72	252		Ripples
	0778103	2841383			51	231		Ripples
	0778103	2841383			72	252		Ripples
	0778103	2841383			43	223		Ripples
	0778103	2841383			38	215		Ripples
	0778103	2841383			55	235		Ripples
	0778103	2841383			96			Cross Lamination
	0778103	2841383			56	236		Ripples
	0778103	2841383			50		10	Asymmetric
	0778103	2841383			50	230		Ripples
	0778103	2841383			48	228		Ripples
	0778103	2841383			51	231		Ripples
	0778103	2841383			49	229		Ripples
	0778103	2841383			49	229		Ripples
	0778103	2841383			49	229		Ripples
	0778103	2841383			259		5	Asymmetric
	0778103	2841383			261		6	Asymmetric

	0778103	2841383			30	210		Ripples
	0778103	2841383			50	230		Ripples
	0778103	2841383			50	230		Ripples
	0778103	2841383			66	246		Ripples
	0778103	2841383			51	2321		Ripples
	0778103	2841383			45	225		Ripples
	0778103	2841383			45	225		Ripples
	0778103	2841383			219		16	Asymmetric
	0778103	2841383			17	197		Ripples
	0778103	2841383			41		29	Asymmetric
	0778103	2841383			52	232		Ripples
	0778103	2841383			67	247		Ripples
	0778103	2841383			63	243		Ripples
	0778103	2841383			53	233		Ripples
	0778103	2841383			63	243		Ripples
	0778103	2841383			53	233		Ripples
	0778103	2841383			47		3	Asymmetric
	0778103	2841383			65	245		Ripples
	0778103	2841383			65	245		Ripples
	0778103	2841383			87	267		Ripples
	0778103	2841383			62	242		Ripples
	0778103	2841383			23		24	Asymmetric
	0778103	2841383			89	269		Ripples
	0778103	2841383			332	152		Ripples
	0778103	2841383			76	256		Ripples
	0778103	2841383			256		26	Asymmetric
	0778103	2841383			60	240		Ripples
	0778103	2841383			95	275		Ripples
	0778103	2841383			98	278		Ripples
	0778103	2841383			43	223		Ripples
	0778103	2841383			35	215		Ripples
	0778103	2841383			55	235		Ripples
	0778103	2841383			52	352		Ripples
	0778103	2841383			63		5	Cross Lamination
	0778103	2841383			63		6	Cross Lamination
	0778103	2841383			63		10	Cross Lamination
	0778103	2841383			238		20	Cross Lamination
	0778103	2841383			238		22	Cross Lamination
	0778103	2841383			48	228		Ripples
	0778103	2841383			45	225		Ripples
	0778103	2841383			56	236		Ripples

	0778103	2841383			56	236		Ripples
	0778103	2841383			56	236		Ripples
	0778103	2841383			358	178		Ripples
	0778103	2841383			353	173		Ripples
	0778103	2841383			19	199		Ripples
	0778103	2841383			1	181		Ripples
	0778103	2841383			1	181		Ripples
	0778103	2841383			19	199		Ripples
	0778103	2841383			299	119		Ripples
	0778103	2841383			171		35	Asymmetric
	0778103	2841383			50	230		Ripples
	0778103	2841383			50	230		Ripples
	0778103	2841383			341	161		Ripples
	0778103	2841383			225	205		Ripples
	0778103	2841383			48	228		Ripples
	0778103	2841383			65	245		Ripples
	0778103	2841383			48	228		Ripples
	0778103	2841383			64	244		Ripples
	0778103	2841383			324	144		Ripples
	0778103	2841383			324	144		Ripples
	0778103	2841383			57	237		Ripples
	0778103	2841383			66	246		Ripples
	0778103	2841383			60	240		Ripples
	0778103	2841383			50	230		Ripples
	0778103	2841383			58	238		Ripples
	0778103	2841383			55	235		Ripples
	0778103	2841383			52	232		Ripples
	0778103	2841383			52	232		Ripples
	0778103	2841383			240	49		Ripples
	0778103	2841383			50	230		Ripples
	0778103	2841383			50	230		Ripples
	0778103	2841383			50	230		Ripples
	0778103	2841383			79	259		Ripples
	0778103	2841383			62	242		Ripples
	0778103	2841383			84	264		Ripples
	0778103	2841383			41	221		Ripples
	0778103	2841383			48	228		Ripples
	0778103	2841383			21	201		Ripples
	0778103	2841383			29	209		Ripples
	0778103	2841383			50	230		Ripples
	0778103	2841383			38	218		Ripples
	0778103	2841383			27	207		Ripples
	0778103	2841383			17	197		Ripples
	0778103	2841383			29	209		Ripples
	0778103	2841383			201		11	Asymmetric

	0778103	2841383			54	234		Ripples
	0778103	2841383			233		15	Asymmetric
	0778103	2841383			42	224		Ripples
	0778103	2841383			46	226		Ripples
	0778103	2841383			37	217		Ripples
	0778103	2841383			43	223		Ripples
	0778103	2841383			44	224		Ripples
	0778103	2841383			34	214		Ripples
	0778103	2841383			30	210		Ripples
	0778103	2841383			351	171		Ripples
	0778103	2841383			26	206		Ripples
	0778103	2841383			33	213		Ripples
	0778103	2841383			37	217		Ripples
	0778103	2841383			47	227		Ripples
	0778103	2841383			63		38	Asymmetric
	0778103	2841383			58	238		Ripples
	0778103	2841383			36	216		Ripples
	0778103	2841383			36	216		Ripples
	0778103	2841383			57	237		Ripples
	0778103	2841383			57	237		Ripples
	0778103	2841383			43	223		Ripples
	0778103	2841383			23	203		Ripples
	0778103	2841383			30	210		Ripples
	0778103	2841383			41	221		Ripples
	0778103	2841383			74	254		Ripples
	0778103	2841383			36	216		Ripples
	0778103	2841383			21	201		Ripples
	0778103	2841383			31	211		Ripples
	0778103	2841383			58	238		Ripples
	0778103	2841383			65	245		Ripples
	0778103	2841383			65	245		Ripples
	0778103	2841383			237		10	Asymmetric
HZB_124	0783236	2853071	45		151		11	Cross Bedding
	0783236	2853071			158		3	Cross Bedding
	0783236	2853071			153		2	Cross Bedding
	0783236	2853071			342		27	Cross Bedding
	0783236	2853071			345		12	Cross Bedding
	0783236	2853071			341		7	Cross Bedding
	0783236	2853071			46		3	Cross Bedding
	0783236	2853071			179		6	Cross Bedding
	0783236	2853071			195		10	Cross Bedding
	0783236	2853071			1		11	Cross Bedding
	0783236	2853071			334		26	Cross Bedding
	0783236	2853071			218		11	Cross Bedding
	0783236	2853071			213		-2	Cross Bedding

	0783236	2853071			287		6	Cross Bedding
	0783236	2853071			290		3	Cross Bedding
	0783236	2853071			155		2	Cross Bedding
	0783236	2853071			138		6	Cross Bedding
	0783236	2853071			321		3	Cross Bedding
	0783236	2853071			325		17	Cross Bedding
	0783236	2853071			339			Cross Bedding
HZB_125	0782608	2852661	46		324			Cross Bedding
	0782608	2852661			333		15	Cross Bedding
	0782608	2852661			323		15	Cross Bedding
	0782608	2852661			342		15	Cross Bedding
	0782608	2852661			345		15	Cross Bedding
	0782608	2852661			337		18	Cross Bedding
	0782608	2852661			331		18	Cross Bedding
	0782608	2852661			342		10	Cross Bedding
	0782608	2852661			315		12	Cross Bedding
	0782608	2852661			322		6	Cross Bedding
	0782608	2852661			341		5	Cross Bedding
	0782608	2852661			193		10	Cross Bedding
	0782608	2852661			190		5	Cross Bedding
	0782608	2852661			170		11	Cross Bedding
	0782608	2852661			329		21	Cross Bedding
	0782608	2852661			169		12	Cross Bedding
	0782608	2852661			158		2	Cross Bedding
	0782608	2852661			341		9	Cross Bedding
	0782608	2852661			94		10	Cross Bedding
	0782608	2852661			274		21	Cross Bedding
	0782608	2852661			282		16	Cross Bedding
	0782608	2852661			102		1	Cross Bedding
	0782608	2852661			172		14	Cross Bedding
	0782608	2852661			334		22	Cross Bedding
	0782608	2852661			106	286		Cross Bedding
	0782608	2852661			98		3	Cross Bedding
	0782608	2852661			279		2	Cross Bedding
	0782608	2852661			98		4	Cross Bedding
	0782608	2852661			349		11	Cross Bedding
	0782608	2852661			344		18	Cross Bedding
	0782608	2852661			356		17	Cross Bedding
	0782608	2852661			303		2	Cross Bedding
	0782608	2852661			304		11	Cross Bedding
	0782608	2852661			262		19	Cross Bedding
	0782608	2852661			73		11	Cross Bedding
	0782608	2852661			77		1	Cross Bedding
	0782608	2852661			104		2	Cross Bedding
	0782608	2852661			255		3	Cross Bedding

	0782608	2852661			170		14	Cross Bedding
	0782608	2852661			172		6	Cross Bedding
	0782608	2852661			348		1	Cross Bedding
	0782608	2852661			131		12	Cross Bedding
	0782608	2852661			173		1	Cross Bedding
	0782608	2852661			119		13	Cross Bedding
	0782608	2852661			262		8	Cross Bedding
	0782608	2852661			269		10	Cross Bedding
	0782608	2852661			263		24	Cross Bedding
	0782608	2852661			202		11	Cross Bedding
	0782608	2852661			200		4	Cross Bedding
	0782608	2852661			205		2	Cross Bedding
	0782608	2852661			217		4	Cross Bedding
	0782608	2852661			24		8	Cross Bedding
	0782608	2852661			11		13	Cross Bedding
HZB_126	0782624	2852174	47		298		1	Cross Bedding
	0782624	2852174			298		8	Cross Bedding
	0782624	2852174			292		3	Cross Bedding
	0782624	2852174			284		18	Cross Bedding
	0782624	2852174			297		12	Cross Bedding
	0782624	2852174			311		8	Cross Bedding
	0782624	2852174			307		1	Cross Bedding
	0782624	2852174			310		23	Cross Bedding
	0782624	2852174			309		24	Cross Bedding
	0782624	2852174			303		1	Cross Bedding
	0782624	2852174			305		1	Cross Bedding
	0782624	2852174			305		8	Cross Bedding
	0782624	2852174			311		11	Cross Bedding
	0782624	2852174			308		16	Cross Bedding
	0782624	2852174			317		7	Cross Bedding
	0782624	2852174			293			Cross Bedding
HZB_127	0782563	2852257	48		276		7	Cross Bedding
	0782563	2852257			258		3	Cross Bedding
	0782563	2852257			297		5	Cross Bedding
	0782563	2852257			143		1	Cross Bedding
	0782563	2852257			323		2	Cross Bedding
	0782563	2852257			143		1	Cross Bedding
	0782563	2852257			86		3	Cross Bedding
	0782563	2852257			272		18	Cross Bedding
	0782563	2852257			142		3	Cross Bedding
	0782563	2852257			280		5	Cross Bedding
	0782563	2852257			287		6	Cross Bedding
	0782563	2852257			98		8	Cross Bedding
	0782563	2852257			282		-2	Cross Bedding
	0782563	2852257			279		2	Cross Bedding

	0782563	2852257			284		18	Cross Bedding
	0782563	2852257			294		20	Cross Bedding
	0782563	2852257			146		12	Asymmetric
	0782563	2852257			155		4	Asymmetric
	0782563	2852257			159		23	Asymmetric
	0782563	2852257			329	149		Cross Bedding
	0782563	2852257			336	156		Cross Bedding
	0782563	2852257			326	146		Cross Bedding
	0782563	2852257			255		11	Cross Bedding
	0782563	2852257			300		20	Cross Bedding
	0782563	2852257			255		10	Cross Bedding
	0782563	2852257			7		15	Cross Bedding
	0782563	2852257			37		6	Cross Bedding
	0782563	2852257			221		9	Cross Bedding
	0782563	2852257			284		14	Cross Bedding
	0782563	2852257			207		19	Cross Bedding
	0782563	2852257			217		8	Cross Bedding
	0782563	2852257		?	124			Cross Bedding
	0782563	2852257			2000			Cross Bedding
	0782563	2852257			328			Cross Bedding
	0782563	2852257			322			Cross Bedding
	0782563	2852257			119			Cross Bedding
	0782563	2852257			142			Cross Bedding
	0782563	2852257			131		1	Cross Bedding
	0782563	2852257			301		6	Cross Bedding
	0782563	2852257			318		1	Cross Bedding
	0782563	2852257			329		3	Cross Bedding
HZB_128	0782804	2852265	49		210		1	Cross Bedding
	0782804	2852265			315		17	Cross Bedding
	0782804	2852265			304		1	Cross Bedding
	0782804	2852265			318		3	Cross Bedding
	0782804	2852265			123		8	Cross Bedding
	0782804	2852265			145		15	Cross Bedding
	0782804	2852265			145		18	Cross Bedding
	0782804	2852265			301		11	Cross Bedding
	0782804	2852265			281		9	Cross Bedding
	0782804	2852265			281		13	Cross Bedding
	0782804	2852265			281		15	Cross Bedding
	0782804	2852265			290		6	Cross Bedding
	0782804	2852265			288		17	Cross Bedding
	0782804	2852265			293		24	Cross Bedding
	0782804	2852265			289		25	Cross Bedding
	0782804	2852265			286		26	Cross Bedding
	0782804	2852265			283		5	Cross Bedding
	0782804	2852265			251		25	Cross Bedding

	0782804	2852265			232		20	Cross Bedding
	0782804	2852265			277		10	Cross Bedding
	0782804	2852265			273		23	Cross Bedding
	0782804	2852265			274		7	Cross Bedding
	0782804	2852265			277		6	Cross Bedding
	0782804	2852265			91		1	Cross Bedding
	0782804	2852265			93		3	Cross Bedding
	0782804	2852265			257	77		Ripples
	0782804	2852265			261	81		Ripples
	0782804	2852265			110		9	Cross Bedding
HZB_129	0782478	2852455			237		2	Cross Bedding
	0782478	2852455			236		17	Cross Bedding
	0782478	2852455			233		36	Cross Bedding
	0782478	2852455			233		15	Cross Bedding
	0782478	2852455			50		1	Cross Bedding
	0782478	2852455			48		-2	Cross Bedding
	0782478	2852455			229		9	Cross Bedding
	0782478	2852455			231		13	Cross Bedding
	0782478	2852455			224		13	Cross Bedding
	0782478	2852455			217		10	Cross Bedding
	0782478	2852455			235		5	Cross Bedding
	0782478	2852455			238		10	Cross Bedding
	0782478	2852455			247		14	Cross Bedding
	0782478	2852455			245		5	Cross Bedding
	0782478	2852455			238		7	Cross Bedding
HZB_130	0782397	2852370	50		140		1	Cross Bedding
	0782397	2852370			326		8	Cross Bedding
	0782397	2852370			333		5	Cross Bedding
	0782397	2852370			230		2	Cross Bedding
	0782397	2852370			165		0	Cross Bedding
	0782397	2852370			20		2	Cross Bedding
	0782397	2852370			7		6	Cross Bedding
	0782397	2852370			338		1	Cross Bedding
	0782397	2852370			335		15	Cross Bedding
	0782397	2852370			158		2	Cross Bedding
	0782397	2852370			330		4	Cross Bedding
	0782397	2852370			342		10	Cross Bedding
	0782397	2852370			169		6	Cross Bedding
	0782397	2852370			183		10	Cross Bedding
	0782397	2852370			183		3	Cross Bedding
	0782397	2852370			343		6	Cross Bedding
	0782397	2852370			192	12		Ripples
	0782397	2852370			183	3		Ripples
	0782397	2852370			183	3		Ripples
	0782397	2852370			313		9	Low Angle

								Cross Bedding
	0782397	2852370			314		9	Low Angle Cross Bedding
	0782397	2852370			318		6	Low Angle Cross Bedding
	0782397	2852370			321		4	Low Angle Cross Bedding
	0782397	2852370			316		5	Low Angle Cross Bedding
	0782397	2852370			317		3	Low Angle Cross Bedding
	0782397	2852370			323		1	Low Angle Cross Bedding
	0782397	2852370			210		20	Cross Bedding
	0782397	2852370			34		3	Cross Bedding
	0782397	2852370			299		13	Cross Bedding
	0782397	2852370			310		5	Cross Bedding
	0782397	2852370			318		0	Cross Bedding
	0782397	2852370			311		20	Cross Bedding
	0782397	2852370			315		3	Cross Bedding
	0782397	2852370			315		15	Cross Bedding
	0782397	2852370			125		8	Cross Bedding
	0782397	2852370			313		20	Cross Bedding
	0782397	2852370			309		18	Cross Bedding
HZB_131	0779904	2842062	51		53	233		Ripples
	0779904	2842062			54		21	Asymmetric
	0779904	2842062			52	232		Ripples
	0779904	2842062			41	221		Ripples
	0779904	2842062			51	231		Ripples
	0779904	2842062			58	238		Ripples
	0779904	2842062			96	276		Ripples
	0779904	2842062			228		17	Asymmetric
	0779904	2842062			228		20	Asymmetric
	0779904	2842062			36	216		Ripples
	0779904	2842062			41	221		Ripples
	0779904	2842062			41	221		Ripples
	0779904	2842062			9	189		Ripples
	0779904	2842062			57		20	Asymmetric
	0779904	2842062			49	229		Ripples
	0779904	2842062			220		8	Cross Bedding
	0779904	2842062			63		0	Cross Bedding
	0779904	2842062			82		3	Cross Bedding
	0779904	2842062			75		5	Cross Bedding
	0779904	2842062			85		5	Cross Bedding
	0779904	2842062			55	235		Ripples
	0779904	2842062			81	261		Ripples

	0779904	2842062			81	261		Ripples
	0779904	2842062			57	237		Ripples
	0779904	2842062			29	209		Ripples
	0779904	2842062			3	183		Ripples
	0779904	2842062			220		35	Asymmetric
	0779904	2842062			100	280		Ripples
	0779904	2842062			49	229		Ripples
	0779904	2842062			39	259		Ripples
	0779904	2842062			44	224		Ripples
	0779904	2842062			254		40	Asymmetric
	0779904	2842062			9	189		Ripples
	0779904	2842062			287		3	Ripples
	0779904	2842062			23		16	Asymmetric
	0779904	2842062			60	240		Ripples
	0779904	2842062			48	228		Ripples
	0779904	2842062			226		10	Asymmetric
	0779904	2842062			29	209		Ripples
	0779904	2842062			32	212		Ripples
	0779904	2842062			39		24	Asymmetric
	0779904	2842062			28	208		Ripples
	0779904	2842062			25	205		Ripples
	0779904	2842062			216		34	Asymmetric
	0779904	2842062			7	187		Ripples
	0779904	2842062			356	176		Ripples
	0779904	2842062			360	180		Ripples
	0779904	2842062			32	212		Ripples
	0779904	2842062			188		48	Asymmetric
	0779904	2842062			191		40	Asymmetric
	0779904	2842062			91	271		Ripples
	0779904	2842062			91	271		Ripples
	0779904	2842062			9	189		Ripples
	0779904	2842062			9	189		Ripples
	0779904	2842062			26	206		Ripples
	0779904	2842062			39	219		Ripples
	0779904	2842062			79	259		Ripples
HZB_134	0778299	2841427	52		47	227		Ripples
	0778299	2841427			55	235		Ripples
	0778299	2841427			338	158		Ripples
	0778299	2841427			16	196		Ripples
	0778299	2841427			52	232		Ripples
	0778299	2841427			52	232		Ripples
	0778299	2841427			37	217		Ripples
	0778299	2841427			29	209		Ripples
	0778299	2841427			33	213		Ripples
	0778299	2841427			48	228		Ripples

	0778299	2841427			41	221		Ripples
	0778299	2841427			41	221		Ripples
	0778299	2841427			51	231		Ripples
	0778299	2841427			54	234		Ripples
	0778299	2841427			53	233		Ripples
	0778299	2841427			53	233		Ripples
	0778299	2841427			56	236		Ripples
	0778299	2841427			35	215		Ripples
	0778299	2841427			41		35	Asymmetric
	0778299	2841427			40	220		Ripples
	0778299	2841427			40	220		Ripples
	0778299	2841427			40	220		Ripples
	0778299	2841427			31		19	Asymmetric
	0778299	2841427			31	213		Ripples
	0778299	2841427			47	227		Ripples
	0778299	2841427			47	227		Ripples
	0778299	2841427			44	224		Ripples
	0778299	2841427			23	203		Ripples
	0778299	2841427			64	244		Ripples
	0778299	2841427			55		40	Asymmetric
	0778299	2841427			45	225		Ripples
	0778299	2841427			79		30	Asymmetric
	0778299	2841427			35	215		Ripples
	0778299	2841427			49	229		Ripples
	0778299	2841427			44	224		Ripples
	0778299	2841427			51	231		Ripples
	0778299	2841427			47	227		Ripples
	0778299	2841427			63	243		Ripples
	0778299	2841427			50	230		Ripples
	0778299	2841427			22	202		Ripples
	0778299	2841427			22	202		Ripples
	0778299	2841427			37	217		Ripples
	0778299	2841427			37	217		Ripples
	0778299	2841427			37	217		Ripples
	0778299	2841427			47		27	Asymmetric
	0778299	2841427			44	224		Ripples
	0778299	2841427			27	207		Ripples
	0778299	2841427			49	229		Ripples
	0778299	2841427			60		32	Asymmetric
	0778299	2841427			13	193		Ripples
	0778299	2841427			13	193		Ripples
	0778299	2841427			30	210		Ripples
	0778299	2841427			27	207		Ripples
	0778299	2841427			81		36	Asymmetric
	0778299	2841427			24	204		Ripples

	0778299	2841427			51	231		Ripples
	0778299	2841427			60	240		Ripples
	0778299	2841427			53	233		Ripples
	0778299	2841427			40	220		Ripples
	0778299	2841427			21	201		Ripples
	0778299	2841427			35	215		Ripples
	0778299	2841427			29	209		Ripples
	0778299	2841427			50	230		Ripples
	0778299	2841427			51	231		Ripples
	0778299	2841427			76	256		Ripples
	0778299	2841427			76	256		Ripples
	0778299	2841427			62	242		Ripples
	0778299	2841427			33	213		Ripples
	0778299	2841427			40	220		Ripples
	0778299	2841427			50	230		Ripples
	0778299	2841427			24	204		Ripples
	0778299	2841427			31	211		Ripples
	0778299	2841427			38	218		Ripples
	0778299	2841427			41	221		Ripples
	0778299	2841427			24	204		Ripples
	0778299	2841427			42	222		Ripples
	0778299	2841427			4	184		Ripples
	0778299	2841427			34	214		Ripples
	0778299	2841427			34		20	Asymmetric
	0778299	2841427			17		40	Asymmetric
	0778299	2841427			35	215		Ripples
	0778299	2841427			31	211		Ripples
	0778299	2841427			10	190		Ripples
	0778299	2841427			31	211		Ripples
	0778299	2841427			10	190		Ripples
	0778299	2841427			34	214		Ripples
	0778299	2841427			29	209		Ripples
	0778299	2841427			207		50	Asymmetric
	0778299	2841427			21	201		Ripples
	0778299	2841427			37		17	Ripples
	0778299	2841427			218		15	Ripples
	0778299	2841427			10	190		Ripples
	0778299	2841427			45	225		Ripples
	0778299	2841427			20	200		Ripples
	0778299	2841427			351	171		Ripples
	0778299	2841427			25	205		Ripples
	0778299	2841427			24	204		Ripples
	0778299	2841427			9	189		Ripples
	0778299	2841427			31	211		Ripples
	0778299	2841427			89	269		Ripples

	0778299	2841427			53	233		Ripples
	0778299	2841427			200		15	Cross Bedding
	0778299	2841427			205		16	Cross Bedding
	0778299	2841427			233		17	Cross Bedding
	0778299	2841427			206		10	Cross Bedding
	0778299	2841427			215		12	Cross Bedding
	0778299	2841427			219		14	Cross Bedding
	0778299	2841427			215		5	Cross Bedding
	0778299	2841427			210		10	Cross Bedding
HZB_135	0777801	2841812	53		34		6	Cross Lamination
	0777801	2841812			28		20	Ripples
	0777801	2841812			32	213		Ripples
	0777801	2841812			49	229		Ripples
	0777801	2841812			68	248		Ripples
	0777801	2841812			345	165		Ripples
	0777801	2841812			82	262		Ripples
	0777801	2841812			82	262		Ripples
	0777801	2841812			341	161		Ripples
	0777801	2841812			341	161		Ripples
	0777801	2841812			341	161		Ripples
	0777801	2841812			70	250		Ripples
	0777801	2841812			35	215		Ripples
	0777801	2841812			357	177		Ripples
	0777801	2841812			351	171		Ripples
	0777801	2841812			355	175		Ripples
	0777801	2841812			354	174		Ripples
	0777801	2841812			348		9	Cross Lamination
	0777801	2841812			73		9	Cross Lamination
	0777801	2841812			41	221		Ripples
	0777801	2841812			45	225		Ripples
	0777801	2841812			11	171		Ripples
	0777801	2841812			56	236		Ripples
	0777801	2841812			62	242		Ripples
	0777801	2841812			68	248		Ripples
	0777801	2841812			344	164		Ripples
	0777801	2841812			344	164		Ripples
	0777801	2841812			357	177		Ripples
	0777801	2841812			20		35	Asymmetric
	0777801	2841812			206		29	Cross Lamination
	0777801	2841812			211		28	Cross Lamination
	0777801	2841812			31	211		Ripples

	0777801	2841812			35	215		Ripples
	0777801	2841812			34	214		Ripples
	0777801	2841812			23	203		Ripples
	0777801	2841812			214		18	Cross Lamination
	0777801	2841812			205		21	Cross Lamination
	0777801	2841812			33	213		Ripples
	0777801	2841812			33	213		Ripples
	0777801	2841812			13	193		Ripples
	0777801	2841812			13	193		Ripples
	0777801	2841812			30	210		Ripples
	0777801	2841812			352	172		Ripples
	0777801	2841812			38	218		Ripples
	0777801	2841812			16	196		Ripples
	0777801	2841812			18	198		Ripples
	0777801	2841812			40	220		Ripples
	0777801	2841812			67	247		Ripples
	0777801	2841812			35	215		Ripples
	0777801	2841812			90	270		Ripples
	0777801	2841812			71	271		Ripples
	0777801	2841812			60	240		Ripples
	0777801	2841812			67		1	Cross Lamination
	0777801	2841812			73		3	Cross Lamination
HZB_136	0778661	2842347	54		55	235		Ripples
	0778661	2842347			48		8	Cross Lamination
	0778661	2842347			234		10	Cross Lamination
	0778661	2842347			59	239		Ripples
	0778661	2842347			59	239		Ripples
	0778661	2842347			74		38	Asymmetric
	0778661	2842347			55	235		Ripples
	0778661	2842347			63	243		Ripples
	0778661	2842347			54	234		Ripples
	0778661	2842347			65	245		Ripples
	0778661	2842347			61	241		Ripples
	0778661	2842347			54	234		Ripples
	0778661	2842347			57		27	Asymmetric
	0778661	2842347			72	252		Ripples
	0778661	2842347			247		50	Asymmetric
	0778661	2842347			247		25	Asymmetric
	0778661	2842347			236		7	Ripple Accretion

	0778661	2842347			51		7	Asymmetric
	0778661	2842347			20	200		Ripples
	0778661	2842347			51	231		Ripples
	0778661	2842347			73	253		Ripples
	0778661	2842347			186		18	Asymmetric
	0778661	2842347			65	245		Ripples
	0778661	2842347			33	213		Ripples
	0778661	2842347			75	255		Ripples
	0778661	2842347			75	255		Ripples
	0778661	2842347			30	210		Ripples
	0778661	2842347			330	150		Ripples
	0778661	2842347			40	220		Ripples
	0778661	2842347			62	242		Ripples
	0778661	2842347			35	215		Ripples
	0778661	2842347			57	237		Ripples
	0778661	2842347			239		21	Asymmetric
	0778661	2842347			59		15	Asymmetric
	0778661	2842347			54	234		Ripple Accretion
	0778661	2842347			55		25	Asymmetric
	0778661	2842347			48	228		Ripples
	0778661	2842347			314	134		Ripples
	0778661	2842347			239		15	Asymmetric
	0778661	2842347			42		20	Asymmetric
	0778661	2842347			59	239		Ripples
	0778661	2842347			50	230		Ripples
	0778661	2842347			55	235		Ripples
	0778661	2842347			43	223		Ripples
	0778661	2842347			225		25	Asymmetric
	0778661	2842347			48		6	Asymmetric
	0778661	2842347			229			Ripples
	0778661	2842347			45	225		Ripples
	0778661	2842347			50	230		Ripples
	0778661	2842347			51	231		Ripples
	0778661	2842347			67	247		Ripples
	0778661	2842347			50	230		Ripples
	0778661	2842347			54	234		Ripples
	0778661	2842347			61	241		Ripples
	0778661	2842347			57	237		Ripples
	0778661	2842347			71	251		Ripples
	0778661	2842347			45	245		Ripples
	0778661	2842347			55		15	Ripple Accretion
	0778661	2842347			237		5	Asymmetric
	0778661	2842347			253		5	Asymmetric

	0778661	2842347			66	246		Ripples
	0778661	2842347			56	236		Ripples
	0778661	2842347			84	264		Ripples
	0778661	2842347			62	242		Ripples
	0778661	2842347			55		10	Asymmetric
	0778661	2842347			262		1	Ripple Accretion
	0778661	2842347			236		9	Ripple Accretion
	0778661	2842347			64	244		Ripples
	0778661	2842347			55	235		Ripples
	0778661	2842347			63	243		Ripples
	0778661	2842347			60	240		Ripples
	0778661	2842347			72	252		Ripples
	0778661	2842347			60	240		Ripples
	0778661	2842347			258		18	Asymmetric
	0778661	2842347			244		12	Ripple Accretion
	0778661	2842347			65	245		Ripples
	0778661	2842347			255		13	Ripple Accretion
	0778661	2842347			259		30	Asymmetric
	0778661	2842347			72	252		Ripples
	0778661	2842347			230			Ripples
	0778661	2842347			59	239		Ripples
	0778661	2842347			85	265		Ripples
	0778661	2842347			103	183		Ripples
	0778661	2842347			60	240		Ripples
	0778661	2842347			63	243		Ripples
	0778661	2842347			89	269		Ripples
	0778661	2842347			66	246		Ripples
	0778661	2842347			12	192		Ripples
	0778661	2842347			50	230		Ripples
HZB_137	0783354	2853040			61		20	Cross Bedding
	0783354	2853040			57		19	Cross Bedding
	0783354	2853040			79		20	Cross Bedding
	0783354	2853040			75		17	Cross Bedding
	0783354	2853040			76		21	Cross Bedding
	0783354	2853040			206		8	Cross Bedding
	0783354	2853040			32		11	Cross Bedding
	0783354	2853040			278		5	Cross Bedding
HZB_138	0783511	2853276	55		342		10	Cross Bedding
	0783511	2853276			342		10	Cross Bedding
	0783511	2853276			342		1	Cross Bedding
	0783511	2853276			341		9	Cross Bedding
	0783511	2853276			8		8	Cross Bedding

	0783511	2853276			2		10	Cross Bedding
	0783511	2853276			179		5	Cross Bedding
	0783511	2853276			8		9	Cross Bedding
	0783511	2853276			186		17	Cross Bedding
	0783511	2853276			188		18	Cross Bedding
	0783511	2853276			146			Cross Bedding
	0783511	2853276			162		9	Cross Bedding
	0783511	2853276			339		14	Cross Bedding
	0783511	2853276			168		6	Cross Bedding
	0783511	2853276			344		6	Cross Bedding
	0783511	2853276			167		9	Cross Bedding
	0783511	2853276			172		3	Cross Bedding
	0783511	2853276			1		7	Cross Bedding
	0783511	2853276			359		15	Cross Bedding
	0783511	2853276			187		3	Cross Bedding
	0783511	2853276			191		9	Cross Bedding
	0783511	2853276			187		3	Cross Bedding
	0783511	2853276			192		1	Cross Bedding
	0783511	2853276			11		8	Cross Bedding
	0783511	2853276			1		13	Cross Bedding
	0783511	2853276			353		16	Cross Bedding
	0783511	2853276			172		2	Cross Bedding
	0783511	2853276			350		9	Cross Bedding
	0783511	2853276			346		11	Cross Bedding
	0783511	2853276			145		9	Cross Bedding
	0783511	2853276			149		13	Cross Bedding
	0783511	2853276			138		13	Cross Bedding
	0783511	2853276			147		10	Cross Bedding
	0783511	2853276			143		13	Cross Bedding
	0783511	2853276			143		15	Cross Bedding
	0783511	2853276			145		0	Cross Bedding
	0783511	2853276			141		6	Cross Bedding
	0783511	2853276			140		11	Cross Bedding
	0783511	2853276			145		5	Cross Bedding
	0783511	2853276			137		9	Cross Bedding
	0783511	2853276			147		2	Cross Bedding
	0783511	2853276			139		5	Cross Bedding
	0783511	2853276			149		7	Cross Bedding
	0783511	2853276			152		8	Cross Bedding
	0783511	2853276			148		2	Cross Bedding
	0783511	2853276			158		11	Cross Bedding
	0783511	2853276			145		2	Cross Bedding
	0783511	2853276			139		3	Cross Bedding
	0783511	2853276			140		3	Cross Bedding
	0783511	2853276			334		5	Cross Bedding

	0783511	2853276			339		15	Cross Bedding
	0783511	2853276			337		0	Cross Bedding
	0783511	2853276			339		10	Cross Bedding
	0783511	2853276			327		13	Cross Bedding
	0783511	2853276			152		46	Asymmetric
	0783511	2853276			141		40	Asymmetric
	0783511	2853276			156		21	Asymmetric
	0783511	2853276			346		-1	Cross Bedding
	0783511	2853276			345		5	Cross Bedding
	0783511	2853276			343		13	Cross Bedding
	0783511	2853276			345		18	Cross Bedding
	0783511	2853276			217			Trough Cross Bedding
	0783511	2853276			214			Trough Cross Bedding
	0783511	2853276			249			Trough Cross Bedding
	0783511	2853276			340		3	Cross Bedding
	0783511	2853276			153		1	Cross Bedding
	0783511	2853276			165		8	Cross Bedding
	0783511	2853276			376		3	Cross Bedding
	0783511	2853276			186			Trough Cross Bedding
	0783511	2853276			188			Trough Cross Bedding
	0783511	2853276			251			Trough Cross Bedding
	0783511	2853276			164		-2	Cross Bedding
	0783511	2853276			162		20	Cross Bedding
	0783511	2853276			132		18	Cross Bedding
	0783511	2853276			142		5	Cross Bedding
	0783511	2853276			145		5	Cross Bedding
	0783511	2853276			331		15	Cross Bedding
	0783511	2853276			140			Trough Cross Bedding
	0783511	2853276			125			Trough Cross Bedding
	0783511	2853276			125			Trough Cross Bedding
	0783511	2853276			131		20	Cross Bedding
	0783511	2853276			150		10	Cross Bedding
	0783511	2853276			143		5	Cross Bedding
	0783511	2853276			341		2	Cross Bedding
	0783511	2853276			334		8	Cross Bedding
HZB_139	0783794	2853324			242		19	Cross Bedding
	0783794	2853324			29		2	Cross Bedding
	0783794	2853324			87		22	Cross Bedding

	0783794	2853324			95		20	Cross Bedding
	0783794	2853324			75		10	Cross Bedding
	0783794	2853324			266		-1	Cross Bedding
	0783794	2853324			255		18	Cross Bedding
	0783794	2853324			25		8	Cross Bedding
	0783794	2853324			40		11	Cross Bedding
	0783794	2853324			239		9	Cross Bedding
	0783794	2853324			233		2	Cross Bedding
	0783794	2853324			237		5	Cross Bedding
	0783794	2853324			46		16	Cross Bedding
	0783794	2853324			55		8	Cross Bedding
	0783794	2853324			235		10	Cross Bedding
	0783794	2853324			224		10	Cross Bedding
	0783794	2853324			339		22	Cross Bedding
	0783794	2853324			211		35	Cross Bedding
	0783794	2853324			90		8	Cross Bedding
	0783794	2853324			106		7	Cross Bedding
	0783794	2853324			106		7	Cross Bedding
	0783794	2853324			116		5	Cross Bedding
	0783794	2853324			118		8	Cross Bedding
	0783794	2853324			105		15	Cross Bedding
	0783794	2853324			90		16	Cross Bedding
	0783794	2853324			103		7	Cross Bedding
	0783794	2853324			103		26	Cross Bedding
	0783794	2853324			106		3	Cross Bedding
	0783794	2853324			157		3	Cross Bedding
	0783794	2853324			110		6	Cross Bedding
	0783794	2853324			82		9	Cross Bedding
	0783794	2853324			92		3	Cross Bedding
	0783794	2853324			76		4	Cross Bedding
	0783794	2853324			71		9	Cross Bedding
	0783794	2853324			75		3	Cross Bedding
	0783794	2853324			247		4	Cross Bedding
	0783794	2853324			93		20	Cross Bedding
	0783794	2853324			138		3	Cross Bedding
	0783794	2853324			134		19	Cross Bedding
	0783794	2853324			117		11	Cross Bedding
	0783794	2853324			155		19	Cross Bedding
	0783794	2853324			120		23	Cross Bedding
	0783794	2853324			113		10	Cross Bedding
	0783794	2853324			113		9	Cross Bedding
	0783794	2853324			127		8	Cross Bedding
	0783794	2853324			118		16	Cross Bedding
	0783794	2853324			276		3	Cross Bedding
	0783794	2853324			122		12	Cross Bedding

	0783794	2853324			111		21	Cross Bedding
	0783794	2853324			126		8	Cross Bedding
	0783794	2853324			133		8	Cross Bedding
	0783794	2853324			109		16	Cross Bedding
	0783794	2853324			108		14	Cross Bedding
	0783794	2853324			109		19	Cross Bedding
	0783794	2853324			103		12	Cross Bedding
	0783794	2853324			281		12	Cross Bedding
	0783794	2853324			69		6	Cross Bedding
	0783794	2853324			69		3	Cross Bedding
	0783794	2853324			71		7	Cross Bedding
	0783794	2853324			215		13	Cross Bedding
	0783794	2853324			239		11	Cross Bedding
	0783794	2853324			234		4	Cross Bedding
	0783794	2853324			215		19	Cross Bedding
	0783794	2853324			231		17	Cross Bedding
	0783794	2853324			217		19	Cross Bedding
	0783794	2853324			238		22	Cross Bedding
	0783794	2853324			231		21	Cross Bedding
HZB_140	0783794	2853040	55		5		11	Cross Bedding
	0783794	2853040			179		9	Cross Bedding
	0783794	2853040			177		8	Cross Bedding
	0783794	2853040			351		11	Cross Bedding
	0783794	2853040			174		6	Cross Bedding
	0783794	2853040			185		9	Cross Bedding
	0783794	2853040			181		8	Cross Bedding
	0783794	2853040			185		1	Cross Bedding
	0783794	2853040			128		22	Cross Bedding
	0783794	2853040			137		28	Cross Bedding
	0783794	2853040			193		12	Cross Bedding
	0783794	2853040			191		9	Cross Bedding
	0783794	2853040			184		12	Cross Bedding
	0783794	2853040			193		-1	Cross Bedding
	0783794	2853040			174		22	Cross Bedding
	0783794	2853040			173		1	Cross Bedding
	0783794	2853040			180		12	Cross Bedding
	0783794	2853040			182		1	Cross Bedding
	0783794	2853040			184		14	Cross Bedding
	0783794	2853040			183		2	Cross Bedding
	0783794	2853040			184		9	Cross Bedding
	0783794	2853040			191		25	Asymmetric
	0783794	2853040			303	123		Ripples
	0783794	2853040			272	152		Ripples
	0783794	2853040			86		3	Asymmetric
	0783794	2853040			291	15		Ripples

	0783794	2853040			346		8	Cross Bedding
	0783794	2853040			334		3	Cross Bedding
	0783794	2853040			341		9	Cross Bedding
	0783794	2853040			347		18	Cross Bedding
	0783794	2853040			350		3	Cross Bedding
	0783794	2853040			171		13	Cross Bedding
	0783794	2853040			345		3	Cross Bedding
	0783794	2853040			350		10	Cross Bedding
	0783794	2853040			169		4	Cross Bedding
	0783794	2853040			9		7	Cross Bedding
	0783794	2853040			191		5	Cross Bedding
	0783794	2853040			176		5	Cross Bedding
	0783794	2853040			138		7	Cross Bedding
	0783794	2853040			182		5	Cross Bedding
	0783794	2853040			145		9	Cross Bedding
	0783794	2853040			175		6	Cross Bedding
	0783794	2853040			153		2	Cross Bedding
	0783794	2853040			150		11	Cross Bedding
	0783794	2853040			103		4	Cross Bedding
	0783794	2853040			131		10	Cross Bedding
HZB_141	0782030	2845429			106		9	Cross Bedding
	0782030	2845429			105		10	Cross Bedding
	0782030	2845429			294		2	Cross Bedding
	0782030	2845429			187		10	Cross Bedding
	0782030	2845429			292		17	Cross Bedding
	0782030	2845429			305		5	Cross Bedding
	0782030	2845429			299		2	Cross Bedding
	0782030	2845429			285		7	Cross Bedding
HZB_142	0781997	2845426			66		19	Cross Bedding
	0781997	2845426			68		15	Cross Bedding
	0781997	2845426			39		20	Cross Bedding
	0781997	2845426			41		15	Cross Bedding
	0781997	2845426			37		12	Cross Bedding
	0781997	2845426			135		8	Cross Bedding
	0781997	2845426			142		2	Cross Bedding
	0781997	2845426			42		17	Cross Bedding
	0781997	2845426			47		26	Cross Bedding
	0781997	2845426			37		11	Cross Bedding
	0781997	2845426			115		7	Cross Bedding
	0781997	2845426			51		18	Cross Bedding
	0781997	2845426			40		6	Cross Bedding
	0781997	2845426			32		12	Cross Bedding
	0781997	2845426			180		2	Cross Bedding
	0781997	2845426			360		19	Cross Bedding
	0781997	2845426			107		15	Cross Bedding

	0781997	2845426			111		14	Cross Bedding
	0781997	2845426			33		9	Cross Bedding
	0781997	2845426			28		21	Cross Bedding
	0781997	2845426			29		10	Cross Bedding
HZB142b	0781959	2845432			22		11	Cross Bedding
	0781959	2845432			218		3	Cross Bedding
	0781959	2845432			35		11	Cross Bedding
	0781959	2845432			32		10	Cross Bedding
	0781959	2845432			25		10	Cross Bedding
	0781959	2845432			27		19	Cross Bedding
	0781959	2845432			33		9	Cross Bedding
HZB_143	0781874	2845515	57		28		3	Cross Bedding
	0781874	2845515			53		12	Cross Bedding
	0781874	2845515			50		5	Cross Bedding
	0781874	2845515			197		1	Cross Bedding
	0781874	2845515			25		15	Cross Bedding
	0781874	2845515			104		29	Asymmetric
	0781874	2845515			276	96		Ripples
	0781874	2845515			306	126		Ripples
	0781874	2845515			178		2	Cross Bedding
	0781874	2845515			188		3	Cross Bedding
	0781874	2845515			157		11	Cross Bedding
	0781874	2845515			127		12	Cross Bedding
	0781874	2845515			217		7	Cross Bedding
	0781874	2845515			296		7	Cross Bedding
	0781874	2845515			121		9	Cross Bedding
	0781874	2845515			293		1	Cross Bedding
	0781874	2845515			11		2	Cross Bedding
	0781874	2845515			295		11	Cross Bedding
	0781874	2845515			115		3	Cross Bedding
	0781874	2845515			271		4	Cross Bedding
	0781874	2845515			190		8	Cross Bedding
	0781874	2845515			88		1	Cross Bedding
	0781874	2845515			264		2	Cross Bedding
	0781874	2845515			120		7	Cross Bedding
	0781874	2845515			309		8	Cross Bedding
	0781874	2845515			277		7	Cross Bedding
	0781874	2845515			285		18	Cross Bedding
	0781874	2845515			103		2	Cross Bedding
	0781874	2845515			298		11	Cross Bedding
	0781874	2845515			281		7	Cross Bedding
	0781874	2845515			286		2	Cross Bedding
	0781874	2845515			286		5	Cross Bedding
	0781874	2845515			201		2	Cross Bedding
	0781874	2845515			109		4	Cross Bedding

HZB_143c	0781894	2845528			109		6	Cross Bedding
	0781894	2845528			110		4	Cross Bedding
	0781894	2845528			109		10	Cross Bedding
	0781894	2845528			109		10	Cross Bedding
	0781894	2845528			111		1	Cross Bedding
	0781894	2845528			119		15	Cross Bedding
	0781894	2845528			110		4	Cross Bedding
	0781894	2845528			117		3	Cross Bedding
	0781894	2845528			100		10	Cross Bedding
	0781894	2845528			302		6	Cross Bedding
	0781894	2845528			129		9	Cross Bedding
	0781894	2845528			122		8	Cross Bedding
	0781894	2845528			109		2	Cross Bedding
	0781894	2845528			125		13	Cross Bedding
	0781894	2845528			111		13	Cross Bedding
	0781894	2845528			77		22	Cross Bedding
	0781894	2845528			130		11	Cross Bedding
	0781894	2845528			273		12	Cross Bedding
	0781894	2845528			264		9	Cross Bedding
	0781894	2845528			256		10	Cross Bedding
	0781894	2845528			207		13	Cross Bedding
	0781894	2845528			292		11	Cross Bedding
	0781894	2845528			109		3	Cross Bedding
	0781894	2845528			287		1	Cross Bedding
	0781894	2845528			110		10	Cross Bedding
	0781894	2845528			283		4	Cross Bedding
	0781894	2845528			283		0	Cross Bedding
	0781894	2845528			246		8	Cross Bedding
	0781894	2845528			222		12	Cross Bedding
HZB_145	0781693	2845210			74		2	Cross Bedding
	0781693	2845210			248		13	Cross Bedding
	0781693	2845210			258		7	Cross Bedding
	0781693	2845210			260		3	Cross Bedding
	0781693	2845210			232		7	Cross Bedding
	0781693	2845210			265		3	Cross Bedding
	0781693	2845210			263		7	Cross Bedding
	0781693	2845210			271		7	Cross Bedding
	0781693	2845210			258	78		RUC
HB_146	0781744	2845233			130		11	Cross Bedding
	0781744	2845233			132		7	Cross Bedding
	0781744	2845233			130		4	Cross Bedding
	0781744	2845233			145		7	Cross Bedding
	0781744	2845233			132		9	Cross Bedding
	0781744	2845233			1		9	Cross Bedding
	0781744	2845233			189		3	Cross Bedding

	0781744	2845233			197		8	Cross Bedding
HZB_147	0781760	2845267			171		0	Cross Bedding
	0781760	2845267			172		1	Cross Bedding
	0781760	2845267			185		12	Cross Bedding
	0781760	2845267			162		6	Cross Bedding
	0781760	2845267			157		3	Cross Bedding
	0781760	2845267			121		14	Cross Bedding
	0781760	2845267			223		12	Cross Bedding
	0781760	2845267			335		8	Cross Bedding
	0781760	2845267			327		9	Cross Bedding
	0781760	2845267			355		2	Cross Bedding
	0781760	2845267			350		1	Cross Bedding
	0781760	2845267			344		9	Cross Bedding
HZB_148	0778038	2840870			103		13	Cross Bedding
	0778038	2840870			82		12	Cross Bedding
	0778038	2840870			76		11	Cross Bedding
	0778038	2840870			99		11	Cross Bedding
	0778038	2840870			81		22	Cross Bedding
	0778038	2840870			231		0	Cross Bedding
	0778038	2840870			240		3	Cross Bedding
	0778038	2840870			126		17	Cross Bedding
HZB_149	0777947	2840871			239		15	Cross Bedding
	0777947	2840871			122		1	Cross Bedding
	0777947	2840871			46		11	Cross Bedding
	0777947	2840871			241		17	Cross Bedding
	0777947	2840871			233		7	Cross Bedding
	0777947	2840871			21		7	Cross Bedding
	0777947	2840871			63		9	Cross Bedding
	0777947	2840871			222		25	Cross Bedding
	0777947	2840871			218		23	Cross Bedding
	0777947	2840871			253		15	Cross Bedding
	0777947	2840871			45		2	Cross Bedding
HZB_150	0777858	2840806			154			Cross Bedding
	0777858	2840806			170			Cross Bedding
	0777858	2840806			184			Cross Bedding
	0777858	2840806			168			Cross Bedding
	0777858	2840806			180			Cross Bedding
	0777858	2840806			175			Cross Bedding
	0777858	2840806			187		9	Cross Bedding
	0777858	2840806			120		15	Cross Bedding
	0777858	2840806			126		9	Cross Bedding
	0777858	2840806			136		11	Cross Bedding
	0777858	2840806			159		17	Cross Bedding
	0777858	2840806			148		21	Cross Bedding
	0777858	2840806			175		9	Cross Bedding

	0777858	2840806			198		23	Cross Bedding
	0777858	2840806			147		21	Cross Bedding
	0777858	2840806			185		11	Cross Bedding
	0777858	2840806			185		15	Cross Bedding
	0777858	2840806			147		17	Cross Bedding
	0777858	2840806			138		18	Cross Bedding
	0777858	2840806			126		8	Cross Bedding
	0777858	2840806			127		6	Cross Bedding
	0777858	2840806			147		15	Cross Bedding
	0777858	2840806			139		20	Cross Bedding
	0777858	2840806			116		9	Cross Bedding
	0777858	2840806			129		1	Cross Bedding
	0777858	2840806			135		17	Cross Bedding
	0777858	2840806			106		9	Cross Bedding
	0777858	2840806			228		1	Cross Bedding
	0777858	2840806			72		10	Cross Bedding
	0777858	2840806			251		5	Cross Bedding
	0777858	2840806			59		4	Cross Bedding
	0777858	2840806			121		7	Cross Bedding
	0777858	2840806			142		16	Cross Bedding
	0777858	2840806			148		19	Cross Bedding
	0777858	2840806			125		9	Cross Bedding
HZB_151	0777833	2840810	58		128		16	Cross Bedding
	0777833	2840810			130		10	Cross Bedding
	0777833	2840810			146		16	Cross Bedding
	0777833	2840810			139		9	Cross Bedding
	0777833	2840810			308		10	Cross Bedding
	0777833	2840810			266		3	Cross Bedding
	0777833	2840810			103		7	Cross Bedding
	0777833	2840810			282		15	Cross Bedding
	0777833	2840810			138		31	Cross Bedding
	0777833	2840810			129		20	Cross Bedding
	0777833	2840810			169		14	Cross Bedding
	0777833	2840810			173		13	Cross Bedding
	0777833	2840810			231		3	Cross Bedding
	0777833	2840810			206		5	Cross Bedding
	0777833	2840810			218		2	Cross Bedding
	0777833	2840810			357	177		Ripples
	0777833	2840810			203		9	Low Angle Cross Bedding
	0777833	2840810			202		7	Low Angle Cross Bedding
	0777833	2840810			201		10	Cross Bedding
	0777833	2840810			197		11	Cross Bedding
	0777833	2840810			220		11	Cross Bedding

	0777833	2840810			209		18	Cross Bedding
	0777833	2840810			210		15	Cross Bedding
	0777833	2840810			209		16	Cross Bedding
HZB_152	0777780	2840921			348		10	Cross Bedding
	0777780	2840921			172		3	Cross Bedding
	0777780	2840921			166		9	Cross Bedding
	0777780	2840921			263		10	Cross Bedding
	0777780	2840921			265		3	Cross Bedding
	0777780	2840921			327		4	Cross Bedding
	0777780	2840921			148		7	Cross Bedding
	0777780	2840921			146		22	Cross Bedding
	0777780	2840921			140		20	Cross Bedding
	0777780	2840921			150		18	Cross Bedding
	0777780	2840921			114		10	Cross Bedding
	0777780	2840921			104		13	Cross Bedding
	0777780	2840921			65		16	Cross Bedding
	0777780	2840921			65		8	Cross Bedding
	0777780	2840921			75		7	Cross Bedding
	0777780	2840921			259		1	Cross Bedding
HZB_153	0777565	2841047			169		8	Cross Bedding
	0777565	2841047			160		2	Cross Bedding
	0777565	2841047			159		4	Cross Bedding
	0777565	2841047			161		7	Cross Bedding
	0777565	2841047			164		14	Cross Bedding
	0777565	2841047			161		10	Cross Bedding
	0777565	2841047			162		20	Cross Bedding
	0777565	2841047			170		19	Cross Bedding
	0777565	2841047			155		9	Cross Bedding
	0777565	2841047			159		9	Cross Bedding
	0777565	2841047			146		3	Cross Bedding
	0777565	2841047			129		3	Cross Bedding
	0777565	2841047			298		11	Cross Bedding
	0777565	2841047			284		10	Cross Bedding
	0777565	2841047			286		10	Cross Bedding
	0777565	2841047			286		1	Cross Bedding
	0777565	2841047			339		11	Cross Bedding
	0777565	2841047			167		4	Cross Bedding
	0777565	2841047			167		17	Cross Bedding
	0777565	2841047			335		1	Cross Bedding
	0777565	2841047			219		10	Cross Bedding
	0777565	2841047			125		15	Cross Bedding
	0777565	2841047			132		3	Cross Bedding
	0777565	2841047			128		10	Cross Bedding
	0777565	2841047			127		10	Cross Bedding
HZB_154	0777570	2841128	59		201		13	Cross Bedding

	0777570	2841128			201		15	Cross Bedding
	0777570	2841128			190		11	Cross Bedding
	0777570	2841128			201		10	Cross Bedding
	0777570	2841128			187		5	Cross Bedding
	0777570	2841128			200		3	Cross Bedding
	0777570	2841128			9		11	Cross Bedding
	0777570	2841128			196		7	Cross Bedding
	0777570	2841128			151		16	Cross Bedding
	0777570	2841128			150		16	Cross Bedding
	0777570	2841128			155		15	Cross Bedding
	0777570	2841128			34		3	Cross Bedding
	0777570	2841128			190		5	Cross Bedding
	0777570	2841128			326		3	Asymmetric
	0777570	2841128			193		15	Asymmetric
	0777570	2841128			10	190		Ripples
	0777570	2841128			35	175		Ripples
	0777570	2841128			292	112		Ripples
	0777570	2841128			25		12	Asymmetric
	0777570	2841128			344	164		Ripples
	0777570	2841128			114		26	Cross Bedding
	0777570	2841128			105		11	Cross Bedding
HZB_155	0777587	2841261			210		11	Cross Bedding
	0777587	2841261			210		20	Cross Bedding
	0777587	2841261			215		16	Cross Bedding
	0777587	2841261			211		-3	Cross Bedding
	0777587	2841261			224		12	Cross Bedding
	0777587	2841261			178		9	Cross Bedding
	0777587	2841261			233		3	Cross Bedding
	0777587	2841261			189		14	Cross Bedding
	0777587	2841261			183		3	Cross Bedding
	0777587	2841261			278		17	Cross Bedding
	0777587	2841261			187		19	Cross Bedding
	0777587	2841261			202		10	Cross Bedding
	0777587	2841261			22		6	Cross Bedding
	0777587	2841261			188		10	Cross Bedding
	0777587	2841261			193		12	Cross Bedding
	0777587	2841261			179		21	Cross Bedding
	0777587	2841261			196		11	Cross Bedding
	0777587	2841261			199		20	Cross Bedding
	0777587	2841261			190		6	Cross Bedding
	0777587	2841261			189		17	Cross Bedding
	0777587	2841261			189		4	Cross Bedding
	0777587	2841261			222		18	Cross Bedding
	0777587	2841261			223		17	Cross Bedding
	0777587	2841261			204		7	Cross Bedding

	0777587	2841261			221		17	Cross Bedding
HZB_156	0777514	2841213			218			Cross Bedding
	0777514	2841213			210			Cross Bedding
	0777514	2841213			210			Cross Bedding
	0777514	2841213			235			Cross Bedding
	0777514	2841213			246		16	Cross Bedding
	0777514	2841213			72		5	Cross Bedding
	0777514	2841213			229		3	Cross Bedding
	0777514	2841213			245		7	Cross Bedding
	0777514	2841213			245		7	Cross Bedding
	0777514	2841213			245		11	Cross Bedding
	0777514	2841213			251		7	Cross Bedding
	0777514	2841213			241		2	Cross Bedding
	0777514	2841213			68		12	Cross Bedding
	0777514	2841213			241		4	Cross Bedding
	0777514	2841213			62		18	Cross Bedding
	0777514	2841213			235		5	Cross Bedding
	0777514	2841213			8		8	Cross Bedding
	0777514	2841213			243		13	Cross Bedding
	0777514	2841213			251		3	Cross Bedding
	0777514	2841213			60		10	Cross Bedding
	0777514	2841213			248		18	Cross Bedding
	0777514	2841213			227		2	Cross Bedding
	0777514	2841213			246		16	Cross Bedding
	0777514	2841213			72		5	Cross Bedding
	0777514	2841213			251		10	Cross Bedding
	0777514	2841213			260		7	Cross Bedding
	0777514	2841213			214		1	Cross Bedding
	0777514	2841213			229		5	Cross Bedding
	0777514	2841213			219		0	Cross Bedding
	0777514	2841213			220		14	Cross Bedding
	0777514	2841213			230		15	Cross Bedding
	0777514	2841213			14		2	Cross Bedding
	0777514	2841213			11		3	Cross Bedding
	0777514	2841213			19		4	Cross Bedding
	0777514	2841213			203		17	Cross Bedding
	0777514	2841213			230		8	Cross Bedding
	0777514	2841213			211		5	Cross Bedding
	0777514	2841213			214		17	Cross Bedding
	0777514	2841213			264		8	Cross Bedding
	0777514	2841213			263		14	Cross Bedding
	0777514	2841213			64		10	Cross Bedding
	0777514	2841213			244		1	Cross Bedding
	0777514	2841213			69		19	Cross Bedding
	0777514	2841213			59		17	Cross Bedding

	0777514	2841213			82		8	Cross Bedding
	0777514	2841213			84		3	Cross Bedding
	0777514	2841213			235		19	Cross Bedding
	0777514	2841213			245		7	Cross Bedding
	0777514	2841213			248		6	Cross Bedding
	0777514	2841213			218		10	Cross Bedding
	0777514	2841213			217		3	Cross Bedding
	0777514	2841213			203		14	Cross Bedding
	0777514	2841213			217		11	Cross Bedding
	0777514	2841213			243		1	Cross Bedding
	0777514	2841213			220		3	Cross Bedding
	0777514	2841213			119		12	Cross Bedding
	0777514	2841213			47		16	Cross Bedding
	0777514	2841213			231		9	Cross Bedding
	0777514	2841213			232		5	Cross Bedding
	0777514	2841213			229		7	Cross Bedding
	0777514	2841213			30		2	Cross Bedding
	0777514	2841213			36		7	Cross Bedding
	0777514	2841213			208		14	Cross Bedding
	0777514	2841213			202		16	Cross Bedding
	0777514	2841213			241		9	Cross Bedding
	0777514	2841213			257		1	Cross Bedding
	0777514	2841213			63		3	Cross Bedding
	0777514	2841213			81		13	Cross Bedding
	0777514	2841213			249		12	Cross Bedding
	0777514	2841213			236		7	Cross Bedding
	0777514	2841213			268		1	Cross Bedding
	0777514	2841213			80		16	Cross Bedding
	0777514	2841213			247		9	Cross Bedding
	0777514	2841213			248		3	Cross Bedding
	0777514	2841213			275		32	Cross Bedding
	0777514	2841213			275		38	Cross Bedding
	0777514	2841213			275		31	Cross Bedding
	0777514	2841213			268		4	Cross Bedding
	0777514	2841213			41		19	Cross Bedding
	0777514	2841213			83		10	Cross Bedding
	0777514	2841213			241		7	Cross Bedding
	0777514	2841213			74		10	Cross Bedding
	0777514	2841213			259		10	Cross Bedding
	0777514	2841213			77		19	Cross Bedding
	0777514	2841213			243		13	Cross Bedding
	0777514	2841213			261		7	Cross Bedding
	0777514	2841213			279		5	Cross Bedding
HZB_157	0777305	2840873			355		12	Cross Bedding
	0777305	2840873			152		14	Cross Bedding

	0777305	2840873			139		14	Cross Bedding
	0777305	2840873			161		21	Cross Bedding
	0777305	2840873			166		20	Cross Bedding
	0777305	2840873			180		7	Cross Bedding
	0777305	2840873			183		18	Cross Bedding
	0777305	2840873			180		18	Cross Bedding
	0777305	2840873			181		20	Cross Bedding
	0777305	2840873			189		14	Cross Bedding
HZB_158	0777374	2840994			186		7	Cross Bedding
	0777374	2840994			189		11	Cross Bedding
	0777374	2840994			176		13	Cross Bedding
	0777374	2840994			183		13	Cross Bedding
	0777374	2840994			133		11	Cross Bedding
	0777374	2840994			145		10	Cross Bedding
	0777374	2840994			120		11	Cross Bedding
	0777374	2840994			149		11	Cross Bedding
	0777374	2840994			125		15	Cross Bedding
	0777374	2840994			163		2	Cross Bedding
	0777374	2840994			145		20	Cross Bedding
	0777374	2840994			154		6	Cross Bedding
	0777374	2840994			155		10	Cross Bedding
	0777374	2840994			159		25	Cross Bedding
	0777374	2840994			161		16	Cross Bedding
	0777374	2840994			298		3	Cross Bedding
	0777374	2840994			283		5	Cross Bedding
	0777374	2840994			119		9	Cross Bedding
	0777374	2840994			168		21	Cross Bedding
	0777374	2840994			111		18	Cross Bedding
	0777374	2840994			120		11	Cross Bedding
	0777374	2840994			105		28	Cross Bedding
	0777374	2840994			107		10	Cross Bedding
	0777374	2840994			278		5	Cross Bedding
	0777374	2840994			275		5	Cross Bedding
	0777374	2840994			273		3	Cross Bedding
	0777374	2840994			83		2	Cross Bedding
	0777374	2840994			279		12	Cross Bedding
	0777374	2840994			207		18	Cross Bedding
	0777374	2840994			129		10	Cross Bedding
	0777374	2840994			145		10	Cross Bedding
	0777374	2840994			135		9	Cross Bedding
	0777374	2840994			153		10	Cross Bedding
HZB_159	0777452	2840922	60		360		10	Cross Bedding
	0777452	2840922			348	168		Asymmetric
	0777452	2840922			338	158		Asymmetric
	0777452	2840922			116		3	Cross Bedding

	0777452	2840922			308		5	Cross Bedding
	0777452	2840922			330		3	Cross Bedding
	0777452	2840922			145		8	Cross Bedding
	0777452	2840922			316		12	Cross Bedding
	0777452	2840922			278		7	Cross Bedding
	0777452	2840922			116		10	Cross Bedding
	0777452	2840922			267		12	Cross Bedding
	0777452	2840922			257		3	Cross Bedding
	0777452	2840922			95		10	Cross Bedding
	0777452	2840922			301		1	Cross Bedding
	0777452	2840922			357		3	Cross Bedding
	0777452	2840922			175		1	Cross Bedding
	0777452	2840922			118		15	Cross Bedding
	0777452	2840922			212			Cross Bedding
	0777452	2840922			132		12	Cross Bedding
	0777452	2840922			129		13	Cross Bedding
	0777452	2840922			126		17	Cross Bedding
	0777452	2840922			150		18	Cross Bedding
	0777452	2840922			348		20	Cross Bedding
	0777452	2840922			155		17	Cross Bedding
HZB_160	0778156	2842034			208		11	Cross Bedding
	0778156	2842034			74			Cross Bedding
	0778156	2842034			242			Cross Bedding
	0778156	2842034			250			Cross Bedding
	0778156	2842034			259			Cross Bedding
	0778156	2842034			78			Cross Bedding
	0778156	2842034			247			Cross Bedding
	0778156	2842034			257		10	Cross Bedding
	0778156	2842034			132		12	Cross Bedding
	0778156	2842034			101		15	Cross Bedding
	0778156	2842034			99		16	Cross Bedding
	0778156	2842034			261		12	Cross Bedding
	0778156	2842034			81		4	Cross Bedding
	0778156	2842034			249		2	Cross Bedding
	0778156	2842034			243		9	Cross Bedding
	0778156	2842034			274		10	Cross Bedding
	0778156	2842034			86		11	Cross Bedding
	0778156	2842034			227		10	Cross Bedding
	0778156	2842034			225		11	Cross Bedding
	0778156	2842034			286		2	Cross Bedding
	0778156	2842034			265		1	Cross Bedding
	0778156	2842034			261		12	Cross Bedding
	0778156	2842034			81		4	Cross Bedding
	0778156	2842034			260		12	Cross Bedding
	0778156	2842034			265		1	Cross Bedding

	0778156	2842034			257		1	Cross Bedding
	0778156	2842034			254		9	Cross Bedding
	0778156	2842034			203		8	Cross Bedding
	0778156	2842034			253		2	Cross Bedding
	0778156	2842034			78		15	Cross Bedding
	0778156	2842034			91		3	Cross Bedding
	0778156	2842034			270		10	Cross Bedding
	0778156	2842034			64		0	Cross Bedding
	0778156	2842034			75		4	Cross Bedding
	0778156	2842034			267		8	Cross Bedding
	0778156	2842034			88		12	Cross Bedding
	0778156	2842034			290		2	Cross Bedding
	0778156	2842034			243		6	Cross Bedding
	0778156	2842034			247		2	Cross Bedding
	0778156	2842034			258		2	Cross Bedding
	0778156	2842034			255		0	Cross Bedding
	0778156	2842034			266		24	Cross Bedding
	0778156	2842034			276		2	Cross Bedding
	0778156	2842034			269		2	Cross Bedding
	0778156	2842034			261		4	Cross Bedding
	0778156	2842034			259		1	Cross Bedding
	0778156	2842034			284		12	Cross Bedding
	0778156	2842034			297		0	Cross Bedding
	0778156	2842034			294		4	Cross Bedding
	0778156	2842034			253		7	Cross Bedding
	0778156	2842034			249		12	Cross Bedding
	0778156	2842034			287		0	Cross Bedding
	0778156	2842034			293		17	Cross Bedding
	0778156	2842034			290		3	Cross Bedding
	0778156	2842034			252		8	Cross Bedding
	0778156	2842034			240		6	Cross Bedding
	0778156	2842034			248		4	Cross Bedding
	0778156	2842034			254		16	Cross Bedding
	0778156	2842034			257		2	Cross Bedding
	0778156	2842034			248		2	Cross Bedding
	0778156	2842034			64		10	Cross Bedding
	0778156	2842034			68		7	Cross Bedding
	0778156	2842034			61		8	Cross Bedding
	0778156	2842034			43		4	Cross Bedding
	0778156	2842034			227		7	Cross Bedding
	0778156	2842034			229		9	Cross Bedding
	0778156	2842034			232		8	Cross Bedding
	0778156	2842034			211		27	Cross Bedding
	0778156	2842034			290		3	Cross Bedding
	0778156	2842034			261		18	Cross Bedding

	0778156	2842034			303		2	Cross Bedding
	0778156	2842034			244		1	Cross Bedding
	0778156	2842034			212		8	Cross Bedding
	0778156	2842034			164		22	Cross Bedding
	0778156	2842034			164		4	Cross Bedding
	0778156	2842034			250		3	Cross Bedding
HZB_161	0778049	2841986			222			Cross Bedding
	0778049	2841986			224			Cross Bedding
	0778049	2841986			206			Cross Bedding
	0778049	2841986			218			Cross Bedding
	0778049	2841986			219		28	Cross Bedding
	0778049	2841986			221		18	Cross Bedding
	0778049	2841986			224		1	Cross Bedding
	0778049	2841986			210		12	Cross Bedding
	0778049	2841986			221		17	Cross Bedding
	0778049	2841986			293		6	Cross Bedding
	0778049	2841986			241		21	Cross Bedding
	0778049	2841986			245		15	Cross Bedding
	0778049	2841986			261		5	Cross Bedding
	0778049	2841986			240		10	Cross Bedding
	0778049	2841986			237		12	Cross Bedding
	0778049	2841986			240		13	Cross Bedding
	0778049	2841986			234		15	Cross Bedding
	0778049	2841986			115		8	Cross Bedding
	0778049	2841986			221		7	Cross Bedding
	0778049	2841986			224		25	Cross Bedding
	0778049	2841986			227		7	Cross Bedding
	0778049	2841986			225		9	Cross Bedding
	0778049	2841986			210		24	Cross Bedding
	0778049	2841986			195		17	Cross Bedding
	0778049	2841986			203		8	Cross Bedding
	0778049	2841986			227		3	Cross Bedding
	0778049	2841986			17		1	Cross Bedding
	0778049	2841986			53		1	Cross Bedding
	0778049	2841986			231		2	Cross Bedding
	0778049	2841986			242		10	Cross Bedding
	0778049	2841986			206		2	Cross Bedding
	0778049	2841986			21		20	Cross Bedding
	0778049	2841986			207		1	Cross Bedding
	0778049	2841986			183		22	Cross Bedding
	0778049	2841986			207		24	Cross Bedding
	0778049	2841986			192		19	Cross Bedding
	0778049	2841986			245		2	Cross Bedding
	0778049	2841986			187		1	Cross Bedding
	0778049	2841986			214		3	Cross Bedding

	0778049	2841986			214		32	Cross Bedding
	0778049	2841986			206		21	Cross Bedding
	0778049	2841986			208		9	Cross Bedding
	0778049	2841986			231		7	Cross Bedding
	0778049	2841986			1		12	Cross Bedding
	0778049	2841986			168		10	Cross Bedding
	0778049	2841986			174		3	Cross Bedding
	0778049	2841986			219		19	Cross Bedding
	0778049	2841986			214		2	Cross Bedding
	0778049	2841986			200		1	Cross Bedding
	0778049	2841986			217		21	Cross Bedding
	0778049	2841986			218		17	Cross Bedding
	0778049	2841986			215		11	Cross Bedding
	0778049	2841986			210		14	Cross Bedding
	0778049	2841986			237		1	Cross Bedding
	0778049	2841986			225		24	Cross Bedding
	0778049	2841986			221		7	Cross Bedding
	0778049	2841986			242		19	Cross Bedding
	0778049	2841986			256		22	Cross Bedding
	0778049	2841986			259		3	Cross Bedding
	0778049	2841986			209		7	Cross Bedding
	0778049	2841986			119		21	Cross Bedding
	0778049	2841986			236		1	Cross Bedding
	0778049	2841986			217		11	Cross Bedding
	0778049	2841986			249		12	Cross Bedding
	0778049	2841986			245		12	Cross Bedding
	0778049	2841986			242		17	Cross Bedding
	0778049	2841986			69		3	Cross Bedding
	0778049	2841986			241		9	Cross Bedding
	0778049	2841986			62		12	Cross Bedding
	0778049	2841986			242		1	Cross Bedding
	0778049	2841986			238		4	Cross Bedding
	0778049	2841986			124		22	Cross Bedding
	0778049	2841986			125		10	Cross Bedding
	0778049	2841986			294		12	Cross Bedding
	0778049	2841986			294		23	Cross Bedding
	0778049	2841986			228		37	Cross Bedding
	0778049	2841986			247		24	Cross Bedding
	0778049	2841986			211		14	Cross Bedding
	0778049	2841986			177		1	Cross Bedding
	0778049	2841986			220		14	Cross Bedding
HZB_162	0777896	2841845	61		263		0	Cross Bedding
	0777896	2841845			271		11	Cross Bedding
	0777896	2841845			90		9	Cross Bedding
	0777896	2841845			269		2	Cross Bedding

	0777896	2841845			260		17	Cross Bedding
	0777896	2841845			265		5	Cross Bedding
	0777896	2841845			263		12	Cross Bedding
	0777896	2841845			81		9	Cross Bedding
	0777896	2841845			80		4	Cross Bedding
	0777896	2841845			252		3	Cross Bedding
	0777896	2841845			219		7	Cross Bedding
	0777896	2841845			230		20	Cross Bedding
	0777896	2841845			236		2	Cross Bedding
	0777896	2841845			230		10	Cross Bedding
	0777896	2841845			236		6	Cross Bedding
	0777896	2841845			223		6	Cross Bedding
	0777896	2841845			244		2	Cross Bedding
	0777896	2841845			235		11	Cross Bedding
HZB_163	0777569	2841335			268		8	Cross Bedding
	0777569	2841335			265		3	Cross Bedding
	0777569	2841335			267		15	Cross Bedding
	0777569	2841335			82		22	Cross Bedding
	0777569	2841335			73		18	Cross Bedding
	0777569	2841335			255		1	Cross Bedding
	0777569	2841335			228		10	Cross Bedding
	0777569	2841335			48		2	Cross Bedding
	0777569	2841335			49		16	Cross Bedding
	0777569	2841335			45		17	Cross Bedding
	0777569	2841335			47		20	Cross Bedding
	0777569	2841335			230		2	Cross Bedding
	0777569	2841335			230		9	Cross Bedding
	0777569	2841335			226		7	Cross Bedding
	0777569	2841335			212		17	Cross Bedding
	0777569	2841335			227		18	Cross Bedding
	0777569	2841335			38		2	Cross Bedding
	0777569	2841335			70		8	Cross Bedding
	0777569	2841335			238		9	Cross Bedding
	0777569	2841335			231		10	Cross Bedding
	0777569	2841335			236		20	Cross Bedding
	0777569	2841335			190		10	Cross Bedding
	0777569	2841335			147		34	Cross Bedding
	0777569	2841335			155		18	Cross Bedding
	0777569	2841335			321		2	Cross Bedding
	0777569	2841335			27	207		Cross Bedding
HZB_164	0779578	2841849	62		7	187		Ripples
	0779578	2841849			192		26	Cross Bedding
	0779578	2841849			194		22	Cross Bedding
	0779578	2841849			183		32	Cross Bedding
	0779578	2841849			173		31	Cross Bedding

	0779578	2841849			213		33	Cross Bedding
	0779578	2841849			204		30	Cross Bedding
	0779578	2841849			213		10	Cross Bedding
	0779578	2841849			210		13	Cross Bedding
	0779578	2841849			206		2	Cross Bedding
	0779578	2841849			193		15	Cross Bedding
	0779578	2841849			206		14	Cross Bedding
	0779578	2841849			193		11	Cross Bedding
	0779578	2841849			203		20	Cross Bedding
	0779578	2841849			204		18	Cross Bedding
	0779578	2841849			198		19	Cross Bedding
	0779578	2841849			196		15	Cross Bedding
	0779578	2841849			202		30	Cross Bedding
	0779578	2841849			204		16	Cross Bedding
	0779578	2841849			210		26	Cross Bedding
	0779578	2841849			208		20	Cross Bedding
	0779578	2841849			23		8	Cross Bedding
	0779578	2841849			191		18	Cross Bedding
	0779578	2841849			210		30	Cross Bedding
	0779578	2841849			207		21	Cross Bedding
	0779578	2841849			4		1	Cross Bedding
	0779578	2841849			201		11	Cross Bedding
	0779578	2841849			207		19	Cross Bedding
	0779578	2841849			210		13	Cross Bedding
	0779578	2841849			3		3	Cross Bedding
	0779578	2841849			14		2	Cross Bedding
	0779578	2841849			19		7	Cross Bedding
	0779578	2841849			177		24	Cross Bedding
	0779578	2841849			188		20	Cross Bedding
	0779578	2841849			191		10	Cross Bedding
	0779578	2841849			11		1	Cross Bedding
	0779578	2841849			360		0	Cross Bedding
	0779578	2841849			201		2	Cross Bedding
	0779578	2841849			183		19	Cross Bedding
	0779578	2841849			200		25	Cross Bedding
	0779578	2841849			186		12	Cross Bedding
	0779578	2841849			186		12	Cross Bedding
	0779578	2841849			187		23	Cross Bedding
	0779578	2841849			187		16	Cross Bedding
	0779578	2841849			185		12	Cross Bedding
	0779578	2841849			160		13	Cross Bedding
	0779578	2841849			192		20	Cross Bedding
	0779578	2841849			206		29	Cross Bedding
	0779578	2841849			205		1	Cross Bedding
	0779578	2841849			27		2	Cross Bedding

	0779578	2841849			16		3	Cross Bedding
	0779578	2841849			184		9	Cross Bedding
	0779578	2841849			187		3	Cross Bedding
	0779578	2841849			353		1	Cross Bedding
	0779578	2841849			1		3	Cross Bedding
	0779578	2841849			358		5	Cross Bedding
	0779578	2841849			10		8	Cross Bedding
	0779578	2841849			15		8	Cross Bedding
	0779578	2841849			19		5	Cross Bedding
	0779578	2841849			198		18	Cross Bedding
	0779578	2841849			184		15	Cross Bedding
	0779578	2841849			195		20	Cross Bedding
165	0783067	2853464	65		227		28	Asymmetric
	0783067	2853464			239		24	Asymmetric
	0783067	2853464			280		27	Cross bed
	0783067	2853464			287		10	Cross bed
	0783067	2853464			277		23	Cross bed
	0783067	2853464			287		10	Cross bed
	0783067	2853464			280		23	Cross bed
	0783067	2853464			107		-3	Cross bed
	0783067	2853464			287		14	Cross bed
	0783067	2853464			292		15	Cross bed
	0783067	2853464			291		18	Cross bed
	0783067	2853464			50		6	Cross bed
	0783067	2853464			119		12	Cross bed
	0783067	2853464			296		8	Cross bed
	0783067	2853464			308		20	Cross bed
	0783067	2853464			300		12	Cross bed
	0783067	2853464			314		14	Cross bed
	0783067	2853464			285		15	Cross bed
	0783067	2853464			121		6	Cross bed
	0783067	2853464			120		10	Cross bed
	0783067	2853464			329		11	Cross bed
	0783067	2853464			276		10	Cross bed
	0783067	2853464			296		11	Cross bed
	0783067	2853464			274		11	Bounding Surface
	0783067	2853464			356		16	Bounding Surface
	0783067	2853464			93		10	Cross bed
	0783067	2853464			298		20	Cross bed
	0783067	2853464			112		8	Cross bed
	0783067	2853464			314		5	Bounding Surface
	0783067	2853464			148		7	Bounding Surface

	0783067	2853464			276		14	Cross bed
	0783067	2853464			276		10	Cross bed
	0783067	2853464			289		11	Cross bed
	0783067	2853464			329		15	Cross bed
	0783067	2853464			302		3	Cross bed
	0783067	2853464			308		5	Cross bed
	0783067	2853464			265		13	Cross bed
	0783067	2853464			258		16	Cross bed
167	0782803	2852372	66		217		10	Cross bed
	0782803	2852372			214		8	Cross bed
	0782803	2852372			207		17	Cross bed
	0782803	2852372			27		4	Cross bed
	0782803	2852372			190		18	Bounding Surface
	0782803	2852372			193		23	Cross bed
	0782803	2852372			181		18	Cross bed
	0782803	2852372			197		23	Cross bed
	0782803	2852372			210		8	Cross bed
	0782803	2852372			200		20	Cross bed
	0782803	2852372			190		20	Cross bed
	0782803	2852372			220		10	Cross bed
	0782803	2852372			208		10	Cross bed
	0782803	2852372			221		20	Cross bed
	0782803	2852372			208		18	Cross bed
	0782803	2852372			240		30	Cross bed
	0782803	2852372			68		6	Cross bed
	0782803	2852372			268		13	Cross bed
	0782803	2852372			230		7	Cross bed
	0782803	2852372			233		17	Cross bed
	0782803	2852372			200		10	Bounding Surface
	0782803	2852372			240		22	Cross bed
	0782803	2852372			207		22	Cross bed
	0782803	2852372			227		18	Cross bed
	0782803	2852372			219		19	Cross bed
	0782803	2852372			202		15	Cross bed
	0782803	2852372			224		20	Cross bed
168	0782718	2852430			219		10	Bounding Surface
	0782718	2852430			178		4	Bounding Surface
	0782718	2852430			214		8	Cross bed
	0782718	2852430			190		6	Cross bed
	0782718	2852430			182		10	Cross bed
	0782718	2852430			195		9	Bounding Surface

	0782718	2852430			176		8	Bounding Surface
	0782718	2852430			168		11	Bounding Surface
169	0782724	2852528			276		18	Cross bed
	0782724	2852528			255		10	Cross bed
	0782724	2852528			287		6	Cross bed
	0782724	2852528			280		22	Cross bed
	0782724	2852528			276		8	Bounding Surface
	0782724	2852528			320		2	Cross bed
	0782724	2852528			315		8	Cross bed
	0782724	2852528			276		6	Cross bed
	0782724	2852528			76		6	Bounding Surface
	0782724	2852528			298		20	Cross bed
	0782724	2852528			118		5	Bounding Surface
	0782724	2852528			321		14	Cross bed
	0782724	2852528			288		10	Bounding Surface
	0782724	2852528			286		18	Bounding Surface
	0782724	2852528			310		2	Bounding Surface
	0782724	2852528			299		18	Bounding Surface
	0782724	2852528			314		8	Cross bed
170	0782718	2852582			217		20	Cross bed
	0782718	2852582			222		2	Cross bed
	0782718	2852582			211		3	Cross bed
	0782718	2852582			220		10	Cross bed
172	0782610	2852628			183			Cross bed
	0782610	2852628			321			Cross bed
	0782610	2852628			328			Cross bed
	0782610	2852628			322			Bounding Surface
	0782610	2852628			337		24	Cross bed
	0782610	2852628			328		16	Cross bed
	0782610	2852628			334		22	Cross bed
	0782610	2852628			339		28	Cross bed
	0782610	2852628			324		14	Bounding Surface
	0782610	2852628			334		20	Cross bed
	0782610	2852628			322		8	Cross bed
	0782610	2852628			158		2	Cross bed
	0782610	2852628			342		26	Cross bed

173	0782828	2852671	68		331		10	Cross bed
	0782828	2852671			327		10	Cross bed
	0782828	2852671			316		10	Cross bed
	0782828	2852671			2	182		Ripples
	0782828	2852671			198		18	Asymmetric
	0782828	2852671			166		24	Asymmetric
174	0782788	2852673	69		310		32	Cross bed
	0782788	2852673			212		3	Cross bed
	0782788	2852673			210			Bounding Surface
	0782788	2852673			170		3	Cross bed
	0782788	2852673			210		12	Cross bed
	0782788	2852673			212		12	Bounding Surface
	0782788	2852673			218		28	Cross bed
	0782788	2852673			200		30	Cross bed
	0782788	2852673			199		20	Cross bed
175	0782755	2852839		32	320		17	Cross bed
	0782755	2852839			140			Cross bed
	0782755	2852839			4		3	Cross bed
	0782755	2852839			30			Bedform - foreset
	0782755	2852839			214		10	Cross bed
	0782755	2852839			250		8	Bounding Surface
	0782755	2852839			226			Cross bed
	0782755	2852839			210		20	Cross bed
	0782755	2852839			180		20	Cross bed
	0782755	2852839			26			Cross bed
	0782755	2852839			306	126		Channel
	0782755	2852839			303	123		Channel
177	0782691	2852924	70		320	140		Ripples
	0782691	2852924			320	140		Ripples
	0782691	2852924			320	140		Ripples
179	0782577	2851951			353		3	Bounding Surface
	0782577	2851951			180		2	Bounding Surface
	0782577	2851951			258		15	Cross Bed
	0782577	2851951			91		3	Cross Bed
	0782577	2851951			88		15	Cross Bed
180	0782518	2852007	71		251			Cross bed
	0782518	2852007			249			Cross bed
	0782518	2852007			189		11	Cross bed
	0782518	2852007			199		26	Asymmetric
	0782518	2852007			189	9		Ripples

	0782518	2852007			180	360		Ripples
	0782518	2852007			167	347		Ripples
	0782518	2852007			172	352		Ripples
	0782518	2852007			200	20		Ripples
	0782518	2852007			21		18	Asymmetric
181	0782522	2852146	72		290			Cross bed
	0782522	2852146			289			Bounding Surface
	0782522	2852146			286		8	Cross bed
	0782522	2852146			246		11	Cross bed
	0782522	2852146			249		8	Cross bed
	0782522	2852146			233		17	Cross bed
	0782522	2852146			67		3	Cross bed
	0782522	2852146			156		3	Cross bed
	0782522	2852146			153			Cross bed
	0782522	2852146			150			Cross bed
	0782522	2852146			181		10	Cross bed
	0782522	2852146			183		10	Cross bed
	0782522	2852146			196			Cross bed
	0782522	2852146			266			Cross bed
	0782522	2852146			250			Cross bed
	0782522	2852146			258			Cross bed
	0782522	2852146			259			Cross bed
	0782522	2852146			230			Cross bed
	0782522	2852146			249			Cross bed
182	0782460	2852211			270		10	Cross bed
	0782460	2852211			220		10	Bounding Surface
	0782460	2852211			25		8	Bounding Surface
	0782460	2852211			230		12	Cross bed
	0782460	2852211			180		22	Cross bed
	0782460	2852211			250			Cross bed
	0782460	2852211			277			Txb
	0782460	2852211			277			Txb
183	0782449	2852222			338			Cross bed
	0782449	2852222			341			Cross bed
	0782449	2852222			335			Cross bed
	0782449	2852222			320			Cross bed
	0782449	2852222			334			Cross bed
184	0782331	2852319	73		33		3	Cross bed
	0782331	2852319			293		26	Cross bed
	0782331	2852319			310		23	Cross bed
	0782331	2852319			314		23	Cross bed
	0782331	2852319			320		20	Cross bed

185	0782318	2852340			231		10	Cross bed
	0782318	2852340			234		6	Cross bed
	0782318	2852340			30		20	Cross bed
186	0782450	2851920			251		16	Cross bed
	0782450	2851920			281		20	Cross bed
	0782450	2851920			286		1	Cross bed
	0782450	2851920			289		17	Cross bed
187	0782414	2851983	74		229		17	Cross bed
	0782414	2851983			236		18	Cross bed
	0782414	2851983			250		10	Cross bed
	0782414	2851983			28		20	Cross bed
	0782414	2851983			320		20	Cross bed
	0782414	2851983			322		20	Cross bed
	0782414	2851983			30	210		Channel
	0782414	2851983			151		16	Cross bed
	0782414	2851983			300		2	Cross bed
	0782414	2851983			140		10	Cross bed
	0782414	2851983			320		20	Cross bed
	0782414	2851983			326		18	Cross bed
	0782414	2851983			230		2	Cross bed
	0782414	2851983			237		6	Cross bed
	0782414	2851983			159		6	Cross bed
	0782414	2851983			301		12	Cross bed
	0782414	2851983			300		11	Cross bed
	0782414	2851983			320			Cross bed
	0782414	2851983			300			Cross bed
	0782414	2851983			146		11	Cross bed
	0782414	2851983			153		5	Cross bed
	0782414	2851983			248		2	Cross bed
	0782414	2851983			332		8	Cross bed
	0782414	2851983			128		16	Cross bed
	0782414	2851983			215		20	Cross bed
	0782414	2851983			188		12	Cross bed
	0782414	2851983			321		20	Cross bed
	0782414	2851983			210		24	Cross bed
188	0782404	2852080		35	330		10	Cross bed
	0782404	2852080			150		5	Cross bed
	0782404	2852080			322		10	Cross bed
	0782404	2852080			324		15	Cross bed
	0782404	2852080			300		20	Cross bed
	0782404	2852080			342		6	Cross bed
	0782404	2852080			344		2	Cross bed
	0782404	2852080			298		15	Cross bed
	0782404	2852080			339		6	Cross bed
	0782404	2852080			341		10	Cross bed

	0782404	2852080			334		21	Cross bed
	0782404	2852080			306			Cross bed
	0782404	2852080			300			Cross bed
189	0782397	2852143			276		22	Cross bed
	0782397	2852143			284		21	Cross bed
190	0782403	2852282			301			Cross bed
	0782403	2852282			301			Cross bed
	0782403	2852282			306			Cross bed
	0782403	2852282			300			Cross bed
	0782403	2852282			131			Bounding Surface
	0782403	2852282			315			Cross bed
	0782403	2852282			320			Cross bed
	0782403	2852282			302			Cross bed
	0782403	2852282			310			Cross bed
	0782403	2852282			333			Cross bed
	0782403	2852282			330			Cross bed
	0782403	2852282			329			Cross bed
	0782403	2852282			330			Cross bed
	0782403	2852282			345			Cross bed
191	0782464	2852328	75		332			Cross bed
	0782464	2852328			151		9	Bounding Surface
	0782464	2852328			148			Cross bed
	0782464	2852328			300			Cross bed
	0782464	2852328			285			Cross bed
	0782464	2852328			153			Cross bed
	0782464	2852328			350			Cross bed
	0782464	2852328			207		3	Cross bed
	0782464	2852328			200		6	Cross bed
	0782464	2852328			20		5	Cross bed
	0782464	2852328			10		2	Cross bed
	0782464	2852328			310			Cross bed
	0782464	2852328			228			Asymmetric
	0782464	2852328			302			Cross bed
	0782464	2852328			298			Cross bed
	0782464	2852328			129			Cross bed
192	0782429	2852389			298		20	Cross bed
	0782429	2852389			357			Cross bed
	0782429	2852389			346			Cross bed
	0782429	2852389			266		3	Cross bed
	0782429	2852389			256			Cross bed
	0782429	2852389			309			Cross bed
	0782429	2852389			317		15	Cross bed
	0782429	2852389			317		6	Cross bed

	0782429	2852389			317		3	Cross bed
	0782429	2852389			288		2	Cross bed
194	0782682	2852333			163			Cross bed
195	0783927	2853017			95		35	Asymmetric
	0783927	2853017			271	91		Ripple
	0783927	2853017			296	116		Ripple
196	0783948	2853020			297		2	Cross bed
	0783948	2853020			106		6	Cross bed
	0783948	2853020			299		3	Cross bed
	0783948	2853020			296		2	Cross bed
	0783948	2853020			301		4	Cross bed
197	0783947	2853086	77		171		7	Cross bed
	0783947	2853086			63		6	Cross bed
	0783947	2853086			94		3	Cross bed
	0783947	2853086			272			Cross bed
	0783947	2853086			228		3	Cross bed
	0783947	2853086			217		2	Cross bed
	0783947	2853086			347		18	Cross bed
	0783947	2853086			213	33		Ripples
	0783947	2853086			200			Cross bed
	0783947	2853086			200		6	Cross bed
	0783947	2853086			196		6	Cross bed
	0783947	2853086			13		17	Cross bed
	0783947	2853086			268			Cross bed
	0783947	2853086			269		38	Cross bed
	0783947	2853086			271		10	Cross bed
	0783947	2853086			200		10	Cross bed
	0783947	2853086			281		22	Cross bed
198	0783898	2853208	78		178		10	Cross bed
	0783898	2853208			319		17	Cross bed
	0783898	2853208			317		10	Cross bed
	0783898	2853208			339		48	Cross bed
	0783898	2853208			339		5	Cross bed
	0783898	2853208			359			Cross bed
	0783898	2853208			250	70		Channel
	0783898	2853208			341		8	Cross bed
	0783898	2853208			341		29	Cross bed
	0783898	2853208			164		9	Cross bed
	0783898	2853208			342		19	Cross bed
	0783898	2853208			290		24	Cross bed
199	0783872	2853225			175			Cross bed
	0783872	2853225			186			Cross bed
	0783872	2853225			177			Cross bed
	0783872	2853225			198			Cross bed
	0783872	2853225			199			Cross bed

200	0783861	2853284			145		35	Cross bed
	0783861	2853284			121		28	Cross bed
	0783861	2853284			128		32	Cross bed
	0783861	2853284			150		35	Cross bed
201	0783828	2853291	79		181			Trough Cross Beds
	0783828	2853291			178			Trough Cross Beds
	0783828	2853291			179			Trough Cross Beds
	0783828	2853291			175			Trough Cross Beds
	0783828	2853291			187			Trough Cross Beds
	0783828	2853291			192			Trough Cross Beds
	0783828	2853291			174			Trough Cross Beds
	0783828	2853291			179			Trough Cross Beds
	0783828	2853291			176			Trough Cross Beds
	0783828	2853291			157			Trough Cross Beds
	0783828	2853291			168			Trough Cross Beds
	0783828	2853291			178			Trough Cross Beds
	0783828	2853291			193			Cross beds
	0783828	2853291			188			Cross beds
	0783828	2853291			188			Cross beds
	0783828	2853291			197			Cross beds
	0783828	2853291			199			Cross beds
	0783828	2853291			199			Cross beds
	0783828	2853291			191			Cross beds
	0783828	2853291			185		40	Cross beds
	0783828	2853291			192		20	Cross beds
	0783828	2853291			197		28	Cross beds
	0783828	2853291			191		28	Cross beds
202	0783698	2853306			270		20	Cross beds
	0783698	2853306			256		25	Cross beds
	0783698	2853306			267		18	Cross beds
	0783698	2853306			265			Cross beds
	0783698	2853306			257		10	Cross beds
	0783698	2853306			213		10	Cross beds
204	0783784	2853323	80		158			Tought Cross Bedding
	0783784	2853323			151			Tought Cross

								Bedding
	0783784	2853323			189		30	Tought Cross Bedding
	0783784	2853323			196		27	Tought Cross Bedding
	0783784	2853323			167		27	Tought Cross Bedding
	0783784	2853323			171		25	Tought Cross Bedding
	0783784	2853323			183		26	Tought Cross Bedding
	0783784	2853323			170		38	Tought Cross Bedding
	0783784	2853323			173		19	Tought Cross Bedding
	0783784	2853323			168		19	Tought Cross Bedding
	0783784	2853323			171		26	Tought Cross Bedding
	0783784	2853323			168		11	Tought Cross Bedding
	0783784	2853323			164		13	Tought Cross Bedding
	0783784	2853323			164		25	Tought Cross Bedding
	0783784	2853323			190		15	Tought Cross Bedding
	0783784	2853323			192		21	Tought Cross Bedding
	0783784	2853323			203		16	Tought Cross Bedding
	0783784	2853323			198			Tought Cross Bedding
	0783784	2853323			209			Tought Cross Bedding
	0783784	2853323			197			Tought Cross Bedding
	0783784	2853323			207			Tought Cross Bedding
	0783784	2853323			185			Tought Cross Bedding
	0783784	2853323			188		7	Tought Cross Bedding
	0783784	2853323			188		7	Tought Cross Bedding
	0783784	2853323			182		18	Tought Cross Bedding
	0783784	2853323			167		23	Cross Beds
	0783784	2853323			166		21	Cross Beds
	0783784	2853323			179		19	Cross Beds

	0783784	2853323			174		12	Cross Beds
	0783784	2853323			176		20	Cross Beds
205	0783749	2853265			139		35	Cross beds
	0783749	2853265			135		23	Cross beds
	0783749	2853265			213		17	Cross beds
	0783749	2853265			242		13	Cross beds
	0783749	2853265			235		15	Bounding Surface
206	0783772	2853200			217		10	Cross beds
	0783772	2853200			179		10	Cross beds
	0783772	2853200			201		1	Cross beds
	0783772	2853200			321	141		Ripple
207	0783597	2853271	81		220		16	Tought Cross Bedding
	0783597	2853271			271		10	Tought Cross Bedding
	0783597	2853271			280		9	Tought Cross Bedding
	0783597	2853271			277		10	Tought Cross Bedding
	0783597	2853271			249		16	Tought Cross Bedding
	0783597	2853271			269		18	Tought Cross Bedding
	0783597	2853271			266		18	Tought Cross Bedding
	0783597	2853271			238		20	Tought Cross Bedding
	0783597	2853271			235		20	Tought Cross Bedding
	0783597	2853271			185		11	Tought Cross Bedding
	0783597	2853271			180		17	Tought Cross Bedding
	0783597	2853271			198			Tought Cross Bedding
	0783597	2853271			330	150		Channel
	0783597	2853271			304	124		Channel
208	0783635	2853192	82		186		25	Tought Cross Bedding
	0783635	2853192			259		10	Tought Cross Bedding
	0783635	2853192			242		8	Tought Cross Bedding
	0783635	2853192			57		22	Tought Cross Bedding
	0783635	2853192			292		1	Tought Cross Bedding
	0783635	2853192			251		17	Tought Cross

								Bedding
	0783635	2853192			261		19	Tought Cross Bedding
	0783635	2853192			108		16	Cross Beds
	0783635	2853192			207			Cross Beds
	0783635	2853192			204			Cross Beds
	0783635	2853192			190			Cross Beds
	0783635	2853192			203			Cross Beds
	0783635	2853192			210			Cross Beds
	0783635	2853192			148		37	Cross Beds
	0783635	2853192			198		9	Cross Beds
	0783635	2853192			188		9	Cross Beds
	0783635	2853192			195		3	Cross Beds
209	0783661	2853168			207		20	Cross Beds
	0783661	2853168			181		13	Cross Beds
	0783661	2853168			154		7	Cross Beds
	0783661	2853168			180		27	Cross Beds
	0783661	2853168			198		28	Cross Beds
	0783661	2853168			188		27	Cross Beds
	0783661	2853168			123		20	Cross Beds
	0783661	2853168			103		21	Cross Beds
	0783661	2853168			183		24	Cross Beds
210	0783640	2853098	83		137		2	Cross Beds
	0783640	2853098			332		19	Cross Beds
	0783640	2853098			335		15	Cross Beds
	0783640	2853098			357		4	Cross Beds
	0783640	2853098			345			Cross Beds
	0783640	2853098			337		20	Cross Beds
	0783640	2853098			171			Cross Beds
	0783640	2853098			350		1	Cross Beds
	0783640	2853098			334		1	Cross Beds
	0783640	2853098			320		1	Cross Beds
	0783640	2853098			326	146		Ripples
213	0783771	2853120	84		11		18	Cross Beds
	0783771	2853120			360		11	Cross Beds
	0783771	2853120			212		6	Cross Beds
	0783771	2853120			213		17	Cross Beds
	0783771	2853120			186		8	Cross Beds
	0783771	2853120			196		7	Cross Beds
	0783771	2853120			87		6	Cross Beds
	0783771	2853120			267		10	Cross Beds
	0783771	2853120			268		13	Cross Beds
	0783771	2853120			270		18	Cross Beds
	0783771	2853120			285			Cross Beds
	0783771	2853120			298			Cross Beds

	0783771	2853120			289			Cross Beds
214	0783859	2853121			213			Cross Beds
	0783859	2853121			195		2	Cross Beds
	0783859	2853121			196		26	Cross Beds
	0783859	2853121			155		22	Cross Beds
215	0783817	2853205			203			Cross Beds
216	0783780	2853192		38	127			Cross Beds
	0783780	2853192			146		18	Cross Beds
	0783780	2853192			163		24	Cross Beds
	0783780	2853192			121		22	Cross Beds
	0783780	2853192			258		10	Cross Beds
	0783780	2853192			156		12	Cross Beds
	0783780	2853192			157			Cross Beds
217	0783350	2853211			192		10	Cross Beds
	0783350	2853211			187		10	Cross Beds
	0783350	2853211			177		16	Cross Beds
	0783350	2853211			181		17	Cross Beds
	0783350	2853211			157		17	Cross Beds
	0783350	2853211			224		12	Trough Cross Bedding
	0783350	2853211			223		6	Trough Cross Bedding
	0783350	2853211			194		8	Trough Cross Bedding
218	0783234	2853298	85		206			Trough Cross Bedding
	0783234	2853298			199			Trough Cross Bedding
	0783234	2853298			199		10	Trough Cross Bedding
	0783234	2853298			205		22	Trough Cross Bedding
	0783234	2853298			266		21	Cross Beds
	0783234	2853298			254		21	Cross Beds
	0783234	2853298			256		15	Cross Beds
	0783234	2853298			210		1	Low anlge cross beds
	0783234	2853298			204		4	Low anlge cross beds
	0783234	2853298			206		15	Low anlge cross beds
	0783234	2853298			253			Trough Cross Bedding
	0783234	2853298			260		5	Trough Cross Bedding
	0783234	2853298			225			Trough Cross Bedding
	0783234	2853298			238			Trough Cross

								Bedding
	0783234	2853298			222			Trough Cross Bedding
	0783234	2853298			33		35	Trough Cross Bedding
	0783234	2853298			60		18	Trough Cross Bedding
	0783234	2853298			54		38	Trough Cross Bedding
	0783234	2853298			43		32	Trough Cross Bedding
219	0783228	2853403			207		26	Cross Beds
	0783228	2853403			198		24	Cross Beds
	0783228	2853403			194		10	Cross Beds
	0783228	2853403			195		14	Cross Beds
	0783228	2853403			278		10	Cross Beds
	0783228	2853403			236		20	Cross Beds
220	0783141	2853423			20			Cross Beds
	0783141	2853423			45			Cross Beds
	0783141	2853423			27			Cross Beds
	0783141	2853423			37			Cross Beds
	0783141	2853423			35			Cross Beds
	0783141	2853423			15			Cross Beds
	0783141	2853423			17			Cross Beds
	0783141	2853423			21			Cross Beds
221	0783082	2853411			76			Cross Beds
	0783082	2853411			190			Cross Beds
222	0783094	2853233			15			Cross Beds
	0783094	2853233			45			Cross Beds
225	0783182	2853052			243		15	Cross Beds
226	0783218	2853005			185			Cross Beds
	0783218	2853005			113			Cross Beds
227	0783305	2853054			307		10	Cross Beds
	0783305	2853054			264			Cross Beds
	0783305	2853054			282			Cross Beds
	0783305	2853054			269			Cross Beds
	0783305	2853054			288			Cross Beds
228	0782708	2853454		40	331			Cross Beds
	0782708	2853454			315			Cross Beds
	0782708	2853454			327			Cross Beds
	0782708	2853454			317			Cross Beds
	0782708	2853454			160			Cross Beds
	0782708	2853454			310			Cross Beds
	0782708	2853454			305			Cross Beds
	0782708	2853454			318			Cross Beds
	0782708	2853454			228		15	Cross Beds

229	0782738	2853376		41	359		15	Cross beds
	0782738	2853376			185			Cross beds
	0782738	2853376			317			Trough Cross Bedding
	0782738	2853376			315			Trough Cross Bedding
	0782738	2853376			197		10	Cross beds
	0782738	2853376			202		2	Cross beds
230	0782753	2853321	86		49		12	Cross beds
	0782753	2853321			39		20	Cross beds
	0782753	2853321			44		17	Cross beds
	0782753	2853321			51		21	Cross beds
	0782753	2853321			47		15	Cross beds
	0782753	2853321			59		26	Cross beds
	0782753	2853321			67		22	Cross beds
	0782753	2853321			63		25	Cross beds
	0782753	2853321			62		20	Cross beds
	0782753	2853321			66		10	Cross beds
	0782753	2853321			70		16	Cross beds
	0782753	2853321			61		22	Cross beds
	0782753	2853321			67		23	Cross beds
	0782753	2853321			71		15	Cross beds
231	0782802	2853267			322		28	Cross beds
	0782802	2853267			249		18	Cross beds
	0782802	2853267			257		8	Cross beds
	0782802	2853267			58		9	Cross beds
232	0782878	2853210			300			Cross beds
	0782878	2853210			297			Cross beds
	0782878	2853210			302			Cross beds
233	0782911	2853223			208		17	Cross beds
	0782911	2853223			218		9	Cross beds
	0782911	2853223			267		12	Cross beds
	0782911	2853223			30		1	Cross beds
235	0782824	2853132			262		20	Cross beds
	0782824	2853132			266		16	Cross beds
	0782824	2853132			263		19	Cross beds
	0782824	2853132			220		21	Cross beds
	0782824	2853132			211		13	Cross beds
	0782824	2853132			198		11	Cross beds
237	0783019	2853246			190			Cross beds
	0783019	2853246			198			Cross beds
	0783019	2853246			183			Cross beds
	0783019	2853246			15			Cross beds
238	0783041	2853366			168			Cross beds
	0783041	2853366			195			Cross beds

	0783041	2853366			167			Cross beds
239	0783020	2853409			269			Cross beds
	0783020	2853409			262			Cross beds
	0783020	2853409			243			Cross beds
240	0782912	2853340			213			Cross beds
	0782912	2853340			209			Cross beds
241	0782880	2853305			214		21	Cross beds
	0782880	2853305			211		22	Cross beds
	0782880	2853305			236			Cross beds
	0782880	2853305			224		5	Cross beds
242	0782788	2853227		42	230		5	Cross beds
	0782788	2853227			221		7	Cross beds
	0782788	2853227			218		19	Cross beds
	0782788	2853227			224		22	Cross beds
	0782788	2853227			188		30	Cross beds
	0782788	2853227			231		28	Cross beds
243	0782774	2853175			193		5	Cross beds
	0782774	2853175			188		5	Cross beds
	0782774	2853175			214		9	Cross beds
	0782774	2853175			211		10	Cross beds
	0782774	2853175			135		1	Bounding Surface
244	0782699	2853117	87		161		5	Cross beds
	0782699	2853117			184		21	Cross beds
	0782699	2853117			181		17	Cross beds
	0782699	2853117			200		17	Cross beds
	0782699	2853117			147		15	Cross beds
	0782699	2853117			358		14	Cross beds
	0782699	2853117			341		10	Cross beds
	0782699	2853117			311		20	Cross beds
	0782699	2853117			3		10	Cross beds
	0782699	2853117			336		8	Cross beds
	0782699	2853117			291		20	Cross beds
	0782699	2853117			342		10	Cross beds
245	0782645	2853137	88		171		15	Cross beds
	0782645	2853137			275		4	Cross beds
	0782645	2853137			237		16	Cross beds
	0782645	2853137			229		2	Cross beds
	0782645	2853137			232		28	Cross beds
	0782645	2853137			54		15	Cross beds
246	0782548	2853177	89		334		12	Cross beds
	0782548	2853177			345		3	Cross beds
247	0782468	2853064			119		6	Cross beds
	0782468	2853064			126		10	Cross beds
	0782468	2853064			122		13	Cross beds

	0782468	2853064			110		17	Cross beds
	0782468	2853064			93		14	Bounding Surface
248	0782455	2853144			227		10	Cross beds
	0782455	2853144			222		12	Cross beds
249	0782518	2853362		43	2240			Cross beds
	0782518	2853362			244			Cross beds
	0782518	2853362			238			Cross beds
	0782518	2853362			236			Cross beds
	0782518	2853362			220			Cross beds
249b	0782532	2853384			52		13	Cross beds
	0782532	2853384			212		6	Cross beds
	0782532	2853384			221		31	Cross beds
	0782532	2853384			161		10	Cross beds
250	0782603	2853372			222		12	Cross beds
	0782603	2853372			226		18	Cross beds
	0782603	2853372			45		2	Cross beds
	0782603	2853372			213		20	Cross beds
	0782603	2853372			234		20	Cross beds
	0782603	2853372			236		24	Cross beds
251	0782523	2853339	90		198			Cross beds
	0782523	2853339			208			Cross beds
	0782523	2853339			31			Cross beds
	0782523	2853339			199			Cross beds
	0782523	2853339			27			Cross beds
	0782523	2853339			211			Cross beds
253	0782440	2853210	91		216		12	Cross beds
	0782440	2853210			224		10	Cross beds
	0782440	2853210			191		24	Cross beds
	0782440	2853210			182		25	Cross beds
254	0782423	2853182			240		16	Cross beds
	0782423	2853182			240		18	Cross beds
	0782423	2853182			241		24	Cross beds
	0782423	2853182			229		13	Cross beds
	0782423	2853182			227		20	Cross beds
257	0782351	2853218	92		183			Cross beds
	0782351	2853218			37			Cross beds
	0782351	2853218			360		2	Cross beds
	0782351	2853218			4		6	Cross beds
	0782351	2853218			190		10	Cross beds
	0782351	2853218			200		5	Cross beds
	0782351	2853218			184		6	Cross beds
258	0781954	2852821	93		299		13	Cross beds
	0781954	2852821			310		12	Cross beds
	0781954	2852821			337		19	Cross beds

	0781954	2852821			284		12	Cross beds
	0781954	2852821			283		19	Cross beds
260	0782257	2852848			232		45	Cross beds
	0782257	2852848			334		10	Cross beds
	0782257	2852848			220		14	Cross beds
	0782257	2852848			243		12.5	Cross beds
	0782257	2852848			25			Cross beds
	0782257	2852848			25			Cross beds
	0782257	2852848			254		6	Cross beds
	0782257	2852848			243		22	Cross beds
	0782257	2852848			262			Cross beds
	0782257	2852848			257		19	Cross beds
261	0782288	2852832	94		198		4	Cross beds
	0782288	2852832			297		10	Cross beds
	0782288	2852832			205		20	Cross beds
	0782288	2852832			231		16	Cross beds
	0782288	2852832			233		2	Cross beds
	0782288	2852832			250		2	Bounding Surface
	0782288	2852832			222		10	Cross beds
	0782288	2852832			222		10	Cross beds
	0782288	2852832			225		9	Cross beds
	0782288	2852832			215		14	Cross beds
262	0782348	2852761			281		10	Trough Cross Bedding
	0782348	2852761			298		13	Cross beds
	0782348	2852761			235		5	Cross beds
	0782348	2852761			232		15	Cross beds
263	0782421	2852672			281		10	Cross beds
	0782421	2852672			269		8	Cross beds
	0782421	2852672			296		10	Cross beds
	0782421	2852672			257		10	Cross beds
	0782421	2852672			296		15	Cross beds
264	0782480	2852673	95		38		8	Cross beds
	0782480	2852673			246		6	Cross beds
	0782480	2852673			30		15	Cross beds
	0782480	2852673			40		14	Cross beds
	0782480	2852673			27		9	Cross beds
266	0782556	2852682			238		20	Cross beds
	0782556	2852682			245		10	Bounding Surface
	0782556	2852682			214			Trough Cross Bedding
	0782556	2852682			205		35	Cross beds
	0782556	2852682			205		12	Cross beds
	0782556	2852682			210		9	Cross beds

	0782556	2852682			220		11	Cross beds
	0782556	2852682			203		11	Cross beds
	0782556	2852682			221		2	Cross beds
267	0782656	2852481			216		10	Cross beds
	0782656	2852481			208		7	Cross beds
	0782656	2852481			14		2	Cross beds
	0782656	2852481			234		16	Cross beds
	0782656	2852481			30		2	Cross beds
269	0782365	2852613		47	172		2	Cross beds
270	0782331	2852676			231		18	Cross beds
	0782331	2852676			32		5	Cross beds
	0782331	2852676			309		18	Cross beds
271	0782255	2852692			278		20	Cross beds
	0782255	2852692			210		18	Cross beds
	0782255	2852692			221		17	Cross beds
	0782255	2852692			285		11	Cross beds
	0782255	2852692			257		12	Cross beds
272	0782043	2852766			287		10	Cross beds
	0782043	2852766			130		5	Cross beds
	0782043	2852766			250		20	Cross beds
	0782043	2852766			336		6	Cross beds
	0782043	2852766			170		2	Cross beds
	0782043	2852766			353		6	Cross beds
	0782043	2852766			273		12	Cross beds
	0782043	2852766			265		10	Cross beds
	0782043	2852766			279		12	Cross beds
	0782043	2852766			292		5	Cross beds
	0782043	2852766			213		12	Cross beds
	0782043	2852766			90		3	Cross beds
273	0781986	2852788	96		325		9	Cross beds
	0781986	2852788			286			Cross beds
	0781986	2852788			300		10	Cross beds
	0781986	2852788			46		2	Asymmetric
	0781986	2852788			174		5	Asymmetric
	0781986	2852788			220	40		Ripple
274	0781910	2852799			135		13	Cross beds
	0781910	2852799			236		14	Cross beds
275	0782209	2852499			210		8	Cross beds
	0782209	2852499			357		9	Cross beds
	0782209	2852499			357		12	Cross beds
277	0782311	2852436			33		16	Cross beds
	0782311	2852436			45		25	Cross beds
278	0782335	2852452			320		18	Cross beds
	0782335	2852452			315		11	Cross beds
	0782335	2852452			215		18	Cross beds

279	0782431	2852761			215		3	Trough Cross Bedding
	0782431	2852761			202		3	Cross beds
	0782431	2852761			190		9	Cross beds
	0782431	2852761			130		14	Cross beds
	0782431	2852761			293		20	Cross beds
	0782431	2852761			296		18	Cross beds
283					186		2	Cross beds
					193		3	Cross beds
					199		5	Cross beds
					191		9	Cross beds
285	0777099	2839843			233		6	Cross beds
289	0777329	2839985			344	164		Ripple
	0777329	2839985			349	169		Ripple
	0777329	2839985			343		6	Asymmetric
290	0777331	2839988	97		161		29	Asymmetric
	0777331	2839988			279		16	Asymmetric
	0777331	2839988			348	168		Ripple
	0777331	2839988			2	182		Ripple
	0777331	2839988			349	169		Ripple
	0777331	2839988			280	100		Ripple
	0777331	2839988			36		32	Asymmetric
	0777331	2839988			13	193		Ripple
296	0777482	2840777			201		12	Cross Bed
	0777482	2840777			199		18	Cross Bed
	0777482	2840777			209		4	Cross Bed
297	0777465	2840812			206		2	Cross Bed
	0777465	2840812			206		9	Cross Bed
	0777465	2840812			215		8	Cross Bed
	0777465	2840812			213		7	Cross Bed
	0777465	2840812			199		8	Cross Bed
298	0777430	2840857			213		9	Cross Bed
300	0777545	2840803	98		49		15	Asymmetric
	0777545	2840803			65	245		Ripple
	0777545	2840803			57	277		Ripple
	0777545	2840803			29	209		Ripple
	0777545	2840803			93		20	Asymmetric
	0777545	2840803			114	294		Ripple
	0777545	2840803			42	222		Ripple
	0777545	2840803			44	224		Ripple
	0777545	2840803			44	224		Ripple
304	0777783	2841056			205		22	Cross Bed
	0777783	2841056			188		22	Cross Bed
	0777783	2841056			192		22	Cross Bed
	0777783	2841056			195		23	Cross Bed

305	0777805	2841053			186		27	Cross Bed
	0777805	2841053			170		28	Cross Bed
	0777805	2841053			166		22	Cross Bed
	0777805	2841053			174		22	Cross Bed
306	0777906	2841054			186		17	Cross Bed
309	0778019	2841075			187		27	Cross Bed
312	0777950	2841272			203		12	Cross Bed
318	0778086	2841574			204		12	Cross Bed
	0778086	2841574			42		5	Cross Bed
	0778086	2841574			33		14	Cross Bed
319	0778107	2841850			222		20	Cross Bed
	0778107	2841850			171		13	Cross Bed
320	0778136	2841939			221		5	Cross Bed
	0778136	2841939			70		3	Cross Bed
321	0778099	2841898			179		5	Cross Bed
	0778099	2841898			216		5	Cross Bed
	0778099	2841898			196		10	Cross Bed
	0778099	2841898			248		6	Bounding Surface
323	0778315	2841630			49	229		Ripples
	0778315	2841630			48	228		Ripples
	0778315	2841630			14	194		Ripples
	0778315	2841630			14	194		Ripples
324	0778344	2841658			303	123		Ripples
	0778344	2841658			318	138		Ripples
	0778344	2841658			301	121		Ripples
325	0778412	2841788			201		10	Cross Beds
	0778412	2841788			25		3	Cross Beds
326	0778598	2841957			184		12	Cross Beds
	0778598	2841957			175		17	Cross Beds
327	0778617	2841931			82		18	Bounding Surface
331	0778591	2842109			8		18	Asymmetric
	0778591	2842109			160	340		Ripples
	0778591	2842109			222	42		Ripples
337	0781689	2845678			154		18	Cross Beds
	0781689	2845678			27		17	Cross Beds
338	0781670	2845628			181		10	Cross Beds
	0781670	2845628			146		13	Cross Beds
339	0781598	2845579			224		6	Cross Beds
	0781598	2845579			241		14	Cross Beds
	0781598	2845579			239		19	Cross Beds
	0781598	2845579			53		2	Cross Beds
	0781598	2845579			235		8	Cross Beds
340	0781616	2845619		51	337		10	Cross beds

341	0781560	2845679			164		19	Cross Beds
	0781560	2845679			172		12	Cross Beds
343	0781416	2845758			358		14	Cross Beds
	0781416	2845758			180		8	Cross Beds
	0781416	2845758			170		10	Cross Beds
	0781416	2845758			336		6	Cross Beds
344	0781632	2845503		52	44		5	Cross Beds
	0781632	2845503			210		14	Cross Beds
	0781632	2845503			242		18	Cross Beds
	0781632	2845503			236		22	Cross Beds
346	0781699	2845435			338		14	Cross Beds
	0781699	2845435			221		10	Cross Beds
348	0781644	2845334			182		13	Cross Beds
	0781644	2845334			181		24	Cross Beds
349	0781608	2845285			211		9	Cross Beds
350	0781522	2845080			211		13	Cross Beds
	0781522	2845080			183		22	Cross Beds
	0781522	2845080			224		8	Cross Beds
353	0780957	2844965			132		22	Trough Cross Beds
	0780957	2844965			106		22	Trough Cross Beds
354	0781021	2844975			226		22	Cross Beds
	0781021	2844975			223		30	Cross Beds
	0781021	2844975			238		18	Cross Beds
	0781021	2844975			223		20	Cross Beds
356	0780821	2844662	103		67	247		Ripples
	0780821	2844662			80	260		Ripples
	0780821	2844662			44	224		Ripples
	0780821	2844662			61	241		Ripples
	0780821	2844662			62	242		Ripples
	0780821	2844662			62	242		Ripples
	0780821	2844662			45	225		Ripples
	0780821	2844662			86	266		Ripples
359	0780867	2844534			73		6	Cross Beds
	0780867	2844534			72		3	Cross Beds
360	0780919	2844467			188		5	Cross Beds
	0780919	2844467			23		3	Cross Beds
361	0780859	2844388			228		20	Cross Beds
	0780859	2844388			192		22	Cross Beds
364	0777201	2841094	104		244		13	Cross Beds
	0777201	2841094			217		10	Cross Beds
	0777201	2841094			244		10	Cross Beds
	0777201	2841094			221		9	Cross Beds
	0777201	2841094			234		10	Cross Beds

	0777201	2841094			198		10	Cross Beds
	0777201	2841094			201		11	Cross Beds
	0777201	2841094			232		2	Cross Beds
	0777201	2841094			29		20	Cross Beds
	0777201	2841094			218		15	Cross Beds
	0777201	2841094			46	226		Ripple
	0777201	2841094			63	243		Ripple
	0777201	2841094			359	179		Ripple
	0777201	2841094			349	169		Ripple
	0777201	2841094			209	29		Ripple
	0777201	2841094			49		11	Asymmetrical
	0777201	2841094			30		10	Asymmetrical
	0777201	2841094			360	180		Ripple
	0777201	2841094			37	217		Ripple
365	0778129	2842137	105		107	297		Ripples
	0778129	2842137			113	293		Ripples
	0778129	2842137			174	354		Ripples
	0778129	2842137			166	346		Ripples
	0778129	2842137			349		12	Asymmetric
	0778129	2842137			161	341		Ripples
	0778129	2842137			200	20		Ripples
	0778129	2842137			140	320		Ripples
	0778129	2842137			160	340		Ripples
	0778129	2842137			124	343		Ripples
	0778129	2842137			177	357		Ripples
	0778129	2842137			155	335		Ripples
	0778129	2842137			77	257		Ripples
	0778129	2842137			43	223		Ripples
	0778129	2842137			71		6	Cross bed
	0778129	2842137			259		10	Cross bed
366	0778133	2842095		54	71	251		Ripples
367	0778582	2842142	106		48	228		Ripples
	0778582	2842142			103	283		Ripples
368	0778687	2842098	107		288		18	Cross Bed
370	0777181	2841039	109		54	234		Ripple
					269			Trough Cross Beds
					13		29	Cross bed
					20		13	Cross bed
					157		40	Cross bed
					207		28	Cross bed
					208		8	Cross bed
					222		15	Cross bed
					237		18	Cross bed
1	0778617	2842373	114		170		17	Cross bed

Appendix 5: Core logs

Key for logs and three-dimensional diagrams

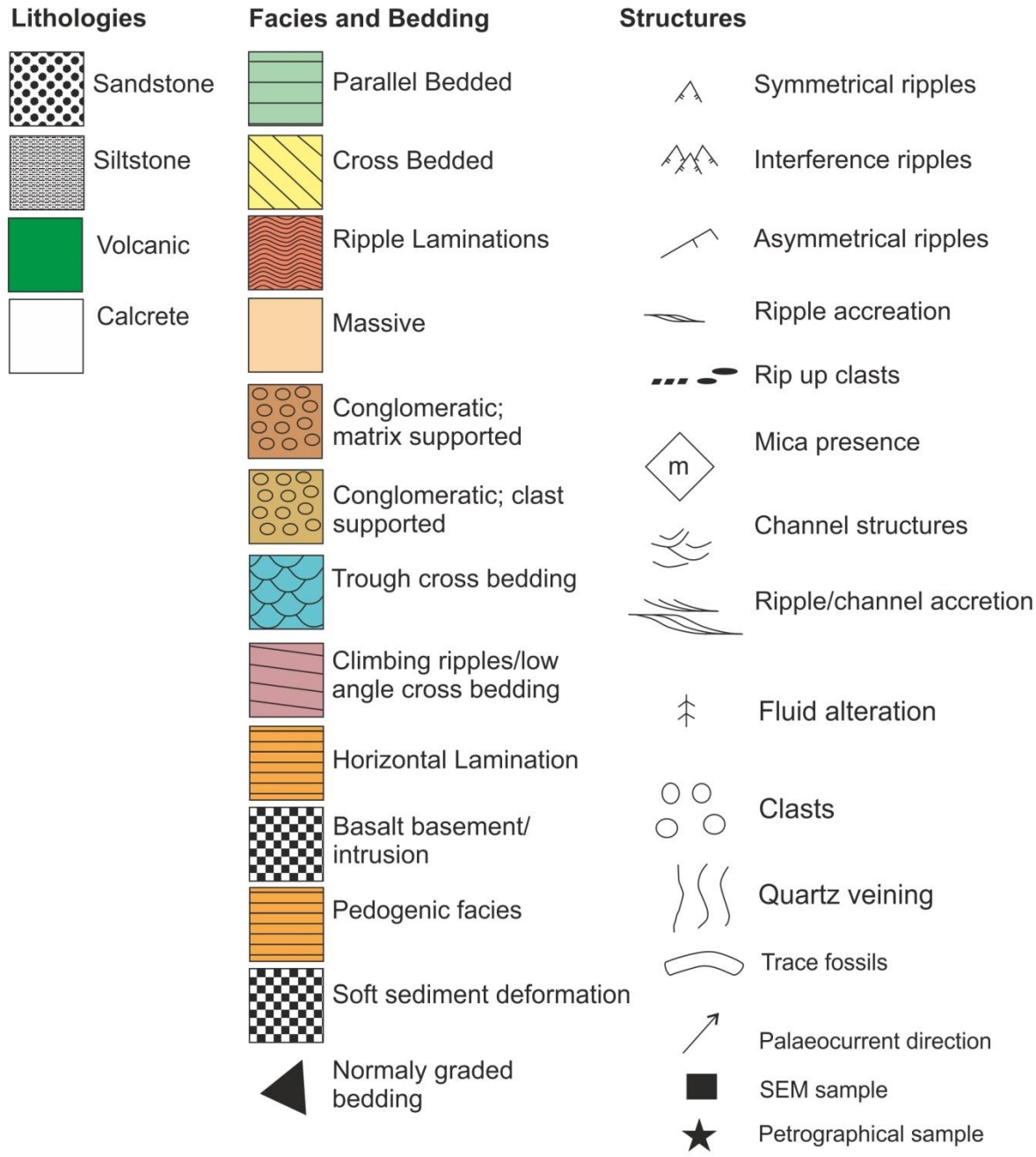

Unless otherwise stated all logs are in metres

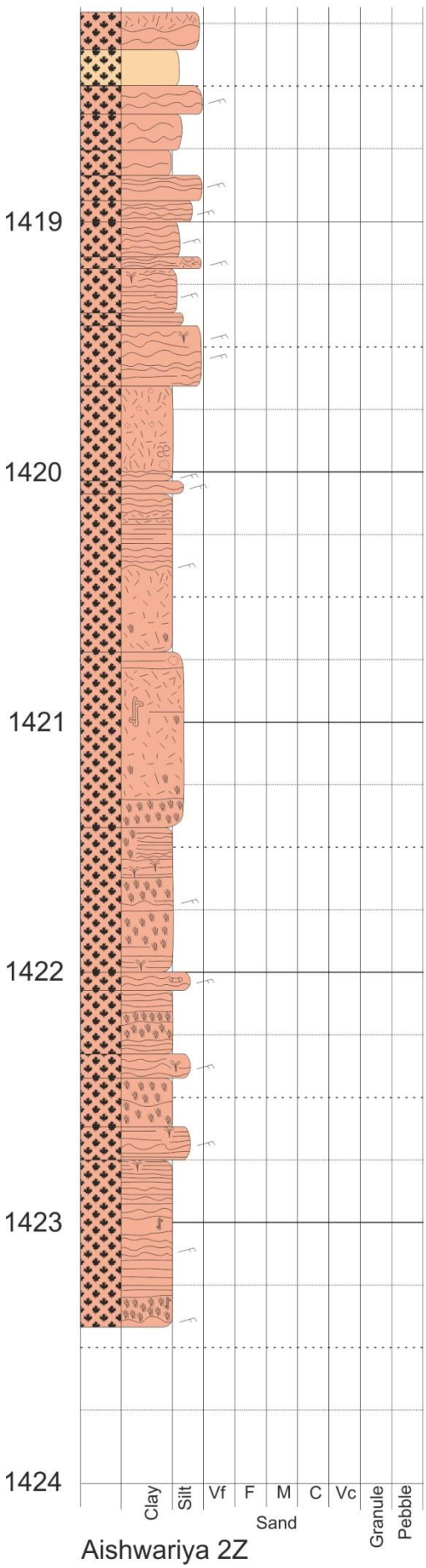

Aishwariya 2Z

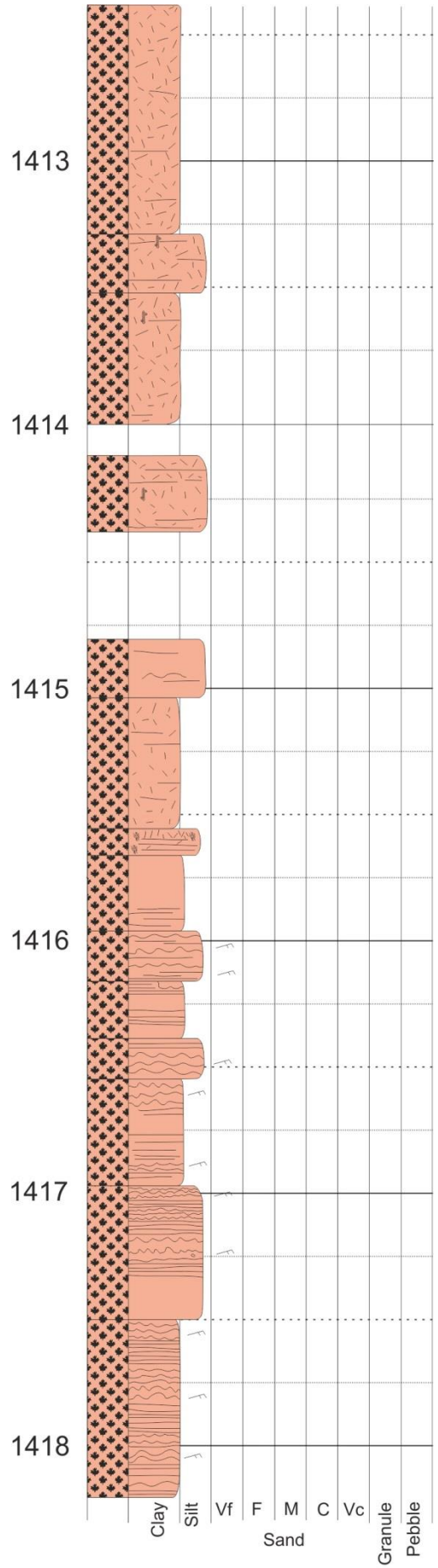

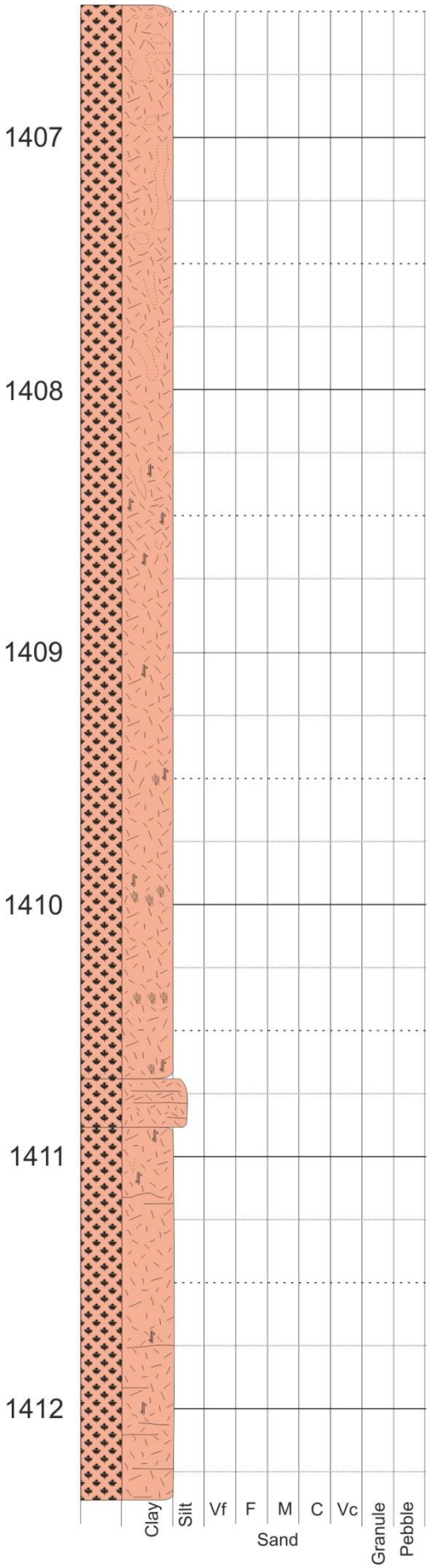
1407
1408
1409
1410
1411
1412
Clay
Silt
Vf
F
M
C
Vc
Granule
Pebble
Sand

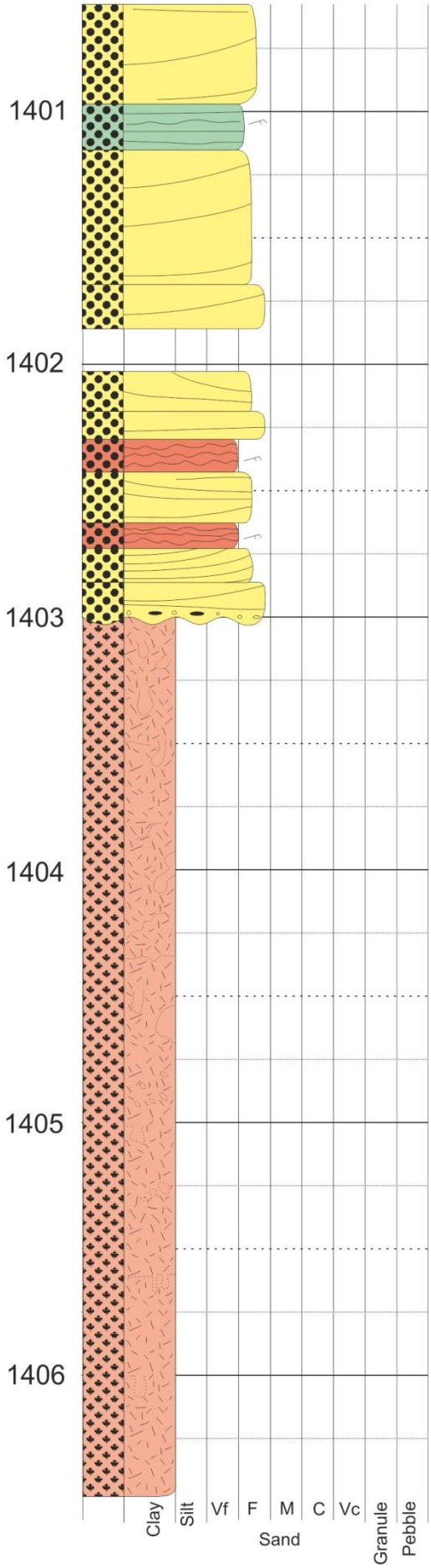
1401
1402
1403
1404
1405
1406
Clay
Silt
Vf
F
M
C
Vc
Granule
Pebble
Sand

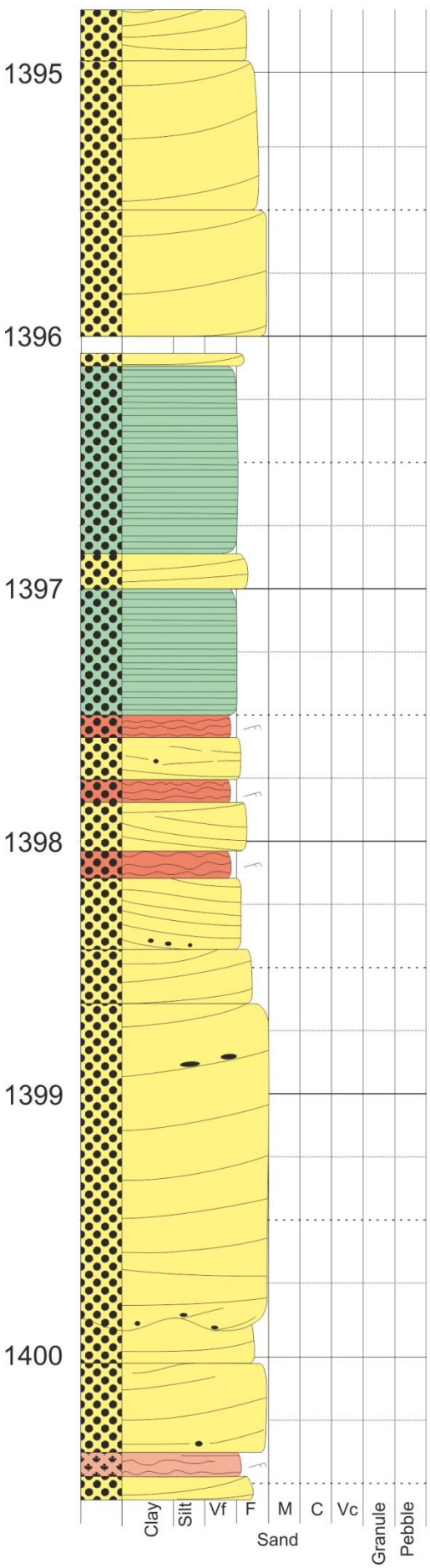
1395
1396
1397
1398
1399
1400
Clay
Silt
Vf
F
M
C
Vc
Granule
Pebble
Sand

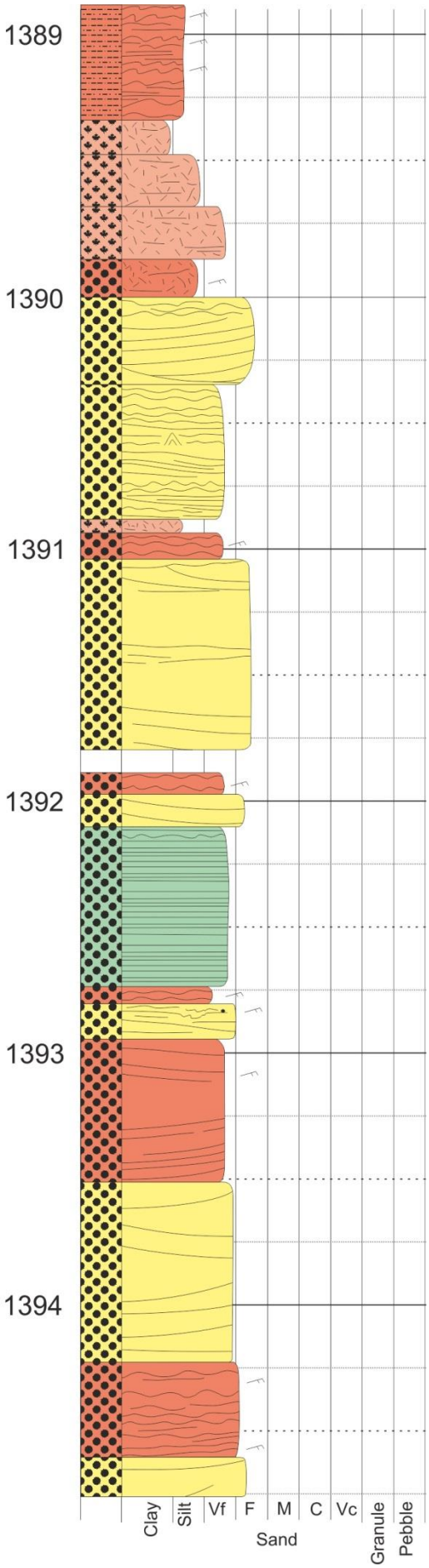
1389
1390
1391
1392
1393
1394
Clay
Silt
Vf
F
M
C
Vc
Granule
Pebble
Sand

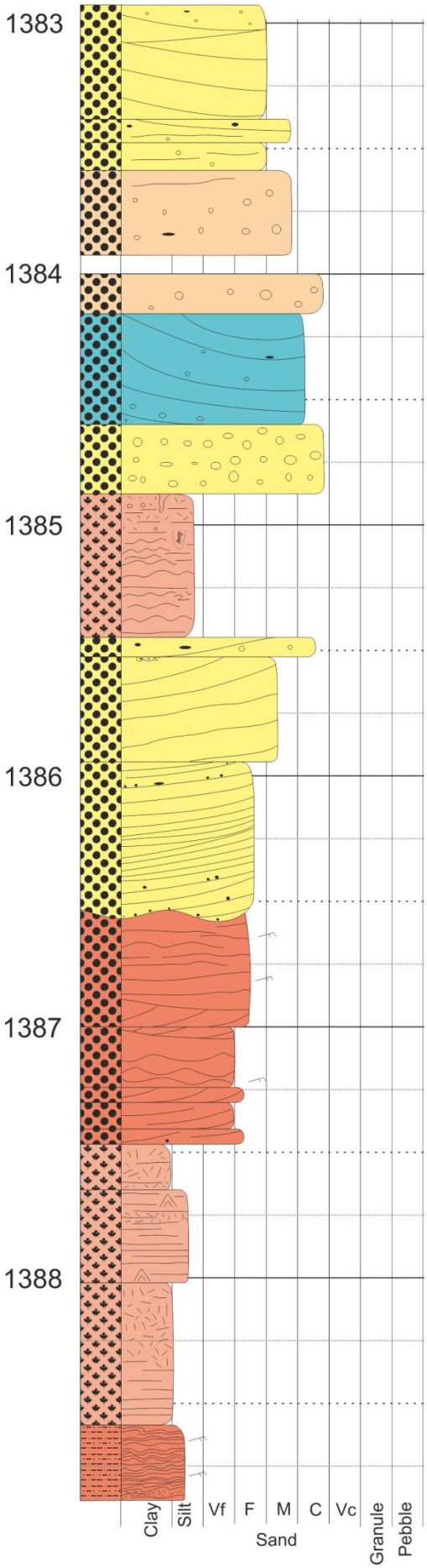
1383
1384
1385
1386
1387
1388
Clay
Silt
Vf
F
M
C
Vc
Granule
Pebble
Sand

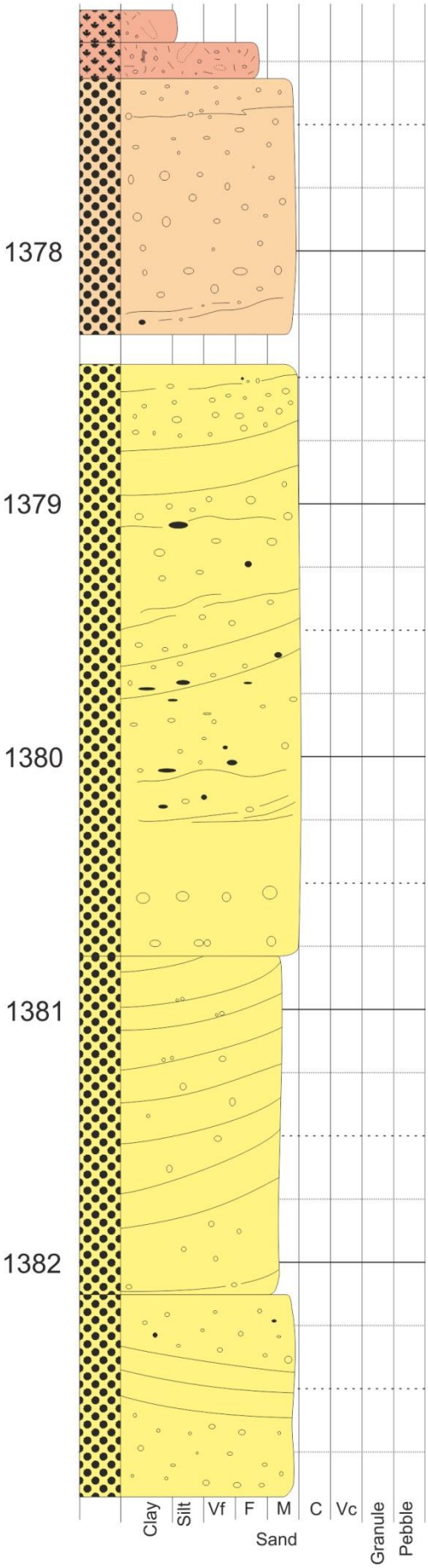
1378
1379
1380
1381
1382
Clay
Silt
Vf
F
M
C
Vc
Granule
Pebble
Sand

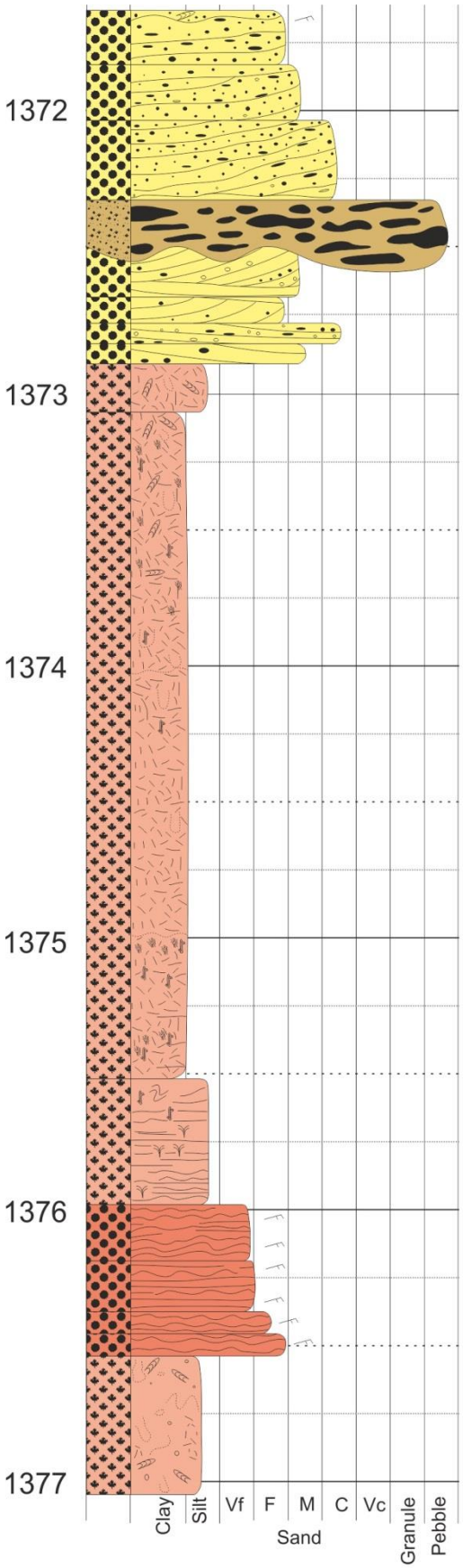
1372
1373
1374
1375
1376
1377
Clay
Silt
Vf
F
M
C
Vc
Granule
Pebble
Sand

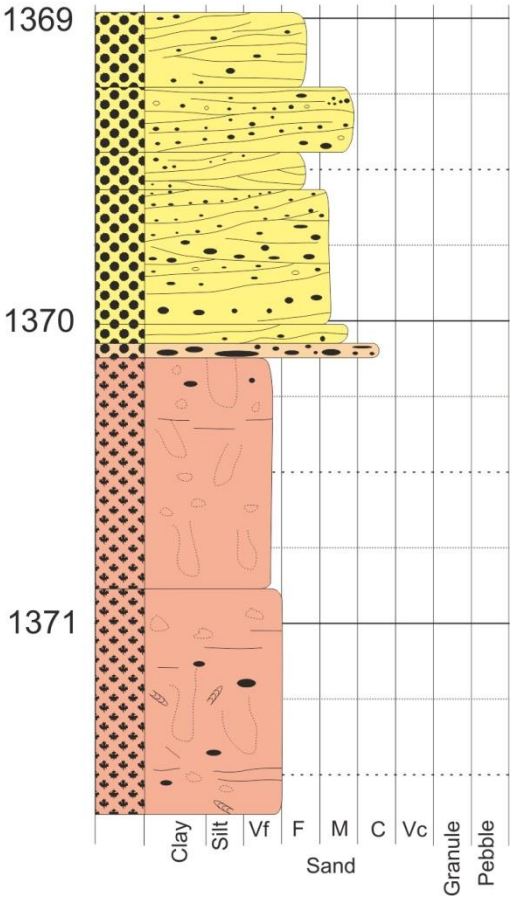
1369
1370
1371
Clay
Silt
Vf
F
M
C
Vc
Granule
Pebble
Sand

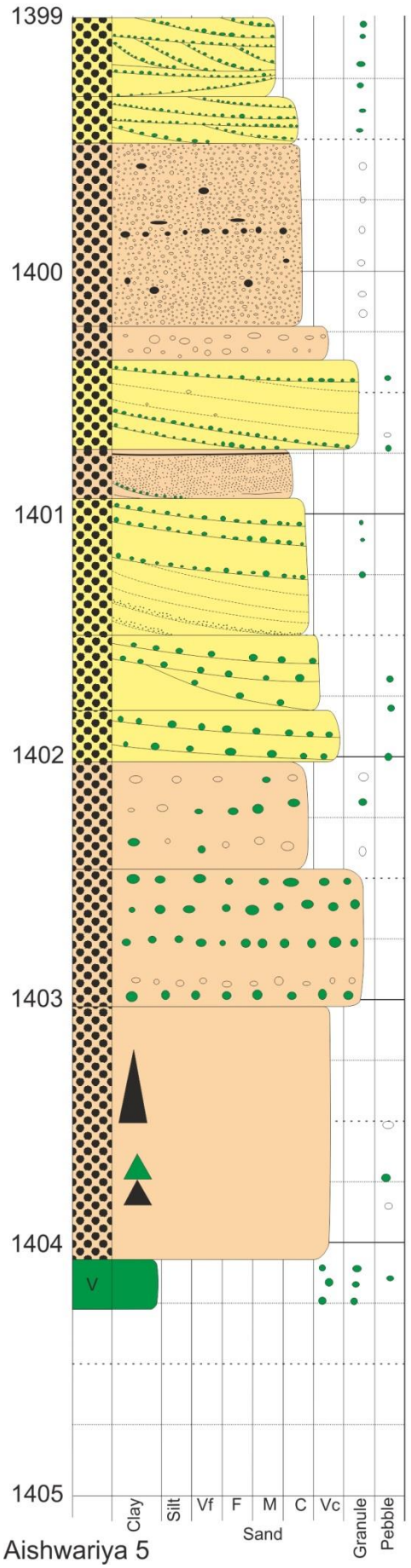

Aishwariya 5

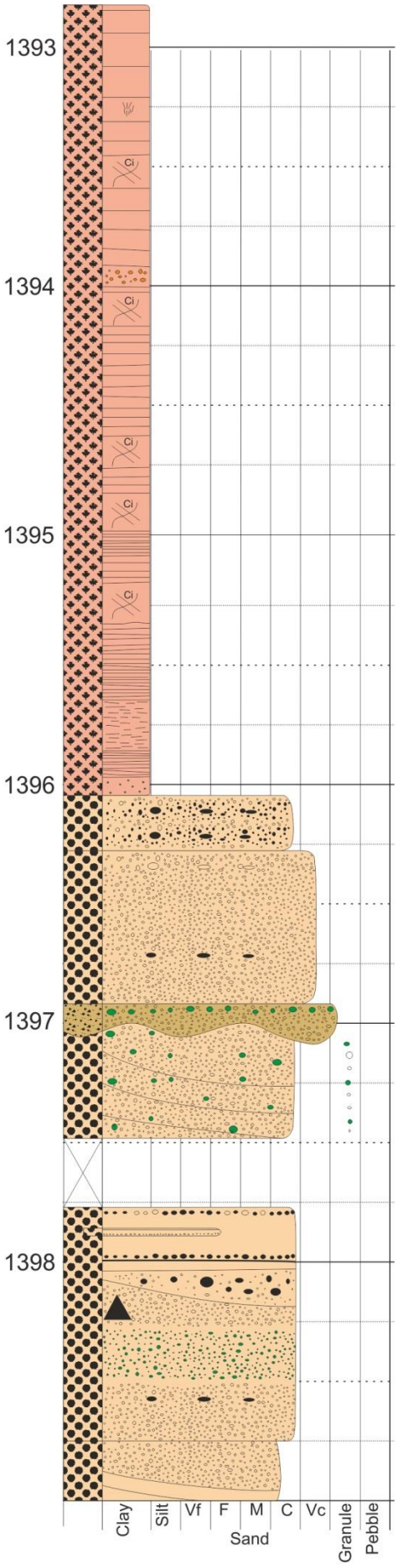

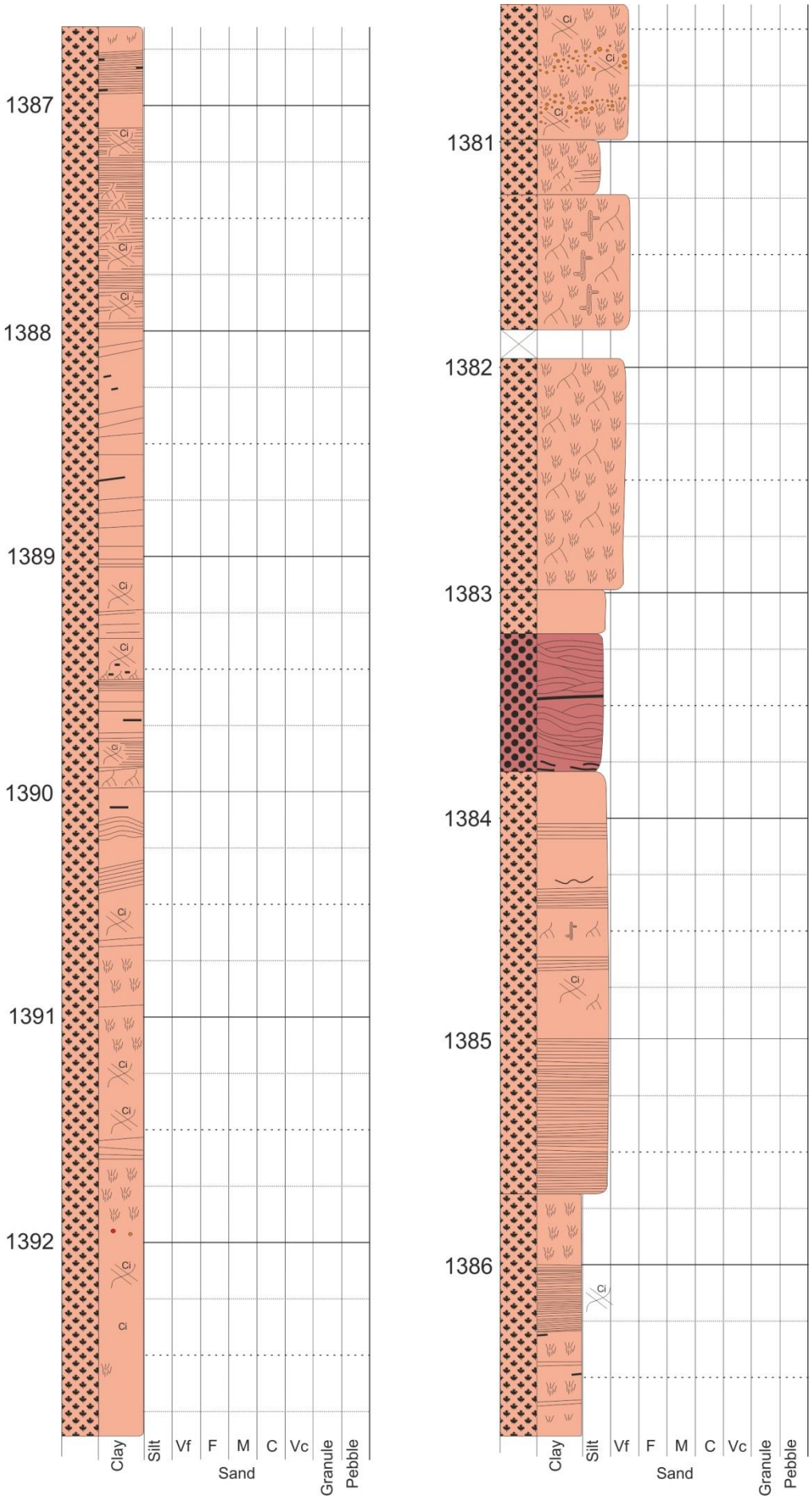
1387
1388
1389
1390
1391
1392
1381
1382
1383
1384
1385
1386
Ci
Clay
Silt
Vf
F
M
C
Vc
Sand
Granule
Pebble

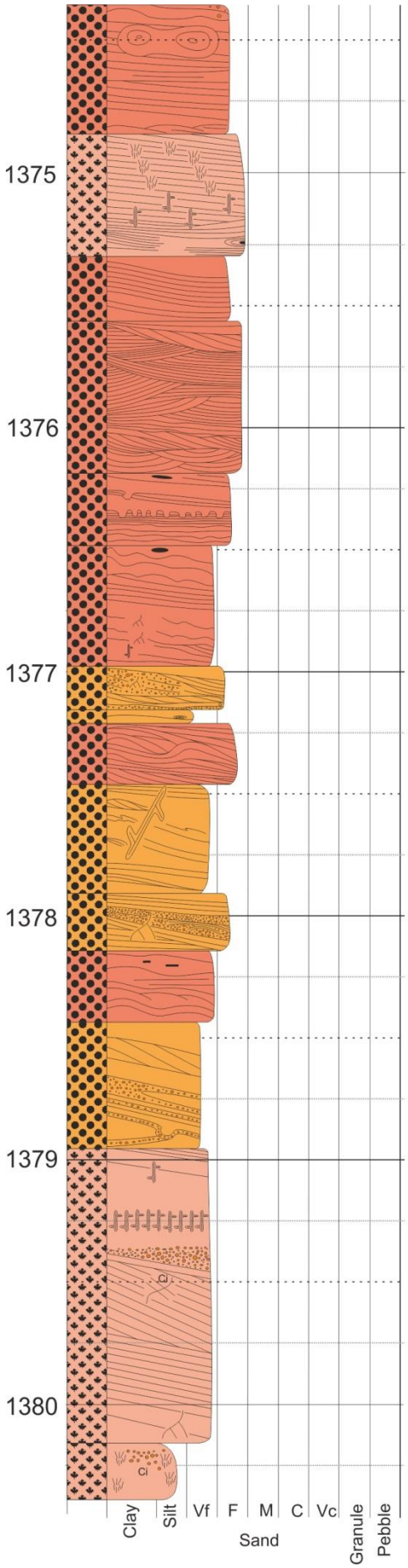
1375
1376
1377
1378
1379
1380
Clay
Silt
Vf
F
M
C
Vc
Granule
Pebble
Sand

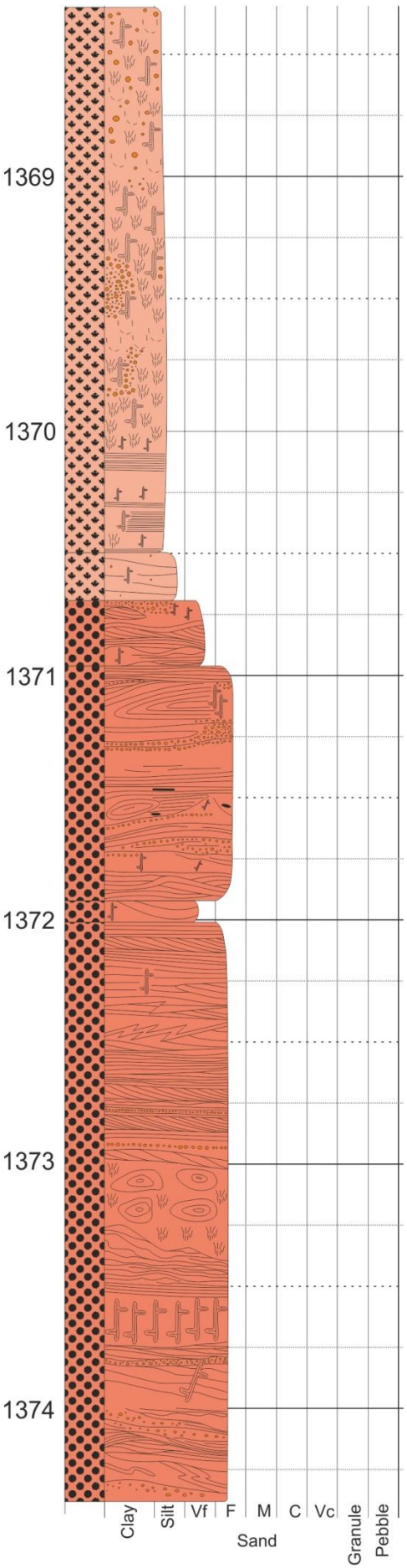
1369
1370
1371
1372
1373
1374
Clay
Silt
Vf
F
M
C
Vc
Granule
Pebble
Sand

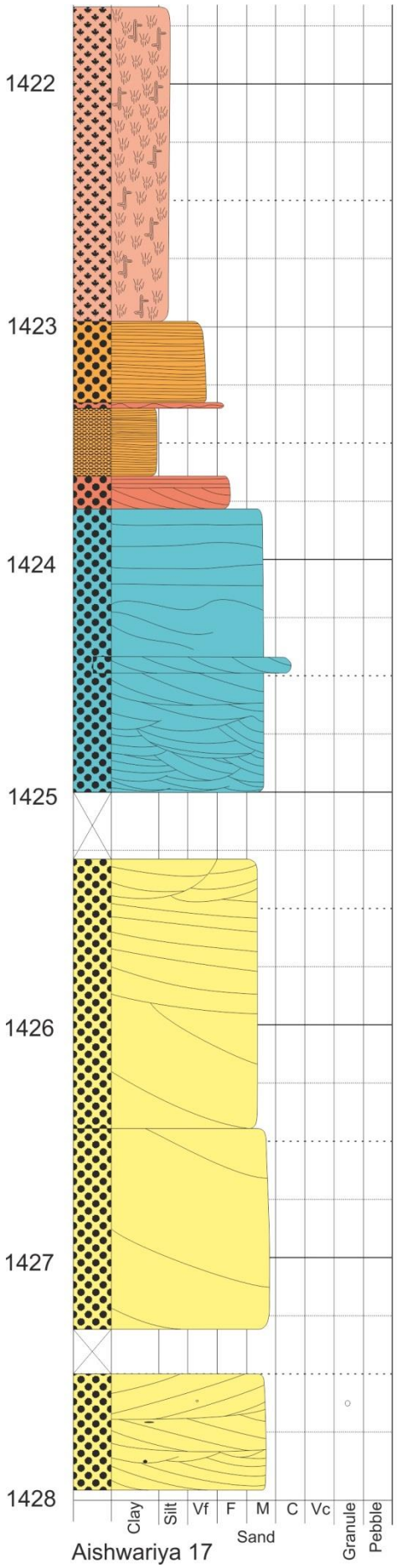
1422
1423
1424
1425
1426
1427
1428
Clay
Silt
Vf
F
M
C
Vc
Granule
Pebble
Sand
Aishwariya 17

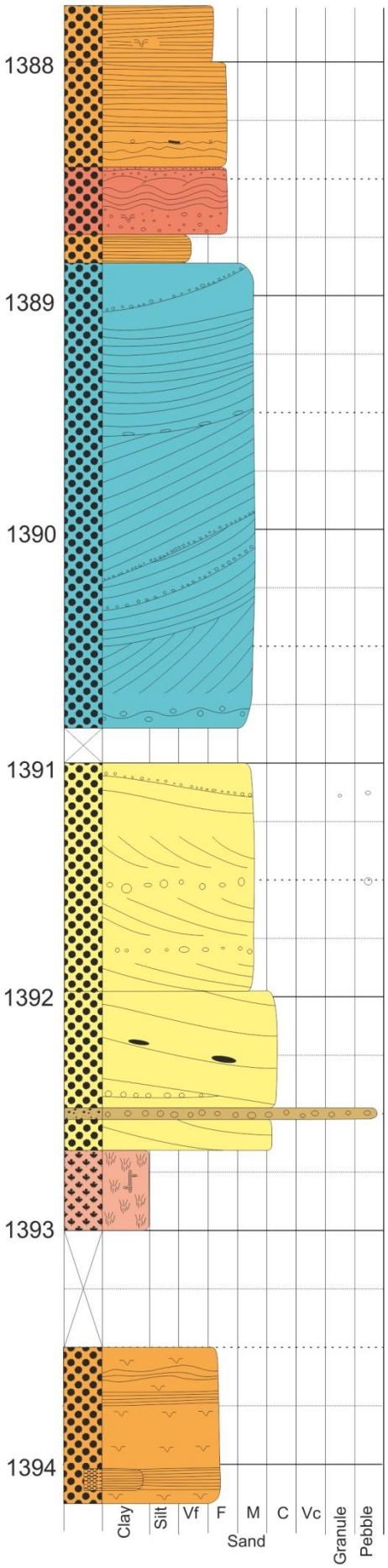
1388
1389
1390
1391
1392
1393
1394
Clay
Silt
Vf
F
M
C
Vc
Granule
Pebble
Sand

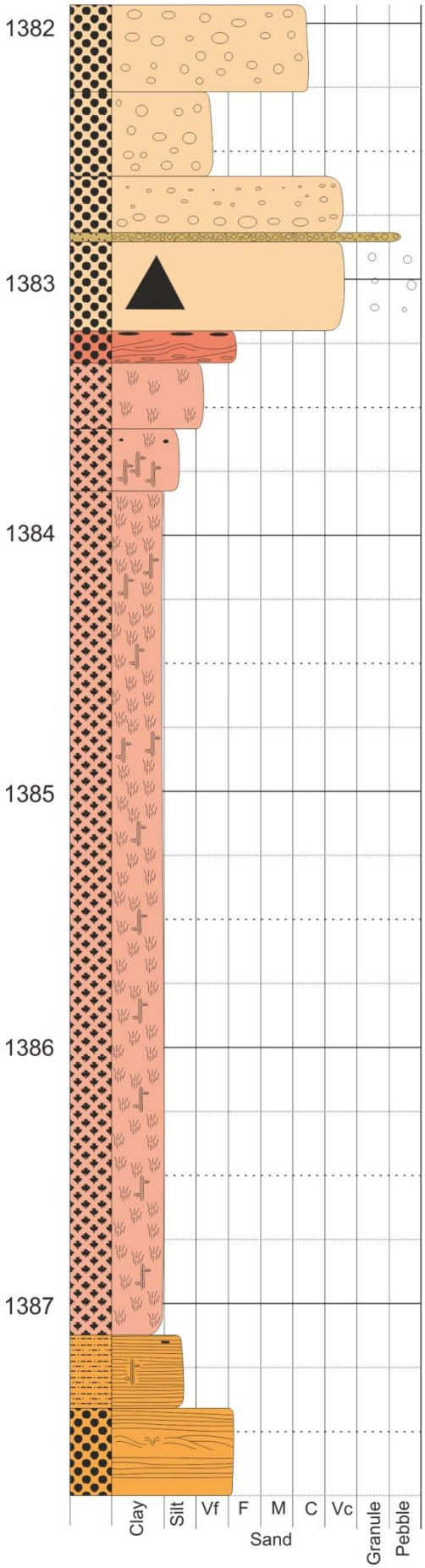
1382
1383
1384
1385
1386
1387
Clay
Silt
Vf
F
M
C
Vc
Granule
Pebble
Sand

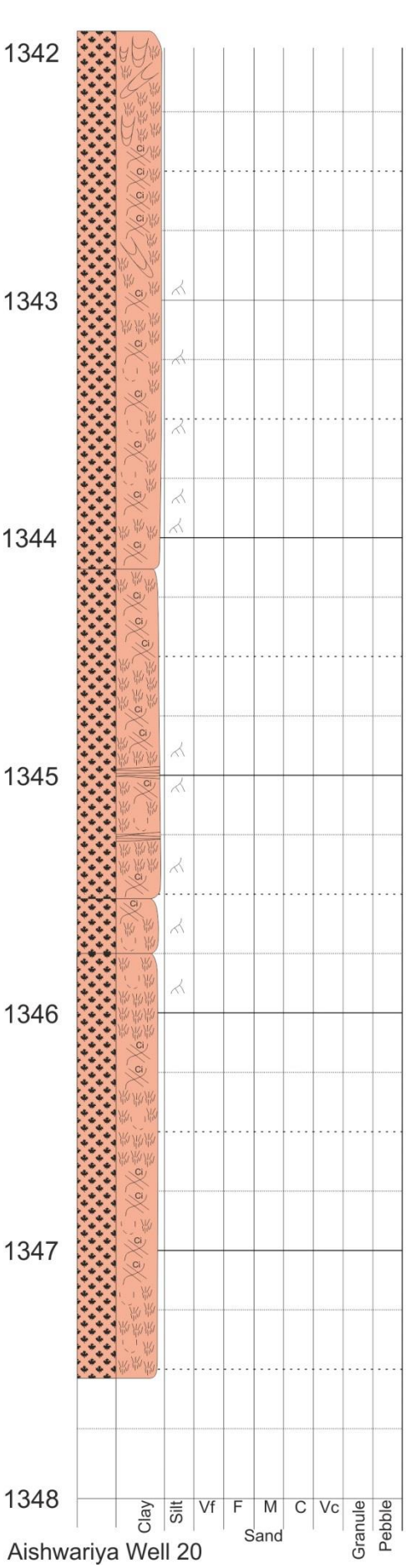

Aishwariya Well 20

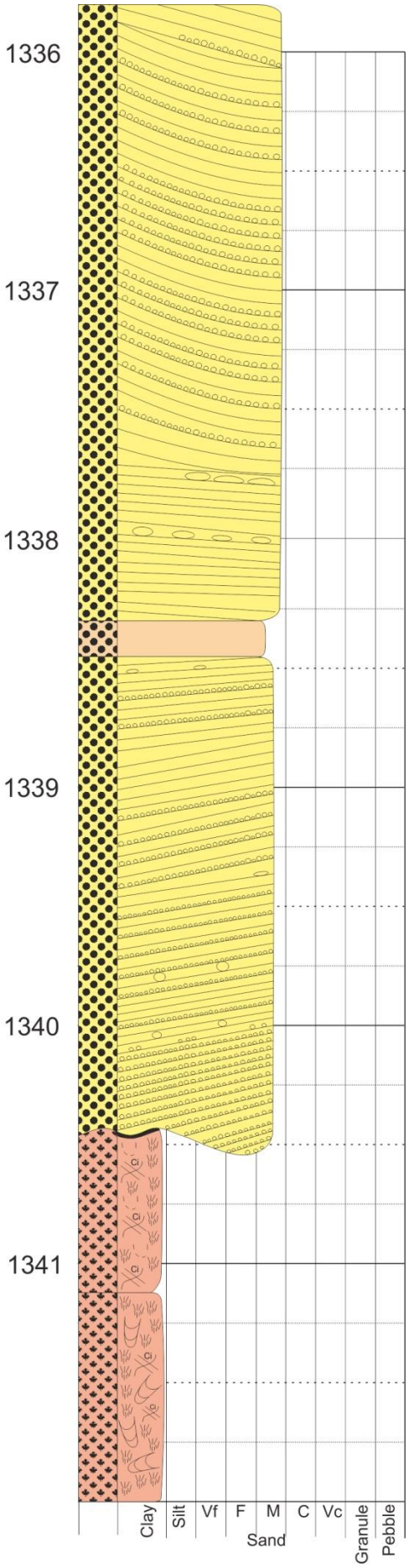

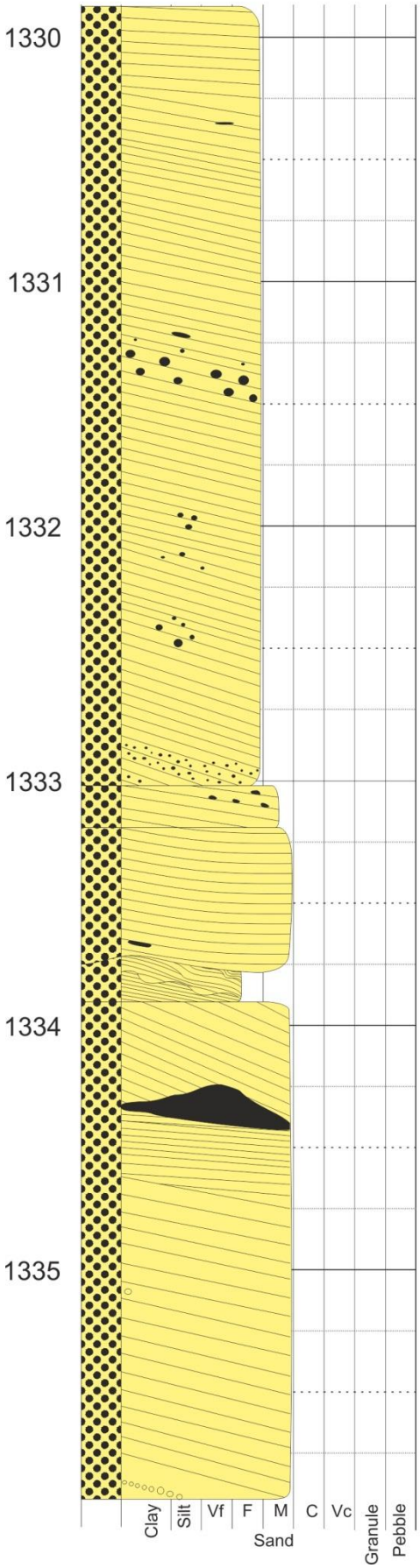
1330
1331
1332
1333
1334
1335
Clay
Silt
Vf
F
M
C
Vc
Granule
Pebble
Sand

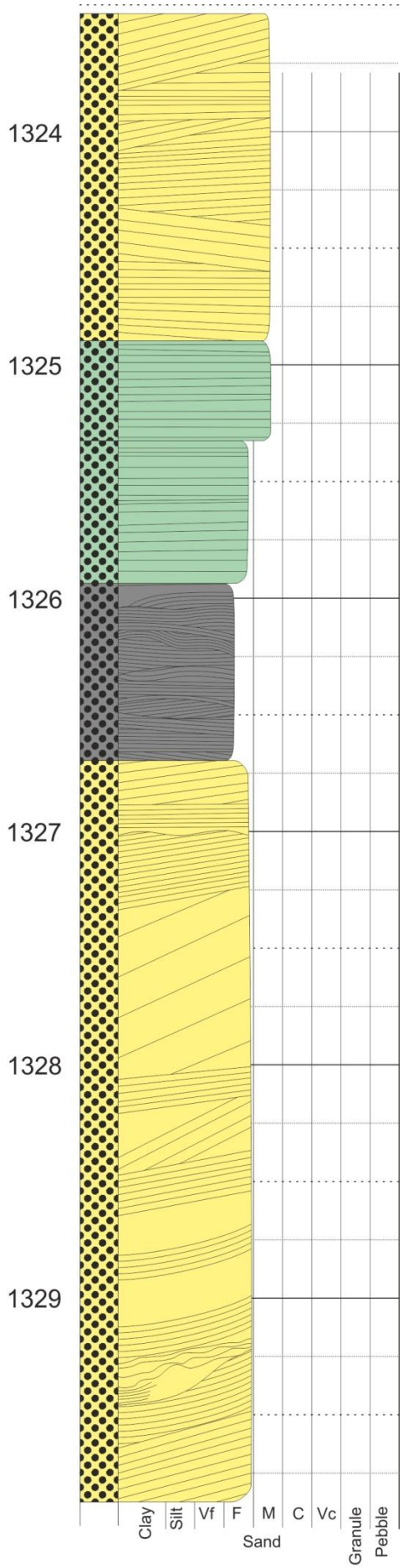
1324
1325
1326
1327
1328
1329
Clay
Silt
Vf
F
M
C
Vc
Granule
Pebble
Sand

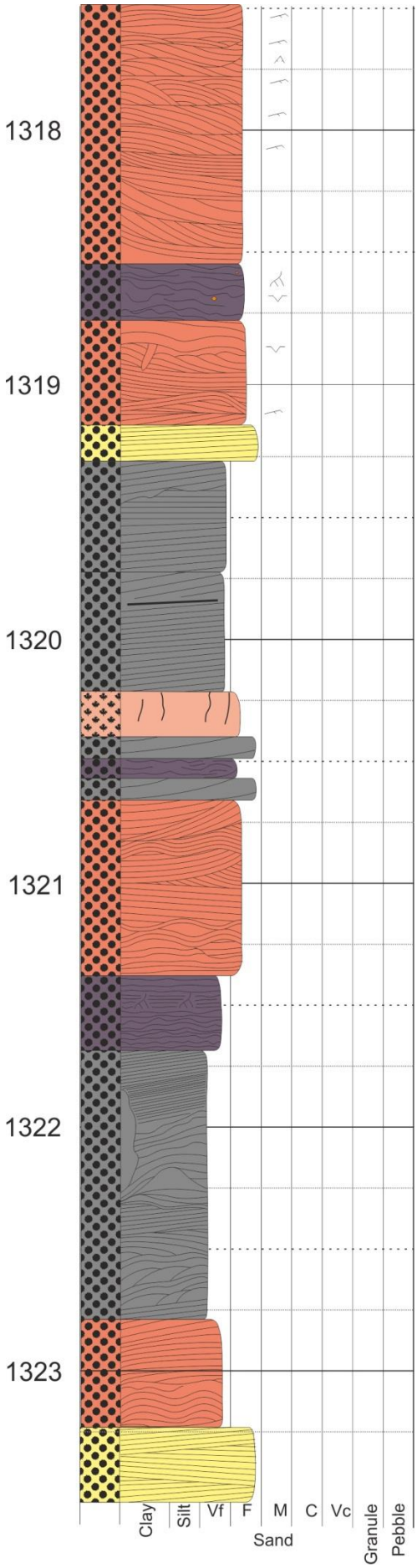
1318
1319
1320
1321
1322
1323
Clay
Silt
Vf
F
M
C
Vc
Granule
Pebble
Sand

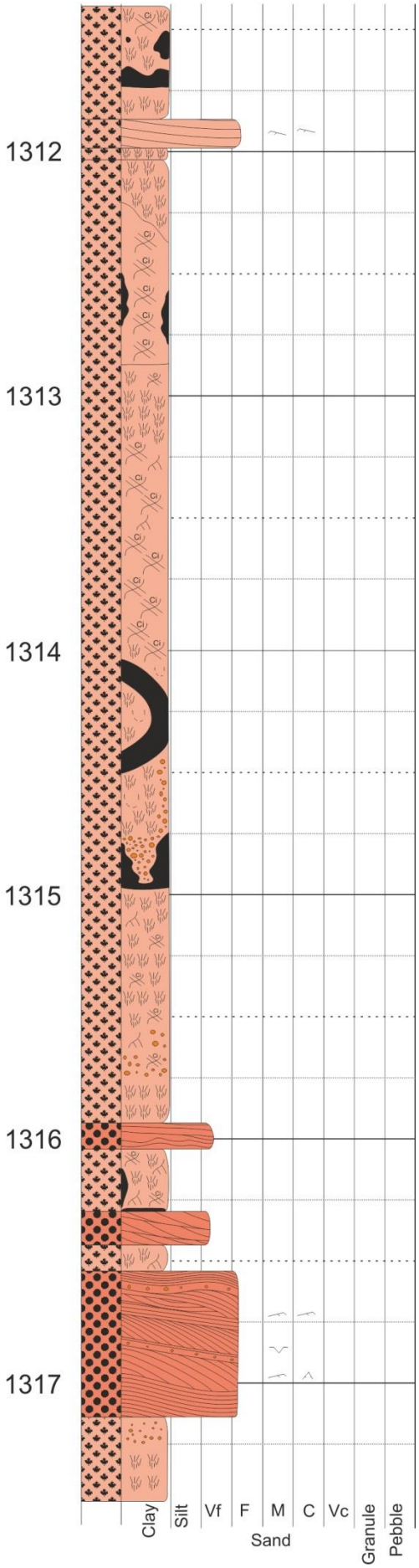
1312
1313
1314
1315
1316
1317
Clay
Silt
Vf
F
M
C
Vc
Granule
Pebble
Sand

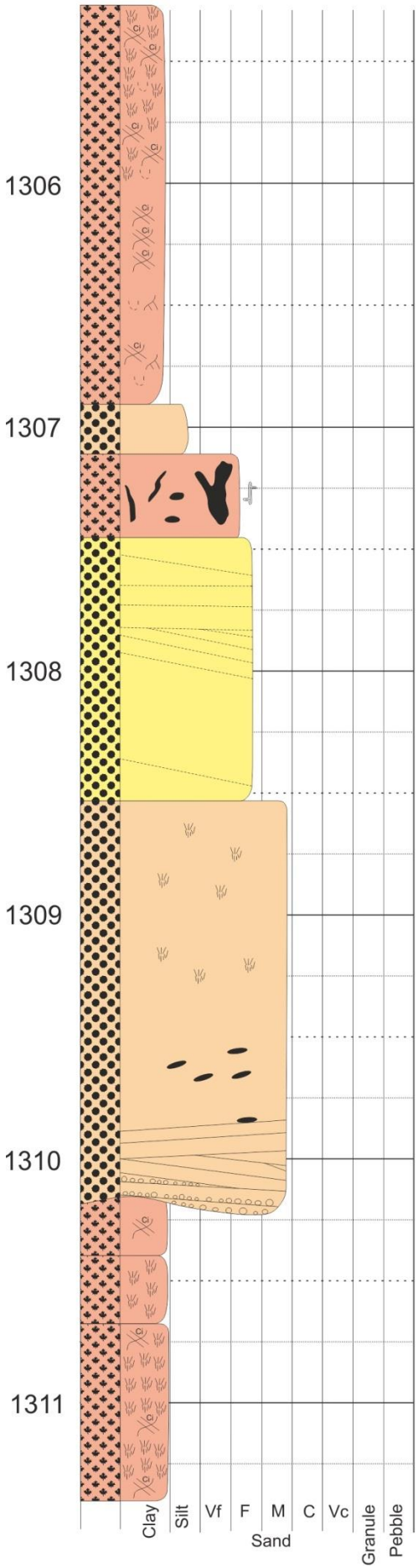
1306
1307
1308
1309
1310
1311
Clay
Silt
Vf
F
M
C
Vc
Granule
Pebble
Sand

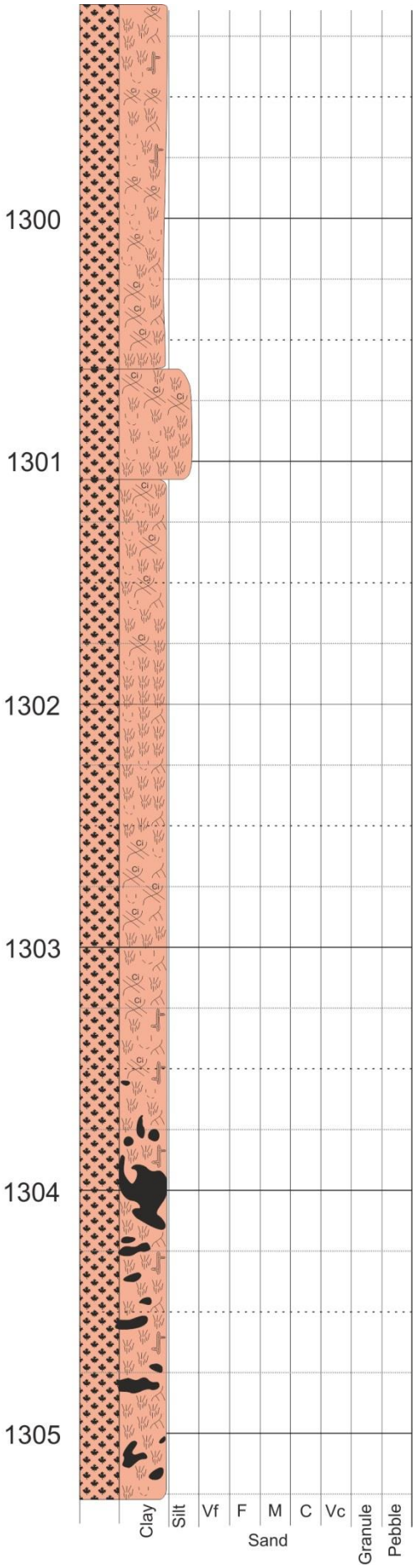
1300
1301
1302
1303
1304
1305
Clay
Silt
Vf
F
M
C
Vc
Granule
Pebble
Sand

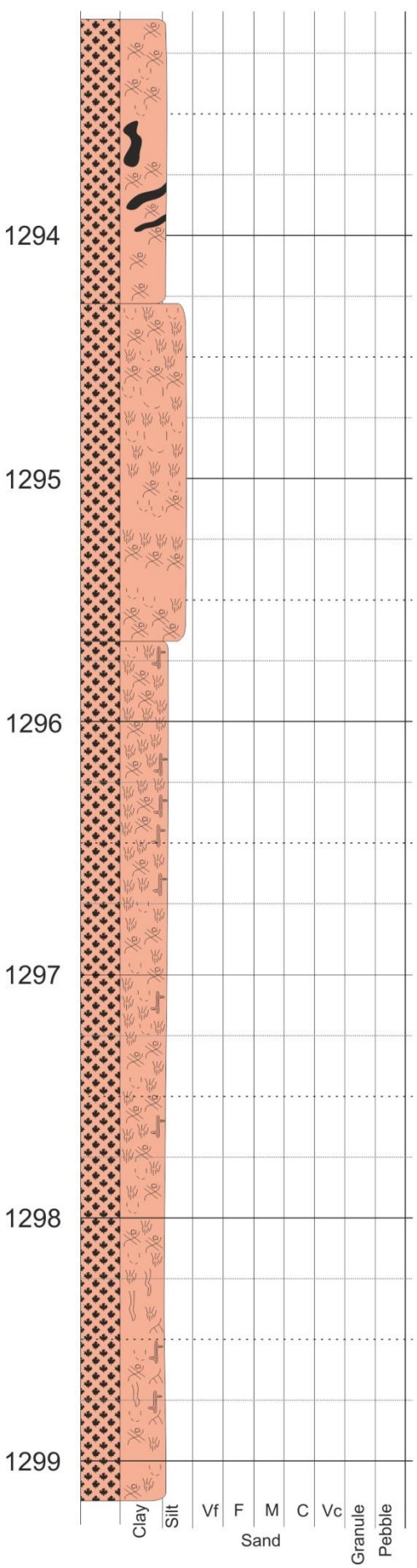
1294
1295
1296
1297
1298
1299
Clay
Silt
Vf
F
M
C
Vc
Granule
Pebble
Sand

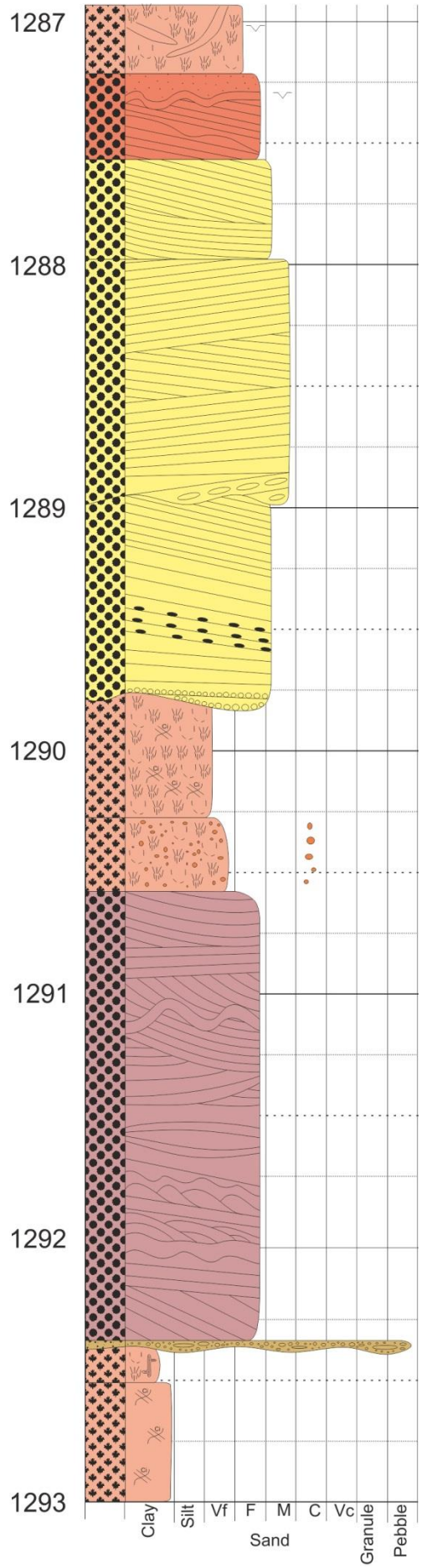
1287
1288
1289
1290
1291
1292
1293
Clay
Silt
Vf
F
M
C
Vc
Granule
Pebble
Sand

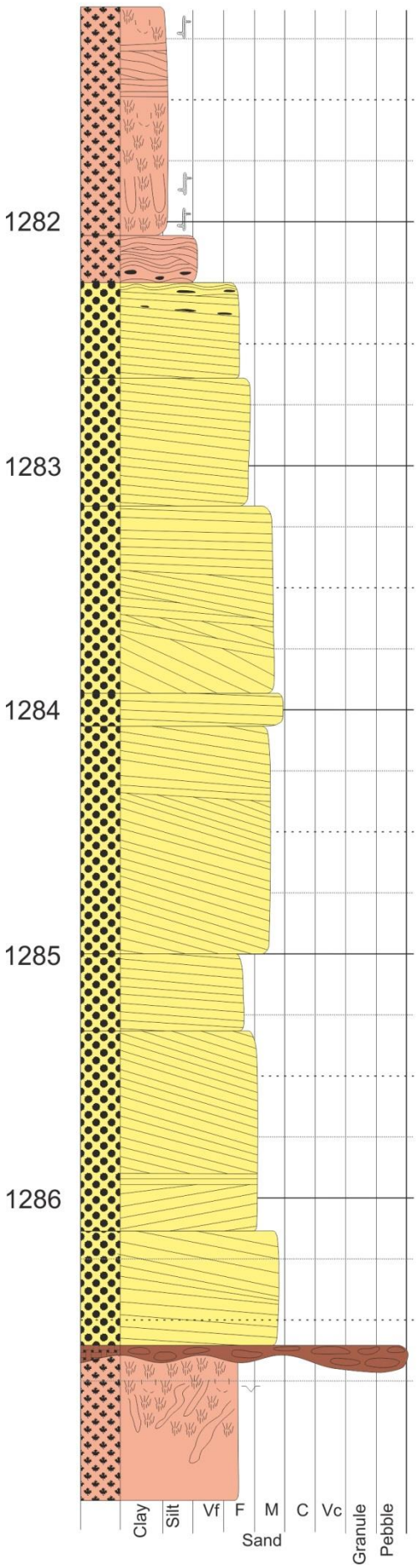
1282
1283
1284
1285
1286
Clay
Silt
Vf
F
M
C
Vc
Granule
Pebble
Sand

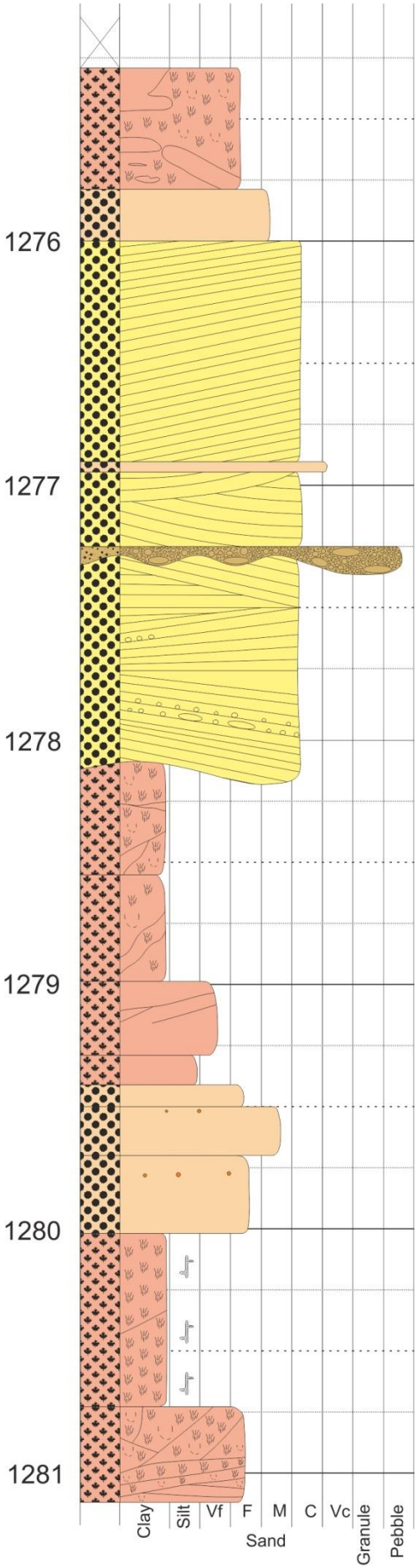
1276
1277
1278
1279
1280
1281
Clay
Silt
Vf
F
M
C
Vc
Granule
Pebble
Sand

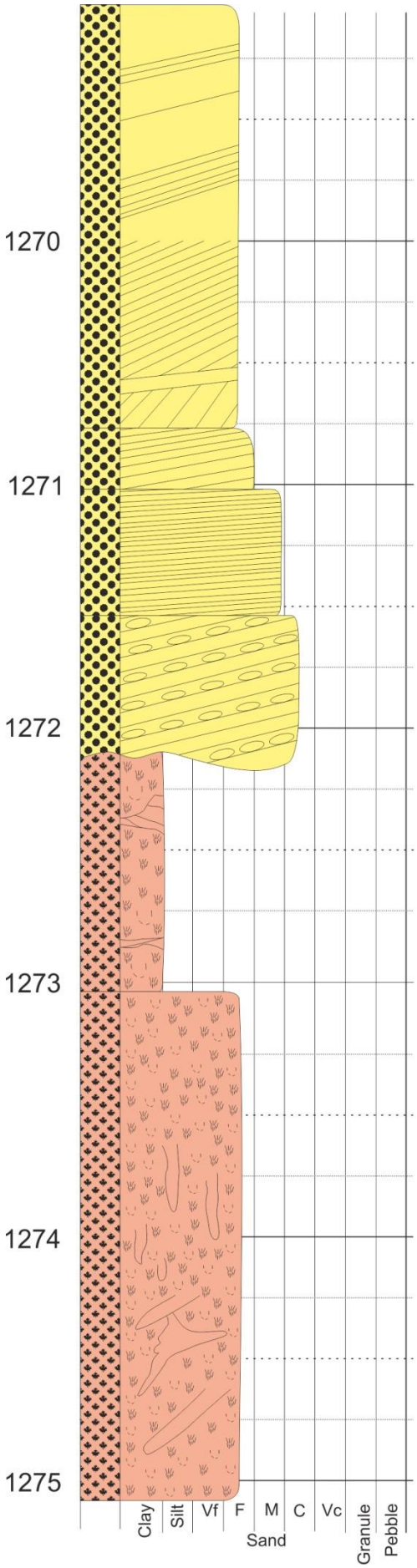
1270
1271
1272
1273
1274
1275
Clay
Silt
Vf
F
M
C
Vc
Granule
Pebble
Sand

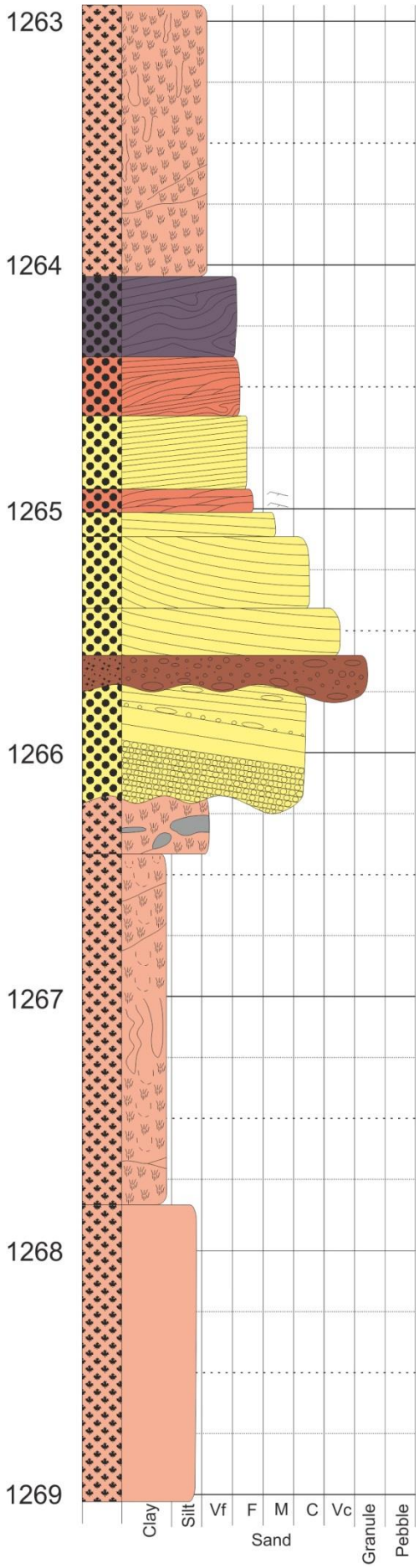
1263
1264
1265
1266
1267
1268
1269
Clay
Silt
Vf
F
M
C
Vc
Granule
Pebble
Sand

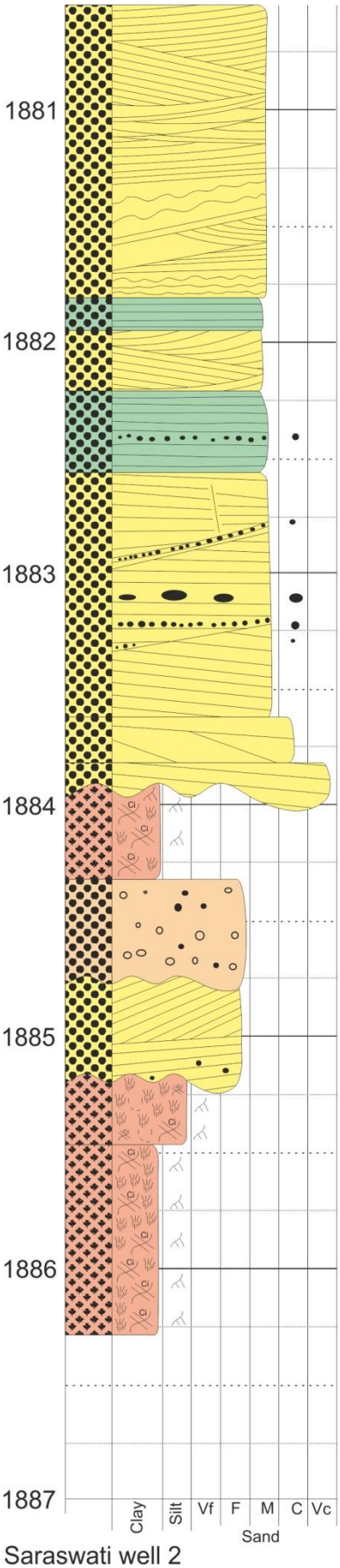

Saraswati well 2

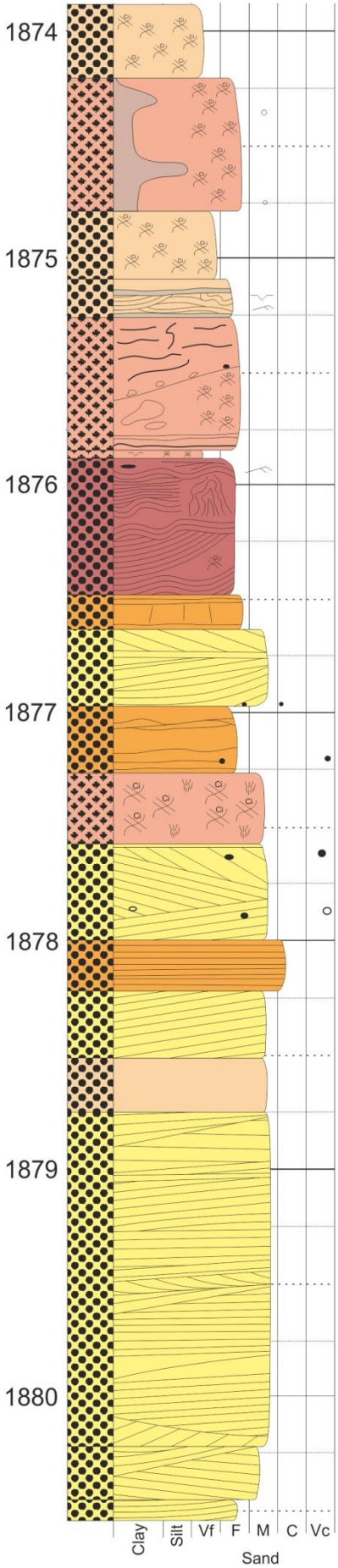

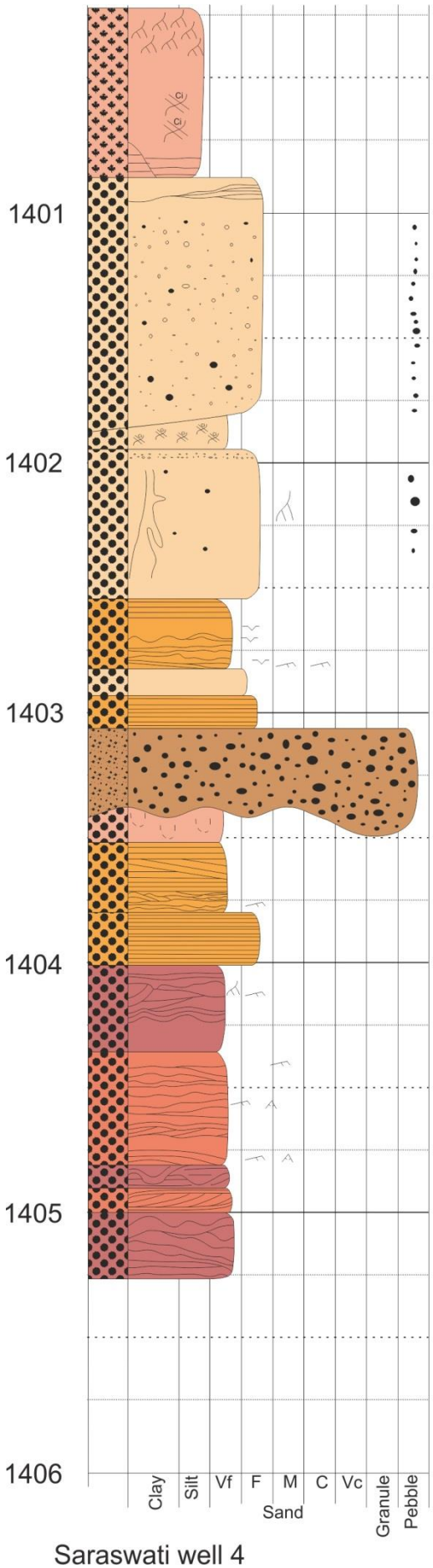

Saraswati well 4